Synthesis of Densely-Functionalized Multicyclic Ring Systems from Bicyclobutanes

by

Kyla J. Woelk

A Dissertation Submitted in Partial Fulfillment of the

Requirements for the Degree of

DOCTOR OF PHILOSOPHY

in the Department of Chemistry

University of Victoria

Synthesis of Densely-Functionalized Multicyclic Ring Systems from Bicyclobutanes

by

Kyla J. Woelk

Supervisory Committee

Dr. David Leitch, Supervisor
Department of Chemistry

Dr. Jeremy Wulff, Departmental Member
Department of Chemistry

Dr. Fraser Hof, Departmental Member
Department of Chemistry

Dr. Alisdair Boraston, Outside Member
Department of Biochemistry and Microbiology

Abstract

The discovery and development of novel small molecule drug candidates is essential to the advancement of the pharmaceutical industry. One area of focus for drug development is increasing the molecular complexity and number of Csp^3 centers in pharmaceutical candidates. Saturated multicyclic structures have been proposed as bioisosteres to replace portions of pharmaceutical molecules that lack these Csp^3 centers. Incorporating these bioisosteres in existing pharmaceuticals has been shown to improve pharmacokinetic properties and in some cases even increase the drug's potency. The syntheses to access these bioisosteres is limited and thus, efforts to develop more syntheses of these motifs is crucial in progressing the development of new drugs.

This thesis explores the development of new methods to access these saturated multicyclic bioisosteres, specifically bridging bicycloalkanes. Bicyclo[1.1.0]butanes are used as a common starting material to access the different bicyclic compounds. Focus is placed on the use of readily available starting materials and straightforward reaction conditions. Reaction discovery, optimization and viability is reported for a variety of different bicyclic compounds. The types of bicyclic compounds that were synthesized include 2-azabicyclo[2.1.1]hexanes, 2-oxo-bicyclo[2.1.1]hexanes and 3-azabicyclo[3.1.1]heptanes. High-throughput experimentation was used to aid in reaction discovery and optimization in a streamlined manner. Reaction scopes were developed to demonstrate the applicability of these methods.

Finally, this thesis demonstrates the potential for application of these bicyclic bioisosteres in pharmaceuticals *via* target-based synthesis. This was done through the functionalization of the products synthesized. This demonstrates their ability to be modified so they can be incorporated into drug candidates. With more syntheses of these bioisosteres available to medicinal chemists, the ability for these motifs to be applied in future drug development processes can be improved.

Contents

List of Tables

List of Figures

List of Abbreviations

Ac	Acetyl
ADME	Absorption, Distribution, Metabolism and Elimination
Ak	Alkyl
aq	Aqueous
Ar	Aryl
ATR	Attenuated Total Reflectance
azaBCH	Azabicyclohexane
BCB	Bicyclobutane
BCH	Bicyclo[2.1.1]hexane
BCO	Bicyclo[2.2.2]octane
BCP	Bicyclo[1.1.1]pentane
BHT	Butylated Hydroxytoluene
BINAP	2,2'-bis(diphenylphosphino)-1,1'-binaphthyl
Bn	Benzyl
Boc	*tert*-Butyloxycarbonyl
bpy	2,2'-Bipyridine
Bu	Butyl
CAN	Cerium Ammonium Nitrate
Cbz-Cl	Benzyl Chloroformate
CCDC	Cambridge Crystallographic Data Centre
CCW	Counter-Clockwise
CDI	1,1'-Carbonyldiimidazole
CIF	Crystallographic Information File
COSY	Homonuclear Correlation Spectroscopy
CPME	Cyclopentyl Methyl Ether
CW	Clockwise
d	Doublet

DBU	1,8-Diazabicyclo[5.4.0]undec-7-ene
DCM	Dichloromethane
DIH	1,3-Diiodo-5,5-Dimethylhydantoin
DIPEA	*N,N*-Diisopropylethylamine
DMAP	4-Dimethylaminopyridine
DMF	Dimethyl Formamide
DMP	2,2-Dimethoxypropane
DMSO	Dimethylsulfoxide
dppe	1,2-Bis(diphenylphosphino)ethane
dppf	1,1'-Bis(diphenylphosphino)ferrocene
d.r.	Diastereomeric Ratio
E	Electrophile
EDG	Electron Donating Group
EI	Electron Ionization
ESI	Electrospray Ionization
Et	Ethyl
EtOAc	Ethyl Acetate
Equiv	Equivalent
EWG	Electron Withdrawing Group
HMBC	Heteronuclear Multiple Bond Correlation
HOMO	Highest Occupied Molecular Orbital
HPLC	High Performance Liquid Chromatography
HRMS	High Resolution Mass Spectrometry
HSQC	Heteronuclear Single Quantum Coherence
HTE	High-Throughput Experimentation
iPr	Isopropyl
IR	Infrared
KHMDS	Potassium Bis(trimethylsilyl)amide
LCMS	Liquid Chromatography Mass Spectrometry
LDA	Lithium Diisopropylamide

LG	Leaving Group
LiHMDS	Lithium Bis(trimethylsilyl)amide
LRMS	Low Resolution Mass Spectrometry
LUMO	Lowest Unoccupied Molecular Orbital
m	Multiplet
mCPBA	*meta*-Chloroperbenzoic acid
Me	Methyl
MeCN	Acetonitrile
Mesyl	Methanesulfonyl
NCS	*N*-Chlorosuccinimide
NHC	*N*-heterocyclic carbene
NIS	*N*-Iodosuccinimide
NMI	*N*-Methylimidazole
NMR	Nuclear Magnetic Resonance
NOE	Nuclear Overhauser Effect
NOESY	Nuclear Overhauser Effect Spectroscopy
Nosyl	*N*-Alkyl Nitrobenzenesulfonamide
Nu	Nucleophile
2-Oxo-BCH	2-Oxo-Bicyclo[2.1.1]hexane
Ph	Phenyl
Piv	Pivalate
PMB	*p*-Methoxybenzyl
PMP	*p*-Methoxyphenyl
ppm	Parts Per Million
PTFE	Polytetrafluoroethylene
q	Quintet
rt	Room Temperature
s	Singlet
SC-XRD	Single Crystal X-ray Diffraction
SFC	Supercritical Fluid Chromatography

t	Triplet
TBME	Methyl *Tert*-Butyl Ether
*t*Bu	*tert*-Butyl
Tf	Triflate
THF	Tetrahydrofuran
TMB	1,3,5-Trimethoxybenzne
TMGA	*N,N,N,N*-Tetramethylguandinium Azide
TMSA	Trimethylsilyl Azide
TMS-OTf	Trimethylsilyl Trifluoromethanesulfonate
TOCSY	Total Correlation Spectroscopy
Ts	Tosyl
vol	Volume
v/v	Volume Per Volume
XRD	X-ray Diffraction

Acknowledgements

I would like to sincerely thank Dr. David Leitch for his supervision over the last four years. All of his support, guidance and expertise throughout my degree exceeded my expectations. I am beyond grateful to have had him as my mentor.

Further, I wish to thank all of the members of the Leitch group over the years for their support and kindness. I want to specifically thank Kushal for all of his co-collaboration and advice with the bicyclobutane project and Nahia for her friendship and support throughout my degree. Thank you to the wonderful undergraduates Jae, Faith, Jesse and Liam that have worked with me on this research.

I am extremely grateful to my family and friends for their constant support and understanding throughout all of my academic journey. I am lucky to have such loving and encouraging parents with undeniable support. Their eagerness to hear and learn about my research was so meaningful (and learning what bicyclobutanes are!). Kaden, I can't thank you enough for being by my side for everything and supporting me throughout my degree.

1 Introduction

1.1 Molecular Complexity in Pharmaceuticals

Small molecules are extremely important as active pharmaceutical ingredients as they make up 90% of all pharmaceutical drugs.[1] One promising area in synthetic chemistry is the exploration of new "chemical space" to discover structurally novel drug candidates. Chemical space is a concept from cheminformatics that refers to the property of space that is spanned by all possible molecules or chemical compounds. The estimated number of possible organic molecules with a molecular weight <500 Da is on the order of 10^{60}.[2] According to the Chemical Abstracts Service database, the total number of all registered organic and inorganic substances as of 2024, is 63,909,687.[3] Clearly, we have only began to explore all of the possible chemical space relevant to drug discovery.

Despite enormous efforts in drug discovery, less than 10% of potential pharmaceuticals succeed in clinical trials.[4–6] To improve our ability to treat cancers, infectious diseases, and other currently incurable medical problems, advances in synthetic organic chemistry are critical. In particular, drug candidates with more three-dimensional character (i.e. those with more sp^3-carbons) tend to be more successful in clinical trials.[7;8] Due to the challenges of accessing molecules with more sp^3-carbons, this area of chemical space is underexplored in medicinal chemistry.

Medicinal chemists look for tools to help predict whether a molecule will have favourable pharmaceutical properties for it to succeed as a potential drug candidate. This is important because about 40% of drug candidiates fail due to these properties such as poor solubility, permeability and metabolic stability.[9;10] A common tool for evaluating whether an orally administered drug will have these favourable pharmaceutical properties is Lipinski's "Rule of Five".[11;12] These guidelines have been implemented across the pharmaceutical industry, lead-

ing to compounds being pre-screened to flag any that do not meet two or more of the following descriptors: molecular weight <500 Da, number of hydrogen bond acceptors <10, number of hydrogen bond donors <10, and calculated n-octanol-water partition coefficient (Clog P) <5.[13] Despite these rules, there has been increasing research on drug candidiates that reach beyond the rule of five in an effort to expand the scope of pharmaceutical development.[14;15]

More recent studies have shown that increasing the molecular complexity measured in terms of fraction of sp^3 hydrbridized carbons and the number of stereogenic carbon centers is also correlated to drug success.[7;8;16] Fsp^3 is defined as:

$$Fsp^3 = (number\ of\ sp^3\ hybridized\ carbons/total\ carbon\ count) \tag{1.1}$$

Molecules with a low Fsp^3 - i.e. those with a significant fraction of sp^2 hybridized carbons - dominate the synthetic pharmaceutical industry, which contributes to a lack of molecular complexity.[17] This is due to the relative simplicity of synthesizing molecules containing sp^2 centers compared to sp^3 centers.[17] This is because the coupling of sp^2-sp^2 centers is well developed and widely used, with both S_NAr and Suzuki-Miyaura coupling being in the top 5 most frequent reactions used in medicinal chemistry.[18] Dabrafenib, used for treating cancer, is an example of a synthetic drug that is almost completely comprised of sp^2-carbons (Figure 1.1). This can be compared to a natural product anti-cancer drug, paclitaxel, which is an example of 3D structural complexity in a successful pharmaceutical (Figure 1.1). With more syntheses of sp^3-rich molecules being developed, the focus on incorporating these saturated structures into pharmaceuticals is becoming more common.

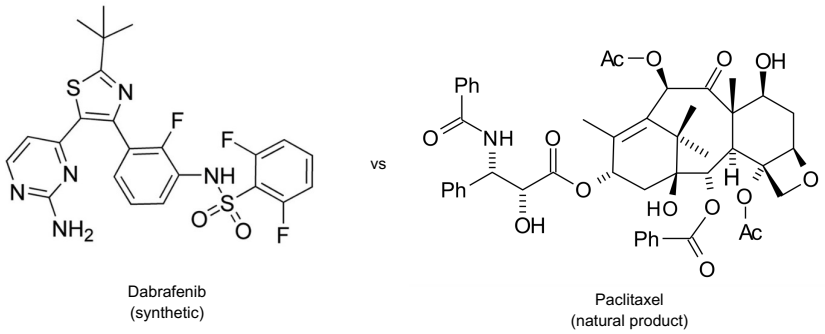

Figure 1.1: Dabrafenib (synthetic) vs Paclitaxel (natural product)

In addition to drug potency, another important aspect for evaluating drug success is by assessing the molecule's overall pharmacokinetic properties. The pharmacokinetic properties of a drug are the measurements of four processes that the drug undergoes in the body, which are absorption, distribution, metabolism and elimination (ADME) (Figure 1.2).[19–21] For an orally administered drug, the physiochemical properties are ultimately what determines how well the drug will perform in the ADME studies.[19;20] Absorption refers to the drug absorption by the walls of the gastrointestinal (GI) tract to enter the blood stream following an oral administration of the pharmaceutical.[20] For the drug to have high absorption, the lipophillicity and solubility of the drug is crucial. These properties can be greatly affected by the molecular substituents and functional groups present in the molecule.[20] Distribution of the drug throughout the blood stream and tissues follows absorption and is also influenced by the properties of the molecule. These properties can affect whether the drug stays in the blood plasma or if it is transported throughout the entire body.[19;20] Controlling the distribution of the drug based on its properties will also affect its relative toxicity and off-target delivery.[19] Metabolism of the drug is also controlled largely by the structure and properties of the given pharmaceutical. Metabolism is highly dependent on the types functional groups present in the molecule. Further, it is crucial that the drug is metabolised at the right step of administration and that no unwanted metabolic reactions occur prior to drug binding/delivery at the desired tissues.[19] For elimination, metabolic clearance is one of the major routes, thus having a molecule that will be metabolized safely in the liver following the desired binding/treatments and that will not be metabolized prior to that is extremely important.[19] Lastly, the other most common method of elimination is renal clearance, controlled by the kidneys, where the drug must be filtered and secreted into the urine, which also depends on its pharmacokinetic molecular properties.[19] The ability of a given pharmaceutical to undergo these four ADME processes describes its overall pharmacokinetic behaviour.

Researchers have established a correlation that relates a higher degree of saturation (i.e. more sp^3-carbons) to improved pharmacokinetic properties, including lipophilicity, solubility, and/or metabolic stability.[22–24] These pharmacokinetic properties can improve the likelihood that the drug molecules will reach the desired target in the body. In addition, having more molecular complexity has been shown to help reduce off-target affects including drug toxic-

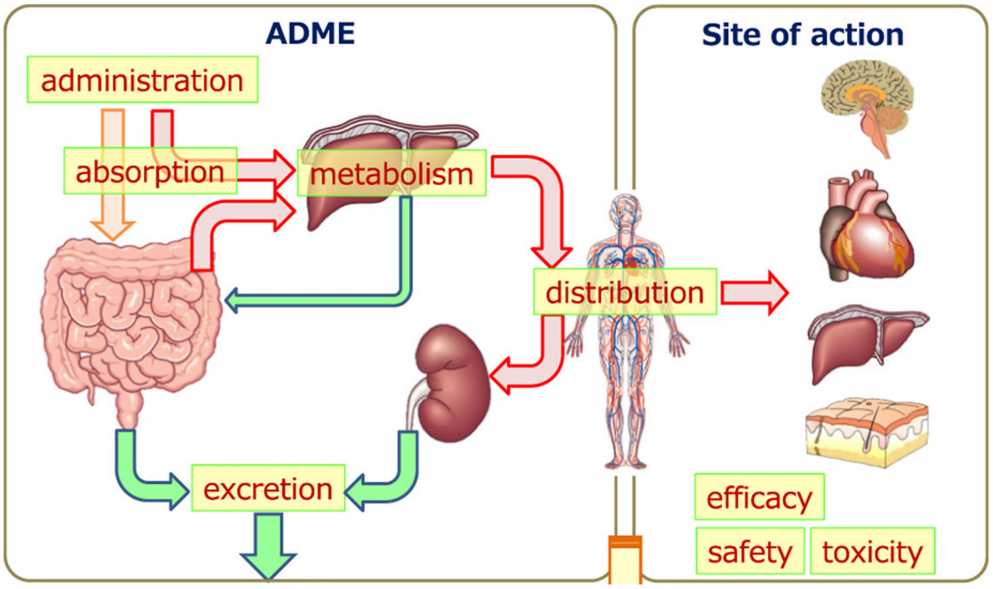

Figure 1.2: ADME processes. Reprinted (adapted) with permission from Ishida, S. *Drug Metabolism and Pharmacokinetics* **2018**, *33*, 49–54. Copyright 2024 Elsevier.[21]

ity.[7;8] Further, having more molecular complexity and three-dimensionality in pharmaceuticals will allow them to better interact with the binding pockets of the target enzymes/proteins in the body.[25] Studies have shown that when the number of sp^3-hybridized atoms as well as stereogenic centers are increased, the frequency and selectivity of drug-protein binding is typically higher.[25;26]

1.2 Bioisosteres

1.2.1 Classical vs Non-Classical Bioisosteres

One way to increase the degree of saturation and sp^3 character in pharmaceuticals is through the use of bioisosteres. Bioisosteres are replacements for structurally similar motifs that have similar biological properties.[27–29] Although biologically similar, these changes can affect the pharmacokinetics of a given pharmaceutical. In some cases, a biosteric replacement can cause an increase in the activity of a drug.

The concept of bioisosterism started in 1919 when Langmuir noted that chemically different substances can have similar physical properties.[30] For example, CO, N_2O, CO_2, and NCO^- all have similar physical properties and have the same number and arrangement of valence

electrons.[30] This finding was classified as isosterism and defined as groups of atoms having the same number and arrangement of valence electrons.[28;30] This differers from isoelectronic species, where the molecules have the same arrangement and total number of electrons. Using this classification method, groups of isosteres were determined by Langmuir (Table 1.1).[30] This definition was applied to biological systems when it was noted that some antibodies could not differentiate between phenyl/thienyl or $O/NH/CH_2$ substituents.[31] This was the first classification of bioisosterism,[31] and now bioisosteres are a key concept in medicinal chemistry. Bioisosteres can be classified into two main groups: classical and non-classical bioisosteres.

Table 1.1: Isosteres determined by Langmuir.[30]

Entry	Isosteres
1	H^-, He, Li^+
2	O^{2-}, F^-, Ne, Na^+, Mg^{2+}, Al^{3+}
3	N_2, CO, CN^-
4	CH_4, NH_4^+
5	CO_2, N_2O, N_3^-, CNO^-
6	MnO_4^-, CrO_4^{2}

Classical bioisosteres are isosteric replacements that do not significantly change the structure of the target molecule.[28;32] The most common example of a classical bioisostere is replacing a hydrogen atom with a fluorine (Figure 1.3).[32] Other examples include exchanging between hydroxyl, amino, thiol, chloro and bromo substituents to alter the biological properties (Figure 1.3).[28;32–34] All of these changes fall under the category of a monovalent substitution. Other types of substitution can take also place such as, divalent (interchange of atoms in a double bond), trivalent (interchange of atoms involving three bonds) and tetravalent substitutions (interchange of atoms involving four bonds) (Figure 1.3).[28;29;33]

On the other hand, non-classical bioisosteres involve a more complex structural change to the substituents and can include a conformational change or ring replacements (Figure 1.3).[28;29;34] These non-classical bioisosteres typically have a different number of atoms than the original substituent. These can be any replacement for a functional group or molecule that do not fall under the classification of a "classical" bioisostere and still maintain similar

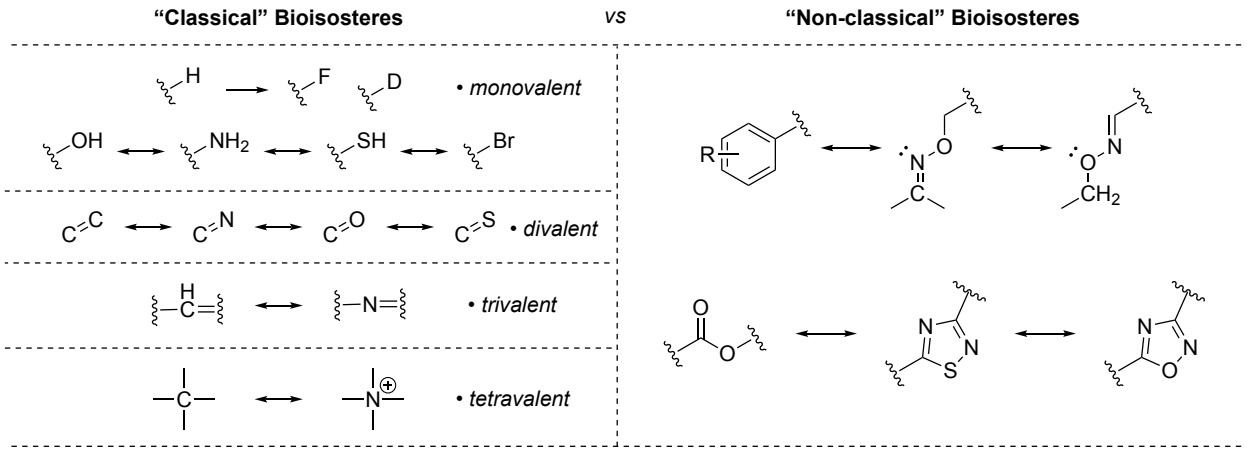

Figure 1.3: Examples of classical vs non-classical bioisosteres.

biologicial activity to the parent molecule. Biosisosteres can do this by having simlar spacial arrangement, electronic properties, or any other physiochemical property that allows them to reproduce the desired biological activity.[28;29] This can include noncyclic or cyclic replacements and the biological activity can be assessed after a replacement to determine if the structural change is viable as a successful bioisostere.[28;29;34]

1.2.2 Saturated Multicyclic Bioisosteres

Bicyclic sp^3-rich structures are being used as bioisosteres for aromatic rings in pharmaceuticals.[35–39] Replacing benzene rings has been challenging as it was difficult to replicate the geometry and substitution vectors of the ring. The most commonly used bicyclic bioisosteres being used in drug discovery now are bicyclo[1.1.1]pentane (BCP, unless explicitly stated, the [1.1.1] herein is implicit), cubane, and bicyclo[2.2.2]octane (BCO, unless explicitly stated, the [2.2.2] herein is implicit).[16] These have been used to replace 1,4-disubstituted phenyl rings and have shown to have improvements of pharmacokinetic properties and in some cases, improved drug activity (Figure 1.4).[37;40;41] Bicyclopentane was used as a bioisostere for a *para*-substituted benzene ring in Darapladib (an atherosclerosis treatment).[37] The bicyclopentane analogue showed improved solubility with retained potency compared to Darapladib.[37] Cubane was incorporated into the drug, Leteprinim (treatment for neurodegenerative disorders such as Alzheimer's disease, Parkinson's disease and strokes), where improved activity was observed.[40] Lastly, bicyclooctane was incorporated into a potential anti-tumour agent,

which improved metabolic stability and increased potency.[41] These examples highlight the potential for bicyclic bioisosteres to improve drug development capabilities and expand methods to discover new pharmaceuticals and treatments. Although improvement of these properties is not always observed, having these as tools for future drug development is crucial. However, all of these bioisosteres are mostly applied to 1,4-substituted benzene rings and the syntheses of these structures still prove to be challenging, making them difficult to incorporate in pharmaceuticals.

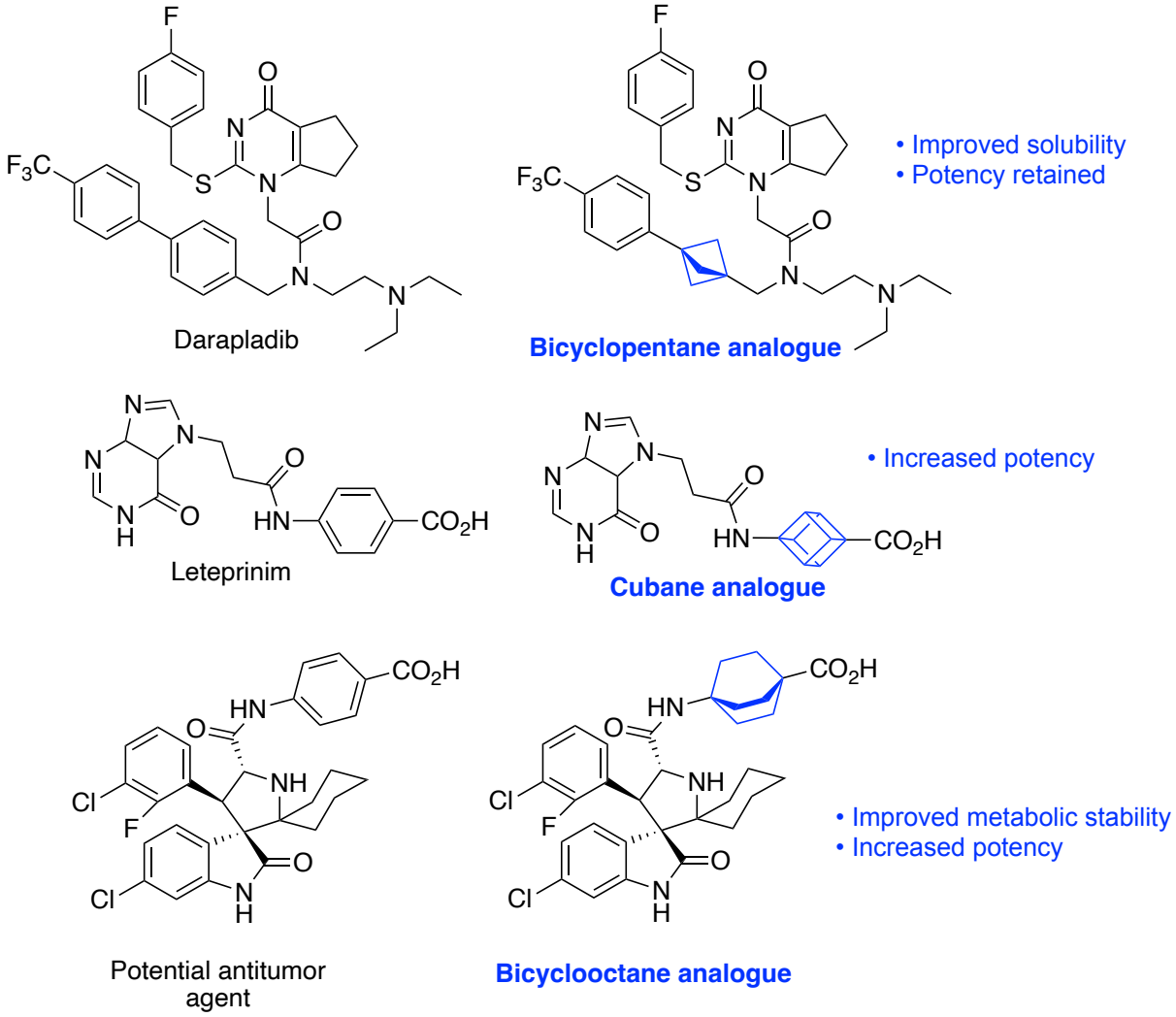

Figure 1.4: Bicyclic bioisostere replacements for 1,4-diphenyl motifs.[37;40;41]

Bicyclopentanes

Bicyclopentanes were one of the first rings that were used as a bioisostere for benzene rings.[16] The bicyclopentane perfectly represents the 180° angle between substituents on a 1,4-substituted benzene ring with only a ∼1 Å shortening of the overall length.[42] The first example of bicyclopentane being used in medicinal chemistry was in 1993 when a bicyclopentane was used to help improve the potency of an antibacterial drug, ciprofloxacin (Figure 1.5).[43] Shortly after, bicyclopentane was used as a bioisostere to mimic a benzene ring for a metabolic glutamate receptor antagonist, (*S*)-(4-carboxyphenyl)glycine where the biological activity of the drug was retained (Figure 1.5).[44]

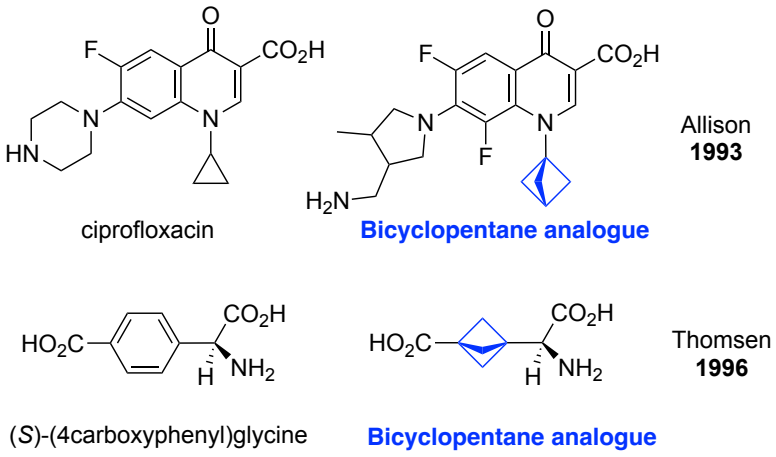

Figure 1.5: First use of bicyclopentane as a bioisostere for benzene.[43;44]

This finding was neglected initially and bicyclopentanes were not used again as bioisosteres until 2012 when Pfizer showed that bicyclopentane could be used to replace a 1,4-benzene ring in a γ-secretase inhibitor, Avagacestat (Figure 1.6).[36] They observed a retention of biological activity but the drug had improved solubility, membrane permeability and metabolic stability.[36] This highlights the ability of bicyclopentanes to improve pharmacokinetic properties compared to a simple benzene ring.

Although less common, bicyclopentanes have also been used occasionally to replace alkynes and *tert*-butyl groups (Figure 1.7).[38;45] In one example, the replacement of an alkyne with a bicyclopentane caused increased basicity of the drug.[38] In another example, a *tert*-butyl group was replaced by a bicyclopentane in bosentan, and improved potency was observed.[45]

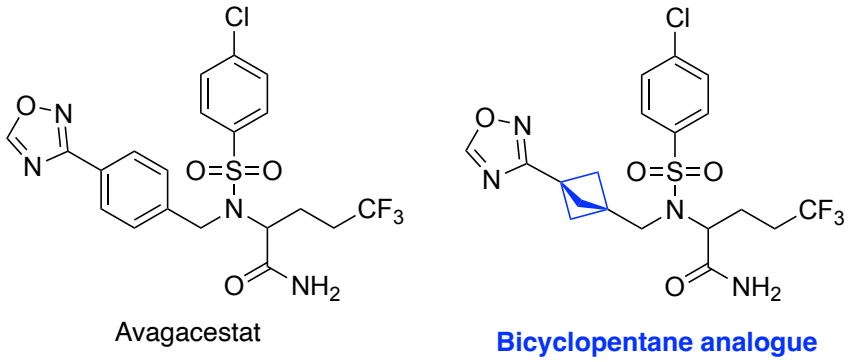

Figure 1.6: Bicyclopentane as a bioisostere for benzene in Avagacestat.[36]

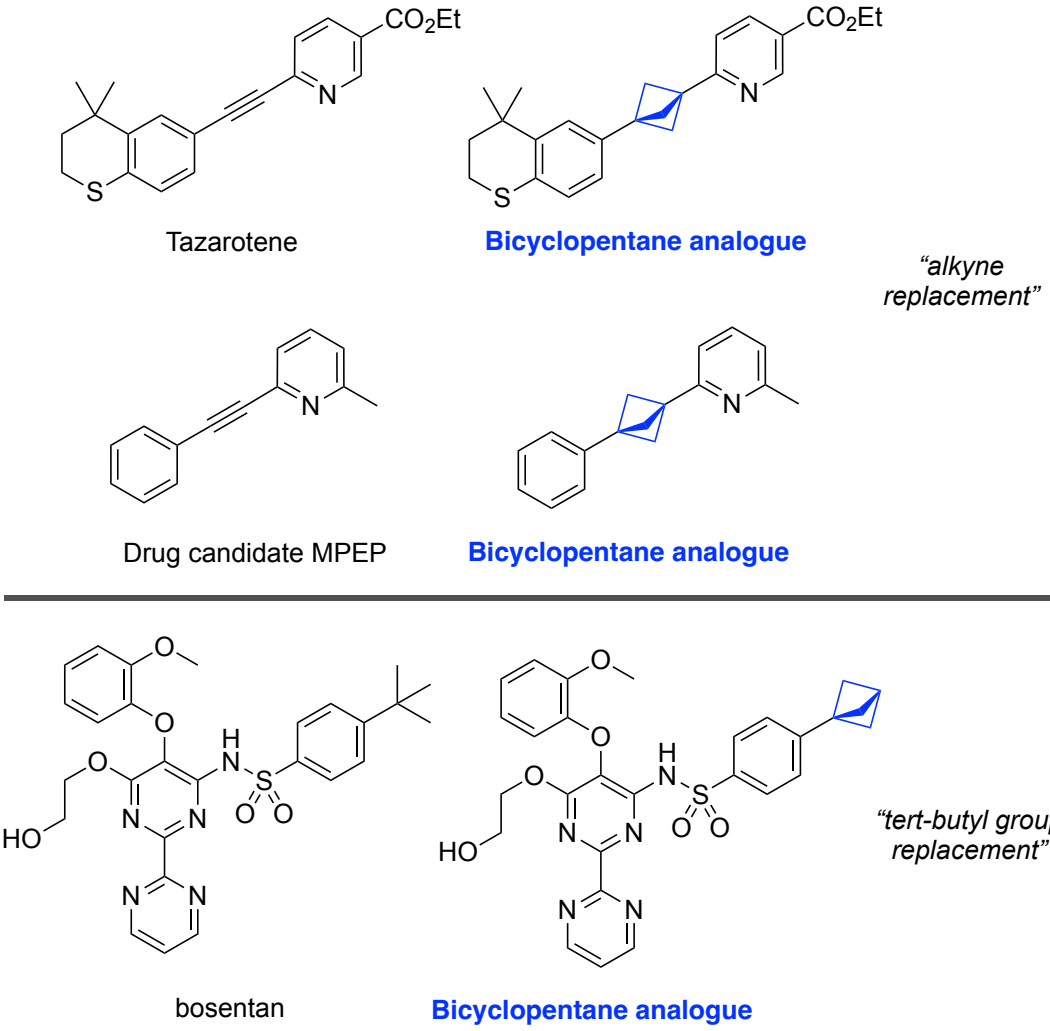

Figure 1.7: Bicyclopentane as a bioisostere for alkynes and *tert*-butyl groups.[38;45]

More recently, 1,2-bicyclopentanes have been tested as bioisosteres for *ortho*- and *meta*-substituted benzene rings.[46] Two examples where 1,2-bicyclopentane derivatives were used as bioisosteres were in lomitapide (*ortho*-substitution) and sonidegib (*meta*-substitution) where the replacement showed improved solubility of the drugs (Figure 1.8).[46]

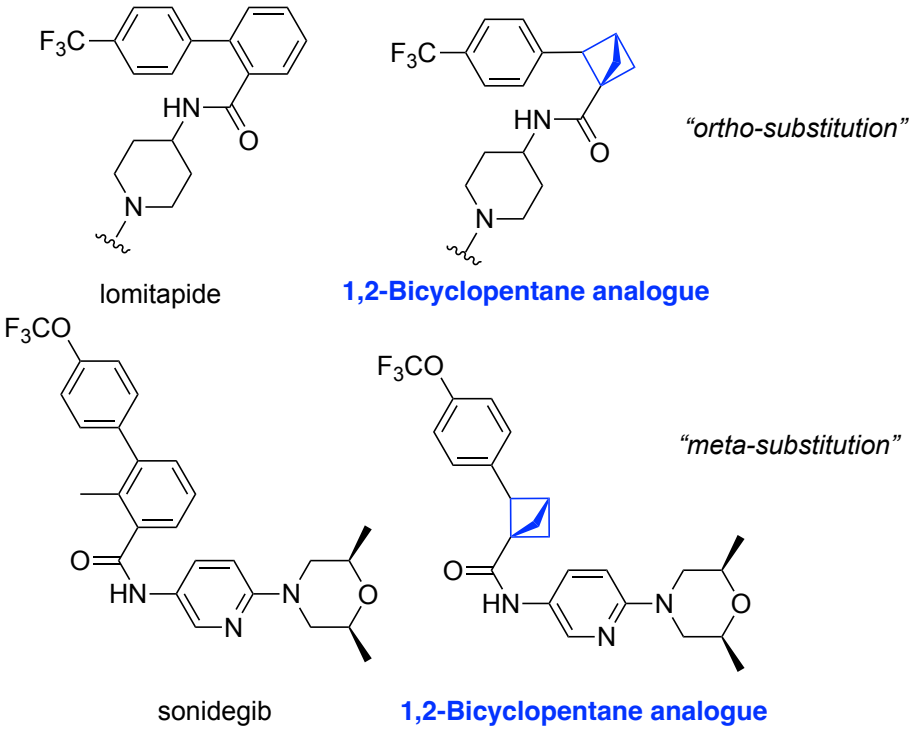

Figure 1.8: Bicyclopentane as a potential bioisostere for meta- and *ortho*-benzene rings.[46]

The main obstacle with bicyclopentanes has been their synthesis and this has limited their applicability in pharmaceuticals. Syntheses of bicyclopentanes are challenging and typically require photochemistry or the use of [1.1.1]propellane as a starting point, which is a volatile and potentially explosive compound (Figure 1.9).[42;47] Regardless, many research groups have developed the chemistry of propellane to generate a variety of substituted bicyclopentanes.

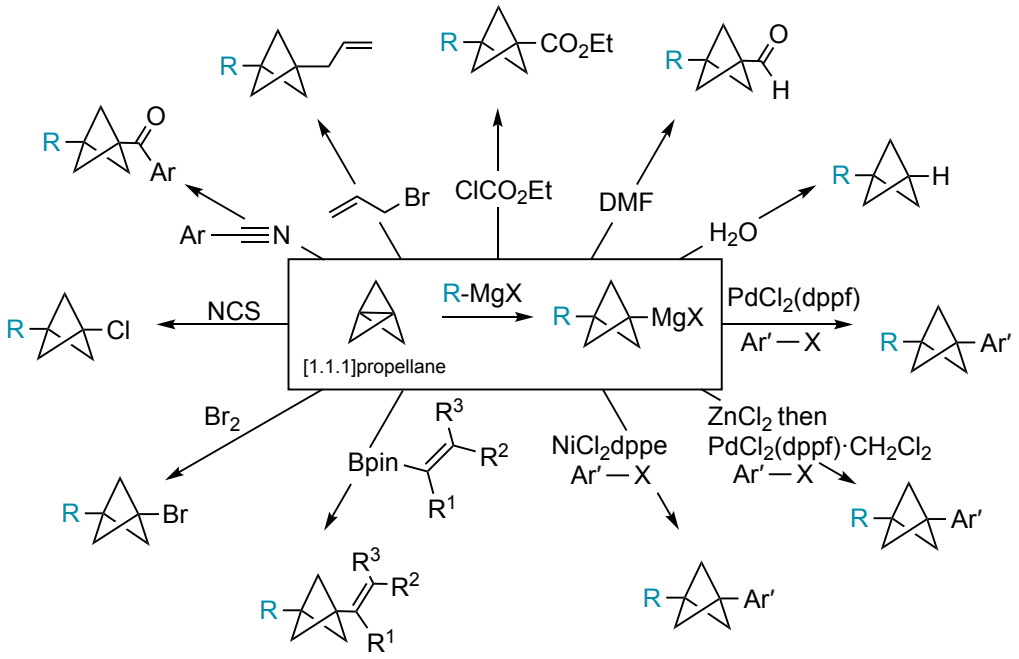

Figure 1.9: Typical syntheses and derivatizations of bicyclopentane.[42]

Cubane

Cubane has also been explored as a bioisostere for benzene rings in pharmaceuticals.[16] Most commonly, 1,4-cubane derivatives are used to replace *para*-substituted benzene rings.[16;40;48–50] 1,2-Cubane has been proposed as a bioisostere for *ortho*-substituted benzene rings, but no biological data has been obtained for the *ortho*-substituted replacement as of now. Recently, a 1,3-cubane derivative was used as a replacement for a *meta*-substituted benzene rings in lumacaftor (a cystic fibrosis drug) where improved solubility with the cubane analogue was observed (Figure 1.10).[51] A drawback of using cubane as a bioisostere is synthetic accessibility. Most syntheses start from a cubane skeleton, which makes specific functionalization challenging, or the synthesis is long and requires very specific conditions that make derivatizations difficult.[52] Additionally, some cubane structures have stability issues, making it a concern for metabolic stability in the body.[53–57] Specifically, contact of cubane with some transition metals caused molecular decomposition,[53–56] and decomposition was also observed under thermal and mechanochemical conditions.[57]

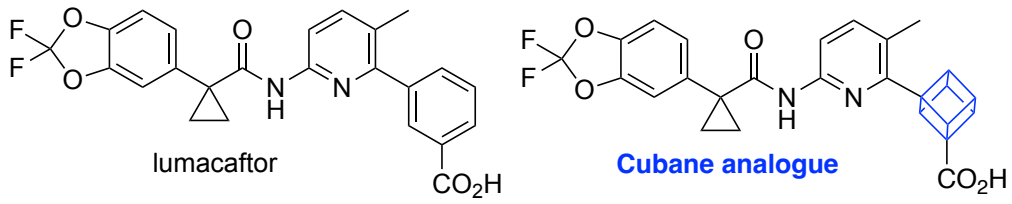

Figure 1.10: 1,3-Cubane bioisostere for *meta*-benzene.[51]

Bicyclooctanes

Bicyclooctanes have also been used as bioisosteres for benzene rings in drugs.[16;58] Bicyclooctanes have only been reported as bioisosters for *para*-substituted benzene rings, likely due to the difficulty in functionalizing the bridging carbons.[16] Bicyclooctane bioisosteres have been shown to improve pharmacokinetic properties when incorporated into a variety of drugs. Most commonly, these saturated structures will increase the lipophilicty of the drug with one major drawback being that they can sometimes cause the drug to become too lipophilic.[16;59] 2-Oxabicyclo[2.2.2]octane is one molecule that has been proposed to help mediate the increased lipohilicity of bicyclooctanes.[58] When bicyclooctane and 2-oxabicyclooctane were used to replace a *para*-substituted benzene in imantinib (an anticancer drug), the bicyclooctane derivative had a drop in solubility whereas the 2-oxabicyclooctane analogue gave improved solubility (Figure 1.11).[58] Both the bicyclooctane analogue and 2-oxabicyclooctane analogue showed reduced lipophilicity while maintaining biological activity.[58] The 2-oxabicyclooctane also had improved metabolic stability.[58] Developing more routes to synthesize these types of structures continues to be of importance for future application of these bioisosteres.

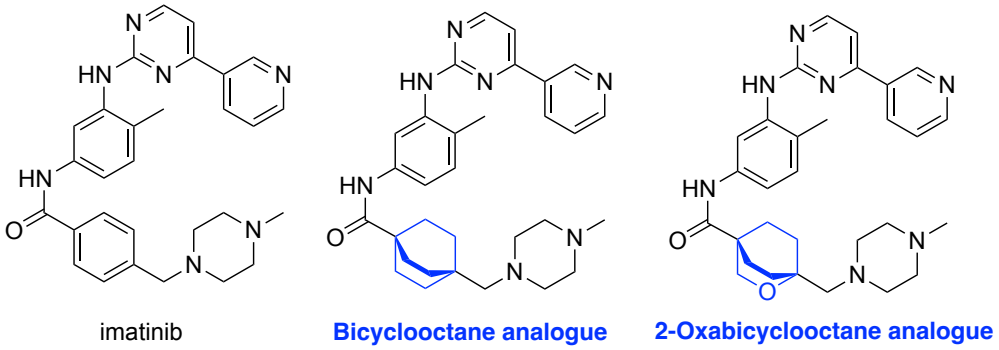

Figure 1.11: Bicyclooctane compared to 2-oxabicyclooctane as bioisosteres.[58]

1.2.3 Bicyclohexane Bioisosteres

After being proposed by Mykhailiuk in 2019,[16] a promising bicyclic bioisostere that is emerging in the literature is bicyclo[2.1.1]hexane (BCH, unless explicitly stated, the [2.1.1] herein is implicit). These motifs proved to be challenging to synthesize in the past, with the rare examples of bicyclohexanes generated via intramolecular photochemical [2+2] cycloadditions.[60–64] This limited the derivatives of bicyclohexane structures that could be accessed, with densely functionalized derivatives especially challenging to obtain. Since 2022, more syntheses of bicyclohexanes have been developed, which involve cycloaddition reactions with bicyclobutanes (See Section 1.4.5 for more details).[65–68] However, as this area is expanding and the need for these motifs grows, more efforts need to be placed on synthetic routes to access these potential bioisosteres.

Depending on the substitution on the bicyclohexane, they have been proposed to replace *ortho*, *meta* and even multisubstituted benzene rings (Figure 1.12).[16] The proposal to replace other substitution patterns of benzene rings is because of the angle vectors of the different substitution patterns possible on bicyclo[2.1.1]hexanes.[16]

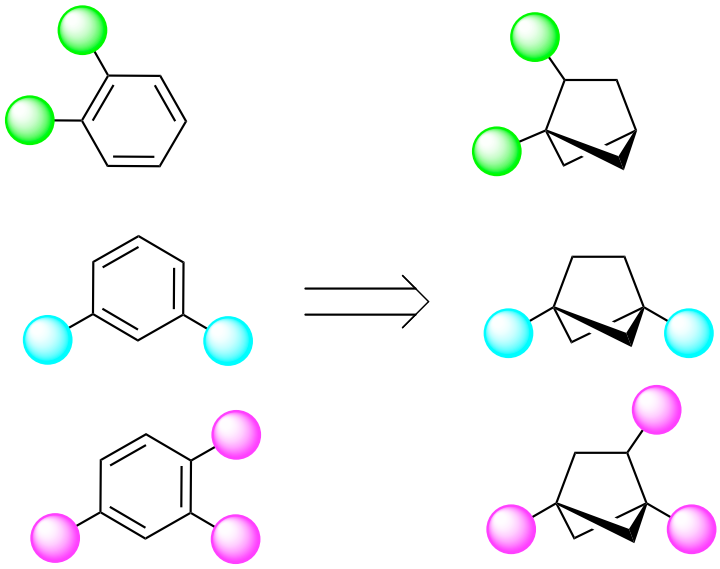

Figure 1.12: Bicyclohexanes as potential bicyclic bioisosteres for different substituted benzene rings.

So far, the two most explored bicyclo[2.1.1]hexanes as bioisosteres of *ortho*-substituted

benzene rings are the 1,2- and 1,5-bicyclo[2.1.1]hexanes.[69] Exit vector analysis of the 1,2-bicyclo[2.1.1]hexanes was done when a BCH was used as a biosisostere for an *ortho*-benzene ring in telmisartan (Figure 1.13 - Left).[70;71] These studies showed that the bond distances and angles between the substituents matched closely but the dihedral angles did not (58° in BCH versus 0° benzene).[70] These findings were confirmed independently by Mykhailiuk when they studied the exit vector for 1,2-bicyclo[2.1.1]hexane in both telmisartan and valsartan.[71]

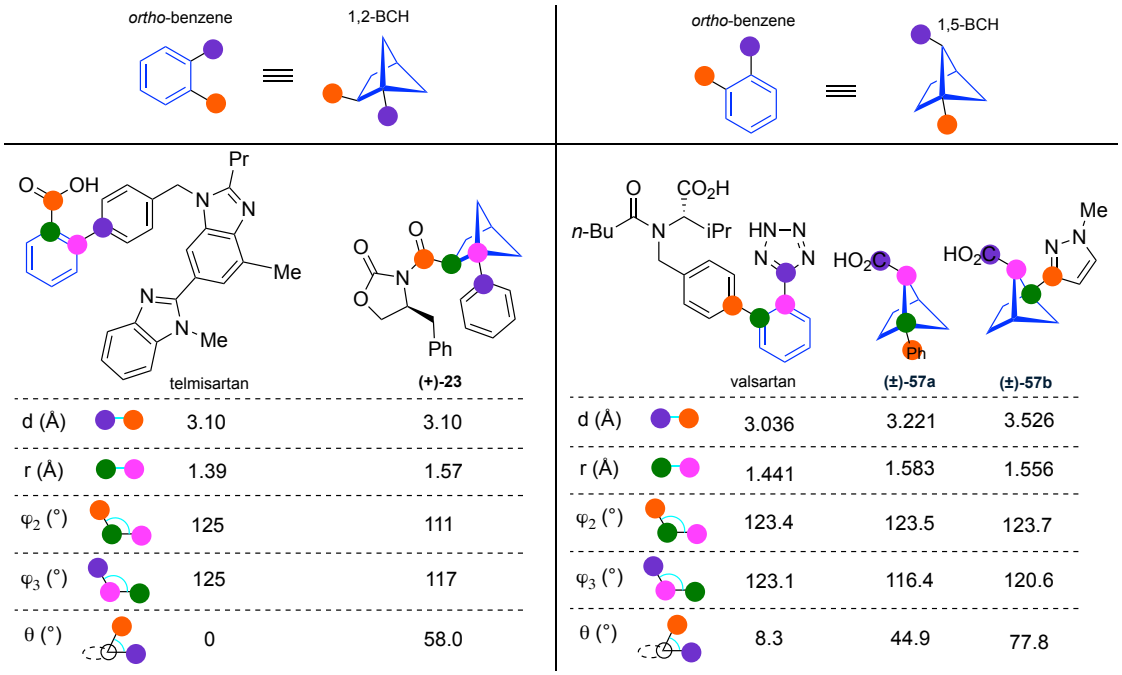

Figure 1.13: Exit vector analysis of 1,2- and 1,5-bicyclo[2.1.1]hexanes comapred to *ortho*-substituted benzene.[23;70] - Adapted from Diepers, H. E.; Walker, J. C. L. *Beilstein J. Org. Chem.* **2024**, *20*, 859–890. Copyright 2024 Beilstein-Institut Open Access License Agreement.[69]

Regardless of the discrepancies in the dihedral angles, 1,2-bicyclo[2.1.1]hexanes are being used to replace *ortho*-substituted phenyl rings pharmaceuticals and some examples are highlighted in Figure 1.14.[71;72] In phthalylsulfathiazole (antibacterial drug), the drug showed improved activity with the bicyclohexane;[72] in conivaptan (a hyponatremia treatment) it showed improved solubility and metabolic stability; finally, in lomitapide (a lipid-lowering agent) it showed improved solubility (Figure 1.14).[71] In all cases, the potency of the drug was also retained.[71;72] These examples highlight the potential for using these bicyclohexanes in other existing and new pharmaceuticals as their synthesis becomes more accessible.

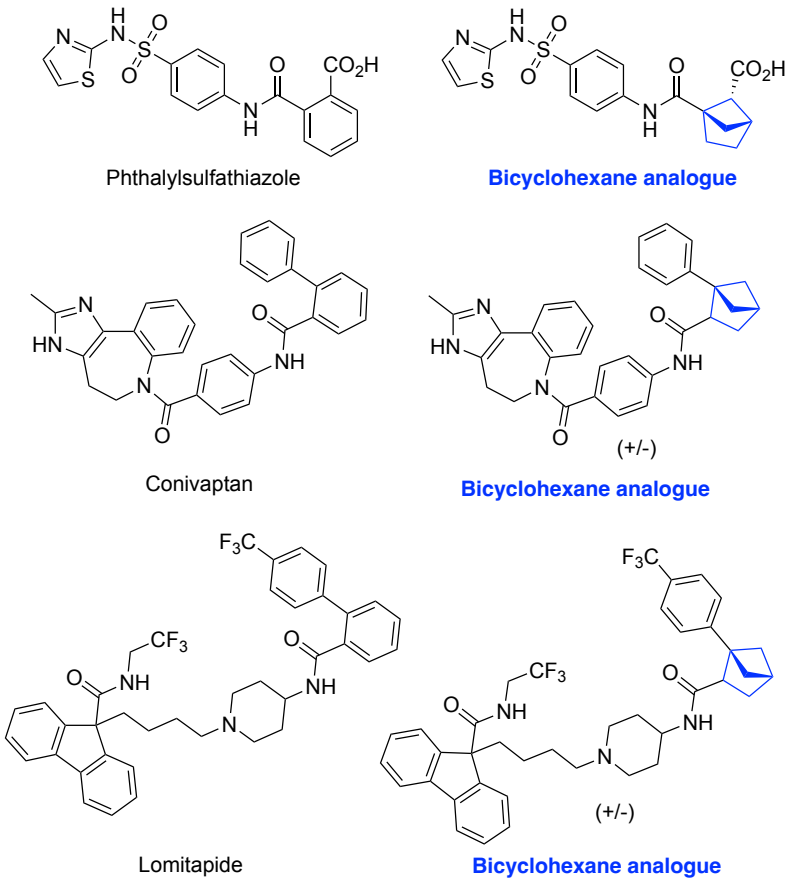

Figure 1.14: Examples of 1,2-bicyclo[2.1.1]hexane replacements in pharmaceuticals.[71;72]

For 1,5-bicyclo[2.1.1]hexanes, exit vector studies were done with a 1,5-bicyclo[2.1.1]hexane replacement in valsartan (Figure 1.13 - Right).[23] These results indicated that the substituent angles match closely to *ortho*-substituted benzene rings but the bond distance between the two substituents was slightly larger and the dihedral angle was significantly larger for the 1,5-bicyclohexane derivatives (Figure 1.13 - Right).[23] This 1,5-substitution of the bicyclohexane has been incorporated into drugs as a bioisostere for *ortho*-substituted benzene rings (Figure 1.15).[73] When the bicyclohexane replaced the *ortho*-benzene in fluxapyroxad (a fungicide), the solubility increased.[73] For boscalid (a fungicide), the solubility and metabolic stability was improved with the BCH replacement.[73] In addition to the pharmacokinetic properties being improved with BCH incorporation, the biological activity of the drug was maintained.[73] This further supports the potential of these motifs as bioisosteres in pharmaceuticals.

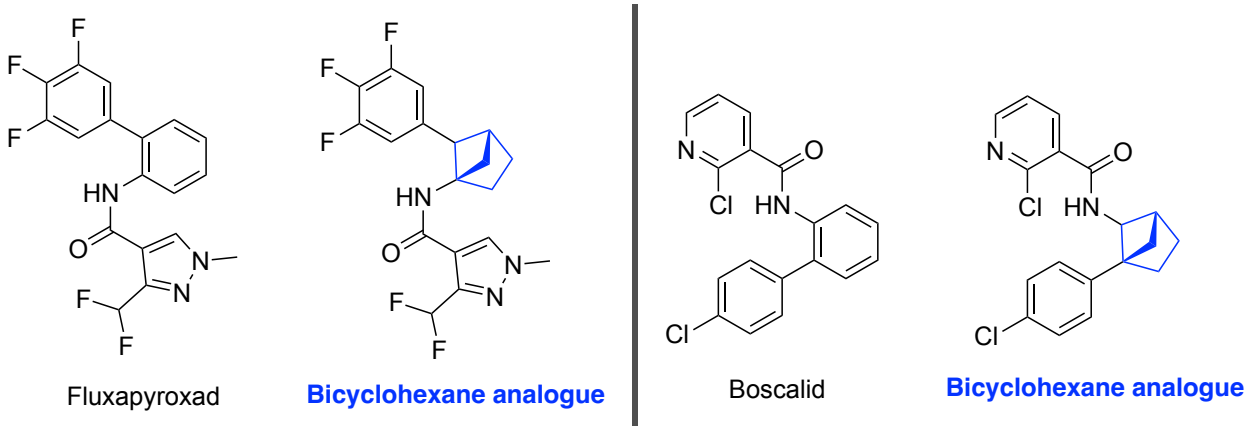

Figure 1.15: Examples of 1,5-bicyclo[2.1.1]hexane replacements in pharmaceuticals.[73]

To replace *meta*-substituted benzene rings, 1,3- and 1,4-bicyclo[2.1.1]hexanes have been proposed.[16;69;70] For 1,3-substituted bicyclohexane, the bond distances and angles are very similar to a *meta*-substituted benzene ring; however, the difference in dihedral angle between substituents is 78° in the bicyclohexane compared to ∼1° for *meta*-benzene (Figure 1.16 - Left).[70] Currently, there are no biological comparisons when using 1,3-bicyclohexane to replace *meta*-substituted benzene. For the 1,4-BCH, the bond distance between the substituted carbons on the bicyclohexane are ∼15% smaller than in *meta*-substituted benzene and the bond angles are increased in comparison (Figure 1.16 - Right).[70] However, the dihedral angle between substituents in the bicyclohexane is almost identical to a *meta*-substituted benzene (Figure 1.16 - Right).[70] Depending on the binding pocket of the target drugs, choosing between 1,3- and 1,4-substituted bicyclohexane could affect the biological activity and must be tested. 1,4-Bicyclohexanes also lack biological comparisons to *meta*-substituted benzene, likely due to the current lack of synthetic routes to access these derivatives. This further emphasizes the need to develop more synthetic routes to access bicyclo[2.1.1]hexanes with a variety of substitution patterns.

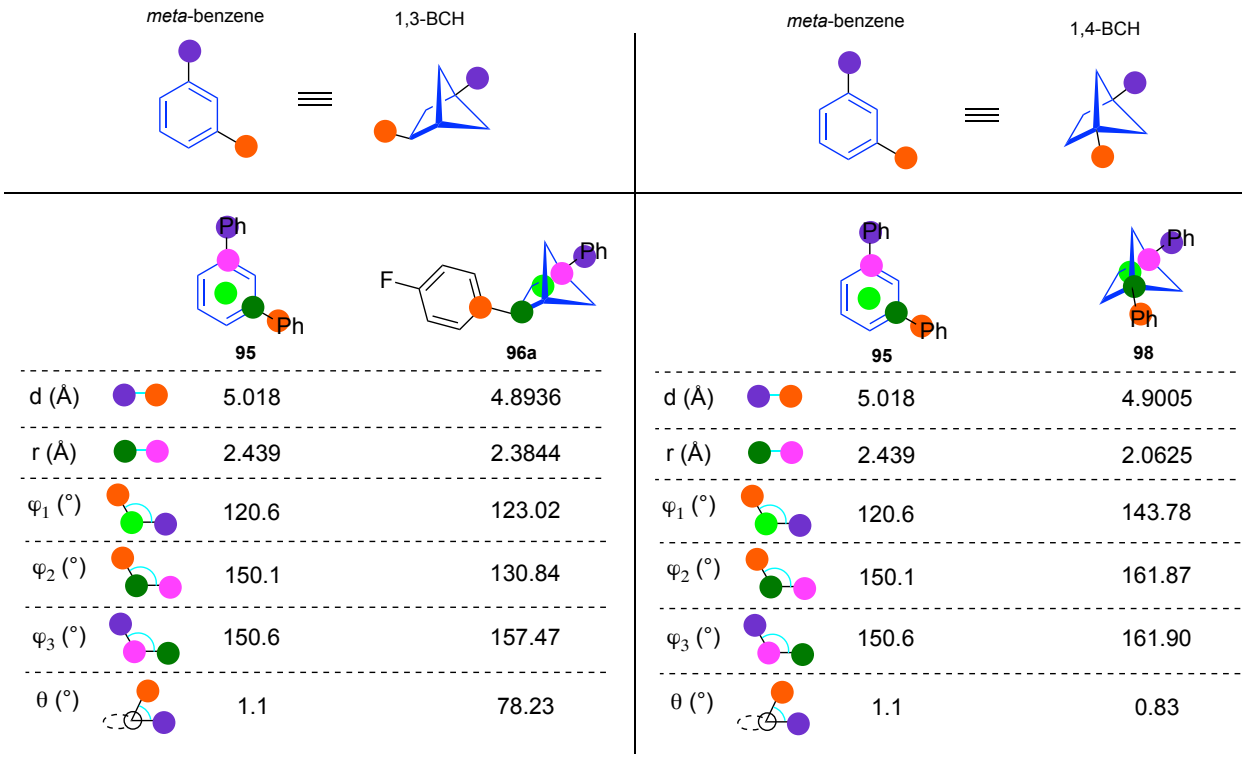

Figure 1.16: Exit vector analysis of 1,3- and 1,4-bicyclo[2.1.1]hexanes comapred to *meta*-substituted benzene[70] - Adapted from Diepers, H. E.; Walker, J. C. L. *Beilstein J. Org. Chem.* **2024**, *20*, 859–890. Copyright 2024 Beilstein-Institut Open Access License Agreement.[69]

1.2.4 Azabicyclic Bioisosteres

Nitrogen containing heterocycles are an extremely important and common motif found in successful drug candidates.[74;75] In a study done in 2014, it was found that 59% of all small molecule drugs contain at least one nitrogen heterocycle,[74] with this statistic being updated in 2024 to 82% of drugs.[75] In addition, it was observed that the number of nitrogen heterocycles per drug has been increasing in frequency.[75] These heterocyclic structures, especially the aromatic heterocycles, have the potential to be replaced with saturated azabicyclic biosisosteres. This would help to increase the number of Csp^3 centers in these pharmaceuticals. Therefore, the development of using azabicyclic structures as bioisosteres is another significant area of focus for improving drug-like properties.

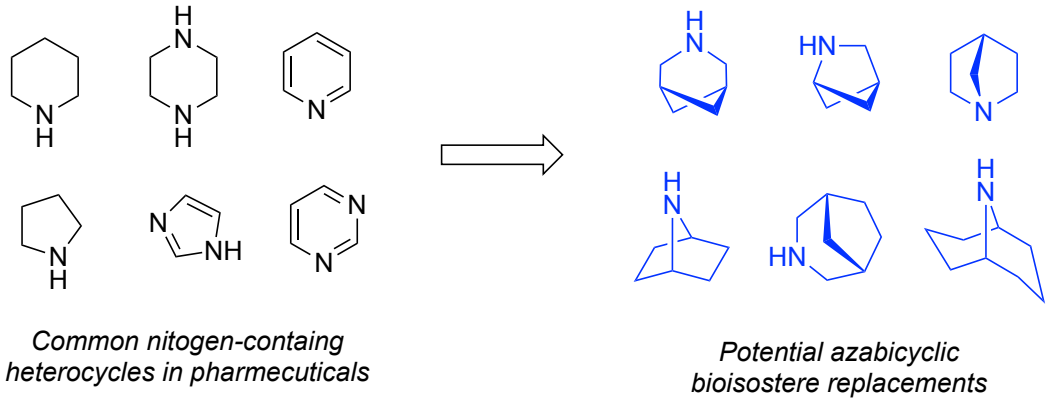

Figure 1.17: Azabicyclic Bioisosteres

Azabicyclic bioisosteres are being proposed as bioisosteres of nitrogen containing heterocycles to increase the fraction of sp^3 carbons and molecular complexity (Figure 1.17). Similarly to other saturated systems, a major limitation of these bioisosteres is their lack of synthetic availability. So far, the most focus has been placed on using naturally-occurring azabicyclics such as tropanes (2-azabicyclo[3.2.1]octanes) as potential bioisosteres. Some other examples of azabicyclic bioisosteres that have been used or tested in pharmaceutical molecules are diazabicycloheptanes (piperazine replacement),[76] azabicycloheptanes (piperazine/pyrrolidine/pyridine replacement)[77] and a variety of other azabicyclics.[78–82] More specifically, azabicyclic structures have commonly been tested as a bioisosteres for binding in nicotinic acetylcholine receptors with 2-azabicyclo[2.2.1]heptanes and tropane derivatives being commonly used (Figure 1.18).[78–82] The potential to expand the types of replacements is substantial but requires the synthesis of these motifs to become more readily available for medicinal chemists to utilize these for pharmaceutical development.

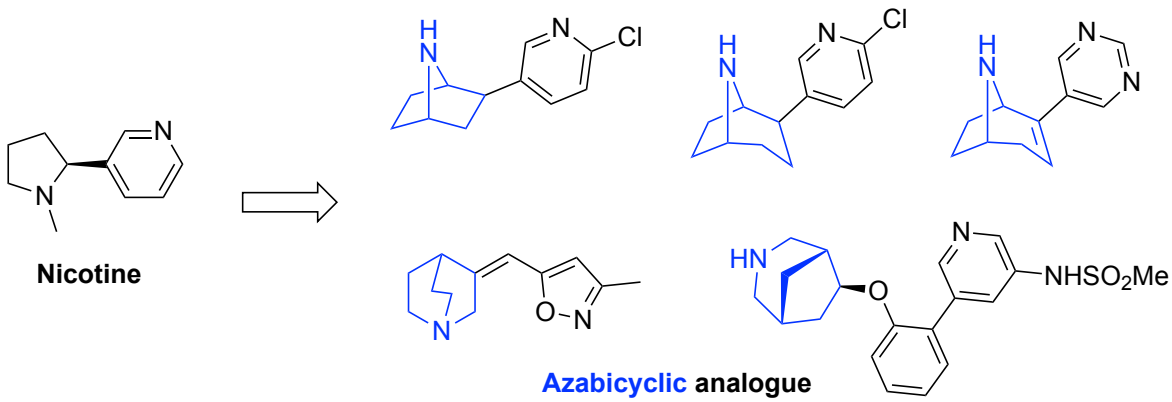

Figure 1.18: Azabicyclic bioisostere analogues for nicotine.[78–82]

A bioisostere that has been proposed for *ortho*- and *meta*-substituted benzne rings are bicyclo[3.1.1]heptanes,[83] where again, synthesis is a major limitation. Expanding this to heterocycles, an azabicycloheptane could be used as a bioisostere for substituted pyridine or even other nitrogen containing heterocycles (Figure 1.19).[77] Once syntheses of these structures are more developed, their bioisostere potential can be further explored. New synthetic approaches toward azabicycloheptanes have emerged recently and will be discussed further in Chapter 4.

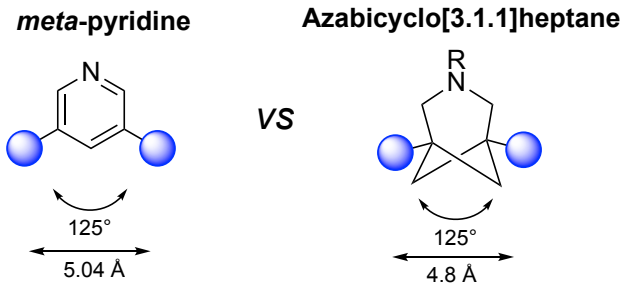

Figure 1.19: Proposed azabicycloheptane bioisostere for *meta*-substituted pyridine.[77]

1.3 Bicyclobutane Structure and Synthesis

1.3.1 Structure

Bicyclo[1.1.0]butanes (BCBs) are a common motif used to access bicyclic bioisosteres recently.[84] These molecules are comprised of two cyclopropane rings fused together along a central C–C bond. The bridgehead carbons are at each end of the central C–C bond with the bridging carbons located between each bridgehead position (Figure 1.20). After the first attempts at making a bicyclobutane were unsuccessful, the first genuine example was synthesized and characterized in 1959 by Wilberg and Ciula.[85] The first solid state molecular structure of bicyclobutane was determined by X-ray crystallography in 1972 by Johnson and Schaefe.[86] They observed that the bicyclobutane takes on a "butterfly" shape where the two bridging CH_2 carbons bend out of the plane of the central C–C bond that fuses the two rings together (Figure 1.20).[86;87] This leads to two sets of signals for the CH_2 hydrogens in the ^{1}H NMR spectrum with two of the hydrogens being *pseudo*-equatorial and two *pseudo*-axial (Figure 1.20). Small coupling can be observed between the axial and equatorial protons, leading to two small triplets for each set of hydrogen signals in the ^{1}H NMR spectrum.[88] At higher temperatures (∼120 °C) ring-flipping has been observed between the two different configurations, causing the two inequivalent NMR signals to coalesce.[89]

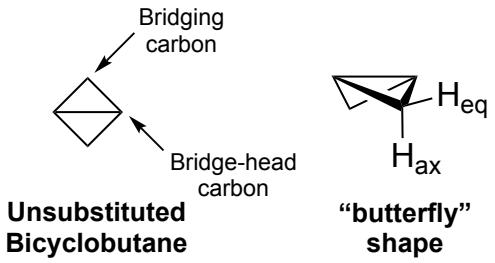

Figure 1.20: Bicyclobutane structure.[85–87]

All five of the C–C bond lengths in the bicyclobutane have been shown to have a similar length of ∼1.50 Å with an angle of 120-125° between the bridging carbons (Figure 1.21).[87] However, the bond lengths and angles are flexible and change depending on the substitution of the bicyclobutane core.[90] The internal cyclopropane angles are between 58-62°, which is

significantly less than a typical Csp^3 bond angle of 109° (Figure 1.21).[87]

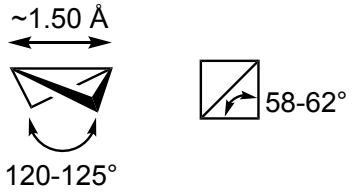

Figure 1.21: Bond lengths and angles of bicyclobutane.[87]

The bond angles of the bicyclobutane cause significant strain on the central C–C bond, contributing to its reactive nature.[91] The strain energy is ∼63.9 kcal mol^{-1} for bicyclobutane, compared to 27.5 kcal mol^{-1} and 26.5 kcal mol^{-1} for a single cyclopropane and cyclobutane ring respectively (Figure 1.22).[91] This strain was hypothesized to arise from the 1,3-carbon-carbon interactions that take place due to the butterfly shape of the bicyclobutane as well as the strain from the smaller bond angles (Baeyer strain[92]). It was found that substituting the bridgehead position of the bicyclobutane with alkyl or aryl substitution can decrease the strain energy and additionally, conjugation of the C–C bond with an aryl group will elongate the central bond.[90]

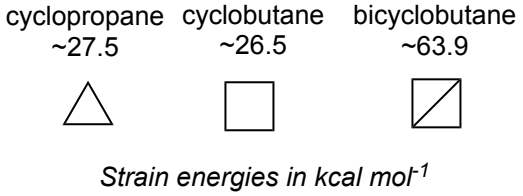

Figure 1.22: Comparative ring strain in cyclic structures.[91]

The butterfly shape of the bicyclobutane causes the 2p-orbitals of the bridging carbon atoms to overlap in the highest occupied molecular orbital (HOMO) and lowest unoccupied molecular orbital (LUMO) as demonstarted in a simplified orbital picture in Figure 1.23.[93] Molecular orbital calculations indicate that there is substantial p-character in the central C–C bond, which allows it to react like an alkene.[94;95] Initially it was shown that the bicyclic bond has up to 96% p-character,[94] which was later calculated to be about a 5:1 p-π to p-σ based on Walsh's rules of orbital rotational symmetry around an axis.[95]

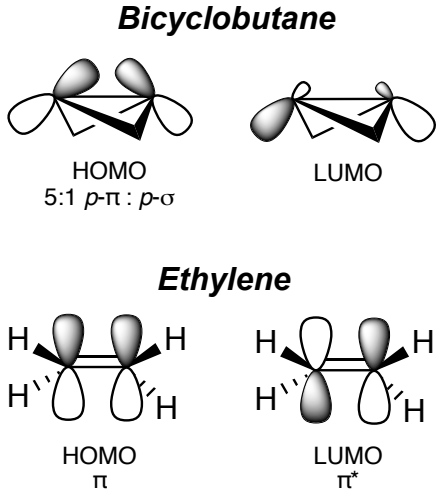

Figure 1.23: Simplified orbital shape for the bicyclobutane HOMO and LUMO compared to ethylene.[93]

1.3.2 Synthesis

Since first being discovered, the synthesis of bicyclo[1.1.0]butanes has been extensively developed. These syntheses typically require a multiple step sequence *via* either a one-pot or linear route. The first synthetic route was developed by Wilberg and Ciula (Figure 1.24).[85] The synthesis starts with the preparation of 3-carbethoxycyclobutanol-1 tosylate, which was developed previously by Maxim starting from epibromohydrin.[96] Ethyl 3-bromocyclobutane-1-carboxylate was then prepared using lithium bromide followed by base-mediated ring closing using sodium triphenylmethide in ether.[85] This afforded the desired product, ethyl bicyclo[1.1.0]butane-1-carboxylate. (Figure 1.24)[85] Following this initial synthesis, efforts have been placed to develop many different ways to access a variety of bicyclobutane derivatives.

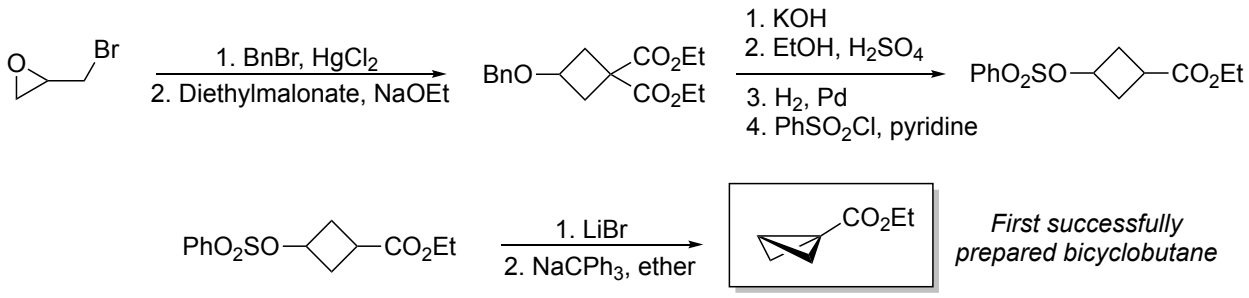

Figure 1.24: The first successful synthesis of bicyclo[1.1.0]butane.[85;96]

Currently, bicyclobutanes are synthesized following one of three different pathways. The routes differ by the starting material structure and can lead to different substitution patterns. The three main syntheses are: side chain cyclization of cyclopropanes (Route **A**), cyclopropanation (Route **B**) and transannular cyclization of cyclobutanes (Route **C**) (Figure 1.25).[84] The first reported synthesis described earlier (Figure 1.24) was a combination of side chain cyclization (Route **A**) and transannular cyclization (Route **C**) starting from an epoxide to give an ethyl ester monosubstituted bicyclobutane.[85] Since then, the different routes to access these structures have been extensively developed.

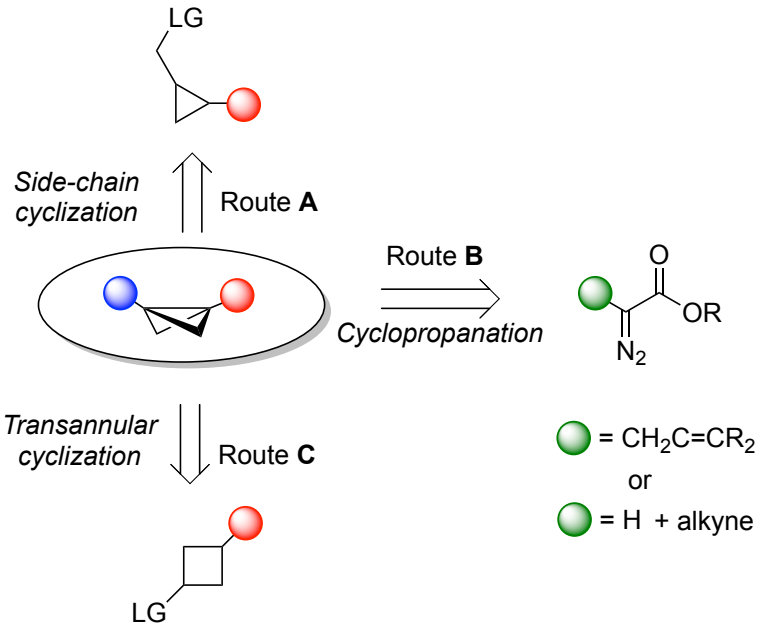

Figure 1.25: Different routes to access bicyclobutanes

The first method using side chain cyclization (Route A) typically starts with an epoxide or allyl chloride (Figure 1.26).[84] The main type of bicyclobutanes synthesized starting from the epoxide are sulfonyl substituted and the synthesis takes place as a one-pot reaction (Figure 1.26).[97–99] Most commonly, products isolated are monosubstituted. On the other hand, when starting from allyl chloride, the first cyclization reaction leads to a cyclopropane where an alkyl bromide side chain undergoes a second cyclization to form the bicyclobutane substituted with a bromine (Figure 1.26).[100–107] This intermediate then undergoes lithium halogen exchange followed by electrophilic substitution to access the final bicyclobutane product (Figure 1.26). Similarly to the epoxide route, most of the products obtained are

monosubstituted bicyclobutanes with a variety of electron withdrawing groups including esters, amides and boronates. To access more substituted bicyclobutanes, the reaction must start with a functionalized allyl chloride where the functionality can be carried through the synthesis to the final product structure.[108;109]

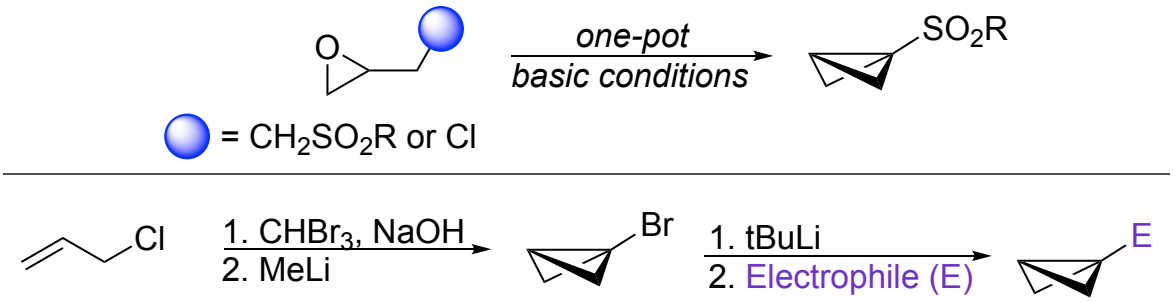

Figure 1.26: Side chain cyclization synthesis of bicyclobutanes (Route A).[97–109]

Synthesizing bicyclobutanes following the cyclopropanation route (Route B) is much less common (Figure 1.27).[84] This synthesis can be done starting from a molecule containing both an α-diazo ester and alkene that undergoes an intramolecular cyclopropanation or *via* an intermolecular reaction between an alkyne and an α-diazo ester (Figure 1.27).[110;111] These routes require specific conditions, which limits their applicability; however, they allow access to enantioenriched bicyclobutanes with bridging substitution.

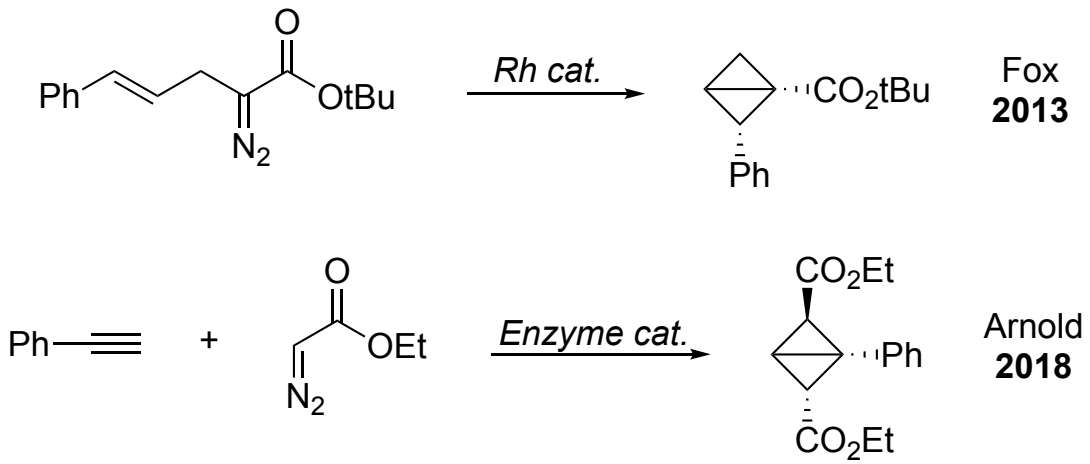

Figure 1.27: Synthesis of bicyclobutanes *via* cyclopropanation (Route B).[110;111]

Arguably, the most commonly used method to syntheszie bicyclobutanes is *via* the transannular cyclization of cyclobutanes (Route C). The three main starting cyclobutanes are 3-methylenecyclobutanecarbonitrile **I**, 1,1-cyclobutanedicarboxylic acid **II** and 3-oxocyclobutanecarboxylic acid **III** (Figure 1.28).[84] All three starting materials follow different synthetic routes and can lead to different bicyclobutane derivatives. Starting from compound **I** gives access to a disubstituted nitrile bicyclobutanes but harsh reagents such as hydrogen bromide and sodium hydride are required (route C-1, Figure 1.28).[108] From compound **II** as a starting material, monosubstituted amide or ester bicyclobutanes can be made (route C-2, Figure 1.28).[112;113] Using sulfuryl chloride and benzoyl peroxide, compound **II** will undergo singular decarboxylation and transannular chlorination. The carbonyl is then converted to the corresponding amide or ester through an acyl chloride intermediate before a base-mediated ring closing reaction to form the bicyclobutane. Finally, using compound **III** as a starting material allows access to both mono and disubstituted bicyclobutanes depending on the synthetic pathway followed (routes C-3 and C-4, Figure 1.28).[22;114;115] When the disubstituted bicyclobutane is desired, first a Grignard reaction is performed. This is followed by functionalization of the carboxylic acid, chlorination and then finally base-mediated ring closing to give the final bicyclobutane (route C-3, Figure 1.28).[114] For the monosubstituted bicyclobutane, the functionalization of the carboxylic acid is done first followed by cyclobutanone reduction to the alcohol. The hydroxyl group is then tosylated followed by base-mediated ring closing to give the monosubstituted bicyclobutane (route C-4, Figure 1.28).[22] Depending on the bicyclobutane derivative needed, specific conditions may be altered to achieve the desired product. Further details regarding specific bicyclobutane syntheses will be discussed in subsequent Chapters.

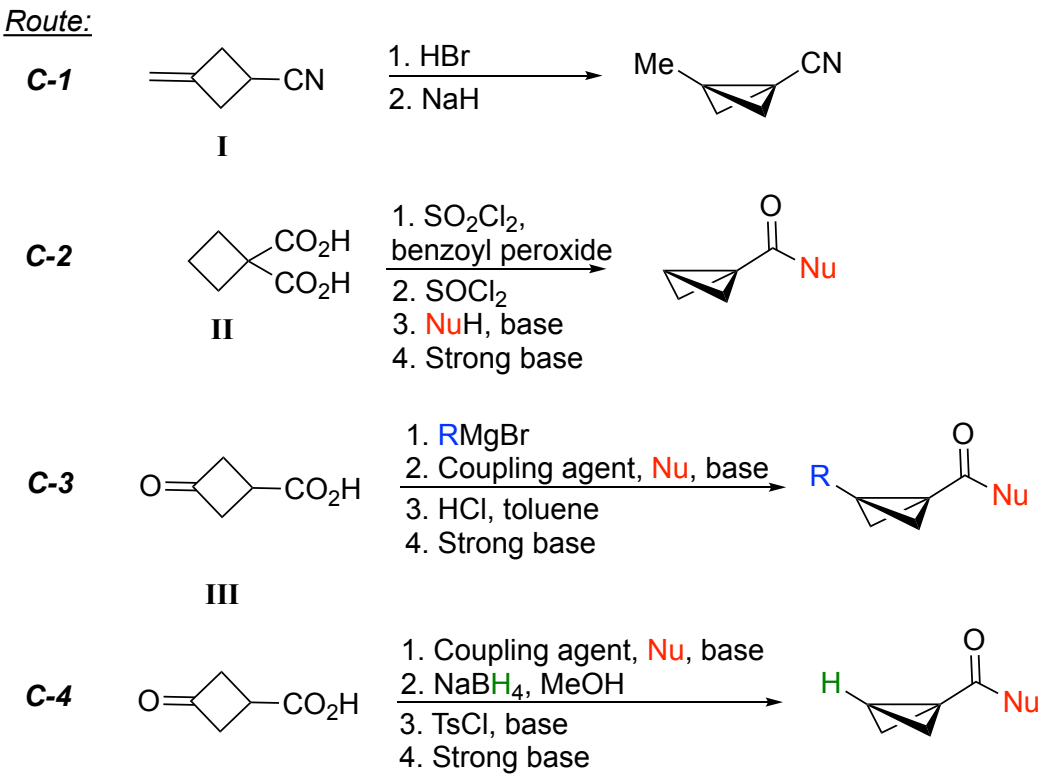

Figure 1.28: Different routes for the syntheses of bicyclobutanes *via* transannular cyclization (Route C).[22;108;112–115]

1.4 Bicyclobutane Reactivity

1.4.1 Strain-Release of Bicyclobutanes

As discussed earlier, bicyclobutanes have significant ring strain across the cental C–C bond.[91] This strain can be released and utilized for reactivity following either a 2 electron polar pathway or radical pathway (Figure 1.29).[84] Following the polar pathway, the bicyclobutane can react with either nucleophiles or electrophiles to form functionalized cyclobutanes or cycloaddition products. This typically requires activation of the bicyclobutane using the electron donating group (EDG) and/or electron withdrawing group (EWG) and/or a reactive electrophile/nucleophile. The high strain energy also makes bicyclobutanes great candidates as radical acceptors. This type of reactivity typically requires some form of activation such as thermal, photochemical or redox conditions.[84]

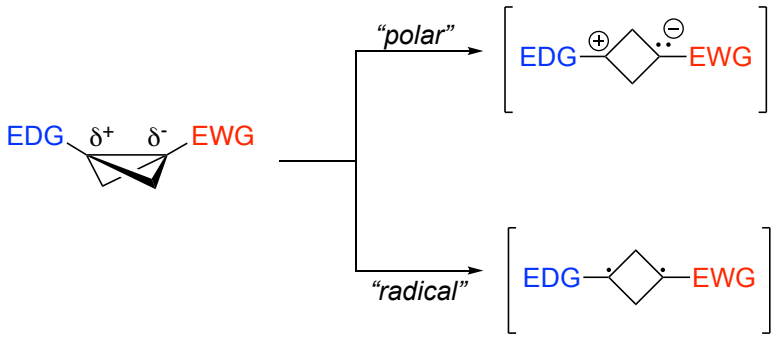

Figure 1.29: Polar vs radical strain release of bicyclobutanes

1.4.2 Donor-Acceptor Cyclopropane Reactivity

It has been established that the substituents on the bridgehead positions of the bicyclobutane play an important role in its reactivity.[116–118] When an EDG and EWG are installed on each side of the ring, reactivity analogous to donor-acceptor cyclopropanes is observed. The presence of both the EWG and EDG causes the bridging C–C bond of the bicyclobutane to be polarized. Analogous to donor-acceptor cyclopropanes, this creates a partial positive charge of one side of the bicyclobutane and a partial negative on the other side (Figure 1.30).[119;120]

Figure 1.30: Donor-acceptor cyclopropane versus bicyclobutane

With donor-acceptor cyclopropanes, the three main types of reactivity observed are ring-opening, cycloaddition and rearrangement reactions (Figure 1.31).[119;120] Due to the analagous structure of bicyclobutanes, this has led to the discovery of new reactions with these bicyclobutanes following similar conditions to those observed for donor-acceptor cyclopropanes.

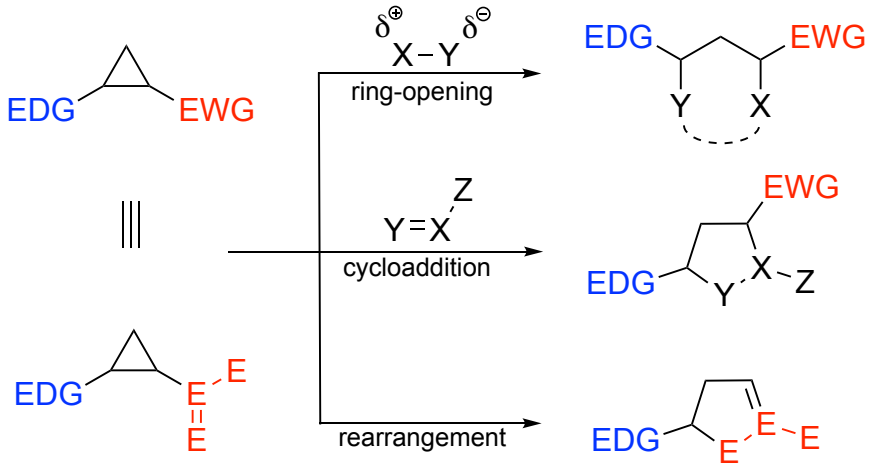

Figure 1.31: Reactivity of donor-acceptor cyclopropanes.[119]

1.4.3 Early Studies of Bicyclobutane Reactivity

Following their synthesis and characterization, the reactivity of bicyclobutanes has been explored.[88] Due to the substantial strain energy of the central C–C bond[91] and its π character,[94;95] it has many possibilities for chemical reactivity. Although not always the case, a difference in strain energy between substrates and products can be a driving force for a reaction to occur. Since bicyclobutanes are proposed to be highly reactive due to their strained structure, the stability of bicyclobutanes have to also be considered for synthetic applicability. The stability/reactivity of the bicyclobutane can be tuned based on the substituents on the ring. It has been shown that having 1,3-disubstituted bicyclobutanes and more sterically hindered substituents can increase the bicyclobutane stability. Balancing controlled reactivity vs stability of the bicyclobutanes for isolation is extremely important for these structures.

Initially, it was hypothesized that the central C–C bond or side C–C bond could be cleaved photochemically to give either a di-secondary radical or a primary and cyclopropyl radical respectively (Figure 1.32).[88;94] The formation of the di-secondary radical would be more thermodynamically favoured. Consequently, this method of radical reactivity has been confirmed and will be discussed in more detail in Section 1.4.7.[94]

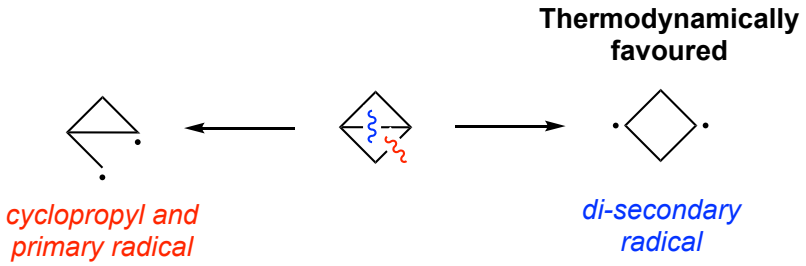

Figure 1.32: Routes for radical initiation of bicyclobutane.[88]

In addition to radical formation, initial studies showed that bicyclobutanes are cleaved in aqueous acidic conditions.[85;88] Under these conditions, the bicyclobutane can be hydrated to form the cyclobutane (Figure 1.33).[88] If the bicyclobutane is subjected to acidic conditions in an alcohol solvent, the alcohol will substitute and give cyclobutyl ether (Figure 1.33).[88] More recently, it was also observed that under Lewis acidic conditions, the bicyclobutane can isomerize to the cyclobutene *via* protonation followed by E1 elimination (Figure 1.33).[121] This reactivity is more prominent with the disubstituted bicyclobutanes, whereas the monosubstituted bicyclobutanes are typically more stable to Lewis acidic conditions. Early on, it was also observed that other groups can be added across the C–C bond including iodine, bromide and chlorine.[88] This set the foundation for further reactivity of the bicyclobutanes being explored.

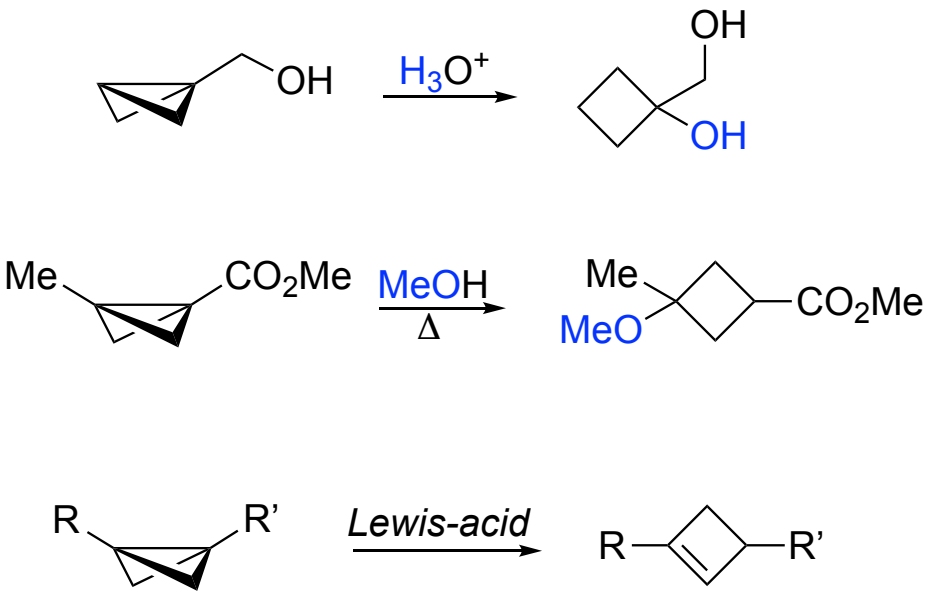

Figure 1.33: Initial reactivity of bicyclobutanes.[85;88;121]

It was hypothesized that a methylene could be inserted into the central C–C bond to make bicyclo[1.1.1]pentane derivatives.[88] Initial attempts to insert methylene *via* a [2+2] reaction were unsuccessful, where ring-opening to pentadiene was the major product instead.[88] Unsuccessful attempts were also observed when trying to insert oxygen across the C–C bond using meta-chloroperbenzoic acid (mCPBA).[88] Finally, using dichlorocarbene also only yielded 1,5-diene products and initial attempts to add ethylene also failed.[88] Despite the initial failed attempts, other additions across the C–C bond continued to be tested. Finally, in 1966, Cairncross and Blanchard showed a successful addition of alkenes with 3-methylbicyclo[1 1.0]butanecarbonitrile to form a bicyclo[2.1.1]hexane (Figure 1.34).[122] Shortly after, it was shown that carbenes could also be inserted in the bicyclobutane when Applequist and Wheeler reported a dichlorocarbene addition to form 1,1-dichlorobicyclo[1.1.1]pentane (Figure 1.34).[123] Other carbene insertions to bicyclobutane were later developed when 1,1-difluorobicyclo-[1.1.1]pentanes were synthesized *via* a difluorocarbene insertion reaction.[22;114]

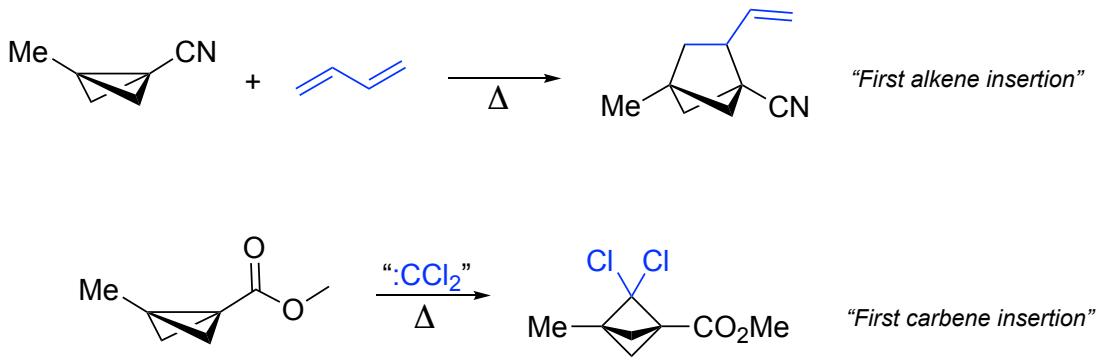

Figure 1.34: First successful insertion reactions with bicyclobutane.[122;123]

1.4.4 Polymerization

When bicyclobutanes were discovered, one hypothesized application was use as polymer building blocks.[124] Monosubstituted bicyclobutanes were found to be prone to polymerization through free radical chain processes.[88;124;125] To inhibit the polymerization, *t*-butylcatechol and butylated hydroxytoluene (BHT) were shown to be effective.[88;124;125] The polymerization occurs spontaneously for the monosubstituted 1-cyano bicyclobutane at room temperature to form a hard plug of polymer material (Figure 1.35).[125] It was shown that this polymer can be dissolved in dimethyl formamide (DMF), which will then form stringy fibres in methanol.[125]

This polymerization was found to be inhibited when electron donating groups such as methyl or phenyl are added to make the disubstituted bicyclobutane.[124;125]

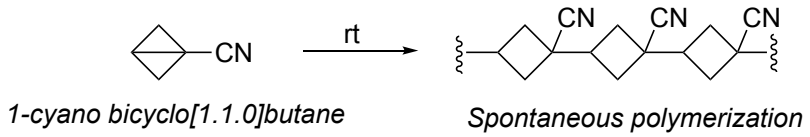

Figure 1.35: Polymerization of the monosubstituted 1-cyano bicyclobutane.[125]

1.4.5 Electrophilic Addition

The addition of a carbene across the bicyclobutane C–C bond discussed in Section 1.4.3 showed that bicyclobutanes can act as nucleophiles and will react with activated electrophiles in addition reactions. When electron donating and electron withdrawing groups are placed on either side of the bicyclobutane ring, the dipole of the central C–C bond is increased and the reactivity is greater. The bridgehead carbon that is attached to the electron withdrawing group can act as a nucleophile and attack certain electrophiles (Figure 1.36). This then leaves behind a carbocation on the opposite bridgehead position that is stabilized by the electron donating group and is susceptible to attack by another nucleophile (intramolecular or intermolecular) or elimination (Figure 1.36). If a nucleophile is present on the carbocation intermediate, this can lead to a stepwise (3+2) reaction to access bicyclic structures. Alternatively, if instead intermolecular nucleophilic attack or elimination occurs, the cyclobutane or cyclobutene product can be formed respectively.

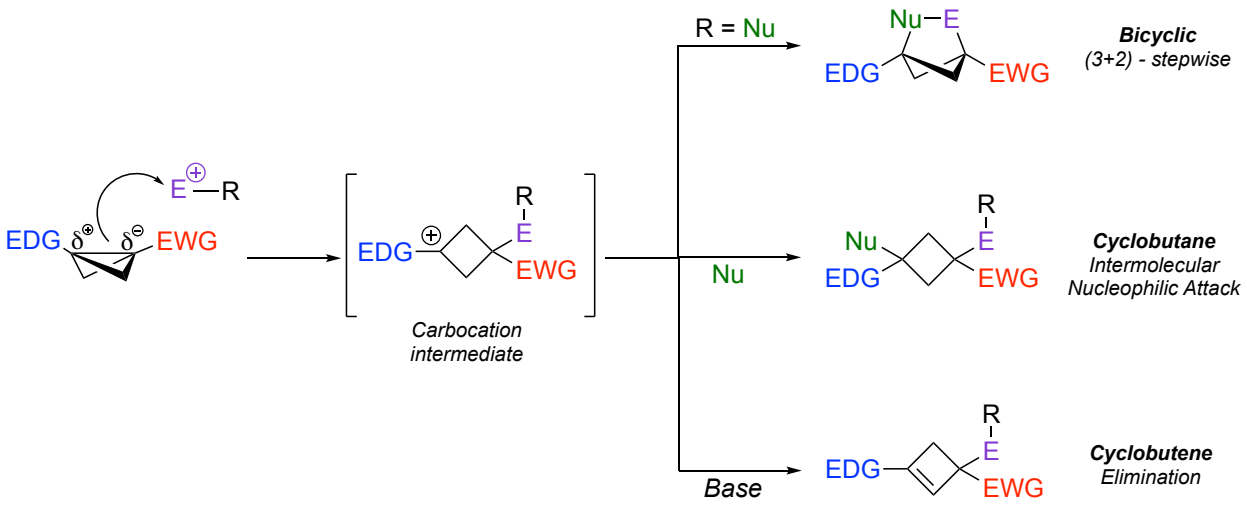

Figure 1.36: Reactivity of bicyclobutanes with electrophiles

The mechanism for the carbene insertion with bicyclobutanes to form bicyclopentanes was studied (Figure 1.37).[22;113;114] It was proposed that the bicyclobutane **I** attacks the electophilic carbene to form the carbocation intermediate **II** (Figure 1.37). If the cyclobutane stays in the intermediate conformation, the carbanion can cause ring opening to form the diene byproduct **IV**. Alternatively, if the ring undergoes a flip in geometry to intermediate **III** then the carbanion can attack the carbocation to form the bicyclopentane **V** (Figure 1.37).[113]

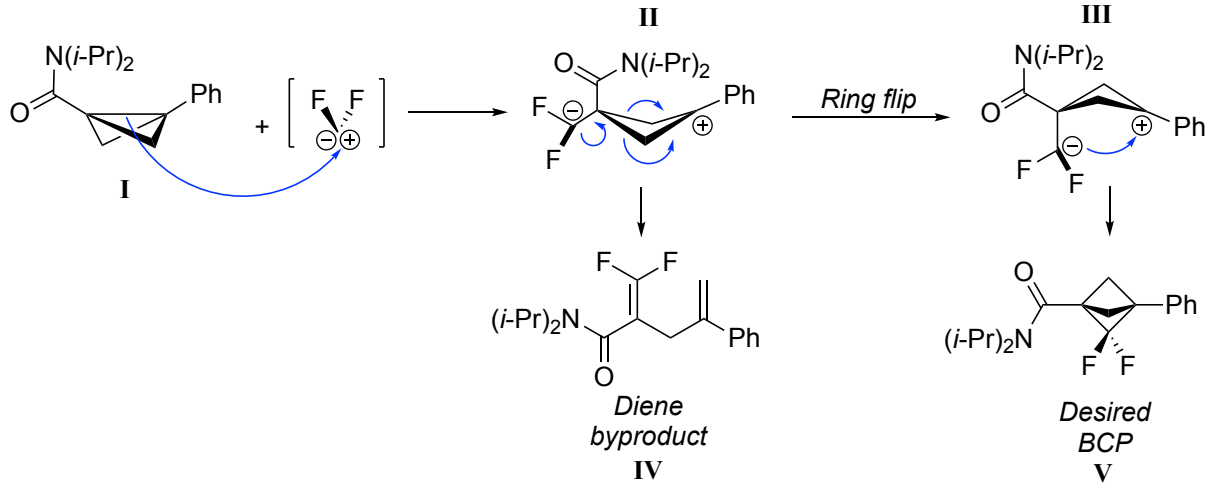

Figure 1.37: Proposed mechanism for carbene insertion to bicyclobutanes.[113]

1.4.6 Cycloadditions

Following the initial reactivity with bicyclobutanes, there was a gap in the published work until 2016 when Baran highlighted the wide range of potential for strain release functionalization.[98] This sparked interest in the area of bicyclobutanes, and since then many different reactions have been developed to add substituents across the central C–C bond (including the previously discussed difluorocarbene insertion to form bicyclopentanes[22;114]). Although it was reported early on that alkenes could be added to bicyclobutanes to form the bicyclohexane,[122] a major drawback is that the alkenes had to be very electron poor to see any reactivity with bicyclobutanes, limiting the potential for this reactivity. Later, Glorius developed a photochemical cycloaddition with bicyclobutanes utilizing blue-light and a photocatalyst.[65] This enabled access to bicyclohexanes with less electron deficient alkenes; however, the substrate scope was still very limited and specific to the type of alkene (coumarin derivatives). This was followed shortly after by three more examples of an alkene insertion into bicyclobutane to form bicyclohexane derivatives (Figure 1.38).[65–68]

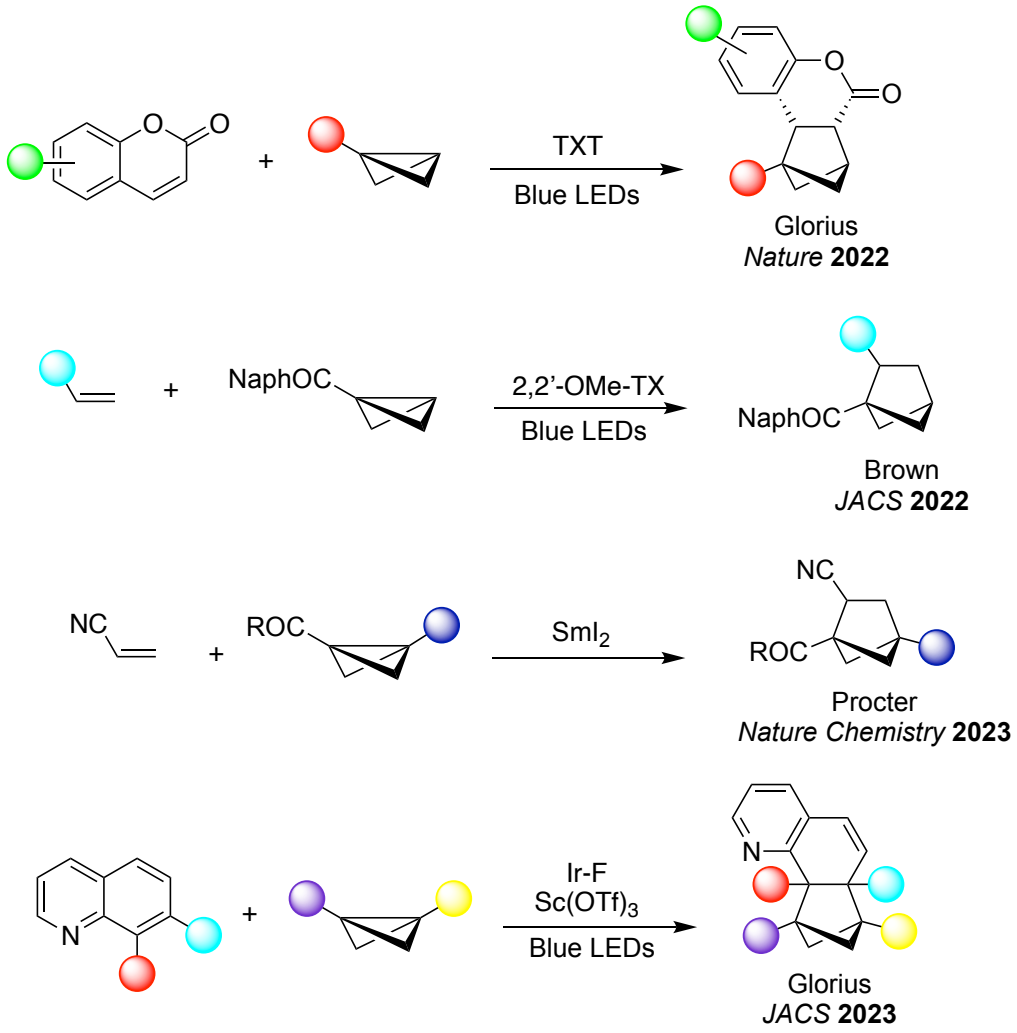

Figure 1.38: Previous alkene additions to bicyclobutane.[65–68]

After the first examples of cycloaddition reactions with bicyclobutanes, there continued to be examples of other addition reactions. Some examples of Lewis acid catalyzed additions to bicyclobutanes include imines (Chapter 2)[121], aldehydes[126] and ketenes[127] to form azabicyclohexanes, oxobicyclohexanes, and 2-oxobicyclohexanes respectively. Additionally, using diboron compounds as catalysts, alkenes and one example of an alkyne[128] have been added to form bicyclohexanes and bicyclohexenes (Figure 1.39).[128;129]

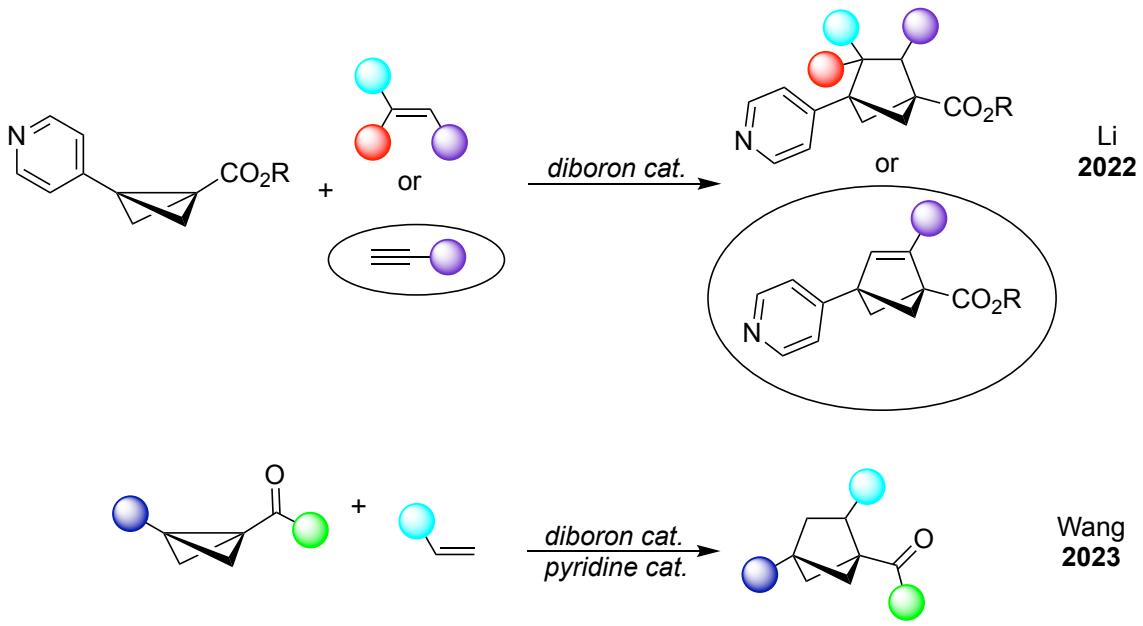

Figure 1.39: Diboron catalyzed additions with bicyclobutane.[128;129]

Two methods of adding indoles across bicyclobutanes have also been developed.[130;131] Using Lewis acid catalysis, the indole will add across the bicyclobutane C–C bond and form indole-fused bicyclohexanes (Figure 1.40). Some differences between these two syntheses are the Lewis acid catalyst used, bicyclobutane scope, and substitution on the indole nitrogen; however, the main difference that sets these apart is the substitution regioselectivity. Deng focuses on one type of bicyclobutane (monosubstituted naphthyl ketone), with $Yb(OTf)_3$ for the catalyst and only *N*-substituted indoles.[130] On the other hand, Feng tested a variety of disubstituted bicyclobutanes, AgOTf as the catalyst with only *N*-unsubstituted indoles.[131] Interestingly, the two methods have opposite selectivity for the regiochemistry of the addition. The indole addition by Deng has the indole-nitrogen adjacent to the electron withdrawing (partial negative) side of the bicyclobutane whereas Feng obtains the indole-nitrogen adjacent to the electron donating (partial positive) side of the bicyclobutane (Figure 1.40).[130;131]

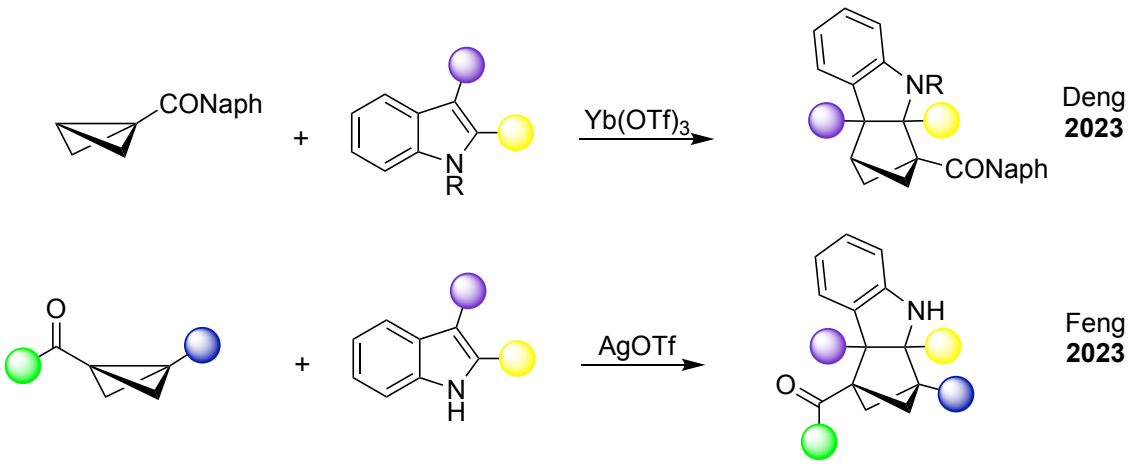

Figure 1.40: Indole additions with bicyclobutane.[130;131]

Since then many papers are still continuing to be published showing different types of additions to bicyclobutanes, further expanding the chemical tool kit for these compounds. This includes recent examples where titanium catalysts enables cycloadditions of 2-azadienes and 1,3-dienes to bicyclobutanes to form 2-aminobicyclohexanes and bicyclohexanes respectively (Figure 1.41).[132;133] Other cycloadditions with bicyclobutanes where three or more atoms are incorporated into the bicyclic product have also been developed and this will be discussed in Chapter 4.

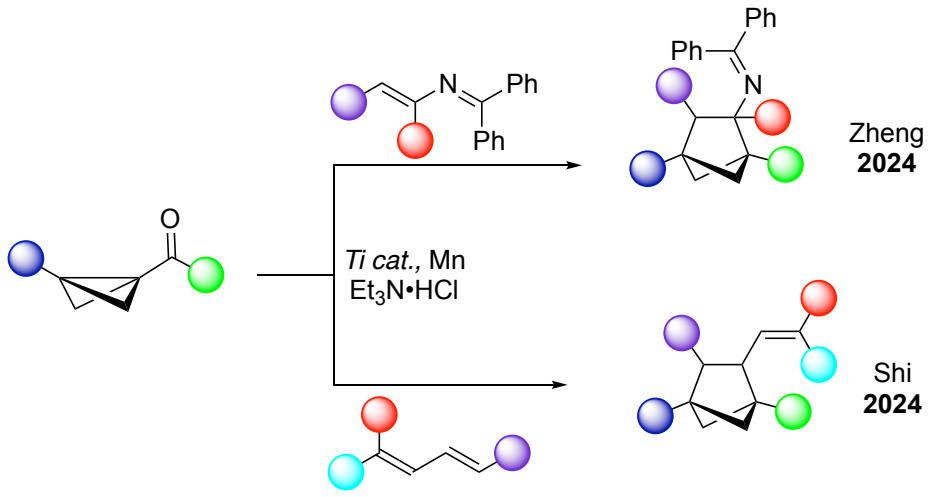

Figure 1.41: Ti-catalyzed cycloadditions to bicyclobutane.[132;133]

1.4.7 Nucleophilic addition

Polar nucleophilic addition

Bicyclobutanes can also react directly with nucleophiles, typically leading to functionalized cyclobutane products. The nucleophile will react at the electron deficient bridgehead carbon that is attached to the electron donating group (Figure 1.42). This will then give an anionic intermediate with a negative charge next to the electron withdrawing group (Figure 1.42). Similarly to how bicyclobutanes react with electrophiles, the intermediate can follow two possible pathways. If the nucleophilic substrate has an electrophilic center, the bicyclobutane anion can react there to give a bicyclohexane (Figure 1.42). Alternately, the anion intermediate can be protonated to form a functionalized cyclobutane (Figure 1.42).

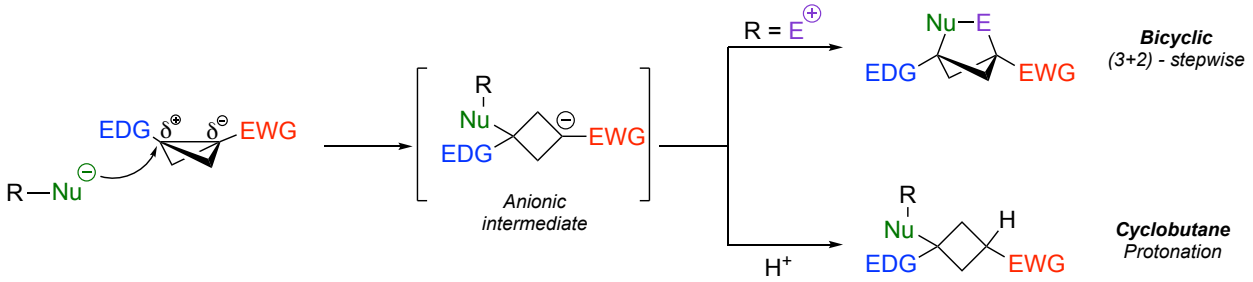

Figure 1.42: Reactivity of bicyclobutanes with nucleophiles

Nucleophile addition to bicyclobutanes is common, with many nucleophile classes reported. The first types of nucleophiles that were reported to undergo addition to bicyclobutane were oxygen and nitrogen-based (Figure 1.43).[134] Hoz developed a methoxide addition with monosubstituted bicyclobutanes (Figure 1.43).[135] Gaoni developed azide additions to bicyclobutanes with *N,N,N,N*-tetramethylguandinium azide (TMGA) or trimethylsilyl azide (TMSA), which could be further reduced to the amine derivative (Figure 1.43).[136] In addition, Gaoni also demontrated that amines could be added directly to bicyclobutanes using heat and the amine as a solvent (Figure 1.43).[137] These conditions were later expanded by Baran when he showed that amines could be added to various monosubstituted sulfonyl bicyclobutane derivatives at room temperature (Figure 1.43).[98;138]

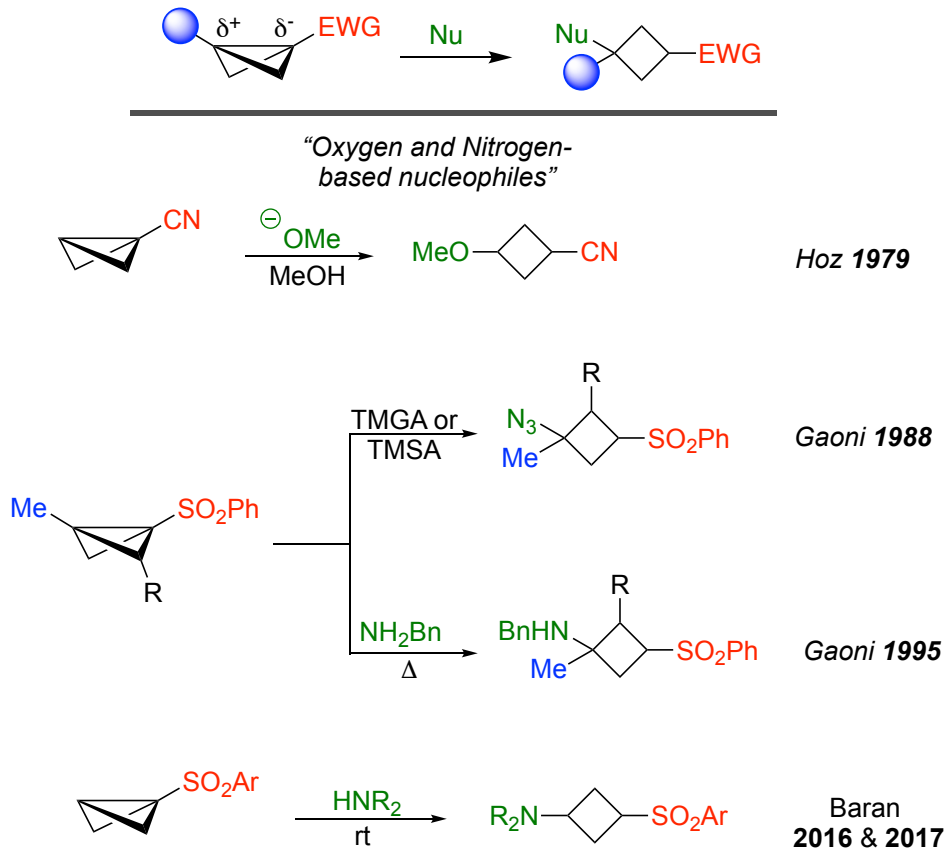

Figure 1.43: Reactivity of bicyclobutanes with oxygen and nitrogen-based nucleophiles.[98;135–138]

Organometallics are another class of nucleophiles that have been added to bicyclobutanes. This reactivity was first investigated by Gaoni from 1982-1989 where he saw successful additions using organo-copper catalysts on sulfonyl bicyclobutanes (Figure 1.44).[139–142] This was later expanded to other bicyclobutane derivatives by Fox using Grignard and organo-copper reagents (Figure 1.44).[110] Fox also showed that if an electrophile is added to quench the reaction, functionalization across the cyclobutane ring at the anionic center can be achieved.[110] Other types of nucleophiles that have been added to bicyclobutanes are phosphines[108] and thiols.[106]

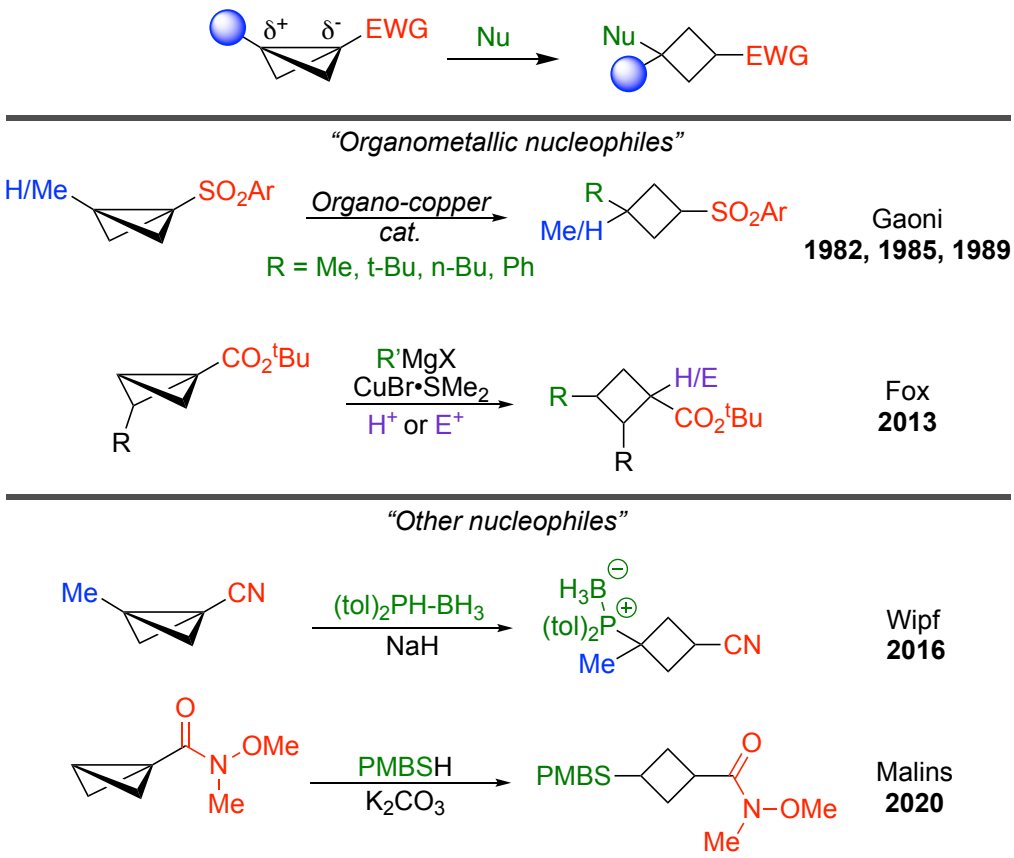

Figure 1.44: Reactivity of bicyclobutanes with organometallic and other nucleophiles.[106;108;110;139–142]

Radical nucleophilic addition

In addition to polar reactions of bicyclobutane with nucleophiles, examples of radical nucleophilic addition syntheses have been reported.[143–146] This also gives access to functionalized cyclobutane products that include substituents containing alkyl carbon chains,[143] alkyl amines[145], ethers,[144] amines,[144] and silyl groups[146] (Figure 1.45).

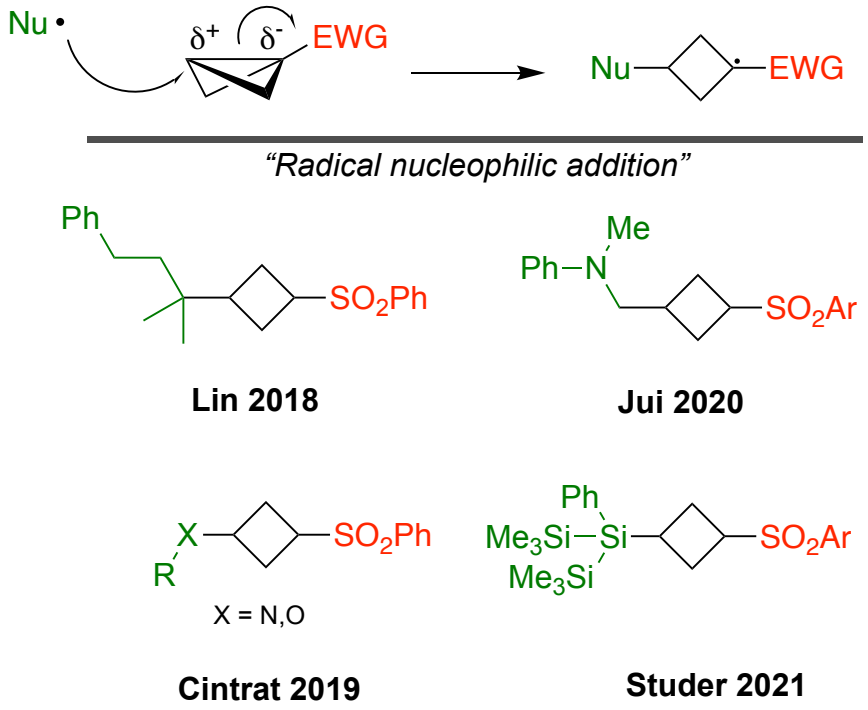

Figure 1.45: Radical reactivity of nucleophiles with bicyclobutanes.[143–146]

1.4.8 Other Classes of Bicyclobutane Reactivity

In addition to the reactivity of bicyclobutanes already discussed, other types of reactivity have also been observed from these compounds. The central C–C bond can rearrange to form fused ring systems or spirocyclic products that also have potential applications in pharmaceuticals.[107;147;148] Using boronate bicyclobutane derivatives, ring rearrangement can occur to give access to other functionalized cyclobutane products.[101–104] Further, with the use of a cobalt catalyst it has been shown that the polarity of the bicyclobutane can be inverted and a nucleophilic radical can form at the usually electrophilic side of the bicyclobutane.[149] This radical can then undergo coupling reactions with electrophilic aromatic and alkene substrates to obtain functionalized cyclobutanes.[149]

Reactions have been developed to further functionalize bicyclobutanes themselves at either the bridgehead or bridging carbons.[113;140;150] It has proven more difficult to substitute at the bridging carbons than the bridgehead.[84] One reason for this is that the cyclobutanone starting material that is most commonly used in the bicyclobutane synthetic pathway is not able to make a stable enolate due to the ring strain of the cyclobutane. This makes it more

challenging to install functionality before the bicyclobutane structure is formed. Furthermore, once the bicyclobutane is synthesized, the reactivity of the compound also makes it difficult to react at the bridging positions without unwanted side reactivity occurring.

1.5 Scope of Thesis

The development of more saturated multicyclic bioisosteres is crucial for the advancement of the pharmaceutical industry. Having a larger library of bioisosteres available will allow the potential for discovering new drug candidates to increase. In addition, the more methods that are available to synthesize these bioisosteres, the greater chance they will be incorporated during the drug discovery process. Therefore, discovering and developing new synthetic methods for saturated bicyclic bioisosteres would have a positive impact on the advancement of the pharmaceutical industry. This thesis focuses on the development of new syntheses to these bioisosteres with additional emphasis on derivatization and further functionalization of these motifs. Bicyclobutanes play a crucial role as a central intermediate that allows access to a variety of different multicyclic structures.

Chapter 2 focuses on the development of an imine addition to bicyclobutanes to synthesize azabicyclo[2.1.1]hexanes and cyclobutenyl methanamines. Azabicyclohexanes are potential bioisosteres for *N*-containing heterocycles and have been used in drug candidates. The cyclobutenyl methanamines are synthesized diastereoselectively and can be converted to the corresponding azabicyclohexane *via* an iodoamination reaction. This transformation installs an iodine on the azabicyclohexane that allows further functionalization of the bicyclic structure.

In Chapter 3, the development for the synthesis of 2-oxo-bicyclo[2.1.1]hexanes is described. The synthesis is achieved through a base-mediated enolate addition and cyclization with bicyclobutanes. The products have an endocyclic carbonyl functional handle for further derivatization. Additionally, glycine-derived enolates were used to install a protected nitrogen synthetic handle that can also be used to derivatize the bicyclohexane products. Bicyclohexanes have been proposed as bioisosteres for different substituted benzene rings. The

development of this synthesis provides another means to access these potential bioisosteres.

Chapter 4 describes a 1,3-dipolar cycloaddition reaction of pyridinium ylides with bicyclobutanes to form 3-azabicyclo[3.1.1]heptanes. Azabicyclo[3.1.1]heptanes have been proposed as bioisosteres for pyridine rings or other *N*-containing heterocycles; however, previous synthesis of these motifs has been limited. The reaction developed proceeds diastereoselectively in the presence of a base without the need for a catalyst. The azabicyclo[3.1.1]heptane products are highly substituted with a fused dihydropyridine ring and can be further derivatized.

Finally, Chapter 5 explores the synthesis of 3-oxo-2-azabicyclo[2.1.1]hexanes and 3-oxo-2-azabicyclo[2.2.1]heptanes *via* an intramolecular substitution reaction. These motifs both have potential uses as bioisosteres for *N*-containing heterocycles and contain an endocyclic carbonyl for further functionalization. The starting material for this reaction is also a precursor to either bicyclobutanes or bicyclopentanes. The selectivity of the reaction could be controlled to access either the azabicycle or the bicyclobutane/bicyclopentane depending on the base and conditions used.

Overall, the research from this thesis allows more synthetic routes to the desired saturated bicyclic bioisosteres. Demonstrations for the diversification of these bicyclic structures highlights the potential for these motifs to be utilized in pharmaceutical development. With more tools developed to access these bioisosteres, their use in future drug candidates can become more frequent.

2 Synthesis of Azabicyclohexanes and Cyclobutenyl Methanamines

This chapter has been adapted from:

Dhake, K.; Woelk, K. J.; Becica, J.; U, A.; Jenny, S. E.; Leitch, D. C. Beyond Bioisosteres: Divergent Synthesis of Azabicyclohexanes and Cyclobutenyl Amines from Bicyclobutanes. *Angew. Chem. Int. Ed.* **2022**, *61*, e202204719

Contributions:
This work is done with equal contribution from Kushal Dhake.

Optimization of the iodoamination reaction and reported solution yields in Section 2.8 was done by Jaelyn Bjornerud-Brown.

Intellectual contributions: Kyla Woelk and Kushal Dhake: Co-lead for data curation, formal analysis, investigation and methodology. Supporting conceptualization.
Dr. David Leitch: Lead conceptualization.

My contributions to this work are:

- High-throughput screening at room temperature (Figure 2.8).
- Product interconversion experiments (Figure 2.9).
- Complete sections 2.4.2,2.6.1,2.6.2, 2.9.2
- Synthesis, purification and characterization of azaBCH scope examples: **3e**, **3i**, **3k**, **3m** and **3p-3u**.
- Synthesis, purification and characterization of cyclobutenyl methanamine scope examples: **4aa-4dd**, **4gg**, and **4ii-4pp**.

- Synthesis, purification and characterization of iodoamination scope examples: **6ii** and **6nn**.
- Synthesis, purification and characterization of products **7a**, **7d-7g**, and **8g**.

2.1 Abstract

Divergent reactivity from the addition of imines to bicyclobutanes to form azabicyclo-[2.1.1]hexanes (azaBCHs) and cyclobutenylmethanamines is reported. AzaBCHs have been used in pharmaceuticals and are bioisosteres of nitrogen-containing heterocycles. Cyclobutenyl methanamines are highly functionalized cyclobutenes that can be further functionalized. High-throughout experimentation was used for reaction discovery and optimization. With *N*-aryl derived imines, a Lewis acid catalyzed formal (3+2) cycloaddition with bicyclobutanes directly formed the azabicyclo[2.1.1]hexanes. Using *N*-alkyl derived imines, a diastereoselective imine addition/elimination reaction with bicyclobutanes is observed to give cyclobutenyl methanamine products. The cyclobutenyl methanamines were then converted to the corresponding azabicyclohexanes *via* an intramolecular iodoamination reaction. The resulting azabicyclohexanes are highly functionalized and contain synthetic handles for further derivatization, allowing them to be useful synthetic motifs for pharmaceutical synthesis. The divergent reactivity observed was attributed to a difference in the basicity/nucleophilicity of the nitrogen from the imine starting material.

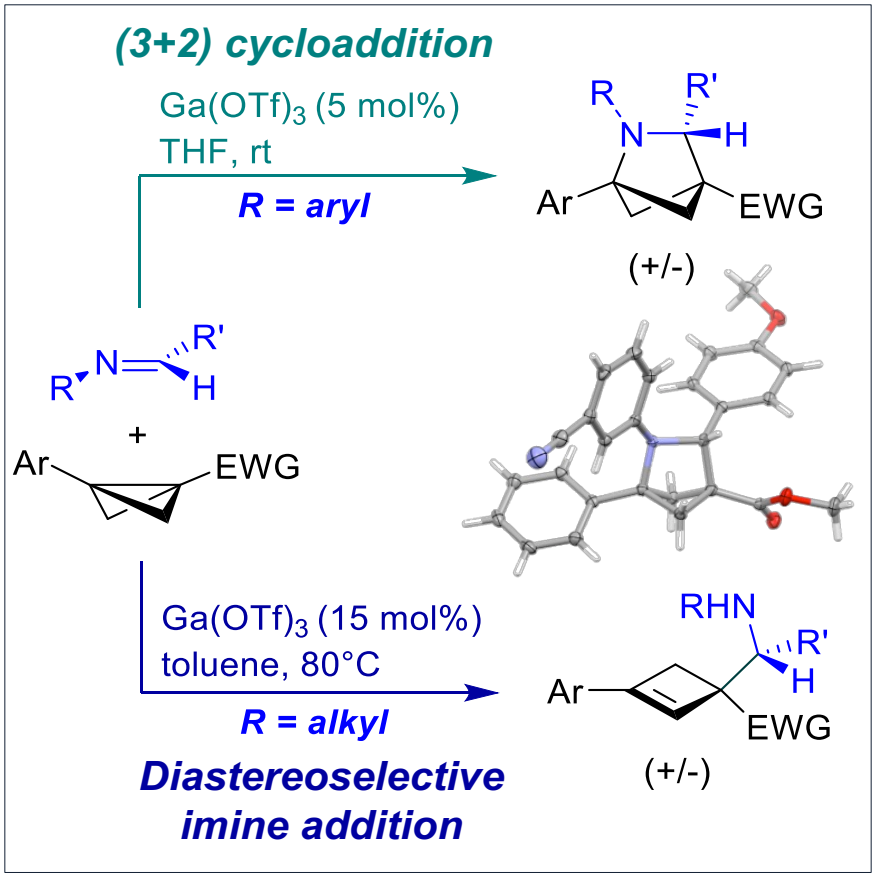

Figure 2.1: Synthesis of azabicyclohexanes and cyclobutenylmethanamines *via* imine addition to bicyclobutanes.[121]

2.2 Background

2.2.1 2-Azabicyclo[2.1.1]hexane Bioisosteres

One class of bicyclic motif that is being used in drug discovery is azabicyclo[2.1.1]-hexanes. These structures have been incorporated in three recent drug candidates (Figure 2.2).[151–153] AzaBCHs can be used as bioisosteres to nitrogen-containing heterocyles and give the pharmaceutical molecules a more three-dimensional shape and a higher fraction of sp^3 to sp^2 carbons. As discussed in Section 1.1, this can help with target binding and pharmacokinetic properties of the molecule.[114;154–156] AzaBCHs have been proposed to be used as bioisosteres for pyrrole, pyrrolidine or other *N*-heterocyclic rings in existing pharmaceuticals to increase three-dimensionality.[157]

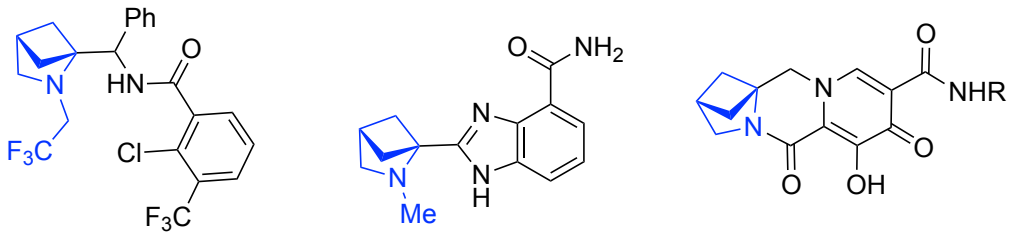

Figure 2.2: AzaBCHs in drug candidates.[151–153]

Methods to access azaBCHs have been limited in the literature. Current synthetic routes to these motifs involve either photochemistry, intramolecular substitution, or modifications of already existing azaBCHs (Figure 2.3).[157–164] These approaches all have challenges associated with them, which leaves opportunities for improvement. Photochemistry poses an issue on industrial scales and requires the molecule to be stable under photochemical conditions. Intramolecular substitution and modifying existing azaBCHs limits the diversity of the products that can be obtained. These limitations hinder the synthesis of different derivatives and makes pharmaceutical development with these motifs more challenging. A more efficient and direct method to access these structures is needed.

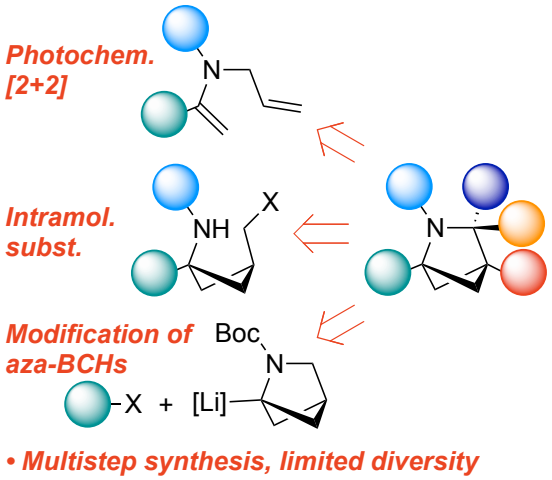

Figure 2.3: Limitations in existing azaBCH syntheses.[157–164]

2.2.2 Bicyclobutane Reactivity

Bicyclobutanes display reactivity that could be exploited to form azaBCHs *via* a direct route. As discussed in Chapter 1, alkenes can be inserted in the central C–C bond of bicyclobutanes to form bicyclic structures. In addition, bicyclobutanes are known to show reactivity similar to donor-acceptor cyclopropanes. Donor-acceptor cyclopropanes can undergo cycloaddition reactions to form heterocyclic structures,[119;165] with one class being Lewis acid catalyzed addition of imines to cyclopropanes to form pyrrolidines (Figure 2.4).[166–169] Imines are dipolarophiles that will react as both an electrophile and nucleophile (similar to bicyclobutanes) and undergo cycloaddition reactions (Figure 2.4). The carbon center of the imine is electrophilic and the nitrogen can react as a nucleophile. The Lewis acid helps to activate the imine and allows it to undergo cycloaddition reactions with donor-acceptor cyclopropanes to form pyrrolidines. This type of reactivity was first seen by Carreira[166] in 1999 and further developed later by Kerr (Figure 2.4).[167;168]

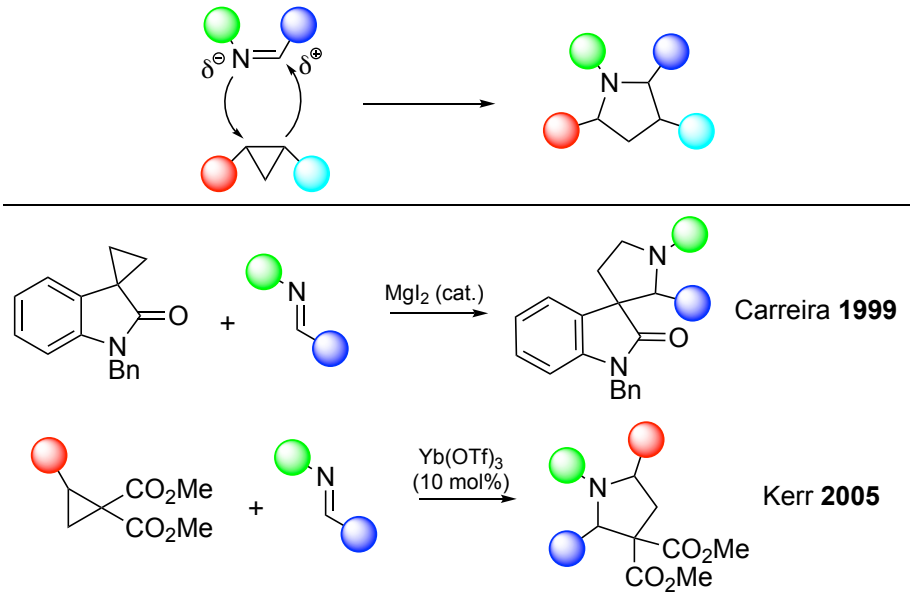

Figure 2.4: Imine cycloaddition with donor-acceptor cyclopropanes.[166;167]

Considering the analogous reactivity of bicyclobutanes to donor-acceptor cyclopropanes, we hypothesized that imines would add to bicyclobutanes to form multisubstituted azaBCHs (Figure 2.5). Upon activation with Lewis acid, the bicyclobutane would react with imines, which are electrophilic, *via* nucleophilic addition. The nitrogen would then react at the

carbocation position of the bicyclobutane to form azabicyclo[2.1.1]hexanes. This is a direct route to azaBCHs that would allow access to functionalized bicyclic structures with potential for more diversity. If this reactivity could be exploited to form azabicyclohexanes, access to these structures would be more readily available.

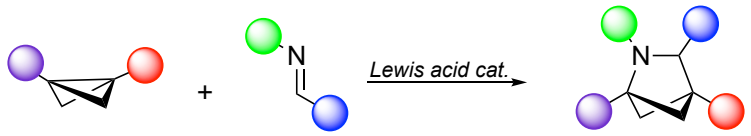

Figure 2.5: Proposed imine addition to bicyclobutanes to form azabicyclo[2.1.1]hexanes.

2.3 Reaction Optimization: High-throughput Experimentation

To establish the best reaction conditions for the imine addition to BCB, high-throughput experimentation (HTE) was used and the results were analyzed by ^{1}H NMR spectroscopy. The first HTE screen used *N*-benzylideneaniline (*N*-phenyl imine) **1a** and methyl 3-phenylbicyclo[1.1.0]butane-1-carboxylate **2a** (Figure 2.6). Three different solvents (tetrahydrofuran (THF), dichloromethane (DCM), and toluene) and eight Lewis acid catalysts (AgOTF, $Bi(OTf)_3$, $Ga(OTf)_3$, $Mg(OTf)_2$, $Sc(OTf)_3$, $Sn(OTf)_2$, $Yb(OTf)_3$, $Zn(OTf)_2$) at 20 mol% were screened over a 24 hour reaction time at room temperature (Figure 2.6). The desired 2-azabicyclo[2.1.1]hexane **3a** was formed as the major product in every case, but a cyclobutenyl methanamine product **4a** was also formed as a minor product as a mixture of diastereomers (for simplicity, d.r. was not reported until the scope in Section 2.7 and the assumed stereochemistry is shown (See section 2.9)). Using gallium triflate and silver triflate with THF as a solvent both gave the lowest percentage of the minor product **4a**. Both the gallium and silver triflate in THF conditions were scaled up to a 0.5 mmol scale with the catalyst loading reduced to 5 mol%, where gallium triflate gave a higher percent yield of the azaBCH product **3a** and lowest yield of minor product **4a**. Based on these results, gallium triflate was selected as the Lewis acid with THF as the solvent as the optimized conditions moving forward.

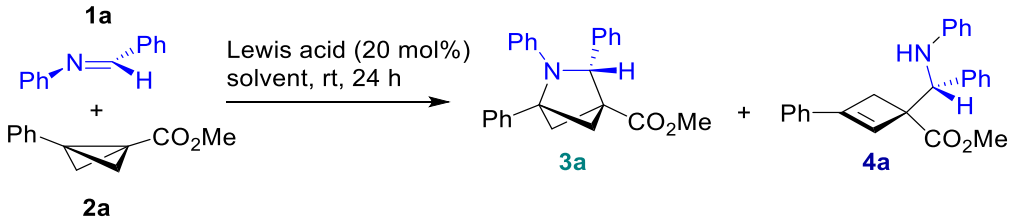

	THF		DCM		toluene	
	3a	4a	3a	4a	3a	4a
AgOTf	93%	2%	54%	10%	58%	16%
$Bi(OTf)_3$	71%	5%	57%	16%	53%	25%
$Ga(OTf)_3$	85%	2%	76%	17%	61%	20%
$Mg(OTf)_2$	48%	24%	75%	23%	44%	31%
$Sc(OTf)_3$	74%	3%	55%	14%	63%	25%
$Sn(OTf)_2$	81%	7%	59%	18%	50%	21%
$Yb(OTf)_3$	95%	6%	71%	20%	65%	28%
$Zn(OTf)_2$	93%	8%	56%	16%	52%	21%

Figure 2.6: High-throughput screen for *N*-phenyl imine **1a**. Solution yields are obtained by ^{1}H NMR spectroscopy by relative integration vs. internal standard, 1,3,5-trimethoxybenzene. Product **4a** was formed as a mixture of diastereomers.

To better understand the cause of product distribution for the azaBCH and cyclobutenyl methanamine, the reaction of **1a** with **2a** was monitored over time with *in situ* ^{1}H NMR spectroscopy (Figure 2.7). The reaction showed great mass balance and the formation of **3a** and **4a** appeared to happen in parallel with a consistent ration of 11:1 of **3a**:**4a** over the course of the reaction.

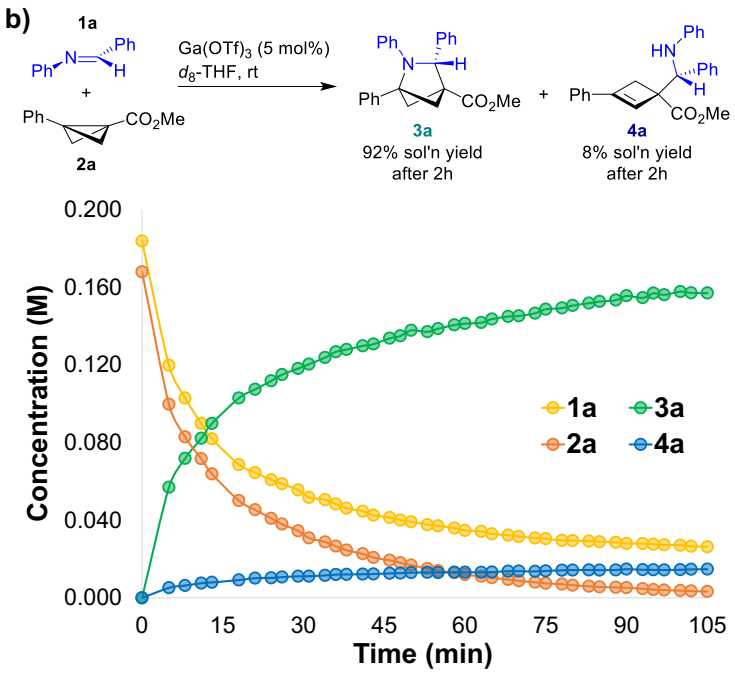

Figure 2.7: ^{1}H NMR reaction monitoring plot for *N*-phenyl imine addition.

Similarly to the high-throughput screen for *N*-phenyl imine, *N*-benzylidenebenzylamine (*N*-benzyl imine) **1b** was also screened with the three solvents and eight Lewis acid catalysts for 24 hours at room temperature (Figure 2.8). The azaBCH **3b** was formed in low yields and both the starting material as well as the cyclobutenyl methanamine product **4b** were also observed. In addition, a cyclobutene product **5** was formed, which is from isomerization of the BCB starting material. With the same conditions that were successful for the *N*-phenyl imine, gallium triflate and THF, only 20% of the desired azaBCH was formed. To test the reactivity further, an additional screen of the eight Lewis acids was done in deuterated benzene at 80 °C for 24 hours (Figure 2.8). This screen showed reversed selectivity for the cyclobutenyl methanamine product **4b** over the azaBCH and overall, less of the cyclobutene byproduct was formed. The conditions with the highest percentage of cyclobutenyl methanamine product were with gallium triflate as the Lewis acid. The reaction was scaled up to 0.5 mmol with toluene as the solvent and gallium triflate at 15 mol% to obtain an 86% solution yield of the cyclobutenyl methanamine product. Gallium triflate at 80 °C in toluene was used as the optimized conditions carried forward for the *N*-alkyl imines.

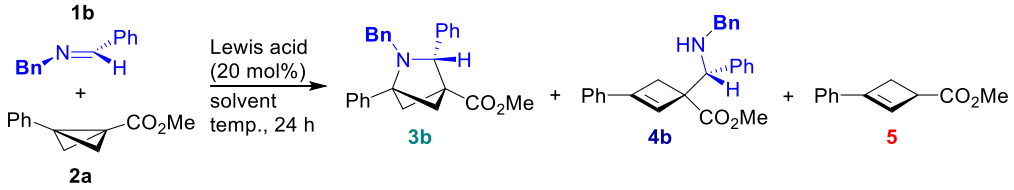

	THF				DCM			
	2a	3b	4b	5	2a	3b	4b	5
AgOTf	65%	0%	0%	1%	39%	0%	0%	1%
$Bi(OTf)_3$	8%	12%	2%	20%	5%	7%	2%	26%
$Ga(OTf)_3$	6%	20%	2%	22%	5%	5%	2%	21%
$Mg(OTf)_2$	61%	0%	0%	3%	58%	1%	1%	7%
$Sc(OTf)_3$	6%	11%	2%	21%	4%	5%	2%	24%
$Sn(OTf)_2$	0%	16%	1%	14%	21%	4%	2%	20%
$Yb(OTf)_3$	6%	0%	3%	21%	8%	0%	1%	29%
$Zn(OTf)_2$	7%	3%	3%	19%	9%	4%	2%	25%

	toluene				d_6-benzene (80 °C)			
	2a	3b	4b	5	2a	3b	4b	5
AgOTf	53%	0%	0%	0%	23%	8%	59%	1%
$Bi(OTf)_3$	3%	5%	2%	26%	4%	16%	81%	2%
$Ga(OTf)_3$	67%	5%	4%	38%	4%	12%	83%	2%
$Mg(OTf)_2$	88%	0%	0%	2%	80%	2%	15%	4%
$Sc(OTf)_3$	1%	3%	1%	15%	1%	14%	85%	1%
$Sn(OTf)_2$	1%	4%	2%	19%	7%	12%	70%	3%
$Yb(OTf)_3$	0%	0%	0%	16%	10%	12%	74%	2%
$Zn(OTf)_2$	10%	3%	2%	16%	24%	9%	57%	2%

Figure 2.8: High throughput screen for *N*-benzyl imine. Solution yields are obtained by ^{1}H NMR spectroscopy by relative integration vs. internal standard, 1,3,5-trimethoxybenzene (See Section A.3). Product **4a** was formed as a mixture of diastereomers.

2.4 Control Reactions

2.4.1 Bicyclobutane Isomerization to Cyclobutene

To determine what is causing the isomerization of the BCB **2a** into the cyclobutene **5**, a set of control reactions was done (Table 2.1). Firstly, the BCB was subjected to the reaction temperature of 80 °C in deuterated benzene for 24 hours and 54% of the cyclobutene was observed (entry 1). This indicates that the BCB will start to decompose at high temperatures on its own. The first experiment was then repeated with the imine **1b** added to the reaction mixture and no cyclobutene was formed (entry 2). This indicated that trace Brønsted acid

may be causing the isomerization to occur and having the imine together with the BCB, as a Brønsted base, prevents the acid from reacting with the BCB and causing isomerization. To test this further, gallium triflate was added to the BCB in both deuterated benzene and THF and left for 20 minutes at room temperature which gave 63% and 60% of the cyclobutene respectively (entry 3 and 4). Since gallium triflate may generate trace amounts of triflic acid, this supports the hypothesis that trace acid may be causing the isomerization to the cyclobutene. To test this hypothesis further, experiments similar to entries 1, 3 and 4 were repeated with 2,6-lutidine added to mimic the basicity of the imine substrate (entries 5-7). In every case, no reactivity occurs and the BCB starting material remains intact. These control experiments indicate that trace Brønsted acid is likely causing the isomerization to the BCB. Further, this reveals a key order-of-addition for the reaction; the Lewis acid catalyst must be added last to avoid BCB decomposition.

Table 2.1: Decomposition of BCB **2a** into cyclobutene **5**.

2a **5**

Entry	Conditions	Yield **5**(%)[a]
1	d_6-benzene, 80 °C, 24 h	54
2	**1b** (1.5 equiv), d_6-benzene, 80 °C, 24 h	n.r.[b]
3	$Ga(OTf)_3$ (15 mol%), d_6-benzene, rt, 20 min	63
4	$Ga(OTf)_3$ (5 mol%), THF, rt, 20 min	60
5	2,6-lutidine (1.5 equiv), d_6-benzene, 80 °C, 24 h	n.r.[b]
6	2,6-lutidine (1.5 equiv), $Ga(OTf)_3$ (15 mol%), d_6-benzene, 80 °C, 24 h	n.r.[b]
7	2,6-lutidine (1.1 equiv), $Ga(OTf)_3$ (5 mol%),THF, rt, 24 h	n.r.[b]

[a] Determined by ^{1}H NMR spectroscopy versus TMB internal standard. [b] ^{b}n.r. = no reaction (**5** not observed, 95% **2a** remaining).

2.4.2 Interconversion of Products

One possible pathway to form the cyclobutenyl methanamine could be through ring-opening elimination of the azaBCH. To test this, **4aa** and **3aa** were isolated and subjected to the reaction conditions (Figure 2.9). To isolate **3aa**, the reaction of **1b** and **2a** in THF with gallium triflate from the screening was repeated on a larger scale. **3aa** was then isolated as the

minor product from that reaction through column chromatography. Subjecting either **3aa** and **4aa** to the reaction conditions for 24 hours showed no sign of conversion or decomposition (Figure 2.9). This test eliminates the possibility for a ring-opening elimination pathway and further suggests that the two products form *via* parallel pathways, supporting the results found in the ^{1}H NMR spectroscopy reaction monitoring experiment.

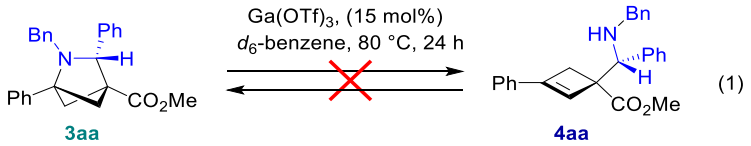

Figure 2.9: Test for interconversion between **3aa** and **4aa**.

2.5 Proposed Mechanism

Based on the control reactions and previous mechanisms for additions to BCBs, a mechanism was proposed (Figure 2.10). First, the BCB can coordinate to gallium to form an enolate and a carbocation. This is consistent with the formation of the cyclobutene product **5** that forms when the BCB is subjected to the gallium triflate without the imine present. This enolate can then attack the imine (that may also be coordinated to gallium to make it more electrophilic) and leave a carbocation intermediate with the gallium coordinated to the nitrogen. This intermediate can then split into two pathways, one where the nitrogen directly attacks the carbocation and forms the azaBCH product **3** and one where the nitrogen acts as a base and performs an elimination to form the cyclobutenyl methanamine product **4**. The divergent reactivity between the *N*-phenyl and *N*-alkyl imine can be explained by the basicity of the nitrogen. In the *N*-phenyl imine, the nitrogen is more nucleophilic than basic and will act as a nucleophile to form **3**. On the other hand, the *N*-alkyl imine is more basic than nucleophilic, so the elimination mechanism to form **4** will be favoured instead. This mechanism is consistent with the ^{1}H NMR spectroscopy monitoring experiment (Figure 2.7) and the interconversion control reaction (Figure 2.9) shown earlier that indicate these products are formed *via* parallel pathways.

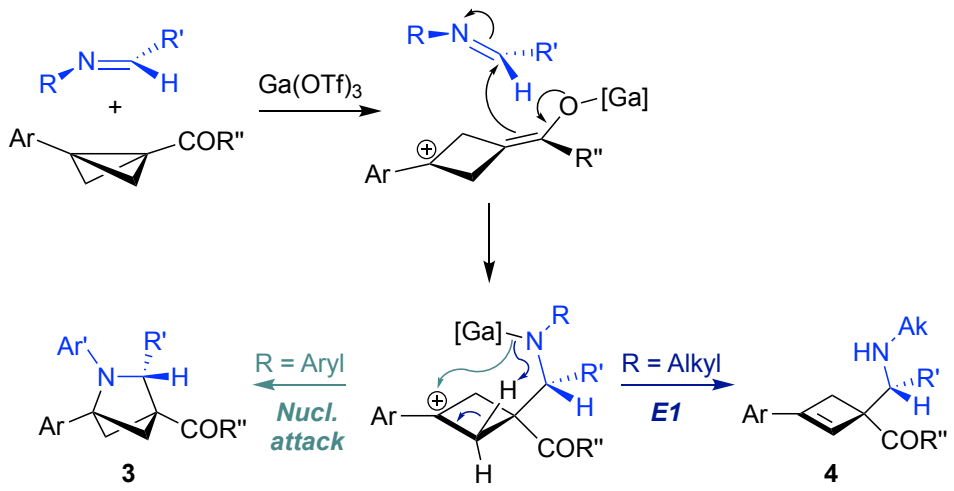

Figure 2.10: Proposed mechanism for imine addition to BCB.

2.6 Bicyclobutane Derivatives

2.6.1 Bicyclobutane Synthesis

The synthesis of the prototype methyl ester BCB **2a** follows four steps starting from a cheap and commercially available starting material, 3-oxocyclobutane carboxylic acid (Figure 2.11). The first step is a Grignard reaction with phenyl magnesium bromide in diethyl ether to give compound **I**. This is followed by a substitution reaction using concentrated hydrochloric acid to convert the hydroxyl group into a chloride and give **II**. In the third step, the carboxylic acid is subjected to an acid-catalyzed esterification using *p*-toluene sulfonic acid and methanol in 2,2'-dimethyoxypropane (DMP) to generate the methyl ester **III**. The product is purified for the first and only time after the methylation reaction using column chromatography. Finally, the methylated product can undergo an intramolecular substitution reaction using lithium bis(trimethylsilyl)amide (LiHMDS) to generate BCB **2a** that can be used in the catalysis without any further purification.

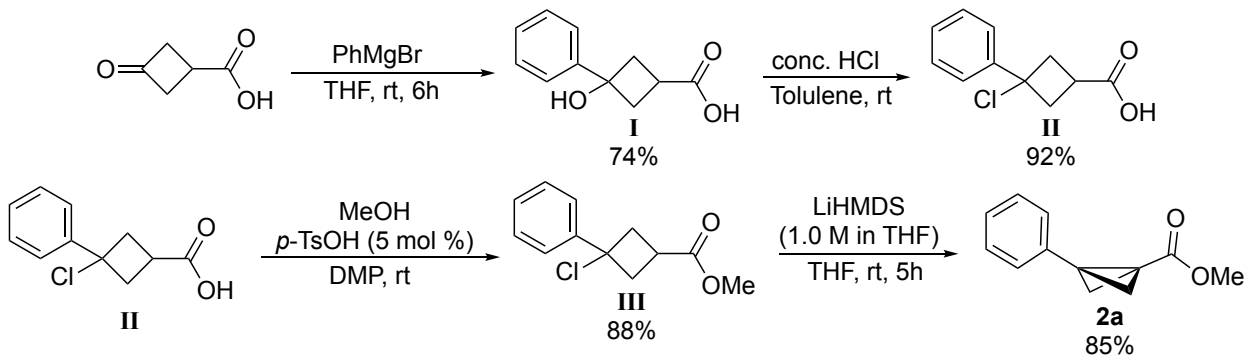

Figure 2.11: Synthesis of the prototype BCB **2a**.

To access other BCBs needed to test the scope of the imine addition reaction, an alternative pathway was developed (Figure 2.12). This pathway also requires four steps starting from 3-oxocyclobutane carboxylic acid with the first step being the Grignard reaction to give compound **V**. Using different Grignard reagents allows for other aryl substituents to be incorporated in the BCB. For step two, the hydroxy carboxylic acid is treated with oxalyl chloride and dimethyl formamide (DMF) to convert the carboxylic acid to a carbonyl chloride. At the same time, the hydrochloric acid byproduct that is produced will also convert the hydroxyl group to a chloride to give compound **VI**. The next step uses *N,N*-diisopropylethylamine (DIPEA) and either an alcohol or an amine to convert the acyl chloride to the corresponding ester or amide **VII** respectively. Similarly to the methyl ester, the product is purified after the esterification/amidation reaction using column chromatography. This product can then undergo the same last step as the prototype BCB pathway, using LiHMDS, to give the new BCB derivatives **2**. Following this procedure, six other BCBs were obtained with four being novel bicyclobutanes (**2b**, **2d**, **2e** and **2g**) (Figure 2.12).

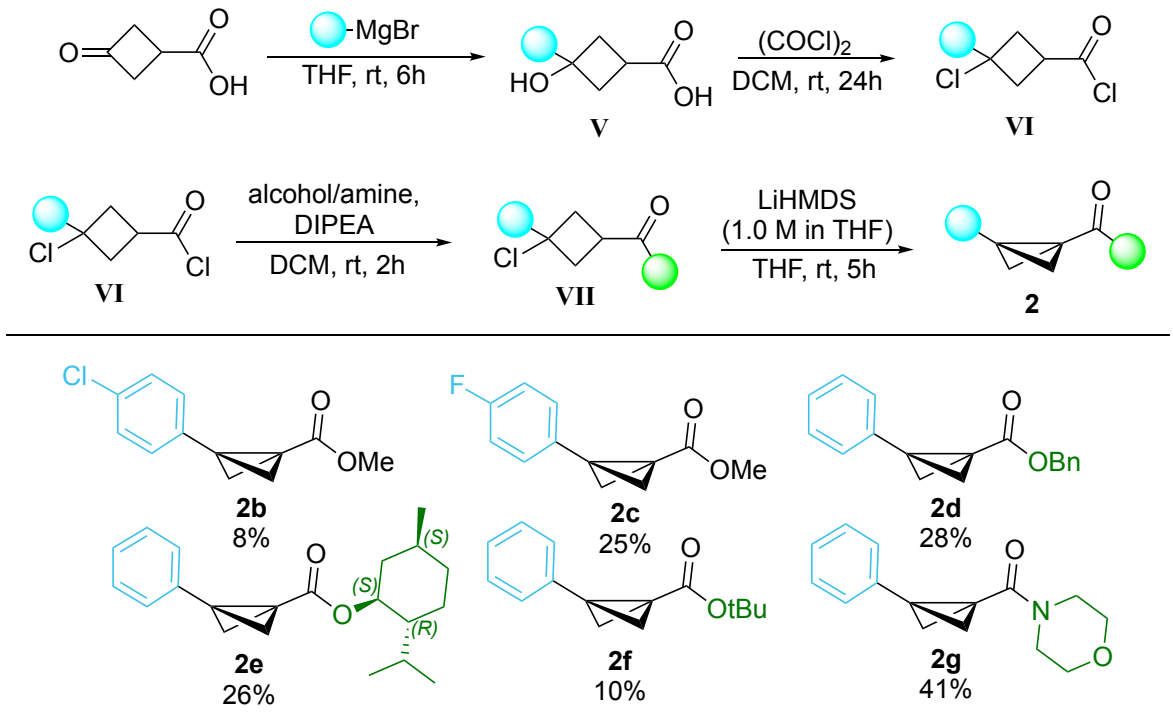

Figure 2.12: Synthetic pathway for other BCB derivatives.

2.6.2 1,2-Addition

To aid in accessing more BCB derivatives, the first step of the BCB synthesis can be optimized. The first step in the synthesis of BCBs is a Grignard addition to 3-oxocyclobutane-carboxylic acid (Figure 2.13). This step determines the aryl group that will be on the final BCB product. A drawback of this reaction is every time a new aryl derivative is required, a new Grignard must be acquired. This limits the derivatives of bicyclobutane that can be accessed. Additionally, excess Grignard reagent is required to quench the acidic proton of the carboxylic acid. Alternatively, the cyclobutanone could be arylated using a catalytic 1,2-addition reaction (Figure 2.13). This would allow easier access to more BCB derivatives.

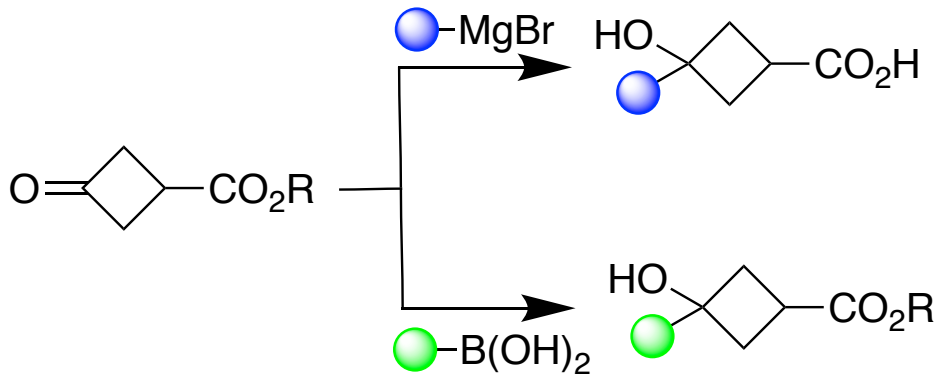

Figure 2.13: Grignard addition compared to aryl boronic acid 1,2-addition to cyclobutanone.

1,2-Additions have been done previously on aldehydes and ketones using aryl boronic acids with different metal catalysts including palladium, rhodium and nickel.[170–174] The advantage of this method is that there is a large set of diverse aryl boronic acids that are readily available. Using a rhodium catalyst, cyclobutanones specifically have been arylated with aryl boronic acids, but ring opened products were obtained instead.[173] Therefore, optimization for obtaining the cyclobutane product would be necessary.

The 1,2-addition of boronic acids to the cyclobutanone was tested using different metal catalysts. The first conditions used a rhodium precatalyst and phenylboronic acid with the methyl ester cyclobutanone (Figure 2.14).[174] By varying solvents, additives and catalyst conditions, the 1,2-addition showed some success; however, the reaction never exceeded 50% conversion (Table A.1). Several high-throughput screens with Pd catalysts were also done, where the ligand, Pd source, additives, and solvents were varied (Table A.2 and A.3). The only conditions that showed any conversion of ketone involved an *N*-heterocyclic carbene ligand; however, that catalyst generated the undesired product where the cyclobutane ring was opened (Figure 2.14). Even with subsequent optimization, only this ring opened product was observed using palladium.

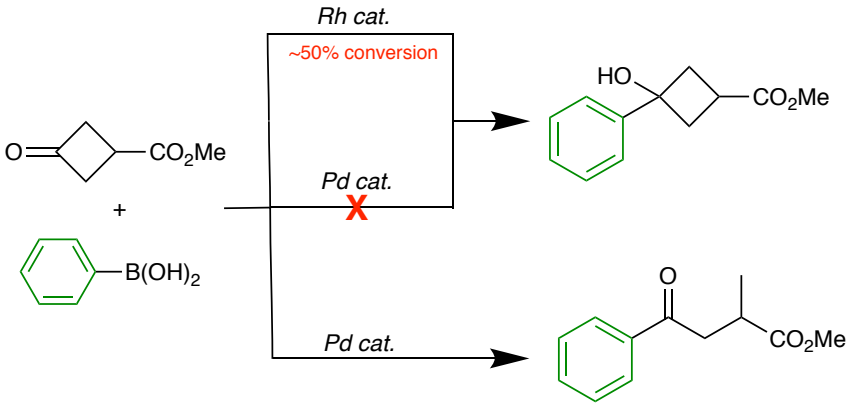

Figure 2.14: Preliminary results for 1,2-addition with Rh and Pd catalysts.

An alternative method to the metal catalyzed aryl boronic acid 1,2-addition uses organozinc reagents. Specifically, aryl zinc pivalates can be readily made from halogenated aromatics using isopropyl magnesium chloride lithium chloride complex solution and zinc pivalate (Figure 2.15).[175;176] These air-stable aryl zinc pivalates can then be treated with trimethylaluminum to give aryl methyl zinc reagents that can undergo 1,2-addition to aldehydes to give arylated products (Figure 2.15).[174] This method works for both electron rich and electron poor aryl groups and different brominated and iodinated aromatic compounds are compatible.

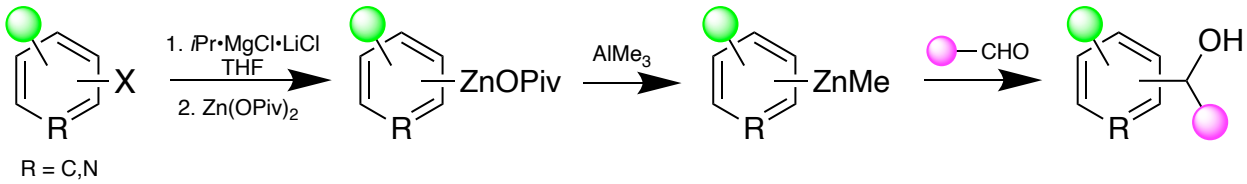

Figure 2.15: Literature zinc pivalate synthesis from aryl halides and 1,2-addition to aldehydes.[175;176]

Using this organozinc methodology, a 1,2-addition was attempted on the cyclobutanone (Figure 2.16). This would allow easier access to diverse BCBs. Preliminary results using benzyl 3-oxocyclobutane carboxylate and 4-bromobenzonitrile indicate that the 1,2-addition was successful, albiet with a low 2% yield. Product was isolated by column chromatography and characterized by ^{1}H NMR spectroscopy (See Section A.2). Upon further optimization, the scope of the reaction can be tested and then these compounds can be converted to the corresponding BCBs. While this appears promising, this route was not pursued due to

prioritizing the BCB reactivity. All of the BCBs discussed going forward were prepared using the general route from Figure 2.12.

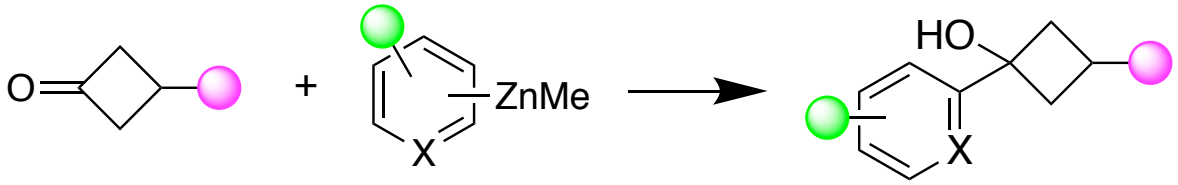

Figure 2.16: Proposed organozinc 1,2-addition to cyclobutanones.

2.7 Reaction Scope

The scope of the azaBCHs (Method A) accessed from *N*-aryl imines and BCBs containing a variety of pharmaceutically relevant substituents was explored using the optimized conditions (Figure 2.17). The characterization for these products are reported in Appendix A. The prototype azaBCH **3a** was recrystallized and obtained with a 57% yield on a 1.0 mmol scale. To test the steric bulk on the nitrogen, *o*-tolyl (**3b**) and 2-naphthyl (**3c**) were incorporated and both worked well under the reaction conditions. However, incorporating a 2,6-dimethylphenyl group on the nitrogen resulted in no reaction. Electron donating (**3d, 3e**) and withdrawing groups (**3e, 3g, 3h**) on the *N*-aryl ring were also successful. Multisubstituted aryl imines (**3i, 3j**) were also successful with electron donating and electron withdrawing groups on both rings. Both 5- and 6-membered heterocycles (**3k-3o**) also worked in this reaction including halogenated substituents (**3l, 3m**). Importantly, a 2-chloropyrid-5-yl substituent (**3l**) works well in this reaction with no competing reactivity at the electrophilic 2-Cl-pyridyl group. Finally, other BCB substituents were also successful in this reaction with *p*-Cl-phenyl (**3p**), *p*-F-phenyl (**3q**), primary (**3r**), secondary (**3s**), tertiary (**3t**) alkyl esters and morpholine amide (**3u**). Unfortunately, some of the products also contain some of the cyclobutenyl methanamine (**4**) as a minor product that co-elutes during column chromatography; these are reported as mixtures in Figure 2.17. The connectivity of the azaBCH product was confirmed by X-ray crystallography **3j** (Figure 2.18).

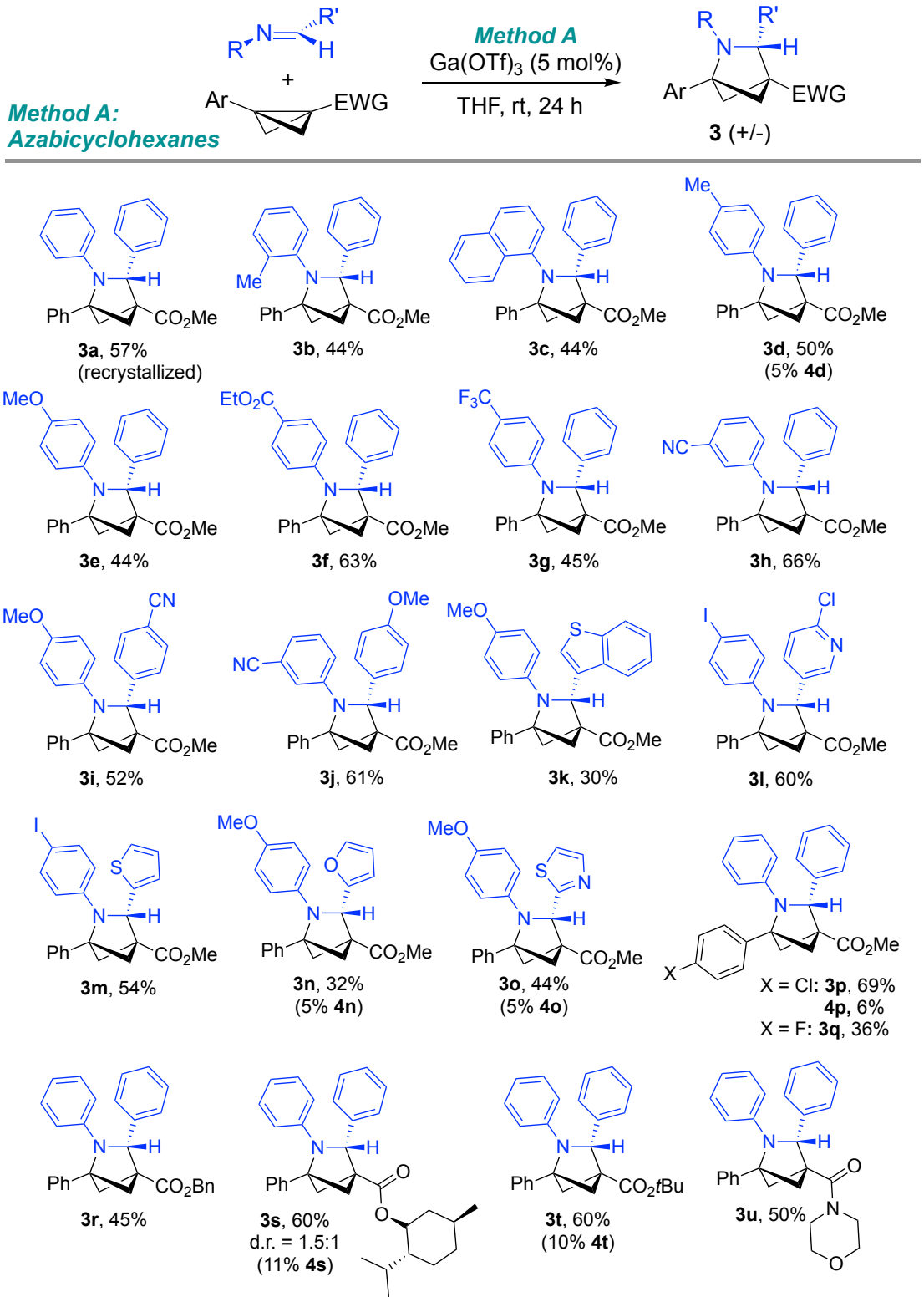

Figure 2.17: The azaBCH Reaction Scope.

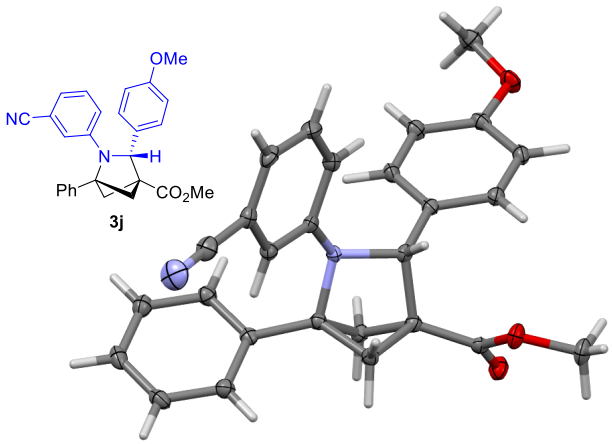

Figure 2.18: Solid state molecular structure of **3j** obtained by X-ray crystallography. Ellipsoids plotted at 50% probability.

The scope of the cyclobutenyl methanamines (Method B) accessed from *N*-alkyl imines and BCBs containing a variety of pharmaceutically relevant substituents was also explored (Figure 3.9). The elimination to form the cyclobutenyl methanamines is diastereoselective, which will be discussed in more detail in Section 2.7, with the pictured diastereomer as the major product. The products were isolated to maximize diastereomeric purity over percentage yield. The diastereomeric ratio (d.r.) of the crude reaction mixture is listed in brackets and in all cases, the d.r. was the same or better upon purification and isolation. Prototype **4aa** was isolated with a 66% yield and a d.r. of 27:1 (crude 11:1). A *p*-methoxybenzyl (PMB) group (**4bb**) on the nitrogen is compatible, providing potential for diversification at the nitrogen. Increasing steric bulk on the nitrogen with cyclohexyl (**4cc**) and *tert*-butyl (**4cc**) groups is feasible with a drop in yield but an increase in the diastereoselectivity. A variety of C-aryl groups are also compatible including naphthyl (**4ee**) and various heterocycles (**4ff, 4gg, 4hh**). Notably, when using a less sterically hindered 5-membered heterocycle (**4ff**), the diastereoselectivity decreased (d.r. 5:1). To control absolute stereochemistry, an (*S*)-α-methylbenzyl chiral auxiliary on the nitrogen was employed (**4ii, 4jj, 4kk**). In all cases, only two of the four potential diastereomers were observed in moderate diastereoselectivity (d.r. 6:1-8:1). Finally, changing substituents on the BCB with *p*-Cl (**4ll**), *p*-F (**4mm**), primary (**4nn**), secondary (**4pp**), and tertiary (**4oo**) alkyl ester were successful.

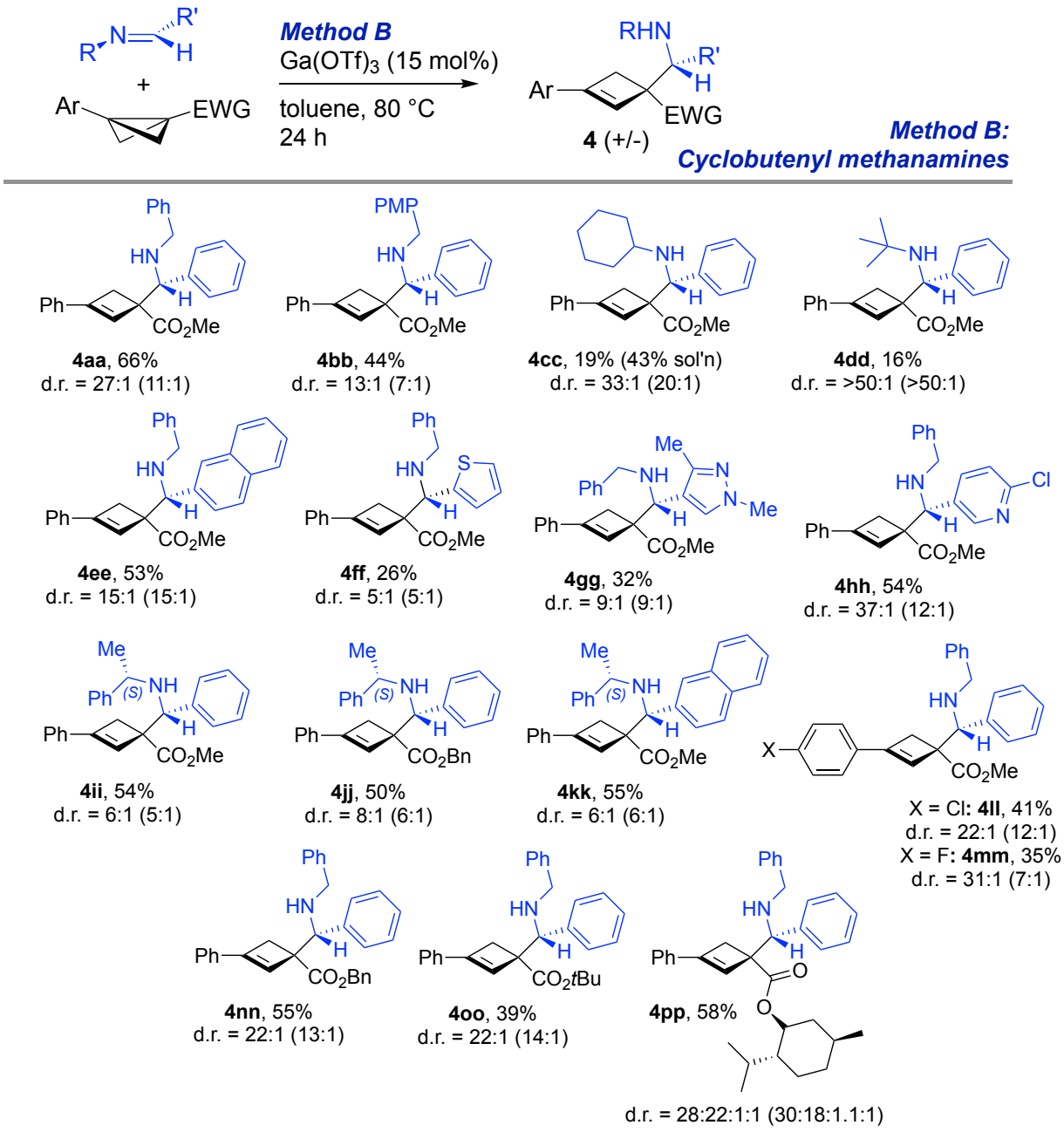

Figure 2.19: Cyclobutenyl methanamine reaction scope. All yields are for isolated compounds after purification by column chromatography. The d.r. values in parentheses determined by ^{1}H NMR spectroscopy of crude products prior to purification.

2.8 Intramolecular Iodoamination

To demonstrate the conversion of the cyclobutenyl methanamines to the desired azaBCH scaffold, an unoptimized iodoamination reaction was used (Figure 2.20).[177] Three cyclobutenyl methanamines (**4aa, 4ii, 4nn**) were selected and reacted with iodine and sodium bicarbonate in acetonitrile (MeCN) at room temperature to afford the iodo-azaBCHs **6aa, 6ii**, and **6nn**. These compounds are obtained as single diastereomers with four contiguous stereocenters, two of which are tetrasubstituted. The relative stereochemistry of **6aa** was determined by 2D NOESY spectroscopy. Using this reaction we can obtain *N*-alkyl azaBCHs that contain iodide as a synthetic handle for further functionalization.

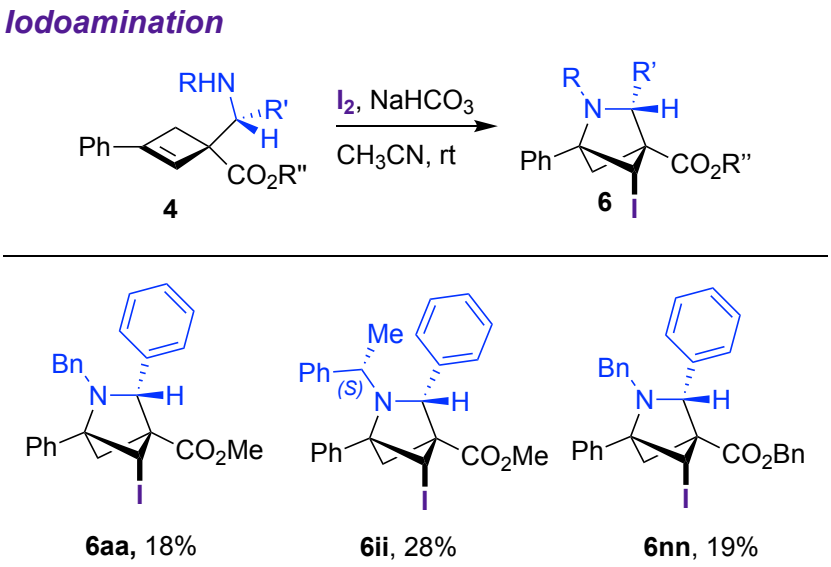

Figure 2.20: Iodoamination reaction.

To try and improve the yield for the iodoamination reaction, the reaction was optimized. Starting with a 12-well HTE screen, three different iodine sources (I_2 with $NaHCO_3$, 1,3-diiodo-5,5-Dimethylhydantoin (DIH), and *N*-Iodosuccinimide (NIS)) and four solvents were screened with cyclobutenyl methanamine **4ii** (Table 2.2). Overall, the yields were relatively low, with $I_2/NaHCO_3$ giving the highest value of 28%. However, with I_2 for the iodine souce there was significantly poorer mass balance compared to when NIS was used.

Table 2.2: 12-well HTE screen for iodoamination optimization with α-methyl benzyl product **4ii**.

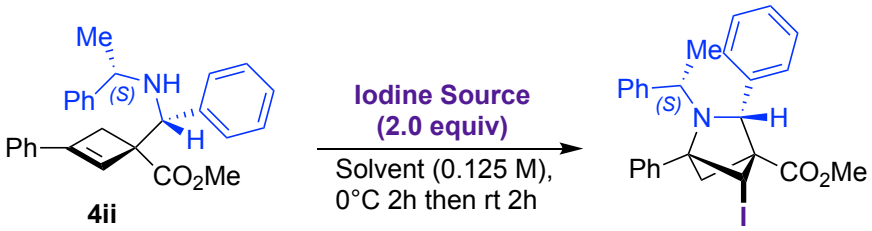

Entry	Iodine Source	Solvent	Yield **6ii**(%)[a]	**4ii**(%)[a] remaining
1	I_2 and $NaHCO_3$	EtOAc	4	6
2	I_2 and $NaHCO_3$	Toluene	27	28
3	I_2 and $NaHCO_3$	MeCN	27	16
4	I_2 and $NaHCO_3$	DCM	16	27
5	DIH	EtOAc	11	0
6	DIH	Toluene	6	0
7	DIH	MeCN	9	7
8	DIH	DCM	12	2
9	NIS	EtOAc	16	66
10	NIS	Toluene	3	0
11	NIS	MeCN	15	63
12	NIS	DCM	11	53

[a]Determined by ^{1}H NMR spectroscopy versus internal standard.

Using NIS as an iodine source was carried forward for further optimization. The reaction temperature was screened for both room temperature and 40 °C with two solvents (DCM and MeCN) and the reaction was run for 20 hours (Table 2.3). With these conditions, we observed that using MeCN as a solvent at rt (Entry 2) give the best yield of 33%; heating the reaction had a negative effect on the yields.

Table 2.3: Further optimization for iodoamination with α-methyl benzyl product **4ii**.

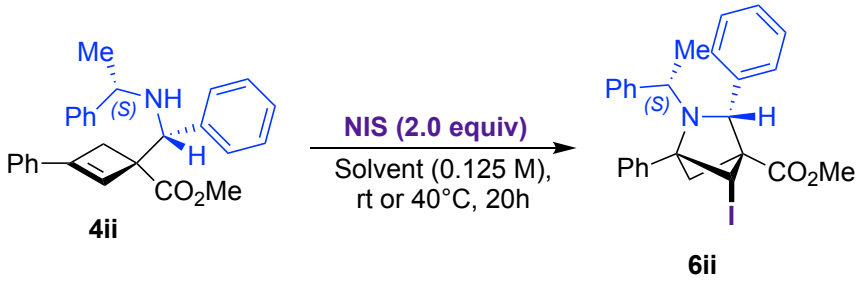

Entry	Temperature	Solvent	Yield **6ii**(%)[a]
1	rt	DCM	28
2	**rt**	**MeCN**	**33**
3	40 °C	DCM	21
4	40 °C	MeCN	0

[a]Determined by ^{1}H NMR spectroscopy versus internal standard.

These conditions from Table 2.3, Entry 2 were carried forward and tested with *N*-benzyl cyclobutenyl methanamine **4aa** (Figure 2.21). Switching the substrate caused a significant increase in yield to 74% of the iodoamination product **6aa**. These conditions were selected as the optimized iodoamination reaction variables that were carried forward.

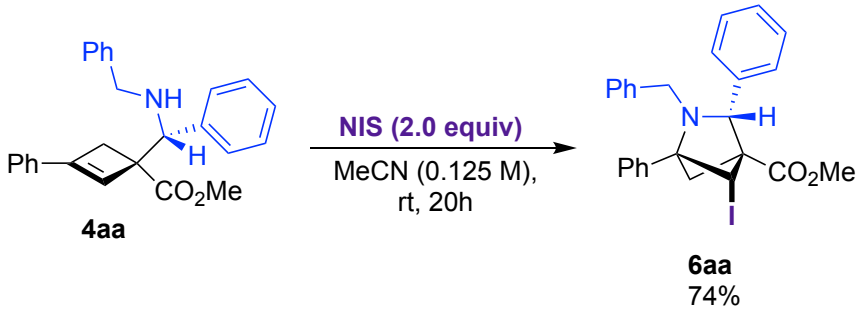

Figure 2.21: Optimized iodoamination conditions with *N*-benzyl imine **4aa**.

The scope of the optimized iodoamination was explored, and the solution yields were determined by ^{1}H NMR spectroscopy (Figure 2.22). The products were obtained with moderate to excellent yields. Bulky *N*-*tert*-butyl **6dd** and *N*-cyclohexyl **6cc** groups were well tolerated giving a 64% and 62% yield respectively. For the scope of the bicyclobutane, *p*-fluoroaryl product **6mm** and *tert*-butyl ester **6oo** were successful with 72% and 64% yields respectively. Other C-aryl groups from the imine are also compatible (**6hh**, and **6qq-6tt**), with electron withdrawing groups, electron donating groups and a variety of heterocycles

giving great yields. Utilizing this optimized iodoamination reaction can provide access to more azaBCH derivatives that are not limited to *N*-aryl derived imines.

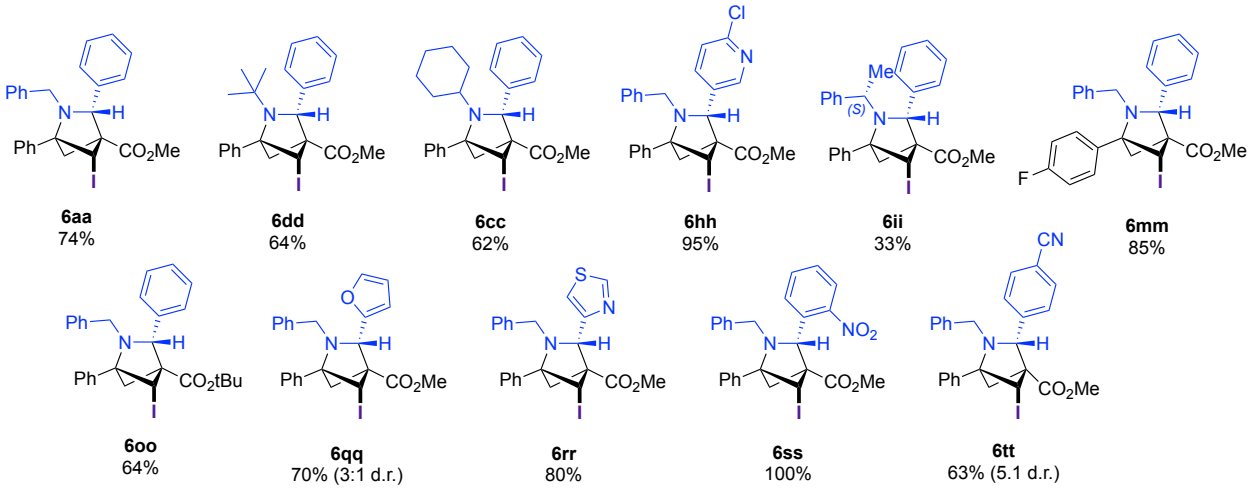

Figure 2.22: Optimized iodoamination scope. Yields reported as ^{1}H NMR spectroscopy solution yields using 1,3,5-trimethoxybenzene as internal standard.

2.9 Stereochemistry

2.9.1 Stereochemical Model for Cyclobutenyl Methanamines

A stereochemical model was proposed to explain the diastereoselectivity of the cyclobutenyl methanamine formation (Figure 2.23). Starting from a Newman projection of the carbocation intermediate proposed in the reaction mechanism (Figure 2.10), the nitrogen can deprotonate either H_a or H_b on the cyclobutane ring. If the nitrogen rotates clockwise (CW) to remove H_b, there is torsional strain between the R' alpha to nitrogen and the EWG on the cyclobutane. However, if it rotates counter clockwise (CCW) to remove H_a, the torsional strain is minimized, leading to the major diastereomer. This hypothesis is consistent with the major diastereomer of **4aa**, which was confirmed by X-ray crystallography (Figure 2.24).

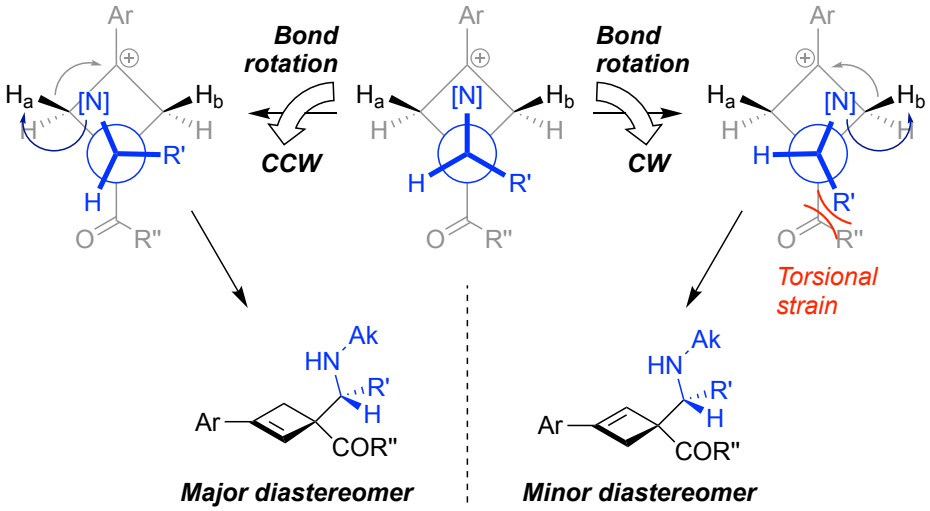

Figure 2.23: Stereochemical model for cyclobutenyl methanamine synthesis.

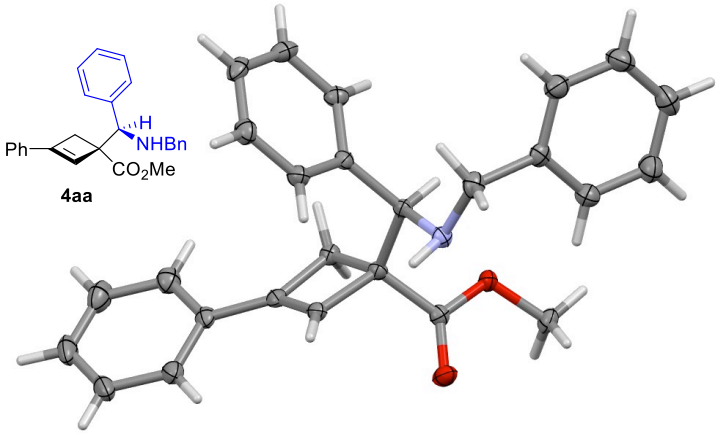

Figure 2.24: Solid state molecular structure of **4aa** obtained by X-ray crystallography. Ellipsoids are plotted at 50% probability.

2.9.2 Stereochemistry of Major Iodoamination Products

To confirm the stereochemistry of the major diastereomer of the iodoamination product, NOESY spectra of compounds **6aa** and **6ii** were obtained (Figure 2.25). The predicted stereochemistry shows the iodine adding to the bottom of the cyclobutene to avoid steric clash with the imine-derived substituent. This would give a *syn* arrangement of the hydrogen alpha to the nitrogen (H_a) and the hydrogen attached to the same carbon as iodine (H_b). Consistent with this, we observe a NOESY correlation between H_a and H_b (shown in red,

Figure 2.25). In addition, we observe a NOESY correlation between H_b and a hydrogen on the benzyl -CH_2 group (shown in purple), further supporting that H_b is *pseudo*-equatorial and the iodine is *pseudo*-axial (Figure 2.25).

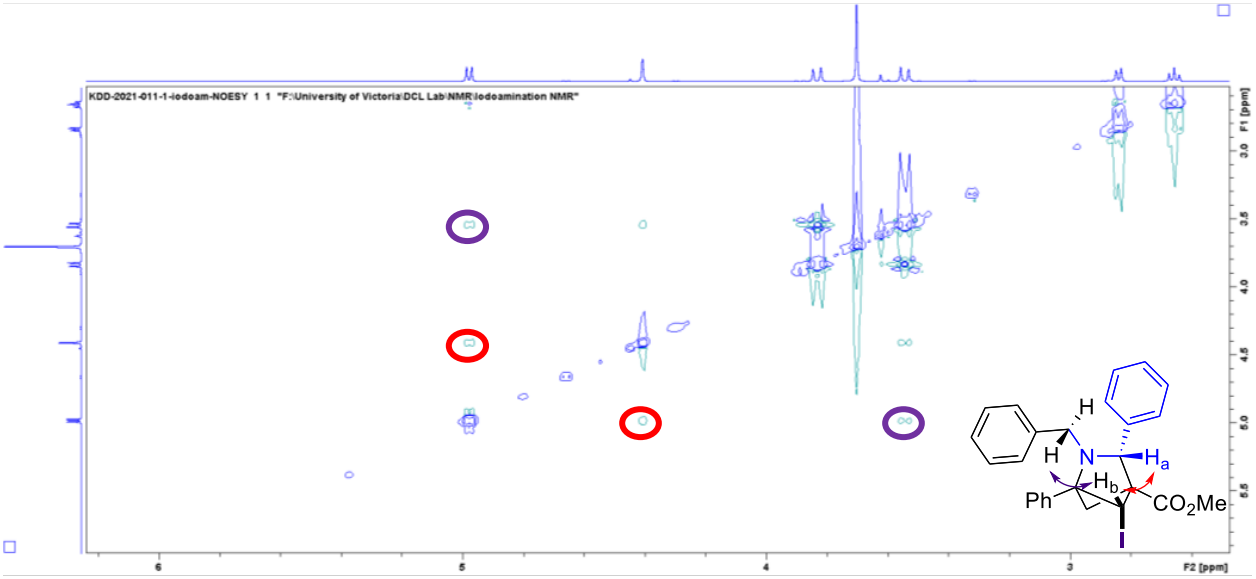

Figure 2.25: Excerpt of NOESY spectrum of compound **6aa**.

Similarly to **6aa**, to deduce the absolute stereochemistry of the enantioenriched **6ii**, the NOESY spectrum was analyzed (Figure 2.26) and 2.27). Key correlations are seen between the hydrogen attached the iodine carbon (H_c) and the two hydrogens alpha to nitrogen (H_a and H_b shown in green and red, respectively, Figure 2.26). These indicate that H_c is *pseudo*-equatorial and on the same side of the ring as H_a and H_b. In addition, a correlation can be seen between H_a and H_b (shown in purple) indicating these two hydrogen are also on the same side of the ring (Figure 2.26). To further support the proposed structure, correlations can be seen between the *ortho* protons on the phenyl ring with the methyl group (shown in red) and the and the *pseudo*-equatorial hydrogen on the methylene carbon of the bicyclic system (shown in purple) (Figure 2.27). All of these NOESY correlations support the proposed absolute stereochemistry of compound **6ii**.

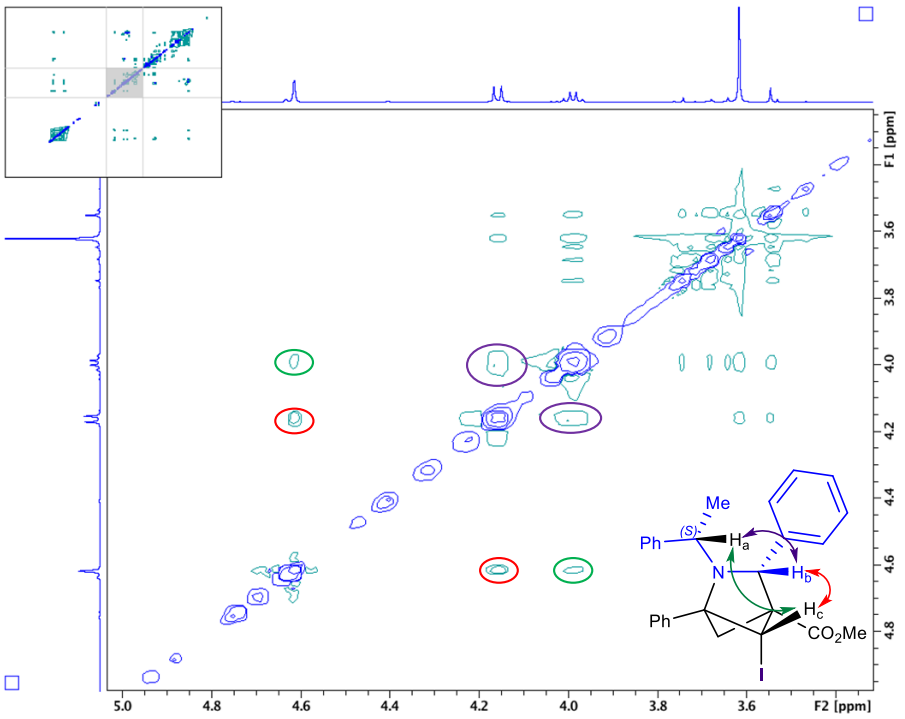

Figure 2.26: NOESY correlations in compound **6ii**.

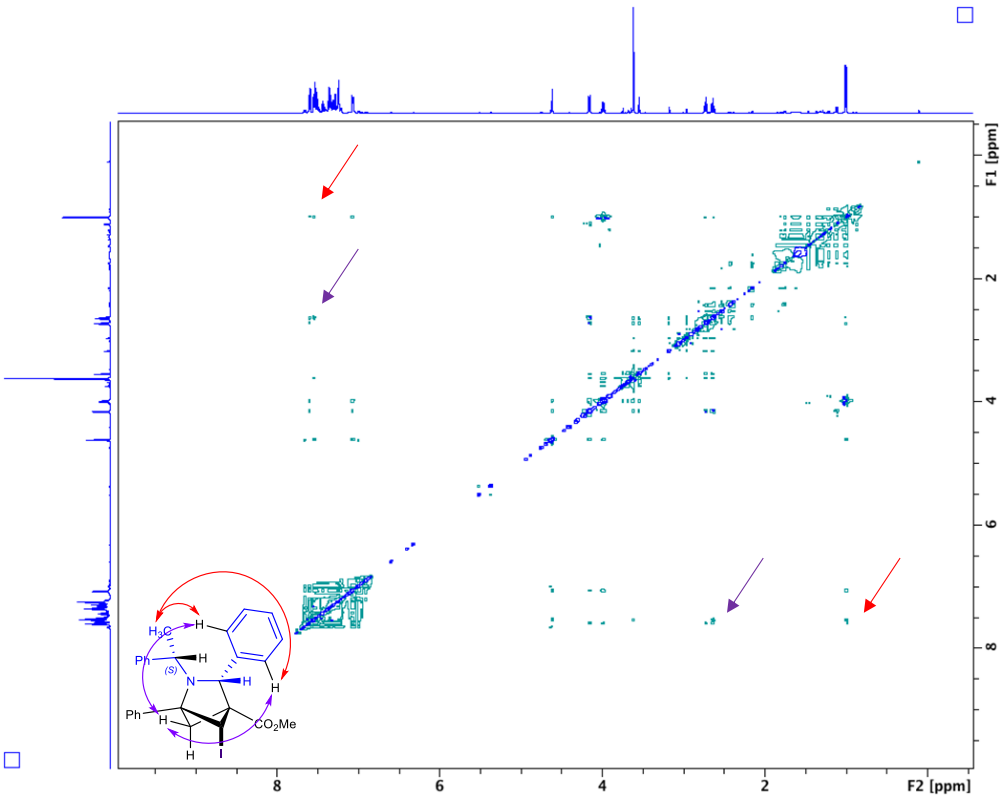

Figure 2.27: Additional NOESY correlations in compound **6ii**.

2.9.3 Stereochemical Assignment of the Minor Diastereomer

The minor diastereomer of **4kk** was isolated to determine its absolute stereochemistry when using (*S*)-α-methylbenzyl (Figure 2.28). The proposed stereochemistry has the two cyclobutenyl methanamine stereocenters inverted relative to the major diastereomer, where the cyclobutene and α-methylbenzyl group are still on the same side of the molecule, but the R group (naphthyl in this case) is on the opposite side as depicted in (Figure 2.28).

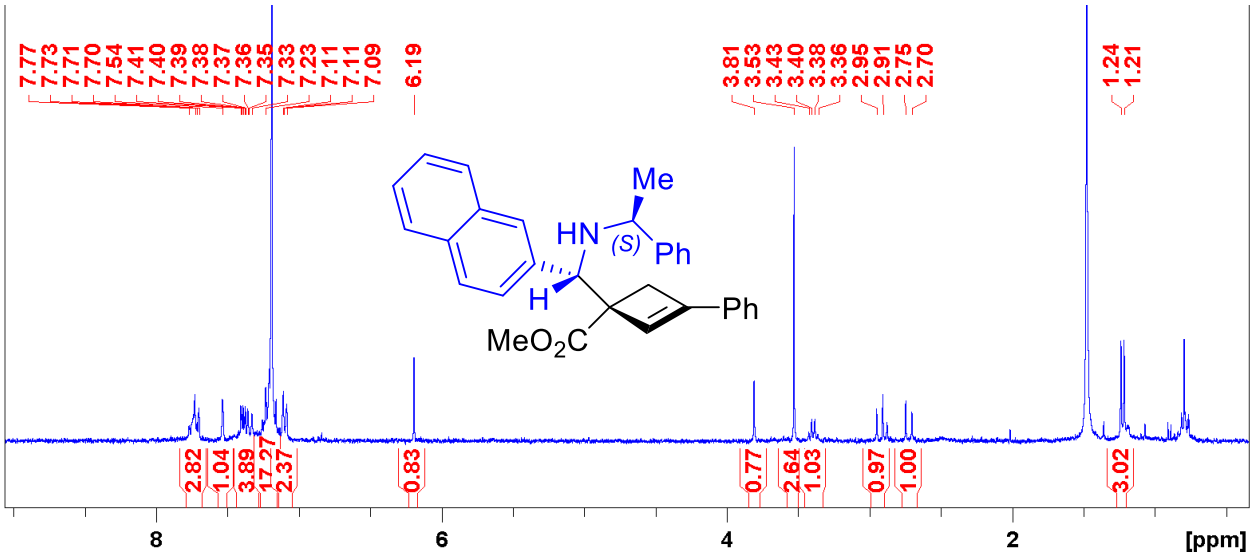

Figure 2.28: ^{1}H NMR of the minor diastereomer of **4kk′**.

To determine the absolute stereochemistry, the isolated product **4kk′** was subjected to the iodoamination conditions and a NOESY spectrum was taken. Key correlations are observed between the hydrogen attached to the iodine carbon (H_a) and the hydrogen alpha to the nitrogen (H_b), indicating that they are on the same side of the ring (Figure 2.29). In addition, the hydrogen on the "front" of the cyclobutane ring (H_e) show correlations to the *ortho* protons on the naphthyl ring (H_g), further supporting the stereochemistry predicted (Figure 2.29). These NOESY correlations are consistent with the minor product having inverted stereochemistry at the two variable stereocenters relative to the major stereoisomer.

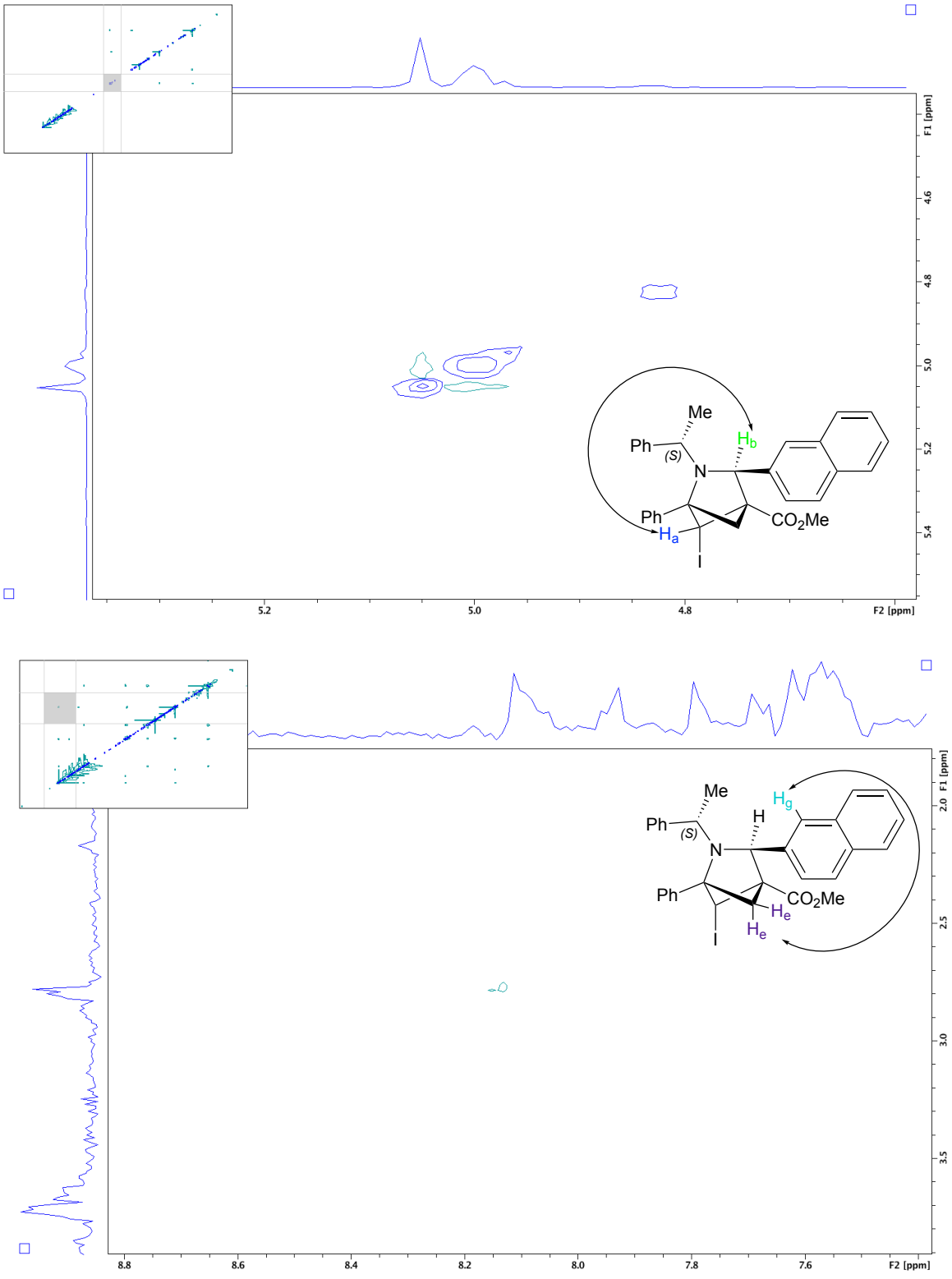

Figure 2.29: Key NOESY correlations for the iodoamination production of **4kk′**.

2.10 Synthetic Transformations of AzaBCHs

To demonstrate the potential synthetic utility of these azaBCHs, three functional group interconversions of **3a** and **3e** were conducted (Figure 2.30). The first transformation starts with azaBCH **3e**, which has a *p*-methoxyphenyl (PMP) group on the nitrogen. Using ceric ammonium nitrate (CAN) in acetonitrile and water, the PMP group of **3e** was removed to give product **7a** (Figure 2.30). This provides a secondary nitrogen on the azaBCH that could undergo further synthetic transformations. The methyl ester group in **3a** can also be hydrolyzed to the carboxylic acid **7b** using lithium hydroxide in THF and water (Figure 2.30). Finally, the methyl ester in **3a** can be reduced to the primary alcohol using lithium aluminum hydride in THF (Figure 2.30). These transformations highlight the stability of the azaBCHs in chemical reactions and reinforce their potential usefulness in pharmaceuticals.

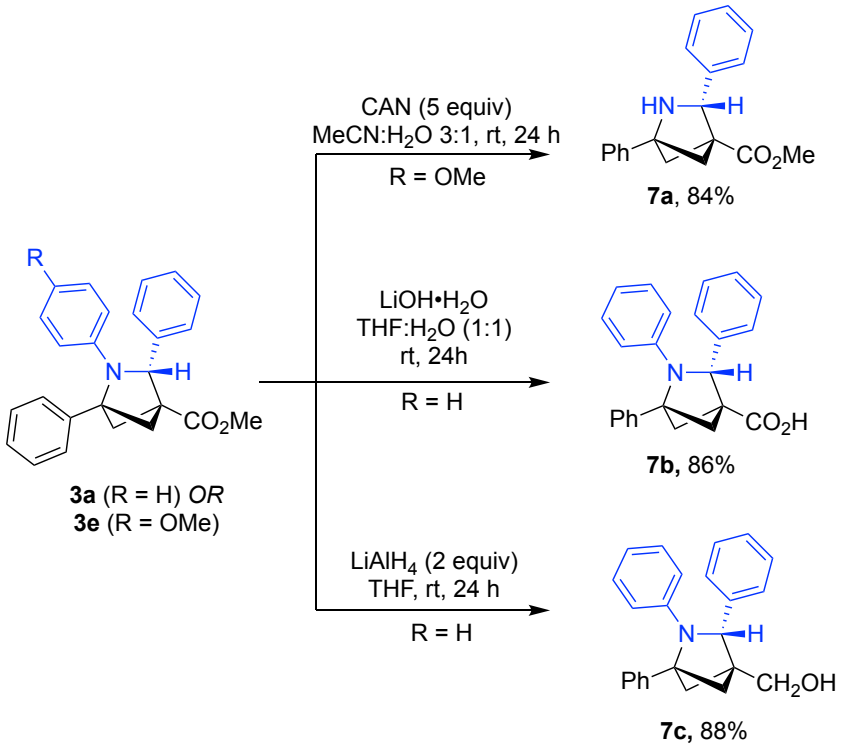

Figure 2.30: Synthetic transformations of the azaBCHs.

Additional transformations of the azaBCHs were also explored. The scope of the hydrolysis reaction was tested and products **7d-7g** were synthesized with excellent yields (Figure 2.31). The hydrolyzed product **7g** was then taken into an unoptimized CDI coupling reaction

to install a 3,5-dimethyl *N*-acyl pyrazole group, giving product **8g** (Figure 2.31). This provides a relatively labile synthetic handle that can be used to further diversify the azaBCHs.

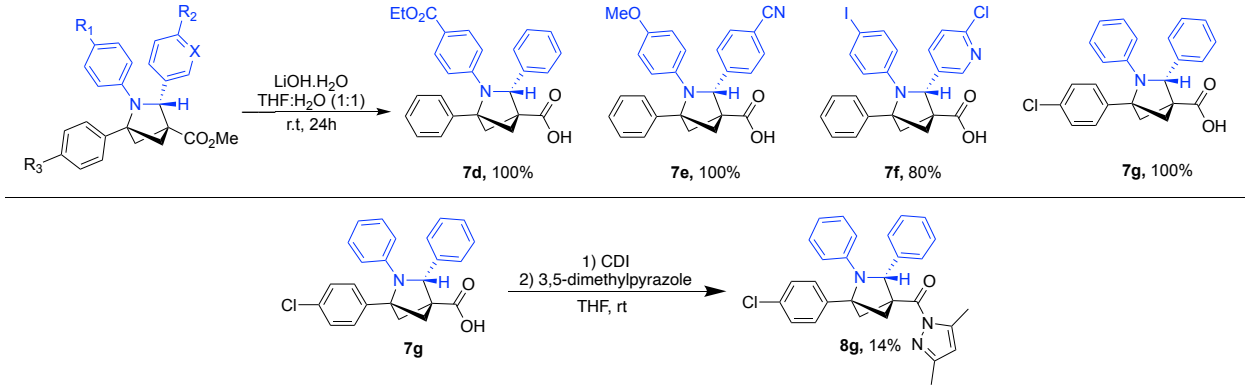

Figure 2.31: Additional synthetic transformations of the azaBCHs.

2.11 Conclusions

In summary, the synthesis of azabicyclohexanes and cyclobutenyl methanamines *via* imine addition to bicyclobutanes was developed. Divergent reactivity was acheieved using either *N*-aryl or *N*-alkyl derived imines. The reactivity was determined to be due to a divergence in the mechanism based on the basicity/nucleophilicity of the nitrogen atom where either nucleophilic addition (to form the azaBCHs) or deprotonation/elimination (to form the cyclobutenyl methanamines) was observed. The cyclobutenyl methanamines can be converted to the corresponding azabicyclohexane *via* an intramolecular iodoamination where an addition iodine synthetic handle was installed. Synthetic transformations of the azaBCH products were demonstrated. The azabicyclohexane structures have potential applications in pharmaceuticals. Work is ongoing to apply these techniques toward other complex molecule synthesis *via* additions to bicyclobutanes. This is crucial for the discovery of new active pharmaceutical ingredients containing these bicyclic scaffolds.

3 Synthesis of 2-Oxo-Bicyclohexanes Through Enolate Addition to Bicyclobutanes

This chapter has been adapted from:
Woelk, K. J.; Dhake, K.; Schley, N. D.; Leitch, D. C. Enolate addition to bicyclobutanes enables expedient access to 2-oxo-bicyclohexane scaffolds. *Chem. Commun.* **2023**, *59*, 13847–13850.

Contributions: The experimental work was completed independently. Support for substrate synthesis and methodology from Kushal Dhake.
Intellectual contributions: Kyla Woelk: Lead conceptualization, data curation, formal analysis, investigation and methodology. Kushal Dhake: Supporting investigation and methodology.

3.1 Abstract

The synthesis of 2-oxo-bicyclo[2.1.1]hexanes (2-oxo-BCHs) from bicyclobutanes and readily available enolate precursors is reported. We propose this reaction proceeds *via* initial enolate addition to the bicyclobutane, which is followed by an intramolecular acyl substitution by the resulting enolate intermediate to form the 2-oxo-BCHs. Arylacetate derivatives are used as enolate precursors, giving 2-oxo-3-aryl-BCH scaffolds from easy to obtain starting materials. Glycine-derived enolates are also viable precursors, which give access to protected 2-oxo-3-amino-BCH derivatives with a nitrogen synthetic handle that can be further functionalized. Different transformations on the 2-oxo-3-amino-BCH derivative nitrogen are demonstrated including deprotection to the free primary amine.

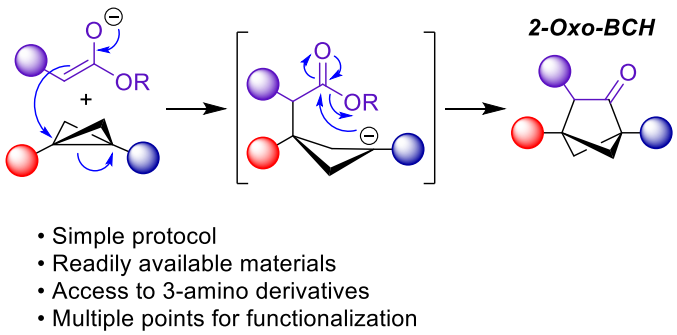

Figure 3.1: Synthesis of 2-oxo-bicyclohexanes *via* enolate addition to bicyclobutanes.[178]

3.2 Background

One class of Csp^3-rich scaffolds of current interest are bicyclo[2.1.1]hexanes. As described in Chapter 1, these structures are relevant benzene bioisosteres, mimicking a variety of substitution patterns.[16] Until recently, syntheses of substituted BCHs were scarce, and relied on intramolecular photochemical [2+2] cycloaddition.[60–64] This was followed by a surge in synthesis of bicyclohexanes *via* intermolecular formal [2+2] cycloadditions with BCBs, through either radical-based mechanisms[65–68] or Lewis acid catalysis.[121;126]

To effectively use BCHs as versatile scaffolds for medicinal chemistry, access to molecules with synthetic handles for vector elaboration is critical. 2-Oxo-bicyclohexanes, which contain a carbonyl group in the bicyclic system, provide such a handle. The initial direct route to these motifs, reported by Carpenter, requires UV photochemical intramolecular [2+2] of oxygen-functionalized dienes (Figure 3.2).[61;179] Fessard and Salomé reported a modification that uses a photocatalyst to enable use of lower-energy light (Figure 3.2).[180] These methods are very specific and limit the diversity of accessible bicyclohexanes. In addition to intramolecular synthesis, Studer recently reported an intermolecular cycloaddition using a Lewis acid catalyzed [2+2] cycloaddition of ketenes to bicyclobutanes, enabling access to 2-oxo-BCHs with quaternary stereocenters alpha to the carbonyl (Figure 3.2).[127] This demonstrates the ability for bicyclobutanes to be viable starting materials to synthesize 2-oxo-bicyclohexanes; however, a downside to this reactivity is the requirement of highly reactive ketene starting materials.

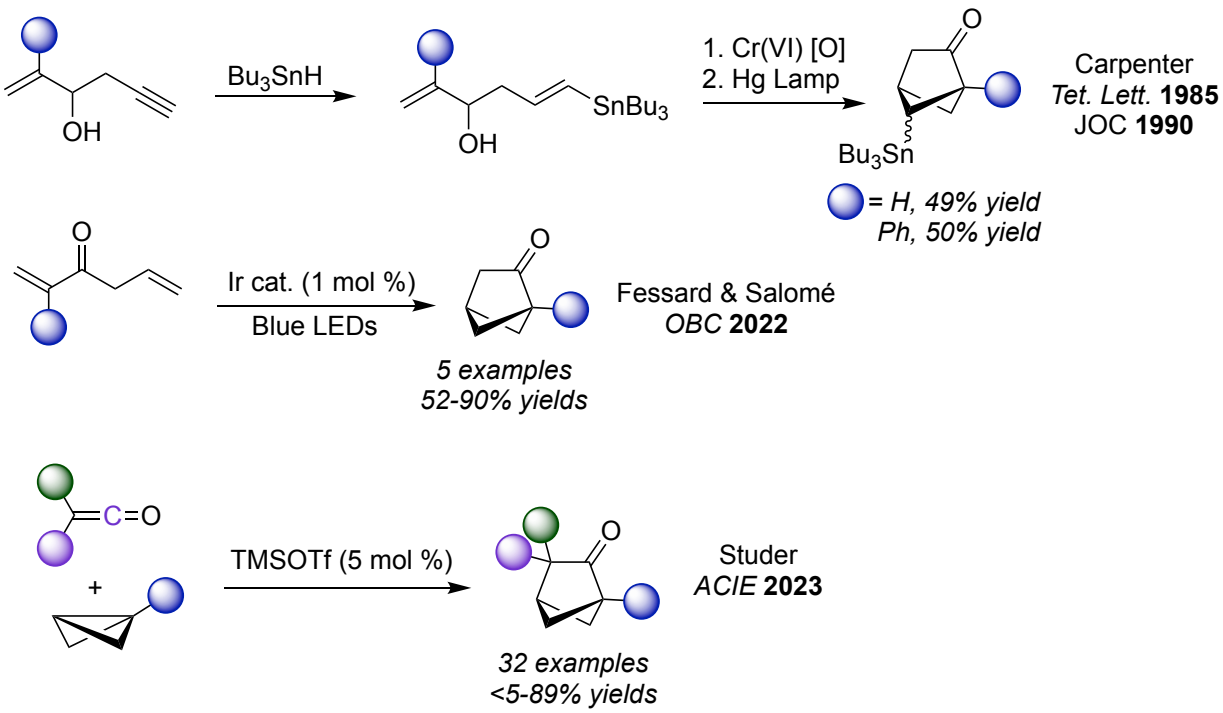

Figure 3.2: Previous syntheses of 2-oxo-bicyclo[2.1.1]hexanes.[61;127;179;180]

As discussed in Chapter 1, bicyclobutanes are susceptible to attack by nucleophiles, with a variety of different examples reported in the literature; however, enolates are one class of nucleophile that have not been previously reported to react with bicyclobutanes. We hypothesized that a combination of ester-derived enolates and bicyclobutanes in the presence of a base could result in 2-oxo-BCHs **3** (Figure 3.3). Nucleophilic attack of an enolate to the electrophilic carbon of a bicyclobutane would result in ring opening and generation of another enolate intermediate. This enolate could then undergo intramolecular acyl substitution at the ester to form a 2-oxo-bicyclo[2.1.1]hexane product. This would be a favoured 5-exo-trig cyclization to form the bicyclohexane bicyclic structure.

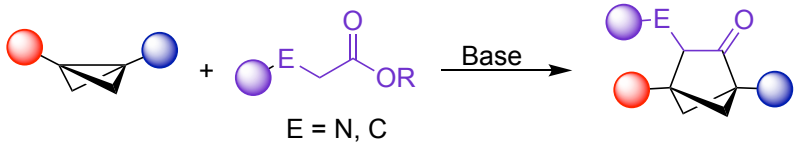

Figure 3.3: Proposed enolate addition to bicyclobutanes to form 2-oxo-bicyclo[2.1.1]hexanes.

3.3 Reaction Optimization

To assess the viability of the proposed addition/cyclization sequence, a variety of conditions were tested. The conditions were optimized using a monosubstituted bicyclobutane containing a morpholine amide (**1a**), and an ethyl glycinate derivative with the nitrogen protected as the benzaldimine (**2a**) (Table 3.1). We used the amide electron withdrawing group on the BCB to avoid competitive 1,2-addition of the enolate to that carbonyl, and the benzaldimine was used as a convenient protected NH_2 equivalent without acidic hydrogens. The first conditions of soft enolization using Lewis acid/weak base combinations failed to generate any desired product (entries 1 and 2). Following this, hard enolization using lithium diisopropylamide (LDA), NaH, and potassium bis(trimethylsilyl)amide (KHMDS) also failed to generate 2-oxo-bicyclohexane **3a** (entries 3, 4 and 5). In these cases, only decomposition of **1a** and/or **2a** was observed.

Table 3.1: Reaction optimization for synthesis of bicyclo[2.1.1]hexane **3a** from **1a** and **2a**.

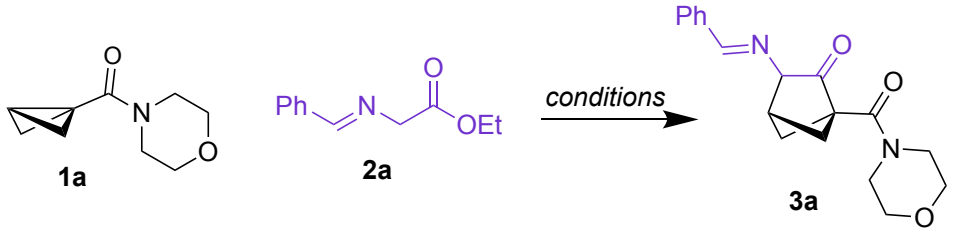

Entry	Conditions	**1a**	**2a**	**3a**
1	AgOAc (10 mol%), NEt_3, DCM	72	24	0
2	$Ga(OTf)_3$ (15 mol%),NEt_3, THF	100	78	0
3	LDA (1.1 equiv), −78 °C, THF	0	0	0
4	NaH (2 equiv), THF,1.5 equiv **2a**	99	68	0
5	KHMDS (1.5 equiv), THF,1.2 equiv **2a**	67	35	0
6	LiHMDS (1 equiv), THF	0	17	20
7	LiHMDS (1 equiv), THF, (0.30 mmol **1a**)	15	9	11
8	LiHMDS (1.5 equiv), THF, 1.2 equiv **2a**, (0.30 mmol **1a**)	11	17	39
9	LiHMDS (1.5 equiv), THF, 0.30 M, 1.2 equiv **2a**, (0.30 mmol **1a**)	21	0	47

[a]Unless otherwise noted, reactions are performed at room temperature for 24 hours with 0.05 mmol of **1a**, 1 equiv of **2a**, and 1 mL of solvent ([**1a**] = 0.05 M). [b] Amounts of **1a**, **2a**, and **3a** are obtained by ^{1}H NMR spectroscopy (rel. integration vs. internal standard, 1,3,5-trimethoxybenzene (TMB)).

Using LiHMDS as a base gave a 20% solution yield of **3a** on a 0.05 mmol scale (entry 6). On larger scale (0.30 mmol of bicyclobutane), keeping all other variables constant, the yield of **3a** dropped to 11% (entry 7). Using a slight excess of LiHMDS and enolate (1.5 and 1.2 equiv respectively), the yield increased to 39% (entry 8). Finally, increasing the reaction concentration from 0.05 M to 0.30 M of **1a** further improves the yield of **3a** to 47% (entry 9). This gives the optimized conditions using LiHMDS as a base with 1.5 equiv, 0.30 M concentration with THF as a solvent.

3.4 Imine-BCH Modifications

The optimized conditions were carried forward to explore the reactivity of **3a** toward functionalization of the amine and ketone synthetic handles (Figure 3.4). A solution of **3a** was generated using the optimized conditions from Table 5.1, entry 9, and then subject to a mild aqueous workup ($NaHCO_3$) prior to functionalization. The yields of the resulting products are calculated over two steps from **1a** (solution yield of **3a** ∼50%). To reveal the unprotected primary amine, imine hydrolysis was performed by stirring **3a** over silica to give **4a** in 35% yield over two steps (Figure 3.4). Both the imine and ketone were reduced using sodium borohydride in methanol to give aminoalcohol product **4b** in 35% yield (Figure 3.4). Notably, **4b** was obtained as a single diastereomer, with *syn* relative stereochemistry between the amino and hydroxyl groups. The stereochemistry was determined by 2D NOESY NMR spectroscopy (Figure 3.5) and confirmed by X-ray crystallography. In the NOESY spectrum, an NOE correlation can be seen between the hydrogens alpha to the hydroxyl and amino groups (shown in blue) (Figure 3.5). In addition, the two hydrogens both show NOE correlations to the same bicyclic hydrogen (shown in red and grey), indicating that the two hydrogens are *syn* to each other (Figure 3.5). Tandem acylation and hydrolysis of the imine was achieved using either benzyl chloroformate (Cbz-Cl) or *p*-toluoyl chloride, giving the corresponding carbamate **4c** and amide **4d** in 47% and 28% yield, respectively (Figure 3.4). A solid state molecular structure of **4d** was also obtained by X-ray diffraction, confirming the proposed connectivity.

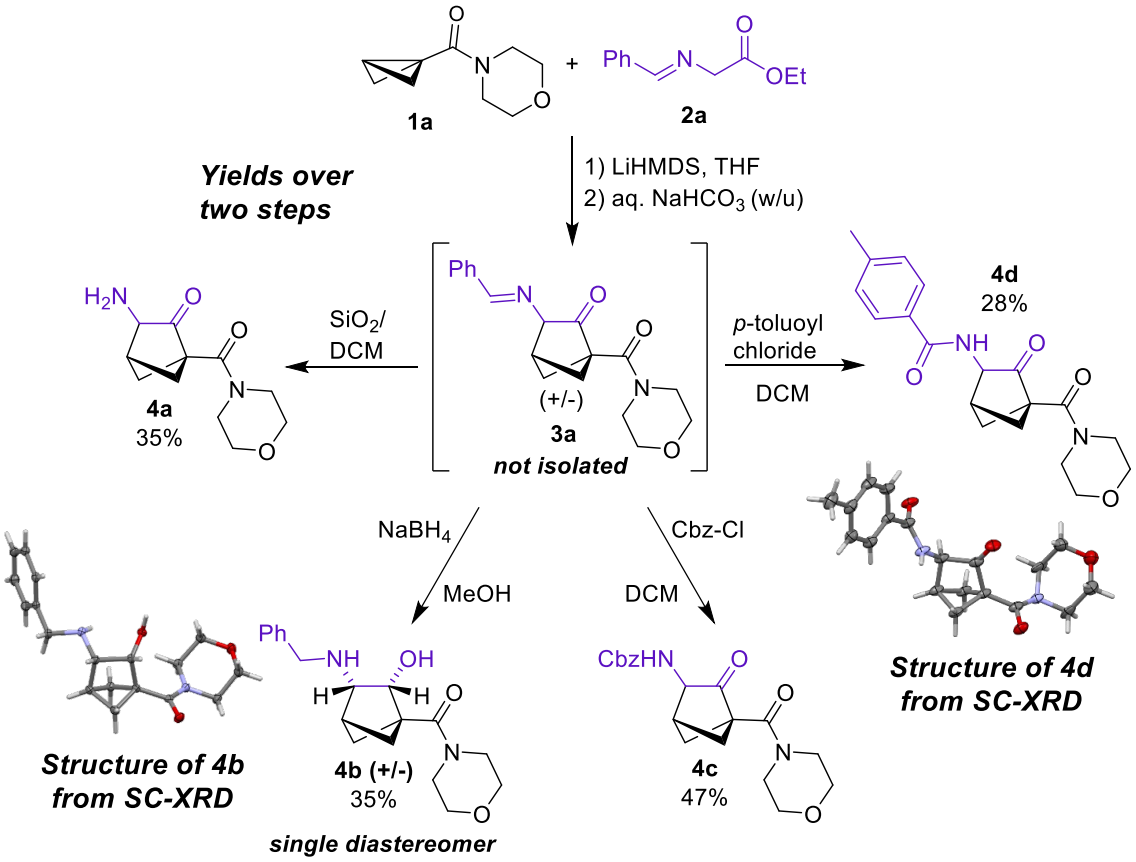

Figure 3.4: Synthesis of **3a** followed by modifications of the imine (and ketone) synthetic handles.

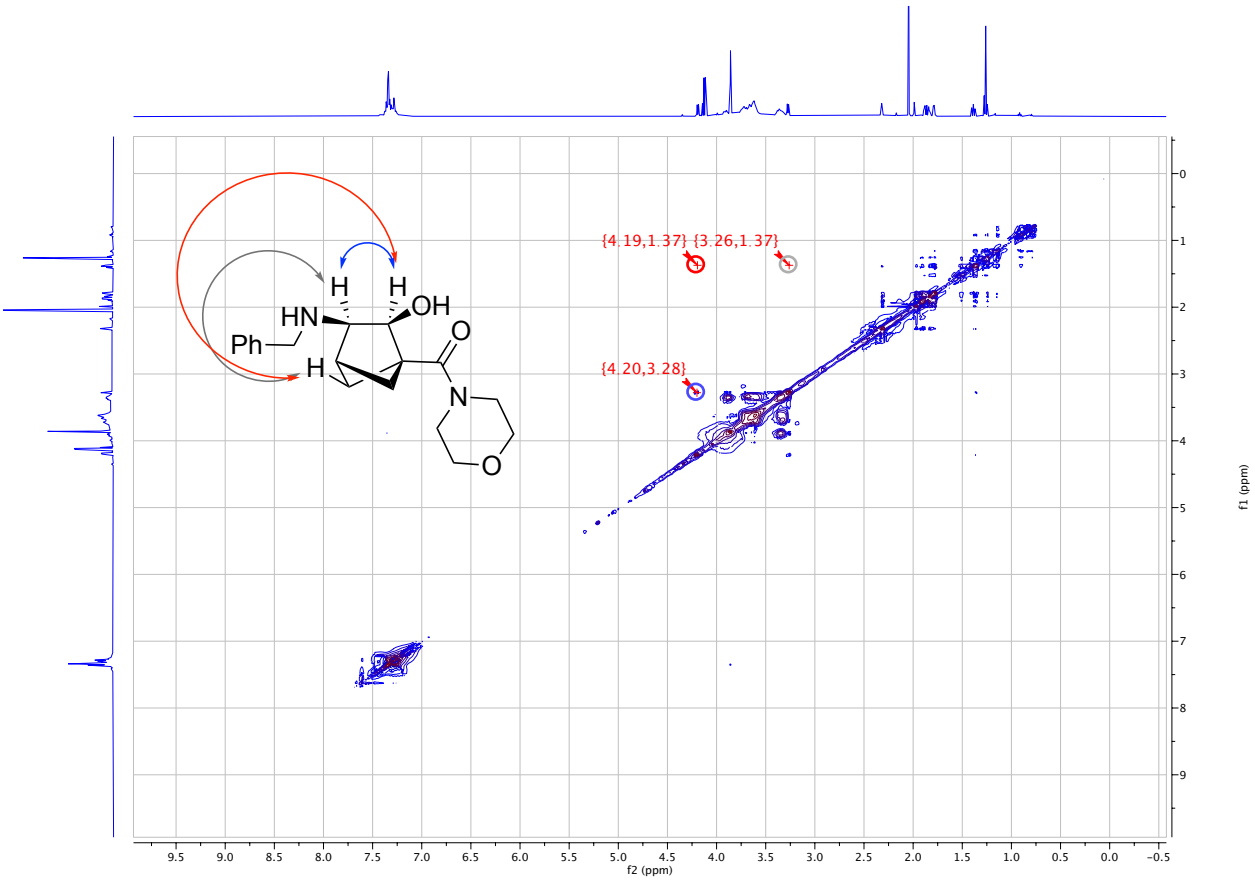

Figure 3.5: 2D NOESY NMR spectrum for assigned stereochemistry of **4b**.

3.5 Substrate Synthesis

3.5.1 Enolate Precursor Synthesis

To assess the scope of enolates viable in this reaction, acetate derivatives were synthesized. The imine containing derivatives were made *via* a condensation reaction between an aldehyde (or ketone) and glycinate esters in the presence of a drying agent (Na_2SO_4) giving glycinate imine derivatives (Figure 3.6 - (1)). In addition to imines, aryl acetates were synthesized *via* an acid catalyzed esterification reaction of acetic acid derivatives to form ethyl esters (Figure 3.6 - (2)). Experimental details are reported in Appendix B, Sections B.3.1 and B.3.2.

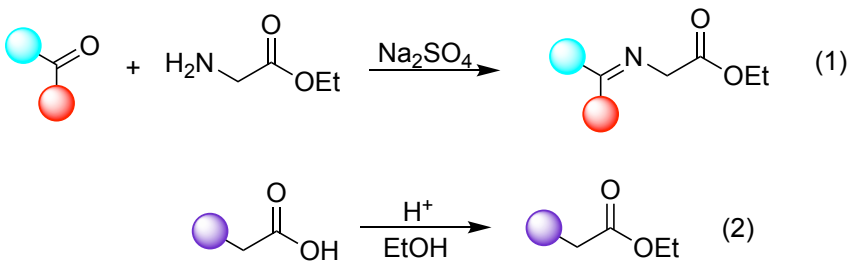

Figure 3.6: Synthesis of enolate precursor derivatives.

3.5.2 Monosubstituted Bicyclobutane Synthesis

The synthesis of different bicyclobutane derivatives was developed to explore the scope of the reaction. Experimental details are reported in Appendix B, Section B.3.3. The synthesis of disubstituted bicyclobutanes was discussed in Chapter 2. The synthesis of monosubstituted bicyclobutanes was optimized from literature procedures (Figure 3.7). Starting from 3-oxocyclobutanecarboxylic acid, there are two pathways that can be used to synthesize the amide derivative **II**. Following the blue pathway, carbonyl diimidazole (CDI) can be used as the coupling agent to synthesize the amide directly from the carboxylic acid (Figure 3.7).

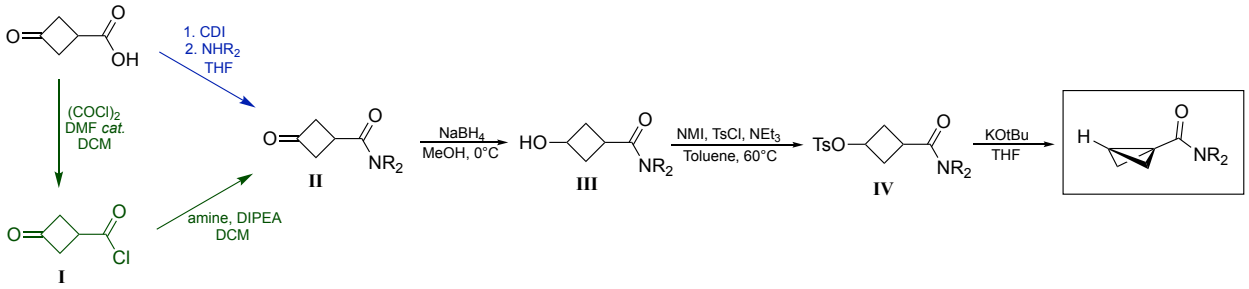

Figure 3.7: Synthesis of monosubstituted bicyclobutane derivatives.

Alternatively, following the green pathway, first the acyl chloride **I** can be synthesized using oxalyl chloride with DMF as a catalyst. This is then followed by amide synthesis using the appropriate amine and DIPEA as a base to give compound **II** (Figure 3.7). Once amide **II** is synthesized, the ketone is reduced using sodium borohydride in methanol to give alcohol **III**. The alcohol was then converted to a good leaving group using tosyl chloride. Literature procedures typically report 4-dimethylaminopyridine (DMAP) as the catalyst, triethylamine as the base and tosyl chlorde in DCM;[65;149] however, this procedure consis-

tently gave low yields (<40%) of the tosylated product **IV**. Instead, after optimization it was found that using *N*-methylimidazole (NMI) as an additive in toluene at 60 °C gave the product **IV** with consistent yields of ∼80-90%. The bicyclobutane was then formed using potassium *tert*-butoxide as a base in THF. Additional optimization was required, as polymerization of the bicyclobutane upon synthesis was observed. Using a THF solvent that contained 250 ppm BHT as an inhibitor was used for the reaction to help prevent polymerization. In addition, once synthesized, the bicyclobutane was stored under N_2 at −20 °C. Following this procedure, a set of monosubstitued bicyclobutanes were synthesized, along with one disubstituted bicyclobutane **1l** (Figure 3.8). These substrates were tested in the scope of the enolate addition reaction.

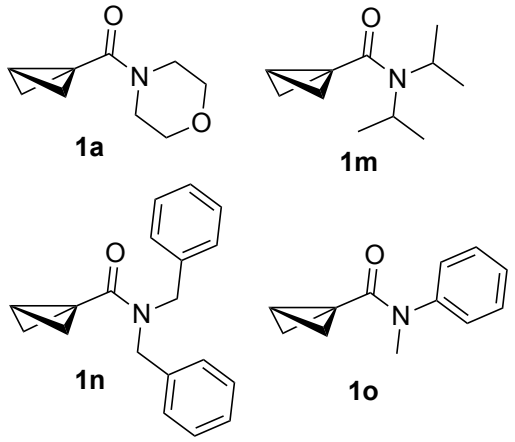

Figure 3.8: Set of monosubstituted amide bicyclobutanes synthesized.

3.6 Reaction Scope

Using the optimized enolate-addition conditions, we performed an initial survey of the reaction scope with respect to the BCB (**1**) and enolate precursors (**2**) (Figure 3.9). Unless otherwise noted, yields are for isolated compounds. Automated purification and product characterization is reported in Appendix B, Section B.5. Imine-containing product **3a** is acid labile, and decomposes during chromatography on silica, so the reported yield of 47% is obtained by ^{1}H NMR spectroscopy (using 1,3,5-trimethoxybenzene as an internal standard). Using the more stable benzophenone imine as a protecting group, we were able to isolate analogue **3b** in 42% yield. In addition to enolates from glycinate ester derivatives,

we assessed a variety of readily available arylacetate esters as enolate precursors. Ethyl phenylacetate is an excellent reactant, giving BCH **3c** with an isolated yield of 85% on a 0.5 mmol scale, and 60% on a 3.0 mmol scale. Single crystal X-ray diffraction of **3c** confirmed the proposed structure (CCDC 2290170). We also tested other arylacetates with a variety of (hetero)aromatic substituents. Electron rich aromatics including *p*-tolyl (**3d**), 3-naphthyl (**3e**), and *p*-methoxyphenyl (**3f**) were all successfully incorporated. In addition, halobenzenes *p*-fluorophenyl (**3g**) and *p*-bromophenyl (**3h**) as well as heterocycles 3-thiophenyl (**3i**) and 3-pyridyl (**3j**) are also compatible with moderate to good isolated yields.

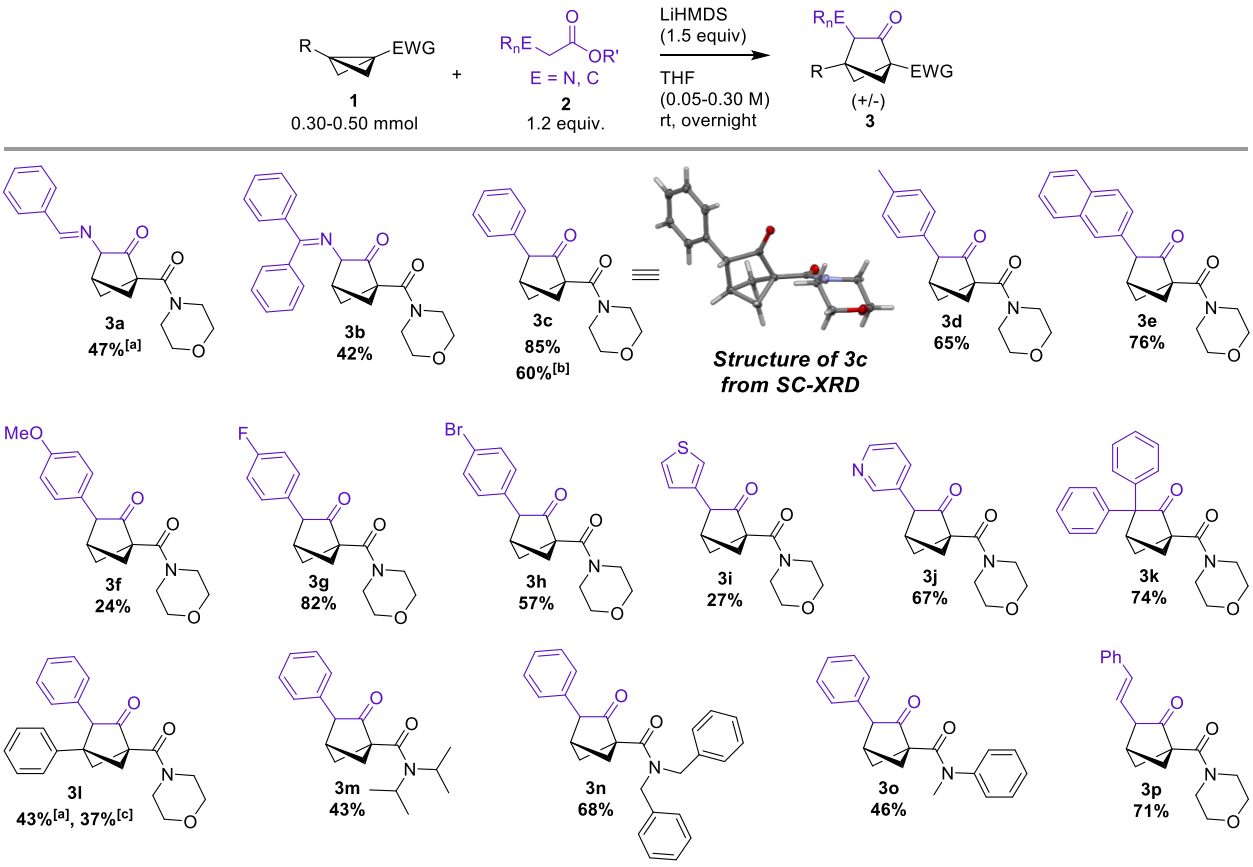

Figure 3.9: Scope of 2-oxo-bicyclo[2.1.1]hexanes enolate addition to bicyclobutanes. [a]Yields determined by ^{1}H NMR spectroscopy (rel. integration vs. internal standard TMB). [b]Isolated yield on 3.0 mmol 1 scale, 0.60 M. [c]Isolated yield as part of a mixture with unreacted bicyclobutane (32%), which could not be separated by column chromatography.

An α,α-disubstituted enolate precursor was also added successfully to give product **3k** with an excellent 74% yield, despite the additional steric bulk. A disubstituted BCB is

also compatible with this reaction, giving **3l** in 43% solution yield (determined by ^{1}H NMR spectroscopy); however, attempts to purify this compound by column chromatography under multiple conditions led to isolation of a mixture of **3l** (37% yield) and unreacted bicyclobutane (32%). Other tertiary amides are supported, such as *N,N*-diisopropyl (**3m**), dibenzyl (**3n**) and *N,N*-methylphenyl (**3o**) with good yields. Finally, an alkenyl substituted enolate was successfully added (**3p**); however, attempts to use alkyl-substituted enolates (e.g. from ethyl propionate) led to no product formation. A bicyclobutane substituted with a benzyl ester was also tested, leading to multiple products; we were able to isolate a small amount of the corresponding ethyl ester BCH. Thus product was likely formed *via* transesterification of the benzyl ester with ethoxide (12% isolated yield) (Figure 3.10).

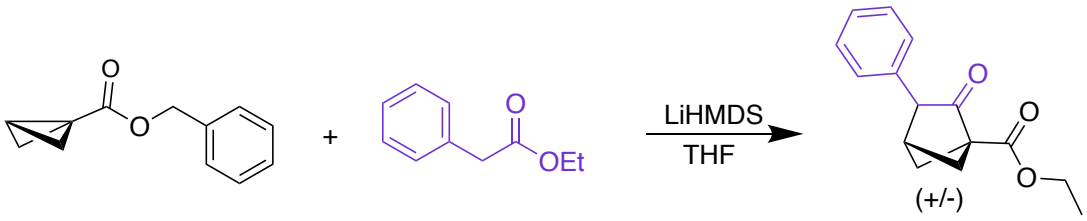

Figure 3.10: Isolation of 2-oxo-bicyclohexane from an ester bicyclobutane derivative.

3.7 Mechanistic Insight

The proposed mechanism for this reaction is a step-wise double enolate addition (Figure 3.11). Starting from deprotonation of the enolate precursor **2** with strong base, the enolate will attack at the electrophilic position of the bicyclobutane **1**. This then forms a second enolate intermediate that can attack at the acetate carbonyl and undergo an acyl substitution to give bicyclohexane **3** with an alkoxide leaving group.

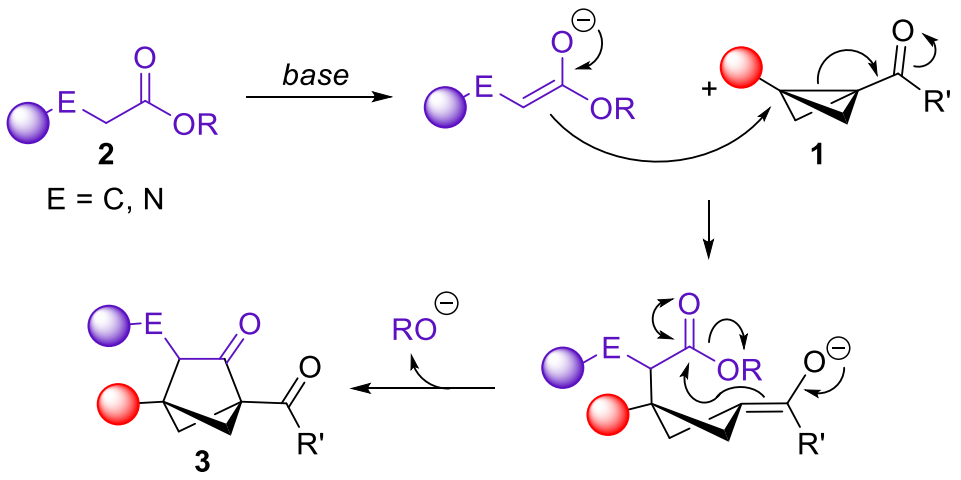

Figure 3.11: Proposed mechanism for synthesis of bicyclo[2.1.1]hexanes **3**.

To support the mechanism, during larger scale preparation of bicyclohexane **3a** and **3c**, we isolated and characterized byproducts of the enolate addition. These byproducts are a result of only the first enolate addition occurring, giving functionalized cyclobutane products **3aa** and **3cc** as mixtures of diastereomers (Figure 3.12). The mass of **3cc** was confirmed by high resolution mass spectrometry (HRMS). For **3aa**, since the imine is labile, the product was converted to the *p*-tolyl amide product **3ab** *via* an acylation/hydrolysis reaction. The mass of **3ab** was confirmed *via* liquid chromatography-mass spectrometry (LCMS) (Figure 3.12).

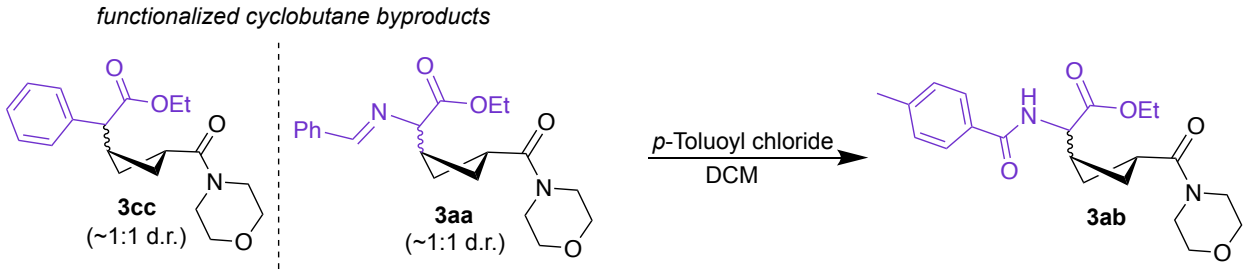

Figure 3.12: Monoenolate addition byproducts isolated.

With respect to the reaction mechanism, we also considered the possibility of *in situ* ketene formation and formal [2+2] cycloaddition catalyzed by Li^+ as a Lewis acid, analogous to Studer's system.[127] Notably, Studer's system does not proceed with amide-based BCBs, or

with disubstituted BCBs, or with *in situ* ketene formation. We therefore tested phenylacetyl chloride as a ketene precursor toward **3e**. Performing a reaction in THF with NEt_3 (with or without LiOTf present as a potential Lewis acid catalyst) led to complete consumption of the acyl chloride, but no conversion of **1a**, ruling out a ketene-based mechanism (Figure 3.13).

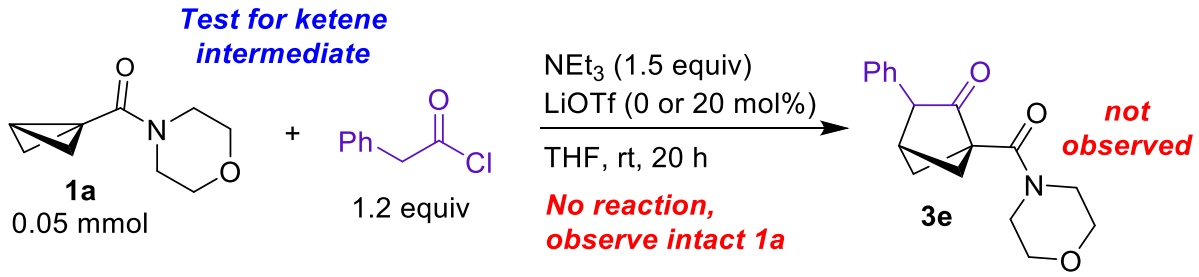

Figure 3.13: Test *in situ* ketene addition to **1a**.

3.8 Additional Synthetic Pathways

We noted that the strongly basic reaction conditions to generate **3a** should be compatible with the formation of BCB **1a** itself from the tosylcyclobutane precursor **1aa**. Therefore, we explored two alternative pathways to prepare BCH **3a** *via in situ* formation of **1a** (Figure 3.14). Starting from **1aa**, product **3a** can be made in 54% solution yield using 1.5 equiv of LiHMDS, followed by the addition of **2a** (1.2 equiv) and more LiHMDS (1.5 equiv) in a telescoped, one-pot procedure (Figure 3.14). BCH **3a** can even be formed by simply mixing **1aa** and **2a** in THF, and adding excess LiHMDS (2.5 equiv) to both generate **1a** and the enolate of **2a** (Figure 3.14). This avoids the need to isolate bicyclobutane **1a**, and has the potential to enable reactions involving less stable and/or difficult to isolate BCBs.

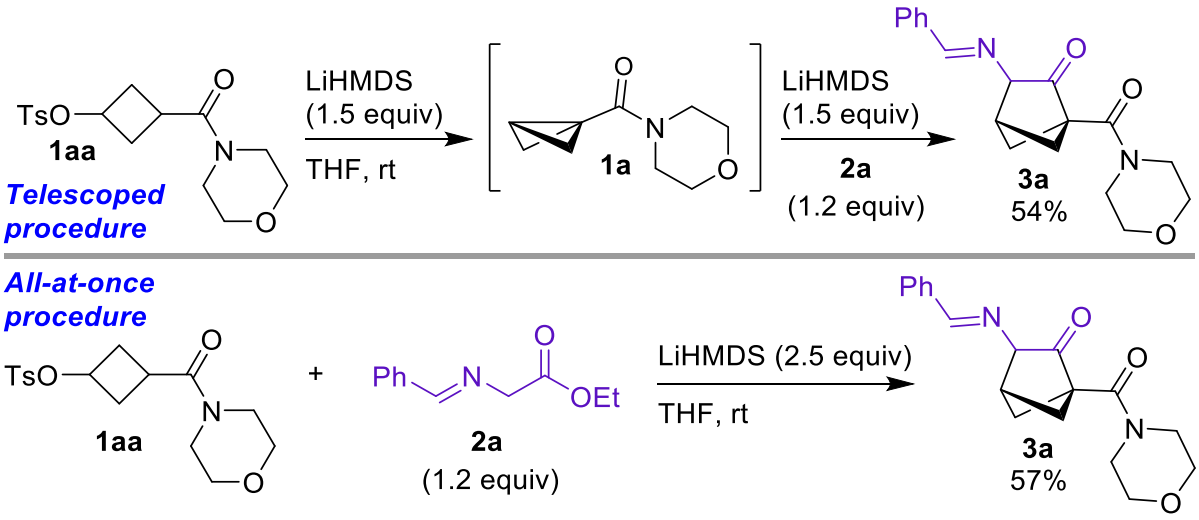

Figure 3.14: Alternative synthetic pathways to access bicyclo[2.1.1]hexanes without isolation of bicyclobutane.

3.9 Other Enolate Additions to Bicyclobutane

To push the scope of the reaction further, other enolates and bicyclic structures were tested under the reaction conditions. The enolate precursor **2c** was tested in a reaction with bicyclo[2.1.0]pentane ("housane") where successful product formation was detected *via* ^{1}H NMR spectroscopy (Figure 3.15 - Top). The product **5a**, a bicyclo[2.2.1.]heptane, was formed in a 26% yield with 60% of the starting bicyclo[2.1.0]pentane remaining (Figure 3.15 - Top). This transformation requires further optimization, but demonstrates that the reactivity is viable with other bicyclic starting materials. In addition, enolate precursor **2c** was tested in a reaction with a disubstituted 3,5-dimethyl *N*-acyl pyrazole bicyclobutane **1i** under the reaction conditions (Figure 3.15 - Top). This pyrazole can be labile under basic conditions; therefore, similarly to when the ester derived bicyclobutanes are used (Figure 3.10), the pyrazole was replaced by an ethyl ester during the reaction to give product **5b**. This product was isolated as a 42% yield on a 1.0 mmol scale and allows access to ester-containing bicyclohexane derivatives with an addition aryl substitution (Figure 3.15 - Top). To see if the *N*-acyl pyrazole bicyclohexane could be isolated, enolate precursor **2i** was prepared with a 3,5-dimethyl pyrazole leaving group. This substrate would not generate ethoxide

during the reaction and instead the free pyrazole anion would be the only byproduct. This enolate precursor was tested with pyrazole bicyclobutane **1i** under the reaction conditions; unfortunately, no product was observed (Figure 3.15 - Bottom).

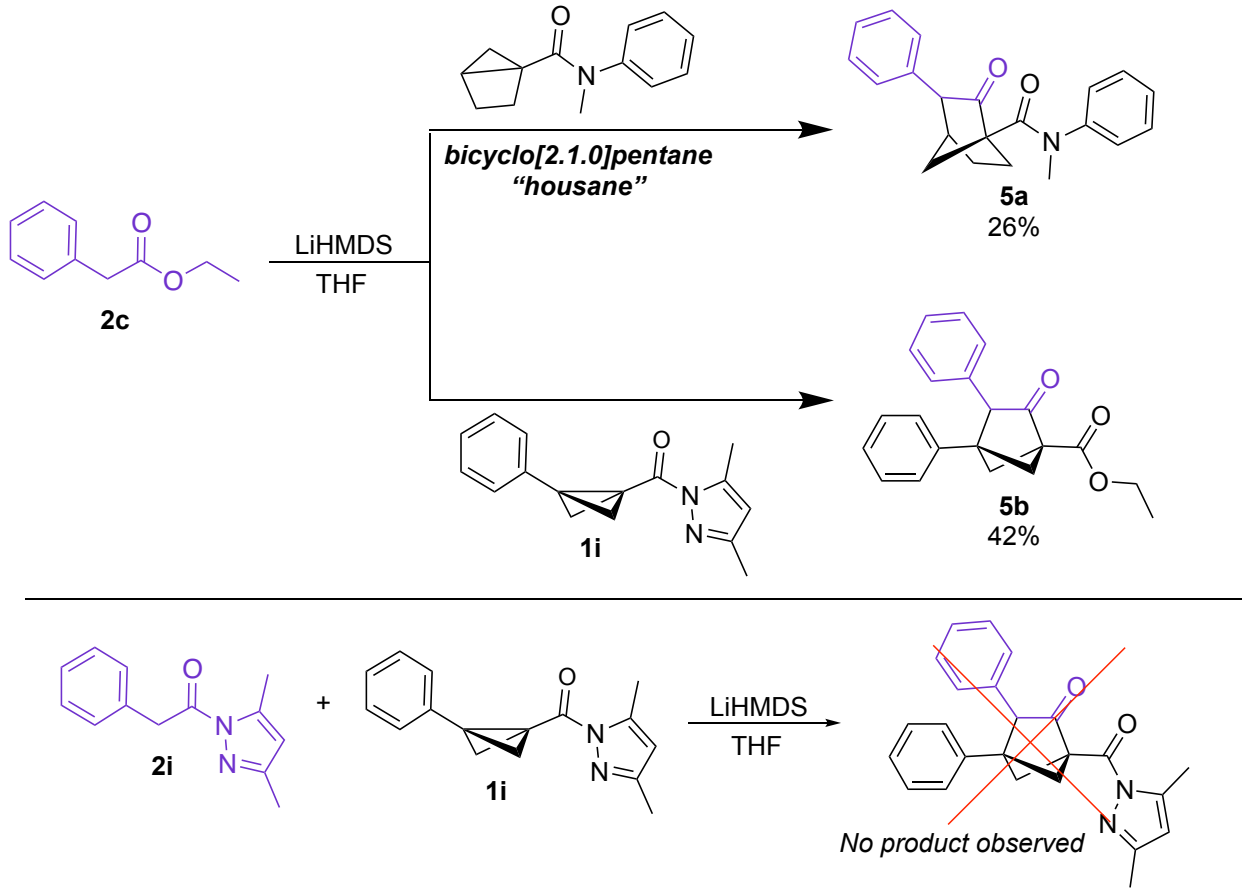

Figure 3.15: Test enolate additions of **3c** with bicyclo[2.1.0]pentane (housane) and disubstituted pyrazole bicyclobutane.

Other enolate precursors were tested with the optimized reaction conditions using bicyclobutane **1a** (Figure 3.16). No product was observed using alkyl or alkoxy-substituted acetate derivatives (Figure 3.16 - Top). Ketone and aldehyde derivatives were also unsuccessful, failing to generate 2-hydroxyl-BCHs (**6**) (Figure. 3.16 - Bottom). This indicates a need to develop additional reaction conditions to try and expand the scope of enolate additions to bicyclobutanes.

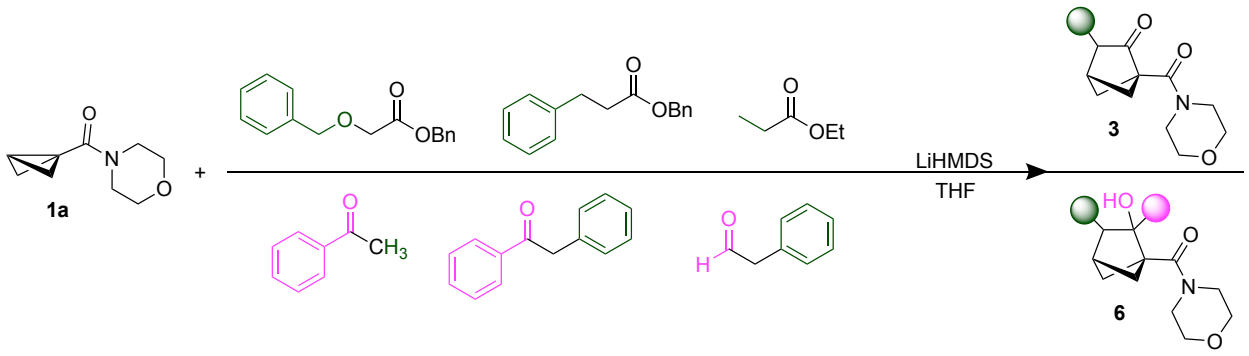

Figure 3.16: Unsuccessful enolate precursors with the optimized conditions.

Other types of carbon-based nucleophiles were tested to see if they would react with the *N*-acyl pyrazole bicyclobutane **1i** (Figure 3.17). Horner–Wadsworth–Emmons-like phosphonates **I** and **II** and ethyl ester malonate **III** were tested with LiHMDS as a base and using scandium triflate as a Lewis acid to attempt formation of cyclobutane **7** (Figure 3.17). The phosphonate derivatives showed no reactivity; however, the malonate derivative **III** gave trace amounts of product as determined by ^{1}H NMR spectroscopy and LCMS. These findings also indicate a need to develop the reaction conditions further to allow other types of carbon-based nucleophiles to react with bicyclobutane.

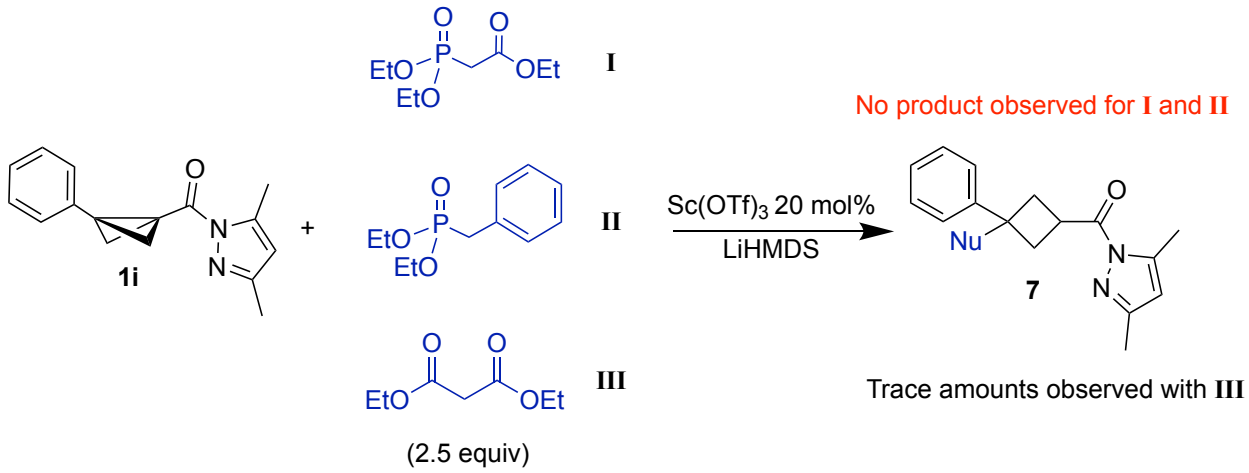

Figure 3.17: Test for other enolate additions to bicyclobutane with the optimized conditions and Lewis acid catalysis.

3.10 Conclusions

An enolate addition reaction with bicyclobutanes to form 2-oxo-BCH products was developed. The products contain an endocyclic carbonyl that can be used for further functionalization of the bicyclic core. This will help with the development of these motifs for use as Csp^3-rich bioisosteres in pharmaceuticals. Glycine-derived enolate precursors were used to synthesize 2-oxo-3-amino-BCH derivatives, giving an additional protected amine synthetic handle. Transformations at this protected amine were demonstrated including deprotection, reduction and acylation. The mechanism is proposed to proceed through an enolate addition to the bicyclobutane followed by a secondary enolate addition and acyl substitution of the intermediate to give the bicyclohexane product. Experiments showed evidence of the acyclic addition intermediate and lack of evidence for ketene addition, which supports the proposed mechanism. The reaction can also be performed in telescoped or one-pot procedures with *in situ* formation of the BCB substrate. Additional optimization is needed to expand the scope of this reactivity to other enolate or enolate-like nucleophiles.

4 Synthesis of Azabicycloheptanes Through Pyridinium Ylide Addition to Bicyclobutanes

This chapter has been adapted from:

Dhake K.; Woelk K. J.; Krueckl, L. D. N.; Alberts F.; Mutter, J.; Pohl, M. O.; Thomas, G. T.; Sharma, M.; Bjornerud-Brown, J.; Fernández, N. P.; Schley, N. D.; and Leitch, D. C. Diastereoselective dearomative cycloaddition of bicyclobutanes with pyridinium ylides: a modular approach to multisubstituted azabicyclo[3.1.1]heptanes. *Chem. Commun.*, **2024**, *60*, 13008-13011.

Contributions:
This work is done with equal contribution from Kushal Dhake.

Intellectual contributions: Kyla Woelk and Kushal Dhake: Co-lead for data curation, formal analysis, investigation and methodology. Kushal Dhake: Lead conceptualization.

Synthesis of bicyclobutanes **1b-1d**, synthesis of pyridinium salts **2q**, **2v**, **2w-3y** and test cycloaddition reactions were done by Faith Alberts. Synthesis of bicyclobutanes **1h-1i** and synthesis of pyridinium salts **2** were done by Liam D. N. Krueckl. Synthesis of bicyclobutane **1g** and test cycloaddition reaction were done by James Mutter. Grignard reactions for the synthesis of bicyclobutanes **1b-1d** were done by Gilian T. Thomas. Synthesis of pyridinium salts **2** were done by Matthew O. Pohl. Synthesis and optimization of bicyclobutane **1a** was done by Muskan Sharma. X-ray crystallography was done by Prof. Nathan D. Schley.

My contributions to this work are:

- High-throughput screening (Figures 4.1 and 4.2).
- ^{1}H NMR spectroscopy reaction monitoring (Figure 4.14).

- Control reactions (Figure 4.15 and Table 4.4).
- Synthesis of bicyclobutane **1a** and development of synthetic route to bicyclobutane **1e**
- Synthesis, purification and characterization of: **3a-3i**, **3m-3t**, **3v-3ab**, **4i**, **4q**, **4ab**, and **4o**
- Purification of cyclobutane **4m**.
- Section 4.9

4.1 Abstract

The synthesis of 3-azabicyclo[3.1.1]heptanes *via* a (3+3) cycloaddition of bicyclobutanes with pyridinium ylides is developed. The reaction proceeds diastereoselectively with dearomatization of the pyridinium ring to give dihydropyridine-containing azabicycloheptanes. High-throughput experimentation was used for reaction development and showed the reaction proceeds with base and without the need for a catalyst. The resulting ring-fused azabicyclo[3.1.1]heptanes have diverse synthetic handles for further transformations. Additionally, a photochemical rearrangement to a highly functionalized cyclobutane was demonstrated.

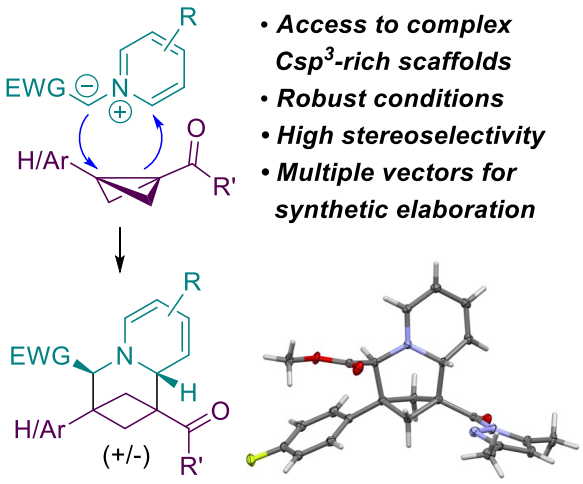

Figure 4.1: Synthesis of azabicycloheptanes from bicyclobutanes and pyridinium ylides.

4.2 Background

4.2.1 Bicycloheptane Bioisosteres

Expanding on the topic of bicyclic bioisosteres discussed in Chapter 1, bicyclo[3.1.1]-heptanes have been considered as bioisosteres for *meta*-substituted benzene rings. Structural studies on bicyclo[3.1.1]heptanes have revealed that they have similar geometry to *meta*-substituted benzene rings as shown in Figure 4.2.[83] However, current limitations of these motifs is the lack of synthetic routes available. For example, the first reported synthesis requires [3.1.1]propellane.[83;181]

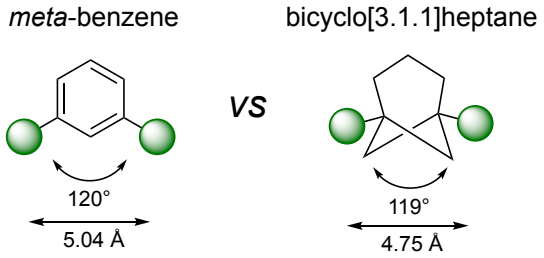

Figure 4.2: Geometries of bicyclo[3.1.1]heptanes compared to *meta*-substituted benzene rings.[83]

The bicyclo[3.1.1]heptane substituted derivatives of two drug analogues (Sonidegib, an anticancer drug; and URB597, an anti seizure drug) were synthesized and their biological activities and pharmacokinetic properties measured (Figure 4.3).[83] It was found that the solubility was retained while the membrane permeability and biological activities were improved for the bicycloheptane containing analogues.[83] These studies demonstrate the potential applications for bicycloheptanes as bioisosteres in future drug candidates.

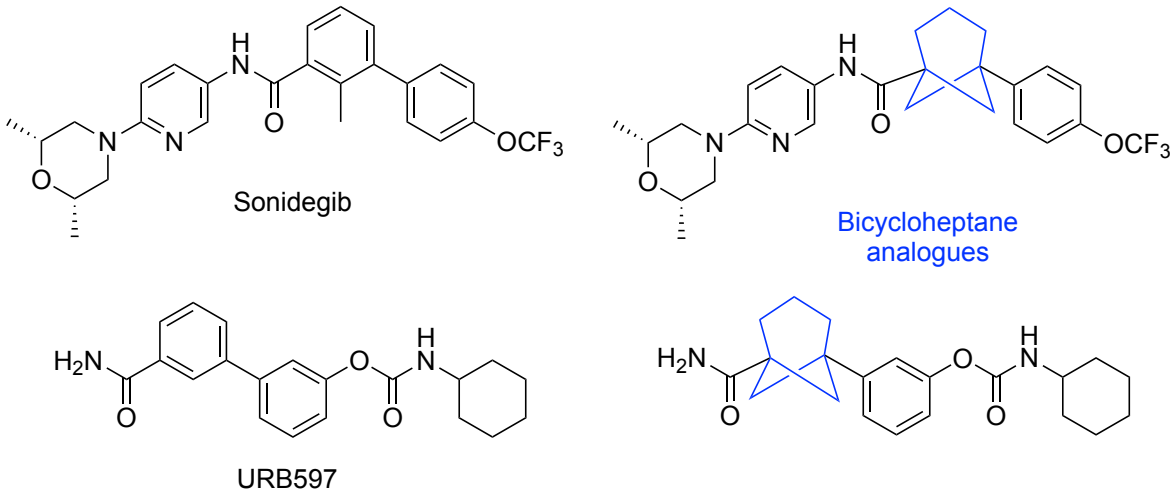

Figure 4.3: Bicyclo[3.1.1]heptane replacements in pharmaceuticals.[83]

4.2.2 Bicycloheptane Syntheses *via* Bicyclobutanes

In addition to the formal (3+2) additions to bicyclobutanes discussed earlier, bicyclobutanes have been shown to undergo formal (3+3) cycloadditions to form bicycloheptane structures. The first example of using a bicyclobutane to access a bicyclo[3.1.1]heptane was reported by Molander in 2022.[182] They reacted cyclopropanes with bicyclobutanes using photocatalysis with blue LEDs and an iridium photocatalyst (Figure 4.4).[182] This was followed shortly after by two more reactions of cyclopropanes with bicyclobutanes to form bicyclo[3.1.1]heptanes by Li and Waser (Figure 4.5).[183;184] Both reactions have similar substrate scope but use different conditions. The reactions developed use either a diboron/pyridine catalytic system or photocatalysis with an Ir catalyst and blue light.

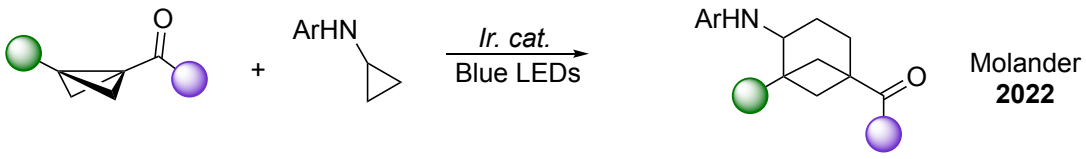

Figure 4.4: First synthesis of bicyclo[3.1.1]heptane from bicyclobutanes.[182]

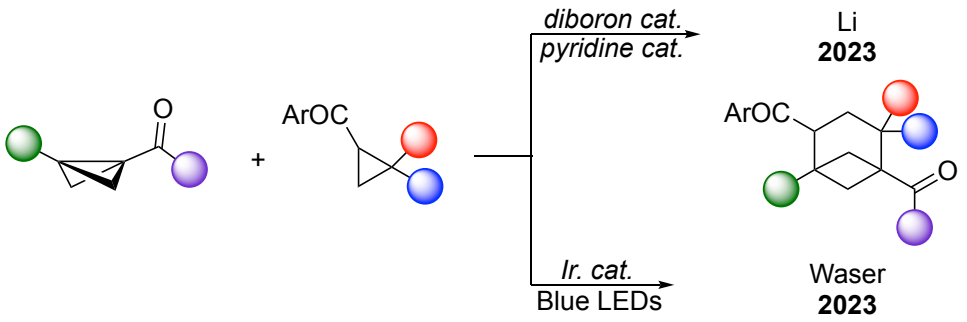

Figure 4.5: Additional syntheses of bicyclo[3.1.1]heptanes from bicyclobutane.[183;184]

Following these reports of routes to all-carbon bicycloheptanes, syntheses of heteroatom-containing bicycloheptanes have also emerged in the literature. Deng reported the synthesis of 2-oxa-3-azabicyclo[3.1.1]heptanes *via* a Lewis acid catalyzed nitrone cycloaddition with bicyclobutanes (Figure 4.6).[185] Later, two more syntheses were developed for 2-azabicyclo[3.1.1]heptenes using a diboron/pyridine catalytic system, or a titanium catalyst to afford a cycloaddition of vinyl azides with bicyclobutanes (Figure 4.6).[186;187]

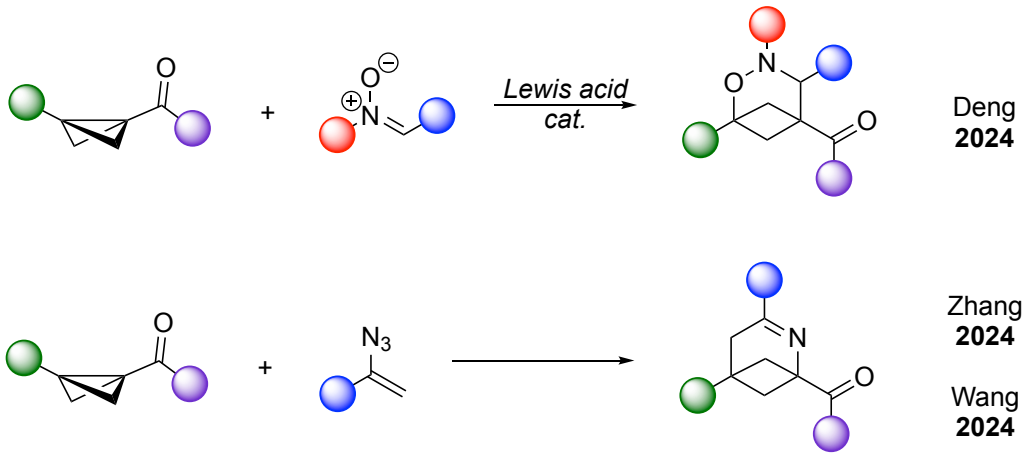

Figure 4.6: Syntheses of heteroatom-bicyclo[3.1.1]heptanes from bicyclobutane.[185–187]

The synthesis of 3-azabicyclo[3.1.1]heptanes has received a lot of attention recently. Mykhailiuk reported a synthesis of the 3-azabicyclo[3.1.1]heptane motif from an unexpected reduction of spirocyclic oxetanyl nitriles (Figure 4.7).[77] In addition to the synthesis of the azabicyclo[3.1.1]heptane derivatives, an analogue of Rupatadine, an antihistamine drug, was synthesized with the replacement of the pyridine with an azabicyclo[3.1.1]heptane (Figure 4.7).[77] The biological properties of this analogue were studied, with improved solubility,

metabolic stability and lipophilicity compared to Rupatadine. These results encourage the use of these motifs as bioisosteres in pharmaceuticals and the development of more synthetic routes to access these molecules. After this synthesis was reported, two more syntheses of azabicyclo[3.1.1]heptanes followed (Figure 4.7).[188;189] Both reactions are cycloadditions with bicyclobutane. The first reaction is a Lewis acid catalyzed cycloaddition with isocyanides,[188] and the second reaction is a copper catalyzed cycloaddition with imines (Figure 4.7).[189]

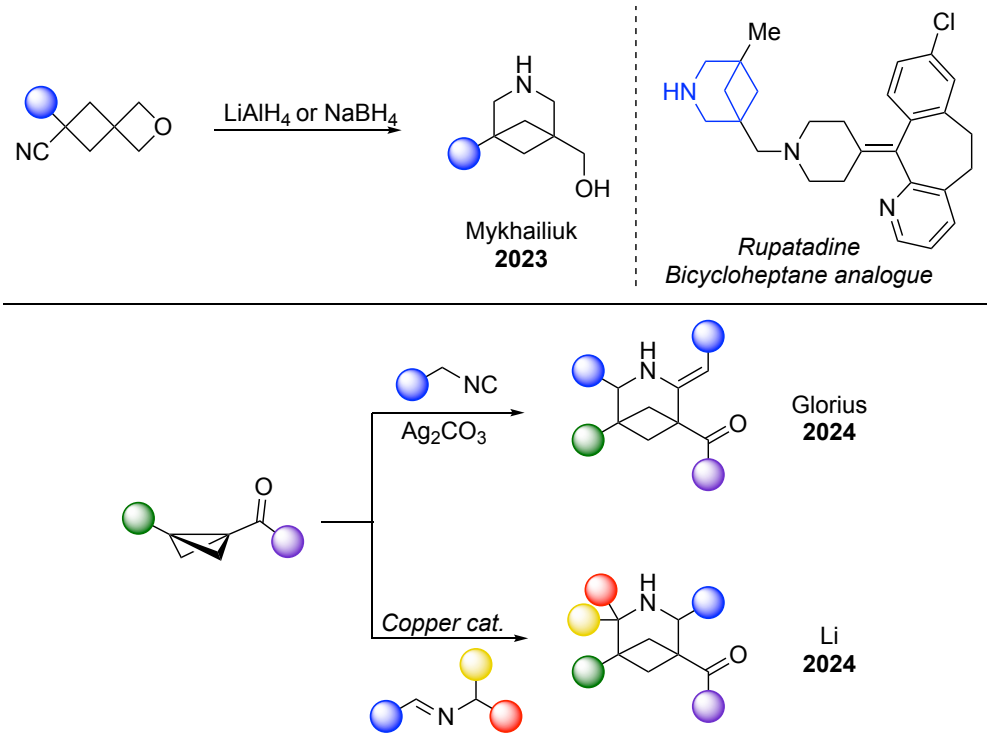

Figure 4.7: Recent syntheses of 3-azabicyclo[3.1.1]heptanes.[77;188;189]

4.2.3 Pyridinium Ylides

Pyridinium ylides are useful reagents for cycloaddition reactions and the synthesis of heterocycles.[190] These zwitterionic molecules have both a nucleophilic carbon and an electrophilic carbon adjacent to a positively charged nitrogen, making them ideal candidates for 1,3-dipolar cycloaddition reactions. The ylide is typically formed *in situ via* deprotonation of a pyridinium salt (Figure 4.8). An electron withdrawing group is typically present beside the nucleophilic carbon to help stabilize the ylide.

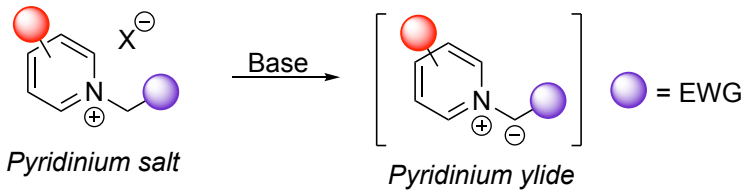

Figure 4.8: Preparation of pyridinium ylides from pyridinium salts.

Pyridinium ylides have been used for the synthesis of different heterocycles.[190] In these syntheses, the pyridine portion of the ylide can have two different roles in the reaction. The pyridinium ring can be incorporated in the product, or it can act as a leaving group. When the pyridine from the ylide is present in the product, the most commonly reported heterocycles formed after the cycloaddition are pyrroles, indolizines, and other azole derivatives (Figure 4.9). The synthesis of pyrroles has been done *via* a cycloaddition of the pyridinium ylide with azirines (Figure 4.10). For the indolizine synthesis, the pyridinium ylide will undergo a cycloaddition with an alkene or alkyne dipolarophile followed by oxidation to the indolizine (Figure 4.10).

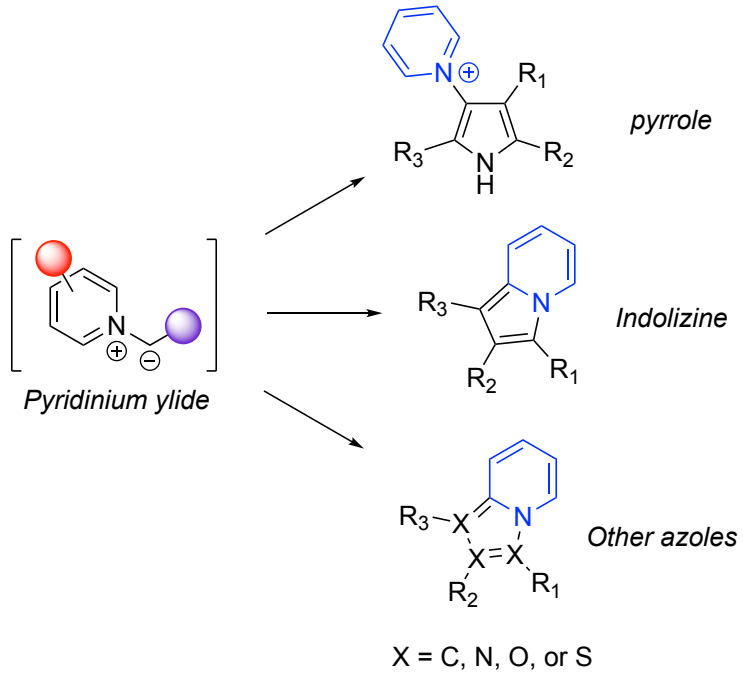

Figure 4.9: Examples of heterocycle syntheses from pyridinium ylide intermediates.

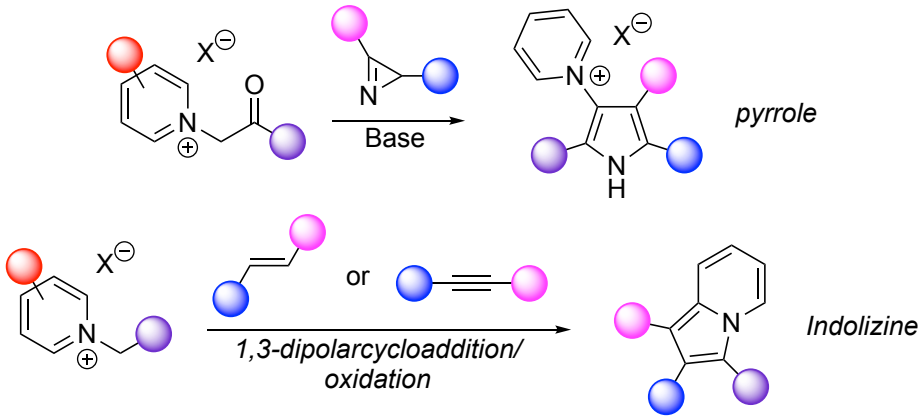

Figure 4.10: Synthesis of pyrroles and indolizines from pyridinium ylide cycloadditions.

The reactivity of the pyridinium ylide is influenced by the electron withdrawing group and the substitution on the pyridinium ring. The initial studies on pyridinium ylides used pK_a values of the corresponding pyridinium ions to determine the pyridinium nucleophilicities.[191;192] However, using pK_a to determine the nucleophilicity is not the best indicator for reactivity. Kinetic studies have been done with different pyridinium ylides towards reactivity with electrophiles.[193] Mayr developed a log scale to rank the reactivity of different pyridinium ylides with the electrophile quinone methide **3a** (Figure 4.11).[193] Changing both the electron withdrawing group and substitution on the pyridine led to large differences in observed reactivity.

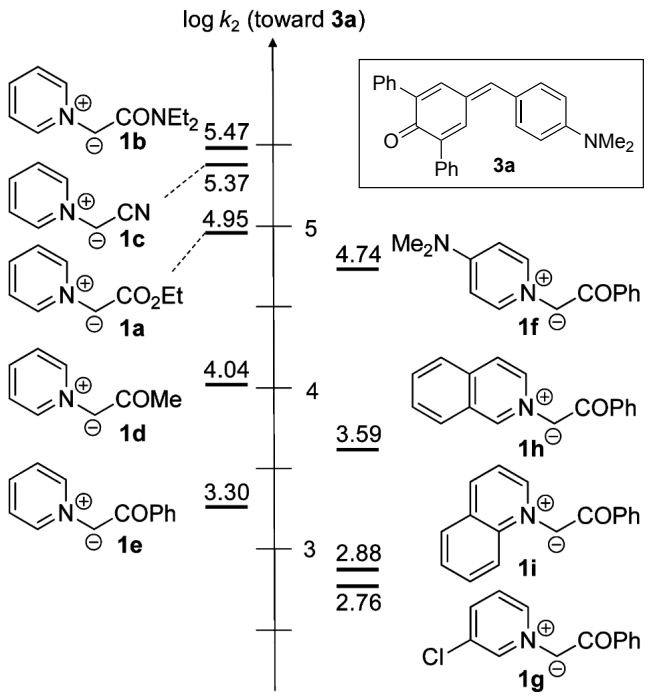

Figure 4.11: Reactivity scale for the reactions of ylides **1a-1i** with the quinone methide **3a** in DMSO at 20 °C. Reprinted (adapted) with permission from *J. Am. Chem. Soc.* **2013**, *135*, 15216–15224. Copyright {2024} American Chemical Society.[193]

4.2.4 Proposed Reactivity of Pyridinium Ylides with Bicyclobutanes

With the established reactivity of bicyclobutanes and pyridinium ylides in mind, we hypothesized that azabicycloheptanes could be formed *via* a formal (3+3) cycloaddition reaction (Figure 4.12). A pyridinium ylide could undergo nucleophilic attack to the electrophilic site of a bicyclobutane. Then, the resulting bicyclobutane enolate would attack the electrophilic carbon of the pyridinium group. This would result in dearomatization of the pyridinium ring and formation of a 3-azabicyclo[3.1.1]heptane with a fused dihydropyridine ring (Figure 4.12). The development of this reactivity will be discussed below.

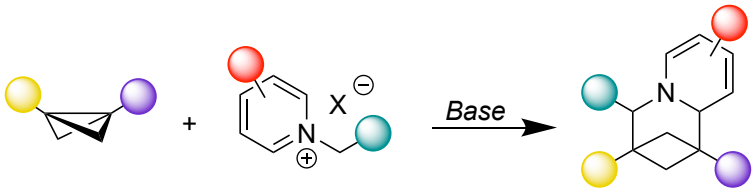

Figure 4.12: Proposed cycloaddition of pyridinium ylides with bicyclobutanes.

4.3 Reaction Optimization

4.3.1 High-Throughput Screening

Initial reaction discovery was explored using microscale high-throughput experimentation and the results were analyzed by ^{1}H NMR spectroscopy (See Section C.2). We hypothesized that deprotonation of the pyridinium **2a** with base to form the ylide, combined with Lewis acid activation of the bicyclobutane **1a** would form the azabicycloheptane **3a**. To investigate this reactivity, a multivariate array of 12 Lewis acids, 4 bases and two solvents were screened at 60 °C for a 96-well screen (Table 4.1). We observed that four Lewis acids (LiOTf, $Mg(OTf)_2$, $Zn(OTf)_2$, and AgOTf) gave the highest amounts of **3a**, with diastereomeric ratios (d.r.) ranging from 1:1-4:1. Using triethylamine as an organic based showed little to no reactivity, whereas inorganic bases were broadly similar; overall, Cs_2CO_3 and K_3PO_4 were superior. Product yields or diastereomeric ratios did not seem to be affected by the solvent.

Based on the results from the 96-well screen, a more focused 30-well screen was conducted at room temperature selecting the best four Lewis acids (LiOTf, $Mg(OTf)_2$, $Zn(OTf)_2$, and AgOTf,) two bases (Cs_2CO_2 and K_3PO_4) and the two solvents (THF and MeCN) (Table 4.2). In addition, the conditions were tested without the addition of a Lewis acid to determine the effect on the reaction outcome. We observed that running the reaction at room temperature did not decrease the yields. While the diastereoselectivity in THF remained low, in acetonitrile we only observed the formation of a single diastereomer in all cases. In addition, it was determined that the use of a Lewis acid is not required for this transformation, and in some cases it even caused a drop in yield. Overall, K_3PO_4 as a base with no Lewis acid in acetonitrile gave the highest yield of 86%, with **3a** formed as a single diastereomer.

Table 4.1: 96-well HTE optimization of pyridinium ylide addition to bicyclobutane

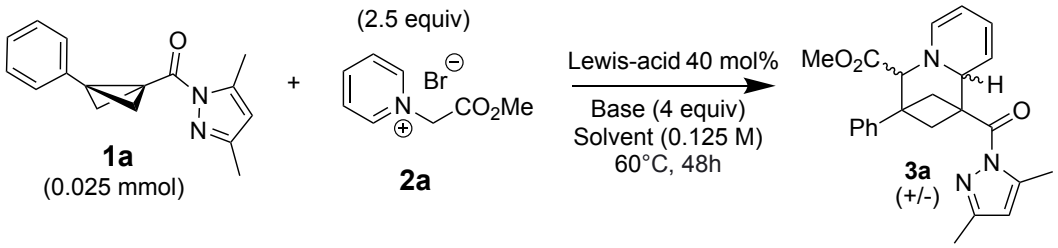

3a % Yield		THF				MeCN			
		K_2CO_3	Cs_2CO_3	K_3PO_4	NEt_3	K_2CO_3	Cs_2CO_3	K_3PO_4	NEt_3
		1	2	3	4	5	6	7	8
LiOTf	A	51%	65%	56%	14%	34%	53%	45%	0%
$Mg(OTf)_2$	B	44%	53%	56%	1%	0%	53%	55%	0%
$Sc(OTf)_3$	C	2%	14%	6%	0%	3%	0%	0%	0%
$Fe(OTf)_3$	D	0%	0%	0%	0%	0%	0%	0%	0%
$Zn(OTf)_2$	E	8%	53%	51%	3%	15%	11%	0%	0%
$Ga(OTf)_3$	F	0%	0%	0%	0%	0%	8%	0%	0%
AgOTf	G	31%	45%	35%	0%	23%	30%	28%	0%
$Sn(OTf)_2$	H	4%	5%	0%	0%	0%	0%	0%	0%
$La(OTf)_3$	I	0%	0%	2%	0%	0%	0%	0%	0%
$Eu(OTf)_3$	J	0%	4%	0%	0%	0%	0%	0%	0%
$Yb(OTf)_3$	K	0%	0%	0%	0%	0%	0%	0%	0%
$Bi(OTf)_3$	L	0%	0%	0%	0%	0%	0%	0%	0%
Diastereomeric Ratio (d.r.)		THF				MeCN			
		K_2CO_3	Cs_2CO_3	K_3PO_4	NEt_3	K_2CO_3	Cs_2CO_3	K_3PO_4	NEt_3
		1	2	3	4	5	6	7	8
LiOTf	A	4.1 : 1	3.1 : 1	4.6 : 1	1.8 : 1	3.9 : 1	3.4 : 1	3.5 : 1	-
$Mg(OTf)_2$	B	3.4 : 1	1.2 : 1	1.7 : 1	>20 : 1	-	3.4 : 1	4.0 : 1	-
$Sc(OTf)_3$	C	>20 : 1	1.3 : 1	>20 : 1	-	>20 : 1	-	-	-
$Fe(OTf)_3$	D	-	-	-	-	-	-	-	-
$Zn(OTf)_2$	E	7.0 :1	1.8 : 1	2.4 : 1	2.0 : 1	2.0 : 1	1.8 : 1	-	-
$Ga(OTf)_3$	F	>20 : 1	-	-	-	-	>20 : 1	-	-
AgOTf	G	3.4 : 1	2.0 : 1	4.8 : 1	-	1.9 : 1	2.3 : 1	2.5 : 1	-
$Sn(OTf)_2$	H	>20 : 1	>20 : 1	-	-	-	-	-	-
$La(OTf)_3$	I	-	-	>20 : 1	-	-	-	-	-
$Eu(OTf)_3$	J	-	>20 : 1	-	-	-	-	-	-
$Yb(OTf)_3$	K	-	-	-	-	-	-	-	-
$Bi(OTf)_3$	L	-	-	-	-	-	-	-	-
1a % Remaining		THF				MeCN			
		K_2CO_3	Cs_2CO_3	K_3PO_4	NEt_3	K_2CO_3	Cs_2CO_3	K_3PO_4	NEt_3
		1	2	3	4	5	6	7	8
LiOTf	A	0%	0%	1%	50%	0%	7%	3%	4%
$Mg(OTf)_2$	B	0%	5%	1%	0%	0%	0%	0%	0%
$Sc(OTf)_3$	C	0%	1%	2%	25%	0%	0%	0%	0%
$Fe(OTf)_3$	D	0%	0%	0%	0%	0%	0%	0%	0%
$Zn(OTf)_2$	E	35%	7%	3%	1%	38%	13%	7%	44%
$Ga(OTf)_3$	F	0%	0%	0%	0%	0%	0%	0%	0%
AgOTf	G	0%	21%	0%	0%	0%	0%	0%	0%
$Sn(OTf)_2$	H	0%	12%	0%	0%	0%	0%	0%	0%
$La(OTf)_3$	I	3%	8%	5%	4%	0%	0%	0%	4%
$Eu(OTf)_3$	J	0%	6%	16%	36%	0%	0%	0%	0%
$Yb(OTf)_3$	K	0%	3%	5%	0%	0%	0%	0%	70%
$Bi(OTf)_3$	L	0%	0%	0%	0%	0%	1%	0%	0%

Yields and d.r. values are obtained by ^{1}H NMR spectroscopy by relative integration vs. internal standard, 1,3,5-trimethoxybenzene (See Section C.2)

Table 4.2: 30-well HTE optimization of pyridinium ylide addition to bicyclobutane

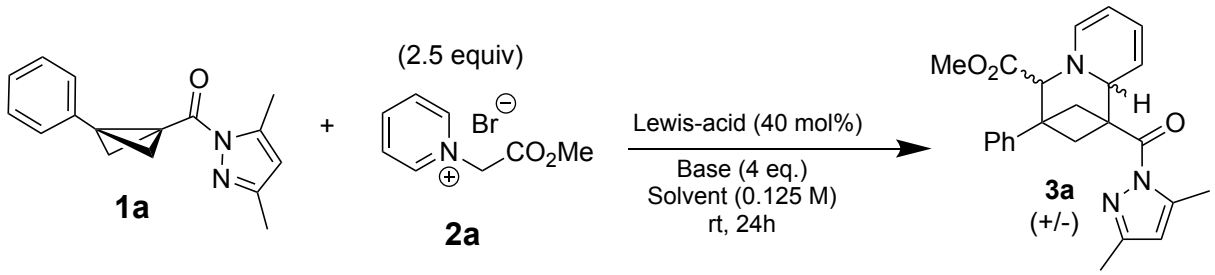

3a % Yield		THF			MeCN		
		Cs_2CO_3	K_3PO_4	NEt_3	Cs_2CO_3	K_3PO_4	NEt_3
		1	2	3	4	5	6
LiOTf	A	57%	46%	0%	57%	30%	0%
$Mg(OTf)_2$	B	**61%**	38%	0%	56%	**82%**	6%
$Zn(OTf)_2$	C	52%	25%	0%	**65%**	50%	0%
AgOTf	D	31%	**68%**	0%	**64%**	36%	0%
none	E	**69%**	**70%**	0%	**73%**	**86%**	0%

Diastereomeric Ratio (d.r.)		THF			MeCN		
		Cs_2CO_3	K_3PO_4	NEt_3	Cs_2CO_3	K_3PO_4	NEt_3
		1	2	3	4	5	6
LiOTf	A	2.4 : 1	5.6 : 1	-	>20 : 1	>20 : 1	-
$Mg(OTf)_2$	B	3.1 : 1	2.8 : 1	-	>20 : 1	>20 : 1	>20 : 1
$Zn(OTf)_2$	C	4.8 : 1	4.0 : 1	-	>20 : 1	>20 : 1	-
AgOTf	D	3.4 : 1	8.7 : 1	-	>20 : 1	>20 : 1	-
none	E	1.1 : 1	1.6 : 1	-	>20 : 1	>20 : 1	-

1a % Remaining		THF			MeCN		
		Cs_2CO_3	K_3PO_4	NEt_3	Cs_2CO_3	K_3PO_4	NEt_3
		1	2	3	4	5	6
LiOTf	A	15%	37%	90%	15%	3%	>99%
$Mg(OTf)_2$	B	17%	50%	81%	0%	0%	74%
$Zn(OTf)_2$	C	24%	60%	80%	3%	6%	58%
AgOTf	D	32%	18%	94%	5%	16%	68%
none	E	3%	3%	>99%	3%	3%	70%

Yields and d.r. values are obtained by ^{1}H NMR spectroscopy by relative integration vs. internal standard, 1,3,5-trimethoxybenzene (See Section C.2)

4.3.2 Full Factorial Analysis

The best screening conditions were carried forward into a full factorial screen to optimize the reagent loading and reaction concentration (Table 4.3). Overall, increasing or decreasing the equivalents of base, equivalents of pyridinium or reaction concentration did not have a significant effect on the yield of the reaction, which ranged from 65-76%. These results indicate that the reaction is quite robust to changes in reagent loading and concentration. Based on these data, the lower reagent/base loading (1.25 equiv pyridinium and 2.5 equiv base) and higher concentration (0.25 M) were chosen to carry forward. These conditions gave a yield of 75%, while requiring less starting materials and solvent quantities. The resulting yields of **3a** observed for this screening were plotted for visualization and shown in Figure 4.13.

Table 4.3: Full factorial screening for reagent loading and concentration

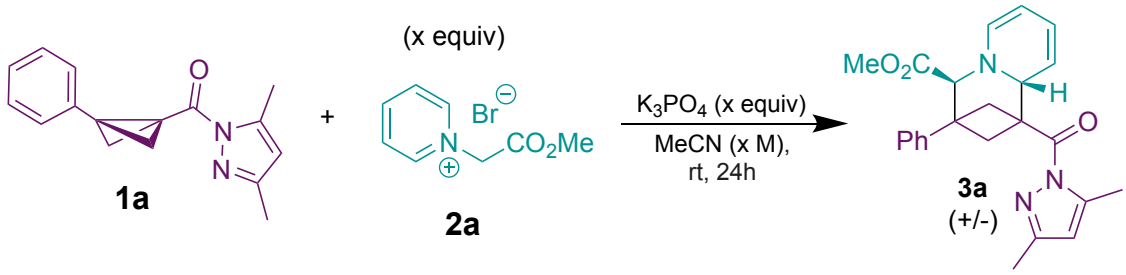

Entry	Base Loading (equiv)	Concentration (M)	Pyridinium **2a** (equiv)	Yield **3a** (%)	Leftover **1a** (%)
1	1.25	0.125	1.25	65	16
2	2.50	0.125	1.25	71	6
3	1.25	0.250	1.25	73	13
4	2.50	0.250	1.25	75	<5
5	1.25	0.125	0.250	70	16
6	2.50	0.125	0.250	75	<5
7	1.25	0.250	0.250	74	<5
8	2.50	0.250	0.250	75	<5
9	1.88	0.188	1.88	76	<5

Yields and d.r. values are obtained by ^{1}H NMR spectroscopy by relative integration vs. internal standard, 1,3,5-trimethoxybenzene

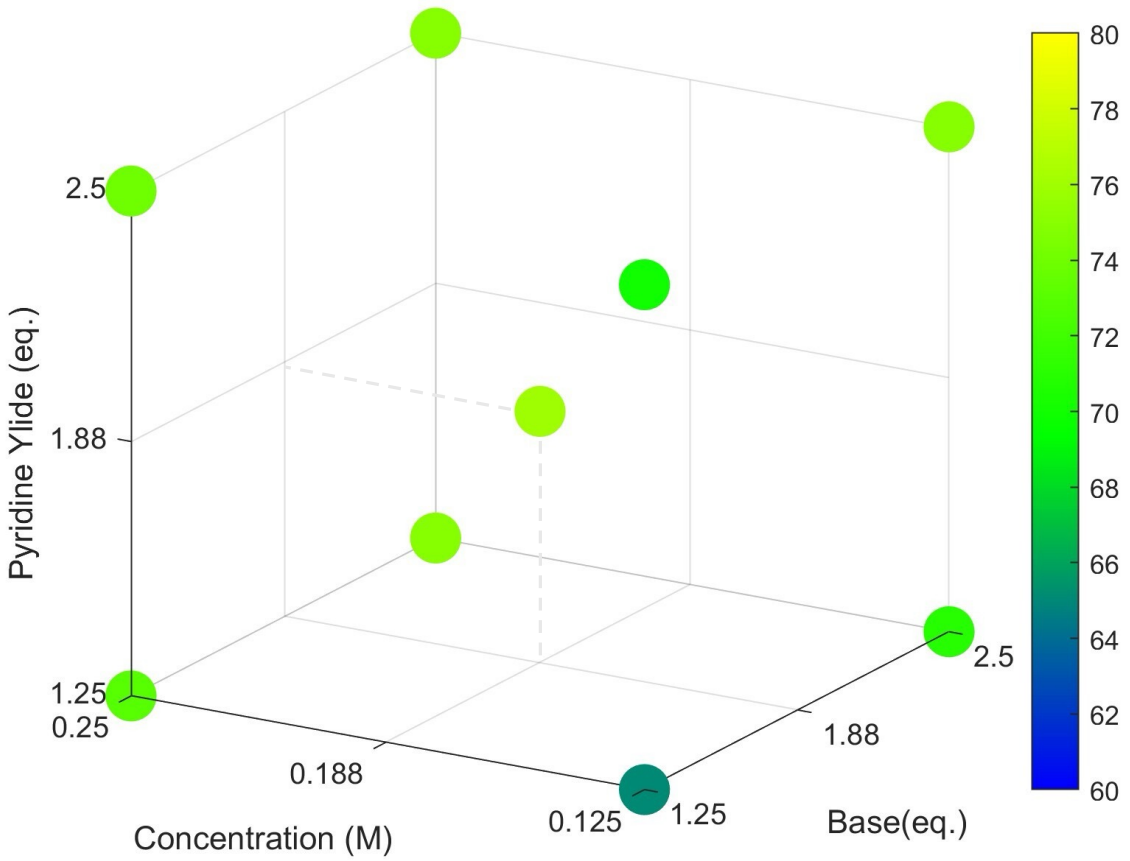

Figure 4.13: Visualization of **3a**% yield for full factorial screening.

4.3.3 Reaction Monitoring by ^{1}H NMR Spectroscopy

The reaction progress was monitored by ^{1}H NMR spectroscopy to assess mass balance and stereoselectivity as a function of time (Figure 4.14). We observed the formation of **3a** to occur quite quickly with a 30% solution yield after 15 minutes. Throughout the course of reaction monitoring, we observed no clear intermediates, and no evidence of the minor diastereomer being formed. Tracking the mass balance further supports these observations, with the %**1a** + %**3a** averaging 93% with a standard deviation of only 2% (excluding t = 0). The reaction conversion was complete at ∼4 h and remained steady until 5.5 h.

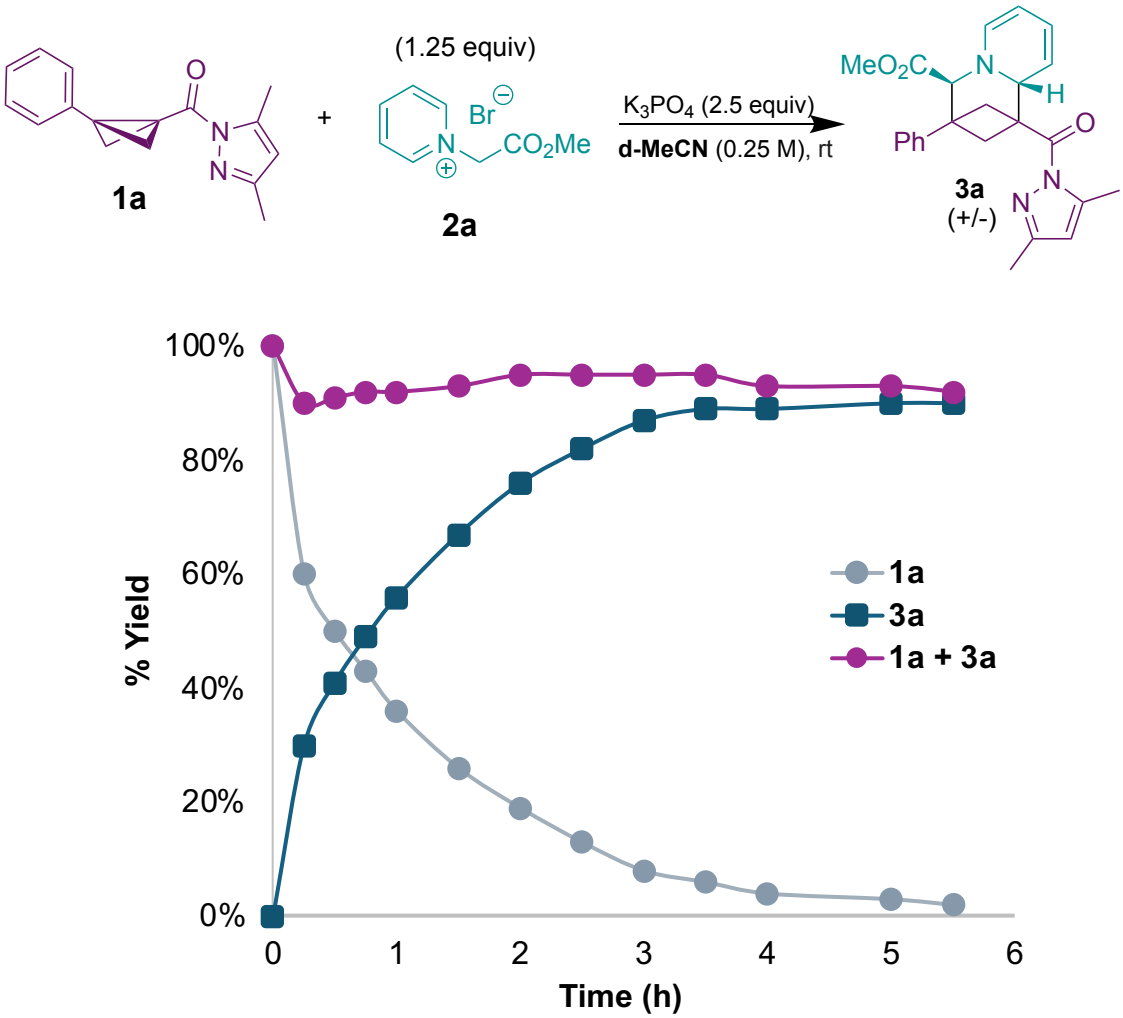

Figure 4.14: Reaction progress plot, with % yield determined by ^{1}H NMR spectroscopy (integration versus internal standard, 1,3,5-trimethoxybenzene).

4.3.4 Control Reactions

To investigate the origin of the diastereoslectivity, the possibility of product epimerization under the reaction conditions was explored. A nearly 1:1 diastereomeric mixture of product **3a** was isolated using THF as the reaction solvent. This mixture of diastereomers was then subjected to the reaction conditions (K_3PO_4 in MeCN, rt, 24 h) and no change in the diastereomeric ratio was observed (Figure 4.15). This indicates that the observed diastereoselectivity is due to kinetic control, rather than thermodynamic control.

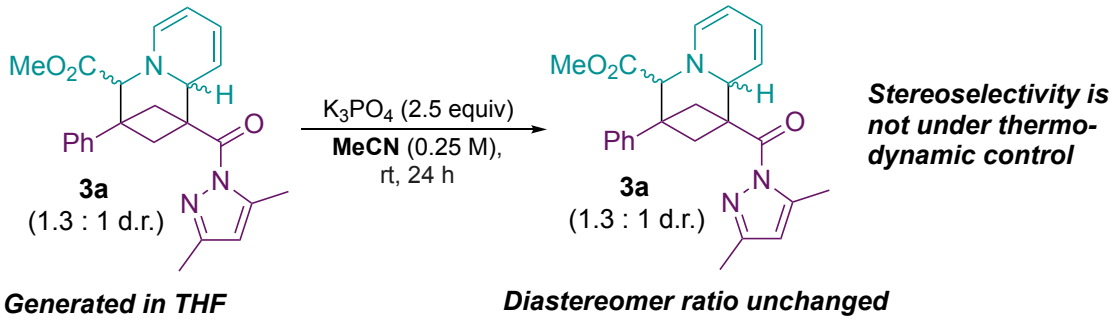

Figure 4.15: Test for control of diastereoselectivity *via* epimerization of **3a** under the optimized conditions

With the optimized conditions determined, a set of control reactions were carried out (Table 4.4). When no base is used, 84% of the bicyclobutane **1a** is retained (Entry 1) and no product is observed. With the reaction run at 30 ^{o}C or with the addition of 10 equiv water (from $Na_2SO_4{\cdot}10H_2O$), no significant change to the reaction yield is observed (Entries 2 and 3). When 4 Å molecular sieves are added, a drop in product yield to 66% is observed (Entry 4). This may be due to inefficient mixing occurring due to the addition of more insoluble material to the reaction. Overall, the reaction is insensitive to oxygen, water and slight changes to the reaction temperature, further demonstrating its robustness.

Table 4.4: Control reactions for the synthesis of **3a** with optimized conditions.

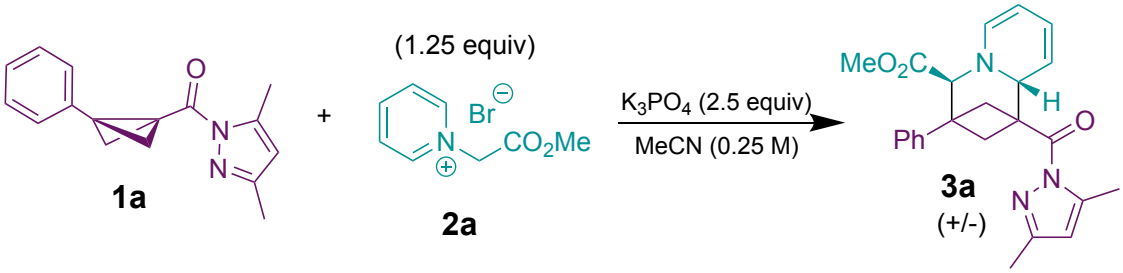

Entry	Deviation from standard[a]	**3a**[b][c]	**1a**[b]
1	No K_3PO_4 added	0	84
2	Run at 30 °C	81	5
3	$Na_2SO_4{\cdot}10H_2O$ (1 equiv)	81	6
4	4 Å molecular sieves	66	12

[a]Unless otherwise notes, reactions are performed at room temperature for 24 hours with 0.05 mmol of **1a**. [b]Amounts of **1a** and **3a** are obtained by ^{1}H NMR spectroscopy by relative integration vs. internal standard, 1,3,5-trimethoxybenzene (TMB). [c]Only one diastereomer of **3a** is observed.

4.4 Bicyclobutane Synthesis

To explore the scope of the pyridinium addition, a library of bicyclobutanes was synthesized. Ketone bicyclobutane derivatives and the disubstituted pyrazole bicyclobutane derivatives were prepared according to previously reported literature conditions (Figure 4.16).[126;132]

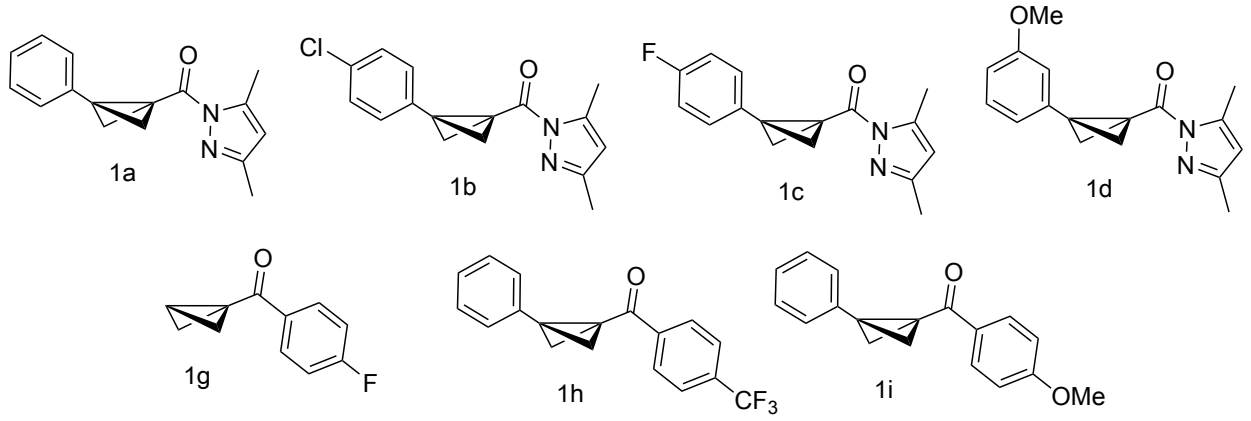

Figure 4.16: Bicyclobutanes synthesized according to literature procedures.[126;132]

Additionally, we developed the synthesis of a new, unreported monosubstituted bicyclobutane **1e** with the 3,5-dimethyl *N*-acylpyrazole electron withdrawing group (Figure 4.17). Starting from 3-oxocyclobutanecarboxylic acid, acid-catalyzed esterification to the methyl ester **I** was done in methanol, followed by reduction of the ketone to the alcohol **II** using $NaBH_4$. The hydroxyl group was then converted to a tosyl leaving group using *p*-toluenesulfonyl chloride, triethylamine, and NMI as an additive. The methyl ester from compound **III** was then hydrolyzed using sodium hydroxide followed by amidation using CDI to install the 3,5-dimethylpyrazole amide and give compound **V**. This intermediate was then converted to the bicyclobutane using potassium *tert*-butoxide as a base at −78 °C to obtain the final bicyclobutane **1e**. This bicyclobutane is prone to polymerization upon formation; therefore, precautions were taken during the synthesis and work-up to prevent this from occurring (see experimental details in Appendix C). Additionally, for long-term storage, the bicyclobutane was stored as a frozen stock solution in acetonitrile at −80 °C.

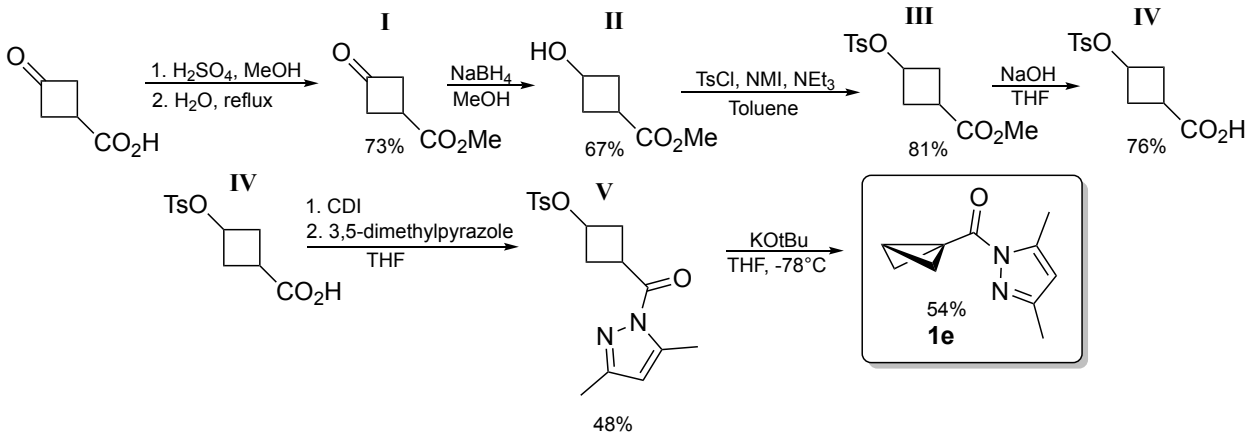

Figure 4.17: Synthetic route developed for novel monosubstituted pyrazole bicyclobutane **1e**.

4.5 Azabicycloheptane Scope

The reaction scope was explored using a diverse set of bicyclobutanes and pyridinium salts. Initial attempts at isolation of the products showed that the dihydropyridine-containing products were not stable to silica gel chromatography. Alternatively, the products were isolated using basic alumina following evaporation of the reaction solvent and using re-solubilization with DCM. DCM was used as the mobile phase to pass the products through the basic alumina plugs. Using this method, the first product **3a** was isolated on a 0.30 mmol scale with a 88% yield and on a 2.0 mmol scale with a 66% isolated yield (Figure 4.18). Following isolation, the products obtained are stable in their respective physical state.

4.5.1 Diversification of Bicyclobutanes

The scope of the bicyclobutane was investigated (Figure 4.18). Aryl groups with both electron donating and electron withdrawing groups worked well, giving products **3b**, **3c** and **3d** with modest yields. Additionally, single crystals of **3c** were obtained and the stereochemistry was confirmed using X-ray diffraction analysis. Importantly, both disubstituted and monosubstituted bicyclobutanes are compatible with this reactivity, which is relatively rare in the literature. Using the monosubstituted bicyclobutane **1e** discussed earlier with both the methyl ester pyridinium **2a** and a ketone-based pyridinium gave products **3e** and **3f** respectively. Product **3f** was obtained as a 6:1 mixture of diastereomers. Further, both mono and disubstituted aryl ketone bicyclobutanes also react with this chemistry, giving products **3g**, **3h** and **3i**. Unfortunately, other bicyclobutanes with weaker electron withdrawing groups (e.g. esters and amides) do not react under these conditions.

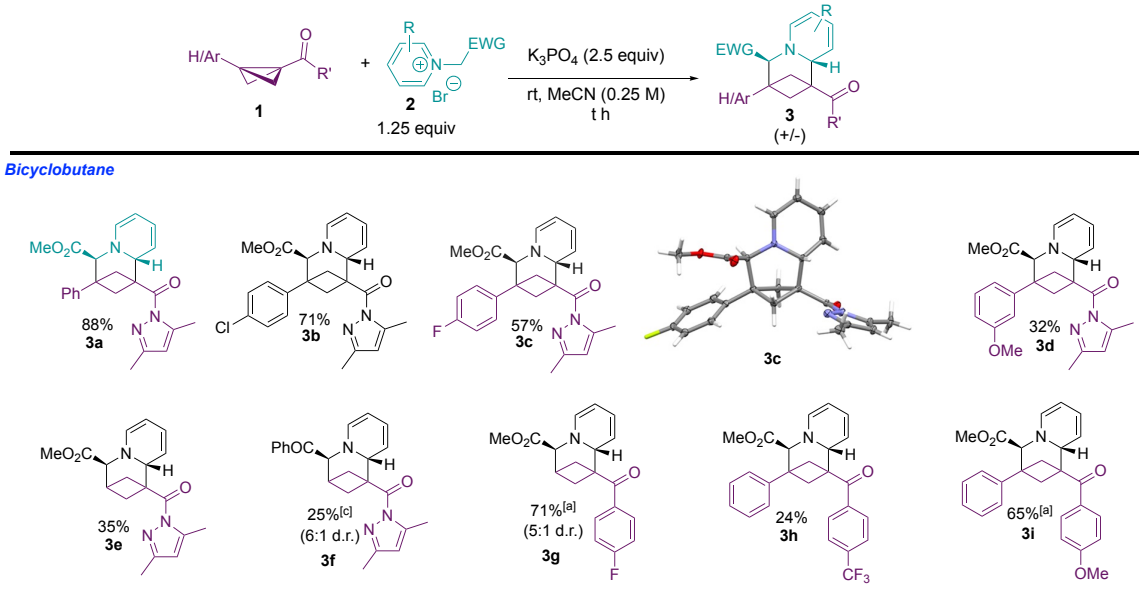

Figure 4.18: Scope of azabicyclo[3.1.1]heptanes **3** *via* pyridinium ylide addition to bicyclobutanes - bicyclobutane derivatives. Yields are for isolated compounds following a basic alumina plug purification and are obtained as a single diastereomer unless otherwise noted with d.r. values in parentheses (determined by ^{1}H NMR spectroscopy). Single crystal XRD structures are deposited with the CCDC: 2374388. [a]Yield determined by ^{1}H NMR spectroscopy (with internal standard 1,3,5-trimethoxybenzene).[c]Reaction performed using $NaPF_6$ (1.3 equiv) as an additive.

4.5.2 Diversification of Pyridinium Ring

The effect of substitution on the pyridine ring of the pyridinium salts was also investigated (Figure 4.19). We observed that substitution on the pyridine greatly affected the reactivity. Using 4-phenyl and 4-methyl pyridiniums we were able to isolate products **3j** and **3k** with 63% and 57% yields respectively; however when using a 4-CF_3 pyridinium, only a 7% solution yield was observed with mostly unreacted bicyclobutane remaining. Based on previous reactivity of pyridinium ylides and the effects observed with solvent and base combinations,[194;195] we tested the use of a protic solvent to try and increase the reactivity. With methanol as a solvent, the cycloaddition reaction was achieved in addition to methanolysis of the *N*-acylprazole to give product **3l-OMe** with a 60% yield (with 15% of unreacted bicyclobutane methyl-ester co-eluting during isolation). Since the ester bicyclobutane derivatives are unreactive with this chemistry, we hypothesize that the cyclization occurs more rapidly than the methanolysis.

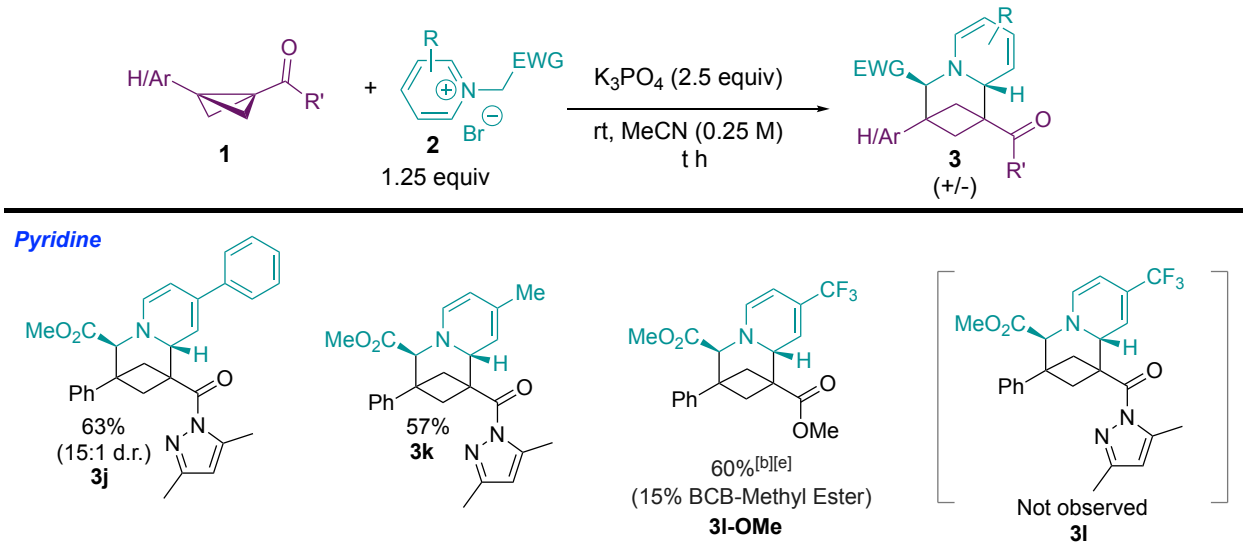

Figure 4.19: Scope of azabicyclo[3.1.1]heptanes **3** *via* pyridinium ylide addition to bicyclobutanes - pyridinium ring derivatives. Yields are for isolated compounds following a basic alumina plug purification and are obtained as a single diastereomer unless otherwise noted with d.r. values in parentheses (determined by ^{1}H NMR spectroscopy). [b]Isolated yield as part of a mixture with unreacted bicyclobutane starting material. [e]Reaction performed with methanol as the solvent.

4.5.3 Diversification of Pyridinium Ester Functional Group

In general, ester-based pyridinium ylides are the most compatible substrates for this chemistry (**3p**-**3v**) (Figure 4.20). Primary (**3q**, **3s**), secondary (**3t**, **3u**, **3v**), and even tertiary (**3r**) substituents at oxygen are viable. Additionally, a highly substituted lactone is successful in this reaction to give product **3p**. Notably, this derivative is formed as a nearly 1:1 mixture of diastereomers. Chiral esters were used to obtain products **3t** and **3v**, though they do not induce any significant stereocontrol over the absolute stereochemistry of the resulting products. The d.r. values reported reflect the ratio between the two different *anti* diastereomers of the product.

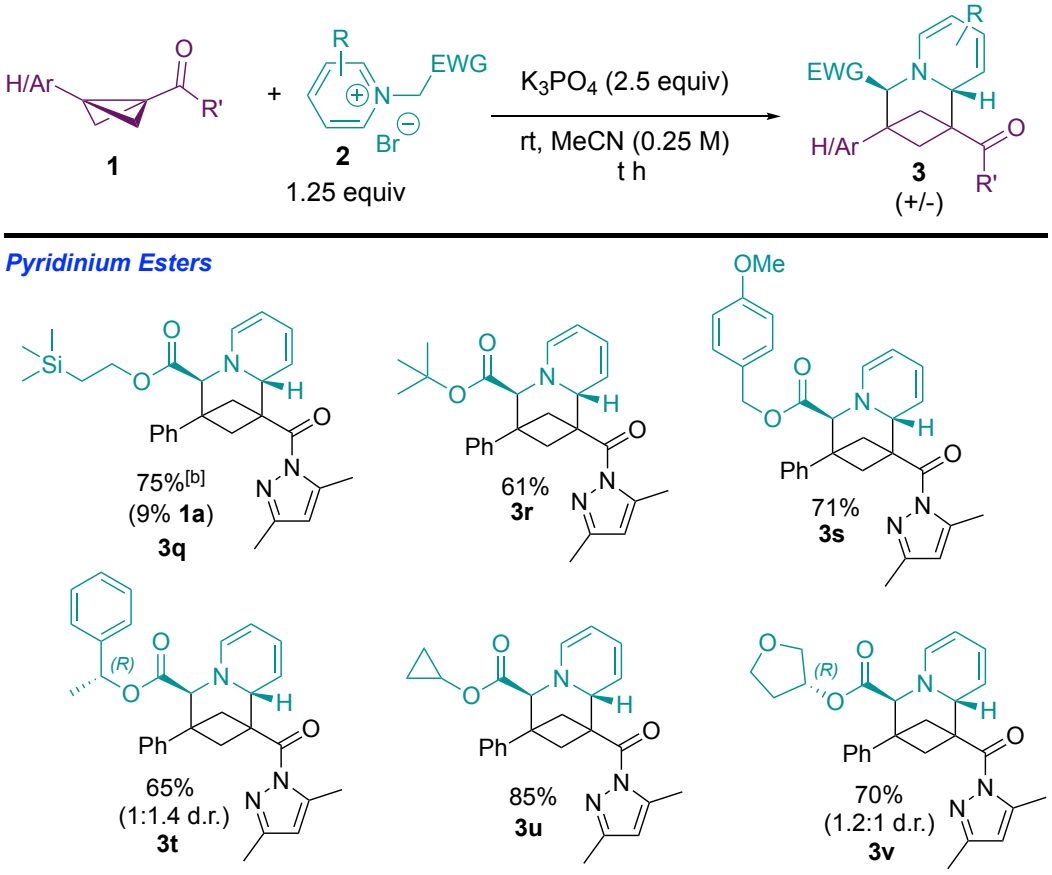

Figure 4.20: Scope of azabicyclo[3.1.1]heptanes **3** *via* pyridinium ylide addition to bicyclobutanes - pyridinium ester derivatives. Yields are for isolated compounds following a basic alumina plug purification and are obtained as a single diastereomer unless otherwise noted with d.r. values in parentheses (determined by ^{1}H NMR spectroscopy) [b]Isolated yield as part of a mixture with unreacted bicyclobutane starting material.

4.5.4 Diversification of Pyridinium EWG

Different electron withdrawing groups on the pyridinium ylide were also explored (Figure 4.21). Both amide and nitrile electron withdrawing groups are successful, giving products **2n** and **3o** respectively. The ketone containing electron withdrawing group to give product **3m** initially showed low conversion, so $Mg(OTf)_2$ was tested as a catalyst based on its reactivity in the screening experiments (Figure 2.7). This improved the solution yield to 80%. The low solubility of $Mg(OTf)_2$ in acetonitrile led us to consider the possibility of salt metathesis rather than Lewis acid catalysis as a possible cause for the improved yield. To test this, $NaPF_6$ was used as an additive. If salt-metathesis occurs, the resulting NaBr would be almost completely insoluble in acetonitrile, leaving only the hexafluorophosphate pyridinium salt in solution. Using 1.3 equiv of $NaPF_6$ allowed formation of product **3m** with an isolated yield of 75%, supporting the salt-metathesis hypothesis. This method was used for all ketone-based pyridinium ylides where both (hetero)aryl and alkyl ketones were suitable (**3w-3ab**). This includes the cyclopropyl ketone resulting in **3aa** in 75% isolated yield. In all cases, we observe a single diastereomer, except for the *tert*-butyl-substituted ketone product **3ab**. This product is generated as a mixture of diastereomers and does contain additional impurities after alumina treatment. However, the fact that such a sterically-encumbered ylide can still undergo cycloaddition to some degree is notable.

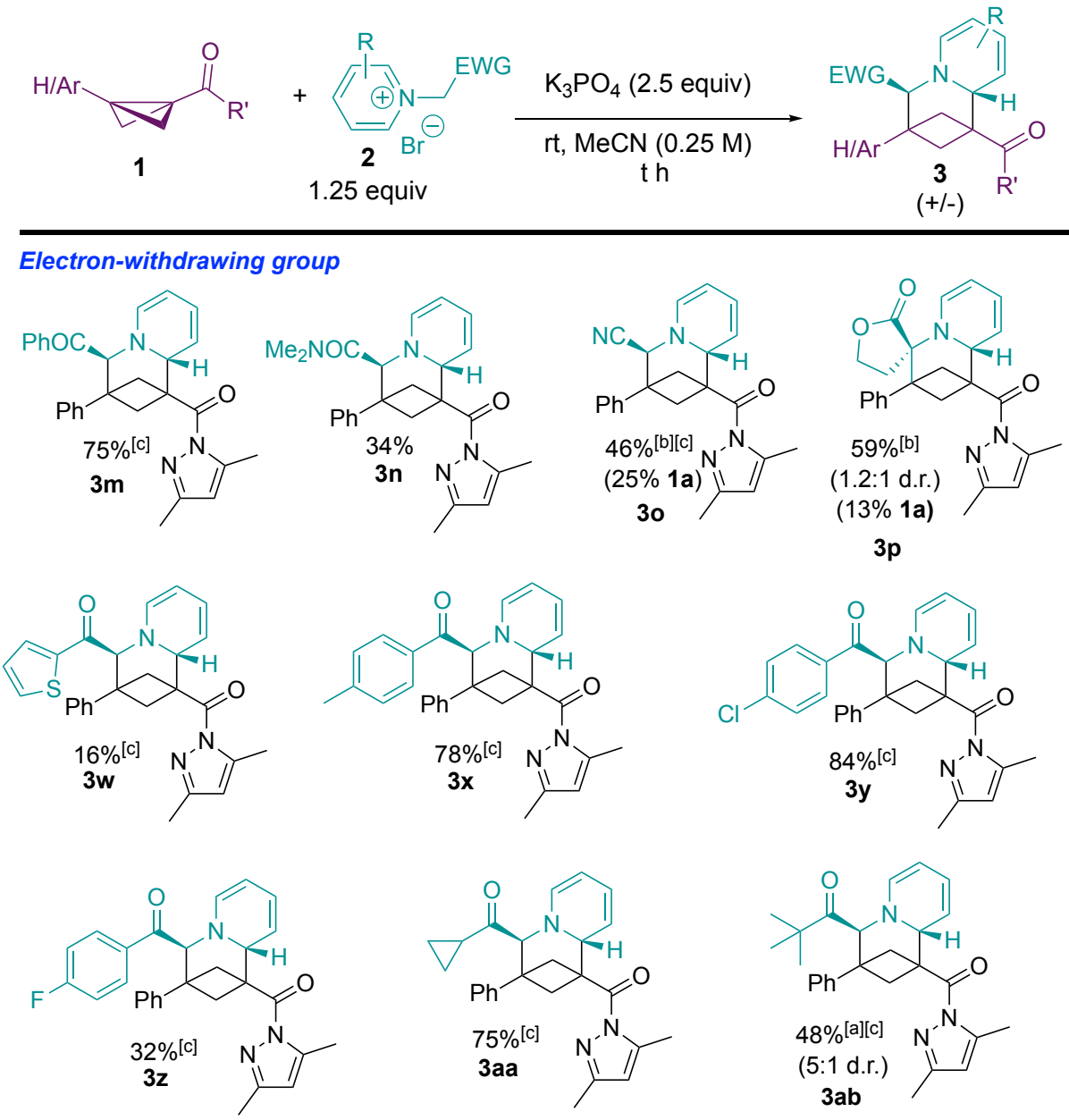

Figure 4.21: Scope of azabicyclo[3.1.1]heptanes **3** *via* pyridinium ylide addition to bicyclobutanes - pyridinium EWG derivatives. Yields are for isolated compounds following a basic alumina plug purification and are obtained as a single diastereomer unless otherwise noted with d.r. values in parentheses (determined by ^{1}H NMR spectroscopy). [a]Yield determined by ^{1}H NMR spectroscopy (with internal standard 1,3,5-trimethoxybenzene).[b]Isolated yield as part of a mixture with unreacted bicyclobutane starting material. [c]Reaction performed using $NaPF_6$ (1.3 equiv) as an additive.

4.6 Additional Synthetic Transformations

Additional transformations of the azabicyclo[3.1.1]heptane products were demonstrated. On a 1-gram scale synthesis, the prototype reaction of bicyclobutane **1a** and **2a** to generate **3a** was performed. This was followed by an *in situ* methanolysis using methanol and additional base to generate the methyl ester product **4a** *via* a telescoped synthesis with a 71% isolated yield (Figure 4.22-A). Following isolation of **4a**, reduction of the dihydropyridine was done using sodium cyanoborohydride ($NaBH_3CN$) and acetic acid in methanol to give compound **4b** with a 58% purified yield (Figure 4.22-B). Significantly, this compound is stable to silica-column chromatography and X-ray crystallography was used to confirm its structure. Based on literature precedent,[196] we subjected the ketone pyridinium product **3m** to blue light (470 nm) where it underwent a rearrangement reaction (aza-Norrish type II) *via* C-N cleavage and hydrogen atom transfer to form a highly functionalized cyclobutane product (Figure 4.22-C). This product is obtained as a single diastereomer containing two quaternary centers on the cyclobutane ring with a 47% yield after purification.

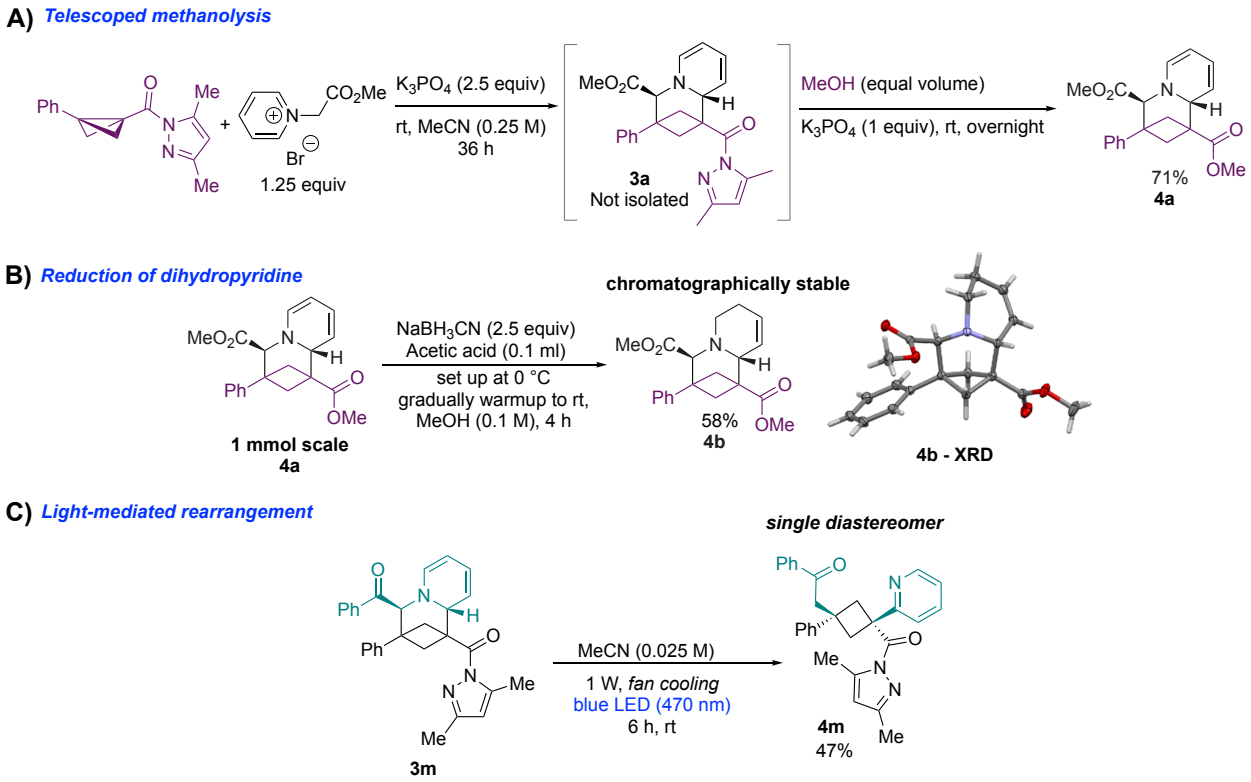

Figure 4.22: Additional synthetic transformations of the azabicyclo[3.1.1]heptanes. Single crystal XRD structure of **4b** is deposited with the CCDC: 2374389.

In further attempts to isolate azabicyclo[3.1.1]heptane derivatives that are chromatographically stable, a telescoped pathway was developed (Figure 4.23). With the ketone-derived bicyclobutane **1i**, a two-step process was done with the first step being the cycloaddition with the pyridinium ylide to form the azabicycloheptane product **3i**. This product was not isolated and instead the solvent was swapped to methanol and the reduction of the dihydropyridine was performed to give product **4i** (Figure 4.23). Notably, the ketone from the bicyclobutane was intact after the reduction conditions. From the *N*-acyl pyrazole bicyclobutane **1a**, a three-step telescoped synthesis to the column stable, reduced product was completed. The first step was the pyridinium ylide cycloadditition to give products **3q** and **3ab** *in situ* after 24 hours (Figure 4.23). An additional equivalent of base and methanol was added to cause methanolysis of the *N*-acyl pyrazole to the methyl ester. After an additional 24 hours, the reaction was subjected to the reduction conditions directly to give the products **4q** and **4ac** with an 11% and 25% yield respectively after three-steps and purification by column chromatography (Figure 4.23). Similarly to the ketone in product **4i**, the *tert*-butyl

ketone in product **4ab** was also intact after the reduction. It is also worth noting that the silyl ester in **4q** remained after the methanolysis step of the reaction pathway. These syntheses highlight the possible transformations available to these products and the capability to purify them by column chromatography.

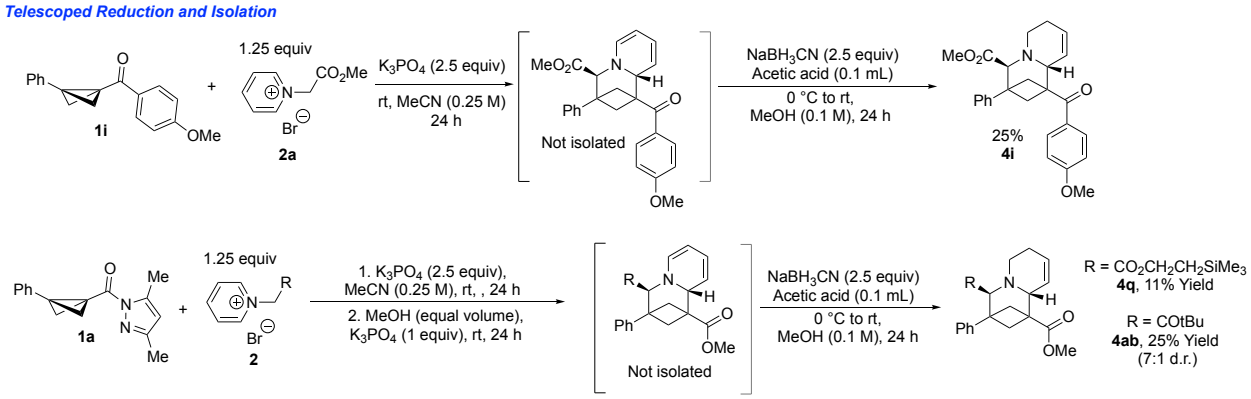

Figure 4.23: Telescoped methanolysis, reduction and isolation of the azabicyclo[3.1.1]heptane products.

The telescoped reduction and isolation conditions were applied to attempt isolation of a column stable version of the nitrile azabicycloheptane product **4o** (Figure 4.24). After the synthesis, we discovered that the isolated product was the decyanated azabicycloheptane (5% overall yield) (Figure 4.24). Upon further examination, we realized that the product after the reduction of the dihydropyridine is an α-aminonitrile, which are known to undergo decyanation reactions under acidic conditions.[197] This route provides a method to access unsubstituted azabicyclo[3.1.1]heptanes that would otherwise require the use of a pyridinium ylide without an EWG; however, the low overall yield means further optimization is required.

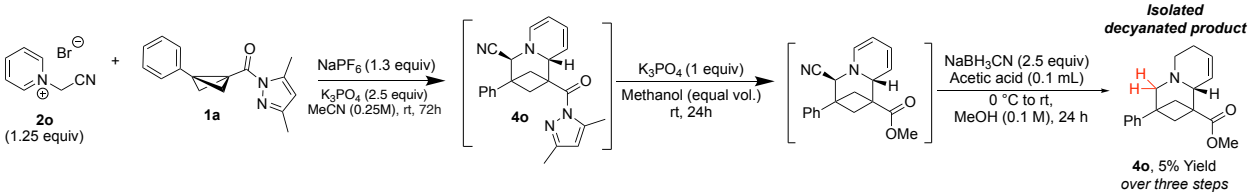

Figure 4.24: Isolation of the decyanation azabicyclo[3.1.1]heptane product

4.7 Proposed Mechanism

The proposed mechanism for the pyridinium ylide addition to bicyclobutane is shown in Figure 4.25. Following the addition of base (K_3PO_4), the carbon between the electron withdrawing group (ester in this case) and the pyridinium is deprotonated to form the pyridinium ylide intermediate **I**. Analogous to our previous work on enolate addition to bicyclobutanes discussed in Chapter 3, the enolate can attack the electrophilic position of bicyclobutane **1** to form the zwitterionic intermediate **II**. The resulting enolate can then attack the electrophilic carbon of the pyridinium ring (analogous to our bicyclobutane reaction with imines in Chapter 2), causing dearomatization of the pyridine ring and formation of the azabicyclo[3.1.1]heptane product **3**. This stepwise pathway is presumed to occur rapidly, as the quenched product of intermediate **II** has not been observed. Notably, this contrasts with the enolate addition reaction described in Chapter 3, where acyclic intermediates were observed in some cases.

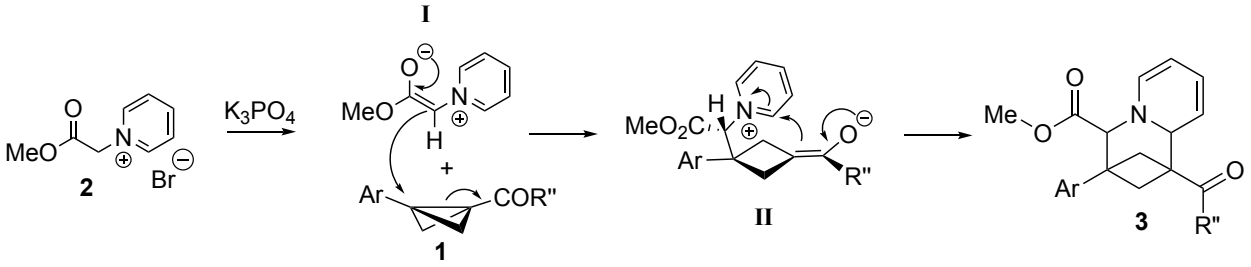

Figure 4.25: Proposed mechanism for the synthesis of azabicyclo[3.1.1]hepatnes *via* ylide addition to bicyclobutane.

4.8 Proposed Stereochemical Model

Based on the proposed mechanism and previous stereochemical model for the imine addition reaction (Chapter 2), we propose a stereochemical model to explain the observed diastereoselectivity (Figure 4.26). After the formation of zwitterionic intermediate **II**, the enolate can attack at two different positions on the pyridinium ring. From the Newmann projection of intermediate **II**, it is clear that following a counter-clockwise bond rotation for nucleophilic addition would cause torsional strain between the ester group from the pyri-

dinium and the aryl group from the bicyclobutane (Figure 4.26). On the other hand, a clockwise bond rotation for nucleophilic addition would minimize torsional strain, leading to the major diastereomer where H_a and H_b are in an *anti* configuration (Figure 4.26). This stereochemical assignment was confirmed by the crystal structure obtained for product **3c**. The role of the solvent on the diastereoselectivity could be due to stabilization of zwitterionic intermediate **II** by the more polar solvents, allowing the lower energy conformation to form and give only the major diastereomer observed. More studies should be done to support this hypothesis.

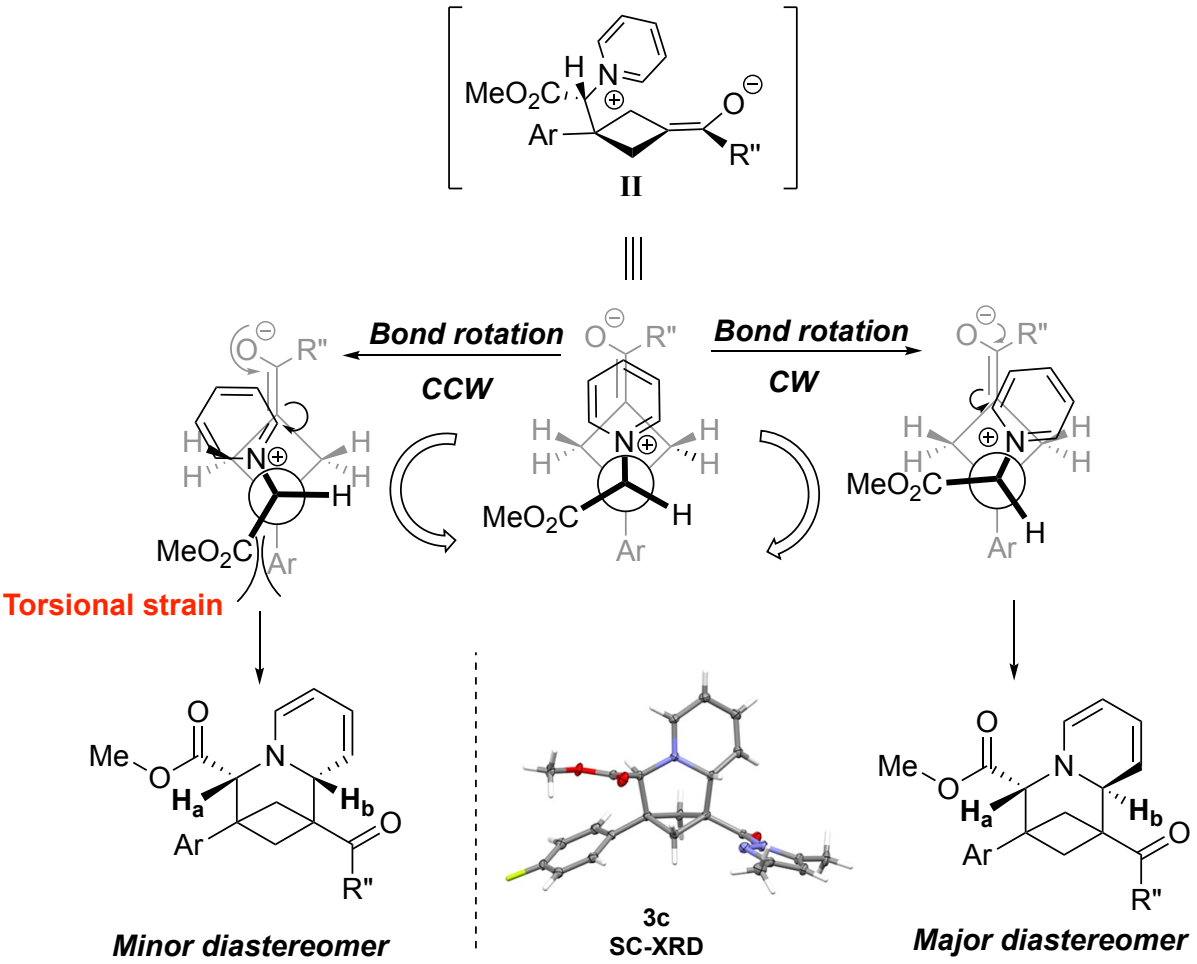

Figure 4.26: Proposed stereochemical model for the synthesis of azabicyclo[3.1.1]hepatnes *via* ylide addition to bicyclobutane.

4.9 Other Ylide Additions to Bicyclobutane

In addition to the pyridinium ylides, other ylide additions to bicyclobutane have been explored. Prior to the copper-catalyzed azomethine ylide addition to bicyclobutanes that was reported by Li,[189] we explored the possibility of forming the azabicycloheptane *via* azomethine ylides (Figure 4.27). From a suitable imine, an azomethine ylide could be formed *in situ* with either a weak base and catalyst or a strong base. This ylide could then react with the bicyclobutane analogously to the pyridinium ylide addition to form 3-azabicyclo[2.1.1]heptanes (Figure 4.27).

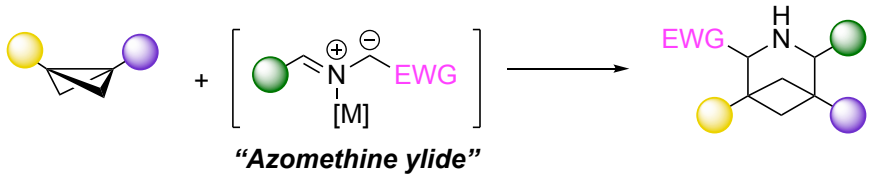

Figure 4.27: Proposed azomethine ylide additions to bicyclobutane to form azabicycloheptanes.

Starting from an ethyl ester derived imine and morpholine amide bicyclobutane, the first set of conditions tested to form the azomethine ylide were using weak base/catalyst combinations (Table 4.5). Variations of base, catalyst and solvent were tested with both the monosubstituted and disubstituted bicyclobutane; however, no product was observed in any case. Instead, we observed homocoupling of the azomethine ylide with another equivalent of imine. This homocoupling reaction has been reported in the literature.[198] Notably, when strongly basic conditions were tested (LiHMDS), we only observed the enolate addition reaction to form the bicyclohexane that was discussed in Chapter 3.

Table 4.5: Test for azomethine ylide addition to bicyclobutanes.

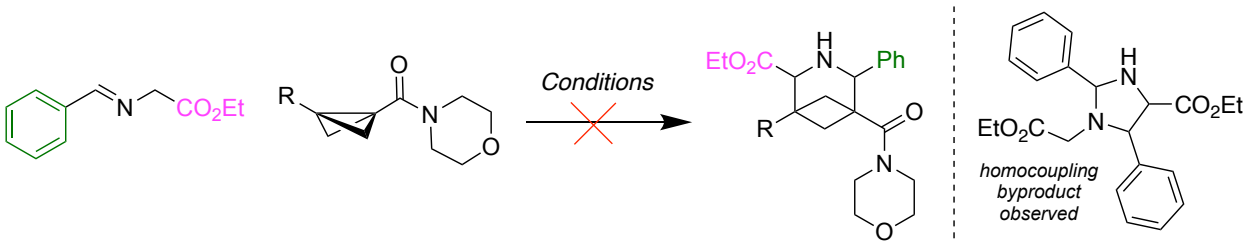

Entry	R =	Base	Lewis acid	Solvent	Temperature
1	Ph	DIPEA (1.0 equiv)	$Ga(OTf)_3$ (0.2 equiv)	THF	rt
2	Ph	NEt_3 (1.0 equiv)	$Ga(OTf)_3$ (0.2 equiv)	Toluene	80 °C
3	Ph	NEt_3 (1.5 equiv)	AgOAc (1.5 equiv)	MeCN	rt
4	Ph	NEt_3 (0.3 equiv)	AgOAc (0.1 equiv)	DCM	rt
5	H	NEt_3 (0.3 equiv)	AgOAc (0.1 equiv)	DCM	rt
6	H	NEt_3 (0.3 equiv)	$Ga(OTf)_3$ (0.1 equiv)	THF	rt
7	H	NEt_3 (0.3 equiv)	$Ga(OTf)_3$ (0.2 equiv)	THF	70 °C

Reactions are performed at 0.1 M concentration with 1 equiv of both imine and bicyclobutane. Results are analyzed by ^{1}H NMR spectroscopy with internal standard, 1,3,5-trimethoxybenzene (TMB).

Due to the competitive enolate addition reaction to form the bicyclohexane (Chapter 3), the ethyl ester group on the imine was swapped for an amide derivative. This imine was tested under the strongly basic reaction conditions with LiHMDS as a base; however, no azabicycloheptane product was observed (Figure 4.28). Instead, only a monoenolate addition cyclobutane byproduct was detected.

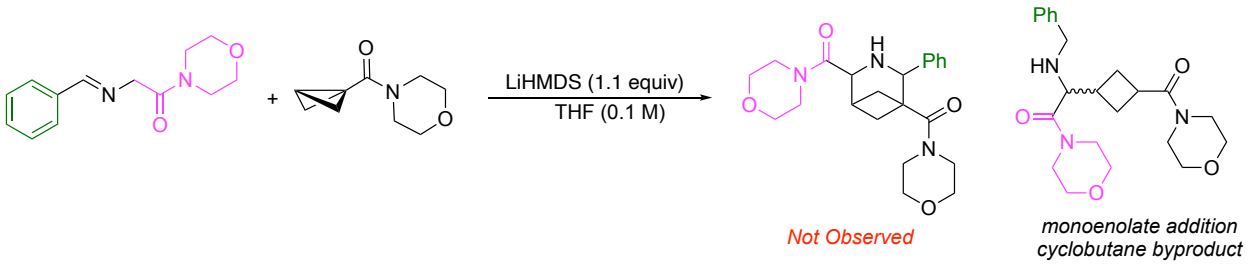

Figure 4.28: Test for azomethine ylide addition with amide electron withdrawing group with strongly basic conditions (optimized conditions from Chapter 3)

To explore the reactivity with the amide derived imine further, a 48-well high-throughput screen was designed (Figure 4.29). For this screen, the morpholine amide derived imine and a monosubstituted amide bicyclobutane were tested. The variables screened were four bases (NEt_3, DIPEA, DBU, LiHMDS), six catalysts/additives (AgOAc, LiBr, $Zn(OAc)_2$, AgOTf,

$Zn(OTf)_2$, CuOAc) and two solvents (THF and toluene). No product was observed for any of the combinations and only trace amounts of the monoaddition cyclobutane product was observed.

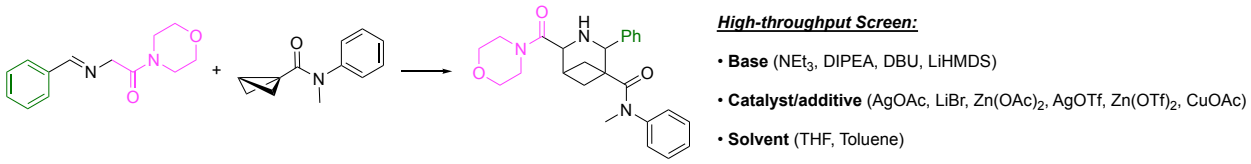

Figure 4.29: 48-well HTE screen for azomethine ylide addition with amide electron-withdrawing group

The focus was shifted to test for azomethine ylide reactivity using the disubstituted pyrazole bicyclobutane used for the pyridinium ylide addition reaction. This bicyclobutane was tested with the ethyl ester imine derivative using two different sets of reaction conditions (Figure 4.30). Neither silver acetate with triethylamine in DCM nor silver carbonate in DMF showed any product formation.

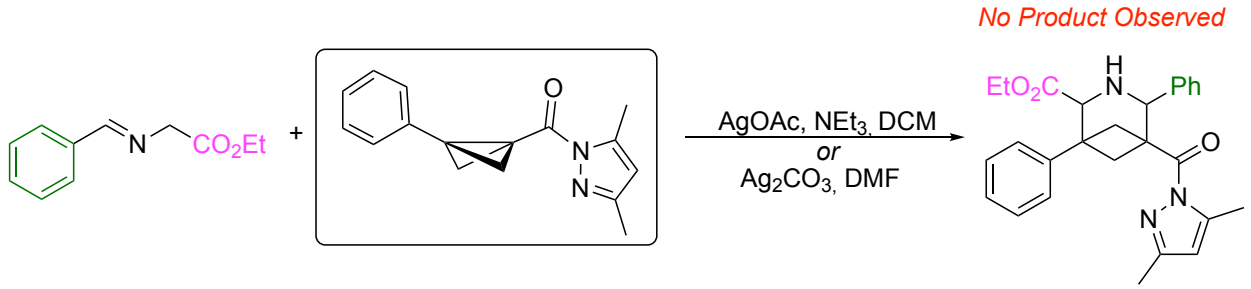

Figure 4.30: Test for azomethine ylide addition with disubstituted pyrazole bicyclobutane.

Continuing with the disubstituted pyrazole bicyclobutane, formation of *N*-acyl iminiums *in situ* was explored. Under a N_2 atmosphere, the *N*-acyl iminium of the ethyl ester imine was generated *in situ via* acylation with an acyl chloride reagent (Figure 4.31). The pyrazole bicyclobutane was then added under various reaction conditions ($Sc(OTf)_3$ and K_2CO_3 or LiHMDS or K_2CO_3); however, no product formation was observed (Figure 4.31).

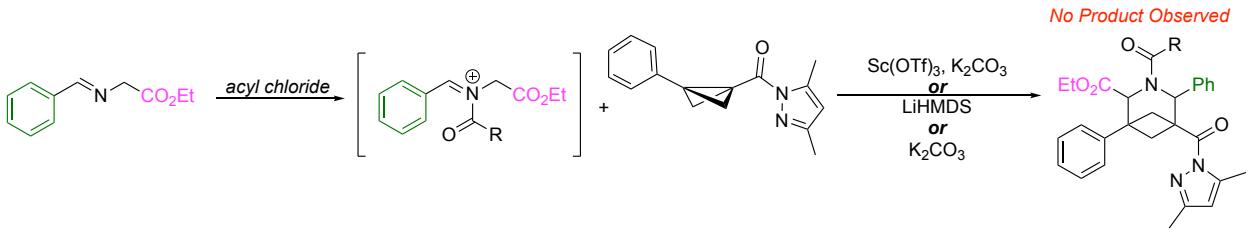

Figure 4.31: Test for azomethine ylide addition *via* an *N*-acyl iminium intermediate with disubstituted pyrazole bicyclobutane.

Unfortunately, no reaction conditions/substrate combinations explored were able to produce the azabicycloheptane *via* azomethine ylides. This highlights the difficulties of designing new syntheses of bicyclic structures and the potential sensitivity of already delevoped transformations.

4.10 Conclusions

A diastereoselective dearomatization of pyridinium ylides through a cycloaddition reaction with bicyclobutanes to form 3-azabicyclo[3.1.1]heptanes was described. Reaction monitoring and epimerization studies indicate that the diastereoselectivity is not from thermodynamic control and thus is kinetically controlled. A stereochemical model explains how torsional strain of the cyclization step leads to the major diastereomer observed. The reaction tolerates a set of pyrazole and ketone containing bicyclobutanes with both mono and disubstituted examples being viable. Examples of substitution of the pyridinium ring and different EWGs on the ylide (such as nitrile, amide and ketone) were also compatible under the reaction conditions. Further transformations of the azabicyclo[3.1.1]heptanes were demonstrated including a photochemical rearrangement reaction to afford a highly-functionalized cyclobutane product.

5 Synthesis of Azabicyclics Through Intramolecular Substitution

Contributions: Synthesis of starting materials **1a-1c** and reaction discovery for the synthesis of compound **2a** was completed by Jesse Delmage. All other experimental work was completed independently.

Intellectual contributions: Kyla Woelk: Lead conceptualization, data curation, formal analysis, investigation and methodology. Jesse Delmage: Supporting data curation, formal analysis, and investigation.

5.1 Background

5.1.1 Previous Syntheses of 3-Oxo-2-Azabicyclo[2.1.1]hexanes

3-Oxo-2-azabicyclo[2.1.1]hexanes are an azaBCH derivative that contain an endocyclic carbonyl adjacent to the nitrogen. As discussed in Chapter 2, azaBCHs have potential applications in pharmaceuticals as bioisosteres and have been incorporated into potential drug candidates. The 3-oxo-2-azabicyclo[2.1.1]hexane derivative is especially interesting since the carbonyl in the bicyclic core would provide a synthetic handle for further derivitizations of these azaBCH motifs.

Syntheses of 3-oxo-2-azabicyclo[2.1.1]hexane derivatives are very scarce in the literature, with only two reports (Figure 5.1).[199;200] The first example, from 1988, used a photochemical [2+2] addition to form the 3-oxo-2-azabicyclo[2.1.1]hexane.[200] The other example was done recently by Grygorenko, and involves an intramolecular coupling reaction between an acetate and an amine using trimethylaluminum.[200] Both of these reaction conditions are extremely limited by the starting material required to perform the synthesis. Further, the

syntheses of these motifs would require either photochemical conditions or trimethylaluminum, which is a highly reactive and pyrophoric reagent. If the syntheses of these 3-oxo-2-azabicyclo[2.1.1]hexane structures could be further developed, they could be used more readily as bioisosteres in pharmaceuticals.

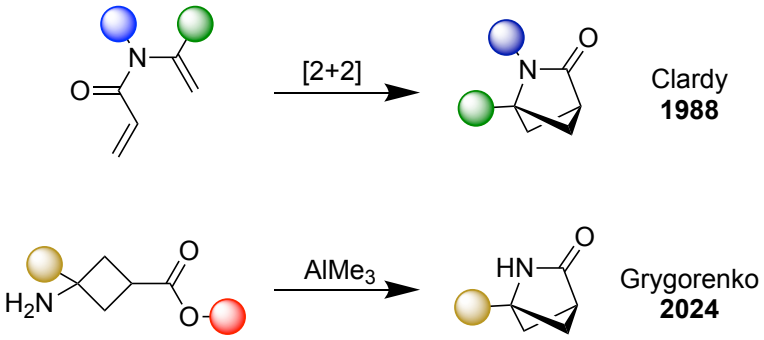

Figure 5.1: Previous syntheses of 3-oxo-2-azabicyclo[2.1.1]hexanes.[199;200]

5.1.2 3-Oxo-2-Azabicyclo[2.2.1]heptane

Another potential azabicyclic bioisostere is the 3-oxo-2-azabicyclo[2.2.1]heptane. The synthesis of the 3-oxo-2-azabicyclo[2.2.1]heptane typically involves a reduction of the 3-oxo-2-azabicyclo[2.2.1]heptene derivative (Figure 5.2).[201] This lactam is referred to as the "Vince lactam" and has been developed as a starting material for the synthesis of nucleoside derivatives.[202] This lactam is prepared through a Diels–Alder reaction between a tosyl cyanide and cyclopentadiene, followed by hydrolysis to give the lactam (Figure 5.2).[202] Using the Vince lactam, various clinical candidates have been prepared, highlighting the importance of this azabicyclic motif (Figure 5.3)[202]

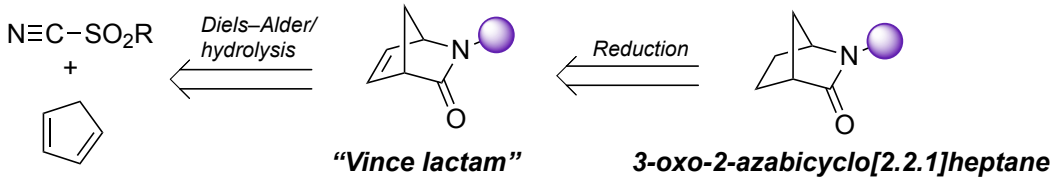

Figure 5.2: 3-oxo-2-azabicyclo[2.2.1]heptane prepared from 3-oxo-2-azabicyclo[2.2.1]hept-5-ene.[202]

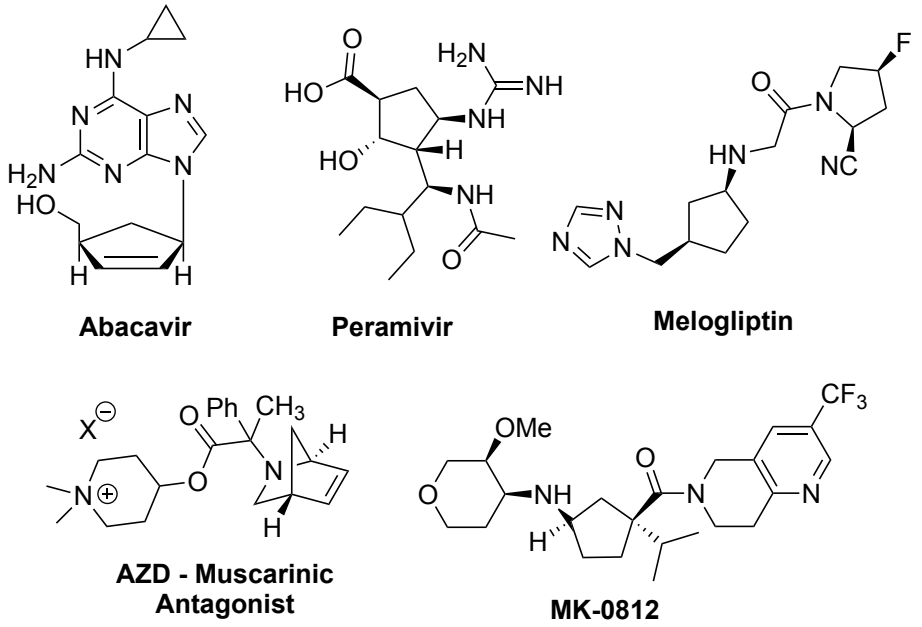

Figure 5.3: Clinical candidates prepared from 3-oxo-2-azabicyclo[2.2.1]hept-5-ene (Vince lactam).[202]

Although the synthesis of the Vince lactam is well reported, synthetic routes to this motif are limited. The main synthetic route to these important structures is *via* a Diels–Alder reaction that requires a highly toxic cyanide reagent which limits their applicability.[202] Alternatively, if the saturated 3-oxo-2-azabicyclo[2.2.1]heptane could be synthesized first, followed by an oxidation to the Vince lactam, it would provide the opportunity to diversify the products we could access. There is one example of a direct synthesis of the 3-oxo-2-azabicyclo[2.2.1]heptane, which uses an intramolecular amidation reaction (Figure 5.4).[203] However, this reaction requires the use of an acyl azide, which is quite reactive. Considering the current syntheses in the literature, there is still room for improvement to develop more synthetic routes to access these 3-oxo-2-azabicyclo[2.2.1]heptane motifs.

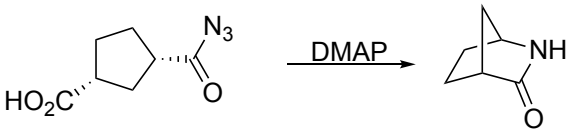

Figure 5.4: Alternative synthesis of 3-oxo-2-azabicyclo[2.2.1]heptane.[203]

5.1.3 Proposed Reactivity

Considering the intramolecular amidation reactivity seen by Grygorenko,[199] it was hypothesized that 3-oxo-2-azabicyclo[2.1.1]hexanes could also be synthesized *via* a similar intramolecular substitution reaction where an amide is the nucleophile with a leaving group across the ring (Figure 5.5). This starting material would resemble an intermediate to the synthesis of bicyclo[1.1.0]butanes. Ideally, from this intermediate, the reaction conditions could be tuned to synthesize either the 3-oxo-2-azabicyclo[2.1.1]hexane or the secondary amide bicyclo[1.1.0]butane (Figure 5.5). This reactivity could be expanded further to synthesize either 3-oxo-2-azabicyclo[2.2.1]heptanes or bicyclo[2.1.0]pentanes (also known as housanes) by expanding the ring size of the starting material to a cyclopentane (Figure 5.5). The reaction discovery and optimization of this reactivity will be discussed below.

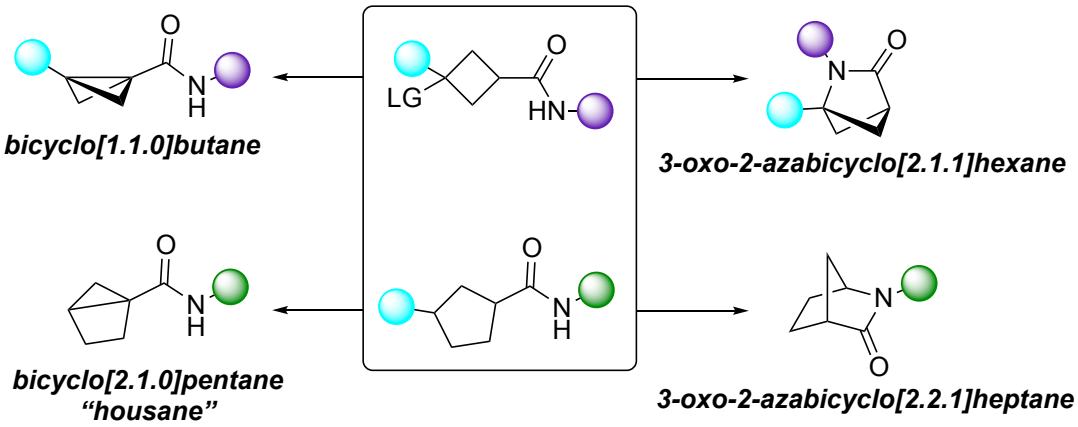

Figure 5.5: Proposed reactivity to form 3-oxo-2-azabicyclo[2.1.1]hexanes and 3-oxo-2-azabicyclo[2.2.1]heptanes *via* an intramolecular substitution reaction.

5.2 Starting Material Synthesis

To test for the synthesis of 3-oxo-2-azabicyclo[2.1.1]hexanes, first the synthesis of the secondary amide cyclobutane **1** was optimized (Figure 5.6). Similarily to the synthesis of monosubstituted bicyclobutanes described in Chapter 3, the first step involves 3-oxocyclobutanecarboxylic acid undergoing an amidation reaction using CDI and a primary amine. This will give the secondary amide intermediate, which can be reduced with sodium cyanoborohydride to give the secondary alcohol. The alcohol is then converted to the toluenesulfonyl leaving group

using triethylamine as a base in DCM to give starting material **1**. Using this procedure, starting materials **1a-1f** were synthesized (Figure 5.6).

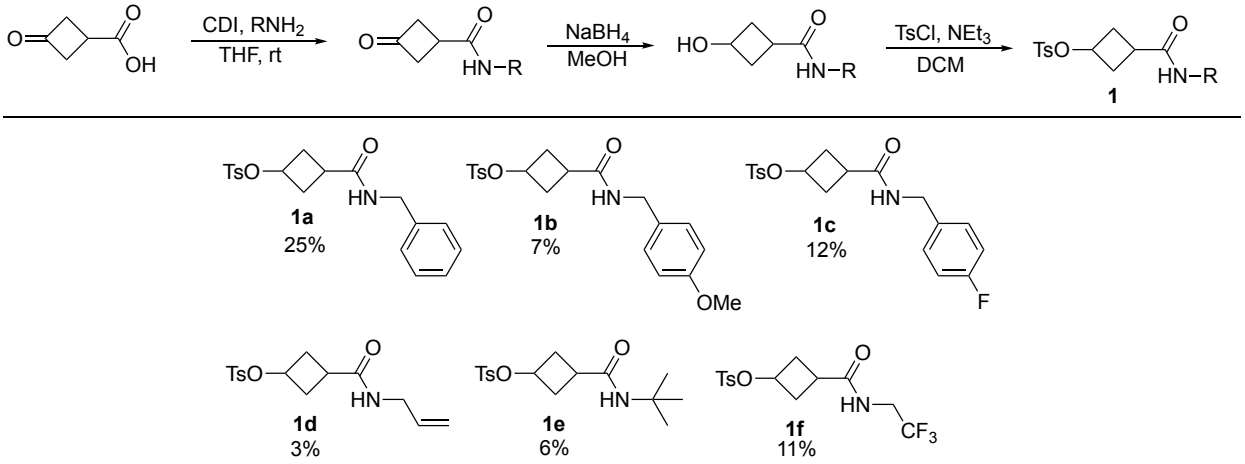

Figure 5.6: Synthesis of cyclobutane amide **1** starting material. Yields are reported as a total yield over three steps.

For the 3-oxo-2-azabicyclo[2.2.1]heptanes, a cyclopentane starting material was synthesized (Figure 5.7). The synthetic route is the same as the one described for the cyclobutane **1** route, with the only difference being the conditions to access the penultimate intermediate. Using 4-toluenesulfonyl chloride with triethylamine as a base in toluene at 60 °C converts the hydroxyl group to a chlorine to give compound **4**. Using this synthetic route, compounds **4a-4e** were prepared (Figure 5.7).

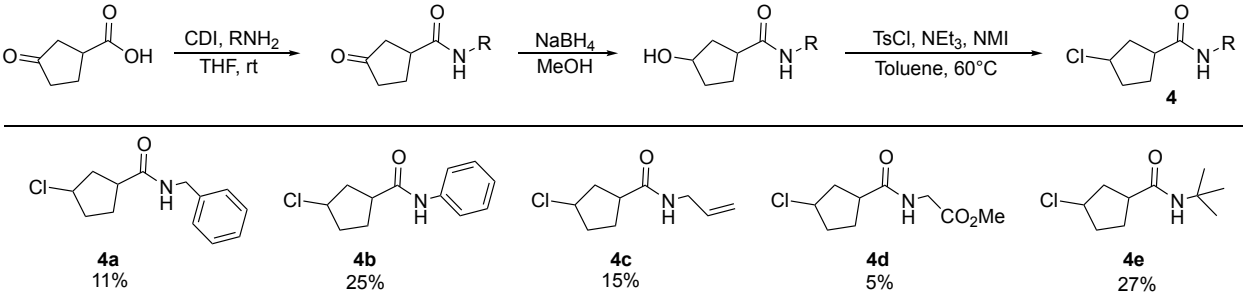

Figure 5.7: Synthesis of cyclopentane amide **4** starting material.Yields are reported as a total yield over three steps.

5.3 Investigations of Reactivity

Starting from compound **1a**, different bases were screened to explore the synthesis of 3-oxo-2-azabicyclo[2.1.1]hexane **2a** and bicyclo[1.1.0]butane **3a** (Table 5.1). The reaction was carried out in THF as the solvent (0.25 M) at 60 °C. When using *tert*-butoxide as a base, formation of the bicyclo[1.1.0]butane was preferred. Sodium *tert*-butoxide performed better than potassium *tert*-butoxide, giving 59% of product **3a** (Entries 1 and 2). When a weaker inorganic base Cs_2CO_3 was used, no reactivity was observed (Entry 3). Stronger bases LDA and NaH showed no product formation, with only consumption/decomposition of the starting material in the case of LDA (Entries 4 and 5). With LiHMDS, a 26% yield of 3-oxo-2-azabicyclo[2.1.1]hexane **2a** was obtained with no starting material remaining (Entry 6). In an effort to optimize this result, the temperature and concentration were adjusted with no significant improvement of the yield (Entries 8-10). Using a weaker organic base (DIPEA) and a Lewis acid (trimethylsilyl trifluoromethanesulfonate (TMSOTf)), gave no products with only starting material observed (Entry 11). Other solvents such as toluene, CPME, DMSO, DMA, DMF and MeCN showed similar or worse reactivity compared to THF. Other Lewis acid catalysts were added along with the best reaction conditions (Entry 6) but only trace amounts of **3a** was observed. Overall, we found that by using either sodium *tert*-butoxide or LiHMDS as the base, the selectivity of the reaction can be controlled to give either the bicyclobutane **3a** or 3-oxo-2-azabicyclo[2.1.1]hexane **2a** products respectively.

Table 5.1: Optimization for synthesis of 3-oxo-2-azabicyclo[2.1.1]hexanes.

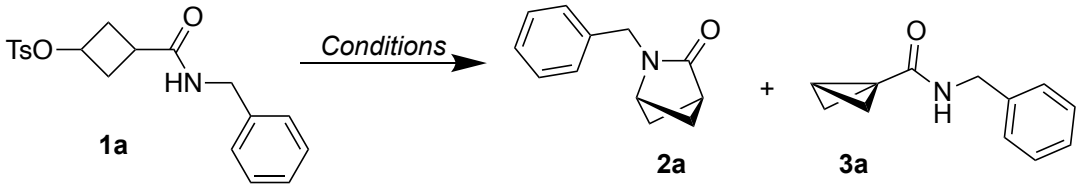

Entry	Conditions	Yield **1a**(%)	Yield **2a**(%)	Yield **3a**(%)
1	KOtBu, 40 °C	0	5	20
2	**NaOtBu (1.1 equiv)**	**0**	**0**	**59**
3	Cs_2CO_3 (1.1 equiv)	100	0	0
4	LDA	0	12	0
5	NaH	84	0	0
6	**LiHMDS**	**0**	**26**	**0**
7	LiHMDS, rt	67	6	6
8	LiHMDS, 40 °C	24	19	0
9	LiHMDS, 0.05 M	0	23	0
10	LiHMDS, 1.0 M	0	21	0
11	DIPEA, TMSOTf	64	0	0

Unless otherwise noted, reactions were performed at 60 °C in THF (0.25 M) and 2.0 equiv of base. Yields determined by ^{1}H NMR spectroscopy versus 1,3,5-trimethoxybenzene as internal standard.

The conditions from Table 5.1, entry 6 were carried forward to test the potential of the reaction. The optimized conditions for the 3-oxo-2-azabicyclo[2.1.1]hexane **2a** synthesis were employed on the cyclopentane starting material **4a** (Figure 5.8). These conditions formed the 3-oxo-2-azabicyclo[2.2.1]heptane **5a** with an improved solution yield of 56% (obtained by ^{1}H NMR spectroscopy analysis), and a 41% isolated yield.

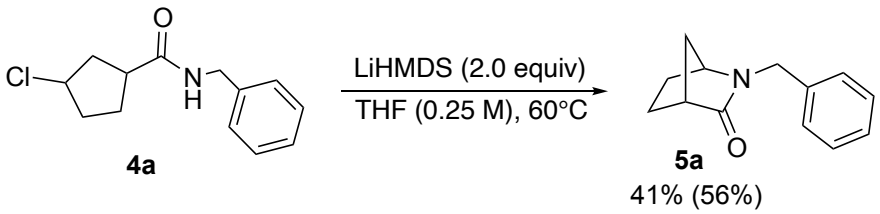

Figure 5.8: Synthesis of 3-oxo-2-azabicyclo[2.2.1]heptanes from cyclopentane. Yield reported after isolation and purification with ^{1}H NMR solution yield using 1,3,5-trimethoxybenzene as internal standard in brackets.

The conditions from Table 5.1, entry 2 that favoured the bicyclo[1.1.0]butane formation were tested on the cyclopentane **4a** derivative to try and form the bicyclo[2.1.0]pentane **6a**

(Figure 5.9). Unfortunately, under these conditions, the bicyclo[2.1.0]pentane **6a** was only formed as a minor product with a 22% yield and the 3-oxo-2-azabicyclo[2.2.1]heptane **5a** was the major product with a 41% yield (Figure 5.9).

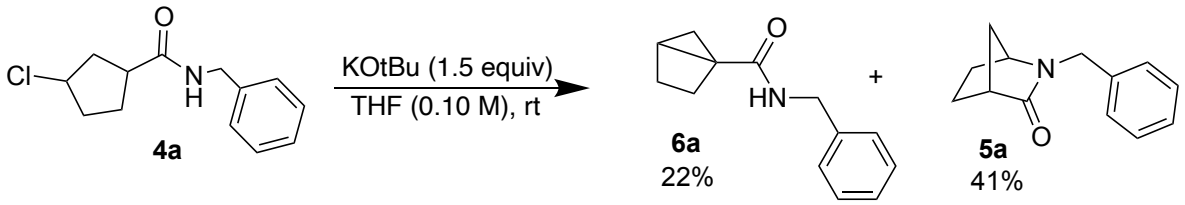

Figure 5.9: Test synthesis of bicyclo[2.1.0]pentane (housane) from cyclopentane. Yields reported as ^{1}H NMR solution yields using 1,3,5-trimethoxybenzene as internal standard.

5.4 Reaction Scope

With the best conditions determined for the synthesis of 3-oxo-2-azabicyclo[2.1.1]hexane **2**, the scope of the reaction was explored (Figure 5.10). Due to low yields and difficulties with isolations, yields are reported as ^{1}H NMR solution yields using 1,3,5-trimethoxybenzene as internal standard. Both electron withdrawing (**2b**) and electron donating (**2c**) benzyl groups were viable to give an 18% and 14% yield respectively. An allyl amide **2d** and bulky *tert*-butyl amide (**2d**) also gave product, although with a drop in yield. Finally, an alkyl CF_3 amide (**2e**) was able to give the 3-oxo-2-azabicyclo[2.1.1]hexane product.

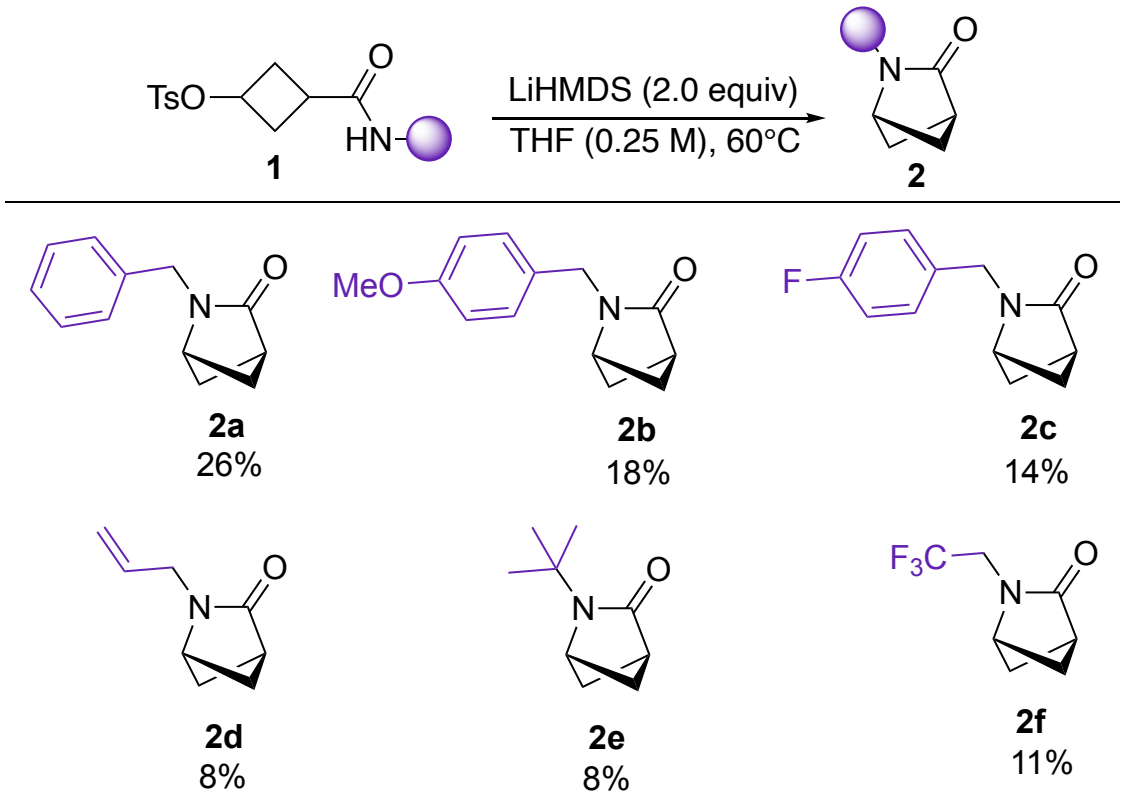

Figure 5.10: Scope of 3-oxo-2-azabicyclo[2.1.1]hexanes reported as ^{1}H NMR solution yields using 1,3,5-trimethoxybenzene as internal standard.

The scope of the 3-oxo-2-azabicyclo[2.2.1]heptanes was also explored with yields determined by ^{1}H NMR spectroscopy with 1,3,5-trimethoxybenzene as internal standard (Figure 5.11). Using an *N*-phenyl amide was compatible with this reactivity to give product **5b** with a 70% yield. Allyl amide **5c** and bulky *tert*-butyl amide **5e** were also successful and gave the 3-oxo-2-azabicyclo[2.2.1]heptane products with a 58% and 51% yield respectively. Notably, a methyl ester alkyl amine was also able to give product **5d**, albeit with a drop in yield to 9%. Overall, the synthesis of the 3-oxo-2-azabicyclo[2.2.1]heptanes gave higher yields than the 3-oxo-2-azabicyclo[2.1.1]hexane products.

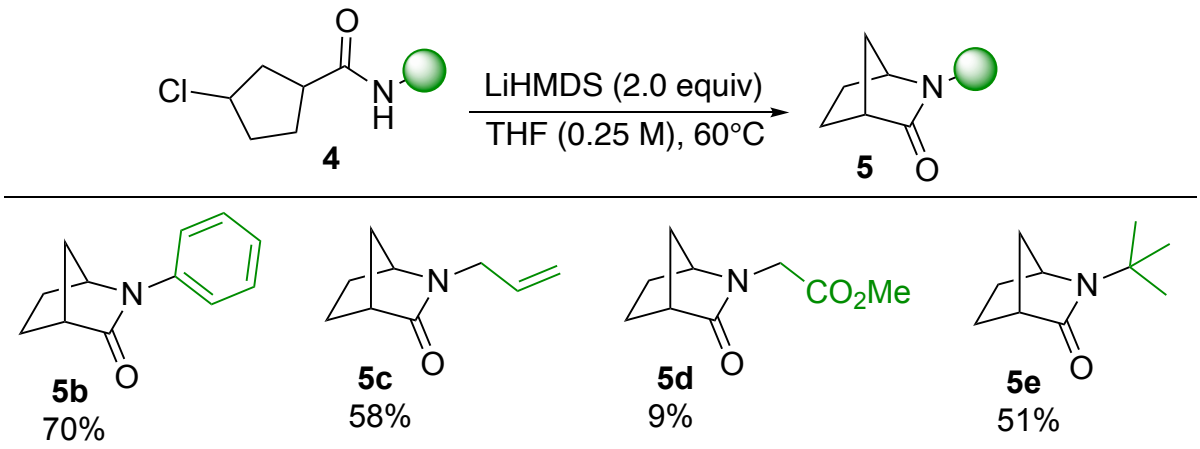

Figure 5.11: Scope of 3-oxo-2-azabicyclo[2.2.1]heptanes reported as ^{1}H NMR solution yields using 1,3,5-trimethoxybenzene as internal standard.

5.5 Additional Studies

Additional experiments were performed to see if the yields of the 3-oxo-2-azabicyclo-[2.1.1]hexane synthesis could be improved. One hypothesis was that if the stereochemistry of the starting material is not the *anti* configuration, then the intramolecular substitution could be slow or unfavoured, leading to low yields. Since the stereochemistry is set after the reduction with sodium borohydride and only one diastereomer is observed, a NOESY spectrum of the cyclobutyl alcohol intermediate was analyzed. No NOE correlations were observed between the two chiral hydrogen, H_a and H_b, suggesting that the product is formed with the *anti* configuration (Figure 5.12). To test this hypothesis further, the alcohol was converted to a bromine with PBr_3, which will invert the stereochemistry of the leaving group (Figure 5.12). The brominated (proposed *syn* configuration) product was then subjected to the reaction conditions for the intramolecular substitution reaction and no product formation was observed (Figure 5.12). These findings suggest that we do in fact have the *anti* stereochemistry that is favoured for the intramolecular substitution to proceed.

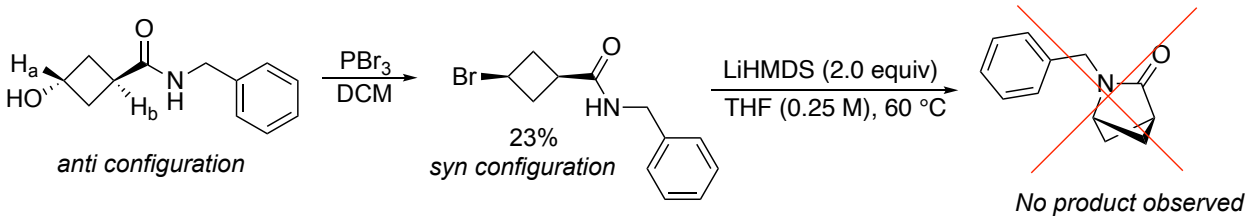

Figure 5.12: Test for stereochemical effect on 3-oxo-2-azabicyclo[2.1.1]hexane synthesis.

Other reaction conditions to achieve the intramolecular substitution were explored. We hypothesized that starting from the alcohol, an intramolecular Mitsunobu reaction could give the desired 3-oxo-2-azabicyclo[2.1.1]hexane product. Unfortunately, under these conditions no product was observed (Figure 5.13). To see if other leaving groups would affect the reaction, a triflate derivative of the starting material was tested but no product was observed under the optimized reaction conditions (Figure 5.13).

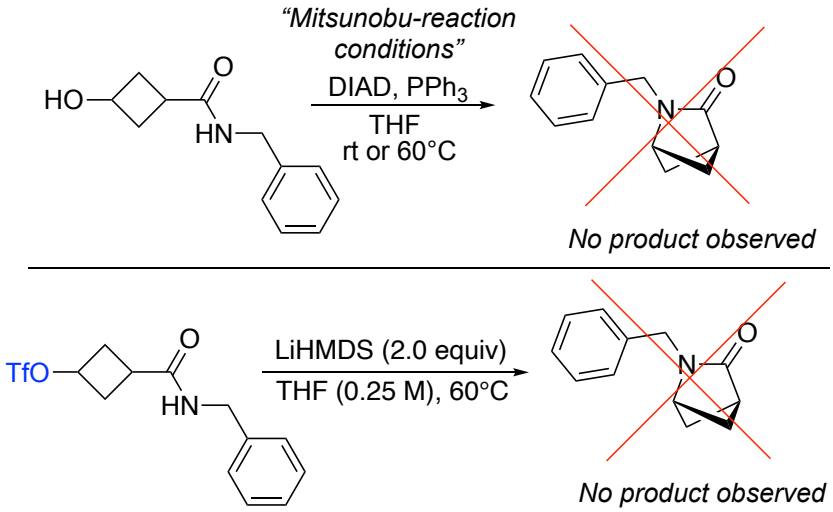

Figure 5.13: Mitsunobu conditions and test with triflate leaving group for 3-oxo-2-azabicyclo[2.1.1]hexane synthesis.

5.6 Conclusions and Future Work

To summarize, a synthesis of 3-oxo-2-azabicyclo[2.1.1]hexanes and 3-oxo-2-azabicyclo-[2.2.1]heptanes *via* an intramolecular substitution reaction was developed. Depending on the base used, the reactivity can be controlled to select for either the bicyclo[1.1.0]butane

or 3-oxo-2-azabicyclo[2.1.1]hexane products. Starting from the cyclopentane derivatives to synthesize the 3-oxo-2-azabicyclo[2.2.1]heptanes gives a higher yield with isolable products. Scope studies *via* ^{1}H NMR spectroscopy analysis show that the reaction is compatible with a variety of other cyclobutane and cyclopentane amide derivatives. Additional studies were completed to try and improve the yields for the 3-oxo-2-azabicyclo[2.1.1]hexane synthesis but the optimized conditions with LiHMDS as a base from the tosylated starting material still gave the best conversion to product.

Further optimization could be done to improve the 3-oxo-2-azabicyclo[2.1.1]hexane synthesis. Trying other leaving groups such as halides in the *anti* configuration (Cl, Br, I), *N*-alkyl nitrobenzenesulfonamides (ONosyl), or methanesulfonyl (OMesyl) could improve the reactivity. Different Lewis acid/base conditions could also be explored and optimized using high-throughput experimentation to screen for higher product yields. Additionally, other reactivity could be explored to try and form the 3-oxo-2-azabicyclo[2.1.1]hexane. One possible reaction would be a carbamate addition to bicyclo[1.1.0]butanes (Figure 5.14). Analogous to the enolate addition to bicyclobutanes discussed earlier,[178] the nitrogen could act as a nucleophile and attack the electrophilic position of the bicyclobutane. This would be followed by the bicyclobutane attacking the carbonyl in an acyl substitution reaction to form the 3-oxo-2-azabicyclo[2.1.1]hexane. Preliminary studies with a *tert*-butyl *N*-benzyl carbamate and monosubstituted morpholine amide bicyclobutane with various bases (LiHMDS, iPrMgCl·LiCl, and $TiCl_4$·2THF) showed no product formation (Figure 5.14). To assess the viability of this reactivity, high-throughput experimentation should be employed to screen different reaction condition combinations.

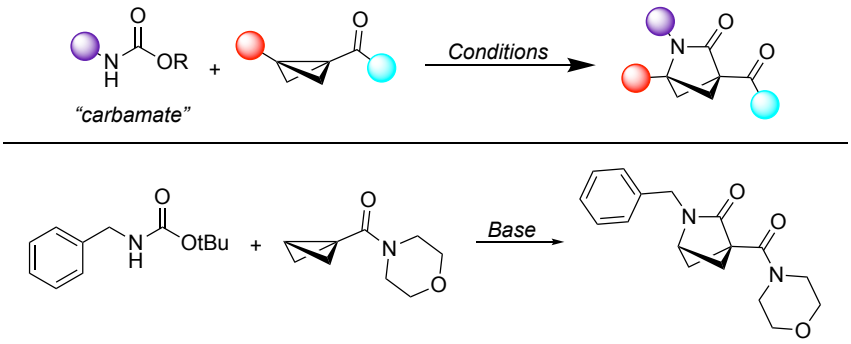

Figure 5.14: Proposed carbamate addition to bicyclobutanes to form 3-oxo-2-azabicyclo[2.1.1]hexanes.

6 Conclusions and Future Work

6.1 Thesis Conclusions

The objective of this thesis was to develop syntheses of highly-functionalized bicyclic motifs. These type of structures are important molecules that are used as bioisosteres in pharmaceuticals.[7;8] Syntheses of these structures are just beginning to be explored in the literature and more ways to access these molecules must continue to be developed. Bicyclo[1.1.0]butanes played a crucial role in this research as a central intermediate to synthesize different bicyclic structures. From bicyclobutanes, we developed the addition of imines to form 2-azabicyclo[2.1.1]hexanes (Chapter 2), addition of enolates to form 2-oxo-bicyclo[2.1.1]hexanes (Chapter 3) and addition of pyridinum ylides to form 3-azabicyclo[3.1.1]heptanes (Chapter 4)(Figure 6.1). All three syntheses required a different set of conditions to be optimized, and the bicyclic products obtained all have applications as bioisosteres in pharmaceuticals. The reactions developed in this thesis provide more ways to access these highly sought-after bicyclic structures. High-throughput experimentation was a key aspect for reaction discovery and/or optimization of these new reactions. The reactivity of the bicyclobutane can continue to be explored to find new and different ways to access these functionalized bicyclic structures.

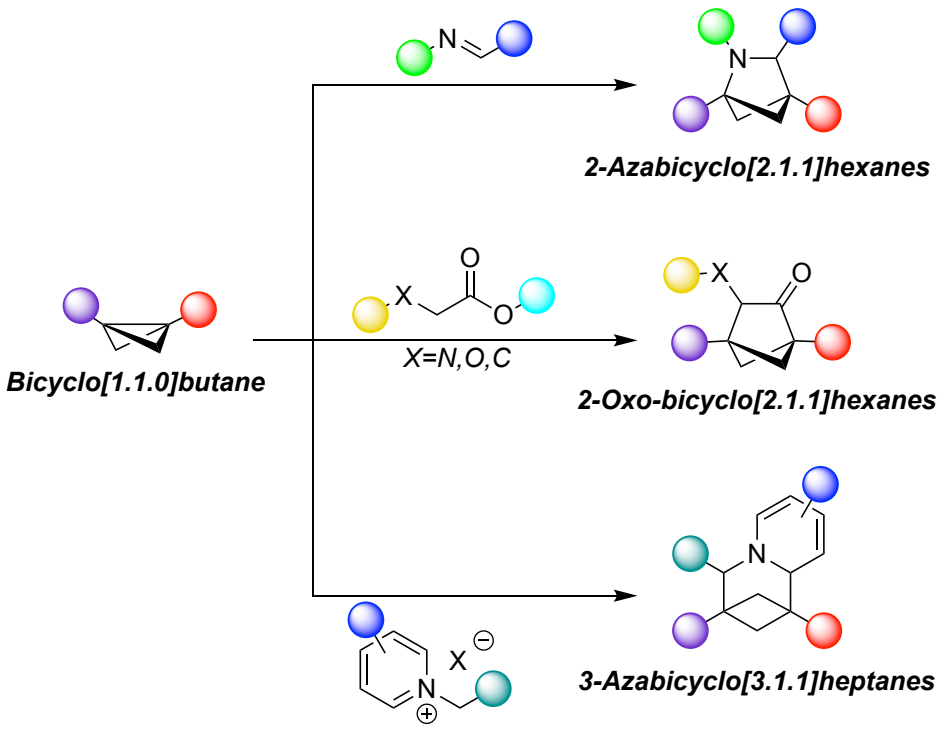

Figure 6.1: Summary of bicyclic structures synthesized from bicyclobutane.

Additional syntheses of bicyclic structures were developed from precursors to bicyclobutane (and housane) that also have applications in pharmaceuticals. Chapter 5 describes the synthesis of 3-oxo-2-azabicyclo[2.1.1]hexanes and 3-oxo-azabicyclo[2.2.1]heptanes from cyclobutane and cyclopentane derivatives respectively *via* an intramolecular substitution reaction. This method provided an alternative route to the products from the established literature procedures.[199–202]

6.2 Future Work

6.2.1 Enantioselectivity

In Chapter 2, the imine addition to bicyclobutanes was performed to generate racemic products. Chiral auxiliaries were installed on both the bicyclobutane (menthol) and the imine (α-methyl benzyl), but only modest enantioinduction was observed with the latter in the cyclobutenyl methanamine synthesis. A next step would be to explore ways to achieve this imine addition enantioselectively. The first approach to test would be exploring other

chiral auxiliaries on the imine and bicyclobutane. Using the chiral auxiliaries with the *N*-alkyl imine reaction conditions to make cyclobutenyl methanamines would be ideal as a starting point, as it allows the potential for more types of chiral imines to be used. Examples of chiral auxiliaries to try for the bicyclobutane would be the Evans auxillary (an oxazolidinone) or camphorsultam. For the imine, more bulky α-benzyl groups such as isopropyl, *tert*-butyl or norephedrine could be explored (Figure 6.2).

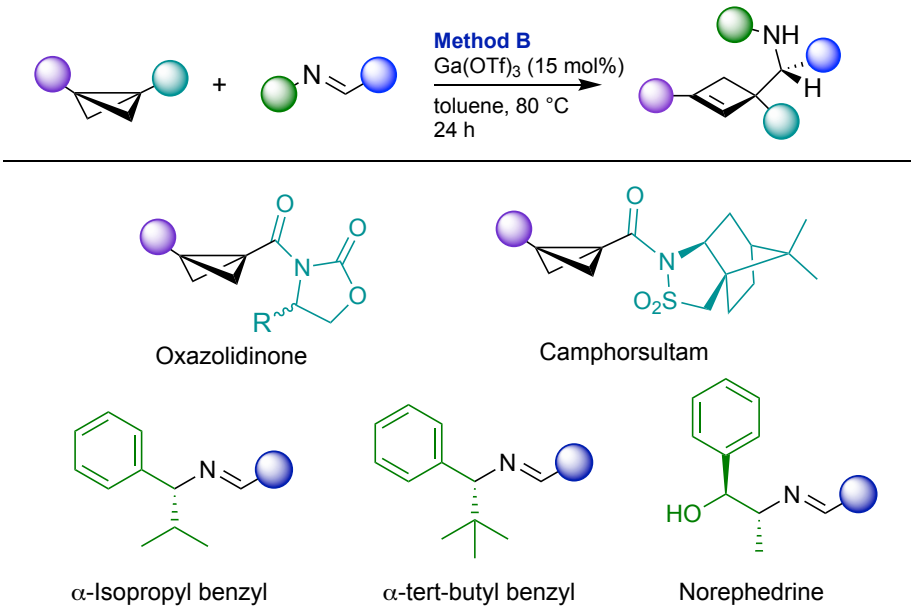

Figure 6.2: Proposed chiral auxiliaries for the imine addition to bicyclobutane.

Alternatively, discovering a chiral gallium Lewis acid catalyst would potentially be a more general approach to enantioselective synthesis. This could be done by pairing chiral ligands and gallium triflate (Figure 6.3).[204] The resulting mixtures of enantiomers could be separated by chiral high performance liquid chromatography (HPLC) or supercritical fluid chromatography (SFC), and the resulting enantioselectivity could be determined.

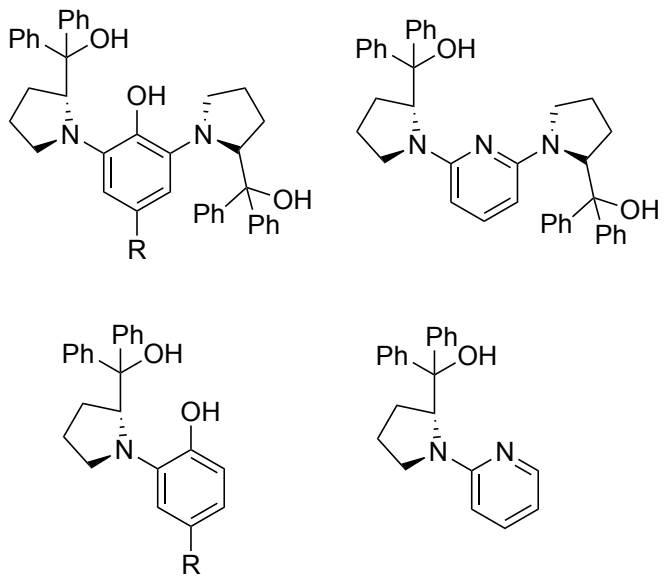

Figure 6.3: Chiral ligands that have been paired with $Ga(OTf)_3$ previously.[204]

In Chapter 3, the enolate addition to bicyclobutanes to form 2-oxo-bicyclohexanes was described; however, the products obtained were also mixtures of enantiomers. Since this reaction only requires base, using a chiral catalyst to control enantioselectivity would be challenging. Alternatively, one way to achieve enantioselectivity could be with chiral auxiliaries. Using chiral esters on the enolate could induce selectivity during the second, intramolecular enolate addition that take place in the proposed mechanism (Figure 6.4). Examples of chiral esters that could be synthesized are (*R*)-1-phenylethanol, (*S*)-2-methyl-1-butanol and (−)-menthol derived acetates (Figure 6.4). Alternatively, chiral ligands such as sparteine could be added to coordinate to Li center of the enolate.

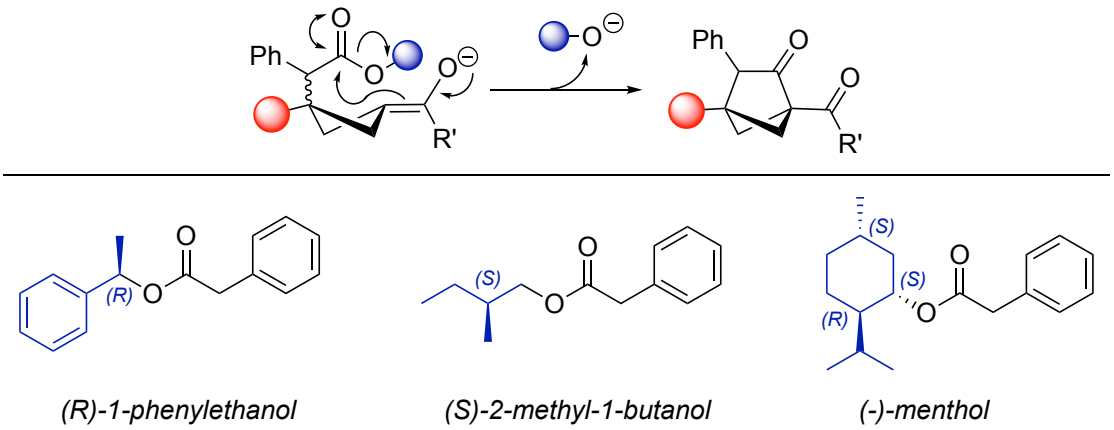

Figure 6.4: Mechanism for intramolecular enolate addition with bicyclobutane and proposed chiral enolates.

6.2.2 Chemoselectivity for Imine Addition to Bicyclobutane

The divergent reactivity observed for the imine addition to bicyclobutanes to give either the azabicycloheptanes (*N*-aryl) or cyclobutenyl methanamines (*N*-alkyl) in Chapter 2 was proposed to be due to the difference in basicity/nucleophilicity of the imine nitrogen. To help support the proposed mechanism, additional studies to explore this hypothesis should be performed. For the *N*-alkyl imine, various electron donating and electron withdrawing groups can be installed to see if the ratio of the azabicyclohexane to cyclobutenyl methanamine can be controlled, ideally with selectivity pushed completely to favour the azabicyclohexane product. A preliminary test was done using an ethyl ester substituted *N*-alkyl imine derivative **1q** under the **Method B** reaction conditions (Figure 6.5). This imine gave a 2:1 ratio of cyclobutenyl methanamine to azabicyclohexane (**4qq : 3q**). This suggests that an electron withdrawing group attached to the nitrogen will help it react more like a nucleophile than a base compared to the standard *N*-benzyl imine. Understanding this selectivity could help us design the reaction to allow the formation of only the azabicyclohexane product when using the *N*-alkyl imine derivatives.

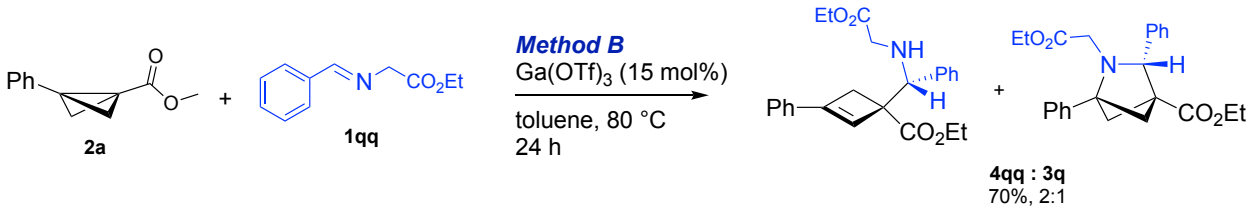

Figure 6.5: Ethyl ester *N*-alkyl imine addition to bicyclobutane.

6.2.3 Expanding Bicyclobutane Scope for Imine Addition

For the imine addition to bicyclobutanes described in Chapter 2, only disubstituted bicyclobutanes were used for the scope. One limitation with many reported bicyclobutane addition reactions is that they are only compatible with either mono or disubstituted bicyclobutanes. Ideally, the imine addition could be expanded to work for monosubstituted bicyclobutanes (Figure 6.6). Preliminary studies were done with the amide monosubstituted bicyclobutanes from Chapter 3 under the standard imine addition conditions from Chapter 2 for both the *N*-alkyl and *N*-aryl imines; however, no product formation was observed. This could be due to the fact that the intermediate carbocation for this reaction would be a less stable secondary carbocation rather than a tertiary carbocation formed when the disubstituted bicyclobutanes are used (Figure 6.6). This reaction requires further optimization, and high-throughput experimentation could be used to find suitable reaction conditions. An array of different Lewis acid and solvent conditions should be explored to find the optimal conditions for these bicyclobutanes to react. Alternatively, conditions could be developed to favour nucleophilic attack by the imine nitrogen to the bicyclobutane itself, which would remove the need to generate a carbocation intermediate.

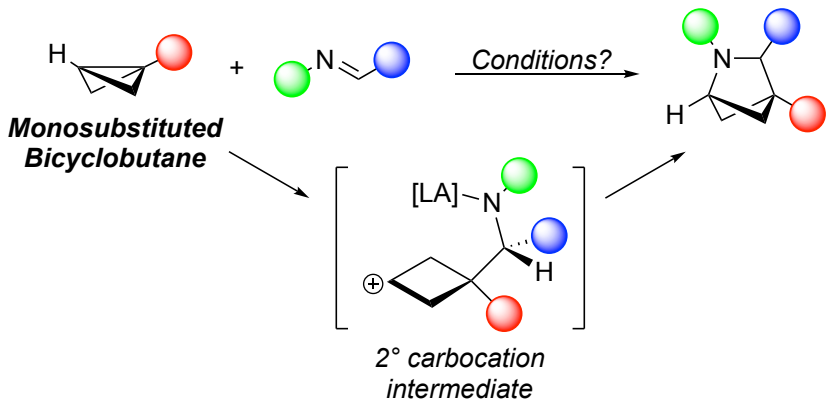

Figure 6.6: Proposed imine addition to monosubstituted bicyclobutanes.

6.2.4 Additional Transformations for Cyclobutenyl Methanamines

We demonstrated in Chapter 2, Section 2.8 that the cyclobutenyl methanamine products could be converted to azabicyclohexanes *via* an intramolecular iodoamination reaction. Alternative methods to form the azabicyclohexane from the cyclobutenyl methanamine can be explored. Two potential pathways would be a hydroamination of the amine with the cyclobutene and/or epoxidation of the cyclobutene followed by ring closing *via* intramolecular attack of the amine at the epoxide (Figure 6.7). The formation of an epoxide followed by ring closure would provide a hydroxyl group on the azabicyclohexane as a synthetic handle for further derivitization. Literature conditions for hydroamination with alkenes,[214] and epoxidation of alkenes[215;216] can be tested to explore these reactions to form the azabicyclohexane.

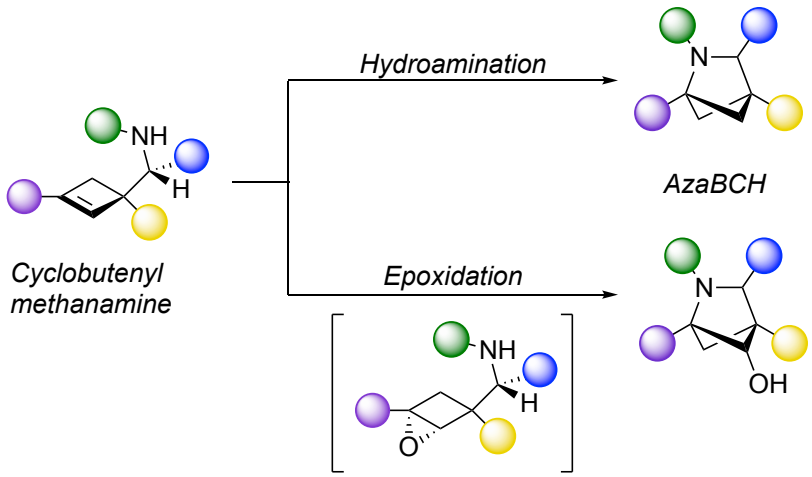

Figure 6.7: Additional transformations proposed for cyclobutenyl methanamines.

6.2.5 Nucleophilicity vs Bicyclobutane Electrophilicity Studies

It was discussed in Chapter 3, Section 3.9, that many enolates and nucleophiles do not react with the bicyclobutane. In addition, until we published the enolate addition to bicyclobutanes discussed in Chapter 3, there were no reports of enolate addition reactions with bicyclobutanes despite reports of many other types of nucleophilic reactions. This indicates an area where improvements could be made to explore how nucleophilicity can be paired with the electrophilicity of the bicyclobutane for successful reactivity. Unfortunately, more electrophilic bicyclobutanes (such as ketones) may pose a problem for certain enolates/nucleophiles since they may be prone to undergo an undesired 1,2-addition reaction at the carbonyl. To explore this reactivity further, computational studies could be done to rank both bicyclobutanes and nucleophiles based on their electrophilicity and nucleophilicity respectively. This would provide insight to what different types of reactions are possible between different bicyclobutanes/enolates and where the limit of potential reactivity is. These theoretical calculations could be paired with experimental studies to create a model for reactivity of nucleophiles with bicyclobutanes.

6.2.6 Diastereoselectivity for Pyridinium Ylide Addition to Bicyclobutane

The pyridinium ylide addition to bicyclobutanes developed in Chapter 4 proceeded diastereoselectively. This was true when acetonitrile was the solvent at room temperature; however, when THF was used as a solvent and/or the reaction was heated to 60 °C, a mixture of diastereomers was obtained. The stereochemical model proposed explains how sterics played a role in the major diastereomer that we observed, but it does not take into account how the solvent plays a role in the diastereoselectivity (Figure 6.8). In addition, using the less hindered monosubstituted bicyclobutanes or a more hindered *tert*-butyl ketone pyrdinium gave mixtures of diastereomers.

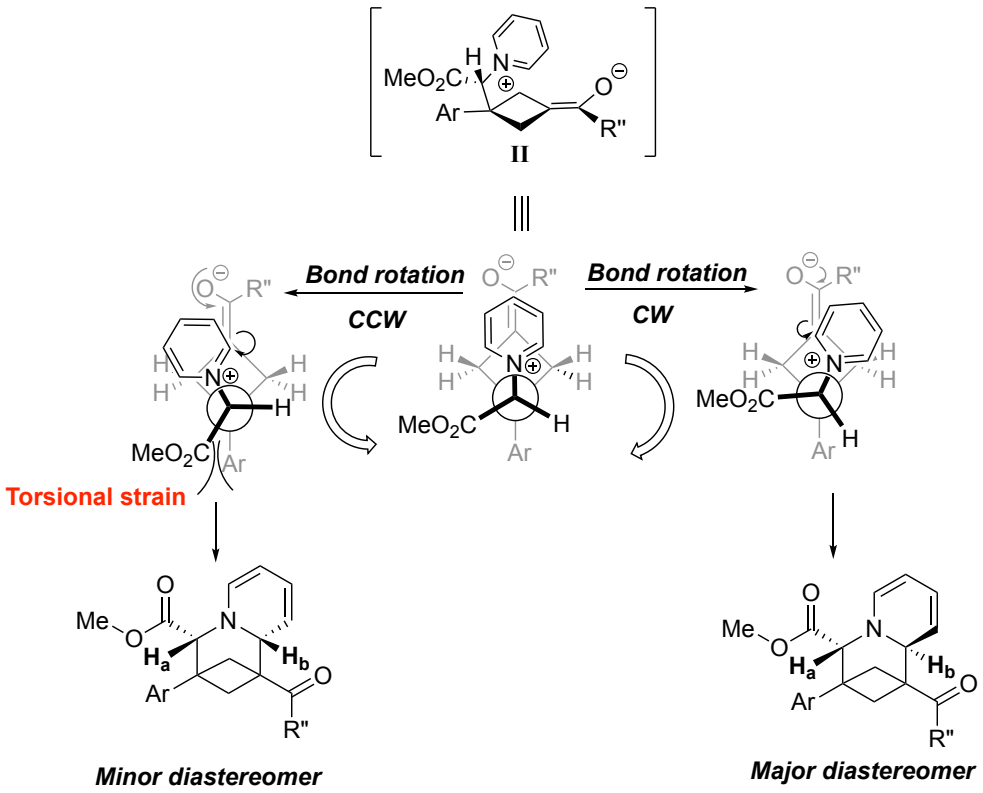

Figure 6.8: Proposed stereochemical model for the synthesis of azabicyclo[3.1.1]hepatnes via ylide addition to bicyclobutane.

More experiments should be done to further test the effects that sterics play on the diasteroselectivity of the reaction, as well as the role that solvent plays. Various other solvents can be used under the reaction conditions and the diastereoselectivity can be monitored. For the sterics, a variety of different types of bulky substituents can be tested on both the bicyclobutane and the pyrdinium ylide to see how they affect the selectivity. As seen in the stereochemical model (Figure 6.8), one of the most prominent steric clashes is between the electron withdrawing group of the pyridinium and the aryl group from the bicyclobutane. In addition to the findings that the monosubstituted bicyclobutane and *tert*-butyl pyridinium give more of the minor diastereomer, it would be useful to see how a more bulky group in either of those positions effects the diastereomeric ratio. For example, if a *tert*-butyl group was installed on the bicyclobutane instead of the aromatic ring, how would that effect the ratio of diastereomers? These studies would help us get a better understanding of both the mechanism and stereochemical model for this cycloaddition reaction.

References

[1] Nagaraju, G. P.; Bonavida, B. *Breaking Tolerance to Pancreatic Cancer Unresponsiveness to Chemotherapy*, 1st ed.; Elsevier, 2019.

[2] Reymond, J. L.; Deursen, R. V.; Blum, L. C.; Ruddigkeit, L. Chemical space as a source for new drugs. *Med. Chem. Commun.* **2010**, *1*, 30–38.

[3] Chemical Abstracts Service - Database Counter. *Retrieved 13 Sept 2024*, https://archive.ph/lNvqE.

[4] DiMasi, J.; Hermann, J.; Twyman, K.; Kondru, R.; Stergiopoulos, S.; Getz, K.; Rackoff, W. A tool for predicting regulatory approval after phase II testing of new oncology compounds. *Clin Pharmacol Ther.* **2015**, *98*, 506–513.

[5] Thomas, D.; Micklus, A.; LaFever, S. Clinical development success rates and contributing factors 2011-2020. *QLS Advisors* **2021**,

[6] Kim, E.; Yang, J.; Park, S.; Shin, K. Factors Affecting Success of New Drug Clinical Trials. *Therapeutic Innovation and Regulatory Science.* **2023**, *57*, 737–750.

[7] Lovering, F. Escape from Flatland 2: Complexity and promiscuity. *Med. Chem. Commun.* **2013**, *4*, 515.

[8] Lovering, F.; Bikker, J.; Humblet, C. Escape from Flatland: Increasing Saturation as an Approach to Improving Clinical Success. *J. Med. Chem.* **2009**, *52*, 6752–6756.

[9] Venkatesh, S.; Lipper, R. A. Role of the Development Scientist in Compound Lead Selection and Optimization. *Journal of Pharmaceutical Sciences* **2000**, *89*, 145–154.

[10] Di, L.; Kerns, A. H. Profiling drug-like properties in discovery research. *Current Opinion in Chemical Biology* **2003**, *4*, 402–408.

[11] Lipinski, C. A. Drug-like properties and the causes of poor solubility and poor permeability. *J. Pharmacy Toxic Methods* **2000**, *44*, 235–249.

[12] Lipinski, C. A.; Lombarado, F.; Domino, B. W.; Feeney, P. J. Experimental and computational approaches to estimate solubility and permeability in drug discovery and development settings. *Adv. Drug Delivery Rev.* **1997**, *23*, 3–25.

[13] Varma, M. V.; Perumal, O. P.; Panchagnula, R. Functional role of P-glycoprotein in limiting peroral drug absorption: optimizing drug delivery. *Current Opinion in Chemical Biology* **2006**, *10*, 367–373.

[14] DeGoey, D. A.; Chen, H. J.; Cox, P. B.; Wendt, M. D. Beyond the Rule of 5: Lessons Learned from AbbVie's Drugs and Compound Collection. *J. Med. Chem.* **2018**, *61*, 2636–2651.

[15] Price, E.; Weinheimer, M.; Rivkin, A.; Jenkins, G.; Nijsen, M.; Cox, P. B.; DeGoey, D. Beyond Rule of Five and PROTACs in Modern Drug Discovery: Polarity Reducers, Chameleonicity, and the Evolving Physicochemical Landscape. *J. Med. Chem.* **2024**, *67*, 5683–5698.

[16] Mykhailiuk, P. K. Saturated bioisosteres of benzene: where to go next? *Org. Biomol. Chem.* **2019**, *17*, 2839–2849.

[17] Taylor, R. D.; Maccoss, M.; Lawson, A. D. Rings in Drugs. *J. Med. Chem.* **2014**, *57*, 5845–5859.

[18] Brown, D. G.; Boström, J. Analysis of Past and Present Synthetic Methodologies on Medicinal Chemistry: Where Have All the New Reactions Gone? *J. Med. Chem.* **2016**, *59*, 4443–4458.

[19] Glassman, P. M.; Muzykantov, V. R. Pharmacokinetic and Pharmacodynamic Properties of Drug Delivery Systems. *J Pharmacol Exp Ther* **2019**, *370*, 570–580.

[20] Talevi, A., Quiroga, P. A., Eds. *ADME Processes in Pharmaceutical Sciences.*, 2nd ed.; Springer Cham: Switzerland, 2024.

[21] Ishida, S. Organs-on-a-chip: Current applications and consideration points for in vitro ADME-Tox studies. *Drug Metabolism and Pharmacokinetics* **2018**, *33*, 49–54.

[22] Ma, X.; Sloman, D. L.; Han, Y.; Bennett, D. J. A Selective Synthesis of 2,2-Difluorobicyclo[1.1.1]pentane Analogues: "BCP-F2". *Org. Lett.* **2019**, *21*, 7199–7208.

[23] Denisenko, A.; Garbuz, P.; Shishkina, S. V.; Voloshchuk, N. M.; Mykhailiuk, P. K. Saturated Bioisosteres of ortho-Substituted Benzenes. *Angew. Chem. Int. Ed.* **2020**, *59*, 20515–20521.

[24] Levterov, V. V.; Panasyuk, Y.; Pinvytska, V. O.; Mykhailiuk, P. K. Water-Soluble Non-Classical Benzene Mimetics. *Angew. Chem. Int. Ed.* **2020**, *59*, 7161–7167.

[25] Caille, S.; Cue, S.; Paul, M. M.; Mennen, S. M.; Tedrow, J. S.; Walker, S. D. Molecular Complexity as a Driver for Chemical Process Innovation in the Pharmaceutical Industry. *J. Org. Chem.* **2019**, *84*, 4583–4603.

[26] Clemons, P. A.; Bodycombe, N. E.; Carrinksi, J. A., H. A. Wilson; Shamji, A. F.; Wagner, B. K.; Koehler, A. N.; Schreiber, S. L. Small molecules of different origins have distinct distributions of structural complexity that correlate with protein-binding profiles. *Proceedings of the National Academy of Sciences* **2010**, *107*, 18787–18792.

[27] Ripenko, V.; Vysochyn, D.; Klymov, I.; Zhersh, S.; Mykhailiuk, P. K. Large-Scale Synthesis and Modifications of Bicyclo[1.1.1]pentane-1,3-dicarboxylic Acid (BCP). *J. Org. Chem.* **2021**, *86*, 14061–14068.

[28] Patani, G. A.; LaVoie, E. J. Bioisosterism: A Rational Approach in Drug Design. *Chem. Rev.* **1996**, *96*, 3147–3176.

[29] Meanwell, N. A. Synopsis of some recent tactical applications of bioisosteres in drug design. *J. Med. Chem.* **2011**, *54*, 2529–2591.

[30] Langmuir, I. Isomorphism, Isosterism and Covalence. *J. Am. Chem. Soc.* **1919**, *41*, 1543–1559.

[31] Friedman, H. L. Influence of Isosteric Replacements upon Biological Activity. *NASNRS* **1951**, *206*, 295–358.

[32] Meanwell, N. A., Ed. *The Influence of Bioisosteres in Drug Design: Tactical Applications to Address Developability Problems*, 9th ed.; Springer-Verlag Berlin Heidelberg, 2014.

[33] Thornber, C. W. Isosterism and molecular modification in drug design. *Chem. Soc. Rev.* **1979**, *8*, 563–580.

[34] Wermuth, C. G. Similarity in drugs: reflections on analogue design. *Drug Discovery Today* **2006**, *11*, 348–354.

[35] Costantino, G.; Maltoni, K.; Marinozzi, M.; Camaioni, E.; Prezeau, L.; Pin, J.; Pellicciari, R. Synthesis and Biological Evaluation of 2-(3'-(1H-Tetrazol-5-yl)bicyclo[1.1.1]pent-1-yl)glycine (S-TBPG), a Novel mGlu1 Receptor Antagonist. *Bioorg. Med. Chem.* **2001**, *9*, 221–227.

[36] Stepan, A. F. et al. Application of the Bicyclo[1.1.1]pentane Motif as a Nonclassical Phenyl Ring Bioisostere in the Design of a Potent and Orally Active γ-Secretase Inhibitor. *J. Med. Chem.* **2012**, *55*, 3414–3424.

[37] Measom, N. D.; Down, K. D.; Hirst, D. J.; Jamieson, C.; Manas, E. S.; Patel, V. K.; Somers, D. O. Investigation of a Bicyclo[1.1.1]pentane as a Phenyl Replacement within an LpPLA2 Inhibitor. *ACS Med. Chem. Lett.* **2017**, *8*, 43–48.

[38] Makarov, I. S.; Brocklehurst, C. E.; Karaghiosoff, K.; Koch, G.; Knochel, P. Synthesis of Bicyclo[1.1.1]pentane Bioisosteres of Internal Alkynes and para-Disubstituted Benzenes from [1.1.1]Propellane. *Angew. Chem. Int. Ed.* **2017**, *56*, 12774–12777.

[39] Tse, E. G.; Houston, S. D.; Williams, C. M.; Savage, G. P.; Rendina, I., L. M. Ans Hallyburton; Anderson, M.; Sharma, R.; Walker, G. S.; Obach, R. S.; Todd, M. H. Nonclassical Phenyl Bioisosteres as Effective Replacements in a Series of Novel Open-Source Antimalarials. *J. Med. Chem.* **2020**, *63*, 11585–11601.

[40] Chalmers, H., B. A. An Xing et al. Cubane as a Benzene Bioisostere. *Angew. Chem Int. Ed.* **2016**, *128*, 3644–3649.

[41] Aguilar, A. et al. Discovery of 4-((3'R,4'S,5'R)-6"-Chloro-4'-(3-chloro-2-fluorophenyl)-1'-ethyl-2"-oxodispiro[cyclohexane-1,2'-pyrrolidine-3',3"-indoline]-5'-carboxamido)bicyclo[2.2.2]octane-1-carboxylic Acid (AA-115/APG-115): A Potent and Orally Active Murine Double Minute 2 (MDM2) Inhibitor in Clinical Development. *J. Med. Chem.* **2017**, *60*, 2819– 2839.

[42] Shire, B. R.; Anderson, E. A. Conquering the Synthesis and Functionalization of Bicyclo[1.1.1]pentanes. *JACS Au* **2023**, *3*, 1539–1553.

[43] Barbachyn, M. R.; Hutchinson, D. K.; Toops, D. S.; Reid, R. J.; Zurenko, G. E.; Yagi, B. H.; Schaadt, R. D.; Allison, J. W. U-87947E, a protein quinolone antibacterial agent incorporating a bicyclo[1.1.1]pent-1-yl (BCP) subunit. *Bioorganic and Medicinal Chemistry Letters* **1993**, *3*, 671–676.

[44] Pellicciari, R.; Raimondo, M.; Marinozzi, M.; Natalini, B.; Constantine, G.; Thomsen, C. (S)-(+)-2-(3'-Carboxybicyclo[1.1.1]pentyl)- glycine, a Structurally New Group I Metabotropic Glutamate Receptor Antagonist. *J. Med. Chem.* **1996**, *39*, 2874–2876.

[45] Westphalia, M. V.; Wolfstädter, B. T.; Plancher, J.; Garfield, J.; Carreira, E. M. Evaluation of tert-Butyl Isosteres: Case Studies ofPhysicochemical and Pharmacokinetic Properties,Efficacies, and Activities. *ChemMedChem* **2015**, *10*, 461–469.

[46] Zhao, J.; Chang, Y.; He, C.; Burke, B. J.; Collins, M. R.; Bel, M. D.; Elleraas, J.; Galled, G. M.; Montgomery, P.; Mousseau, J. J.; Nair, S. K.; Perry, M. A.; Spangler, J. E.; Vantourout, J. C.; Baran, P. S. 1,2-Difunctionalized bicyclo[1.1.1]pentanes: Long–sought-after mimetics for ortho/meta-substituted arenes. *Proceedings of the National Academy of Sciences* **2021**, *118*, e21088811118.

[47] Anderson, J. M.; Measom, N. D.; Murphy, J. A.; Poole, D. L. Bridge Functionalisation of Bicyclo[1.1.1]pentane Derivatives. *Angew. Chem. Int. Ed.* **2021**, *60*, 24754–24769.

[48] Eaton, P. E. Cubanes: Starting Materials for the Chemistry of the 1990s and the New Century. *Angew. Chem. Int. Ed.* **1992**, *31*, 1421–1436.

[49] Reekie, T. A.; Williams, C. M.; Rendina, L. M.; Kassiou, M. Cubanes in Medicinal Chemistry. *J. Med. Chem.* **2018**, *62*, 1078–1095.

[50] Wlochal, J.; Davies, R. D. M.; Burton, J. Cubanes in Medicinal Chemistry: Synthesis of Functionalized Building Blocks. *Org. Lett.* **2014**, *16*, 4094–4097.

[51] Wang, D.; Lyu, X.; Sun, M.; Liang, Y. Spectral Analysis on Cuba-Lumacaftor: Cubane as Benzene Bioisosteres of Lumacaftor. *ACS Omega* **2023**, *8*, 43332–43340.

[52] Biegasiewicz, K. F.; Griffiths, J. R.; Savage, G. P.; Tsanaktsidis, J.; Priefer, R. Cubane: 50 Years Later. *Chem. Rev.* **2015**, *116*, 6719–6745.

[53] Cassar, L.; Eaton, P. E.; Halpern, J. Catalysis of symmetry-restricted reactions by transition metal compounds. Valence isomerization of cubane. *J. Am. Chem. Soc.* **1970**, *92*, 3515–3518.

[54] Wiesendeldt, M. P.; Rossi-Ashton, J. A.; Perry, I. B.; Diesel, J.; Garry, O. L.; Bartels, F.; Cootee, S. C.; Ma, X.; Yeung, C. S.; Bennett, D. J.; MacMillan, D. W. C. General access to cubanes as benzene bioisosteres. *Nature* **2023**, *618*, 513–518.

[55] Houston, S. D.; Xing, H.; Bernhardt, P. V.; Berg, T. J. V.; Tsanaktsidis, J.; Savage, G. P.; Williams, C. M. Cyclooctatetraenes through Valence Isomerization of Cubanes: Scope and Limitations. *Chem. Eur. J.* **2019**, *25*, 2735–2739.

[56] Takebe, H.; Matsubara, S. Catalytic Asymmetric Synthesis of 2,6-Disubstituted Cuneanes through Enantioselective Constitutional Isomerization of 1,4-Disubstituted Cubanes. *Eur. J. Org. Chem.* **2022**, e202200567.

[57] Wang, L.; Zheng, X.; Kouznetsova, T. B.; Yen, T.; Ouchi, T.; Brown, C. L.; Craig, S. L. Mechanochemistry of Cuban. *J. Am. Chem. Soc.* **2022**, *144*, 22865–22869.

[58] Leterov, V. V. et al. 2-Oxabicyclo[2.2.2]octane as a new bioisostere of the phenyl ring. *Nature* **2023**, *14*, 5608.

[59] Auberson, Y. P.; Brocklehurst, C.; Furegati, M.; Fessard, T. C.; Koch, G.; Decker, A.; Vecchia, L. L.; Briard, E. Improving Nonspecific Binding and Solubility: Bicycloalkyl Groups and Cubanes as para-Phenyl Bioisosteres. *ChemMedChem* **2017**, *12*, 590–598.

[60] Hogeveen, P. K.; Zwart, L. Synthesis and Properties of Functionalized 2,4-Ethano-Bridged Bicyclobutanes. *Isr. J. Chem.* **1981**, *21*, 221–228.

[61] Newman-Evans, R. H.; Carpenter, B. K. Highly Steretoselective Synthesis OF Bicyclo[2.1.1lhexenes-5-d By Transmetallation of a Tetra-alkyl Tin. *Tetrahedron Lett.* **1985**, *26*, 1141–1144.

[62] Saya, J. M.; Vos, K.; Kleinnijenhuis, R. A.; van Maarseveen, J. H.; Ingemann, S.; Hiemstra, H. Total Synthesis of Aquatolide. *Org. Lett.* **2015**, *17*, 3892–3894.

[63] Kleinnijenhuis, R. A.; Timmer, B. J. J.; Lutteke, G.; Smits, J. M.; de Gelder, R.; van Maarseveen, J. H.; Hiemstra, H. Formal Synthesis of Solanoeclepin A: Enantioselective Allene Diboration and Intramolecular [2+2] Photocycloaddition for the Construction of the Tricyclic Core. *Chem. Eur. J.* **2016**, *22*, 1266–12694.

[64] Takao, K.; Kai, H.; Yamada, A.; Fukushima, Y.; Komatsu, D.; Ogura, A.; Yoshida, K. Total Syntheses of (+)-Aquatolide and Related Humulanolides. *Angew. Chem., Int. Ed.* **2019**, *58*, 9851–9855.

[65] Kleinmans, R.; Pinkert, T.; Dutta, S.; Paulisch, T. O.; Keum, H.; Daniliuc, C. G.; Glorius, F. Intermolecular [$2\pi + 2\sigma$]-photocycloaddition enabled by triplet energy transfer. *Nature* **2022**, *605*, 477–482.

[66] Kleinmans, R.; Dutta, S.; Ozols, K.; Shao, H.; Schafer, F.; Thielemann, R. E.; H.T.Chan; C.G.Daniliuc; Houk, K. N.; Glorius, F. ortho-Selective Dearomative [$2\pi + 2\sigma$] Photocycloadditions of Bicyclic Aza-Arenes. *J. Am. Chem. Soc.* **2023**, *145*, 12324–12332.

[67] Guo, R.; Chang, Y.; Herter, L.; Salome, C.; Braley, S. E.; Fessard, T. C.; Brown, M. K. Strain-Release [$2\pi + 2\sigma$] Cycloadditions for the Synthesis of Bicyclo[2.1.1]hexanes Initiated by Energy Transfer. *J. Am. Chem. Soc.* **2022**, *144*, 7988–7994.

[68] Agasti, S.; Beltran, F.; Pye, E.; Kaltsoyannis, N.; Crisenza, G. E. M.; Procter, D. J. A catalytic alkene insertion approach to bicyclo[2.1.1]hexane bioisosteres. *Nat. Chem.* **2023**, *15*, 535–541.

[69] Diepers, H. E.; Walker, J. C. L. (Bio)isosteres of ortho- and meta-substituted benzenes. *Beilstein J. Org. Chem.* **2024**, *20*, 859–890.

[70] Reinhold, M.; Steinebach, J.; Golz, C.; Walker, J. C. Synthesis of polysubstituted bicyclo[2.1.1]hexanes enabling access to new chemical space. *Chem. Sci.* **2023**, *14*, 9885.

[71] Denisenko, A.; Garbuz, P.; Makovetska, Y.; Shablykin, O.; Lesyk, D.; Al-Maali, G.; Korzh, R.; Sadkova, I. V.; Mykhailiuk, P. K. 1,2-Disubstituted bicyclo[2.1.1]hexanes as saturated bioisosteres of ortho-substituted benzene. *Chem. Sci.* **2023**, *14*, 14092.

[72] Garrido-Garcia, P.; Quiros, I.; Milan-Rois, P.; Somoza, A.; Fernandez, I.; Rigotti, T.; Tortosa, M. Enantioselective photocatalytic synthesis of bicyclo[2.1.1]hexanes as ortho disubstituted benzene bioisosteres with improved biological activity. *ChemRxiv*

[73] Denisenko, A.; Garbuz, P.; Voloshchuk, N. M.; Holota, Y.; Al-Maali, G.; Borysko, P.; Mykhailiuk, P. K. 2-Oxabicyclo[2.1.1]hexanes as saturated bioisosteres of the ortho-substituted phenyl ring. *Nature Chemistry* **2023**, *15*, 1155–1163.

[74] Vitaku, E.; Smith, D. T.; Njardarson, J. T. Analysis of the Structural Diversity, Substitution Patterns and Frequency of Nitrogen Heterocycles among U.S. FDA Approved Pharmaceuticals. *J. Med. Chem.* **2014**, *57*, 10257–10274.

[75] Marshall, C. M.; Federice, J. C.; Bell, C. N.; Cox, P. B.; Njardarson, J. T. An Update on the Nitrogen Heterocycle Compositions and Properties of U.S. FDA-Approved Pharmaceuticals (2013-2023). *J. Med. Chem.* **2024**, *67*, 11622–11655.

[76] Xu, K.; Hsieh, C.; Lee, J. L.; Riad, A.; Izzo, N. J.; Look, G.; Catalano, S.; Mach, R. H. Exploration of Diazaspiro Cores as Piperazine Bioisosteres in the Development of σ2 Receptor Ligands. *Int. J. Mol. Sci.* **2022**, *23*, 8259.

[77] Dibchak, D.; Snisarenko, M.; Mishuk, A.; Shablykin, O.; Bortnichuk, L.; Klymenko-Ulianov, O.; Kheylik, Y.; Sadkova, I. V.; Rzepa, H. S.; Mykhailiuk, P. K. General Synthesis of 3-Azabicyclo[3.1.1]heptanes and Evaluation of Their Properties as Saturated Isosteres. *Angew. Chem. Int. Ed.* **2023**, *62*, e202304246.

[78] Bromidge, S. M.; Brown, F.; Cassidy, F.; Clark, M. S.; Dabbs, S.; Hadley, M. S.; Hawkins, J.; Loudon, J. M.; Naylor, C. B.; Orlek, B. S.; Riley, G. J. Design of [R-(Z)]-(+)-r-(Methoxyimino)-1-azabicyclo[2.2.2]octane-3-acetonitrile (SB 202026), a Functionally Selective Azabicyclic Muscarinic M1 Agonist Incorporating the N-Methoxy

Imidoyl Nitrile Group as a Novel Ester Bioisostere. *J. Med. Chem.* **1997**, *40*, 4265–4280.

[79] Lowe III, J. A. et al. A novel series of [3.2.1] azabicyclic biaryl ethers as $\alpha 3\beta 4$ and $\alpha 6/4\beta 4$ nicotinic receptor agonists. *Bioorg. Med. Chem. Lett.* **2010**, *20*, 4749–4752.

[80] Gundisch, D.; Harms, K.; Schwartz, S.; Seitz, G.; Stubbs, M. T.; Wegge, T. Synthesis and Evaluation of Diazine Containing Bioisosteres of (–)-Ferruginine as Ligands for Nicotinic Acetylcholine Receptors. *Bioorg. Med. Chem. Lett.* **2001**, *9*, 2683–2691.

[81] Olesen, P. H.; Swedberg, M. D. B.; Eskesen, K.; Judge, M. E.; Egebjerg, J.; Tonder, J. E.; Rasmussen, T.; Sheardown, M. J.; Rimvall, K. Identification of novel (isoxazole)methylene-1-azabicyclic compounds with high affinity for the central nicotinic cholinergic receptor. *Bioorg. Med. Chem. Lett.* **1997**, *7*, 1963–1968.

[82] Olesen, P. H.; Tonder, J. E.; Hansen, J. B.; Hansen, H. C.; Rimvall, K. Bioisosteric replacement strategy for the synthesis of 1-azacyclic compounds with high affinity for the central nicotinic cholinergic receptors. *Bioorg. Med. Chem. Lett.* **2000**, *8*, 1443–1450.

[83] Frank, N.; Nugent, J.; Shire, B.; Pickford, H.; Rabe, P.; Sterling, A.; Zarganes-Tzitzikas, T.; Grimes, T.; Thompson, A.; Smith, R.; Schofield, C.; Brennan, P.; Duarte, F.; Anderson, E. Synthesis of meta-substituted arene bioisosteres from [3.1.1]propellane. *Nature* **2022**, *611*, 721–726.

[84] Golfmann, M.; Walker, J. C. L. Bicyclobutanes as unusual building blocks for complexity generation in organic synthesis. *Communications Chemistry* **2023**, *6*, doi:10.1038/s42004–022–00811–3.

[85] Wilberg, K. B.; Ciula, R. P. Ethyl Bicyclo[1.1.0]butane-1-carboxylate. *J. Am. Chem. Soc.* **1959**, *81*, 5261–5262.

[86] Johnson, P. L.; Schaefer, J. P. Structure of 1,3-dicyanobicyclo[1.1.0]butane using x-ray analysis. *J. Org. Chem.* **1972**, *37*, 2762–2763.

[87] Meiboom, S.; Snyder, L. C. Nuclear magnetic resonance spectra in liquid crystals and molecular structure. *Acc. Chem. Res.* **1971**, *4*, 81–87.

[88] Wiberg, K. B.; Lampman, G. M.; Ciula, R. P.; Connor, D. S.; Schertler, P.; Lavanish, J. Bicyclo[1.1.0]butane. *Tetrahedron* **1965**, *21*, 2749–2769.

[89] Woodward, R. B.; Dalrymple, D. L. Dimethyl 1,3-diphenylbicyclobutane-2,4-dicarboxylates. *J. Am. Chem. Soc.* **1969**, *91*, 4612–4613.

[90] Gassman, P. G.; Greenlee, M. L.; Dixon, D. A.; Richtsmeier, S.; Gougoutas, J. Z. X-ray and theoretical analysis of the relationship between substituent steric effects and the structure of bicyclo[1.1.0]butane. The unexpected flexibility of the bicyclo[1.1.0]butane skeleton. *J. Am. Chem. Soc.* **1983**, *105*, 5865–5874.

[91] Wilberg, K. B. The Concept of Strain in Organic Chemistry. *Angew. Chem. Int. Ed.* **1986**, *25*, 312–322.

[92] Baeyer, A. v. Ueber Polyacetylenverbindungen, Ber. *Ber. Dtsch. Chem. Ges.* **1885**, *18*, 2278.

[93] Pomerantz, M.; Abrahamson, E. W. The Electronic Structure and Reactivity of Small Ring Compounds. I. Bicyclobutane. *J. Am. Chem. Soc.* **1966**, *88*, 3970–3972.

[94] Newton, M. D.; Schulman, J. M. Theoretical studies of bicyclobutane. *J. Am. Chem. Soc.* **1971**, *94*, 767–773.

[95] Fisanick, G. J.; Schulman, J. M. New model for the bonding in bicyclobutanes. *J. Am. Chem. Soc.* **1970**, *92*, 6653–6654.

[96] Avram, M.; Nenitzescu, C. D.; Maxim, M. Untersuchungen in der Cyclobutanreihe, I. 1.3-Disubstituierte Cyclobutanderivate. *Chemische Berichte* **1957**, *90*, 1424–1432.

[97] Gaoni, Y. A simple one-pot preparation of 1-arylsulfonylbicyclobutanes from γ,δ,-epoxysulfones. *Tetrahedron Letters* **1981**, *22*, 4339–4340.

[98] Gianatassio, R.; Lopchuk, J. M.; Wang, J.; Pan, C.; Malins, L. R.; Prieto, L.; Brandt, T. A.; Collins, M. R.; Gallego, G. M.; Sach, N. W.; Spangler, J. E.; Zhu, H.; Zhu, J.; Baran, P. S. Strain-release amination. *Science* **2016**, *351*, 241–246.

[99] Jung, M.; Lindsay, V. N. G. One-Pot Synthesis of Strain-Release Reagents from Methyl Sulfones. *J. Am. Chem. Soc.* **2022**, *144*, 4764–4769.

[100] Duker, A.; Szeimies, G. 1-Bromobicyclo[1.1.0]butanes and strong bases: products and mechanism. *Tetrahedron Letters* **1985**, *26*, 3555–3558.

[101] Silvi, M.; Aggarwal, V. K. Radical Addition to Strained σ-Bonds Enables the Stereocontrolled Synthesis of Cyclobutyl Boronic Esters. *J. Am. Chem. Sci.* **2019**, *141*, 9511–9515.

[102] Fawcett, A.; Biberger, T.; Aggarwal, V. K. Carbopalladation of C–C σ-bonds enabled by strained boronate complexes. *Nat. Chem.* **2019**, *11*, 117–122.

[103] Bennett, S. H.; Fawcett, A.; Denton, E. H.; Biberger, T.; Fasano, V.; Winter, N.; Aggarwal, V. Difunctionalization of C–C σ-Bonds Enabled by the Reaction of Bicyclo[1.1.0]butyl Boronate Complexes with Electrophiles: Reaction Development, Scope, and Stereochemical Origins. *J. Am. Chem. Soc.* **2020**, *142*, 16766–16775.

[104] Guo, L.; Noble, A.; Aggarwal, V. K. α-Selective Ring-Opening Reactions of Bicyclo[1.1.0]butyl Boronic Ester with Nucleophiles. *Angew. Chem., Int. Ed., 2021, 60, 212–216.* **2021**, *60*, 212–216.

[105] Pinkert, T.; Das, M.; Schrader, M. L.; Glorius, F. Use of Strain-Release for the Diastereoselective Construction of Quaternary Carbon Centers. *J. Am. Chem. Soc.* **2021**, *143*, 7648–7654.

[106] Schwartz, B. D.; Zhang, M. Y.; Attard, R. H.; Gardiner, M. G.; Malins, L. R. Structurally Diverse Acyl Bicyclobutanes: Valuable Strained Electrophiles. *Chem. Eur. J.* **2020**, *26*, 2808–2812.

[107] Walczak, M. A. A.; Wipf, P. Rhodium(I)-catalyzed cycloisomerizations of bicyclobutanes. *J. Am. Chem. Soc.* **2008**, *130*, 6924–6925.

[108] Milligan, J. A.; Busacca, C. A.; Senanayake, C. H.; Wipf, P. Hydrophosphination of Bicyclo[1.1.0]butane-1-carbonitriles. *Org. Lett.* **2016**, *18*, 4300–4303.

[109] Nilsen, N. O.; Skattebol, L.; Baird, M. S.; Buxton, S. R.; Slowey, P. D. A simple route to 1-bromobicyclo[1.1.0]butanes by intramolecular trapping of 1-bromo-1-lithiocyclopropanes. *Tetrahedron Letters* **1984**, *25*, 2887–2890.

[110] Panish, R.; Chintala, S. R.; Boruta, D. T.; Fang, Y.; Taylor, M. T.; Fox, J. M. Enantioselective Synthesis of Cyclobutanes via Sequential Rh-catalyzed Bicyclobutanation/Cu-catalyzed Homoconjugate Addition. *J. Am. Chem. Soc.* **2013**, *135*, 9283–9286.

[111] Chen, K.; Huang, X.; Kan, S. B. J.; Zhang, R. K.; Arnold, F. H. Enzymatic construction of highly strained carbocycles. *Science* **2018**, *360*, 71–75.

[112] Drujon, X.; Riess, G.; Jr., H. H. K.; Padias, A. B. Synthesis and polymerization of alkyl 1-bicyclobutanecarboxylates. *Macromolecules* **1993**, *26*, 1199–1205.

[113] McNamee, R. E.; Thompson, A. L.; Anderson, E. A. Synthesis and applications of polysubstituted bicyclo[1.1.0]butanes. *J. Am. Chem. Soc.* **2021**, *143*, 21246–21251.

[114] Bychek, R. M.; Hutskalova, V.; Bas, Y. P.; Zaporozhets, O. A.; Zozulya, S.; Leterov, V. V.; Mykhailiuk, P. K. Difluoro-Substituted Bicyclo[1.1.1]pentanes for Medicinal Chemistry: Design, Synthesis, and Characterization. *J. Org. Chem.* **2019**, *84*, 15106–15117.

[115] Song, Z. J.; Qi, J.; H., E. M.; Wang, J.; Yang, X.; Xiao, D. Two Scalable Syntheses of 3-(Trifluoromethyl)cyclobutane-1-carboxylic Acid. *Org. Process Res. Dev.* **2021**, *25*, 82–88.

[116] Dill, J. D.; Greenberg, A.; Liebman, J. F. Substituent effects on strain energies. *J. Am. Chem. Soc.* **1979**, *101*, 6814–6826.

[117] Kelly, C. B.; Milligan, J. A.; Tilley, L. J.; Sodano, T. M. Bicyclobutanes: from curiosities to versatile reagents and covalent warheads. *Chem. Sci.* **2022**, *13*, 11721–11737.

[118] Azran, C.; Hoz, S. Bridgehead substituents effect on the reactivity of bicyclobutane in its reactions with nucleophiles. A comparison with olefinic systems. *Tetrahedron* **1995**, *51*, 11421–11430.

[119] Schneider, T. F.; Kaschel, J.; Werz, D. B. A New Golden Age for Donor–Acceptor Cyclopropanes. *Angew. Chem. Int. Ed.* **2014**, *53*, 5504 – 5523.

[120] Pagenkopf, B. L.; Vemula, N. Cycloadditions of Donor–Acceptor Cyclopropanes and Nitriles. *Eur. J. Org. Chem.* **2017**, 2561–2567.

[121] Dhake, K.; Woelk, K. J.; Becica, J.; U, A.; Jenny, S. E.; Leitch, D. C. Beyond Bioisosteres: Divergent Synthesis of Azabicyclohexanes and Cyclobutenyl Amines from Bicyclobutanes. *Angew, Chem, Int. Ed.* **2022**, *61*, e202204719.

[122] Cairncross, A.; Blanchard, E. P. Bicyclo[1.1.0]butane Chemistry. II. Cycloaddition Reactions of 3-Methylbicyclo[1.1.0]butanecarbonitriles. The Formation of Bicyclo[2.1.1]hexanes. *J. Am. Chem. Soc.* **1966**, *88*, 496–504.

[123] Applequist, D. E.; Wheeler, L. W. Synthesis of 1,3-disubstituted bicyclo[1.1.1]pentanes. *Tetrahedron Lett.* **1977**, *18*, 3411–3412.

[124] Hall, H. K. J.; Padias, A. B. Bicyclobutanes and Cyclobutenes: Unusual Carbocyclic Monomers. *J. Polym. Sci. Part A: Polym. Chem.* **2002**, *41*, 625–635.

[125] Hall, H. K.; Blanchard, E. P.; Cherkofsky, S. C.; Sieja, J. B.; Sheppard, W. A. Synthesis and polymerization of 1-bicyclobutanecarbonitriles. *J. Am. Chem. Soc.* **1971**, *93*, 110–120.

[126] Liang, Y.; Paulus, F.; Daniliuc, C. G.; Glorius, F. Catalytic Formal [2π + 2σ] Cycloaddition of Aldehydes with Bicyclobutanes: Expedient Access to Polysubstituted 2-Oxabicyclo[2.1.1]hexanes. *Angew. Chem. Int. Ed.* **2023**, *62*, e202305043.

[127] Radhoff, N.; Daniliuc, C. G.; Studer, A. Lewis Acid Catalyzed Formal (3+2)-Cycloaddition of Bicyclo[1.1.0]butanes with Ketenes. *Angew, Chem, Int. Ed.* **2023**, *62*, e202204719.

[128] Xu, M.; Wang, Z.; Sun, Z.; Ouyang, Y.; Ding, Z.; Yu, T.; Xu, L.; Li, P. Diboron(4)-Catalyzed Remote [3+2] Cycloaddition of Cyclopropanesvia Dearomative/Rearomative Radical Transmission through Pyridine. *Angew. Chem. Int. Ed.* **2022**,

[129] Liu, Y.; Lin, S.; Li, Y.; Xue, J.; Li, Q.; Wang, H. Pyridine-Boryl Radical-Catalyzed [2π + 2σ] Cycloaddition of Bicyclo[1.1.0]butanes with Alkenes. *ACS Canal.* **2023**, *13*, 5096–5103.

[130] Ni, D.; Hu, S.; Tan, X.; Yu, Y.; Li, Z.; Deng, L. Intermolecular Formal Cycloaddition of Indoles with Bicyclo[1.1.0]butanes by Lewis Acid Catalysis. *Angew. Chem. Int. Ed.* **2023**, *62*, e202308606.

[131] Tang, L.; Xiao, Y.; Zhou, J.; Xu, T.; Feng, J. Silver-Catalyzed Dearomative [2π + 2σ] Cycloadditions of Indoles with Bicyclobutanes: Access to Indoline Fused Bicyclo[2.1.1]hexanes. *Angew. Chem. Int. Ed.* **2023**, *62*, e202310066.

[132] Ten, H.; Li, T.; Xing, J.; Li, Z.; Zhang, Y.; Yu, X.; Zheng, J. Ti-Catalyzed Formal [2π + 2σ] Cycloadditions of Bicyclo[1.1.0]butanes with 2-Azadienes to Access Aminobicyclo[2.1.1]hexanes. *Organic Letters* **2024**, *26*, 1745–1750.

[133] Lui, Y.; Wu, Z.; Shan, J.; Yan, H.; Hao, E.; Shi, L. Titanium catalyzed [$2\pi + 2\sigma$] cycloaddition of bicyclo[1.1.0]-butanes with 1,3-dienes for efficient synthesis of stilbene bioisosteres. *Nature Communications* **2024**, *15*, 4374.

[134] Turkowska, J.; Durka, J.; Gryko, D. Strain release – an old tool for new transformations. *Chem. Commun.* **2020**, *56*.

[135] Hoz, S.; Auerbach, D. Cyclobutane-bicyclobutane system—I: The relative reactivity of the central bond in bicyclobutanecarbonitrile and the double bond in crotononitrile in nucleophilic reactions. *Tetrahedron* **1979**, *35*, 881–883.

[136] Gaoni, Y. Regiospecific additions of hydrazoic acid and benzylamine to 1-(arylsulfonyl)bicyclo[1.1.0]Butanes. Application to the synthesis of cis and trans 2,7-methanoglutamic acids. *Tetrahedron Lett.* **1988**, *29*, 1591–1594.

[137] Gaoni, Y. Synthesis of Aminocyclobutane Mono- and Dicarboxylic Acids and Derivatives Thereof from (phenylsulfonyl)bicyclobutanes. *Organic Preparations and Procedures International* **1995**, *27*, 185–212.

[138] Lopchuk, J. M. et al. Strain-Release Heteroatom Functionalization: Development, Scope, and Stereospecificity. *J. Am. Chem. Soc.* **2017**, *139*, 3209–3226.

[139] Gaoni, Y. Conjugate addition of organocopper reagents to 1-arylsulfonylbicyclobutanes. synthesis of the racemic form of the sex pheromone of the citrus mealybug, Planococcus citri (Risso). *Tetrahedron Lett.* **1982**, *23*, 5215–5218.

[140] Gaoni, Y.; Tomažič, A. B. Bridgehead reactivity, nucleophilic and radical additions, and lithium aluminum hydride reduction of 1-(arylsulfonyl) bicyclobutanes: general access to substituted, functionalized cyclobutanes. Syntheses of (±)-citrilol acetate, (±)-junionone, and the tricyclo[3.3.0.01,4] octane and tricyclo[4.3.0.01,7]nonane ring systems. *J. Org. Chem.* **1985**, *50*, 2948–2957.

[141] Gaoni, Y.; Tomazic, A.; Potgieter, E. Stereochemistry of addition of organocopper reagents and of the hydride ion to 1-(arylsulfonyl)bicyclo[1.1.0]butanes. *J. Org. Chem.* **1985**, *50*, 2943–2947.

[142] Gaoni, Y. New bridgehead-substituted 1-(arylsulfonyl)bicyclo[1.1.0]butanes and some novel addition reactions of the bicyclic system. *Tetrahedron* **1989**, *45*, 2819–2840.

[143] Wu, X.; Hat, W.; Ye, K.; Jiang, B.; Pombar, G.; Song, Z.; Lin, S. Ti-Catalyzed Radical Alkylation of Secondary and Tertiary Alkyl Chlorides Using Michael Acceptors. *J. Am. Chem. Soc.* **2018**, *140*, 14836–14843.

[144] Ernouf, G.; Chirkin, E.; Rhyman, L.; Ramasami, P.; Cintrat, J. Photochemical Strain-Release-Driven Cyclobutylation of C(sp^3)-Centered Radicals. *Angew. Chem. Int. Ed.* **2020**, *59*, 2618–2622.

[145] Pratt, C. J.; Ayock, R. A.; King, M. D.; Jui, N. T. Radical σ-C–H cyclobutylation of aniline derivatives. *Synlett* **2020**, *31*, 51–54.

[146] Yu, X.; Lübbesmeyer, M.; Studer, A. Oligosilanes as silyl radical precursors through oxidative Si-Si bond cleavage using redox catalysis. *Angew. Chem. Int. Ed.* **2021**, *60*, 675–679.

[147] Ueda, M.; Walczak, M. A. A.; Wipf, P. Formal Alder-ene reaction of a bicyclo[1.1.0]butane in the synthesis of the tricyclic quaternary ammonium core of daphniglaucins. *Tetrahedron Lett.* **2008**, *49*, 5986–5989.

[148] Kerner, M.; Wipf, P. Semipinacol-typerearrangementsof[3-(Arylsulfonyl) bicyclo[1.1.0]butan-1-yl]alkanols. *Org. Lett.* **2021**, *23*, 3615–3619.

[149] Ociepa, M.; Wierzba, A. J.; Turkowska, J.; Gyro, D. Polarity-Reversal Strategy for the Functionalization of Electrophilic Strained Molecules via Light-Driven Cobalt Catalysis. *J. Am. Chem. Soc.* **2020**, *142*, 5355–5361.

[150] McNamee, R. E.; Haugland, M. M.; Nugent, J.; Chan, R.; Christensen, K. E.; Anderson, E. A. Synthesis of 1,3-disubstituted bicyclo[1.1.0]butanes via directed bridgehead functionalization. *Chem. Sci.* **2021**, *12*, 7480–7485.

[151] Dargazanli, G.; Estenne-Bouhtou, G.; Mafroud, A. K. N-[(2-azabicyclo[2.1.1]hex-1- yl]-aryl-methyl]-benzamide derivatives, preparation thereof, and therapeutic use thereof. US Patent WO2010092286A1, 2010.

[152] Chu, D. Novel inhibitors of poly(adp-ribose)polymerase (parp). US Patent US20090062268A1, 2009.

[153] Desai, M. C.; Ji, M.; Jin, H.; Martin, T. A. T.; Pyun, H.-J. Substituted pyrido[1',2':4,5]pyrazino[1,2-a]azepines for treating viral infections. US Patent US9458159B2, 2016.

[154] Ma, X.; Sloman, D. L.; Han, Y.; Bennett, D. J. A Selective Synthesis of 2,2- Difluorobicyclo[1.1.1]pentane Analogues: "BCP-F2". *Org. Lett.* **2019**, *21*, 7199–7208.

[155] Denisenko, A.; Garbuz, P.; Shishkina, S. V.; Voloshchuk, N. M.; Mykhailiuk, P. K. Saturated Bioisosteres of ortho-Substituted Benzenes. *Angew. Chem. Int. Ed.* **2020**, *59*, 20515–20521.

[156] Levterov, V. V.; Panasyuk, Y.; Pinvytska, V. O.; Mykhailiuk, P. K. Water-Soluble Non-Classical Benzene Mimetics. *Angew. Chem. Int. Ed.* **2020**, *59*, 7161–7167.

[157] Levterov, V. V.; Michurin, O.; Borysko, P. O.; Zozulya, S.; Sadkova, I. V.; Tolmachev, A. A.; Mykhailiuk, P. K. Photo-chemical In-Flow Synthesis of 2,4-Methanopyrrolidines: Pyr-rolidine Analogues with Improved Water Solubility and Reduced Lipophilicity. *J. Org. Chem.* **2018**, *83*, 14350–14361.

[158] Pirrung, M. C. Total Synthesis of 2,4-Methanaproline. *Tetrahedron Lett.* **1980**, *21*, 4577–4578.

[159] Hughes, P.; Martin, M.; Clardy, J. Synthesis of 2,4-Methanoproline. *Tetrahedron Lett.* **1980**, *21*, 4579–4580.

[160] Stevens, C.; De Kimpe, N. A New Entry into 2-Azabicy-clo[2.1.1]Hexanes via 3-(Chloromethyl)Cyclobutanone. *J. Org. Chem.* **1996**, *61*, 2174–2178.

[161] Liao, H.; Li, A.; Chen, X.; Liang, K.; Shen, Y.; Liang, Q.; Xu, K.; Shore, D.; Villemure, E.; Siu, M.; Huestis, M. Preparation of 2-Azabicyclo[2.1.1]Hexane Hydrochloride. *Synlett.* **2016**, *27*, 2251–2253.

[162] Krow, G. R.; Herzon, S. B.; Lin, G.; Qiu, F.; Sonnet, P. E. Complex-Induced Proximity Effects. Temperature-Dependent Regiochemical Diversity in Lithiation-Electrophilic Substitution Reactions of N-BOC-2-Azabicyclo[2.1.1]Hexane. 2,4- and 3,5-Methanoprolines. *Org. Lett.* **2002**, *4*, 3151–3154.

[163] Krow, G. R.; Shoulders, M. D.; Edupuganti, R.; Gandla, D.; Yu, F.; Sonnet, P. E.; Sender, M.; Choudhary, A.; DeBrosse, C.; Ross, C. W.; Carroll, P.; Raines, R. T. Synthesis of 5-Fluoro- and 5-Hydroxymethanoprolines via Lithiation of N-BOCMethanopyrrolidines. Constrained Cy-Exo and Cy-Endo Flp and Hyp Conformer Mimics. *J. Org. Chem.* **2012**, *77*, 5331–5344.

[164] Krow, G. R.; Gandla, D.; Cannon, K. C.; Ross, C. W.; Carroll, P. J. C1-Substituted NTert-Butoxycarbonyl-5-Syn-Tert-Butyl-dimethylsilyloxymethyl-2-Azabicyclo[2.1.1]Hexanes as Conformationally Constrained B-Amino Acid Precursors. *Hetero-cyclic Commun.* **2016**, *22*, 319–328.

[165] Singh, P.; Varshnaya, R. K.; Dey, R.; Banerjee, P. Donor–Acceptor Cyclopropanes as an Expedient Building Block Towards the Construction of Nitrogen-Containing Molecules:An Update. *Adv. Synth. Catal.* **2020**, *362*, 1447–1484.

[166] Alter, P. B.; Meyers, C.; Lerchner, A.; Riegel, D. R.; Carreira, E. M. Eine neuartige Methode zur Synthese von Spiro[pyrrolidin-3,3'-oxindolen]: katalysierte Ringerweiterung von Cyclopropanen mit Aldiminen. *Angew. Chem.* **1999**, *111*, 3379–3381.

[167] Carson, C. A.; Kerr, M. A. Diastereoselective Synthesis ofPyrrolidines via the $Yb(OTf)_3$ Catalyzed Three-Component Reaction of Aldehydes ,Amines, and 1,1-Cyclopropanediesters. *J. Org. Chem.* **2005**, *70*, 8242–8244.

[168] Jackson, S. K.; Karadeolian, A.; Driega, A. B.; Kerr, M. A. Stereodivergent Methodology for the Synthesis of Complex Pyrrolidines. *J. Am. Chem. Soc.* **2008**, *130*, 4196–4201.

[169] Parsons, A. T.; Smith, A. G.; Neil, A. J.; Johnson, J. S. Dynamic Kinetic Asymmetric Synthesis of Substituted Pyrrolidines from Racemic Cyclopropanes and Aldimines: Reaction Development and Mechanistic Insights. *J. Am. Chem. Soc.* **2010**, *132*, 9688–9692.

[170] Bouffard, J.; Itami, K. A Nickel Catalyst for the Addition of Organoboronate Esters to Ketones and Aldehydes. *Org. Lett.* **2009**, *11*, 4410–4413.

[171] Liu, G.; Lu, X. Cationic Palladium Complex Catalyzed Highly Enantioselective Intramolecular Addition of Arylboronic Acids to Ketones. A Convenient Synthesis of Optically Active Cycloalkanols. *J. Am. Chem. Soc.* **2006**, *128*, 16504–16505.

[172] Matsuda, T.; Makino, M.; Murakami, M. Addition/Ring-Opening Reaction of Organoboronic Acids to Cyclobutanones Catalyzed by Rhodium(I)/P(t-Bu)$_3$ Complex. *Bull. Chem. Soc. Jpn.* **2005**, *78*, 1528.

[173] Matsuda, T.; Makino, M.; Murakami, M. Rhodium-Catalyzed Addition/Ring-Opening Reaction of Arylboronic Acids with Cyclobutanones. *Org. Lett.* **2004**, *6*, 1257–1259.

[174] Tan, J.; Kuang, Y.; Wang, Y.; Huang, Q.; Zhu, J.; Wang, Y. Axial Tri-tert-butylphosphane Coordination to $Rh_2(OAc)_4$: Synthesis, Structure, and Catalytic Studies. *Organometallics* **2016**, *35*, 3139–3147.

[175] Manolikakes, S. M.; Ellwart, M.; Stathakis, C. I.; Knochel, P. Air-Stable Solid Aryl and Heteroaryl Organozinc Pivalates: Syntheses and Applications in Organic Synthesis. *Chem Eur, J.* **2014**, *20*, 12289–12297.

[176] Bernhardt, S.; Manolikakes, G.; Kunz, T.; Knochel, P. Preparation of Solid Salt-Stabilized Functionalized Organozinc Compounds and their Application to Cross-Coupling and Carbonyl Addition Reactions. *Angew. Chem. Int. Ed.* **2011**, *50*, 9205–9209.

[177] Feula, A.; Dhillon, S. S.; Byravan, R.; Sangha, M.; Ebanks, R.; Salih, M. A. H.; Spencer, N.; Male, L.; Magyary, I.; Deng, W. P.; Muller, F.; Fossey, J. S. Synthesis of azetidines and pyrrolidines via iodocyclisation of homoallyl amines and exploration of activity in a zebrafish embryo assay. *Org. Biomol. Chem.* **2013**, *11*, 5083–5093.

[178] Woelk, K. J.; Dhake, K.; Schley, N. D.; Leitch, D. C. Enolate addition to bicyclobutanes enables expedient access to 2-oxo-bicyclohexane scaffolds. *Chem. Commun.* **2023**, *59*, 13847–13850.

[179] Newman-Evans, R. H.; Simon, R. J.; Carpenter, B. K. The influence of intramolecular dynamics on branching ratios in thermal rearrangements. *J. Org. Chem* **1990**, *55*, 695–711.

[180] Herter, L.; Koutsopetras, I.; Turelli, L.; Fessard, T.; Salome, C. Preparation of new bicyclo[2.1.1]hexane compact modules: an opening towards novel sp^3-rich chemical space. *Org. Biomol. Chem.* **2022**, *20*, 9108–9111.

[181] Iida, T.; Kanazawa, J.; Matsunaga, T.; Miyamoto, K.; Hirano, K.; Uchiyama, M. Practical and Facile Access toBicyclo[3.1.1]heptanes: Potent Bioisosteres of meta-Substituted Benzenes. *J. Am. Chem. Soc.* **2022**, *144*, 21848–21852.

[182] Zheng, Y.; Huang, W.; Dhungana, R. K.; Granados, A.; Keess, S.; Makvandi, M.; Molander, G. A. Photochemical Intermolecular [3σ +2σ]-Cycloaddition for the Construction of Aminobicyclo[3.1.1]heptanes. *J. Am. Chem. Soc.* **2022**, *144*, 23685–23690.

[183] Nguyen, T. V. T.; Bossonnet, A.; Wodrich, M. D.; Waser, J. Photocatalyzed [2σ + 2σ] and [2σ + 2π] Cycloadditions for the Synthesis of Bicyclo[3.1.1]heptanes and 5-or 6-Membered Carbocycles. *J. Am. Chem. Soc.* **2023**, *145*, 25411–25421.

[184] Yu, T.; Yang, J.; Wang, Z.; Ding, Z.; Xu, M.; Wen, J.; Xu, L.; Li, P. Selective [2σ +2σ] Cycloaddition Enabled by Boronyl Radical Catalysis: Synthesis of Highly Substituted Bicyclo[3.1.1]heptanes. *J. Am. Chem. Soc.* **2023**, *145*, 4304–4310.

[185] Zhang, J.; Su, J.; Zheng, H.; Li, H.; Deng, W. Eu(OTf)$_3$-Catalyzed Formal Dipolar [4π + 2σ] Cycloaddition of Bicyclo-[1.1.0]butanes with Nitrones: Access toPolysubstituted 2-Oxa-3-azabicyclo[3.1.1]heptanes. *Angew. Chem.* **2024**, *136*, e202318476.

[186] Lin, Z.; Ron, H.; Lin, X.; Yu, X.; Zheng, J. Synthesis of Azabicyclo[3.1.1]heptenes Enabled by Catalyst-Controlled Annulations of Bicyclo[1.1.0]butanes with Vinyl Azides. *J. Am. Chem. Soc.* **2024**, *146*, 18565–18575.

[187] Liu, Y.; Lin, S.; Ding, Z.; Li, Y.; Tang, Y. J.; Xue, J. H.; Li, Q.; Li, P.; Wang, H. Pyridine-Boryl Radical-Catalyzed [$3\pi + 2\sigma$] Cycloaddition for the Synthesis of Pyridine Bioisosteres. *ChemRxiv* **2024**,

[188] Liang, Y.; Nematswerani, R.; Daniliuc, C. G.; Glorius, F. Silver-Enabled Cycloaddition of Bicyclobutanes with Isocyanides for the Synthesis of Polysubstituted 3-Azabicyclo[3.1.1]heptanes. *Angew. Chem. Int. Ed.* **2024**, *63*, e202402730.

[189] Wang, X.; Tao, R.; Li, X. Catalytic Asymmetric Construction of Chiral Polysubstituted 3-Azabicyclo[3.1.1]heptanes by Copper-Catalyzed Stereoselective Formal [4π + 2σ] Cycloaddition. *J. Am. Chem. Soc.* **2024**, *136*, 21069–21077.

[190] Funt, L. D.; Novikov, M. S.; Khlebnikov, A. F. New applications of pyridinium ylides toward heterocyclic synthesis. *Tetrahedron.* **2020**, *76*, 131415.

[191] Zhang, X. M.; Bordwell, F. G.; Puy, M. V. D.; Fried, H. E. Equilibrium acidities and homolytic bond dissociation energies of the acidic carbon-hydrogen bonds in N-substituted trimethylammonium and pyridinium cations. *J. Org. Chem.* **1993**, *58*, 3060–3066.

[192] Rates, K. W.; Phillips, W. G. Basicity of N-ylides. *J. Org. Chem.* **1970**, *35*, 3144–3147.

[193] Allgäuer, D. S.; Mayer, P.; Mayr, H. Nucleophilicity Parameters of Pyridinium Ylides and Their Use in Mechanistic Analyses. *J. Am. Chem. Soc.* **2013**, *135*, 15216–15224.

[194] Bonte, S.; Ghinea, I. O.; Dinica, R.; Baussanne, I.; Demeunynck, M. Investigation of the Pyridinium Ylide—Alkyne Cycloaddition as a Fluorogenic Coupling Reaction. *Molecules* **2016**, *21*, 332.

[195] Dega-Szafran, Z.; Schroeder, G.; Szafran, M.; Szwajca, A.; Leska, B.; Lewandowska, M. Experimental and quantum chemical evidences for C–H-N hydrogen bonds involving quaternary pyridinium salts and pyridinium ylides. *Journal of Molecular Structure* **2000**, *555*, 31–42.

[196] Hu, R.-B.; Sun, S.; Su, Y. Visible-Light-Induced Carbo-2-pyridylation of Electron-Deficient Alkenes with Pyridinium Salts. *Angew. Chem. Int. Ed.* **2017**, *56*, 10877–10880.

[197] Grundke, C.; Vierengel, N.; Opatz, T. α-Aminonitriles: From Sustainable Preparation to Applications in Natural Product Synthesis. *Chem. Rec.* **2020**, *20*, 989–1016.

[198] Jia, H.; Liu, H.; Gus, Z.; Huang, J.; Guo, H. Tandem [3 + 2] Cycloaddition/1,4-Addition Reaction of Azomethine Ylides and Aza-*o*-quinone Methides for Asymmetric Synthesis of Imidazolidines. *Org. Lett.* **2017**, *19*, 5236–5239.

[199] Smyrnov, O.; Melnykov, K. P.; Semeno, V.; Liashuk, O. S.; Grygorenko, O. O. α-CF3-Substituted Saturated Bicyclic Amines: Advanced Building Blocks for Medicinal Chemistry. *Eur. J. Org. Chem.* **2024**, *27*, e202300935.

[200] P., H.; Clardy, J. Total synthesis of cyclobutane amino acids from *Atelia herbert smithii*. *J. Org. Chem.* **1988**, *53*, 4793–4796.

[201] Faith, W. C.; Booth, C. A.; Foxman, B. M.; Snider, B. B. An Approach to the Synthesis of Neplanocin A. *J. Org. Chem.* **1985**, *50*, 1983–1985.

[202] Singh, R.; Vince, R. 2-Azabicyclo[2.2.1]hept-5-en-3-one: Chemical Profile of a Versatile Synthetic Building Block and its Impact on the Development of Therapeutics. *Chem. Rev.* **2012**, *112*, 4642–4686.

[203] Smith, S. N.; Trujillo, C.; Connon, S. J. Catalytic, asymmetric azidations at carbonyls: achiral and *meso*-anhydride desymmetrisation affords enantioenriched γ-lactams. *Org, Biomol. Chem.* **2022**, *20*, 6384.

[204] Li, H.; Tian, H.; Chen, Y.; Wang, D.; Li, C. Novel chiral gallium Lewis acid catalysts with semi-crown ligands for aqueous asymmetric Mukaiyama aldol reactions. *Chem. Commun.* **2002**, *24*.

[205] Aimo, G.; Degani, I.; Fochi, R. New Route to Esters from 2-Substituted 1,3-Benzoxathiolium Tetrafluoroborates. An Effective Protection of Esters against Nucleophilic Attack. *Synthesis* **1979**, *3*, 223.

[206] Song, B.; Rudolphi, F.; Hummler, T.; Goossen, L. J. Practical Synthesis of 2-Arylacetic Acid Esters via Palladium- Catalyzed Dealkoxycarbonylative Coupling of Malonates with Aryl Halides. *Adv. Synth. Catal.* **2011**, *353*, 1565.

[207] Matulenko, M. A. et al. 4-Amino-5-aryl-6-arylethynylpyrimidines: Structure-activity relationships of non-nucleoside adenosine kinase inhibitors. *Bioorg. Med. Chem.* **2007**, *15*, 1586.

[208] Hiroshi, Y.; Masayuki, A.; Yoshinori, K.; Takao, S. Studies on Pyrimidine Derivatives. XXXVIII. Cross-Coupling Reaction of N-Heteroaryl Iodides with Ethoxycarbonylmethylzinc Bromide in the Presence of Palladium Catalyst. *Chem. Pharm. Bull.* **1985**, *33*, 4309.

[209] Song, B.; Himmler, T.; Goossen, L. J. Palladium Copper-Catalyzed Di-α-arylation of Acetic Acid Esters. *Adv. Synth. Catal.* **2011**, *353*, 1688.

[210] Kondoh, A.; Odaira, K.; Terada, M. Ring Expansion of Epoxides under Brønsted Base Catalysis: Formal [3+2] Cycloaddition of β,γ-Epoxy Esters with Imines Providing 2,4,5-Trisubstituted 1,3-Oxazolidines. *Angew. Chem. Int. Ed.* **2015**, *54*, 11240.

[211] Wager, T. T. Histamine-3 receptor antagonists. US Patent WO2006136924-A1, 2009.

[212] Schwartz, B. D.; Smyth, A. P.; Nashar, P. E.; Gardiner, M. G.; Malins, L. R. Investigating bicyclobutane-triazolinedione cycloadditions as a tool for peptide modification. *Org. Lett.* **2022**, *24*, 1268.

[213] Tokunaga, K.; Sato, M.; Kuwata, K.; Miura, C.; Fuchida, H.; Matsunaga, N.; Koyanagi, S.; Ohdo, S.; Shindo, N.; Ojida, A. Bicyclobutane Carboxylic Amide as a Cysteine-Directed Strained Electrophile for Selective Targeting of Proteins. *J. Am. Chem. Soc.* **2020**, *142*, 18522–18531.

[214] Muller, T. E.; Hultzsch, K. C.; Yus, M.; Foubelo, F.; Tada, M. Hydroamination: Direct Addition of Amines to Alkenes and Alkynes. *Chem. Rev.* **2008**, *108*, 3795–3892.

[215] Hanson, R. M. The synthetic methodology of nonracemic glycidol and related 2,3-epoxy alcohols. *Chem. Rev.* **1991**, *91*, 437–475.

[216] Thirumalaikumar, M. Ring Opening Reactions of Epoxides. A Review. *Organic Preparations and Procedures International* **2021**, *51*, 1–39.

Appendix A

Supporting Information for Chapter 2

Contributions: The following data reported has been completed **independently** with supporting work from supervised undergraduate students.

A.1 General Considerations

Materials:All solvents and common organic reagents were purchased from commercial suppliers and used without further purification. Organic building blocks and starting materials were purchased from Oakwood Chemicals and used as received. All Lewis acids were purchased from Strem Chemicals and used as received. Anhydrous solvents (SureSeal) were purchased from MilliporeSigma and used as received.

Techniques:All air-free manipulations were performed under a dry nitrogen atmosphere using an MBraun glovebox. High-throughput experimentation was performed using 1 mL capacity glass shell vials in sealable aluminum reaction blocks purchased from Analytical Sales. Heating/stirring was achieved using rare-earth magnetic tumble stirrers acquired from V&P Scientific.

Analysis and Spectroscopy: All NMR spectra were acquired on either a Bruker AVANCE 300 MHz spectrometer or a Bruker AVANCE Neo 500 MHz spectrometer. All ^{1}H and ^{13}C NMR spectra chemical shifts are calibrated to residual protio-solvents. All NMR spectroscopic data is processed using Bruker TopSpin 4.07. High-resolution electrospray ionization mass spectrometric analysis was performed using a Thermo Scientific Ultimate 3000 ESI-Orbitrap Exactive Plus.

A.2 1,2-Addition

General Procedure for Rh catalyzed 1,2-Addition (Table A.1):

Methyl 3-oxocyclobutanecarboxylic acid (20.0 mg, 0.156 mmol, 1 equiv) and phenyl boronic acid (20.9 mg, 0.172 mmol, 1.1 equiv) were weighed into six 4-mL vials with red septa teflon caps containing stir bars. The base (K_2CO_3 (1.1 mg, 0.008 mmol, 5 mol%) or KOAc (0.8 mg, 0.008 mmol, 5 mol%)) was then added to the appropriate vials. The vials were brought into a N_2 glovebox and then the Rh catalyst (either $Rh_2(OAc)_4(P(tBu_3)_2$ precatalyst (1.3 mg, 1 mol %) or $Rh_2(OAc)_4$ (7.0 mg, 1 mol %) plus $P(tBu)_3$ 50 mol% in toluene (1.51 μL, 4 mol %)) was added to the appropriate vials. CPME (0.25 mL) was added to all of the vials and then they were sealed and taken out of the glovebox. Then degassed H_2O (0.25 mL) was injected to all vials and they were stirred at 90 °C for 1 hour. The solvent was evaporated and ^1H NMR spectra were taken. Product conversion was determiend relative to remaining starting material by NMR spectroscopy (Starting material 3.55-3.16 ppm and product 2.97-2.53 ppm).

Table A.1: Rh catalyzed 1,2-Addition Screen

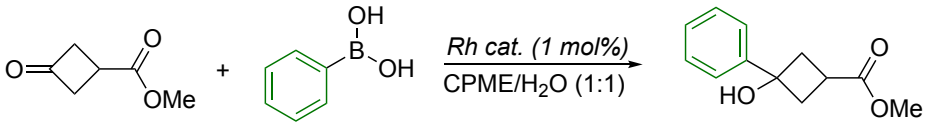

Entry	Catalyst	Base	% Conversion
1	$Rh_2(OAc)_4(P(tBu_3)_2$	no base	37
2	$Rh_2(OAc)_4(P(tBu_3)_2$	K_2CO_3	56
3	$Rh_2(OAc)_4(P(tBu_3)_2$	KOAc	21
4	$Rh_2(OAc)_4$ and $P(tBu)_3$	no base	60
5	$Rh_2(OAc)_4$ and $P(tBu)_3$	K_2CO_3	49
6	$Rh_2(OAc)_4$ and $P(tBu)_3$	KOAc	52

^{1}H NMR (300 MHz, $CDCl_3$, 292K, ppm) Table A.1, Entry 1:

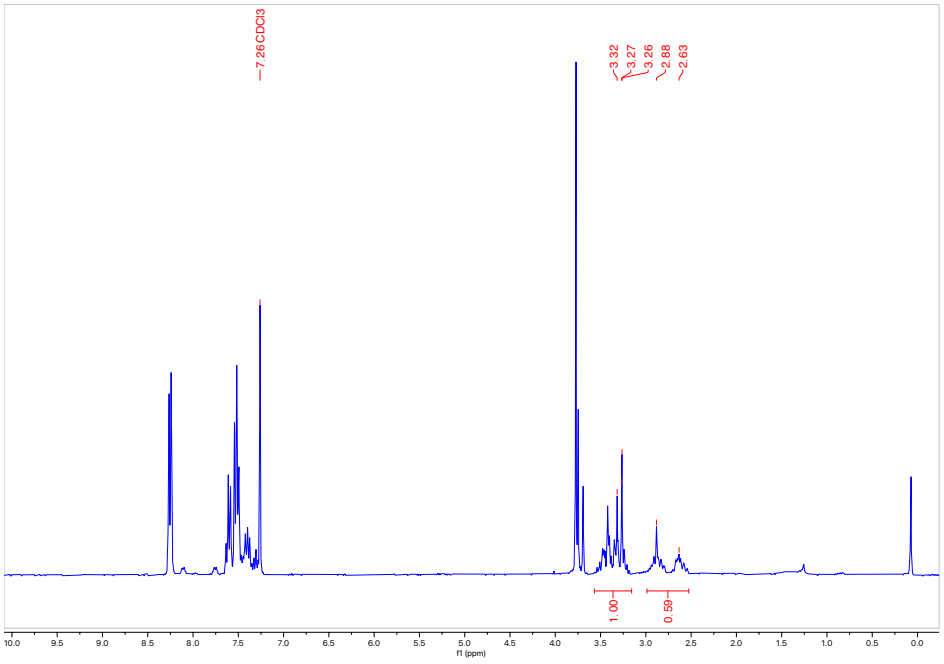

^{1}H NMR (300 MHz, $CDCl_3$, 292K, ppm) Table A.1, Entry 2:

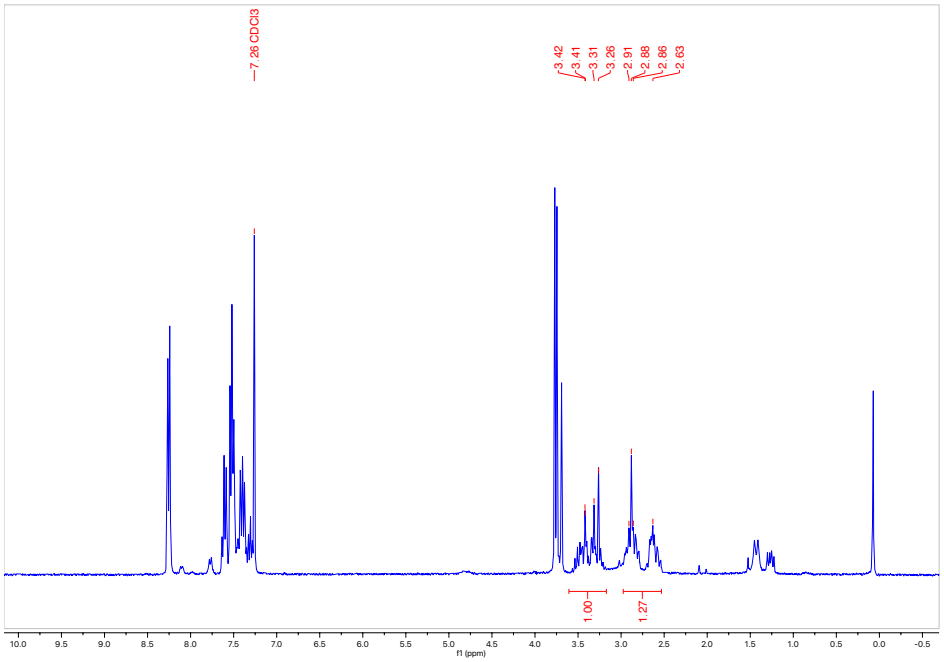

^{1}H NMR (300 MHz, $CDCl_3$, 292K, ppm) Table A.1, Entry 3:

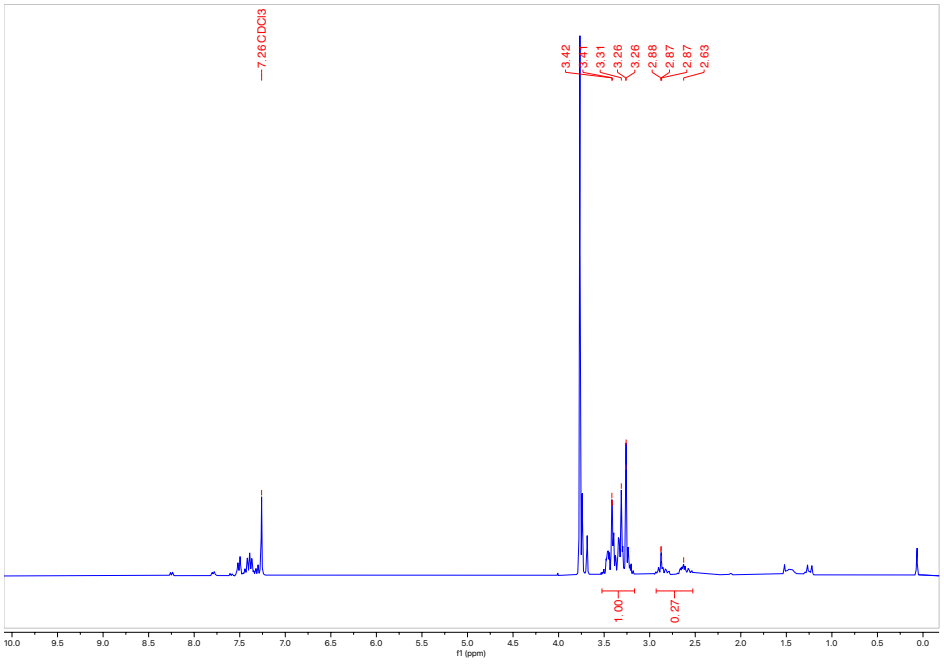

^{1}H NMR (300 MHz, $CDCl_3$, 292K, ppm) Table A.1, Entry 4:

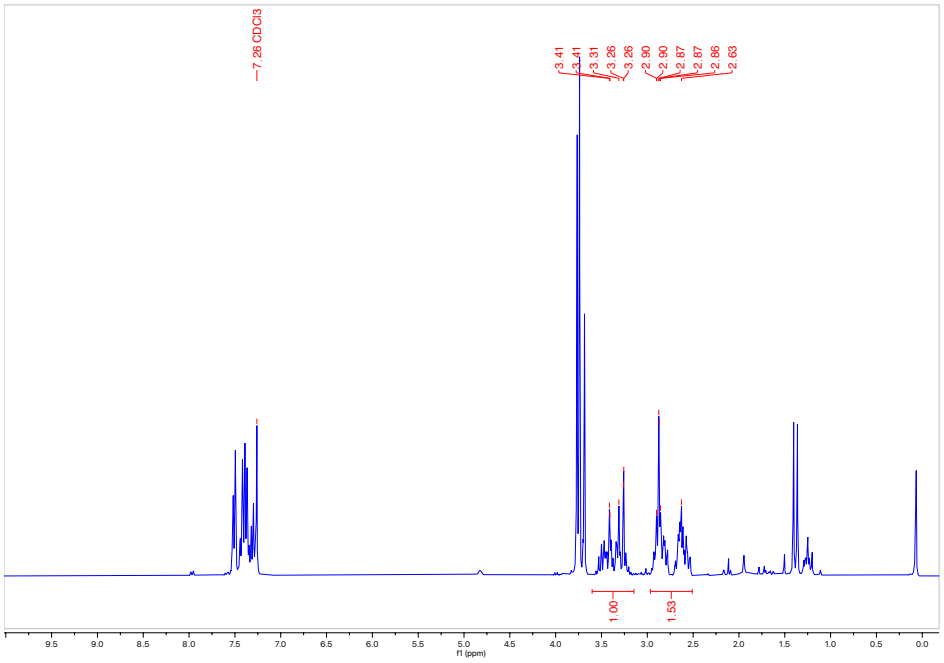

^{1}H NMR (300 MHz, $CDCl_3$, 292K, ppm) Table A.1, Entry 5:

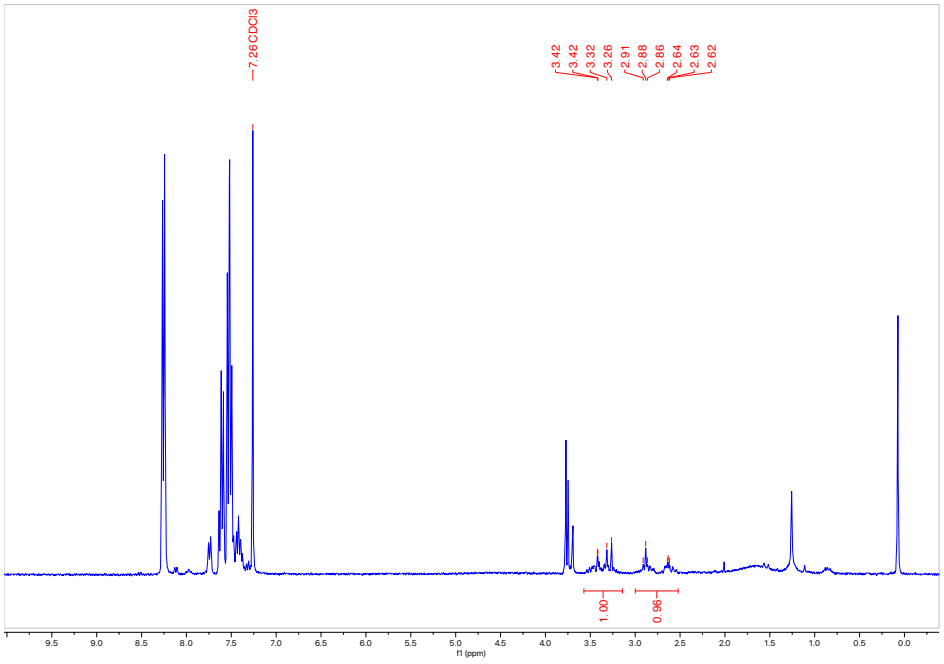

^{1}H NMR (300 MHz, $CDCl_3$, 292K, ppm) Table A.1, Entry 6

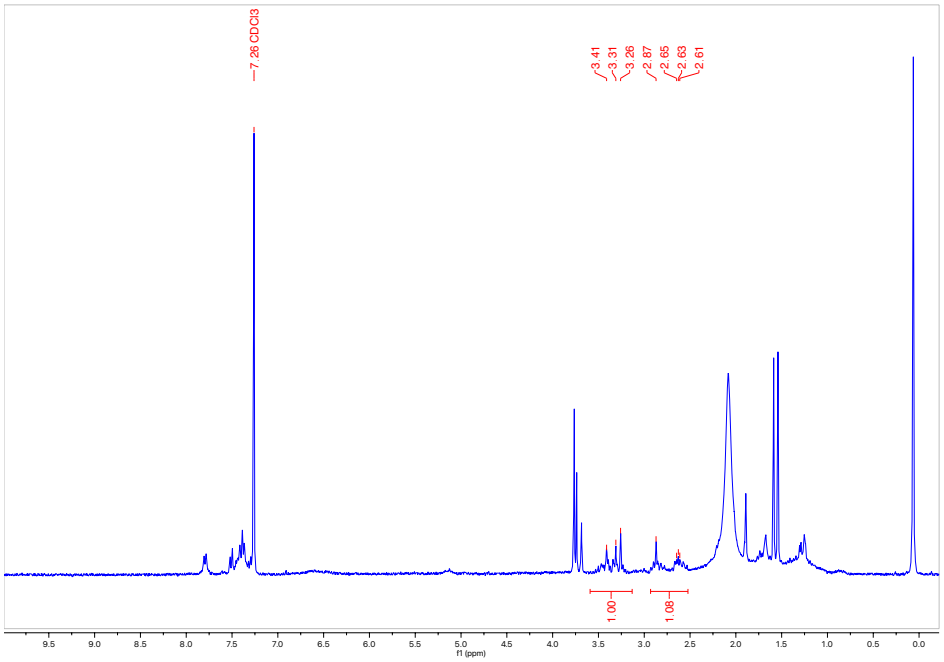

General Procedure for HTE Screening for Pd catalyzed 1,2-Addition (Table A.2):

Under a N_2 atmosphere, the palladium source was dispensed into all 24 reaction vials (1 mL shells) then the ligand was added to the appropriate vials. Two stock solutions of Methyl 3-oxocyclobutanecarboxylic acid (0.04 mmol, 1 equiv) and phenyl boronic acid (0.08 mmol, 2 equiv) were prepared in THF (one with K_2CO_3 and one without base) and the solution was added to all vials. The vials were sealed then stirred at 70 °C for 24 hours. The solvent was then evaporated and the results were analyzed by ^{1}H NMR spectroscopy. Only ring opened product was observed.

Table A.2: Pd catalyzed HTE Screen Variables

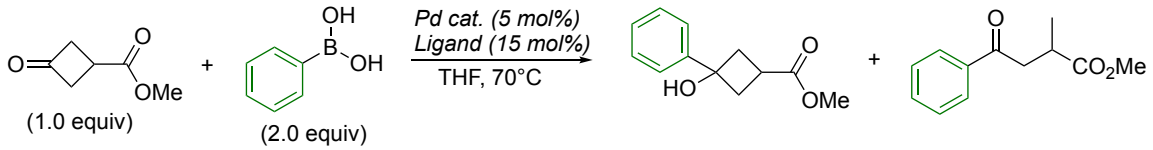

Pd Source (5 mol%)	Ligand	Base (1.5 equiv)
$Pd(OAc)_2$	bpy (15 mol%)	no base
$[Pd(allyl)Cl]_2$	PPh_3 (30 mol%)	K_2CO_3
	NHC (15 mol%)	
	BINAP (30 mol%)	
	dppf (15 mol%)	
	dppp (15 mol%)	

bpy = 2,2'-Bipyridine, NHC = 1,3-Bis(2,6-diisopropylphenyl)-1,3-dihydro-2H-imidazol-2-ylidene, BINAP = 2,2'-bis(diphenylphosphino)-1,1'-binaphthyl, dppf = 1,1'-Bis(diphenylphosphino)ferrocene, and dppe = 1,2-Bis(diphenylphosphino)ethane

General Procedure for HTE Screening for Pd catalyzed 1,2-Addition with NHC ligand (Table A.3):

Under a N_2 atmosphere, the palladium source was dispensed into all 24 reaction vials (1 mL shells) then the ligand was added to the vials. Stock solutions of Methyl 3-oxocyclobutanecarboxylic acid (0.04 mmol, 1 equiv) and phenyl boronic acid (0.08 mmol, 2 equiv) were prepared in the appropriate solvents (one with K_2CO_3 and one without base) and the solution was added to all vials. The additive was then added to the appropriate vials. The vials were sealed then stirred at 70 °C for 24 hours. The solvent was then evaporated and the results were analyzed by ^{1}H NMR spectroscopy. Only ring opened product was observed.

Table A.3: Pd/NHC catalyzed HTE Screen Variables

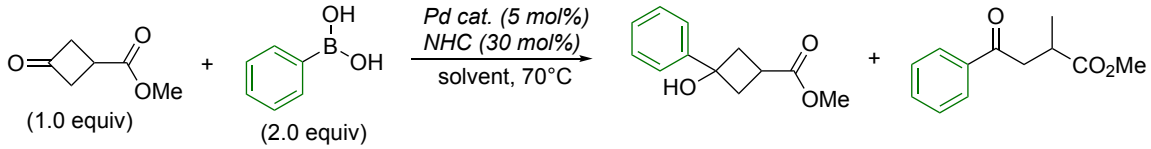

Pd Source (5 mol%)	Solvent	Additive (1.5 equiv)
$Pd(OAc)_2$	Toluene	no base
	THF	K_2CO_3 (1.5 equiv)
	t-amyl alcohol	Ac_2O (0.2 or 1.5 equiv)
	DMA	AcOH (0.2 or 1.5 equiv)

1,2-Addition on benzyl 3-oxocyclobutanecarboxylic acid using zinc:

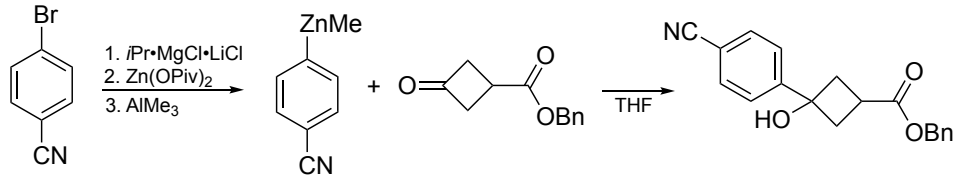

In a 20-mL vial containing a stir bar was added 4-bromobenzonitrile (0.20 g, 1.0 equiv, 1.1 mmol) and brought into a N_2 glovebox. THF (5.0 mL, 0.22 M) was added to the vial and it was cooled down to −20 °C in the glovebox freezer followed by the dropwise addition of 1.3 M *i*Pr·MgCl·LiCl solution in THF (0.93 mL, 1.1 equiv, 1.2 mmol) and the reaction was stirred overnight at room temperature. Solid zinc pivalate (388.2 mg, 1.2 equiv, 1.5 equiv) was added to the reaction and it was left to stir at rt for 15 minutes in the glovebox. A solution of 2.0 M Trimethylaluminium in toluene (0.55 mL, 1.0 equiv, 1.1 mmol) was added to the vial and it was left to stir for 10 minutes at room temperature. Benzyl 3-oxocyclobutanecarboxylic acid (224.4 mg, 1.0 equiv, 1.1 mmol) was dissolved in THF (2 mL) and added quantitatively to the reaction vial and it was left to stir at room temperature for 24 hours. The reaction was quenched with 1M HCl (10 mL) and extracted with diethyl ether (3 x 10 mL). The combined organic layers were dried with Mg_2SO_4, filtered and the solvent was evaporated to give the crude product. The product was purified by column chromatography (Biotage® Sfär 10g Column, 0-100% EtOAc/hexanes). 7 mg of a white solid was obtained (2% Yield).

^{1}H NMR (300 MHz, $CDCl_3$, 292K, ppm): δ 7.77 (s, 2H), 7.71 (s, 2H), 7.37 (m, 5H), 5.19 (s, 2H), 3.53 – 3.24 (m, 5H).

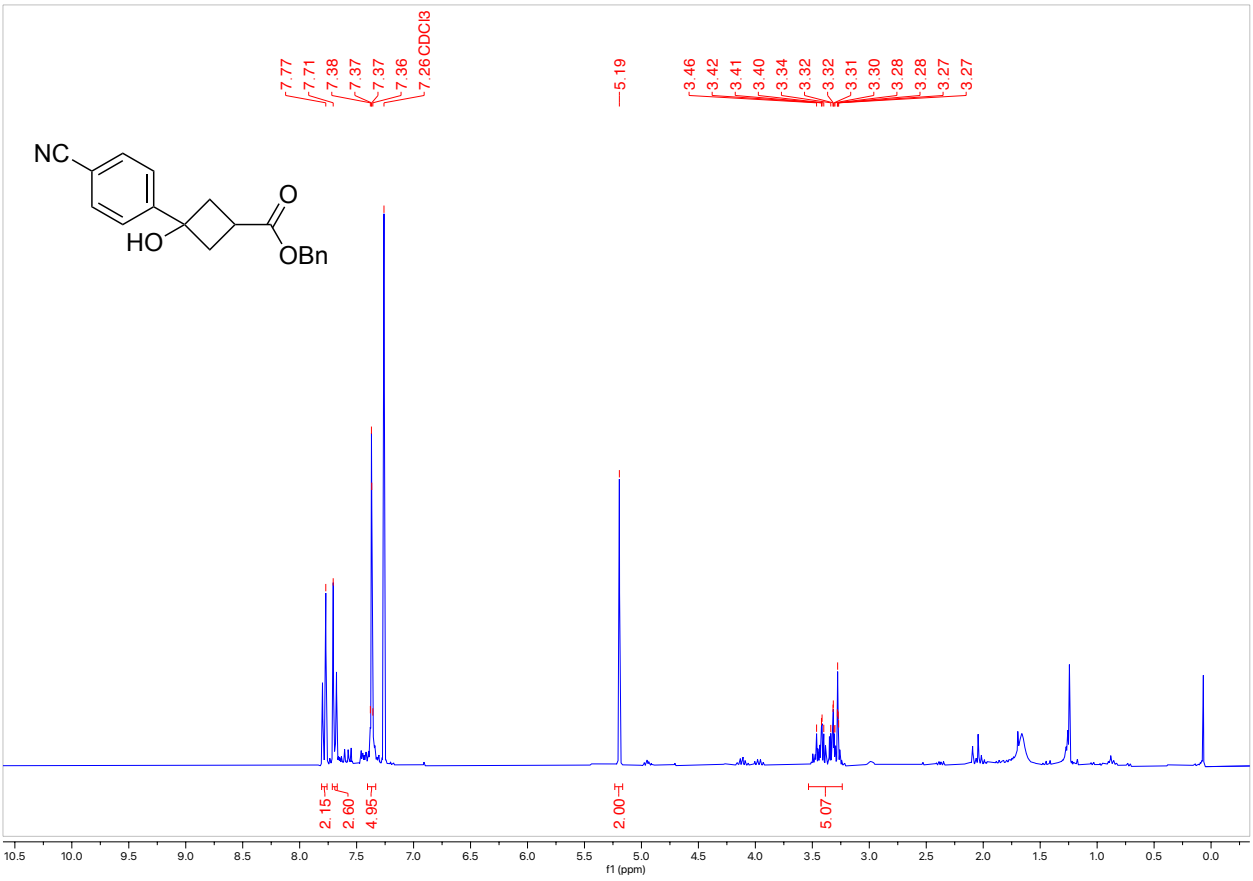

A.3 Screening - *N*-benzylimine

Procedure for Lewis acid screening in DCM, toluene, and THF (Table A.4):

Preparation of reaction stock solutions: six stock solutions (3 for **2a** and 3 for **1aa**) were made for 3 solvents (DCM, toluene and THF). Stock solution for **2a**: To three vials was added **2a** (45.2 mg, 0.240 mmol). 1200 μL of DCM, THF and toluene were added separately to the three vials respectively, ensuring **2a** was solubilized. Stock solution for 1aa: To three vials was added **1aa** (70.3 mg, 0.360 mmol). 1200 μL of DCM, THF and toluene were added separately to the three vials respectively, ensuring **1aa** was solubilized. These stock solutions were taken inside the glovebox. In 2 mL vials, 20 mol% (0.004 mmol) of the appropriate Lewis acid was added as a solid. 24 such vials were prepared: 3 vials of each Lewis acid for 3 different solvents. To each vial, 100 μL of **1aa** stock solution and 100 μL of **2a** stock solution were added. Stock solutions were arrayed to achieve 24 Lewis acid/solvent combinations. Micro stir bars were added to the vials followed by sealing the vials with aluminum crimp caps with a PTFE liner. Vials were taken outside the glovebox and subject to stirring at room temperature for 24 h. After 24 hours, all the vials were unsealed and solvent was evaporated in a GeneVac centrifugal evaporator. After the solvent evaporation was done, a stock solution of 1,3,5-trimethoxybenzene was made (1.85 mg/mL of 1,3,5-trimethoxybenzene in $CDCl_3$). Into each vial was added 0.6 mL (0.0066 mmol, 0.33 equiv) of internal standard stock solution, and ^{1}H NMR spectra were recorded for each sample.

Table A.4: Microscale screening data for the reaction of **1aa** and **2a**. Percentages are solution yields determined by ^{1}H NMR spectroscopy based on relative integration to the internal standard.

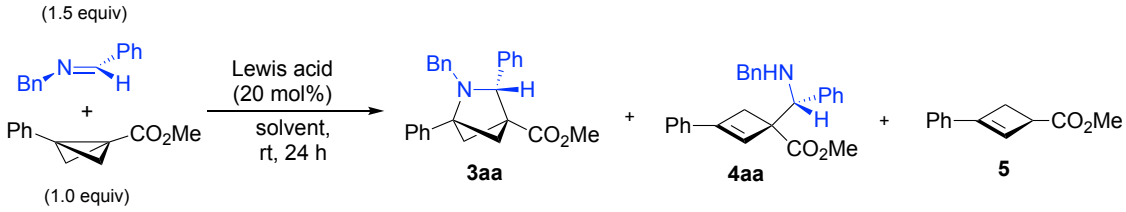

Entry	Solvent	Catalyst	2a	3aa	4aa	5
1	DCM	AgOTf	39%	0%	0%	1%
2	DCM	$Bi(OTf)_3$	5%	7%	2%	26%
3	DCM	$Ga(OTf)_3$	5%	5%	2%	21%
4	DCM	$Mg(OTf)_2$	58%	1%	1%	7%
5	DCM	$Sc(OTf)_3$	21%	4%	2%	20%
6	DCM	$Sn(OTf)_2$	21%	4%	2%	20%
7	DCM	$Yb(OTf)_3$	8%	0%	1%	29%
8	DCM	$Zn(OTf)_2$	9%	4%	2%	25%
9	Toluene	AgOTf	53%	0%	0%	0%
10	Toluene	$Bi(OTf)_3$	3%	5%	2%	26%
11	Toluene	$Ga(OTf)_3$	68%	5%	4%	38%
12	Toluene	$Mg(OTf)_2$	88%	0%	0%	2%
13	Toluene	$Sc(OTf)_3$	1%	3%	1%	15%
14	Toluene	$Sn(OTf)_2$	1%	4%	2%	19%
15	Toluene	$Yb(OTf)_3$	0%	0%	0%	16%
16	Toluene	$Zn(OTf)_2$	10%	3%	2%	16%
17	THF	AgOTf	65%	0%	0%	1%
18	THF	$Bi(OTf)_3$	8%	12%	2%	20%
19	THF	$Ga(OTf)_3$	6%	20%	2%	22%
20	THF	$Mg(OTf)_2$	61%	0%	0%	3%
21	THF	$Sc(OTf)_3$	6%	11%	2%	21%
22	THF	$Sn(OTf)_2$	0%	16%	1%	14%
23	THF	$Yb(OTf)_3$	6%	0%	3%	21%
24	THF	$Zn(OTf)_2$	7%	3%	3%	19%

A.4 Product Interconversion Experiment

Experimental for product interconversion testing

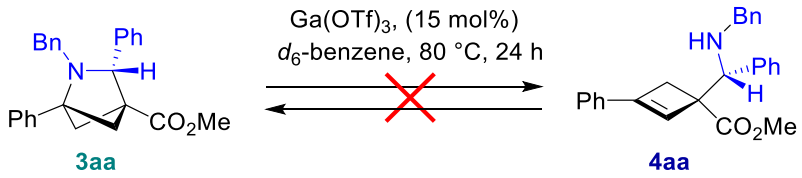

Synthesis and isolation of **3aa**:

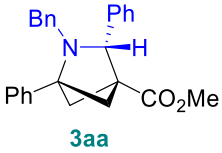

A vial was charged with **2a** (0.1000 g, 0.53 mmol) and **1aa** (0.1556 g, 0.80 mmol, 1.5 equiv) and was taken inside the glovebox. In an another vial, $Ga(OTf)_3$ (0.0549 g, 20 mol%) was added as a solid. THF (3 mL) was added to first vial. Once the solution was homogeneous, it was transferred to the vial containing $Ga(OTf)_3$. A stir bar was added, the vial was capped, and the mixture was stirred outside the glovebox at room temperature for 24 h. After 24 h, the solvent was evaporated. The residue was dissolved in toluene (5 mL) and washed with $NaHCO_3$ (5 mL) and brine (5 mL). The compound was then purified by column chromatography (Biotage® Sfär Amino 11g, 0-100% EtOAc/hexanes, eluted at 10% EtOAc). Compound **3aa** was isolated as a white solid (15.5 mg, 8%).

HRMS(ESI): calc'd for $[C_{26}H_{25}NO_2 + H^+]$, 384.19581; found: 384.19583.

^{1}H NMR of 3aa (500 MHz, $CDCl_3$, 292K, ppm): δ 7.49 (d, J=7.26 Hz, 2H), 7.46-7.35 (m, 4H), 7.35-7.29 (m, 1H), 7.18 (t, J=7.01 Hz, 2H), 7.16-7.09 (m, 3H), 7.06-6.95 (m, 3H), 4.29 (s, 1H), 3.85 (d, J=12.68 Hz, 1H), 3.63 (s, 3H), 3.46 (d, J=12.68 Hz, 1H), 2.87-2.79 (dd, J=7.21, 9.84 Hz 1H), 2.49 (d, J=6.17 Hz, 2H), 1.96 (d, J=6.17 Hz, 1H).

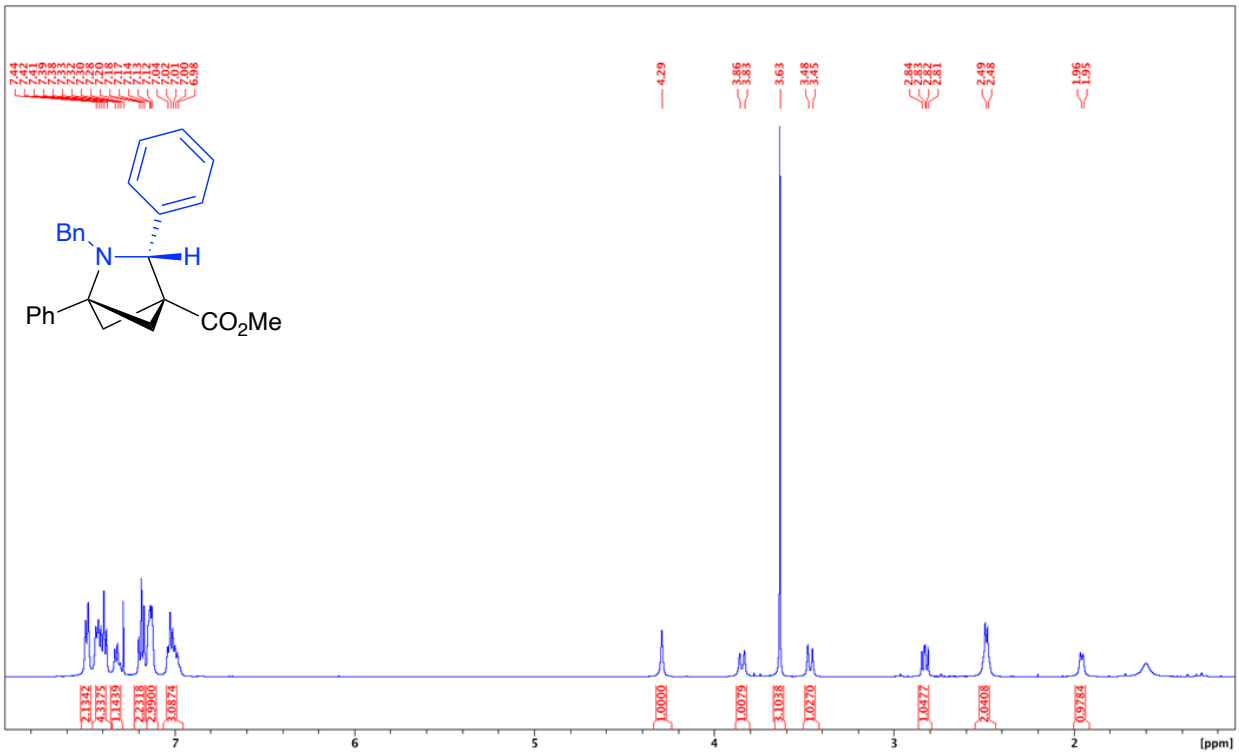

^{13}C NMR of 3aa (126 MHz, $CDCl_3$, 292K, ppm): δ 171.80, 140.82, 138.85, 129.31, 128.40, 127.85, 127.64, 127.53, 127.35, 127.09, 126.78, 126.44, 71.82, 56.97, 54.18, 51.48, 42.81, 42.53.

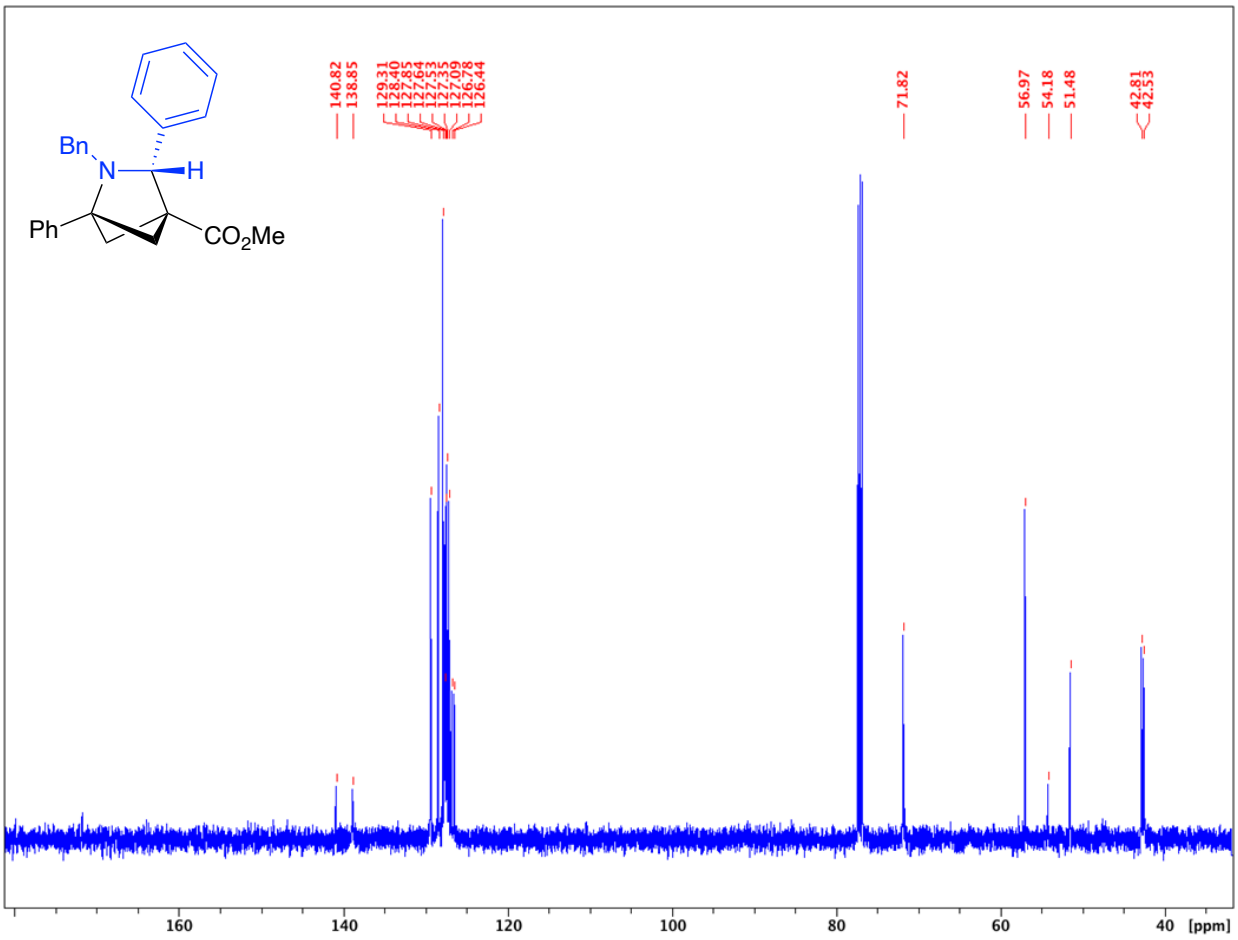

^{1}H-^{13}C HSQC (3aa):

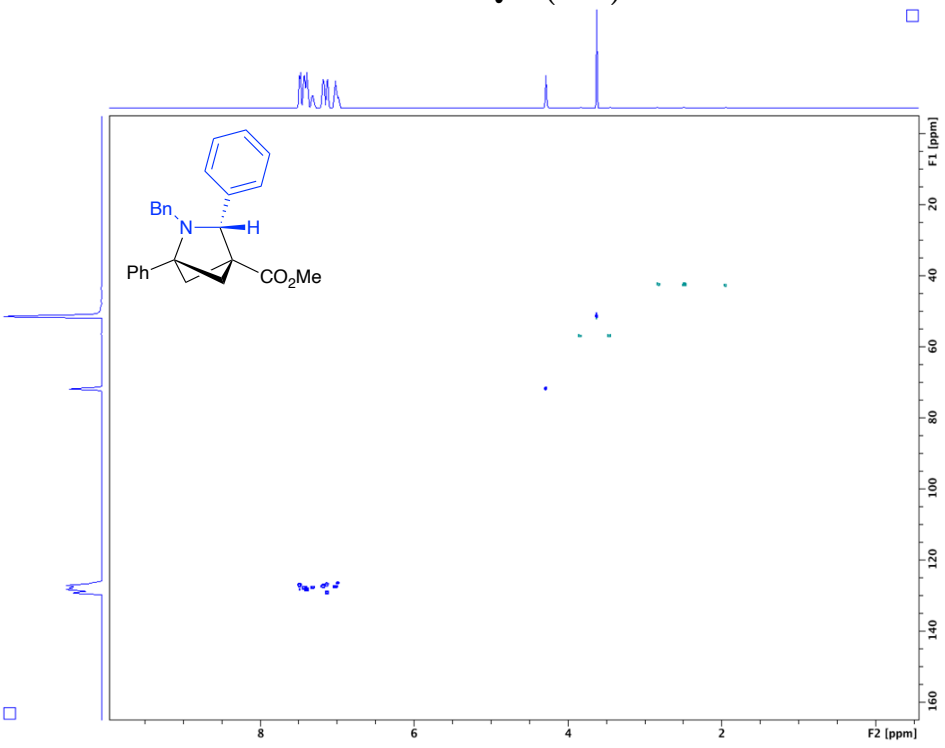

^{1}H-^{13}C HMBC (3aa):

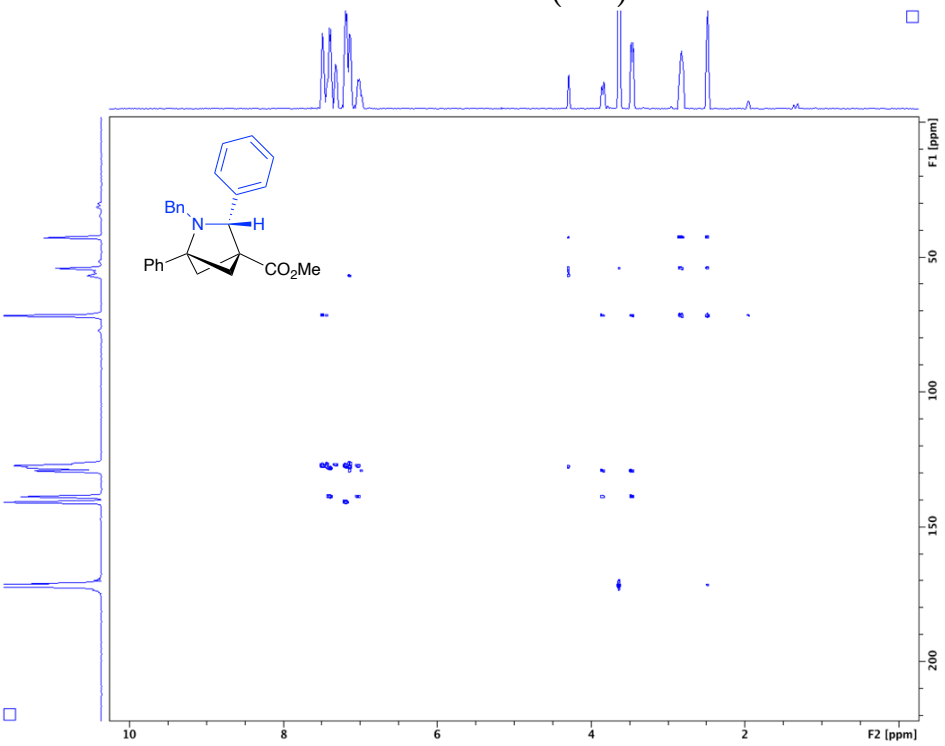

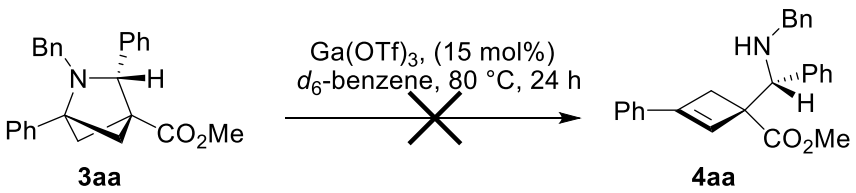

A small vial was charged with **3aa** (0.0155 g, 0.04 mmol) and $Ga(OTf)_3$ (0.0031 g, 15 mol%), which were dissolved in d_6-benzene. The resulting solution was transferred to a J. Young NMR tube. The sealed tube was heated to 80 °C for 24 hours. After 24 hours, a ^{1}H NMR spectrum was recorded, revealing no formation of **4aa**.

^{1}H NMR (300 MHz, $CDCl_3$, 292K)

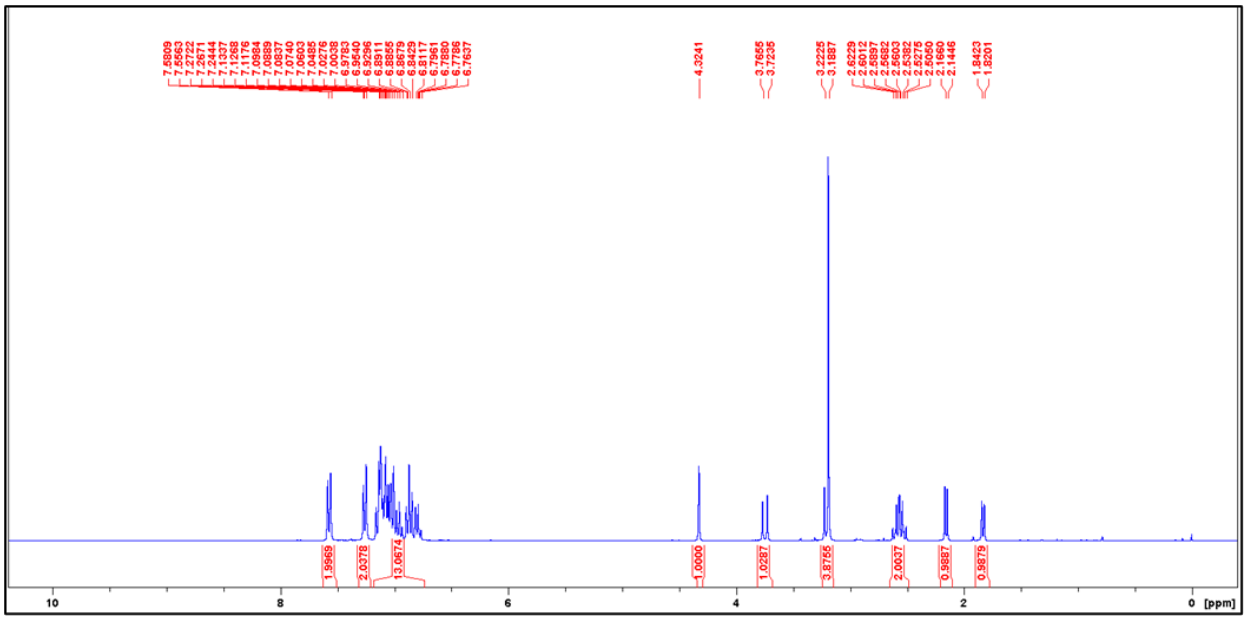

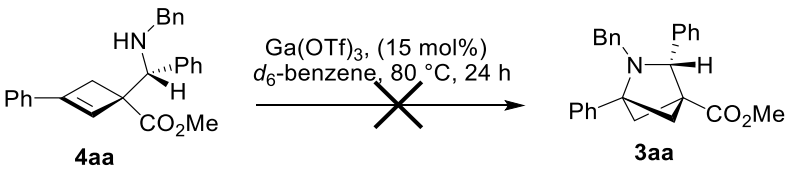

A small vial was charged with **4aa** (0.0383 g, 0.1 mmol) and $Ga(OTf)_3$ (0.0077 g, 15 mol%), which were dissolved in d_6-benzene. The resulting solution was transferred to a J. Young NMR tube. The sealed tube was heated to 80 °C for 24 hours. After 24 hours, a ^{1}H NMR spectrum was recorded, revealing no formation of **3aa**.

^{1}H NMR (300 MHz, $CDCl_3$, 292K)

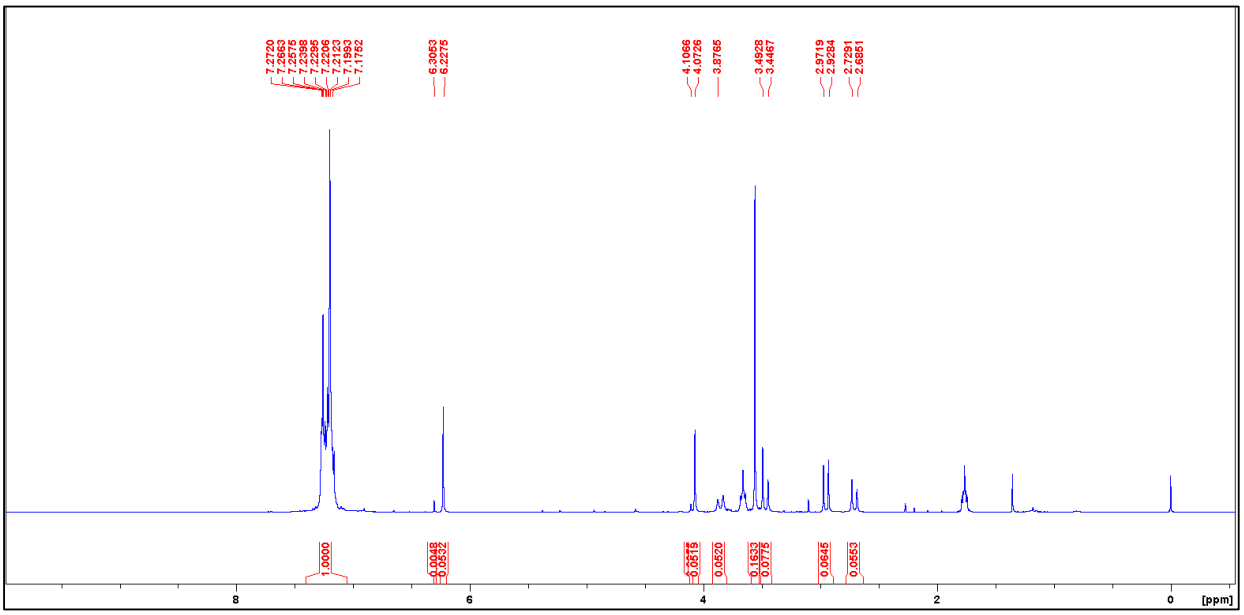

A.5 Substrate Synthesis

A.5.1 Imine Synthesis

General procedure: An aldehyde (1.1 equiv, 1.25-11 mmol) and an amine (1.1 equiv, 1.25-11 mmol) were dissolved in DCM (6-50 ml) in an appropriately-sized vial (20-40 mL) or round bottomed flask (50-250 mL). Anhydrous Na_2SO_4 was added as a drying agent, and the mixture was stirred at room temperature overnight. The drying agent was removed by filtration, and the solvent was evaporated to give the desired imine.

N-aryl Imines

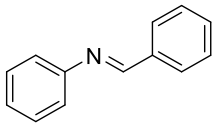

1a

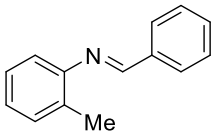

1b

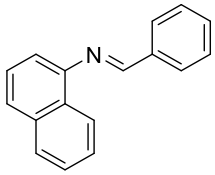

1c

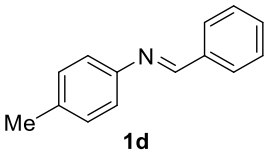

1d

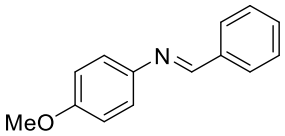

1e

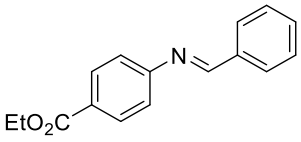

1f

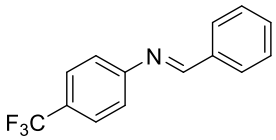

1g

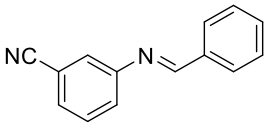

1h

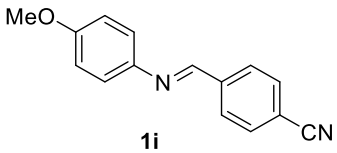

1i

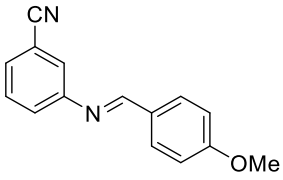

1j

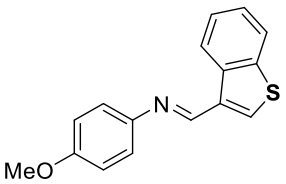

1k

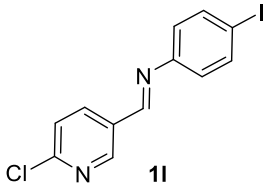

1l

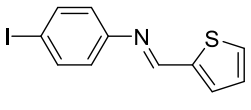

1m

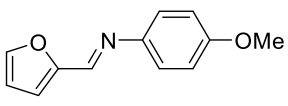

1n

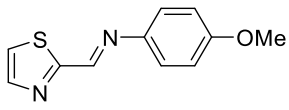

1o

N-alkyl Imines

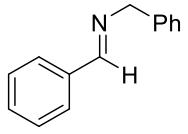

1aa

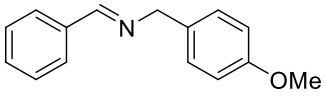

1bb

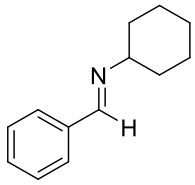

1cc

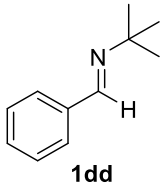

1dd

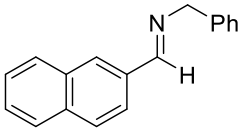

1ee

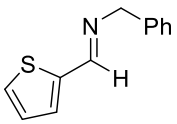

1ff

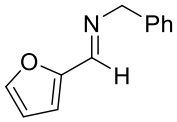

1gg

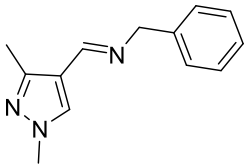

1hh

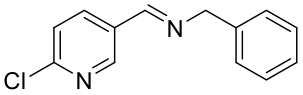

1ii

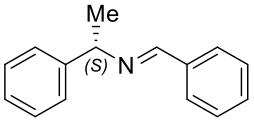

1jj

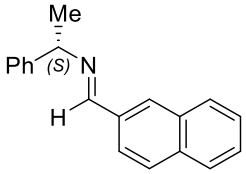

1ll

A.5.2 Bicyclobutane Synthesis

General Procedure 1 (3-Hydroxy-3-arylcyclobutane carboxylic acids)[114;125;154]
Solid 3-oxocyclobutane carboxylic acid was added to a 3-necked round bottom flask containing a stir bar and fitted with a gas inlet adapter, a septum, and an addition funnel. The apparatus was purged with nitrogen gas. Anhydrous THF was transferred to the flask via cannula, and the 3-oxocyclobutane carboxylic acid was dissolved with stirring. A solution of the Grignard reagent (2.05 equiv) was added to an addition funnel via cannula transfer, followed by slow dropwise addition to the reaction mixture over 6 hours. After the addition was complete, the reaction mixture was quenched with 6 M HCl. The aqueous layer was extracted with diethyl ether and the organic layer was dried with Mg_2SO_4. The solvent was removed under vacuum and the product was re-dissolved in saturated $NaHCO_3$. An equal amount of diethyl ether was added to extract the aqueous layer. The aqueous layer was acidified using concentrated HCl and a precipitate was formed which was filtered with vacuum filtration. The product was used in the next step without further purification.

General Procedure 2 (3-Chloro-3-arylcyclobutane carboxylic acids)[114;125;154]
The 3-hydroxy-3-arylcyclobutane carboxylic acid was dissolved in toluene and then an equal volume of concentrated hydrochloric acid was added. The reaction mixture was stirred at room temperature for 6 hours. The two layers were separated, and the aqueous layer was extracted with toluene. The organic layers were combined and washed with water and brine. The solution was then dried with Mg_2SO_4 and the solvent was removed under vacuum. The product was used in the next step without further purification.

General Procedure 3 (Methyl 3-chloro-3-arylcyclobutane carboxylates)[125]
The 3-chloro-3-arylcyclobutane carboxylic acid was dissolved in 2,2-dimethoxypropane (5.12 equiv) and then methanol (2.25 equiv) and *p*-TsOH (5 mol%) were added to the reaction mixture. The reaction was stirred at room temperature for 24 hours. The reaction mixture was washed with $NaHCO_3$ and the aqueous layer was extracted with TBME. The organic layer was dried with Mg_2SO_4 and the solvent was removed under vacuum.

General Procedure 4 (3-Chloro-3-arylcyclobutane esters and amides)
The alcohol or amide (1.2 equiv) and DIPEA (1 equiv) was added to a vial, dissolved in DCM and then cooled to 0 °C. 3-chloro-3-phenylcyclobutane-1-carbonyl chloride (1 equiv) dissolved in DCM was added dropwise to the vial. The reaction mixture was then warmed to room temperature and left to stir for 2 hours. The reaction mixture was washed with water and then the solvent was removed under vacuum to give the crude product.

General Procedure 5 (Bicyclobutane Synthesis)[114;125;154]
The 3-chloro-3-arylcyclobutane ester or amide (1 equiv) was added to a vial and dissolved in THF or toluene under a nitrogen atmosphere. NaHMDS (1.2 equiv) was added to the vial and the reaction mixture was stirred at room temperature or 70 °C for 5 hours. The mixture was cooled to room temperature, diluted with TBME, washed with NH_4Cl and then filtered. The filtrate was collected and washed with $NaHCO_3$ and brine. The organic layer was dried with Mg_2SO_4, filtered and the solvent was removed under vacuum. The product was used without further purification.

3-(4-fluorophenyl)-3-hydroxycyclobutane-1-carboxylic acid

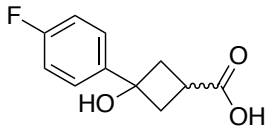

This product was prepared using **General Procedure 1**. 3-oxobutanecarboxylic acid (5.566 g, 48.8 mmol), 4-fluorophenylmagnesium bromide 1.0 M in THF (100 mL, 100 mmol) in 150 mL THF. 5.215 g of a white solid was obtained (51%).

^{1}H NMR (300 MHz, $CDCl_3$/DMSO-d_6, 292K, ppm): δ 7.34-7.27 (m, 2H), 6.89-6.60 (m, 2H), 3.63-2.36 (m, 5H).

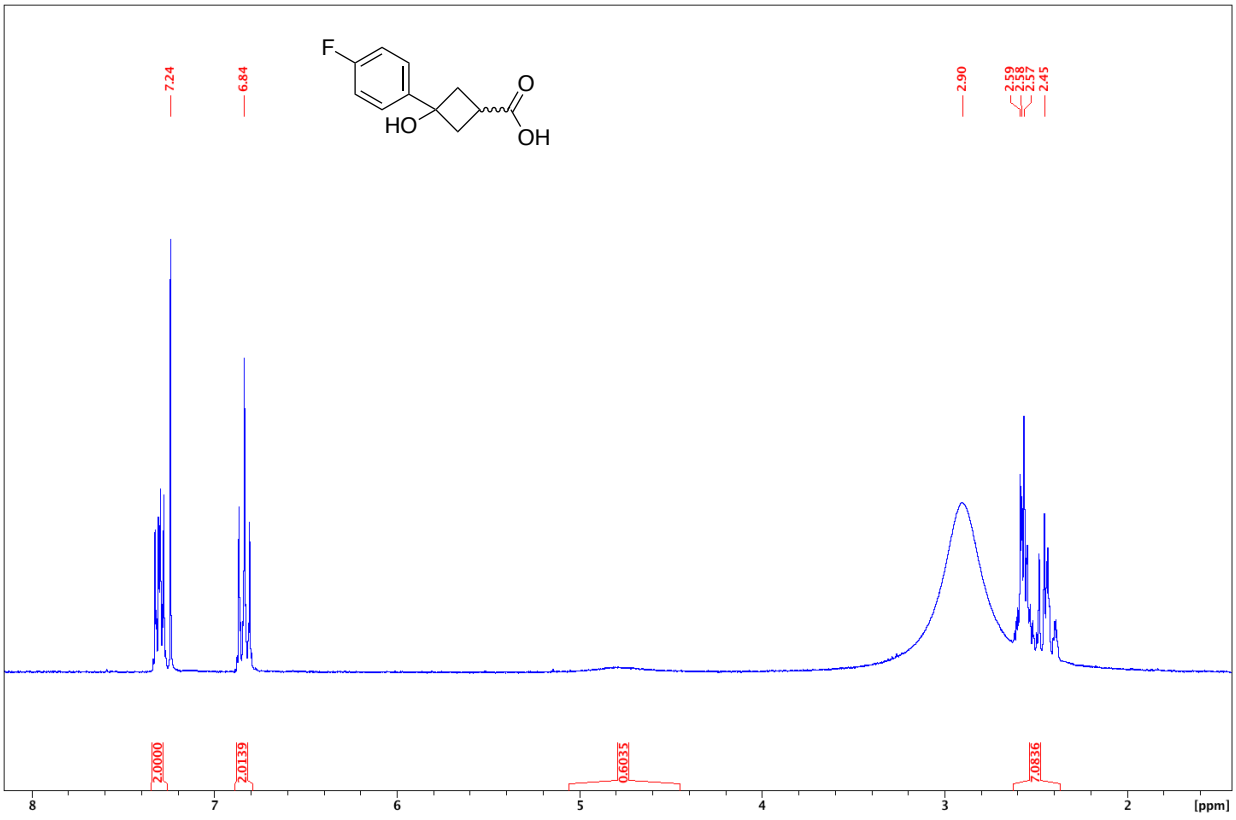

^{19}F NMR (300 MHz, $CDCl_3$/DMSO-d_6, 292K, ppm): δ -115.46

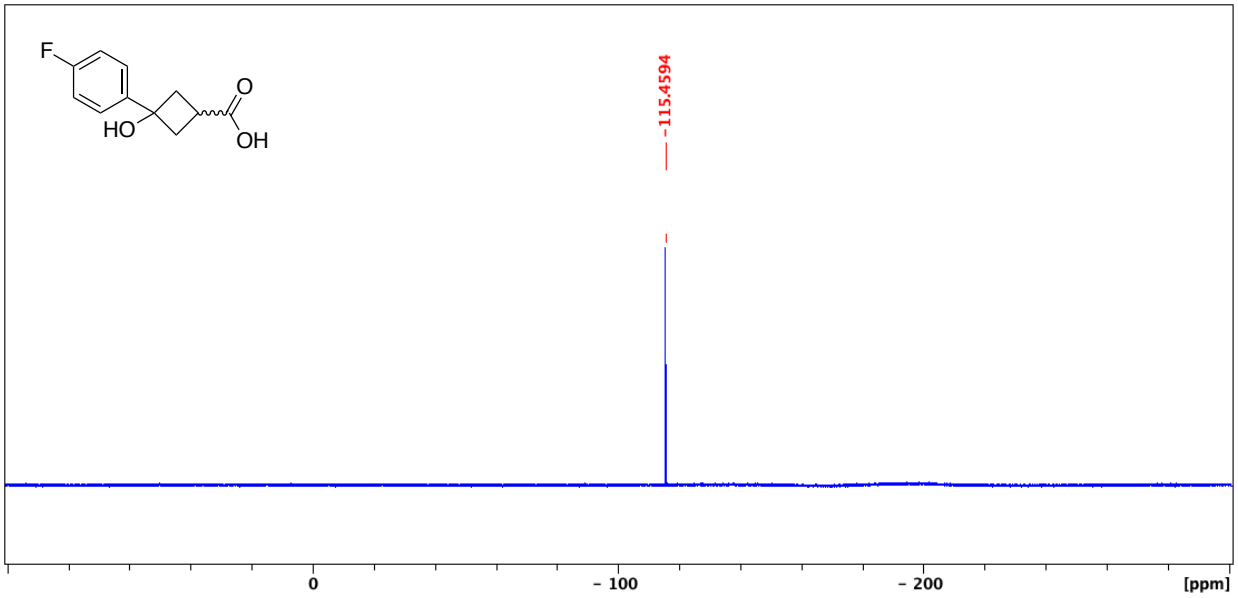

3-(4-chlorophenyl)-3-hydroxycyclobutane-1-carboxylic acid

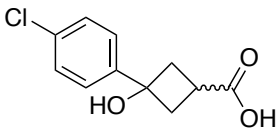

This product was prepared using **General Procedure 1**. 3-oxobutanecarboxylic acid (5.566 g, 48.8 mmol), 4-chlorophenylmagnesium bromide 1.0 M in THF (100 mL, 100 mmol) in 150 mL THF. 5.215 g of a white solid was obtained (51%).

HRMS(ESI): calc'd for $[C_{11}H_{11}{}^{35}ClO_3 - H]^-$, 225.03240; found: 225.03223.

^{1}H NMR (300 MHz, $CDCl_3$, 292K, ppm): δ 7.47-7.38 (d, J=7.05 Hz, 2H), 7.34-7.29 (d, J=7.05 Hz, 2H), 2.89-2.76 (m, 3H), 2.65-2.55 (m, 2H).

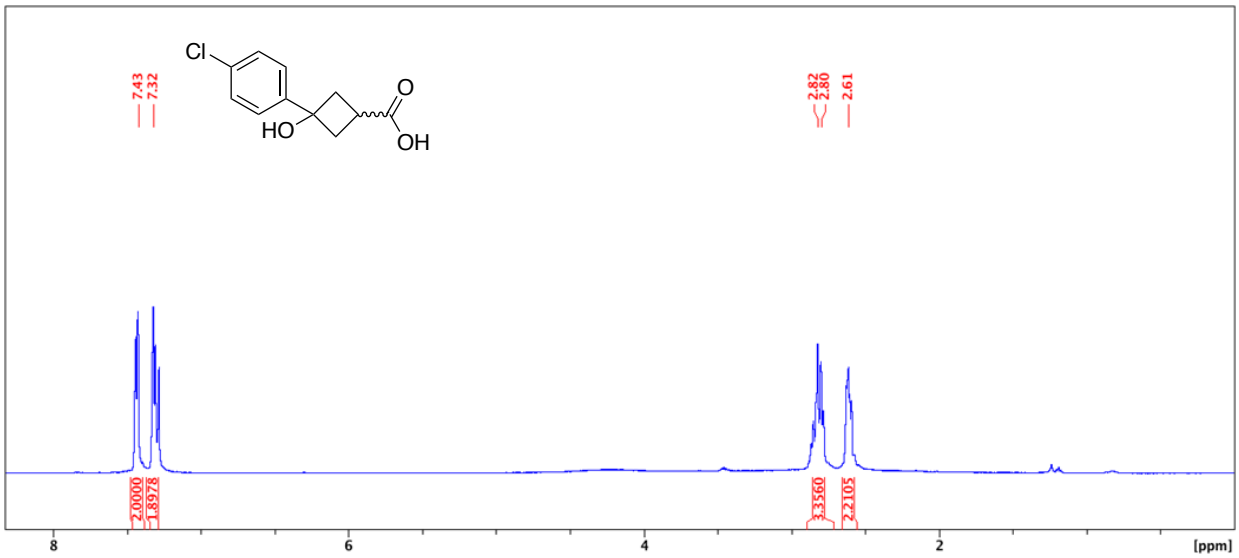

^{13}C NMR (126 MHz, $CDCl_3$, 292K, ppm): δ 178.50, 143.97, 132.97, 128.43, 126.56, 73.21, 40.85, 30.04.

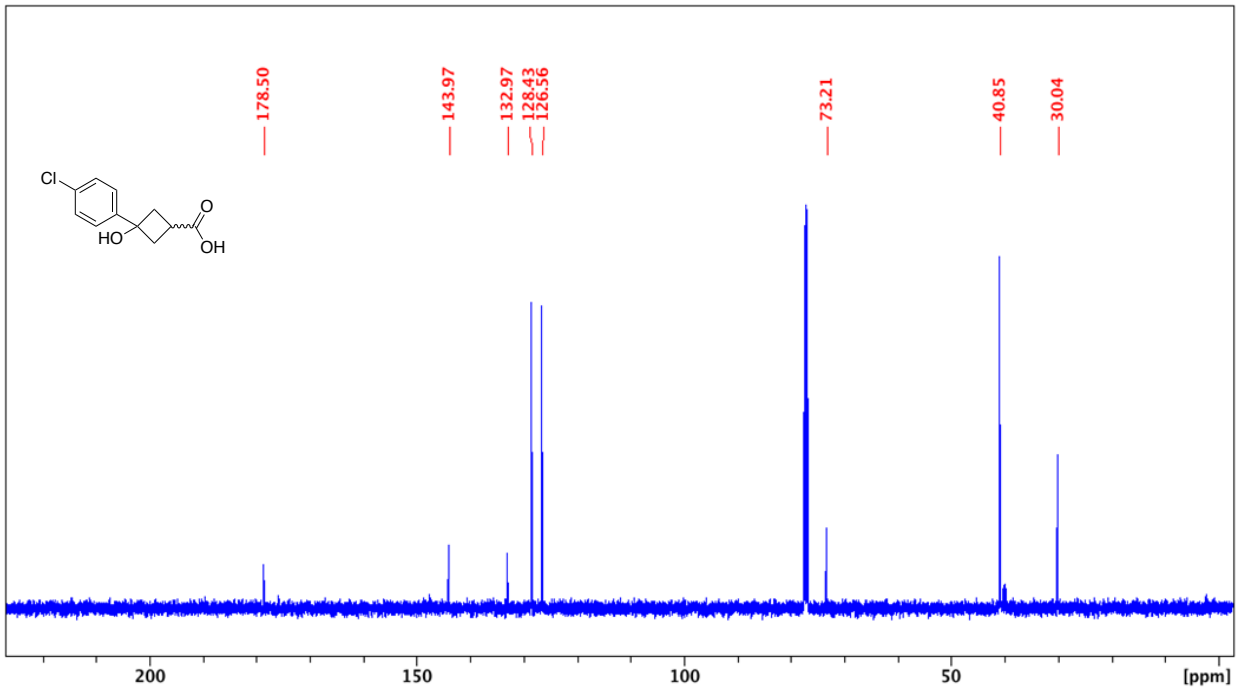

3-Chloro-3-(4-fluorophenyl)cyclobutane-1-carboxylic acid

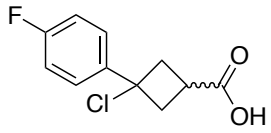

The product was prepared using **General Procedure 2**. 3-(4-fluorophenyl)-3-hydroxycyclobutane-1-carboxylic acid (4.65 g, 22.12 mmol), 50 mL of toluene and 50 mL of conc. HCl. 3.90 g of a white solid was obtained (77%).

^{1}H NMR (300 MHz, $CDCl_3$, 292K, ppm): δ 7.47-6.93 (m, 4H), 3.66 (q, J=8.73, 0.5H), 3.13 (d, J=8.73 Hz, 1H), 2.97 (d, J=8.73 Hz, 2H), 2.91-2.77 (m, 0.32H).

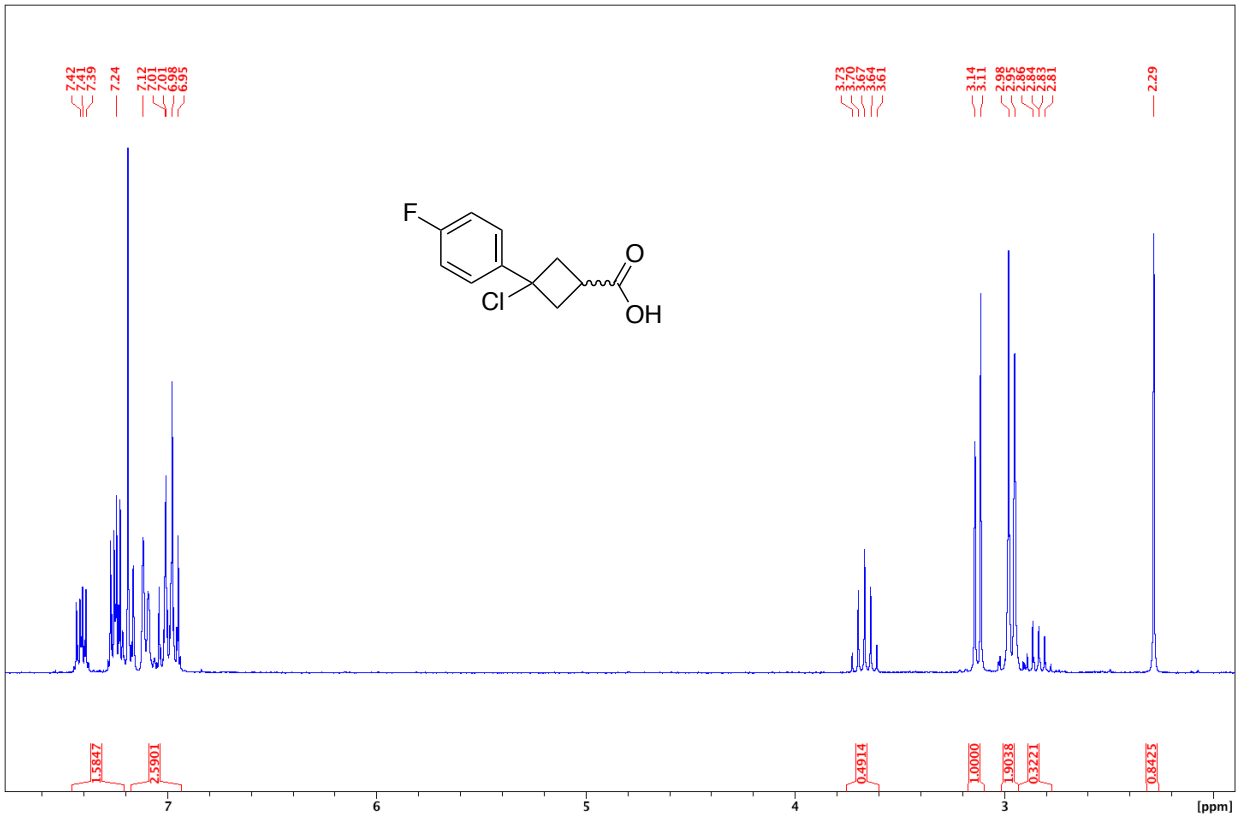

^{19}F NMR (300 MHz, $CDCl_3$, 292K, ppm): δ -113.86.

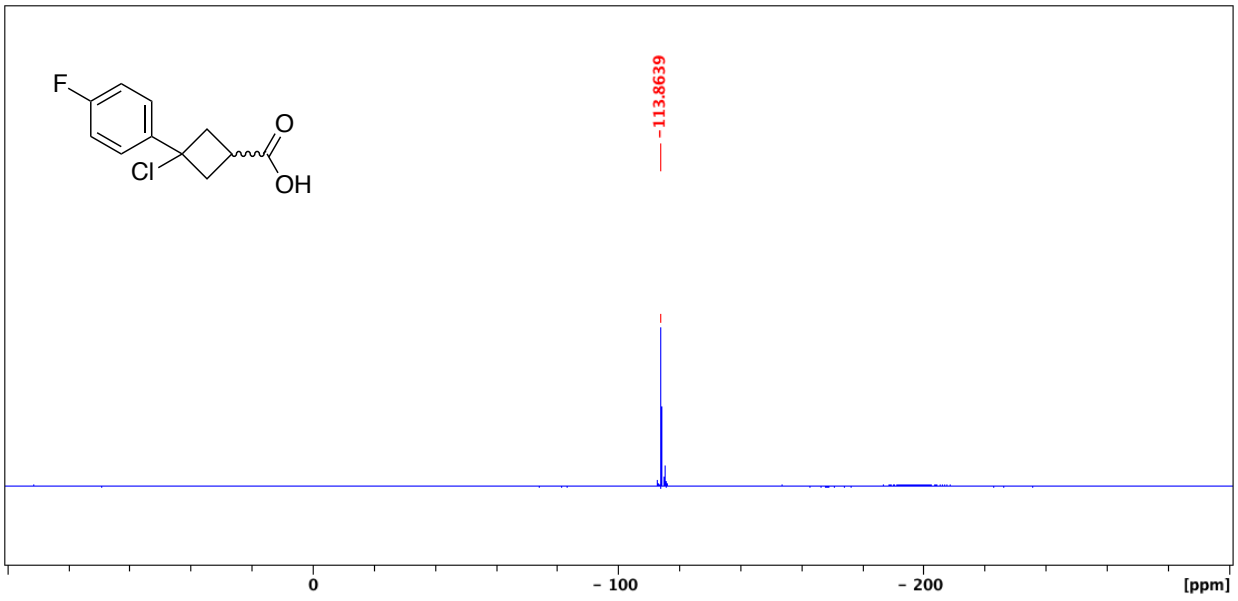

3-chloro-3-(4-chlorophenyl)cyclobutane-1-carboxylic acid

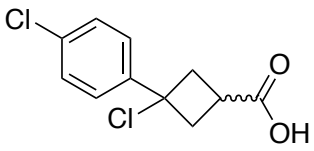

The product was prepared using **General Procedure 2**. 3-(4-chlorophenyl)-3-hydroxy-cyclobutane-1-carboxylic acid (8.89 g, 39.22 mmol), 40 mL of toluene and 40 mL of concentrated HCl. 6.91 g of a white solid was obtained (72%).

HRMS(ESI): calc'd for $[C_{11}H_{10}{}^{35}Cl_2O_2 - H]^-$, 242.99851; found: 242.99881.

^{1}H NMR (300 MHz, $CDCl_3$, 292K, ppm): δ 7.43-7.10 (m, 4H), 3.71-3.55 (m, 2H), 3.16-3.06 (m, 0.5H), 3.02-2.81 (m, 2H), 2.66-2.49 (m, 1.5H).

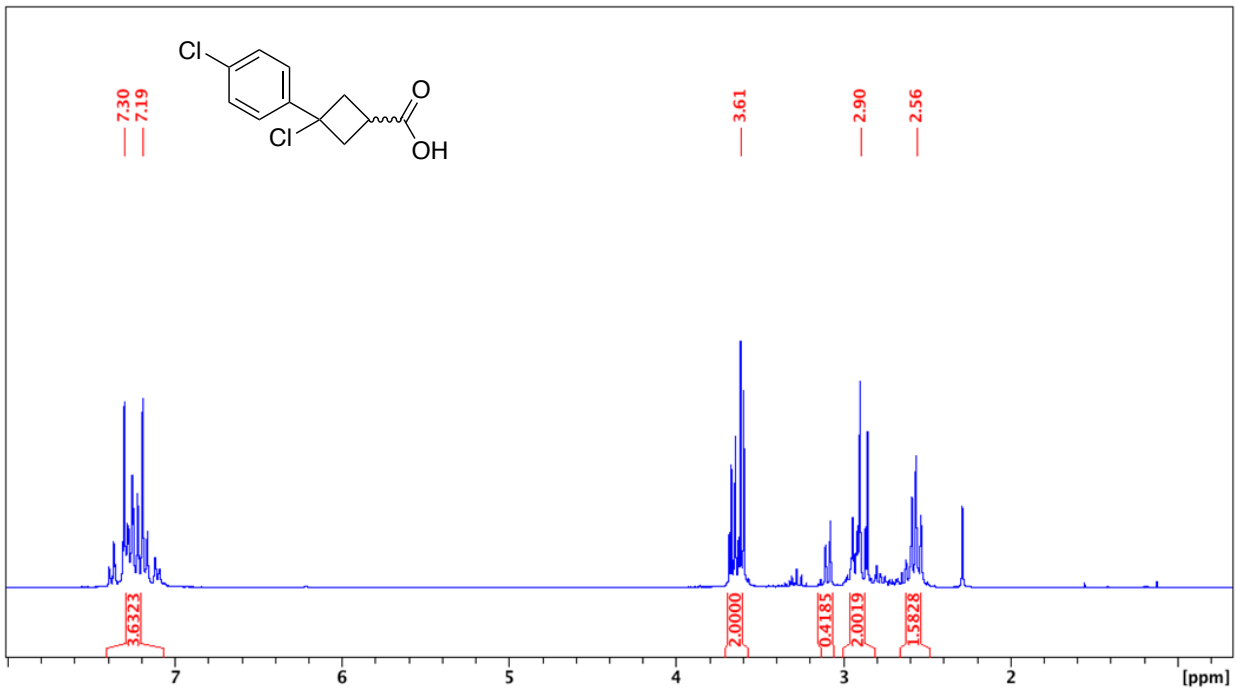

^{13}C NMR (126 MHz, $CDCl_3$, 292K, ppm): δ 180.31, 179.90, 148.45, 138.26, 133.40, 131.47, 130.74, 72.56, 58.53, 54.09, 46.40, 37.36, 37.20, 34.07, 31.74.

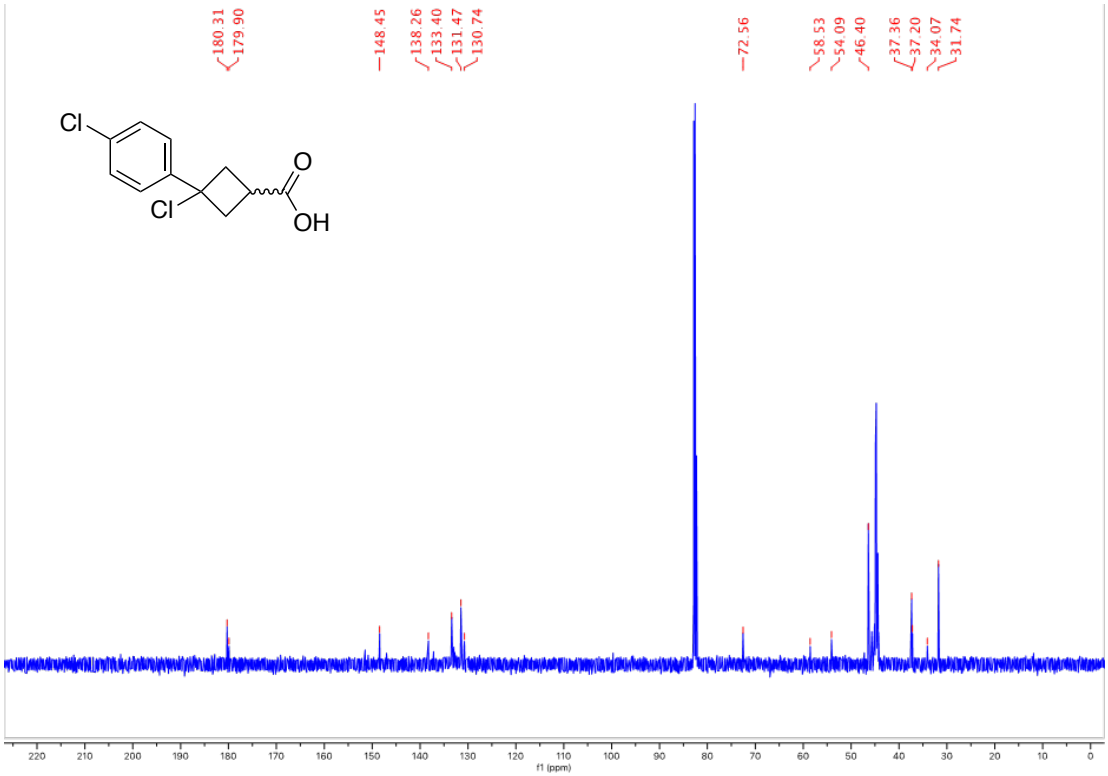

Methyl 3-chloro-3-(4-fluorophenyl)cyclobutane-1-carboxylate

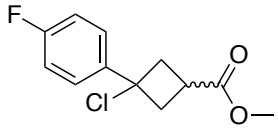

The product was prepared using **General Procedure 3**. 3-chloro-3-(4-fluorophenyl)cyclobutane-1-carboxylic acid (3.90 g, 17.1 mmol), methanol (1.55 mL, 38.4 mmol), *p*-TsOH (0.1622 g, 5 mol%), and 2,2-dimethoxypropane (11 mL, 87.3 mmol). The crude product was purified by column chromatography (SiO_2, 0-100% EtOAc/hexanes, eluted at 25% EtOAc). 3.16 g of a clear colourless oil was obtained as a mixture of diastereomers (76%).

^{1}H NMR (300 MHz, $CDCl_3$, 292K, ppm): δ 7.54-7.29 (m, 2H), 7.13-7.00 (m, 2H), 3.77-3.66 (m, 3.4H), 3.17 (d, 8.39H, 2H), 3.07-2.98 (m, 1.5H), 2.93-2.79 (m, 0.6H).

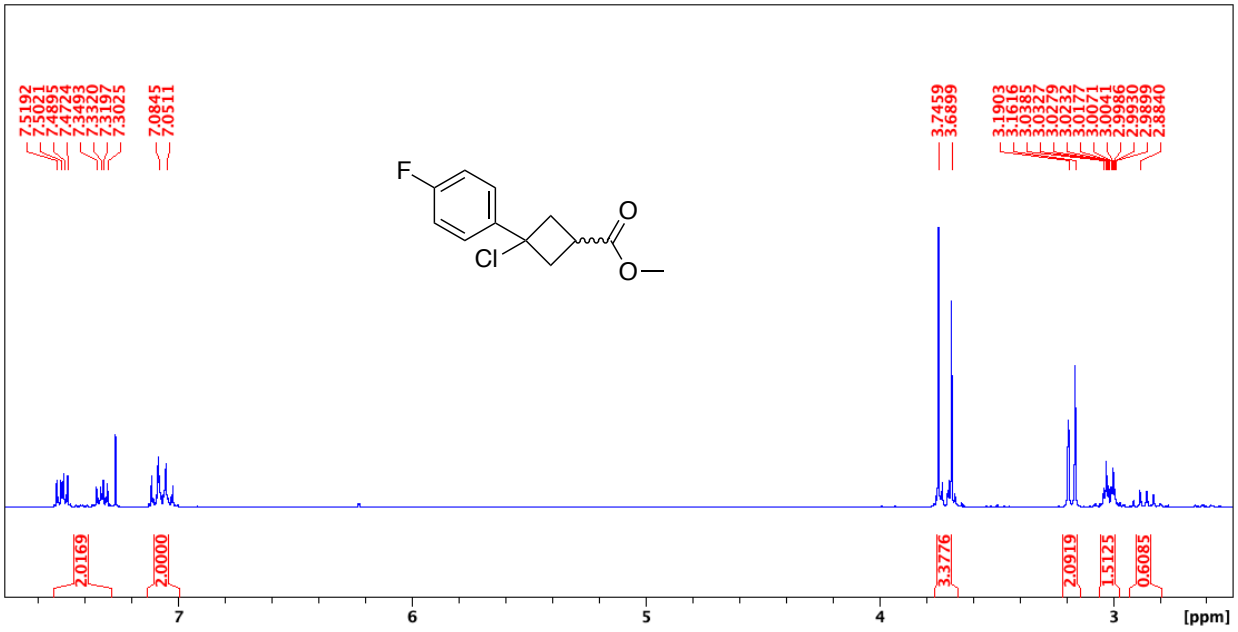

^{19}F NMR (300 MHz, $CDCl_3$ 292K, ppm): δ -113.60, -113.66.

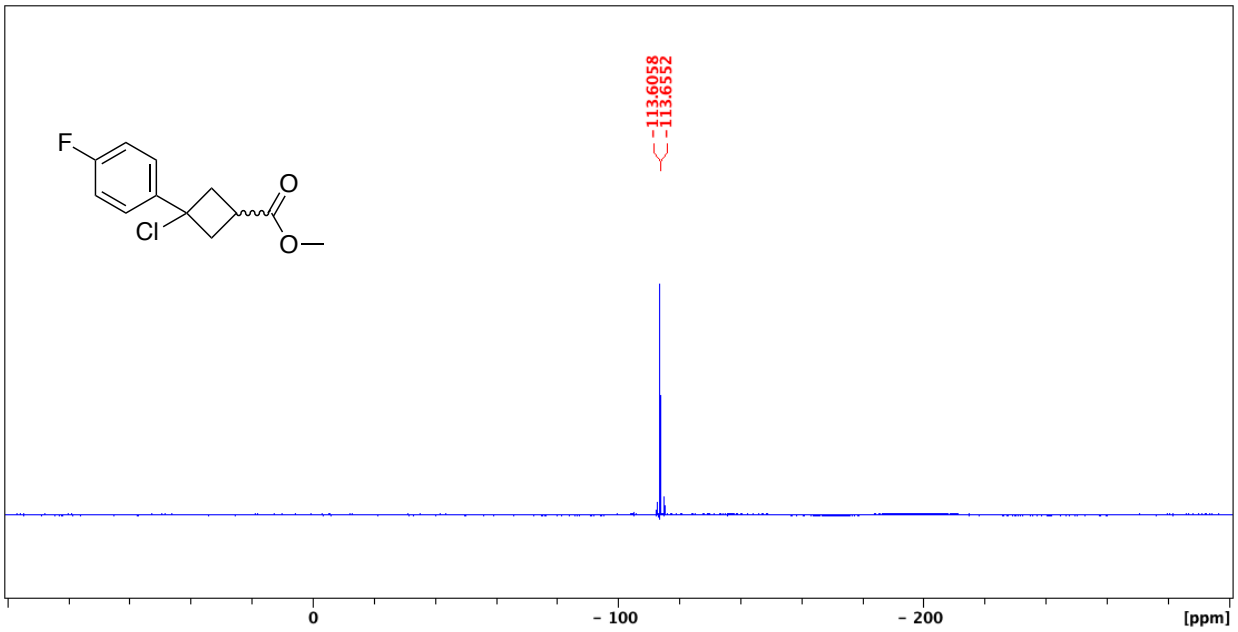

Methyl 3-chloro-3-(4-chlorophenyl)cyclobutane-1-carboxylate

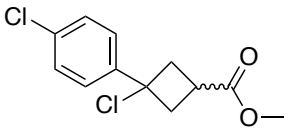

The product was prepared using **General Procedure 3**. 3-chloro-3-(4-chlorophenyl)cyclobutane-1-carboxylic acid (6.47 g, 26.4 mmol), methanol (2.40 mL, 59.39 mmol), *p*-TsOH (0.2511 g, 5 mol%), and 2,2-dimethoxypropane (16.6 mL, 135.15 mmol). The crude product was purified by column chromatography (SiO_2, 0-100% EtOAc/hexanes, eluted at 25% EtOAc). 5.17 g of a yellow solid was obtained as a mixture of diastereomers (76%).

HRMS(ESI): calc'd for $[C_{12}H_{12}{}^{35}Cl_2O_2 - {}^{35}Cl]^+$, 223.05203; found: 223.05208.

^{1}H NMR (300 MHz, $CDCl_3$, 292K, ppm): δ 2.50-7.26 (m, 4H), 3.79-3.67 (m, 3.6H), 3.20-3.15 (m, 0.4H), 3.10-2.54 (m, 4H).

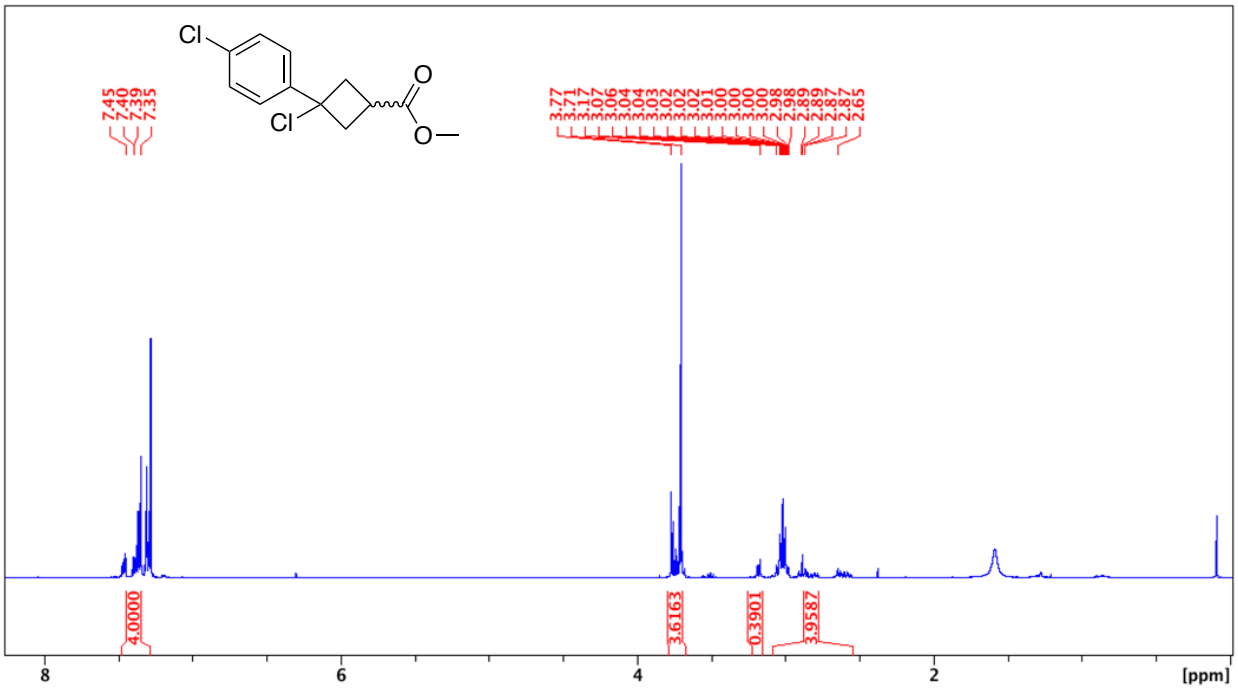

^{13}C NMR (126 MHz, $CDCl_3$, 292K, ppm): δ 174.28, 143.40, 133.92, 128.85, 128.80, 128.65, 128.62, 127.40, 126.57, 126.52, 126.27, 67.63, 52.03, 42.52, 41.73, 40.92, 39.63, 32.61.

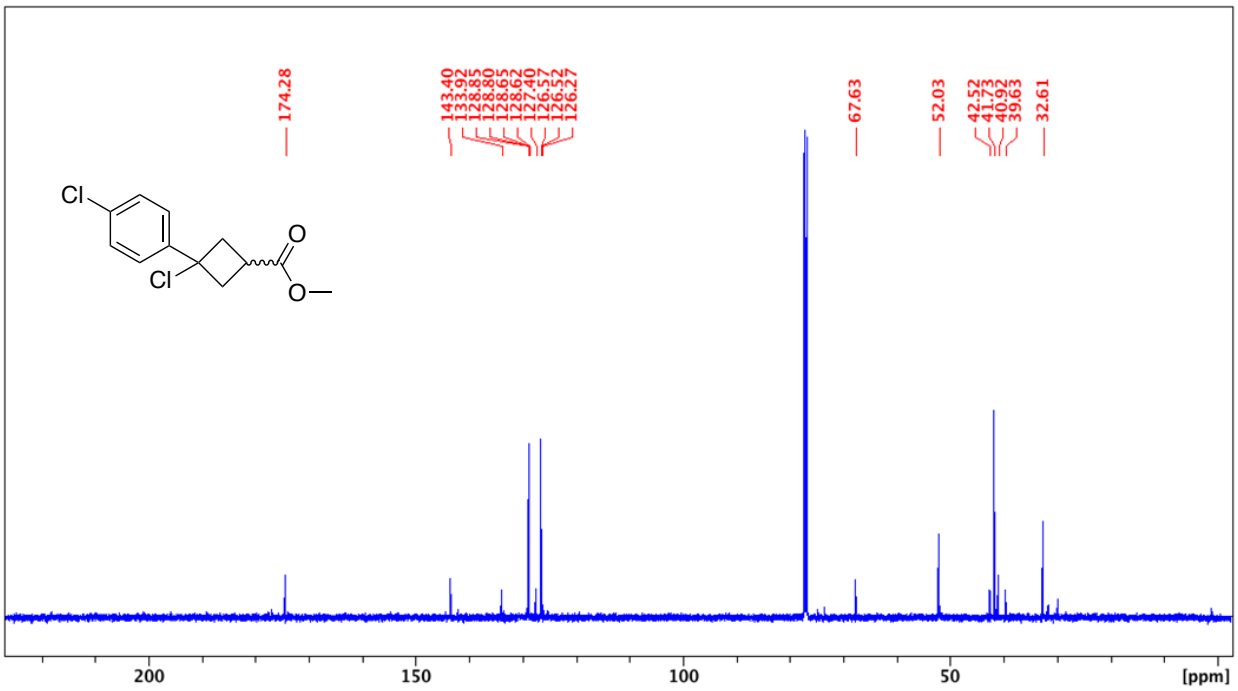

3-chloro-3-phenylcyclobutane-1-carbonyl chloride

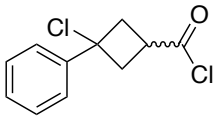

3-hydroxy-3-phenylcyclobutane-1-carboxylic acid (2.98 g, 15.5 mmol) was added to a 100 mL round bottom flask and dissolved in 20 mL of DCM. A drop a DMF was added to the reaction mixture. Oxalyl chloride (3.5 mL, 38.8 mmol) dissolved in 5 mL DCM was added dropwise over a period of 20 minutes at room temperature. The reaction mixture was stirred for 24 hours. Oxalyl chloride (3.5 mL, 38.8 mmol) dissolved in 5 mL DCM was added again dropwise over 20 minutes and the mixture is stirred for another 24 hours. The solvent was removed by vacuum filtration and a brown oil was isolated as a mixture of diastereomers (2.74 g, 77%). The product was used in the next step without further purification.

LRMS (EI): calc'd for $[C_{11}H_{10}Cl_2O]$, 208; found: 208. calc'd for $[C_{18}H_{17}ClO_2$ - $Cl]^+$, 193; found: 193.

^{1}H NMR (500 MHz, $CDCl_3$, 292K, ppm): δ 7.30-7.55 (m, 5H), 7.81-7.74 (q, J=8.70 Hz, 0.8H), 3.30-2.90 (m, 4.1H).

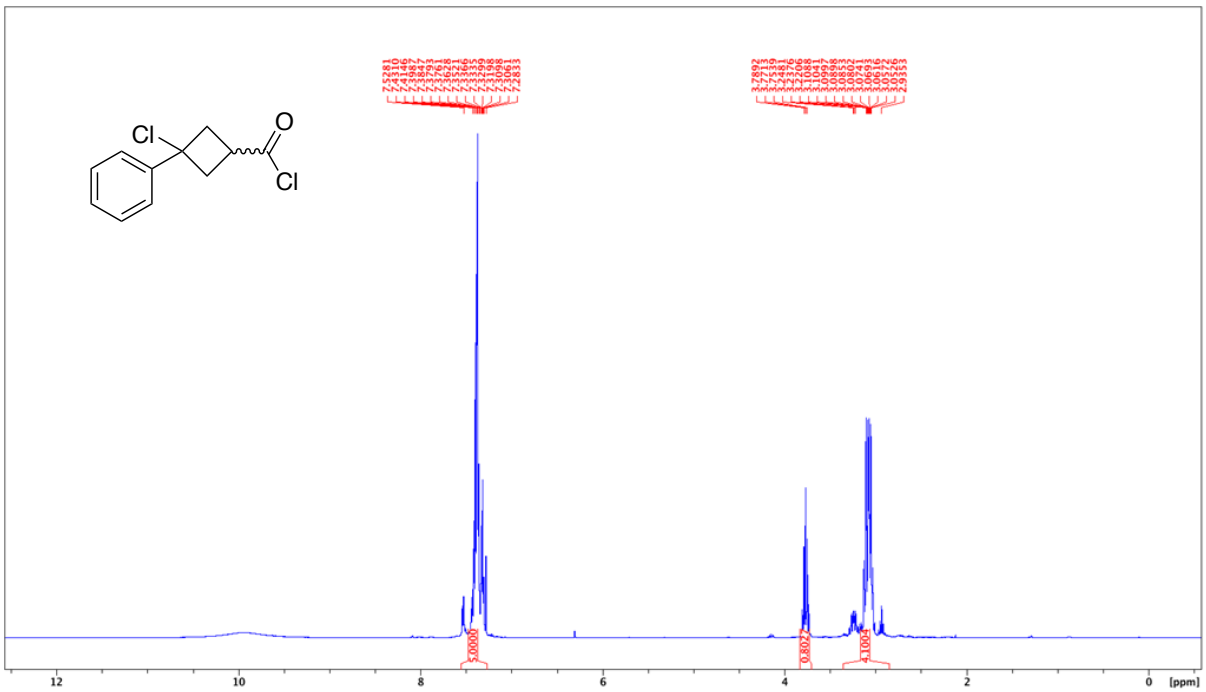

^{13}C NMR (126 MHz, $CDCl_3$, 292K, ppm): δ 180.13, 144.74, 128.71, 128.66, 128.09, 125.84, 124.98, 68.23, 41.64, 32.73.

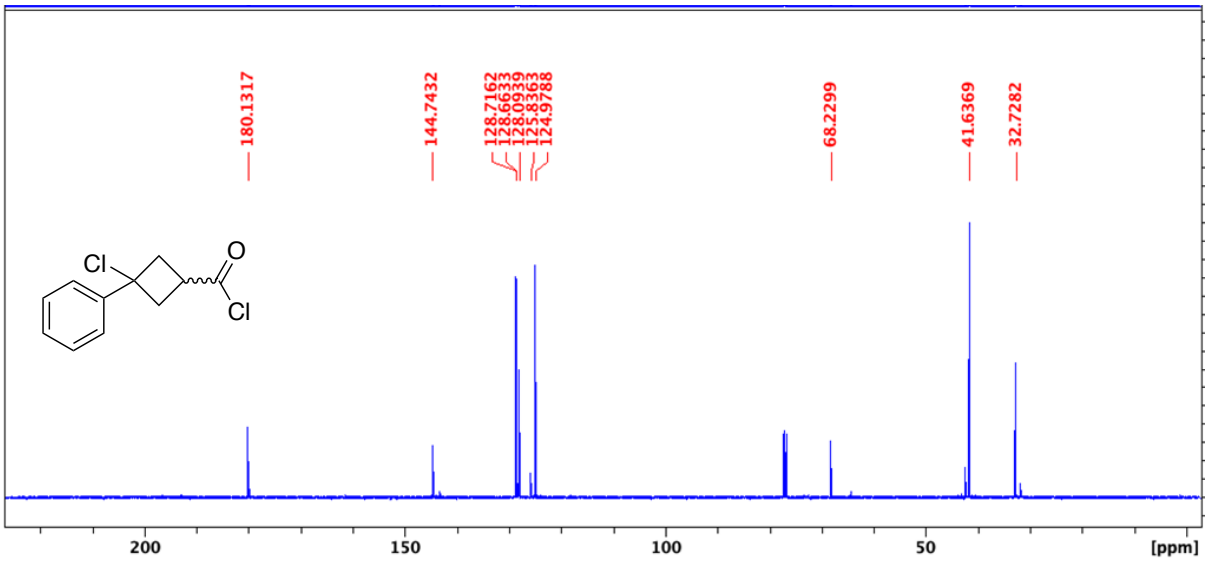

Benzyl 3-chloro-3-phenylcyclobutane-1-carboxylate

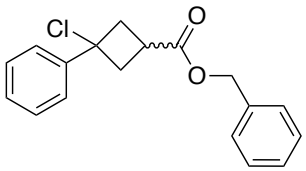

This product was prepared by **General Procedure 4**. benzyl alcohol (250 μL, 2.4 mmol), DIPEA (349 μL, 2.0 mmol), and 3-chloro-3-phenylcarbonyl chloride (0.4582 g, 2.0 mmol) in 15 mL of DCM. The crude product was purified by column chromatography (SiO_2, 0-100% EtOAc/hexanes, eluted at 30% EtOAc). 383 mg of a pale-yellow solid was obtained as a mixture of diastereomers (64%).

HRMS(ESI): calc'd for $[C_{18}H_{17}ClO_2 - Cl]^+$, 265.12231; found: 265.12233.

^{1}H NMR (500 MHz, $CDCl_3$, 292K, ppm): δ 7.55-7.43 (m, 10H), 5.20 (s, 0.83H), 5.14 (s, 1.17), 3.82-3.73 (q, J=8.70 Hz, 0.65H), 3.27-3.19 (m, 1.37H), 3.12-3.01 (m, 2.49H), 2.90-2.75 (q, J=8.70 Hz, 0.34).

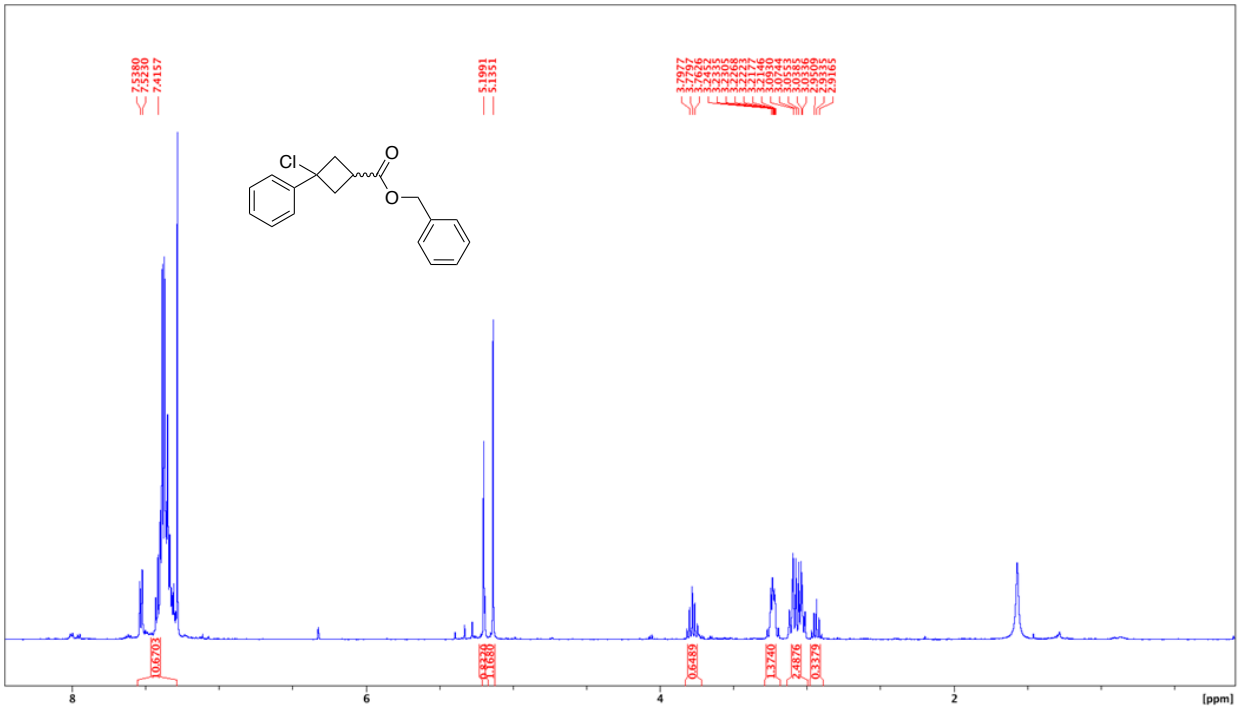

^{13}C NMR (126 MHz, $CDCl_3$, 292K, ppm): δ 173.80, 144.86, 135.75, 135.72, 128.66, 128.62, 128.35, 128.21, 128.20, 128.13, 128.01, 125.86, 125.03, 66.60, 42.53, 41.73, 32.95, 32.09.

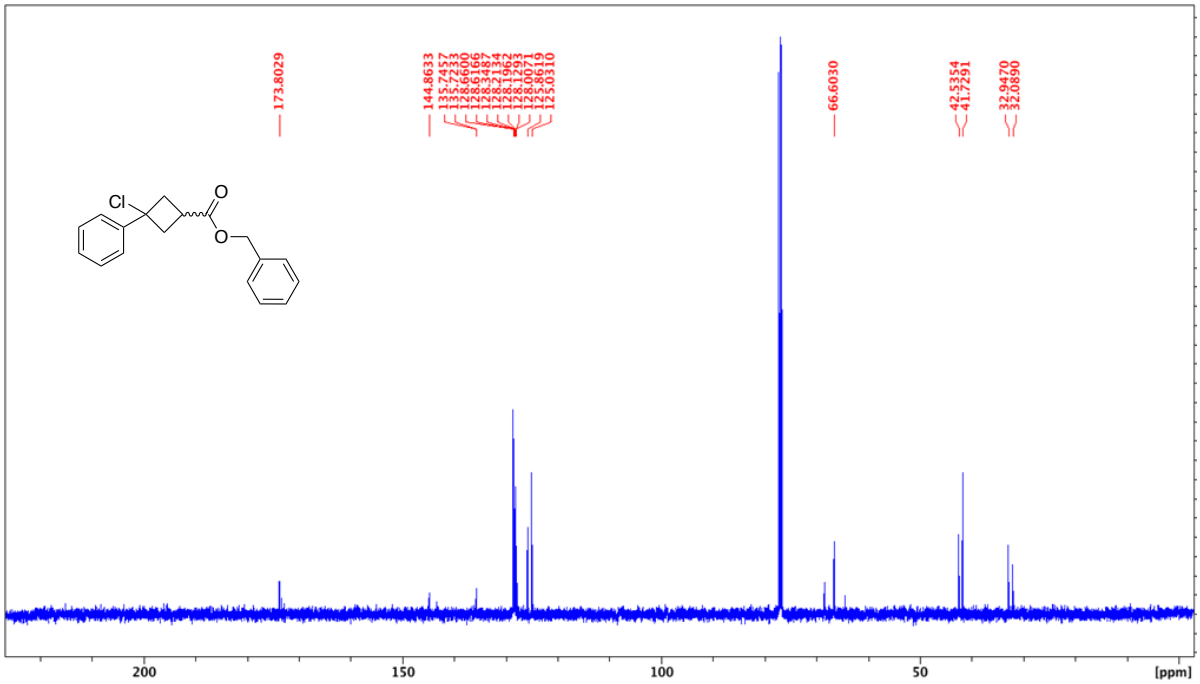

(1*S*,2*R*,5*S*)-2-isopropyl-5-methylcyclohexyl 3-chloro-3-phenylcyclobutane-1-carboxylate

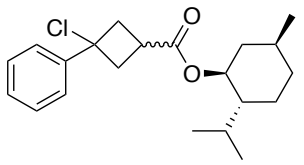

This product was prepared by **General Procedure 4**. (1*S*,2*R*,5*S*)-(+)-Menthol (0.8196 g, 5.24 mmol), DIPEA (763 μL, 4.37 mmol), and 3-chloro-3-phenylcarbonyl chloride (1.0013 g, 4.37 mmol) in 30 mL of DCM. The crude product was purified by column chromatography (SiO_2, 0-100% EtOAc/hexanes, eluted at 30% EtOAc) 1.0675 g of a clear colourless solid was obtained as a mixture of diastereomers (70%).

HRMS(ESI): calc'd for $[C_{21}H_{29}O_2 - Cl]^+$, 313.21621; found: 313.21603

^{1}H NMR (500 MHz, $CDCl_3$, 292K, ppm): δ 7.56-7.30 (m, 5H), 4.81-4.62 (m, 1H), 3.75-3.64 (q, J=9.09 Hz, 0.30H), 3.50-3.42 (q, J=9.09 Hz, 0.35H), 3.27-3.14 (m, 0.95H), 3.10-2.98 (m, 1.17H), 2.96-2.80 (m, 1.31H), 2.67-2.56 (m, 0.92H), 2.12-1.77 (m, 3H), 1.76-1.65 (m, 2.69H), 1.64-1.45 (m, 4H), 1.45-1.34 (m, 1.19H), 1.31-1.24 (m, 0.55H), 1.20-0.97 (m, 2.39H), 0.97-0.83 (m, 9.46H), 0.83-0.78 (m, 1.85H), 0.78-0.73 (m, 1.84H).

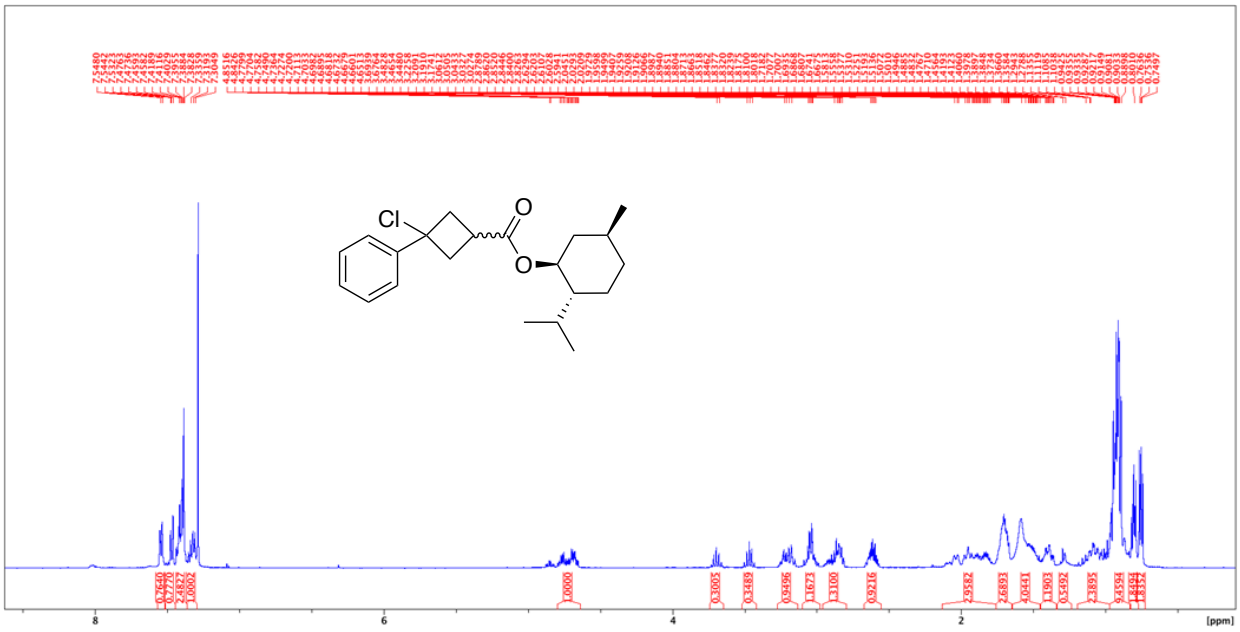

^{13}C NMR (126 MHz, $CDCl_3$, 292K, ppm): δ 174.73, 128.63, 128.59, 128.51, 127.49, 125.89, 125.09, 124.74, 75.16, 74.78, 74.57, 74.30, 47.07, 47.01, 46.97, 42.54, 42.46, 41.75, 41.62, 39.54, 39.44, 34.26, 34.21, 33.18, 32.33, 31.92, 31.43, 31.40, 31.37, 26.32, 23.50, 23.47, 22.03, 20.74, 16.36.

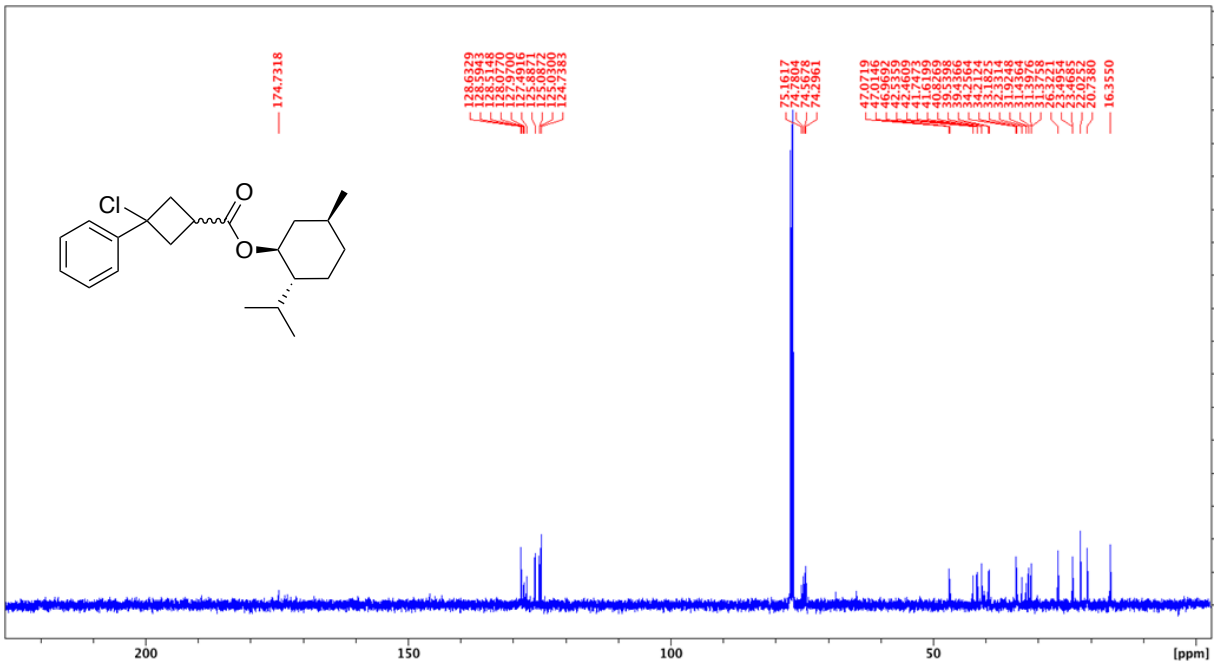

***Tert*-Butyl 3-chloro-3-phenylcyclobutane-1-carboxylate**

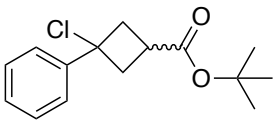

This product is prepared by **General Procedure 4**. *Tert*-butanol (497 μL, 5.24 mmol), DIPEA (762 μL, 4.37 mmol), and 3-chloro-3-phenylcarbonyl chloride (1.0000 g, 4.37 mmol) in 30 mL of DCM. The crude product was purified by column chromatography (SiO_2, 0-100% EtOAc/hexanes, eluted at 15% EtOAc). 290 mg of a yellow oil was obtained as a mixture of diastereomers (25%).

^{1}H NMR (500 MHz, $CDCl_3$, 292K, ppm): δ 7.48-7.20 (m, 5H), 3.58-3.44 (q, J=8.67 Hz, 0.80H), 3.14-2.95 (m, 1.30H), 2.95-2.83 (m, 2.52), 2.75-2.62 (q, J=8.66 Hz, 0.29H), 1.39 (s, 4.29H), 1.33 (s, 4.79H).

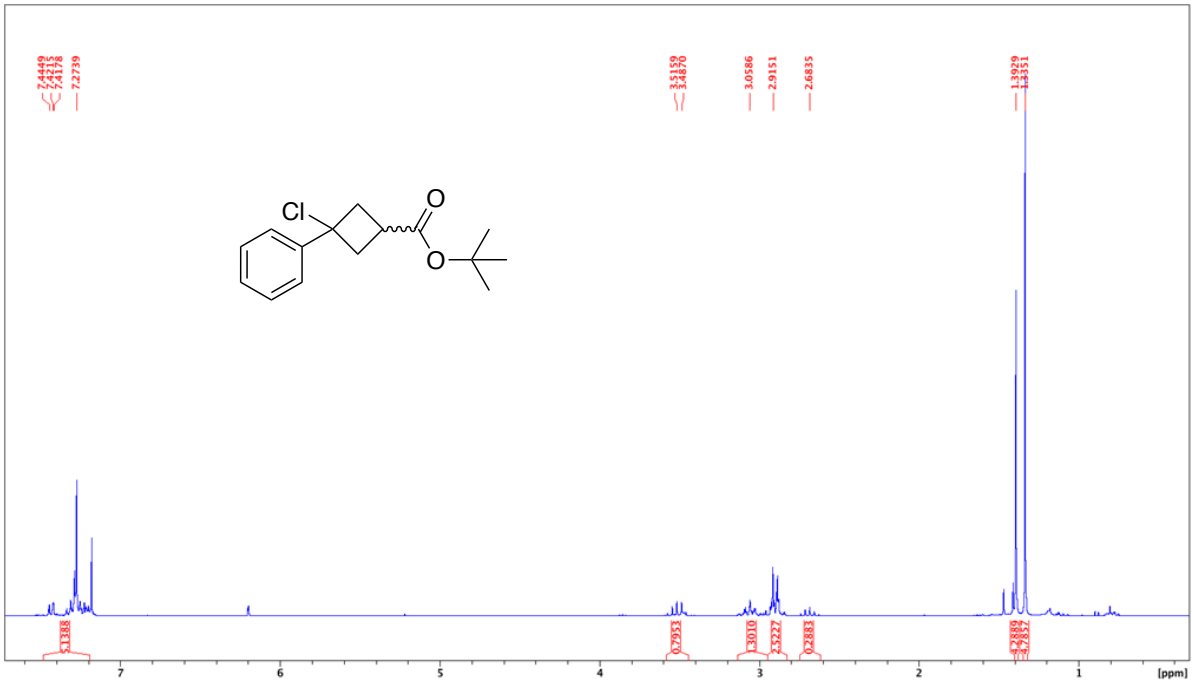

^{13}C NMR (126 MHz, $CDCl_3$, 292K, ppm): δ 1152.24, 128.60, 128.57, 128.02, 127.92, 125.89, 125.10, 80.93, 80.76, 42.54, 42.45, 41.71, 33.92, 33.09, 28.05, 28.01.

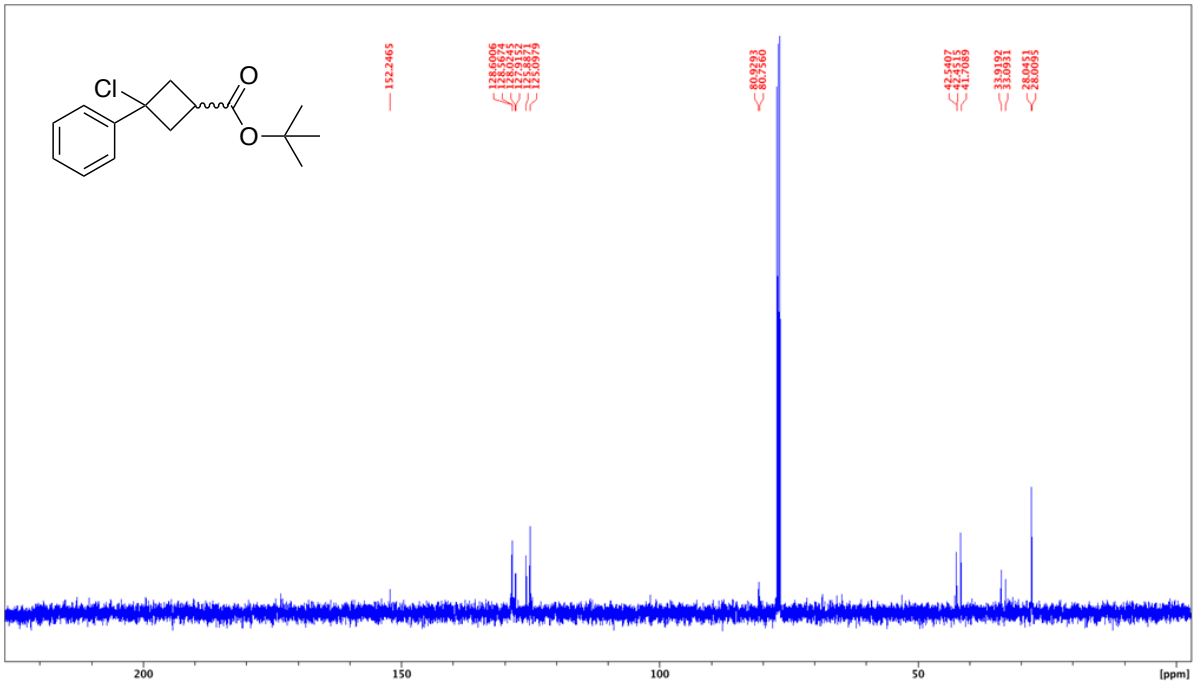

(3-Chloro-3-phenylcyclobutyl)(morpholino)methanone

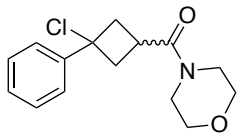

This product is prepared by **General Procedure 4** using morpholine (233 μL, 2.68 mmol), DIPEA (390 μL, 2.23 mmol), and 3-chloro-3-phenylcarbonyl chloride (0.5100 g, 2.23 mmol) in 15 mL of DCM. The crude product is purified by column chromatography (SiO_2, 0-100% EtOAc/hexanes, eluted at 50% EtOAc). 469 mg of a dark orange solid was obtained as a mixture of diastereomers (75%).

HRMS(ESI): calc'd for [$C_{15}H_{18}ClNO_2$ + H+], 280.10989; found: 280.11016.

^{1}H NMR (500 MHz, $CDCl_3$, 292K, ppm): δ 7.60-7.25 (m, 5H), 3.89-3.39 (m, 7.34H), 3.30-2.79 (m, 5H), 2.76-2.48 (m, 0.66H).

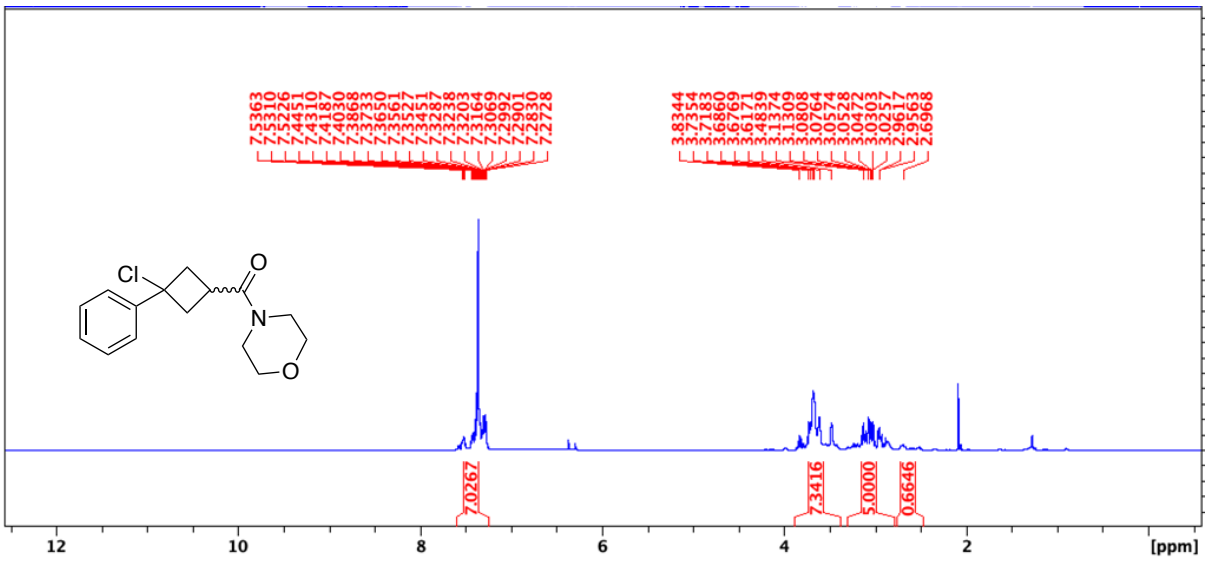

^{13}C NMR (126 MHz, $CDCl_3$, 292K, ppm): δ 178.45, 171.71, 144.84, 128.74, 128.69, 128.66, 128.63, 128.60, 128.58, 128.51, 128.45, 128.37, 128.31, 128.17, 128.04, 128.00, 127.65, 127.46, 127.43, 126.03, 125.86, 125.09, 125.05, 125.03, 125.01, 124.99, 124.09, 68.87, 68.37, 66.86, 66.72, 45.68, 42.45, 42.33, 42.30, 41.66, 41.56, 40.54, 40.42, 39.41, 39.22, 32.70, 31.93, 30.97, 30.71, 29.67, 28.02, 20.75.

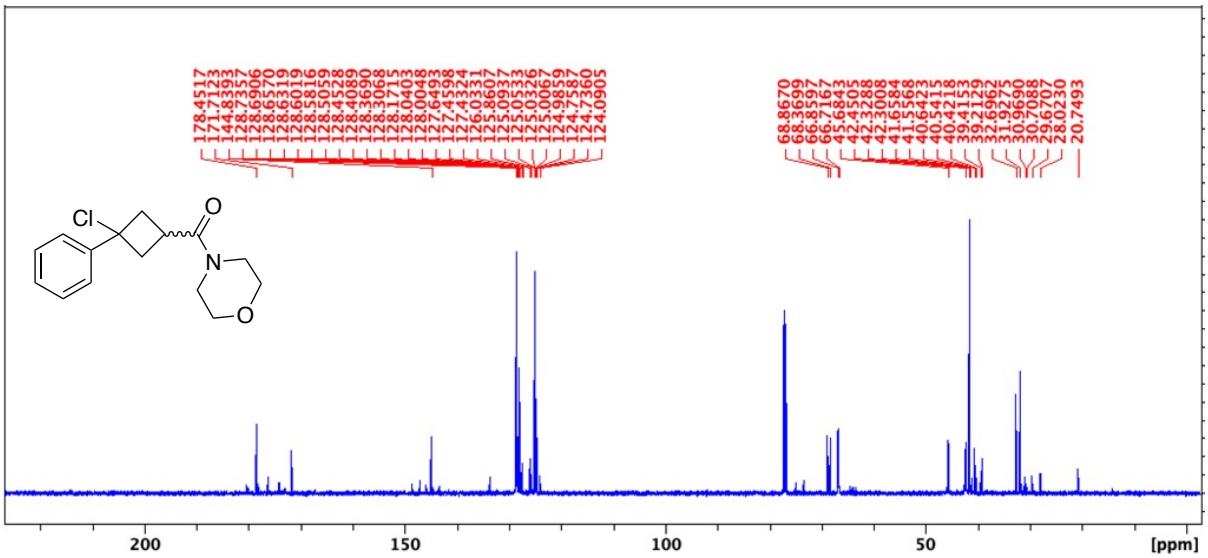

Methyl 3-(4-fluorophenyl)bicyclo[1.1.0]butane-1-carboxylate[114;154]

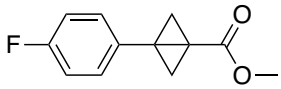

This product is prepared by **General Procedure 5** using toluene as a solvent at room temperature. methyl 3-chloro-3-(4-fluorophenyl)cyclobutane-1-carboxylate (2.072 g, 8.54 mmol), NaHMDS (10 mL, 10.25 mmol) in 20 mL toluene. The product was isolated as a yellow solid (0.4860 g, 28%).

^{1}H NMR (500 MHz, $CDCl_3$, 292K, ppm): δ 7.10 (m, 3H), 6.84 (m, 2H), 3.34 (s, 3H), 2.72 (m, 2H), 1.45 (m, 2H).

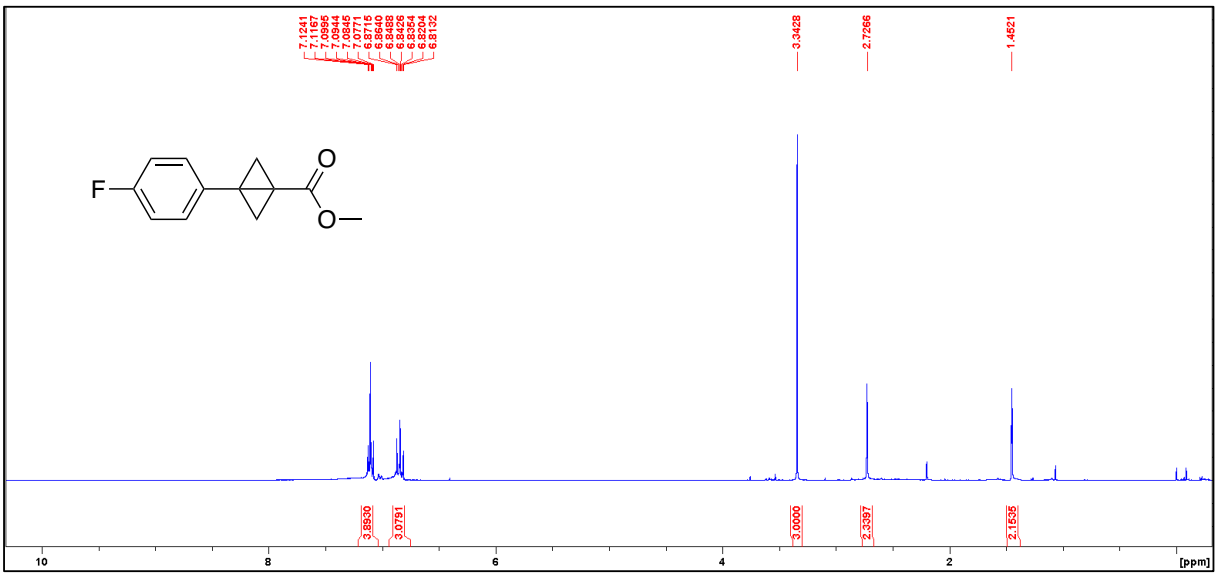

^{19}F NMR (500 MHz, $CDCl_3$, 292K, ppm): δ 115.16.

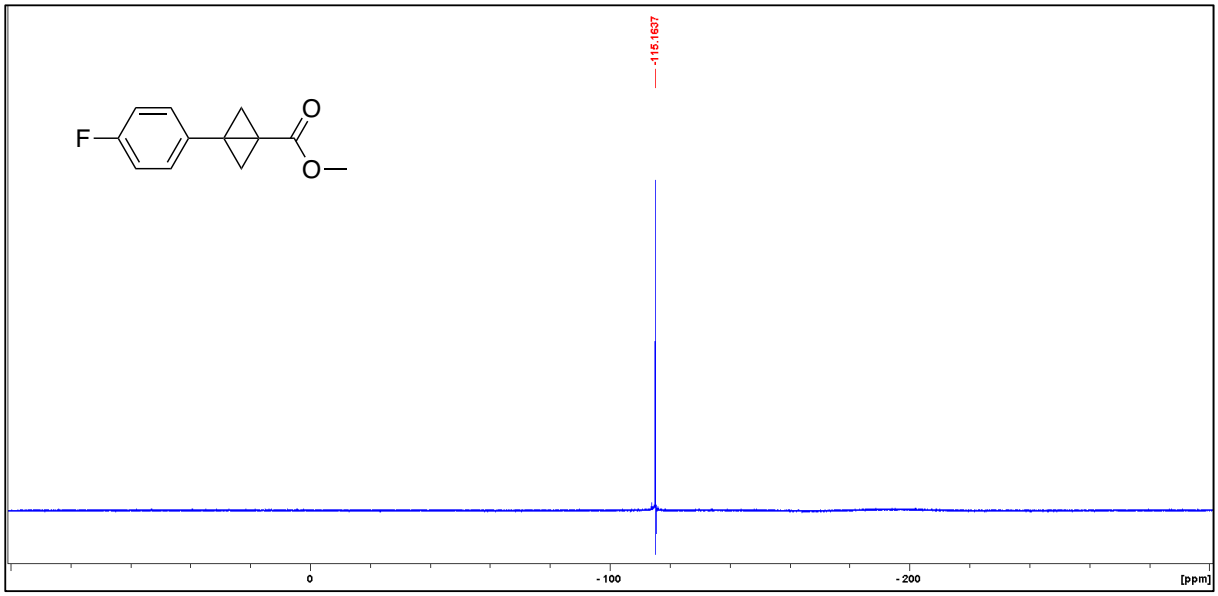

Methyl 3-(4-chlorophenyl)bicyclo[1.1.0]butane-1-carboxylate

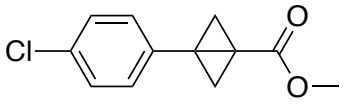

This product was prepared by **General Procedure 5** using THF at room temperature. 3-chloro-3-(4-chlorophenyl)cyclobutane-1-carboxylate (0.39230 g, 1.51 mmol), LiHMDS (1.51 mL, 1.51 mmol) in 17.6 mL THF. The product was isolated as an orange solid (0.3371 g, 90%).

HRMS(ESI): calc'd for $[C_{12}H_{11}{}^{35}ClO_2 + H^+]$, 223.05204; found: 223.05204.

^{1}H NMR (300 MHz, $CDCl_3$, 292K, ppm): δ 7.14 – 7.03 (m, 4H), 3.35 (s, 3H), 2.74 (s, 2H), 1.46 (s, 2H).

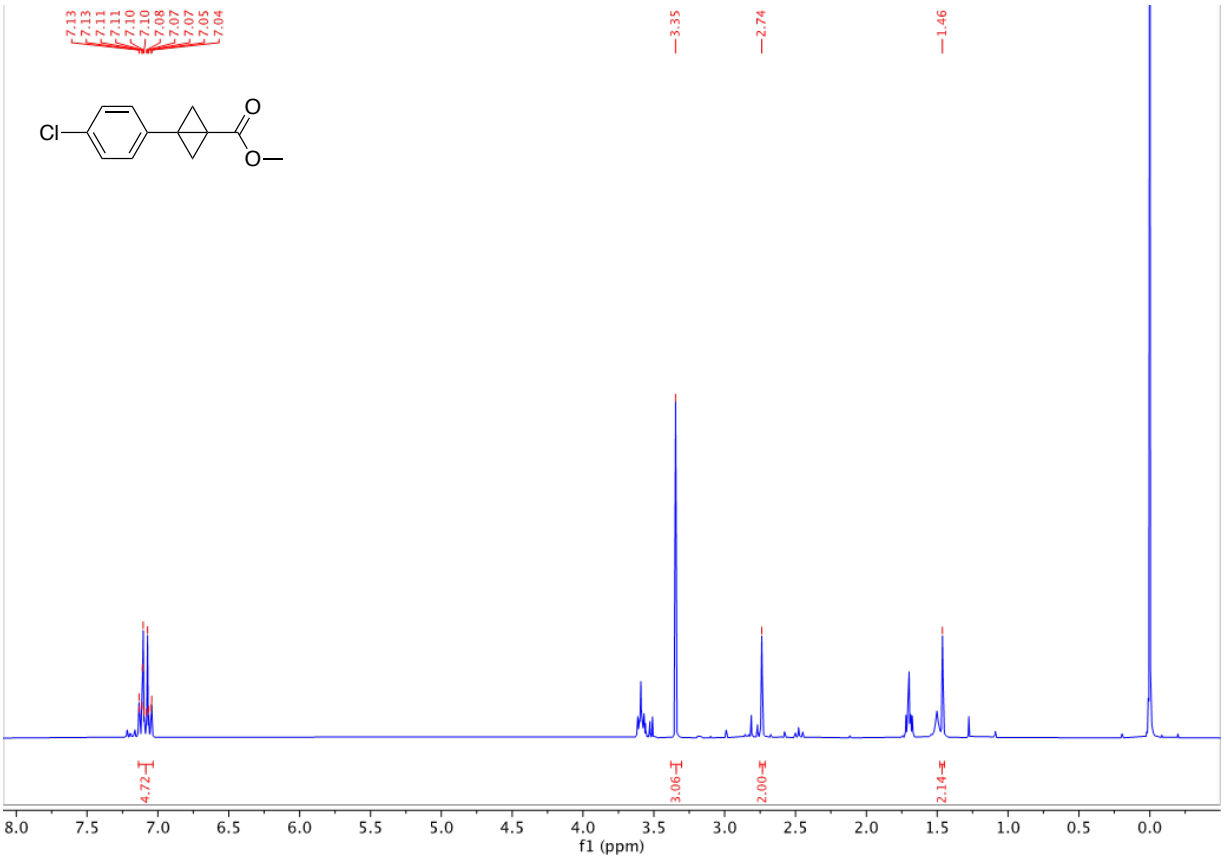

^{13}C NMR (126 MHz, $CDCl_3$, 292K, ppm): δ 168.43, 131.55, 131.06, 127.40, 127.37, 125.86, 50.60, 34.57, 33.56, 30.80, 22.20.

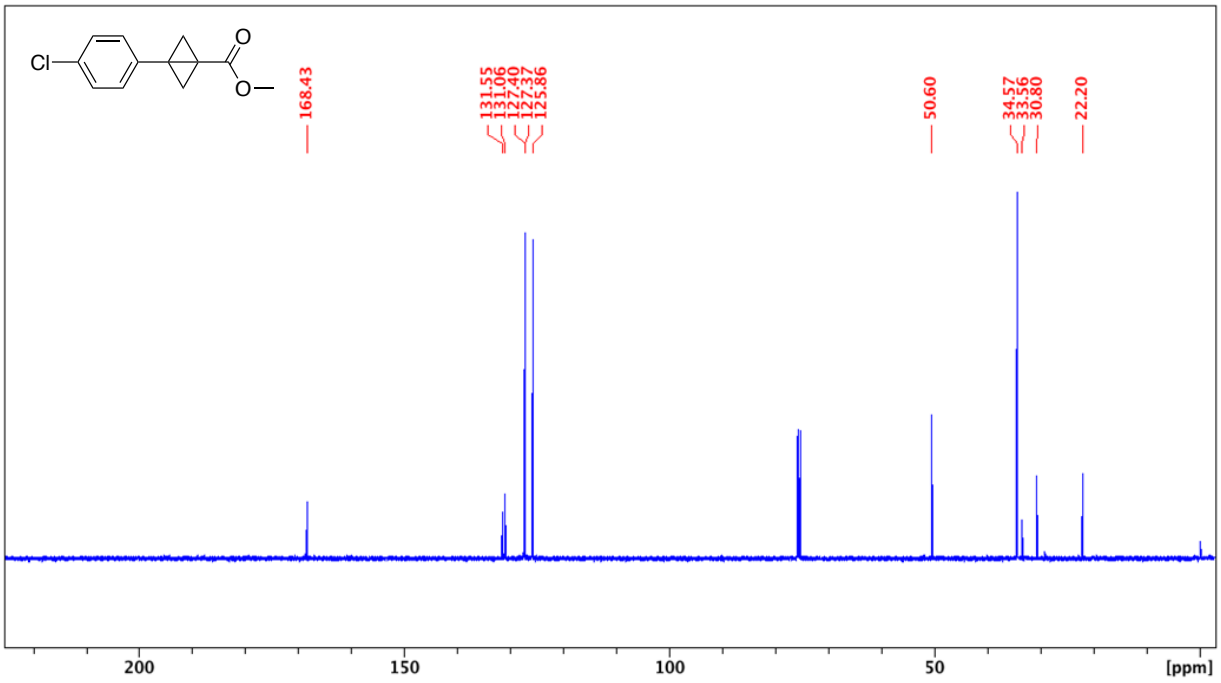

Benzyl 3-phenylbicyclo[1.1.0]butane-1-carboxylate

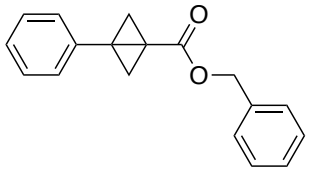

This product was prepared by **General Procedure 5** using THF and a reaction temperature of 70 °C. benzyl 3-chloro-3-phenylcyclobutane-1-carboxylate (0.8619 g, 2.87 mmol), NaHMDS (3.44 mL, 3.44 mmol) in 9 mL THF. The product was isolated as an orange solid (0.577 g, 76%).

HRMS(ESI): calc'd for [$C_{18}H_{16}O_2$ + H^+], 265.12231; found: 265.12229.

^{1}H NMR (500 MHz, $CDCl_3$, 292K, ppm): δ 7.41-7.21 (m, 8H), 7.05-7.00 (m, 2H), 4.96 (s, 2H), 3.00 (s, 2H), 1.65 (s, 2H).

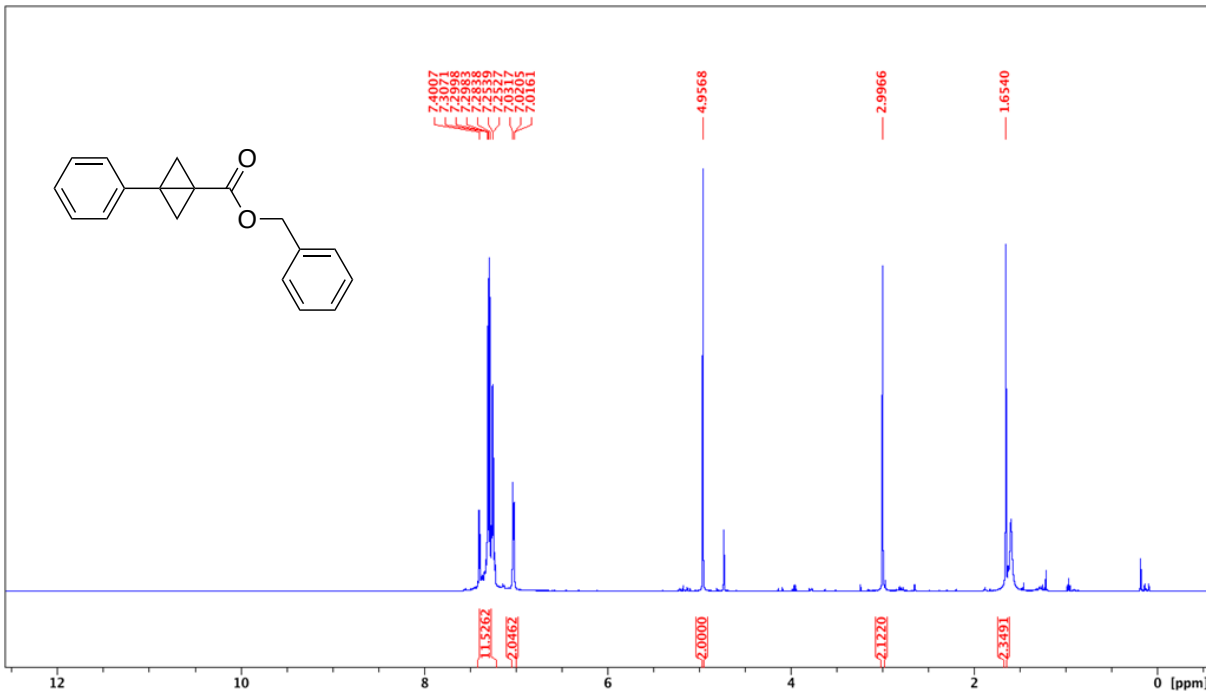

^{13}C NMR (126 MHz, $CDCl_3$, 292K, ppm): δ 169.64, 136.16, 133.44, 128.59, 128.54, 128.52, 128.35, 127.83, 127.75, 127.00, 125.99, 66.16, 35.89, 35.40, 23.18.

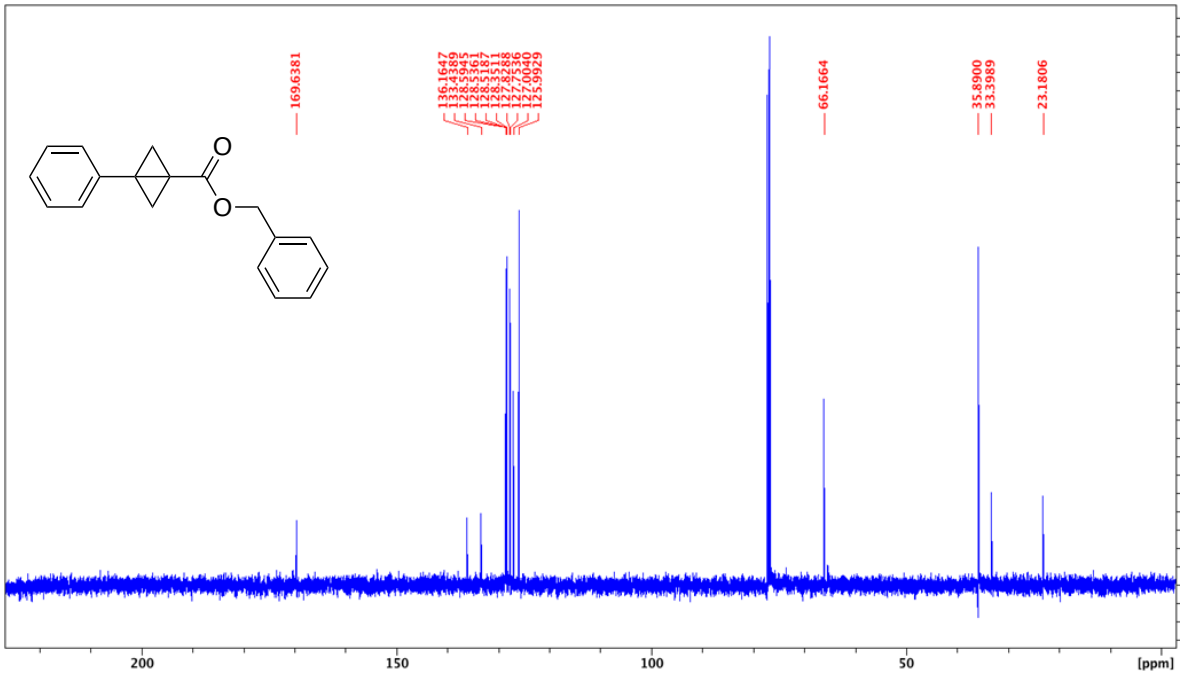

(1*S*,2*R*,5*S*)-2-Isopropyl-5-methylcyclohexyl-3-phenylbicyclo[1.1.0]butane-1-carboxylate

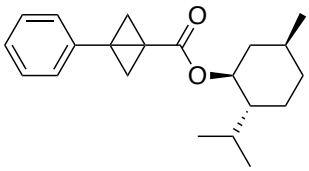

HRMS(ESI): calc'd for [$C_{21}H_{28}O_2$ + H^+], 313.21621; found: 313.21628.

This product was prepared by **General Procedure 5** using THF and a reaction temperature of 70 °C. (1*S*,2*R*,5*S*)-2-isopropyl-5-methylcyclohexyl 3-chloro-3-phenylcyclobutane-1-carboxylate (0.3000 g, 0.86 mmol), NaHMDS (1.03 mL, 1.03 mmol) in 3 mL THF. The product was isolated as a yellow solid (0.2687 g, 65%).

^{1}H NMR (500 MHz, $CDCl_3$, 292K, ppm): δ 7.34-7.19 (m, 5H), 4.54-4.42 (dt, J=11.16,4.34 Hz, 1H), 3.02-2.97 (dd, J=6.79,1.94 Hz, 1H), 2.97-2.91 (dd, 6.69,1.94 Hz, 1H), 1.66-1.53 (m, 5H), 1.53-1.48 (m, 1H), 1.46-1.38 (m, 1H), 1.37-1.27 (m, 1H), 1.25-1.16 (m, 1H), 0.96-0.86 (m, 1H), 0.81-0.71 (m, 7H), 0.72-0.63 (q, J=11.41 Hz, 1H), 0.46-0.40 (d, J=7.03 Hz, 3H).

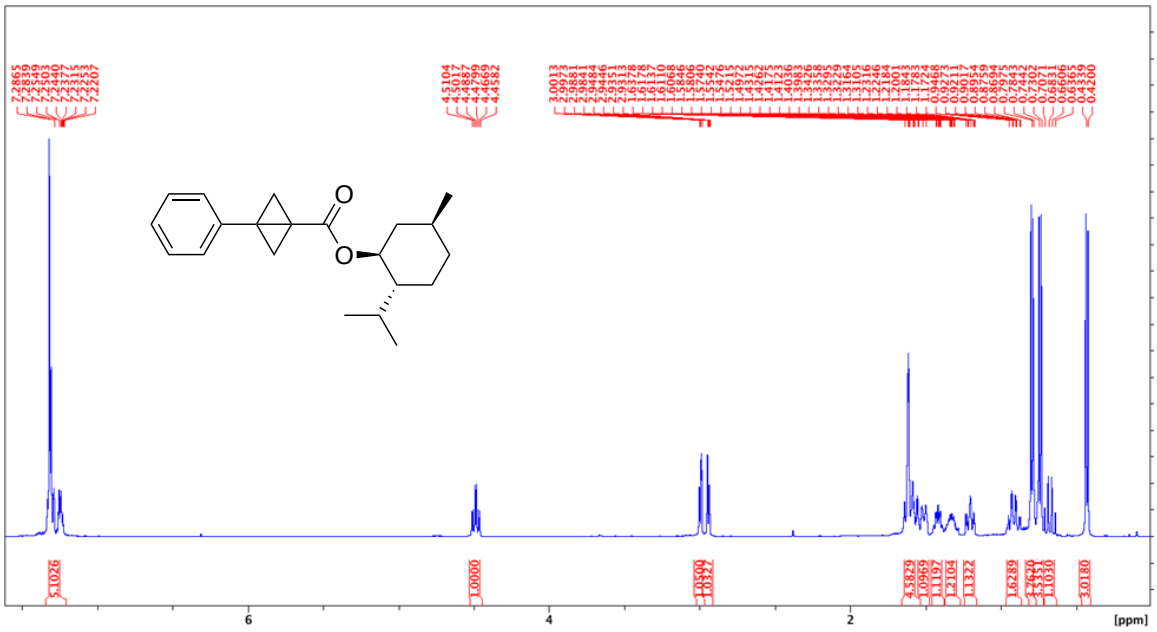

^{13}C NMR (126 MHz, $CDCl_3$, 292K, ppm): δ 1169.22, 133.73, 128.38, 126.87, 125.91, 74.25, 46.72, 41.04, 35.70, 35.48, 34.19, 32.63, 31.21, 25.74, 23.55, 23.10, 21.86, 20.76, 15.72.

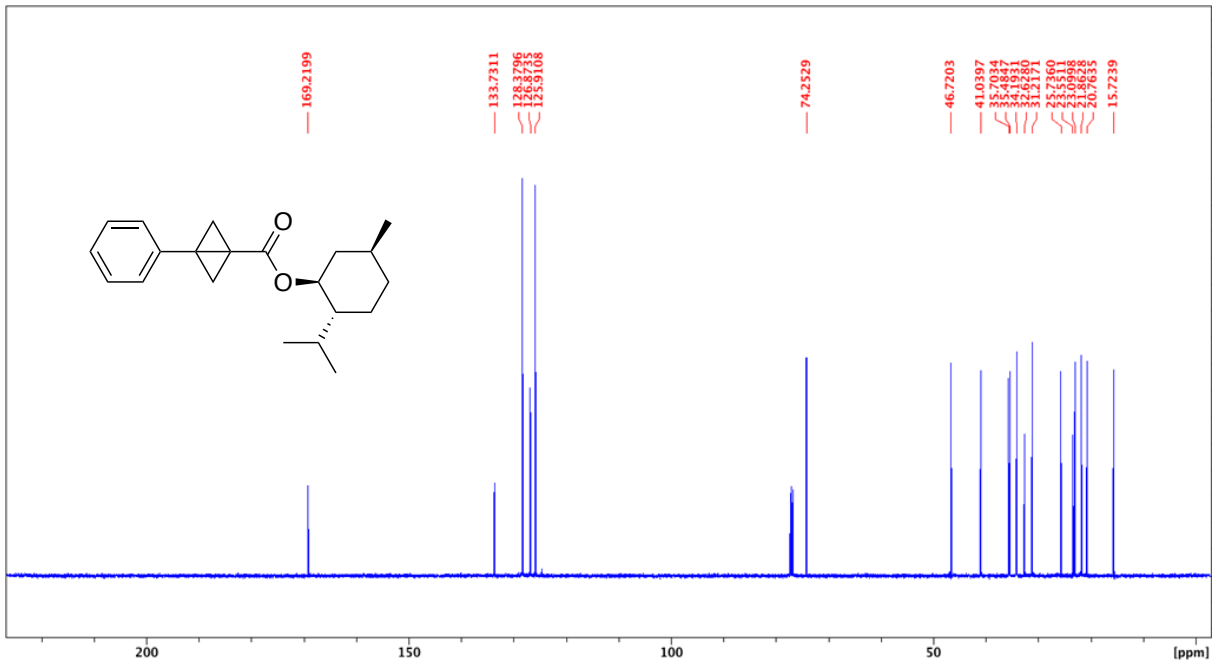

***Tert*-butyl 3-phenylbicyclo[1.1.0]butane-1-carboxylate**

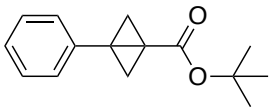

This product was prepared by **General Procedure 5** using THF and a reaction temperature of 70 °C. *Tert*-butyl 3-chloro-3-phenylcyclobutane-1-carboxylate (0.2900 g, 1.09 mmol), NaHMDS (1.30 mL, 1.30 mmol) in 3 mL THF. The product was isolated as a yellow oil (0.167 g, 67%).

^{1}H NMR (500 MHz, $CDCl_3$, 292K, ppm): δ 7.17-7.02 (m, 5H), 2.75 (m, 2H), 1.40 (m, 2H), 0.97 (s, 9H).

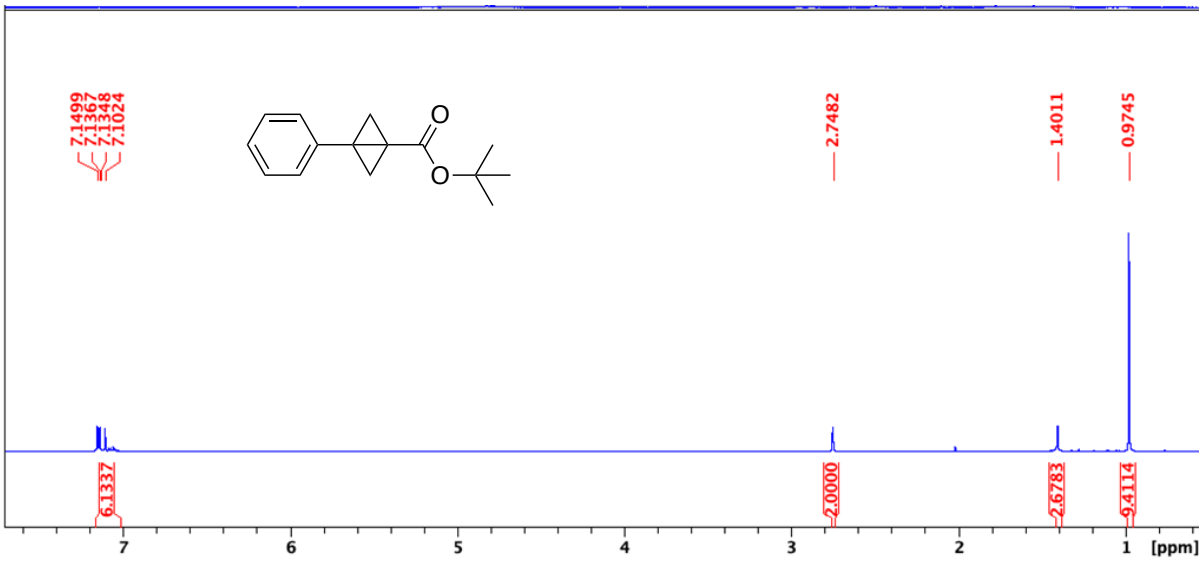

^{13}C NMR (126 MHz, $CDCl_3$, 292K, ppm): δ 136.47, 133.44, 128.70, 128.10, 82.61, 54.45, 51.47, 41.57, 27.79.

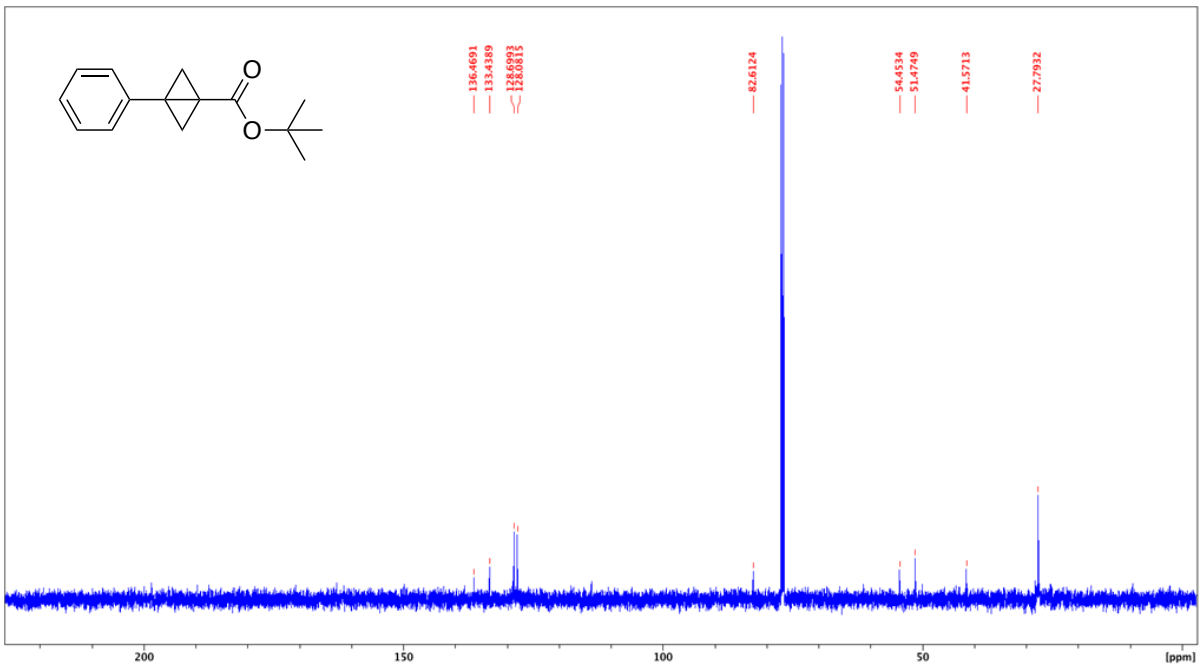

Morpholino(3-phenylbicyclo[1.1.0]butan-1-yl)methanone

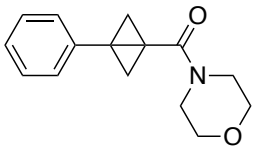

(3-chloro-3-phenylcyclobutyl)(morpholino)methanone (0.4776g, 1.70 mmol) was added to a 20 mL vial and dissolved in 5 mL THF under a N_2 atmosphere at 0 °C. NaHMDS (2.04 mL, 2.04 mmol) was added to the vial and the reaction mixture was stirred at 0 °C for 4 hours. The reaction mixture was diluted with DCM and washed with water. The organic layer was dried with Mg_2SO_4 and the solvent was removed by evaporation. The product was isolated as an orange solid and used without further purification (0.394, 95%).

HRMS(ESI): calc'd for $[C_{15}H_{17}NO_2 + H^+]$, 244.13321; found: 244.13324.

^{1}H NMR (500 MHz, $CDCl_3$, 292K, ppm): δ 7.37-7.18 (m, 5H), 3.61 (s, 8H), 2.77 (s, 2H), 1.60 (s, 2H).

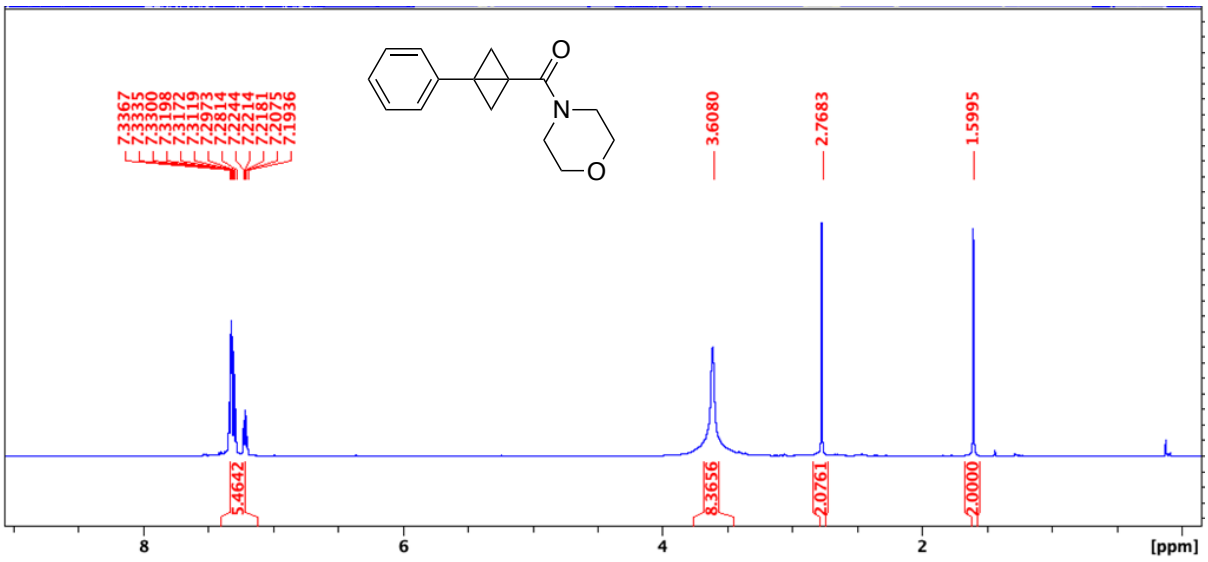

^{13}C NMR (126 MHz, $CDCl_3$, 292K, ppm): δ 166.30, 132.44, 126.89, 125.20, 124.99, 65.56, 35.27, 29.87, 19.88.

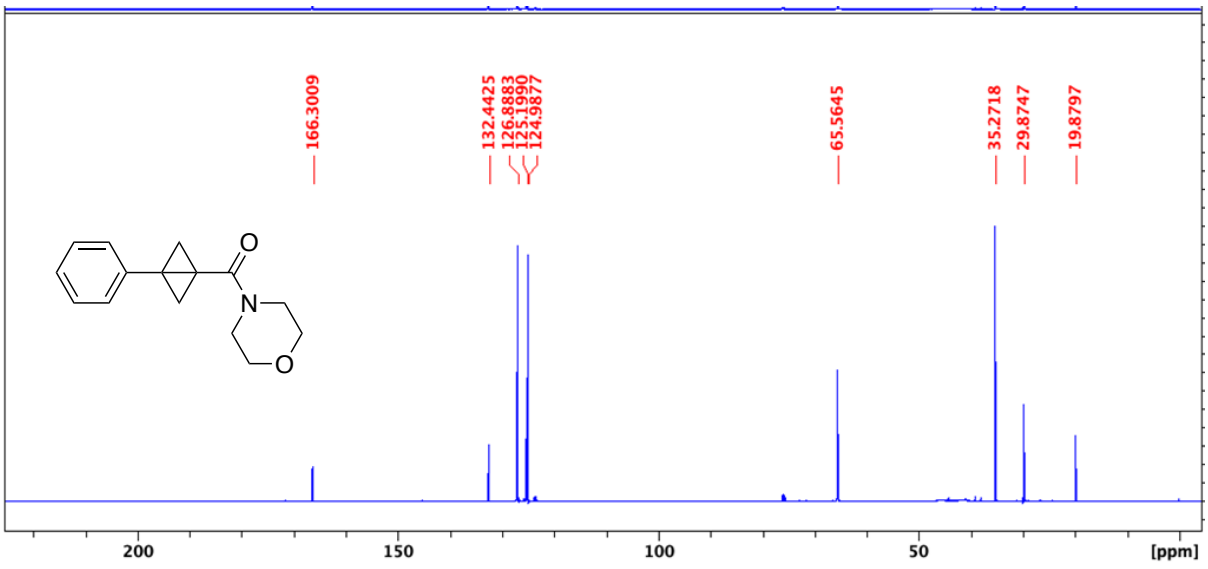

A.6 Azabicyclohexane Synthesis

Method A General Procedure:

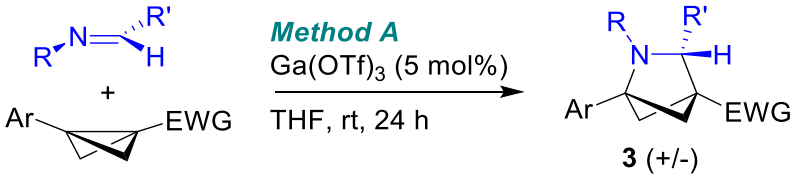

A vial was charged with a bicyclobutane (0.500 mmol) and an *N*-arylimine (1.1 equiv) and then taken inside the glovebox. $Ga(OTf)_3$ (0.025 mmol, 5 mol%) was added to a second vial. The substrates were dissolved in THF (3 mL). Once the substrates were completely dissolved, this solution was transferred to the vial containing $Ga(OTf)_3$. A stir bar was added, the vial was capped, and stirring was commenced outside the glovebox. After stirring at rt for 24 h, the vial was opened and the solvent was evaporated. The resulting residue was dissolved in toluene (5 mL) and washed with saturated $NaHCO_3$ (5 mL) and brine (5 mL). The toluene layer was directly loaded onto a silica gel column for purification.

Methyl-2-(4-methoxyphenyl)-1,3-diphenyl-2-azabicyclo[2.1.1]hexane-4-carboxylate (3e)

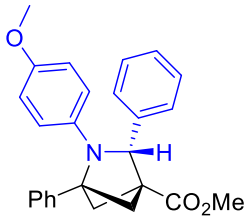

The product was prepared by **Method A** using **2a** (0.1914 g, 1.02 mmol), **1e** (0.2363 g, 1.12 mmol) and $Ga(OTf)_3$ (0.0263 g, 5 mol%). The compound was purified by column chromatography (Biotage® Sfär 10g Column, 0-100% EtOAc/hexanes, eluted at 25% EtOAc). 179 mg of a dark brown solid was obtained (44%). 98% peak area by LCMS.

IR: C=O 1741 cm^{-1}

Melting point range: 119.1 – 121.4 °C

HRMS(ESI): calc'd for $[C_{26}H_{25}NO_3 + H^+]$, 400.19702; found: 400.19702.

^{1}H NMR (500 MHz, $CDCl_3$, 292K, ppm): δ 7.76 (d, J=8.27 Hz, 2H), 7.31-7.56 (m, 8H), 6.55-6.61 (m, 4H), 4.91 (s, 1H), 3.73 (s, 3H), 3.68 (s, 3H), 2.86 (d, J=7.66 Hz, 1H), 2.78 (m, 1H), 2.56 (m, 1H), 2.05 (d, J=7.66 Hz, 1H).

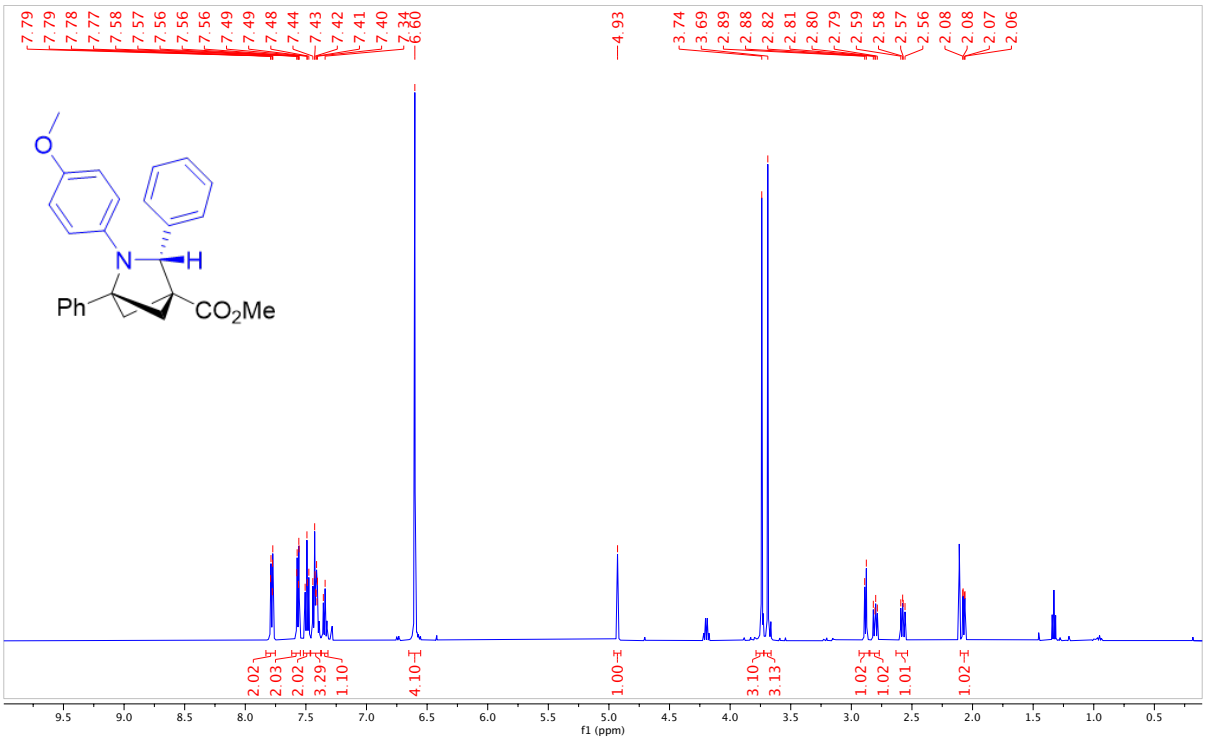

^{13}C NMR (126 MHz, $CDCl_3$, 292K, ppm): δ 171.01, 153.68, 144.62, 141.06, 139.69, 128.78, 128.34, 127.91, 127.61, 127.32, 126.16, 120.45, 113.88, 74.42, 70.48, 55.39, 54.37, 51.65, 45.58, 44.62.

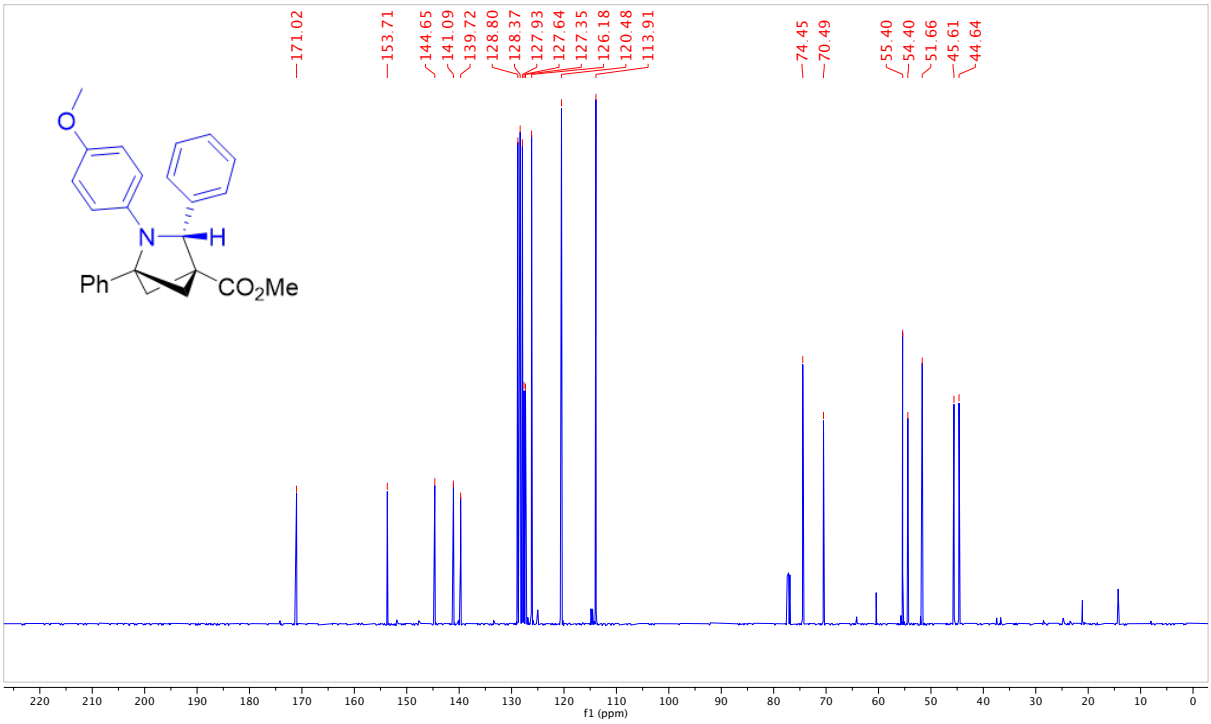

ATR IR spectrum:

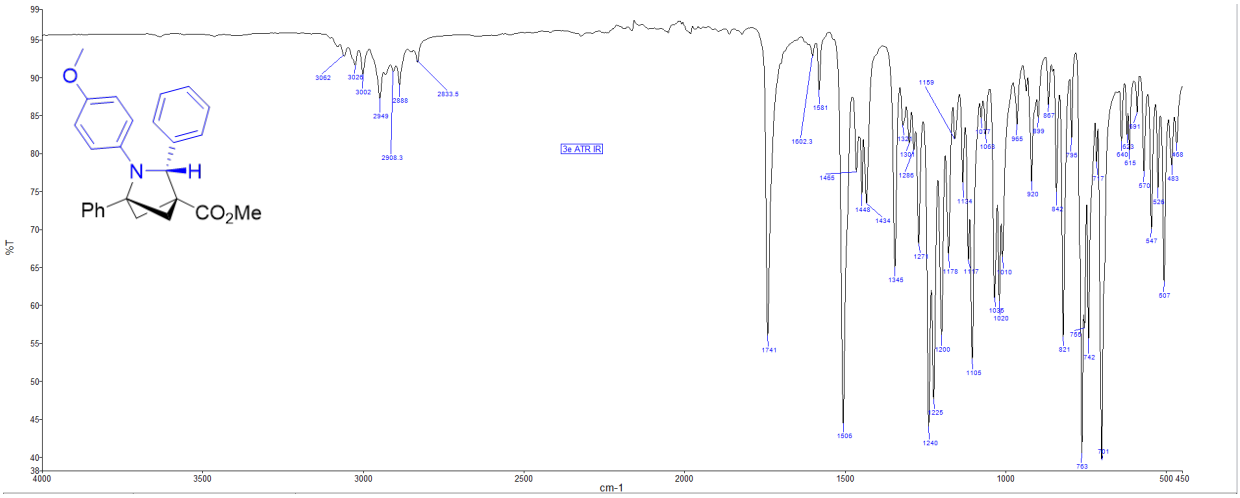

LCMS Chromatogram:

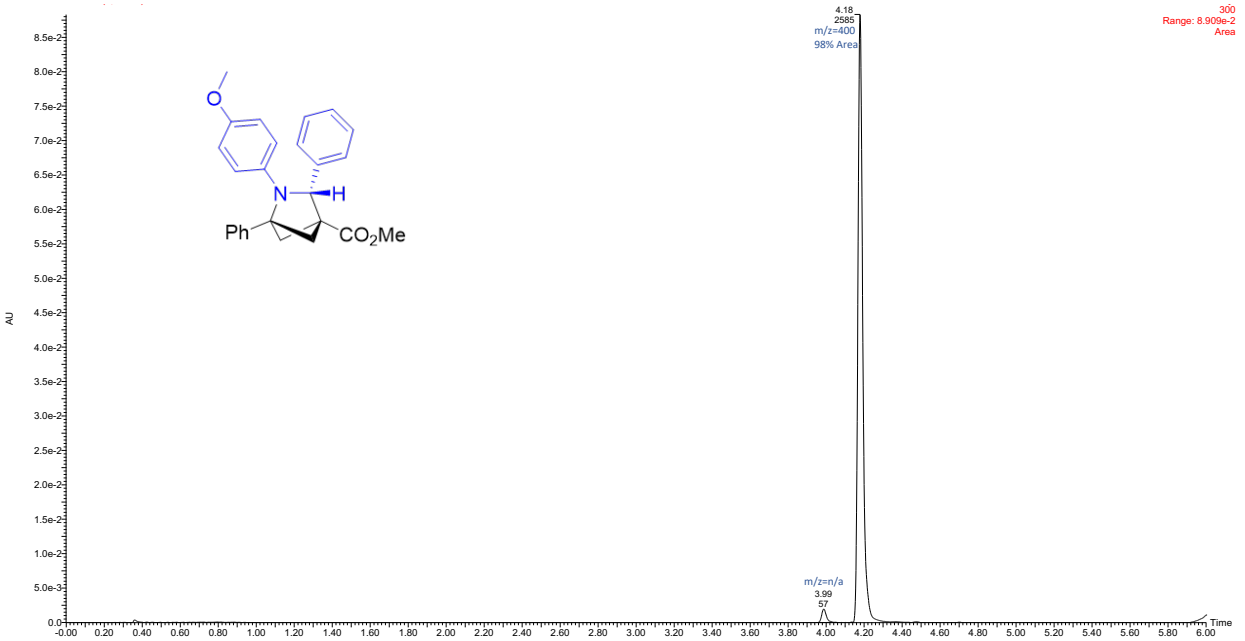

Methyl-3-(4-cyanophenyl)-2-(4-methoxyphenyl)-1-phenyl-2-azabicyclo[2.1.1]-hexane-4-carboxylate (3i)

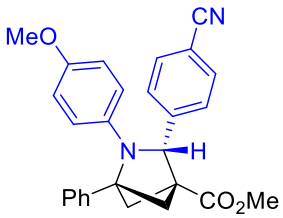

The product was prepared by **Method A** using **2a** (0.0941 g, 0.50 mmol), **1i** (0.1299 g, 0.55 mmol) and $Ga(OTf)_3$ (0.0129 g, 5 mol%). The compound was purified by column chromatography (Biotage® Sfär 10g Column, 0-100% EtOAc/hexanes, eluted at 25% EtOAc). 111.1 mg of a yellow solid was obtained (52%). 98% peak area (2% **4i**) by LCMS

IR: C≡N 2228 cm^{-1}, C=O 1731 cm^{-1}

Melting point range: 95.4 – 98.3 °C

HRMS(ESI): calc'd for [$C_{27}H_{24}N_2O_3$ + H^+], 425.18597; found: 425.18577.

^{1}H NMR (500 MHz, $CDCl_3$, 292K, ppm): δ 77.78 (d, J = 8.18 Hz, 2H), 7.64 (d, J = 8.18 Hz, 2H), 7.36 m, 2H), 7.29 (m, 3H), 6.45 (m, 2H), 6.41 (m, 2H), 4.79 (s, 1H), 3.61 (s, 3H), 3.57 (s, 3H), 2.76 (d, J = 7.10 Hz, 1H), 2.69 (dd, J = 9.9, 7.0 Hz, 1H) 2.30 (dd, J = 9.9, 7.8 Hz, 1H), 1.97 (d, J = 7.66 Hz, 1H).

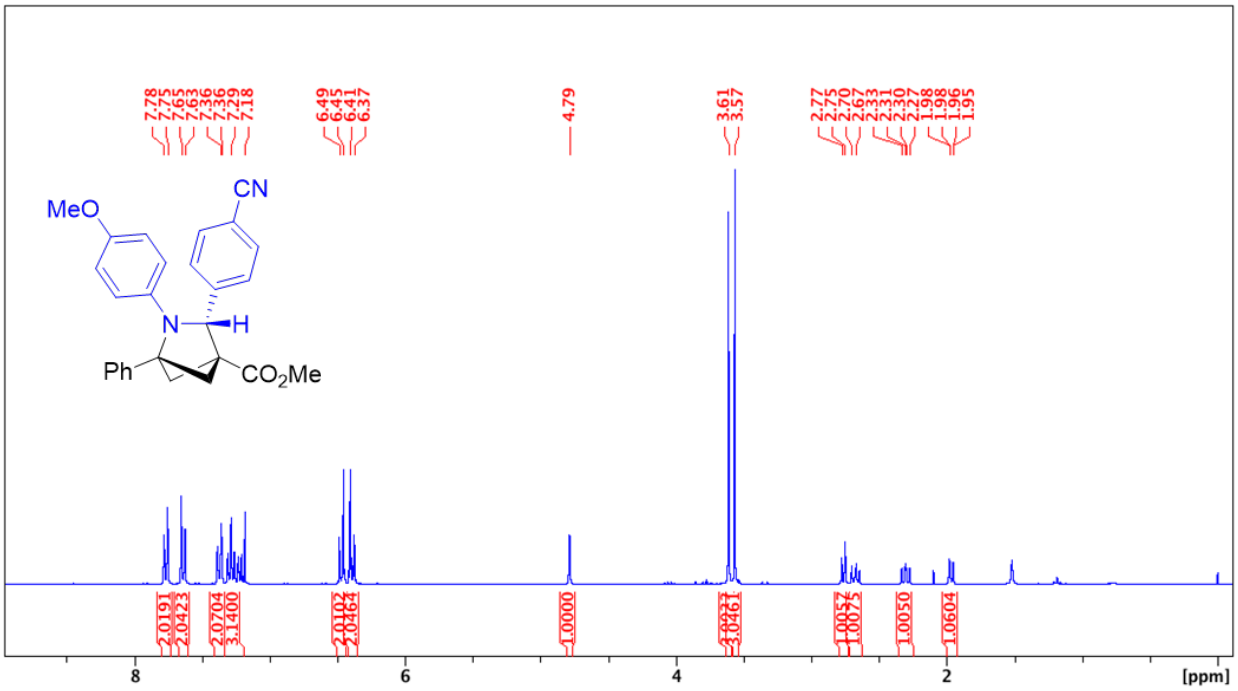

^{13}C NMR (126 MHz, $CDCl_3$, 292K, ppm): δ 170.45, 154.14, 146.55, 143.67, 138.94, 132.16, 128.87,128.80, 127.55,126.14, 120.83, 118.91, 113.97, 111.57, 73.59, 70.91, 55.37, 54.34, 51.86, 45.25, 44.96.

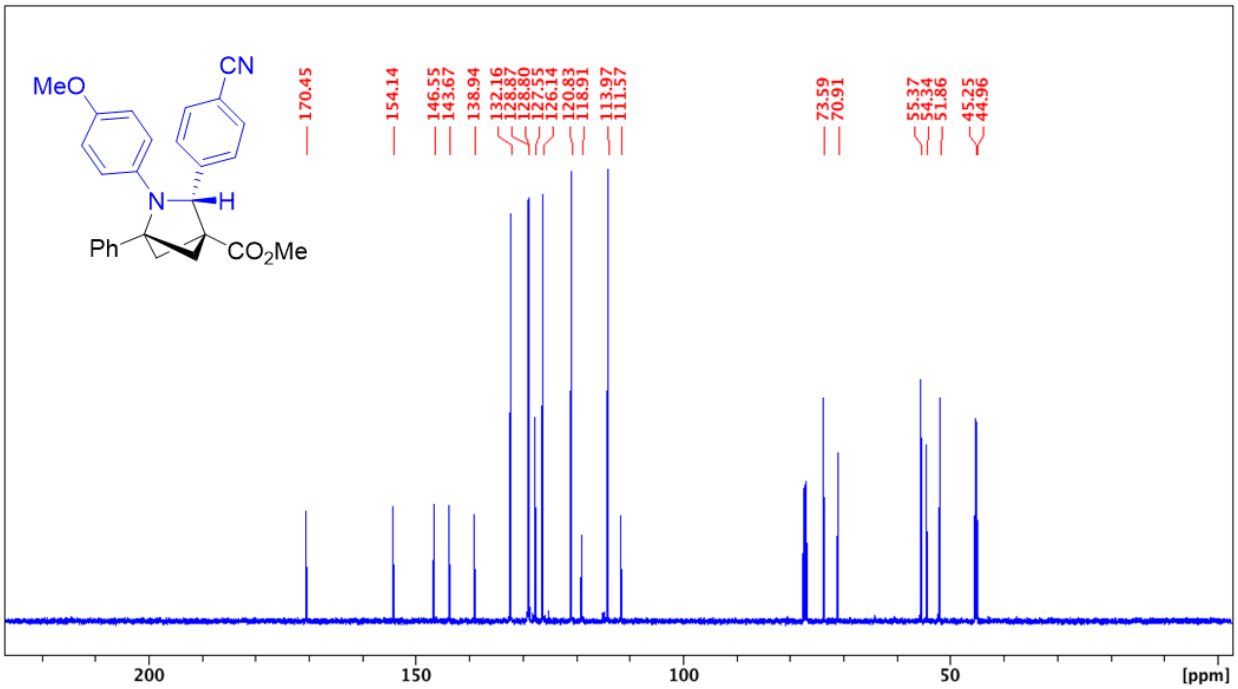

ATR IR spectrum:

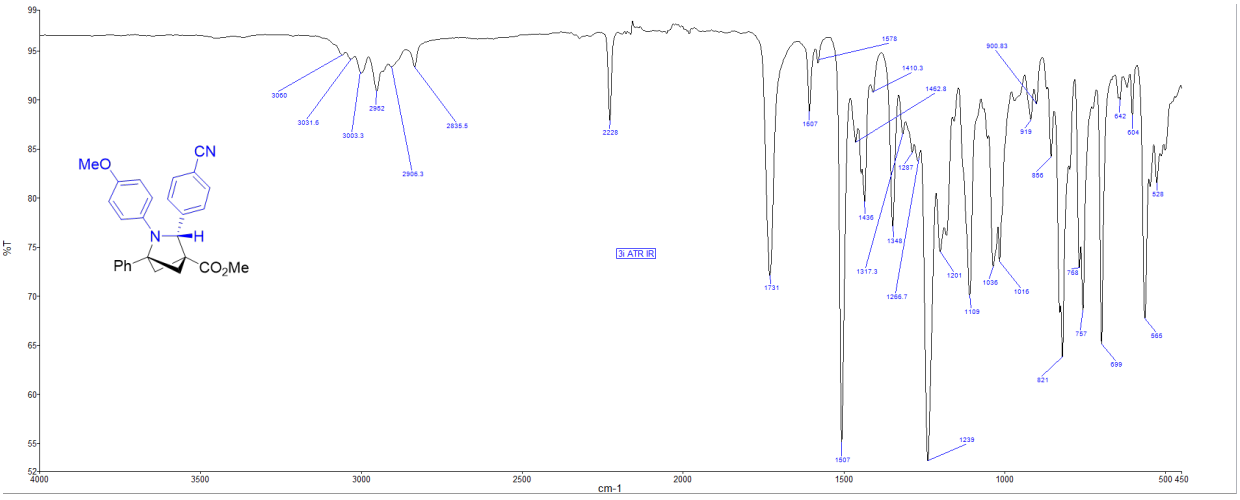

LCMS Chromatogram:

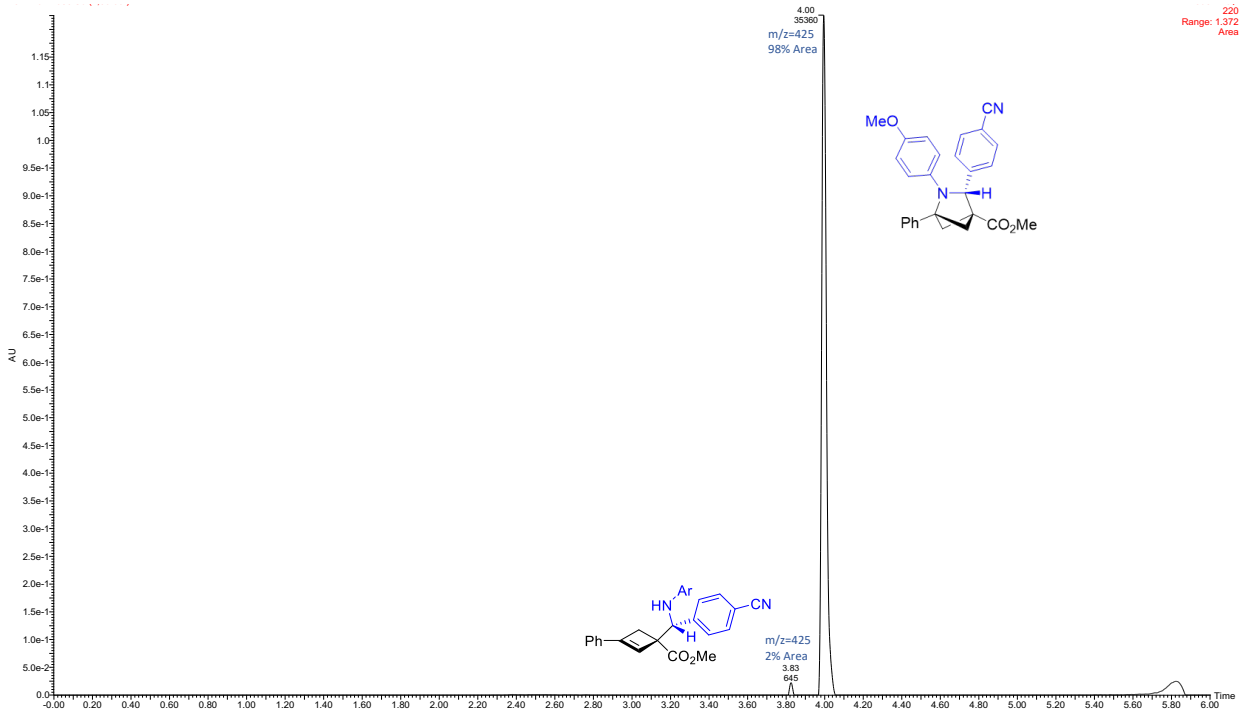

Methyl-3-(benzo[b]thiophen-3-yl)-2-(4-methoxyphenyl)-1-phenyl-2-azabicyclo-[2.1.1]hexane-4-carboxylate (3k)

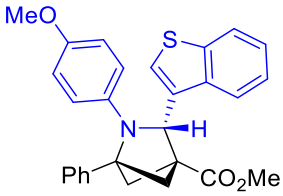

The product was prepared by **Method A** using **2a** (0.0941 g, 0.50 mmol), **1k** (0.1470 g, 0.55 mmol) and $Ga(OTf)_3$ (0.0129 g, 5 mol%). The compound was purified by column chromatography (Biotage® Sfär 10g Column, 0-100% EtOAc/hexanes, eluted at 30% EtOAc). 68 mg of a yellow oil was obtained (30%). 98% peak area by LCMS.

IR: C=O 1727 cm^{-1}

HRMS(ESI): calc'd for $[C_{28}H_{25}NO_3S + H^+]$, 456.16279; found: 456.16265.

^{1}H NMR (500 MHz, $CDCl_3$, 292K, ppm): δ 7.90 (d, J=0.73, 1H), 7.80 (m, 1H), 7.72 (m, 1H), 7.40 (m, 2H), 7.27 (m, 5H), 6.47 (m, 4H), 5.05 (s, 1H), 3.54 (s, 3H), 3.30 (s, 3H), 2.79 (d, J=6.99, 1H), 2.71 (m, 1H), 2.63 (m, 1H), 1.99 (m, 1H).

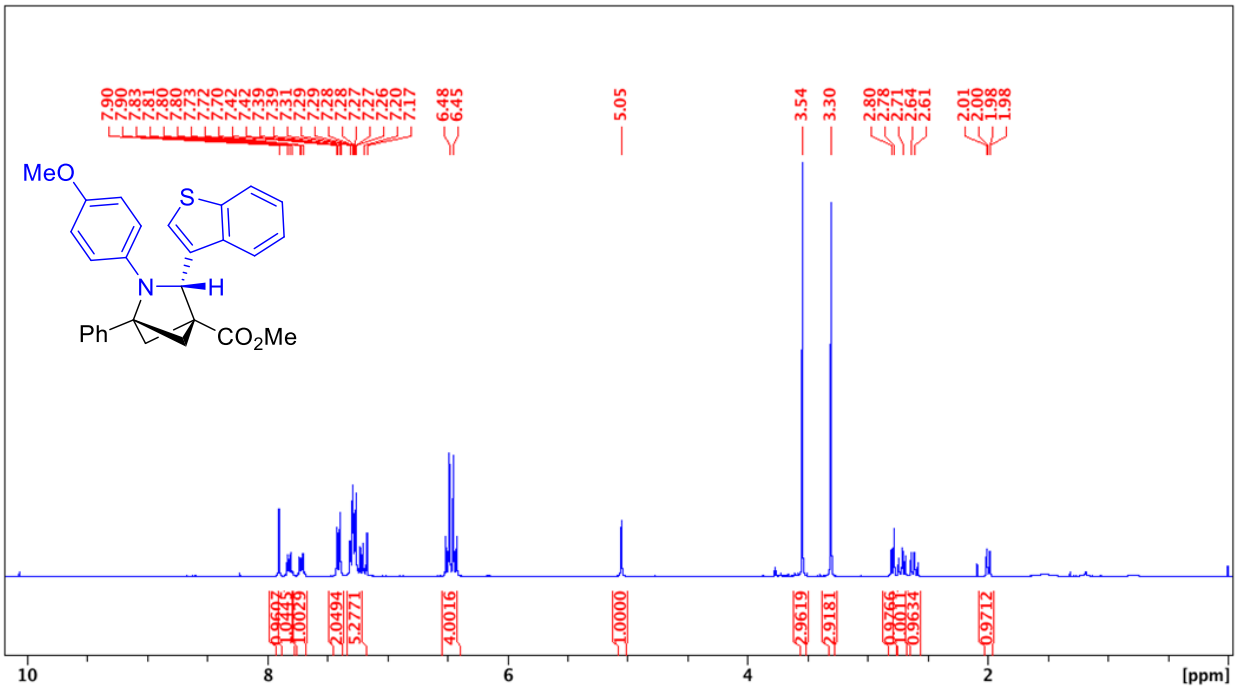

^{13}C NMR (126 MHz, $CDCl_3$, 292K, ppm): δ 171.25, 153.94, 144.32, 141.06, 139.39, 137.76, 136.81, 128.79, 127.37, 126.37, 126.20, 124.34, 123.87, 122.98, 121.89, 120.73, 113.91, 70.47, 69.79, 55.37, 53.38, 21.64, 47.25, 43.65.

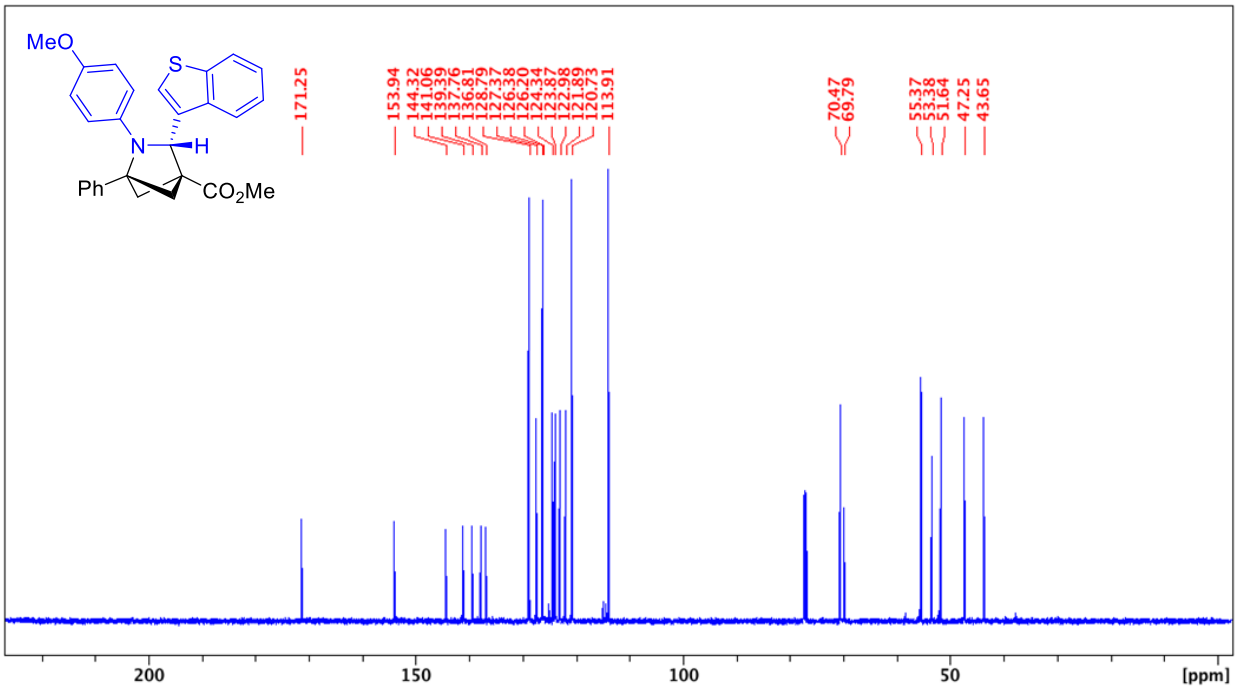

ATR IR spectrum:

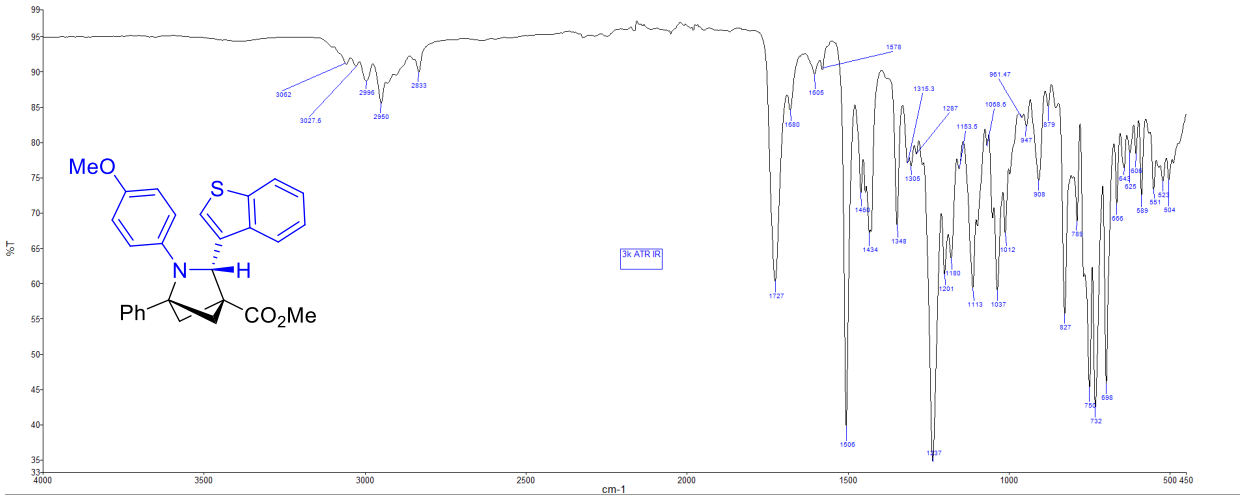

LCMS Chromatogram:

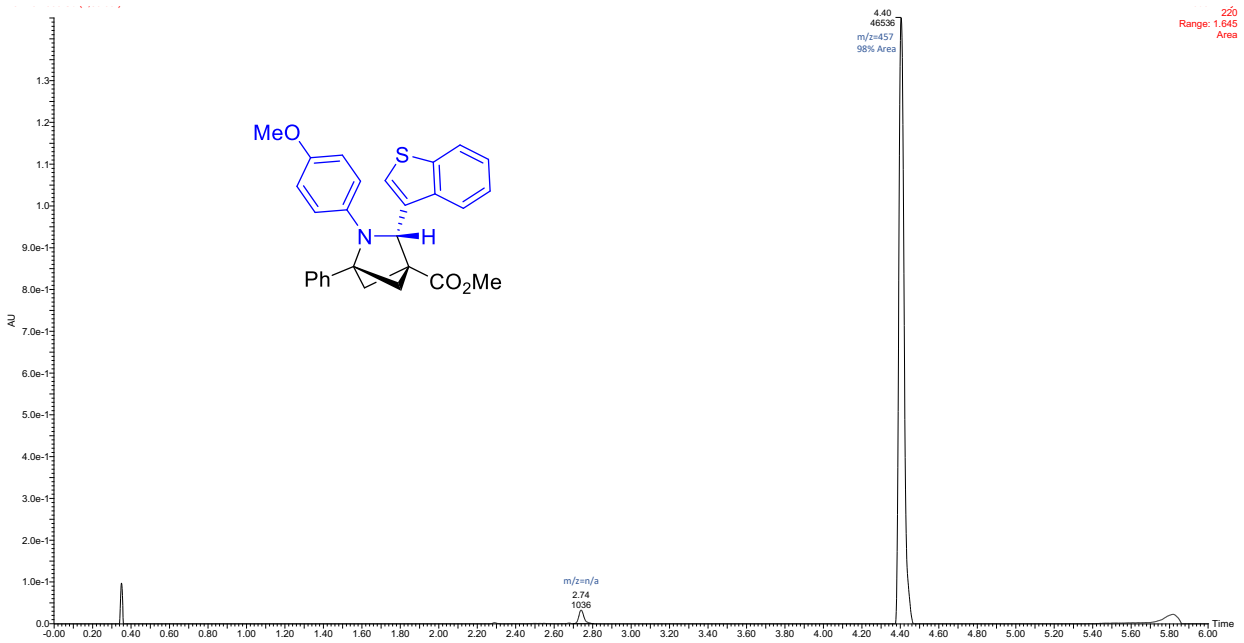

Methyl-2-(4-iodophenyl)-1-phenyl-3-(thiophen-2-yl)-2-azabicyclo[2.1.1]hexane-4-carboxylate (3m)

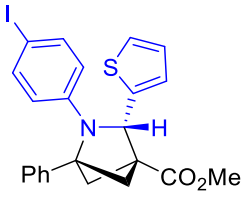

The product was prepared by **Method A** using **2a** (0.0941 g, 0.50 mmol), **1m** (0.1722 g, 0.55 mmol) and $Ga(OTf)_3$ (0.0129 g, 5 mol%). The compound was purified by column chromatography (Biotage® Sfär 10g Column, 0-100% EtOAc/hexanes, eluted at 25% EtOAc). 136 mg of a white solid was obtained (54%). 100% peak area by LCMS.

IR: C=O 1729 cm^{-1}

Melting point range: 152.7 – 154.0 °C

HRMS(ESI): calc'd for $[C_{23}H_{20}INO_2S + H^+]$, 502.03322; found: 502.03318.

^{1}H NMR (500 MHz, $CDCl_3$, 292K, ppm): δ 7.22 (m, 9H), 7.09 (m, 1H), 6.32 (m, 2H), 4.94 (s, 1H), 3.66 (s, 3H), 2.74 (d, J=6.75 Hz, 1H), 2.53 (m, 1H), 2.46 (m, 1H), 2.05 (m, 1H).

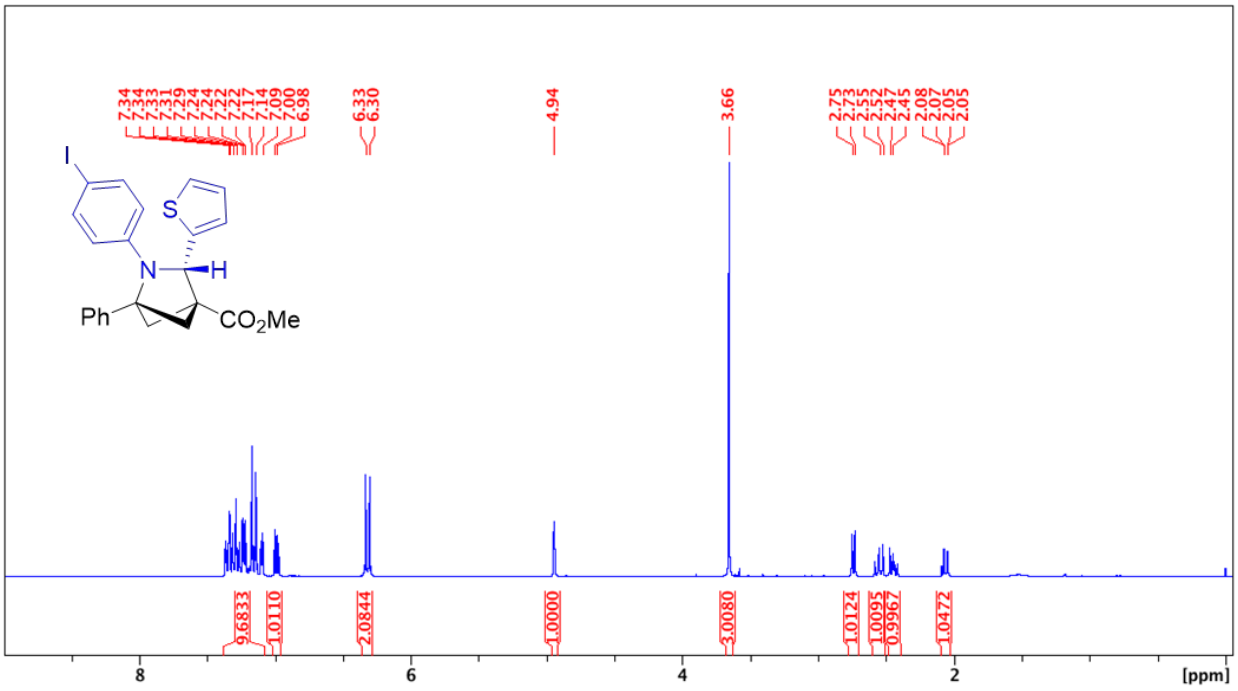

^{13}C NMR (126 MHz, $CDCl_3$, 292K, ppm): δ 170.05, 150.51, 145.19, 137.26, 128.98, 127.67, 127.36, 125.87, 125.36, 125.17, 121.17, 83.22, 70.92, 70.46, 54.37, 51.89, 46.64, 44.38.

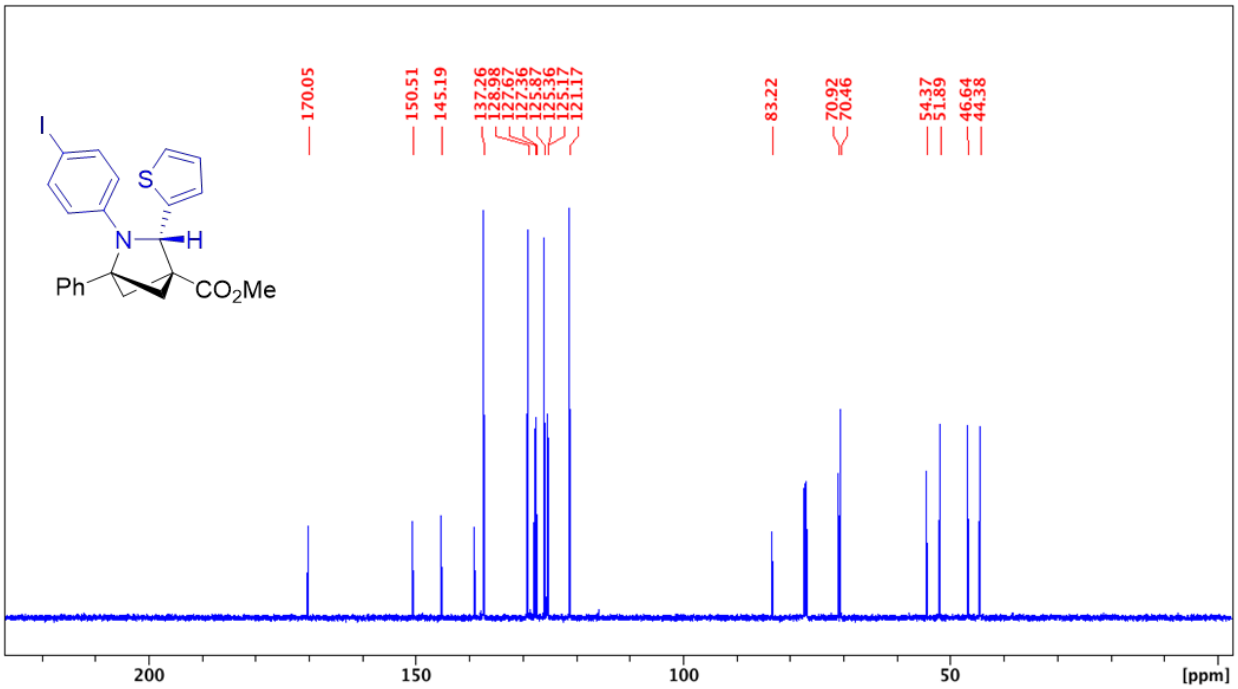

ATR IR spectrum:

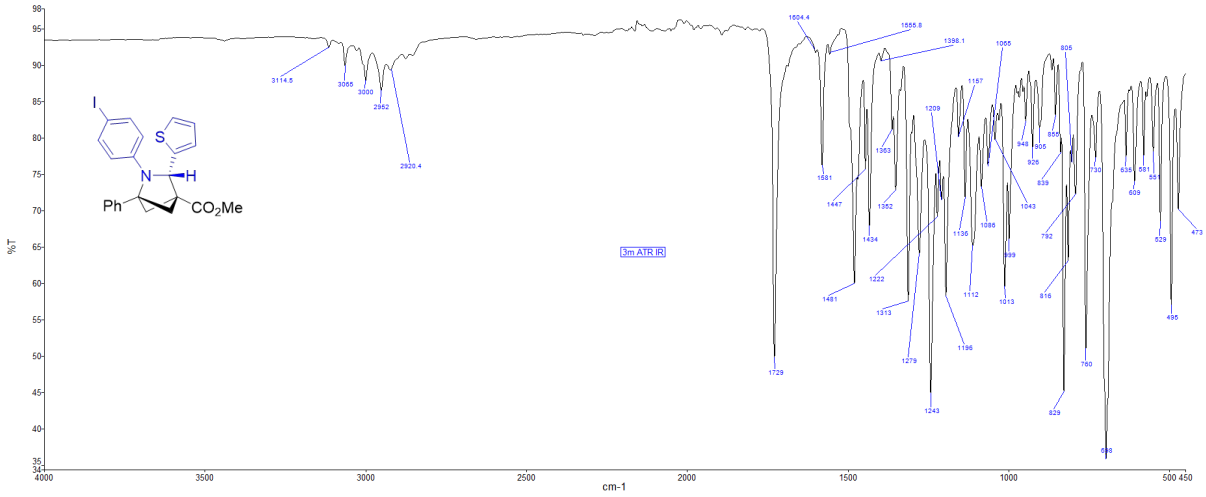

LCMS Chromatogram:

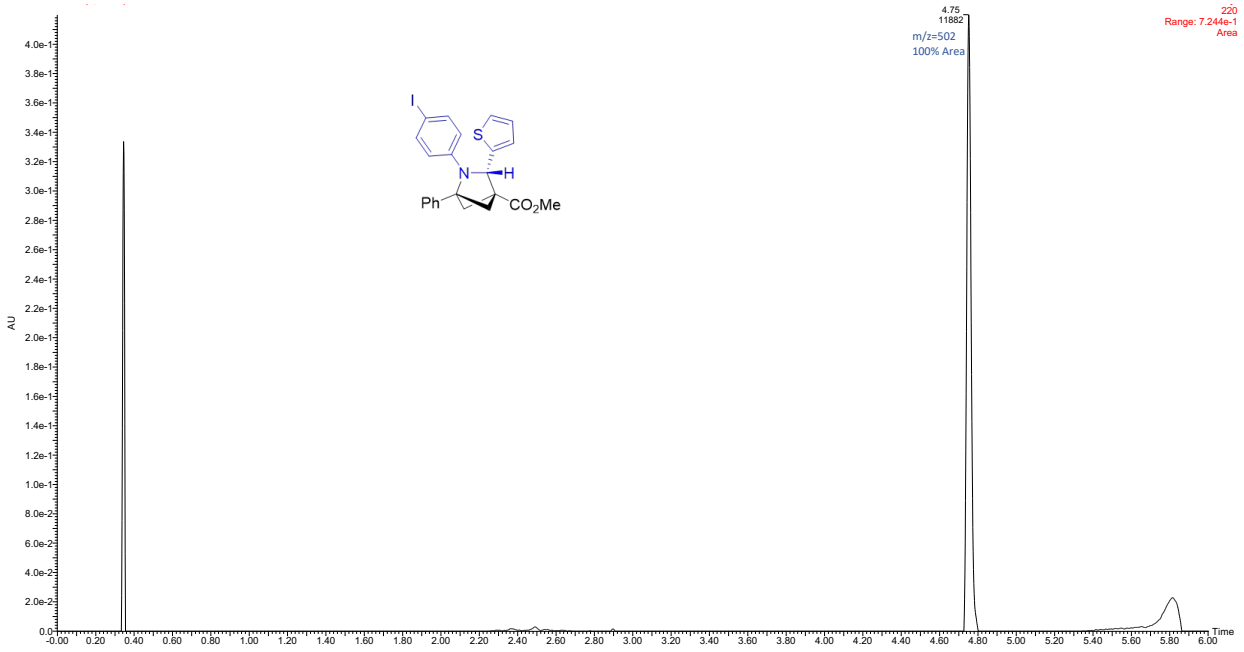

Methyl-1-(4-chlorophenyl)-2,3-diphenyl-2-azabicyclo[2.1.1]hexane-4-carboxylate (3p)

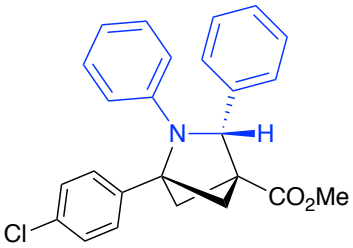

The product was prepared by **Method A** using methyl 3-(4-chlorophenyl)bicyclo[1.1.0]-butane-1-carboxylate (0.1113 g, 0.50 mmol), **2b** (0.0997 g, 0.55 mmol) and $Ga(OTf)_3$ (0.0129 g, 5 mol%). The compound was purified by column chromatography (Biotage® Sfär 10g Column, 0-100% EtOAc/hexanes, eluted at 25% EtOAc).152 mg of a yellow oil was obtained (75%, 69% 3p & 6% 4p by NMR spectroscopy [peaks chosen 4.83 ppm & 6.26 ppm]). 95% product and 5% 4p by LCMS area.

IR: C=O 1738 cm^{-1}

HRMS(ESI): calc'd for $[C_{25}H_{22}{}^{35}ClNO_2 + H^+]$, 404.14119; found: 404.14115.

^{1}H NMR (500 MHz, $CDCl_3$, 292K, ppm): δ 7.65 – 7.56 (m, 2H), 7.42 – 7.21 (m, 7H), 6.96 – 6.83 (m, 2H), 6.74 – 6.63 (m, 1H), 6.43 (m, 2H), 4.83 (s, 1H), 3.61 (s, 3H), 2.72 (d, J = 6.8 Hz, 1H), 2.59 (dd, J = 9.7, 6.9 Hz, 1H), 2.40 (dd, J = 9.8, 7.7 Hz, 1H), 1.89 (dd, J = 7.6, 1.3 Hz, 1H).

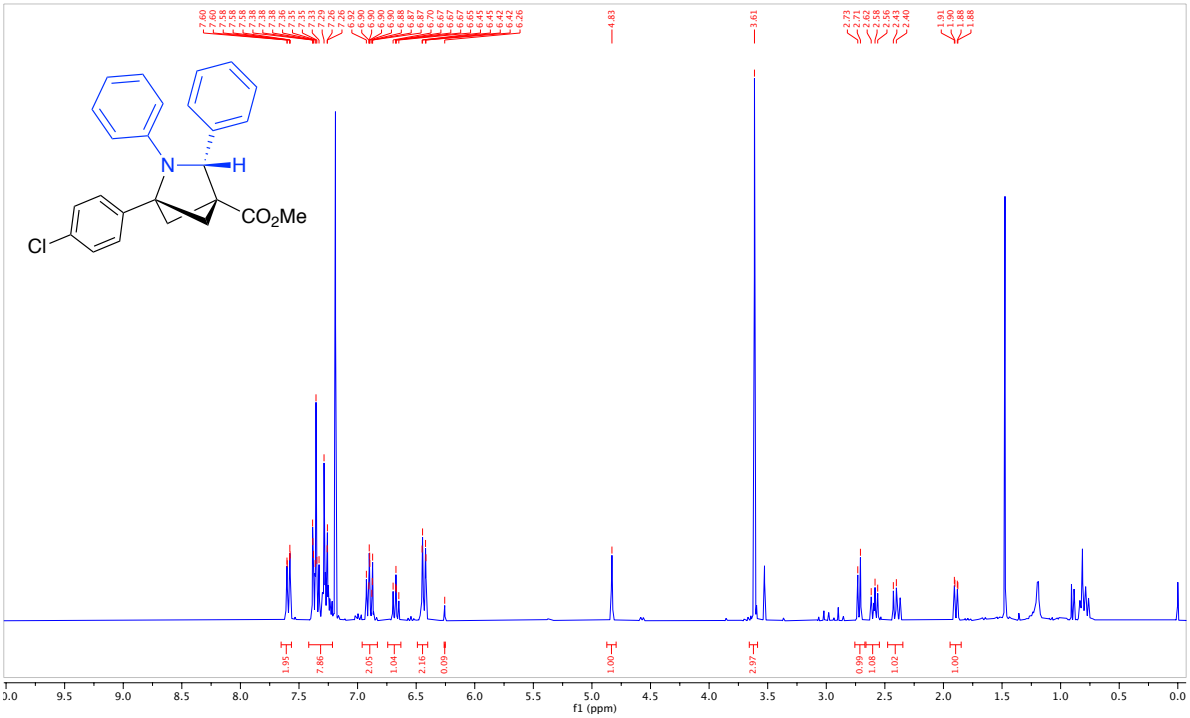

^{13}C NMR (126 MHz, $CDCl_3$, 292K, ppm): δ 170.70, 151.06, 140.76, 138.40, 133.17, 129.16, 128.65, 128.50, 127.82, 127.46, 120.46, 118.96, 74.50, 69.81, 54.46, 51.79, 45.90, 44.75.

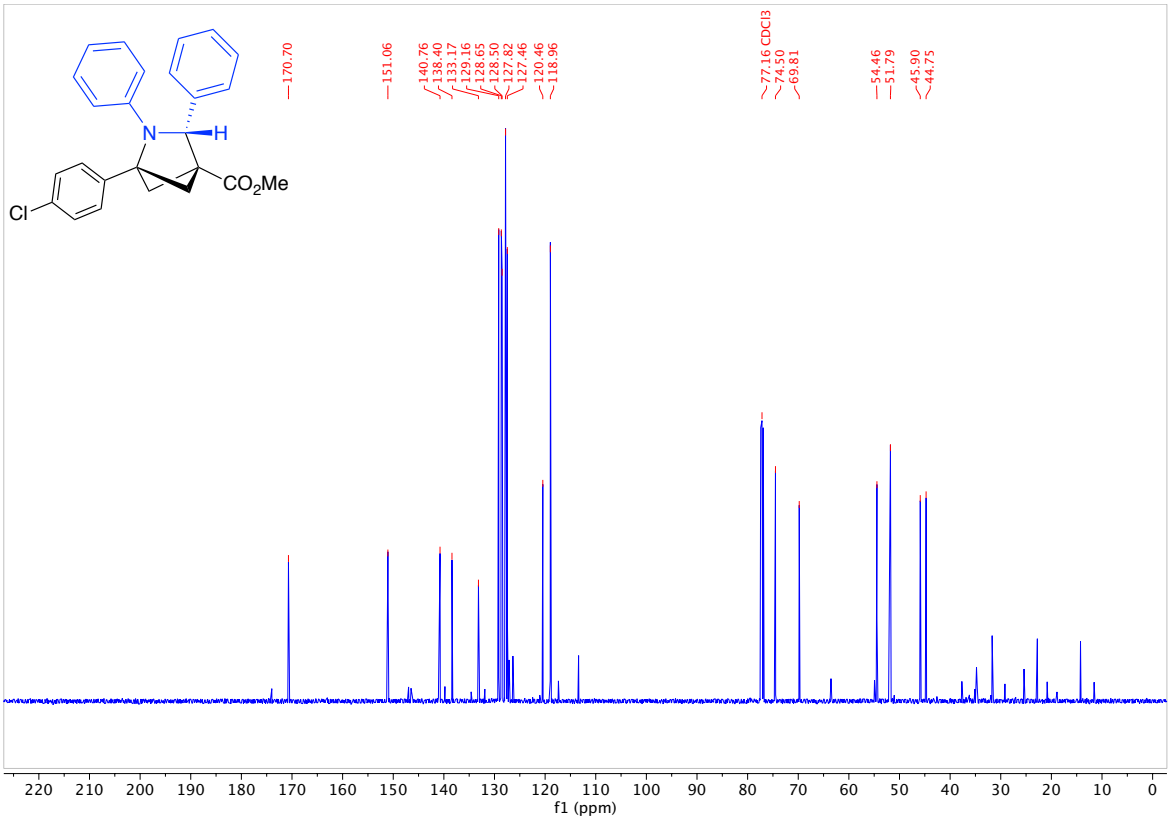

ATR IR spectrum:

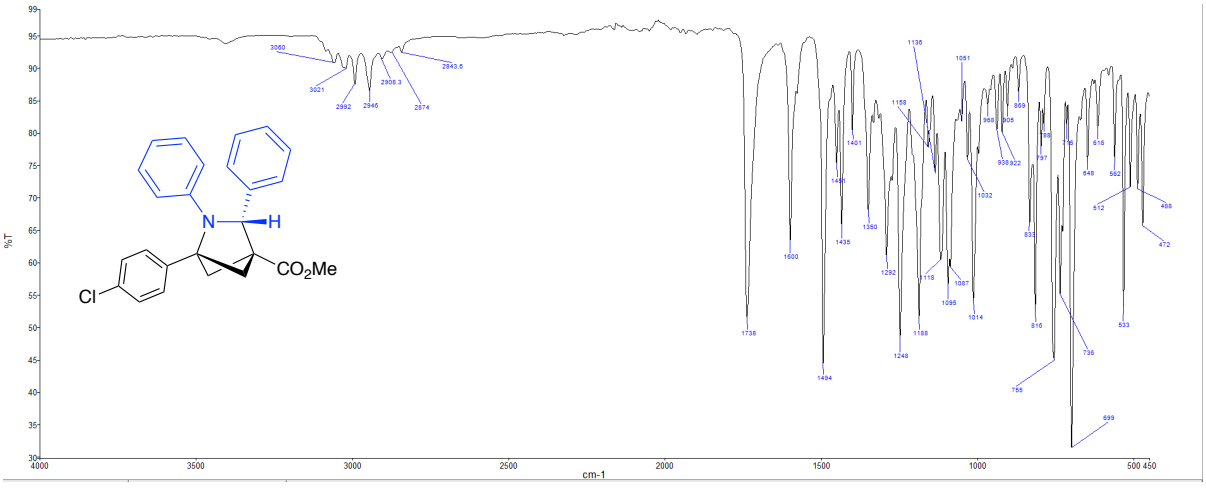

LCMS Chromatogram:

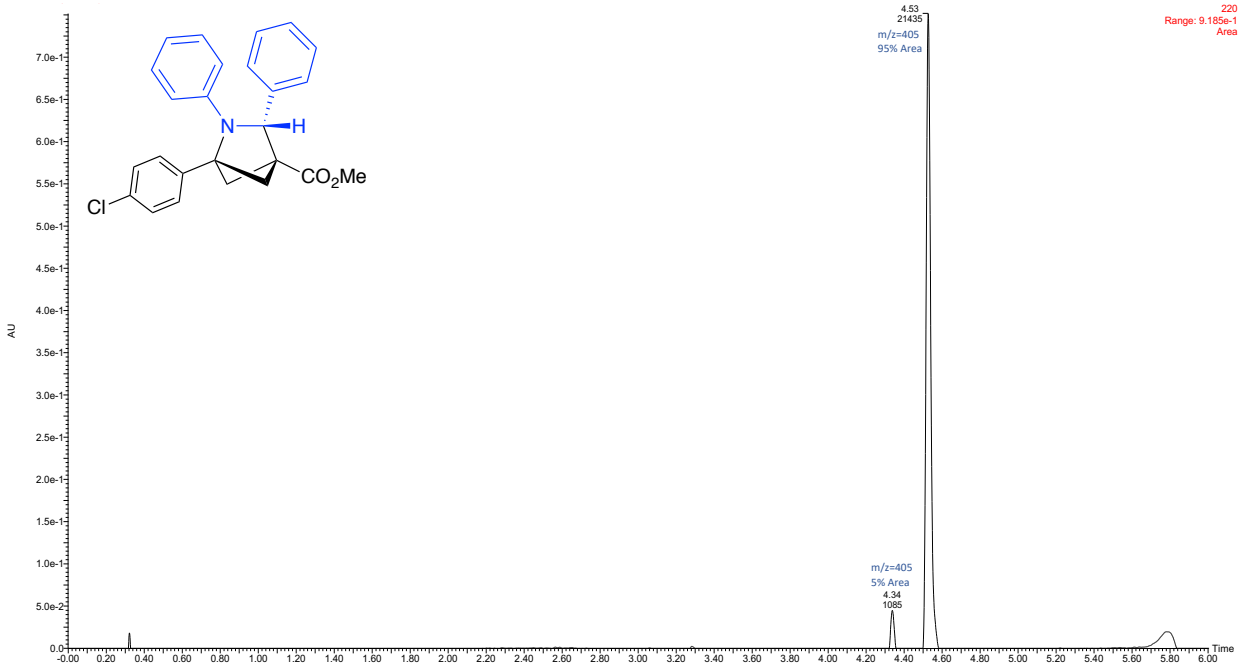

Methyl-1-(4-fluorophenyl)-2,3-diphenyl-2-azabicyclo[2.1.1]hexane-4-carboxylate (3q)

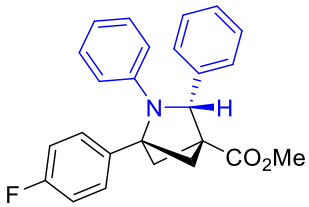

The product was prepared by **Method A** using methyl 3-(4-fluorophenyl)bicyclo[1.1.0]-butane-1-carboxylate (0.1031 g, 0.50 mmol), **2c** (0.0997 g, 0.55 mmol) and $Ga(OTf)_3$ (0.0129 g, 5 mol%). The compound was purified by column chromatography (Biotage® Sfär KP-Amino 11g Column, 0-100% EtOAc/hexanes, eluted at 0% EtOAc). 69.6 mg of a yellow solid was obtained (36%). 97% by LCMS.

IR: C=O 1730 cm^{-1}

HRMS(ESI): calc'd for [$C_{25}H_{22}FNO_2$+ H^+], 388.17074; found: 388.17065.

^{1}H NMR (500 MHz, $CDCl_3$, 292K, ppm): δ7.72 (d, J=7.76 Hz, 2H), 7.53-7.50 (m, 2H), 7.47 (t, J=7.28 Hz, 2H), 7.39 (t, J=7.28 Hz, 1H), 7.11 (t, J=8.68 Hz, 2H), 7.01 (t, J=7.90 Hz, 2H) 6.78 (t, J=7.40 Hz, 1H), 6.57 (d, J=8.21 Hz, 2H), 4.97 (s, 1H), 3.73 (s, 3H), 2.84 (d, J=7.75 Hz, 1H), 2.72 (dd, J= 9.73 Hz & 6.83 Hz, 2H), 2.54 (m, 2H), 2.02 (d, J=7.75 Hz, 1H).

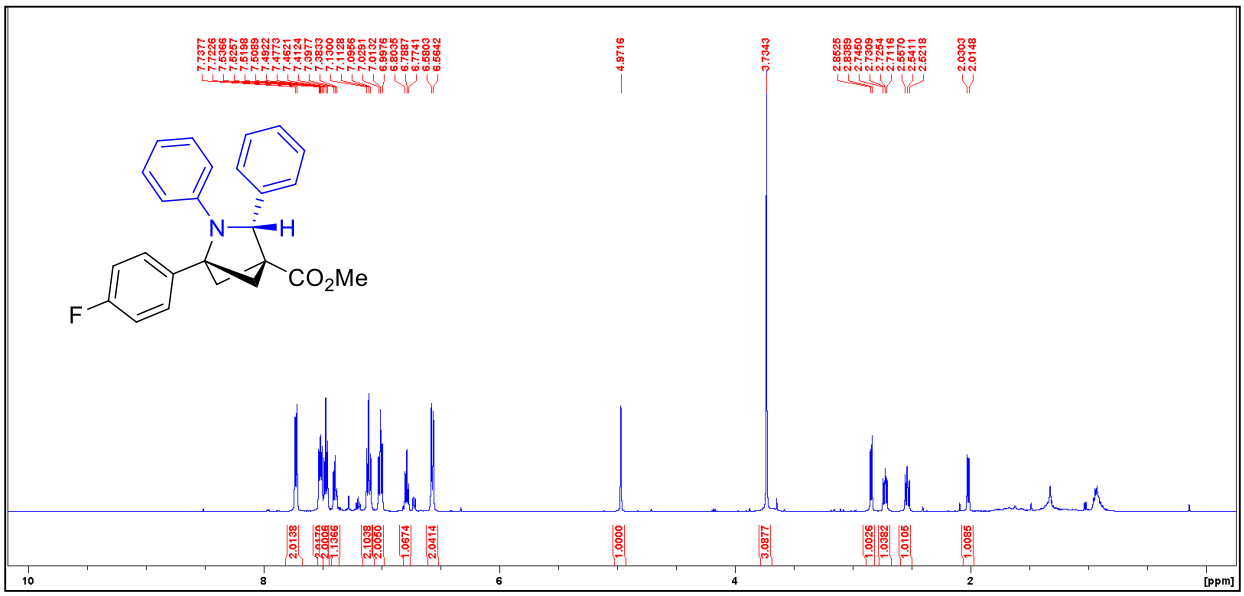

^{19}F NMR (500 MHz, $CDCl_3$, 292K, ppm): δ -114.62

^{13}C NMR (126 MHz, $CDCl_3$, 292K, ppm): δ 170.73, 162.00 (d, J=246.15 Hz, 1C), 151.07, 140.75, 135.61 (d, J=3.23 Hz, 1C), 128.47 (d, J=15.10 Hz, 1C), 127.76, 127.70 (d, J=5.18 Hz, 1C), 127.61, 120.29, 118.92, 115.81 (d, J=21.62 Hz, 1C), 74.36, 69.78, 54.32, 51.71, 45.72, 44.83.

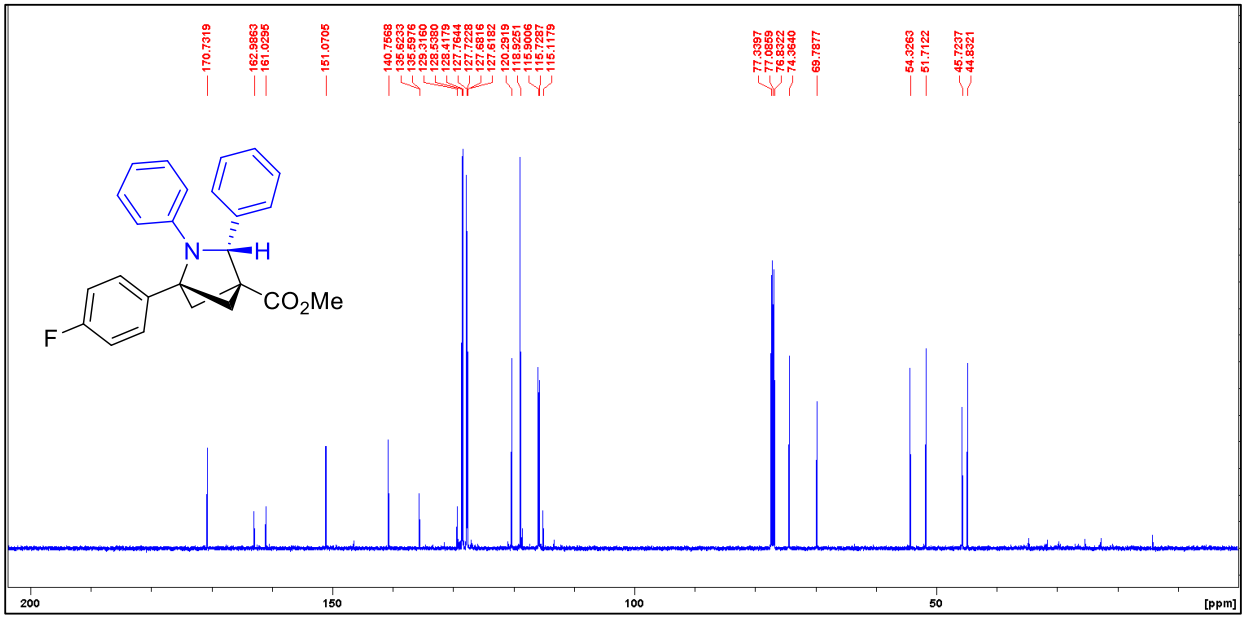

ATR IR spectrum:

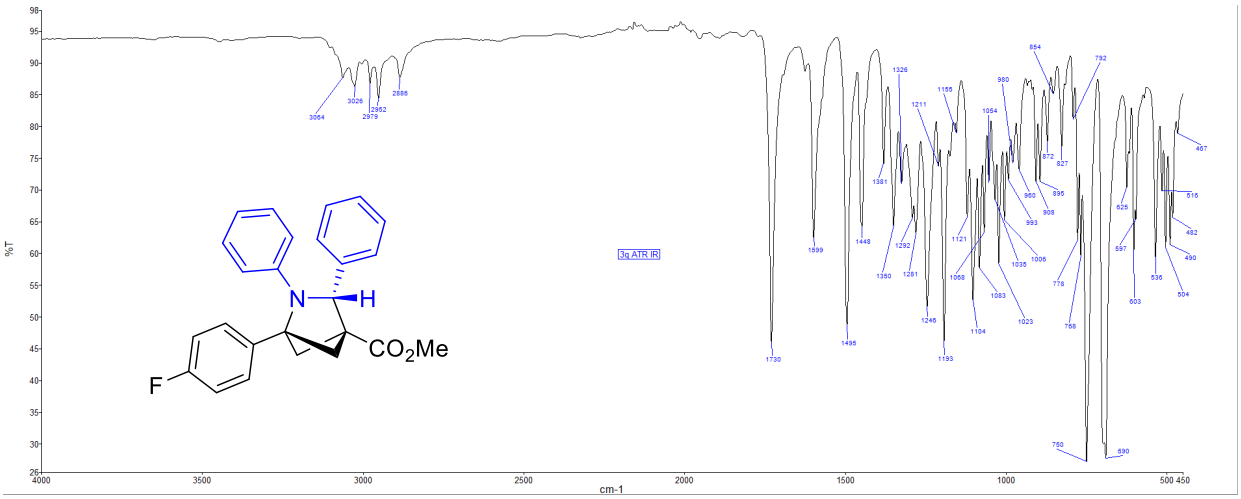

LCMS Chromatogram:

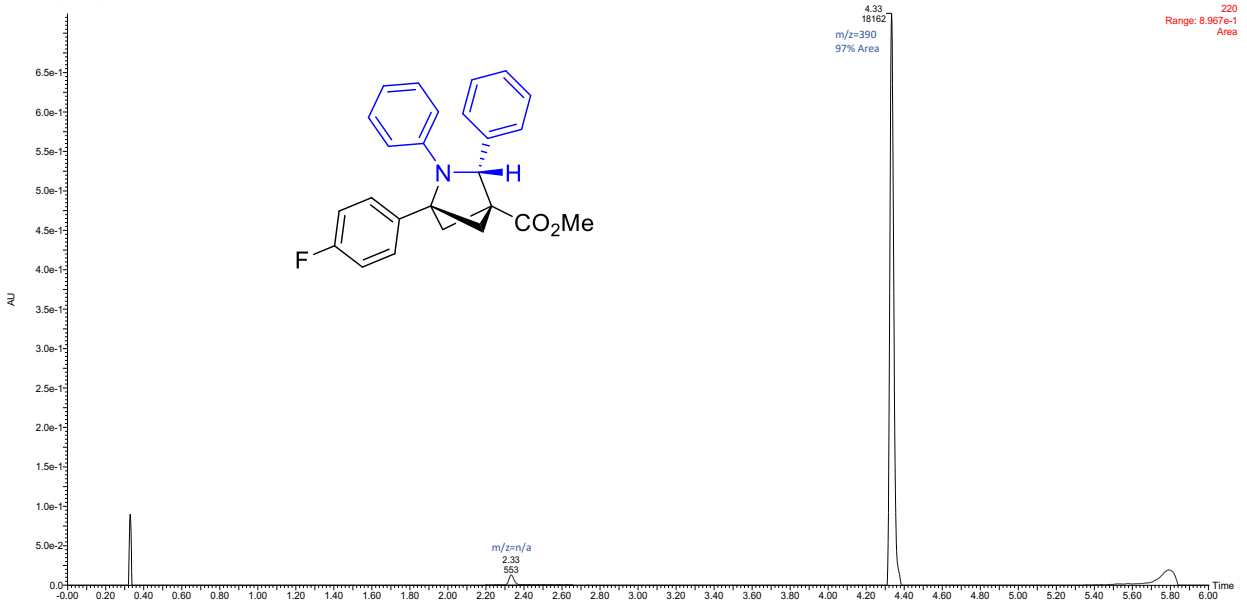

Benzyl-1,2,3-triphenyl-2-azabicyclo[2.1.1]hexane-4-carboxylate (3r)

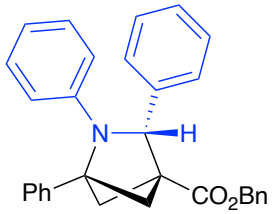

The product was prepared by **Method A** using benzyl 3-phenylbicyclo[1.1.0]butane-1-carboxylate **2d** (0.1322 g, 0.50 mmol), *N*-benzylidene aniline (0.0997 g, 0.55 mmol) and $Ga(OTf)_3$ (0.0129 g, 5 mol%). The compound was purified by column chromatography (Biotage® Sfär KP-Amino 11g Column, 0-100% EtOAc/hexanes, eluted at 1% EtOAc). 100.1 mg of a yellow solid was obtained (45%). 97% peak area by LCMS.

IR: C=O 1730 cm^{-1}

Melting point range: 78.8 – 81.3 °C

HRMS(ESI): calc'd for $[C_{31}H_{27}NO_2 + H^+]$, 446.21146; found: 446.21143.

^{1}H NMR (500 MHz, $CDCl_3$, 292K, ppm): δ 7.67 (d, J=7.37 Hz, 2H), 7.57 (d, J=6.96 Hz, 2H), 7.57-7.27 (m, 11H), 7.00 (t, J=8.11 Hz, 2H), 6.77 (t, J=7.10 Hz, 1H), 6.59 (d, J=8.06 Hz, 2H), 5.28 (d, J=12.18 Hz, 1H), 5.15 (d, J=12.18 Hz, 1H), 4.98 (s, 1H), 2.90 (d, J = 6.70 Hz, 1H), 2.74 (dd, J = 9.9, 6.9 Hz, 1H), 2.59 (dd, J = 9.9, 7.8 Hz, 1H), 2.07 (d, J = 7.88 Hz, 1H).

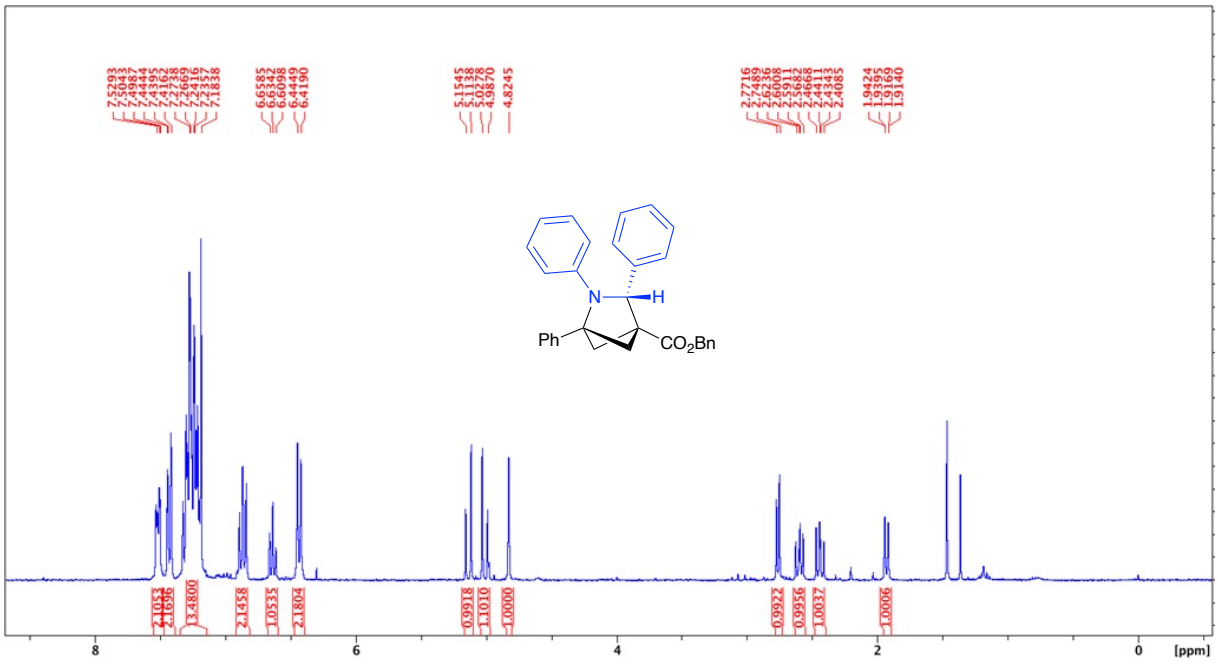

^{13}C NMR (126 MHz, $CDCl_3$, 292K, ppm): δ 170.25,160.45, 151.32, 140.79, 139.79, 131.44, 129.21, 128.90, 128.64, 128.57, 128.50, 128.42, 128.40, 127.84, 127.63, 127.39, 125.97, 120.94, 120.06, 118.76, 74.40, 70.33, 66.45, 54.45, 45.79, 44.76.

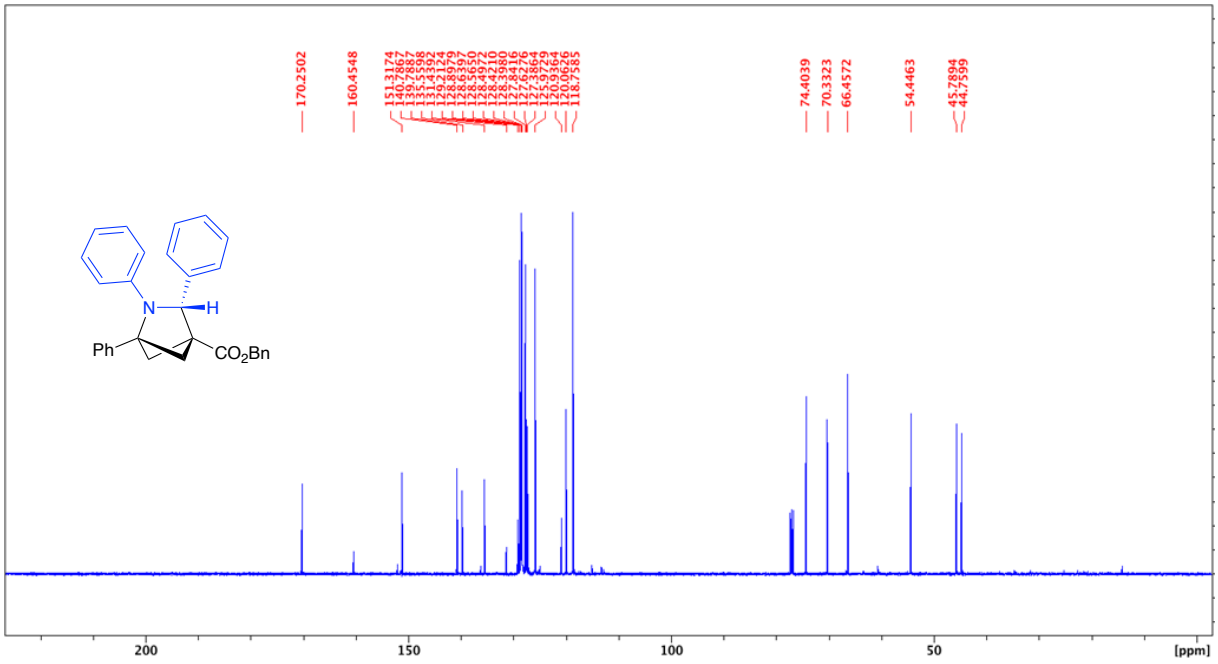

ATR IR spectrum:

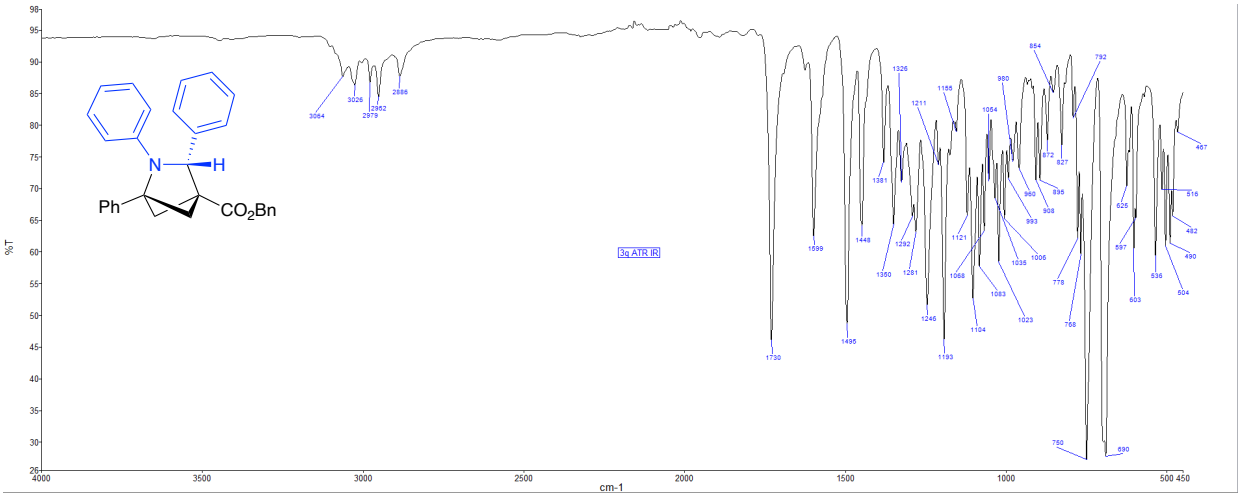

LCMS Chromatogram:

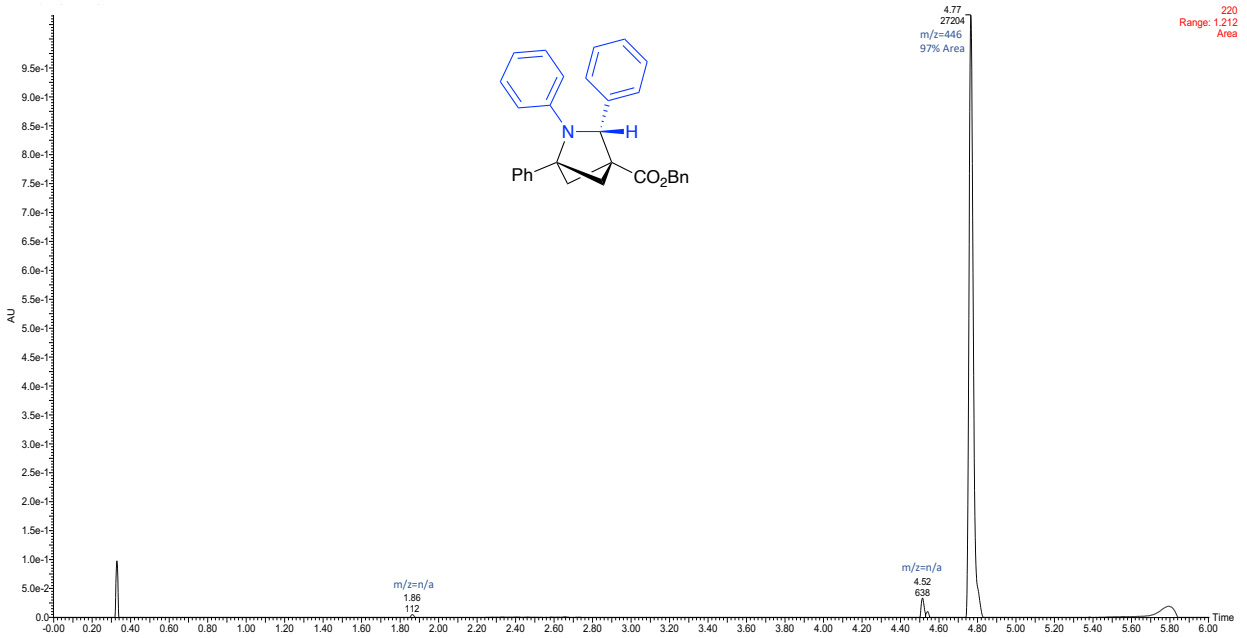

[(1*R*,2*R*,5*S*)-2-isopropyl-5-methylcyclohexyl]-1,2,3-triphenyl-2-azabicyclo[2.1.1]-hexane-4-carboxylate (3s)
[(1*R*,2*R*,5*S*)-2-isopropyl-5-methylcyclohexyl]-3-phenyl-1-(phenyl(phenylamino)-methyl)cyclobut-2-ene-1-carboxylate) (4s)

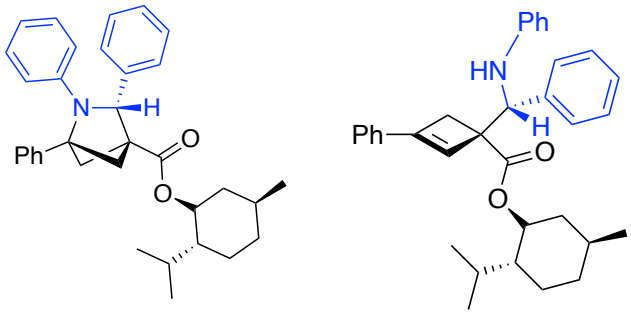

The product was prepared by **Method A** using (1*S*,2*R*,5*S*)-2-isopropyl-5-methylcyclohexyl 3-phenylbicyclo[1.1.0]butane-1-carboxylate **2e** (0.1562 g, 0.50 mmol), **1a** (0.0997 g, 0.55 mmol) and $Ga(OTf)_3$ (0.0129 g, 5 mol%). The compound was purified by column chromatography (Biotage® Sfär KP-Amino 11g Column, 0-100% EtOAc/hexanes, eluted at 0% EtOAc). 176 mg of a white solid was obtained (71% total yield) as a 6:1 mixture of **3s** (60%) to **4s** (11%). Compound **3s** is also a 1.4:1 mixture of diastereomers. A small fraction of **4s** was also isolated during chromatography to enable characterization. 90% peak area (9% **4s**) by LCMS.

IR: C=O 1720 cm^{-1}

HRMS(ESI): calc'd for [$C_{34}H_{39}NO_2$ + H^+], 494.30536; found: 494.30555.

^{1}H NMR (500 MHz, $CDCl_3$, 292K, ppm): δ 7.82 (t, J=7.88 Hz, 2H), 7.59 (d, J=7.88 Hz, 2H), 7.51-7.28 (m, 6H), 7.02 (t, J=7.59 Hz, 2H), 6.79 (t, J=6.90 Hz, 1H), 6.65-6.57 (m, 2H), 5.01 (s, 0.58H), 4.99 (s, 0.41H), 4.84-4.73 (m, 1H), 2.87 (t, J=6.96 Hz, 1H), 2.77-2.71 (m, 1H), 2.59 (t, J=9.05 Hz, 1H), 2.18-2.10 (m, 0.64 H), 2.07 (d, J=11.50 Hz, 0.64H), 2.07-1.91 (m, 1.38H), 1.8-1.67 (m, 2.3H), 1.67-1.48 (m, 2.36H), 1.48-1.32 (m, 1.38H), 1.12 (m, 1.90H), 1.01 (d, J=6.14 Hz, 1.85H), 0.97 (d, J=6.61 Hz, 2.82H), 0.97-0.79 (m, 5.31H), 0.79-0.71 (d, J=6.61 Hz, 1.93H).

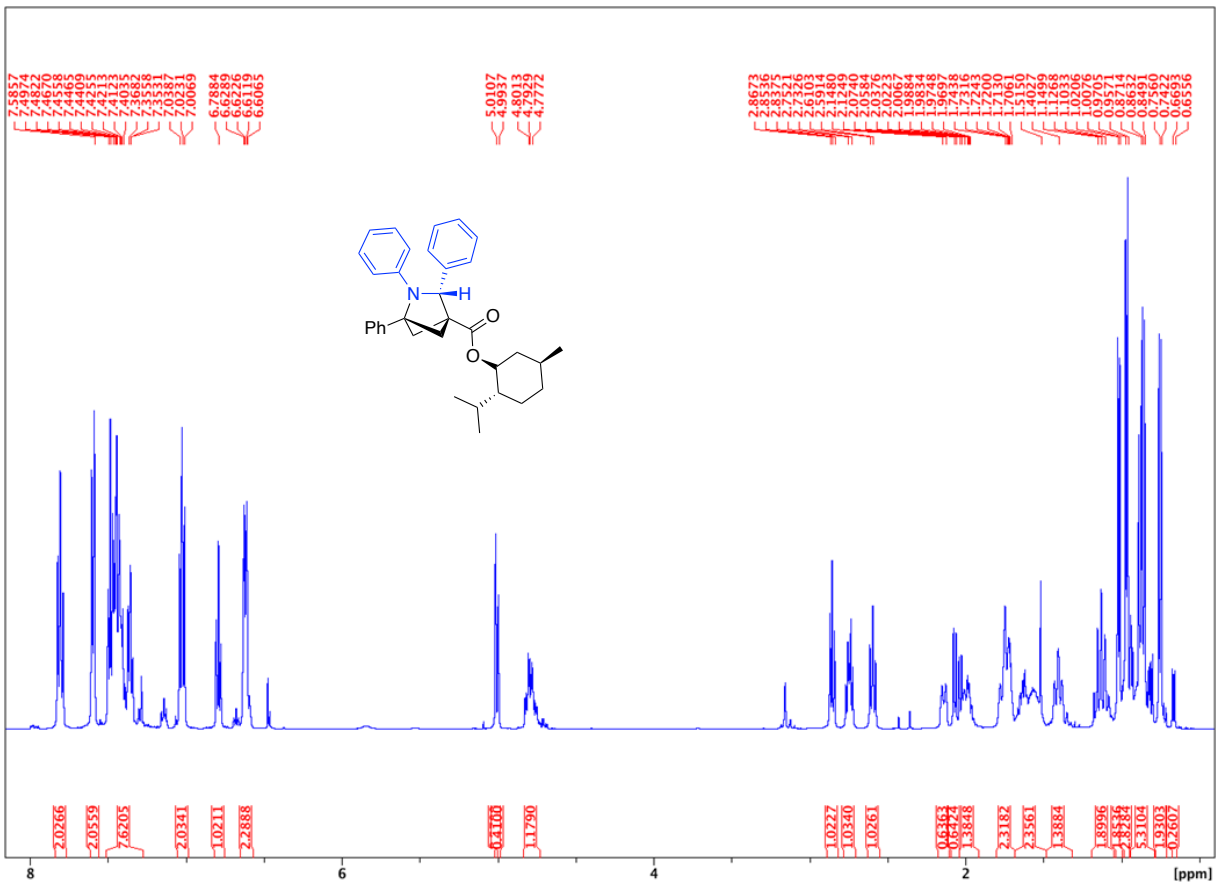

^{13}C NMR (126 MHz, $CDCl_3$, 292K, ppm): δ 170.32 169.93, 151.49, 151.41, 141.03, 140.97, 139.97, 139.94, 129.18, 128.94, 128.91, 128.89, 128.87, 128.64, 128.50, 128.38, 128.33, 128.32, 128.27, 128.03, 127.98, 127.96, 127.94, 127.62, 127.50, 127.36, 127.33, 127.30, 127.27, 126.02, 125.98, 125.001 119.99, 119.97, 118.75, 117.01, 113.15, 74.84, 74.70, 74.39, 74.22, 70.28, 70.07, 54.79, 54.63, 47.03, 46.82, 46.08, 45.66, 45.01, 44.75, 41.05, 40.73, 34.29, 34.20, 31.47, 31.38, 26.32, 26.15, 23.58, 23.32, 22.14, 22.04, 20.93, 20.73, 16.47, 16.25.

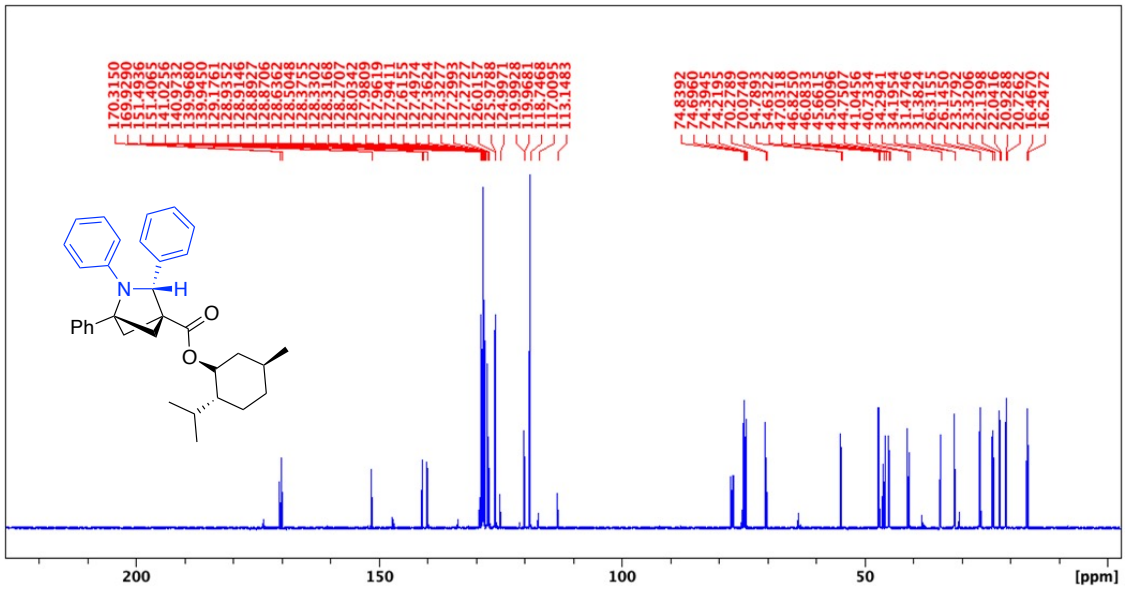

ATR IR spectrum:

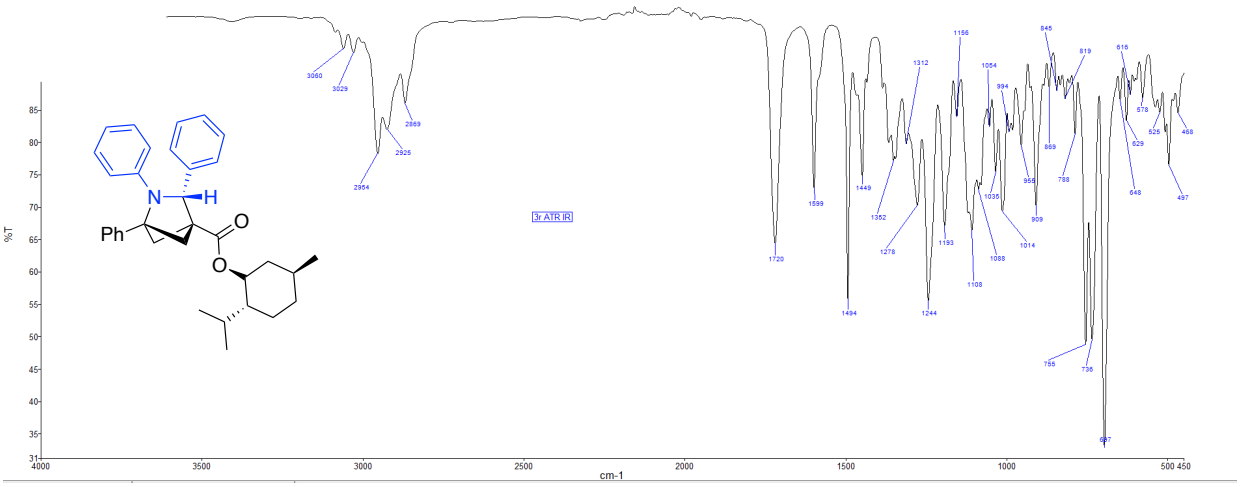

LCMS Chromatogram:

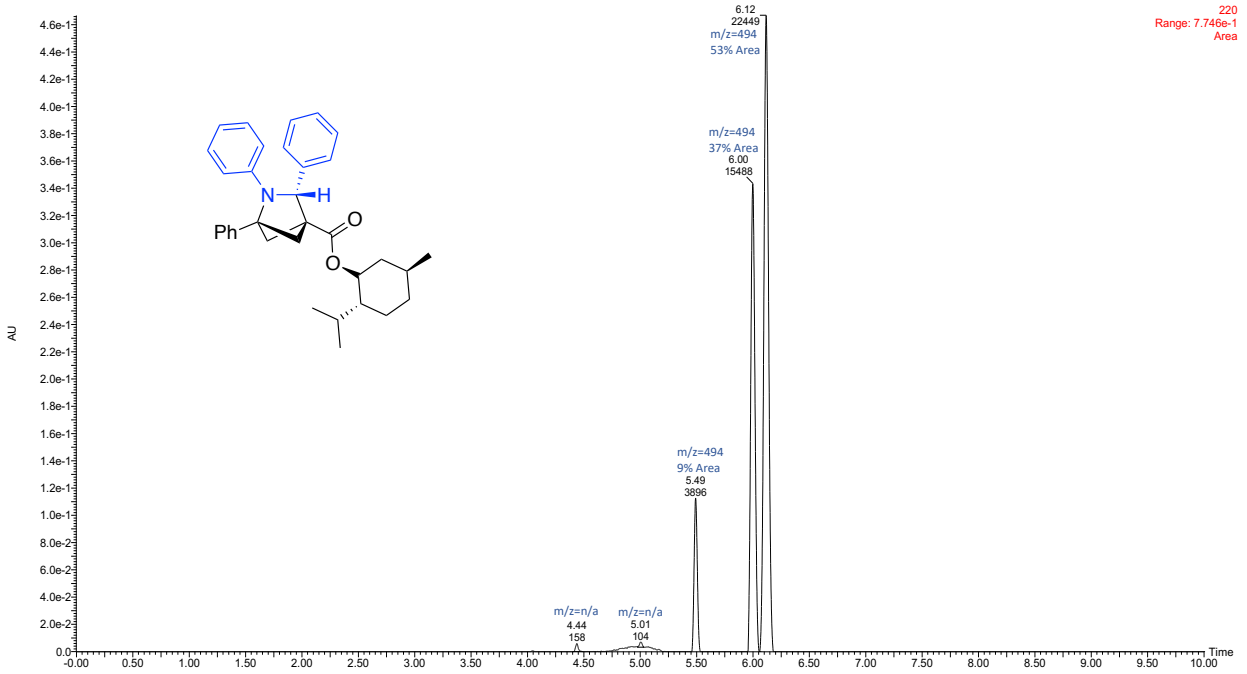

^{1}H-^{1}H COSY (3s):

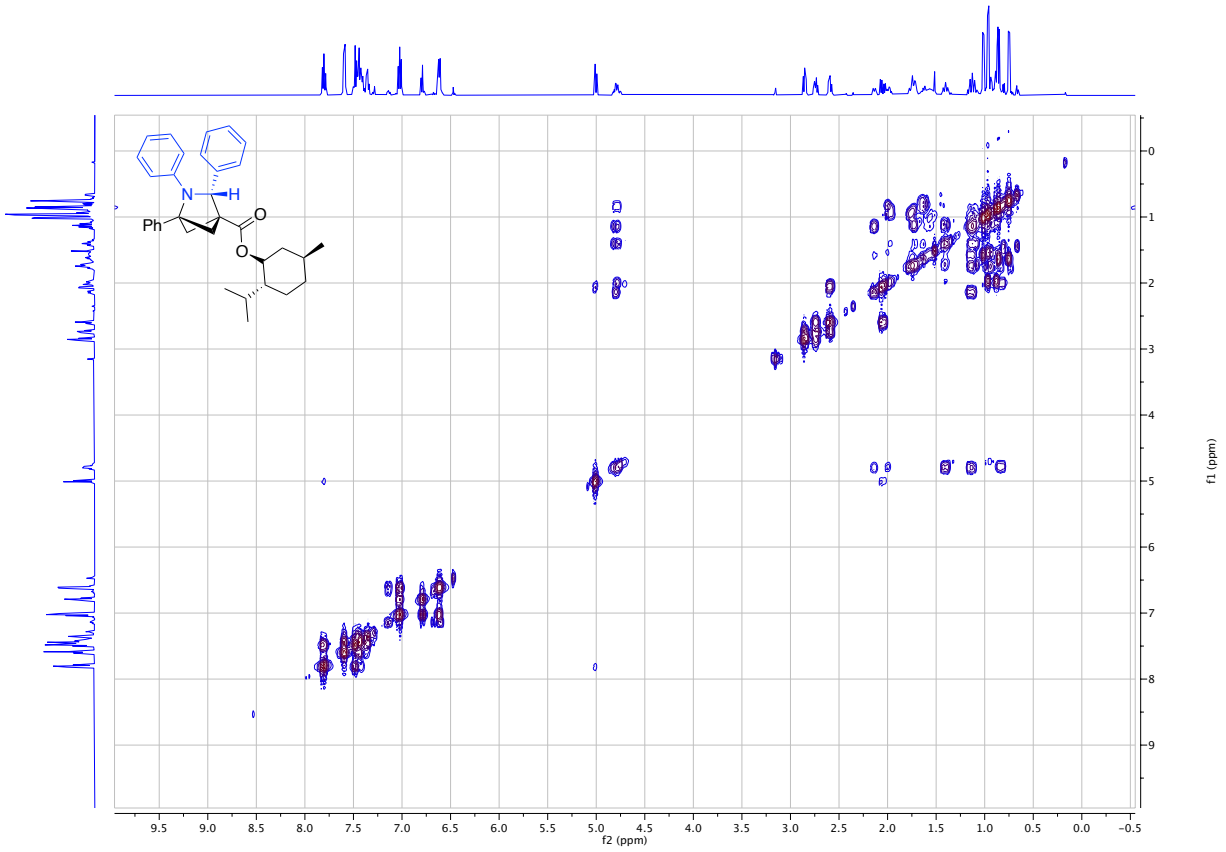

^{1}H-^{13}C HSQC (3s):

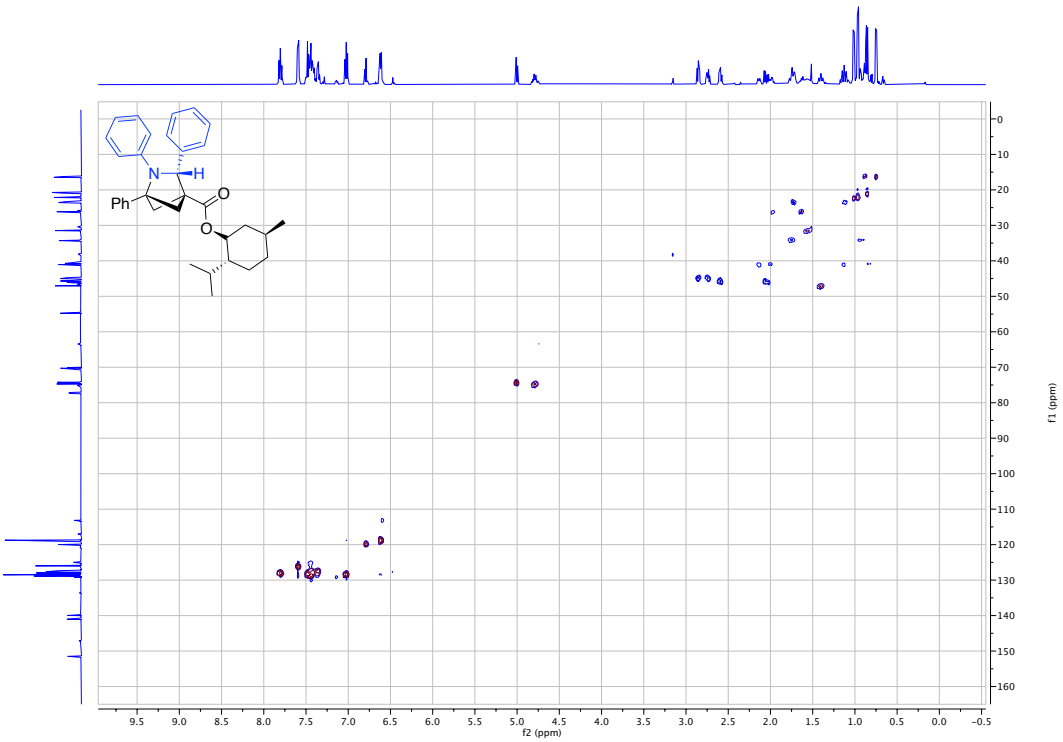

^{1}H-^{13}C HMBC (3s):

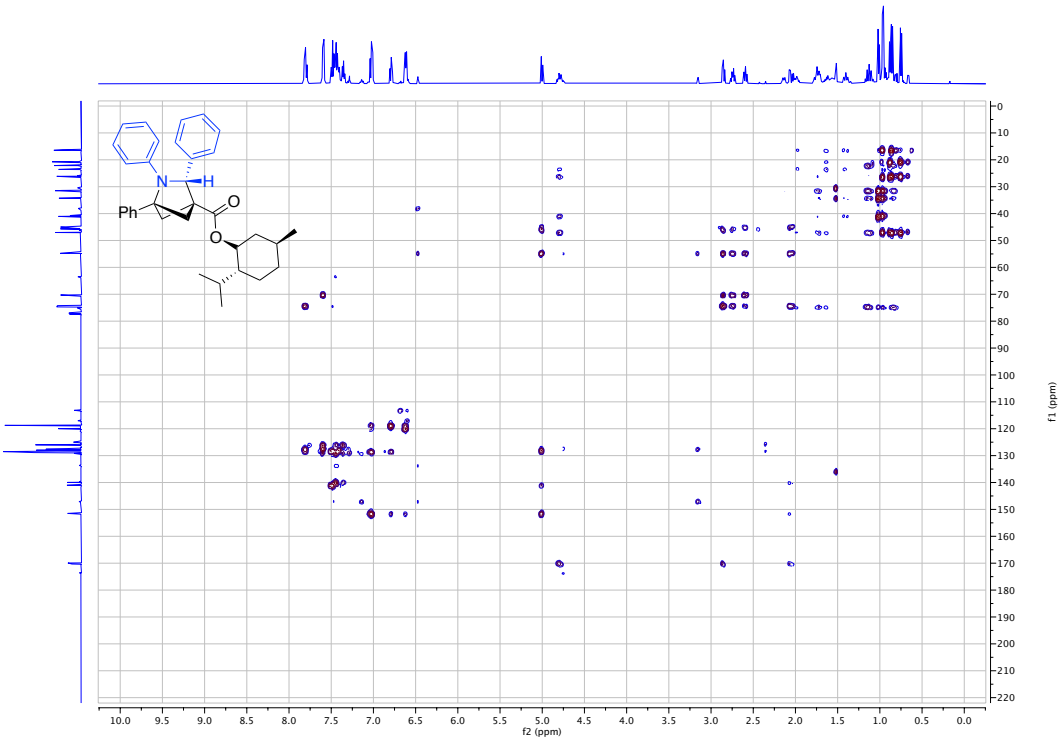

1D sel TOCSY (menthyl spin system for one diastereomer of 3s:

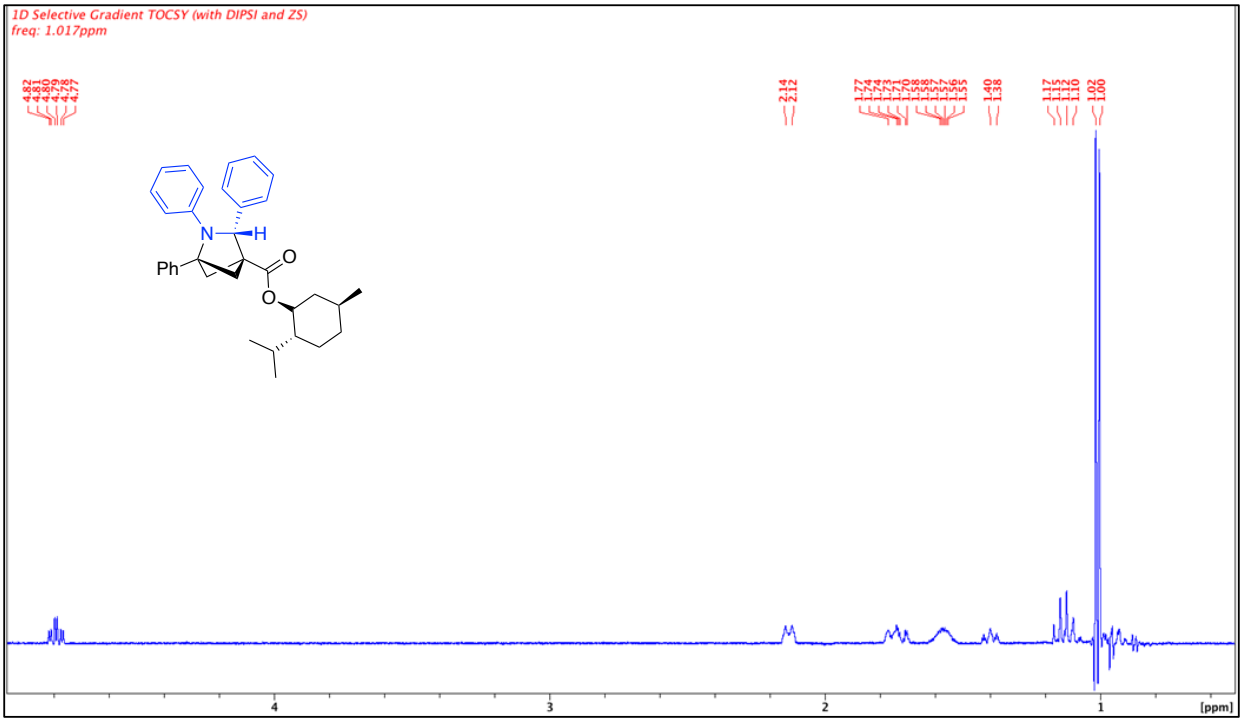

1D sel TOCSY (menthyl spin system for second diastereomer of 3s):

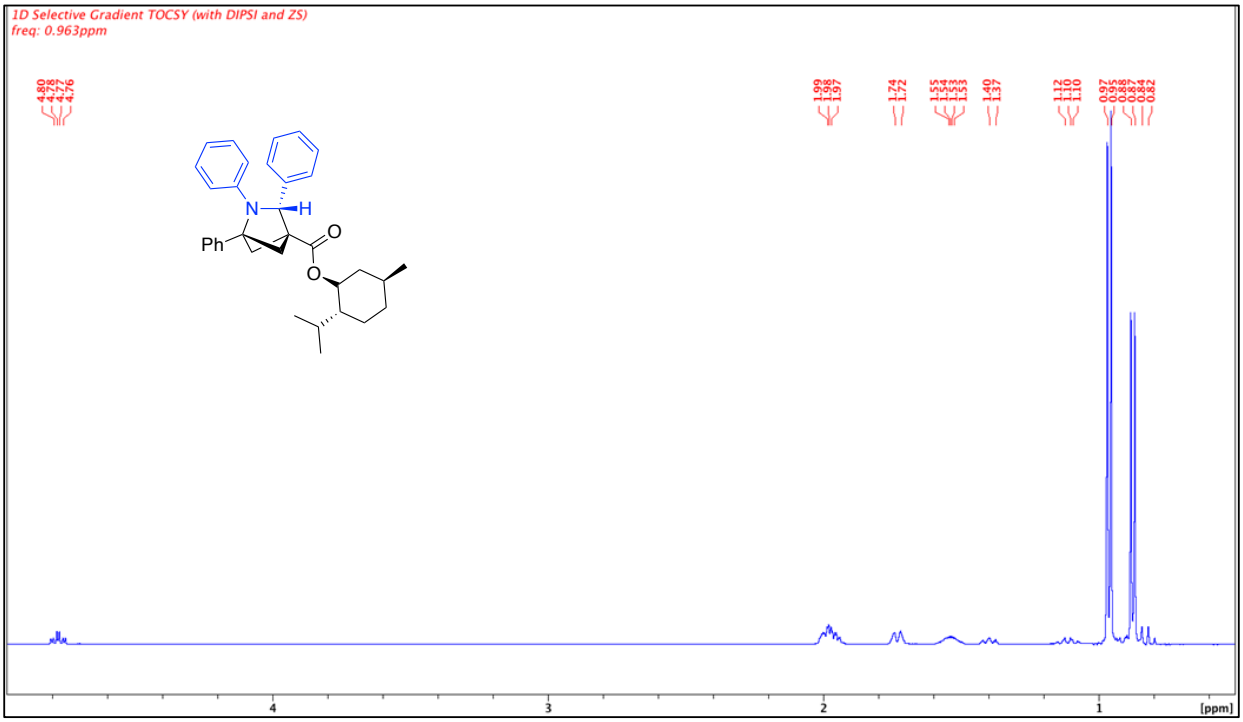

^{1}H NMR spectrum for isolated fraction of 4s:

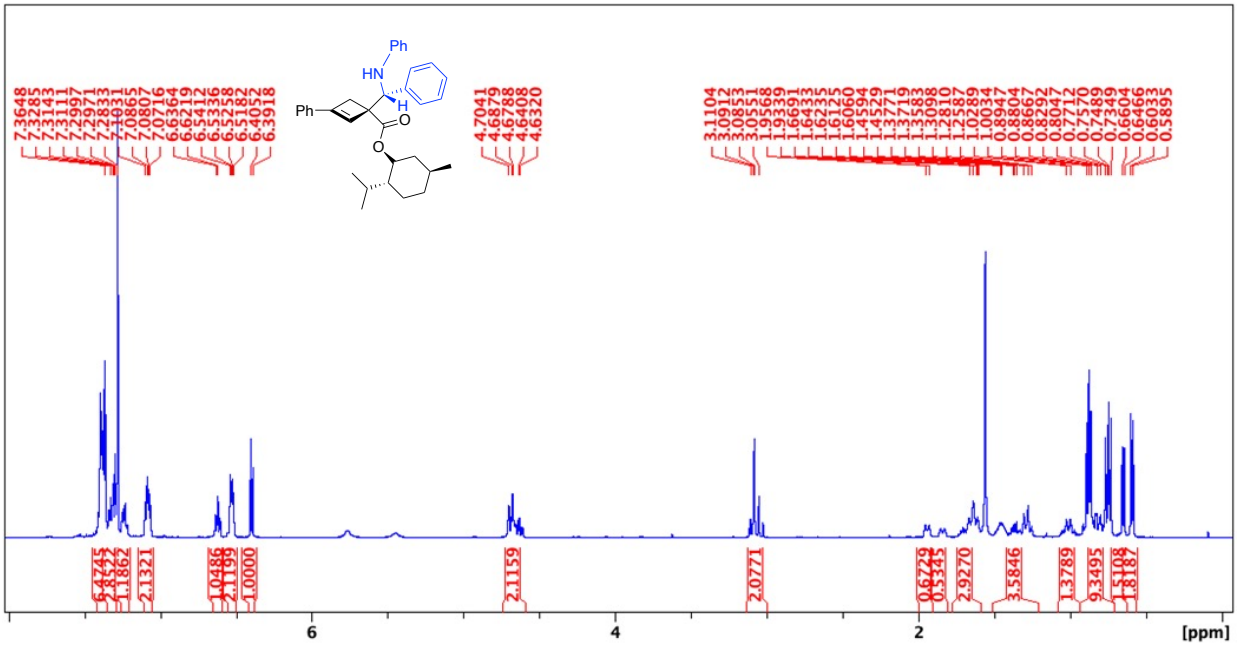

^{13}C NMR spectrum for isolated fraction of 4s:

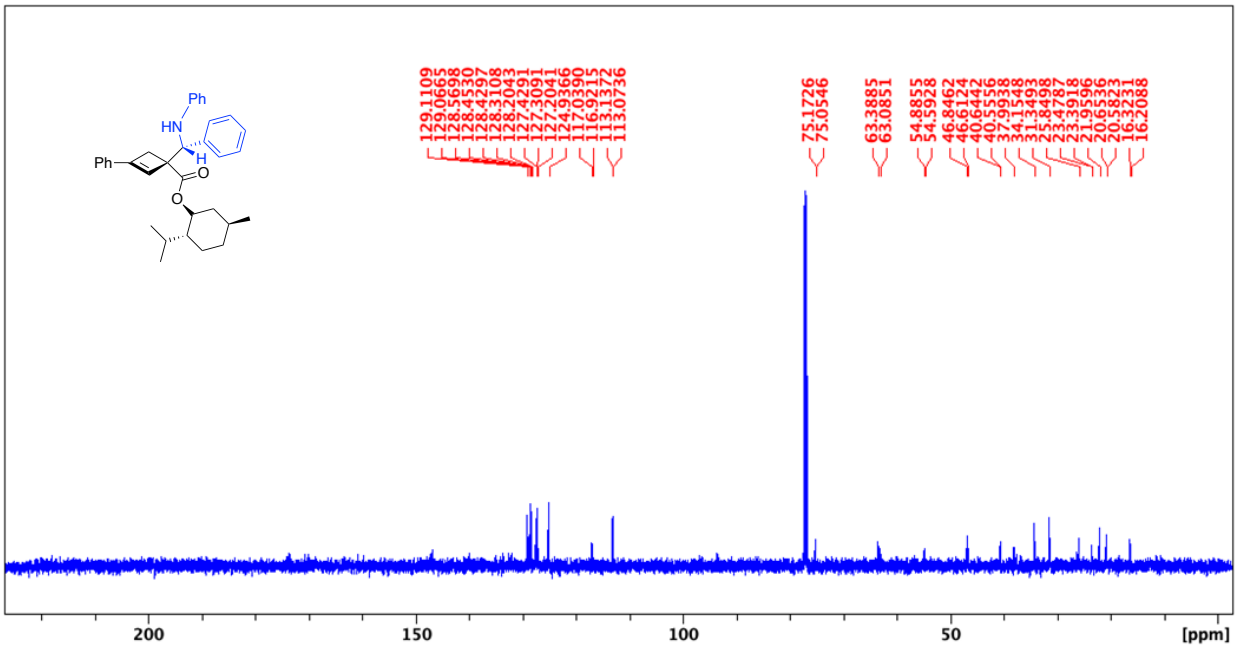

^{1}H-^{1}H COSY (4s):

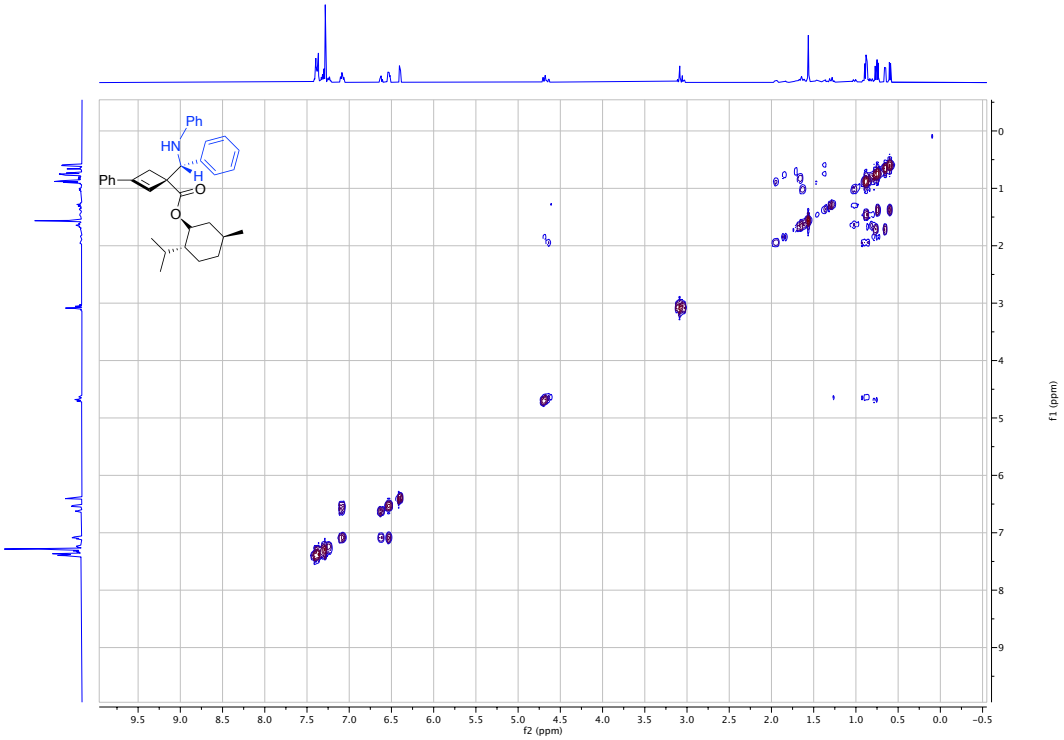

^{1}H-^{13}C HSQC (4s):

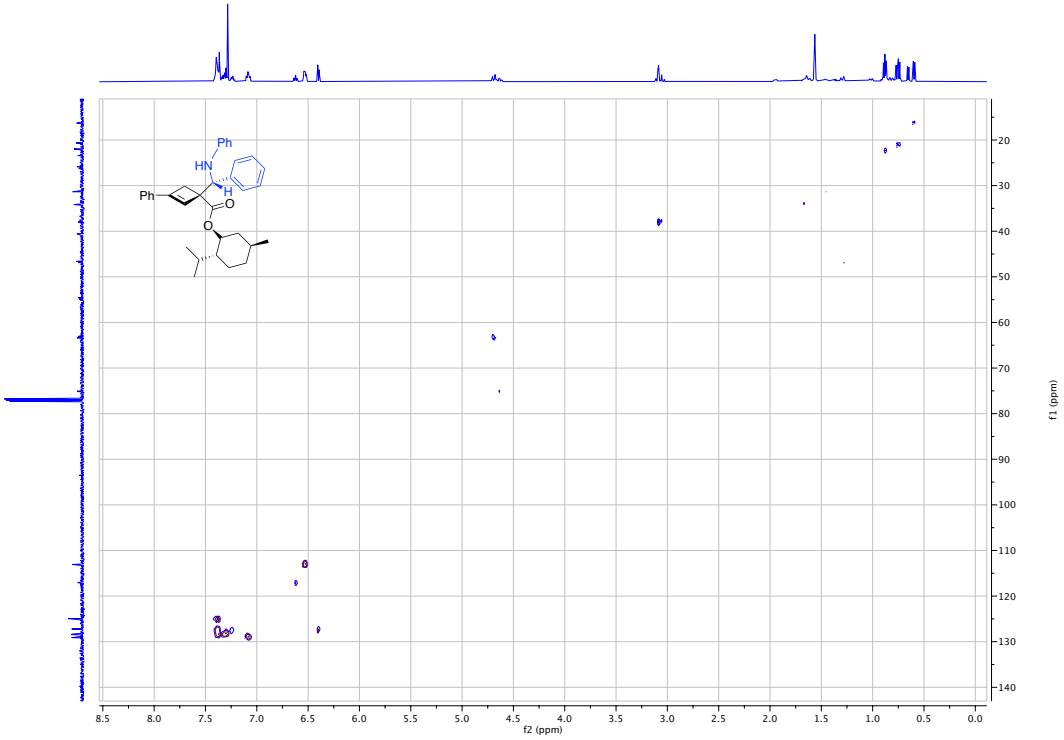

^{1}H-^{13}C HMBC (4s):

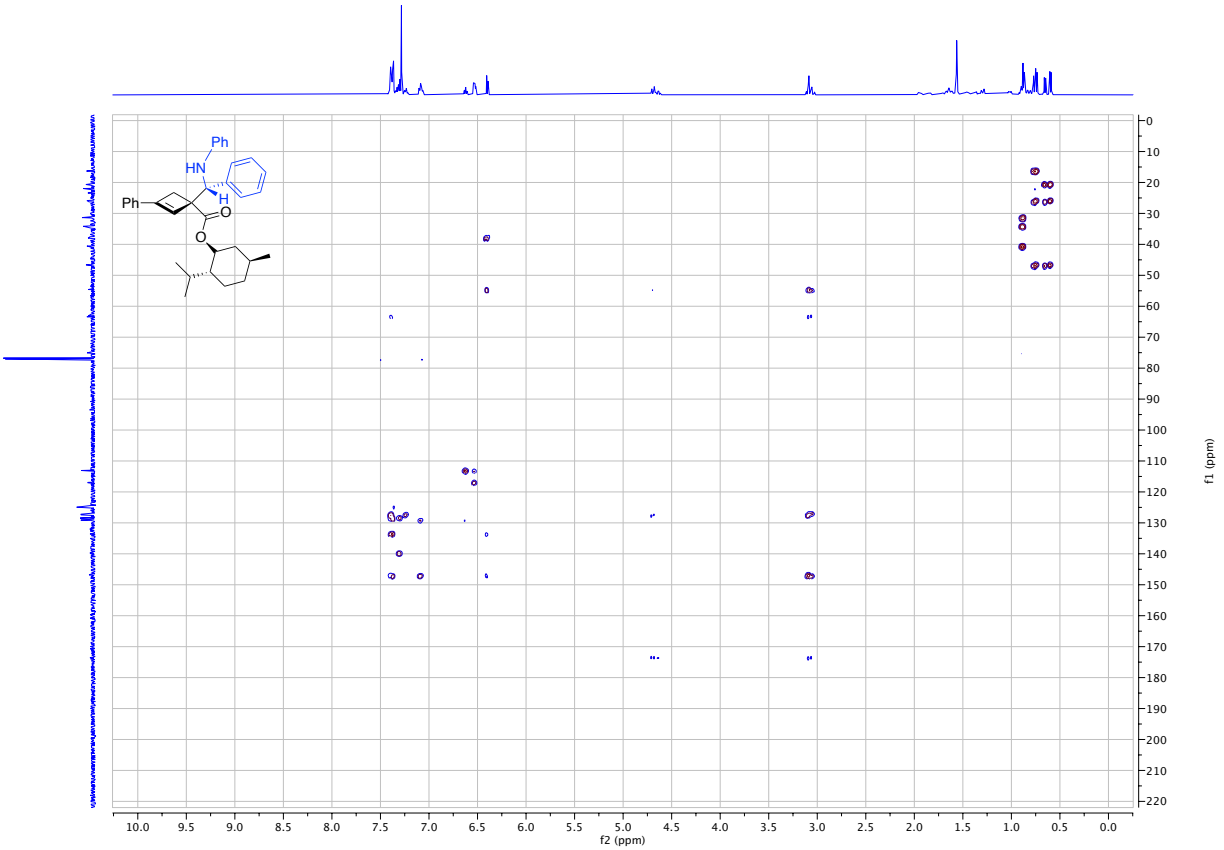

***Tert*-butyl-1,2,3-triphenyl-2-azabicyclo[2.1.1]hexane-4-carboxylate (3t)**

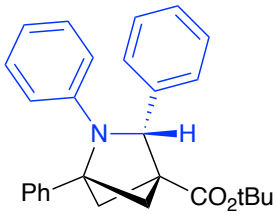

The product was prepared by **Method A** using *tert*-butyl 3-phenylbicyclo[1.1.0]butane-1-carboxylate **2f** (0.0990 g, 0.43 mmol), **1a** (0.0857 g, 0.47 mmol) and $Ga(OTf)_3$ (0.0111 g, 5 mol%). The compound was purified by column chromatography (Biotage® Sfär Column, 0-100% EtOAc/hexanes, eluted at 25% EtOAc). 123 mg of a white solid was obtained (70% total yield) which was a 6:1 mixture of 3t (60%) and the cyclobutenyl amine **4t** (10%). 86% peak area (12% **4t**) by LCMS.

IR: C=O 1724 cm^{-1}

Melting point range: 126.7 – 129.2 °C

HRMS(ESI): calc'd for $[C_{28}H_{29}NO_2 + H^+]$, 412.22711; found: 412.22713.

^{1}H NMR (500 MHz, $CDCl_3$, 292K, ppm): δ 7.80 (d, J=7.55 Hz, 2H), 7.56 (d, J=7.55 Hz, 2H), 7.50-7.25 (m, 6H), 7.00 (t, J=8.01 Hz, 2H), 6.76 (t, J=6.94 Hz, 1H), 6.58 (d, J=7.63 Hz, 2H), 4.94 (s, 1H), 2.83 (d, J=6.62 Hz, 1H), 2.66 (dd, J = 9.9, 6.8 Hz, 1H), 2.52 (dd, J = 9.9, 7.7 Hz, 1H), 1.98 (d, J=7.93 Hz, 1H), 1.49 (s, 9H).

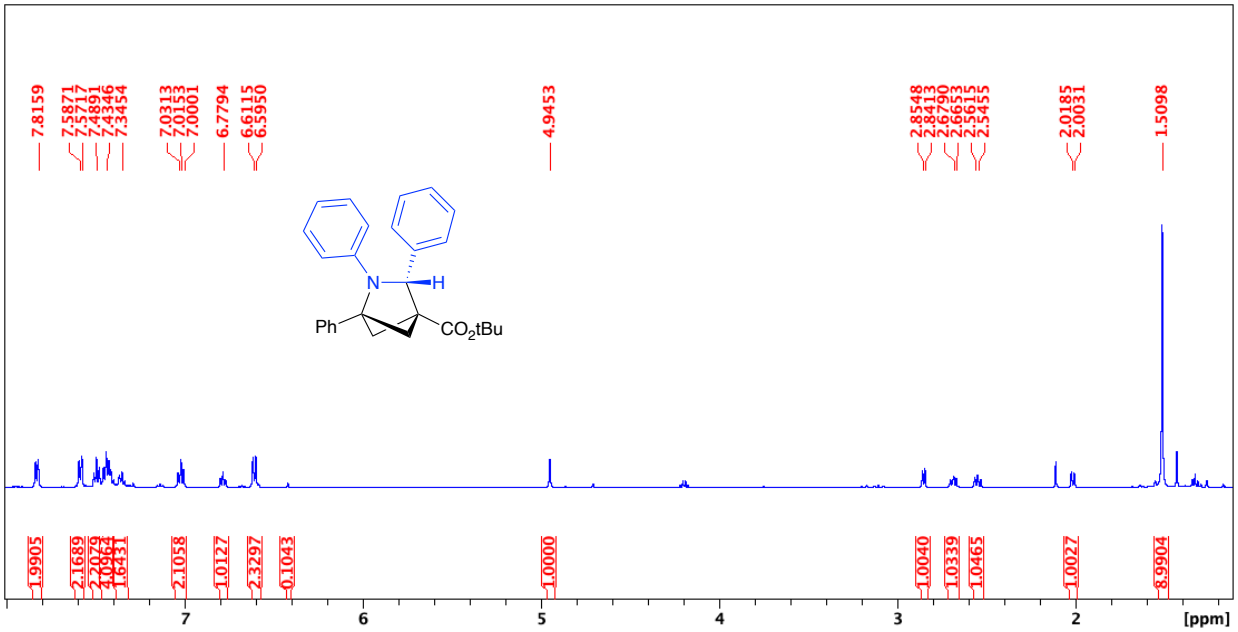

^{13}C NMR (126 MHz, $CDCl_3$, 292K, ppm): δ 168.66, 150.42, 140.07, 138.97, 128.05, 127.76, 127.38, 127.14, 126.94, 126.51, 126.17, 124.86, 123.86, 118.78, 117.62, 112.05, 80.10, 73.26, 68.77, 54.20, 44.68, 43.58, 27.04.

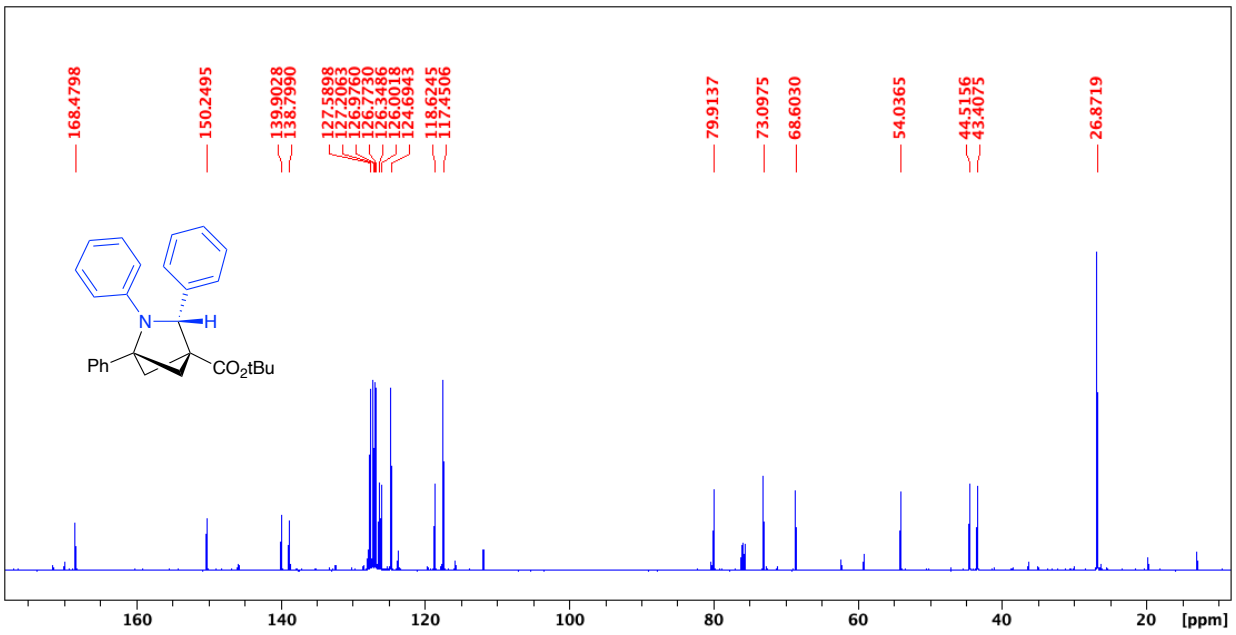

ATR IR spectrum:

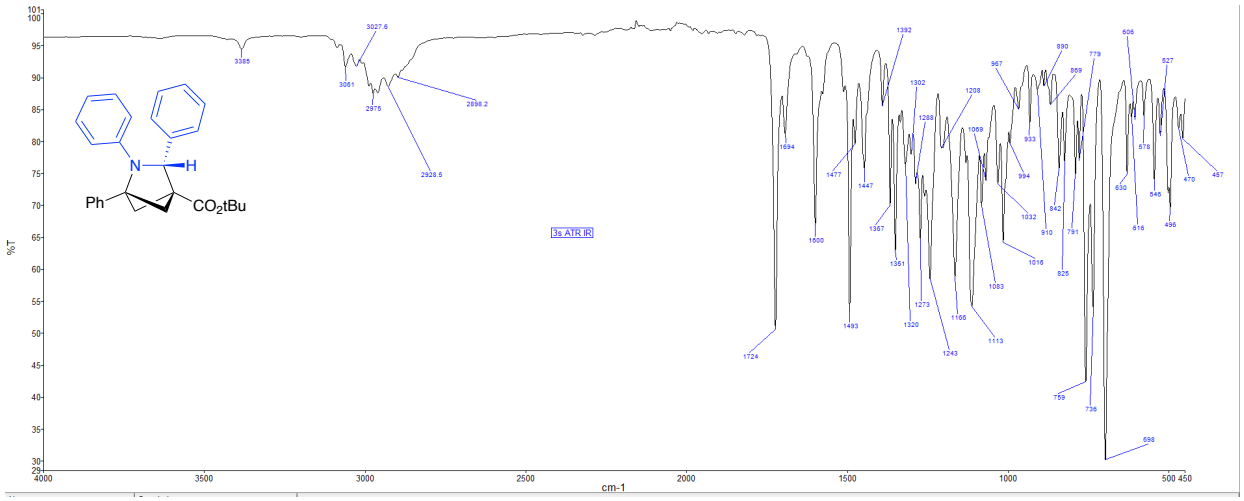

LCMS Chromatogram:

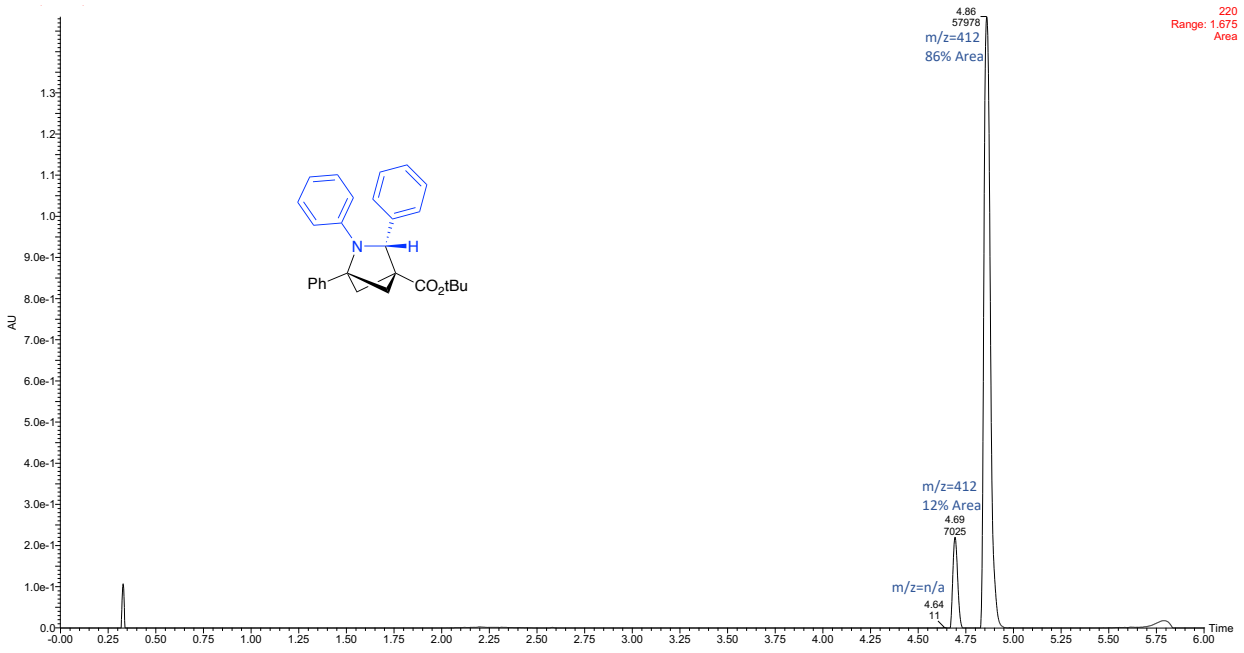

Morpholino-1,2,3-triphenyl-2-azabicyclo[2.1.1]hexan-4-yl)methanone (3u)

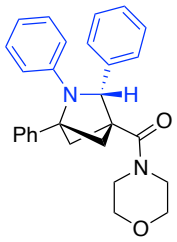

The product was prepared by **Method A** using morpholino(3-phenylbicyclo[1.1.0]butan-1-yl)methanone **2g** (0.1219g, 0.50 mmol), **1a** (0.0997 g, 0.55 mmol) and $Ga(OTf)_3$ (0.0129 g, 5 mol%). The compound was purified by column chromatography (Biotage® Sfär KP-Amino 11g Column, 0-100% EtOAc/hexanes, eluted at 40% EtOAc). 212.6 mg of a yellow solid was obtained (50%). 99% peak area by LCMS.

IR: C=O 1624 cm^{-1}, C-N 1597 cm^{-1}

Melting point range: 210.3 – 211.8 °C

HRMS(ESI): calc'd for [$C_{28}H_{28}N_2O_2$ + H^+], 425.22236; found: 425.22235.

^{1}H NMR (500 MHz, $CDCl_3$, 292K, ppm): δ 7.73 (d, J=7.46 Hz, 2H), 7.56 (d, J=7.46 Hz, 2H), 7.50 (t, J=7.46 Hz, 2H), 7.41 (t, J-7.93 Hz, 3H), 7.33 (t, J=7.40 Hz, 1H), 6.98 (t, J=7.76 Hz, 2H), 6.76 (t, J=7.24 Hz, 2H), 6.58 (d, J=8.28 Hz, 2H), 4.89 (s, 1H), 3.84-3.76 (m, 1H), 3.76-3.65 (m, 1H), 3.65-3.54 (m, 1H), 3.54-3.44 (m, 1H), 3.44-3.33 (m, 1H), 3.14-3.02 (m, 1H), 3.02-2.90 (m, 1H), 2.87 (d, J=7.24 Hz, 1H), 2.80 (t, 7.66 Hz, 1H), 2.77-2.64 (m, 2H), 2.08 (d, J=7.11 Hz, 1H).

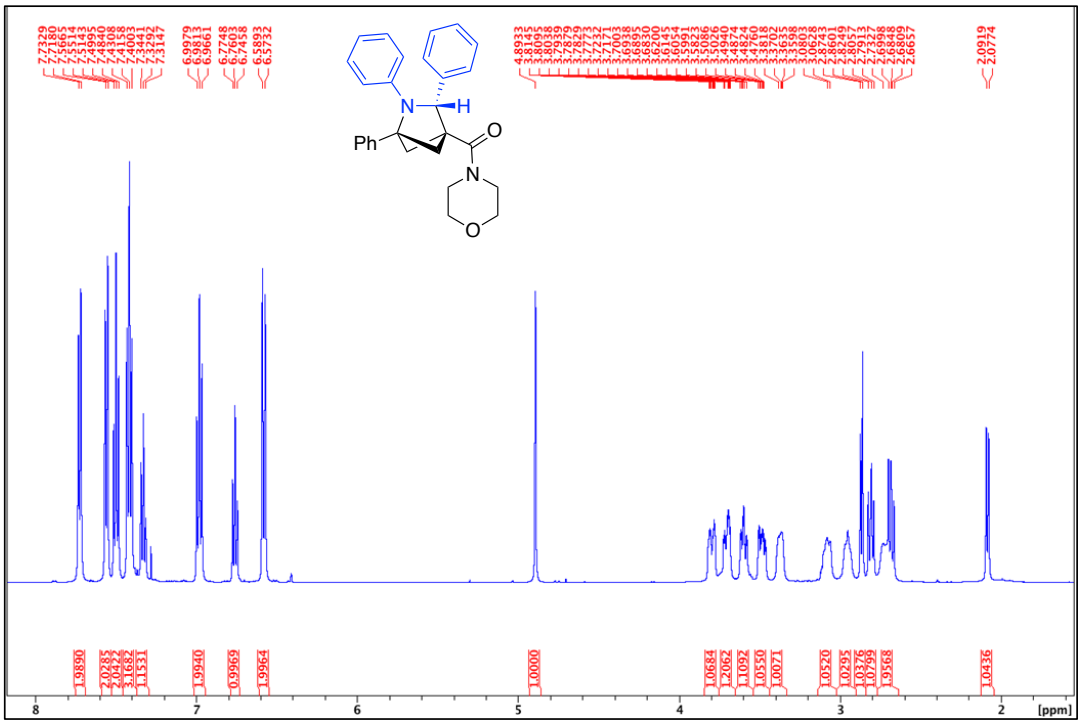

^{13}C NMR (126 MHz, $CDCl_3$, 292K, ppm): δ 168.95, 151.17, 140.89, 139.52, 128.90, 128.69, 128.49, 127.99, 127.63, 127.39, 126.02, 120.22, 118.94, 75.54, 69.69, 66.73, 66.03, 55.27, 48.35, 45.36, 45.30, 42.27.

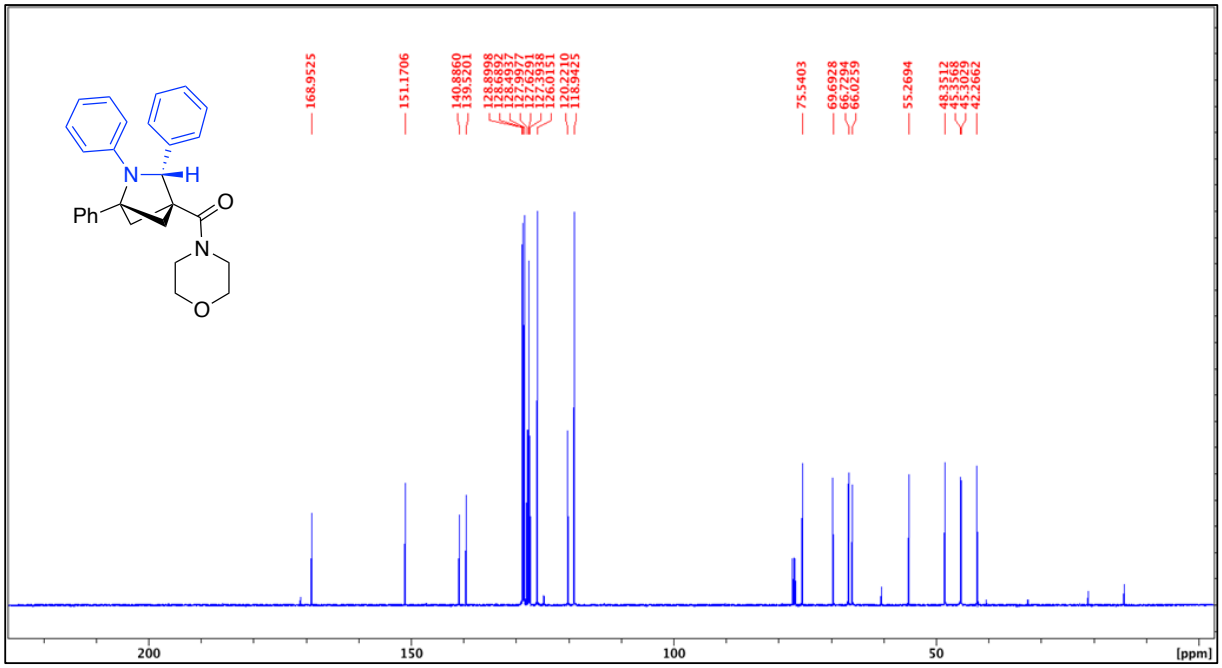

ATR IR spectrum:

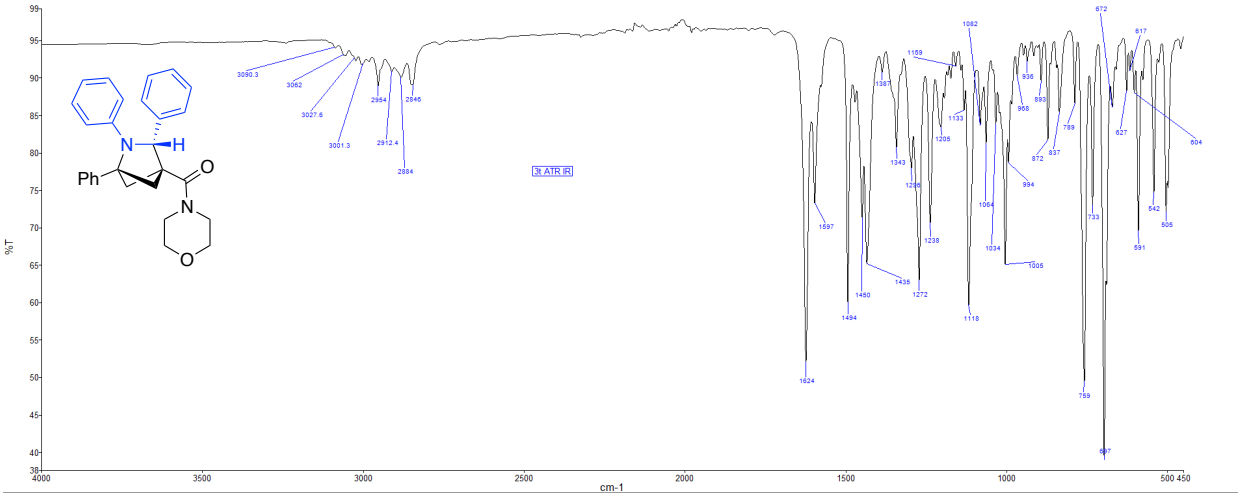

LCMS Chromatogram:

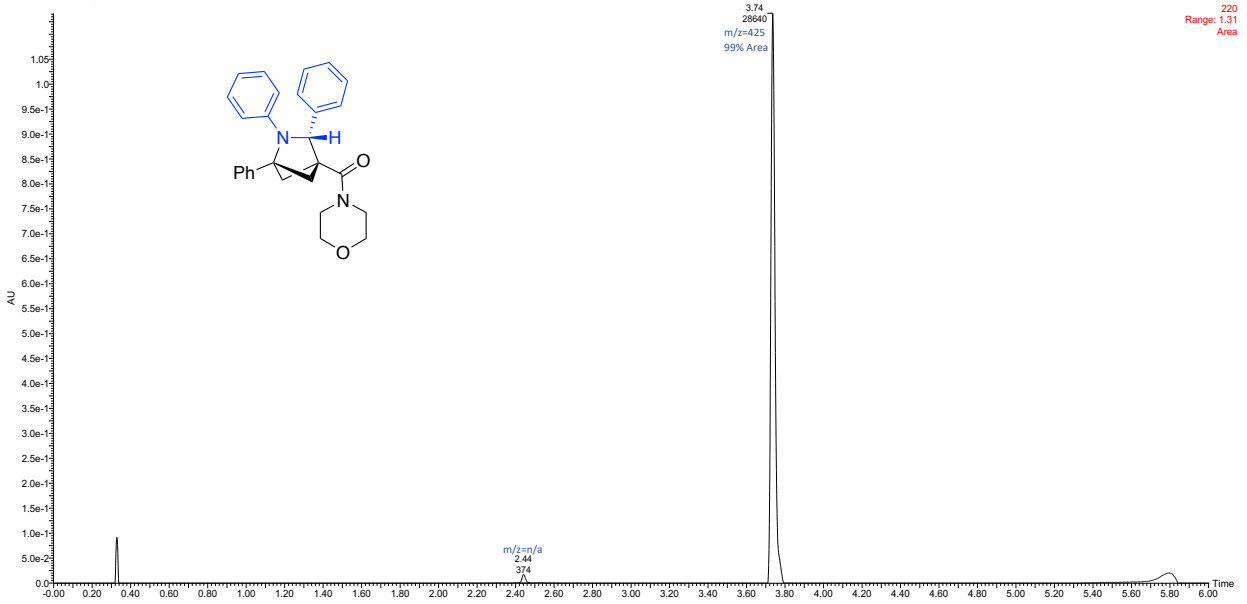

^{1}H-^{1}H COSY (3u):

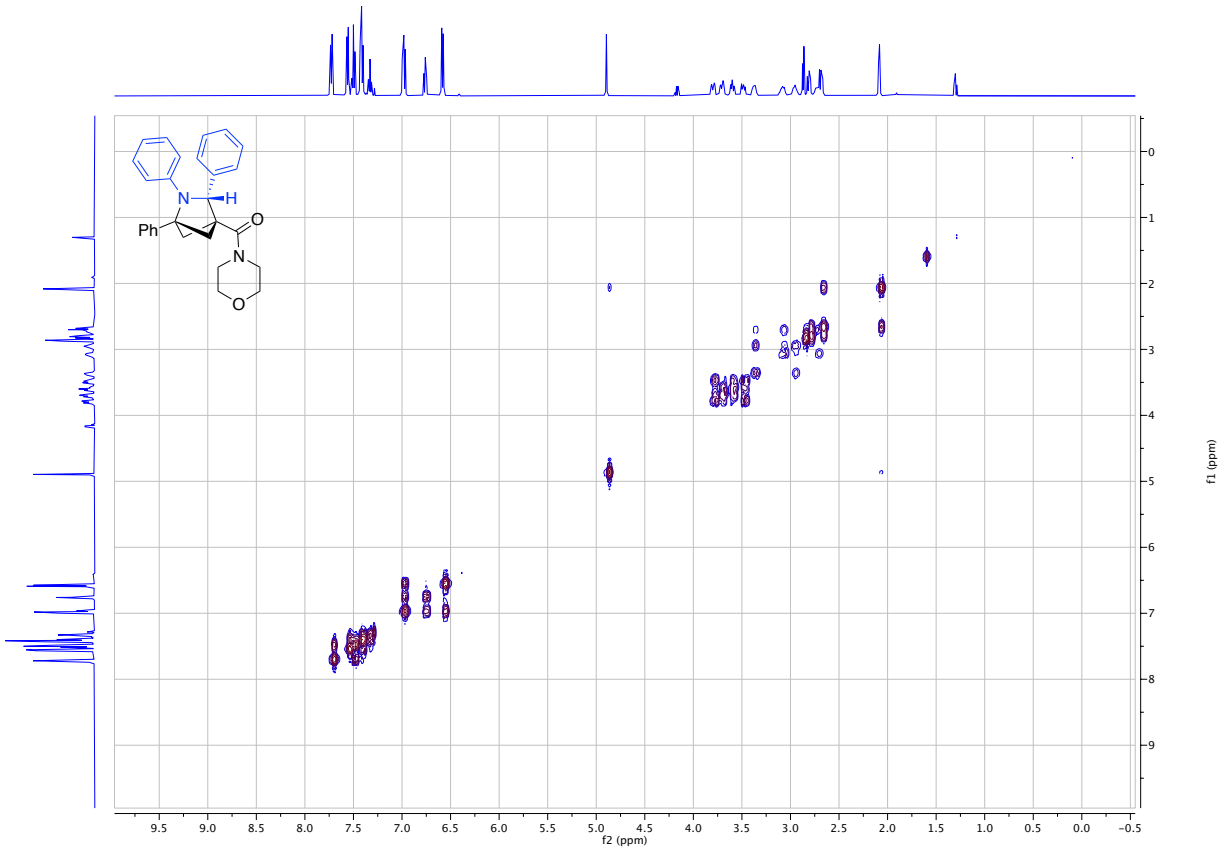

^{1}H-^{13}C HSQC (3u):

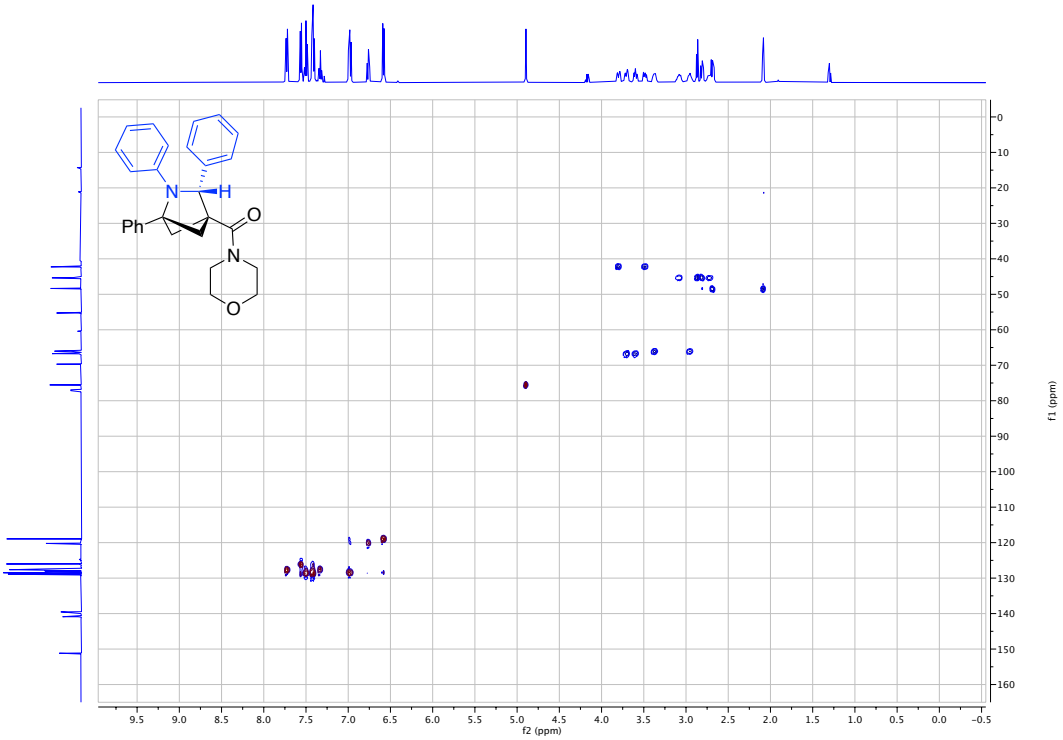

^{1}H-^{13}C HMBC (3u):

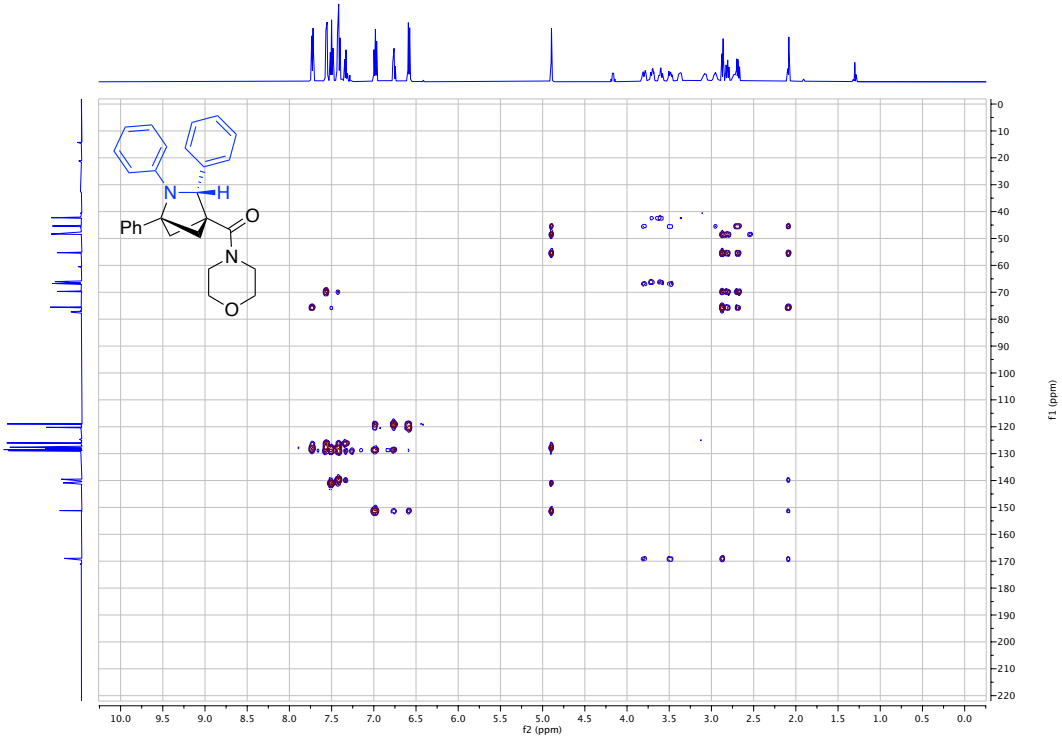

A.7 Cylobutenyl Methanamine Synthesis

Method B General Procedure:

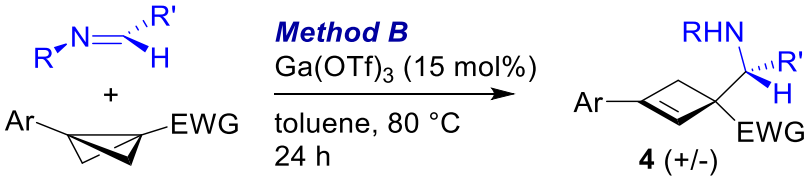

A screw-cap vial was charged with bicyclobutane substrate (0.500 mmol) and *N*-alkylimine substrate (0.550 mmol, 1.1 equiv). The vial was then taken inside an inert-atmosphere (N_2) glovebox. $Ga(OTf)_3$ (38.8 mg, 0.075 mmol, 15 mol%) was added to a second vial, along with a Teflon-coated stirbar. The substrates were dissolved in anhydrous toluene (3 mL) and transferred via syringe to the vial containing $Ga(OTf)_3$. The vial was sealed with a Teflon-lined screw cap, and stirring was commenced in an 80 °C aluminium block outside the glovebox. After stirring at 80 °C for 24 h, the vial was cooled to room temperature, followed by the addition of additional toluene (3 mL). The organic layer was washed with saturated $NaHCO_3$ (5 mL) and brine (5 mL). The toluene solution was directly loaded onto a silica gel column for purification by automated flash chromatography. The diastereomeric ratio from the NMR spectra was calculated using the benzylic proton (s, 4 ppm-5 ppm) at the stereocenter or alkene hydrogen just above 6 ppm from the ^1H NMR spectra.

Methyl-1-((benzylamino)(phenyl)methyl)-3-phenylcyclobut-2-ene-1-carboxylate (4aa)

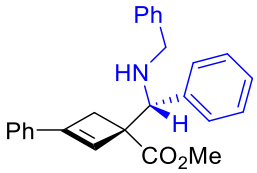

The product was prepared by **Method B** using **2a** (0.1882 g, 1 mmol), **1aa** (0.2929 g, 1.5 mmol) and $Ga(OTf)_3$ (0.0775 g, 15 mol%). The compound was purified by column chromatography (Silica, DCM:Methanol:Et_3N = 97:2:1). 253.1 mg (66%) of a light yellow solid was obtained with a 27:1 d.r.(d.r. by NMR spectra of isolated compound, peaks chosen 4.14 ppm & 4.21 ppm). 95% major and 2% minor diastereomer area from LCMS.

IR: N-H 3324 cm^{-1}, C=O 1712 cm^{-1}

Melting point range: 89.7-91.2 °C

HRMS(ESI): calc'd for [$C_{26}H_{25}NO_2$ + H^+], 384.19581; found: 384.19581.

^{1}H NMR (500 MHz, $CDCl_3$, 292K, ppm): δ 7.39-7.25 (m, 15H), 6.32 (s, 1H), 4.14 (s, 1H), 3.77 (d, J=13.96 Hz, 1H), 3.65 (s, 3H), 3.53 (d, J=13.96 Hz, 1H), 3.06 (d, J=13.32 Hz, 1H), 2.93 (d, J=13.32 Hz, 1H).

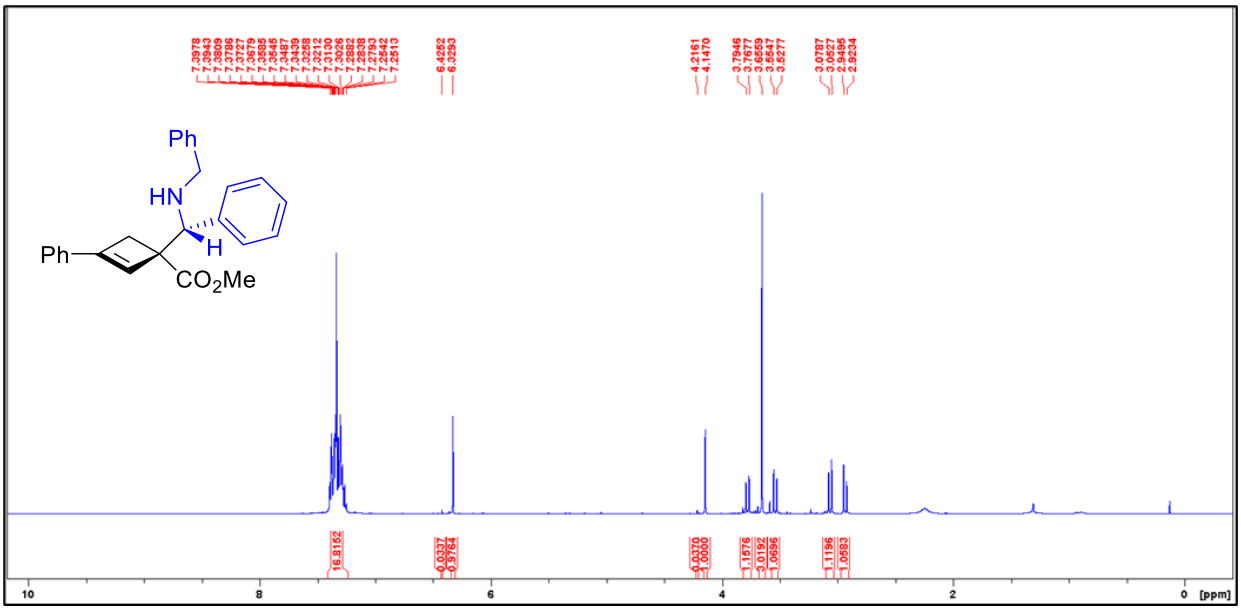

^{13}C NMR (126 MHz, $CDCl_3$, 292K, ppm): δ 174.30, 147.89, 140.48, 139.61, 133.53, 128.45, 128.36, 128.30, 128.20, 128.00, 127.55, 126.87, 126.43, 124.91, 65.84, 55.86, 51.80, 51.33, 36.06.

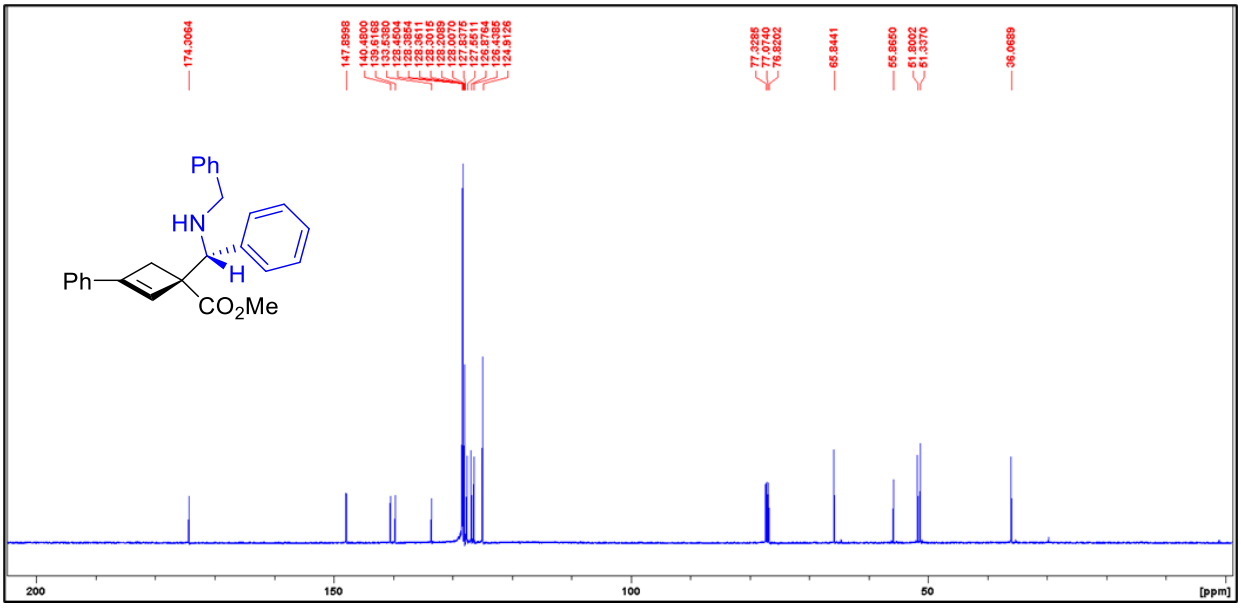

ATR IR spectrum:

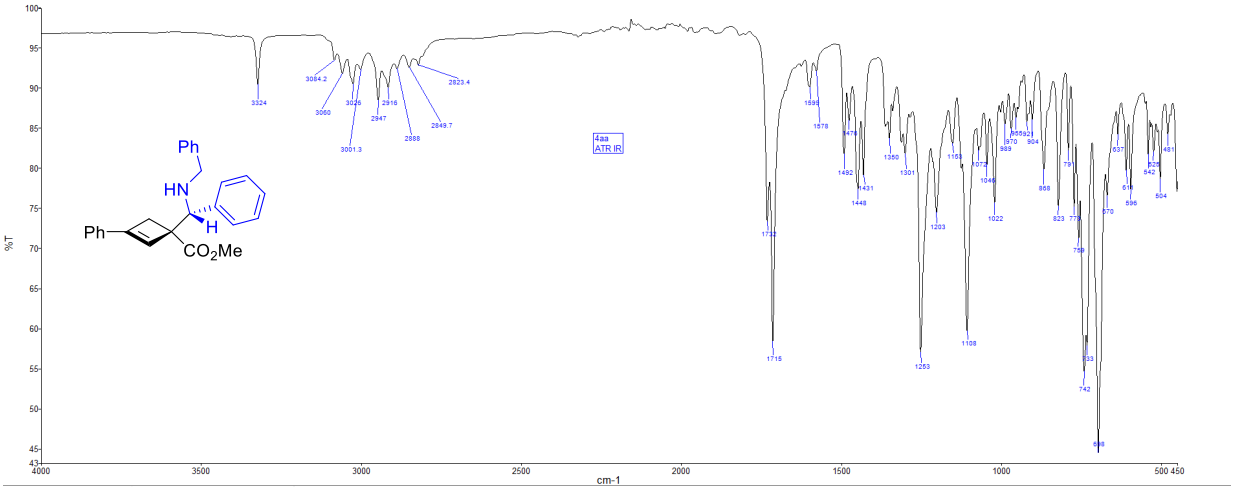

LCMS Chromatogram:

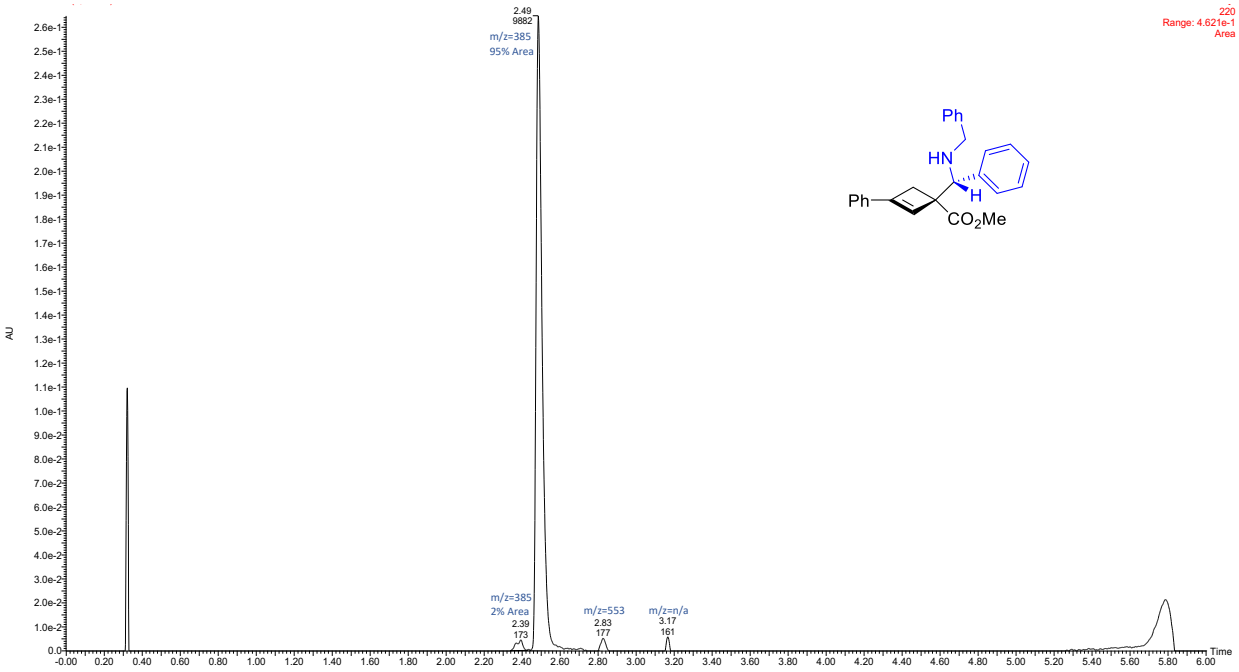

Methyl-1-((4-methoxybenzyl)amino)(phenyl)methyl)-3-phenylcyclobut-2-ene-1-carboxylate (4bb)

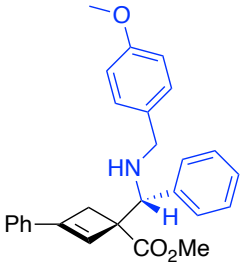

The product was prepared by **Method B** using **2a** (0.0941 g, 0.50 mmol), **1bb** (0.1600 g, 0.75 mmol) and $Ga(OTf)_3$ (0.0388 g, 15 mol%). The compound was purified by column chromatography (Biotage® Sfär KP-Amino 11g Column, 0-100% EtOAc/hexanes, eluted at 30% EtOAc). 88.8 mg of an orange solid was obtained with a 13:1 d.r. (44%). 94% peak area by LCMS.

IR: N-H 3350 cm^{-1}, C=O 1713 cm^{-1}

Melting point range: 99.2 – 101.8 °C

HRMS(ESI): calc'd for $[C_{27}H_{27}NO_3 + H^+]$, 414.20637; found: 414.20656.

^{1}H NMR (500 MHz, $CDCl_3$, 292K, ppm): δ 7.42-7.27 (m, 10H), 7.20 (d, J=8.47 Hz, 2H), 6.87 (d, J=8.47 Hz, 2H), 6.32 (s, 1H), 4.13 (s, 1H), 3.82 (s, 3H), 3.72 (d, J=13.22 Hz, 1H), 3.47 (d, J=13.22 Hz, 1H), 3.06 (d, J=13.13 Hz, 1H), 2.92 (d, J=13.13 Hz, 1H).

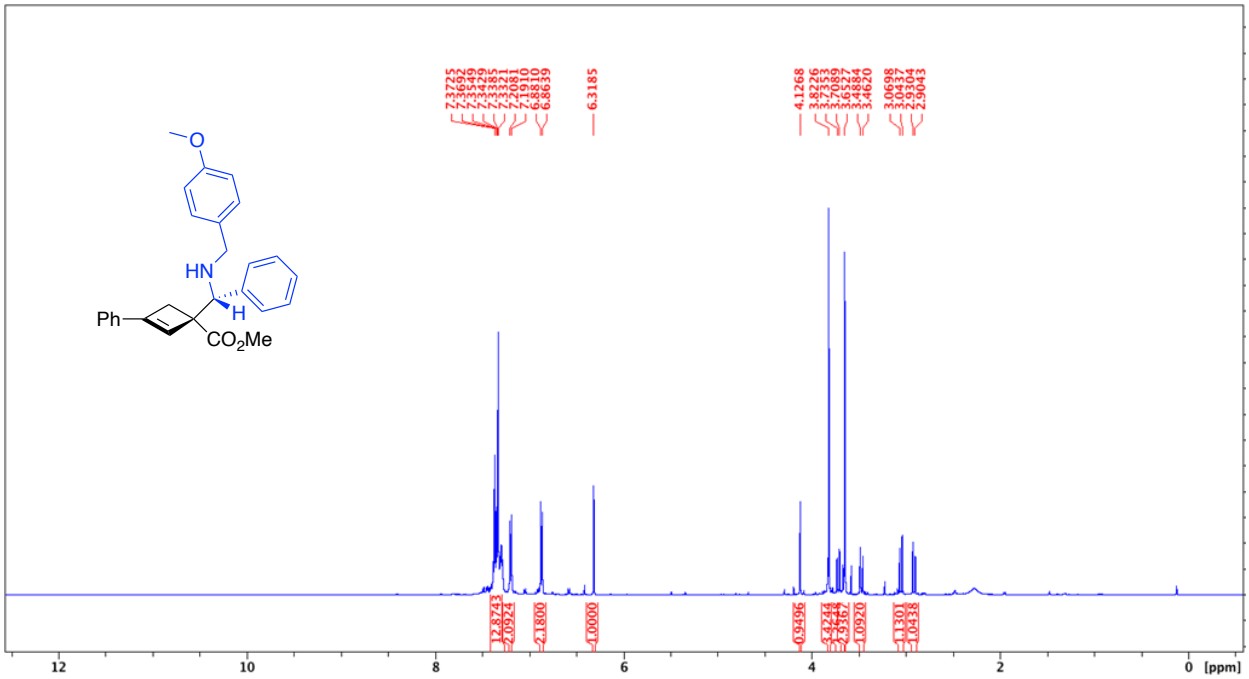

^{13}C NMR (126 MHz, $CDCl_3$, 292K, ppm): δ 174.33, 125.60, 147.87, 1235.54, 132.46, 130.34, 129.37, 128.61, 128.54, 128.17, 127.85, 127.74, 127.60, 127.39, 127.07, 126.77, 126.30, 124.91, 113.71, 65.65, 55.82, 51.80, 50.65, 36.08.

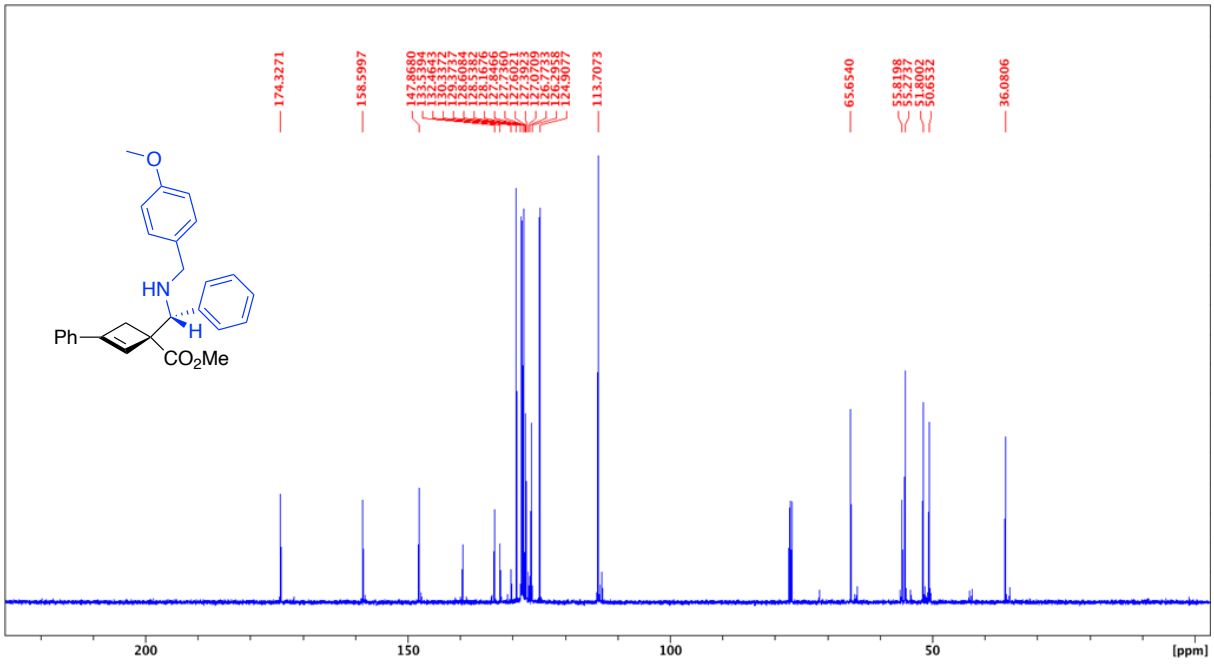

ATR IR spectrum:

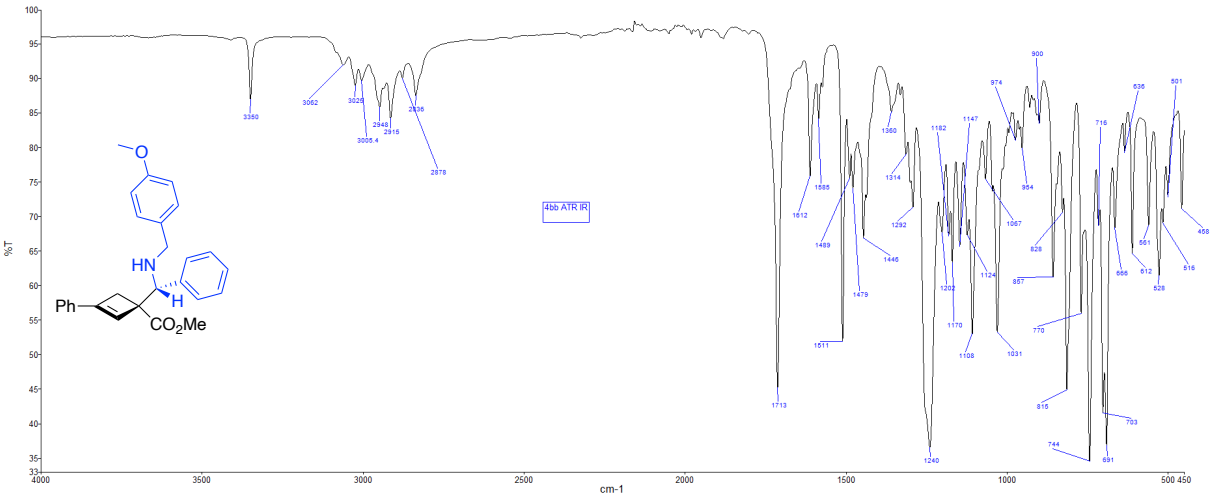

LCMS Chromatogram:

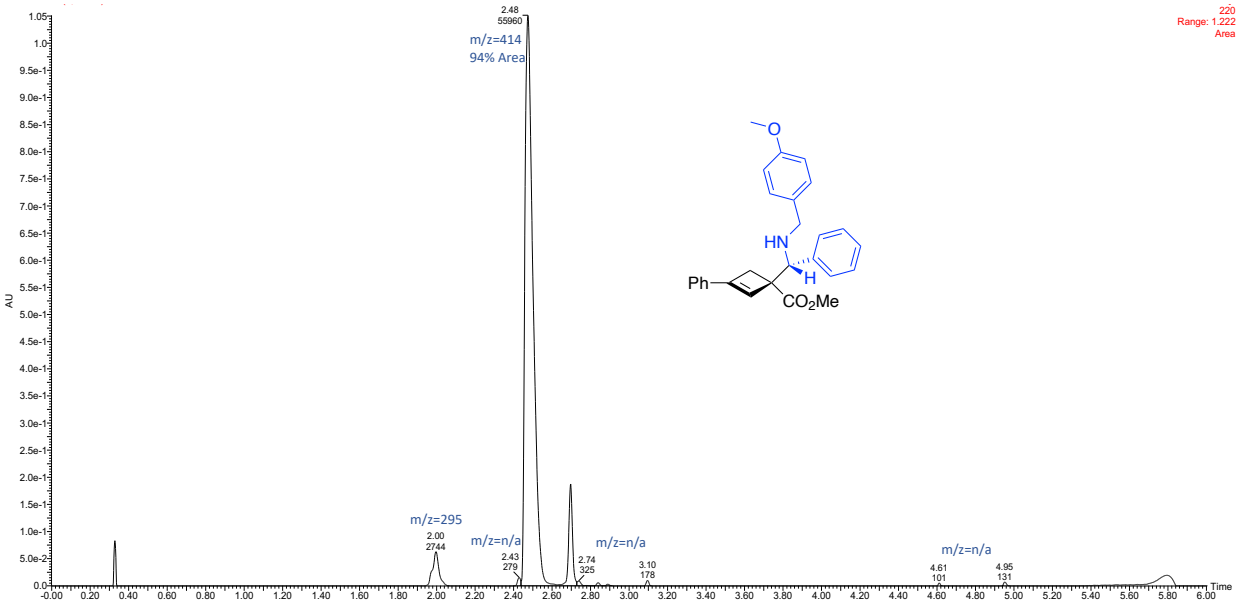

Methyl-1-((cyclohexylamino)(phenyl)methyl)-3-phenylcyclobut-2-ene-1-carboxylate (4cc)

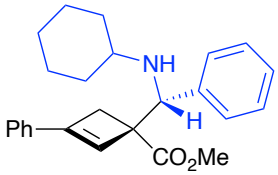

The product was prepared by **Method B** using **2a** (0.0941 g, 0.50 mmol), **1cc** (0.1405 g, 0.75 mmol) and $Ga(OTf)_3$ (0.0388 g, 15 mol%). The compound was purified by column chromatography (Biotage® Sfär KP-Amino 11g Column, 0-100% EtOAc/hexanes, eluted at 0% EtOAc). 36.3 mg of a white solid was obtained with a 33:1 d.r. (19%). 98% major diastereomer and 1% minor diastereomer area by LCMS.

IR: N-H 3313 cm^{-1}, C=O 1724 cm^{-1}

Melting point range: 109.2 – 110.7 °C

HRMS(ESI): calc'd for $[C_{25}H_{29}NO_2 + H^+]$, 376.22711; found: 376.22718.

^{1}H NMR (500 MHz, $CDCl_3$, 292K, ppm): δ 7.37-7.22 (m, 10H), 6.33 (s, 1H), 4.25 (s, 1H), 3.65 (s, 3H), 3.04 (d, J=13.15 Hz, 1H), 2.88 (d, J=13.15 Hz, 1H), 2.27 (m, 1H), 1.99-1.90 (m, 1H), 1.66 (m, 3H), 1.53 (m, 1H), 1.22-1.00 (m, 4H).

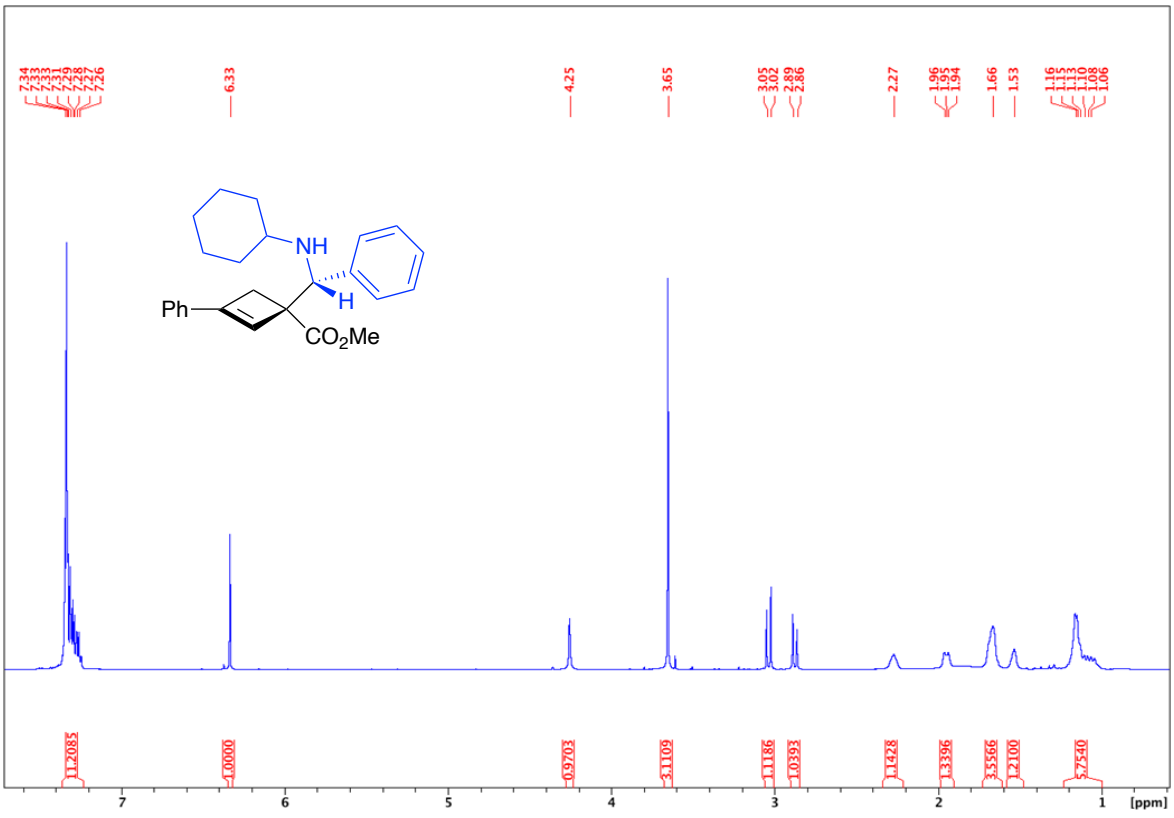

^{13}C NMR (126 MHz, $CDCl_3$, 292K, ppm): δ 174.52, 147.48, 133.62, 128.40, 128.37, 128.34, 128.31, 128.09, 127.81, 127.27, 126.75, 124.87, 63.95, 53.66, 51.76, 36.39, 34.61, 32.51, 26.16, 25.05, 24.60.

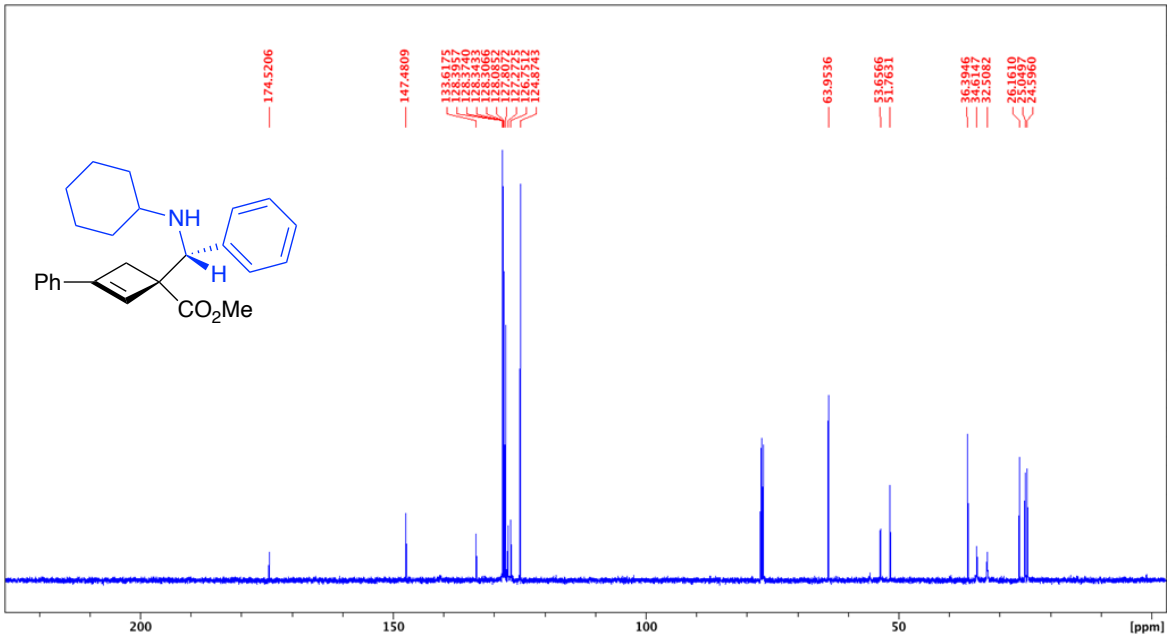

ATR IR spectrum:

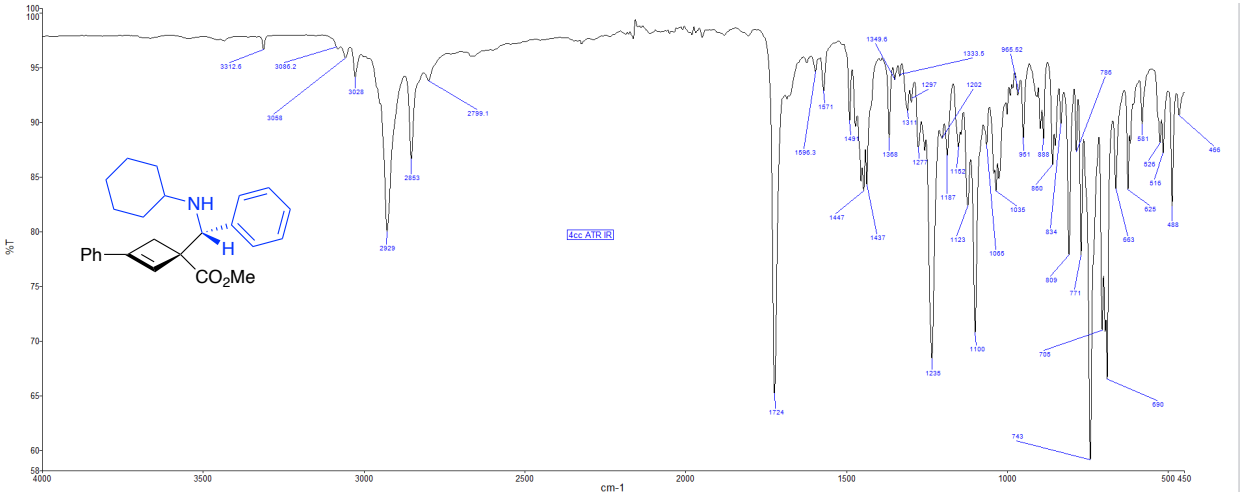

LCMS Chromatogram:

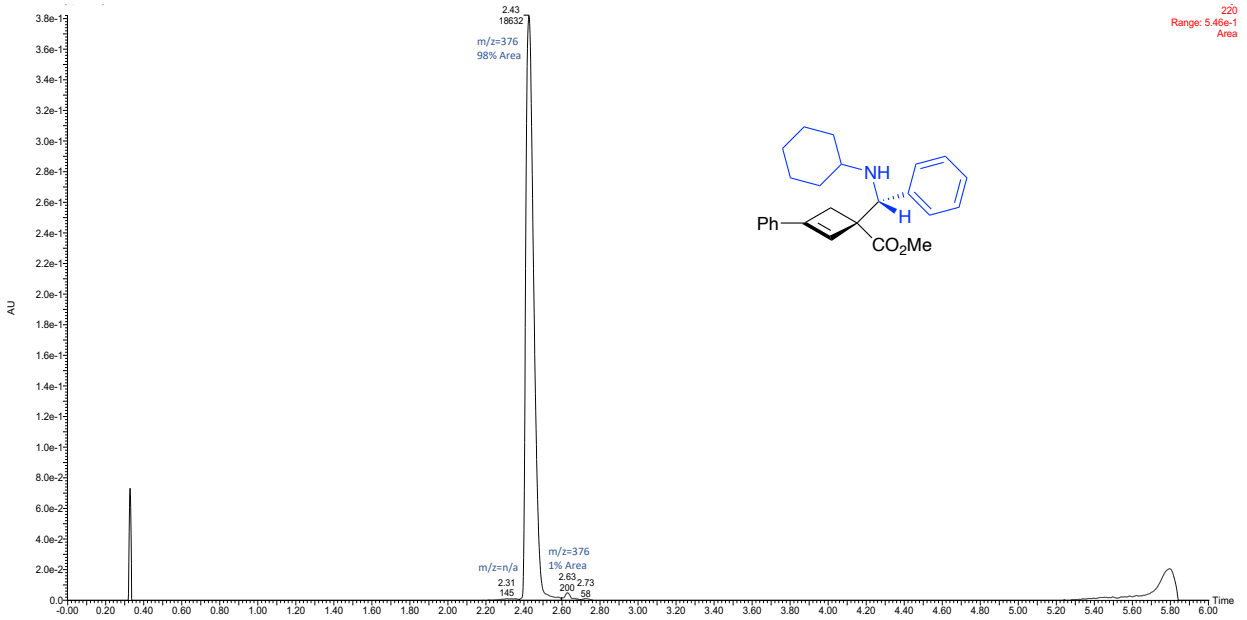

Methyl-1-((*tert*-butylamino)(phenyl)methyl)-3-phenylcyclobut-2-ene-1-carboxylate (4dd)

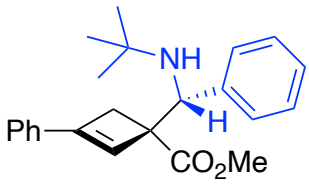

The product was prepared by **Method B** using **2a** (0.0941 g, 0.50 mmol), **1dd** (0.1209 g, 0.75 mmol) and $Ga(OTf)_3$ (0.0388 g, 15 mol%). The compound was purified by column chromatography (Biotage® Sfär KP-Amino 11g Column, 0-100% EtOAc/hexanes, eluted at 0% EtOAc). 27.5 mg of a yellow oil was obtained with a >50:1 d.r. (16%). 95% major diastereomer and 4% minor diastereomer area by LCMS.

IR: C=O 1722 cm^{-1}

HRMS(ESI): calc'd for $[C_{23}H_{27}NO_2 + H^+]$, 350.21146; found: 350.21147.

^{1}H NMR (500 MHz, $CDCl_3$, 292K, ppm): δ 7.42-7.17 (m, 10H), 6.32 (s, 1H), 4.27 (s, 1H), 3.65 (s, 3H), 2.99 (d, J=13.02 Hz, 1H), 2.78 (d, J=13.02 Hz, 1H), 0.98 (s, 9H).

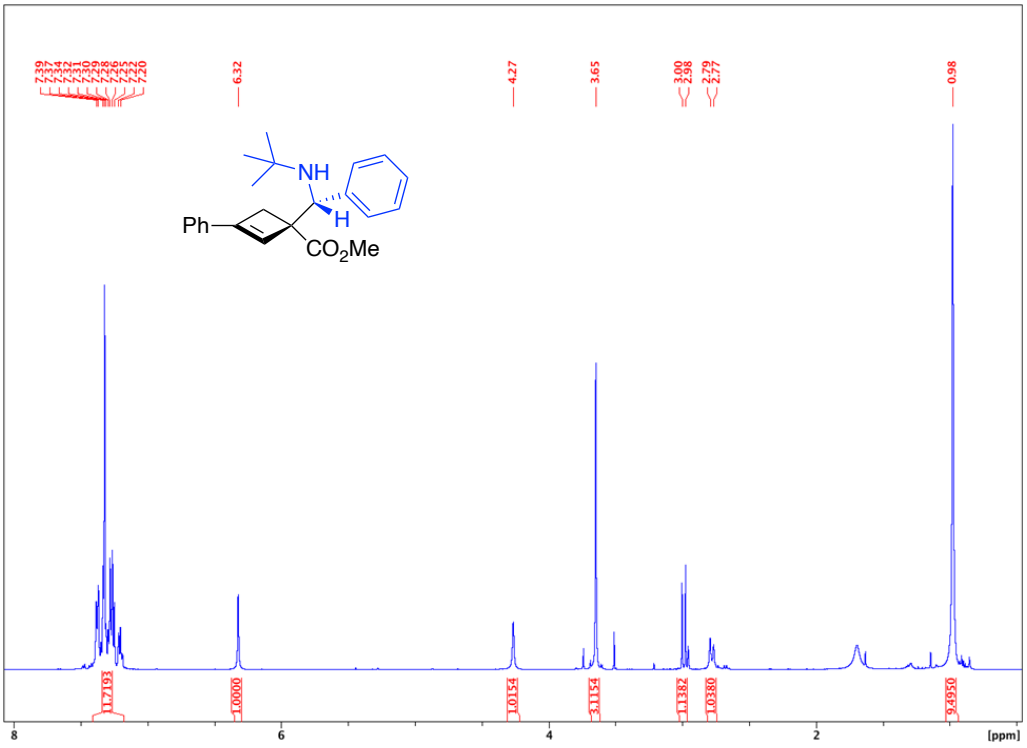

^{13}C NMR (126 MHz, $CDCl_3$, 292K, ppm): δ 174.49, 147.38, 143.56, 133.58, 128.49, 128.39, 128.35, 128.33, 128.05, 127.51, 126.88, 125.95, 124.88, 61.19, 51.82, 51.70, 51.09, 35.81, 30.16.

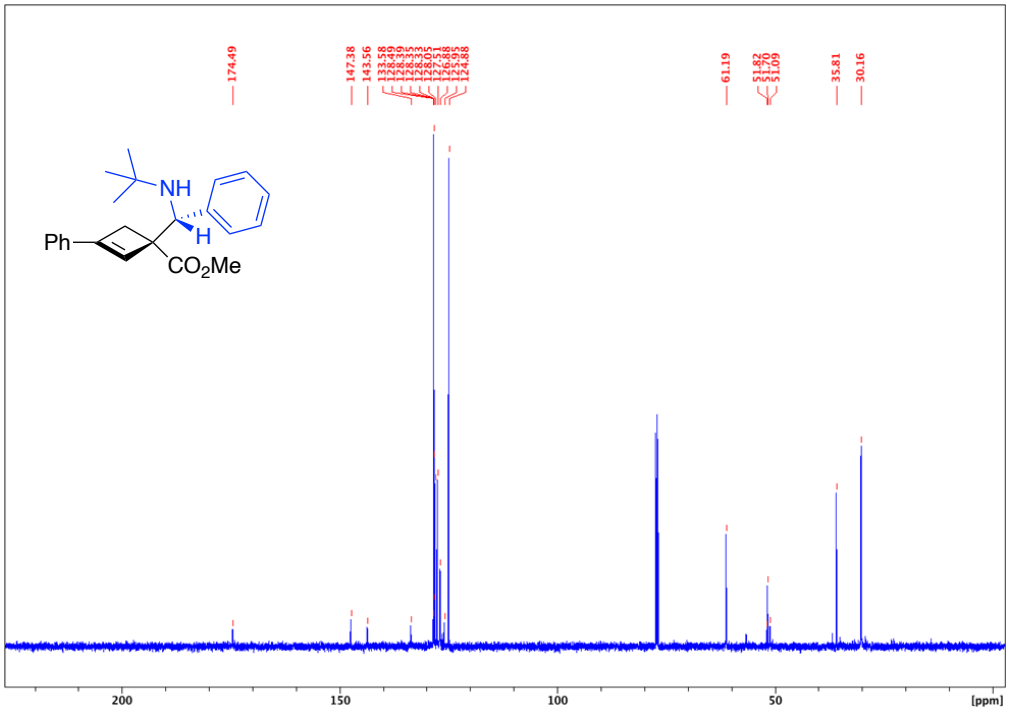

ATR IR spectrum:

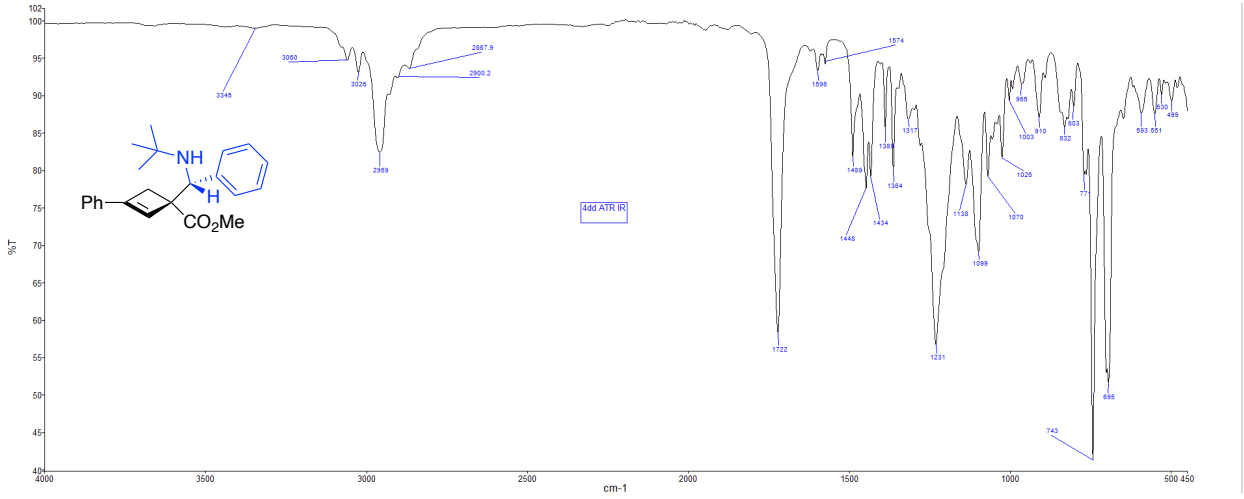

LCMS Chromatogram:

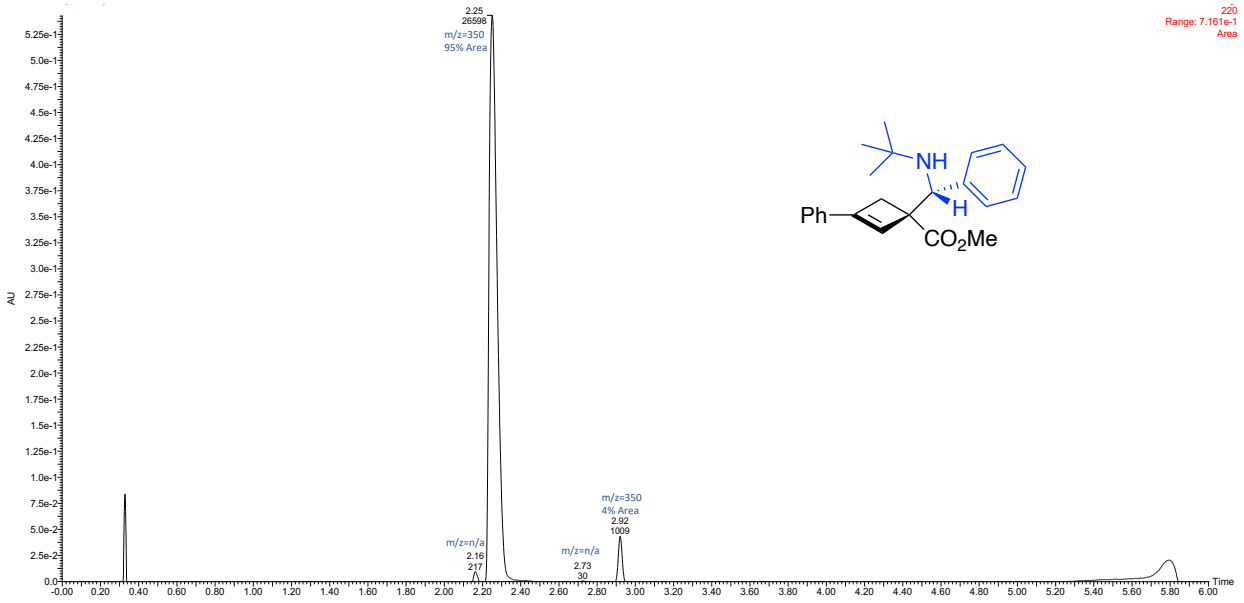

Methyl-1-((benzylamino)(1,3-dimethyl-1H-pyrazol-4-yl)methyl)-3-phenylcyclobut-2-ene-1-carboxylate (4gg)

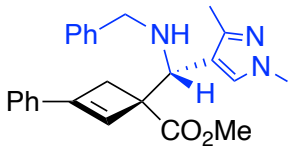

The product was prepared by **Method B** using **2a** (0.0941 g, 0.50 mmol), **1hh** (0.1600 g, 0.75 mmol) and $Ga(OTf)_3$ (0.0388 g, 15 mol%). The compound was purified by column chromatography (Biotage® Sfär KP-Amino 11g Column, 0-100% EtOAc/hexanes, eluted at 25% EtOAc). 64 mg of an colourless oily solid was obtained (32%, d.r. = 9:1 [peaks chosen 2.18 ppm & 2.16 ppm). 96% major diastereomer and 1% minor diastereomer area by LCMS.

IR: N-H 3334.9 cm^{-1}, C=O 1722 cm^{-1}

HRMS(ESI): calc'd for $[C_{17}H_{19}NO + H^+]$, 402.21761; found: 402.21771.

^{1}H NMR (500 MHz, $CDCl_3$, 292K, ppm): δ 7.39-7.24 (m, 14H), 6.32 (s, 1H), 4.07 (s, 1H), 3.82 (d, J= 11.76 Hz, 1H), 3.80 (s, 3H), 3.69 (s, 3H), 3.60 (d, J= 13.45 Hz, 1H), 3.10 (d, J= 12.80 Hz, 1H), 2.84 (d, J= 12.85 Hz, 1H), 2.16 (s, 3H).

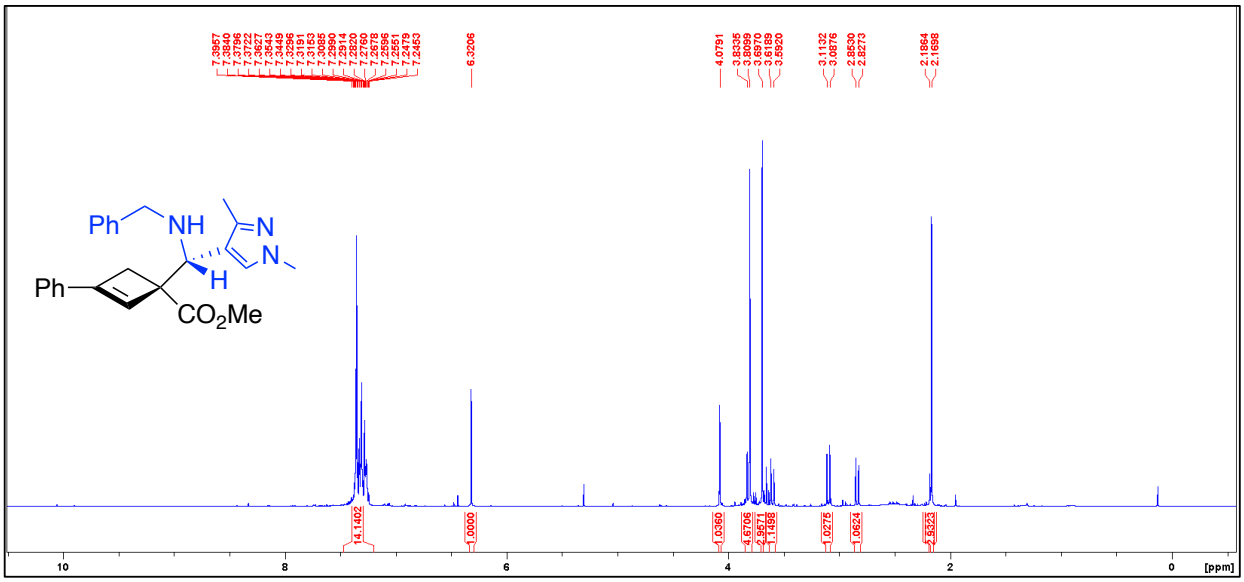

^{13}C NMR (126 MHz, $CDCl_3$, 292K, ppm): δ 174.63, 148.29, 147.76, 140.36, 133.55, 129.46, 128.50, 128.40, 128.32, 128.17, 126.90, 126.39, 124.89, 117.66, 56.42, 55.82, 51.89, 51.35, 38.75, 36.20, 11.99.

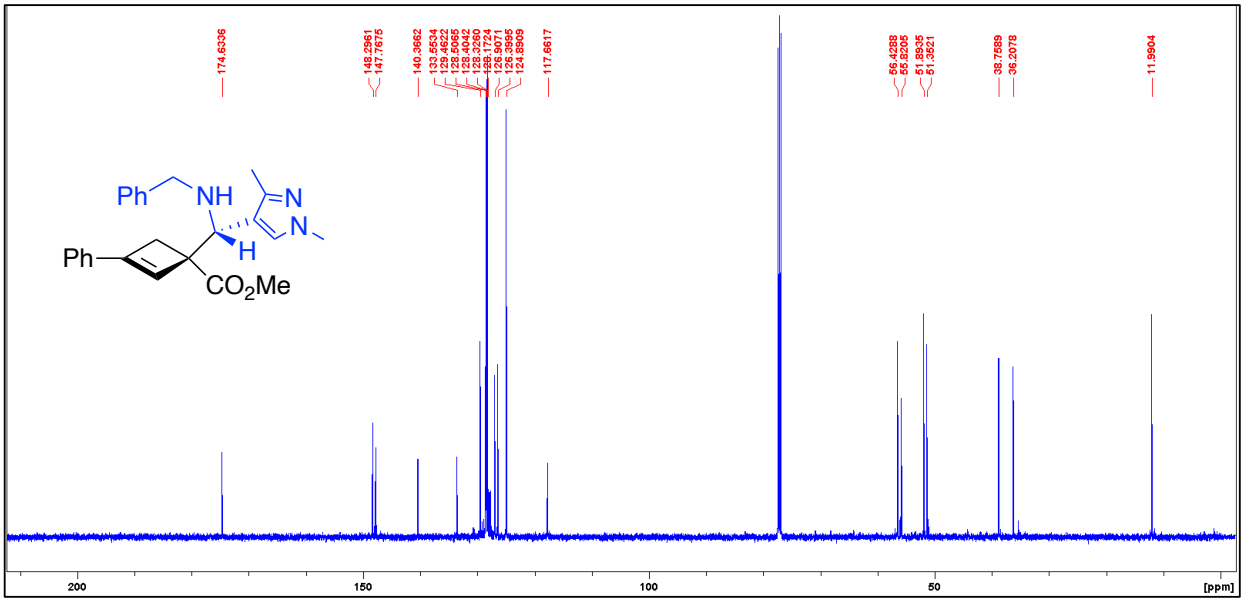

ATR IR spectrum:

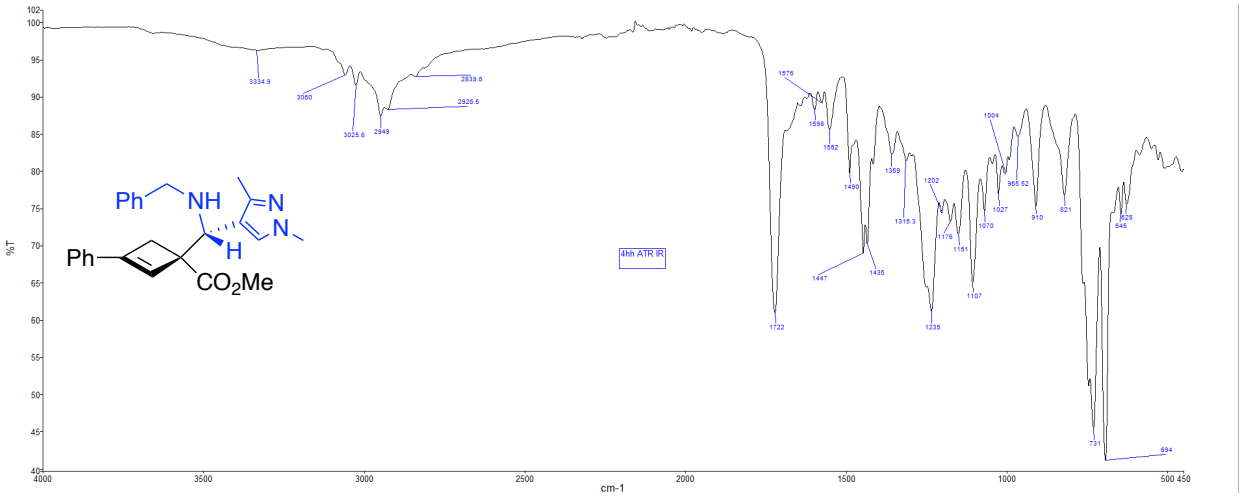

LCMS Chromatogram:

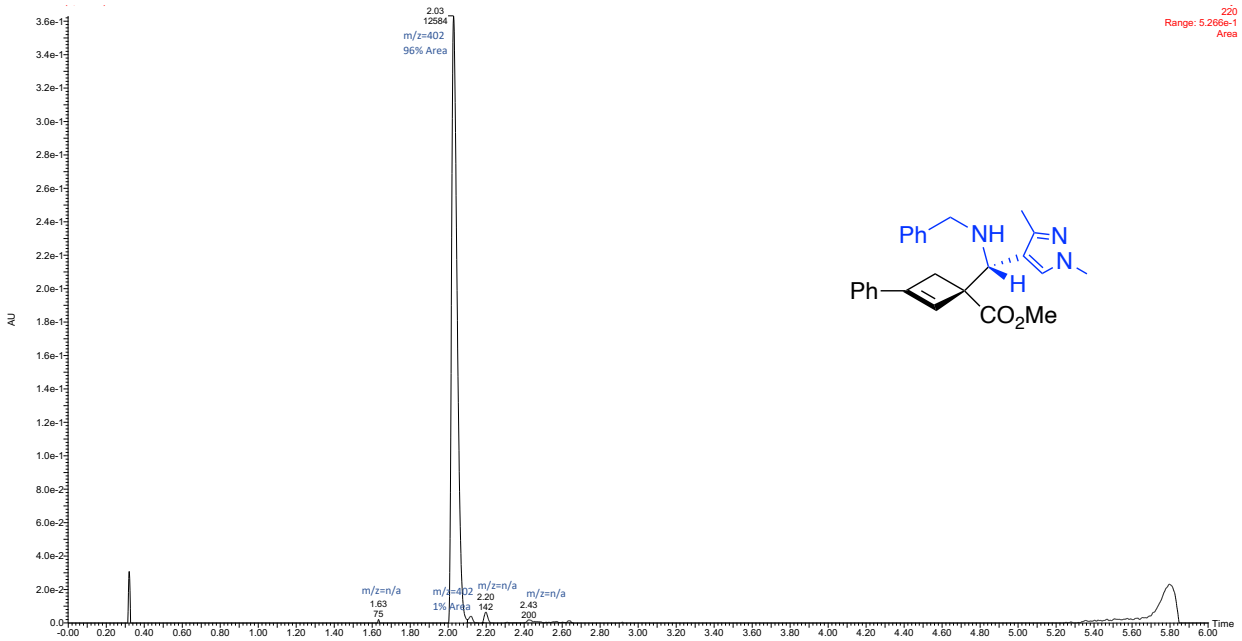

Methyl (*S*)-3-phenyl-1-((*R*)-phenyl(((*S*)-1-phenylethyl)amino)methyl)cyclobut-2-ene-1-carboxylate (4ii)

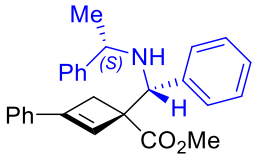

The product was prepared by **Method B** using **2a** (0.0941 g, 0.50 mmol), **1jj** (0.1570 g, 0.75 mmol) and $Ga(OTf)_3$ (0.0388 g, 15 mol%). The compound was purified by column chromatography (Biotage® Sfär Column, 0-100% EtOAc/hexanes, eluted at 25% EtOAc). 106.5 mg of a yellow oil was obtained with a 6:1 d.r. (54%). 95% major diastereomer and 5% minor diastereomers area by LCMS.

IR: N-H (broad) 3349 cm^{-1}, C=O 1721 cm^{-1}

HRMS(ESI): calc'd for $[C_{23}H_{27}NO_2 + H^+]$, 350.21146; found: 350.21147.

^{1}H NMR (500 MHz, $CDCl_3$, 292K, ppm): δ 7.17 (m, 15H), 6.22 (s, 1H), 4.19 (s, 1H), 3.55 (m, 4H), 2.94 (d, J=12.74 Hz, 1H), 2.79 (d, J=12.74 Hz, 1H), 1.20 (d, J=6.03 Hz, 3H).

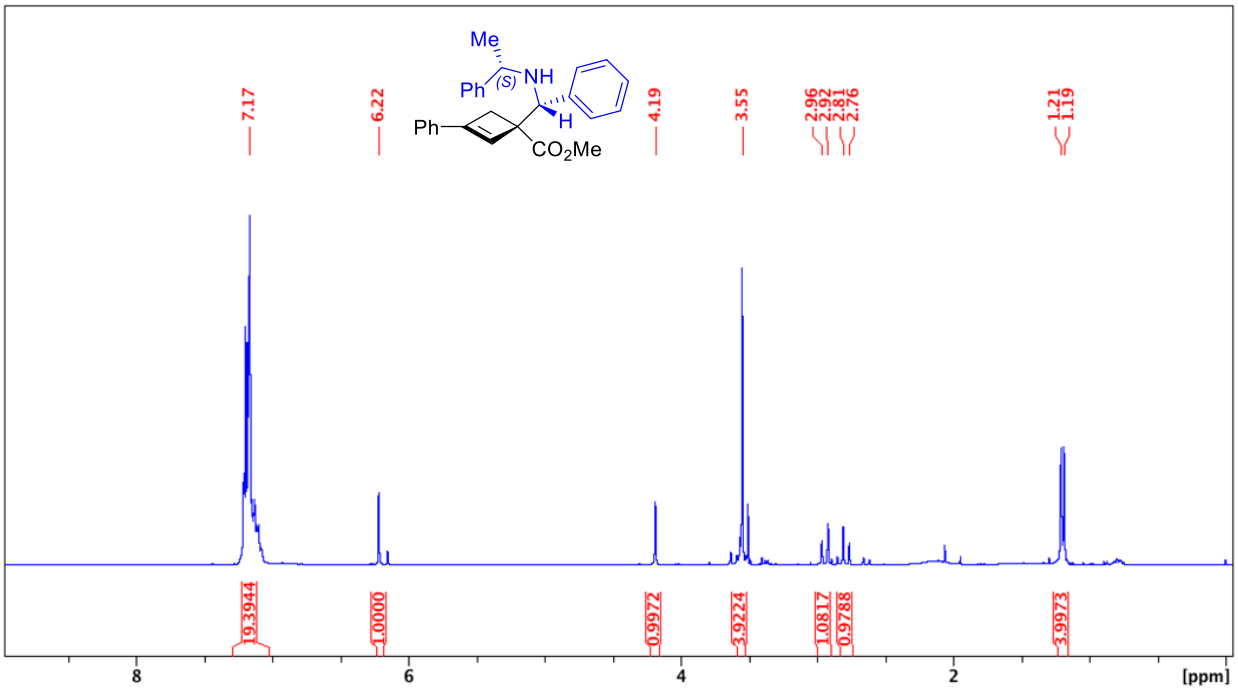

^{13}C NMR (126 MHz, $CDCl_3$, 292K, ppm): δ 174.63, 147.24, 146.40, 139.88, 133.63, 128.39, 128.37, 128.34, 128.19, 127.88, 127.36, 126.95, 126.81, 126.70, 126.61, 124.89, 124.86, 64.56, 55.74, 54.76, 51.80, 36.59, 25.17, 22.11.

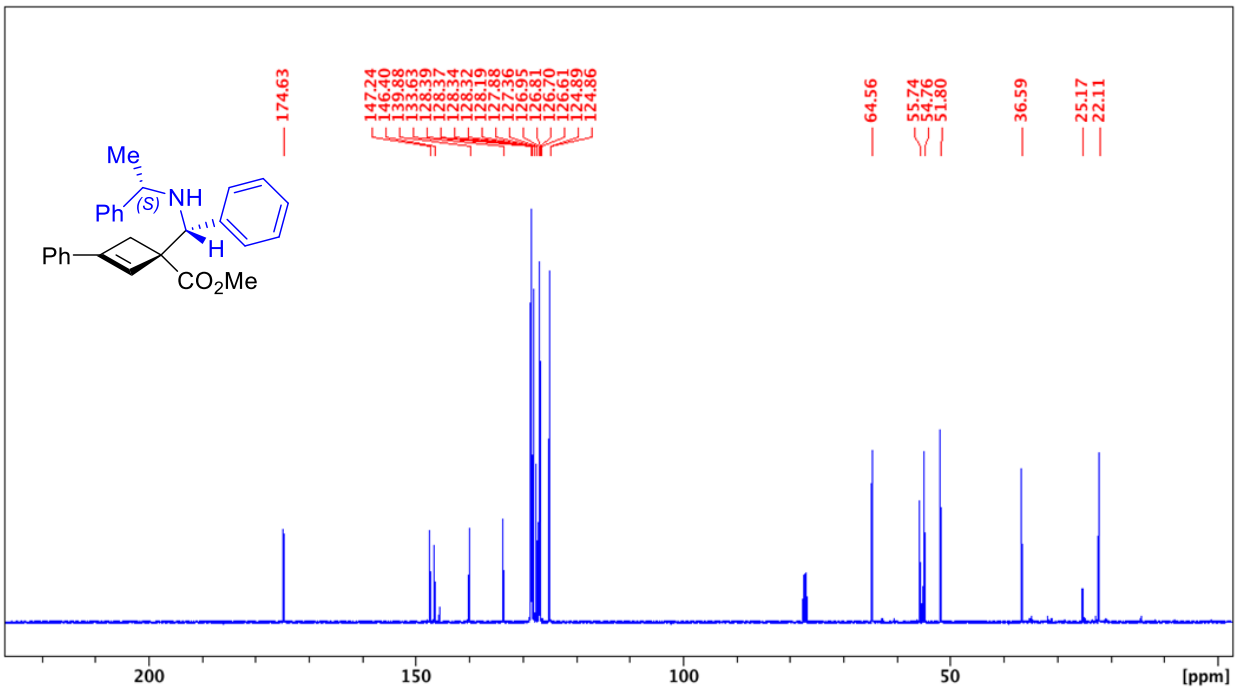

ATR IR spectrum:

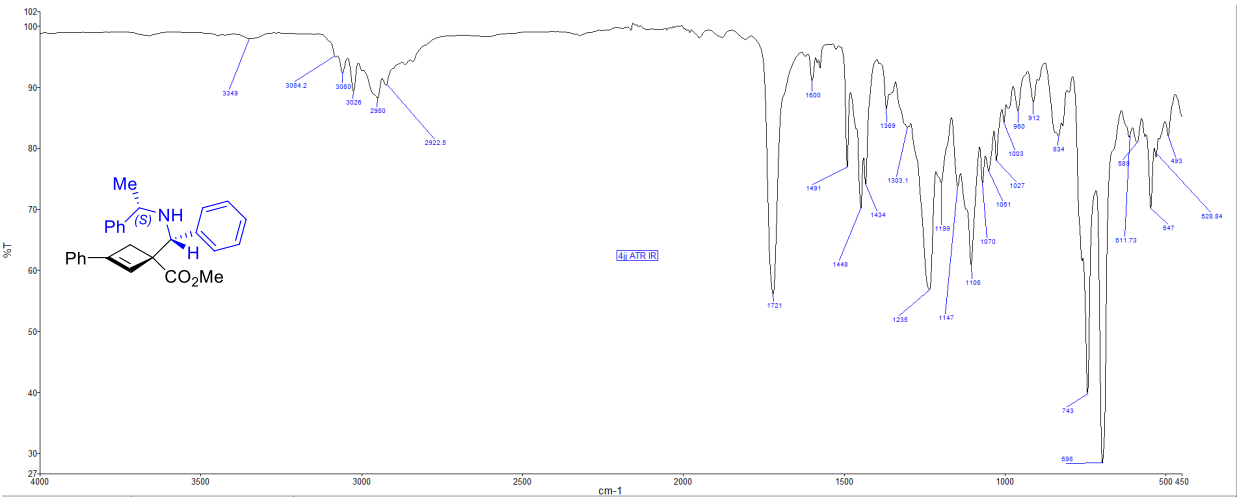

LCMS Chromatogram:

Benzyl (*S*)-3-phenyl-1-((*R*)-phenyl(((*S*)-1-phenylethyl)amino)methyl)cyclobut-2-ene-1-carboxylate (4jj)

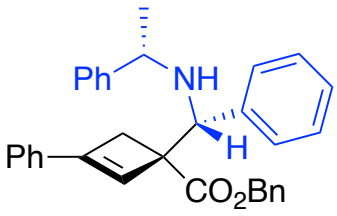

The product was prepared by **Method B** using benzyl 3-phenylbicyclo[1.1.0]butane-1-carboxylate (0.1322 g, 0.50 mmol), **1jj** (0.1570 g, 0.75 mmol) and $Ga(OTf)_3$ (0.0388 g, 15 mol%). The compound was purified by column chromatography (Biotage® Sfär 10g Column, 0-100% EtOAc/hexanes, eluted at 20% EtOAc). 119.4 mg of a yellow oil was obtained with an 8:1 d.r. (50%). 92% major diastereomer, 4% minor diastereomer and 3% **3jj** area by LCMS.

IR: N-H 3349 cm^{-1}, C=O 1721 cm^{-1}

HRMS(ESI): calc'd for $[C_{33}H_{31}NO_2 + H^+]$, 474.24276; found: 474.24277.

^{1}H NMR (500 MHz, $CDCl_3$, 292K, ppm): δ 7.31 – 7.00 (m, 20H), 6.25 (s, 1H), 5.03 (dd, J = 7.7, 1.0 Hz, 2H), 4.23 (s, 1H), 3.53 (q, J = 6.5 Hz, 1H), 2.97 (d, J = 13.1, 1H), 2.78 (d, J = 13.2, 1H), 1.17 (d, J = 6.5, 3H).

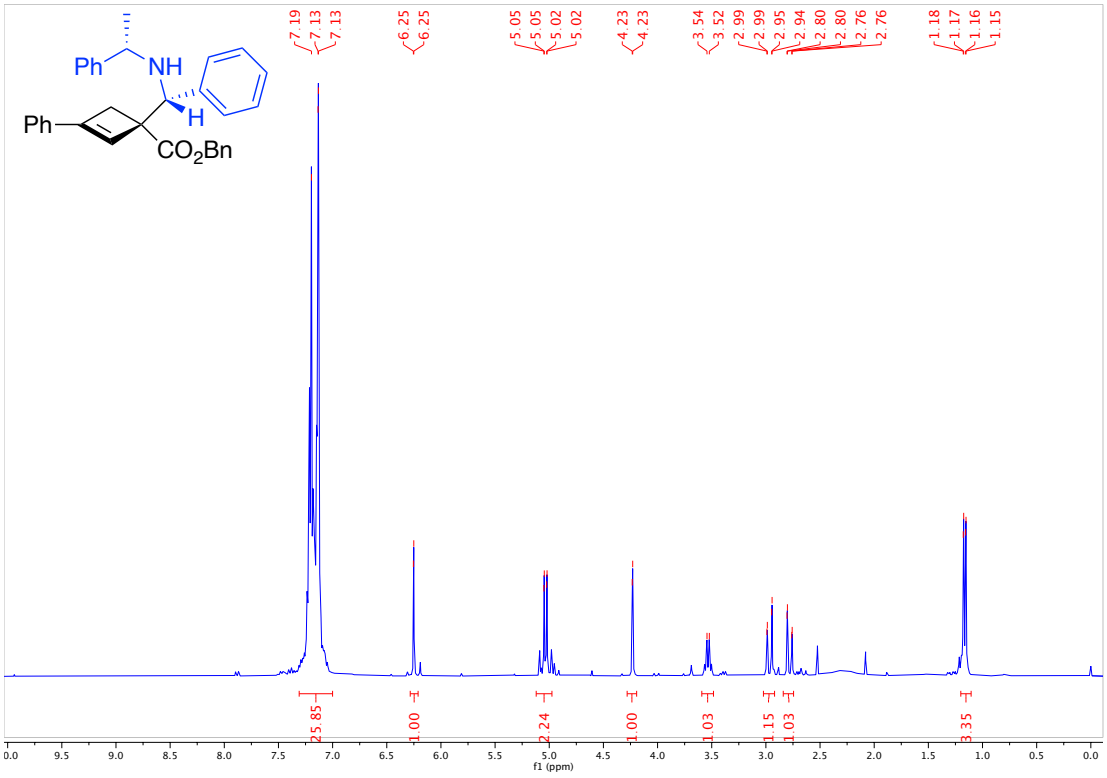

^{13}C NMR (126 MHz, $CDCl_3$, 292K, ppm): δ 174.01, 147.22, 136.04, 133.61, 128.49, 128.38, 128.35, 128.32, 128.26, 128.09, 127.89, 127.38, 126.84, 126.72, 126.47, 124.90, 124.88, 66.45, 64.53, 54.78, 36.63, 21.89.

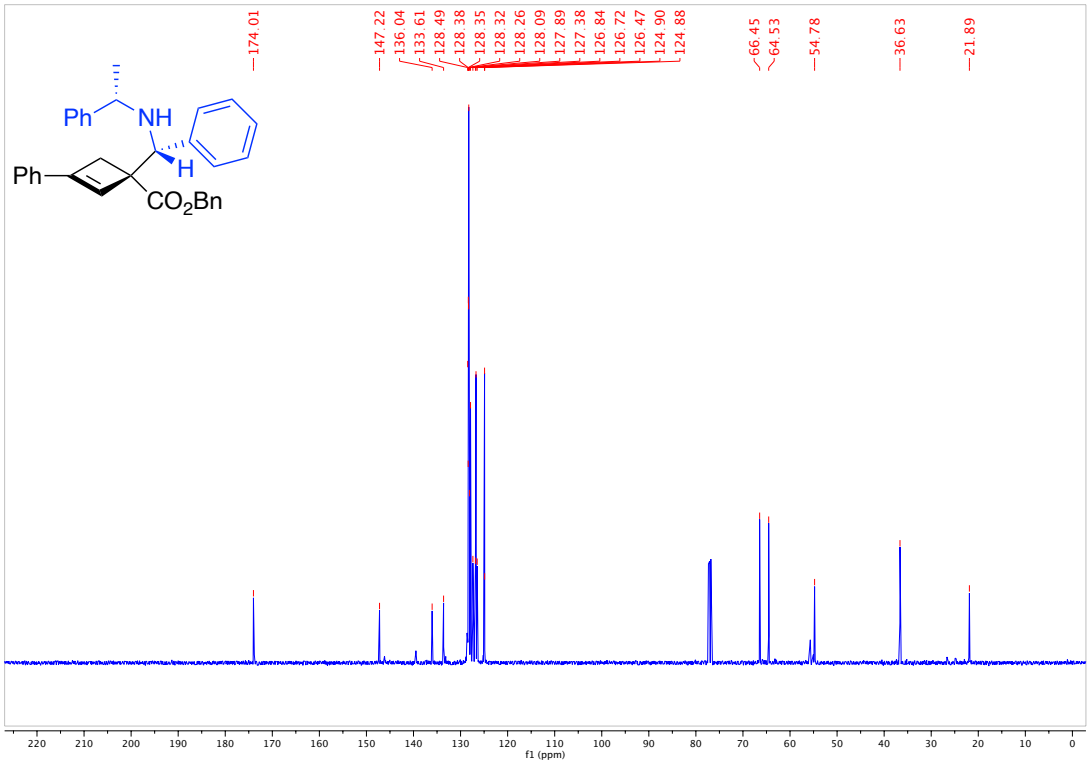

ATR IR spectrum:

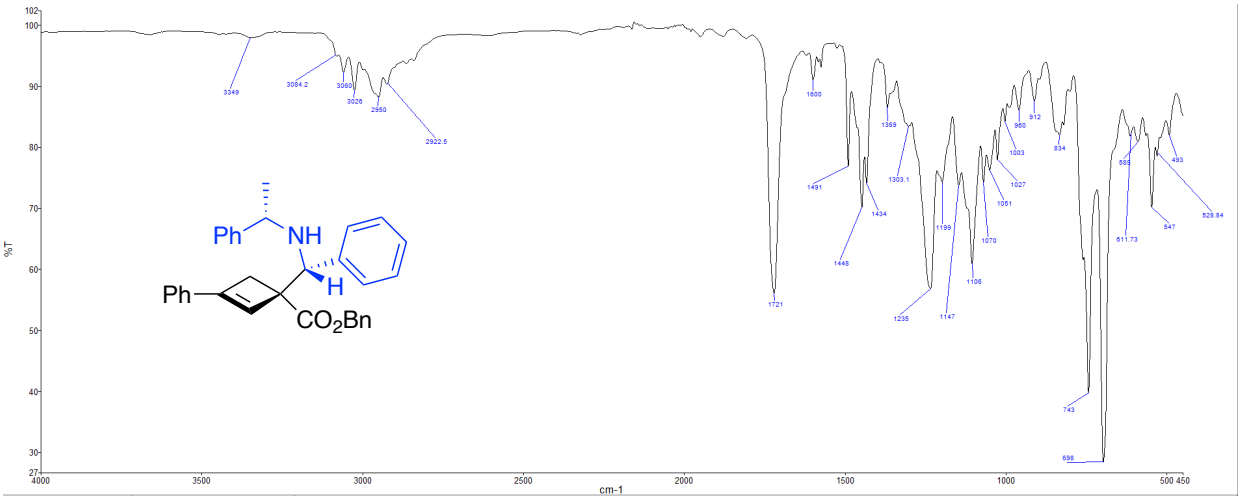

LCMS Chromatogram:

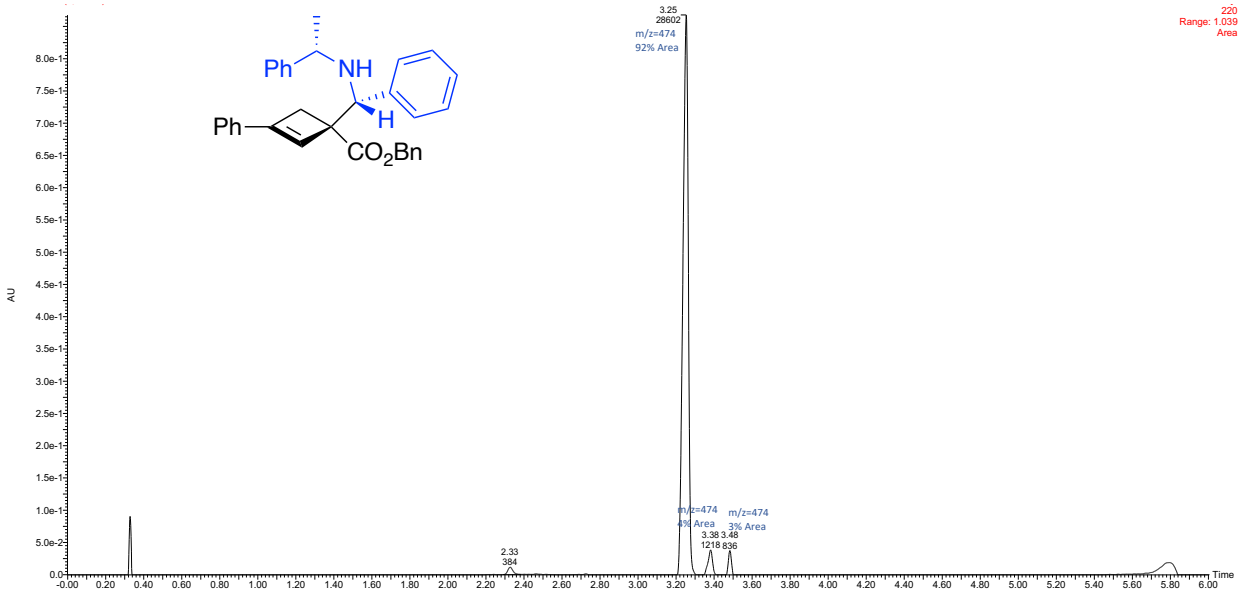

Methyl-1-(naphthalen-2-yl(((*S*)-1-phenylethyl)amino)methyl)-3-phenylcyclobut-2-ene-1-carboxylate (4kk)

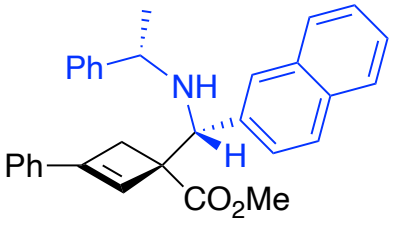

The product was prepared by **Method B** using **2a** (0.0941 g, 0.50 mmol), **1ll** (0.1945 g, 0.75 mmol) and $Ga(OTf)_3$ (0.0388 g, 15 mol%). The compound was purified by column chromatography (Biotage® Sfär 10g Column, 0-100% EtOAc/hexanes, eluted at 25% EtOAc). 123.5 mg of a yellow solid was obtained with a 6:1 d.r. (55%). 81% major diastereomer, 12:3:1% minor diastereomers and 3% **3kk** area by LCMS.

IR: N-H 3291 cm^{-1}, C=O 1727 cm^{-1}

Melting point range: 134.5 – 136.9 °C

HRMS(ESI): calc'd for $[C_{31}H_{29}NO_2 + H_+]$, 448.22711; found: 448.22695.

^{1}H NMR (500 MHz, $CDCl_3$, 292K, ppm): δ 7.90-7.79 (m, 5 H), 7.55-7.47 (m, 4H), 7.42-7.23 (m, 7H), 6.43 (s, 1H), 4.53 (s, 1H), 3.71 (s, 3H), 3.76-3.70 (m, 1H), 3.15 (d, J=12.92 Hz, 1H), 3.02 (d, J=12.92 Hz, 1H), 1.39 (d, J=6.38 Hz, 3H).

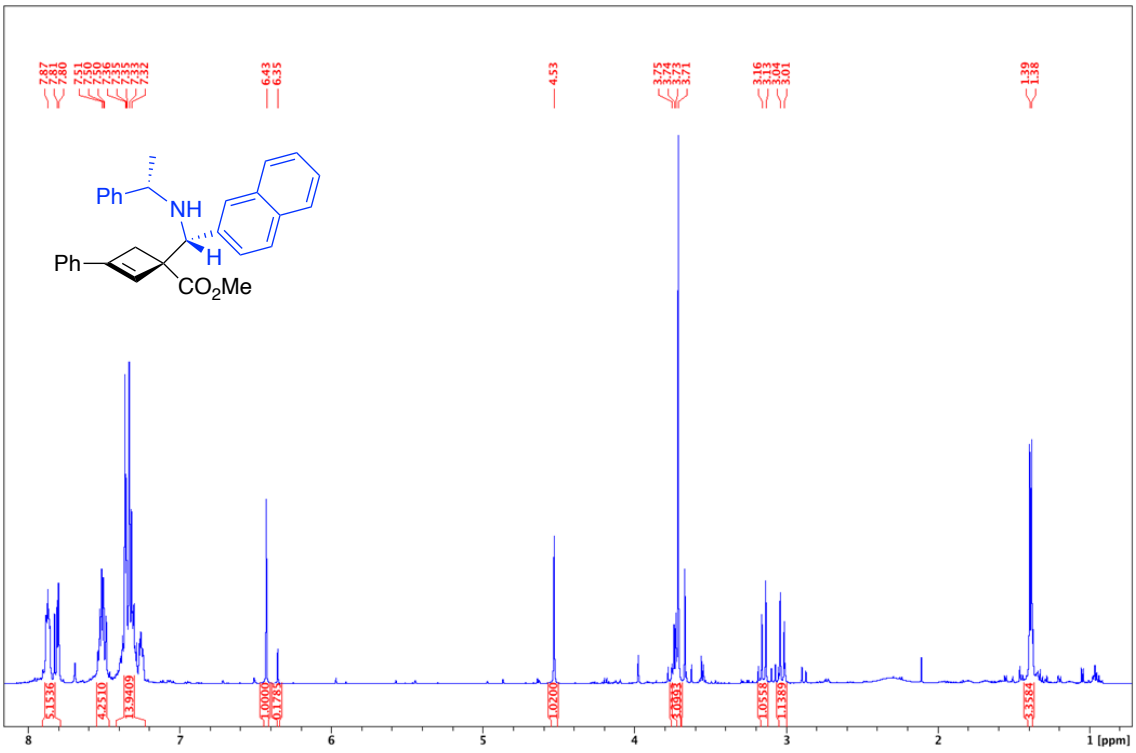

^{13}C NMR (126 MHz, $CDCl_3$, 292K, ppm): δ 174.68, 147.36, 146.36, 137.65, 133.59, 133.16, 133.00, 128.44, 127.92, 127.70, 127.54, 127.53, 126.86, 126.66, 125.95, 125.93, 125.71, 124.93, 64.80, 55.81, 54.81, 51.87, 36.80, 22.10.

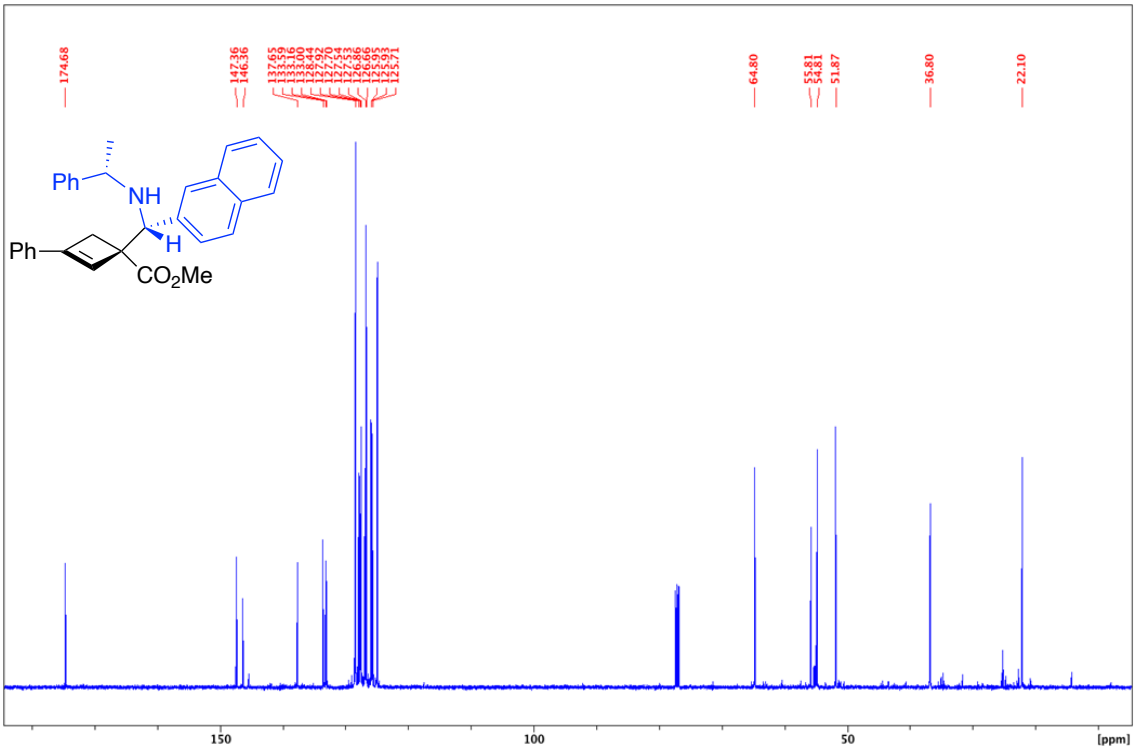

ATR IR spectrum:

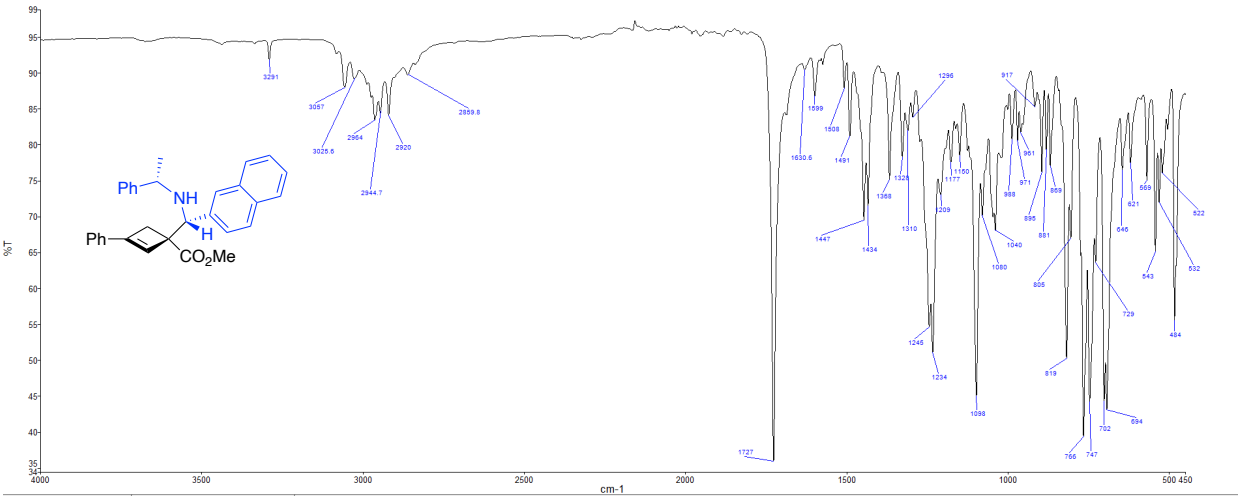

LCMS Chromatogram:

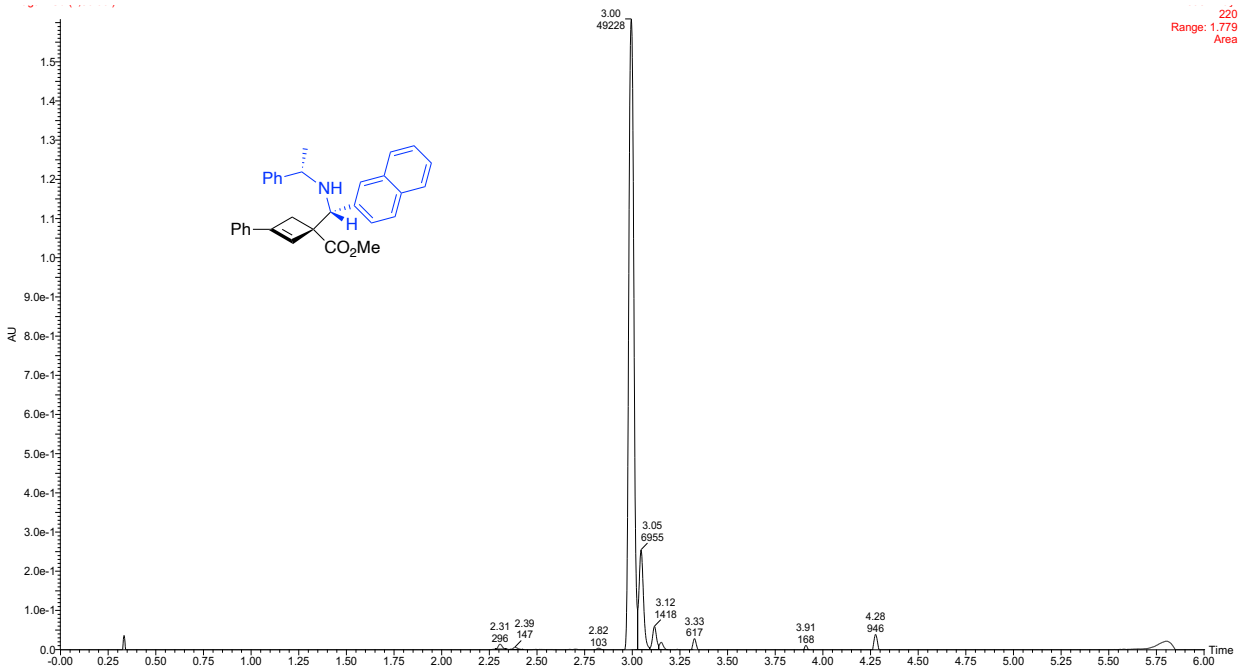

Minor diastereomer of methyl-1-(naphthalen-2-yl(((*S*)-1-phenylethyl)amino)-methyl)-3-phenylcyclobut-2-ene-1-carboxylate (4kk′)

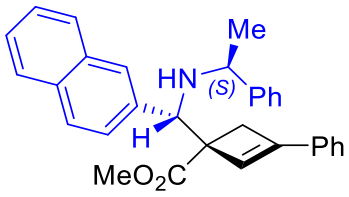

During chromatographic purification of **4kk**, we were able to isolate a small amount of the minor diastereomer to enable further spectroscopic characterization.

^{1}H NMR (300 MHz, $CDCl_3$, 292K, ppm): δ 7.71 (m, 3H), 7.41 (s, 1H), 7.37 (m, 4H), 7.25-7.15 (m, 7H), 7.10 (m, 2H), 6.19 (s, 1H), 3.81 (s, 1H), 3.53 (s, 3H), 3.39 (q, J=6.66 Hz, 1H), 2.93 (d, J=12.97 Hz, 1H), 2.73 (d, J=12.97 Hz, 1H), 1.22 (d, J=6.77 Hz, 3H).

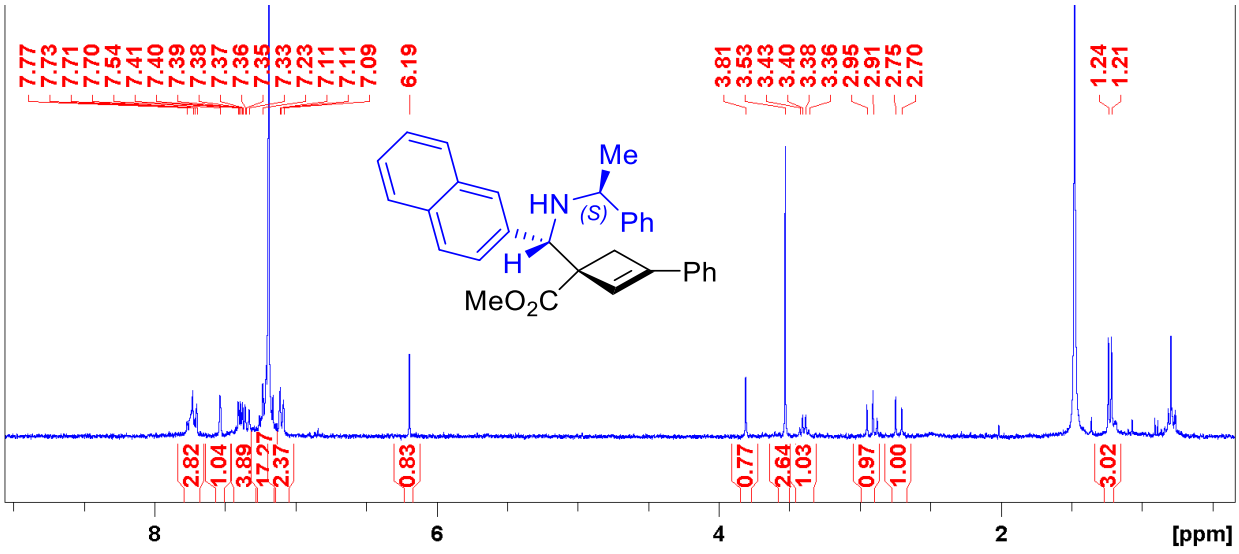

Methyl-1-((benzylamino)(phenyl)methyl)-3-(4-chlorophenyl)cyclobut-2-ene-1-carboxylate (4ll)

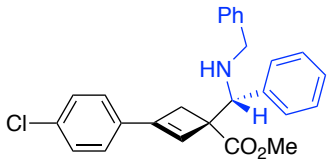

The product was prepared by **Method B** using methyl 3-(4-chlorophenyl)bicyclo[1.1.0]-butane-1-carboxylate (0.1113 g, 0.50 mmol), **1aa** (0.1074 g, 0.55 mmol) and $Ga(OTf)_3$ (0.0388 g, 15 mol%). The compound was purified by column chromatography (Biotage® Sfär 10g Column, 0-100% EtOAc/hexanes, eluted at 25% EtOAc). 86 mg of a yellow oil was obtained with a 22:1 d.r. (41%). 98% product and1% **3ll** area by LCMS.

IR: N-H 3291 cm^{-1}, C=O 1727 cm^{-1}

HRMS(ESI): calc'd for [$C_{26}H_{24}{}^{35}ClNO_2$+ H^+], 418.15684; found: 418.15683.

^{1}H NMR (500 MHz, $CDCl_3$, 292K, ppm): δ 7.29 – 7.07 (m, 14H), 6.21 (s, 1H), 4.02 (s, 1H), 3.65 (d, J = 13.4 Hz, 1H), 3.54 (s, 3H), 3.41 (d, J = 13.4 Hz, 1H), 2.90 (d, J = 13.1 Hz, 1H), 2.75 (d, J = 13.1 Hz, 1H).

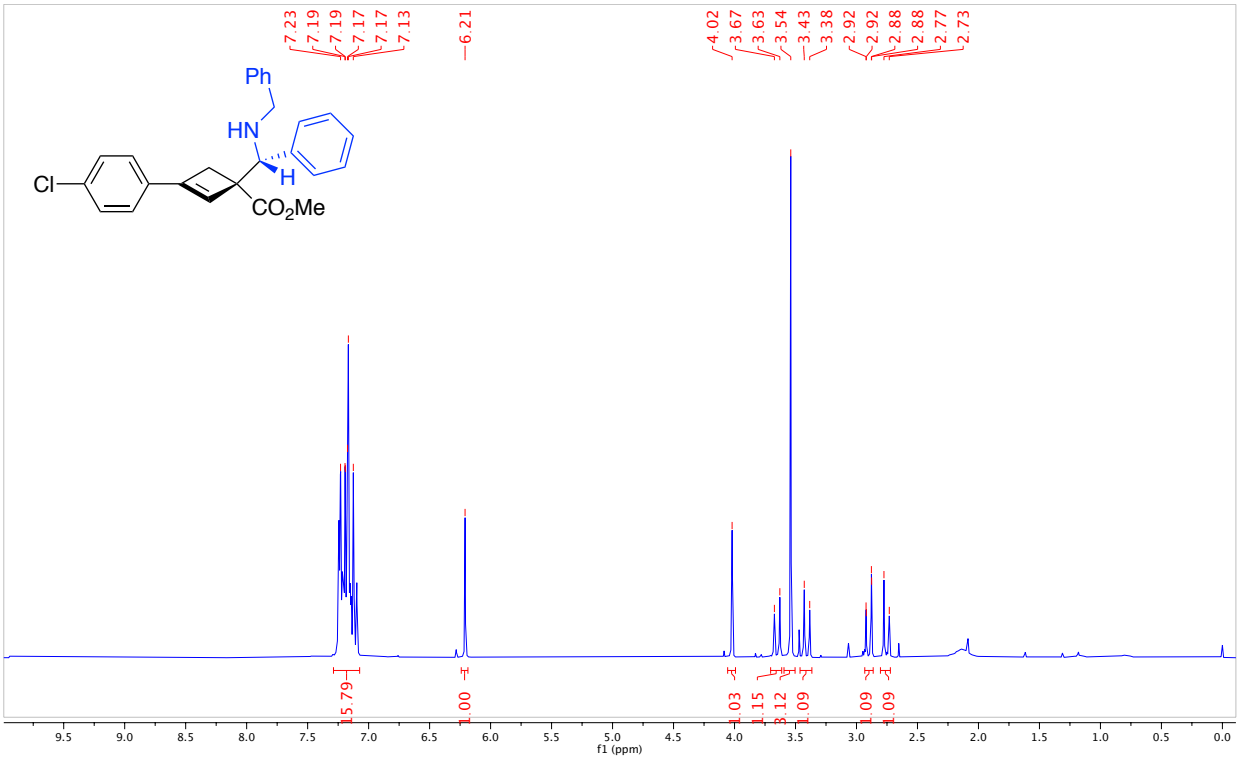

^{13}C NMR (126 MHz, $CDCl_3$, 292K, ppm): δ 174.14, 146.67, 140.39, 139.39, 134.19, 131.98, 128.58, 128.30, 128.28, 128.20, 128.01, 127.62, 127.09, 126.90, 126.22, 65.76, 55.82, 51.86, 51.33, 36.02.

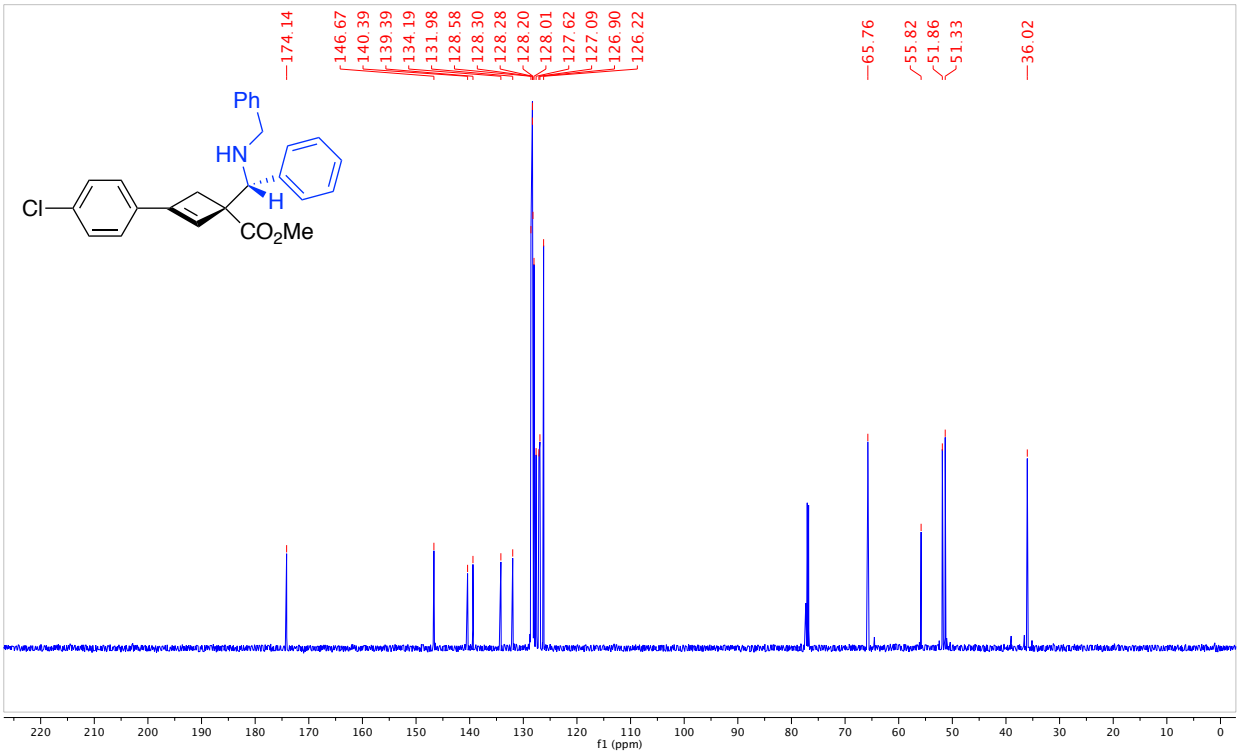

ATR IR spectrum:

LCMS Chromatogram:

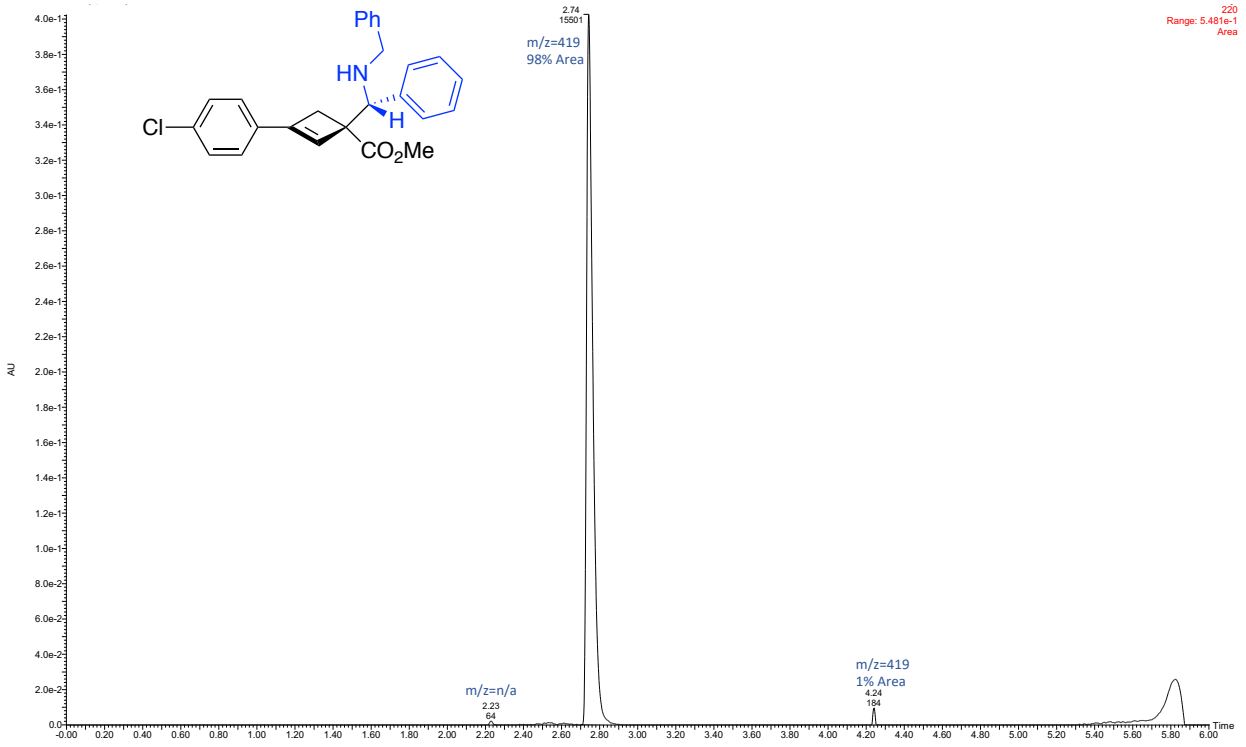

Methyl-1-((benzylamino)(phenyl)methyl)-3-(4-fluorophenyl)cyclobut-2-ene-1-carboxylate (4mm)

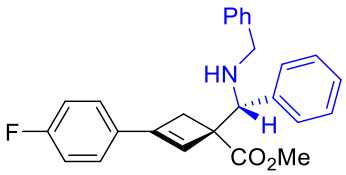

The product was prepared by **Method B** using methyl 3-(4-fluorophenyl)bicyclo[1.1.0]-butane-1-carboxylate (0.1031 g, 0.50 mmol), **1aa** (0.1074 g, 0.55 mmol) and $Ga(OTf)_3$ (0.0388 g, 15 mol%). The compound was purified by column chromatography (Biotage® Sfär 10g Column, 0-100% EtOAc/hexanes, eluted at 30% EtOAc). 70.4 mg of a yellow oil was obtained with a 31:1 d.r. (35%). 99% major diastereomer and 1% minor diastereomer area by LCMS.

IR: N-H 3349 cm^{-1}, C=O 1722 cm^{-1}

HRMS(ESI): calc'd for [$C_{25}H_{22}FNO_2$+ H^+], 402.18639; found: 402.18632.

^{1}H NMR (500 MHz, $CDCl_3$, 292K, ppm): δ 7.43 – 7.23 (m, 12H), 7.06 – 6.97 (m, 2H), 6.27 (s, 1H), 4.17 (s, 1H), 3.82 (d, J = 13.4 Hz, 1H), 3.67 (s, 3H), 3.56 (d, J = 13.4 Hz, 1H), 3.02 (d, J = 13.0 Hz, 1H), 2.90 (d, J = 13.0 Hz, 1H).

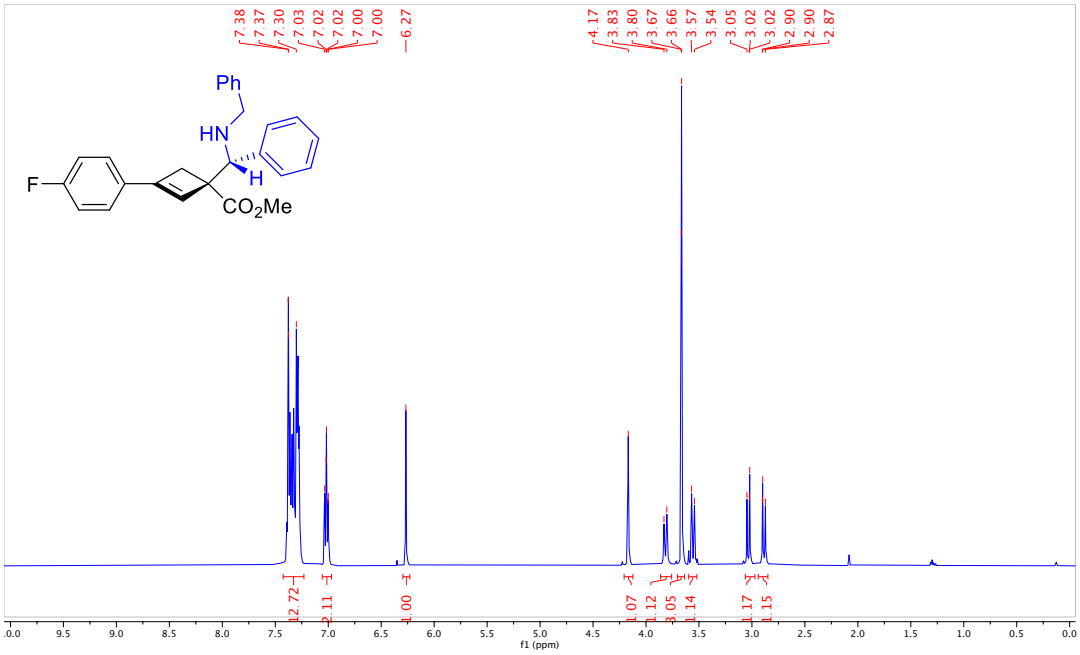

^{19}F NMR (500 MHz, $CDCl_3$, 292K, ppm): δ112.51

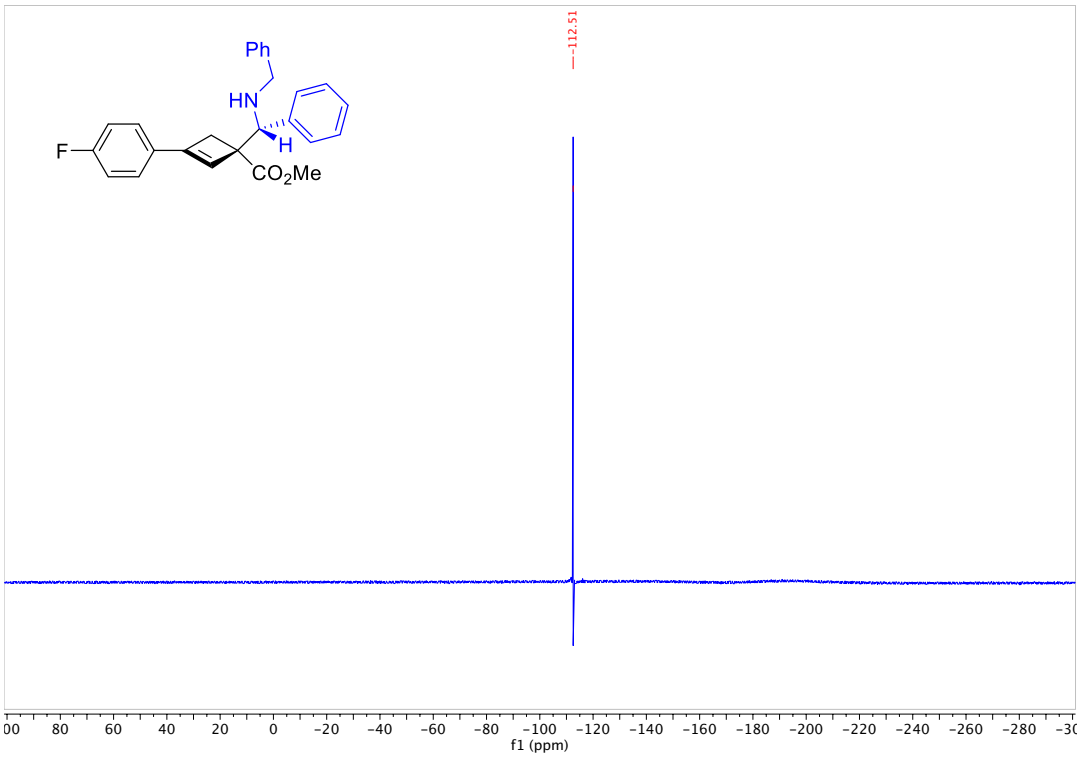

^{13}C NMR (126 MHz, $CDCl_3$, 292K, ppm): δ 174.28, 163.82, 161.84, 146.89, 129.83, 129.81, 128.38, 128.36, 128.33, 128.10, 127.76, 127.10, 126.80, 126.74, 125.68, 115.48, 115.31, 65.65, 51.93, 51.16, 36.15.

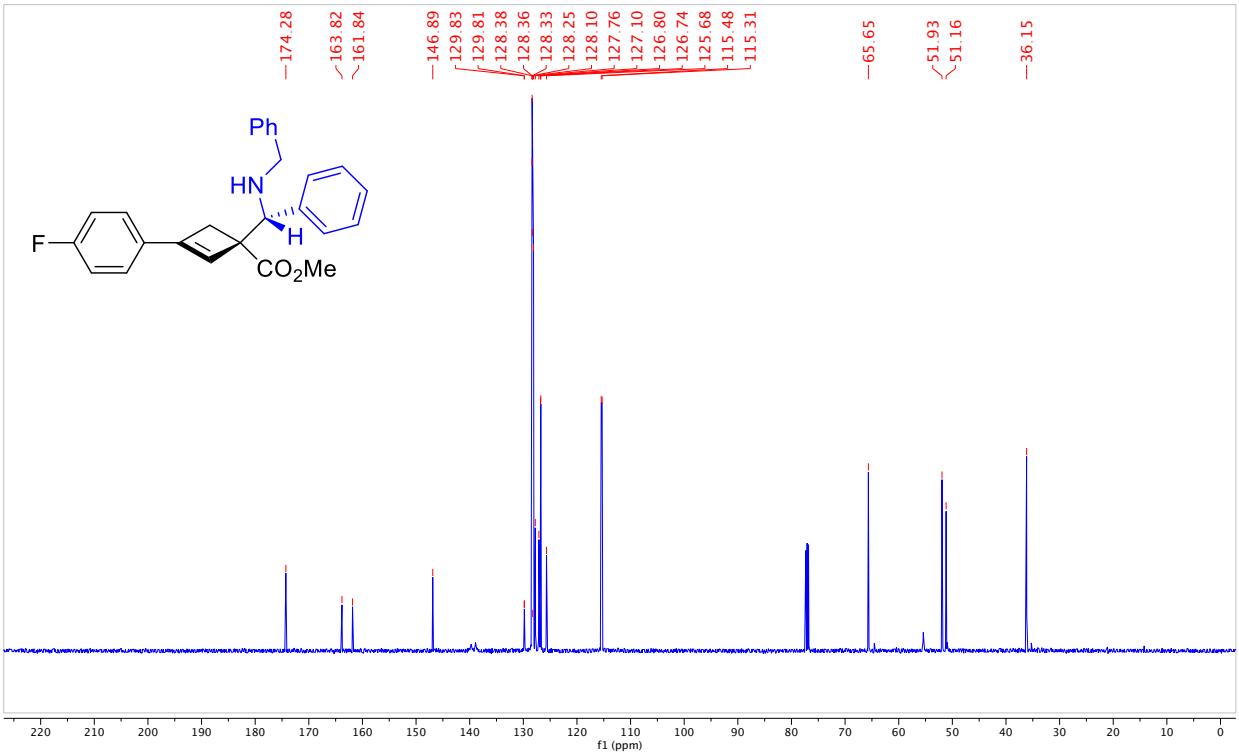

ATR IR spectrum:

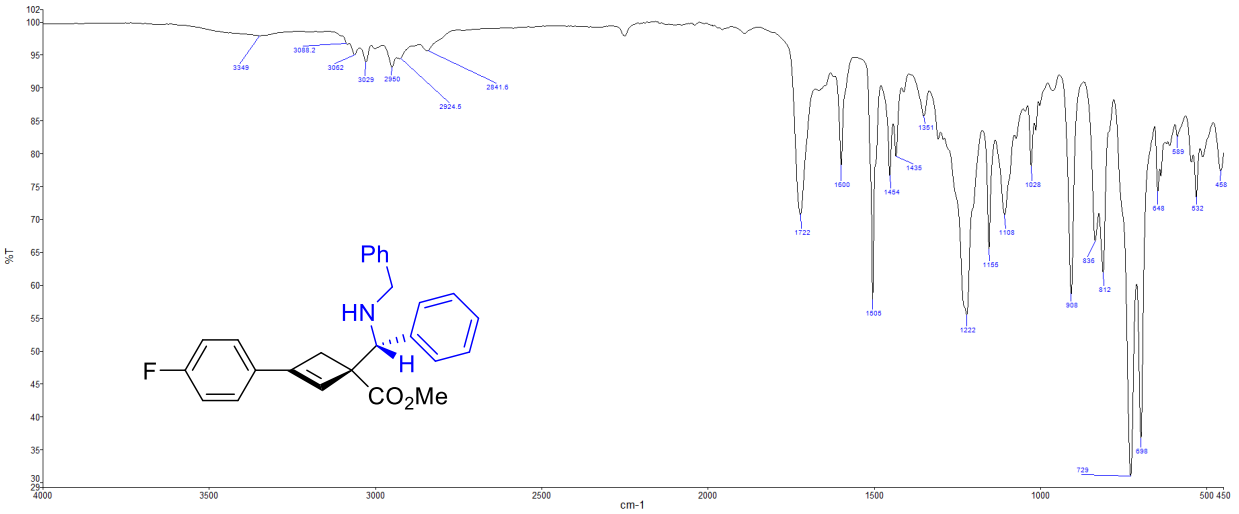

LCMS Chromatogram:

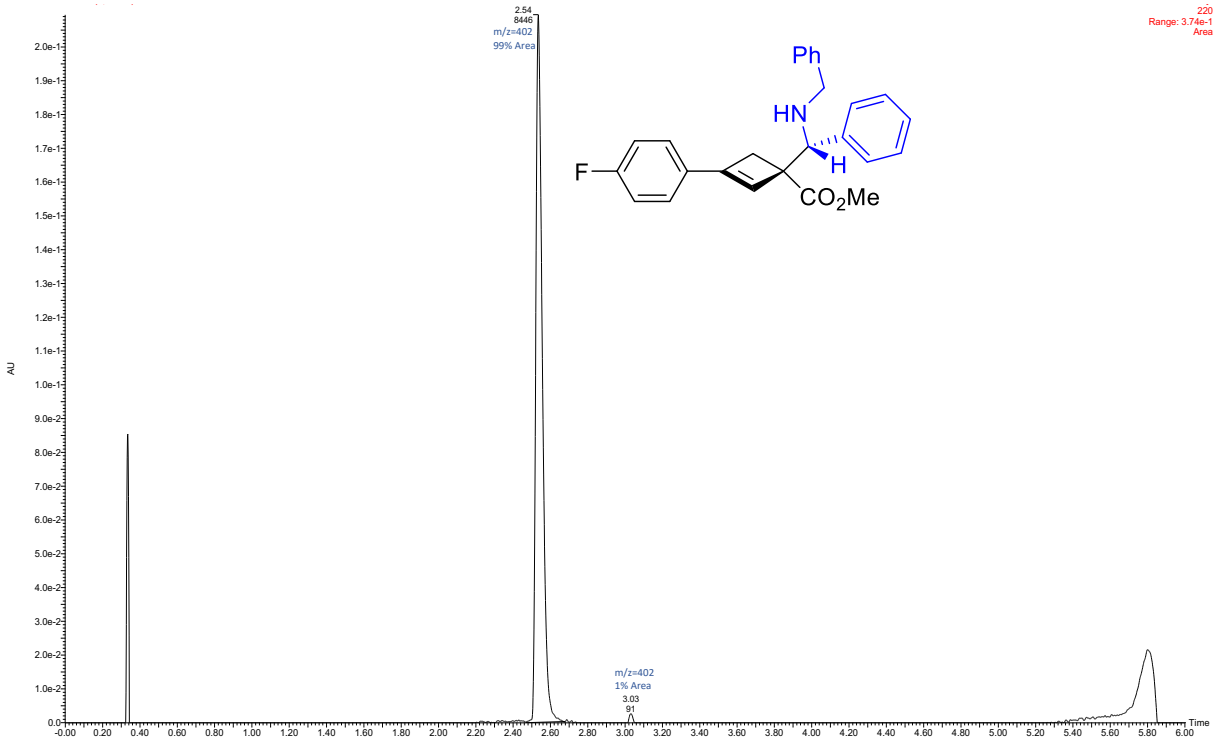

Benzyl-1-((benzylamino)(phenyl)methyl)-3-phenylcyclobut-2-ene-1-carboxylate (4nn)

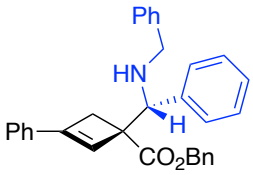

The product was prepared by **Method B** using benzyl 3-phenylbicyclo[1.1.0]butane-1-carboxylate (0.1322 g, 0.50 mmol), **1aa** (0.1464 g, 0.75 mmol) and $Ga(OTf)_3$ (0.0388 g, 15 mol%). The compound was purified by column chromatography (Biotage® Sfär KP-Amino 11g Column, 0-100% EtOAc/hexanes, eluted at 35% EtOAc). 81.2 mg of a yellow oil was obtained with a 22:1 d.r. (55%). 89% major diastereomer and 10% minor diastereomer area by LCMS.

IR: N-H 3333 cm^{-1}, C=O 1719 cm^{-1}

HRMS(ESI): calc'd for $[C_{32}H_{29}NO_2 + H^+]$, 460.22711; found: 460.22712.

^{1}H NMR (500 MHz, $CDCl_3$, 292K, ppm): δ 7.26 – 7.03 (m, 20H), 6.22 (s, 1H), 5.01 (d, J = 12.4 Hz, 1H), 4.95 (d, J = 12.4 Hz, 1H), 4.05 (s, 1H), 3.62 (d, J = 13.4 Hz, 1H), 3.40 (d, J = 13.4 Hz, 1H), 2.97 (d, J = 13.1 Hz, 1H), 2.83 (d, J = 13.1 Hz, 1H).

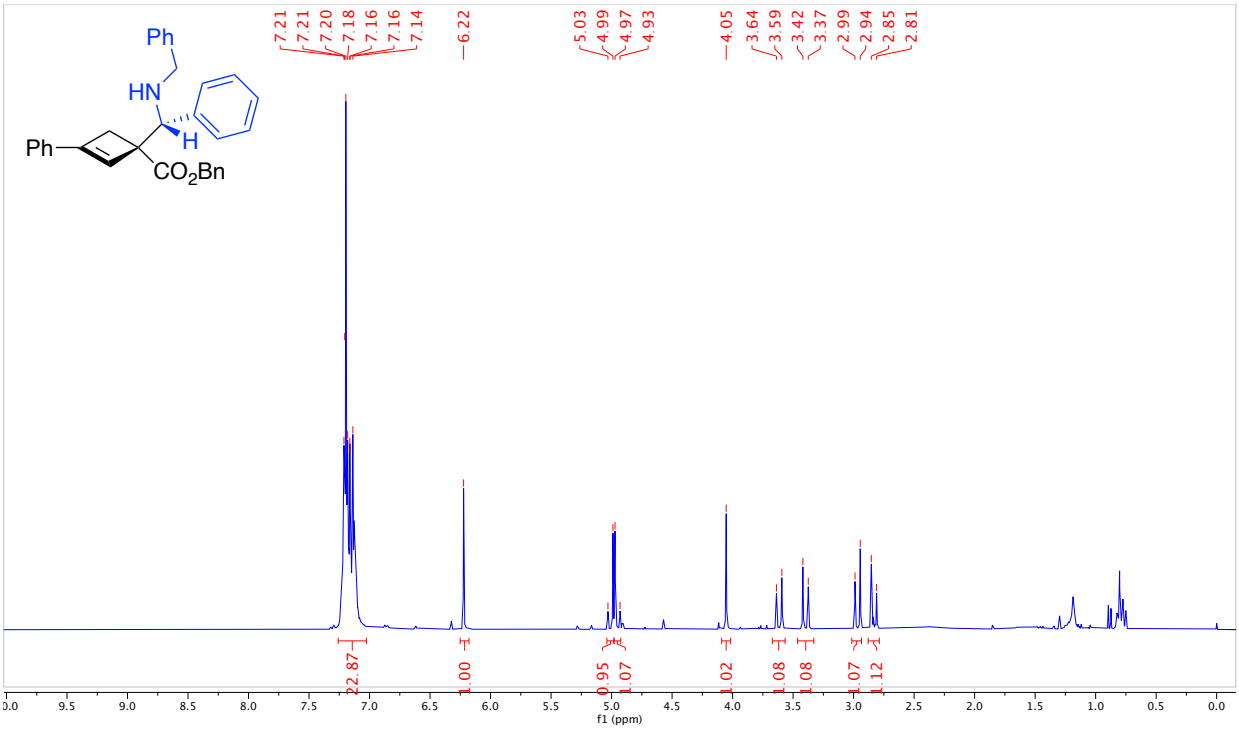

^{13}C NMR (126 MHz, $CDCl_3$, 292K, ppm): δ 173.02, 147.67, 140.68, 139.80, 136.34, 133.63, 128.43, 128.29, 128.23, 128.19, 128.15, 128.10, 127.84, 127.35, 126.77, 126.75, 124.86, 66.34, 66.10, 55.92, 51.38, 36.31.

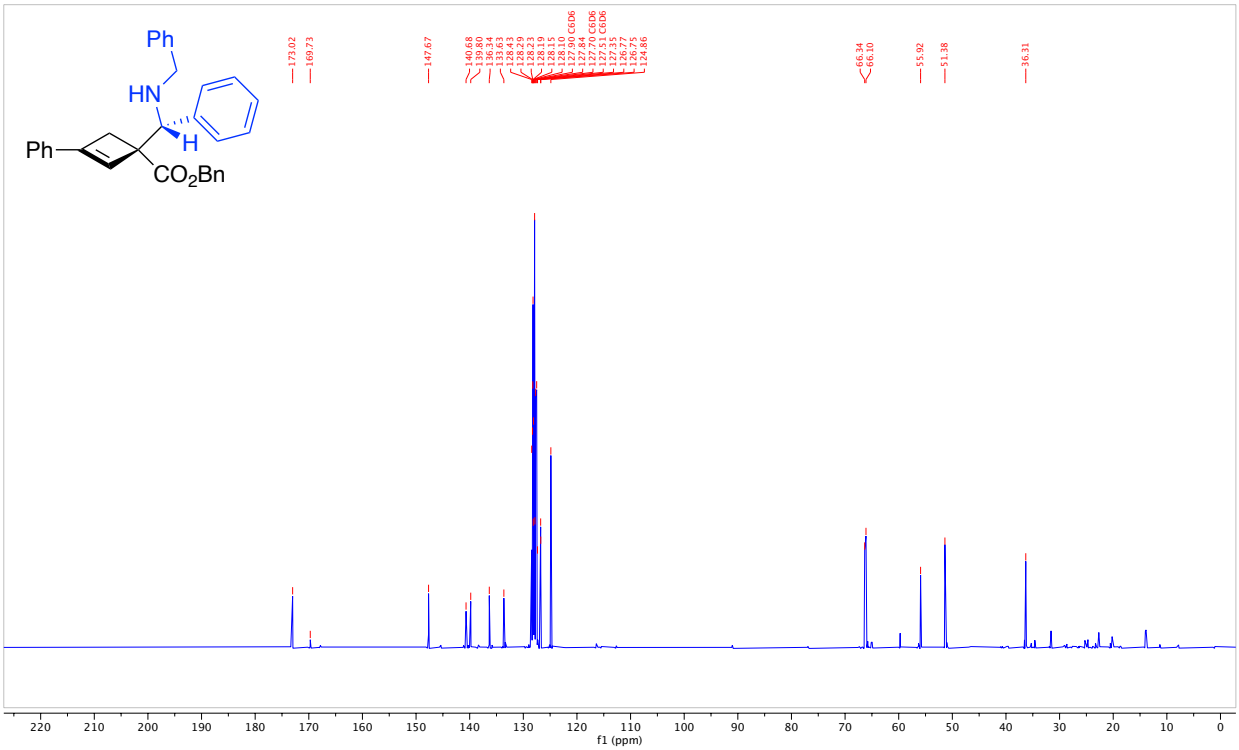

ATR IR spectrum:

LCMS Chromatogram:

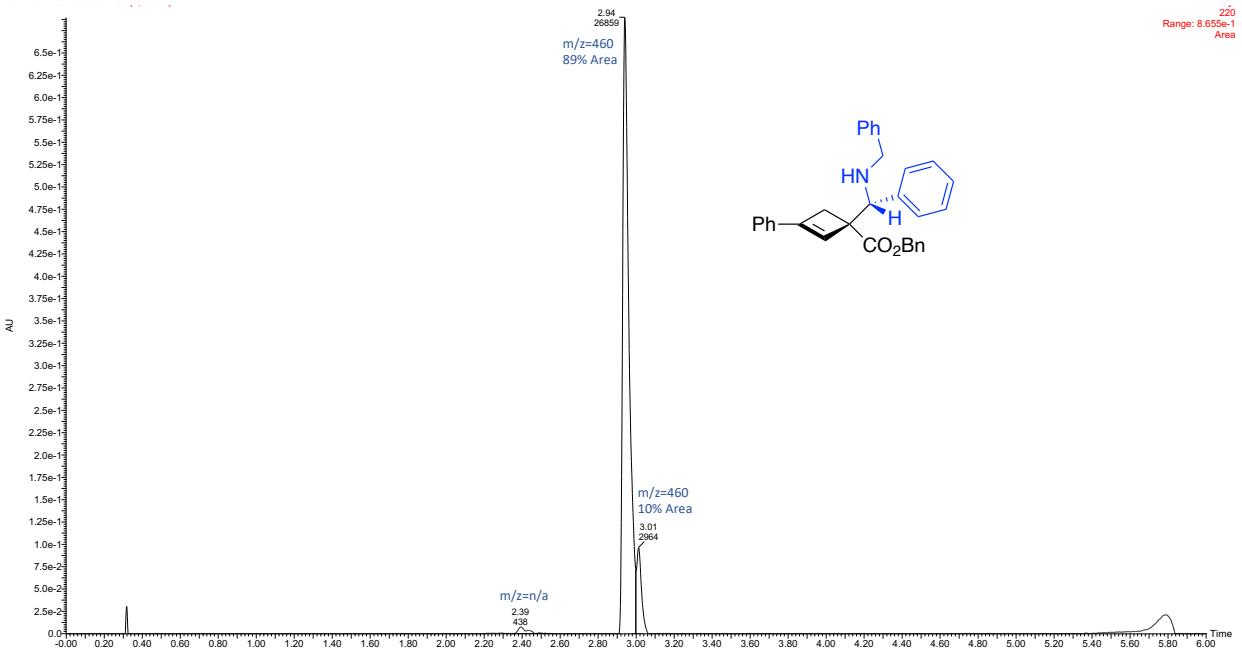

***Tert*-butyl-1-((benzylamino)(phenyl)methyl)-3-phenylcyclobut-2-ene-1-carboxylate (4oo)**

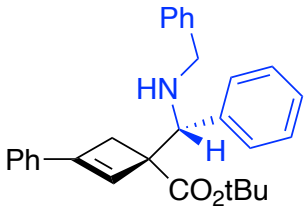

The product was prepared by **Method B** using *tert*-butyl 3-phenylbicyclo[1.1.0]butane-1-carboxylate (0.1152 g, 0.50 mmol), **1aa** (0.1464 g, 0.75 mmol) and $Ga(OTf)_3$ (0.0388 g, 15 mol%). The compound was purified by column chromatography (Biotage® Sfär KP-Amino 11g Column, 0-100% EtOAc/hexanes, eluted at 0% EtOAc). 83 mg of a yellow solid was obtained with a 22:1 d.r. (39%). 95% peak area by LCMS.

IR: N-H 3357 cm^{-1}, C=O 1702 cm^{-1}

Melting point range: 92.3 – 94.5 °C

HRMS(ESI): calc'd for [$C_{29}H_{31}NO_2$ + H^+], 426.24276; found: 426.24298

^{1}H NMR (500 MHz, $CDCl_3$, 292K, ppm): δ 7.47 – 7.23 (m, 15H), 6.33 (s, 1H), 4.16 (s, 1H), 3.77 (d, J = 13.4 Hz, 1H), 3.56 (d, J = 13.4 Hz, 1H), 3.04 (d, J = 12.9 Hz, 1H), 2.93 (d, J = 12.9 Hz, 1H), 1.41 (s, 9H).

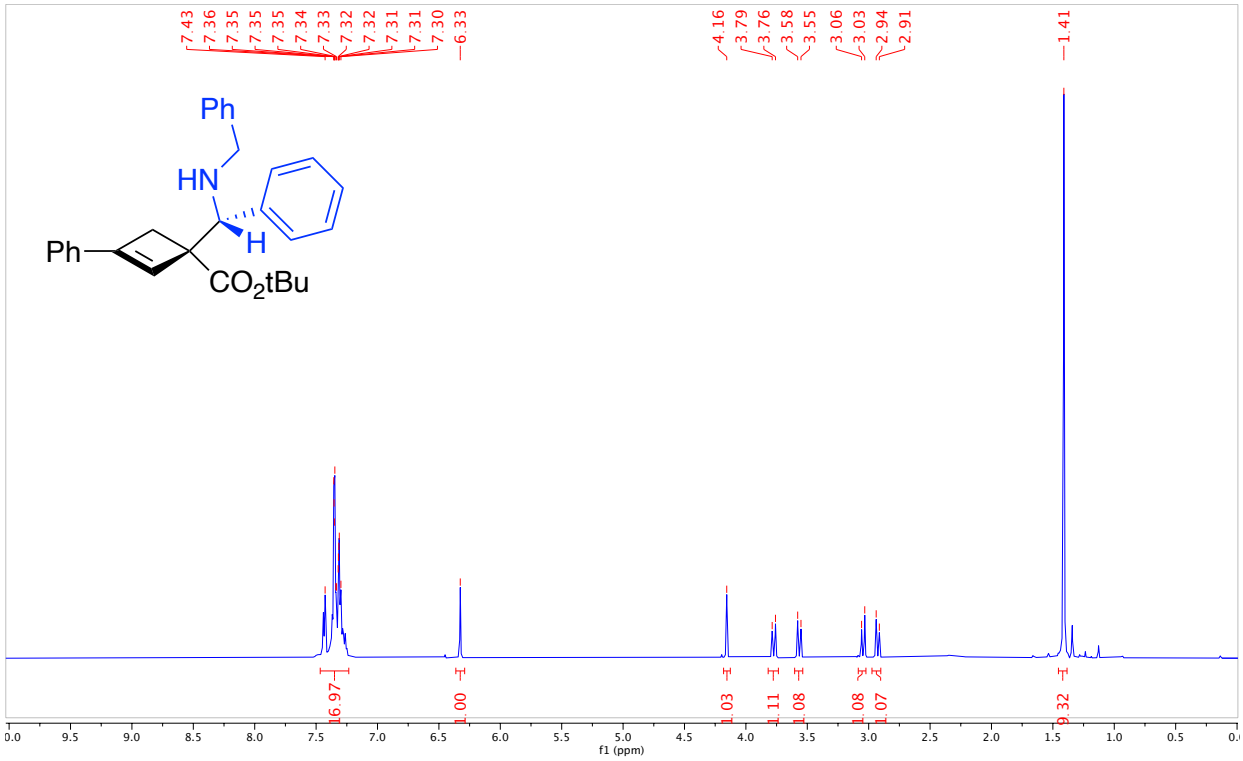

^{13}C NMR (126 MHz, $CDCl_3$, 292K, ppm): δ 173.03, 147.65, 140.58, 139.87, 133.80, 128.64, 128.32, 128.28, 128.26, 128.21, 127.85, 127.42, 127.13, 126.82, 124.90, 80.76, 65.86, 56.45, 51.48, 35.84, 27.98.

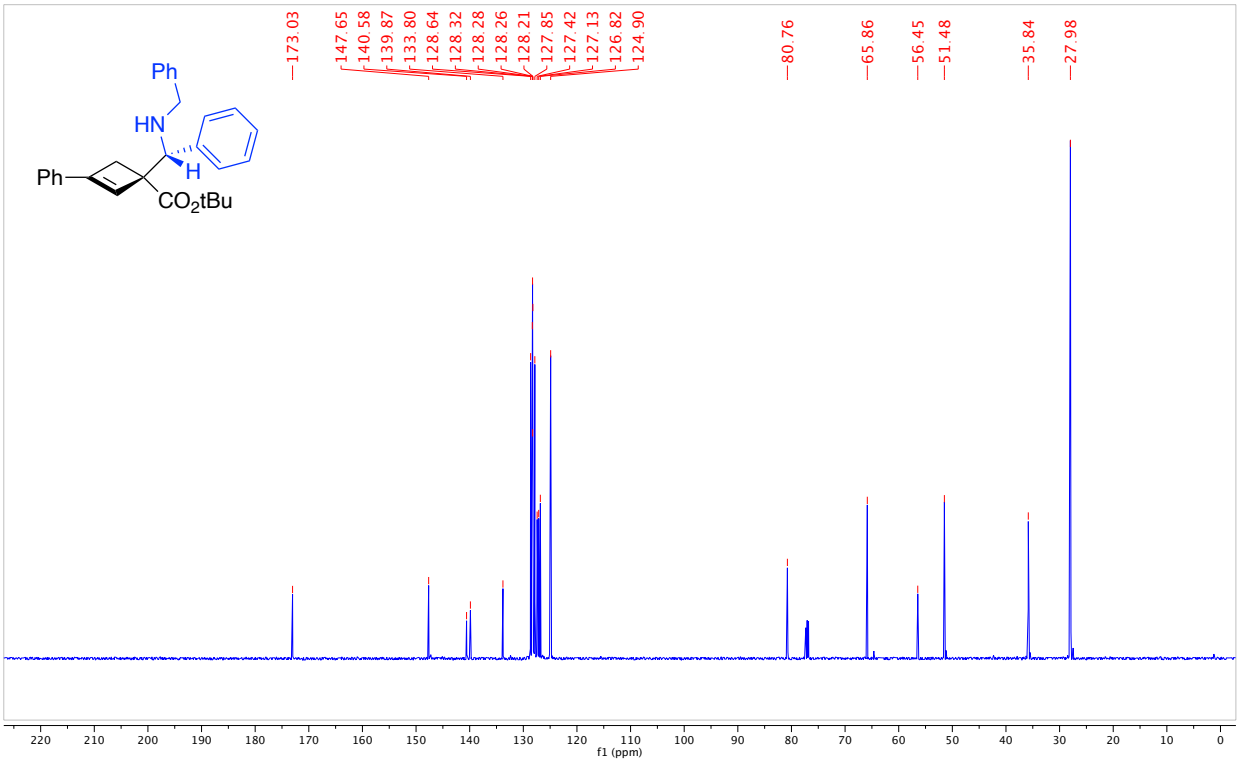

ATR IR spectrum:

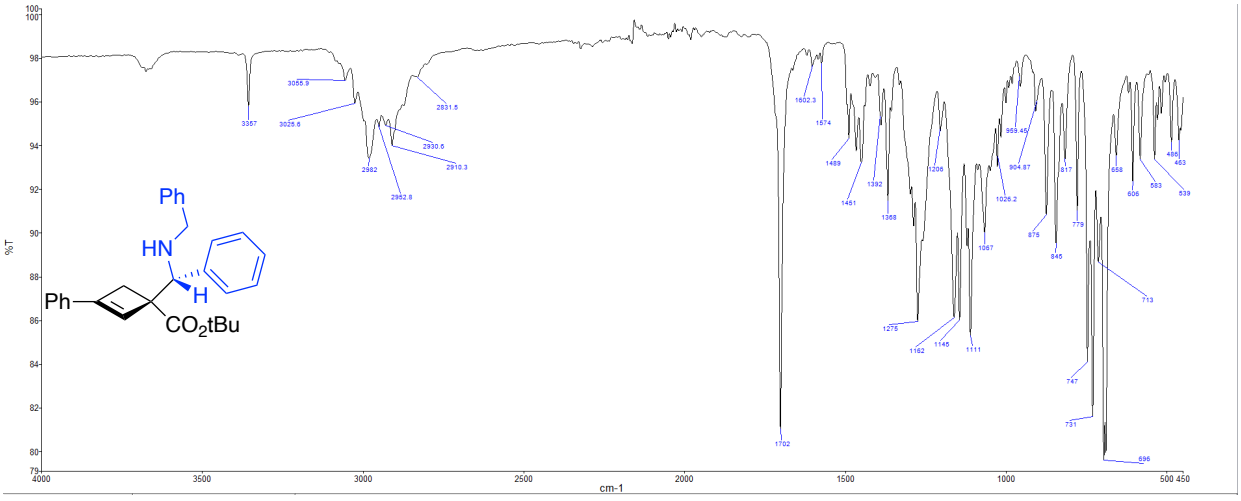

LCMS Chromatogram:

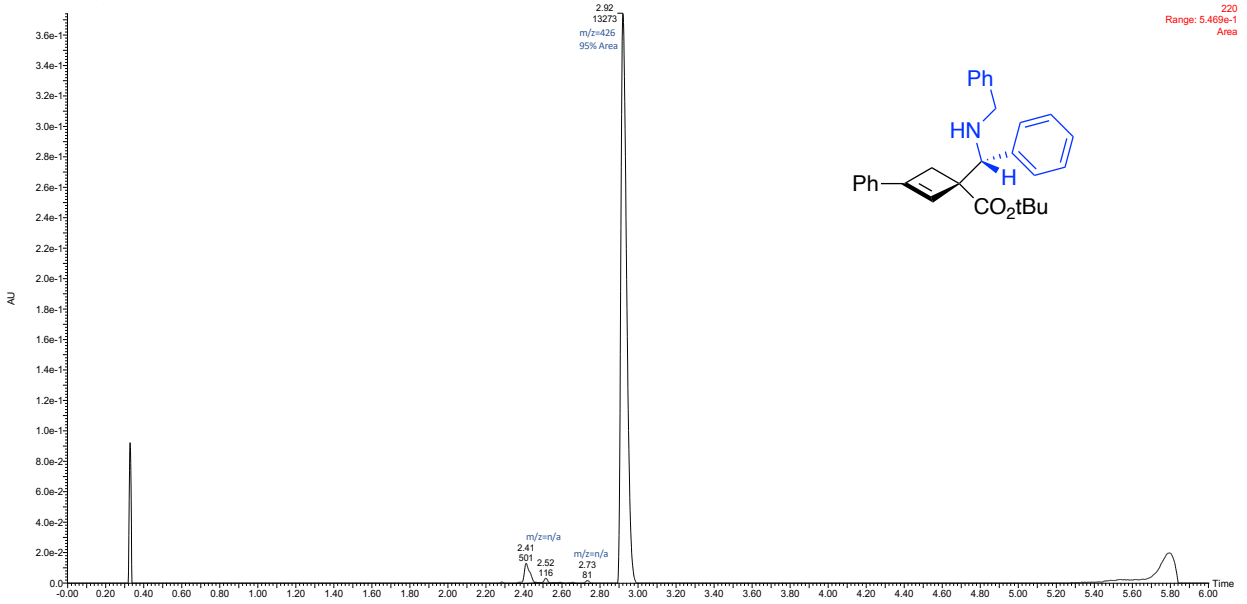

(1*R*,2*R*,5*S*)-2-isopropyl-5-methylcyclohexyl-1-((benzylamino)(phenyl)methyl)-3-phenylcyclobut-2-ene-1-carboxylate (4pp)

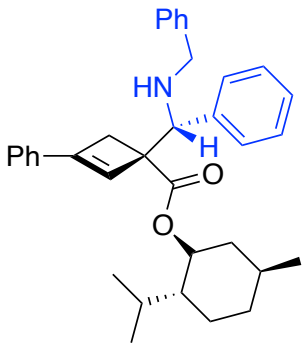

The product was prepared by **Method B** using (1*S*,2*R*,5*S*)-2-isopropyl-5-methylcyclohexyl 3-phenylbicyclo[1.1.0]butane-1-carboxylate (0.1562 g, 0.50 mmol), **1aa** (0.1464 g, 0.75 mmol) and $Ga(OTf)_3$ (0.0388 g, 15 mol%). The compound was purified by column chromatography (Biotage® Sfär KP-Amino 11g Column, 0-100% EtOAc/hexanes, eluted at 0% EtOAc). 148 mg of a yellow solid was obtained with a 28:22:1:1 d.r. (58%). 68% major diastereomer, 28:3:2% minor diastereomers and 3% **3pp** area by LCMS.

IR: N-H 3361 cm^{-1}, C=O 1701 cm^{-1}

Melting point range: 108.9 – 111.7 °C

HRMS(ESI): calc'd for $[C_{35}H_{41}NO_2 + H^+]$, 508.32101; found: 508.32128.

^{1}H NMR (500 MHz, $CDCl_3$, 292K, ppm): δ 7.53-7.25 (m, 15H), 6.48 (s, 0.38H), 6.46 (s, 0.58H), 4.78-4.65 (m, 1H), 4.25 (s, 0.59H), 4.22 (s, 0.39H), 3.81-3.71 (m, 1H), 3.63-3.56 (m, 1H), 3.13-2.90 (m, 2H), 2.46-2.27 (m, 1.25H), 2.05-1.94 (m, 1.23H), 1.84-1.64 (m, 3.88H), 1.57-1.44 (m, 1.52), 1.44-1.31 (m, 1.48H), 1.17-.02 (m, 1.56), 1.00-0.79 (m, 10.59H), 0.79-0.69 (m, 3.40H).

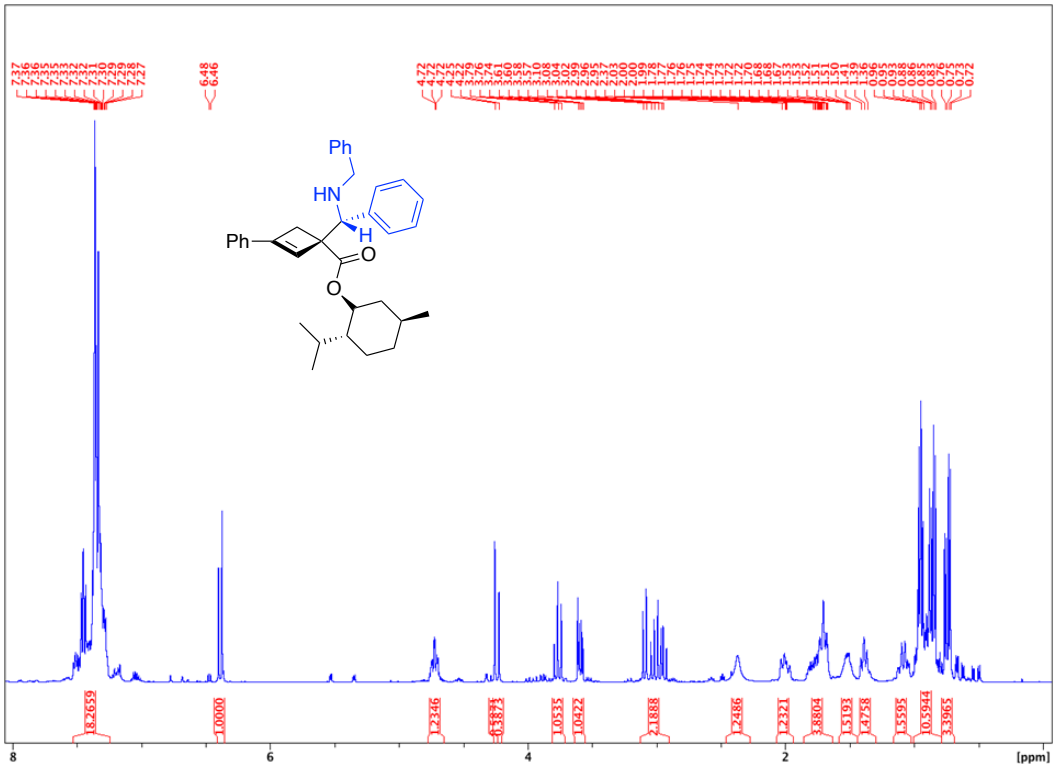

^{13}C NMR (126 MHz, $CDCl_3$, 292K, ppm): δ 173.76, 173.45, 147.84, 147.35, 140.56, 140.53, 139.72, 139.59, 133.77, 139.32, 128.67, 128.63, 128.61, 128.50, 128.43, 128.37, 128.33, 128.30, 128.25, 128.20, 128.12, 127.93, 127.93, 127.62, 127.55, 127, 50, 127.45, 127.42, 127.41, 127.31, 127.15, 127.12, 127.03, 126.86, 126.81, 126.76, 126.74, 126.72, 126.62, 124.94, 124.92, 124.90, 124.78, 74.74, 74.62, 66.08, 66.05, 56.11, 55.70, 51.67, 51.56, 46.96, 46.86, 40.84, 40.62, 36.30, 36.02, 34.32, 34.30, 31.42, 31.39, 26.18, 23.54, 23.45, 22.10, 20.81, 20.76, 16.40, 16.33.

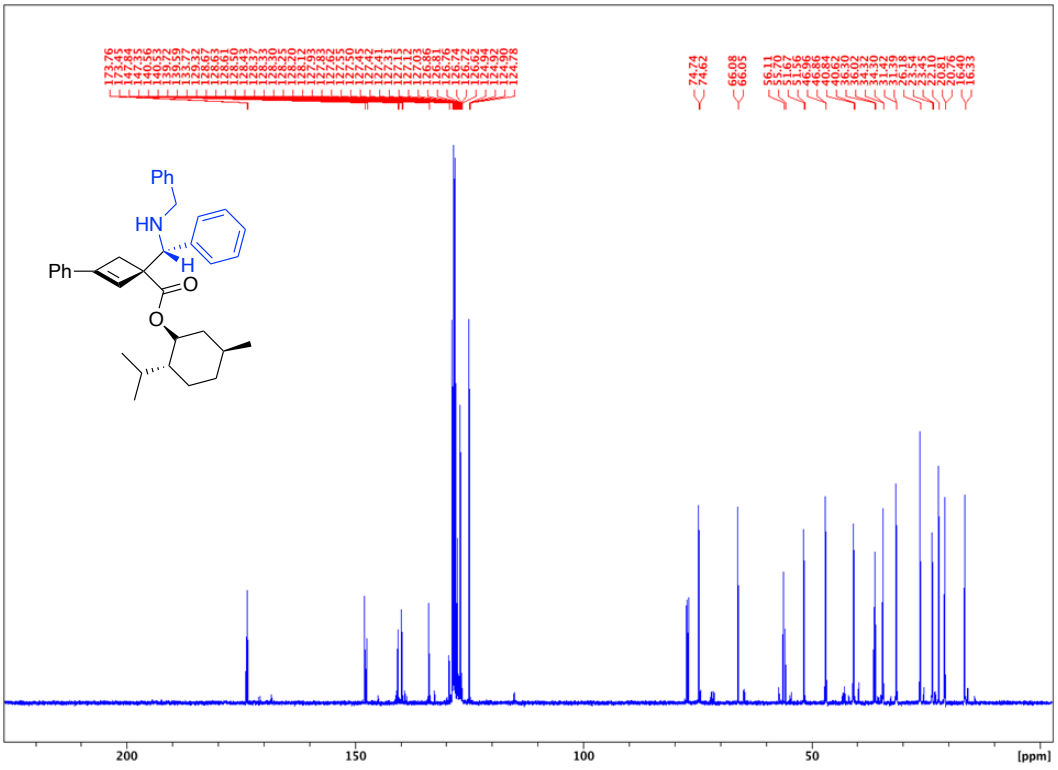

ATR IR spectrum:

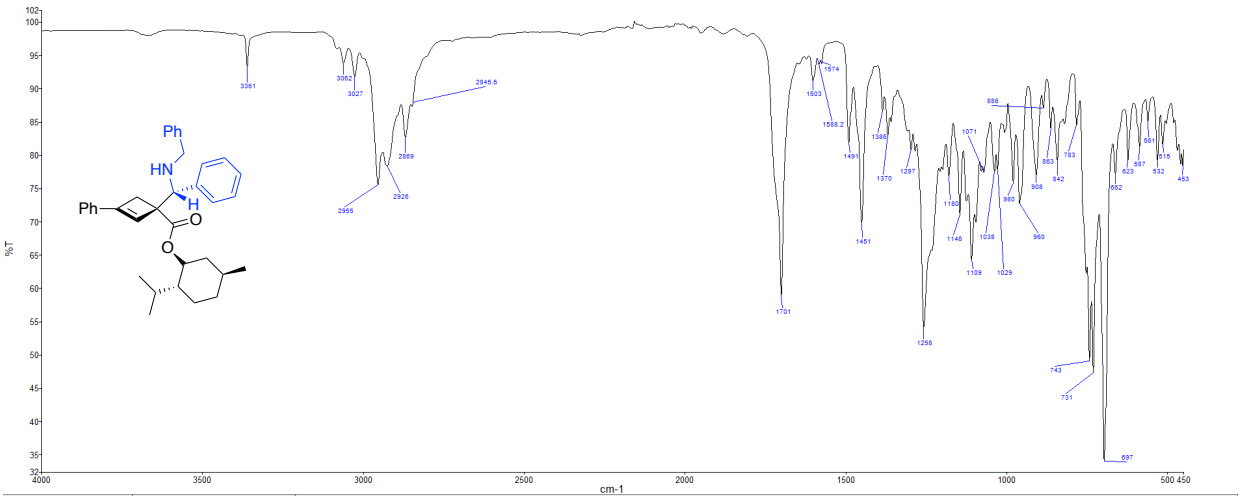

LCMS Chromatogram:

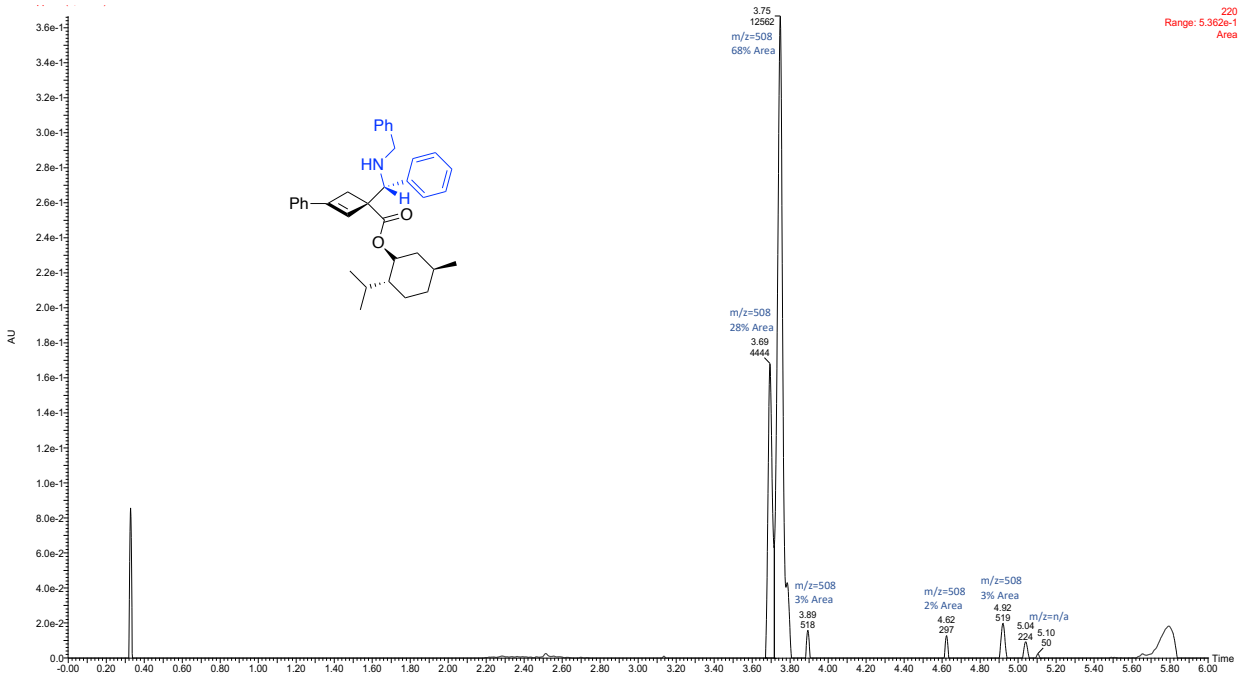

^{1}H-^{1}H COSY (4pp):

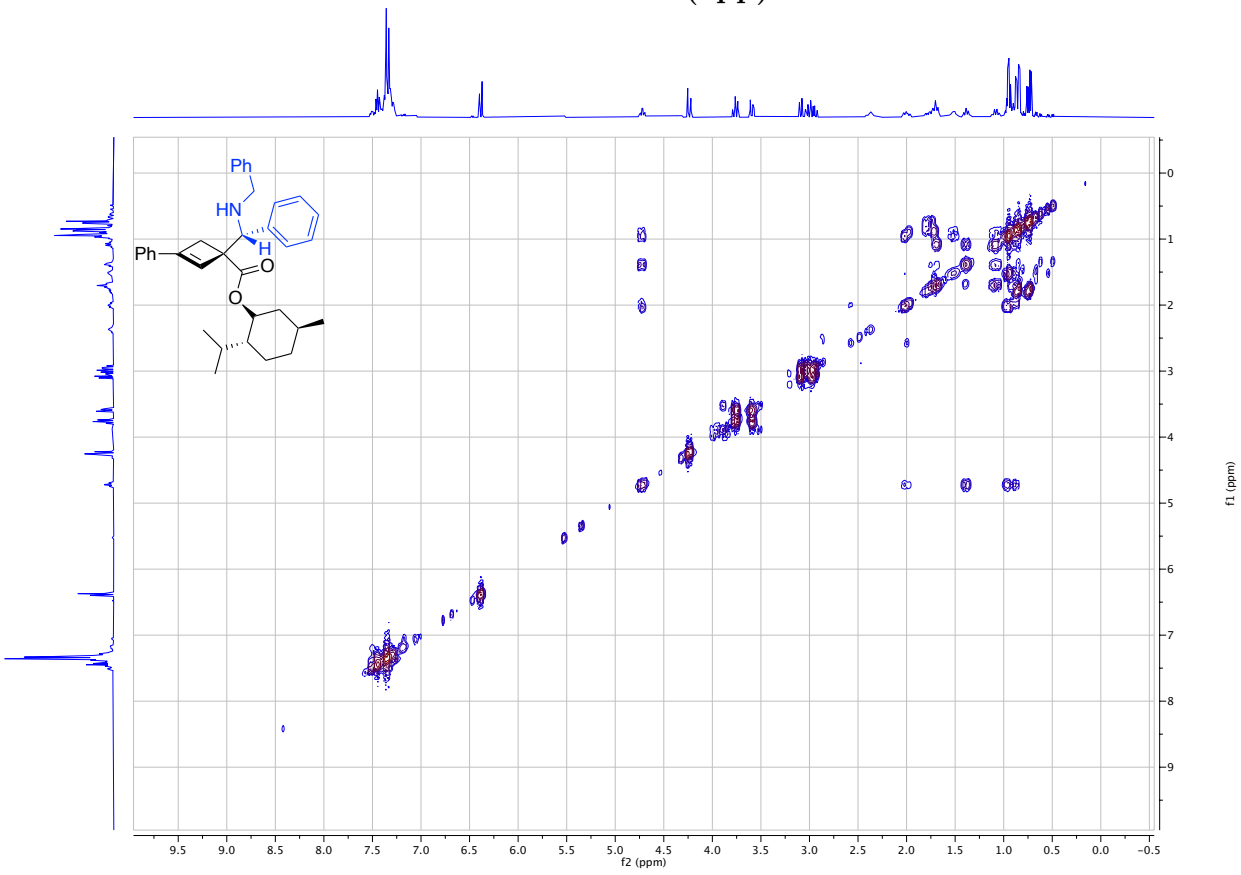

^{1}H-^{13}C HSQC (4pp):

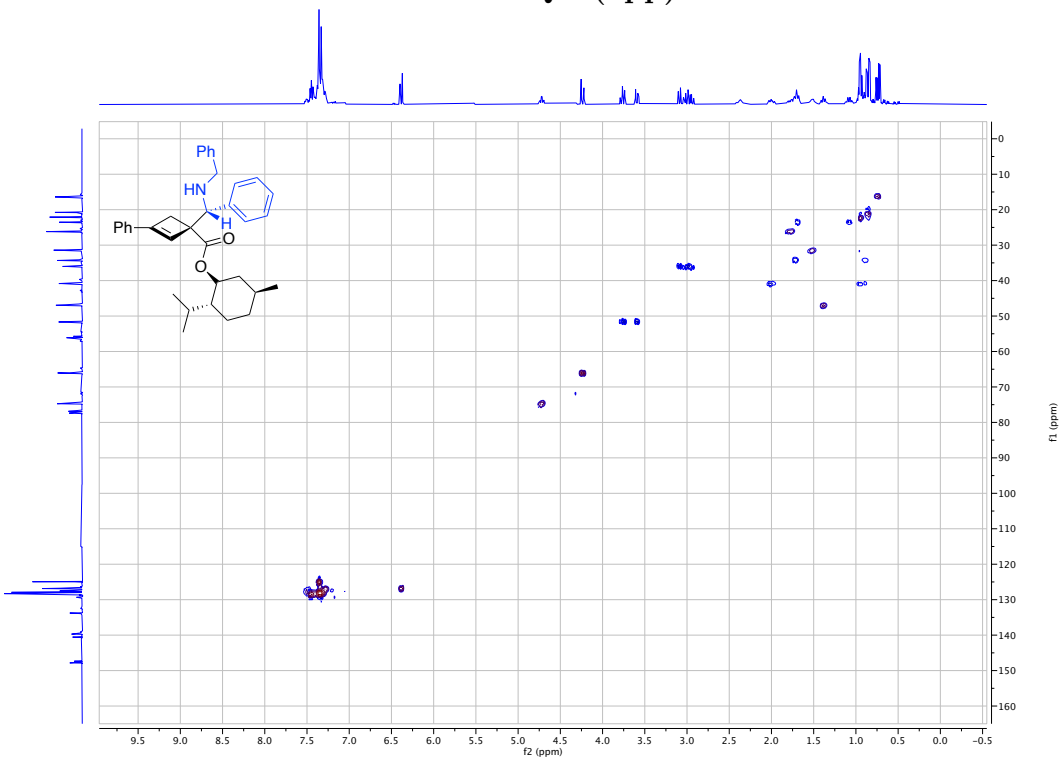

^{1}H-^{13}C HMBC (4pp):

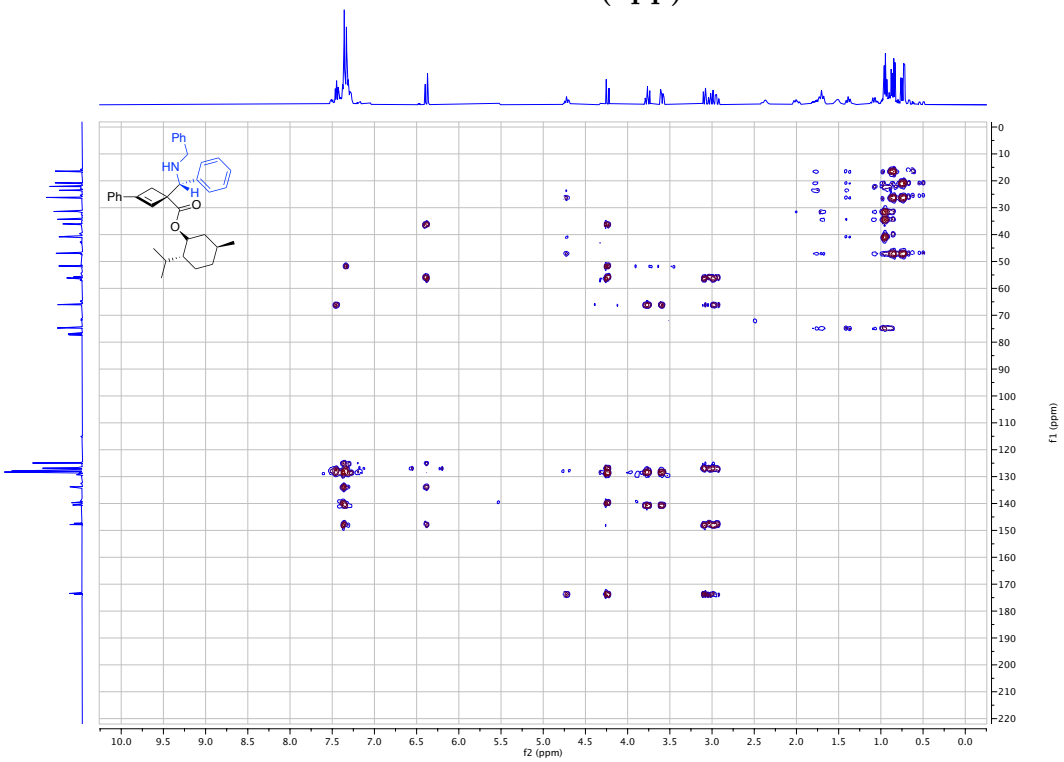

One of the diastereomers of **4pp** was isolated by column chromatography, providing a sample for characterization by NMR spectroscopy.

^{1}H spectrum (4pp, single diastereomer):

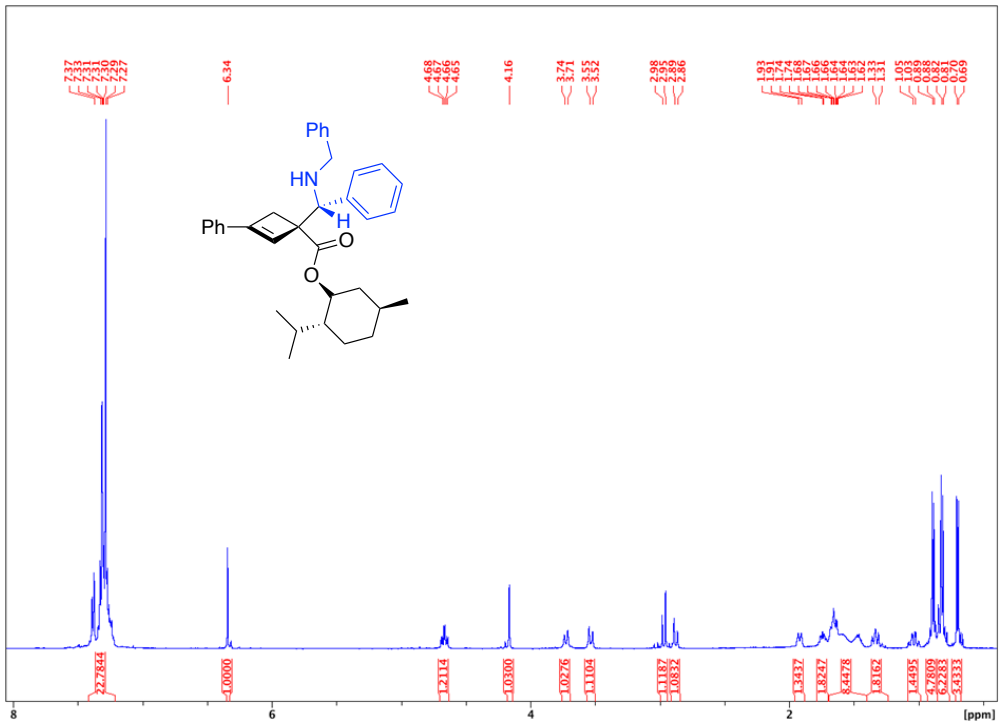

^{13}C spectrum (4pp, single diastereomer):

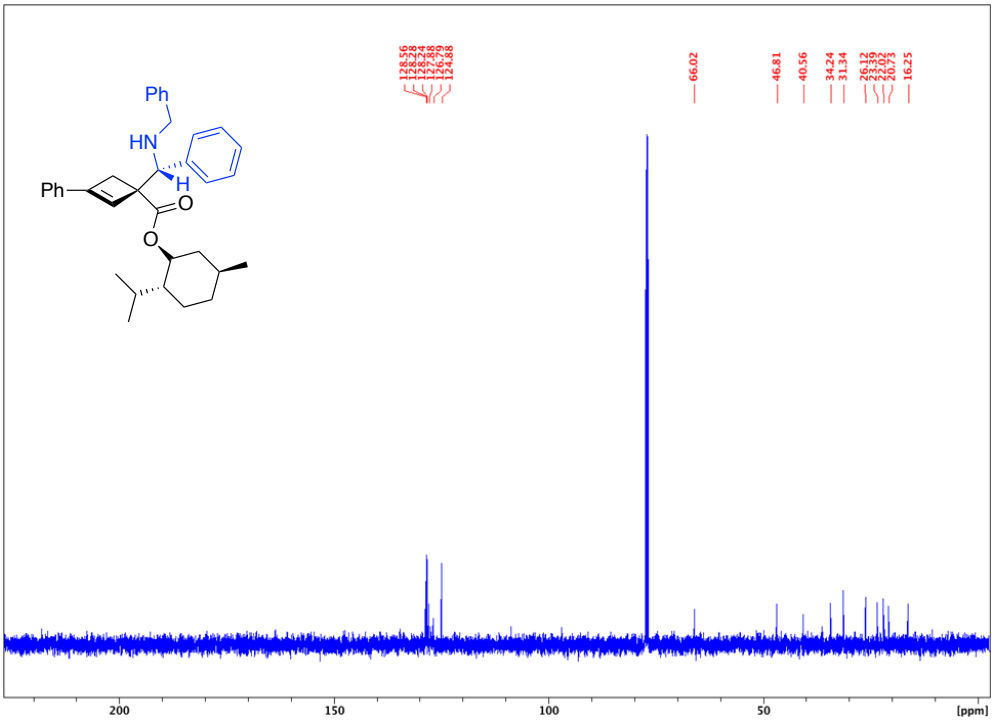

^{1}H-^{1}H COSY (4pp, single diastereomer):

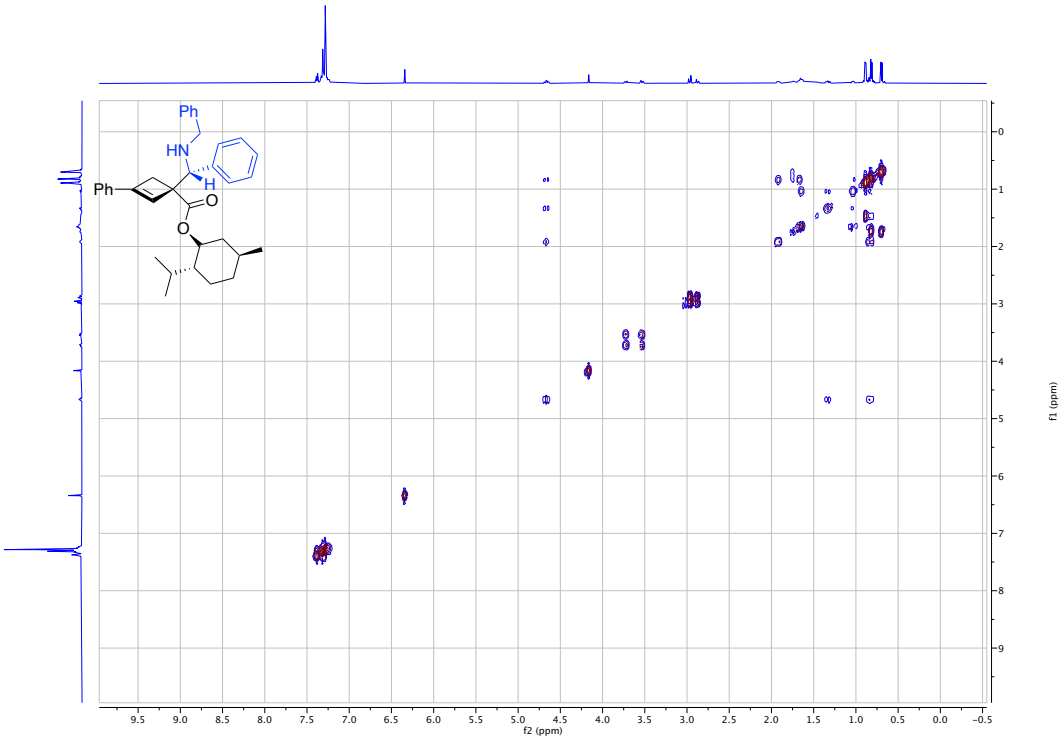

^{1}H-^{13}C HSQC (4pp, single diastereomer):

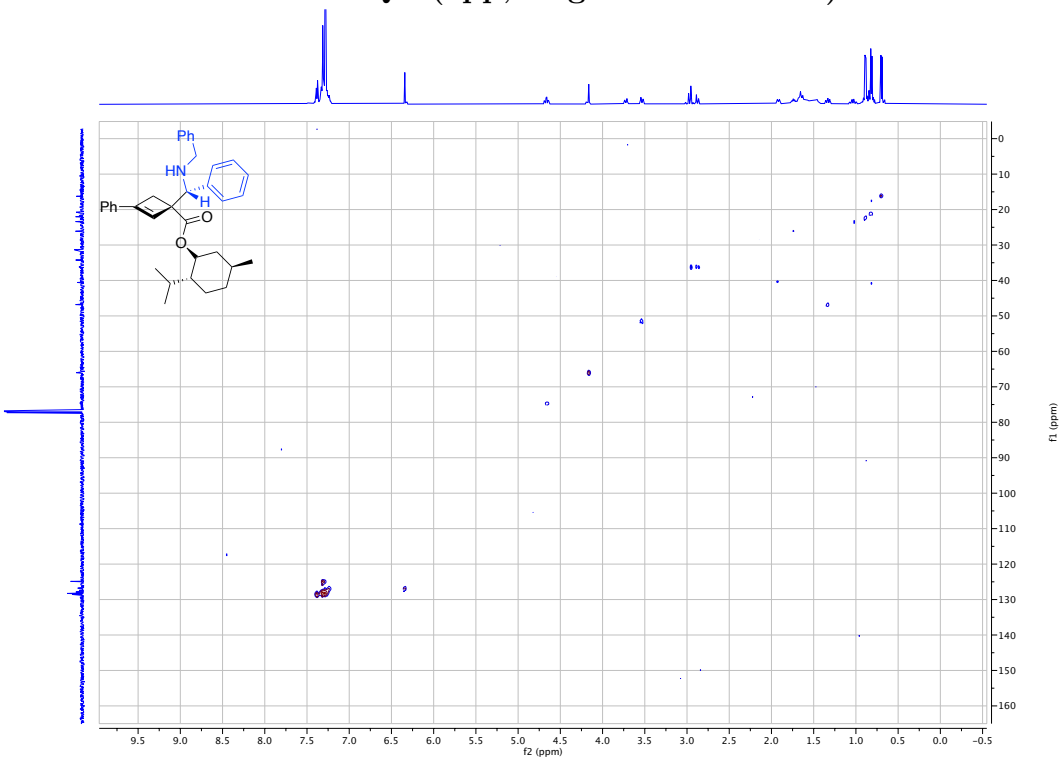

^{1}H-^{13}C HMBC (4pp, single diastereomer):

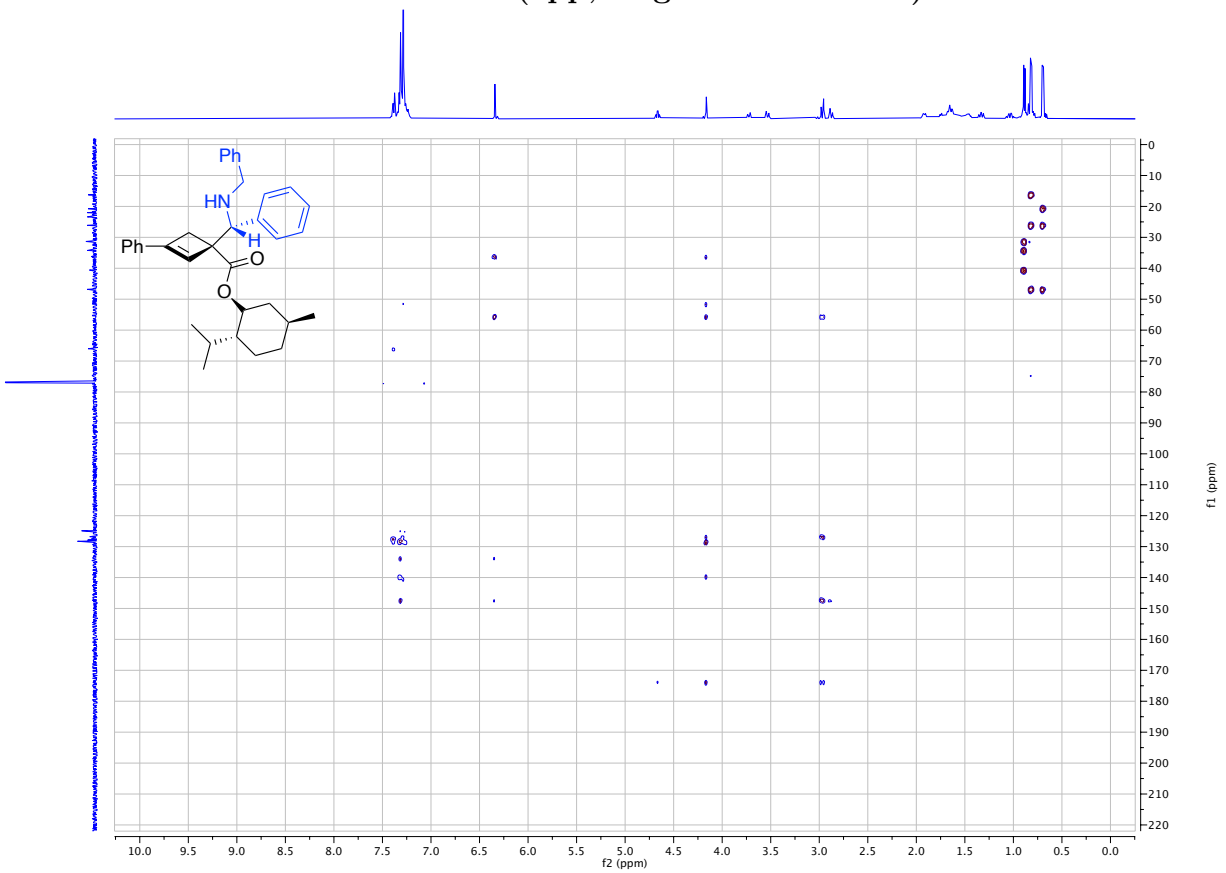

A.8 Iodoamination and Stereochemical Analysis

Initial iodoamination reactions were performed by adapting a literature procedure.[177]

Methyl (1*R*,3s,4S,5*S*)-5-iodo-1,3-diphenyl-2-((*S*)-1-phenylethyl)-2-azabicyclo-[2.1.1]hexane-4-carboxylate (6ii)

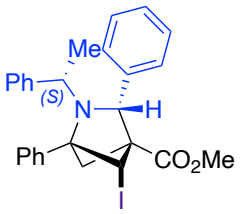

4ii (0.1089 g, 0.275 mmol) was added to a 4 mL vial and dissolved in 1 mL of acetonitrile. I_2 (0.1151 g, 1.37 mmol, 3 equiv) and $NaHCO_3$ (0.2086 g, 0.82 mmol, 5 equiv) were added to the reaction mixture at -20 °C and the solution was stirred for 2 hours. The mixture was then warmed to room temperature and stirred for 22 hours. The solution was quenched with saturated $Na_2S_2O_3$ and the aqueous layer was extracted with ethyl acetate. The organic layers were combined and dried with Mg_2SO_4, the solvent was removed under vacuum and the product was purified by column chromatography (SiO_2, 0-100% EtOAc/hexanes, eluted at 1% EtOAc). 39.6 mg of a yellow oil was obtained (28%). 86% major diastereomer and 5% minor diastereomer area by LCMS.

IR: C=O 1732 cm^{-1}

HRMS(ESI): calc'd for [$C_{27}H_{26}INO_2$ + H^+], 524.10810; found: 524.10816.

^{1}H NMR (500 MHz, $CDCl_3$, 292K, ppm): δ 7.72-7.15 (m, 13H), 7.13-7.02 (m, 2H), 4.61 (s, 1H), 4.16 (d, J=8.54 Hz, 1H), 3.99 (q, J=7.00 Hz, 1H), 3.62 (s, 3H), 2.73 (d, J=8.11 Hz, 1H), 2.64 (t, 8.29 Hz, 1H), 1.01 (d, J=7.00 Hz, 3H).

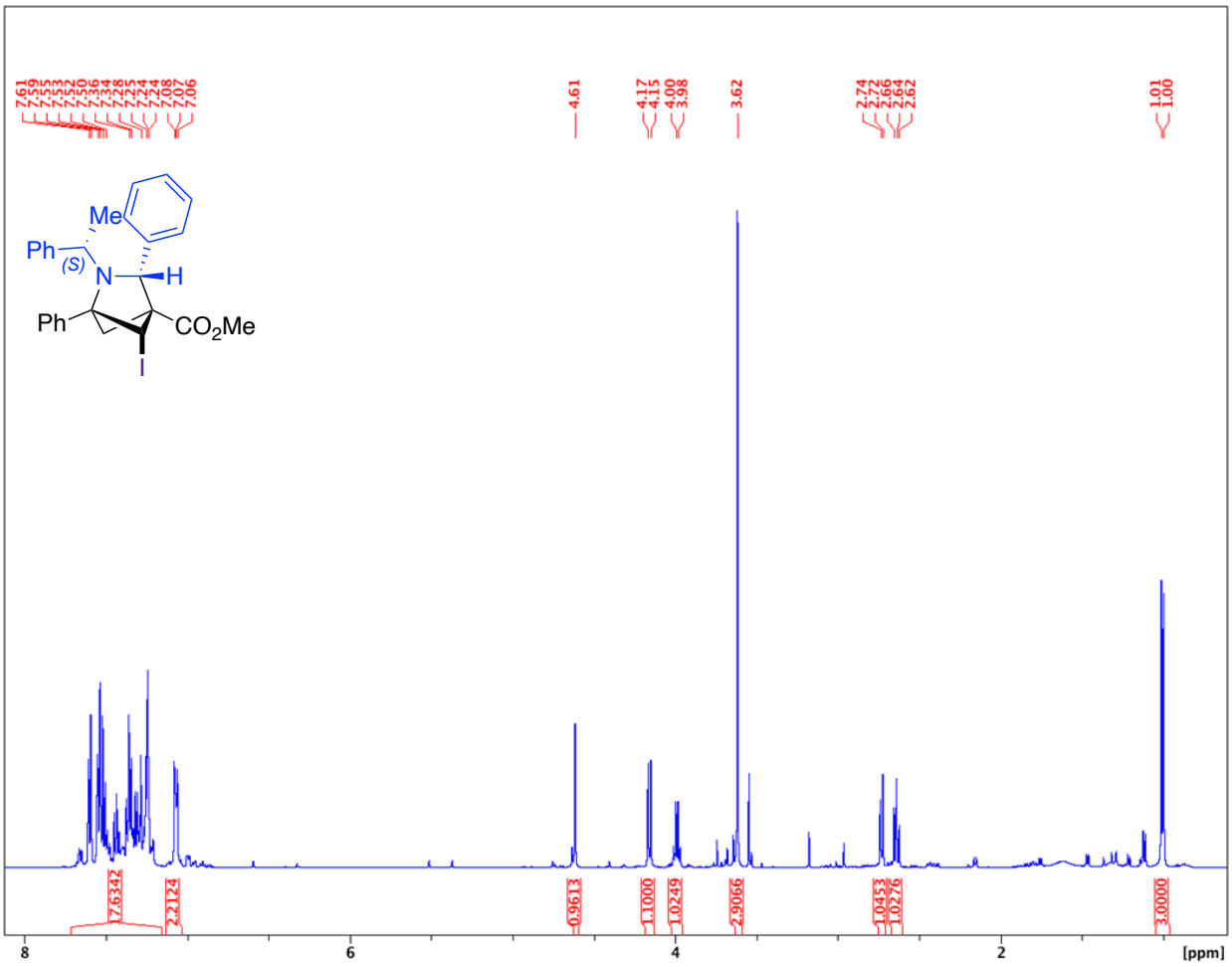

^{13}C NMR (126 MHz, $CDCl_3$, 292K, ppm): δ 169.45, 141.97, 141.22, 136.34, 128.95, 128.69, 128.66, 128.54, 128.49, 128.39, 128.37, 128.32, 128.29, 128.26, 128.23, 128.13, 127.99, 127.91, 127.88, 127.66, 127.60, 127.51, 127.49, 127.27, 127.05, 126.86, 126.77, 73.50, 63.70, 59.45, 57.44, 51.67, 41.22, 36.29, 22.57.

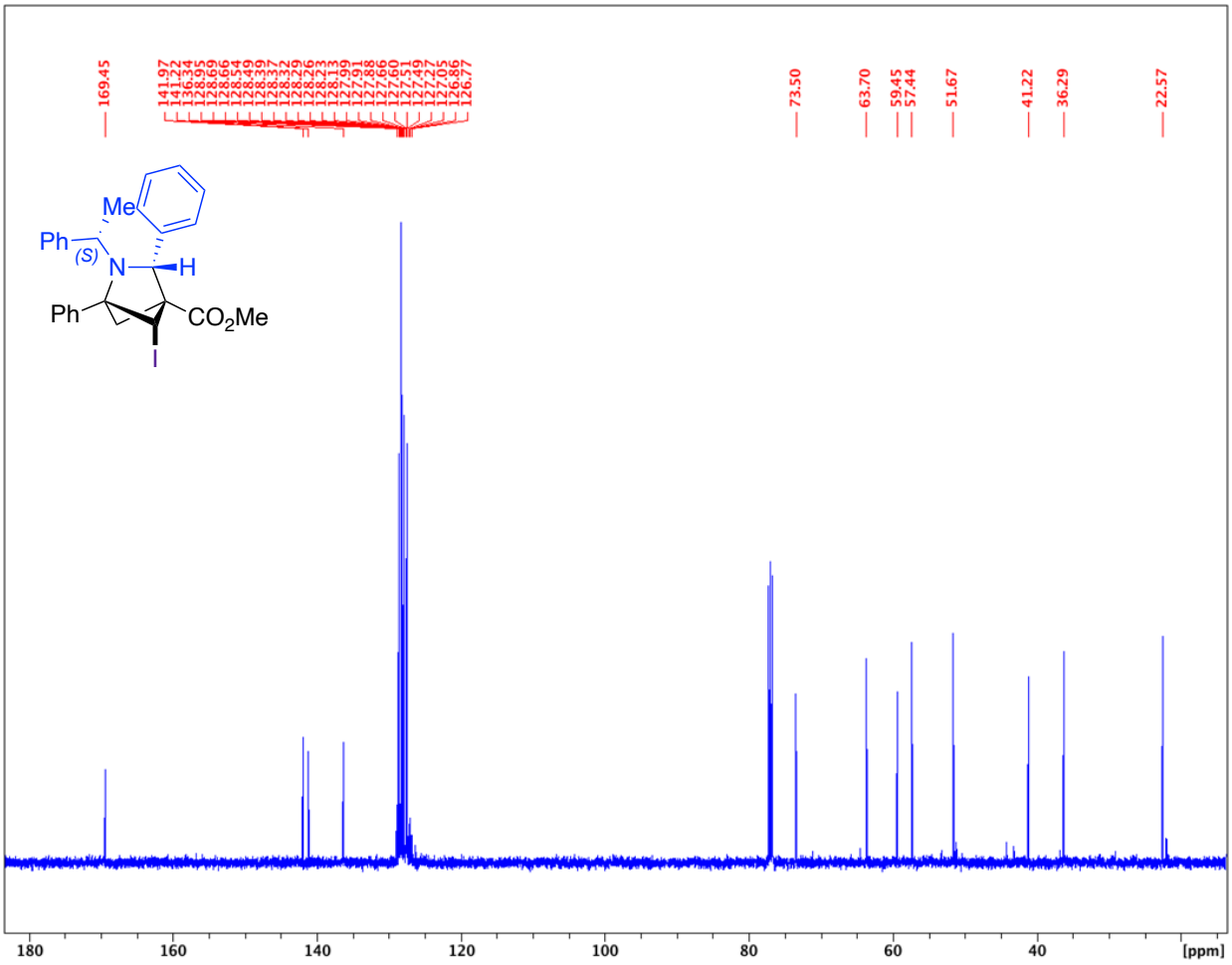

ATR IR spectrum:

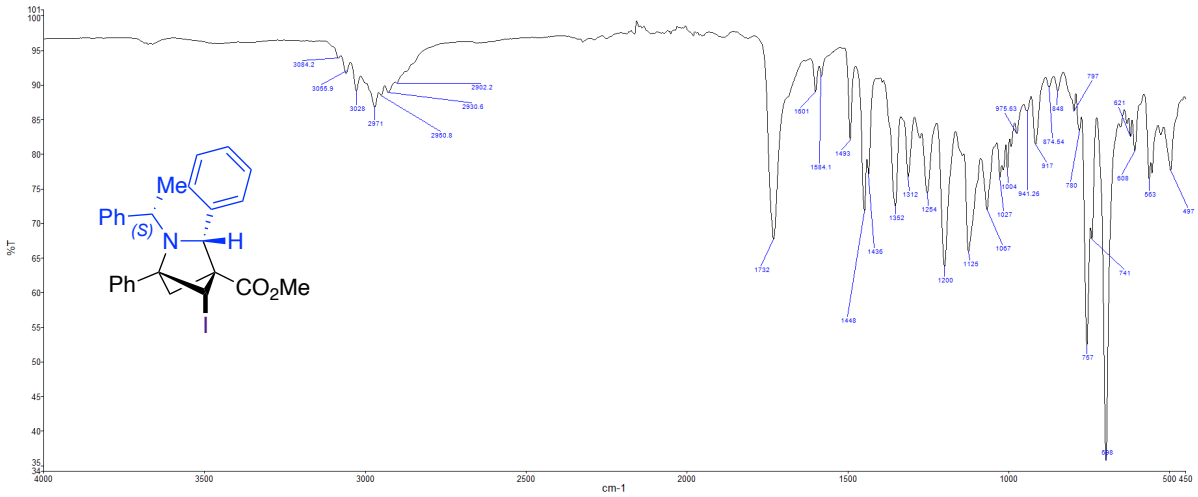

LCMS Chromatogram:

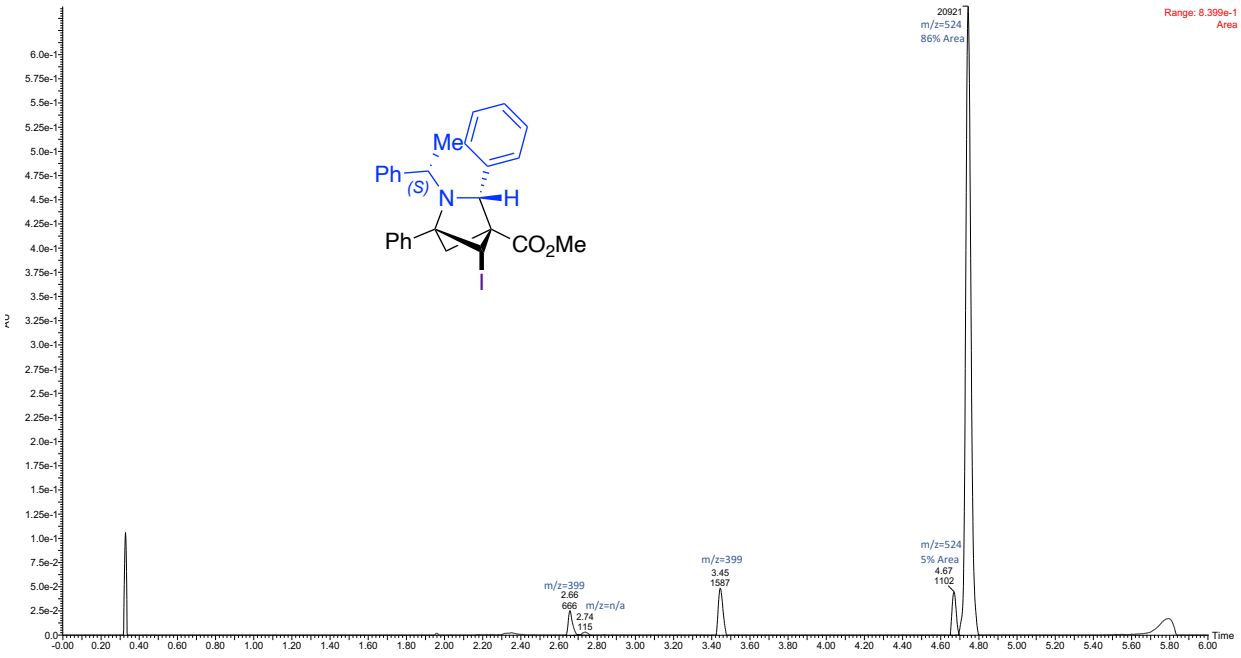

^{1}H-^{13}C HSQC (6ii):

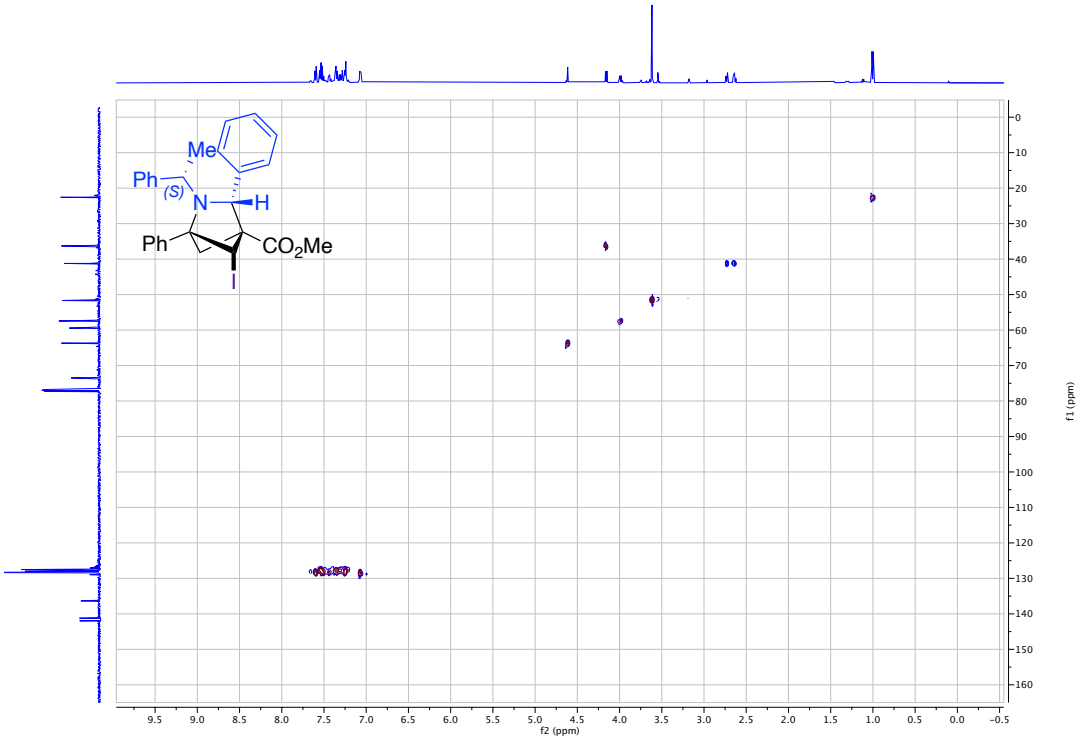

^{1}H-^{13}C HMBC (6ii):

^{1}H-^{1}H NOESY (6ii):

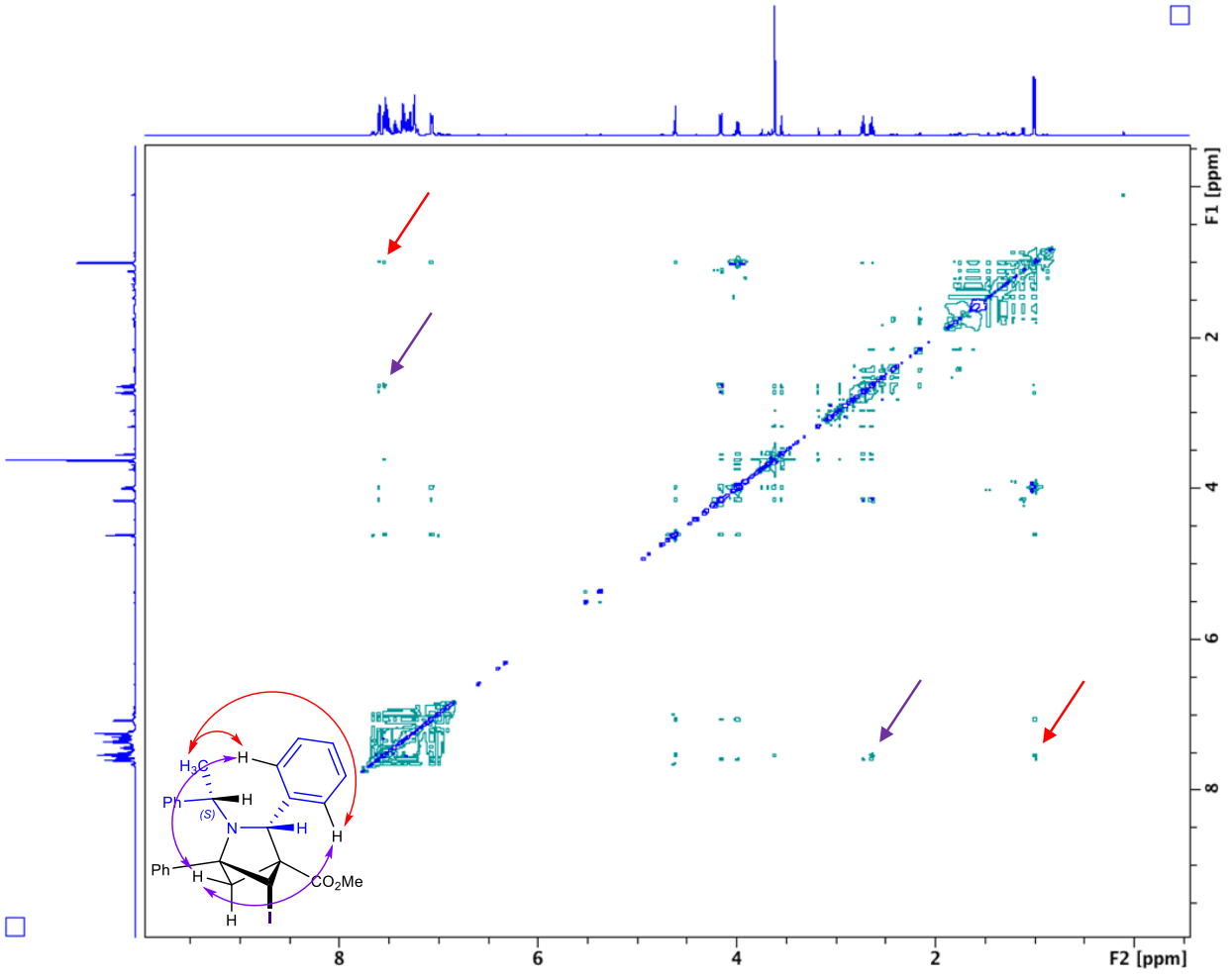

Key correlations are observed for through-space coupling between the *ortho* Ph–H signals shown (7.54 ppm, assigned using HSQC and HMBC data) and the indicated azaBCH ring C–H (2.64 ppm) and the methyl group on the (*S*)-α-methylbenzyl substituent (1.00 ppm). This indicates that all three of these hydrogens are on the same side of the azabicyclohexane ring, consistent with the proposed stereochemistry.

^{1}H-^{1}H NOESY - zoomed (6ii):

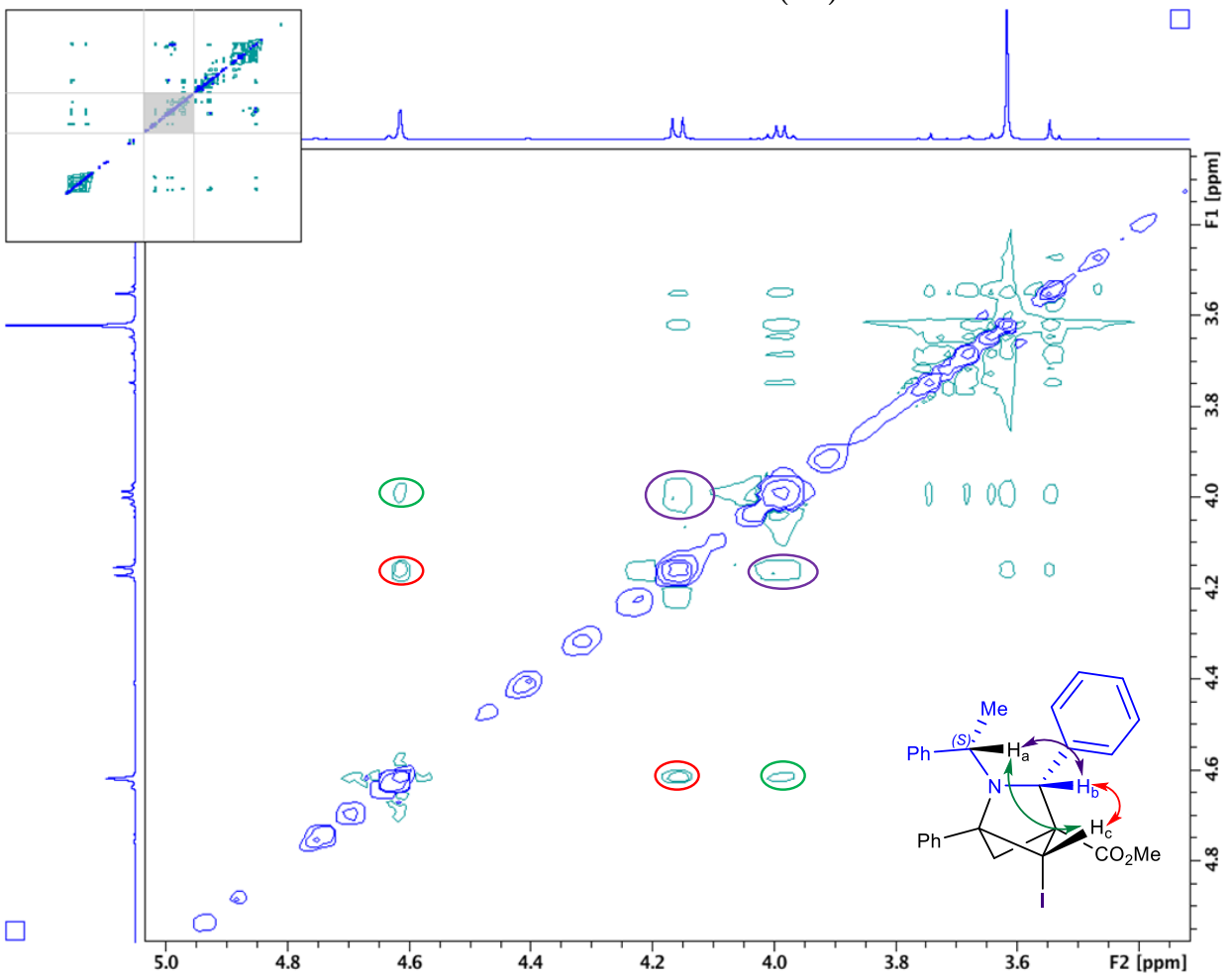

More key correlations are observed between the three indicated methine hydrogens (H_a at 4.00 ppm, H_b at 4.61 ppm, and Hc at 4.17 ppm). These sets of correlations indicate that all three of these hydrogens are on the same side of the azabicyclohexane ring, opposite to the hydrogens discussed above. Thus, the combination of correlations observed between these hydrogens are all consistent with the proposed absolute stereochemical assignment.

Benzyl-2-benzyl-5-iodo-1,3-diphenyl-2-azabicyclo[2.1.1]hexane-4-carboxylate (6nn)

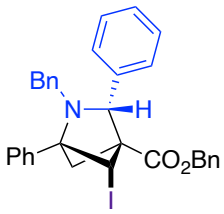

4nn (0.0707 g, 0.154 mmol) was added to a vial and dissolved in 1 mL of acetonitrile. I_2 (0.1171g, 0.46 mmol, 3 equiv) and $NaHCO_3$ (0.0646 g, 0.77 mmol, 5 equiv) were added to the reaction mixture and the solution was stirred for 24 hours at room temperature. The solvent was removed under vacuum and the resulting crude product was purified by column chromatography (SiO_2, 0-100% EtOAc/hexanes, eluted at 20% EtOAc). 15.6 mg of a yellow solid was obtained (19%). 96% major diastereomer and 3% minor diastereomer area by LCMS.

IR: C=O 1728 cm^{-1}

HRMS(ESI): calc'd for [$C_{32}H_{28}INO_2$ + H^+], 586.12375; found: 586.12377.

^{1}H NMR (500 MHz, $CDCl_3$, 292K, ppm): δ 7.46-7.39 (m, 4H), 7.38-7.31 (m, 4H), 7.30-7.25 (m, 4H), 7.15-7.07 (m, 3H), 7.04-6.94 (m, 5H), 5.19 (d, J=12.22 Hz, 1H), 5.13 (d, J=12.22 Hz, 1H), 4.99 (d, J=8.35 Hz, 1H), 4.39 (s, 1H), 3.83 (d, J=12.70 Hz, 1H), 3.54 (d, J=12.70 Hz, 1H), 2.87 (d, J=8.38 Hz, 1H), 2.69 (t, J=8.38 Hz, 1H).

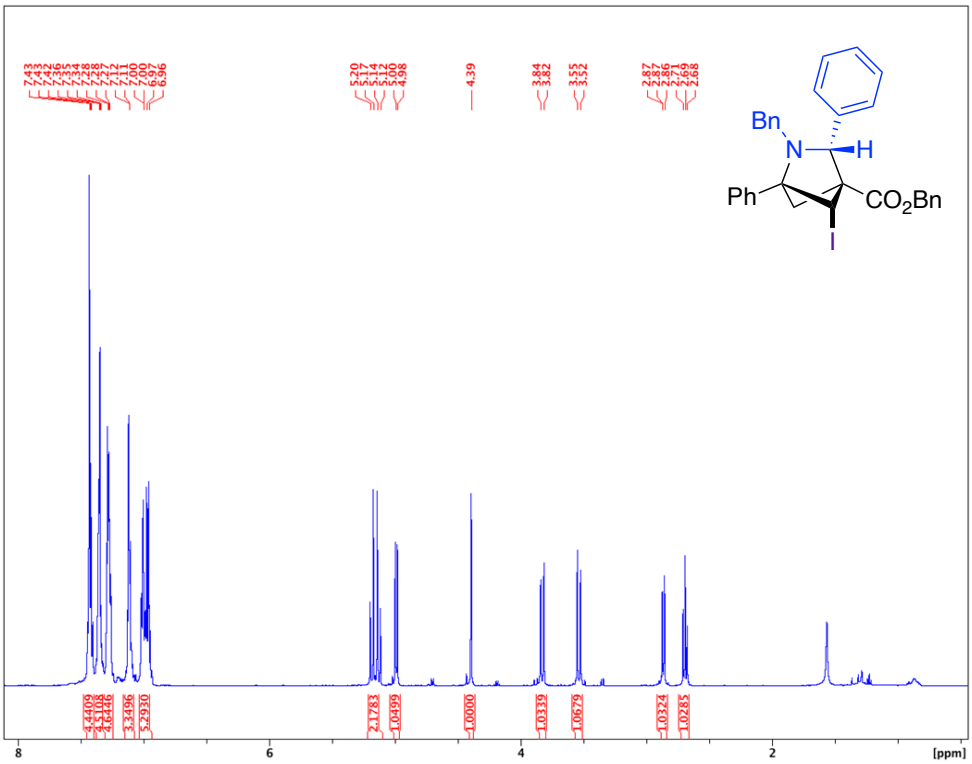

^{13}C NMR (126 MHz, $CDCl_3$, 292K, ppm): δ 168.95, 139.33, 127.78, 125.50, 125.38, 129.20, 128.64, 128.47, 128.31, 128.26, 128.05, 127.62, 127.58, 127.36, 127.23, 126.65, 73.70, 70.16, 66.64, 59.92, 55.63, 39.98, 35.69.

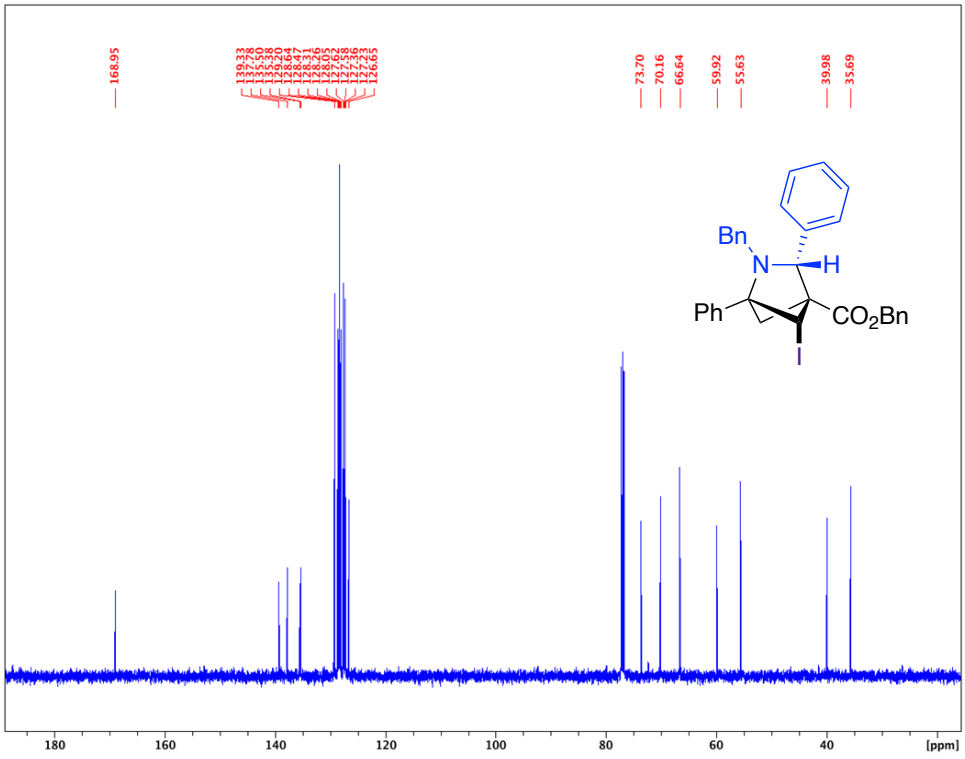

ATR IR spectrum:

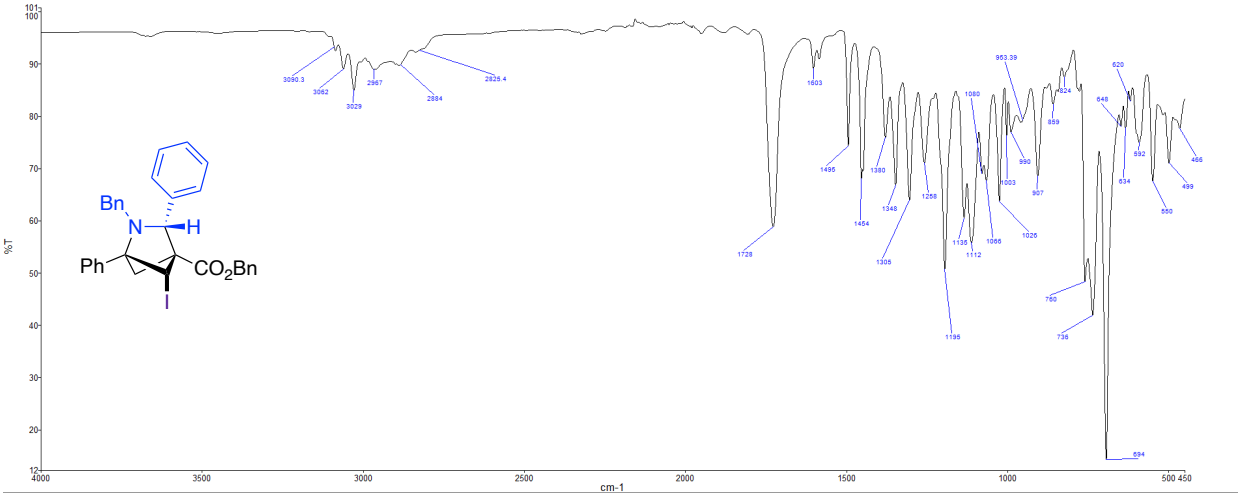

LCMS Chromatogram:

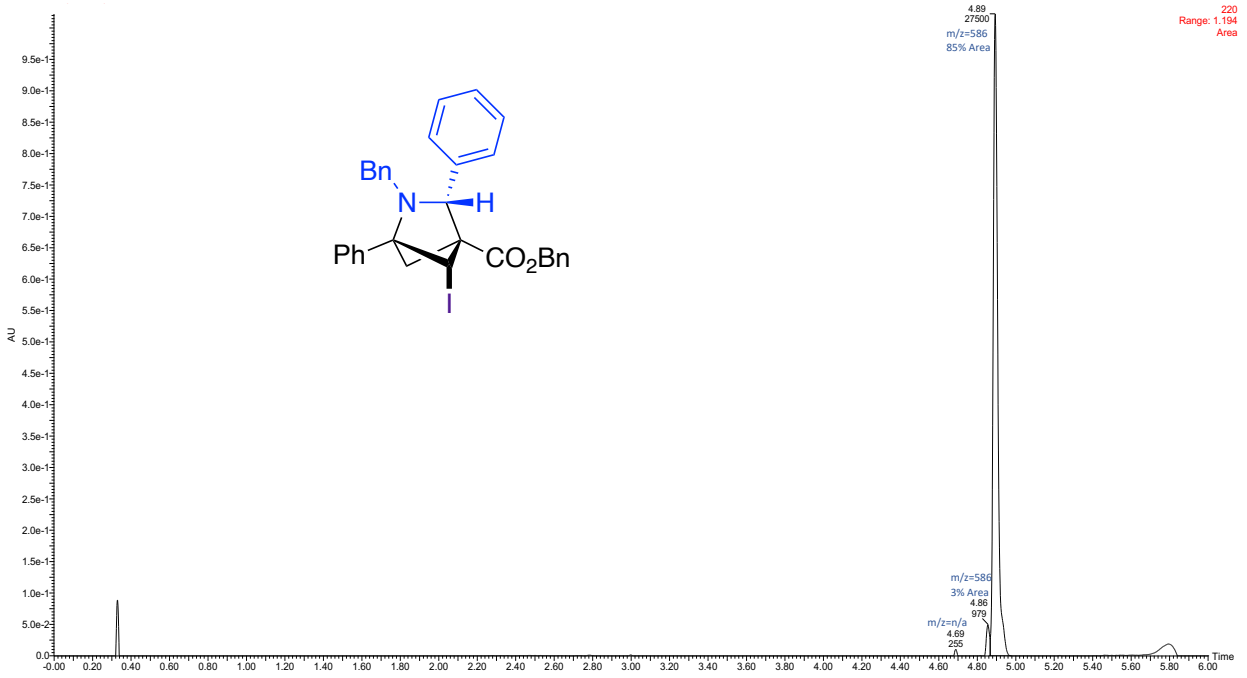

^{1}H-^{13}C HSQC (6nn):

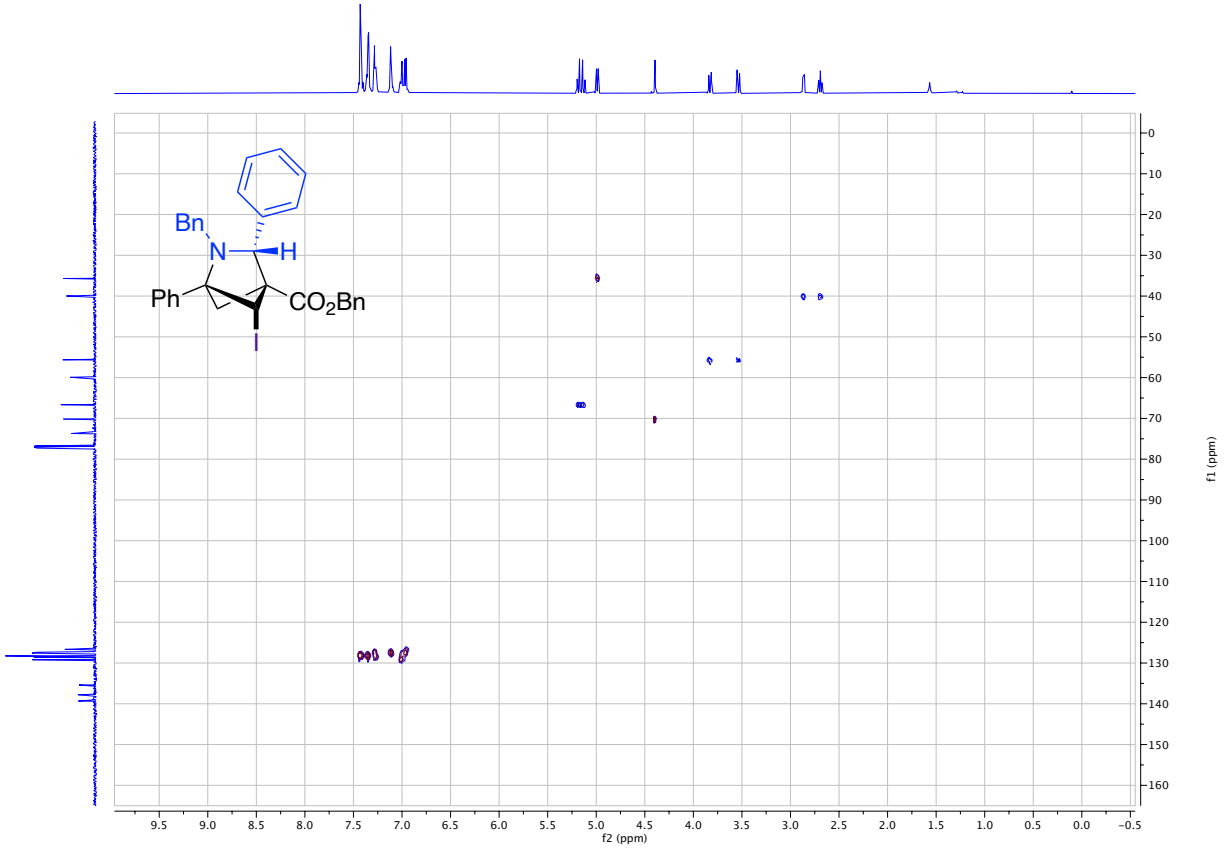

^{1}H-^{13}C HMBC (6nn):

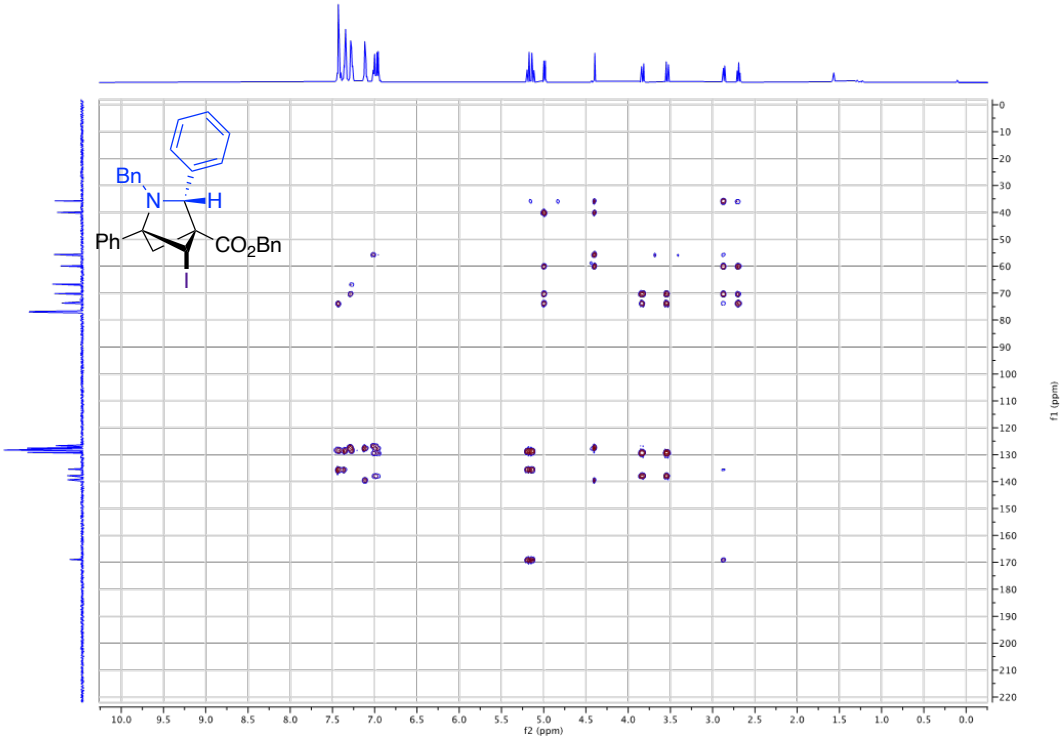

^{1}H-^{1}H NOESY (6nn):

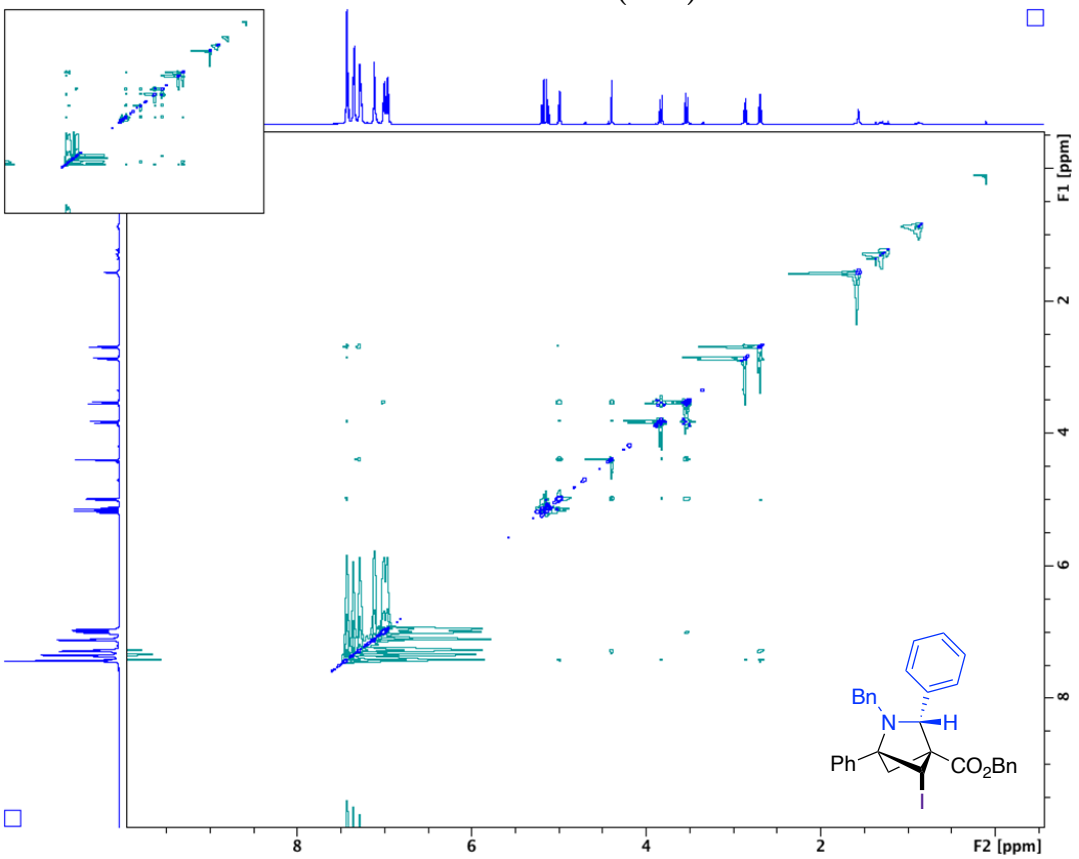

^{1}H-^{1}H NOESY - Zoomed (6nn):

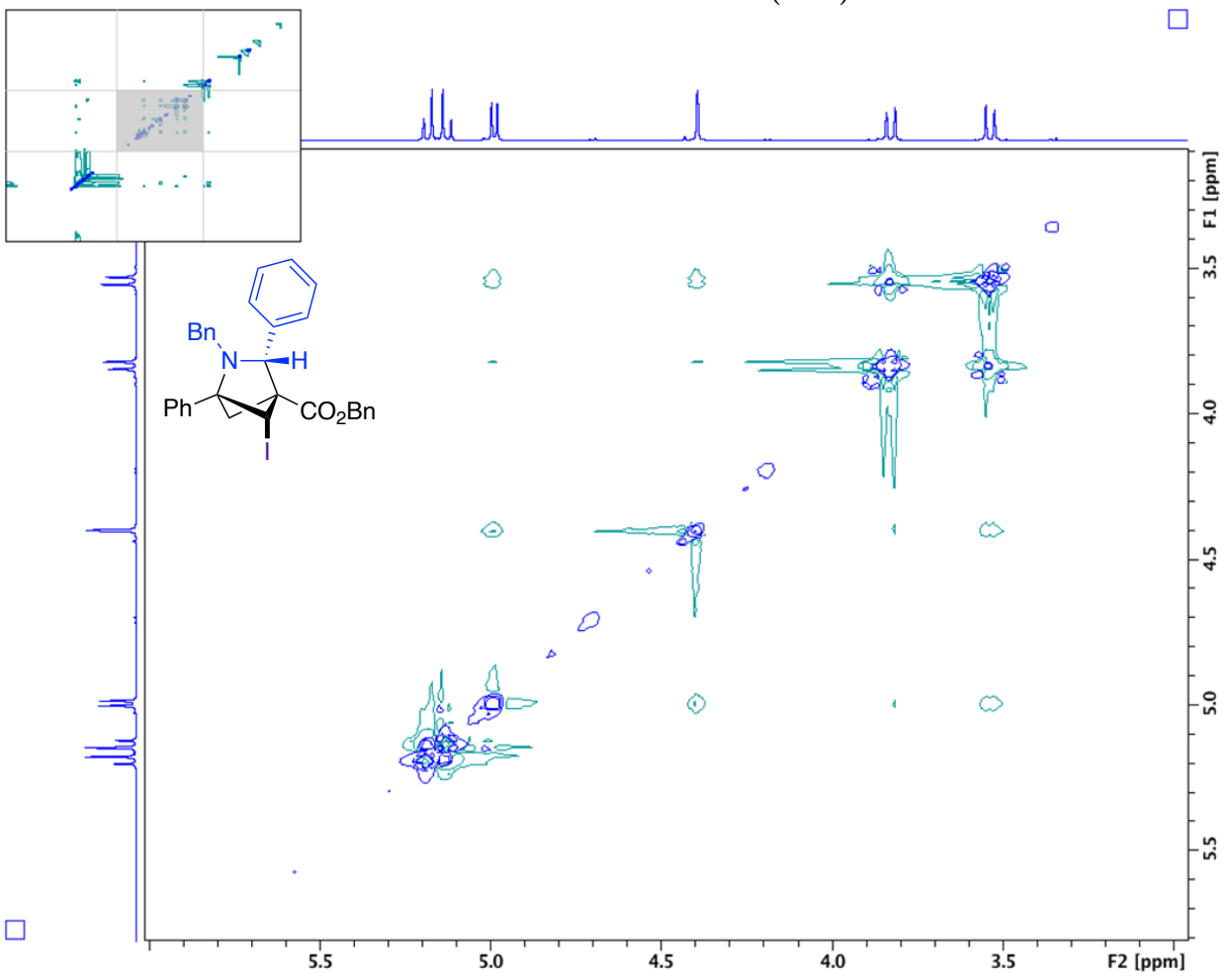

Iodoamination of the minor diastereomer of methyl-1-(naphthalen-2-yl(((*S*)-1-phenylethyl)amino)methyl)-3-phenylcyclobut-2-ene-1-carboxylate (6kk′)

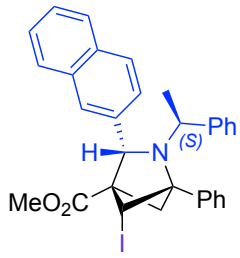

4kk′ (0.021.5 g, 0.048 mmol) was added to a vial and dissolved in 1 mL of acetonitrile and the vial was cooled down to −20 °C. I_2 (0.0366 g, 0.14 mmol, 3 equiv) and $NaHCO_3$ (0.0202 g, 0.24 mmol, 5 equiv) were added to the reaction mixture and the solution was warmed up and stirred for 24 hours at room temperature. The reaction was quenched with 1 mL of saturated Na_2SO_3 and then the aqueous layer was extracted three times with 1 mL of ethyl acetate. The organic layers were dried with Mg_2SO_4, the solution was filtered and then the solvent was removed under vacuum to give the crude product **6kk′**. The product was dissolved in $CDCl_3$ and a ^{1}H NMR and NOESY spectrum was taken.

^{1}H NMR (500 MHz, $CDCl_3$, 292K, ppm):

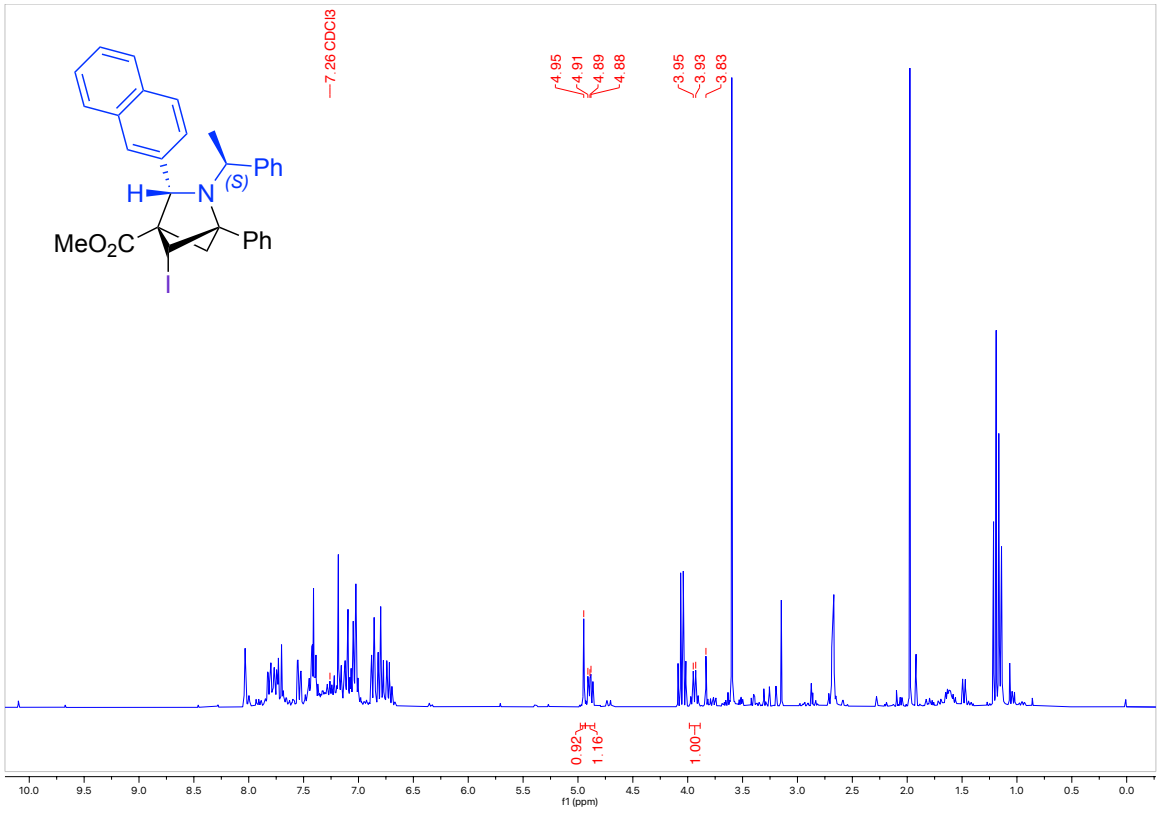

^{1}H-^{1}H NOESY:

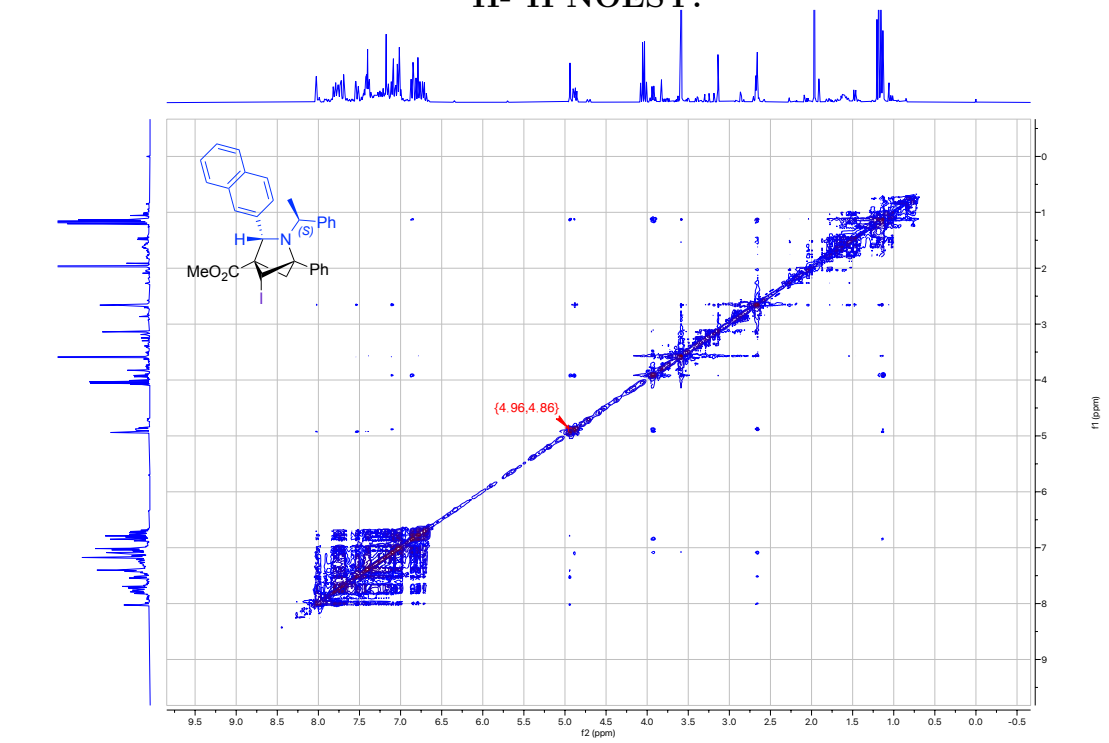

^{1}H-^{1}H NOESY - Zoomed: Key correlation seen between H_a and H_b.

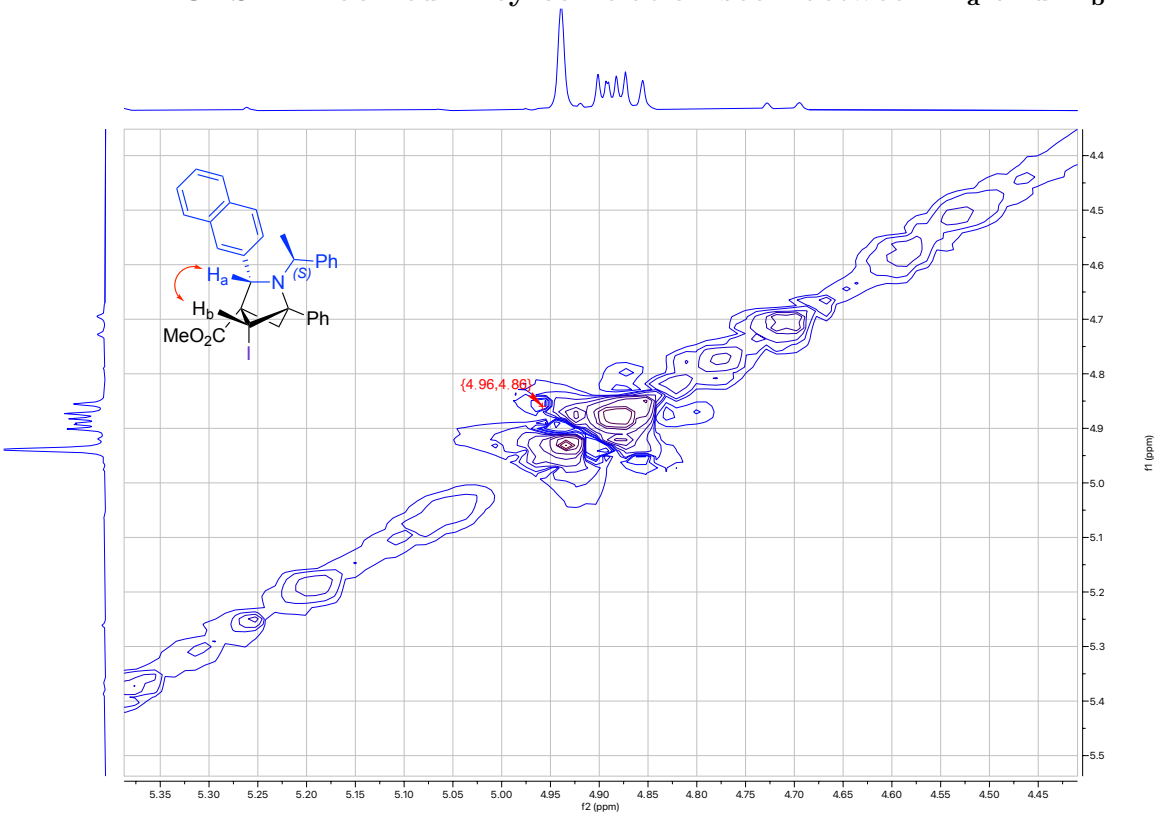

A.9 Synthetic Transformations of AzaBCHs

Methyl-1,3-diphenyl-2-azabicyclo[2.1.1]hexane-4-carboxylate (7a):

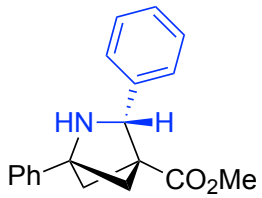

Compound **3e** (0.1487 g, 0.37 mmol) was dissolved in acetonitrile (3.5 mL). Cerium ammonium nitrate (1.0204 g, 1.86 mmol, 5 equiv) was dissolved in water (10 mL) and added dropwise to the acetonitrile mixture. The reaction mixture was stirred at room temperature for 24 hours. The mixture was then diluted with DCM (10 mL) and then quenched with $NaHCO_3$ until basic. The aqueous layer was then extracted with DCM (10 mL), dried with Mg_2SO_4, filtered, and then concentrated under vacuum. The residue was redissolved in 1 M HCl (10 mL) and then extracted with hexanes (10 mL). The aqueous layer was basified with 1 M NaOH, and then extracted with DCM (10 mL). The organic layer was dried with Mg_2SO_4, filtered and the solvent was evaporated under vacuum to give product **7a** as a brown solid (92 mg, 84% yield). 98% peak area by LCMS.

IR: 3302, 1733 cm^{-1}

HRMS(ESI): calc'd for $[C_{19}H_{19}NO_2 + H_+]$, 294.14886; found: 294.14892.

^{1}H NMR (500 MHz, $CDCl_3$, 292K, ppm): δ 7.58(m, 2H), 7.52 (m, 2H), 7.40 (m, 6H), 4.93 (s, 1H), 3.72 (s, 3H), 2.57 (d, J = 6.6 Hz, 1H), 2.40 (m, 1H), 2.26 (m, 1H), 2.10 (d, J = 7.4 Hz, 1H).

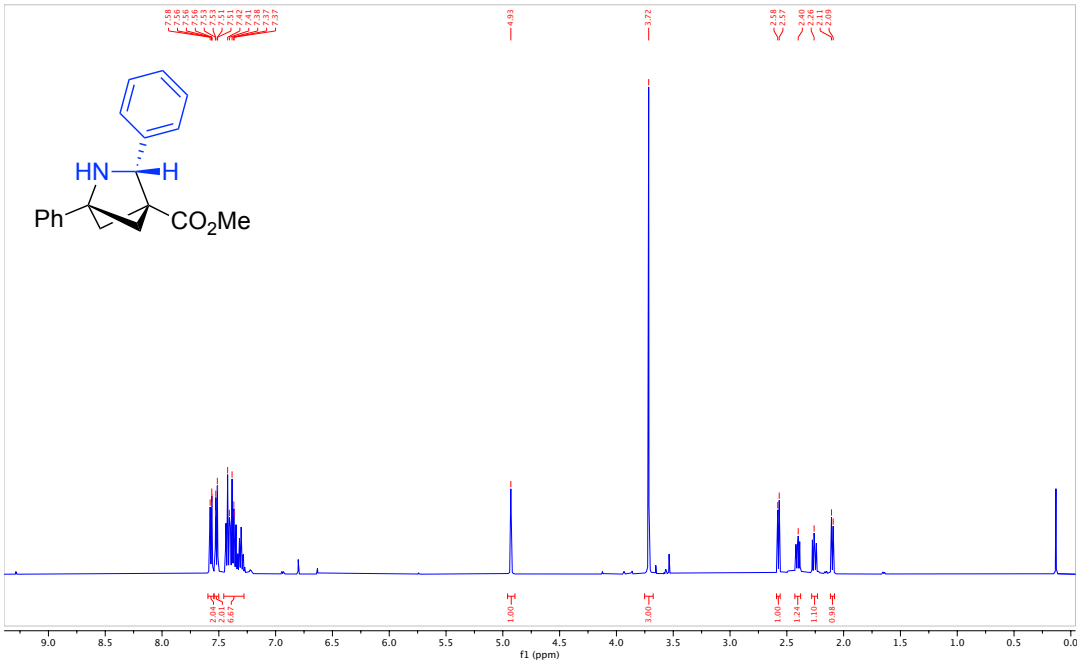

^{13}C NMR (126 MHz, $CDCl_3$, 292K, ppm): δ 170.88, 140.20, 138.41, 127.37, 127.11, 126.62, 126.42, 126.23, 125.22, 66.69, 62.15, 53.48, 50.80, 50.55, 39.26.

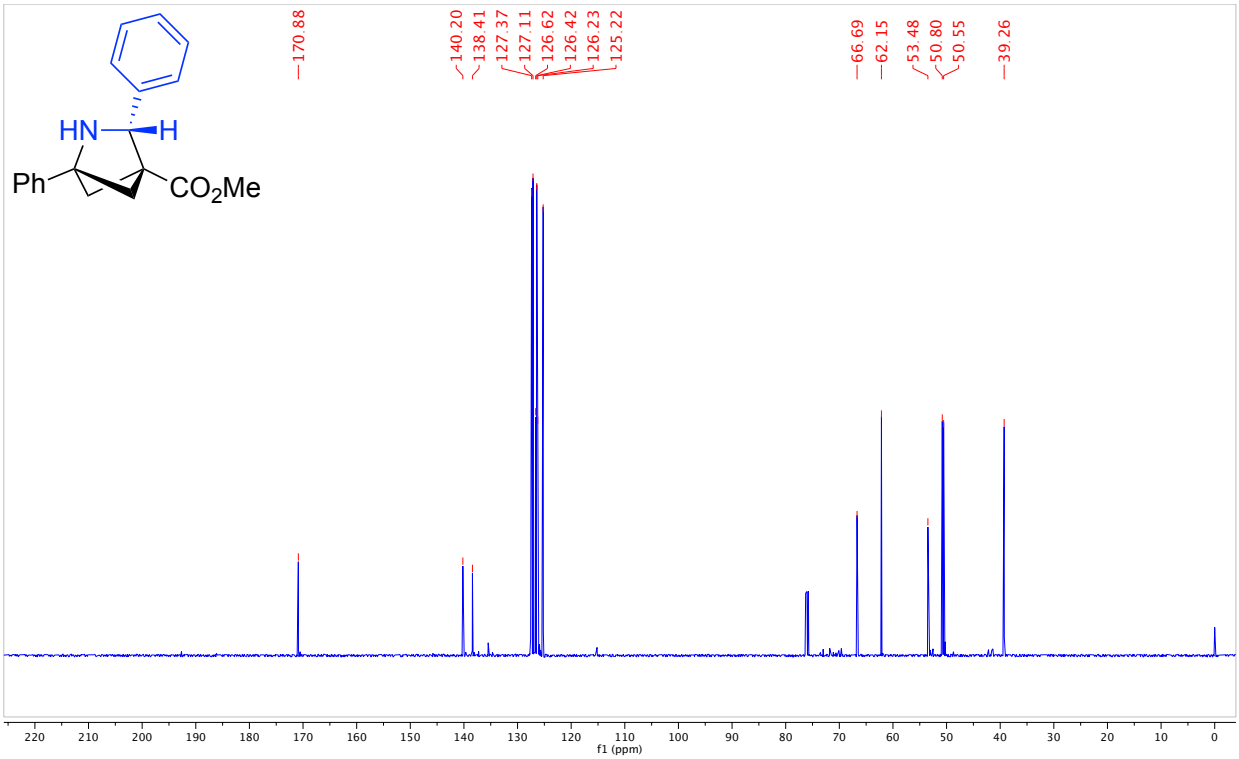

ATR IR spectrum:

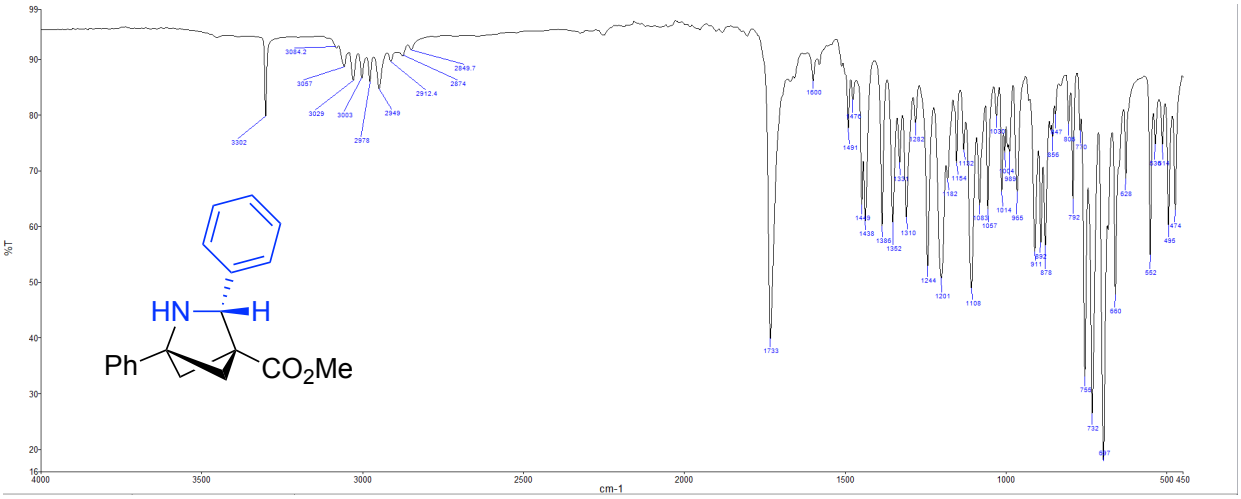

LCMS Chromatogram:

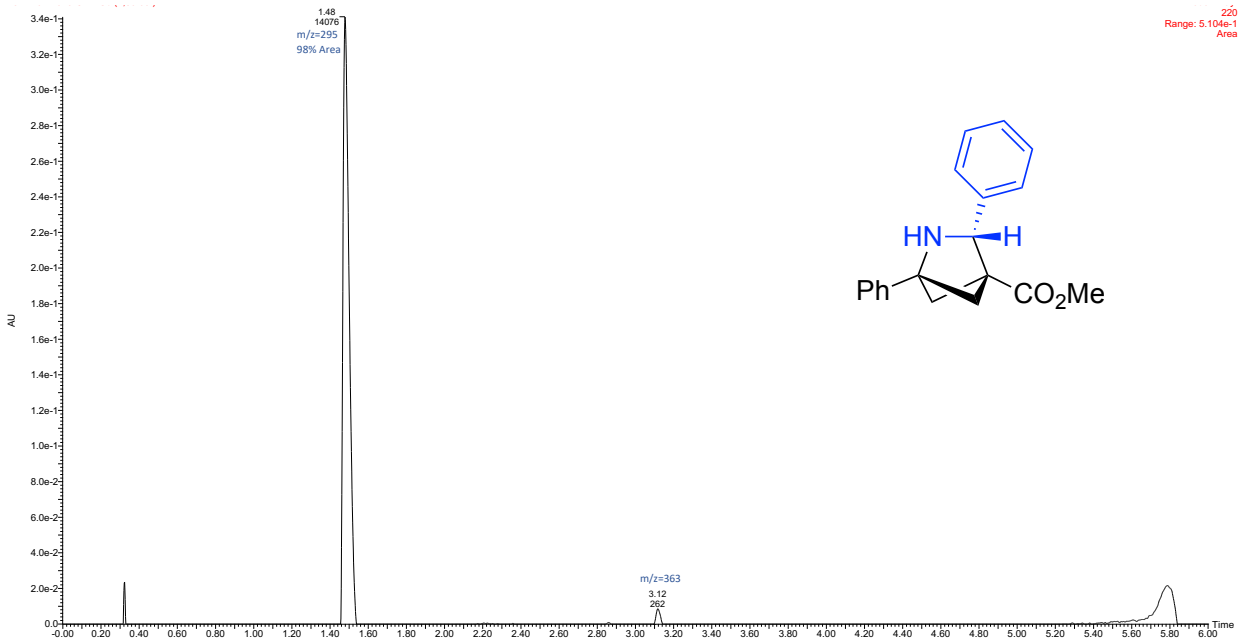

2-(4-(Ethoxycarbonyl)phenyl)-1,3-diphenyl-2-azabicyclo[2.1.1]hexane-4-carboxylic acid (7d)

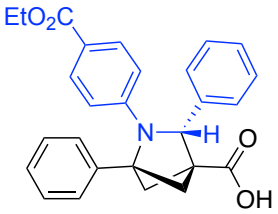

A 1-dram vial was charged with a stirbar, **3f** (86.2 mg, 0.20 mmol), and LiOH•H_2O (16.4 mg, 2 equiv). The solids were dissolved in a 1:1 v/v THF/water mixture (0.5 mL total). The reaction mixture was acidified with 1 M HCl to adjust the pH to 4-6. Once the solution reached the desired pH range, the aqueous phase was extracted with DCM (3 x 2 mL). The organic layer was dried using anhydrous Mg_2SO_4 and concentrated under reduced pressure to give 83.5 mg (100%) of **7d** as a yellow oil.

^{1}H NMR (500 MHz, $CDCl_3$, 292K, ppm): δ 7.71 (d, J = 7.2 Hz, 2H), 7.62 (d, J = 9.0 Hz, 2H), 7.57 – 7.30 (m, 8H), 6.45 (d, J = 9.0 Hz, 2H), 4.99 (s, 1H), 4.24 (q, J = 7.1 Hz, 2H), 2.94 – 2.82 (m, 1H), 2.67 – 2.50 (m, 2H), 2.05 (dd, J = 7.3, 1.4 Hz, 1H), 1.28 (t, J = 7.1 Hz, 3H).

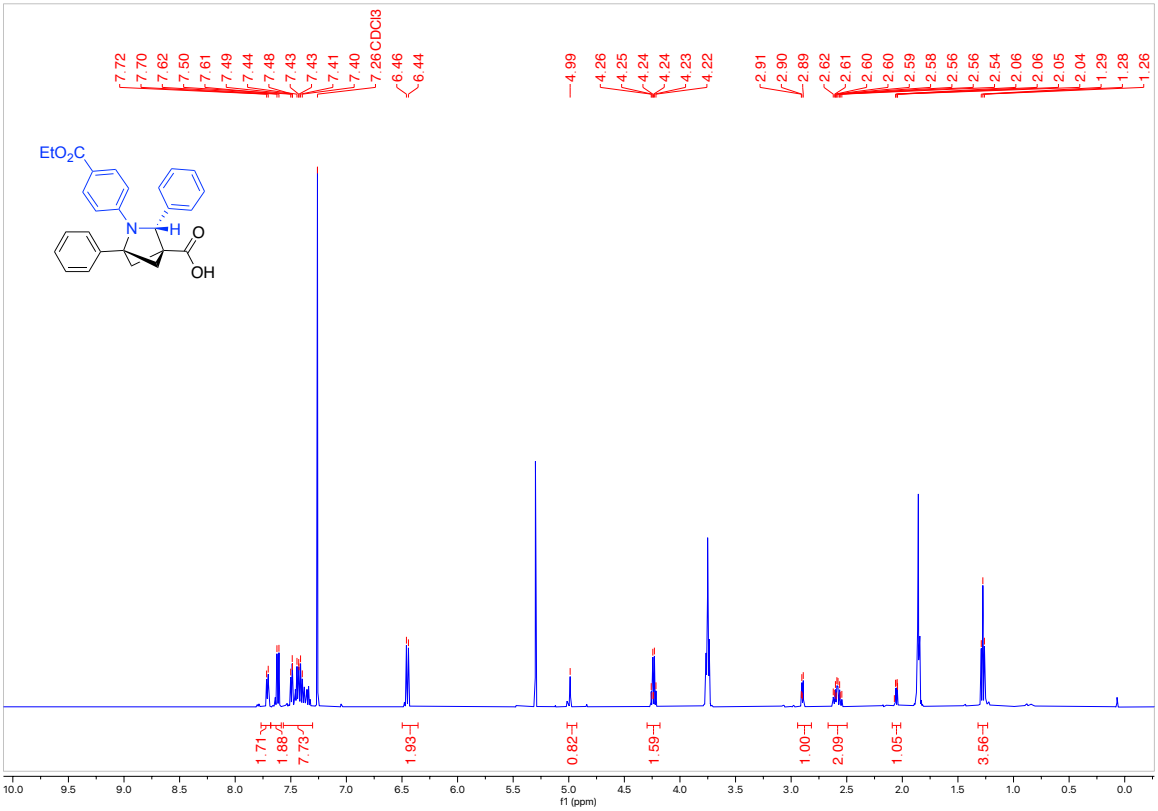

3-(4-Cyanophenyl)-2-(4-methoxyphenyl)-1-phenyl-2-azabicyclo[2.1.1]hexane-4-carboxylic acid (7e)

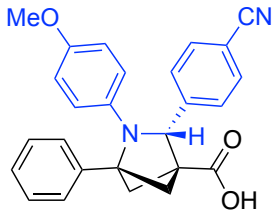

A 1-dram vial was charged with a stirbar, **3i** (70.6 mg, 0.17 mmol), and LiOH•H_2O (14.0 mg, 2 equiv). The solids were dissolved in a 1:1 v/v THF/water mixture (0.5 mL total). The reaction mixture was acidified with 1 M HCl to adjust the pH to 4-6. Once the solution reached the desired pH range, the aqueous phase was extracted with DCM (3 x 2 mL). The organic layer was dried using anhydrous Mg_2SO_4 and concentrated under reduced pressure to give 68.3 mg (100%) of **7e** as a yellow oil.

^{1}H NMR (500 MHz, $CDCl_3$, 292K, ppm): δ 7.91 (d, J = 8.2 Hz, 2H), 7.73 (d, J = 8.2 Hz, 2H), 7.50 – 7.26 (m, 5H), 6.58 – 6.53 (m, 2H), 6.48 (d, J = 9.1 Hz, 2H), 4.88 (s, 1H), 3.64 (s, 3H), 2.91 (d, J = 6.9 Hz, 1H), 2.80 (dd, J = 9.9, 7.0 Hz, 1H), 2.49 – 2.35 (m, 1H), 2.08 (d, J = 7.9 Hz, 1H).

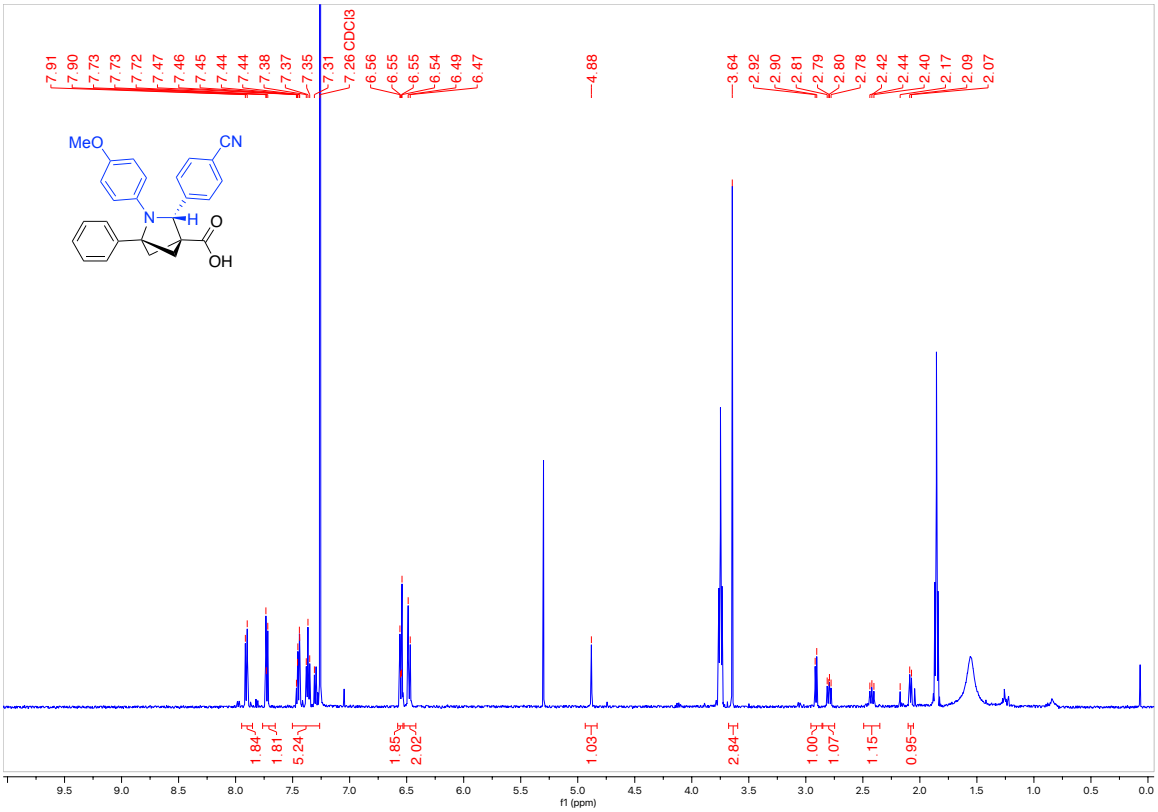

3-(6-chloropyridin-3-yl)-2-(4-iodophenyl)-1-phenyl-2-azabicyclo[2.1.1]hexane-4-carboxylic acid (7f)

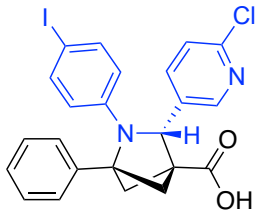

A 1-dram vial was charged with a stirbar, **3l** (59.2 mg, 0.11 mmol), and LiOH•H_2O (9.4 mg, 2 equiv). The solids were dissolved in a 1:1 v/v THF/water mixture (0.5 mL total). The reaction mixture was acidified with 1 M HCl to adjust the pH to 4-6. Once the solution reached the desired pH range, the aqueous phase was extracted with DCM (3 x 2 mL). The organic layer was dried using anhydrous Mg_2SO_4 and concentrated under reduced pressure to give 46.0 mg (80%) of **7f** as a yellow oil.

^{1}H NMR (500 MHz, $CDCl_3$, 292K, ppm): δ 8.75 (d, J = 2.4 Hz, 1H), 8.12 (d, J = 7.7 Hz, 1H), 7.47 – 7.28 (m, 5H), 6.24 (d, J = 9.0 Hz, 2H), 4.88 (s, 1H), 2.94 (d, J = 7.0 Hz, 1H), 2.65 (dd, J = 9.9, 7.2 Hz, 1H), 2.43 – 2.30 (m, 1H), 2.12 (d, J = 8.2 Hz, 1H).

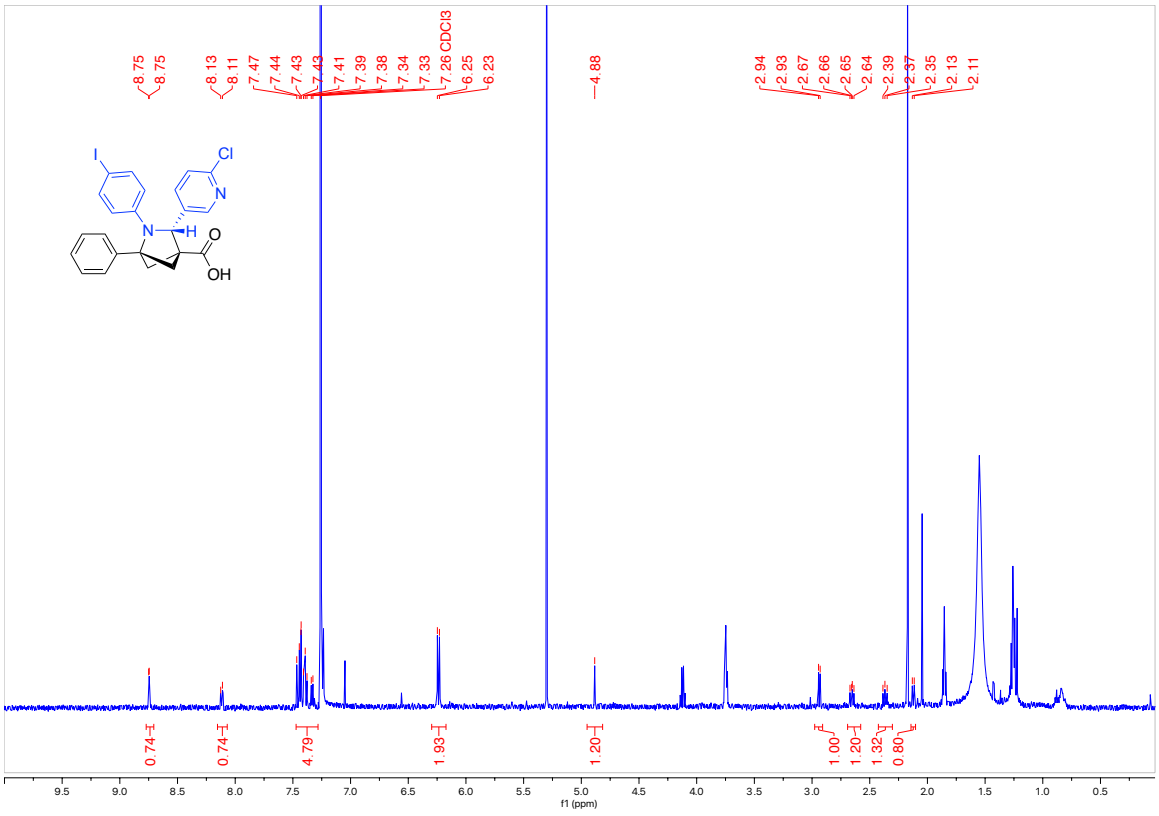

1-(4-Chlorophenyl)-2,3-diphenyl-2-azabicyclo[2.1.1]hexane-4-carboxylic acid (7g)

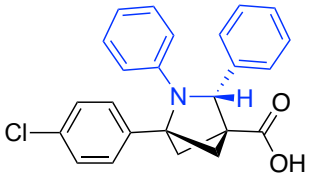

A 1-dram vial was charged with a stirbar, **3p** (89.8 mg, 0.22 mmol), and LiOH•H_2O (18.7 mg, 2 equiv). The solids were dissolved in a 1:1 v/v THF/water mixture (0.5 mL total). The reaction mixture was acidified with 1 M HCl to adjust the pH to 4-6. Once the solution reached the desired pH range, the aqueous phase was extracted with DCM (3 x 2 mL). The organic layer was dried using anhydrous Mg_2SO_4 and concentrated under reduced pressure to give 86.7 mg (100%) of **7g** as a yellow oil.

^{1}H NMR (500 MHz, $CDCl_3$, 292K, ppm): δ 7.73 (d, J = 7.6 Hz, 2H), 7.51 – 7.28 (m, 7H), 7.01 – 6.93 (m, 2H), 6.76 (t, J = 7.3 Hz, 1H), 6.51 (d, J = 8.0 Hz, 2H), 4.92 (s, 1H), 2.86 (d, J = 6.8 Hz, 1H), 2.70 (dd, J = 9.9, 6.8 Hz, 1H), 2.57 – 2.45 (m, 1H), 2.00 (d, J = 7.8 Hz, 1H).

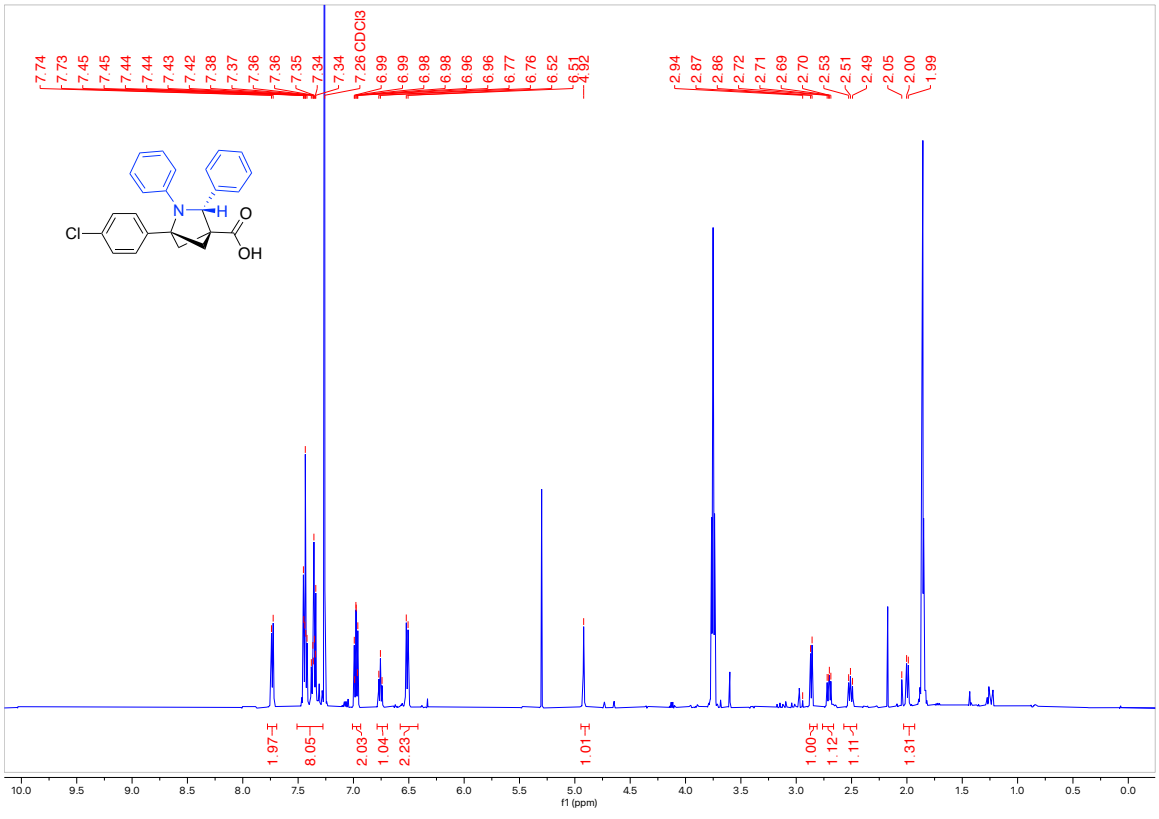

1-(4-chlorophenyl)-2,3-diphenyl-2-azabicyclo[2.1.1]hexan-4-yl)(3,5-dimethyl-1H-pyrazol-1-yl)methanone (8g)

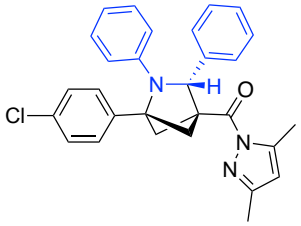

A 1-dram vial was charged with a stirbar and **7g** (89.8 mg, 0.22 mmol) then dissolved in THF (1.0 mL, 0.22 M). Carbonyldiimidazole (37.9 mg, 0.23 mmol, 1.05 equiv) was added as a solid to the reaction mixture and it was left to stir for 1 hour at room temperature. Then 3,5-dimethylpyrazole (37.9 mg, 0.23 mmol, 1.05 equiv) was added to the reaction mixture as a solid and it was left to stir at room temperature overnight. The reaction mixture was quenched with 1 mL of NH_4Cl and the aqueous later was extracted with ethyl acetate (3 x 2 mL). The combined organic laters were washed with 5 mL NH_4Cl and brine (2 x 5 mL). The organic layer was dried using anhydrous Mg_2SO_4 and concentrated under reduced pressure to give the crude product. The product was purified by column chromatography (Biotage® Sfär 5g Column, 0-100% EtOAc/hexanes, eluted at 5% EtOAc). 15.0 mg (14%) of **8g** was obtained as a white solid.

^{1}H NMR (500 MHz, $CDCl_3$, 292K, ppm): δ 7.50 – 7.42 (m, 2H), 7.38 – 7.27 (m, 7H), 7.04 – 6.93 (m, 2H), 6.81 – 6.72 (m, 1H), 6.60 – 6.50 (m, 2H), 6.00 (d, J = 1.1 Hz, 1H), 5.45 – 5.39 (m, 1H), 3.01 (dd, J = 9.6, 7.1 Hz, 1H), 2.96 (d, J = 7.1 Hz, 1H), 2.58 (dd, J = 9.6, 7.8 Hz, 1H), 2.48 (d, J = 1.0 Hz, 3H), 2.19 (s, 3H), 1.98 (dd, J = 7.7, 1.3 Hz, 1H).

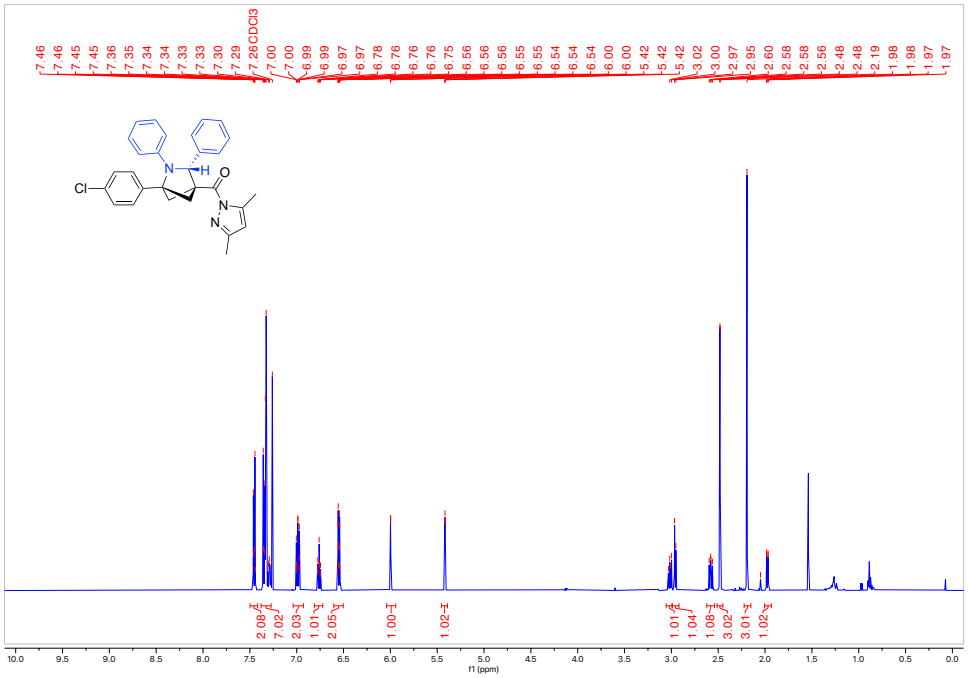

Appendix B

Supporting Information for Chapter 3

Contributions: The following data reported has been completed **independently** with supporting work from supervised undergraduate students.

B.1 General

Materials. All solvents and common organic reagents were purchased from commercial suppliers and used without further purification. Organic building blocks and starting materials were purchased from Oakwood Chemicals and MilliporeSigma and used as received. Anhydrous solvents (SureSeal) were purchased from MilliporeSigma and used as received.

Techniques. All air-free manipulations were performed under a dry nitrogen atmosphere using an MBraun glovebox.

Analysis and Spectroscopy. All NMR spectra were acquired on either a Bruker AVANCE 300 MHz spectrometer or a Bruker AVANCE Neo 500 MHz spectrometer. All ^{1}H and ^{13}C NMR spectroscopy chemical shifts are calibrated to residual protio-solvents. All NMR spectroscopic data is processed using MestReNova v14.2.2. High-resolution electrospray ionization mass spectrometric analysis was performed using a Thermo Scientific Ultimate 3000 ESI-Orbitrap Exactive Plus.

X-Ray Crystallography. A suitable crystal of each sample (**3c, 4b**, and **4d**) was selected for analysis and mounted in a polyimide loop. All measurements were made on a Rigaku Oxford Diffraction Supernova Eos CCD with filtered Cu Kα radiation at a temperature of 100 K. Using Olex2, the structure was solved with the ShelXT structure solution program using Direct Methods and refined with the ShelXL refinement package using Least Squares minimization. The structure of compounds **3c** and **4b** were refined without restraint. The structure of compound **4d** was refined to model conformational disorder. The morpholinyl group was modeled over two positions with similarity restraints placed on bond distances and atomic thermal parameters. CIFs of **3c**, **4b**, and **4d** are available from the Cambridge Crystallographic Data Centre (CCDC): CCDC 2290170-2290171, 2298459.

B.2 Optimization and Control Reactions

Table 3.1 reaction conditions

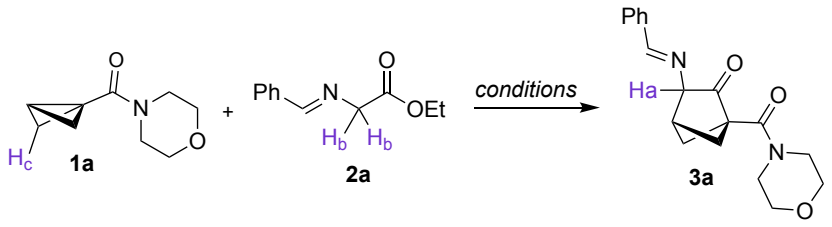

Table 3.1, entry 1

In one vial, the bicyclobutane (8.4 mg, 1 equiv) and 1,3,5-trimethoxybenzene (2.8 mg, 0.33 equiv) were added and to another vial, the imine (9.6 mg, 1 equiv), silver acetate (0.8 mg, 0.1 equiv) and triethylamine (2.1 μL, 0.3 equiv) were added under a nitrogen atmosphere. 50% of the THF solvent (1 mL total, 0.05 mmol) was added to each vial then the imine solution was added to the bicyclobutane, and the reaction was left to stir for 24 hours at room temperature. The solvent was evaporated, and the amounts of product and starting materials were determined by NMR spectroscopy relative to the internal standard (1,3,5-trimethoxybenzene). No product (no peak at 4.06 ppm, H_a), 25% imine (4.39 ppm peak, H_b), 1% benzaldehyde (from imine hydrolysis, 10.02 ppm peak), and 72% bicyclobutane (1.99 ppm peak, H_c).

^{1}H NMR (300 MHz, $CDCl_3$, 292 K, ppm)

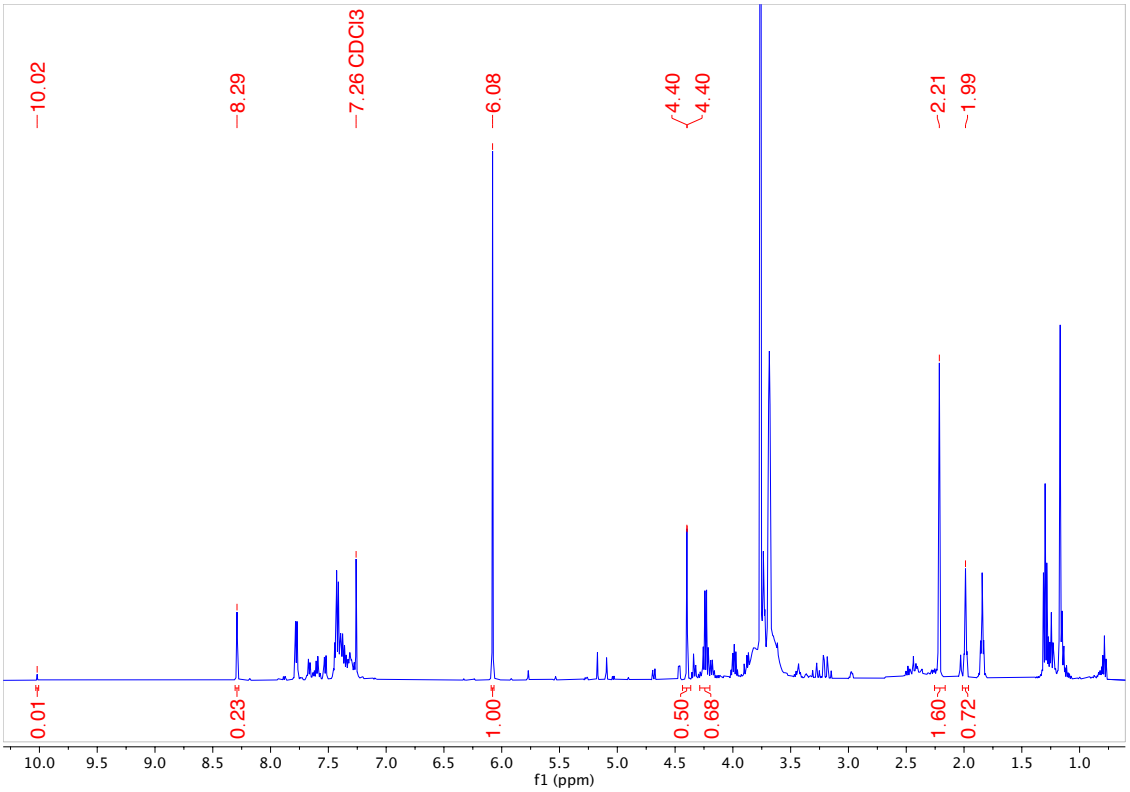

Table 3.1, entry 2

In one vial, the bicyclobutane (8.4 mg, 1 equiv) and 1,3,5-trimethoxybenzene (2.8 mg, 0.33 equiv) were added and to another vial, the imine (9.6 mg, 1 equiv), $Ga(OTf)_3$ (2.6 mg, 0.1 equiv) and triethylamine (2.1 μL, 0.3 equiv) were added under a nitrogen atmosphere. 50% of the THF solvent (1 mL total, 0.05 mmol) was added to each vial then the imine solution was added to the bicyclobutane, and the reaction was left to stir for 24 hours at room temperature. The solvent was evaporated, and the amounts of product and starting materials were determined by NMR spectroscopy relative to the internal standard (1,3,5-trimethoxybenzene). No product (no peak at 4.06 ppm, H_a), 78% imine (4.39 ppm peak, H_b), 14% benzaldehyde (from imine hydrolysis, 10.02 ppm peak), and 100% bicyclobutane (1.99 ppm peak, H_c).

^{1}H NMR (300 MHz, $CDCl_3$, 292 K, ppm)

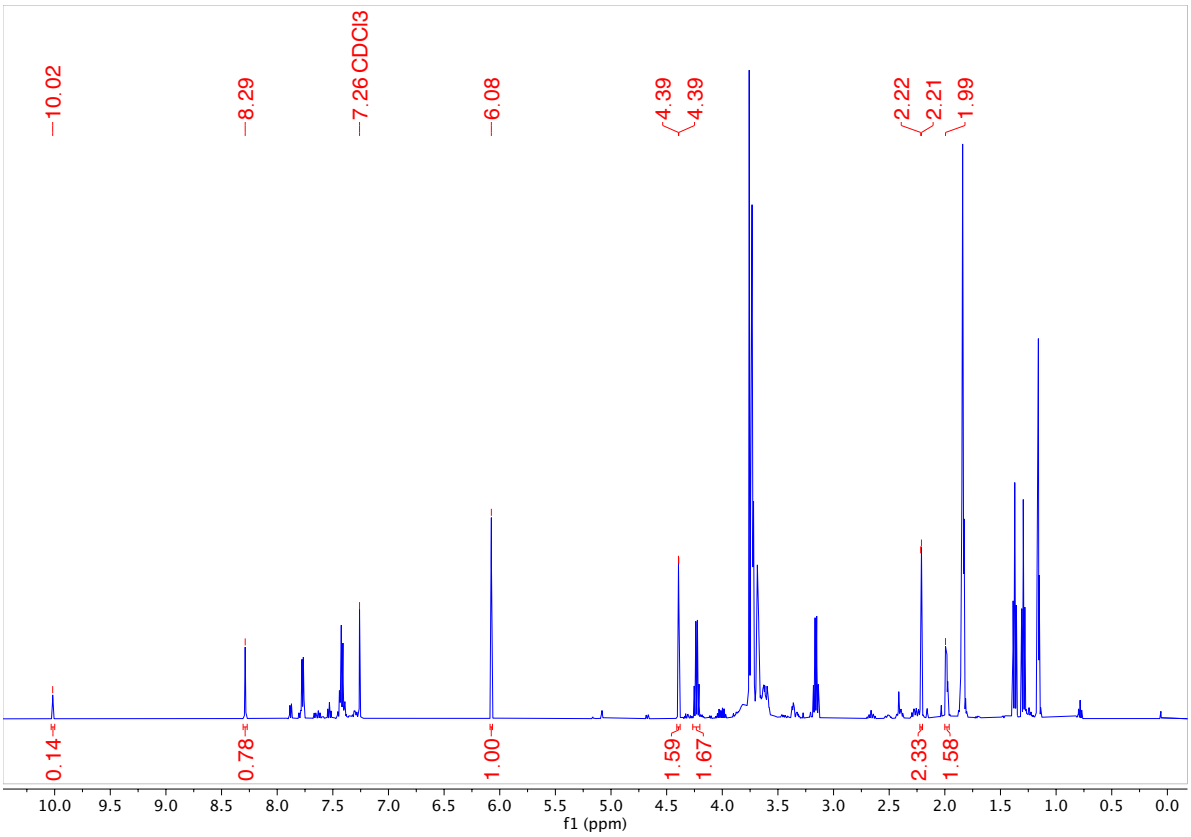

Table 3.1, entry 3

In one vial, the bicyclobutane (8.4 mg, 1 equiv) and 1,3,5-trimethoxybenzene (2.8 mg, 0.33 equiv) were added followed by 50% of the THF solvent (1 mL total, 0.05 M). To another vial, the imine (9.6 mg, 1 equiv), was added under a nitrogen atmosphere and dissolved in 25% of the THF solvent. In another vial n-BuLi (2.5 M in hexanes, 0.022 mL, 1.1 equiv) was added and dissolved in 25% of the THF solvent and placed in the freezer for 10 minutes. Diisopropylamine (8 μL, 1.1 equiv) was then added to the n-BuLi vial and stirred for 10 minutes before the imine dissolved in 25% of the THF vial was added. This mixture was stirred for 10 minutes before being cooled in the freezer for 10 minutes along with the bicyclobutane vial. The imine vial was then added dropwise to the bicyclobutane, and the mixture was left to stir at room temperature overnight. The reaction was quenched with NH_4Cl and extracted with TBME. The organic layers were dried with Mg_2SO_4, filtered and the solvent was evaporated. the amounts of product and starting materials were determined by NMR spectroscopy relative to the internal standard (1,3,5-trimethoxybenzene). No product (no peak at 4.06 ppm, H_a), imine (no peak at 4.39 ppm, H_b), or BCB (no peak at 1.99 ppm, H_c) were observed.

^{1}H NMR (300 MHz, $CDCl_3$, 292 K, ppm)

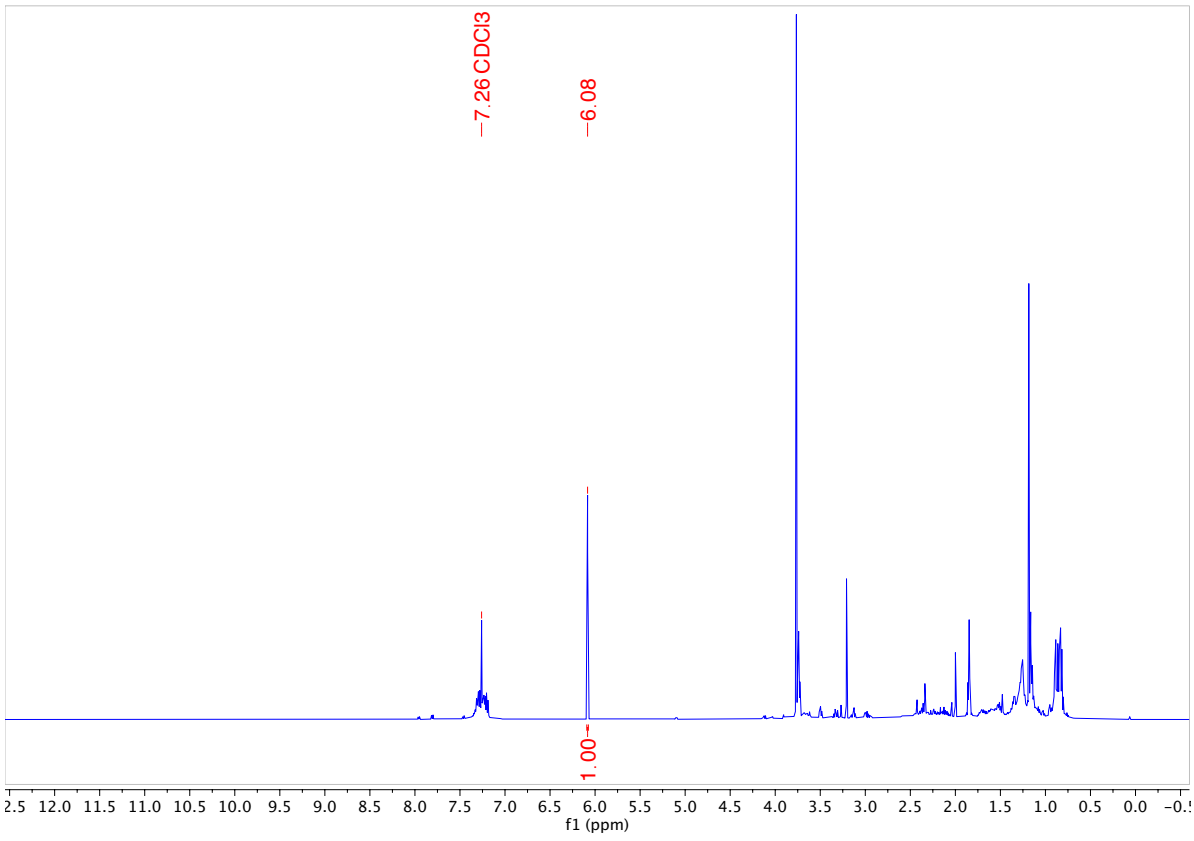

Table 3.1, entry 4

In one vial, the bicyclobutane (8.4 mg, 1 equiv), imine (14.3 mg, 1.5 equiv) and 1,3,5-trimethoxybenzene (2.8 mg, 0.33 equiv) were added and flushed with nitrogen followed by the addition of 50% of the anhydrous THF solvent (1 mL total, 0.05 M). To another vial, NaH in 60% mineral oil (2.2 mg, 2 equiv) was added and flushed with nitrogen and then dissolved in 50% of the anhydrous THF solvent. The NaH solution was then added dropwise to the BCB, and imine solution and the mixture was left to stir at room temperature overnight. The reaction was quenched with water and extracted with ethyl acetate. The organic layers were dried with Mg_2SO_4, filtered and the solvent was evaporated. the amounts of product and starting materials were determined by NMR spectroscopy relative to the internal standard (1,3,5-trimethoxybenzene). No product (no peak at 4.06 ppm, H_a), 68% imine (4.42 ppm peak, H_b) and 99% BCB (1.99 ppm peak, H_c) was observed.

^{1}H NMR (300 MHz, $CDCl_3$, 292 K, ppm)

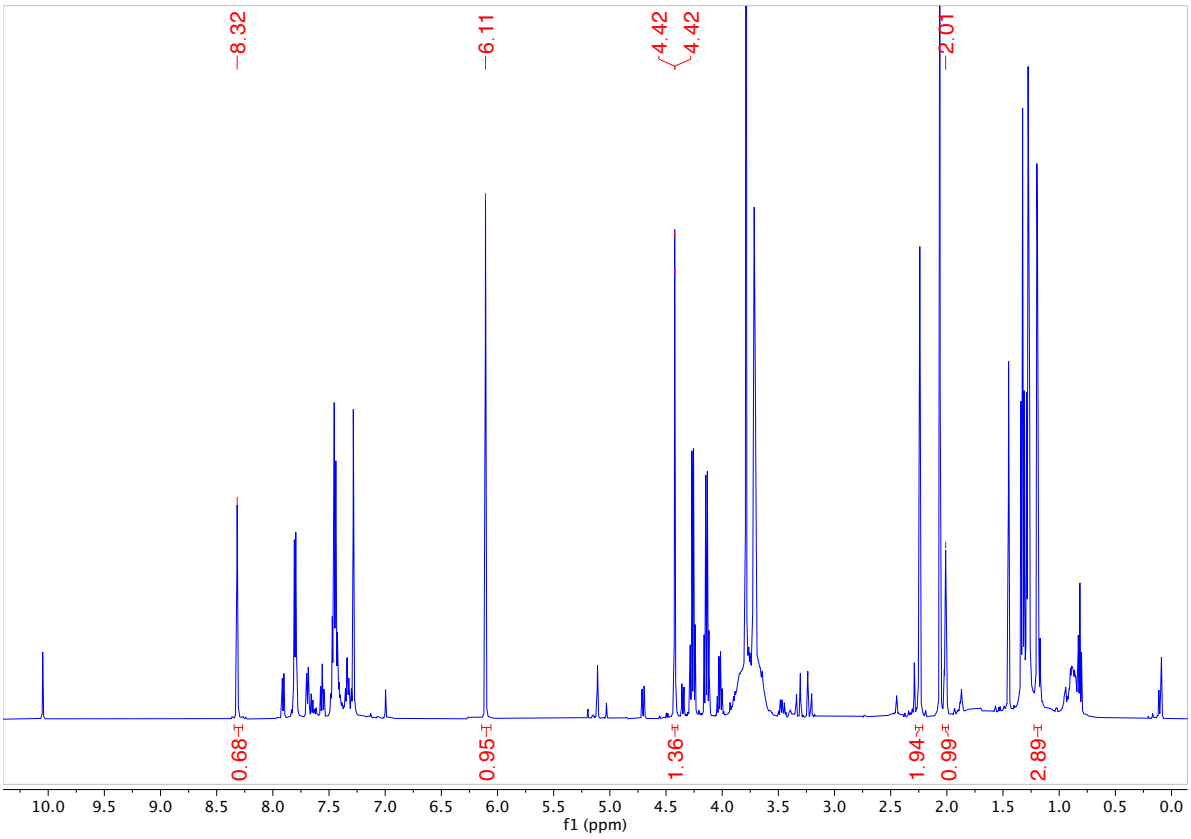

Table 3.1, entry 5

In one vial, the bicyclobutane (8.4 mg, 1 equiv) and 1,3,5-trimethoxybenzene (2.8 mg, 0.33 equiv) were added and to another vial, the imine (11.5 mg, 1.2 equiv), was added under a nitrogen atmosphere. 50% of the THF solvent (1 mL total, 0.05 mmol) was added to the bicyclobutane and 25% of the THF was added to the imine and 25% to a separate vial that contained KHMDS (0.5 M in toluene, 0.15 mL, 1.5 equiv). The imine was added dropwise to the KHMDS and left to stir for 10 minutes at room temperature. The imine/KHMDS mixture was added dropwise to the bicyclobutane vial. The reaction was left to stir for 24 hours at room temperature. The reaction was quenched with water and the organic solvent was dried with Mg_2SO_4, filtered and the solvent was evaporated. The amounts of product and starting materials were determined by NMR spectroscopy relative to the internal standard (1,3,5-trimethoxybenzene). No product (no peak at 4.06 ppm, H_a), 35% imine (4.40 ppm peak, H_b), and 67% bicyclobutane (1.99 ppm peak, H_c) was observed.

^{1}H NMR (300 MHz, $CDCl_3$, 292 K, ppm)

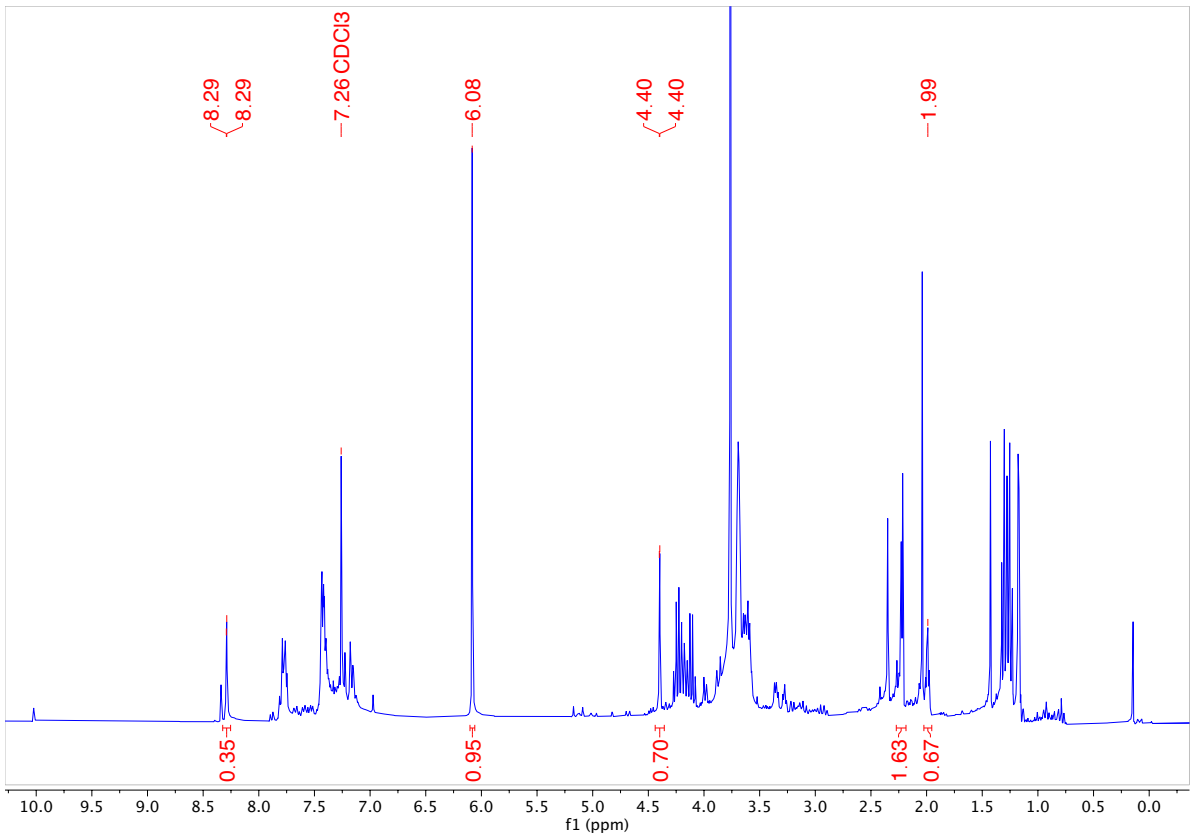

Table 3.1, entry 6

In one vial, the bicyclobutane (8.4 mg, 1 equiv) and 1,3,5-trimethoxybenzene (2.8 mg, 0.33 equiv) were added and to another vial, the imine (9.6 mg, 1 equiv), was added under a nitrogen atmosphere. 50% of the THF solvent (1 mL total, 0.05 mmol) was added to the bicyclobutane and 25% of the THF was added to the imine and 25% to a separate vial that contained LiHMDS (1.0M in THF, 0.05 mL, 1 equiv). The imine was added dropwise to the LiHMDS and left to stir for 10 minutes at room temperature. The imine/LiHMDS mixture was added dropwise to the bicyclobutane vial. The reaction was left to stir for 24 hours at room temperature. The reaction was quenched with NH_4Cl, and the organic solvent was dried with Mg_2SO_4, filtered and the solvent was evaporated. The amounts of product and starting materials were determined by NMR spectroscopy relative to the internal standard (1,3,5-trimethoxybenzene). 20% product (4.06 ppm, H_a peak), 17% imine (4.39 ppm peak, H_b), 18% benzaldehyde (from imine hydrolysis, 10.02 ppm peak), and no bicyclobutane (no 1.99 ppm peak, H_c) was observed.

^{1}H NMR (300 MHz, $CDCl_3$, 292 K, ppm)

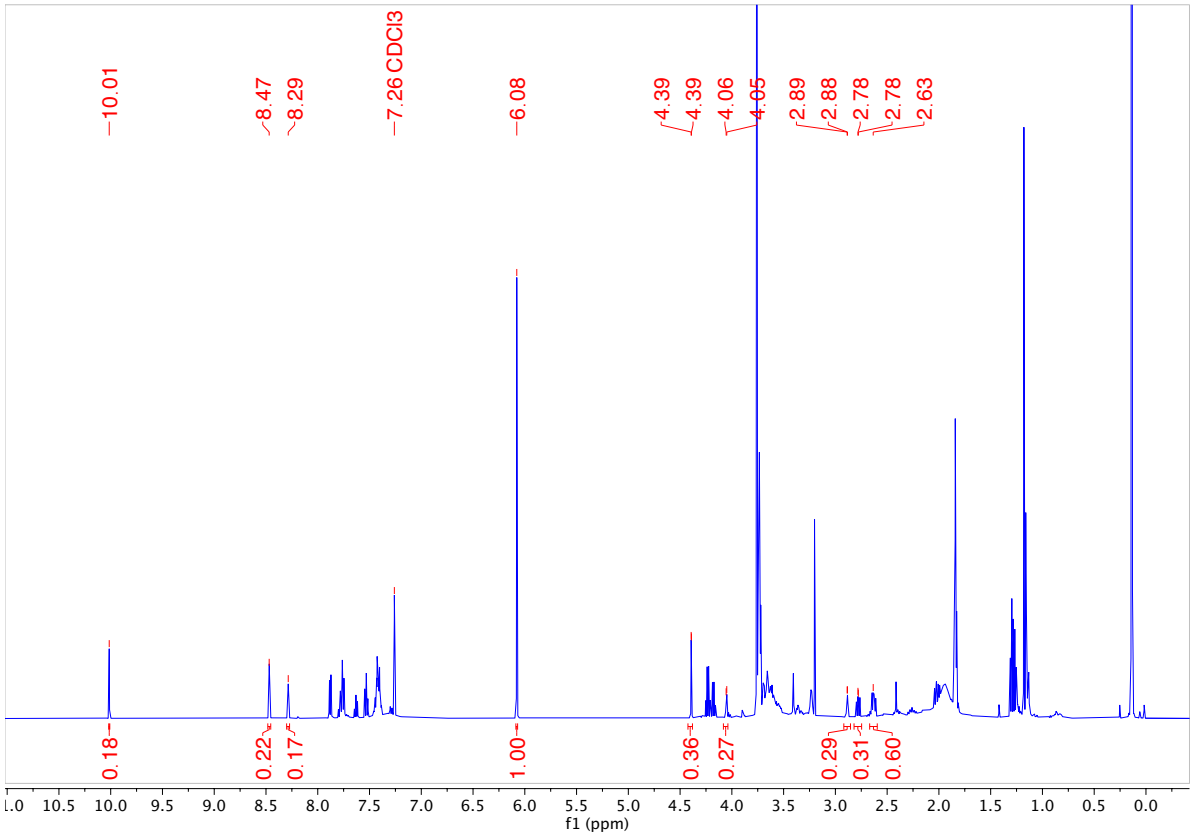

Table 3.1, entry 7

In one vial, the bicyclobutane (50.2 mg, 1 equiv) and 1,3,5-trimethoxybenzene (16.8 mg, 0.33 equiv) were added and to another vial, the imine (57.4 mg, 1 equiv), was added under a nitrogen atmosphere. 50% of the THF solvent (1 mL total, 0.05 mmol) was added to the bicyclobutane and 25% of the THF was added to the imine and 25% to a separate vial that contained LiHMDS (1.0M in THF, 0.30 mL, 1 equiv). The imine was added dropwise to the LiHMDS and left to stir for 10 minutes at room temperature. The imine/LiHMDS mixture was added dropwise to the bicyclobutane vial. The reaction was left to stir for 24 hours at room temperature. The reaction was quenched with NH_4Cl, and the organic solvent was dried with Mg_2SO_4, filtered and the solvent was evaporated. The amounts of product and starting materials were determined by NMR spectroscopy relative to the internal standard (1,3,5-trimethoxybenzene). 11% product (4.06 ppm, H_a peak), 9% imine (4.39 ppm peak, H_b), 4% benzaldehyde (from imine hydrolysis, 10.02 ppm peak), and 15% bicyclobutane (2.22 ppm peak, H_c).

^{1}H NMR (300 MHz, $CDCl_3$, 292 K, ppm)

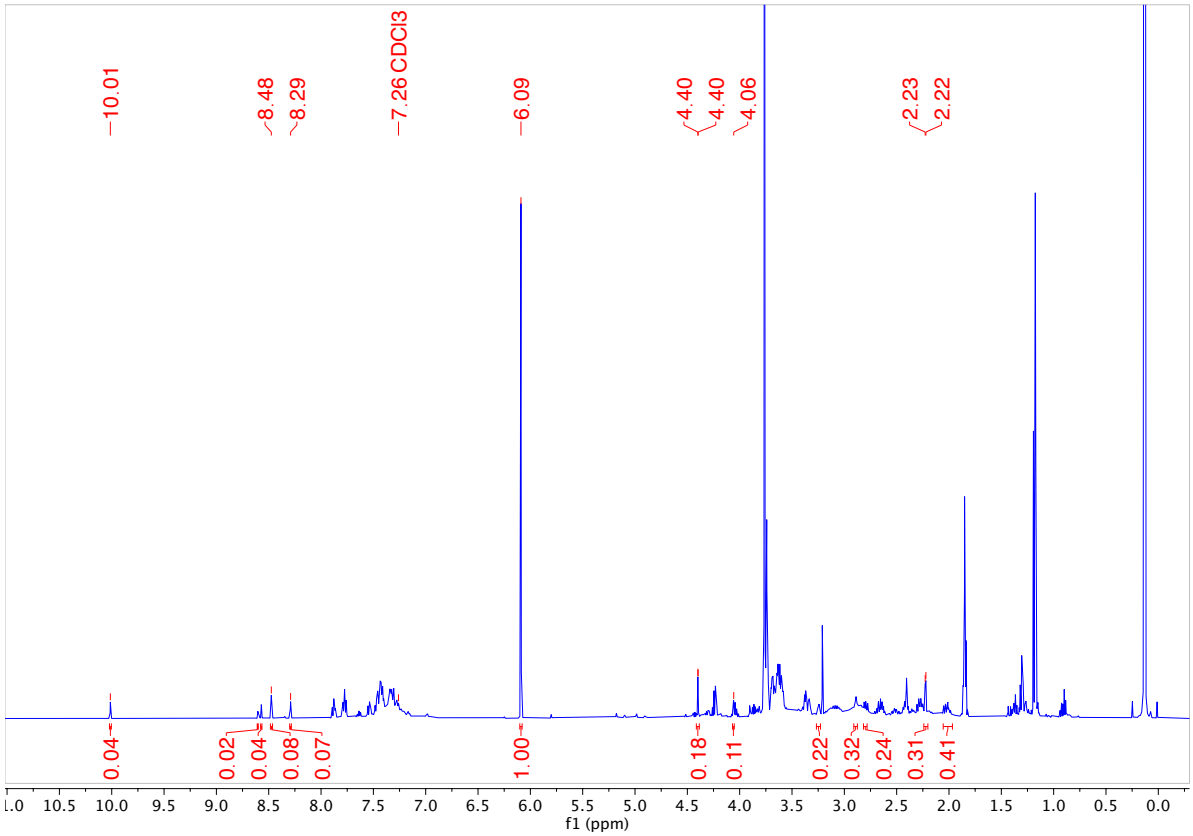

Table 3.1, entry 8

In one vial, the bicyclobutane (50.2 mg, 1 equiv) and 1,3,5-trimethoxybenzene (16.8 mg, 0.33 equiv) were added and to another vial, the imine (68.8 mg, 1.2 equiv), was added under a nitrogen atmosphere. 50% of the THF solvent (6 mL total, 0.05 mmol) was added to the bicyclobutane and 25% of the THF was added to the imine and 25% to a separate vial that contained LiHMDS (1.0M in THF, 0.45 mL, 1.5 equiv). The imine was added dropwise to the LiHMDS and left to stir for 10 minutes at room temperature. The imine/LiHMDS mixture was added dropwise to the bicyclobutane vial. The reaction was left to stir for 24 hours at room temperature. The reaction was quenched with $NaHCO_3$, and the organic solvent was dried with Mg_2SO_4, filtered and the solvent was evaporated. The amounts of product and starting materials were determined by NMR spectroscopy relative to the internal standard (1,3,5-trimethoxybenzene). 39% product (4.01 ppm peak, H_a), 17% imine (4.33 ppm peak, H_b), 10% benzaldehyde (from imine hydrolysis, 9.94 ppm peak), and 11% bicyclobutane (2.15 ppm peak, H_c).

^{1}H NMR (300 MHz, $CDCl_3$, 292 K, ppm)

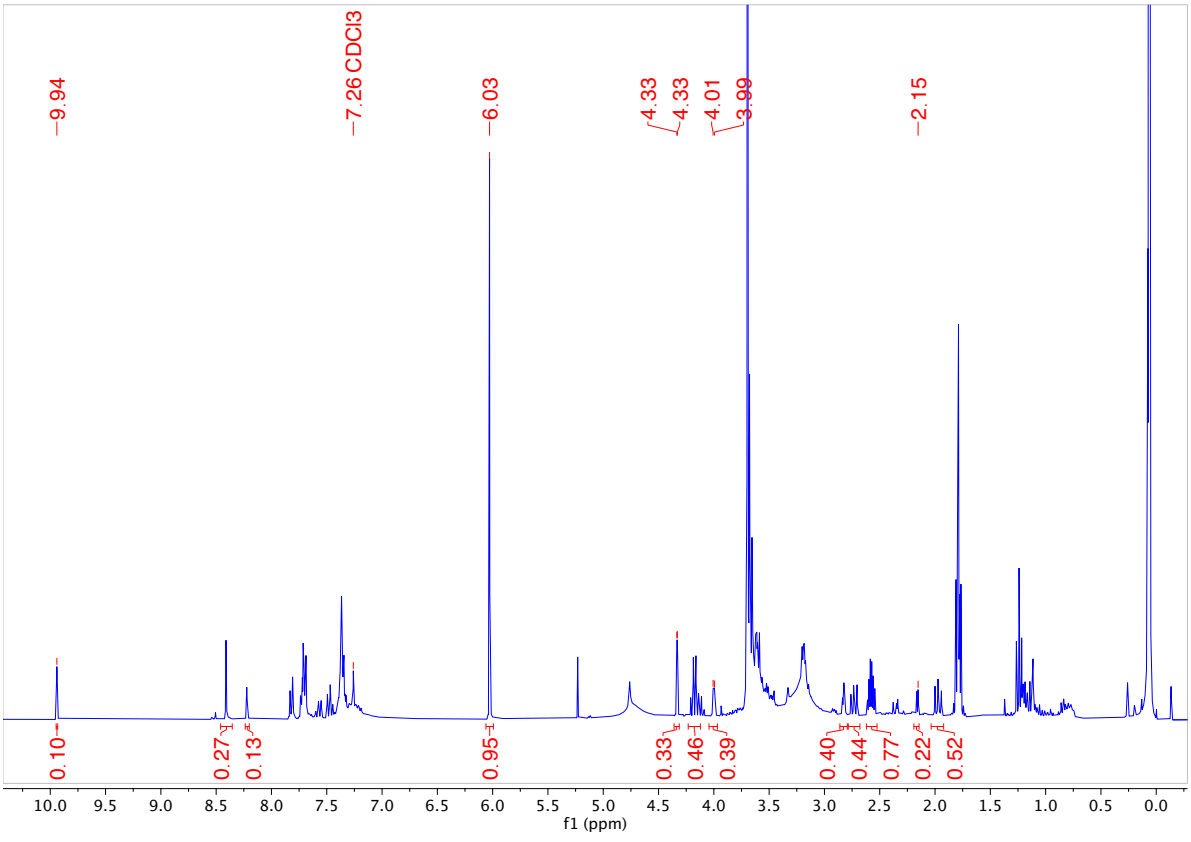

Table 3.1, entry 9

In one vial, the bicyclobutane (50.2 mg, 1 equiv) and 1,3,5-trimethoxybenzene (16.8 mg, 0.33 equiv) were added and to another vial, the imine (68.8 mg, 1.2 equiv), was added under a nitrogen atmosphere. 50% of the THF solvent (1 mL total, 0.3 mmol) was added to the bicyclobutane and 50% of the THF was added to the imine. LiHMDS (1.0M in THF, 0.45 mL, 1.5 equiv) was added to the imine vial and left to stir for 10 minutes at room temperature. The two vials were then cooled in the freezer for 10 minutes followed by a dropwise addition of the BCB to the enolate vial. The reaction was left to stir for 24 hours at room temperature. The reaction was quenched with $NaHCO_3$ and extracted with ethyl acetate 3 times. The organic layers were dried with Mg_2SO_4, filtered and the solvent was evaporated. The amounts of product and starting materials were determined by NMR spectroscopy relative to the internal standard (1,3,5-trimethoxybenzene). 47% product (2.89 ppm peak, H_a), no imine (no peak at 4.33 ppm, H_b) and 21% bicyclobutane (2.22 ppm peak, H_c).

^{1}H NMR (300 MHz, $CDCl_3$, 292 K, ppm)

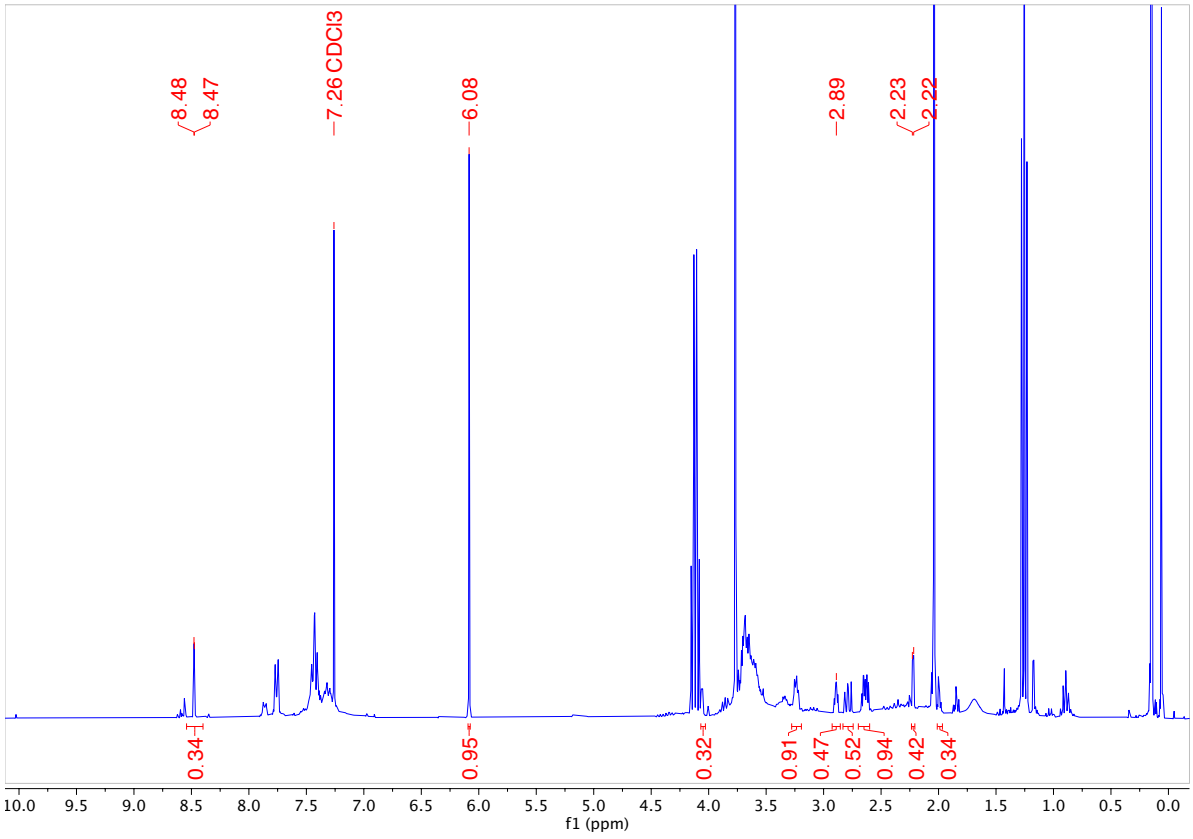

B.3 Substrate Synthesis

B.3.1 Imine Synthesis

General Procedure: The aldehyde (1 equiv) and amine (1.2 equiv) were added to a vial and dissolved in Toluene (0.6 M). Then DIPEA (1.3 equiv) and excess anhydrous Na_2SO_4 was added to the vial, and it was left to stir at room temperature for 24 hours. The solution was then filtered, and the solvent was evaporated to give the desired imine without further purification.

Imine **2b** was purchased from Oakwood chemicals.

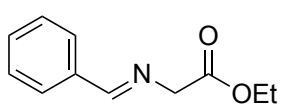

2a

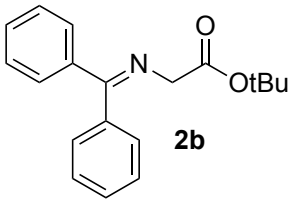

2b

B.3.2 Ethyl Ester Acetate Synthesis

General Procedure: The acetic acid derivative (1 equiv) was dissolved in ethanol in a vial and sulfuric acid was added (0.5 equiv). The vial was heated to 70 °C overnight then the vial was cooled, and the solvent was evaporated. The residue was quenched with $NaHCO_3$ until the solution was basic, determined by pH indicator paper. The solution was then extracted by TBME, dried with Mg_2SO_4, filtered and the solvent was evaporated to give the desired ethyl ester acetate without further purification.[205–210]

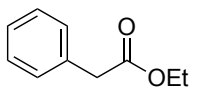

2c

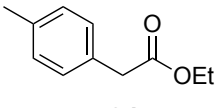

2d

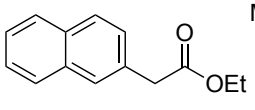

2e

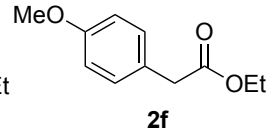

2f

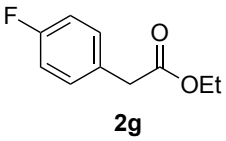

2g

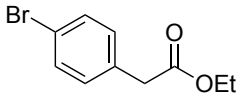

2h

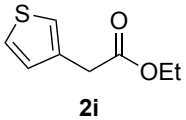

2i

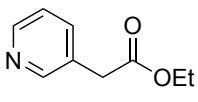

2j

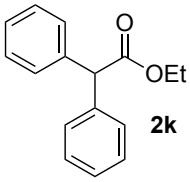

2k

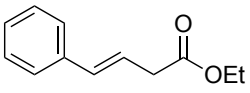

2p

B.3.3 Bicyclobutane Synthesis

Bicyclobutanes synthesized.[65;106;121;144;150;213]

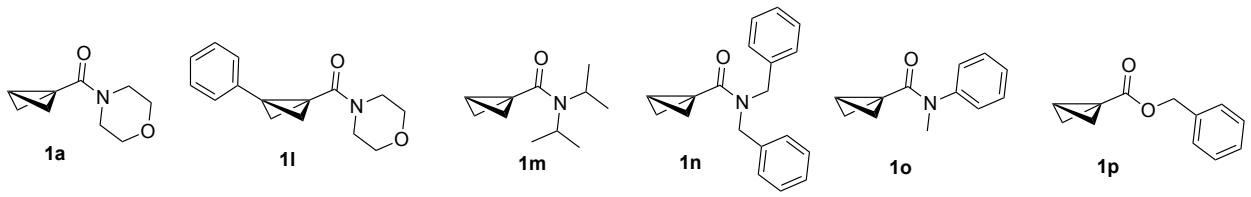

General Procedure 1a (Amidation/Esterification from acyl chloride)[121]
The alcohol or amide (1.2 equiv) and DIPEA (1 equiv) was added to the reaction vessel, dissolved in DCM, and then cooled to 0 °C. 3-oxocyclobutane-1-carbonyl chloride (1 equiv) dissolved in DCM was added dropwise to the solution. The reaction mixture was then warmed to room temperature and left to stir overnight. The reaction mixture was quenched with water and extracted with DCM. The organic solvent was dried with Mg_2SO_4, filtered and the solvent was evaporated to give the crude product. The compound was purified by column chromatography.

General Procedure 1b (Amidation/Esterification from carboxylic acid)[211]
3-Oxocyclobutane-1-carboxylic acid (1 equiv) was dissolved in THF (0.40 M) in a round bottom flask and the solution was cooled down to 0 °C. Carbonyl diimidazole (1.05 equiv) was added to the flask. The solution was warmed to room temperature and left to stir for 2-3 hours before the solution was cooled back down to 0 °C and the amine (1.05 equiv) was added dropwise. The solution was then warmed to room temperature and left to stir overnight. The reaction was then quenched with NH_4Cl and then extracted with DCM. The combined organic layers were dried with Mg_2SO_4, filtered and the solvent was evaporated. The compound was purified by column chromatography.

General procedure 2 (Cyclobutanone reduction)[212]
The cyclobutanone ester or amide (1 equiv) was dissolved in methanol and cooled down to 0 °C. Sodium borohydride was added portion-wise to the reaction mixture. The solution was allowed to warm to room temperature and left to stir for 2-3 hours at room temperature. The solution was quenched with NH_4Cl and extracted with DCM. The organic layer was dried with Mg_2SO_4, filtered and the solvent was evaporated to give the product which was used without further purification.

General procedure 3 (Tosylation)[212]
The cyclobutane alcohol (1 equiv) was dissolved in DCM and cooled down to 0 °C. 4-toluenesulfonyl chloride (1.3 equiv) was added to the reaction mixture followed by triethylamine (1.3 equiv). The solution was then heated to 40 °C for 24 hours. The reaction was quenched with NH_4Cl and then extracted with DCM. The organic solvent was dried with Mg_2SO_4, filtered and the solvent was evaporated to give the crude product. The compound was purified by column chromatography.

General procedure 4 (Bicyclobutane synthesis)[212]
The cyclobutane tosylate (1 equiv) was dissolved in THF (0.15 M) under a nitrogen atmosphere. The reaction was cooled down to 0 °C then potassium *tert*-butoxide (1.1 equiv) was added to the reaction mixture. The reaction was warmed to room temperature and stirred overnight. The reaction was quenched with NH_4Cl and extracted with TBME. The organic layer was washed with $NaHCO_3$, brine before being dried with Mg_2SO_4, filtered and the solvent was evaporated to give the product without further purification.

3-Phenyl-3-hydroxycyclobutane-1-carboxylic acid[114;125;154]

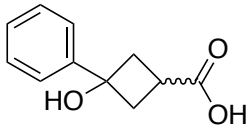

Solid 3-oxocyclobutane carboxylic acid was added to a 3-necked round bottom flask containing a stir bar and fitted with a gas inlet adapter, a septum, and an addition funnel. The apparatus was purged with nitrogen gas. Anhydrous THF was transferred to the flask via cannula, and the 3-oxocyclobutane carboxylic acid was dissolved with stirring. A solution of the Grignard reagent (2.05 equiv) was added to an addition funnel via cannula transfer, followed by slow dropwise addition to the reaction mixture over 6 hours. After the addition was complete, the reaction mixture was quenched with 6 M HCl. The aqueous layer was extracted with diethyl ether and the organic layer was dried with Mg_2SO_4. The solvent was removed under vacuum and the product was re-dissolved in saturated $NaHCO_3$. An equal amount of diethyl ether was added to extract the aqueous layer. The aqueous layer was acidified using concentrated HCl and a precipitate was formed which was filtered with vacuum filtration. The product was used in the next step without further purification.

^{1}H NMR (300 MHz, $CDCl_3$, 292 K, ppm):δ 7.64 – 7.20 (m, 7H), 3.56 (s, 1H), 2.94 (s, 3H), 2.73 (d, J = 0.6 Hz, 3H).

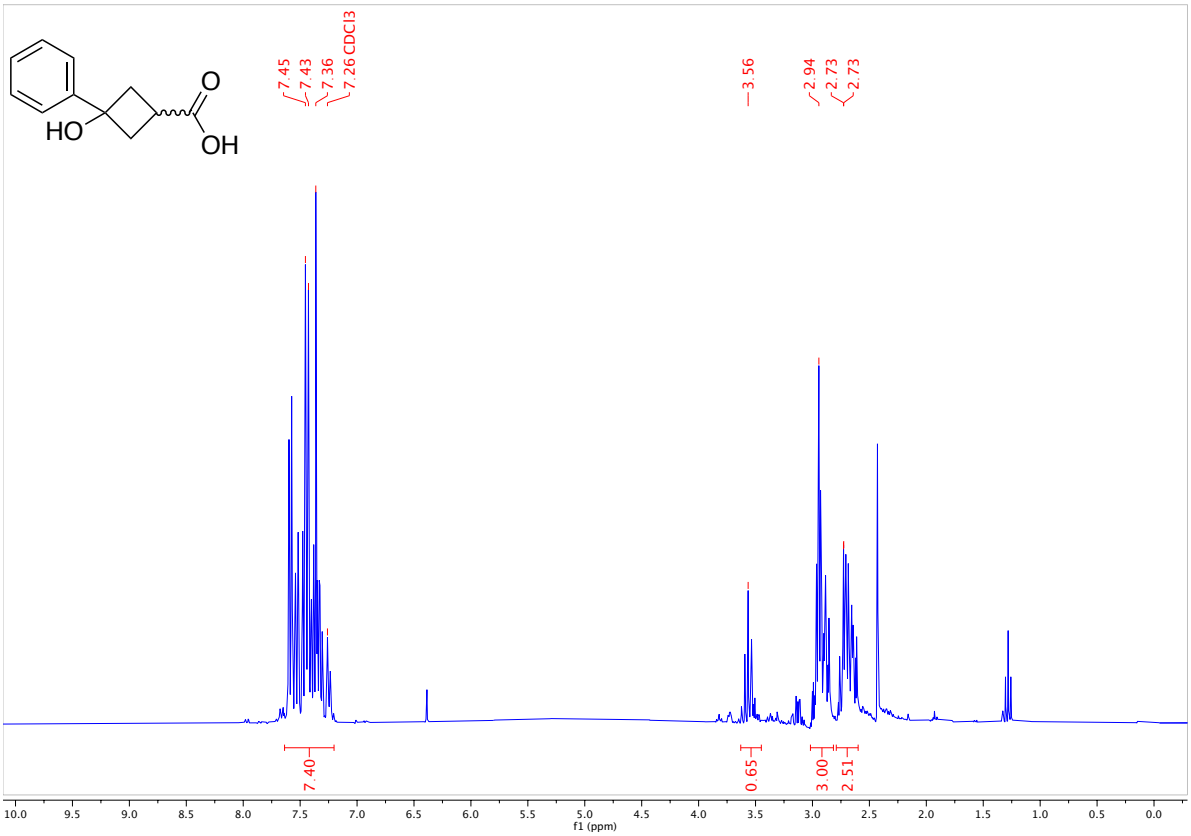

3-Phenyl-3-chlorocyclobutane-1-carboxylic acid[125]

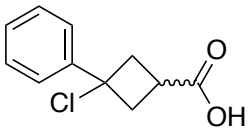

The 3-hydroxy-3-arylcyclobutane carboxylic acid was dissolved in toluene and then an equal volume of concentrated hydrochloric acid was added. The reaction mixture was stirred at room temperature for 6 hours. The two layers were separated, and the aqueous layer was extracted with toluene. The organic layers were combined and washed with water and brine. The solution was then dried with Mg_2SO_4 and the solvent was removed under vacuum. The product was used in the next step without further purification.

^{1}H NMR (300 MHz, $CDCl_3$, 292 K, ppm): δ 7.33 (s, 5H), 3.92 – 3.75 (m, 0.7H), 3.32 (m, 1H), 3.15 (m, 3H), 3.00 (m, 0.4H).

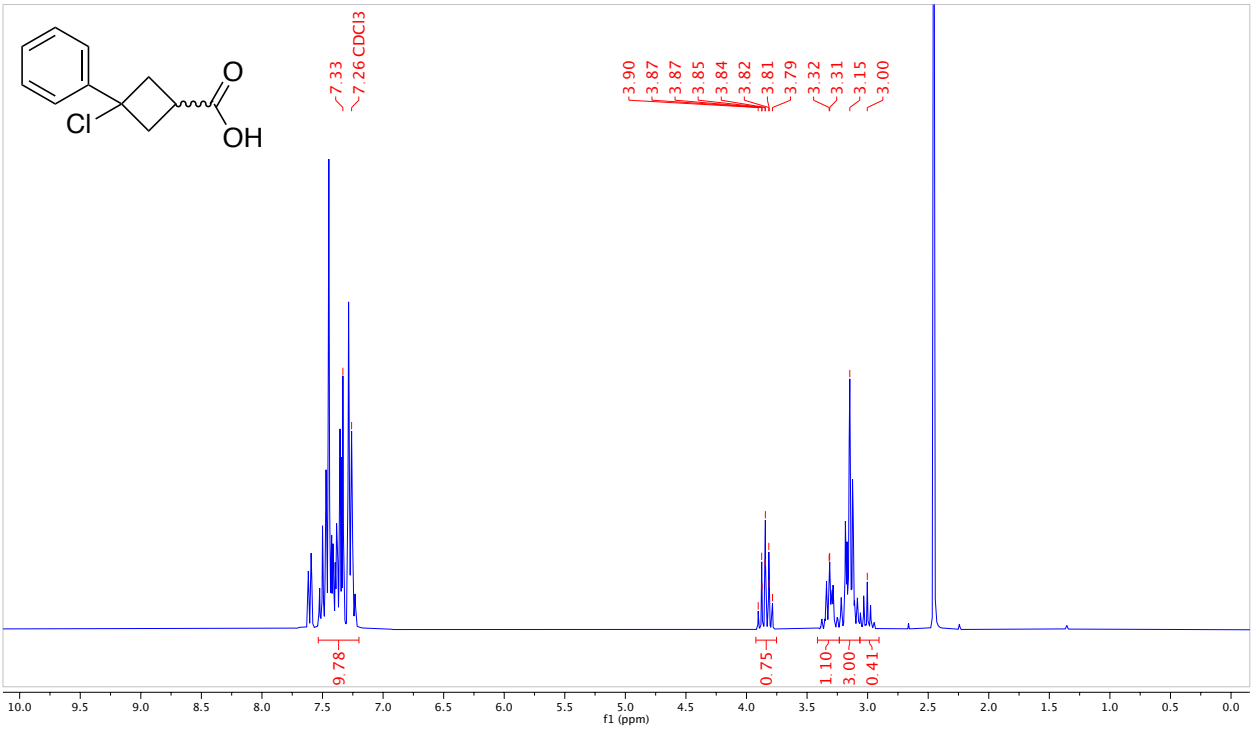

(3-Chloro-3-phenylcyclobutyl)(morpholino)methanone

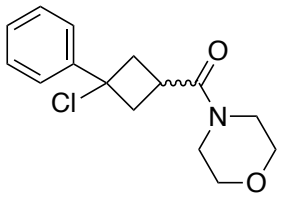

This product was prepared using general procedure **1b**. The compound was purified by column chromatography (Biotage® Sfär 25g Column, 0-100% EtOAc/hexanes, eluted at 43% EtOAc). 876 mg of an orange oil was obtained (66% Yield).

^{1}H NMR (300 MHz, $CDCl_3$, 292 K, ppm): δ 7.34 (m, 5H), 3.89 – 3.73 (m, 1H), 3.66 (m, 6H), 3.46 (m, 2H), 3.11 (m, 2H), 2.96 (m, 2H).

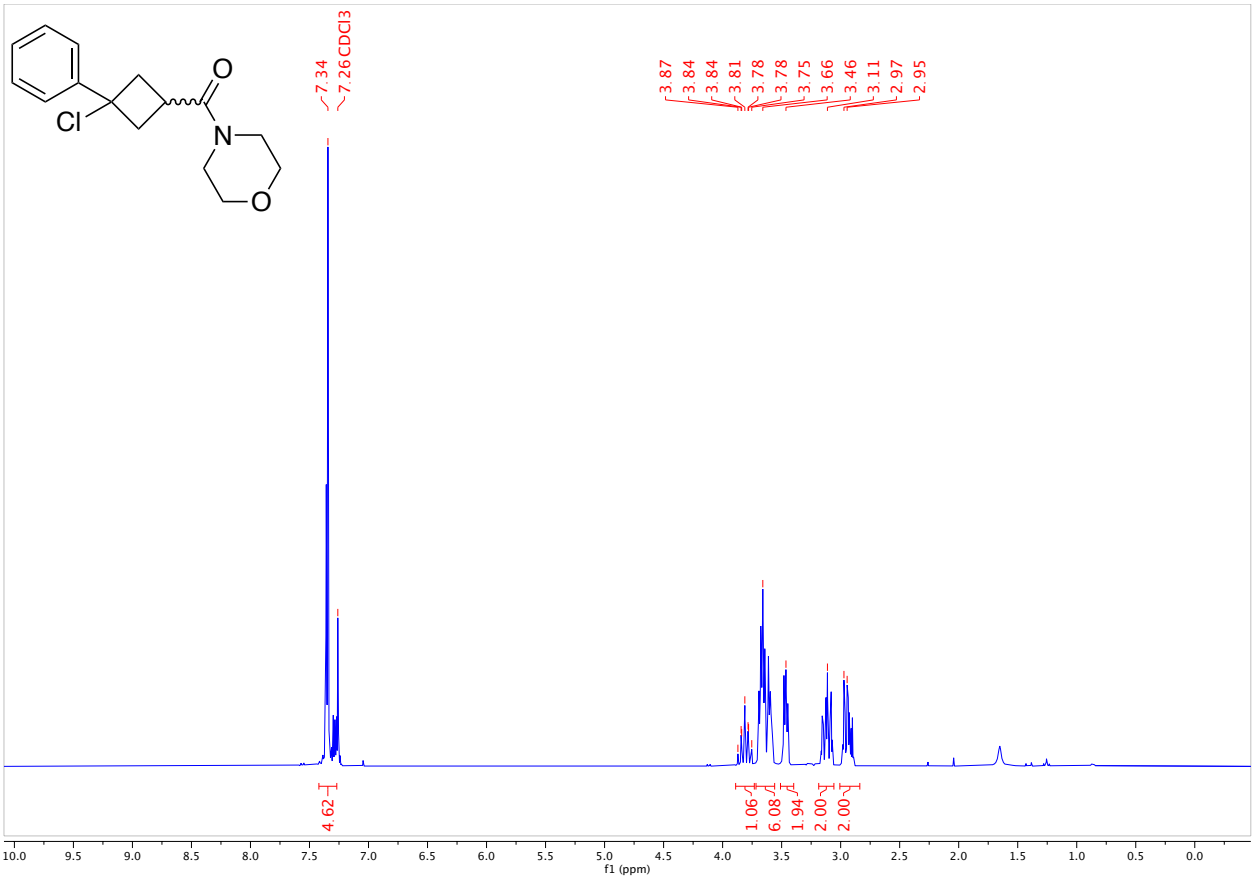

3-Oxocyclobutane-1-carbonyl chloride[121]

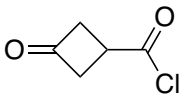

3-oxocyclobutane-1-carboxylic acid (5.0 g. 43.8 mmol) was added to a round bottom flask and dissolved in DCM. A drop of DMF was added and the solution was cooled down to 0 °C. Oxalyl chloride (5.6 mL, 1.5 equiv) was added dropwise to the reaction flask. The solution was allowed to warm to room temperature and was left to stir for 24 hours. The solvent was then evaporated to give the product with quantitative yield as a brown oil.

^{1}H NMR (300 MHz, $CDCl_3$, 292 K, ppm): δ 5.62-5.75 (m, 1H), 5.43-5.57 (m, 2H), 5.28-5.43 (m, 2H).

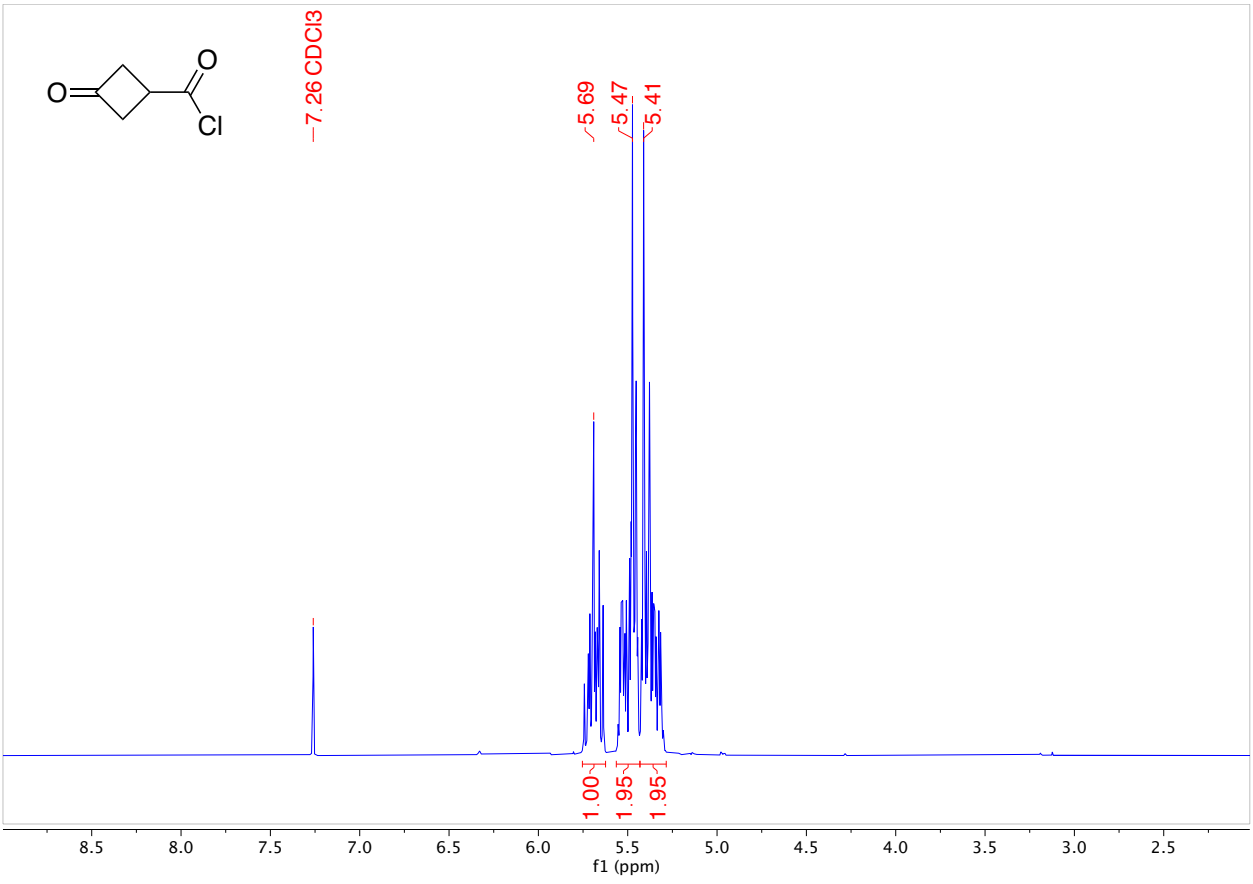

3-(Morpholine-4-carbonyl)cyclobutan-1-one

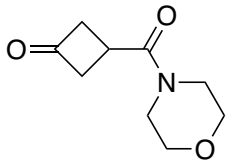

This product was prepared using general procedure **1b**. The compound was purified by column chromatography (Biotage® Sfär 50g Column, 0-100% MeOH/DCM, eluted at 15% MeOH). 3.03 grams of an orange oil was obtained (94% Yield).

^{1}H NMR (300 MHz, $CDCl_3$, 292 K, ppm): δ 3.74-3.62 (m, 6H), 3.58-3.46 (m, 4H), 3.39-3.13 (m, 3H).

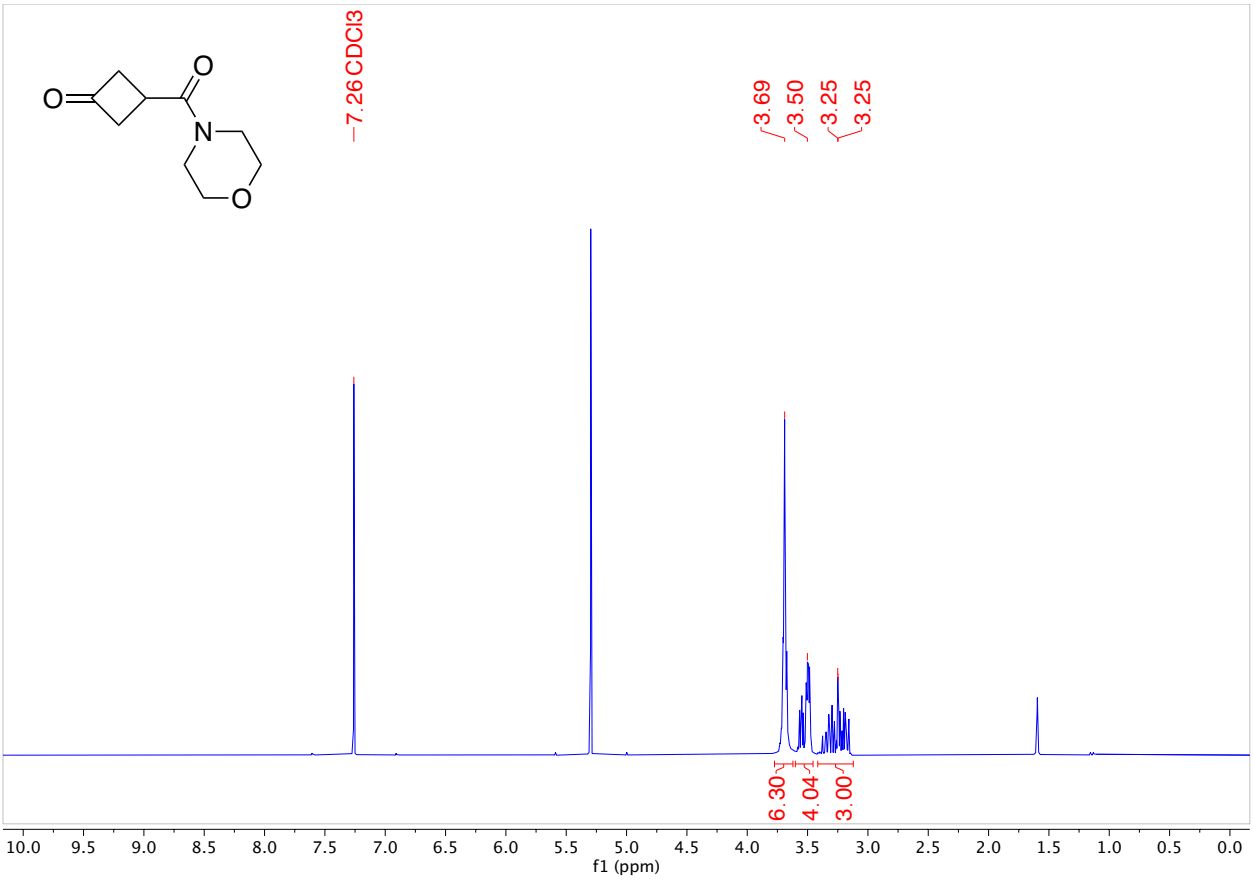

N,*N*-Diisopropyl-3-oxocyclobutane-1-carboxamide

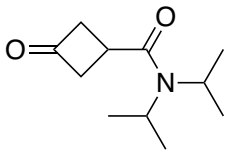

This product was prepared using general procedure **1a**. Isolated 689 mg of an orange oil (93% Yield).

^{1}H NMR (300 MHz, $CDCl_3$, 292 K, ppm): δ 3.98 (septet, 1H), 3.62-3.41 (m, 3H), 3.35-3.21 (m, 1H), 3.20-3.07 (m, 2H), 1.40 (d, 6H), 1.23 (d, 6H).

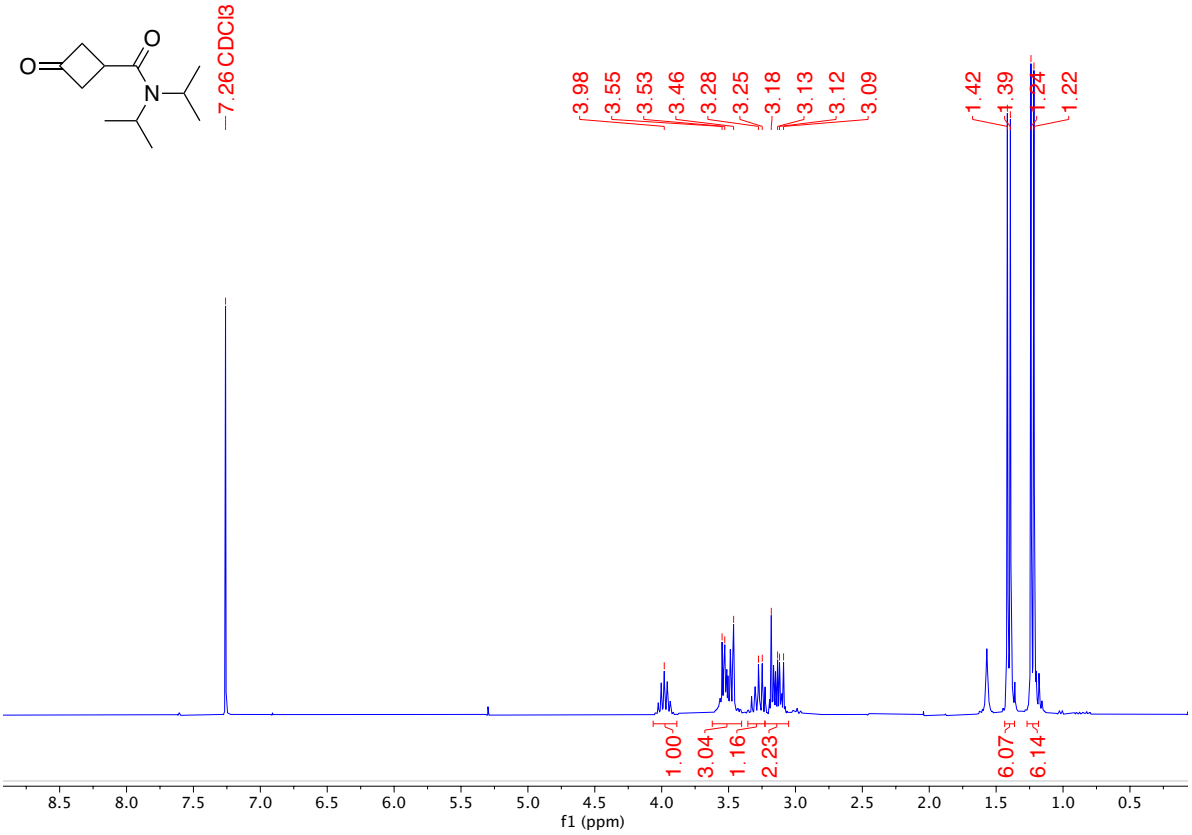

N,*N*-Dibenzyl-3-oxocyclobutane-1-carboxamide

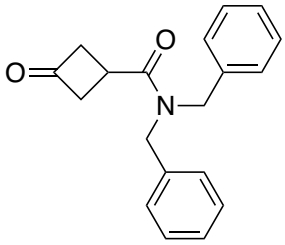

This product was prepared using general procedure **1b**. The compound was purified by column chromatography (Biotage® Sfär 50g Column, 0-100% EtOAc/hexanes, eluted at 24% EtOAc). 3.3 g of a yellow oil was obtained (100% Yield).

^{1}H NMR (300 MHz, $CDCl_3$, 292 K, ppm):δ7.35 (m, 10H), 4.69 (s, 2H), 4.50 (s, 2H), 3.53 (m, 2H), 3.39 (m, 1H), 3.16 (m, 2H).

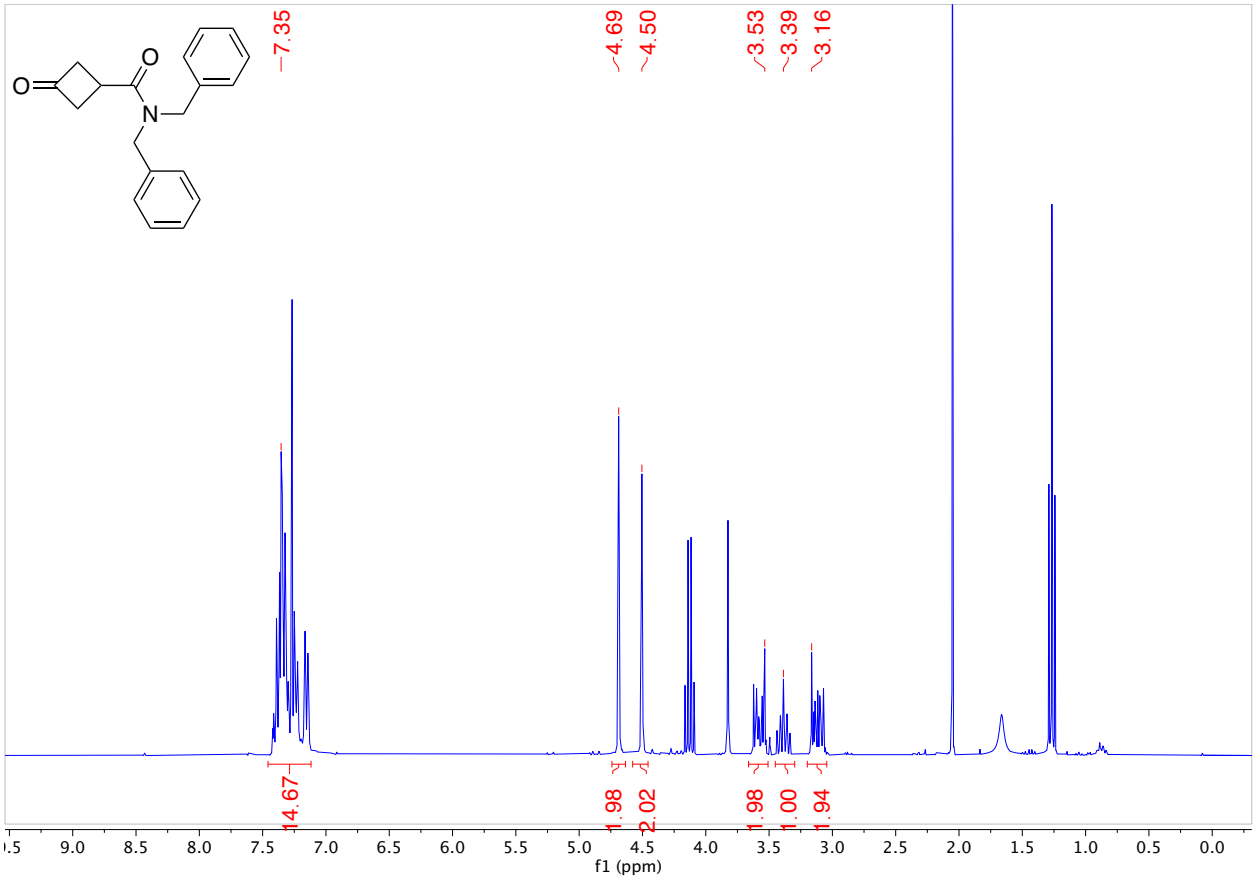

***N*-Methyl-3-oxo-*N*-phenylcyclobutane-1-carboxamide**

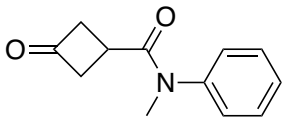

This product was prepared using general procedure **1b**. The compound was purified by column chromatography (Biotage® Sfär 25g Column, 0-100% EtOAc/hexanes, eluted at 35% EtOAc). 890 mg of a yellow oil was obtained (28% Yield).

^{1}H NMR (300 MHz, $CDCl_3$, 292 K, ppm): δ 7.47 (dd, J = 8.4, 6.9 Hz, 2H), 7.44 – 7.35 (m, 1H), 7.20 (d, J = 7.0 Hz, 2H), 3.50 (m, 2H), 3.35 (s, 3H), 3.05 (dq, J = 9.0, 7.2 Hz, 1H), 2.97 – 2.83 (m, 2H).

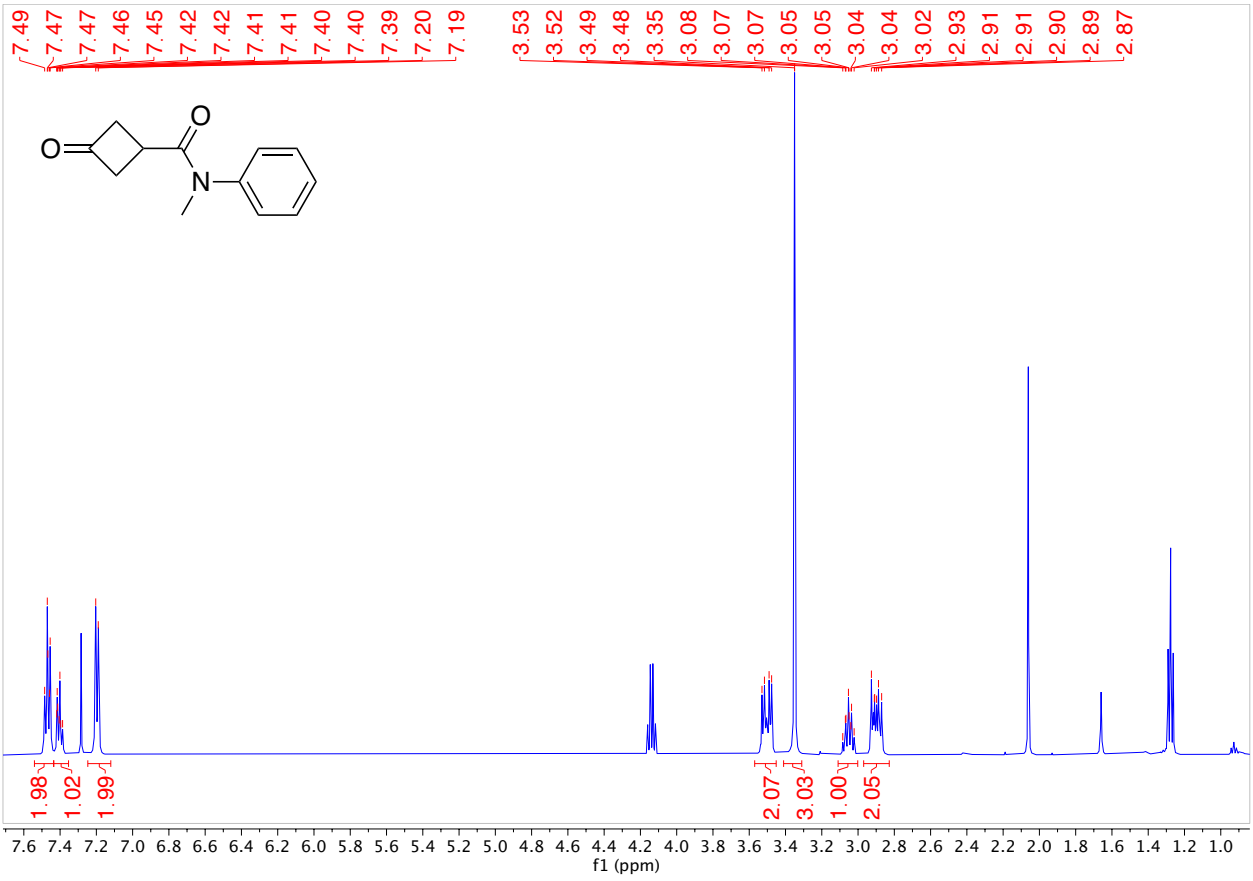

Benzyl 3-oxocyclobutane-1-carboxylate

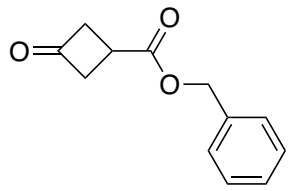

3-Oxocyclobutane carboxylic acid (2.0 g, 17.5 mmol) was dissolved in acetonitrile in a round bottom flask and potassium carbonate (3.63 g, 1.5 equiv) was added. Then benzyl bromide (2.29 mL, 1.1 equiv) was added to the flask and the reaction was left to stir overnight at 50 °C. The reaction was quenched with water and extracted with ethyl acetate. The organic layers were dried with Mg_2SO_4, filtered and the solvent was evaporated to obtain the crude product. The compound was purified by column chromatography (Biotage® Sfär 50g Column, 0-100% EtOAc/hexanes, eluted at 35% EtOAc). 1.84 grams of a white solid was obtained (51% Yield).

^{1}H NMR (300 MHz, $CDCl_3$, 292 K, ppm): δ 7.37 (m, 5H), 5.19 (s, 2H), 3.52 – 3.20 (m, 5H).

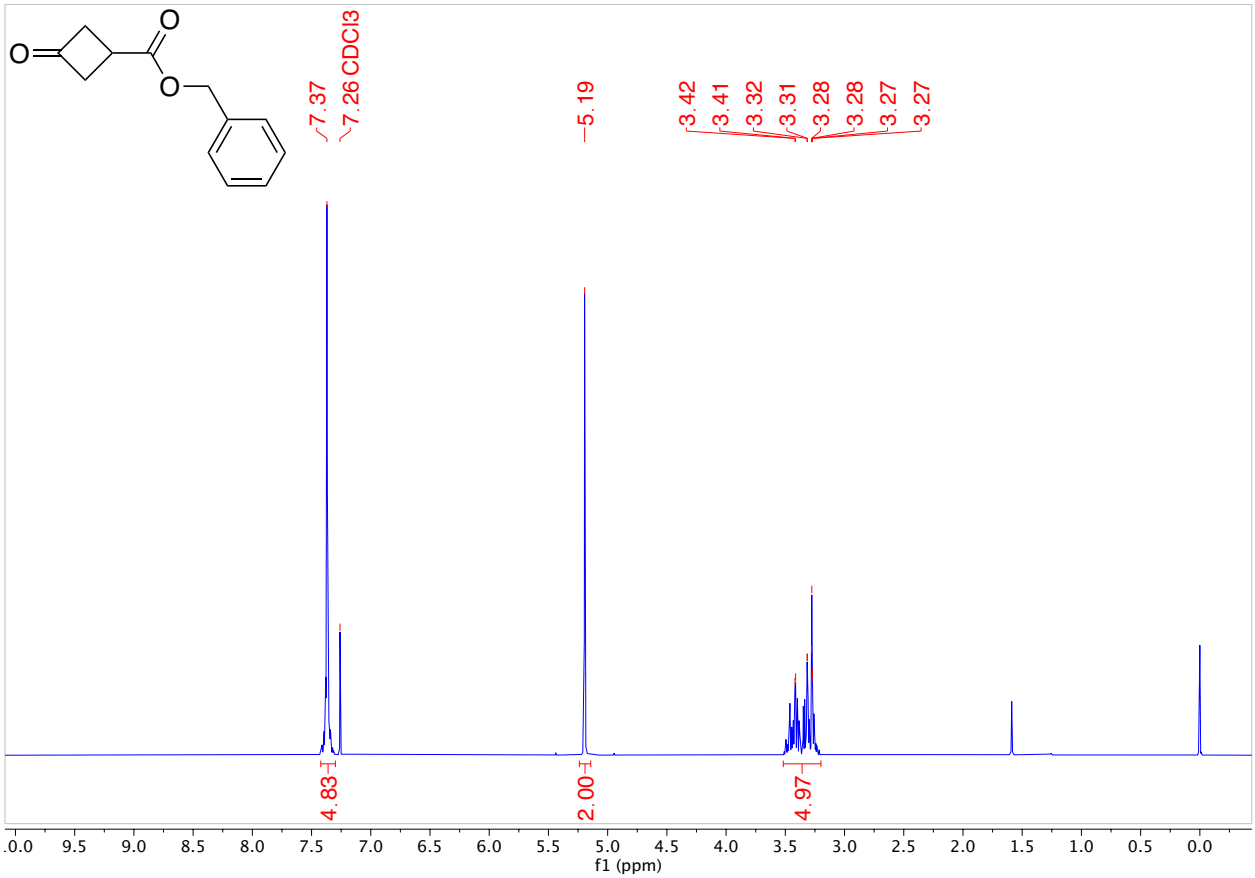

(3-Hydroxycyclobutyl)(morpholino)methanone

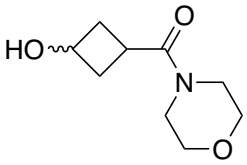

This product was prepared using **general procedure 2**. Isolated 4.21 grams of a white powder (94% Yield).

^{1}H NMR (300 MHz, $CDCl_3$, 292 K, ppm): δ 4.18 (septet, 1H), 3.69-3.58 (m, 6H), 3.43-3.36 (m, 2H), 2.80-2.67 (m, 1H), 2.62-2.49 (m, 2H), 2.28-2.15 (m, 2H).

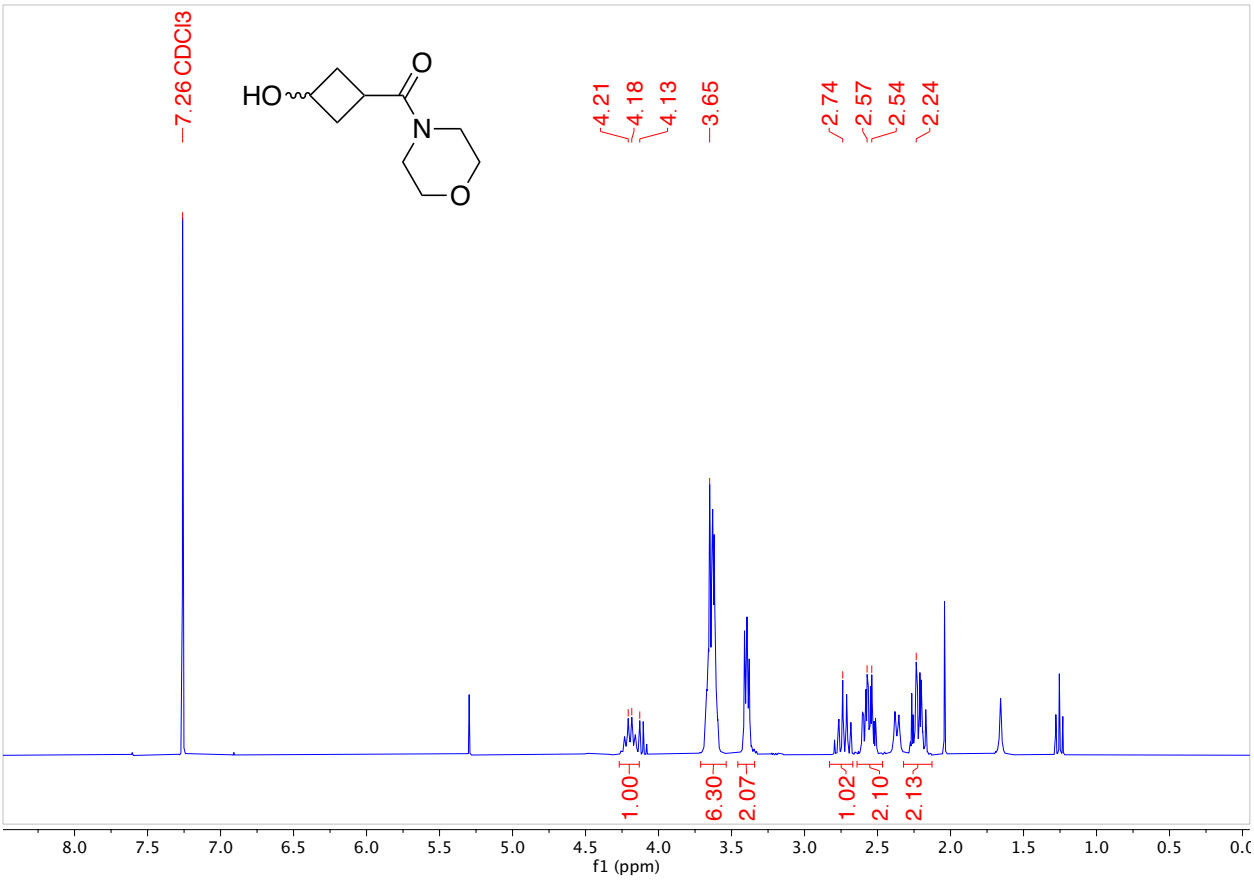

3-Hydroxy-N,*N*-diisopropylcyclobutane-1-carboxamide

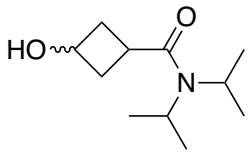

This product was prepared using **general procedure 2**. Isolated 600 mg of a brown solid (86% Yield).

^{1}H NMR (300 MHz, $CDCl_3$, 292 K, ppm):δ 4.17 (sextet, J = 7.3 Hz, 1H), 3.87 (s, 1H), 2.71 (m, 1H), 2.54 (s, 3H), 2.20 (s, 2H), 1.37 (d, J = 6.8 Hz, 7H), 1.16 (d, J = 6.7 Hz, 6H).

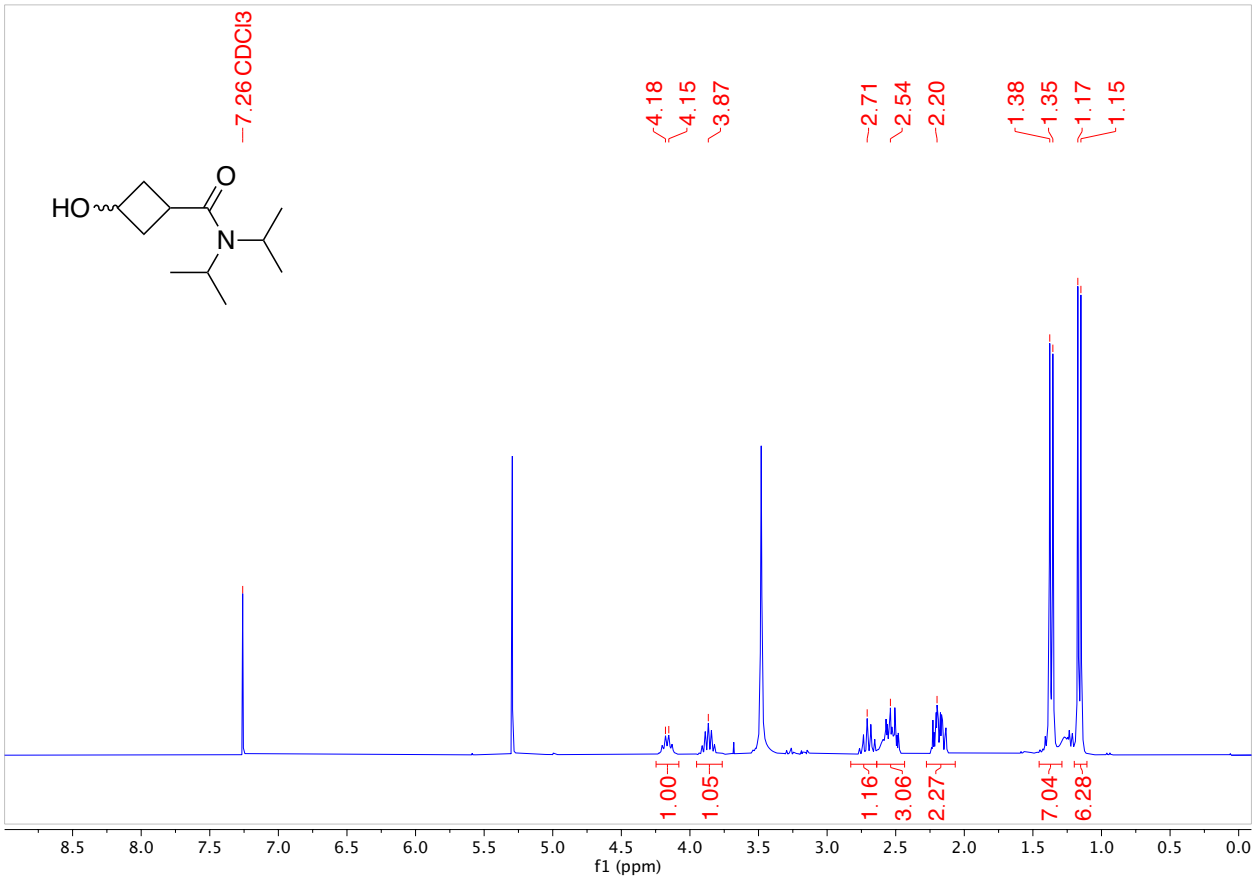

N,*N*-Dibenzyl-3-hydroxycyclobutane-1-carboxamide

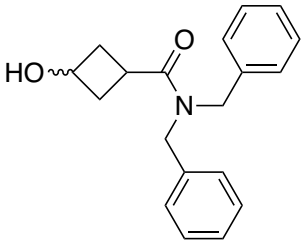

This product was prepared using **general procedure 2**. Isolated 3.23 grams of a clear colourless oil (100% Yield).

^{1}H NMR (300 MHz, $CDCl_3$, 292 K, ppm):δ 7.25 – 6.99 (m, 10H), 4.51 (s, 2H), 4.30 (s, 2H), 4.13 – 3.99 (m, 1H), 2.86 – 2.68 (m, 1H), 2.44 (m, 2H), 2.31 – 2.15 (m, 2H).

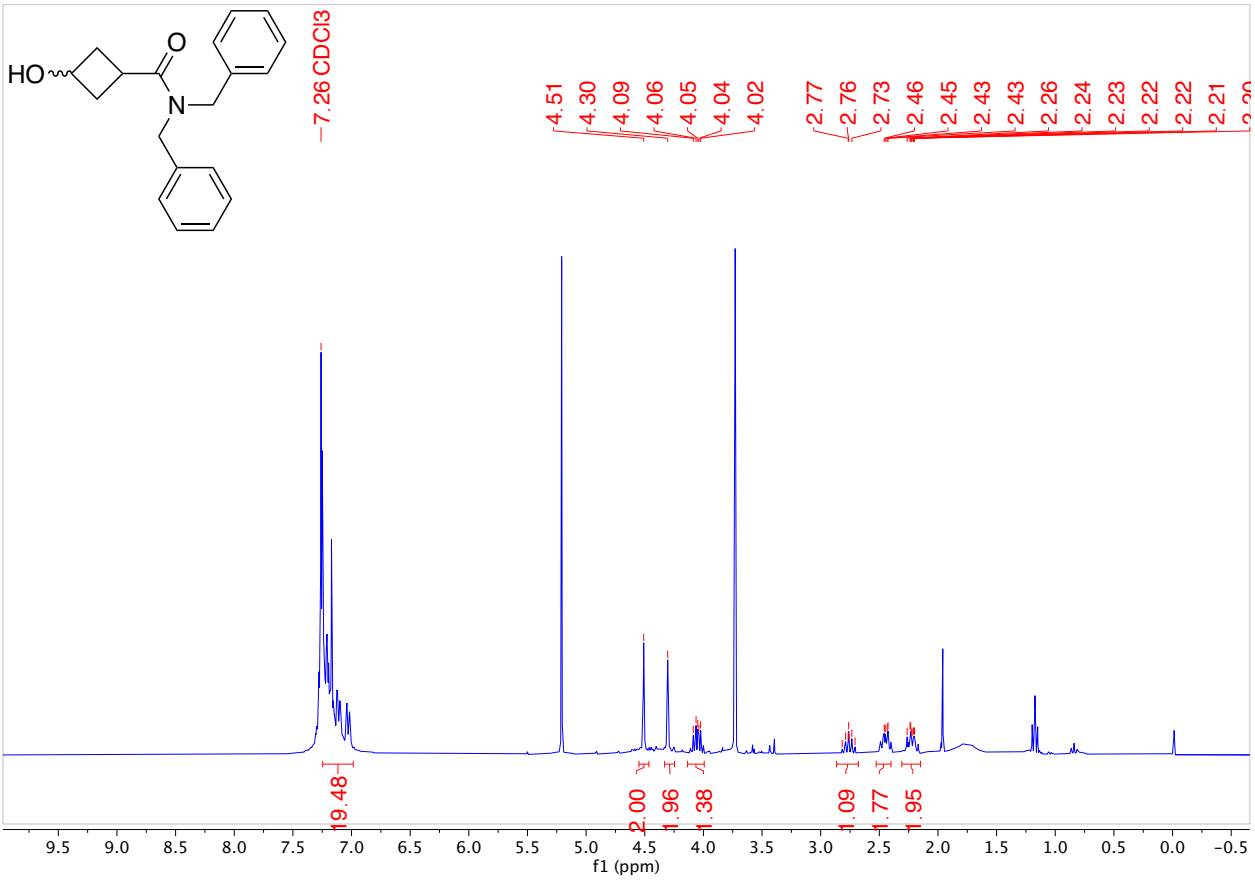

3-Hydroxy-*N*-methyl-*N*-phenylcyclobutane-1-carboxamide

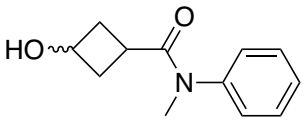

This product was prepared using **general procedure 2**. Isolated 740.7 mg of a white powder (82% Yield).

^{1}H NMR (300 MHz, $CDCl_3$, 292 K, ppm):δ 7.43 (m, 3H), 7.19 – 7.09 (m, 2H), 3.99 (p, J = 7.1 Hz, 1H), 3.29 (s, 3H), 2.58 – 2.44 (m, 1H), 2.28 (m, 2H), 2.22 (m, 2H).

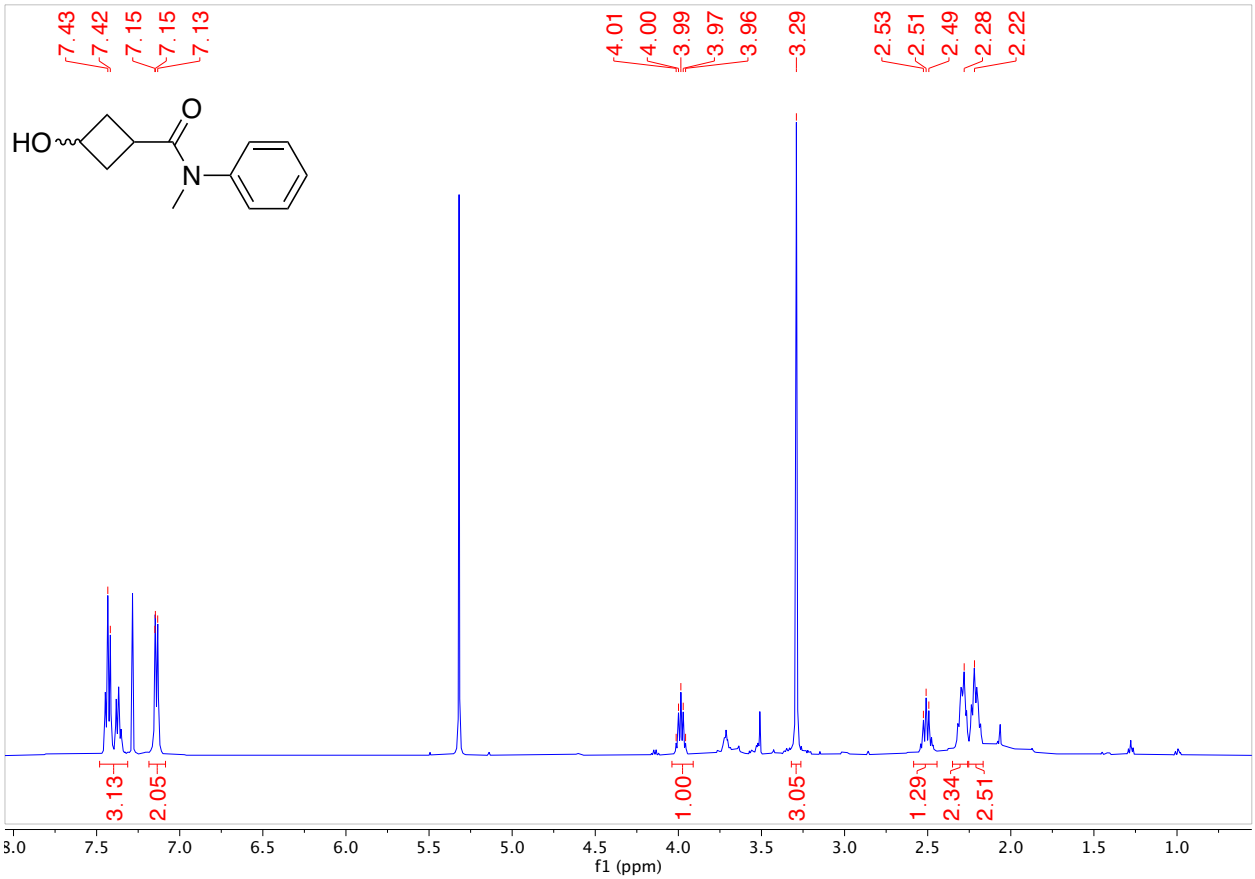

Benzyl 3-hydroxycyclobutane-1-carboxylate

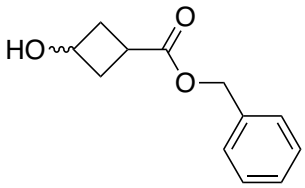

This product was prepared using **general procedure 2**. Isolated 1.32 grams of a white powder (100% Yield).

^{1}H NMR (300 MHz, $CDCl_3$, 292 K, ppm): δ 7.35 (m, 6H), 5.12 (s, 2H), 4.20 (m, 1H), 2.64 (m, 3H), 2.28 – 2.10 (m, 2H).

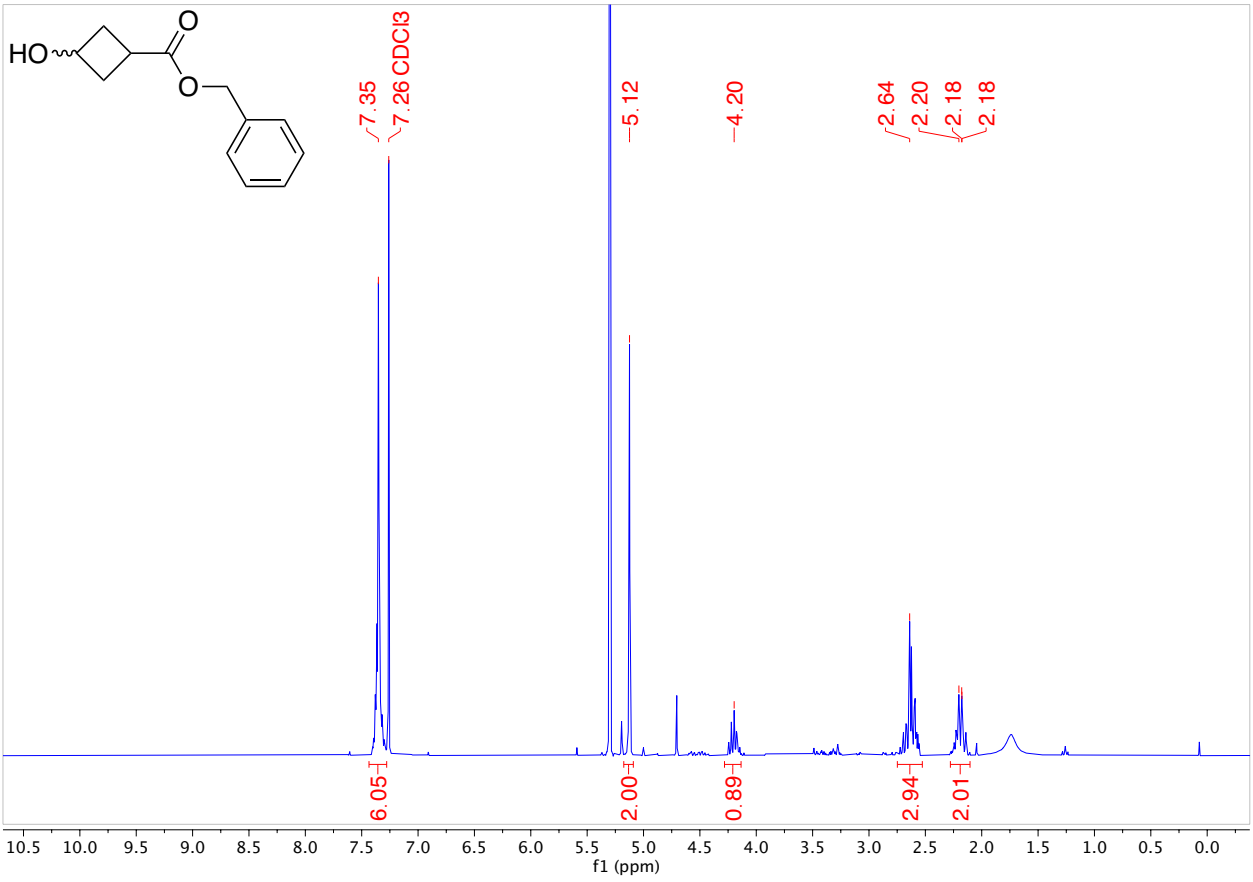

3-(Morpholine-4-carbonyl)cyclobutyl 4-methylbenzenesulfonate

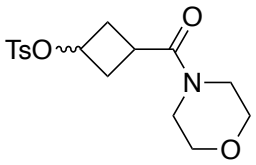

This product was prepared using **general procedure 3**. The compound was purified by column chromatography (Biotage® Sfär 50g Column, 0-100% MeOH/DCM, eluted at 10% MeOH). 6.86 grams of a yellow oil was obtained (89% Yield).

^{1}H NMR (300 MHz, $CDCl_3$, 292 K, ppm): δ 7.76 (d, 2H), 7.35 (d, 2H), 4.80 (quintet, 1H), 3.67-3.53 (m, 6H), 3.34-3.27 (m, 2H), 2.78-2.64 (m, 1H), 2.54-2.39 (m, 7H).

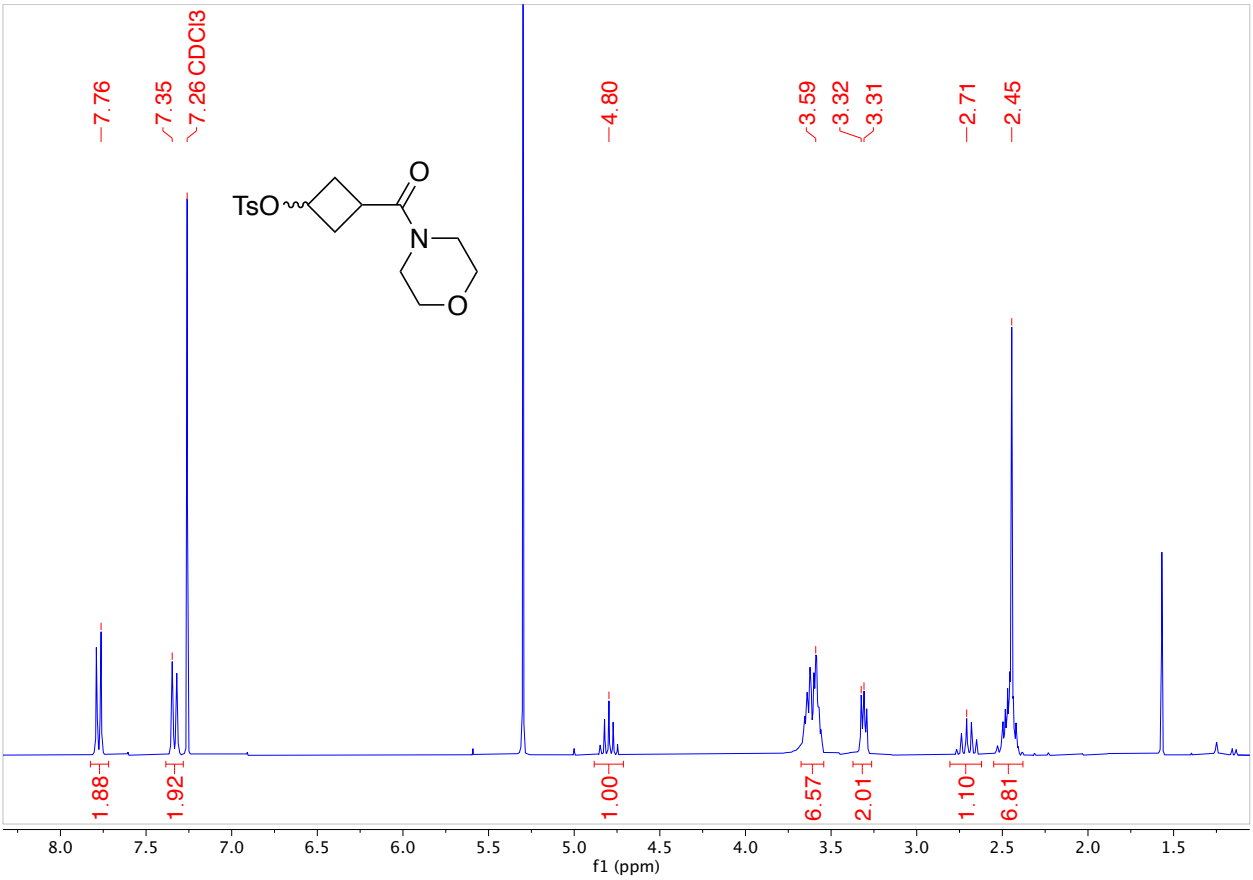

3-(Diisopropylcarbamoyl)cyclobutyl 4-methylbenzenesulfonate

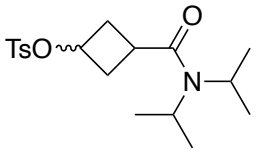

This product was prepared using **general procedure 3**. The compound was purified by column chromatography (Biotage® Sfär 50g Column, 0-100% MeOH/DCM, eluted at 13% MeOH). 2.11 grams of a white solid was obtained (60% Yield).

^{1}H NMR (300 MHz, $CDCl_3$, 292 K, ppm): δ 7.71 (d, J = 8.3 Hz, 2H), 7.26 (d, J = 8.0 Hz, 2H), 4.72 (m, 1H), 3.68 (hept, J = 6.6 Hz, 1H), 3.41 – 3.24 (m, 1H), 2.58 (m, 1H), 2.37 (s, 7H), 1.28 (d, J = 6.8 Hz, 6H), 1.06 (d, J = 6.7 Hz, 6H).

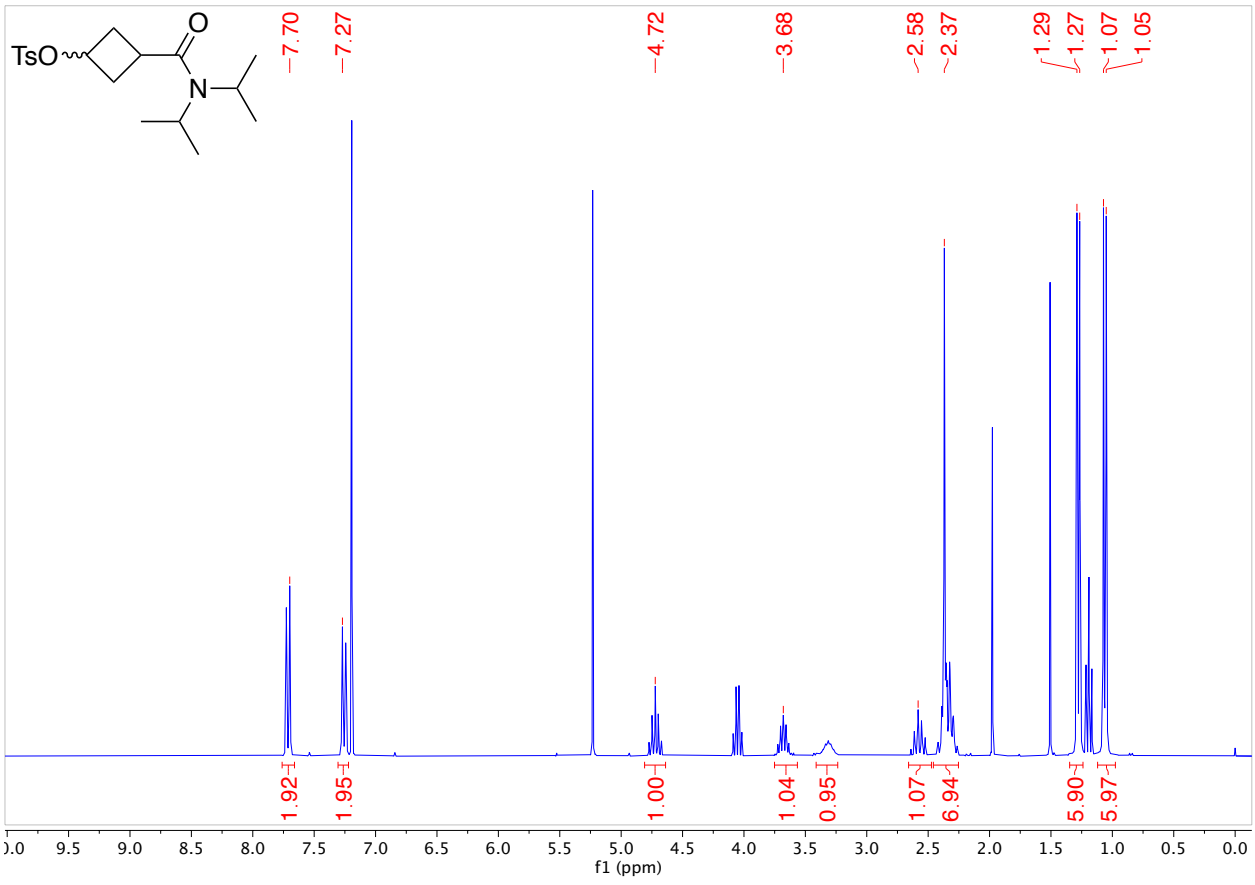

3-(Dibenzylcarbamoyl)cyclobutyl 4-methylbenzenesulfonate

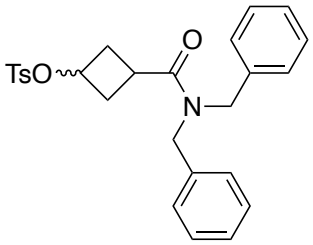

This product was prepared using **general procedure 3**. The compound was purified by column chromatography (Biotage® Sfär 25g Column, 0-100% EtOAc/hexanes, eluted at 30% EtOAc). 2.32 grams of an orange oil was obtained (47% Yield).

^{1}H NMR (300 MHz, $CDCl_3$, 292 K, ppm): δ 7.70 (d, J = 8.3 Hz, 2H), 7.31 – 7.20 (m, 7H), 7.09 (m, 3H), 7.00 – 6.91 (m, 2H), 4.75 – 4.58 (m, 1H), 4.48 (s, 2H), 4.25 (s, 2H), 2.70 (m, 1H), 2.49 (m, 2H), 2.37 (s, 3H), 2.30 (m, 2H).

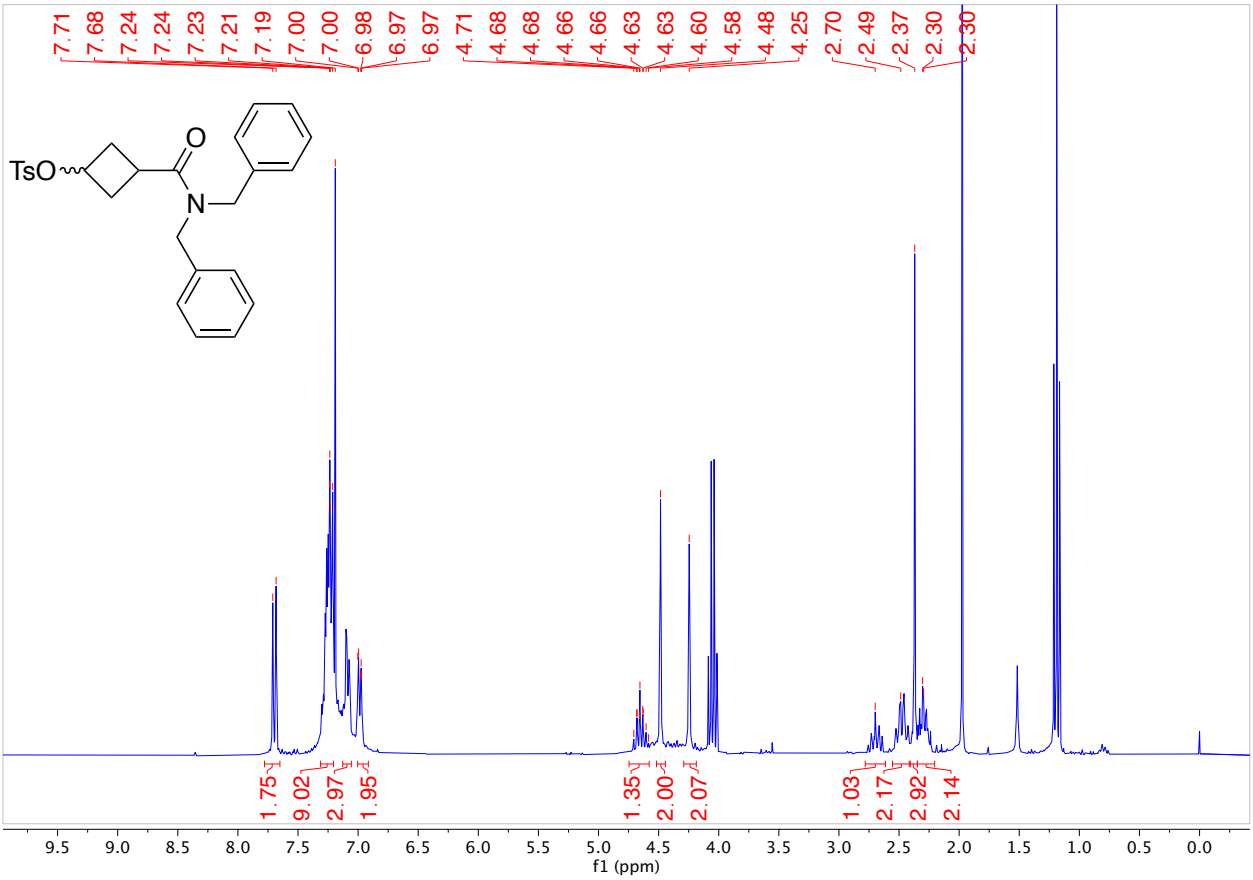

3-(Methyl(phenyl)carbamoyl)cyclobutyl 4-methylbenzenesulfonate

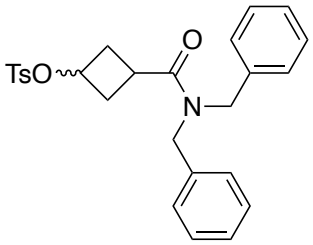

This product was prepared using **general procedure 3**. The compound was purified by column chromatography (Biotage® Sfär 25g Column, 0-100% EtOAc/hexanes, eluted at 40% EtOAc). 1.21 grams of a yellow oil was obtained (93% Yield).

^{1}H NMR (300 MHz, $CDCl_3$, 292 K, ppm): δ 7.73 (d, J = 8.3 Hz, 2H), 7.38 (m, 5H), 7.07 (m, 2H), 4.61 – 4.45 (m, 1H), 3.23 (s, 3H), 2.43 (m, 6H), 2.07 (m, 2H).

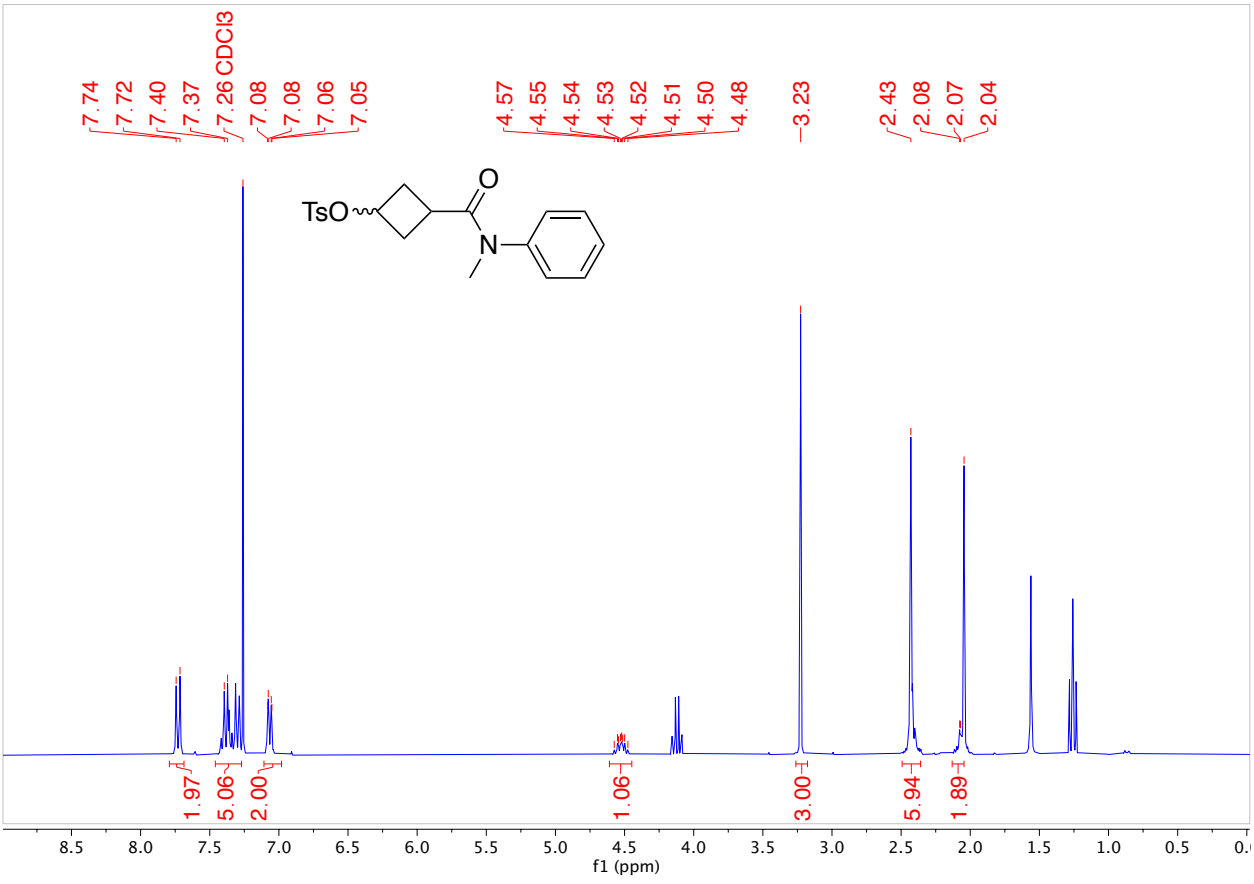

Benzyl 3-(tosyloxy)cyclobutane-1-carboxylate

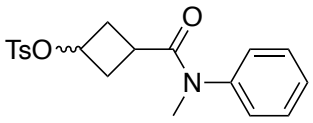

This product was prepared using **general procedure 3**. The compound was purified by column chromatography (Biotage® Sfär 25g Column, 0-100% EtOAc/hexanes, eluted at 35% EtOAc). 1.02 grams of a white solid was obtained (44% Yield).

^{1}H NMR (300 MHz, $CDCl_3$, 292 K, ppm): δ 7.78 (d, J = 8.3 Hz, 2H), 7.33 (m, J = 5.7 Hz, 7H), 5.09 (s, 2H), 4.74 (m, 1H), 2.67 (m, 1H), 2.45 (m, 7H).

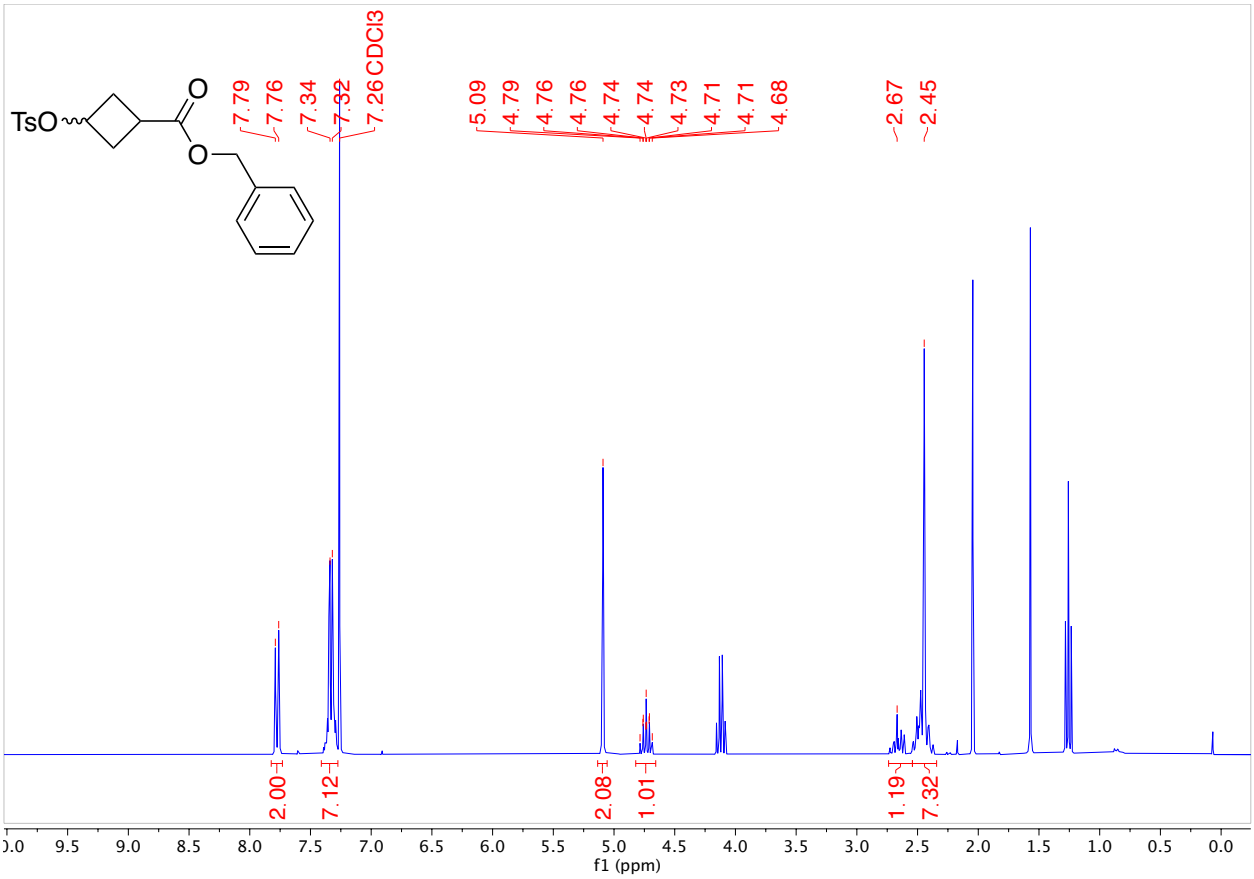

Bicyclo[1.1.0]butan-1-yl(morpholino)methanone (1a)[106]

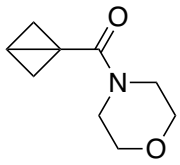

This product was prepared using **general procedure 4**. 338 mg of an orange oil was obtained (89% Yield).

^{1}H NMR (300 MHz, $CDCl_3$, 292 K, ppm): δ 3.54 (m, 8H), 2.07 (d, J = 3.4 Hz, 2H), 1.84 (m, 1H), 1.02 (d, J = 2.5 Hz, 2H).

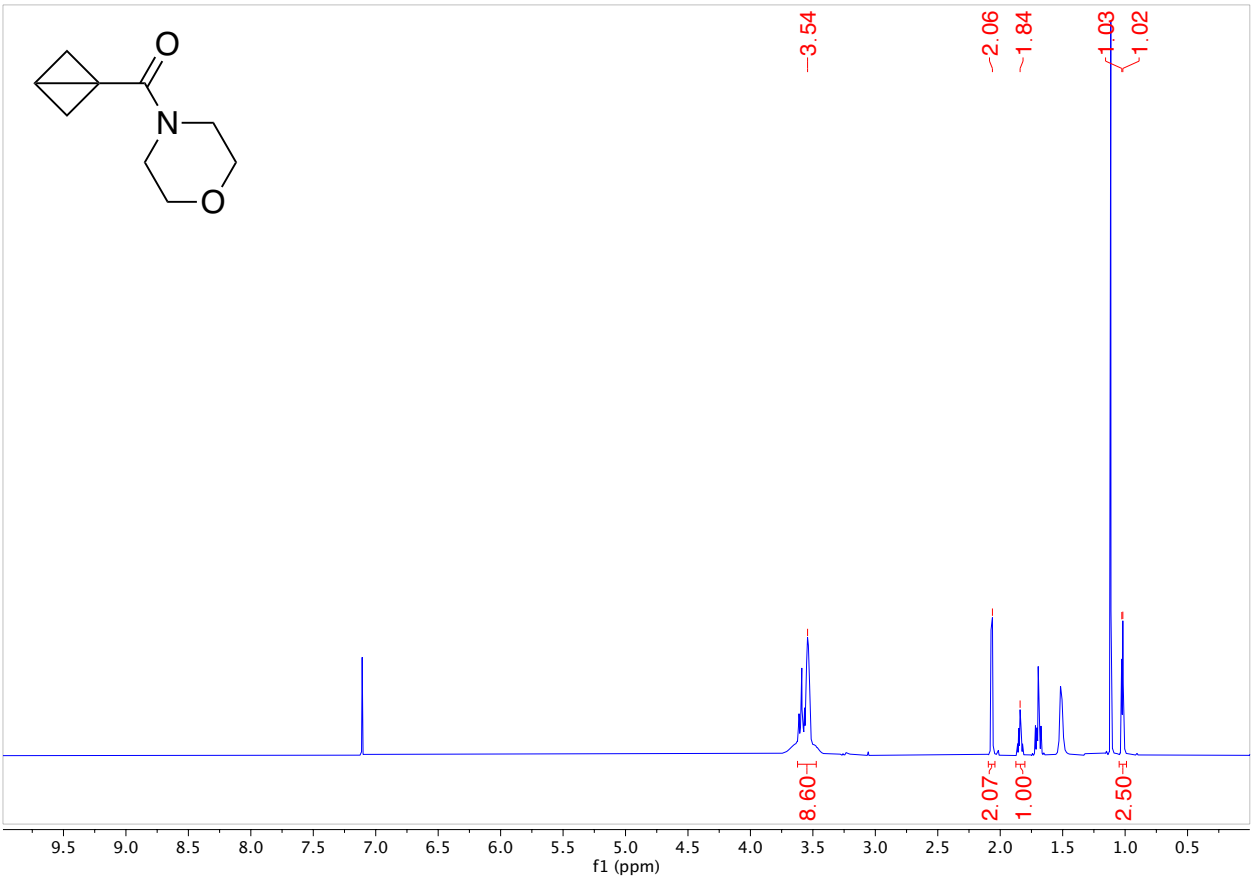

Morpholino(3-phenylbicyclo[1.1.0]butan-1-yl)methanone (1l) [121]

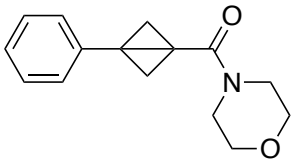

(3-chloro-3-phenylcyclobutyl)(morpholino)methanone (0.4776 g, 1.70 mmol) was added to a 20 mL vial and dissolved in 5 mL THF under a N_2 atmosphere at 0 °C. NaHMDS (2.04 mL, 2.04 mmol) was added to the vial and the reaction mixture was stirred at 0 °C for 4 hours. The reaction mixture was diluted with DCM and washed with water. The organic layer was dried with Mg_2SO_4 and the solvent was removed by evaporation. The product was isolated as an orange solid and used without further purification (0.394 mg, 95%).

^{1}H NMR (500 MHz, $CDCl_3$, 292 K, ppm): δ 7.37-7.18 (m, 5H), 3.61 (s, 8H), 2.77 (s, 2H), 1.60 (s, 2H).

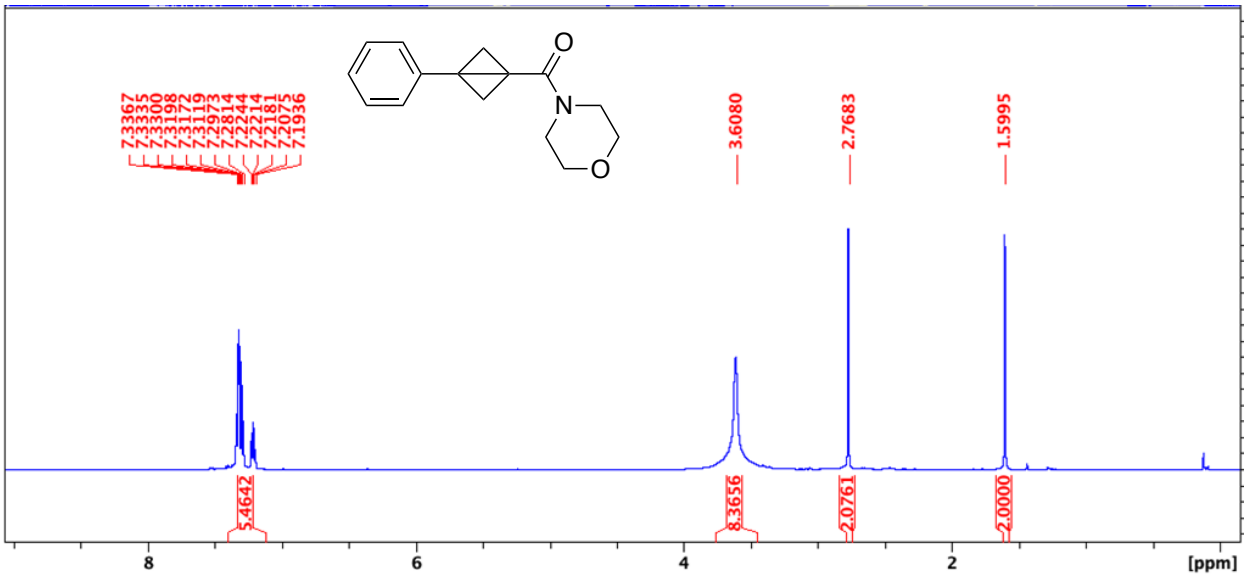

N,*N*-Diisopropylbicyclo[1.1.0]butane-1-carboxamide (1m) [150]

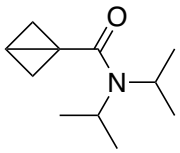

This product was prepared using **general procedure 4**. 896 mg of an orange solid was obtained (83% Yield).

^{1}H NMR (300 MHz, $CDCl_3$, 292 K, ppm): δ 4.71 (broad s, 1H), 3.36 (broad s, 1H), 2.01 (d, J = 3.3 Hz, 2H), 1.72 (m, 1H), 1.24 (m, 6H), 1.07 (m, 6H), 0.90 (d, J = 2.2 Hz, 2H).

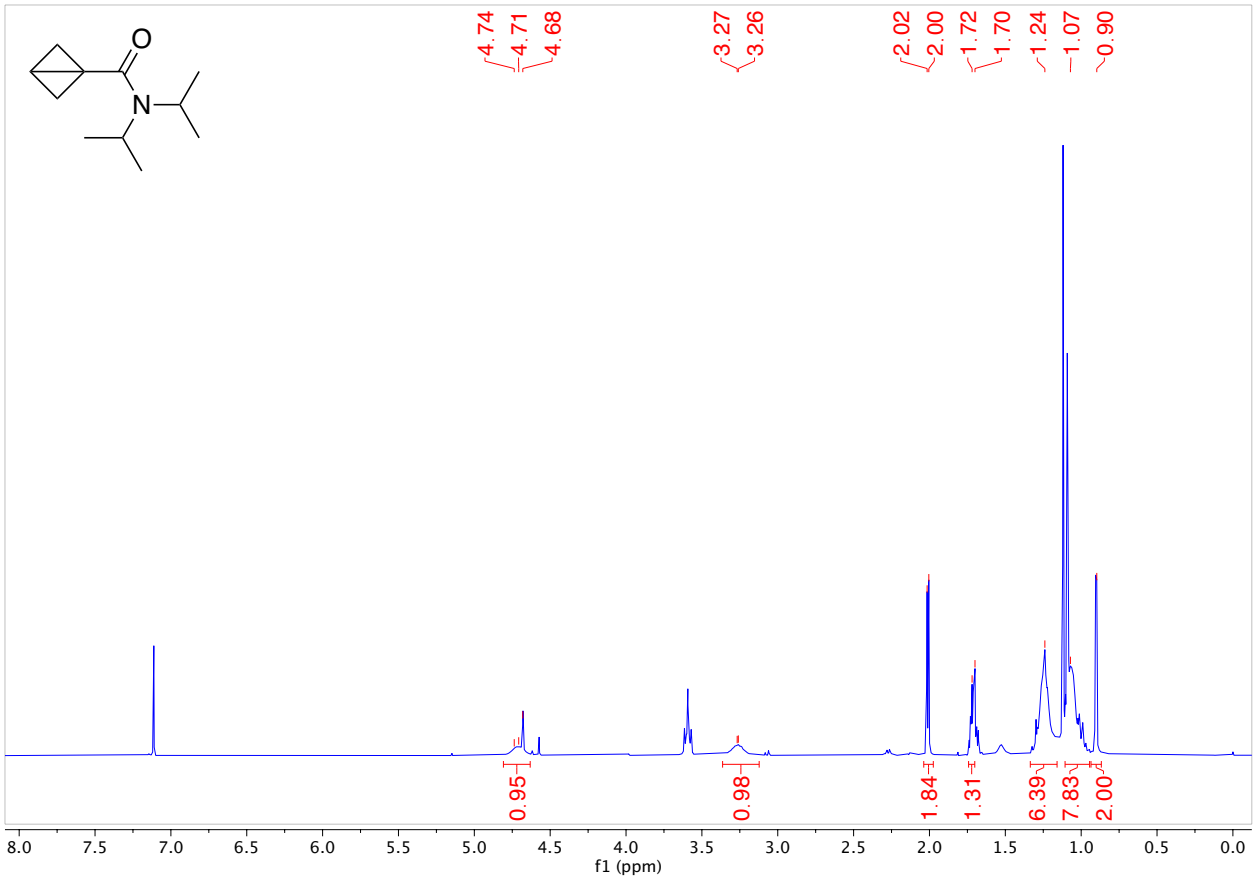

N,*N*-Dibenzylbicyclo[1.1.0]butane-1-carboxamide (1n)[211]

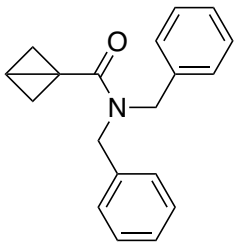

Synthesis adapted from Agasti et al.[68] 3-(Dibenzylcarbamoyl)cyclobutyl 4-methylbenzenesulfonate (1 equiv) was dissolved in THF (0.15 M) under a nitrogen atmosphere. The reaction was cooled down to 0 °C then NaHMDS (1.0M in THF, 1.1 equiv) was added to the reaction mixture. The reaction was stirred at 0 °C for 2 hours. The reaction was quenched with NH_4Cl and extracted with ethyl acetate. The organic layers were washed with $NaHCO_3$ and brine. The organic layer was then dried with Mg_2SO_4, filtered and the solvent was evaporated. The crude compound was purified by column chromatography (Biotage® Sfär 5g Column, 0-100% EtOAc/hexanes, eluted at 28% EtOAc). 109.5 mg of a clear colourless oil was obtained (68% Yield).

^{1}H NMR (300 MHz, $CDCl_3$, 292 K, ppm): δ 7.31 (m, 6H), 7.21 (m, 4H), 4.82 (s, 2H), 4.57 (s, 2H), 2.27 (d, J = 3.4 Hz, 2H), 2.13 – 2.07 (m, 1H), 1.11 (d, J = 2.4 Hz, 2H).

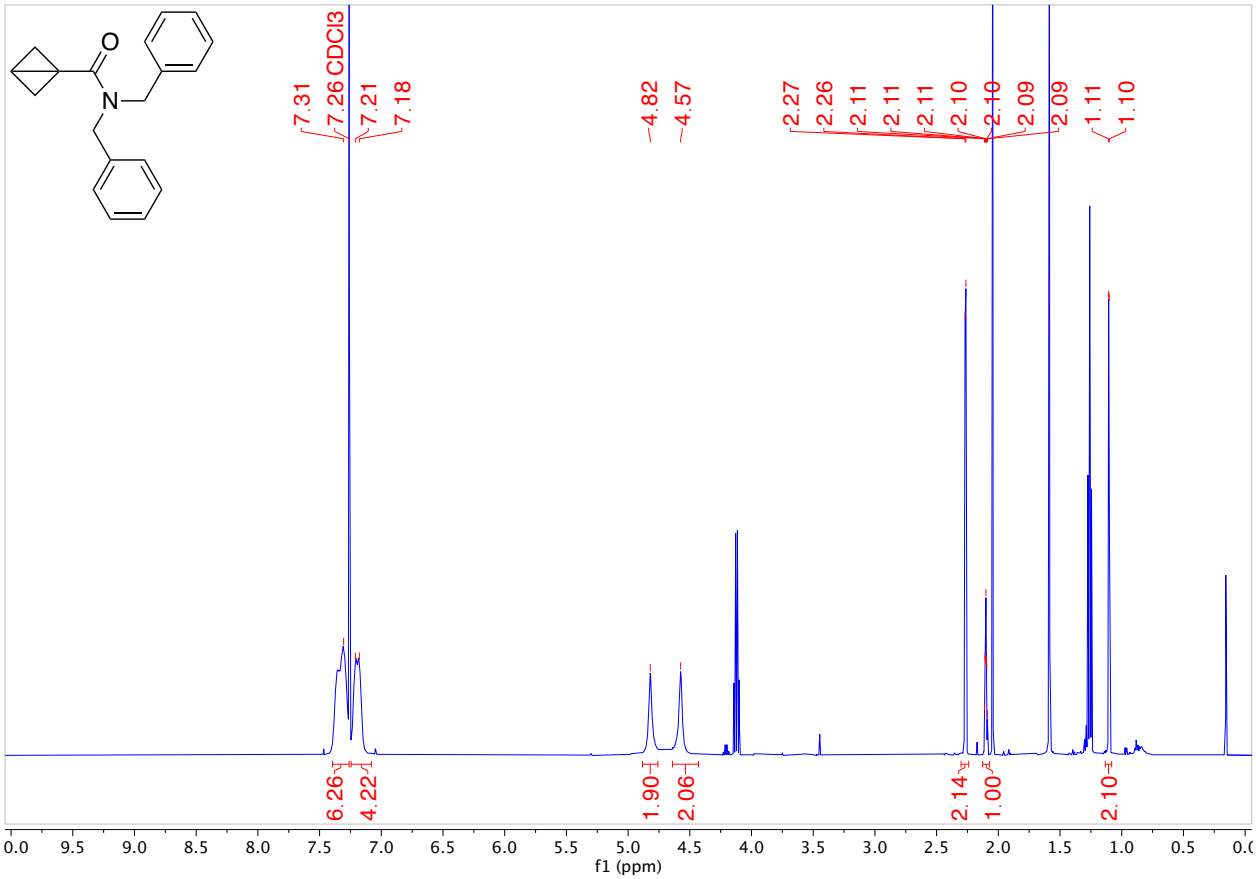

_N_-Methyl-_N_-phenylbicyclo[1.1.0]butane-1-carboxamide (1o)[213]

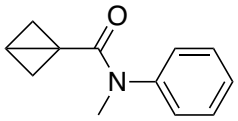

Synthesis adapted from Agasti et al.[68] 3-(Methyl(phenyl)carbamoyl)cyclobutyl 4-methylbenzenesulfonate (1 equiv) was dissolved in THF (0.15 M) under a nitrogen atmosphere. The reaction was cooled down to 0 °C then NaHMDS (1.0M in THF, 1.1 equiv) was added to the reaction mixture. The reaction was stirred at 0 °C for 1.5 hours. The reaction was quenched with NH_4Cl and extracted with ethyl acetate. The organic layers were washed with $NaHCO_3$ and brine. The organic layer was then dried with Mg_2SO_4, filtered and the solvent was evaporated to give the product without further purification. 126 mg of a yellow solid was obtained (80% Yield).

^{1}H NMR (300 MHz, $CDCl_3$, 292 K, ppm): δ 7.44 – 7.30 (m, 2H), 7.23 (m, 3H), 3.34 (s, 3H), 2.02 (ddd, J = 5.8, 3.3, 2.5 Hz, 1H), 1.80 (d, J = 3.3 Hz, 2H), 0.77 (d, J = 2.6 Hz, 2H).

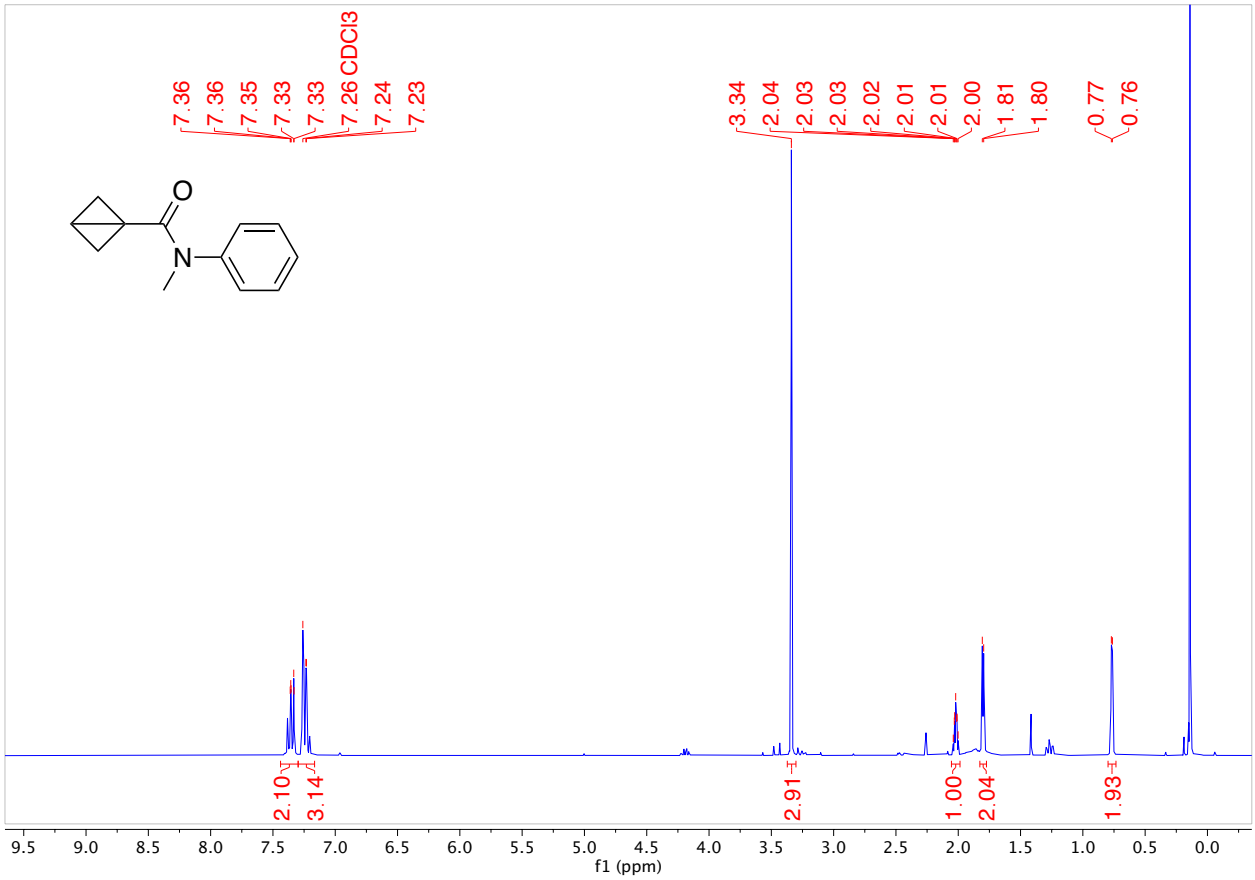

Benzyl bicyclo[1.1.0]butane-1-carboxylate (1p)[144]

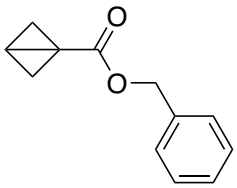

Benzyl 3-(tosyloxy)cyclobutane-1-carboxylate (1 equiv) was dissolved in THF (0.19 M) under a nitrogen atmosphere. The reaction was cooled down to 0 °C then LiHMDS (1.0M in THF, 1.1 equiv) was added to the reaction mixture. The reaction was stirred at rt overnight. The reaction was quenched with NH_4Cl and extracted with ethyl acetate. The organic layer was then dried with Mg_2SO_4, filtered and the solvent was evaporated to give the crude product. The compound was purified by column chromatography (Biotage® Sfär 25g Column, 0-100% EtOAc/hexanes, eluted at 12% EtOAc). 718 mg of a clear colourless oil was obtained (40% Yield).

^{1}H NMR (300 MHz, $CDCl_3$, 292 K, ppm):δ 7.19 (m, 5H), 5.00 (s, 2H), 2.24 (m, 2H), 1.95 (m, 1H), 1.02 (m, 2H).

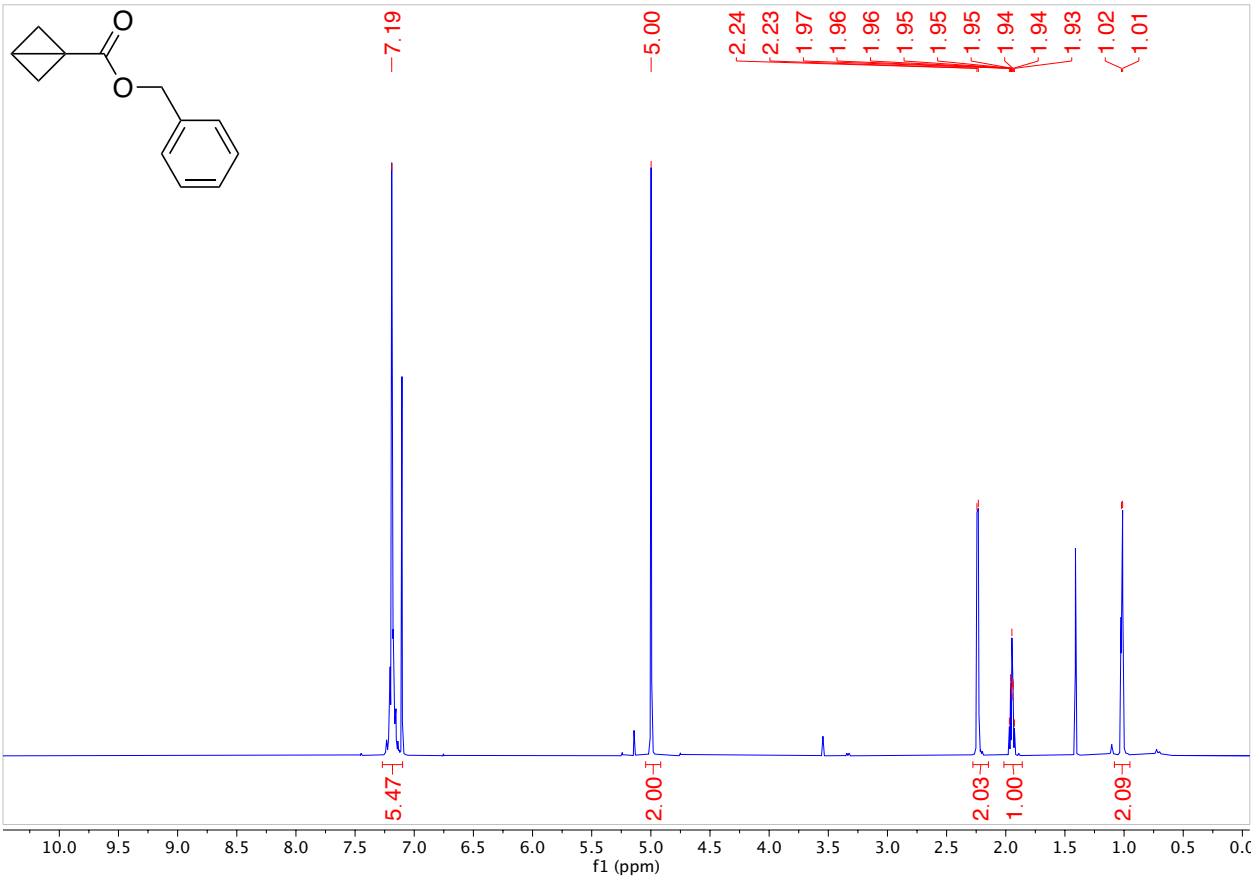

B.4 Imine Bicyclohexane Transformations

General Procedure for Bicyclohexane Synthesis

In two separate vials, the bicyclobutane **1** (1 equiv) and acetate **2** (1.2 equiv) were added and put under a nitrogen atmosphere. The acetate was dissolved in 50% of the THF and LiHMDS (1.0M in THF, 1.5 equiv) was added to the vial and then left to stir for 15 minutes at room temperature to form the enolate. Then 50% of the THF solvent was added to the bicyclobutane vial and then it was cooled in the glovebox freezer for 15 minutes along with the enolate vial. The bicyclobutane was then added dropwise to the enolate vial. The reaction was left to stir at room temperature overnight. The reaction was quenched with $NaHCO_3$ and extracted three times with ethyl acetate. The organic layers were dried with Mg_2SO_4, filtered and the solvent was evaporated to give the crude product **3**.

3-((Benzylidene)amino)-1-(morpholine-4-carbonyl)bicyclo[2.1.1]hexan-2-one (3a)

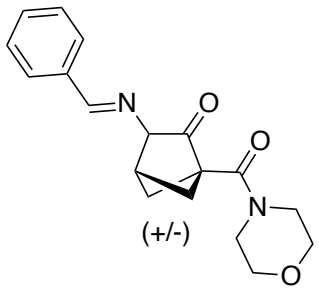

The product was prepared following the general procedure for bicyclohexane synthesis and carried into the next transformation without purification. Amount of reagents used: bicyclo-[1.1.0]butan-1-yl(morpholino)methanone **1a** (83.6 mg, 1 equiv), ethyl (*E*)-2-(benzylidene-amino)acetate **2a** (105.2 mg, 1.1 equiv), LiHMDS (1.0 M in THF, 0.75 mL, 1.5 equiv) and THF (10 mL, 0.06 M). This was used directly in the next step without purification. Crude ^{1}H NMR spectroscopy solution yield of 47% (peak at 2.89 ppm).

One sample was isolated and purified by column chromatography for characterization (Biotage® Sfär 5g Column, 0-100% EtOAc/hexanes, eluted at 100% EtOAc). Isolated 8 mg of a yellow oil (13% yield).

HRMS(ESI): calc'd for [$C_{18}H_{20}N_2O_3$ + H^+], 313.15467; found: 313.15446.

Crude ^{1}H NMR spectrum, including 1,3,5-trimethoxybenzene as internal standard (500 MHz, $CDCl_3$, 292 K):

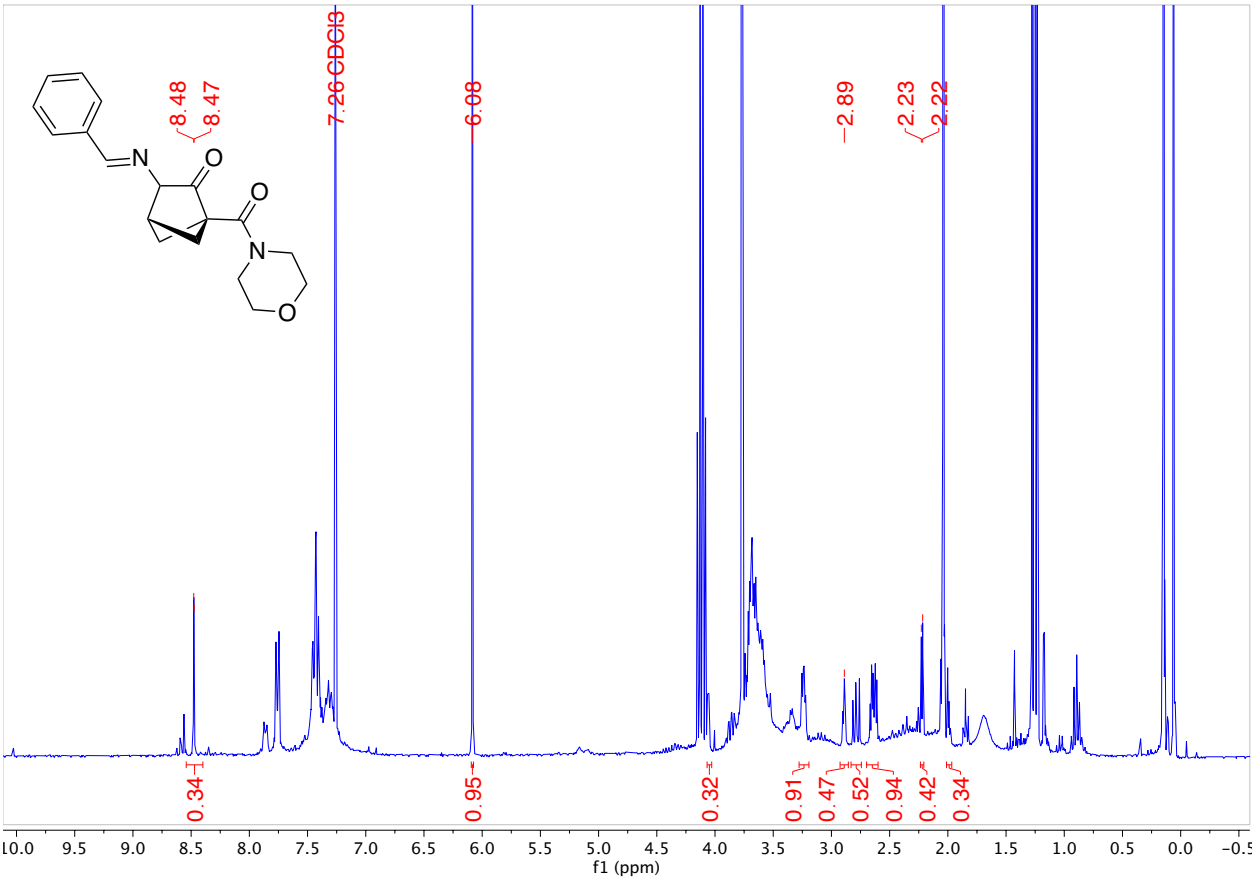

Isolated sample of 3a after chromatography: ^{1}H NMR (500 MHz, $CDCl_3$, 292 K, ppm): δ 8.48 (s, 1H), 7.81 – 7.70 (m, 2H), 7.43 (m, 3H), 4.06 (s, 1H), 3.83 – 3.60 (m, 6H), 3.57 (m, 1H), 3.24 (d, J = 4.4 Hz, 2H), 2.89 (m, 1H), 2.79 (dd, J = 9.4, 7.5 Hz, 1H), 2.64 (m, 2H), 2.03 (t, J = 8.7 Hz, 1H).

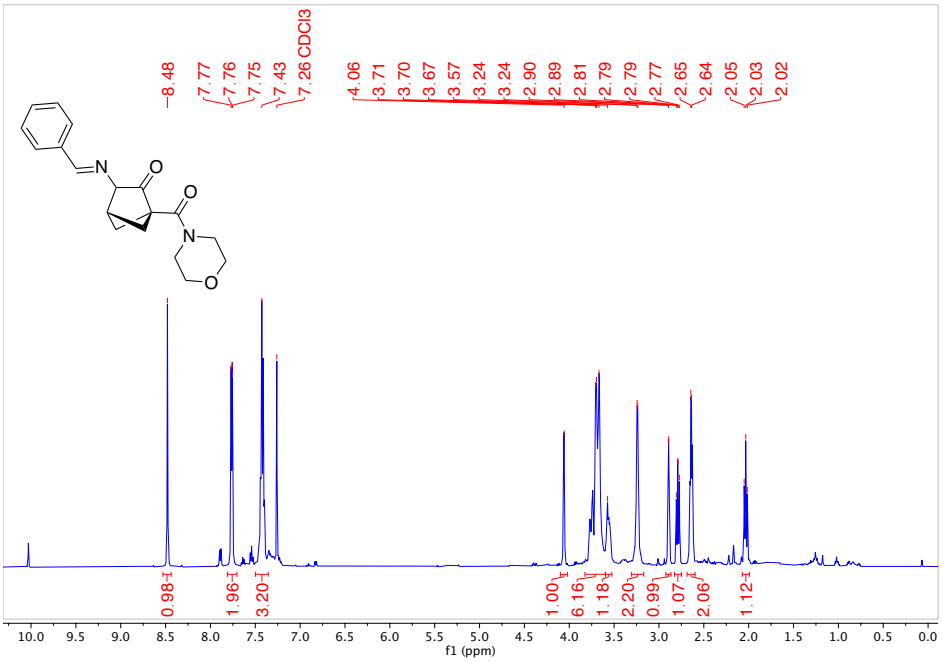

^{13}C NMR (126 MHz, $CDCl_3$, 292 K, ppm): δ 204.60, 166.53, 164.48, 135.90, 131.34, 128.75, 128.59, 75.82, 67.08, 66.98, 66.77, 46.49, 42.54, 41.57, 39.42, 37.35.

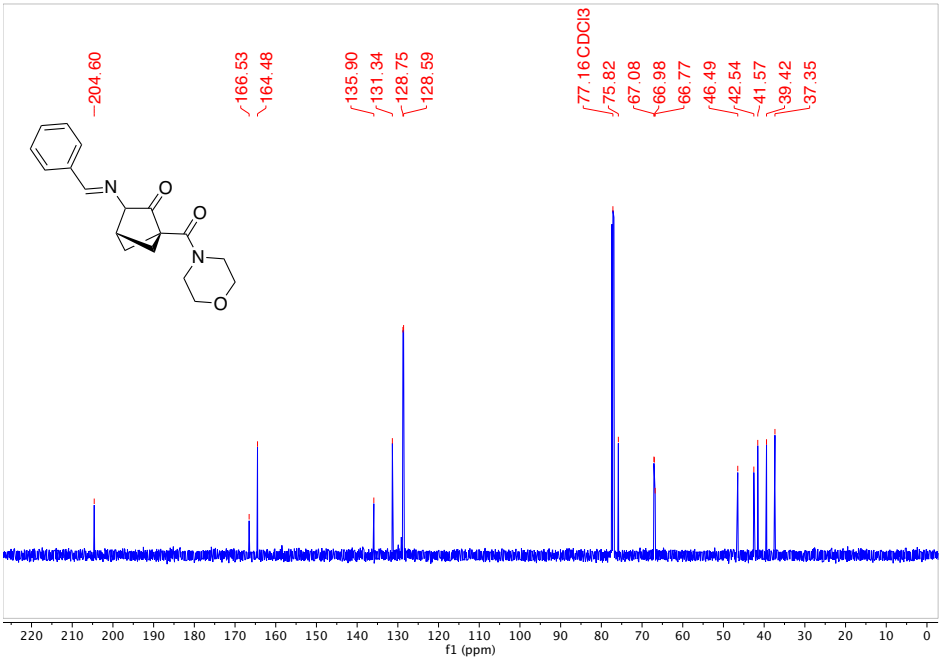

^{1}H-^{1}H COSY (3a):

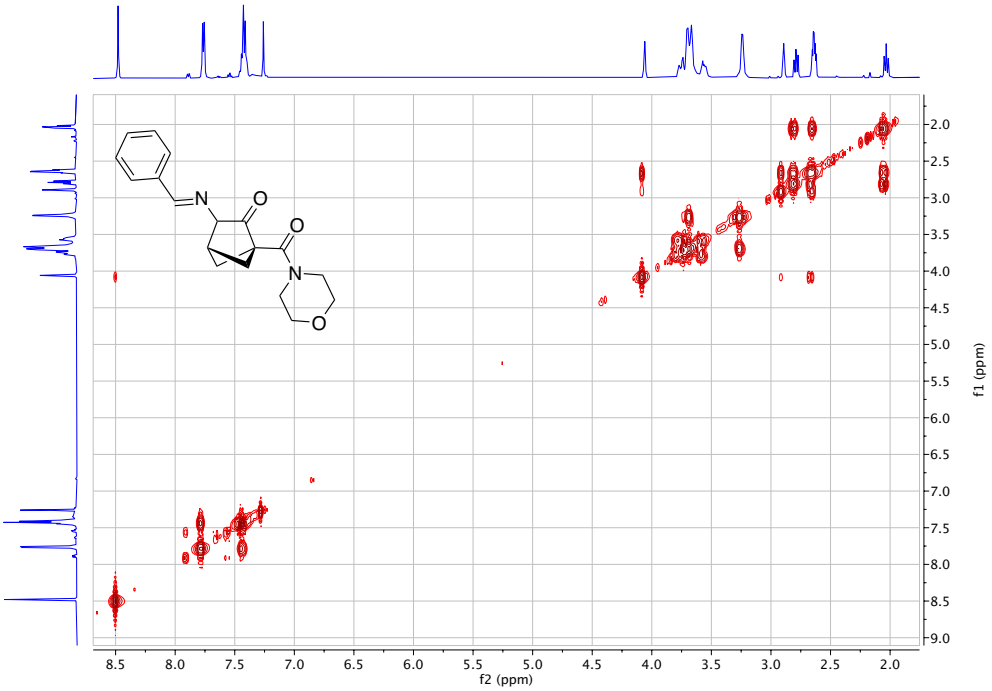

^{1}H-^{13}C HSQC (3a):

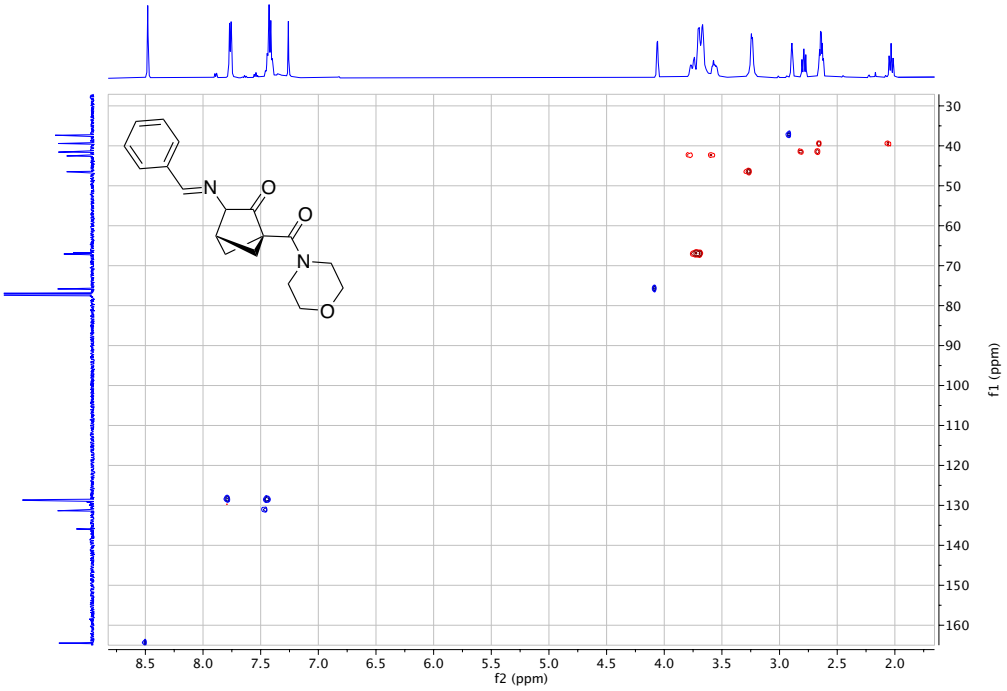

^{1}H-^{13}C HMBC (3a):

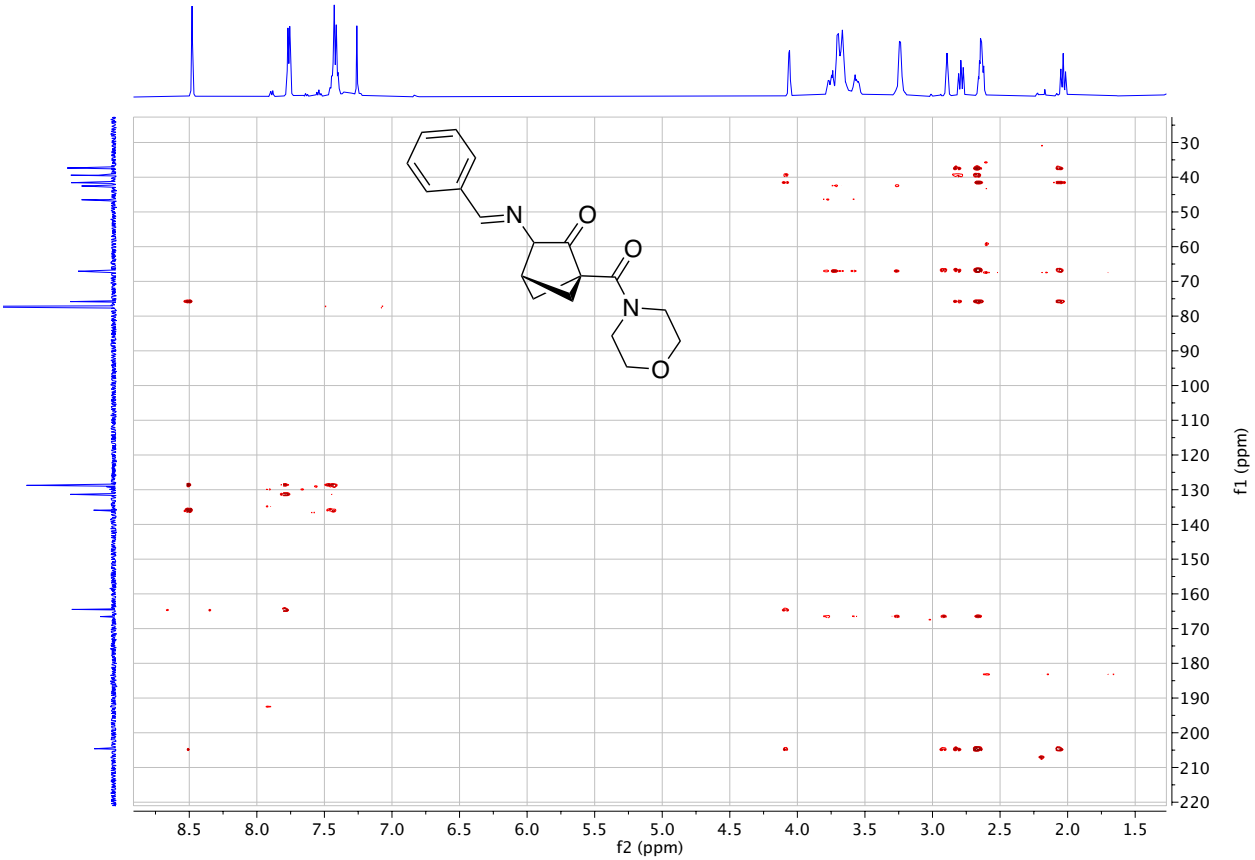

Synthesis of Ethyl 2-(4-methylbenzamido)-2-(3-(morpholine-4-carbonyl)-cyclobutyl)acetate 3ab:

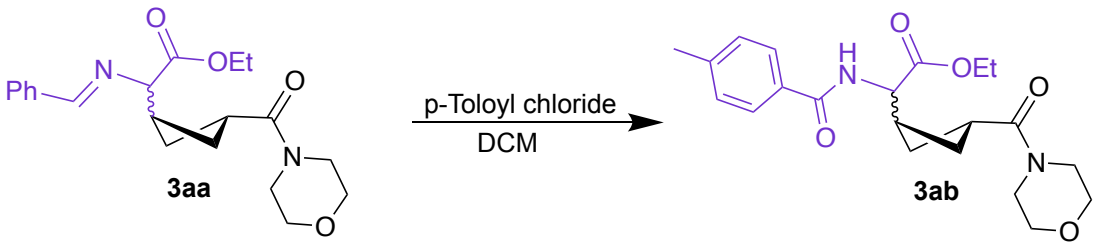

An additional sample of the byproduct **3aa** was isolated. The isolated crude product was acylated by taking **3aa** (17.9 mg, 0.05 mmol, 1 equiv) and dissolving it in DCM. *p*-Toluoyl chloride (0.033 mL, 0.25 mmol, 5 equiv) was added and the reaction was left to stir at rt overnight. The reaction was quenched with $NaHCO_3$ and extracted three times with ethyl acetate. The combined organic layers were dried with Mg_2SO_4, filtered and the solvent was evaporated to give the crude product **3ab**. The mass was confirmed via LCMS (expected 389.5 and found 389.5 m/z)

Crude ^{1}H NMR spectra of 3ab (300 MHz, $CDCl_3$, 292 K, ppm):

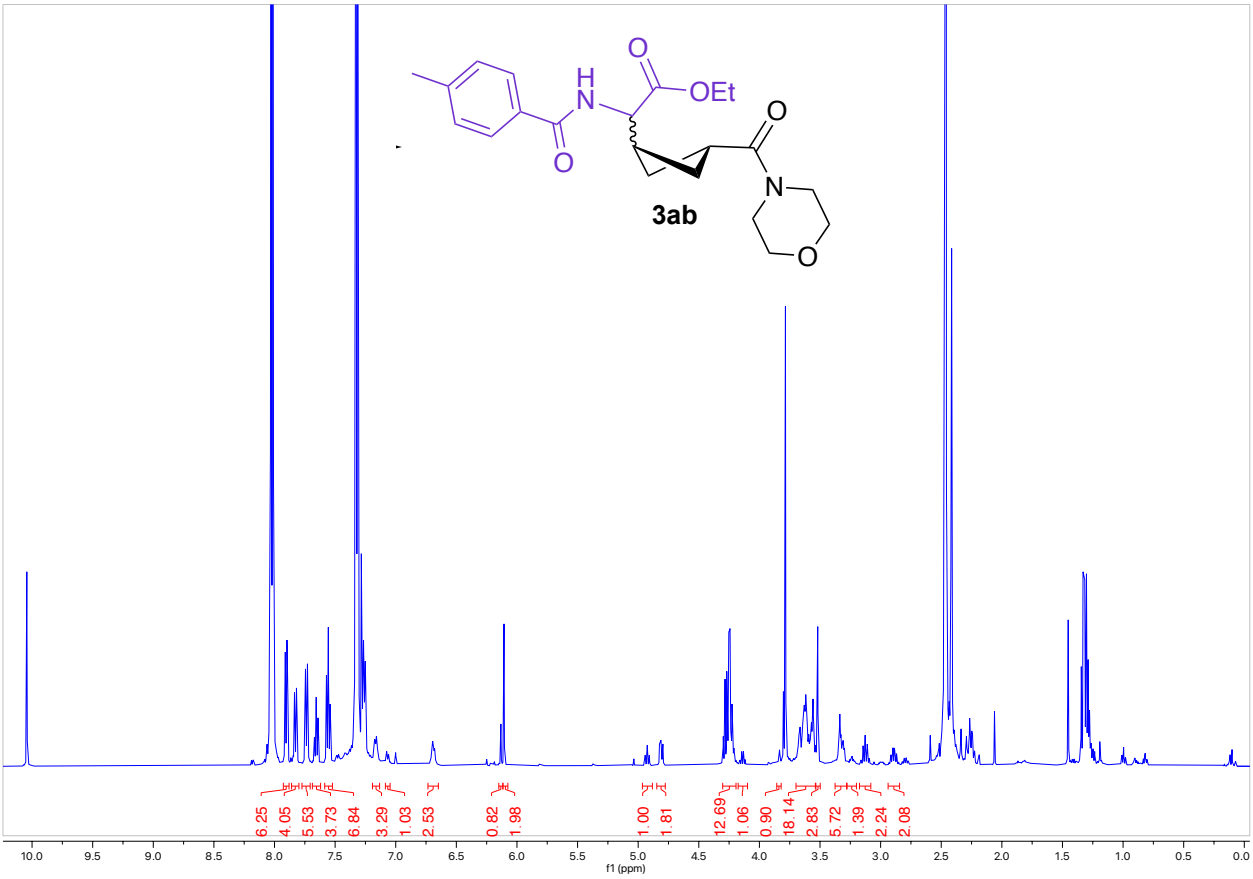

3-Amino-1-(morpholine-4-carbonyl)bicyclo[2.1.1]hexan-2-one (4a)

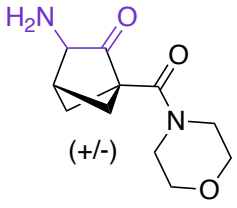

Crude **3a** was dissolved in DCM (3 mL) and silica gel was added to the vial (0.875 g). The mixture was stirred overnight at room temperature. The mixture was then filtered, and the silica was washed with DCM (3 times) to remove benzaldehyde from the hydrolysis and any organic impurities. The silica was then washed with 50% MeOH/DCM and the organic layer was collected, dried with Mg_2SO_4, filtered and evaporated to give the primary amine product **4a**. Isolated 23.3 mg of an orange solid (35% yield over two steps).

HRMS(ESI): calc'd for [$C_{11}H_{17}N_2O_3$ + H^+], 225.12337; found: 225.12335.

^{1}H NMR (500 MHz, $CDCl_3$, 292 K, ppm): δ 3.64 (m, 9H), 3.27 (m, 2H), 3.00 (d, J = 2.9 Hz, 1H), 2.57 (dd, J = 7.6, 3.5 Hz, 1H), 2.48 (m, 1H), 2.14 (dd, J = 9.6, 7.6 Hz, 1H), 1.65 (dd, J = 9.6, 7.5 Hz, 1H).

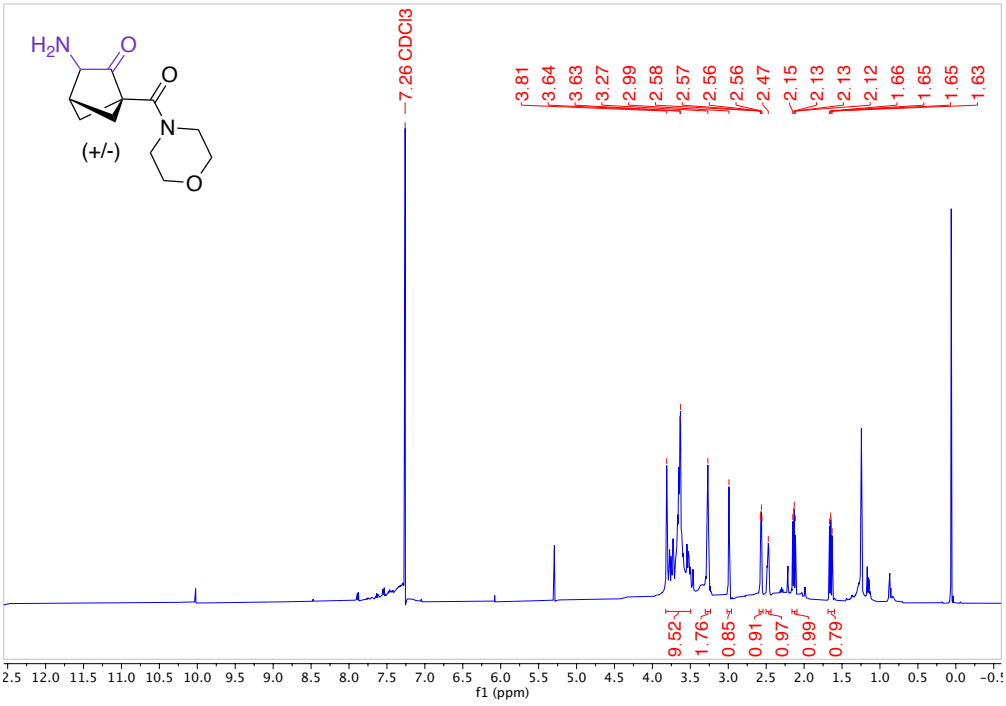

^{13}C NMR (126 MHz, $CDCl_3$, 292 K, ppm): δ 183.22, 167.46, 67.44, 66.94, 59.30, 46.55, 43.29, 43.14, 42.51, 35.69.

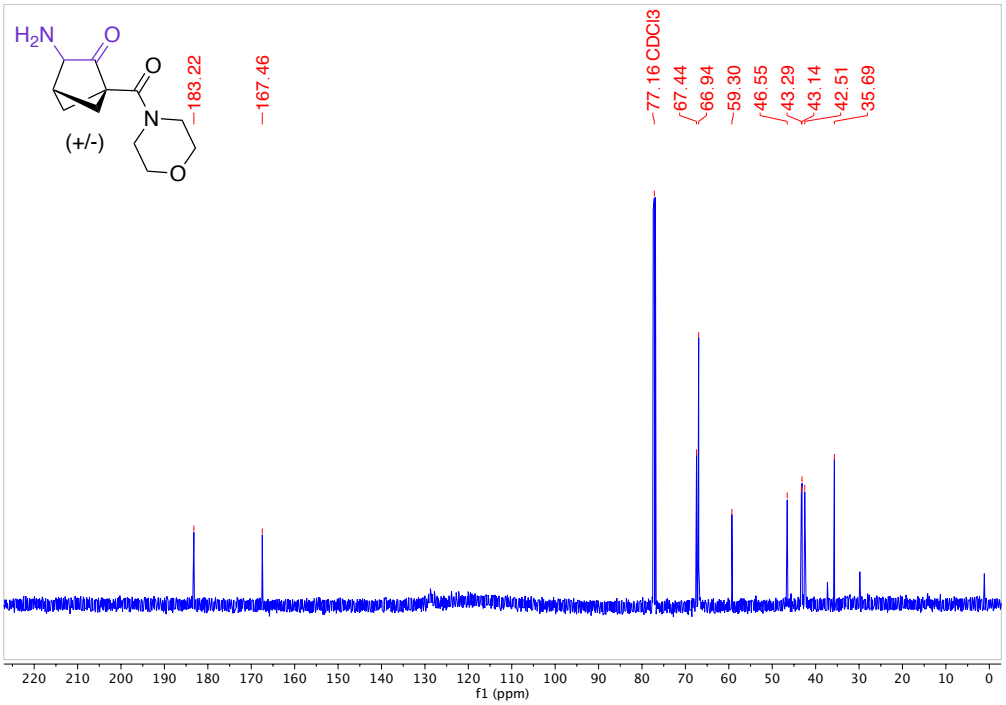

3-(Benzylamino)-2-hydroxybicyclo[2.1.1]hexan-1-yl)(morpholino)methanone (4b)

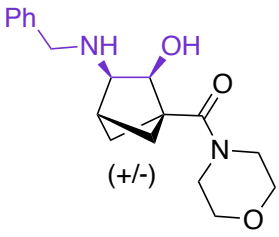

Crude **3a** was dissolved in methanol (5 mL, 0.1 M) then $NaBH_4$ (94.6 mg, 5 equiv) was added and then the reaction was stirred at room temperature overnight. The reaction was quenched with $NaHCO_3$ and extracted with DCM. The organic layers were dried with Mg_2SO_4, filtered and the solvent was evaporated to give the crude product. The compound was purified by column chromatography (Biotage® Sfär 5g Column, 0-100% EtOAc/hexanes, eluted at 20% EtOAc). 60 mg of a red oil was obtained as a single diastereomer (35% Yield over two steps). *syn* stereochemistry was assigned through NOESY and 2D NMR experiments.

HRMS(ESI): calc'd for $[C_{18}H_{24}N_2O_3 + H^+]$,317.18597; found: 317.18601.

^{1}H NMR (500 MHz, $CDCl_3$, 292 K, ppm): δ 7.26 – 7.15 (m, 5H), 4.12 (dd, J = 6.5, 1.5 Hz, 1H), 3.78 (s, 2H), 3.68 – 3.47 (m, 6H), 3.31 – 3.22 (m, 2H), 3.19 (d, J = 6.5 Hz, 1H), 2.24 (s, 1H), 1.84 – 1.79 (m, 1H), 1.75 (m, 1H), 1.71 (dd, J = 7.9, 3.4 Hz, 1H), 1.33 – 1.27 (m, 1H).

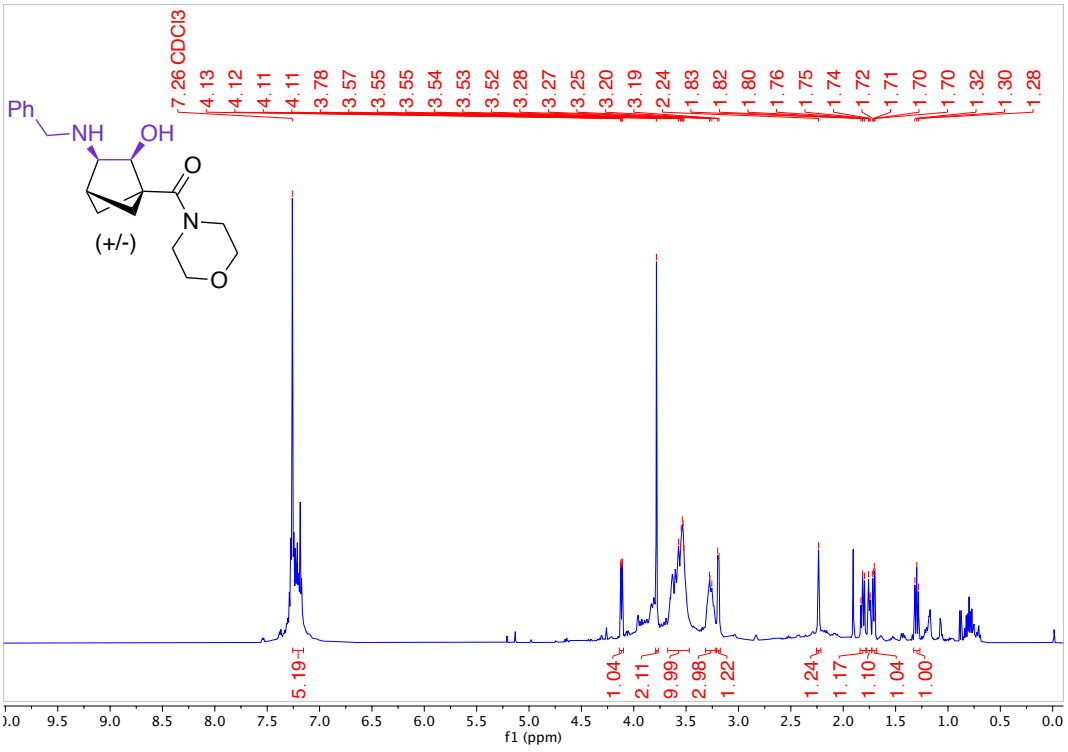

^{13}C NMR (126 MHz, $CDCl_3$, 292 K, ppm): δ 171.25, 138.62, 128.83, 128.38, 127.78, 71.66, 67.30, 67.02, 59.94, 58.08, 53.07, 46.11, 42.51, 39.14, 38.40, 35.27.

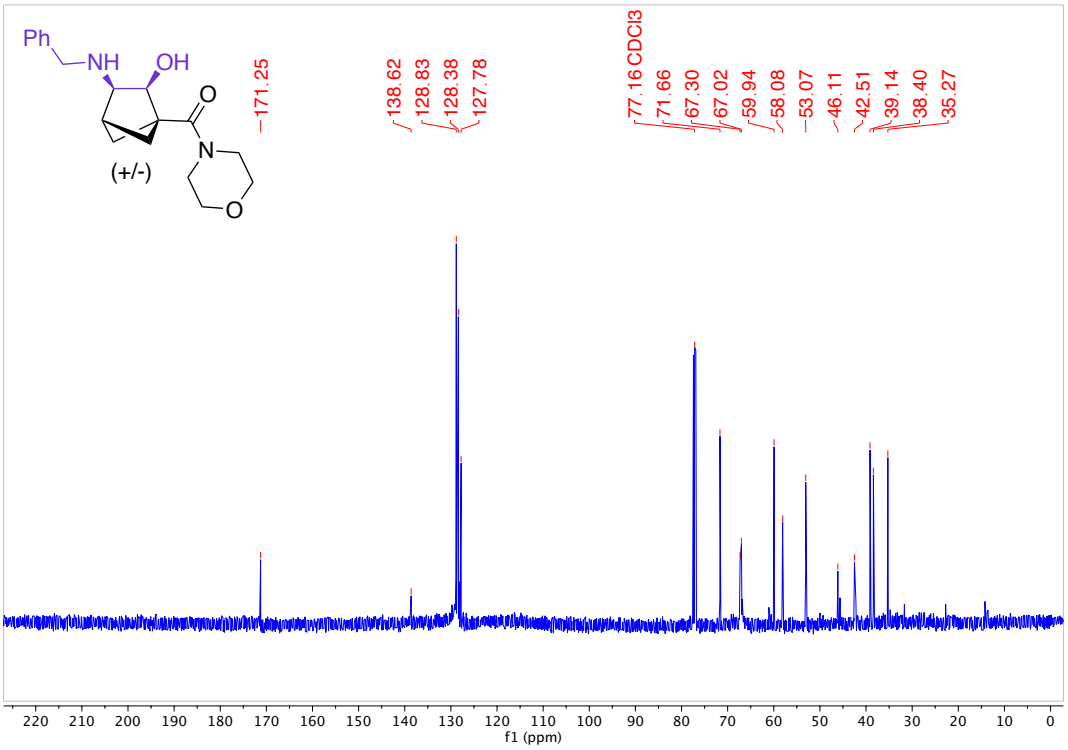

^{1}H-^{1}H COSY (4b):

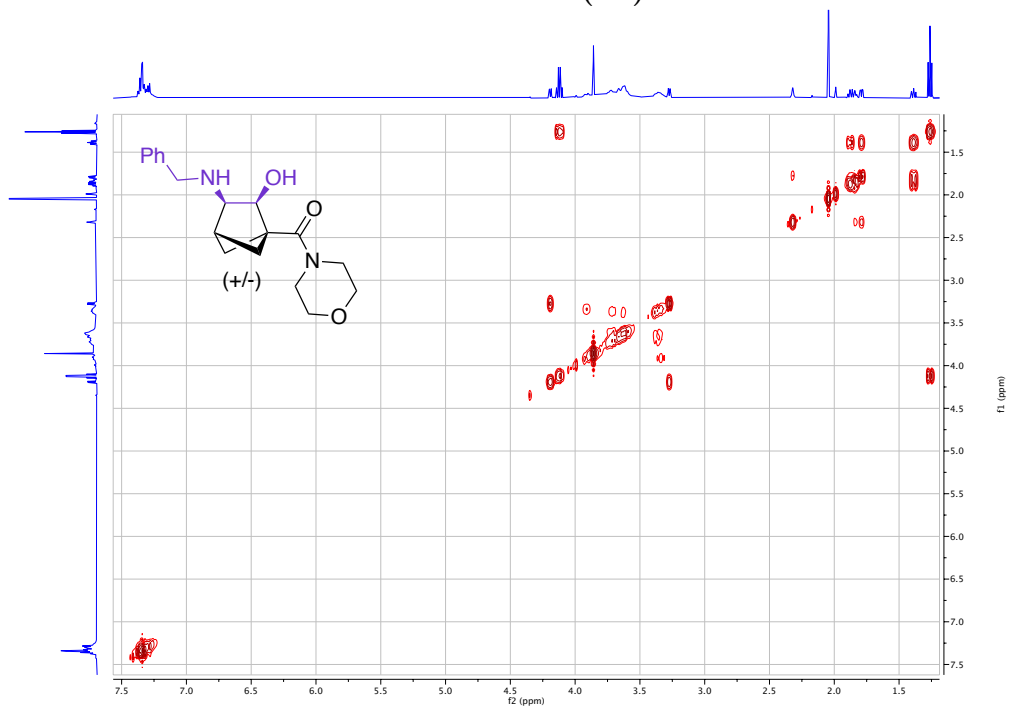

^{1}H-^{13}C HSQC (4b):

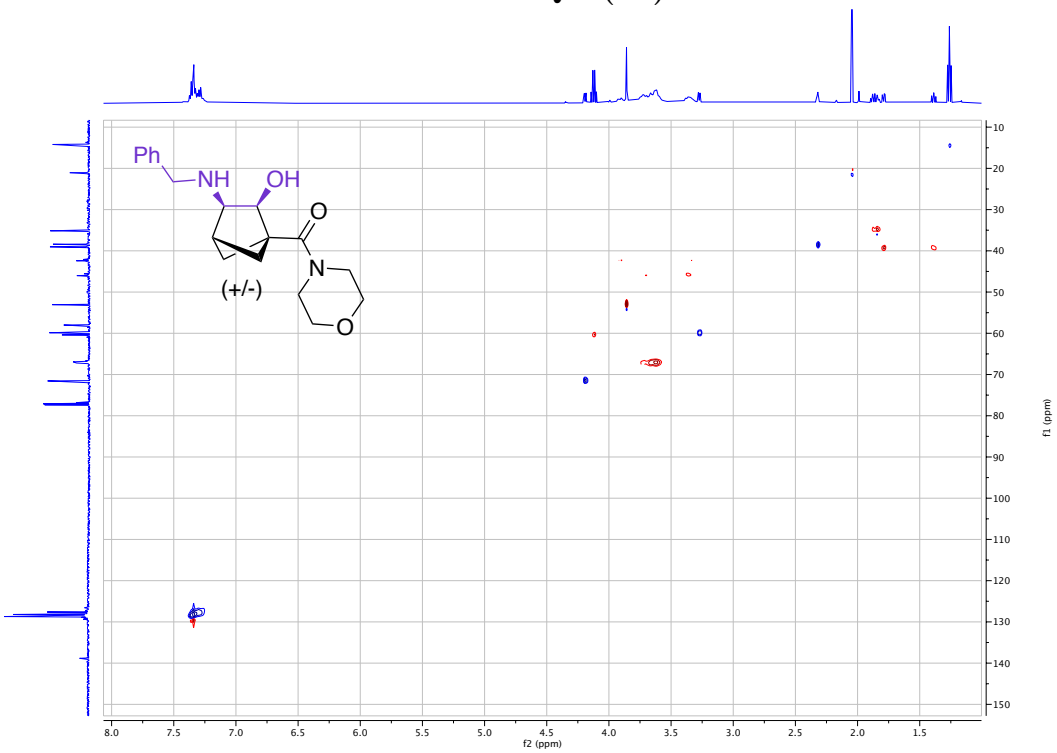

^{1}H-^{13}C HMBC (4b):

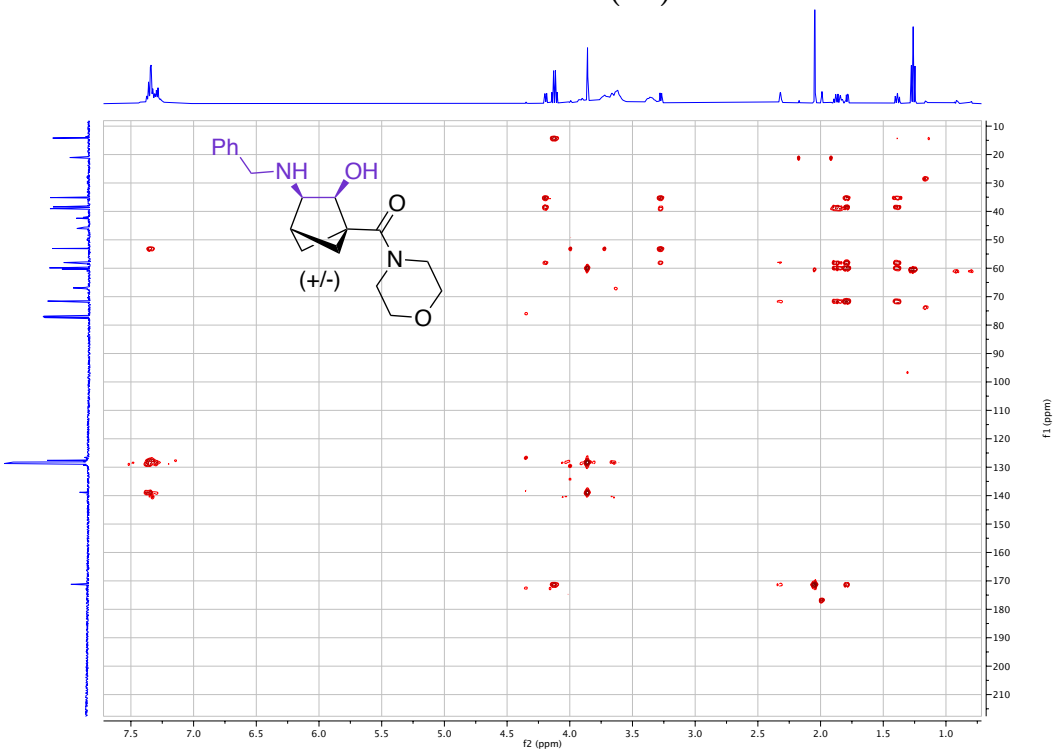

^{1}H-^{1}H NOESY (4b):

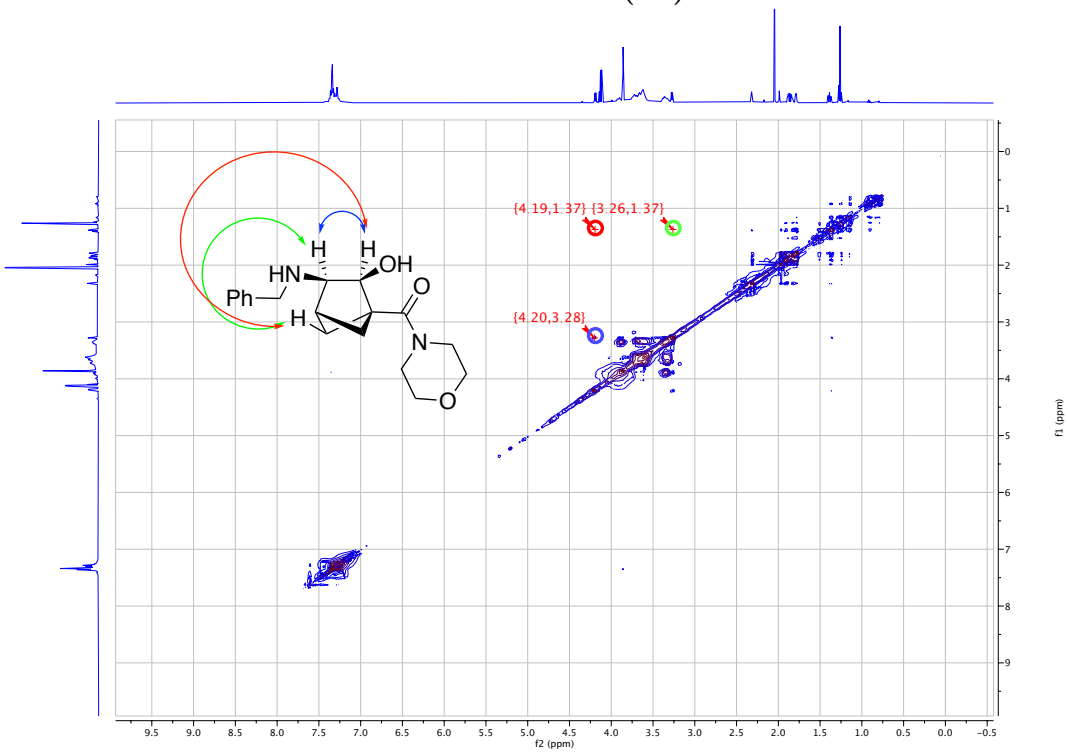

^{1}H-^{1}H NOESY - Zoomed-In (4b):

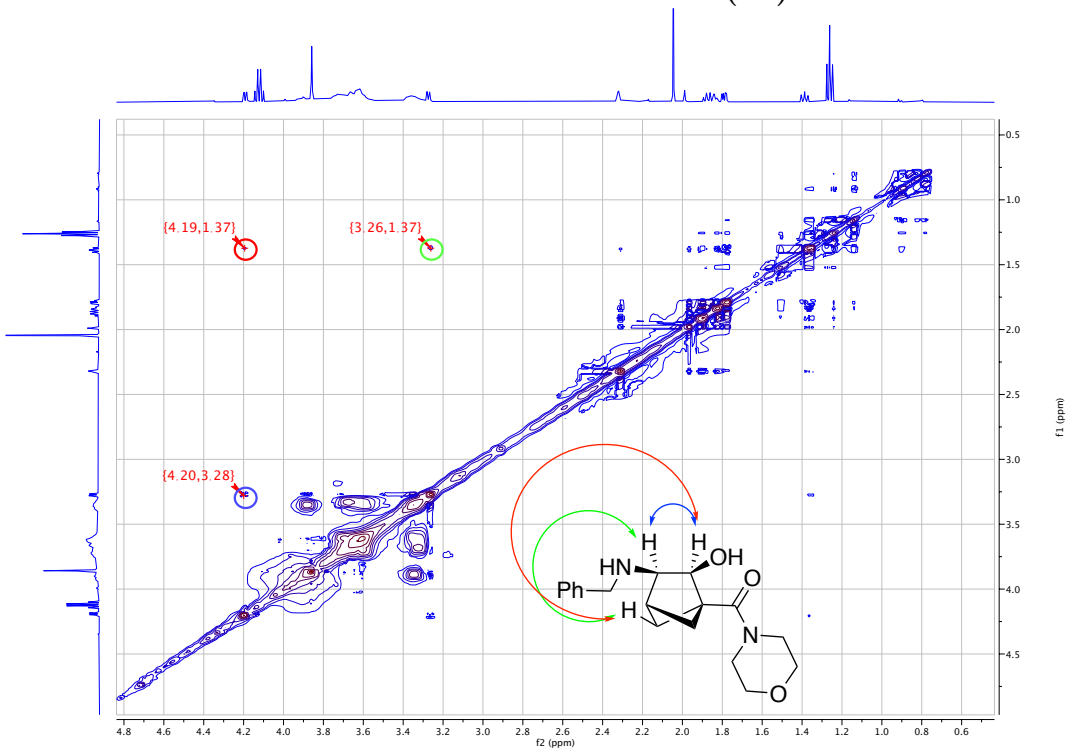

Benzyl (4-(morpholine-4-carbonyl)-3-oxobicyclo[2.1.1]hexan-2-yl)carbamate (4c)

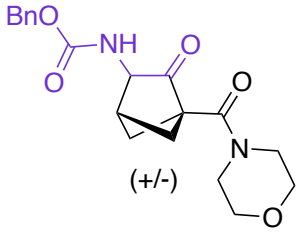

3a was dissolved in DCM (5 mL, 0.1 M) and benzyl chloroformate (0.284 mL, 4 equiv) was added and then the reaction was stirred at room temperature overnight. The reaction was quenched with $NaHCO_3$ and extracted with DCM. The organic layers were dried with Mg_2SO_4, filtered and the solvent was evaporated to give the crude product. The compound was purified by column chromatography (Biotage® Sfär 5g Column, 0-100% MeOH/EtOAc/hexanes, eluted at 8% MeOH). 74 mg of a yellow solid was obtained (47% Yield over two steps).

HRMS(ESI): calc'd for $[C_{19}H_{22}N_2O_5 + Na^+]$, 381.14209; found: 381.14193.

^{1}H NMR (500 MHz, $CDCl_3$, 292 K, ppm): δ 7.36 (m, 5H), 5.13 (s, 2H), 4.26 (m, 1H), 3.68 (m, 7H), 3.21 (m, 2H), 2.97 (m, 1H), 2.56 (m, 2H), 2.19 (t, J = 8.9 Hz, 1H), 1.97 (t, J = 8.7 Hz, 1H).

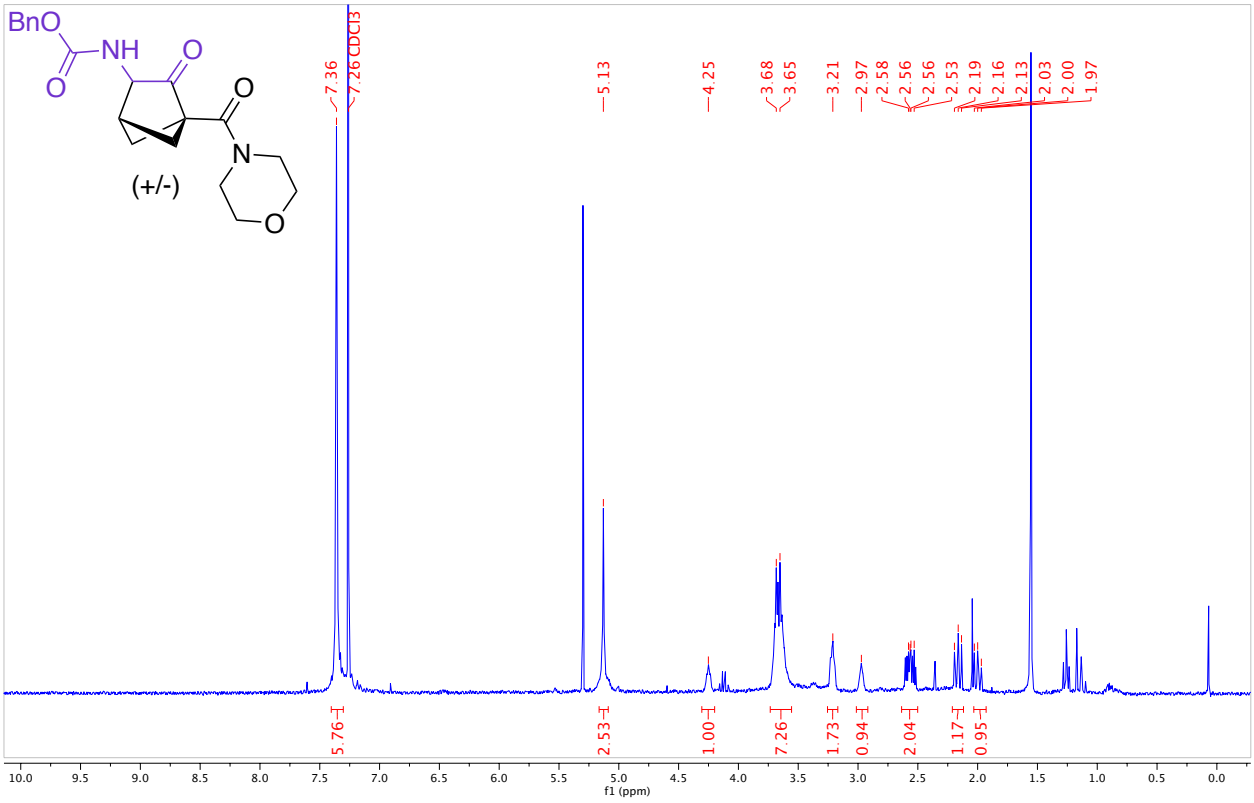

^{13}C NMR (126 MHz, $CDCl_3$, 292 K, ppm): δ 205.70, 165.96, 156.56, 136.10, 128.63, 128.39, 128.35, 67.31, 67.02, 66.83, 66.78, 59.32, 46.38, 42.50, 40.49, 40.22, 36.41, 28.42.

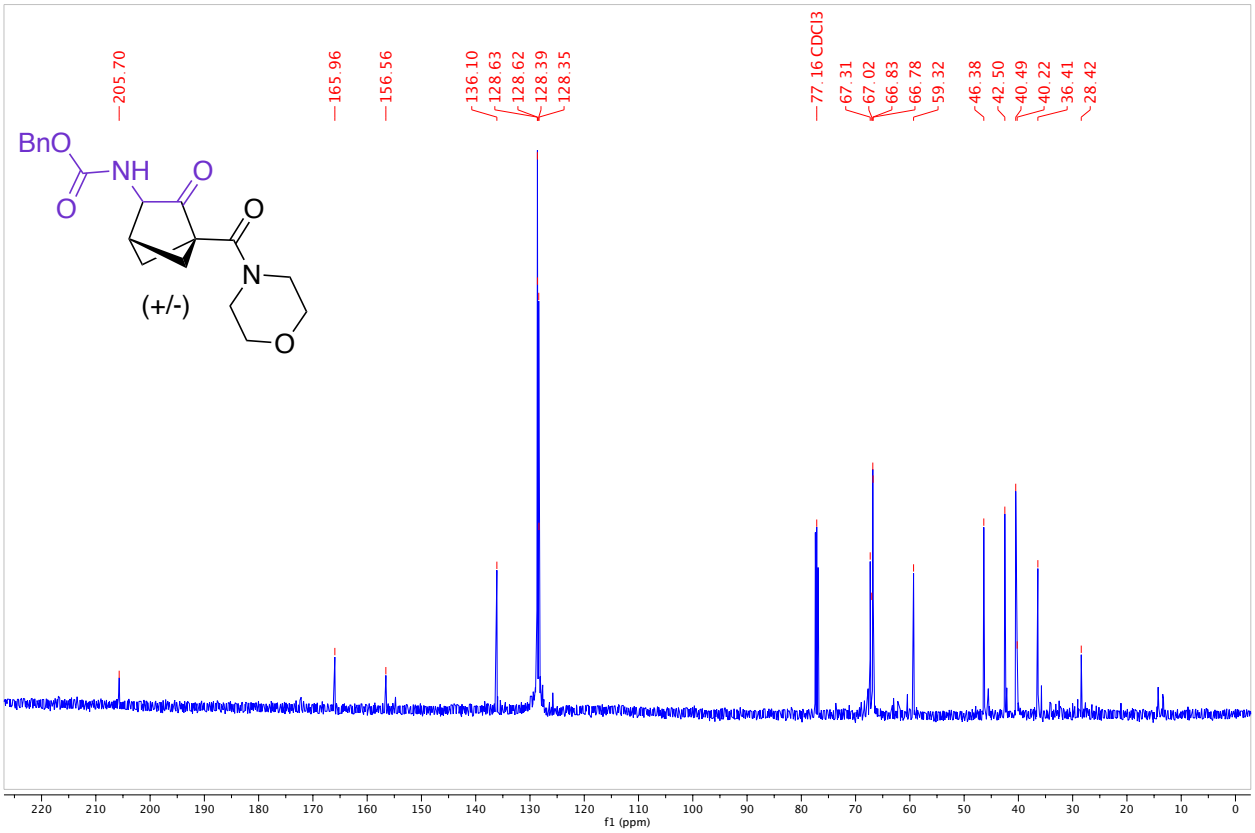

4-methyl-*N*-(4-(morpholine-4-carbonyl)-3-oxobicyclo[2.1.1]hexan-2-yl)-benzamide (4d)

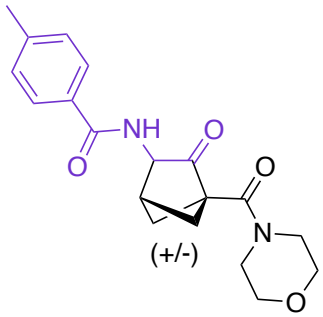

3a was dissolved in DCM (5 mL, 0.1 M) and p-toluoyl chloride (0.264 mL, 4 equiv) was added and then the reaction was stirred at room temperature overnight. The reaction was quenched with $NaHCO_3$ and extracted with DCM. The organic layers were dried with Mg_2SO_4, filtered and the solvent was evaporated to give the crude product. The compound was purified by column chromatography (Biotage® Sfär 5g Column, 0-100% EtOAc/hexanes, eluted at 100% EtOAc). 44 mg of a white solid was obtained (28% Yield over two steps).

HRMS(ESI): calc'd for [$C_{19}H_{22}N_2O_4$ + H^+], 343.16524; found: 343.16528.

^{1}H NMR (500 MHz, $CDCl_3$, 292 K, ppm): δ 7.70 (d, J = 8.3 Hz, 2H), 7.22 (d, J = 7.9 Hz, 2H), 6.91 (d, J = 6.1 Hz, 1H), 4.60 (t, J = 4.7 Hz, 1H), 3.67 (m, 5H), 3.52 (m, 1H), 3.26 (m, 2H), 3.02 (m, 1H), 2.61 (dd, J = 7.9, 3.9 Hz, 1H), 2.53 (dt, J = 7.7, 3.7 Hz, 1H), 2.39 (s, 3H), 2.35 – 2.28 (m, 1H), 2.07 (dd, J = 9.5, 7.9 Hz, 1H).

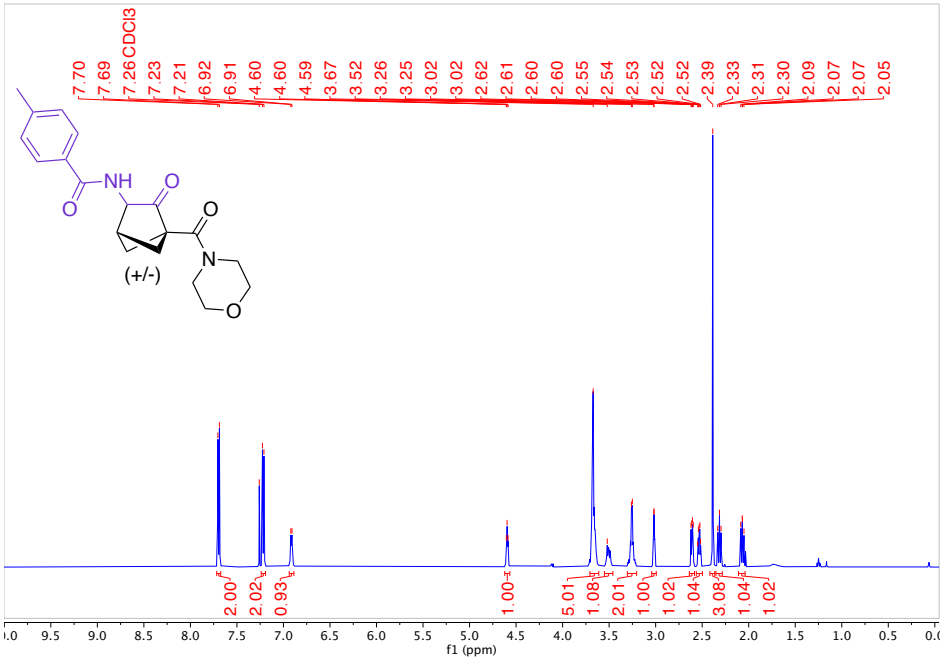

^{13}C NMR (126 MHz, $CDCl_3$, 292 K, ppm): δ 206.36, 168.33, 166.02, 142.63, 130.80, 129.40, 127.35, 67.39, 66.95, 66.88, 58.79, 46.52, 42.60, 40.97, 40.74, 36.57, 21.62.

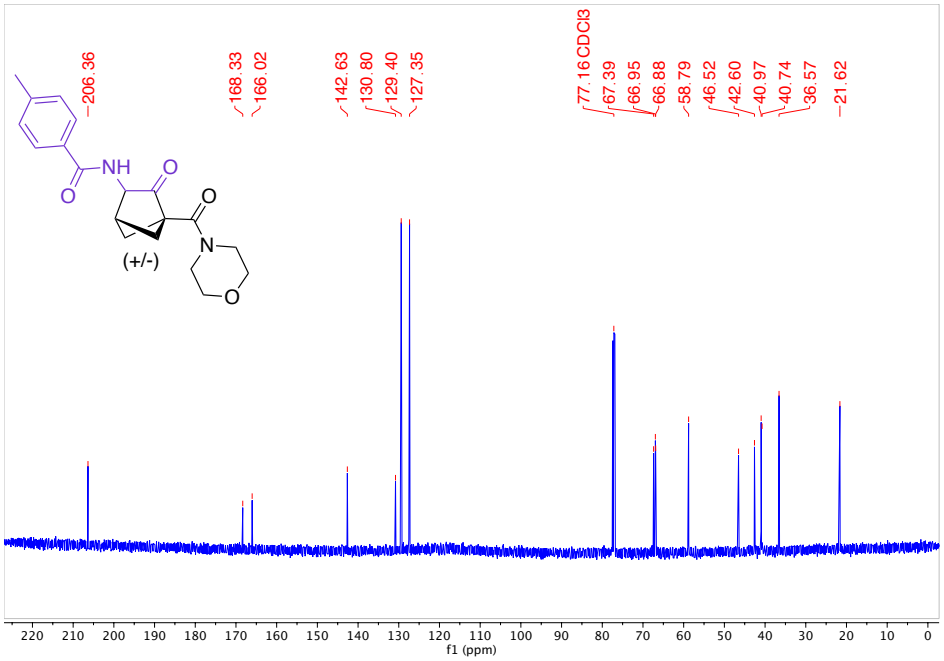

^{1}H-^{1}H COSY (4d):

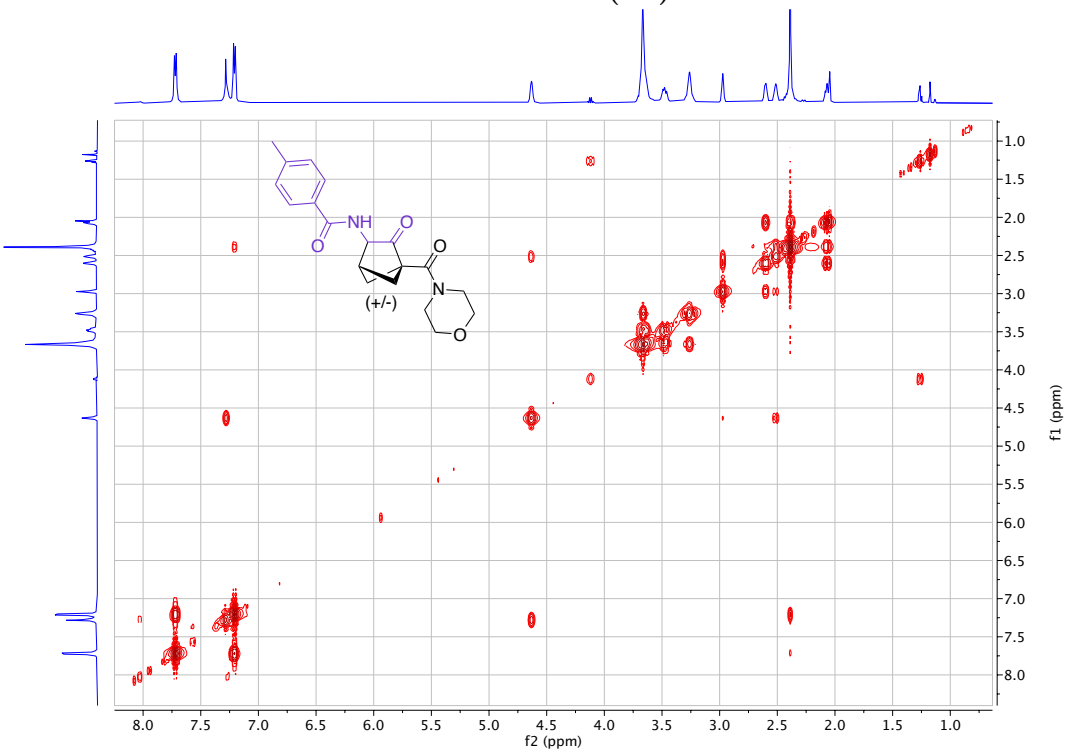

^{1}H-^{13}C HSQC (4d):

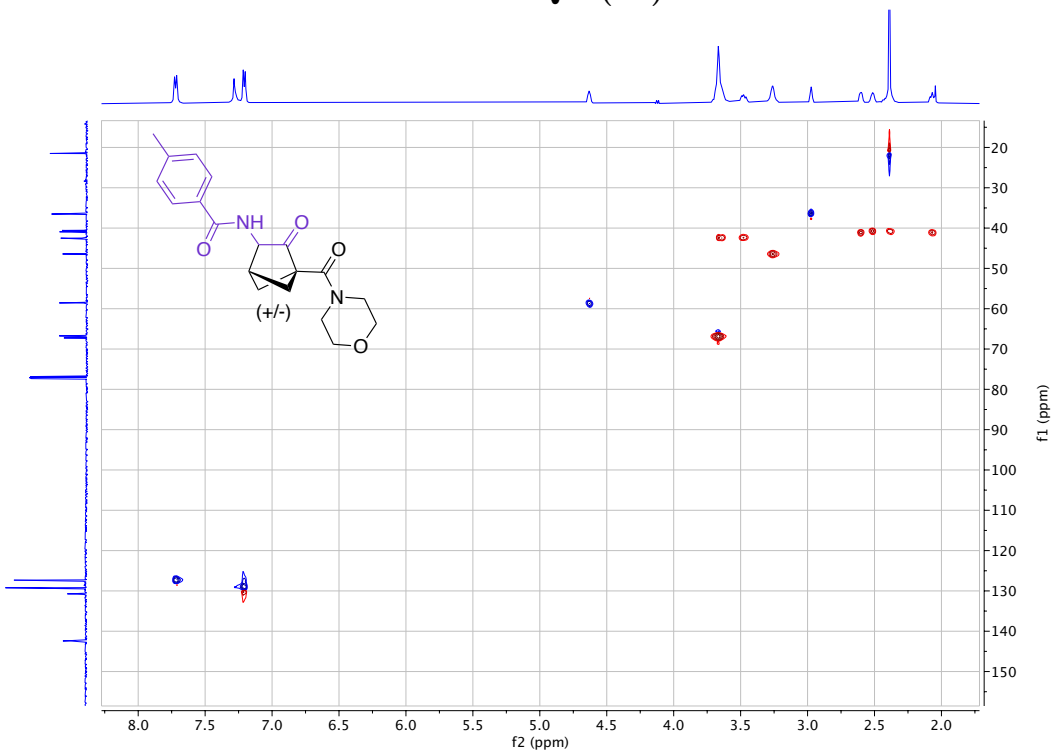

^{1}H-^{13}C HMBC (4d):

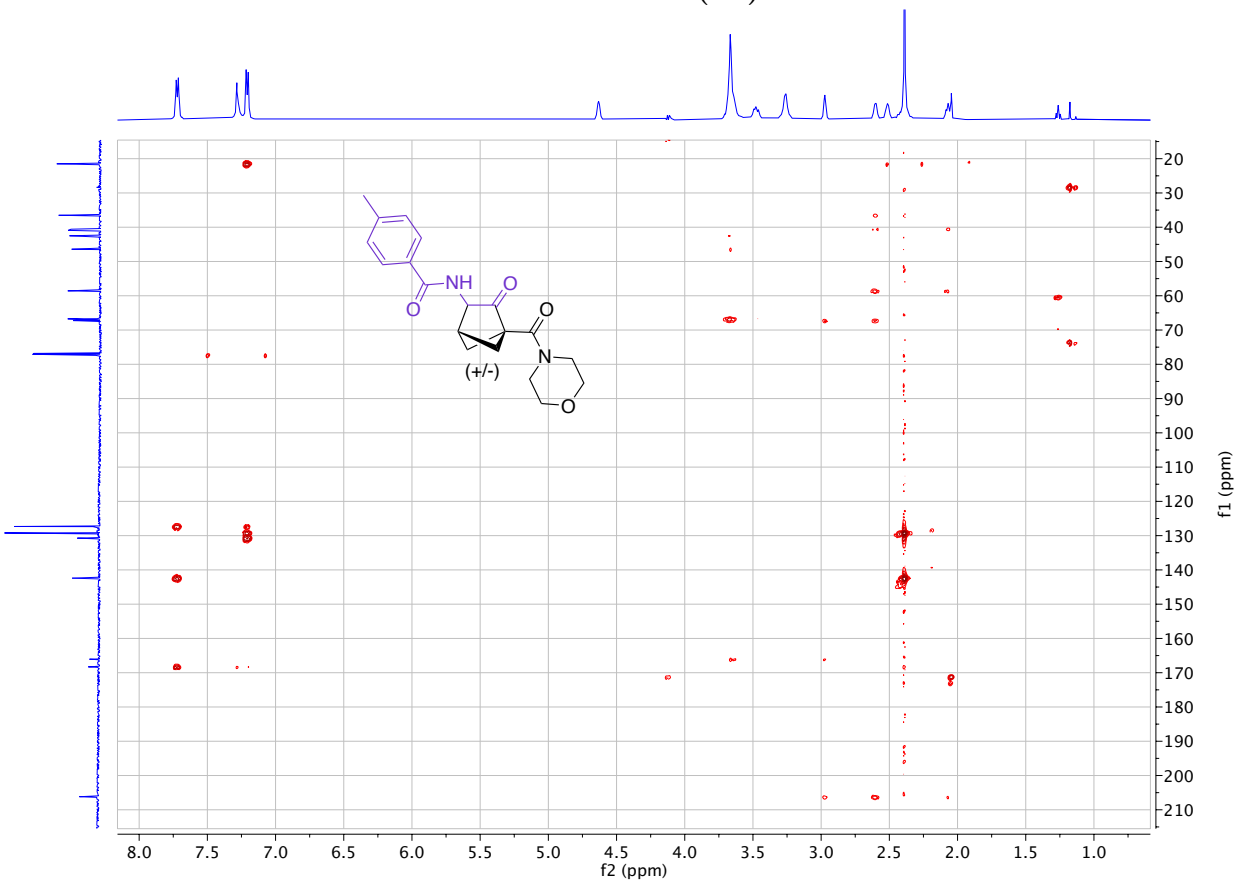

B.5 Bicyclohexane Synthesis Scope

General Procedure for Bicyclohexane Synthesis

In two separate vials, the bicyclobutane **1** (1 equiv) and enolate precursor **2** (1.2 equiv) were added and put under a nitrogen atmosphere. The acetate was dissolved in 50% of the THF (0.3 M) and LiHMDS (1.0M in THF, 1.5 equiv) was added dropwise to the vial containing the acetate and then left to stir for 15 minutes at room temperature to form the enolate. 50% of the THF solvent was added to the bicyclobutane vial and then it was cooled in the freezer for 15 minutes along with the enolate vial. The bicyclobutane was then added dropwise to the enolate. The reaction was left to stir at room temperature overnight. The reaction was quenched with $NaHCO_3$ and extracted with ethyl acetate (3 times). The organic layers were dried with Mg_2SO_4, filtered and the solvent was evaporated to give the crude product. Products were purified by column chromatography.

3-((Benzylidene)amino)-1-(morpholine-4-carbonyl)bicyclo[2.1.1]hexan-2-one (3a)

The product was prepared following the general procedure for bicyclohexane synthesis from **1a** and **2a** on a 0.30 mmol bicyclobutane scale. 1,3,5-Trimethoxybenzene was used as an internal standard for calculating a solution yield of 47% (peak at 2.89 ppm).

^{1}H NMR (500 MHz, $CDCl_3$, 292 K, ppm):

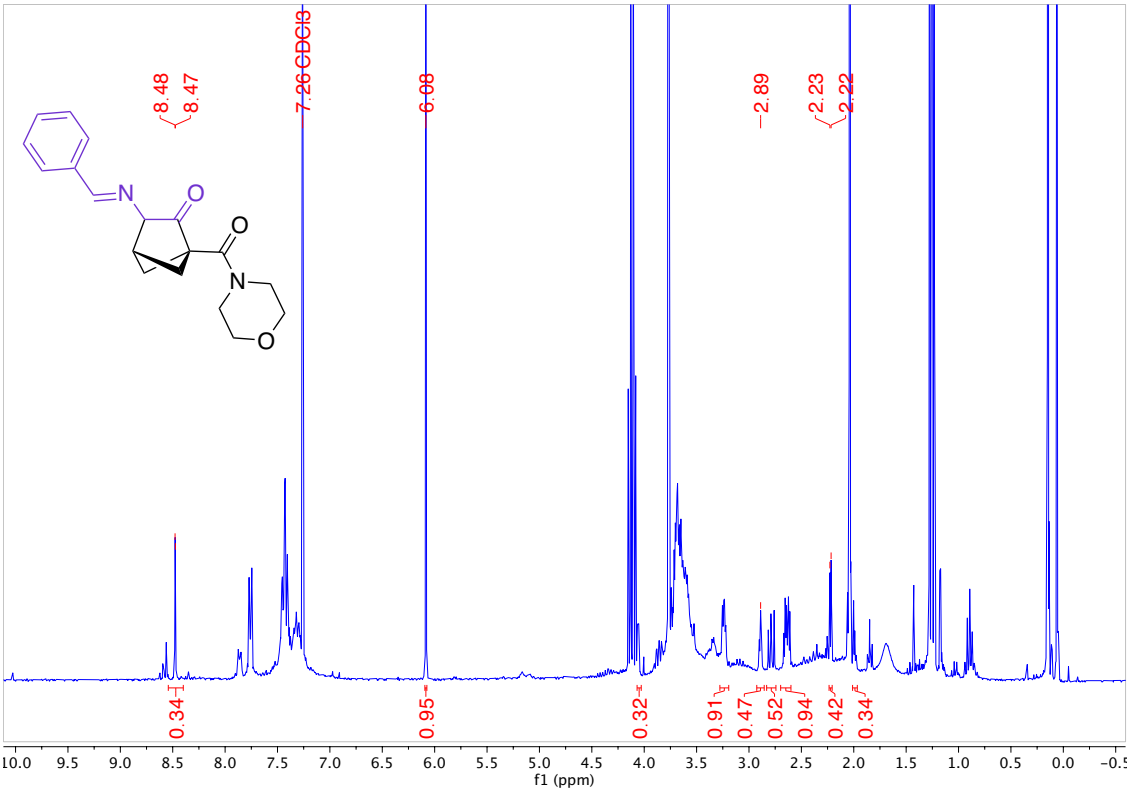

3-((Diphenylmethylene)amino)-1-(morpholine-4-carbonyl)bicyclo[2.1.1]hexan-2-one (3b)

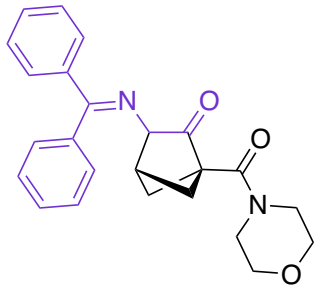

The product was prepared following the general procedure for bicyclohexane synthesis from **1a** and **2b** on a 0.30 mmol bicyclobutane scale with a reaction concentration of 0.1 M. The compound was purified by column chromatography (Biotage® Sfär 5g Column, 0-100% EtOAc/hexanes, eluted at 75% EtOAc). 45 mg of a white solid was obtained (42% Yield).

HRMS(ESI): calc'd for $[C_{24}H_{24}N_2O_3 + H^+]$, 389.18597; found: 389.18601.

^{1}H NMR (500 MHz, $CDCl_3$, 292 K, ppm): δ 7.65 – 7.61 (m, 2H), 7.51 – 7.43 (m, 3H), 7.42 – 7.36 (m, 3H), 7.36 – 7.30 (m, 2H), z14 (m, 1H), 3.79 (m, 1H), 3.68 (m, 4H), 3.55 – 3.44 (m, 1H), 3.28 (m, 2H), 3.02 (dd, J = 9.4, 7.2 Hz, 1H), 2.68 (m, 1H), 2.63 (dt, J = 7.1, 3.5 Hz, 1H), 2.52 (dd, J = 8.1, 3.9 Hz, 1H), 1.87 (dd, J = 9.3, 8.1 Hz, 1H).

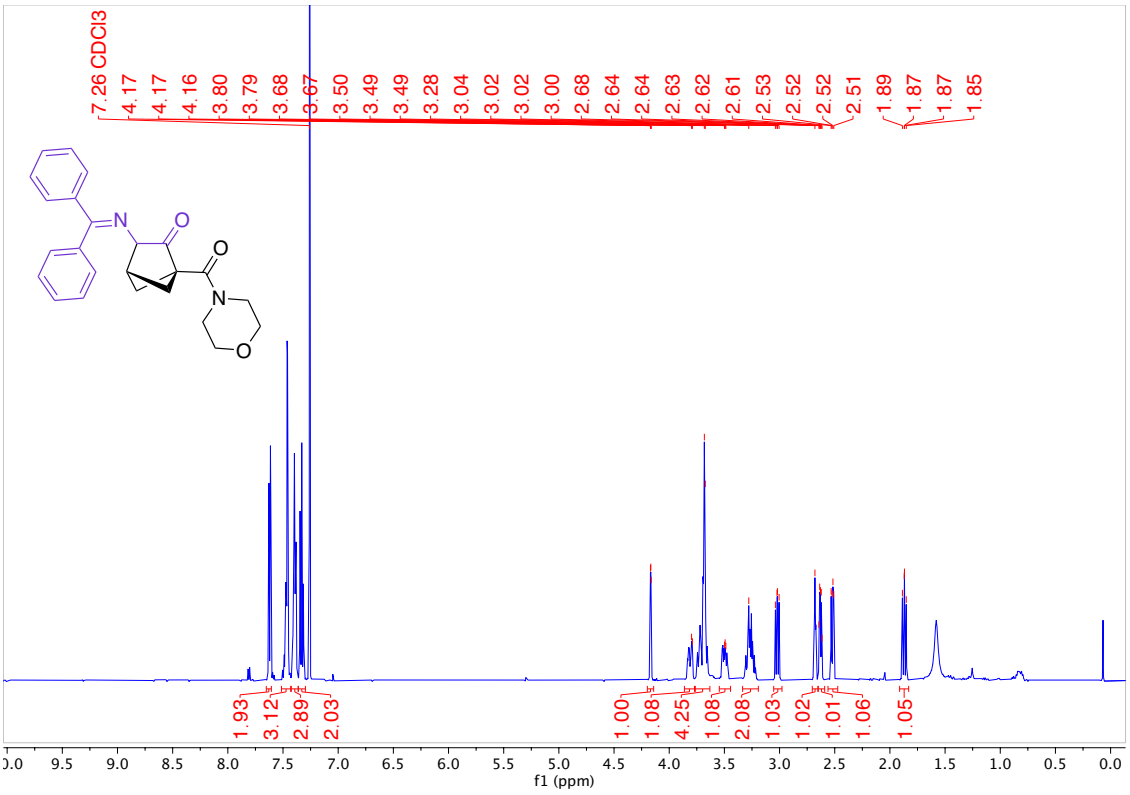

^{13}C NMR (126 MHz, $CDCl_3$, 292 K, ppm): δ 205.14, 171.70, 166.71, 139.67, 136.01, 130.54, 130.22, 129.09, 128.99, 128.80, 128.59, 128.18, 70.30, 67.50, 67.16, 67.02, 46.49, 42.51, 41.98, 39.47, 37.91.

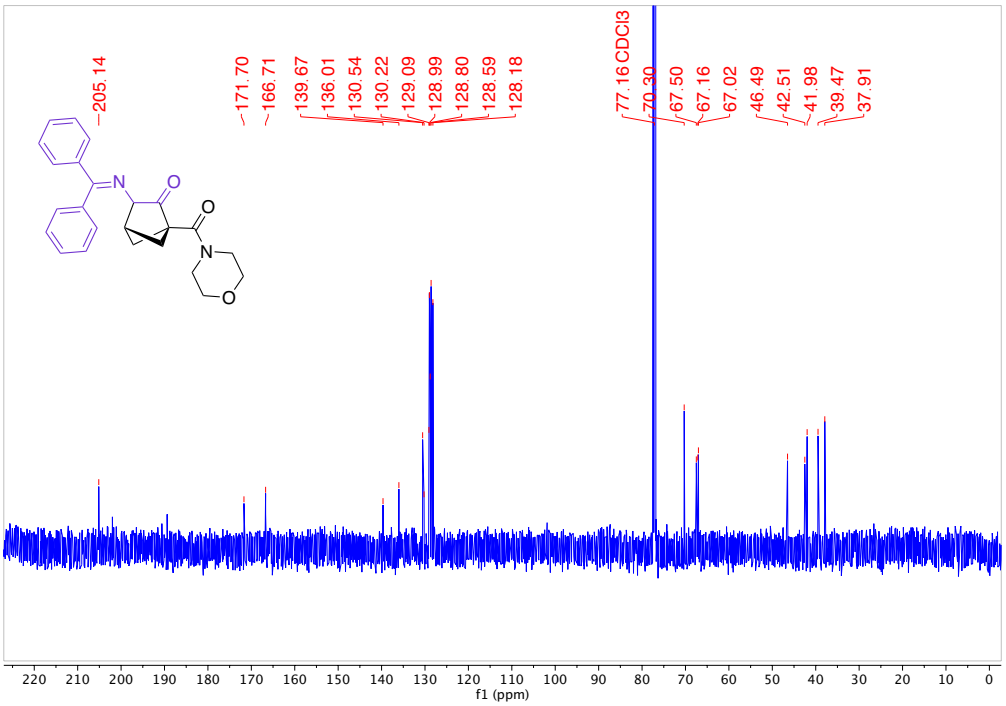

1-(Morpholine-4-carbonyl)-3-phenylbicyclo[2.1.1]hexan-2-one (3c):

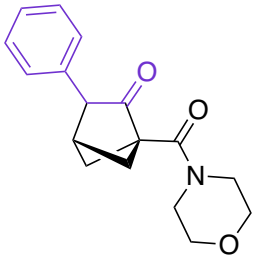

The product was prepared following the general procedure for bicyclohexane synthesis from **1a** and **2c** on a 0.50 mmol bicyclobutane scale. The compound was purified by column chromatography (Biotage® Sfär 5g Column, 0-100% EtOAc/hexanes, eluted at 80% EtOAc). 120.6 mg of a white solid was obtained (85% Yield).

This product was also prepared following the general procedure for bicyclohexane synthesis using 3 mmol of **1a** with an increase of concentration to 0.60 M. The compound was purified by column chromatography (Biotage® Sfär 10g Column, 0-100% EtOAc/hexanes, eluted at 72% EtOAc). 513.5 mg of a white solid was obtained (60% Yield). On larger scale, an enolate addition product **3cc** is also observed as a mixture of diastereomers, but can be separated from the desired product by column chromatography.

HRMS(ESI): calc'd for [$C_{17}H_{19}NO_3$ + H^+], 286.14377; found: 286.14379.

^{1}H NMR (500 MHz, $CDCl_3$, 292 K, ppm): δ 7.37 – 7.22 (m, 5H), 3.75 – 3.57 (m, 7H), 3.20 (t, J = 4.8 Hz, 2H), 3.08 (t, J = 3.7 Hz, 1H), 2.62 (dd, J = 7.6, 3.8 Hz, 1H), 2.51 (dt, J = 7.8, 3.7 Hz, 1H), 2.29 – 2.20 (m, 1H), 2.19 – 2.11 (m, 1H).

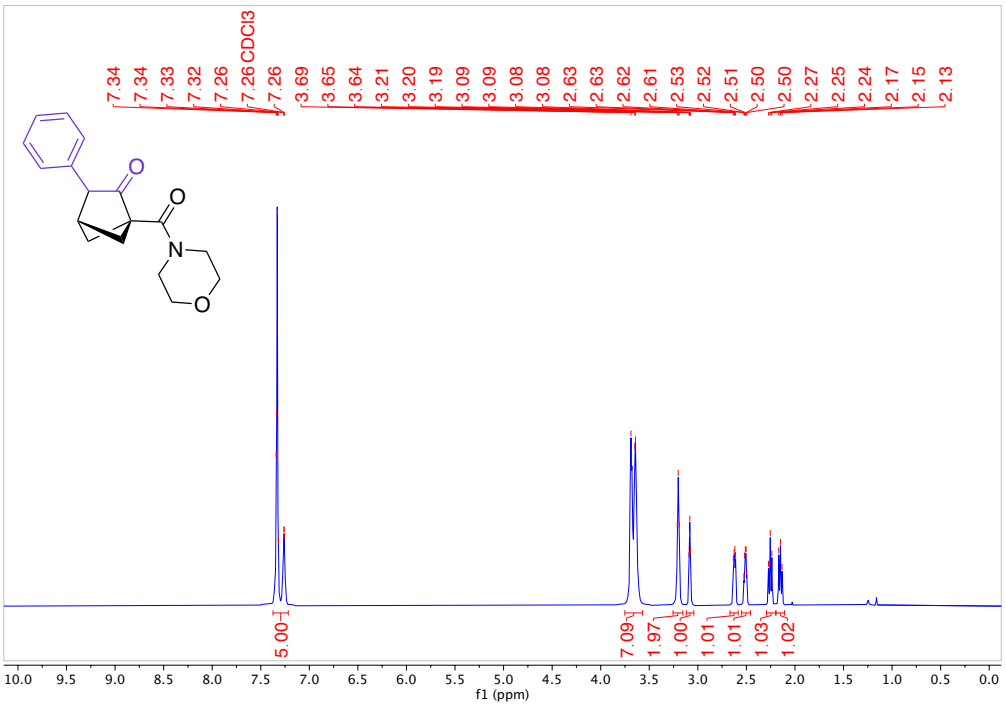

^{13}C NMR (126 MHz, $CDCl_3$, 292 K, ppm): δ 206.74, 166.51, 135.83, 128.76, 127.45, 127.14, 67.85, 66.91, 54.86, 46.42, 43.11, 42.45, 41.65, 35.17.

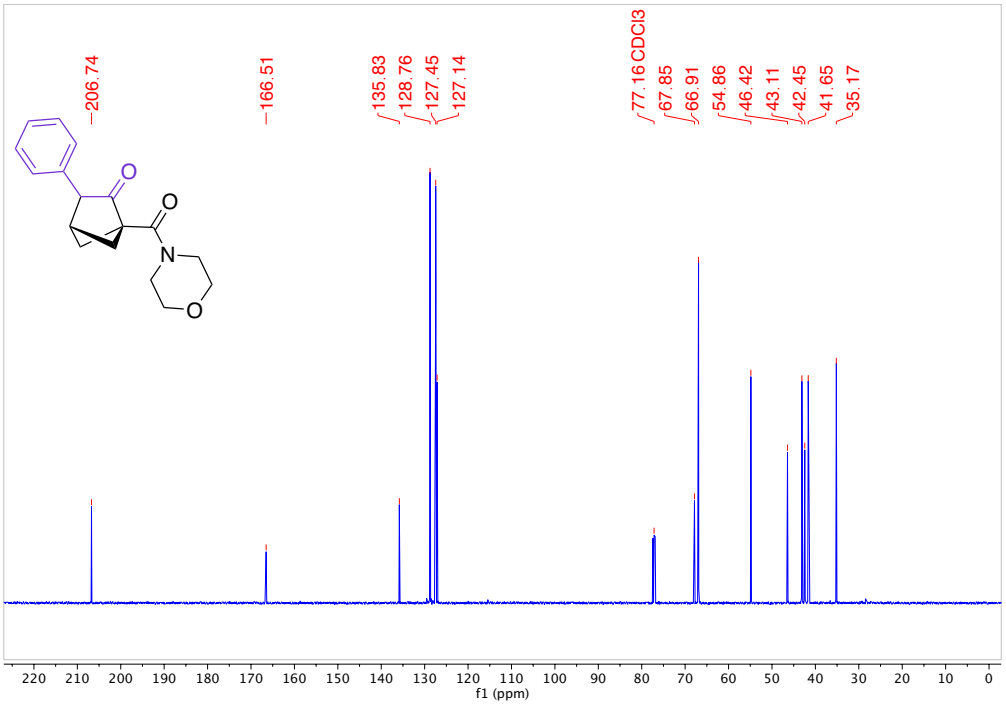

^{1}H-^{1}H COSY (3c):

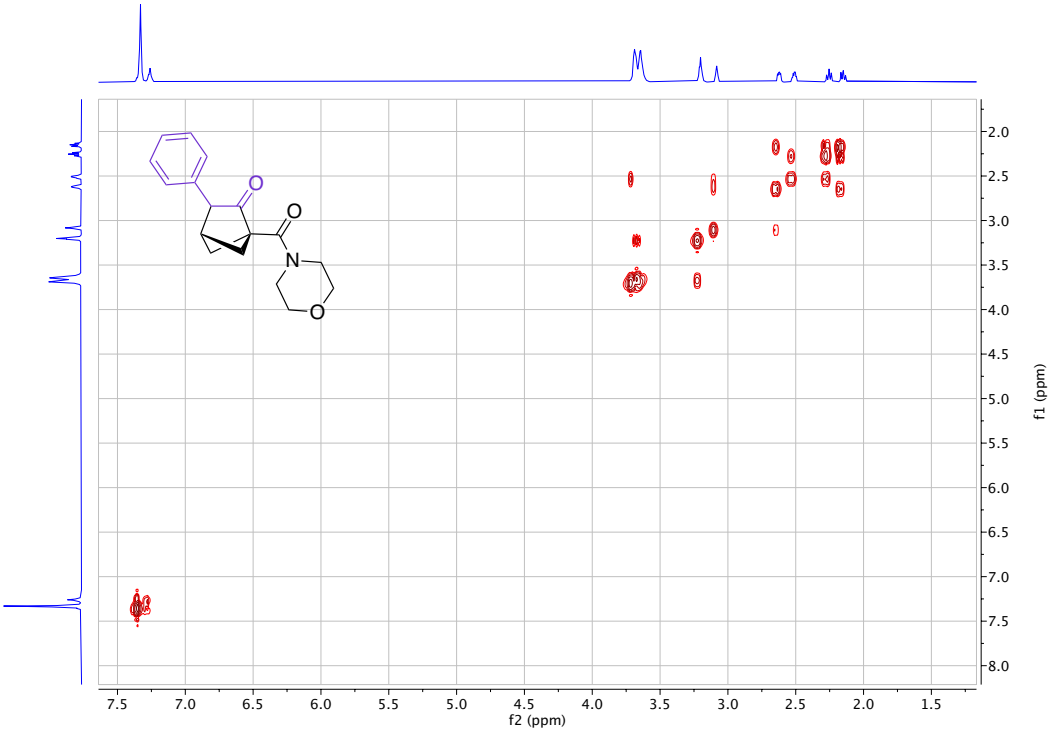

^{1}H-^{13}C HSQC (3c):

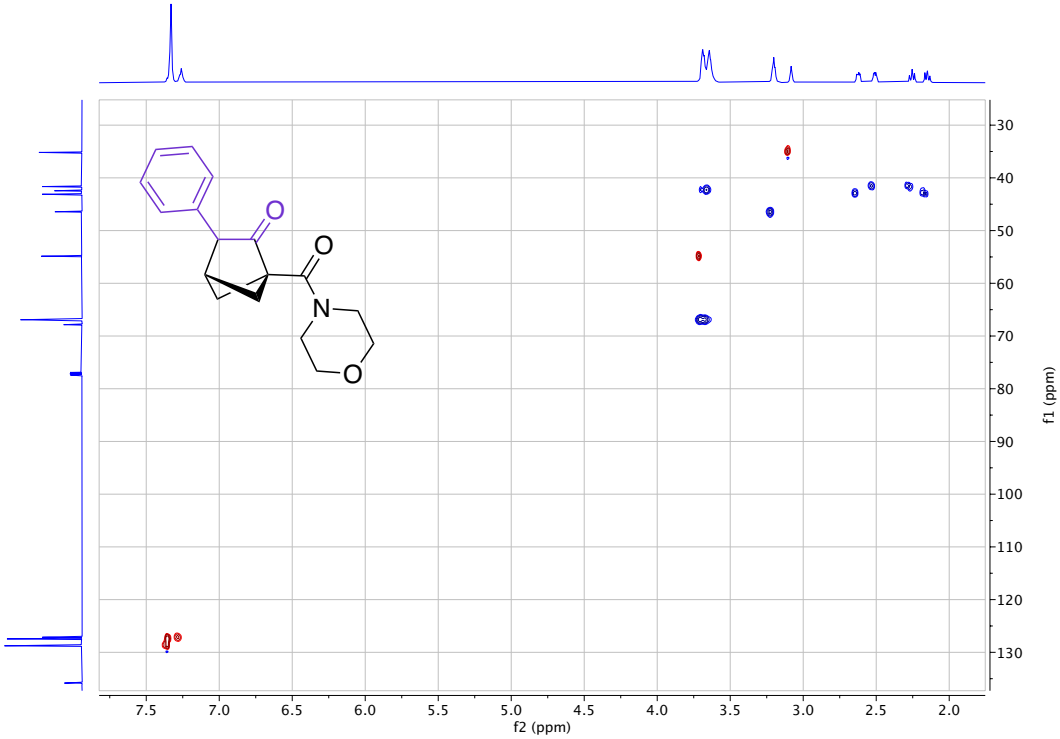

^{1}H-^{13}C HMBC (3c):

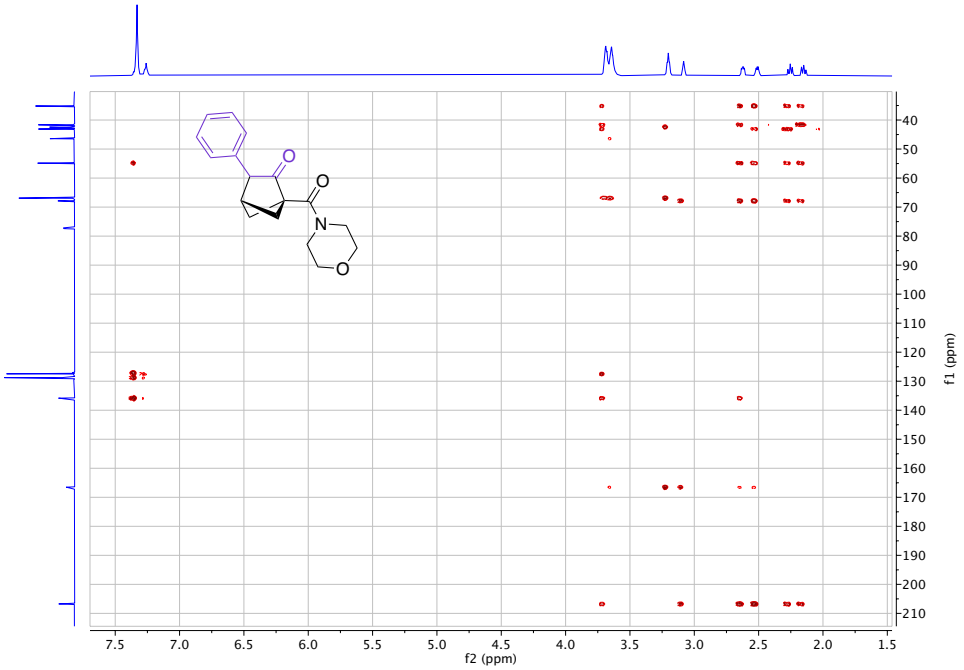

Isolated By-product Ethyl 2-(3-(morpholine-4-carbonyl)cyclobutyl)-2-phenyl-acetate (3cc):

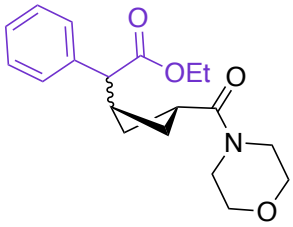

HRMS(ESI): calc'd for $[C_{19}H_{25}NO_4 + H^+]$, 332.18564; found: 332.18565.

^{1}H NMR (500 MHz, $CDCl_3$, 292 K, ppm): δ 7.36 – 7.20 (m, 5H), 4.17 – 3.99 (m, 2H), 3.71 – 3.53 (m, 6H), 3.50 (d, J = 11.0 Hz, 0.6H), 3.31 (d, J = 4.6 Hz, 1.1H), 3.25 (d, J = 3.4 Hz, 0.8H), 3.15 (m, 0.5H), 3.09 – 2.98 (m, 1H), 2.94 – 2.83 (m, 0.6H), 2.57 (m, 0.5H), 2.46 – 2.38 (m, 1H), 2.27 (m, 0.5H), 2.14 (m, 0.6H), 2.03 (m, 1H), 1.95 (m, 1.2H), 1.82 (m, 0.5H), 1.19 (m, 3H).

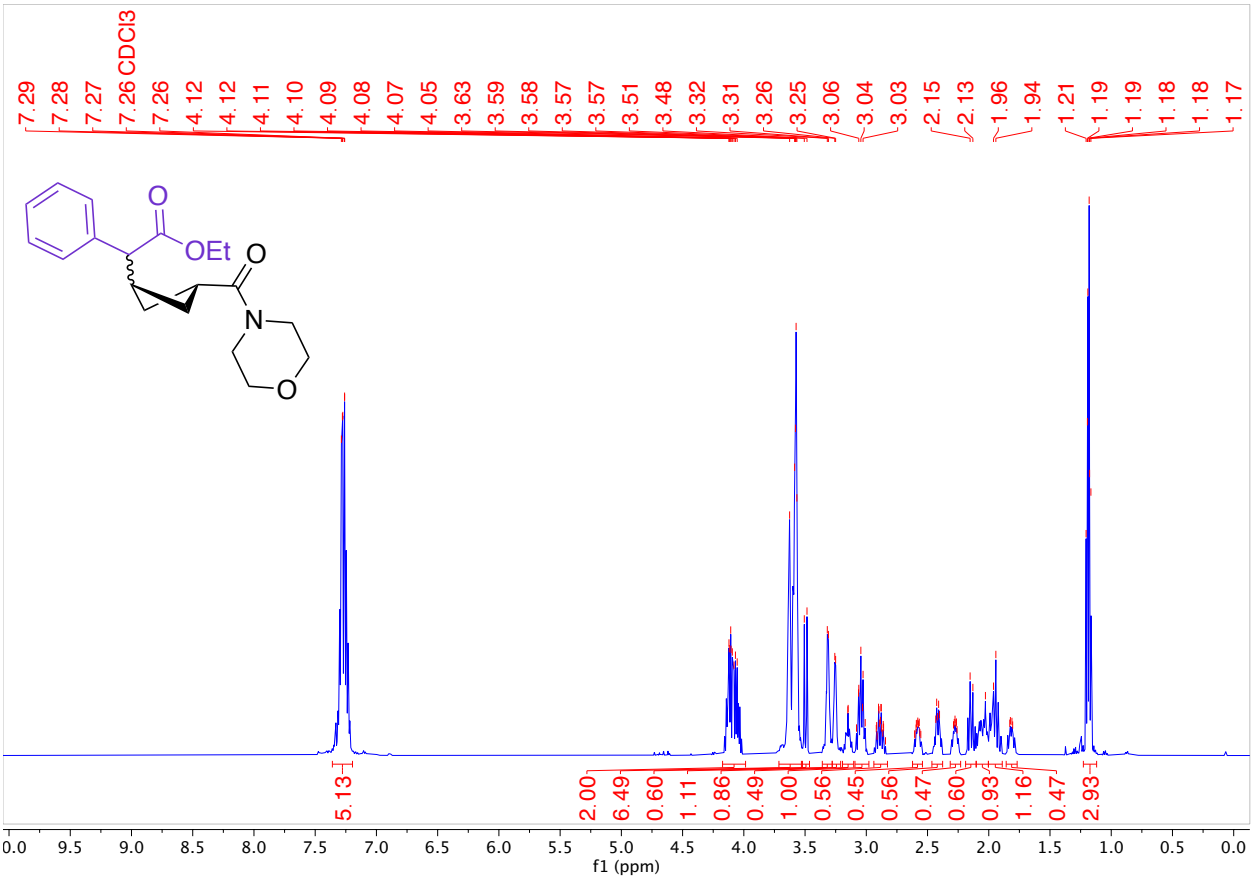

^{13}C NMR (126 MHz, $CDCl_3$, 292 K, ppm): δ 173.09, 172.90, 172.84, 172.73, 137.20, 128.61, 128.25, 127.99, 127.44, 127.33, 66.92, 66.73, 66.60, 60.78, 60.72, 58.11, 57.58, 45.51, 42.13, 42.10, 34.16, 14.12, 32.90, 32.64, 30.63, 29.41, 29.03, 27.98, 14.20, 14.18.

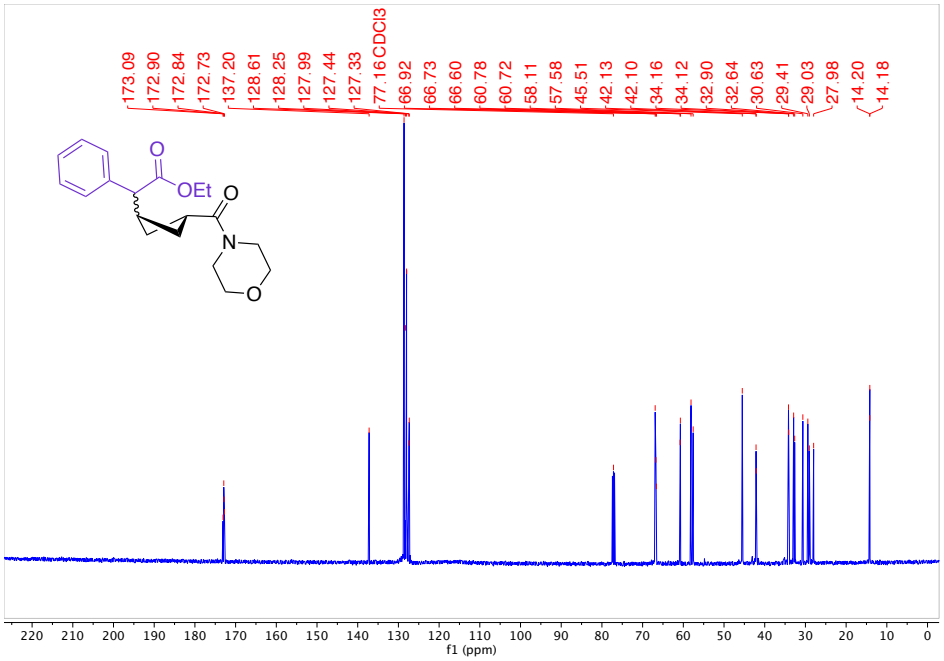

^{1}H-^{1}H COSY (3cc):

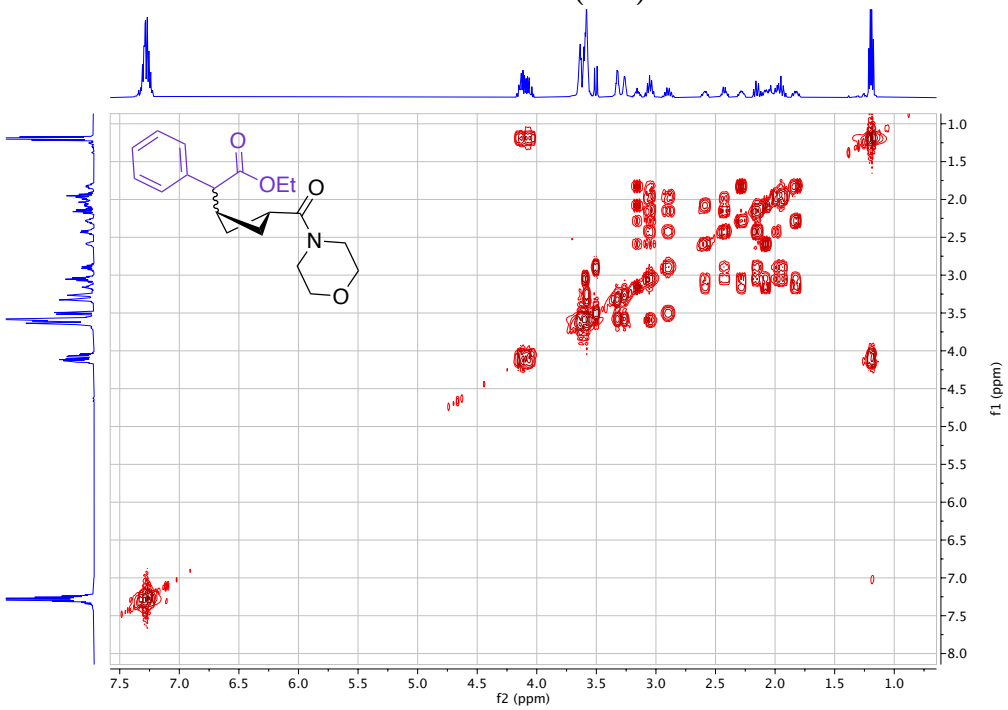

^{1}H-^{13}C HSQC (3cc):

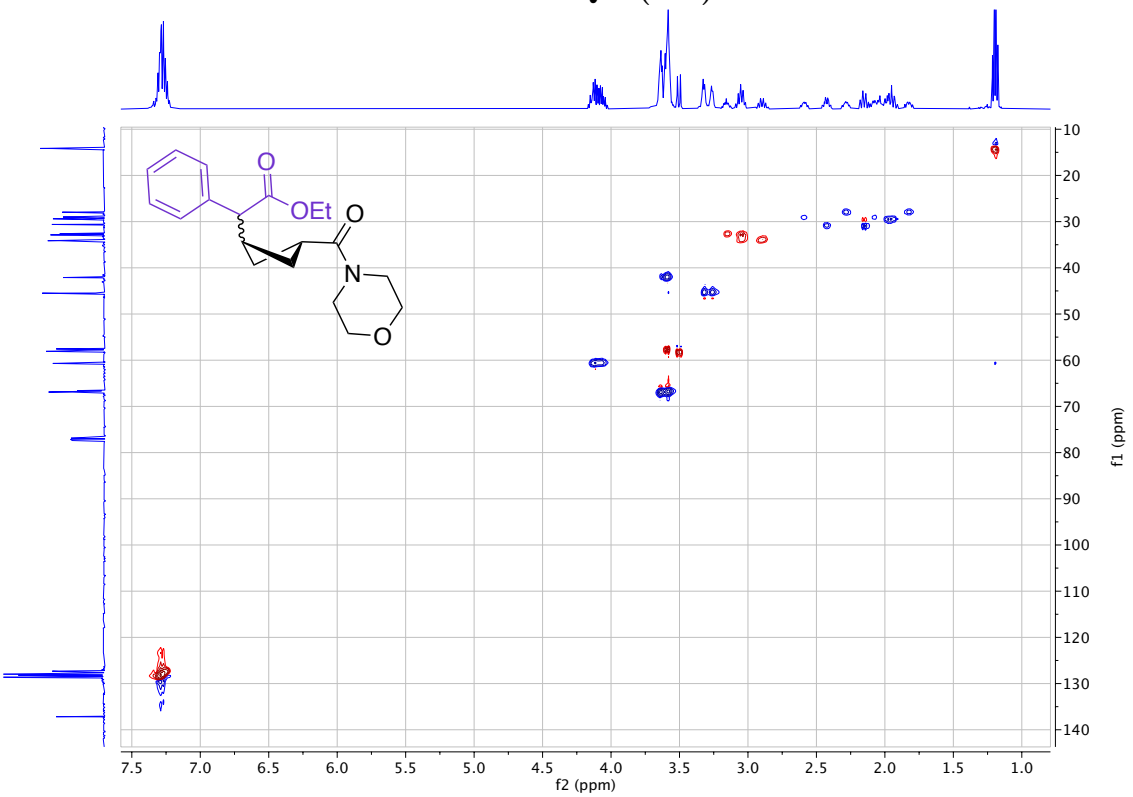

^{1}H-^{13}C HMBC (3cc):

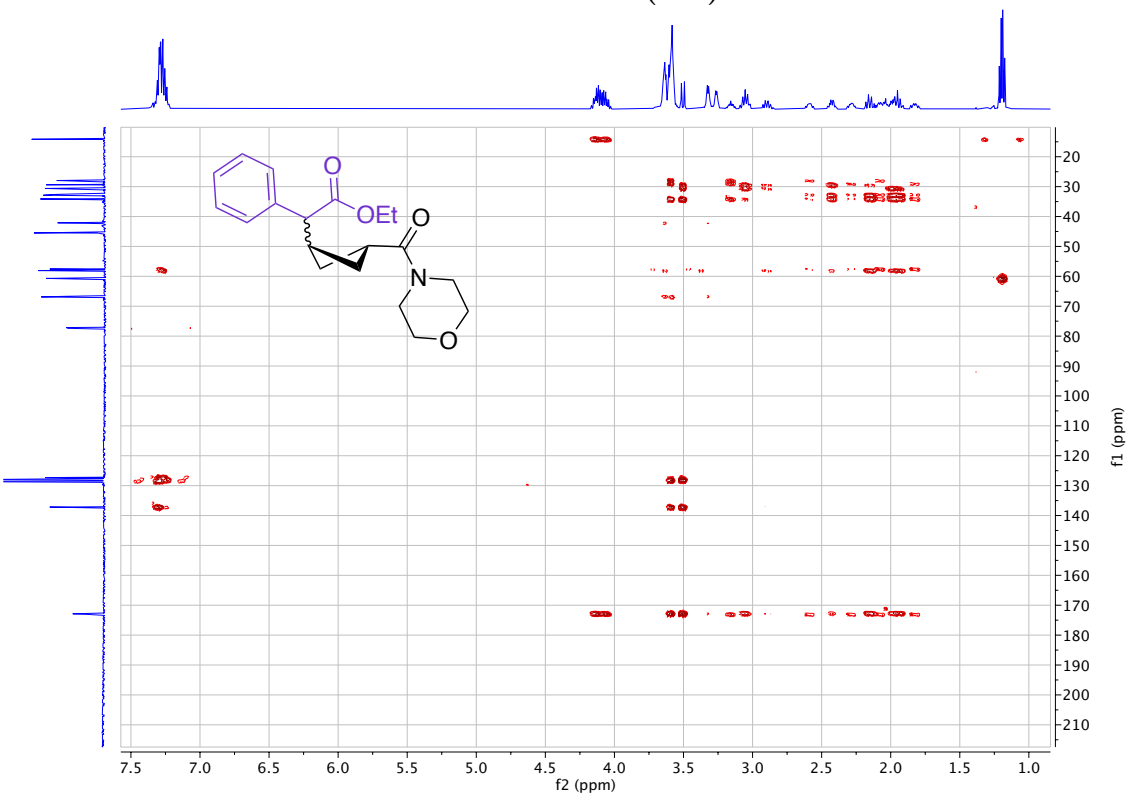

1-(Morpholine-4-carbonyl)-3-(p-tolyl)bicyclo[2.1.1]hexan-2-one (3d)

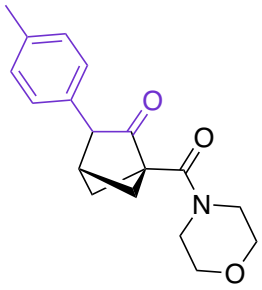

The product was prepared following the general procedure for bicyclohexane synthesis from **1a** and **2d** on a 0.30 mmol bicyclobutane scale. The crude compound was crystallized in a vial and was washed with hexanes. 58 mg of a white solid was obtained (65% Yield).

HRMS(ESI): calc'd for [$C_{18}H_{21}NO_3$ + H^+], 300.15942; found: 300.15946.

^{1}H NMR (500 MHz, $CDCl_3$, 292 K, ppm): δ 7.21 (d, J = 7.6 Hz, 2H), 7.14 (d, J = 7.9 Hz, 2zH), 3.71 – 3.56 (m, 7H), 3.20 (t, J = 4.8 Hz, 2H), 3.05 (td, J = 3.7, 1.4 Hz, 1H), 2.61 (ddd, J = 7.6, 3.9, 1.0 Hz, 1H), 2.49 (dt, J = 7.7, 3.8 Hz, 1H), 2.32 (s, 3H), 2.25 (dd, J = 9.5, 7.7 Hz, 1H), 2.14 (dd, J = 9.5, 7.5 Hz, 1H).

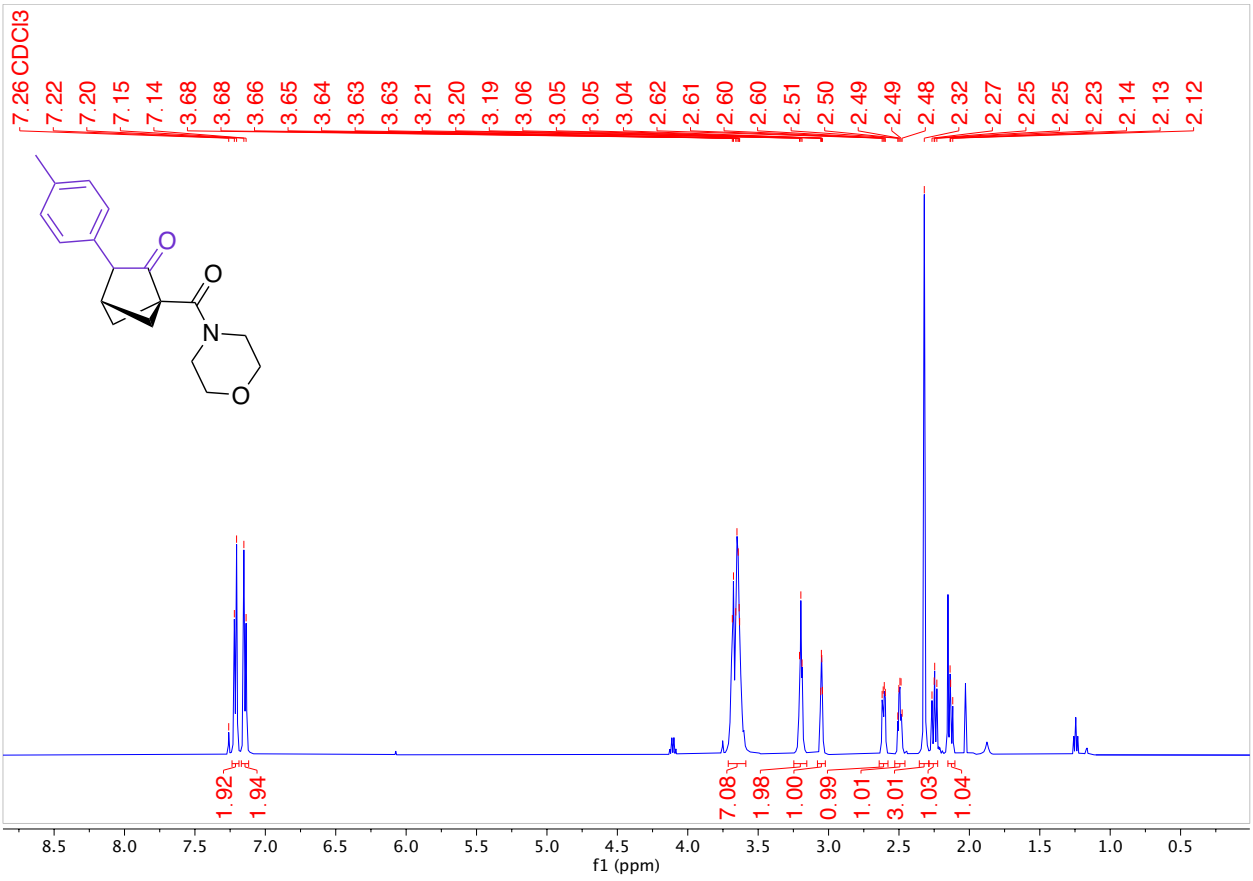

^{13}C NMR (126 MHz, $CDCl_3$, 292 K, ppm): δ 206.99, 166.56, 136.77, 132.81, 129.43, 127.32, 67.85, 66.91, 54.57, 46.41, 43.12, 42.42, 41.66, 35.25, 21.09.

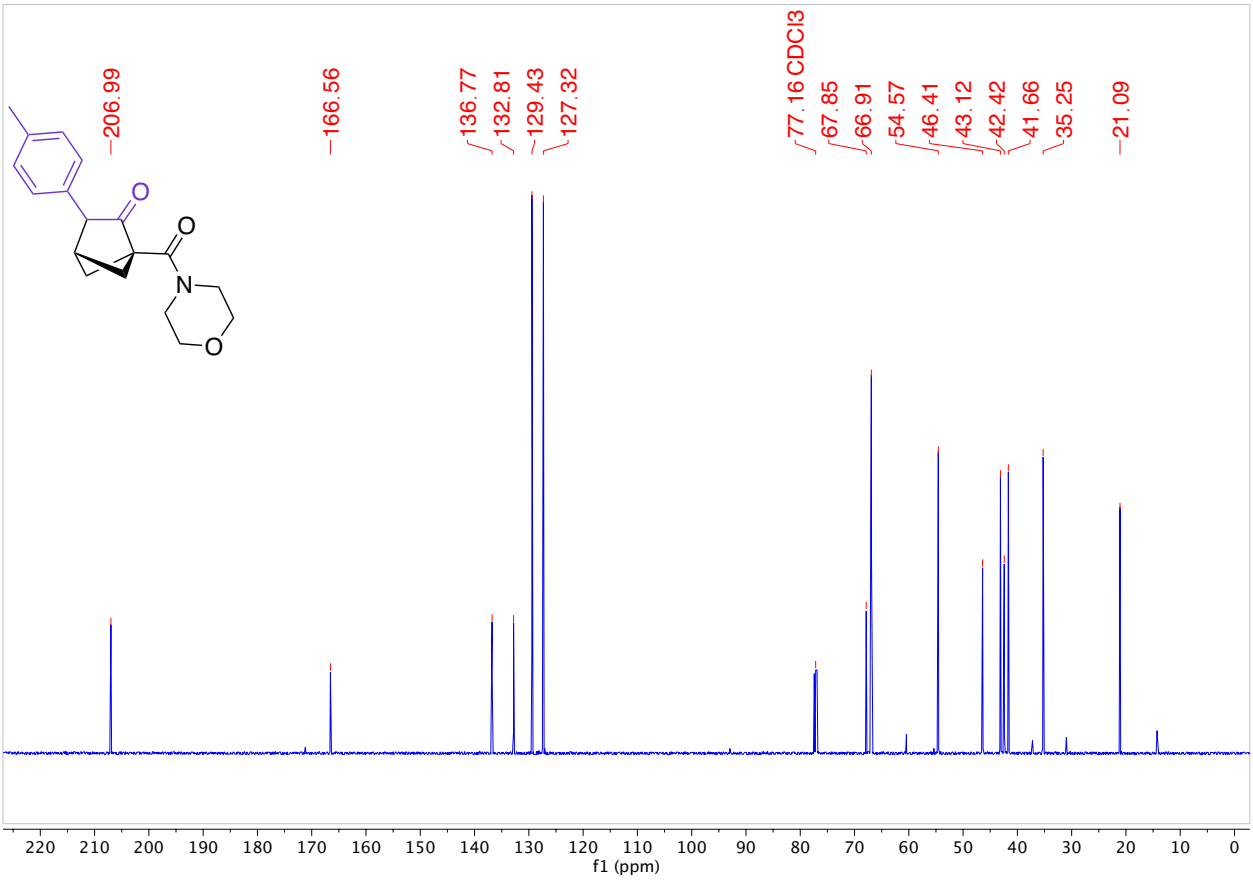

1-(Morpholine-4-carbonyl)-3-(naphthalen-2-yl)bicyclo[2.1.1]hexan-2-one (3e)

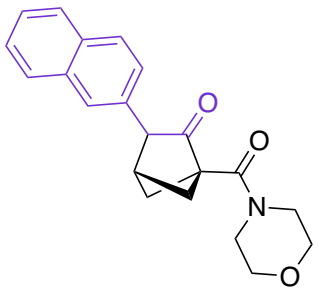

The product was prepared following the general procedure for bicyclohexane synthesis from **1a** and **2e** on a 0.50 mmol bicyclobutane scale using a reaction concentration of 0.05 M. The compound was purified by column chromatography (Biotage® Sfär 5g Column, 0-100% EtOAc/hexanes, eluted at 80% EtOAc). 127 mg of a light brown solid was obtained (76% Yield).

HRMS(ESI): calc'd for [$C_{21}H_{21}NO_3$ + H^+], 336.15942; found: 336.15947.

^{1}H NMR (500 MHz, $CDCl_3$, 292 K, ppm): δ 7.86 – 7.78 (m, 3H), 7.74 (sz, 1H), 7.53 – 7.43 (m, 3H), 3.85 (d, J = 3.9 Hz, 1H), 3.72 – 3.61 (m, 5H), 3.21 (m, 3H), 2.68 (ddd, J = 7.5, 3.9, 1.0 Hz, 1H), 2.56 (dt, J = 7.7, 3.8 Hz, 1H), 2.33 (dd, J = 9.5, 7.8 Hz, 1H), 2.21 (dd, J = 9.5, 7.6 Hz, 1H).

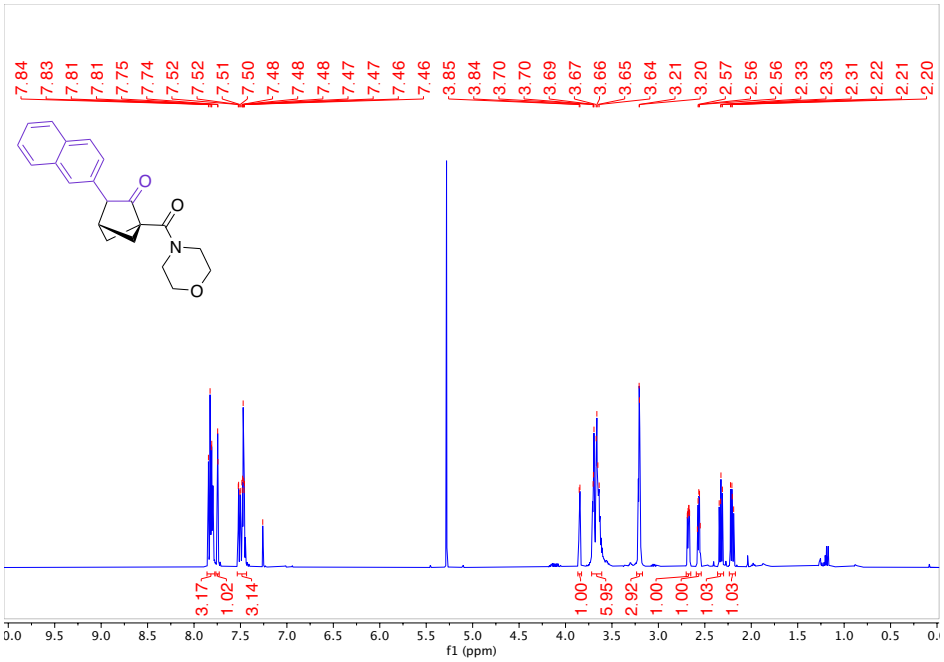

^{13}C NMR (126 MHz, $CDCl_3$, 292 K, ppm): δ 206.72, 166.48, 133.38, 133.33, 132.44, 128.48, 127.88, 127.70, 126.38, 126.05, 125.94, 125.71, 67.94, 66.91, 54.94, 46.43, 43.11, 42.45, 41.79, 35.17.

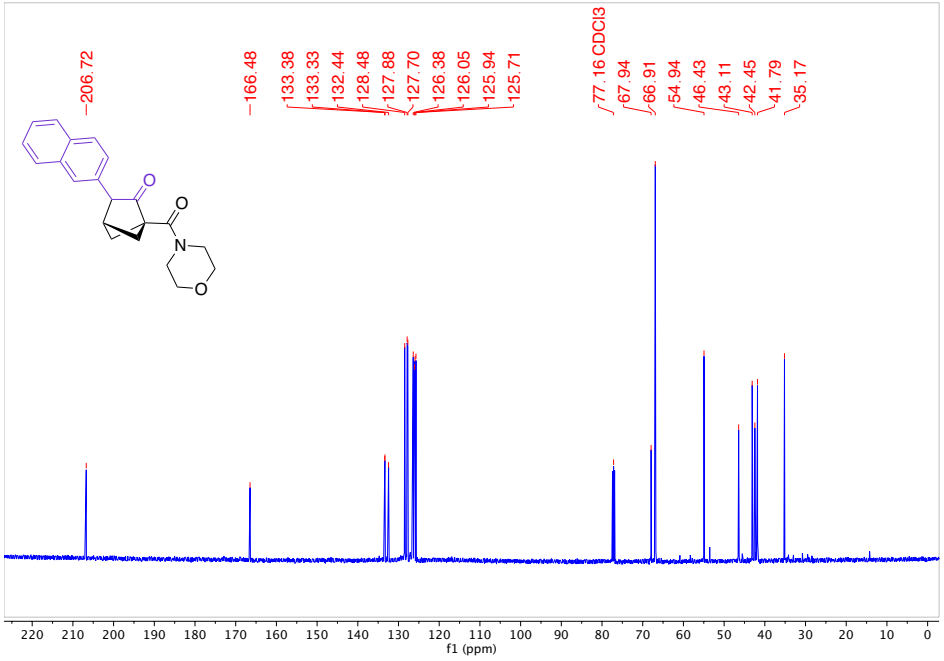

3-(4-Methoxyphenyl)-1-(morpholine-4-carbonyl)bicyclo[2.1.1]hexan-2-one (3f)

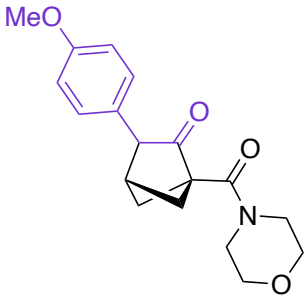

The product was prepared following the general procedure for bicyclohexane synthesis from **1a** and **2f** on a 0.50 mmol bicyclobutane scale using a reaction concentration of 0.1 M. The compound was purified by column chromatography (Biotage® Sfär 10g Column, 0-100% EtOAc/hexanes, eluted at 68% EtOAc). 37.2 mg of a clear colourless oil was obtained (24% Yield).

HRMS(ESI): calc'd for $[C_{18}H_2NO_4 + Na^+]$, 338.13628; found: 338.13626.

^{1}H NMR (500 MHz, $CDCl_3$, 292 K, ppm): δ 7.24 (m, 2H), 6.91 – 6.86 (m, 2H), 3.80 (s, 3H), 3.65 (m, 7H), 3.21 (t, J = 4.8 Hz, 2H), 3.05 (td, J = 3.7, 1.4 Hz, 1H), 2.62 (ddd, J = 7.6, 3.9, 0.9 Hz, 1H), 2.51 (dt, J = 7.7, 3.8 Hz, 1H), 2.25 (dd, J = 9.5, 7.7 Hz, 1H), 2.15 (dd, J = 9.5, 7.6 Hz, 1H).

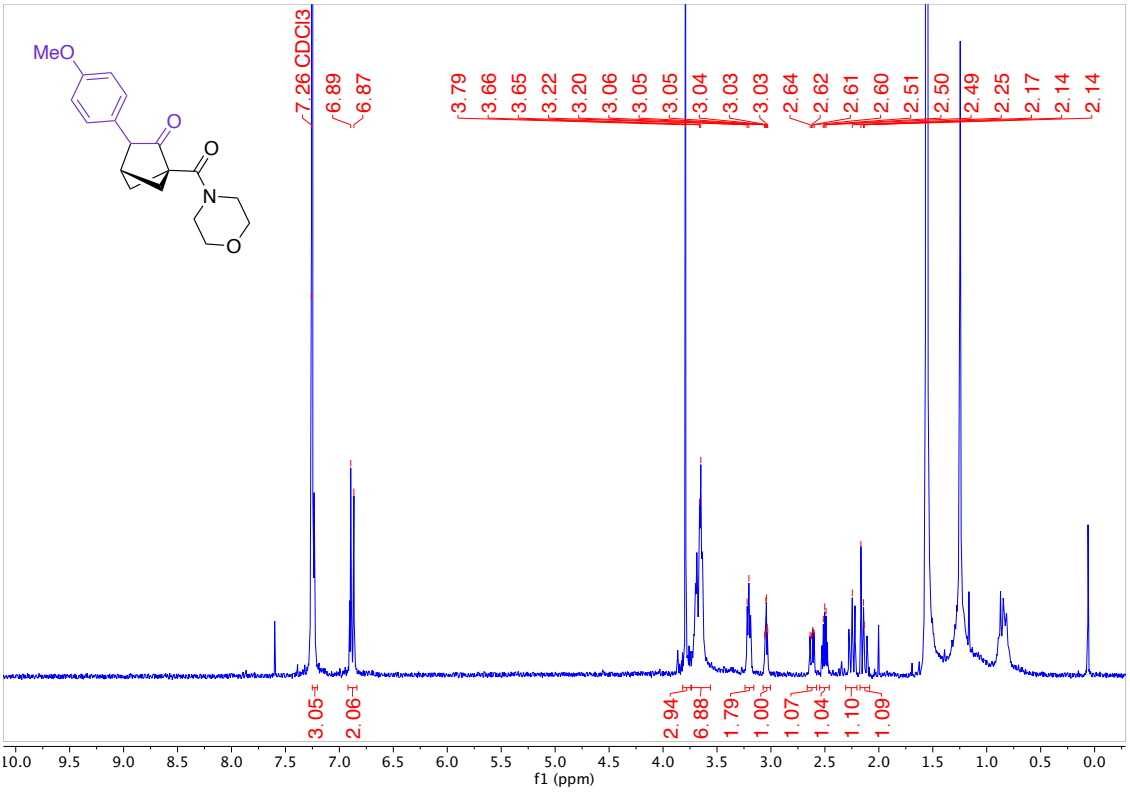

^{13}C NMR (126 MHz, $CDCl_3$, 292 K, ppm): δ 207.11, 166.51, 158.64, 129.42,128.42, 127.82, 114.12, 67.80, 66.85, 55.28, 54.10, 46.36, 43.08, 42.37, 41.56, 36.51, 35.28, 28.37.

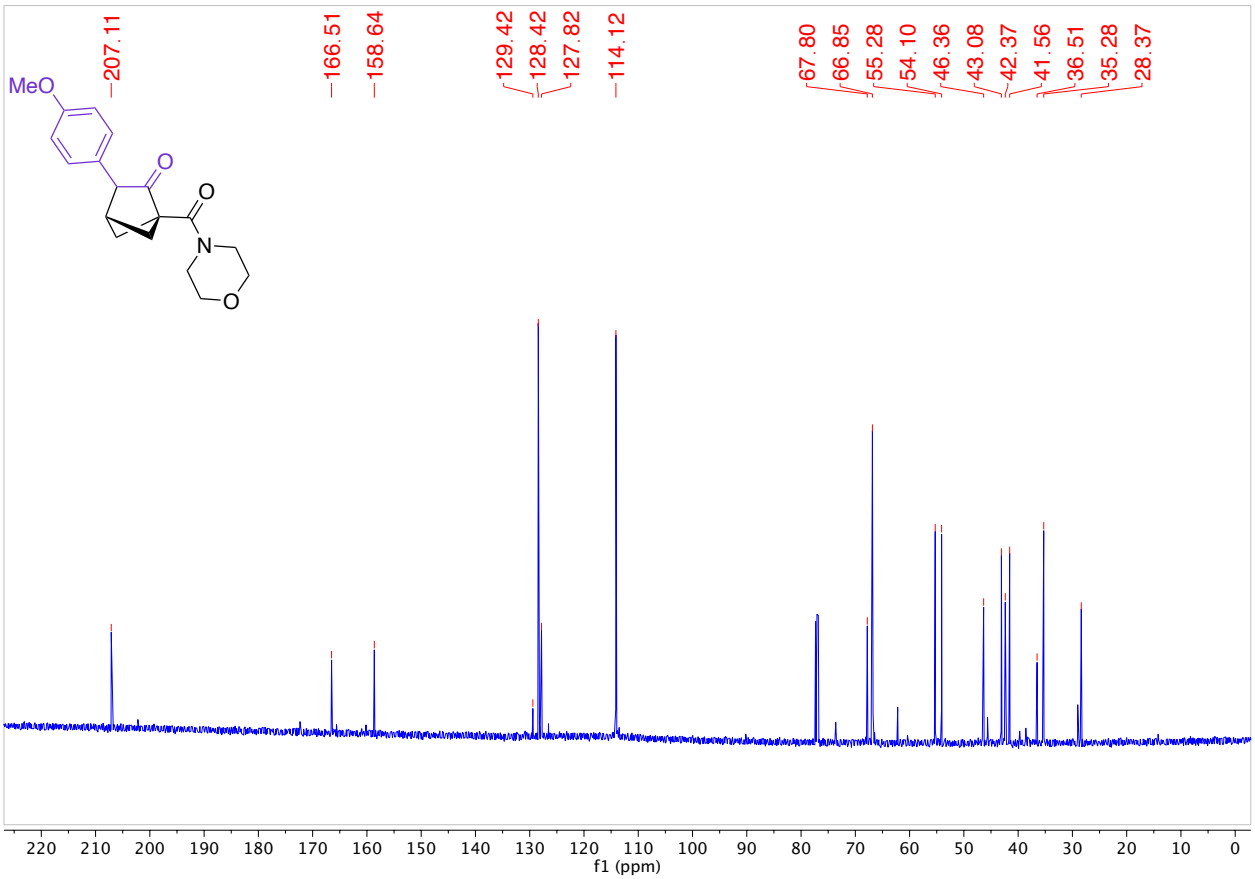

3-(4-Fluorophenyl)-1-(morpholine-4-carbonyl)bicyclo[2.1.1]hexan-2-one (3g)

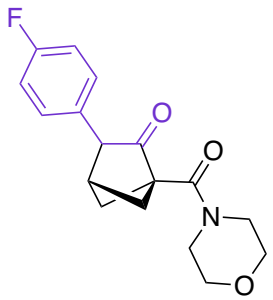

The product was prepared following the general procedure for bicyclohexane synthesis from **1a** and **2g** on a 0.30 mmol bicyclobutane scale. The compound was purified by column chromatography (Biotage® Sfär 5g Column, 0-100% EtOAc/hexanes, eluted at 82% EtOAc). 74 mg of a white solid was obtained (68% Yield).

HRMS(ESI): calc'd for [$C_{17}H_{18}FNO_3$ + H^+], 304.13435; found: 304.13435.

^{1}H NMR (500 MHz, $CDCl_3$, 292 K, ppm): δ 7.32 – 7.26 (m, 2H), 7.01 (m, 2H), 3.70 – 3.59 (m, 7H), 3.18 (t, J = 4.8 Hz, 2H), 3.06 (td, J = 3.7, 1.4 Hz, 1H), 2.62 (ddd, J = 7.5, 3.8, 1.0 Hz, 1H), 2.51 (dt, J = 7.6, 3.8 Hz, 1H), 2.20 (dd, J = 9.6, 7.6 Hz, 1H), 2.13 (dd, J = 9.5, 7.5 Hz, 1H).

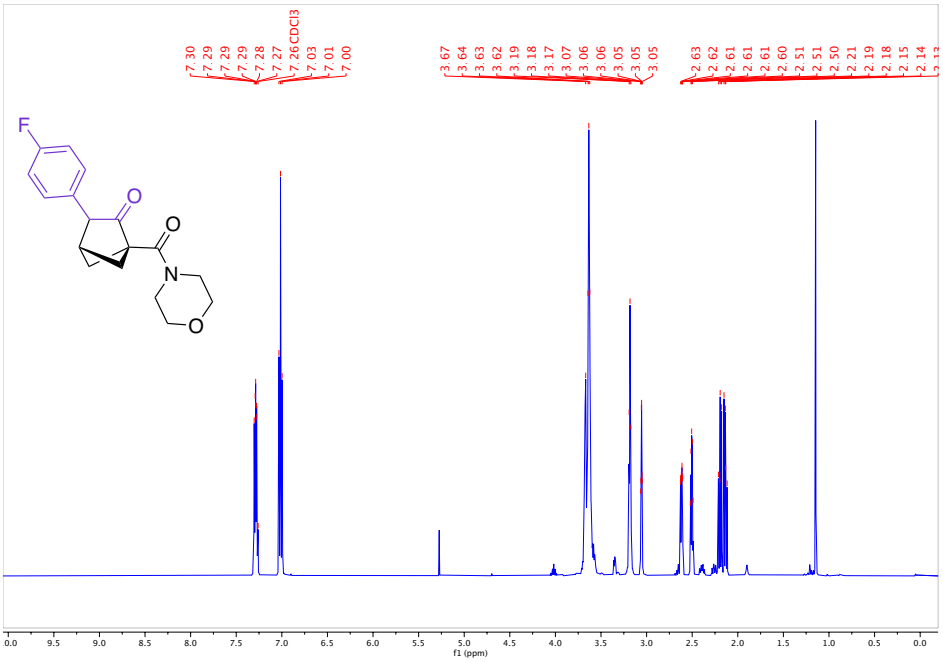

^{13}C NMR (126 MHz, $CDCl_3$, 292 K, ppm): δ 206.56, 166.32, 162.94, 160.99, 131.51, 131.48, 128.99, 128.92, 115.72, 115.55, 67.82, 66.88, 54.05, 46.40, 43.06, 42.43, 41.50, 35.13, 28.42.

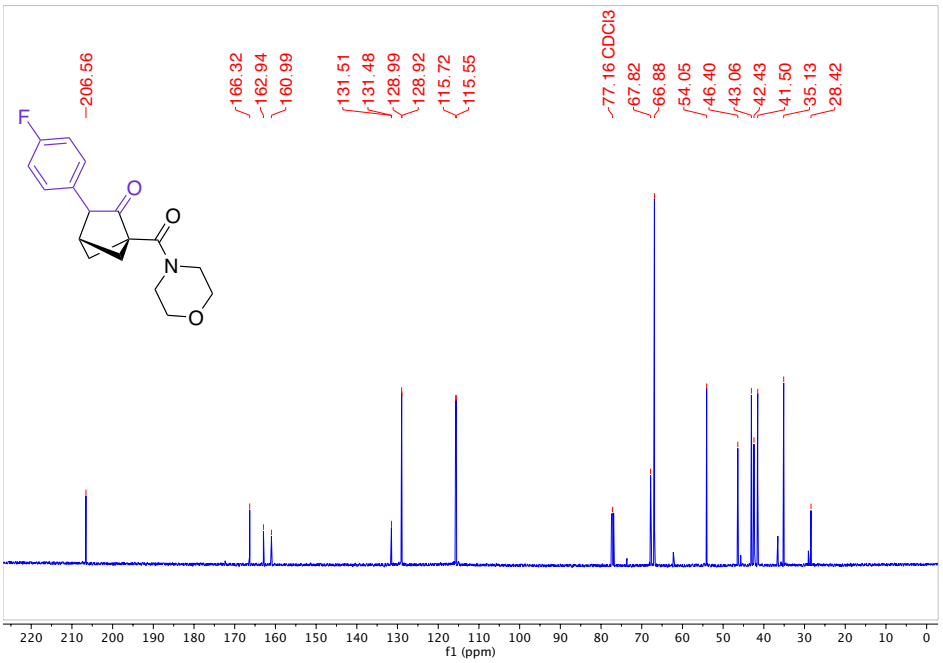

^{19}F NMR (500 MHz, $CDCl_3$, 292 K, ppm): δ 115.44.

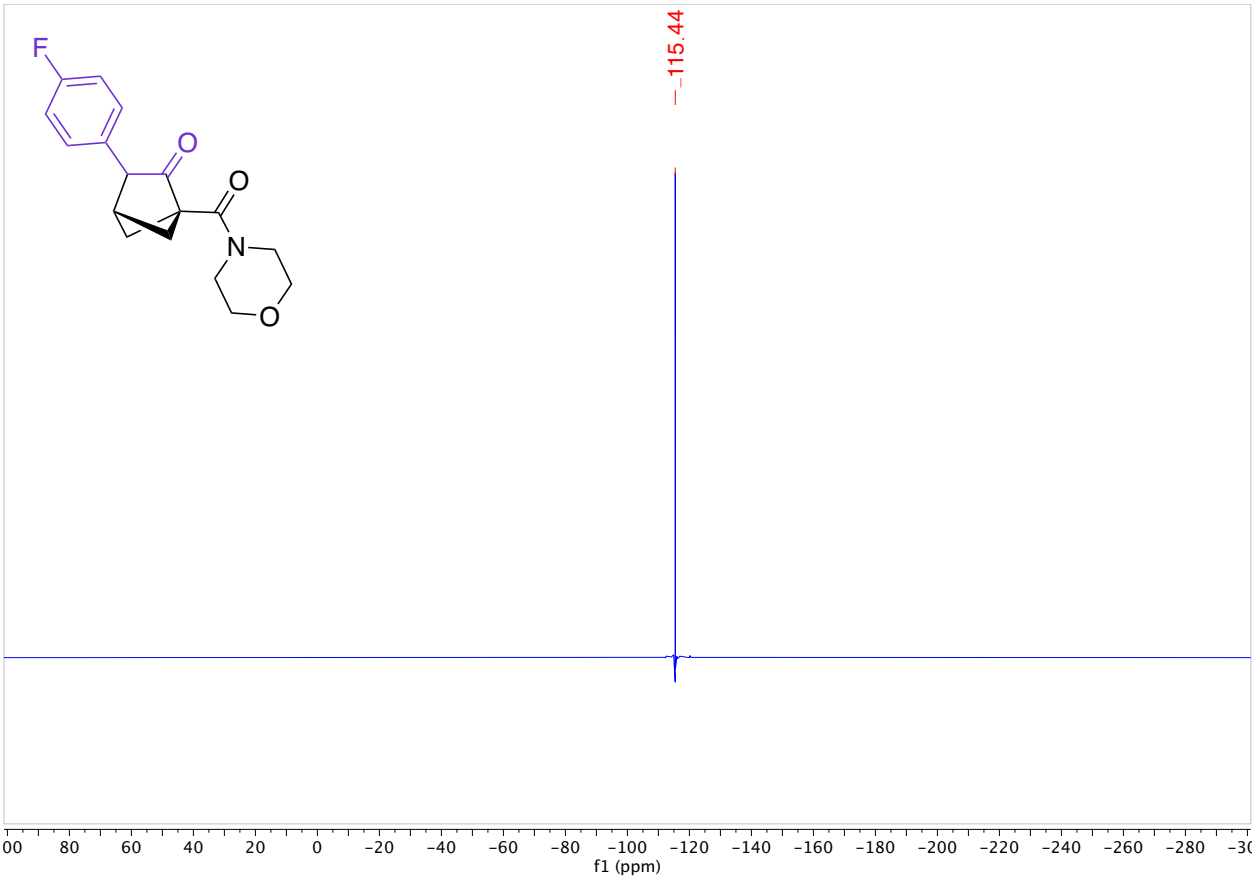

3-(4-Bromophenyl)-1-(morpholine-4-carbonyl)bicyclo[2.1.1]hexan-2-one (3h)

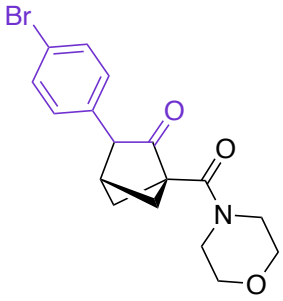

The product was prepared following the general procedure for bicyclohexane synthesis from **1a** and **2h** on a 0.30 mmol bicyclobutane scale. The compound was purified by column chromatography (Biotage® Sfär 5g Column, 0-100% EtOAc/hexanes, eluted at 82% EtOAc). 62 mg of a white solid was obtained (57% Yield).

HRMS(ESI): calc'd for [$C_{17}H_{18}BrNO_3$ + H^+], 364.05429; found: 364.05441.

^{1}H NMR (500 MHz, $CDCl_3$, 292 K, ppm): δ 7.46 (d, J = 8.5 Hz, 2H), 7.23 – 7.19 (m, 2H), 3.70 – 3.59 (m, 7H), 3.17 (m, 2H), 3.07 (m, 1H), 2.62 (ddd, J = 7.3, 3.9, 0.9 Hz, 1H), 2.51 (dt, J = 7.6, 3.8 Hz, 1H), 2.21 – 2.10 (m, 2H).

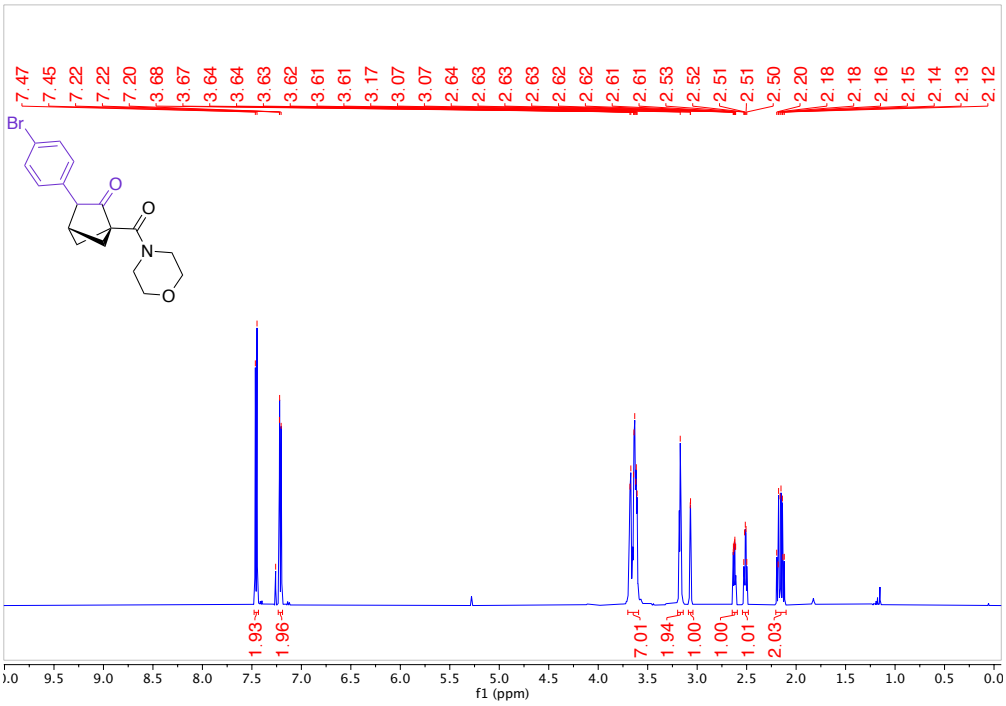

^{13}C NMR (126 MHz, $CDCl_3$, 292 K, ppm): δ 206.12, 166.24, 134.73, 131.87, 129.12, 121.24, 67.78, 66.89, 54.20, 46.40, 42.96, 42.45, 41.55, 34.87.

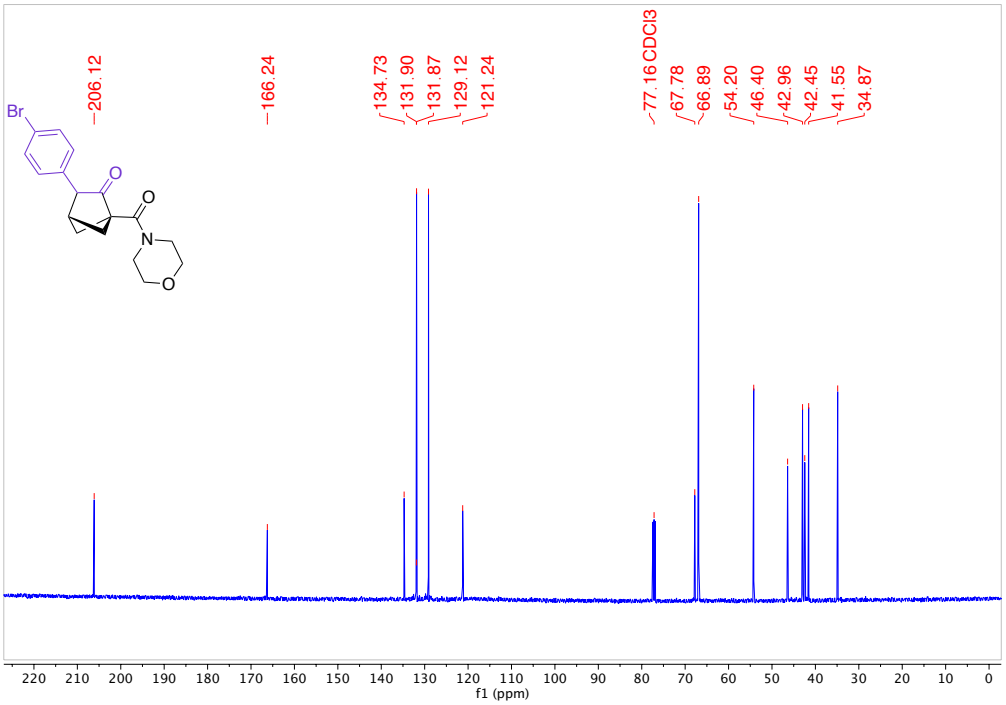

1-(Morpholine-4-carbonyl)-3-(thiophen-3-yl)bicyclo[2.1.1]hexan-2-one (3i)

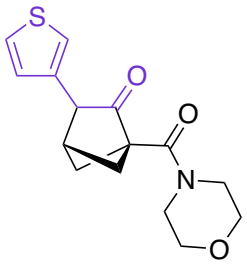

The product was prepared following the general procedure for bicyclohexane synthesis from **1a** and **2i** on a 0.30 mmol bicyclobutane scale. The compound was purified by column chromatography (Biotage® Sfär 5g Column, 0-100% EtOAc/hexanes, eluted at 75% EtOAc). 23 mg of a white solid was obtained (27% Yield).

HRMS(ESI): calc'd for $[C_{15}H_{17}NO_3S + H^+]$, 292.10019; found: 292.10017.

^{1}H NMR (500 MHz, $CDCl_3$, 292 K, ppm): δ 7.22 (m, 1H), 6.97 (m, 1H), 6.95 (m, 1H), 3.85 (d, J = 3.8 Hz, 1H), 3.67 (m, 7H), 3.21 (m, 2H), 3.02 (m, 1H), 2.63 (ddd, J = 7.7, 3.8, 0.9 Hz, 1H), 2.53 (dt, J = 7.7, 3.7 Hz, 1H), 2.30 (dd, J = 9.6, 7.9 Hz, 1H), 2.15 (dd, J = 9.6, 7.7 Hz, 1H).

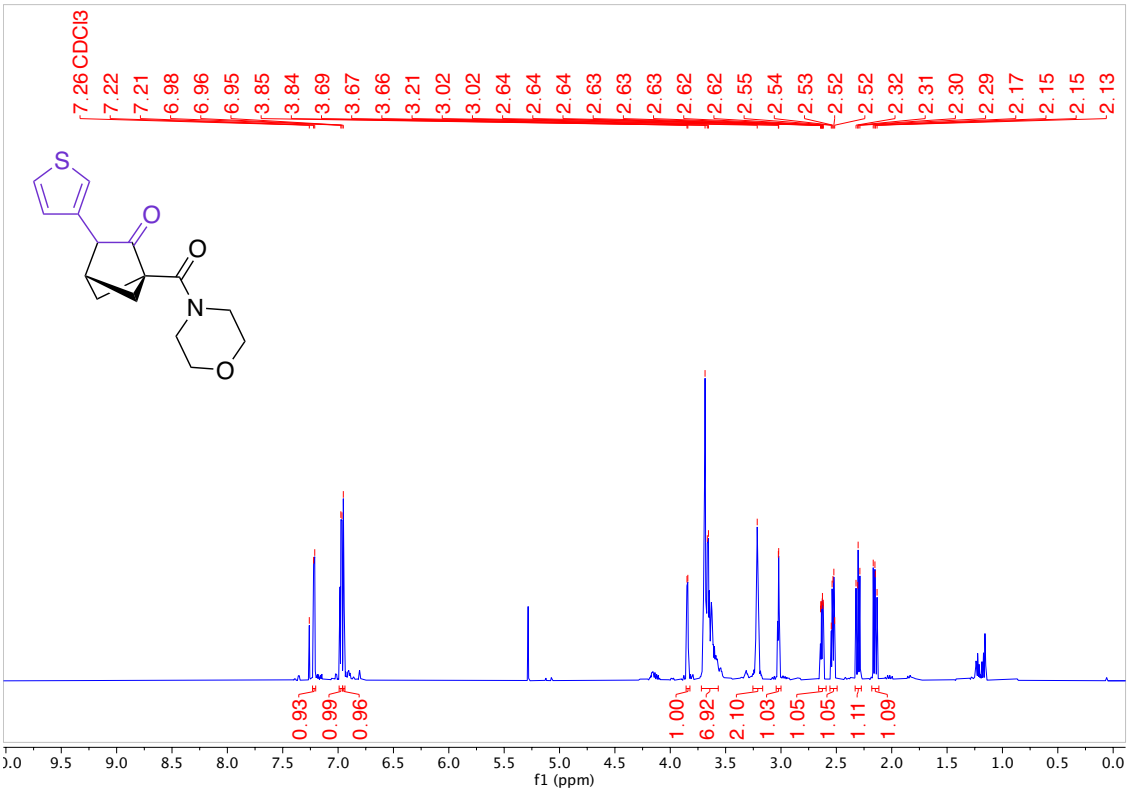

^{13}C NMR (126 MHz, $CDCl_3$, 292 K, ppm): δ 205.57, 166.18, 138.39, 127.05, 125.18, 124.74, 67.92, 66.91, 51.61, 46.47, 43.19, 42.48, 42.19, 37.00.

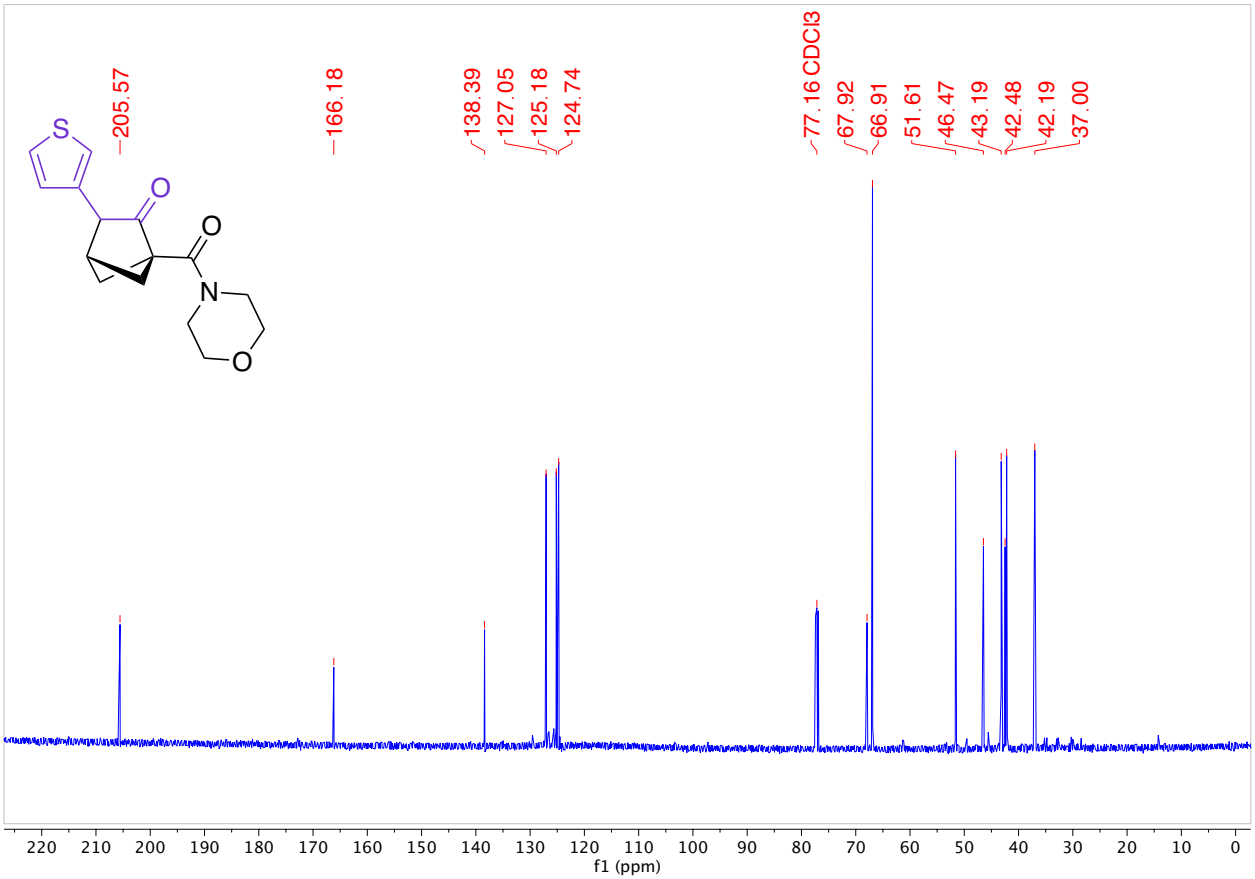

1-(Morpholine-4-carbonyl)-3-(pyridin-3-yl)bicyclo[2.1.1]hexan-2-one (3j)

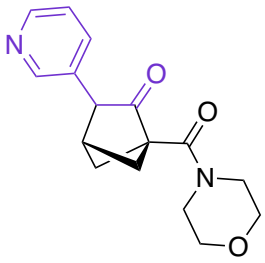

The product was prepared following the general procedure for bicyclohexane synthesis from **1a** and **2j** on a 0.30 mmol bicyclobutane scale. The compound was purified by column chromatography (Biotage® Sfär 5g Column, 0-100% MeOH/EtOAc, eluted at 44% MeOH). 57 mg of a white solid was obtained (67% Yield).

HRMS(ESI): calc'd for [$C_{16}H_{18}N_2O_3$ + H^+], 287.13902; found: 287.13889.

^{1}H NMR (500 MHz, $CDCl_3$, 292 K, ppm): δ 8.59 – 8.54 (m, 1H), 8.51 (m, 1H), 7.73 – 7.67 (m, 1H), 7.30 – 7.26 (m, 1H), 3.74 – 3.59 (m, 7H), 3.19 (t, J = 4.8 Hz, 2H), 3.14 (td, J = 3.7, 1.3 Hz, 1H), 2.66 (d, J = 3.1 Hz, 1H), 2.55 (d, J = 3.7 Hz, 1H), 2.24 – 2.14 (m, 2H).

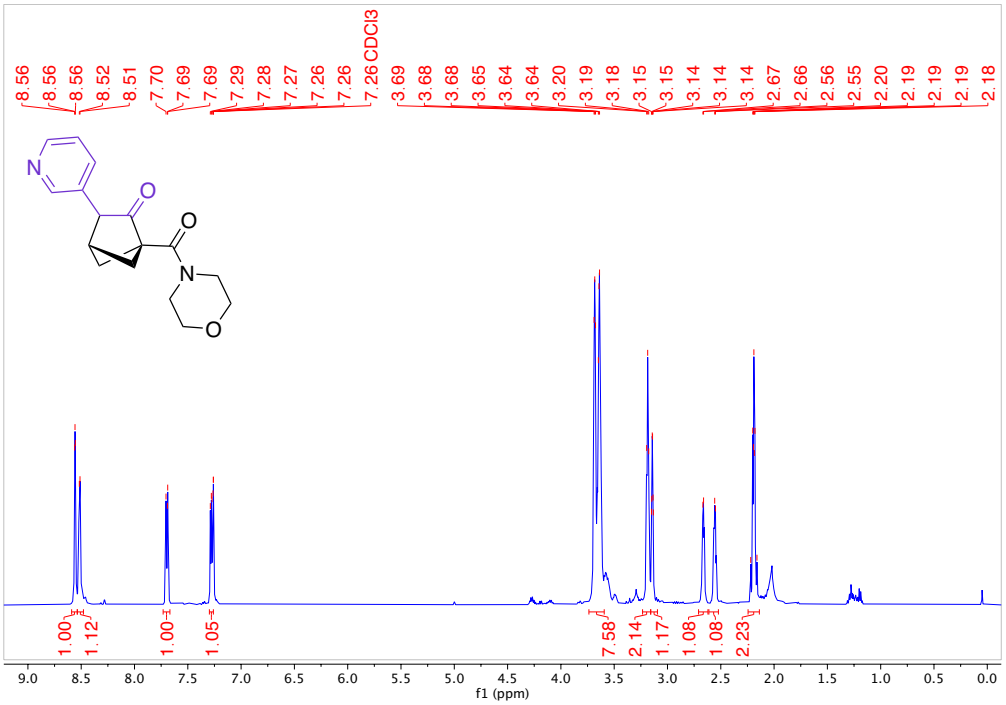

^{13}C NMR (126 MHz, $CDCl_3$, 292 K, ppm): δ 205.75, 166.11, 148.62, 135.30, 131.56, 123.67, 67.87, 66.90, 52.79, 46.45, 43.17, 42.50, 41.41, 34.73.

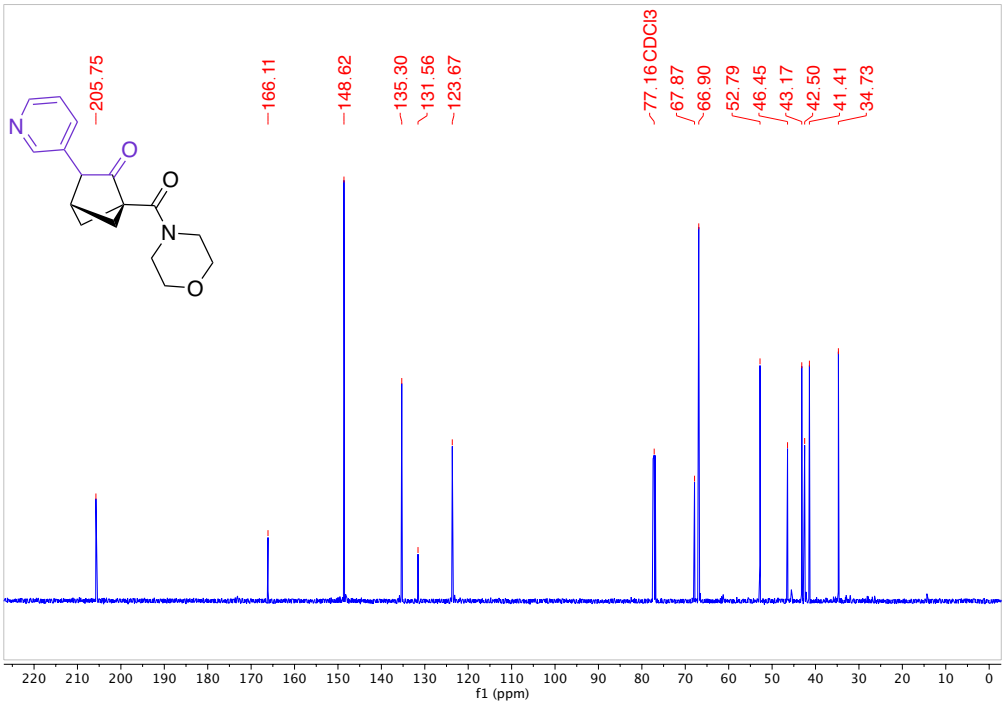

1-(Morpholine-4-carbonyl)-3,3-diphenylbicyclo[2.1.1]hexan-2-one (3k)

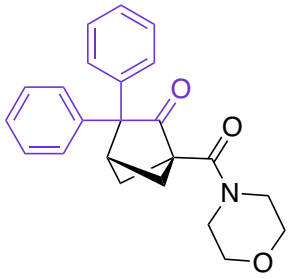

The product was prepared following the general procedure for bicyclohexane synthesis from **1a** and **2k** on a 0.30 mmol bicyclobutane scale. The compound was purified by column chromatography (Biotage® Sfär 5g Column, 0-100% EtOAc/hexanes, eluted at 62% EtOAc). 80 mg of a white solid was obtained (74% Yield).

HRMS(ESI): calc'd for $[C_{23}H_{23}NO_3 + H^+]$, 362.17507; found: 362.17477.

^{1}H NMR (500 MHz, $CDCl_3$, 292 K, ppm): δ 7.49 – 7.41 (m, 4H), 7.28 (t, J = 7.8 Hz, 4H), 7.18 (t, J = 7.4 Hz, 2H), 3.68 (dd, J = 20.8, 5.1 Hz, 6H), 3.58 (t, J = 3.8 Hz, 1H), 3.18 (d, J = 4.8 Hz, 2H), 2.54 (ddd, J = 5.6, 3.7, 2.2 Hz, 2H), 2.19 (dd, J = 5.2, 2.3 Hz, 2H).

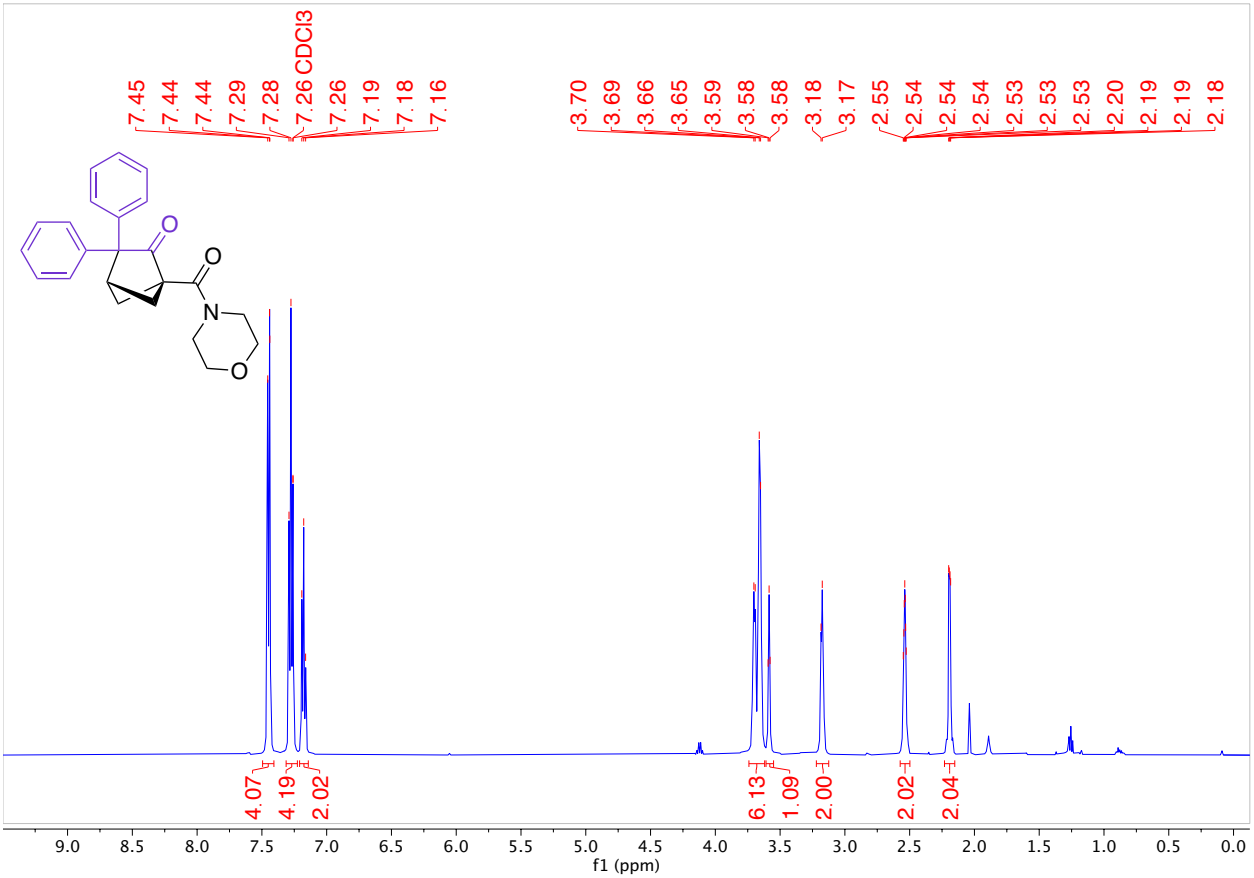

^{13}C NMR (126 MHz, $CDCl_3$, 292 K, ppm): δ 207.22, 166.29, 141.62, 128.80, 126.88, 126.87, 67.34, 66.91, 66.87, 62.21, 46.44, 42.45, 41.15, 39.37, 28.44.

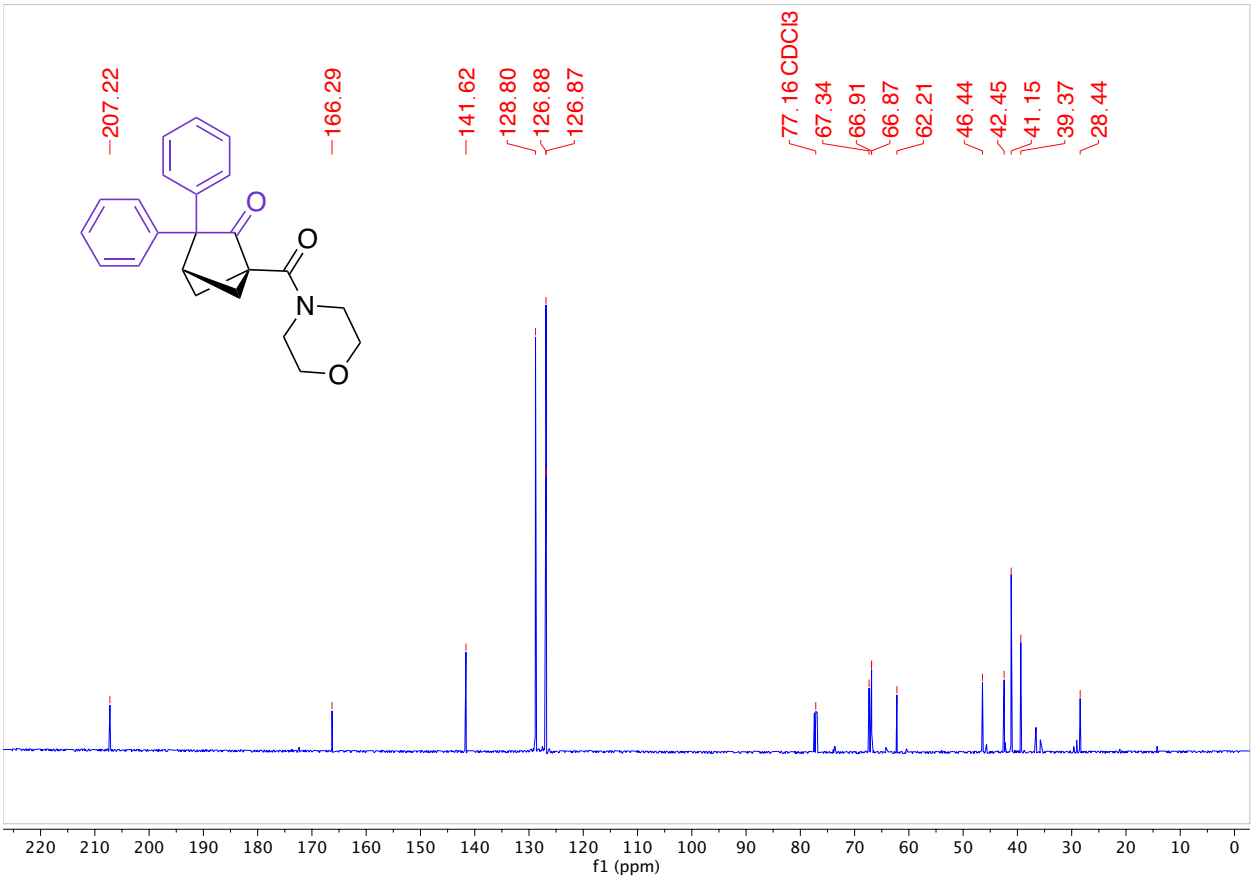

1-(Morpholine-4-carbonyl)-3,4-diphenylbicyclo[2.1.1]hexan-2-one (3l):

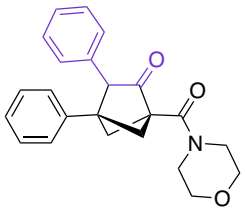

The product was prepared following the general procedure for bicyclohexane synthesis from **1l** and **2c** on a 0.30 mmol bicyclobutane scale. An NMR spectroscopy yield of 43% (3.97 ppm peak) is reported compared to internal standard (1,3,5-trimethoxybenzene). The compound was attempted to be purified by column chromatography (Biotage® Sfär 5g Column, 0-100% EtOAc/hexanes) but the product and bicyclobutane starting material co-eluted at 43% ethyl acetate. 64.3 mg of a yellow solid was obtained as a mixture of **3o** and unreacted bicyclobutane (1 : 0.87 mol ratio, determined by NMR spectrscopy with peak at 2.83 ppm for bicyclobutane and 3.98 ppm for **3l**) (37% Yield of **3o**, 32% of bicyclobutane).

HRMS(ESI): calc'd for [$C_{23}H_{23}NO_3$ + H^+], 362.17507; found: 362.17487.

Crude ^{1}H NMR, including 1,3,5-trimethoxybenzene (500 MHz, $CDCl_3$, 292 K, ppm):

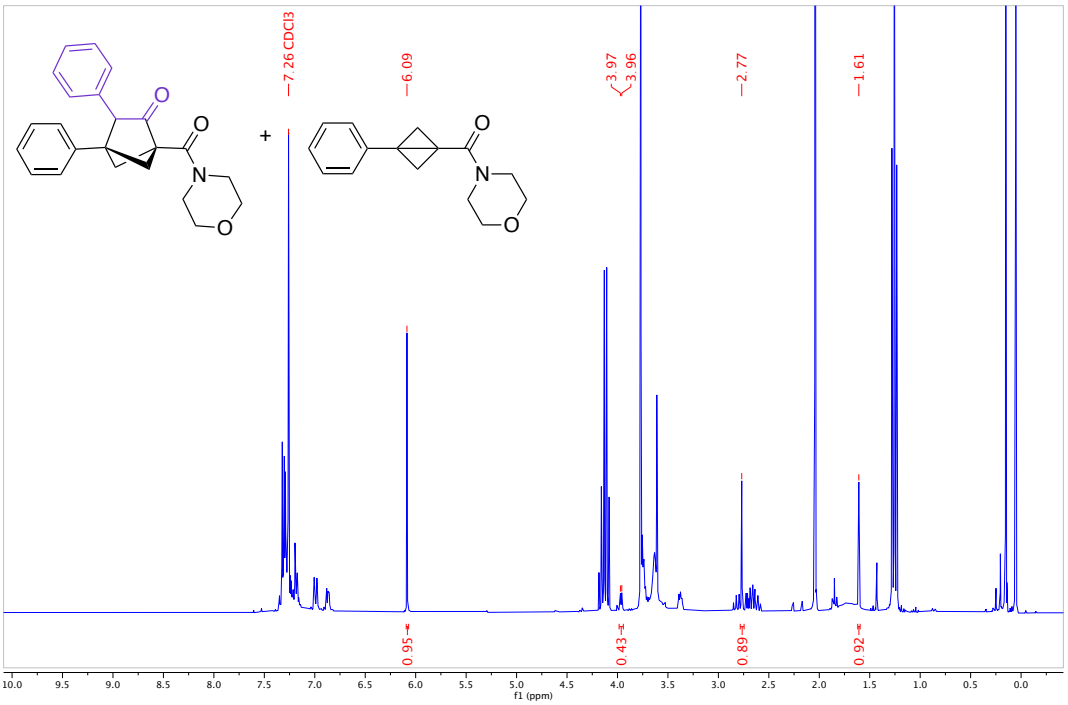

^{1}H NMR (500 MHz, $CDCl_3$, 292 K, ppm): δ 7.33 (m, 6H), 7.00 (m, 2H), 6.89 (m, 2H), 4.02 – 3.92 (m, 1H), 3.76 (m, 6H), 3.38 (m, 2H), 2.83 (m, 1H), 2.75 – 2.53 (m, 3H). Bicyclobutane peaks: 7.27 (m, 5H), 3.64 (m, 8H), 2.78 (t, J = 0.7 Hz, 2H), 1.62 (t, J = 0.7 Hz, 2H).

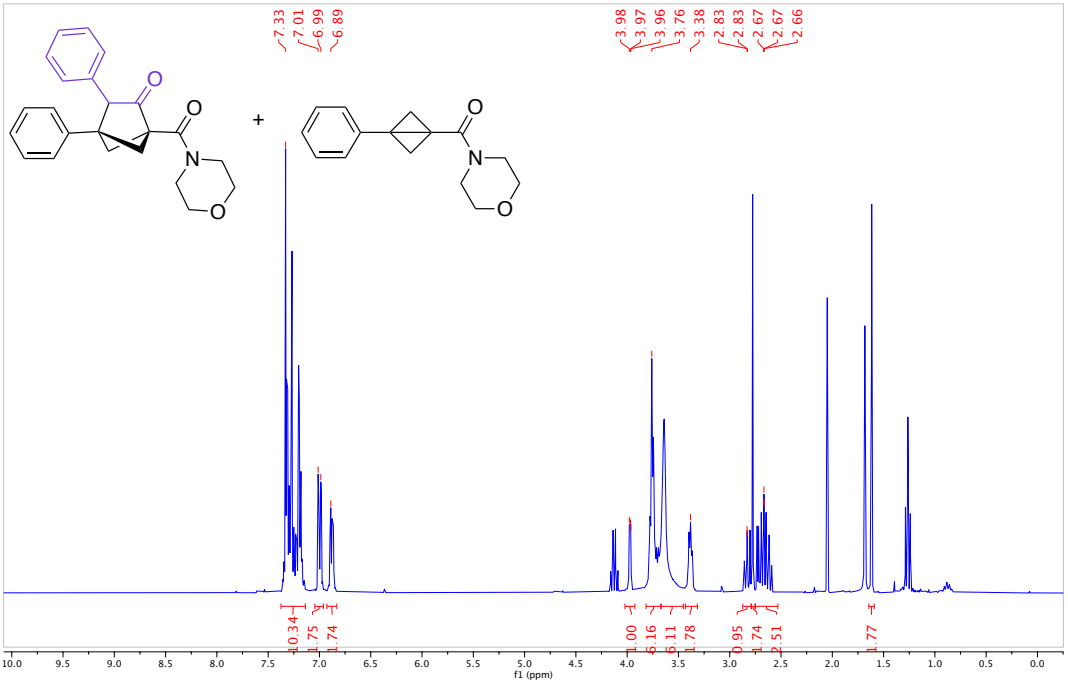

N,*N*-diisopropyl-2-oxo-3-phenylbicyclo[2.1.1]hexane-1-carboxamide (3m)

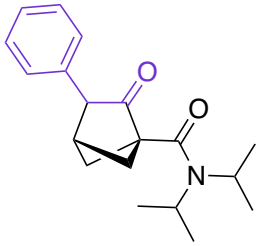

The product was prepared following the general procedure for bicyclohexane synthesis from **1m** and **2c** on a 0.30 mmol bicyclobutane scale. The compound was purified by column chromatography (Biotage® Sfär 5g Column, 0-100% EtOAc/hexanes, eluted at 42% EtOAc). 39 mg of a clear colourless oil was obtained (43% Yield).

HRMS(ESI): calc'd for $[C_{19}H_{25}NO_2 + H^+]$, 300.19581; found: 300.19577.

^{1}H NMR (500 MHz, $CDCl_3$, 292 K, ppm): δ7.29 – 7.21 (m, 4H), 7.21 – 7.14 (m, 1H), 3.60 (d, J = 4.0 Hz, 1H), 3.45 (p, J = 6.6 Hz, 1H), 3.27 (p, J = 6.8 Hz, 1H), 2.93 (s, 1H), 2.54 – 2.49 (m, 1H), 2.39 (dt, J = 7.8, 3.8 Hz, 1H), 2.14 (dd, J = 9.5, 7.7 Hz, 1H), 2.04 (dd, J = 9.5, 7.5 Hz, 1H), 1.35 (t, J = 6.8 Hz, 6H), 1.11 – 1.03 (m, 6H).

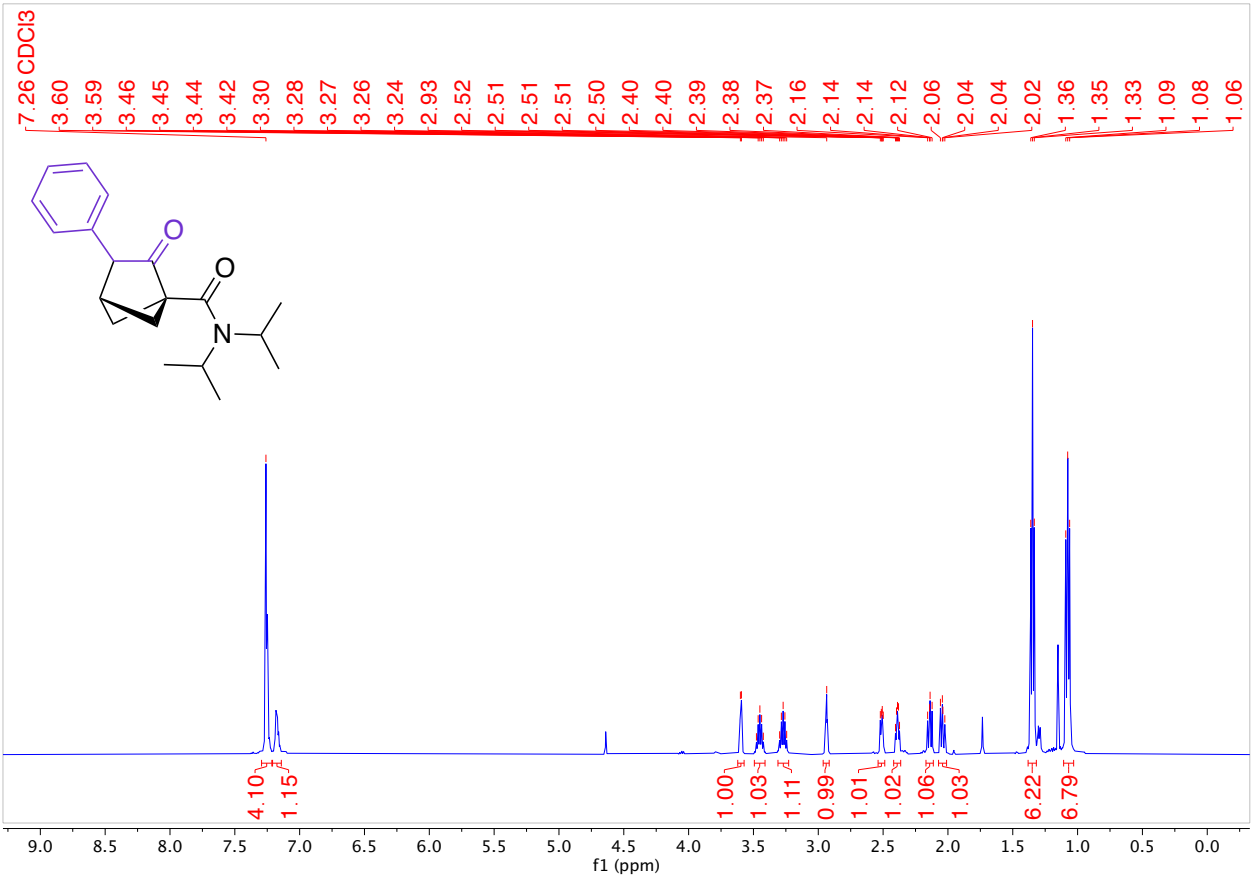

^{13}C NMR (126 MHz, $CDCl_3$, 292 K, ppm): δ 207.14, 166.95, 136.28, 128.68, 127.58, 126.99, 69.53, 54.98, 49.52, 46.24, 43.47, 41.58, 34.71, 20.86, 20.84, 20.64, 20.62.

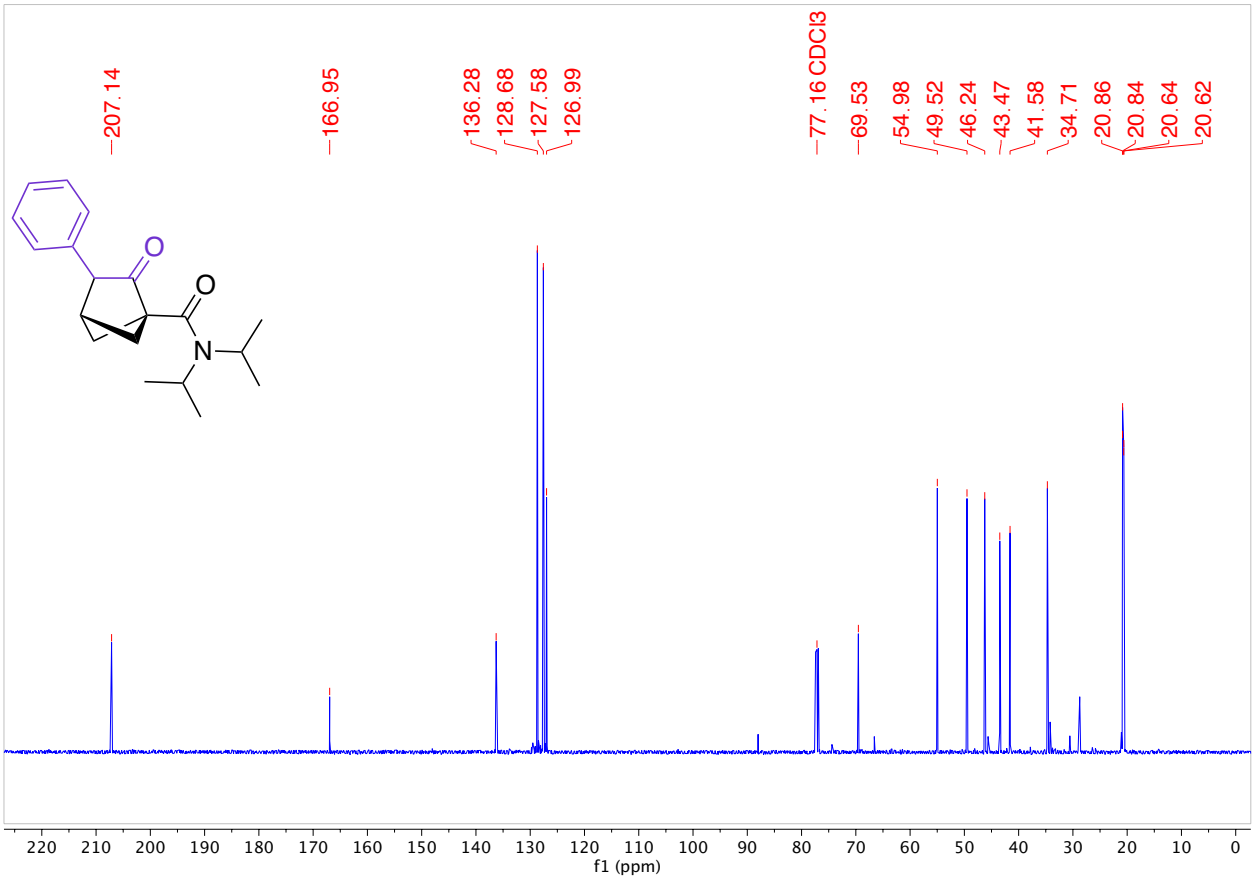

N,*N*-Dibenzyl-2-oxo-3-phenylbicyclo[2.1.1]hexane-1-carboxamide (3n)

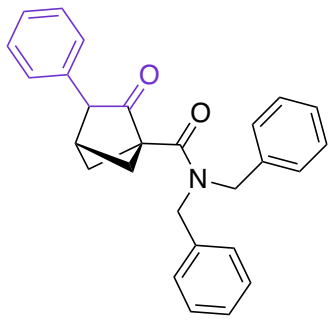

The product was prepared following the general procedure for bicyclohexane synthesis from **1n** and **2c** on a 0.30 mmol bicyclobutane scale. The compound was purified by column chromatography (Biotage® Sfär 5g Column, 0-100% EtOAc/hexanes, eluted at 36% EtOAc). 81 mg of a clear colourless oil was obtained (68% Yield).

HRMS(ESI): calc'd for [$C_{27}H_{25}NO_2$ + H^+], 396.19581; found: 396.19583.

^{1}H NMR (500 MHz, $CDCl_3$, 292 K, ppm): δ 7.33 (m, 8H), 7.28 (m, 5H), 7.12 (d, J = 6.8 Hz, 2H), 4.65 (d, J = 15.1 Hz, 1H), 4.51 (d, J = 15.2 Hz, 1H), 4.29 (d, J = 3.7 Hz, 2H), 3.71 (d, J = 4.0 Hz, 1H), 3.04 (td, J = 3.7, 1.3 Hz, 1H), 2.67 (ddd, J = 7.6, 3.9, 1.0 Hz, 1H), 2.56 (dt, J = 7.8, 3.8 Hz, 1H), 2.25 (dd, J = 9.6, 7.9 Hz, 1H), 2.19 – 2.10 (m, 1H).

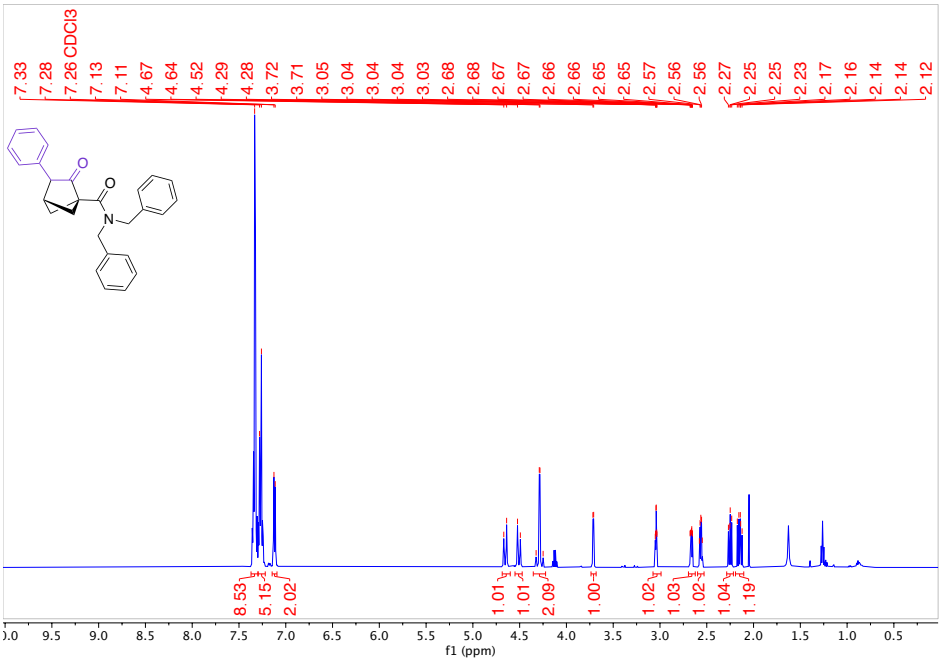

^{13}C NMR (126 MHz, $CDCl_3$, 292 K, ppm): δ 207.27, 168.96, 136.45, 136.25, 135.91, 129.00, 128.79, 128.76, 127.87, 127.84, 127.55, 127.38, 127.16, 126.91, 68.37, 54.84, 50.14, 47.81, 43.95, 42.34, 35.06.

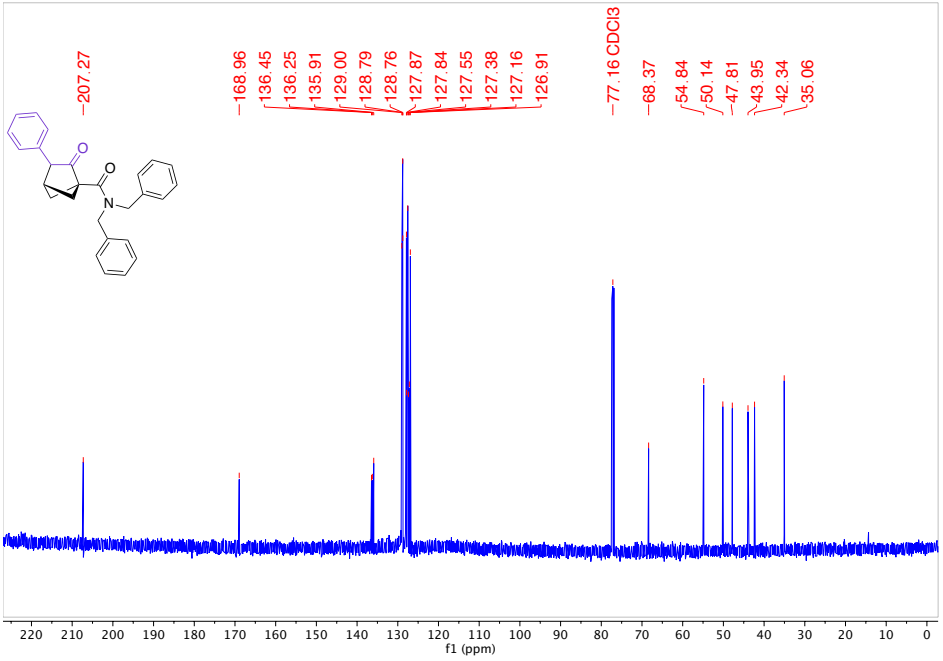

***N*-Methyl-2-oxo-N,3-diphenylbicyclo[2.1.1]hexane-1-carboxamide (3o)**

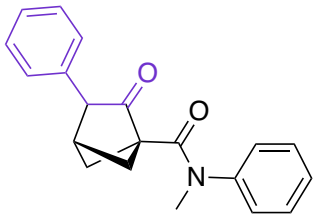

The product was prepared following the general procedure for bicyclohexane synthesis from **1o** and **2c** on a 0.30 mmol bicyclobutane scale. The compound was purified by column chromatography (Biotage® Sfär 5g Column, 0-100% EtOAc/hexanes, eluted at 71% EtOAc). 42 mg of a clear colourless oil was obtained (46% Yield).

HRMS(ESI): calc'd for $[C_{20}H_{19}NO_2 + H^+]$, 306.14886; found: 306.14879.

^{1}H NMR (500 MHz, $CDCl_3$, 292 K, ppm): δ 7.37 – 7.25 (m, 7H), 7.25 – 7.18 (m, 1H), 7.12 (d, J = 7.1 Hz, 2H), 3.46 (s, 1H), 3.33 (s, 3H), 2.74 – 2.67 (m, 1H), 2.27 (d, J = 3.5 Hz, 1H), 2.13 – 2.07 (m, 1H), 1.50 – 1.42 (m, 2H).

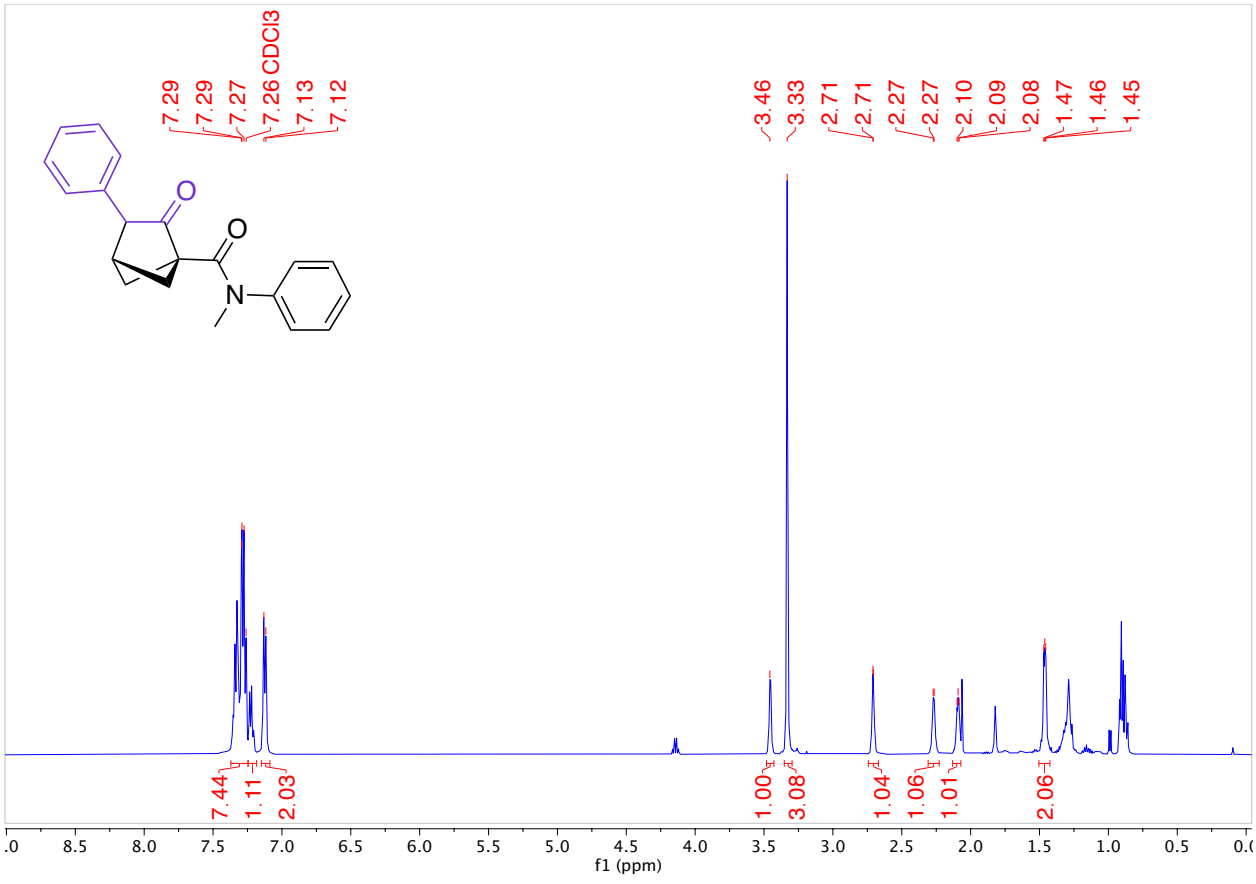

^{13}C NMR (126 MHz, $CDCl_3$, 292 K, ppm): δ 207.76, 168.22, 142.85, 136.30, 129.46, 128.48, 128.46, 128.00, 127.72, 126.90, 69.03, 54.38, 43.72, 41.74, 38.09, 35.54, 31.69, 22.75, 14.22.

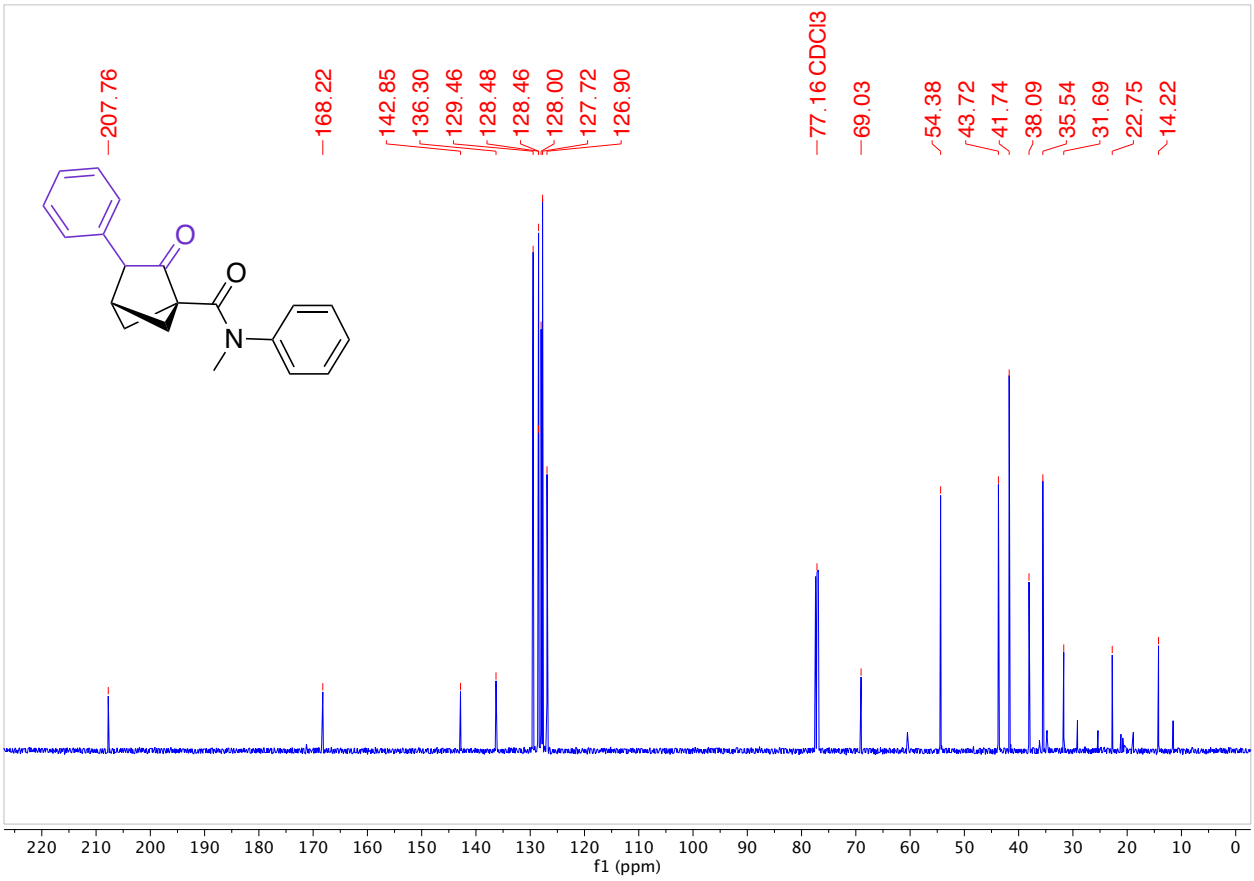

1-(Morpholine-4-carbonyl)-3-((*E*)-styryl)bicyclo[2.1.1]hexan-2-one (3p)

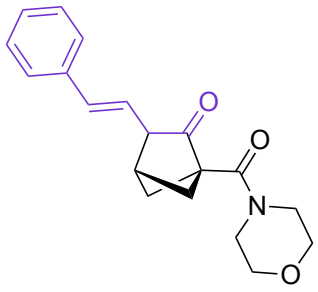

The product was prepared following the general procedure for bicyclohexane synthesis from **1a** and **2p** on a 0.30 mmol bicyclobutane scale. The compound was purified by column chromatography (Biotage® Sfär 5g Column, 0-100% EtOAc/hexanes, eluted at 50% EtOAc). 66 mg of a white solid was obtained (71% Yield).

HRMS(ESI): calc'd for [$C_{19}H_{21}NO_3$ + H^+], 312.15942; found: 312.15937.

^{1}H NMR (500 MHz, $CDCl_3$, 292 K, ppm): δ 7.39 (d, J = 7.3 Hz, 2H), 7.33 (t, J = 7.5 Hz, 2H), 7.27 (m, 1H), 6.61 (d, J = 16.0 Hz, 1H), 6.20 (dd, J = 16.1, 6.2 Hz, 1H), 3.71 (m, 6H), 3.25 (m, 3H), 2.86 (m, 1H), 2.61 (dd, J = 7.7, 3.8 Hz, 1H), 2.55 (dt, J = 7.7, 3.8 Hz, 1H), 2.35 (dd, J = 9.5, 7.8 Hz, 1H), 2.10 (dd, J = 9.5, 7.6 Hz, 1H).

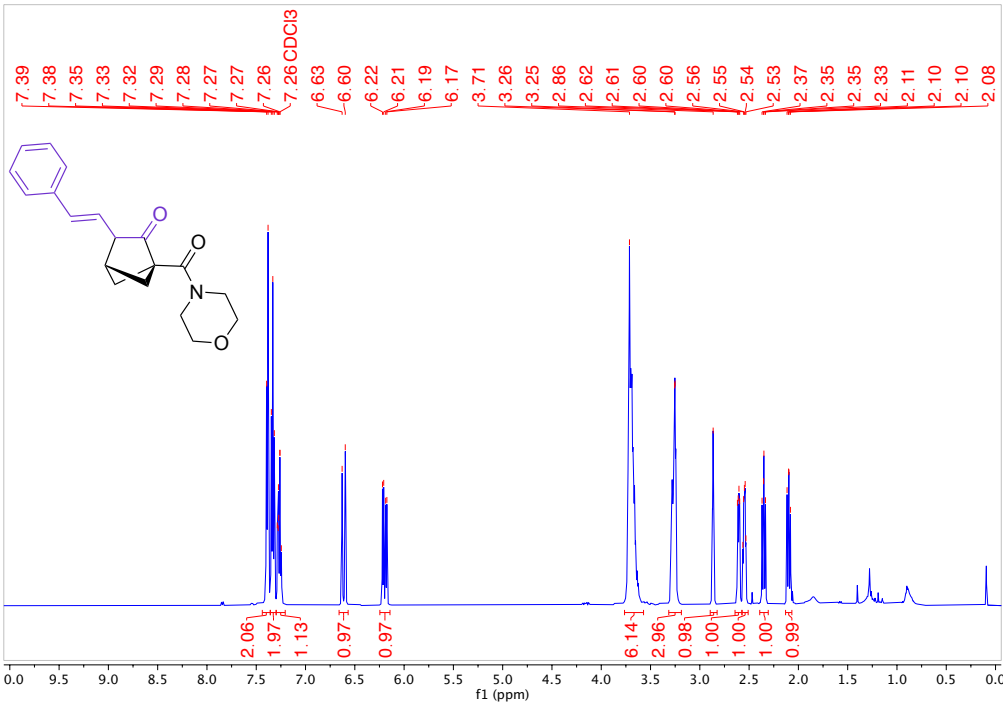

^{13}C NMR (126 MHz, $CDCl_3$, 292 K, ppm): δ 207.26, 166.51, 136.61, 133.55, 128.70, 127.91, 126.35, 123.70, 67.70, 66.95, 66.92, 54.46, 46.44, 43.31, 42.45, 41.66, 35.33.

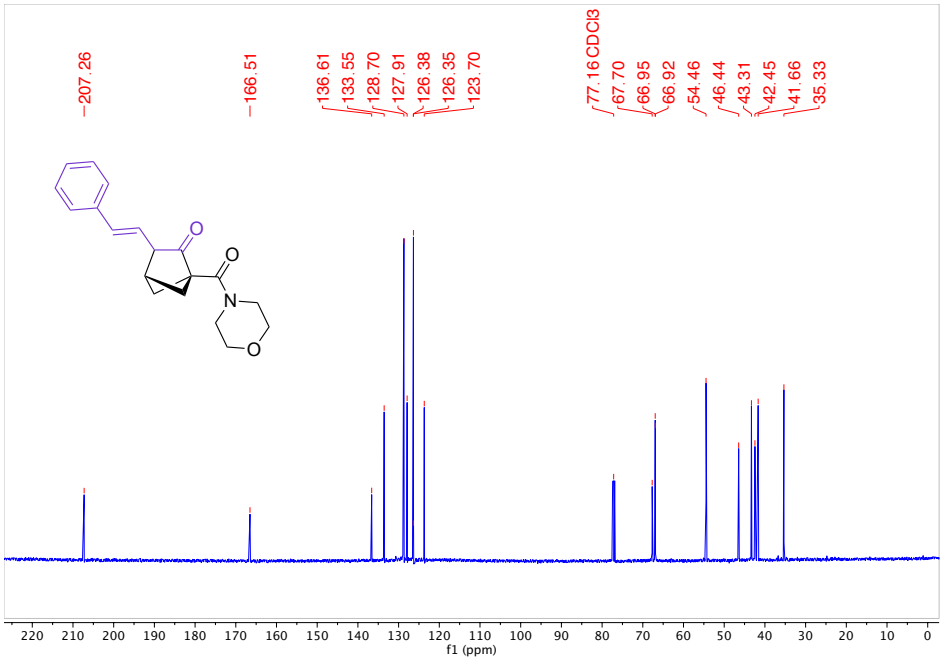

Synthesis of bicyclo[2.1.1]hexane with a benzyl ester bicyclobutane derivative

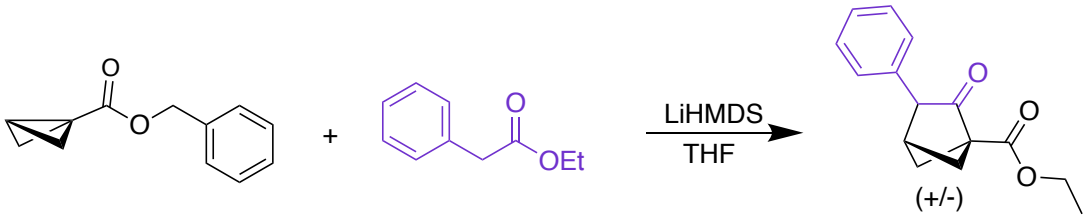

The benzyl ester bicyclobutane and aryl enolate were used following the general procedure for bicyclohexane synthesis from **1p** and **2c** on a 0.70 mmol bicyclobutane scale. With the ester on the bicyclobutane, side reactions with the enolate and intermediates resulted a low solution yield and formation of multiple products, with only the ethyl ester product shown (due to transesterification of the benzyl ester with the ethoxide byproduct of the reaction). The ethyl ester product was purified by column chromatography (Biotage® Sfär 10g Column, 0-100% EtOAc/hexanes, eluted at 8% EtOAc). 21 mg of a clear colourless oil was obtained (12% Yield).

HRMS(ESI): calc'd for $[C_{15}H_{16}O_3 + Na^+]$, 267.09916; found: 267.09924.

Crude ^{1}H NMR (300 MHz, $CDCl_3$, 292 K):

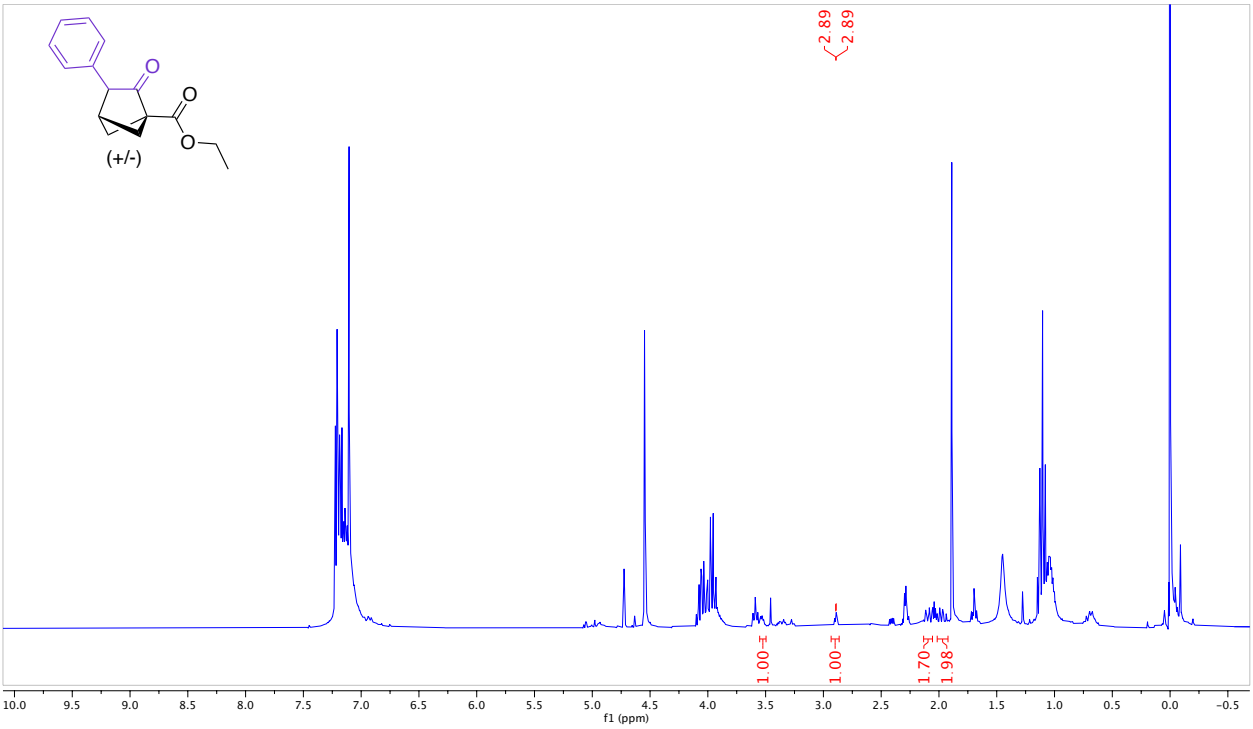

^{1}H NMR (500 MHz, $CDCl_3$, 292 K, ppm): δ 7.39 – 7.31 (m, 5H), 4.22 (q, J = 7.1 Hz, 2H), 3.69 (d, J = 3.6 Hz, 1H), 3.05 (td, J = 3.7, 1.4 Hz, 1H), 2.56 (ddd, J = 7.5, 3.9, 0.9 Hz, 1H), 2.44 (dt, J = 7.7, 3.8 Hz, 1H), 2.24 (dd, J = 9.4, 7.8 Hz, 1H), 2.12 (dd, J = 9.4, 7.5 Hz, 1H), 1.28 (t, J = 7.1 Hz, 4H).

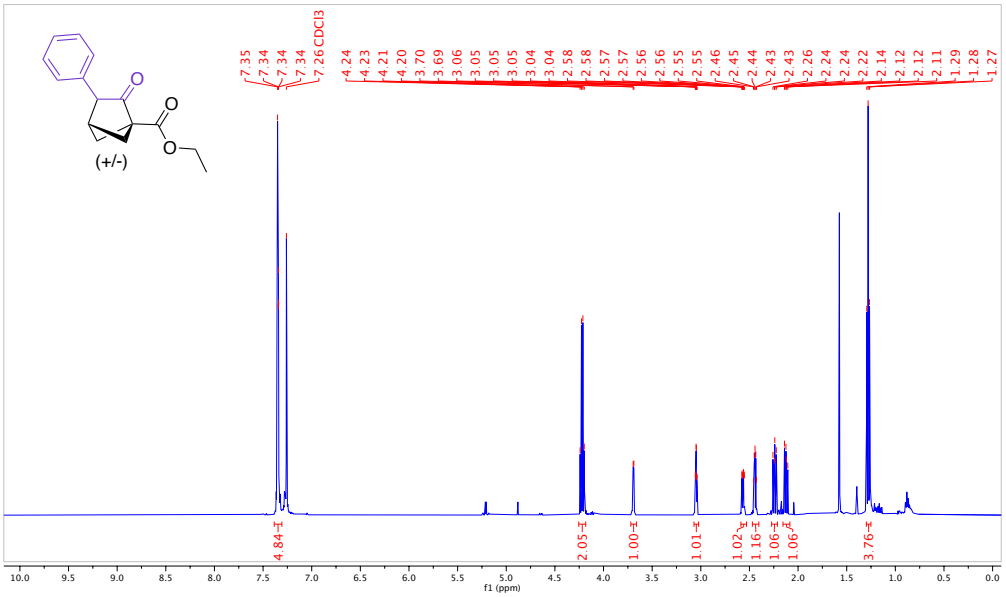

^{13}C NMR (126 MHz, $CDCl_3$, 292 K, ppm): δ 205.48, 168.70, 136.02, 128.74, 127.64, 127.14, 66.03, 61.18, 54.40, 42.22, 40.58, 35.30, 14.35.

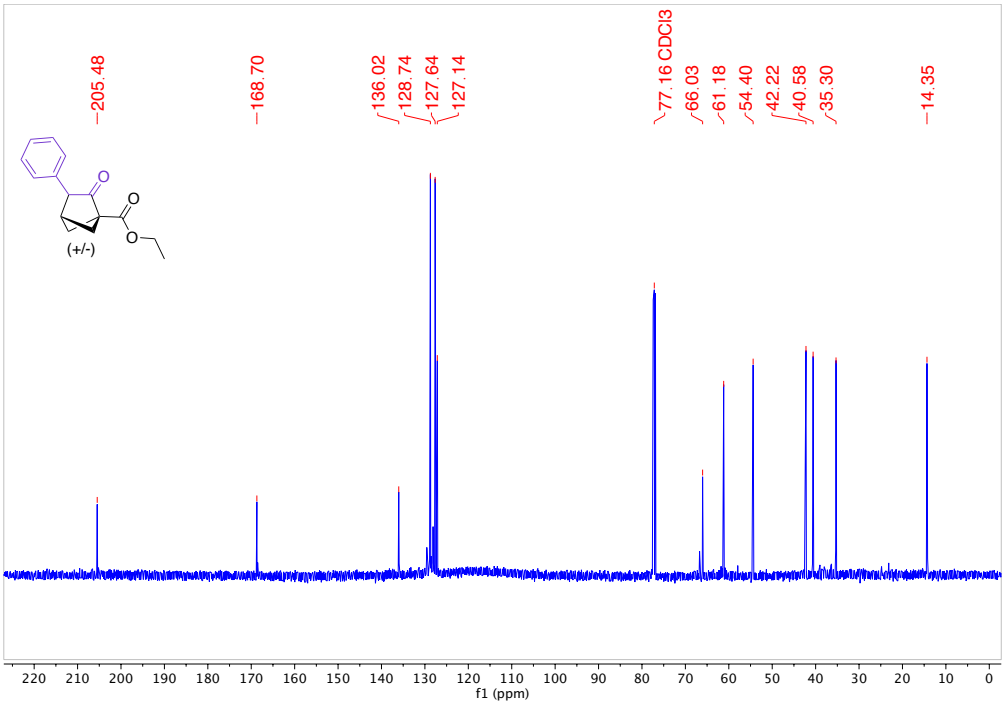

B.6 Additional Reactions

Telescoped synthesis of bicyclohexane 3a:

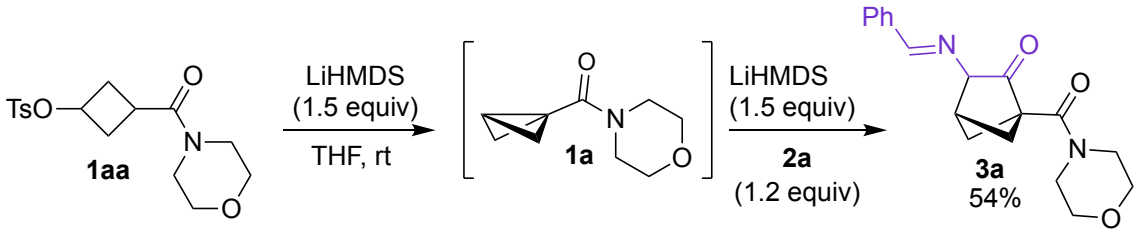

In one vial, 3-(morpholine-4-carbonyl)cyclobutyl 4-methylbenzenesulfonate (33.9 mg, 0.10 mmol) and 1,3,5-trimethoxybenzene (5.6 mg, 0.33 equiv) were added and dissolved in 50% of the THF solvent (1 mL total, 0.10 M) under a nitrogen atmosphere. LiHMDS (1.0M in THF, 0.15 mL, 1.5 equiv) was added to the vial and it was left to stir for 15 minutes at room temperature. In another vial, the imine **2a** (68.8 mg, 1.2 equiv) was dissolved in 50% of the THF solvent. LiHMDS (1.0M in THF, 0.15 mL, 1.5 equiv) was added to the imine vial and left to stir for 10 minutes at room temperature. The two vials were then cooled in the freezer for 10 minutes followed by a dropwise addition of the BCB vial to the enolate vial. The reaction was left to stir for 24 hours at room temperature. The reaction was quenched with $NaHCO_3$ and extracted with ethyl acetate 3 times. The organic layers were dried with Mg_2SO_4, filtered and the solvent was evaporated. The amounts of product and starting materials were determined by NMR spectroscopy relative to the internal standard (1,3,5-trimethoxybenzene). 54% product (2.74 ppm peak).

^{1}H NMR (500 MHz, $CDCl_3$, 292 K, ppm):

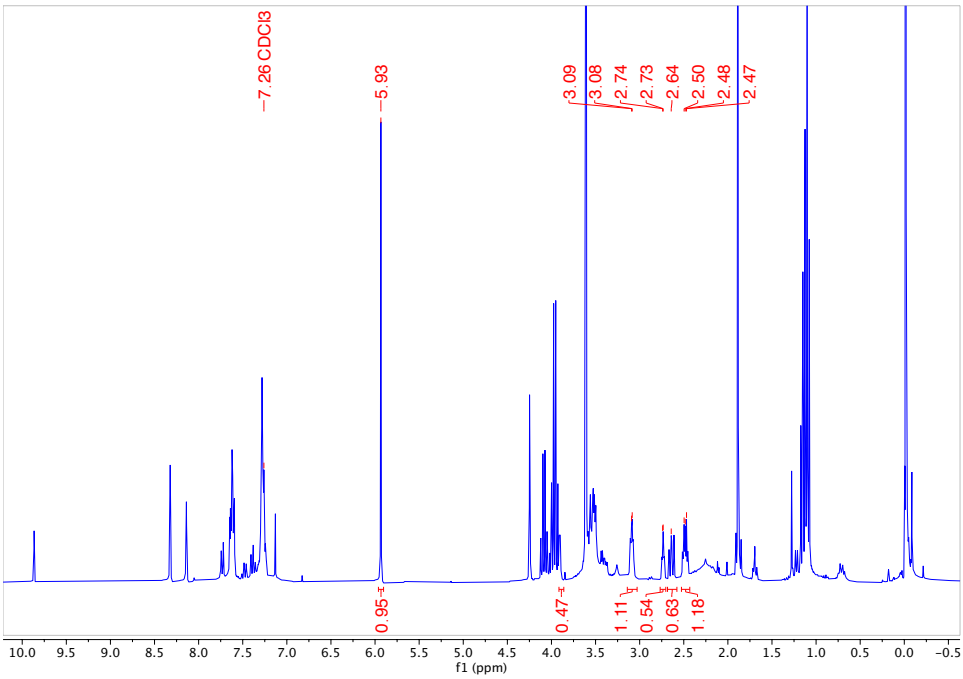

All-at-once one pot synthesis of bicyclohexane 3a:

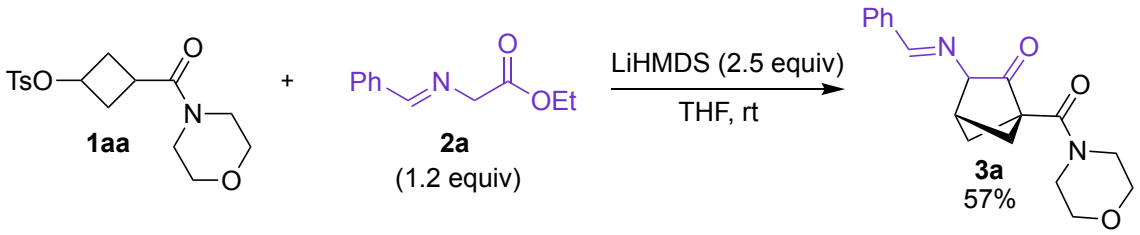

In one vial, the 3-(morpholine-4-carbonyl)cyclobutyl 4-methylbenzenesulfonate (101.8 mg, 0.30 mmol) and 1,3,5-trimethoxybenzene (16.8 mg, 0.33 equiv) were added. In another vial, the imine **2a** (68.8 mg, 1.2 equiv), was added and the vials were put under a nitrogen atmosphere in the glovebox. 50% of the THF solvent (2 mL total, 0.15 M) was added to the tosylated cyclobutane and 50% of the THF was added to the imine vial. LiHMDS (1.0M in THF, 0.75 mL, 2.5 equiv) was added to the imine vial and left to stir for 10 minutes at room temperature. The two vials were then cooled in the freezer for 10 minutes followed by a dropwise addition of the tosylated cyclobutane to the enolate vial. The reaction was left to stir for 24 hours at room temperature. The reaction was quenched with $NaHCO_3$ and extracted with ethyl acetate 3 times. The organic layers were dried with Mg_2SO_4, filtered and the solvent was evaporated. The amounts of product and starting materials were determined by NMR spectroscopy relative to the internal standard (1,3,5-trimethoxybenzene). 57% product (2.74 ppm peak).

^{1}H NMR (500 MHz, $CDCl_3$, 292 K, ppm):

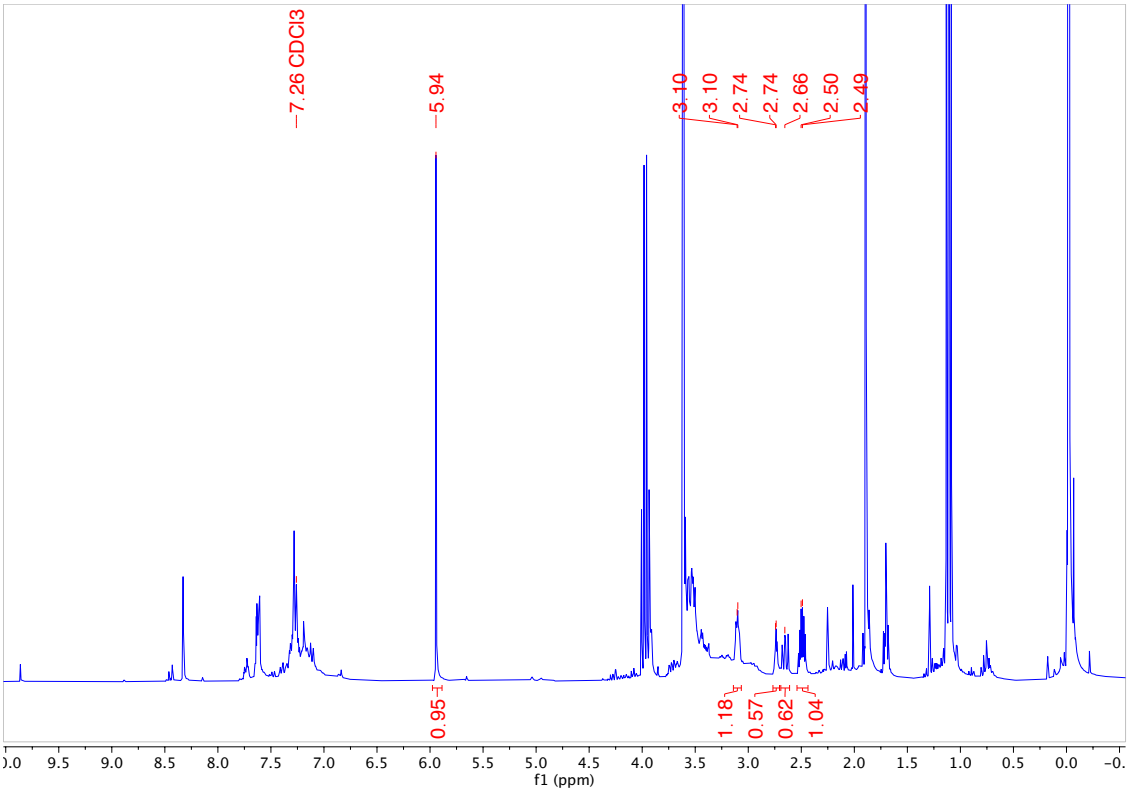

Test for ketene addition to bicyclobutanes:

To test if the mechanism proceeds through a ketene addition to the bicyclobutane, phenyl acetyl chloride was reacted with triethylamine and the bicyclobutane with or without the presence of LiOTf in THF at room temperature as follows:

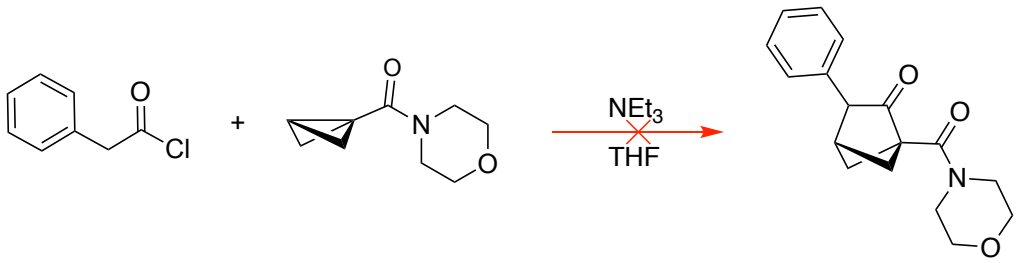

In one vial, phenyl acetyl chloride (7.9 μL, 1.2 equiv) and 1,3,5-trimethoxybenzene (2.8 mg, 0.33 equiv) were added and dissolved in 50% of the THF solvent (0.17 mL total, 0.30 M) under a nitrogen atmosphere. Triethylamine (10.5 μL, 1.5 equiv) was added to the vial and it was left to stir for 5 minutes at room temperature. In another vial, the bicyclobutane **1a** (8.4 mg, 1 equiv, 0.05 mmol) was dissolved in 50% of the THF solvent. The two vials were then cooled in the freezer for 10 minutes followed by a dropwise addition of the BCB vial to the ketene vial. The reaction was left to stir overnight at room temperature. The reaction was quenched with $NaHCO_3$ and extracted with ethyl acetate. The organic layer was dried with Mg_2SO_4, filtered and the solvent was evaporated. Decomposition of the phenyl acetyl chloride was observed and no bicyclohexane product was formed (no peak at 4.06 ppm).

^{1}H NMR (500 MHz, $CDCl_3$, 292 K, ppm):

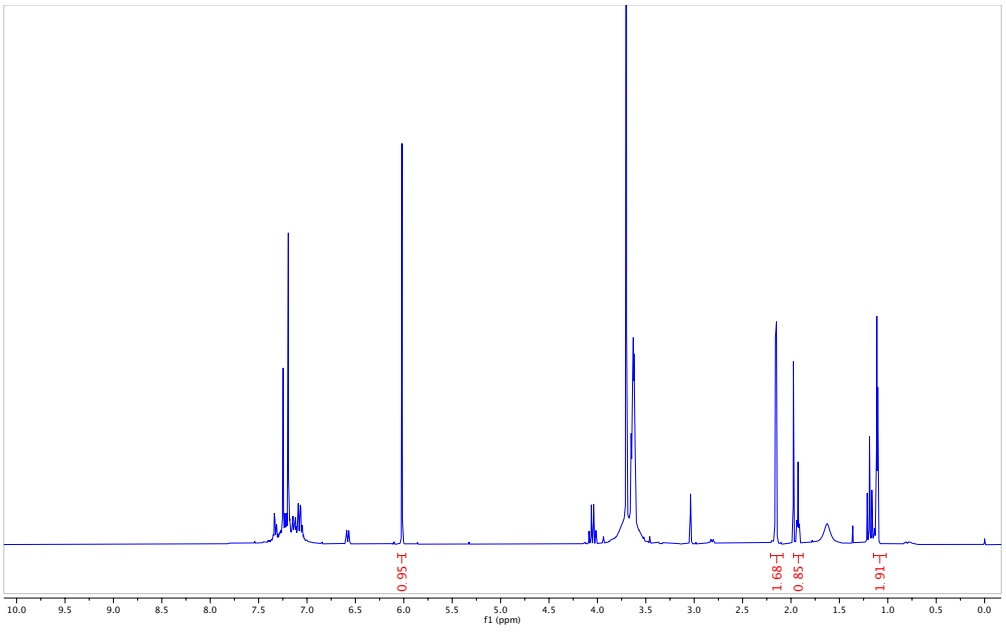

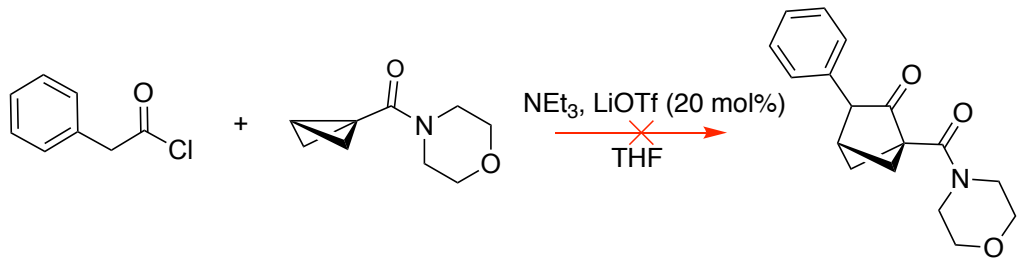

In one vial, phenyl acetyl chloride (7.9 μL, 1.2 equiv) and 1,3,5-trimethoxybenzene (2.8 mg, 0.33 equiv) were added and dissolved in 33% of the THF solvent (0.26 mL total, 0.2 M) under a nitrogen atmosphere. Triethylamine (10.5 μL, 1.5 equiv) was added to the vial and it was left to stir for 5 minutes at room temperature. In another vial, the bicyclobutane **1a** (8.4 mg, 1 equiv, 0.05 mmol) was dissolved in 33% of the THF solvent. The two vials were then cooled in the freezer for 10 minutes followed by a dropwise addition of the BCB vial to the ketene vial. LiOTf was dissolved in 33% of the THF solvent and then added to the reaction mixture. The reaction was left to stir overnight at room temperature. The reaction was quenched with $NaHCO_3$ and extracted with ethyl acetate. The organic layer was dried with Mg_2SO_4, filtered and the solvent was evaporated. Decomposition of the phenyl acetyl chloride was observed and no bicyclohexane product was formed (no peak at 4.06 ppm).

^{1}H NMR (500 MHz, $CDCl_3$, 292 K, ppm):

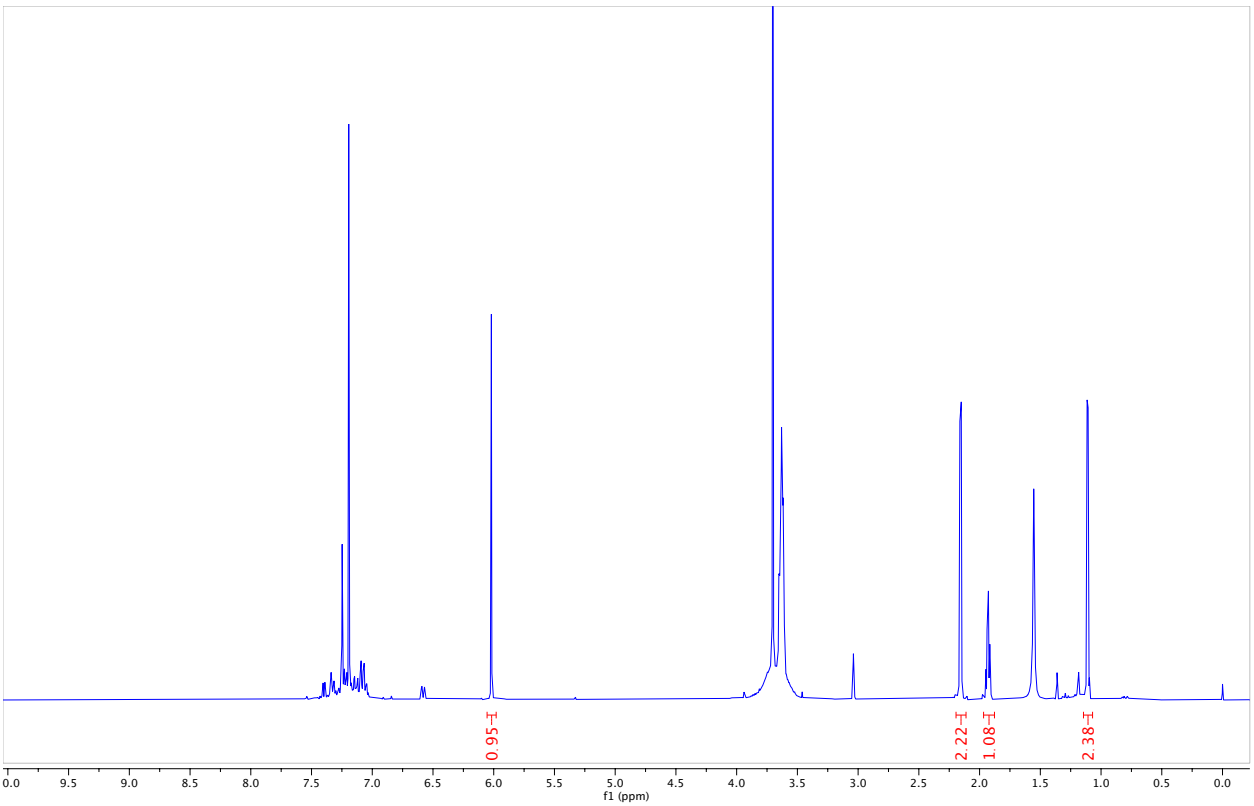

B.7 Other Enolate Additions to Bicyclobutane

Synthesis of *N*-methyl-2-oxo-N,3-diphenylbicyclo[2.2.1]heptane-1-carboxamide (5a)

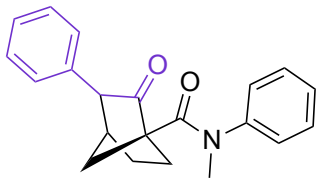

In a 1-dram vial, ethyl ester phenyl acetate **2c** (40.9 mg, 1.2 equiv) and TMB (10.1 mg, 0.06 mmol, 0.33 equiv) were added and put under a nitrogen atmosphere. The starting material was dissolved in THF (0.20 mL, 0.9 M) and 1.0 M LiHMDS in THF (0.269 mL, 0.27 mmol, 1.50 equiv) was added to the vial and it was stirred at rt for 10 minutes. The contents of the vial were then transferred to another 1-dram vial containing *N*-methyl-*N*-phenylbicyclo[2.1.0]pentane-1-carboxamide "housane" (36.1 mg, 0.18 mmol, 1.0 equiv) and the reaction was lfet to stir at rt overnight. The reaction was quenched with $NaHCO_3$ and extracted three times with ethyl acetate. The organic layers were dried with Mg_2SO_4, filtered and the solvent was evaporated to give the crude product **5a** (26% yield (peak at 2.57 ppm) compared to internal standard TMB, 65% starting material remaining (housane, 2.22 ppm peak)).

^{1}H NMR (500 MHz, $CDCl_3$, 292 K, ppm): 2.57 ppm peak is product and 2.22 ppm is starting material, housane.

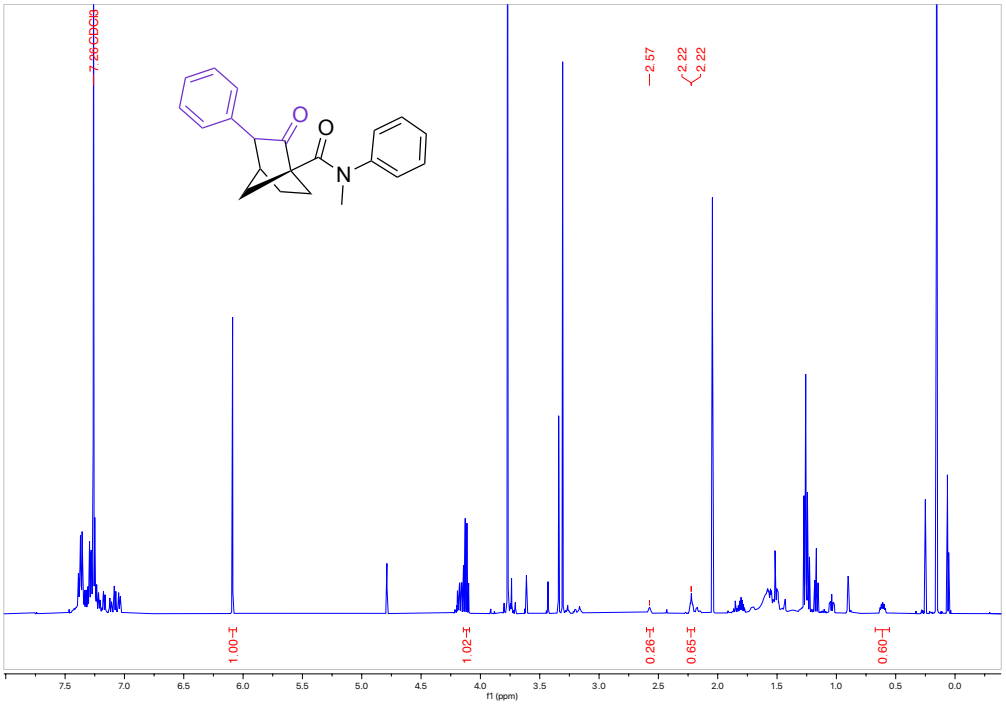

Isolated fraction of product: ^{1}H NMR (500 MHz, $CDCl_3$, 292 K, ppm): δ 7.40 (s, 4H), 7.31 (t, J = 7.7 Hz, 3H), 7.25 (d, J = 7.4 Hz, 1H), 7.10 – 7.03 (m, 2H), 3.36 (s, 3H), 3.19 (s, 1H), 2.60 (s, 1H), 2.25 – 2.20 (m, 1H), 1.73 (d, J = 10.4 Hz, 1H), 1.58 – 1.32 (m, 3H).

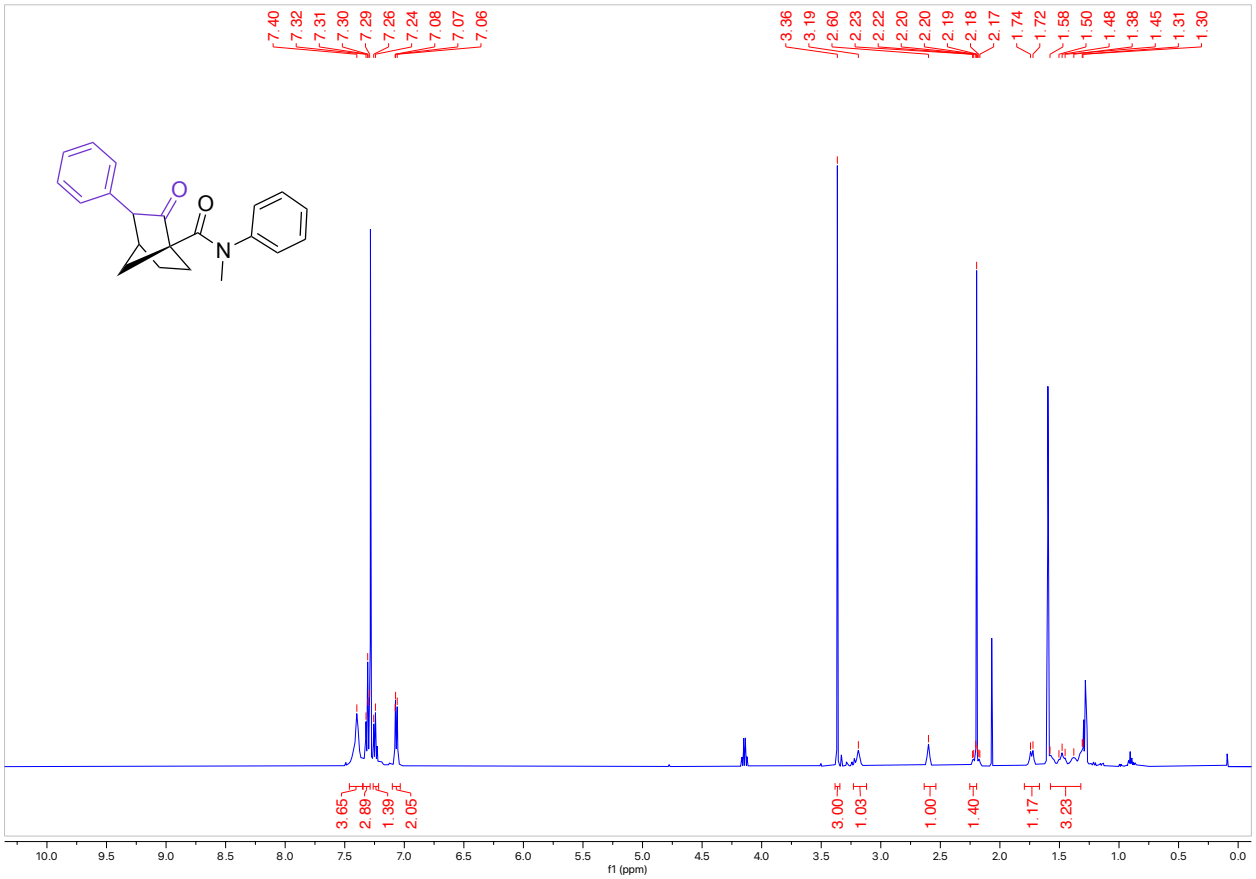

Synthesis of bicyclo[2.1.1]hexane with a *N*-acyl pyrazole bicyclobutane derivative

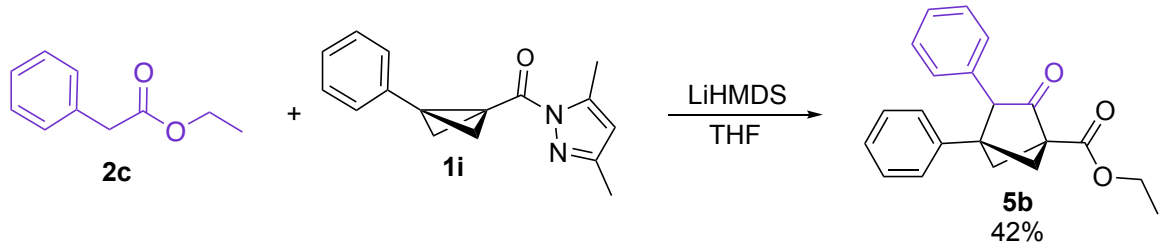

The *N*-acyl pyrazole bicyclobutane and aryl enolate were used following the general procedure for bicyclohexane synthesis from **1i** and **2c** on a 1.20 mmol bicyclobutane scale. With the *N*-acyl pyrazole on the bicyclobutane, side reactions with the enolate resulted with only the ethyl ester product obtained (due to transesterification of the *N*-acyl pyrazole with the ethoxide byproduct of the reaction). The ethyl ester product was purified by column chromatography (Biotage® Sfär 10g Column, 0-100% EtOAc/hexanes, eluted at 8% EtOAc). 133.5 mg of a clear colourless oil was obtained (42% Yield).

^{1}H NMR (500 MHz, $CDCl_3$, 292 K, ppm): δ 7.26 – 7.09 (m, 8H), 7.03 – 6.96 (m, 2H), 4.50 (s, 1H), 4.08 – 3.94 (m, 2H), 3.06 (dd, J = 6.8, 2.5 Hz, 1H), 3.00 (dd, J = 6.8, 2.4 Hz, 1H), 1.66 (dd, J = 6.4, 2.4 Hz, 2H), 1.11 (t, J = 7.1 Hz, 3H).

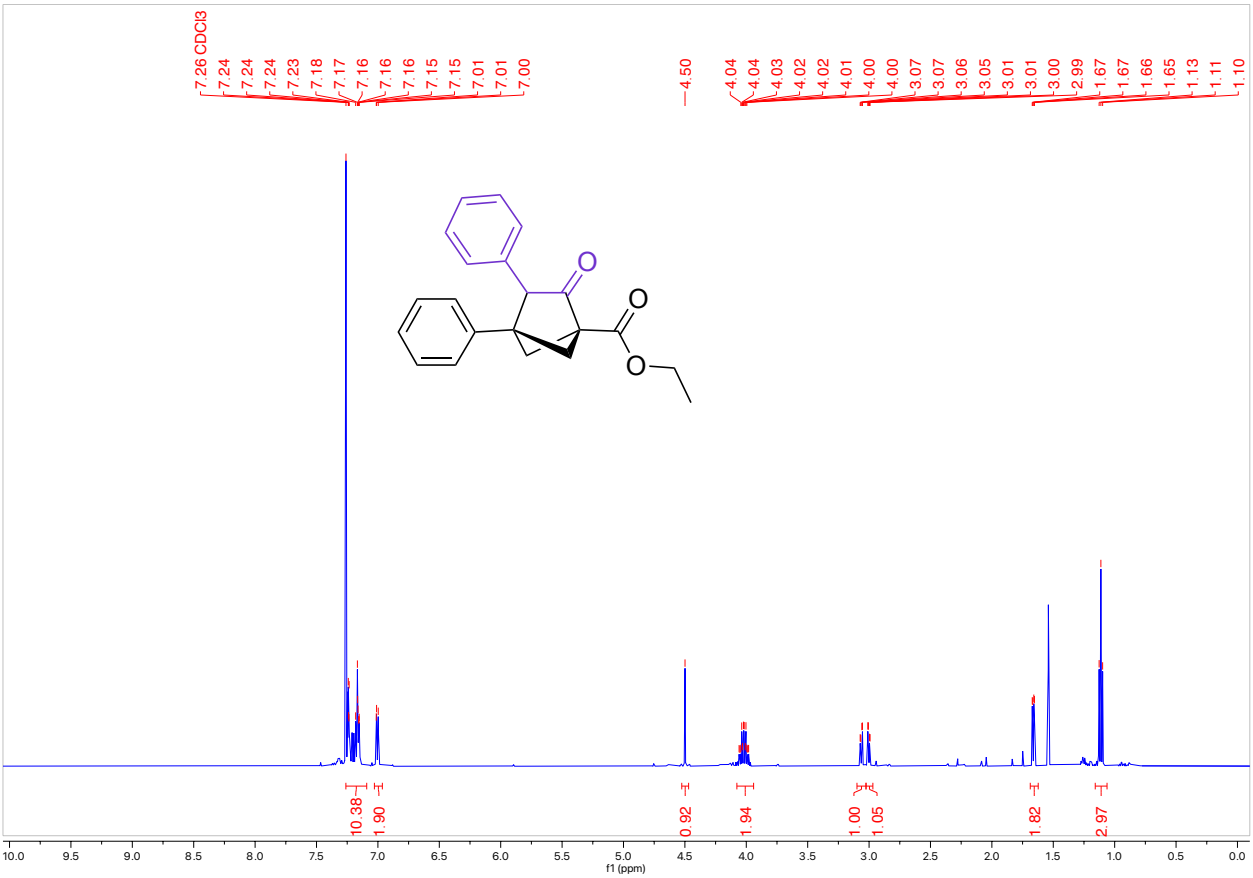

Test for the synthesis of 3,5-dimethylpyrazole bicyclo[2.1.1]hexane with a *N*-acyl pyrazole bicyclobutane and enolate derivatives

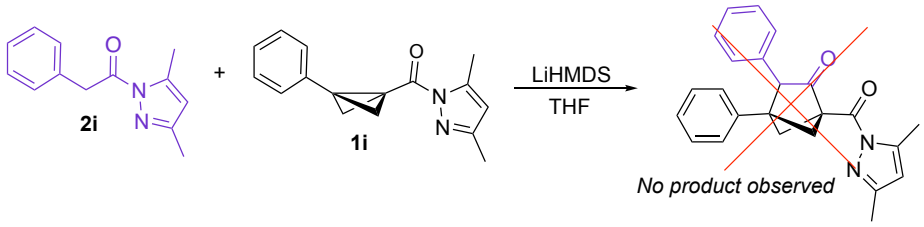

The *N*-acyl pyrazole bicyclobutane and 3,5-dimethyl *N*-pyrazole enolate were used following the general procedure for bicyclohexane synthesis from **1i** and **2i** on a 0.05 mmol bicyclobutane scale with TMB internal standard (0.33 equiv). Under these conditions, no product was formed.

Crude ^{1}H NMR (500 MHz, $CDCl_3$, 292 K):

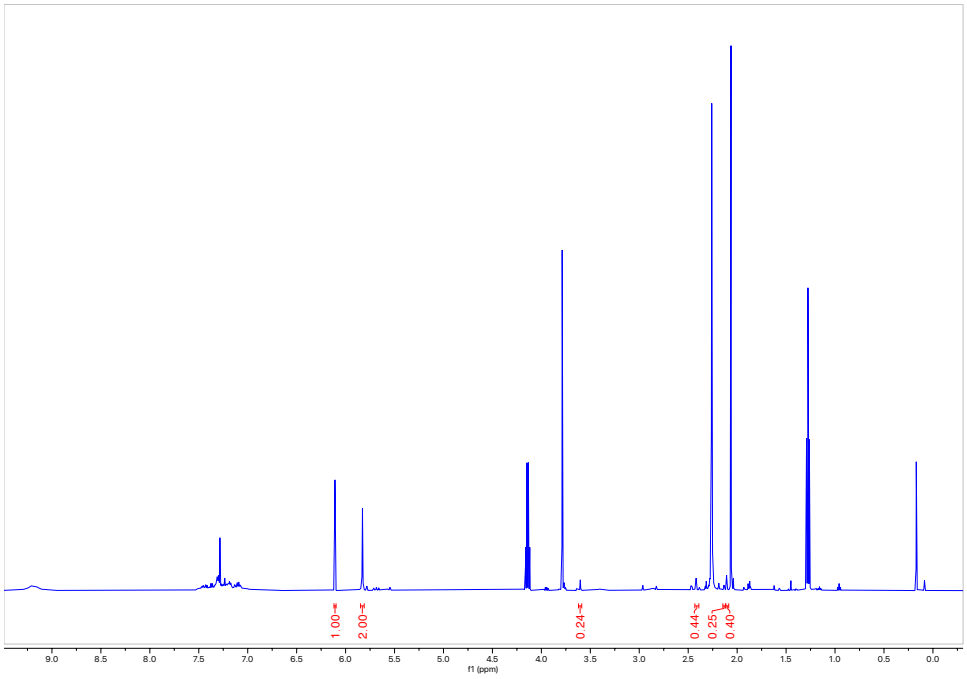

General procedure for Lewis-acid catalyzed nucleophilic addition to bicyclobutane

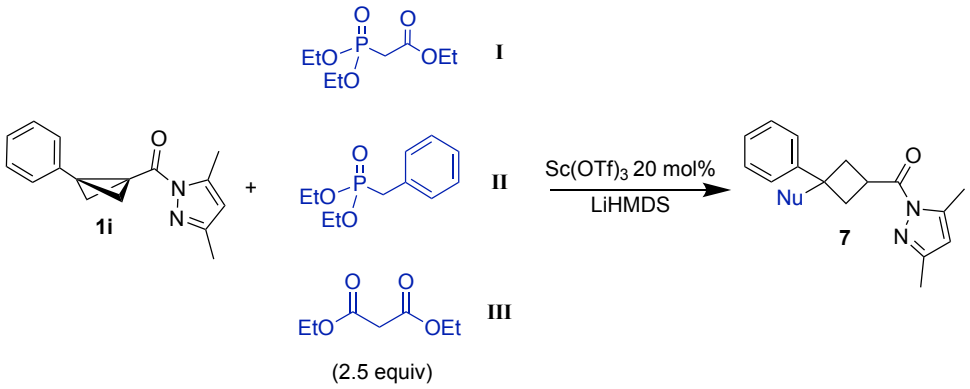

In a N_2 glovebox, the nucleophile (**I-III**, 2.5 equiv, 0.13 mmol) was added to a 4-mL vial with a stir bar and dissolved in THF (0.25 mL) and then 1.0 M LiHMDS in THF (0.15 mL, 3 equiv, 0.15 mmol) was added to the vial and it was left to stir for 10 minutes. In another 4-mL vial the bicyclobutane (12.6 mg, 1.0 equiv, 0.05 mmol) and $Sc(OTf)_3$ (4.9 mg, 20 mol%) was added and dissoled in THF (0.25 mL), stirred for 10 minutes at room temperature and then added to the vial containing the enolate. The reaction mixture was stirred for 2 hours at room temperature and then it was heated to 70 °C for 24 hours. The reaction was quenched with water (1 mL) and extracted with ethyl acetate (2 x 2 mL). The organic layer was dried with Mg_2SO_4, filtered and the solvent was removed. A ^{1}H NMR spectra was taken with internal standard (1,3,5-trimethyoxybenzene, 0.33 equiv).

^{1}H NMR (300 MHz, $CDCl_3$, 292 K): Nucleophile I.

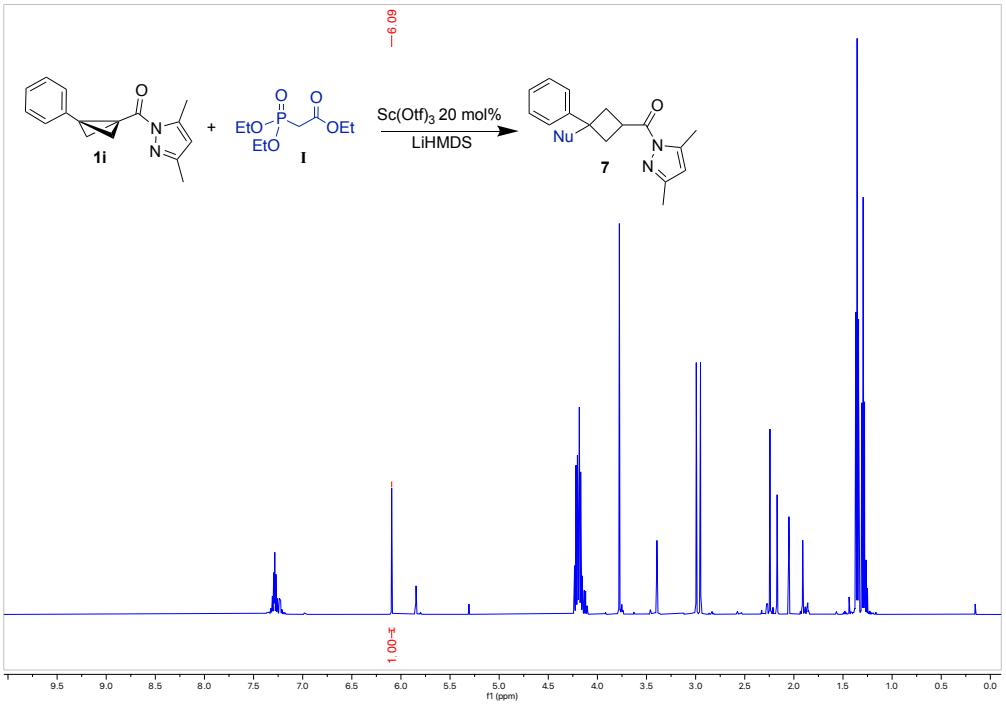

^{1}H NMR (300 MHz, $CDCl_3$, 292 K): Nucleophile II.

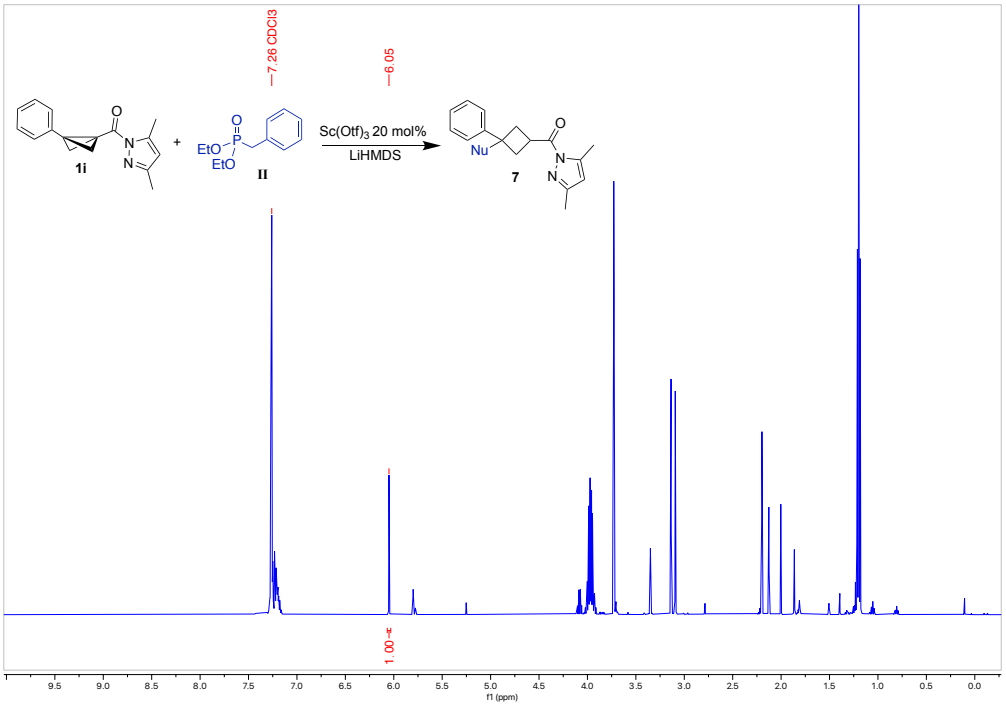

^{1}H NMR (300 MHz, $CDCl_3$, 292 K): Nucleophile III. Detected 413.4 m/z in LCMS (expected 413.5 m/z)

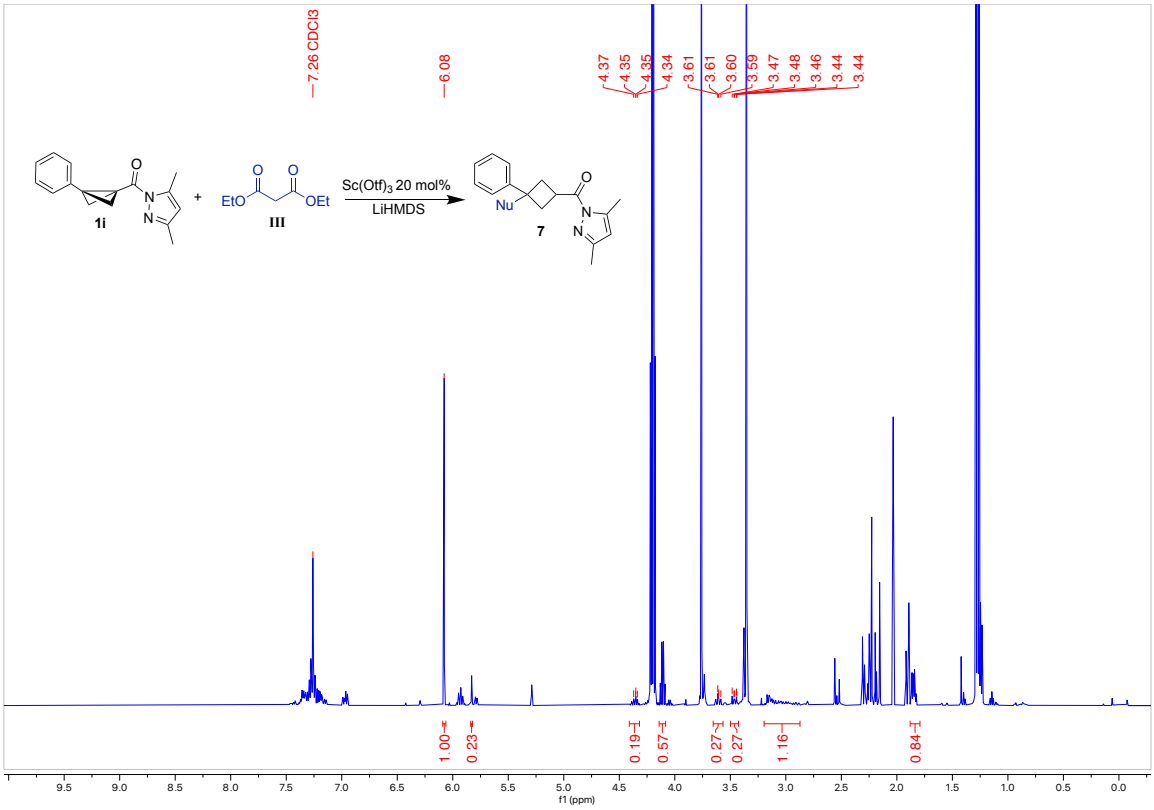

Appendix C

Supporting Information for Chapter 4

Contributions: The following data reported has been completed **independently** with supporting work from supervised undergraduate students.

C.1 General

Materials. All solvents and common organic reagents were purchased from commercial suppliers and used without further purification. Organic building blocks and starting materials were purchased from Oakwood Chemicals, Sigma Aldrich, or AmBeed and used as received. All Lewis acids were purchased from Strem Chemicals and used as received. All non-commerical compounds were prepared using literature procedures, or syntheses as described in Section V.

Techniques. High-throughput experimentation was performed using 1 mL capacity glass shell vials in sealable aluminum reaction blocks purchased from Analytical Sales. Heating/stirring was achieved using rare-earth magnetic tumble stirrers acquired from V&P Scientific. Photochemistry was performed using a Lumidox® II LED Controller and Lumidox® II LumLamp from Analytical Sales.

Analysis and Spectroscopy. All NMR spectra were acquired on either a Bruker AVANCE 300 MHz spectrometer or a Bruker AVANCE Neo 500 MHz spectrometer. All ^{1}H and ^{13}C NMR spectra chemical shifts are calibrated to residual protio-solvents, and ^{19}F NMR spectra chemical shifts are calibrated to an external standard. High-resolution electrospray ionization mass spectrometric analysis was performed using a Thermo Scientific Ultimate 3000 ESI-Orbitrap Exactive Plus.

C.2 Reaction Optimization

96-well HTE Screen Procedure: (From Table 4.1):

A stock solution for the methyl ester pyridinium **2a** in methanol was prepared and dispensed to all 96 x 1 mL shell vials (0.063 mmol, 2.5 equiv), followed by solvent evaporation and the addition of micro stir bars to each vial. Two stock solution were prepared for the bicyclobutane 1a, one in THF and another in MeCN. To two vials was added **1a** (454.2 mg, 1.8 mmol) and then 7.20 mL of THF or MeCN was added to each vial. The inorganic bases were weighed into the reaction vials containing the pyridinium **2a** using calibrated scoops, and triethylamine was added to the remaining vials. To all vials containing the base and 2a, 100 μL of THF or MeCN was added, and the mixtures were left to stir at rt for 10 minutes. Meanwhile, 24 stock solutions were prepared for the 12 triflate Lewis acids in the two solvents by weighing out the Lewis acid into the vial followed by addition of the bicyclobutane **1a** stock solution (0.48 mL to each vial). The bicyclobutane **1a** and Lewis acid mixtures were left to stir for 10 minutes at rt before 100 μL of the mixture was added to each reaction vial. The vials were then sealed and left to stir at 60 °C for 48 hours. The solvent was then evaporated using a Genevac centrifugal evaporator and then a stock solution of 1,3,5-trimethoxybenzene in $CDCl_3$ (1.4 mg, 0.33 equiv, 0.6 mL) was added to each vial. The mixtures were stirred for 5 minutes, and then the samples were centrifuged before the supernatants were removed for analysis by NMR spectroscopy compared to 1,3,5-tromethoxybenzene as internal standard.

Table C.1: 96-well High-throughput screen at 60 °C:

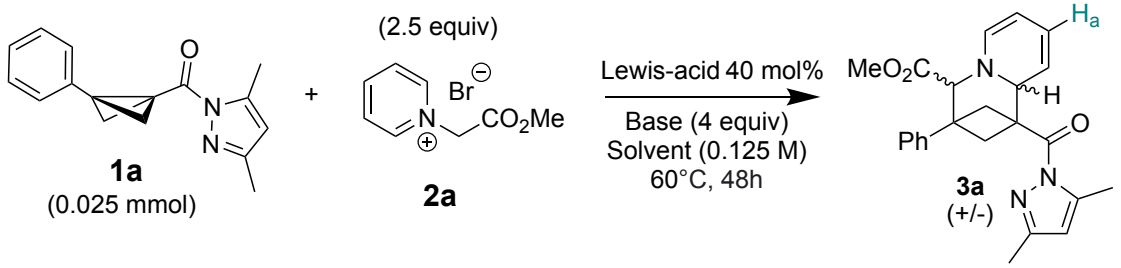

Entry	Catalyst	Solvent	Base	% 3a	d.r. (major : 1)	% 1a left
A1	LiOTf	THF	K_2CO_3	51	4.1	0
B1	$Mg(OTf)_2$	THF	K_2CO_3	44	3.4	0
C1	$Sc(OTf)_3$	THF	K_2CO_3	2	-	0
D1	$Fe(OTf)_3$	THF	K_2CO_3	0	-	0
E1	$Zn(OTf)_2$	THF	K_2CO_3	8	7.0	35
F1	$Ga(OTf)_3$	THF	K_2CO_3	0	-	0
G1	AgOTf	THF	Cs_2CO_3	31	3.4	0
H1	$Sn(OTf)_2$	THF	K_2CO_3	4	-	0
I1	$La(OTf)_3$	THF	K_2CO_3	0	-	3
J1	$Eu(OTf)_3$	THF	K_2CO_3	0	-	0
K1	$Yb(OTf)_3$	THF	K_2CO_3	0	-	0
L1	$Bi(OTf)_3$	THF	K_2CO_3	0	-	0

Entry	Catalyst	Solvent	Base	% 3a	d.r. (major : 1)	% 1a left
A2	LiOTf	THF	Cs_2CO_3	65	3.1	0
B2	$Mg(OTf)_2$	THF	Cs_2CO_3	53	1.2	5
C2	$Sc(OTf)_3$	THF	Cs_2CO_3	14	1.3	1
D2	$Fe(OTf)_3$	THF	Cs_2CO_3	0	-	0
E2	$Zn(OTf)_2$	THF	Cs_2CO_3	53	1.8	7
F2	$Ga(OTf)_3$	THF	Cs_2CO_3	0	-	0
G2	AgOTf	THF	Cs_2CO_3	45	2.0	21
H2	$Sn(OTf)_2$	THF	Cs_2CO_3	5	-	12
I2	$La(OTf)_3$	THF	Cs_2CO_3	0	-	8
J2	$Eu(OTf)_3$	THF	Cs_2CO_3	4	-	6
K2	$Yb(OTf)_3$	THF	Cs_2CO_3	0	-	3
L2	$Bi(OTf)_3$	THF	Cs_2CO_3	0	-	0
A3	LiOTf	THF	K_3PO_4	56	4.6	1
B3	$Mg(OTf)_2$	THF	K_3PO_4	56	1.7	1
C3	$Sc(OTf)_3$	THF	K_3PO_4	6	-	2
D3	$Fe(OTf)_3$	THF	K_3PO_4	0	-	0
E3	$Zn(OTf)_2$	THF	K_3PO_4	51	2.4	3
F3	$Ga(OTf)_3$	THF	K_3PO_4	0	-	0
G3	AgOTf	THF	K_3PO_4	35	4.8	0
H3	$Sn(OTf)_2$	THF	K_3PO_4	0	-	0
I3	$La(OTf)_3$	THF	K_3PO_4	2	-	5
J3	$Eu(OTf)_3$	THF	K_3PO_4	0	-	16
K3	$Yb(OTf)_3$	THF	K_3PO_4	0	-	5
L3	$Bi(OTf)_3$	THF	K_3PO_4	0	-	0
A4	LiOTf	THF	NEt_3	14	1.8	50
B4	$Mg(OTf)_2$	THF	NEt_3	1	-	0
C4	$Sc(OTf)_3$	THF	NEt_3	0	-	25
D4	$Fe(OTf)_3$	THF	NEt_3	0	-	0
E4	$Zn(OTf)_2$	THF	NEt_3	3	2.0	1
F4	$Ga(OTf)_3$	THF	NEt_3	0	-	0
G4	AgOTf	THF	NEt_3	0	-	0
H4	$Sn(OTf)_2$	THF	NEt_3	0	-	0
I4	$La(OTf)_3$	THF	NEt_3	0	-	4
J4	$Eu(OTf)_3$	THF	NEt_3	0	-	36
K4	$Yb(OTf)_3$	THF	NEt_3	0	-	0
L4	$Bi(OTf)_3$	THF	NEt_3	0	-	0
A5	LiOTf	MeCN	K_2CO_3	34	3.9	0
B5	$Mg(OTf)_2$	MeCN	K_2CO_3	0	-	0
C5	$Sc(OTf)_3$	MeCN	K_2CO_3	3	-	0
D5	$Fe(OTf)_3$	MeCN	K_2CO_3	0	-	0
E5	$Zn(OTf)_2$	MeCN	K_2CO_3	15	2.0	38
F5	$Ga(OTf)_3$	MeCN	K_2CO_3	0	-	0

Entry	Catalyst	Solvent	Base	% 3a	d.r. (major : 1)	% 1a left
G5	AgOTf	MeCN	Cs_2CO_3	23	1.9	0
H5	$Sn(OTf)_2$	MeCN	K_2CO_3	0	-	0
I5	$La(OTf)_3$	MeCN	K_2CO_3	0	-	0
J5	$Eu(OTf)_3$	MeCN	K_2CO_3	0	-	0
K5	$Yb(OTf)_3$	MeCN	K_2CO_3	0	-	0
L5	$Bi(OTf)_3$	MeCN	K_2CO_3	0	-	0
A6	LiOTf	MeCN	Cs_2CO_3	53	3.4	7
B6	$Mg(OTf)_2$	MeCN	Cs_2CO_3	53	3.4	0
C6	$Sc(OTf)_3$	MeCN	Cs_2CO_3	0	-	0
D6	$Fe(OTf)_3$	MeCN	Cs_2CO_3	0	-	0
E6	$Zn(OTf)_2$	MeCN	Cs_2CO_3	11	1.8	13
F6	$Ga(OTf)_3$	MeCN	Cs_2CO_3	8	-	0
G6	AgOTf	MeCN	Cs_2CO_3	30	2.3	0
H6	$Sn(OTf)_2$	MeCN	Cs_2CO_3	0	-	0
I6	$La(OTf)_3$	MeCN	Cs_2CO_3	0	-	0
J6	$Eu(OTf)_3$	MeCN	Cs_2CO_3	0	-	0
K6	$Yb(OTf)_3$	MeCN	Cs_2CO_3	0	-	0
L6	$Bi(OTf)_3$	MeCN	Cs_2CO_3	0	-	1
A7	LiOTf	MeCN	K_3PO_4	45	3.5	3
B7	$Mg(OTf)_2$	MeCN	K_3PO_4	55	4.0	0
C7	$Sc(OTf)_3$	MeCN	K_3PO_4	0	-	0
D7	$Fe(OTf)_3$	MeCN	K_3PO_4	0	-	0
E7	$Zn(OTf)_2$	MeCN	K_3PO_4	0	-	7
F7	$Ga(OTf)_3$	MeCN	K_3PO_4	0	-	0
G7	AgOTf	MeCN	K_3PO_4	28	2.5	0
H7	$Sn(OTf)_2$	MeCN	K_3PO_4	0	-	0
I7	$La(OTf)_3$	MeCN	K_3PO_4	0	-	0
J7	$Eu(OTf)_3$	MeCN	K_3PO_4	0	-	0
K7	$Yb(OTf)_3$	MeCN	K_3PO_4	0	-	0
L7	$Bi(OTf)_3$	MeCN	K_3PO_4	0	-	0
A8	LiOTf	MeCN	NEt_3	0	-	4
B8	$Mg(OTf)_2$	MeCN	NEt_3	0	-	0
C8	$Sc(OTf)_3$	MeCN	NEt_3	0	-	0
D8	$Fe(OTf)_3$	MeCN	NEt_3	0	-	0
E8	$Zn(OTf)_2$	MeCN	NEt_3	0	-	44
F8	$Ga(OTf)_3$	MeCN	NEt_3	0	-	0
G8	AgOTf	MeCN	NEt_3	0	-	0
H8	$Sn(OTf)_2$	MeCN	NEt_3	0	-	0
I8	$La(OTf)_3$	MeCN	NEt_3	0	-	4
J8	$Eu(OTf)_3$	MeCN	NEt_3	0	-	0
K8	$Yb(OTf)_3$	MeCN	NEt_3	0	-	70
L8	$Bi(OTf)_3$	MeCN	NEt_3	0	-	0

^{1}H NMR spectrum in $CDCl_3$ for Table C.1, entry A2: 4.94 ppm peak is the major diastereomer of the product and 5.19 ppm is the minor diastereomer of the product (H_a)

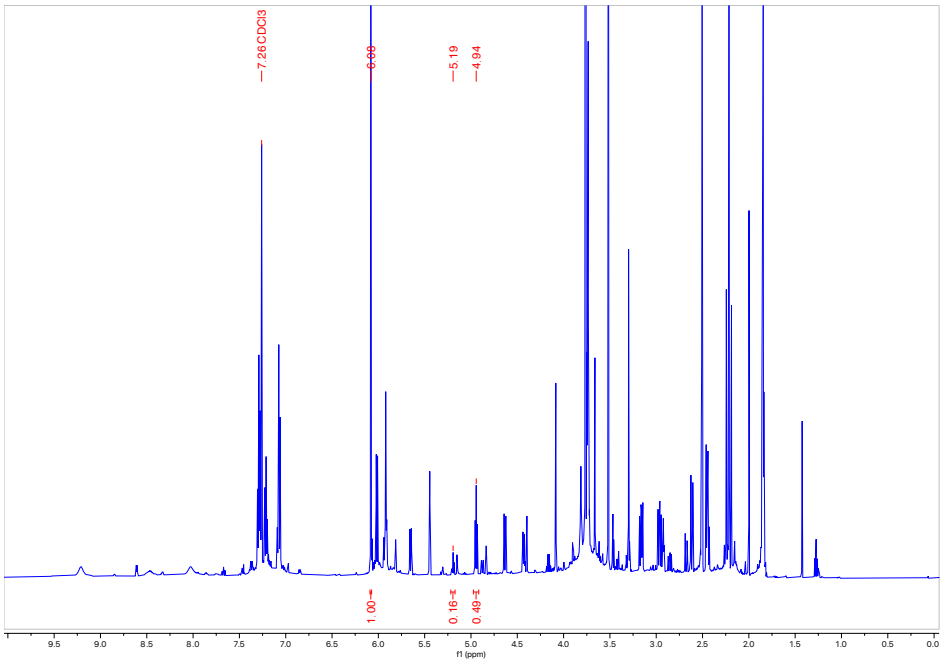

^{1}H NMR spectrum in $CDCl_3$ for Table C.1, entry B7: 4.94 ppm peak is the major diastereomer of the product and 5.19 ppm is the minor diastereomer of the product (H_a)

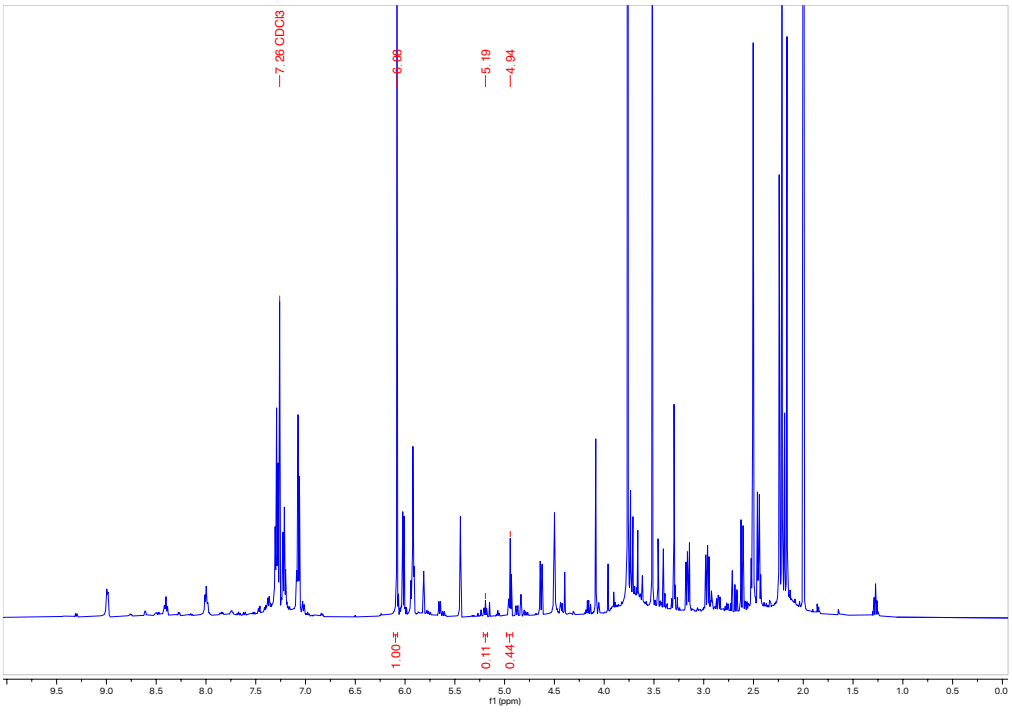

30-well HTE Screen Procedure: (From Table 4.2):

For the vials with Lewis acid (A-D): a stock solution for the methyl ester pyridinium **2a** in methanol was prepared and dispensed to 24 x 1 mL glass shell vials (0.063 mmol, 2.5 equiv) followed by solvent evaporation and the addition of micro parylene-coated stir bars to each vial. Two stock solution were prepared for the bicyclobutane 1a, one in THF and another in MeCN. To two vials was added **1a** (454.2 mg, 1.8 mmol), followed by 7.20 mL of THF or MeCN. The inorganic bases were weighed into the vials containing the pyridinium **2a** using calibrated scoops and triethylamine was added to the remaining vials. To all vials with the base and 2a, 100 μL of THF or MeCN was added, and the vials were left to stir at rt for 10 minutes. Meanwhile, 24 stock solutions were prepared for the 12 triflate Lewis acids in the two solvents by weighing out the Lewis acid into the vial followed by addition of the bicyclobutane **1a** stock solution (0.48 mL to each vial). The bicyclobutane **1a** and Lewis acids were left to stir for 10 minutes at rt before 100 μL of the mixture was added to each vial (0.125 M concentration). The vials were then sealed and left to stir at rt for 24 hours.

For the vials without Lewis acid (E), pyridinium **2a** (14.5 mg, 0.063 mmol, 2.5 equiv) and base was weighed into the 1 mL shell vials followed by the addition of stir bars. Half of the acetonitrile solvent (100 μL) was added to all six vials, and they were left to stir for 10 minutes at rt. Two stock solutions of bicyclobutane were made by adding 22.7 mg of **1a** to two vials followed by 0.36 mL of THF and acetonitrile to the vials. The bicyclobutane stock solution was added to each vial (100 μL, 0.125 M) and the reactions were left to stir at rt for 24 hours.

One the reaction time was complete, the solvent was evaporated using a Genevac centrifugal evaporator. A stock solution of 1,3,5-trimethoxybenzene in $CDCl_3$ (1.4 mg, 0.33 equiv, 0.7 mL) was then added to each vial. The mixtures were stirred for 5 minutes, followed by centrifugation. The supernatant solutions were removed for analysis by NMR spectroscopy compared to 1,3,5-tromethoxybenzene as internal standard.

Table C.2: 30-well High-throughput screen at rt:

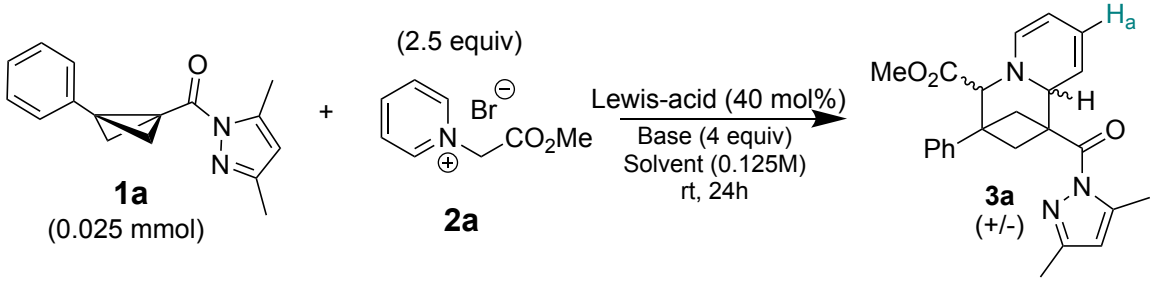

Entry	Catalyst	Solvent	Base	% 3a	d.r. (major : 1)	% 1a left
A1	LiOTf	THF	Cs_2CO_3	57	2.4	15
B1	$Mg(OTf)_2$	THF	Cs_2CO_3	61	3.1	17
C1	$Zn(OTf)_2$	THF	Cs_2CO_3	52	4.8	24
D1	AgOTf	THF	Cs_2CO_3	31	3.4	32
E1	none	THF	Cs_2CO_3	69	1.1	3
A2	LiOTf	THF	K_3PO_4	46	5.6	37
B2	$Mg(OTf)_2$	THF	K_3PO_4	38	2.8	50
C2	$Zn(OTf)_2$	THF	K_3PO_4	25	4.0	60
D2	AgOTf	THF	K_3PO_4	68	8.7	18
E2	none	THF	K_3PO_4	70	1.6	3
A3	LiOTf	THF	NEt_3	0	-	90
B3	$Mg(OTf)_2$	THF	NEt_3	0	-	81
C3	$Zn(OTf)_2$	THF	NEt_3	0	-	80
D3	AgOTf	THF	NEt_3	0	-	94
E3	none	THF	NEt_3	0	-	100
A4	LiOTf	MeCN	Cs_2CO_3	57	>20	15
B4	$Mg(OTf)_2$	MeCN	Cs_2CO_3	56	>20	0
C4	$Zn(OTf)_2$	MeCN	Cs_2CO_3	65	>20	3
D4	AgOTf	MeCN	Cs_2CO_3	64	>20	5
E4	none	MeCN	Cs_2CO_3	73	>20	3
A5	LiOTf	MeCN	K_3PO_4	30	>20	33
B5	$Mg(OTf)_2$	MeCN	K_3PO_4	82	>20	1
C5	$Zn(OTf)_2$	MeCN	K_3PO_4	50	>20	6
D5	AgOTf	MeCN	K_3PO_4	36	>20	16
E5	none	MeCN	K_3PO_4	86	>20	3
A6	LiOTf	MeCN	NEt_3	0	-	100
B6	$Mg(OTf)_2$	MeCN	NEt_3	6	>20	74
C6	$Zn(OTf)_2$	MeCN	NEt_3	0	-	58
D6	AgOTf	MeCN	NEt_3	0	-	68
E6	none	MeCN	NEt_3	0	-	70

^{1}H NMR spectrum in $CDCl_3$ for Table C.2, entry B5: 4.95 ppm peak is the major diastereomer of the product (H_a)

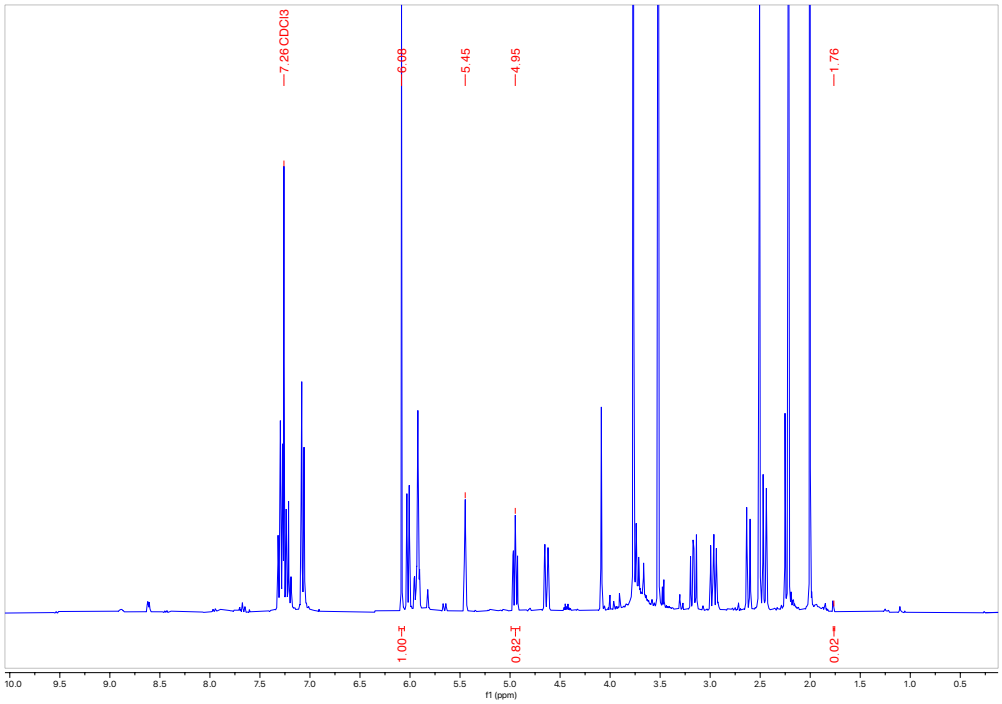

^{1}H NMR spectrum in $CDCl_3$ for Table C.2, entry E5: 4.94 ppm peak is the major diastereomer of the product (H_a)

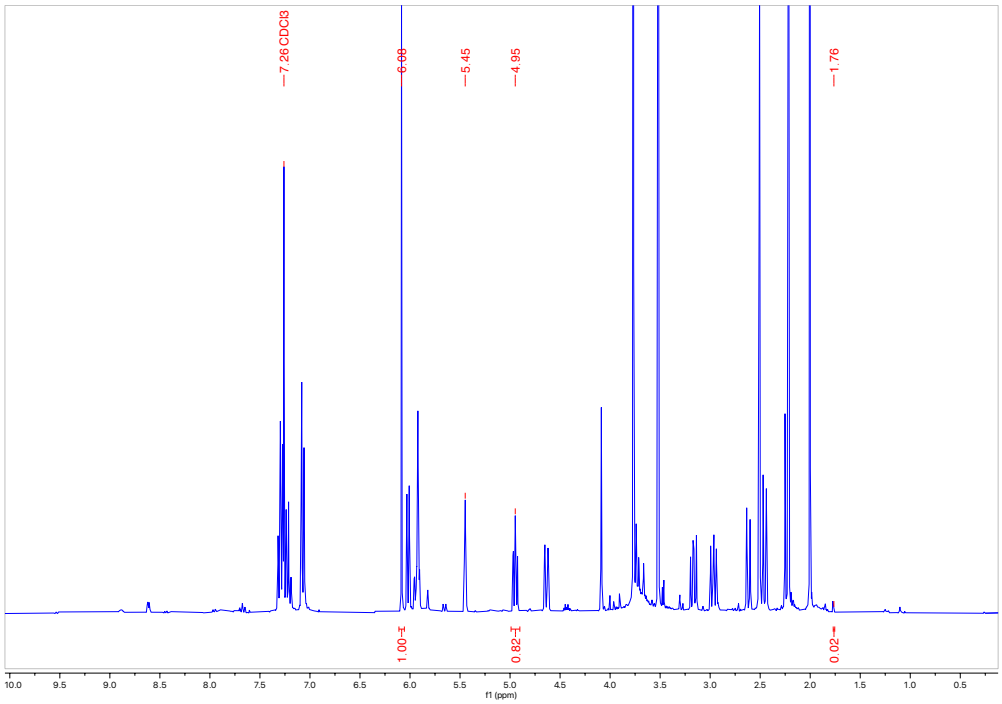

C.3 Reaction Progress Monitoring

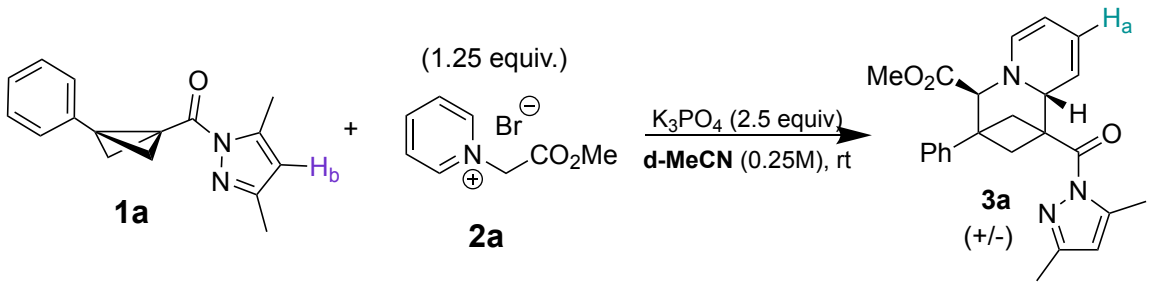

Procedure (Table C.3): Pyridinium **2a** (145.0 mg, 0.63 mmol, 1.25 equiv) and K_3PO_4 (265.4 mg, 0.50 mmol, 2.5 equiv) were weighed into a 20 mL vial, followed by the addition of a Teflon-coated stir bar. d-MeCN (1.0 mL) was added to the vial, and the mixture was stirred for 2 minutes at rt. Then, the bicyclobutane **1a** (126.2 mg, 0.50 mmol, 1 equiv) and 1,3,5-trimethoxybenzene internal standard (28.0 mg, 0.17 mmol, 0.33 equiv) were dissolved in d-MeCN (0.50 mL) in a 4 mL vial, and the solution added to the reaction vial. The bicyclobutane vial was washed with another 0.50 mL of d-MeCN, and this was added to the reaction mixture, which represented t = 0.

At each time point, a 50 μL sample was withdrawn from the reaction mixture via pipette, diluted with d-MeCN, and passed through a 0.45 μm syringe filter. The filter was washed with an additional 0.3 mL of d-MeCN, and then the sample was analyzed by NMR spectroscopy compared to 1,3,5-tromethoxybenzene as internal standard. Peak at 5.94 ppm is the bicyclobutane (H_b) and 4.84 ppm is product (H_a).

Table C.3: Reaction progress monitoring data (From Figure 4.14).

Time (h)	% 1a left	% 3a	% 1a + %3a
0.0	100	0	100
0.25	60	30	90
0.50	50	41	91
0.75	43	49	92
1.0	36	56	92
1.5	26	67	93
2.0	19	76	95
2.5	13	82	95
3.0	8	87	95
3.5	6	89	95
4.0	4	89	93
5.0	3	90	93

^{1}H NMR spectrum in $CDCl_3$ for Table C.3, t = 0 h:

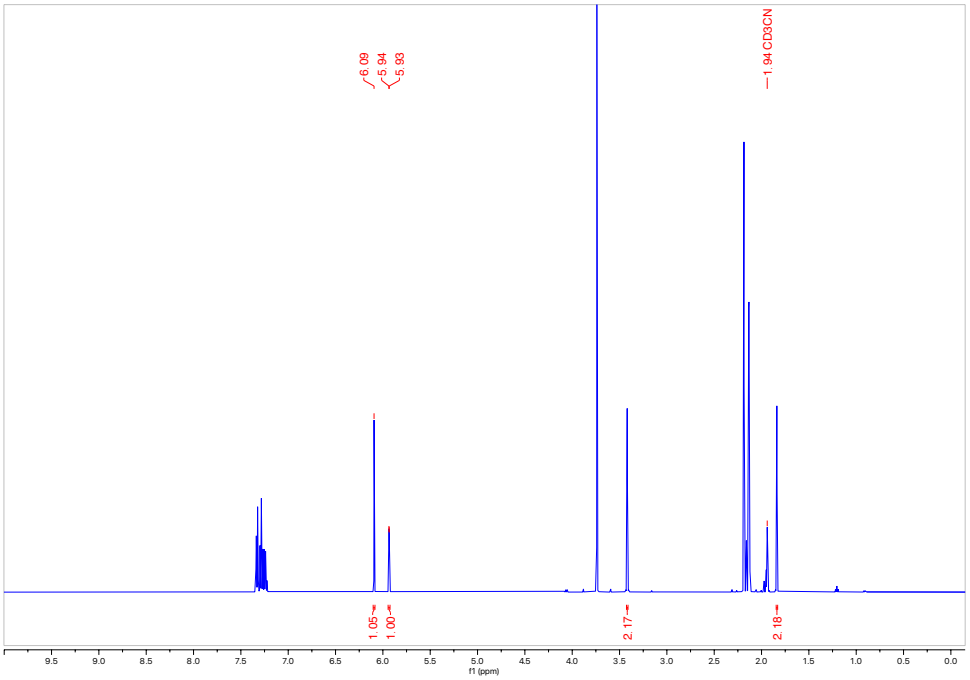

^{1}H NMR spectrum in $CDCl_3$ for Table C.3, t = 0 h, 30% 3a (4.84 ppm peak, H_a):

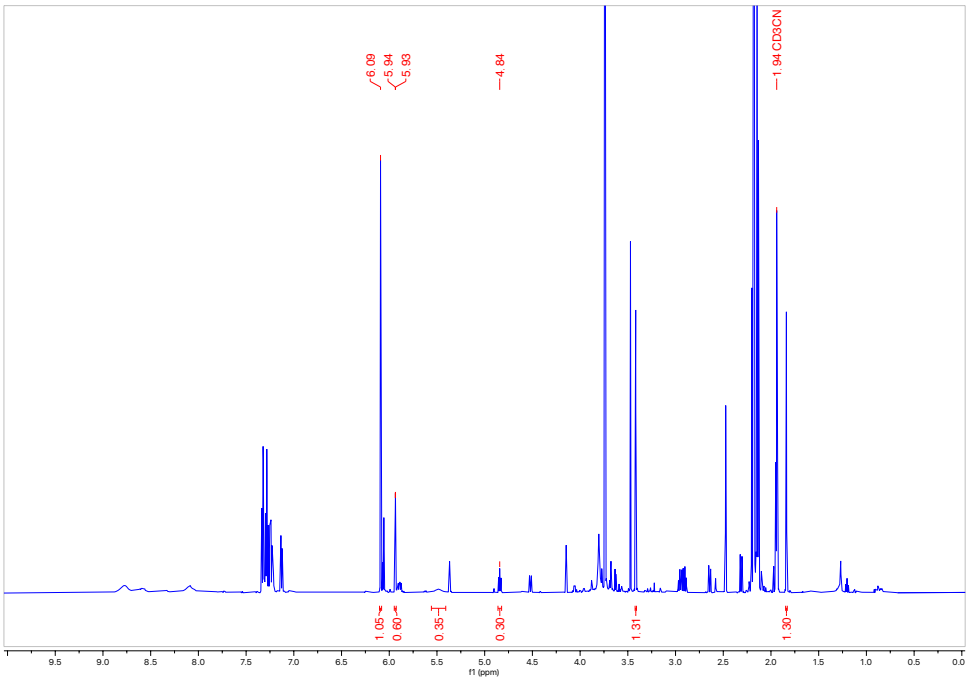

^{1}H NMR spectrum in $CDCl_3$ for Table C.3, t = 1 h, 56% 3a (4.84 ppm peak, H_a):

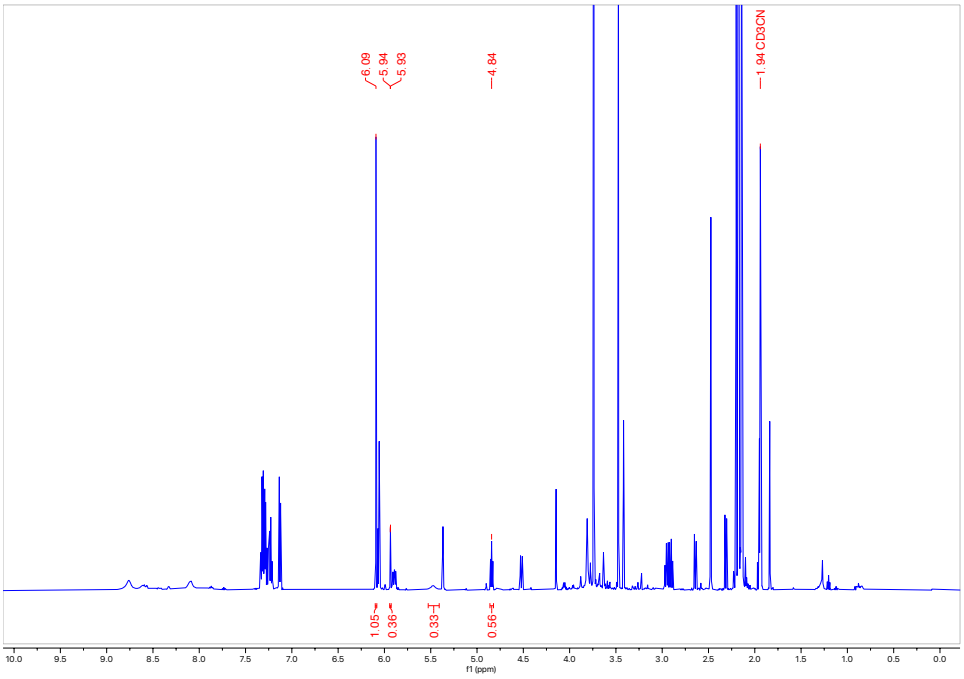

^{1}H NMR spectrum in $CDCl_3$ for Table C.3, t = 5 h, 90% 3a (4.84 ppm peak, H_a):

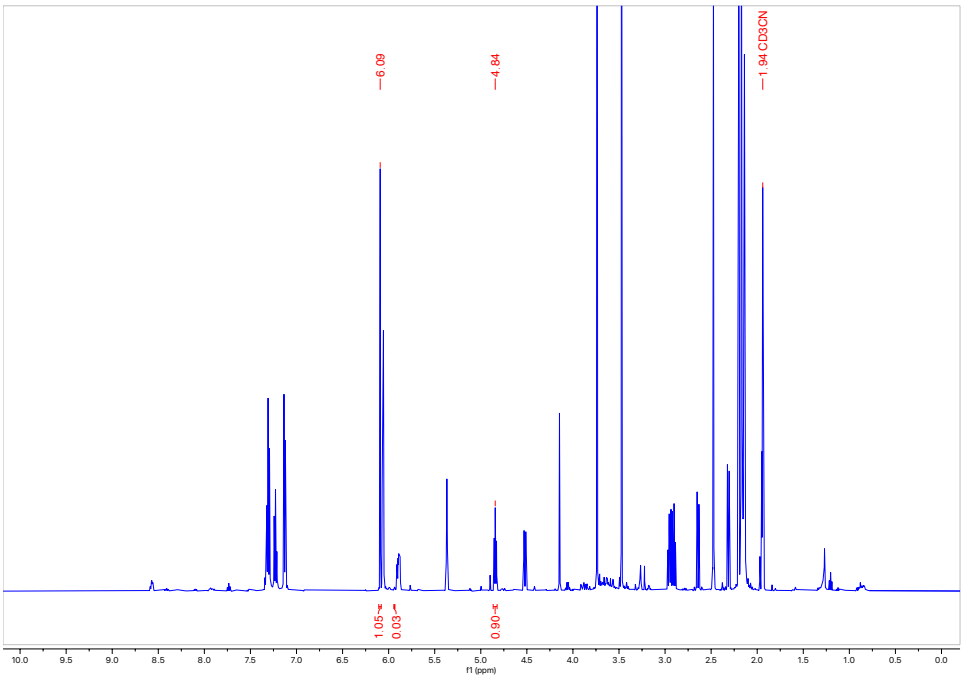

C.4 Control Reactions

General Procedure for Sensitivity Reactions (Table C.4):

Pyridinium **2a** (29.0 mg, 0.13 mmol, 1.25 equiv) and K_3PO_4 (53.1 mg, 0.25 mmol, 2.5 equiv) were weighed into four 4 mL vials, followed by the addition of stir bars. MeCN (0.2 mL) was added to all four vials, and they were left to stir for 5 minutes at rt. A stock solution of **1a** was made from 121.1 mg of **1a** and 0.96 mL of MeCN. The bicyclobutane stock solution was then added to each vial (0.2 mL, 0.25 M) and the reaction mixtures were left to stir at rt for 24 hours. The solvent was then evaporated using a Genevac centrifugal evaporator, followed by dilution with a stock solution of 1,3,5-trimethoxybenzene in $CDCl_3$ (0.7 mL, containing 5.6 mg, 0.33 equiv of internal standard). The mixtures were stirred for 5 minutes, centrifuged, and the supernatant removed for analysis by NMR spectroscopy compared to 1,3,5-tromethoxybenzene as internal standard (peak at 5.81 ppm is bicyclobutane (H_b) and 4.93 ppm is product (H_a)).

Deviations from the general procedure:

Entry 1: No base was added to the reaction.
Entry 2: The reaction mixture was stirred at 30 °C.
Entry 3: $Na_2SO_4{\cdot}10H_2O$ (32.2 mg, 0.10 mmol, 1 equiv) was added to the pyridinium/base vial before solvent was added.
Entry 1: 4 Åmolecular sieves (100 mg) was added to the pyridinium/base vial before solvent was added.

Table C.4: Sensitivity Reactions (From Figure 4.4).

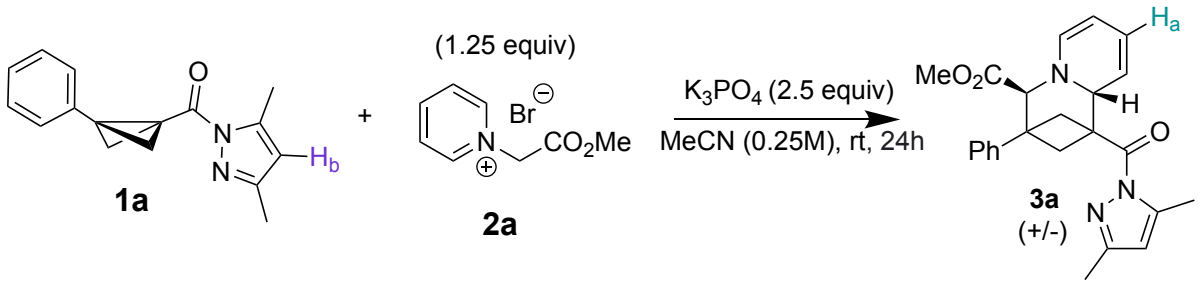

Entry	Conditions[a]	% 3a[b]	% 1a[b]
1	No K_3PO_4 added	0	84
2	Run at 30 °C	81	5
3	$Na_2SO_4{\cdot}10H_2O$ (1 equiv)	81	6
4	Molecular Sieves	66	12

[a]Unless otherwise noted, reactions are performed at room temperature for 24 hours with 0.05 mmol of **1a** and 3a is formed as a single diastereomer. [b]Amounts of **1a** and 3a are obtained by ^{1}H NMR spectroscopy by relative integration vs. internal standard, 1,3,5-trimethoxybenzene (TMB).

^{1}H NMR spectrum in $CDCl_3$ for Table C.4, Entry 1:

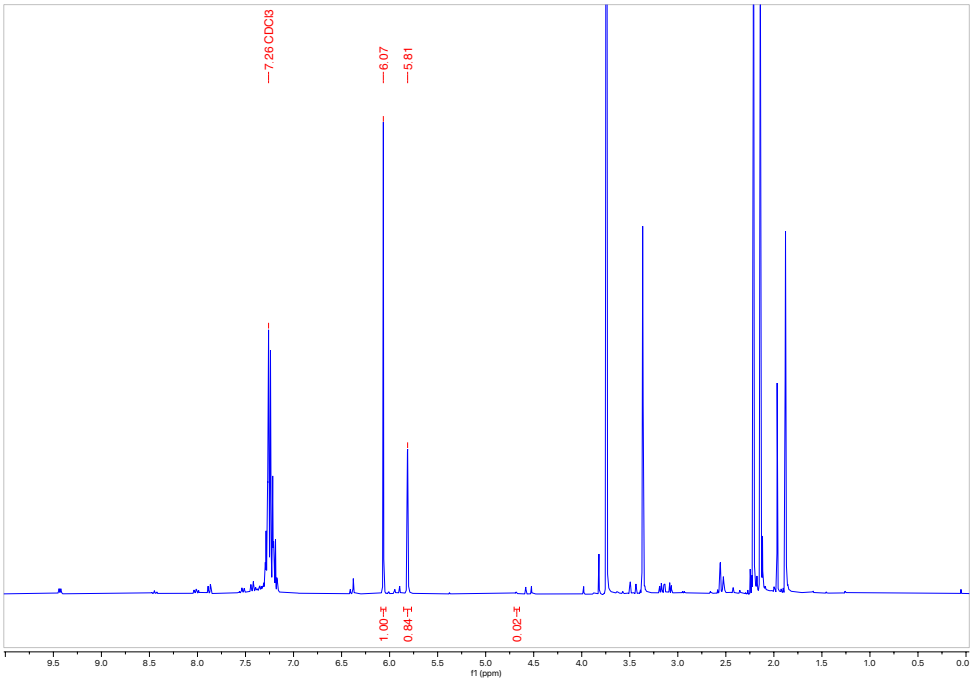

^{1}H NMR spectrum in $CDCl_3$ for Table C.4, Entry 2:

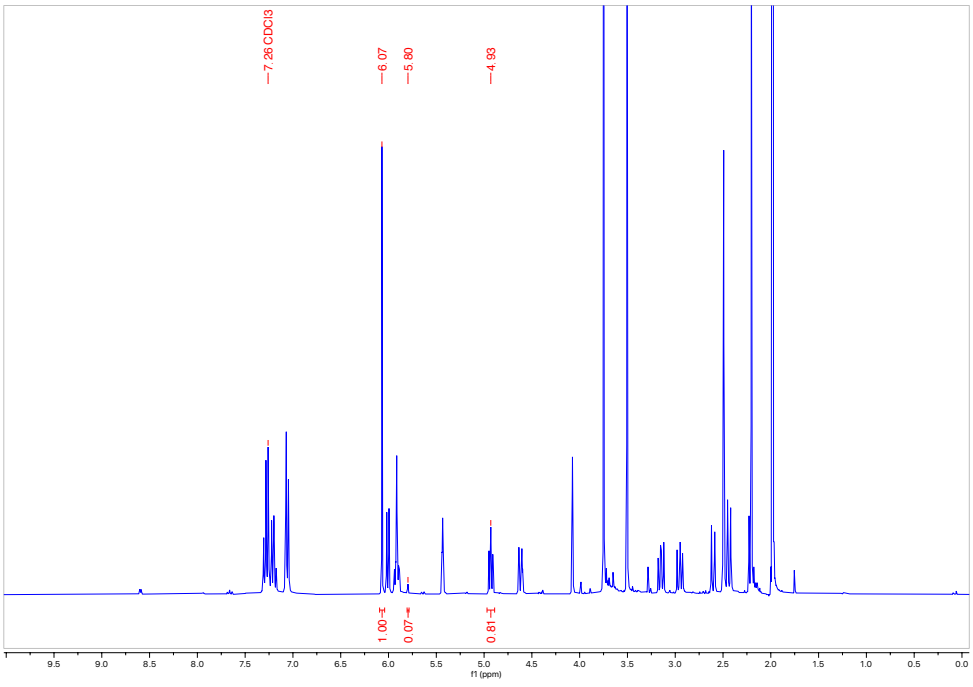

^{1}H NMR spectrum in $CDCl_3$ for Table C.4, Entry 3:

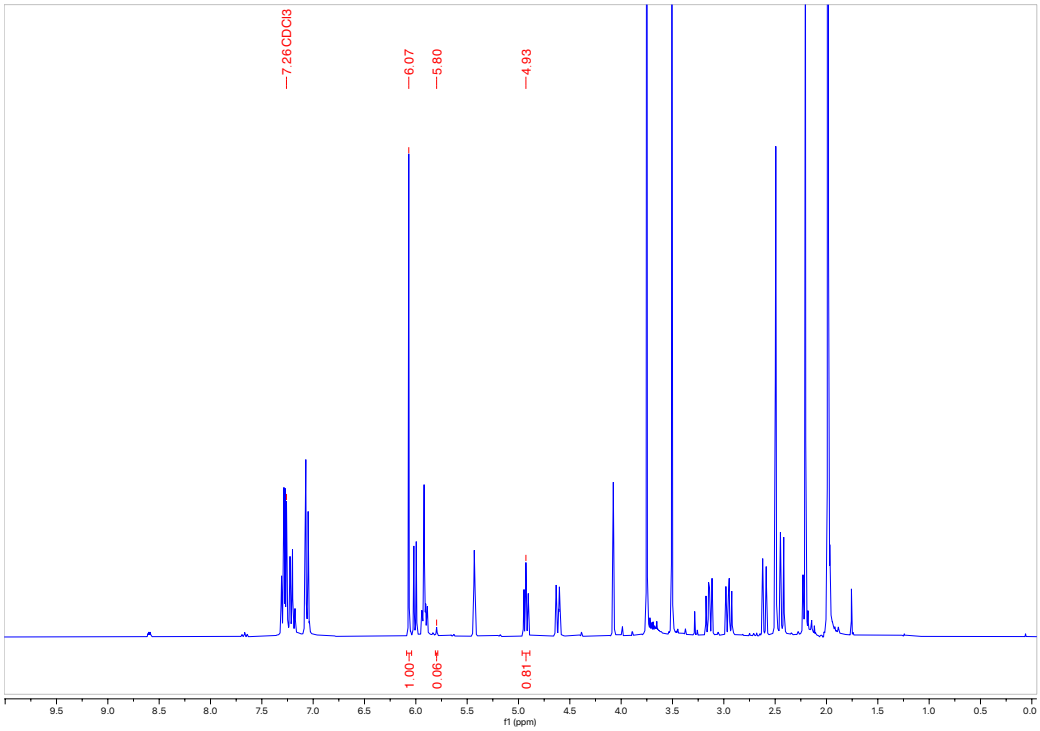

^{1}H NMR spectrum in $CDCl_3$ for Table C.4, Entry 4:

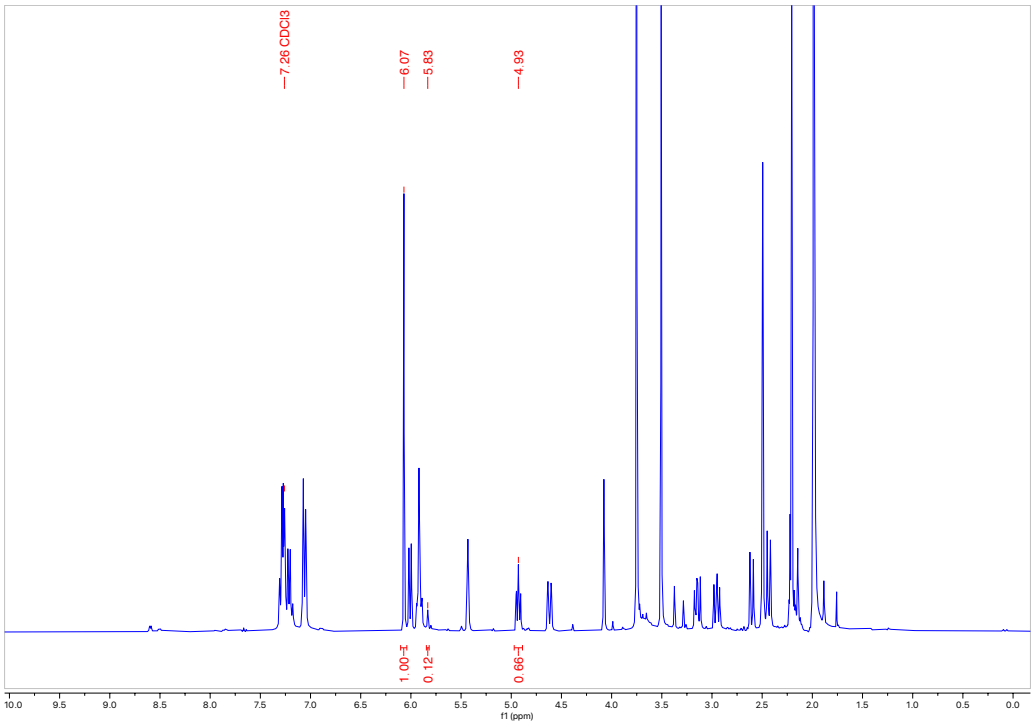

Epimerization test reaction

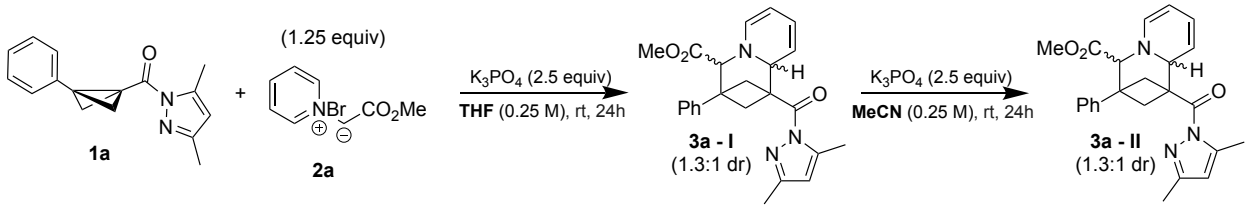

Procedure: Pyridinium **2a** (58.0 mg, 0.25 mmol, 1.25 equiv) and K_3PO_4 (106.1 mg, 0.50 mmol, 2.5 equiv) were weighed into a 4 mL vial, followed by the addition of a stir bar. THF (0.4 mL) was added to the vial, and the mixture stirred for 5 minutes at rt. After 5 minutes, **1a** (50.5 mg, 0.20 mmol) was dissolved in THF (0.4 mL) and added to the reaction mixture. The reaction mixture was stirred at rt for 24 hours. The solvent was then evaporated using a Genevac centrifugal evaporator. The crude **3a – I** obtained was dissolved in dichloromethane and eluted through a plug of basic alumina. Solvent evaporation provided **3a – I** as a mixture of diastereomers as determined by NMR spectroscopy (1.3:1 d.r.). This compound was then dissolved in MeCN (0.8 mL, 0.25 M), and K_3PO_4 (106.1 mg, 0.50 mmol, 2.5 equiv) was added to the vial. The reaction mixture was stirred for 24 hours at rt. The solvent was then evaporated using a Genevac centrifugal evaporator. Analysis by NMR spectroscopy revealed the diastereomeric ratio was unchanged (1.3:1 d.r.).

^{1}H NMR spectrum in $CDCl_3$ for 3a - I: peak at 5.20 ppm is minor diastereomer and 4.95 ppm is major diastereomer

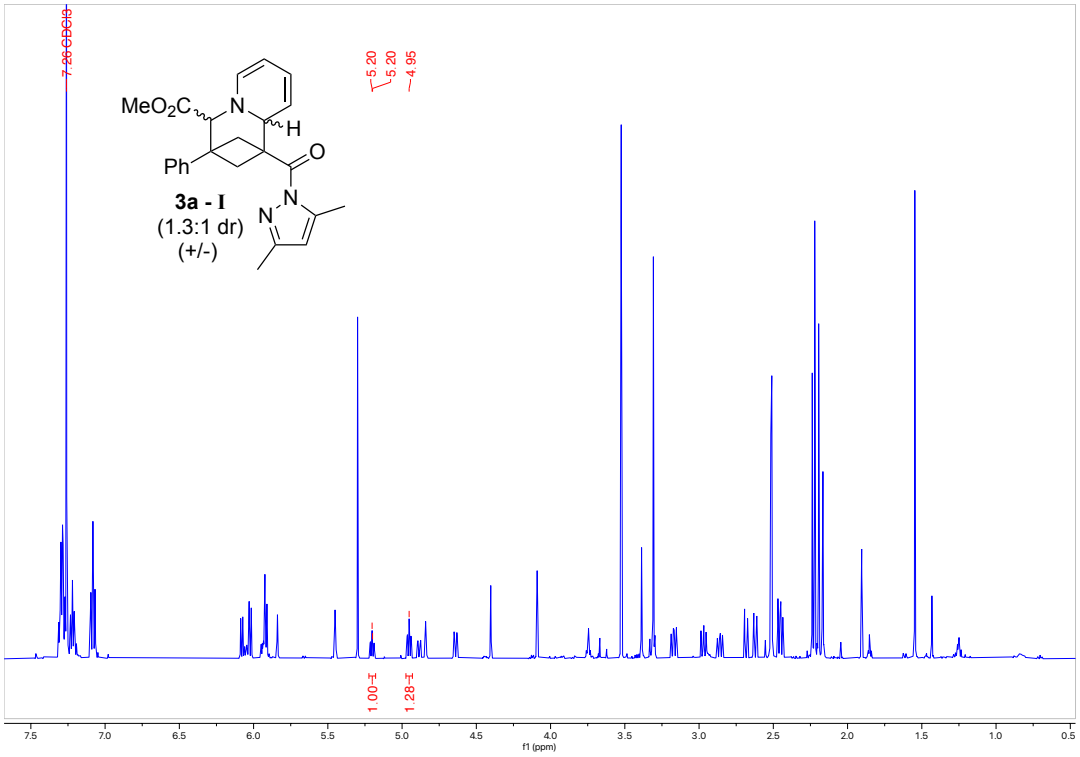

^{1}H NMR spectrum in $CDCl_3$ for 3a - II: peak at 5.19 ppm is minor diastereomer and 4.94 ppm is major diastereomer

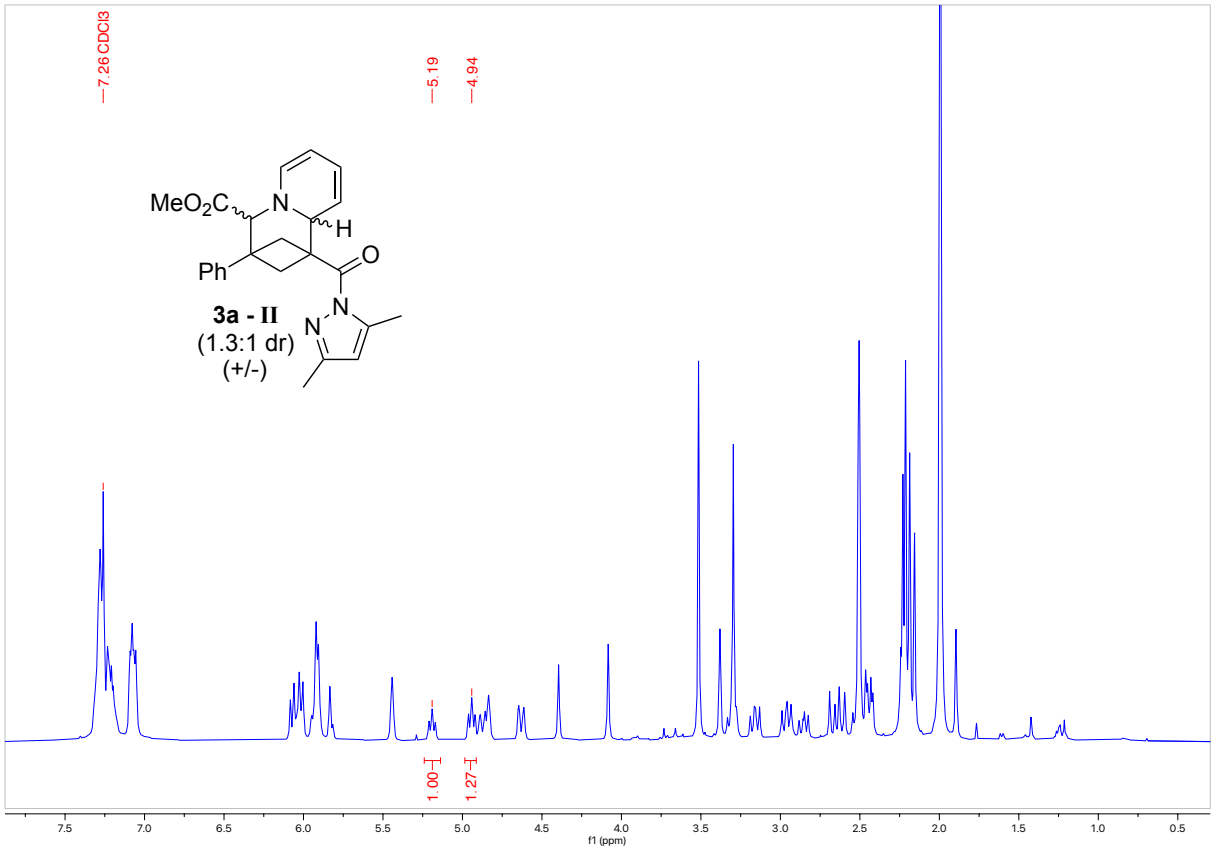

C.5 Substrate Synthesis

C.5.1 Bicyclobutane Synthesis

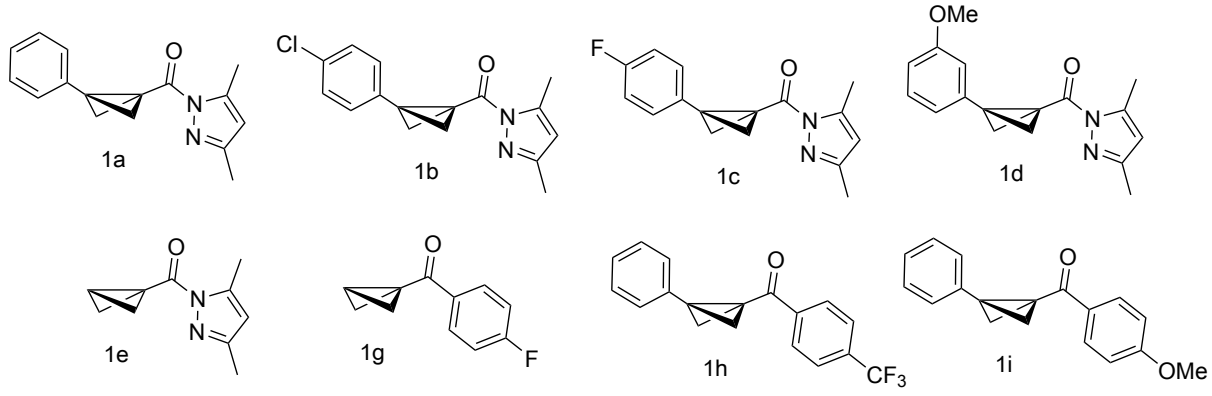

Bicyclobutane substrates **1a-1d**,[126] **1g-h**,[132] have been reported and were prepared according to the literature procedures.

Unsuccessful bicyclobutanes in the cycloaddition reaction are listed below:

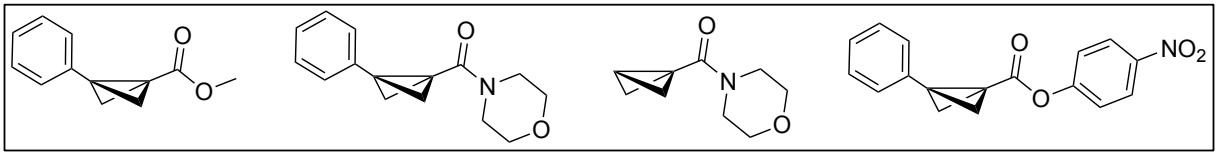

Synthesis of novel bicyclo[1.1.0]butan-1-yl(3,5-dimethyl-1H-pyrazol-1-yl)methanone (1e):

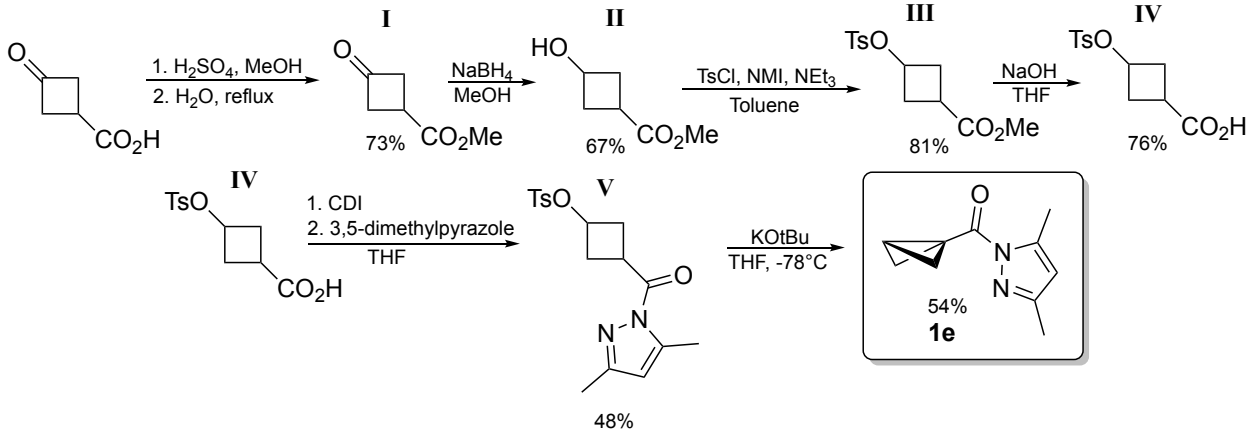

Methyl 3-oxocyclobutane-1-carboxylate (I) synthesis: 3-Oxocyclobutanecarboxylic acid (10.0 g, 87.6 mmol) was dissolved in methanol (100 mL, 0.88 M) and then concentrated sulfuric acid was added dropwise (0.47 mL, 10 mol%). The reaction mixture was left to stir at rt for 4 hours, followed by the addition of water (100 mL). The mixture was then stirred at 90 °C overnight. The acidic mixture was quenched with saturated sodium bicarbonate until the pH was basic (pH > 9), and then the aqueous solution was extracted with DCM (5 x 50 mL). The organic layers were combined, dried with Mg_2SO_4, filtered, and the solvent evaporated to give compound **I** without further purification (8.16 g, 73% yield).

Methyl 3-hydroxycyclobutane-1-carboxylate (II) synthesis: Compound **I** (8.16 g, 63.7 mmol) was dissolved in methanol (80 mL, 0.8 M). The mixture was cooled to 0 °C followed by the portionwise addition of solid $NaBH_4$ (1.20 g, 0.5 equiv, 31.8 mmol). The mixture was warmed to rt and left to stir overnight. The reaction was quenched with saturated ammonium chloride (80 mL) and then extracted with DCM (3 x 80 mL). The organic layers were combined, dried with Mg_2SO_4, filtered and then the solvent was evaporated to give compound **II** without further purification (5.53 g, 67% yield).

Methyl 3-(tosyloxy)cyclobutane-1-carboxylate (III) synthesis: Compound **II** (5.53 g, 42.5 mmol) was dissolved in toluene (80 mL, 0.53 M) followed by the addition of *N*-methylimidazole (3.4 mL, 1.0 equiv, 42.5 mmol). 4-Toluenesulfonyl chloride (12.2 g, 1.5 equiv, 63.7 mmol) was then added, followed by triethylamine (8.9 mL, 1.5 equiv, 63.7 mmol), and the mixture stirred at 60 °C overnight. The reaction was quenched with saturated ammonium chloride (80 mL) and then extracted with toluene (3 x 80 mL). The organic layers were combined, dried with Mg_2SO_4, filtered and then the solvent was evaporated to give compound **III** without further purification (9.8 g, 81% yield).

3-(Tosyloxy)cyclobutane-1-carboxylic acid (IV) synthesis: Compound **III** (9.8 g, 34.5 mmol) was dissolved in THF (40 mL, 0.86 M) and then 1 M NaOH (40 mL) was added to the mixture, which was stirred at rt overnight. The reaction mixture was acidified with 1 M HCl (pH < 3) and then extracted with DCM (3 x 40 mL). The organic layers were combined, dried with Mg_2SO_4, filtered and then the solvent was evaporated to give compound**IV** without further purification (7.11 g, 76% yield).

3-(3,5-dimethyl-1H-pyrazole-1-carbonyl)cyclobutyl 4-methylbenzenesulfonate (VI) synthesis: Compound **IV** (7.11 g, 26.3 mmol) was dissolved in THF (50 mL, 0.53 mmol) and then the solution was cooled to 0 °C before addition of carbonyldiimidazole (4.48 g, 1.05 equiv, 27.6 mmol). The mixture was stirred at rt for 1 hour, followed by the addition of 3,5-dimethylpyrazole (2.65 g, 1.05 equiv, 27.6 mmol). The mixture was then stirred at rt overnight. The reaction was quenched with saturated ammonium chloride (50 mL) and then extracted with ethyl acetate (3 x 50 mL). The organic layers were combined, dried with Mg_2SO_4, filtered and then the solvent was evaporated. The product was purified by column chromatography (Biotage® Sfär 100g Column, 0-100% EtOAc/hexanes, eluted at 20% EtOAc) to give compound **V** as a white solid (4.39 g, 48% yield).

Bicyclo[1.1.0]butan-1-yl(3,5-dimethyl-1H-pyrazol-1-yl)methanone (1e) synthesis:

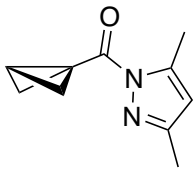

Compound VI (209.5 mg, 0.60 mmol) was dissolved in anhydrous THF containing 250 ppm BHT as inhibitor (12.0 mL, 0.05 M) in a 40 mL vial. The solution was cooled to −78 °C. Potassium tert-butoxide (74.1 mg, 1.1 equiv, 0.66 mmol) was added as a solid, and the reaction was stirred at −78 °C for 2 hours. While keeping the mixture as cold as possible, the reaction was quenched with cold (∼2-4 °C) ammonium chloride (10 mL), and the aqueous layer extracted with cold (∼2-4 °C) THF (containing 250 ppm BHT as inhibitor, 3 x 10 mL). The THF layers were combined and dried with Mg_2SO_4 (being cautious that the solution remained cold AT ALL TIMES), filtered, and then concentrated on a rotary evaporator using a water bath that remained at ∼10-15 °C. The crude product was purified using column chromatography, with the crude material loaded using cold hexanes (Biotage® Sfär 10g Column, 0-100% EtOAc/hexanes, eluted at 10% EtOAc). The product 1e was obtained as a clear colourless oil (57.0 mg, 54% yield). **NOTE:** The neat product is prone to rapid polymerization at ambient temperature. For short term storage, we stored neat 1e in a −20 °C freezer; for long term storage, we stored 1e as a 0.5 M stock solution in frozen acetonitrile in a −80 °C freezer.

HRMS(ESI): calc'd for $[C_{10}H_{12}N_3O + H^+]$, 177.10224; found: 177.10216.

^{1}H NMR (500 MHz, $CDCl_3$, 292 K, ppm): δ 5.94 (d, J = 1.1 Hz, 1H), 2.84 (dt, J = 3.4, 0.9 Hz, 2H), 2.52 (d, J = 1.0 Hz, 3H), 2.50 – 2.46 (m, 1H), 2.22 (s, 3H), 1.40 (dt, J = 3.1, 0.9 Hz, 2H).

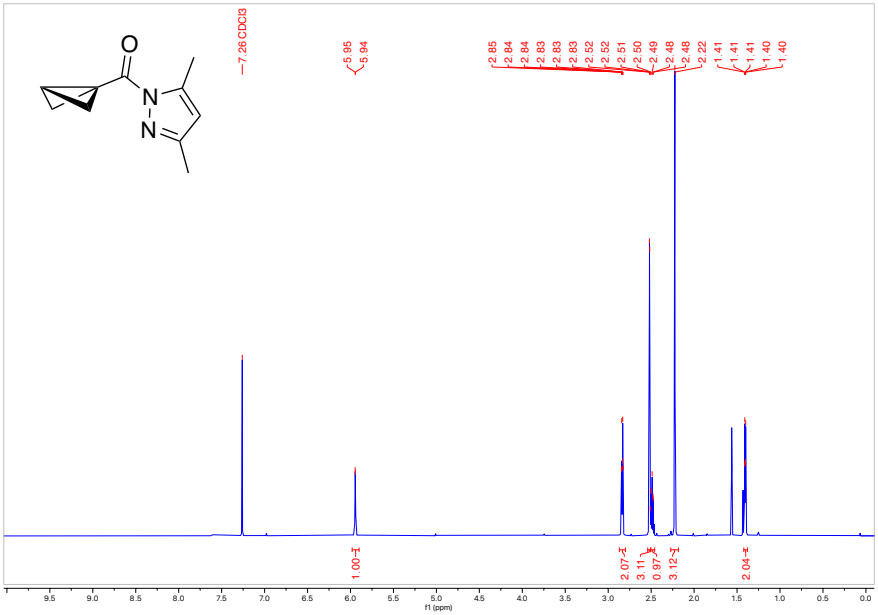

^{13}C NMR (126 MHz, $CDCl_3$, 292 K, ppm): δ 172.57, 151.58, 144.14, 110.45, 38.60, 29.55, 21.30, 14.57, 13.96, 12.32.

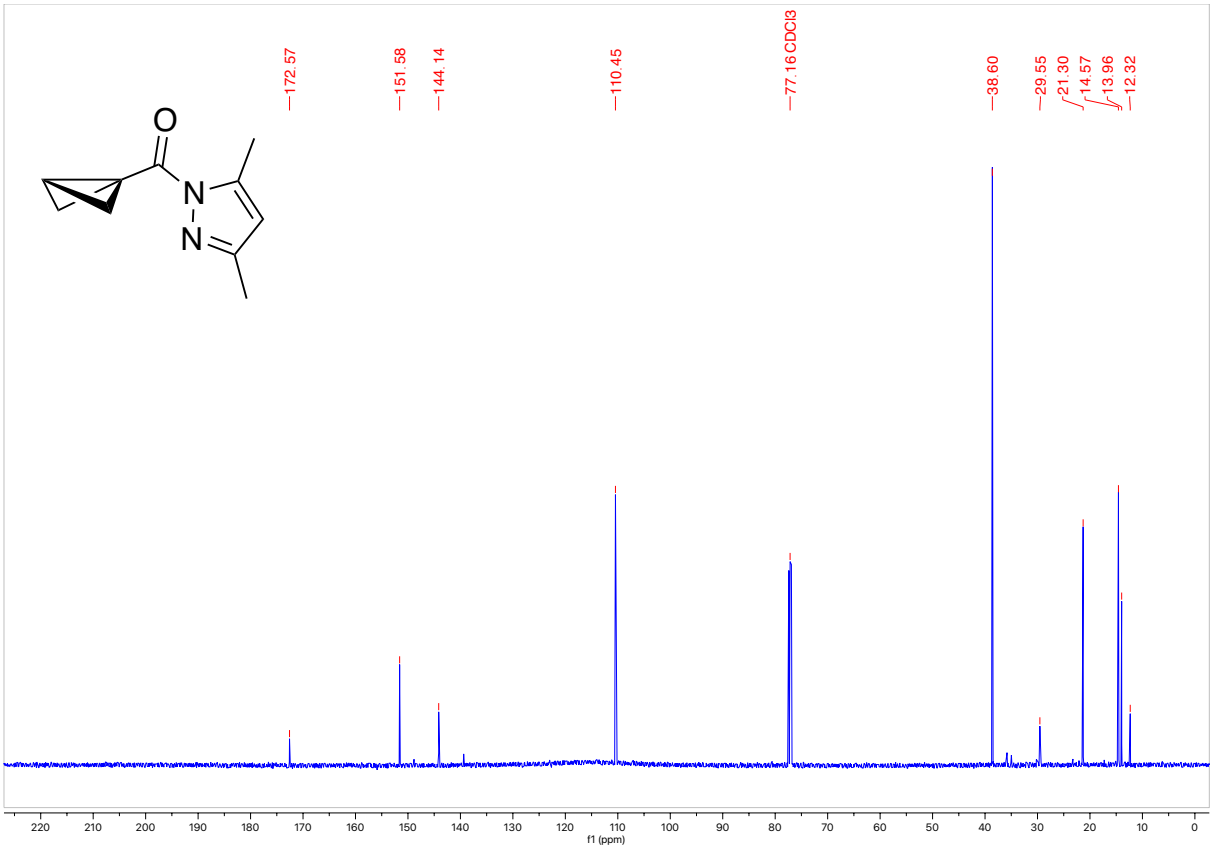

C.5.2 Pyridinium Synthesis

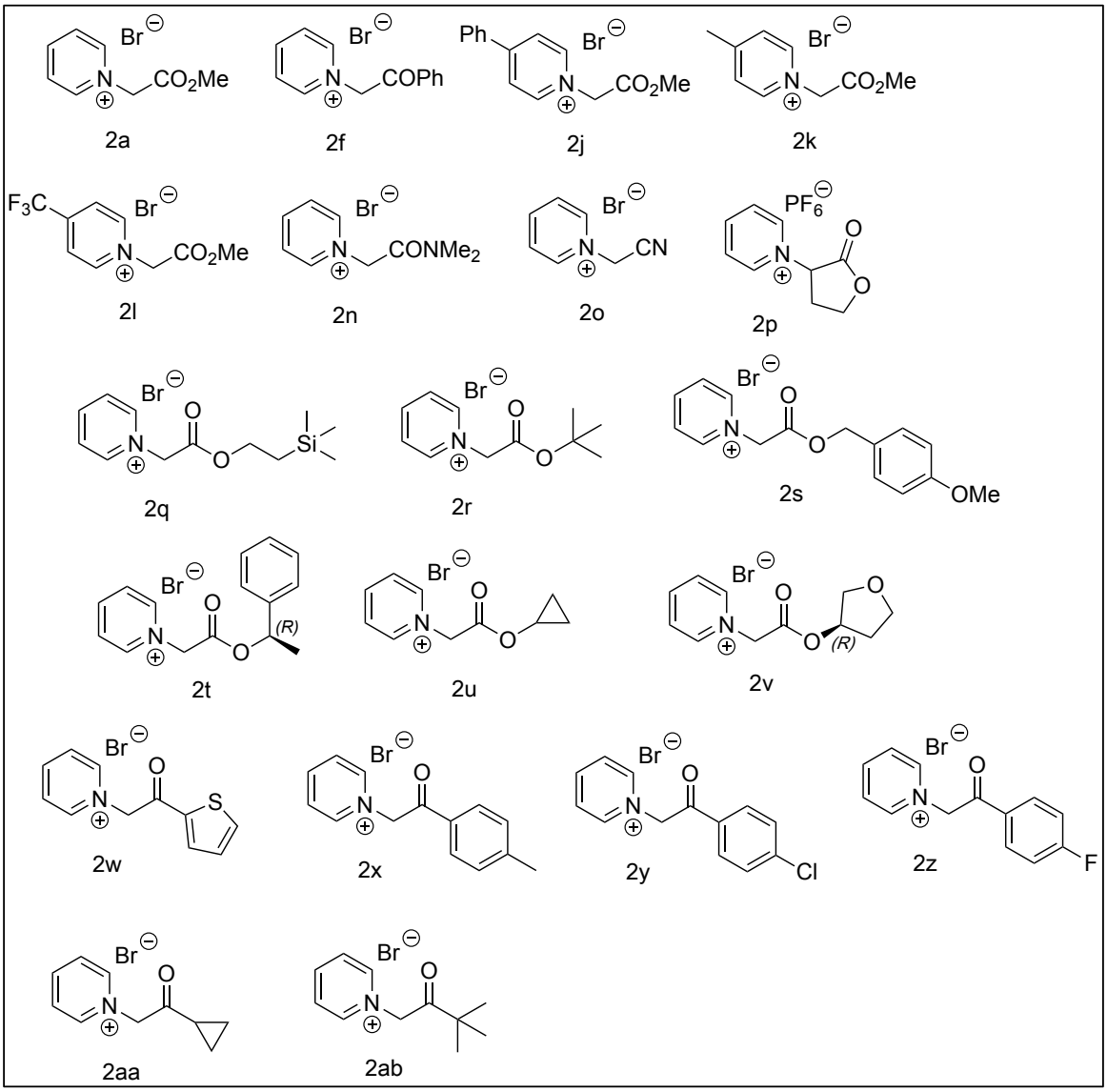

Pyridinium substrates **2a-p, 2r**, and **2w-ab** have been reported and were prepared according to the literature procedures.3-17 Pyridiniums **2q**, and **2s-2v** are not reported previously and were prepared according to the general procedure outlined below.

Unsuccessful pyridiniums in the cycloaddition reaction:

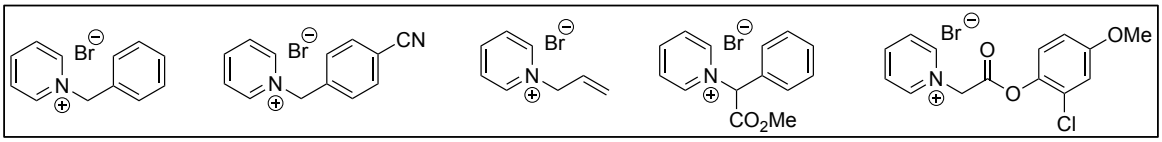

General procedure for pyridinium synthesis: To a 40 mL vial containing a stir bar was added the appropriate bromoester (2.00 mmol, 1 equiv) and ethyl acetate (10 mL, 0.20 M). The reaction mixture was stirred at room temperature for 2 minutes before adding pyridine (158 mg, 161 μL, 2.00 mmol, 1 equiv). The reaction mixture was stirred for 12 h at room temperature. Then, the solvent was evaporated to give the desired pyridinium salt. If required, the crude product was stirred in excess diethyl ether for 1 h, collected by filtration, and dried in vacuo to remove soluble impurities.

Characterization data for new pyridinium salts:

1-(2-Oxo-2-(2-(trimethylsilyl)ethoxy)ethyl)pyridin-1-ium bromide (2q)

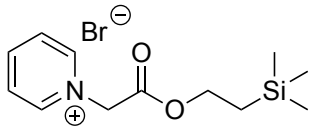

HRMS(ESI): calc'd for [$C_{12}H_{20}BrNO_2Si^+$ - Br^-], 238.12578; found: 238.12605.

^{1}H NMR (500 MHz, DMSO-d$_6$, 292 K, ppm): δ 9.05 – 9.00 (m, 2H), 8.71 – 8.65 (m, 1H), 8.21 (dd, J = 7.9, 6.6 Hz, 2H), 5.63 (s, 2H), 4.29 – 4.20 (m, 2H), 1.03 – 0.92 (m, 2H), 0.00 (s, 9H).

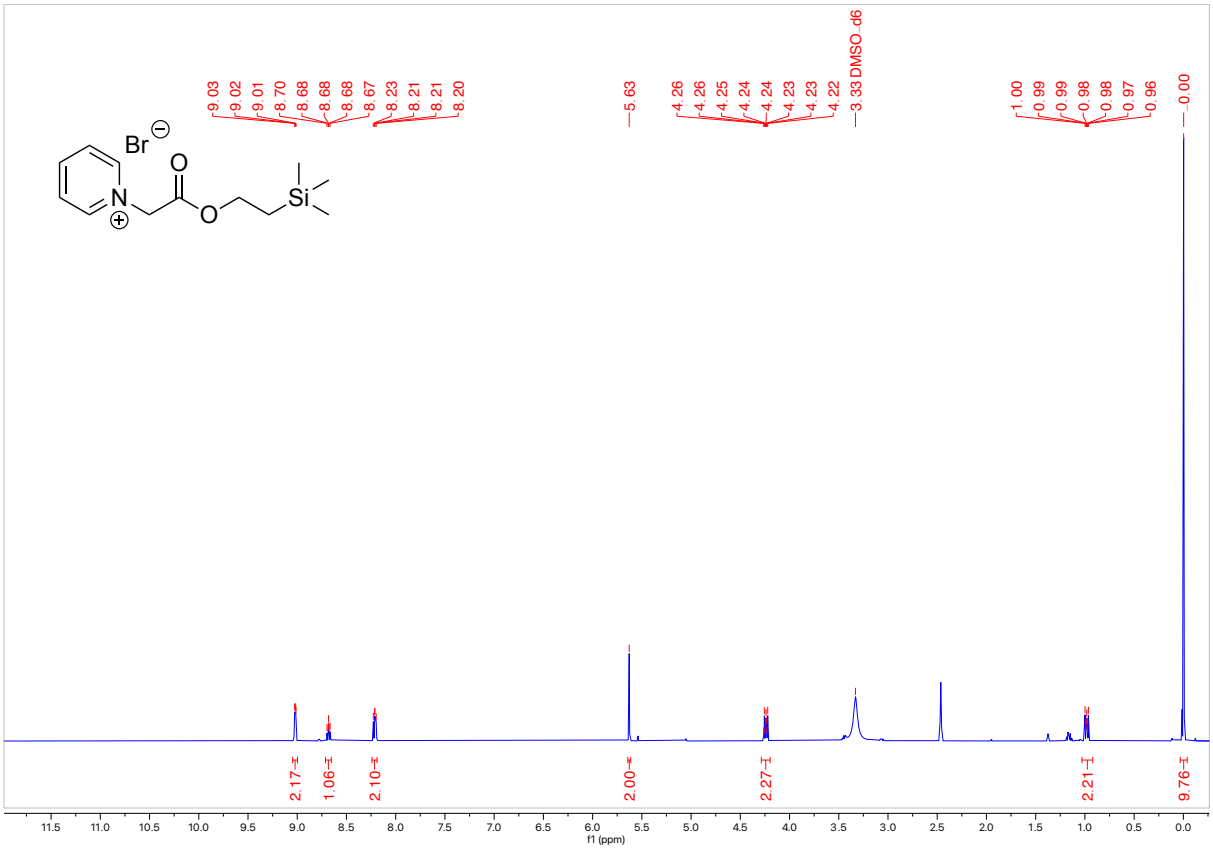

^{13}C NMR (126 MHz, DMSO-d$_6$, 292 K, ppm): δ 166.36, 146.79, 146.27, 127.86, 64.60, 60.36, 16.84.

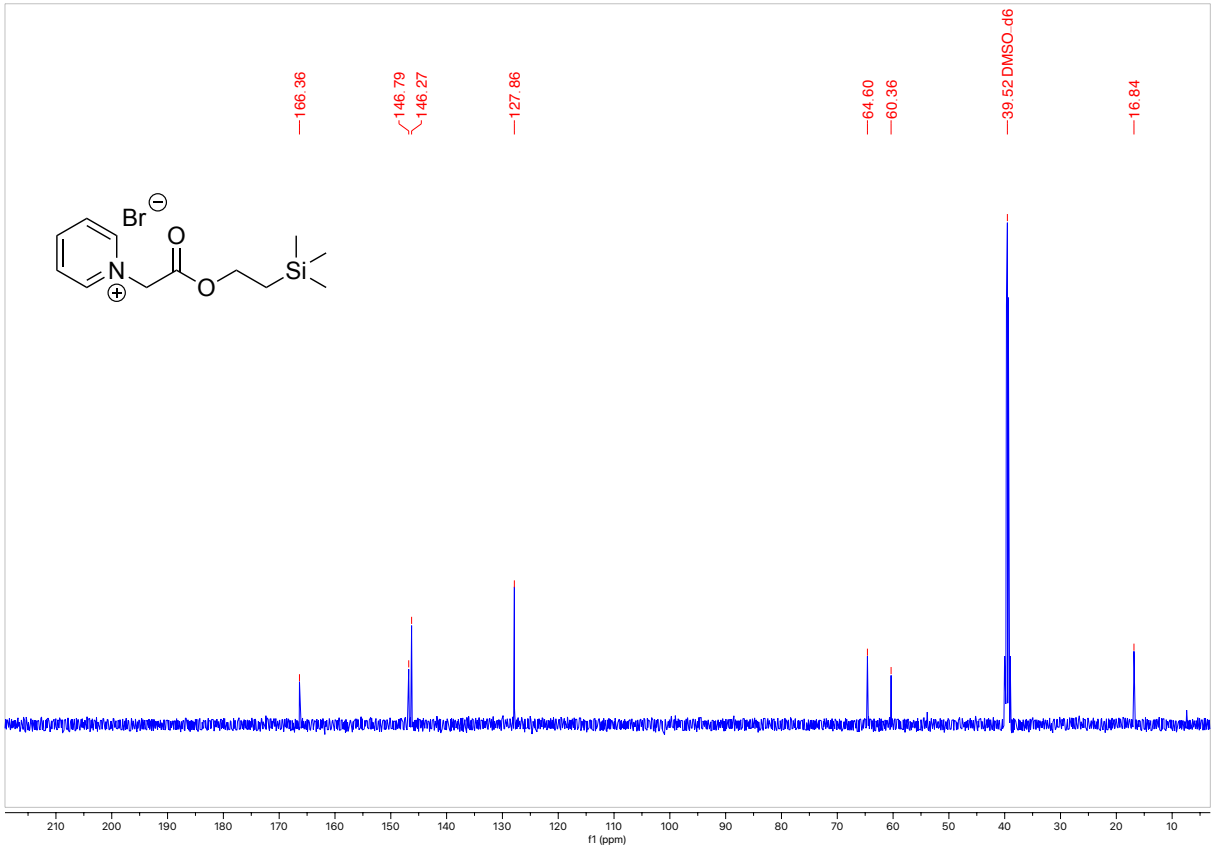

(*R*)-1-(2-Oxo-2-((tetrahydrofuran-3-yl)oxy)ethyl)pyridin-1-ium bromide (2v)

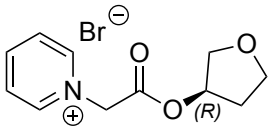

HRMS(ESI): calc'd for [$C_{11}H_{14}BrNO_3$ - Br^-], 208.09682; found: 208.09693.

^{1}H NMR (500 MHz, DMSO-d_6, 292 K, ppm): δ 9.09 – 9.03 (m, 2H), 8.75 – 8.69 (m, 1H), 8.25 (dd, J = 8.0, 6.7 Hz, 2H), 5.68 (s, 2H), 5.37 (ddt, J = 6.0, 3.6, 1.7 Hz, 1H), 3.86 – 3.69 (m, 4H), 2.23 – 2.13 (m, 1H), 2.03 – 1.98 (m, 1H).

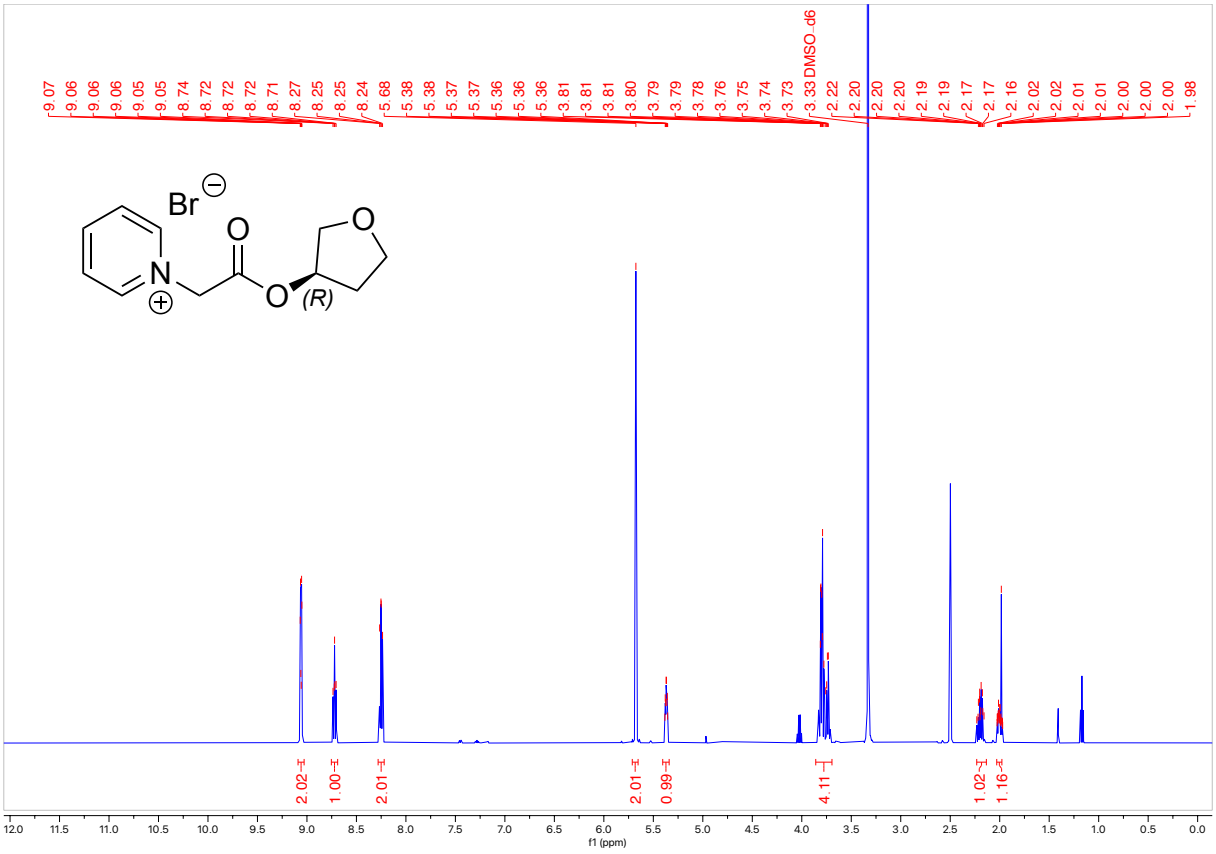

^{13}C NMR (126 MHz, DMSO-d$_6$, 292 K, ppm): δ 166.23, 146.84, 146.31, 127.83, 77.28, 71.93, 66.24, 60.36, 31.97.

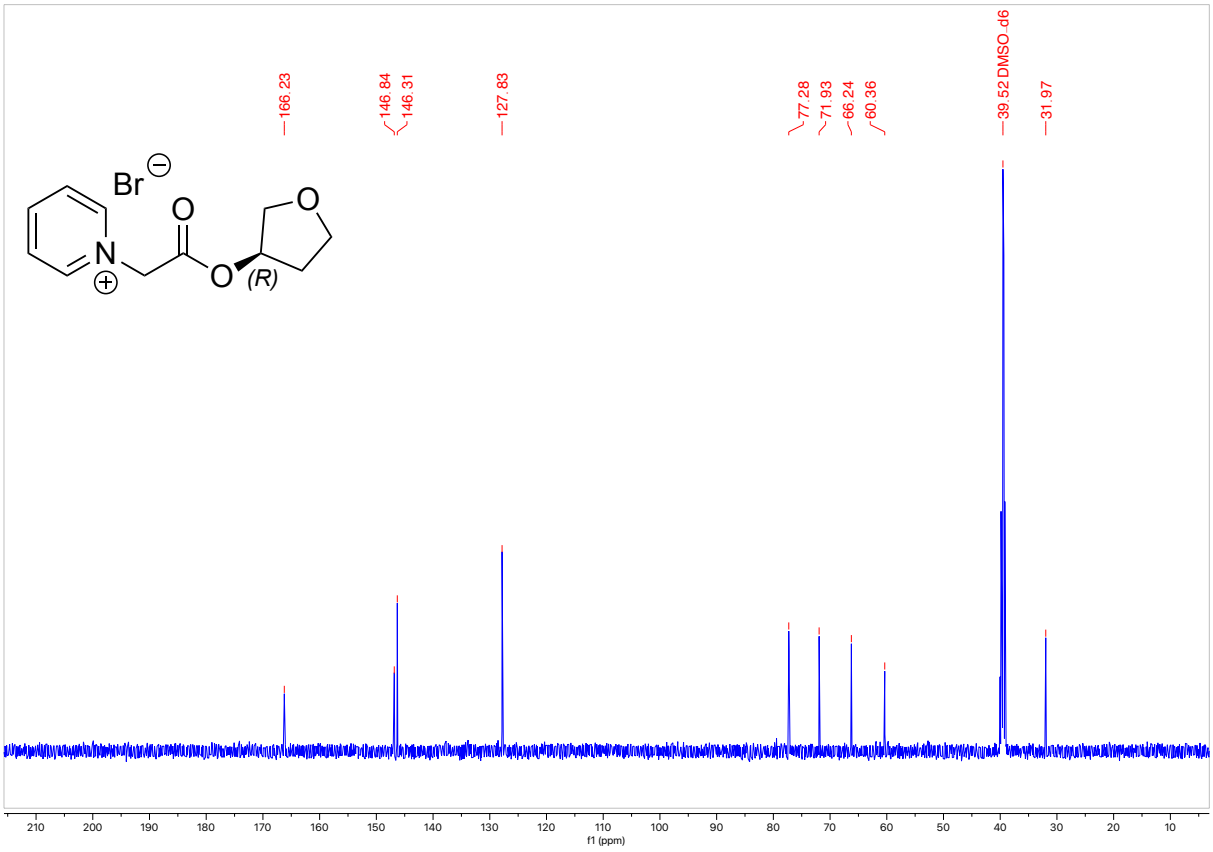

(*R*)-1-(2-Oxo-2-(1-phenylethoxy)ethyl)pyridin-1-ium bromide (2t)

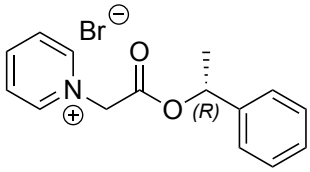

HRMS(ESI): calc'd for [$C_{15}H_{16}BrNO_2$ - Br^-], 242.11755; found: 242.11738.

^{1}H NMR (500 MHz, DMSO-d_6, 292 K, ppm): δ 9.14 – 9.04 (m, 2H), 8.74 – 8.65 (m, 1H), 8.22 (dd, J = 7.9, 6.6 Hz, 2H), 7.39 – 7.26 (m, 5H), 5.91 (q, J = 6.5 Hz, 1H), 5.78 (s, 2H), 1.52 (d, J = 6.6 Hz, 3H).

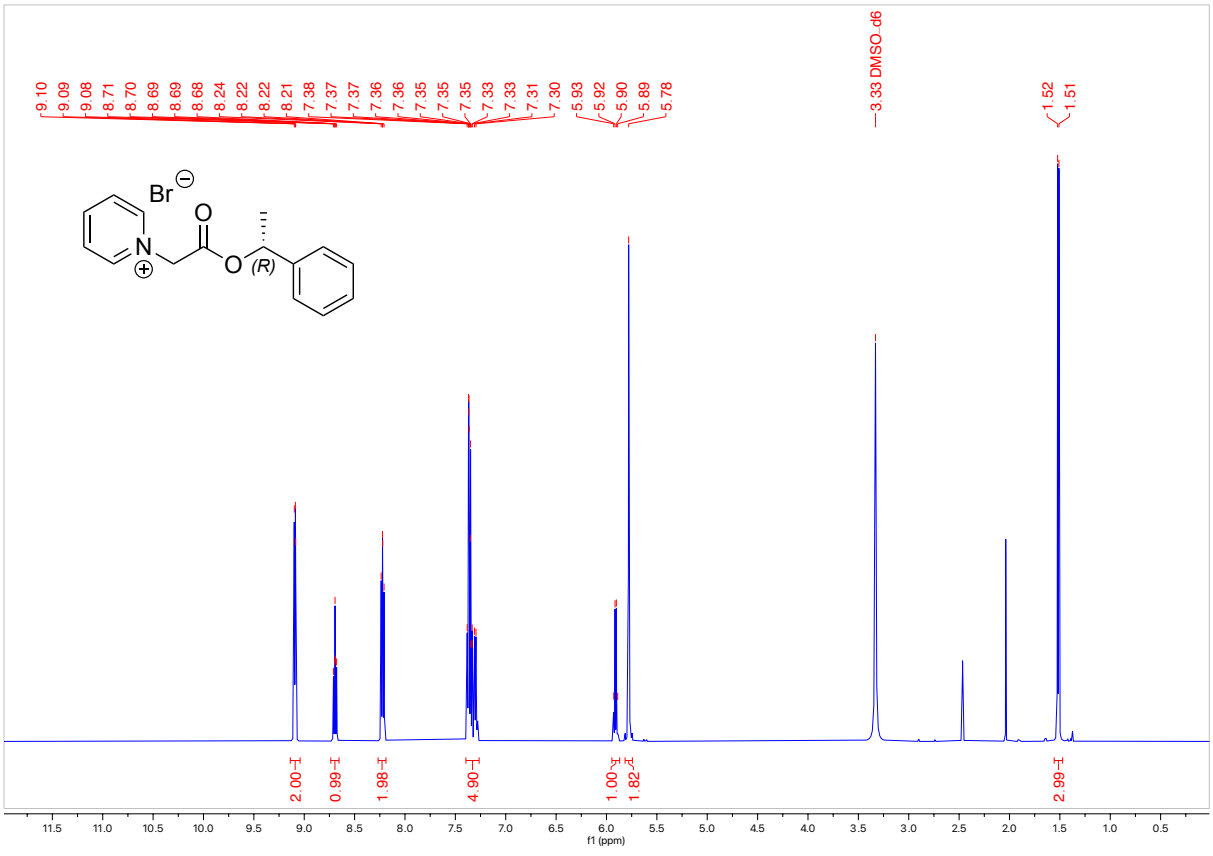

^{13}C NMR (126 MHz, DMSO-d$_6$, 292 K, ppm): δ 165.75, 146.82, 146.28, 146.25, 140.43, 128.50, 128.48, 128.12, 128.11, 127.86, 127.84, 126.03, 74.51, 60.31, 21.96.

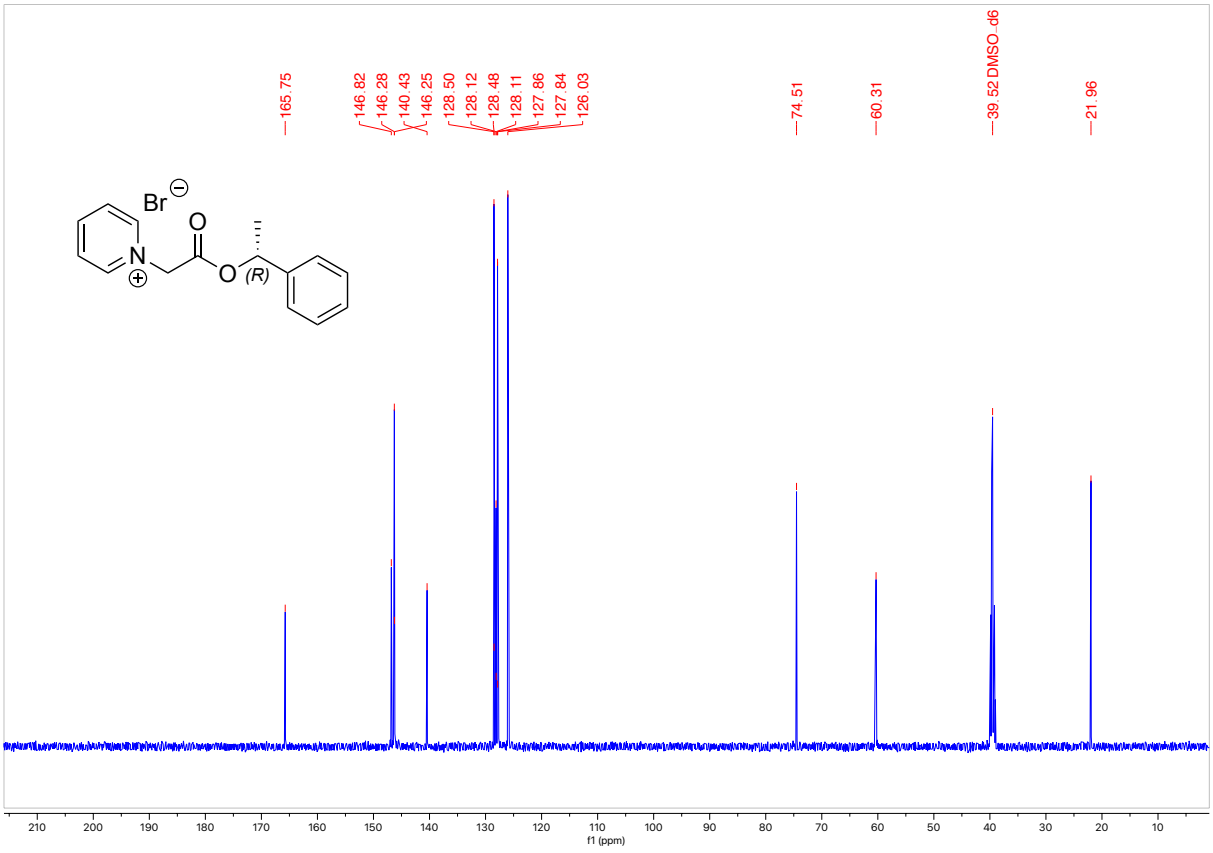

1-(2-((4-Methoxybenzyl)oxy)-2-oxoethyl)pyridin-1-ium bromide (2s)

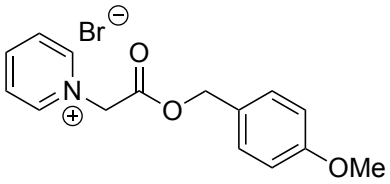

HRMS(ESI): calc'd for [$C_{15}H_{16}BrNO_3$ - Br^-], 258.11247; found: 258.11294.

^{1}H NMR (500 MHz, DMSO-d_6, 292 K, ppm): δ 9.11 – 9.04 (m, 2H), 8.76 – 8.66 (m, 1H), 8.24 (dd, J = 7.8, 6.5 Hz, 2H), 7.34 (d, J = 8.7 Hz, 2H), 6.94 (d, J = 8.7 Hz, 2H), 5.74 (s, 2H), 5.17 (s, 2H), 3.74 (s, 3H).

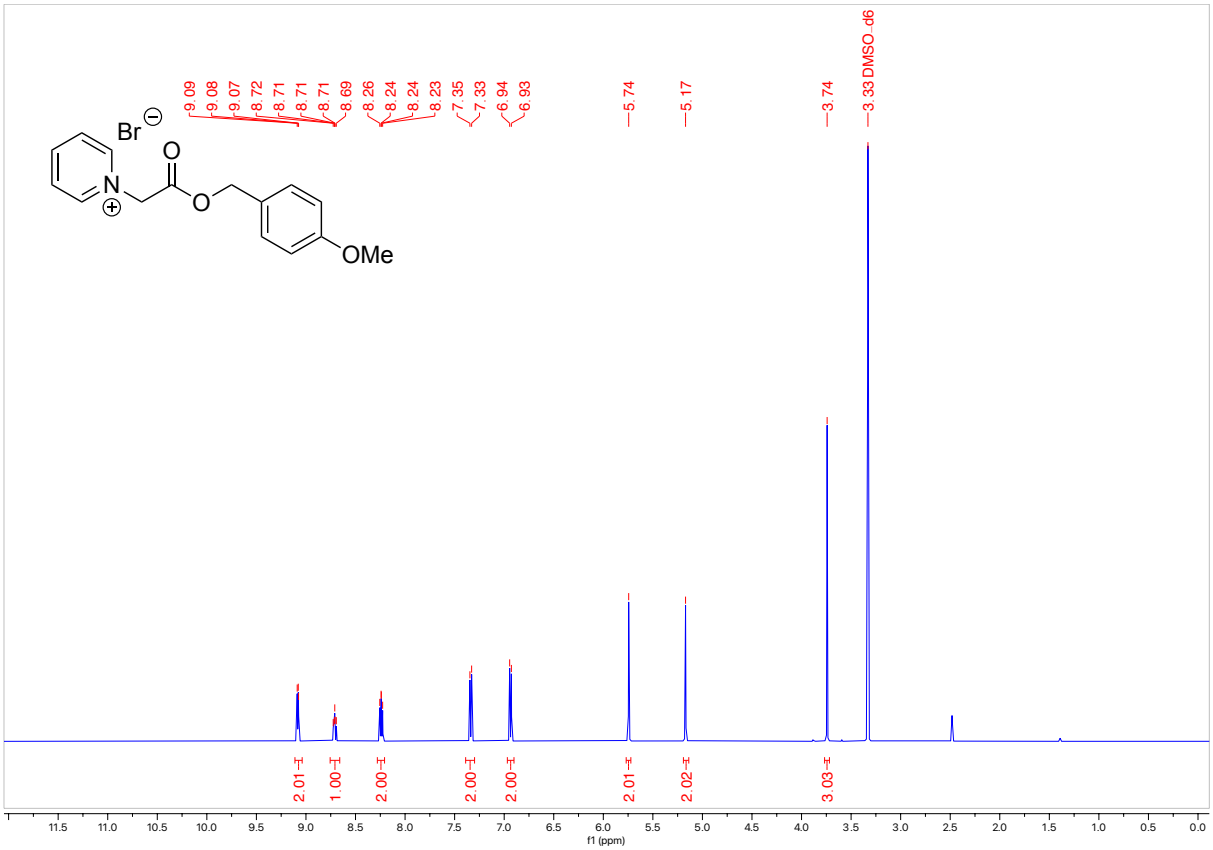

^{13}C NMR (126 MHz, DMSO-d$_6$, 292 K, ppm): δ 166.38, 159.49, 146.84, 146.27, 130.36, 127.88, 126.80, 126.79, 113.90, 67.50, 60.29, 55.19.

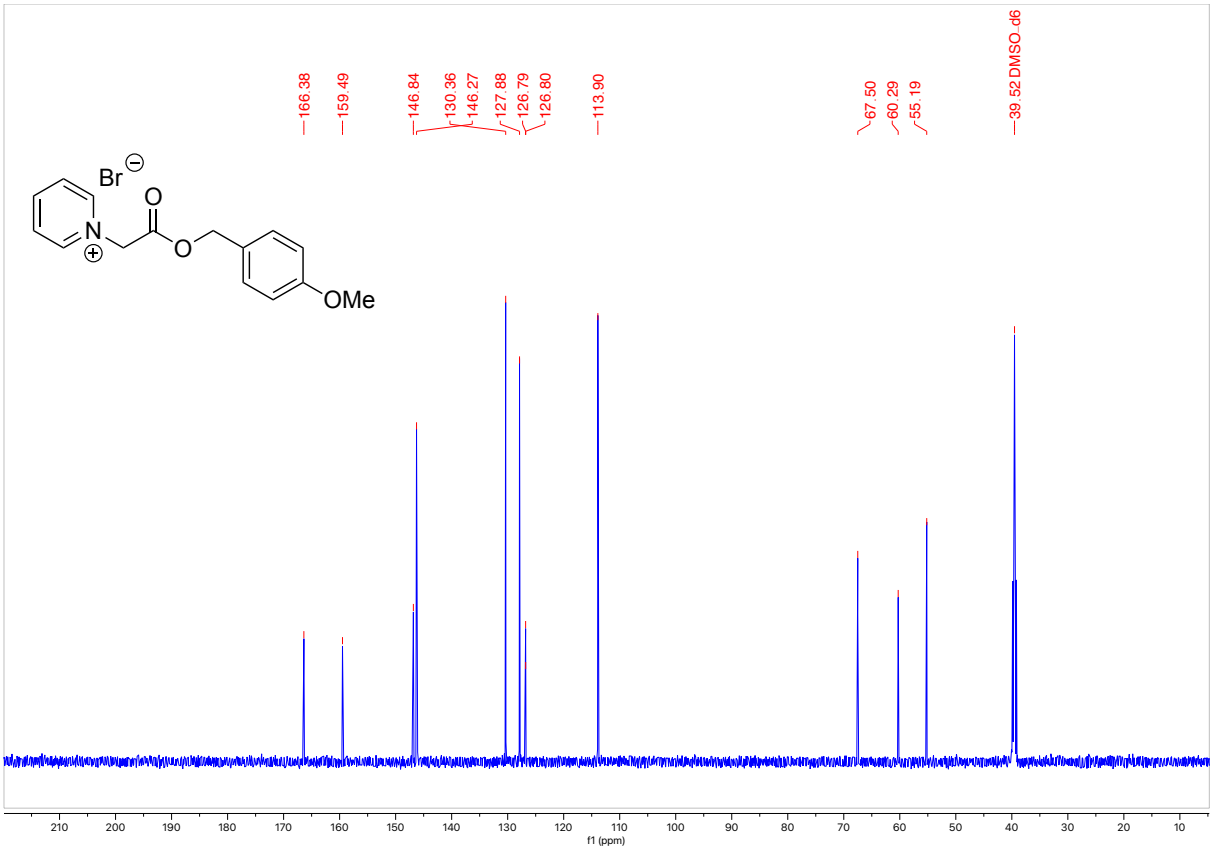

C.6 Azabicyclo[3.1.1]heptane Synthesis

Two general procedures are given below (A and B). Specific amounts of reactants, reagents, and solvents are given for each example.

General Procedure A:

To a 4 mL vial was added the appropriate pyridinium salt **2**, K_3PO_4, and a stir bar. Half of the total acetonitrile solvent was added to this vial, and the mixture stirred for 2 minutes at room temperature. The appropriate bicyclobutane **1** was weighed into another 4 mL vial, and quantitatively transferred to the vial containing pyridinium/base using the other half of the acetonitrile reaction solvent. The reaction mixture was stirred for 24 hours at room temperature. The solvent was then evaporated, the residue dissolved in dichloromethane, and the resulting solution passed through a plug of basic alumina, using excess dichloromethane to elute. Evaporation of the eluent provided the products **3**.

General Procedure B (ketone-based pyridinium salts):

To a 4 mL vial was added the appropriate pyridinium **2**, $NaPF_6$, and a stir bar. Half of the total acetonitrile solvent was added to the vial, and the mixture stirred for 2 hours at room temperature. The K_3PO_4 base was then added to the reaction vial, and the mixture stirred for 2 minutes at room temperature. The appropriate bicyclobutane **1** was weighed into another 4 mL vial, and quantitatively transferred to the vial containing pyridinium/base using the other half of the acetonitrile reaction solvent. The reaction mixture was stirred for 24 hours at room temperature. The solvent was then evaporated, the residue dissolved in dichloromethane, and the resulting solution passed through a plug of basic alumina, using excess dichloromethane to elute. Evaporation of the eluent provided the products **3**.

Methyl 1-(3,5-dimethyl-1H-pyrazole-1-carbonyl)-3-phenyl-1,3,4,9a-tetrahydro-2H-1,3-methanoquinolizine-4-carboxylate (3a)

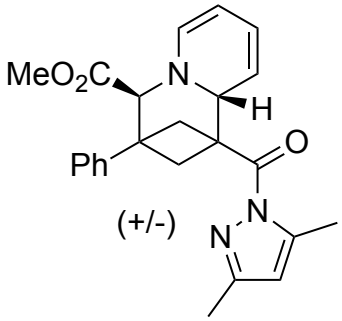

Product was synthesized following general procedure A on a 0.30 mmol scale. Reagent amounts used: bicyclobutane **1a** (75.7 mg, 0.30 mmol), pyridinium **2a** (1.25 equiv, 87.0 mg, 0.38 mmol), and K_3PO_4 (2.5 equiv, 159.2 mg, 0.75 mmol) in 1.2 mL acetonitrile (0.25 M). Isolated 106.4 mg of an orange solid (88% yield).

HRMS(ESI): calc'd for $[C_{31}H_{31}N_3O_4 + H^+]$, 404.19687; found: 404.19668.

^{1}H NMR (500 MHz, $CDCl_3$, 292 K, ppm): δ 7.30 (m, 2H), 7.24 – 7.19 (m, 1H), 7.11 – 7.04 (m, 2H), 6.02 (dt, J = 7.1, 0.9 Hz, 1H), 5.97 – 5.91 (m, 2H), 5.48 – 5.43 (m, 1H), 4.95 (ddd, J = 7.0, 5.4, 1.3 Hz, 1H), 4.64 (ddt, J = 9.4, 2.3, 1.1 Hz, 1H), 4.09 (s, 1H), 3.52 (s, 3H), 3.17 (dd, J = 10.2, 7.4 Hz, 1H), 2.97 (dd, J = 9.7, 7.4 Hz, 1H), 2.62 (dd, J = 10.2, 0.9 Hz, 1H), 2.51 (d, J = 1.1 Hz, 3H), 2.46 (d, J = 9.7 Hz, 1H), 2.22 (s, 3H).

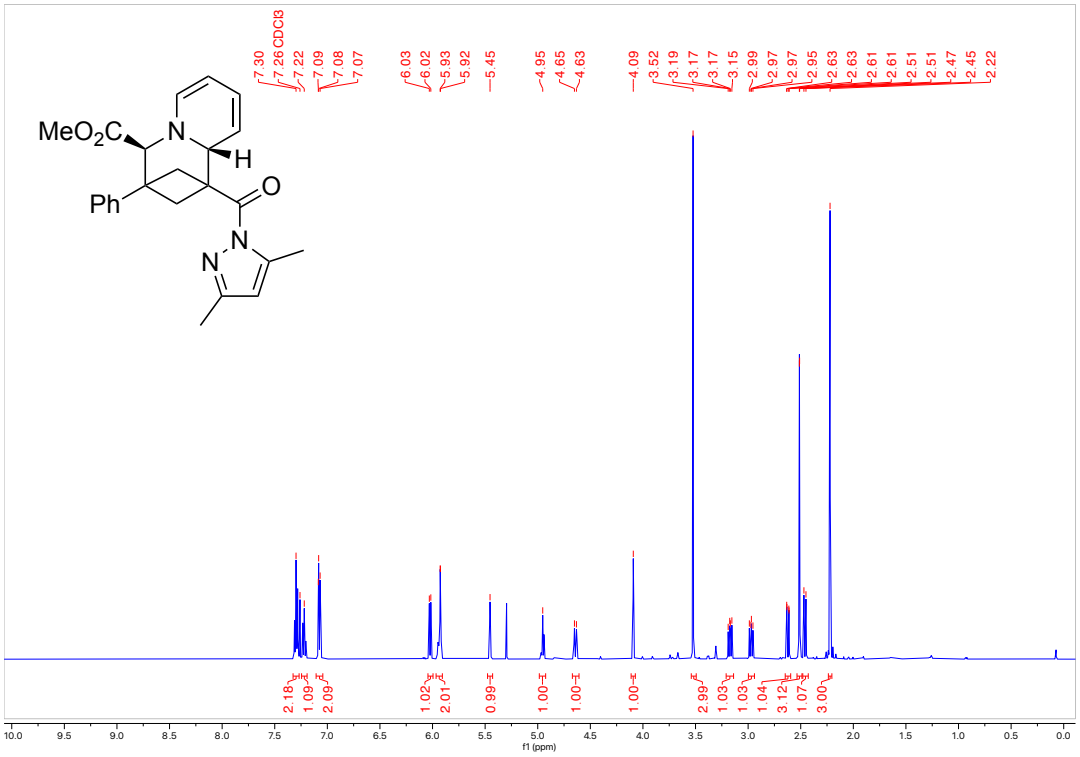

^{13}C NMR (126 MHz, $CDCl_3$, 292 K, ppm): δ 173.05, 172.28, 152.47, 144.10, 144.02, 135.78, 128.34, 128.31, 126.91, 126.35, 125.96, 125.93, 125.93, 111.27, 111.09, 98.30, 70.99, 59.32, 51.61, 49.66, 42.92, 40.24, 37.39, 14.45, 14.09.

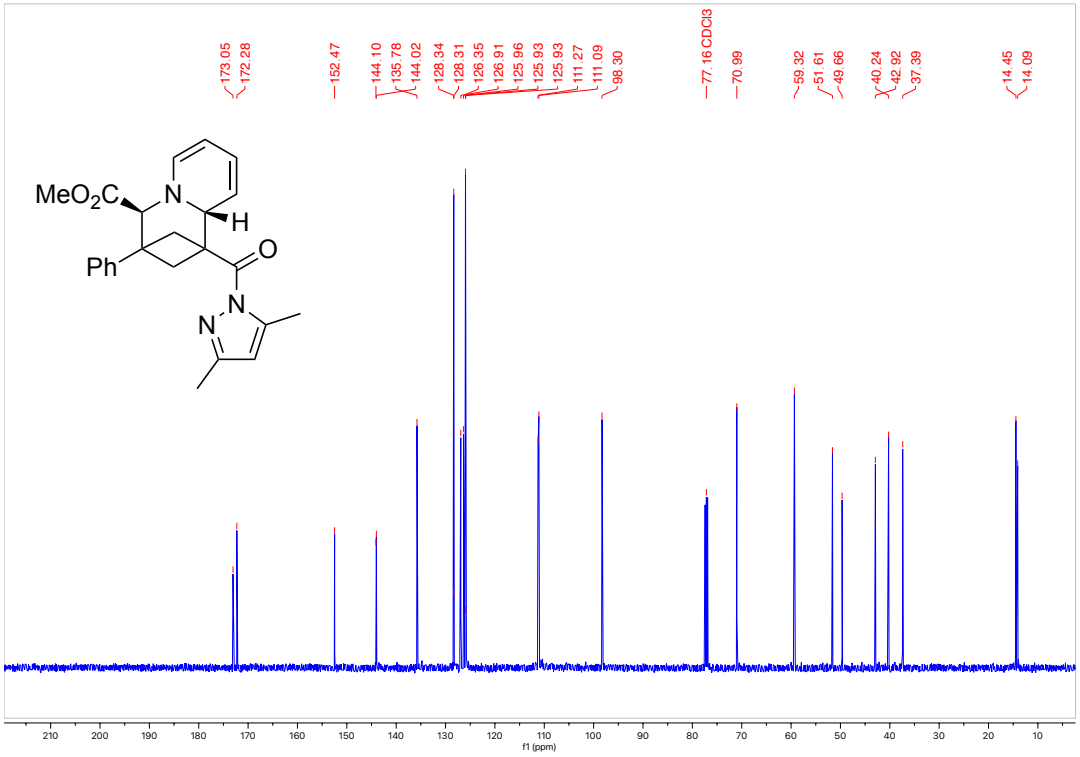

Methyl 3-(4-chlorophenyl)-1-(3,5-dimethyl-1H-pyrazole-1-carbonyl)-1,3,4,9a-tetrahydro-2H-1,3-methanoquinolizine-4-carboxylate (3b)

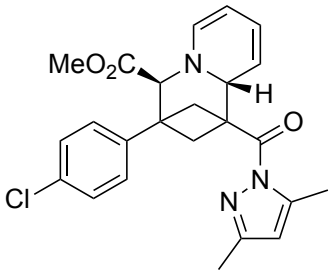

Product was synthesized following general procedure A on a 0.20 mmol scale. Reagent amounts used: bicyclobutane **1b** (57.4 mg, 0.20 mmol), pyridinium **2a** (1.25 equiv, 57.8 mg, 0.25 mmol), and K_3PO_4 (2.5 equiv, 106.1 mg, 0.50 mmol) in 0.8 mL acetonitrile (0.25 M). Isolated 77.9 mg of a yellow oil (71% yield).

HRMS(ESI): calc'd for [$C_{24}H_{24}ClN_3O_3$ + H^+], 438.15790; found: 438.15843.

^{1}H NMR (500 MHz, $CDCl_3$, 292 K, ppm): δ 7.32 – 7.28 (m, 2H), 7.07 – 7.02 (m, 2H), 6.04 (d, J = 7.1 Hz, 1H), 5.99 – 5.92 (m, 2H), 5.47 (s, 1H), 4.97 (ddd, J = 7.0, 5.4, 1.3 Hz, 1H), 4.66 (ddt, J = 9.4, 2.2, 1.1 Hz, 1H), 4.08 (s, 1H), 3.58 (s, 3H), 3.16 (dd, J = 10.2, 7.4 Hz, 1H), 2.99 (dd, J = 9.7, 7.4 Hz, 1H), 2.62 (dd, J = 10.2, 1.0 Hz, 1H), 2.54 (d, J = 1.1 Hz, 3H), 2.44 (d, J = 9.7 Hz, 1H), 2.24 (s, 3H).

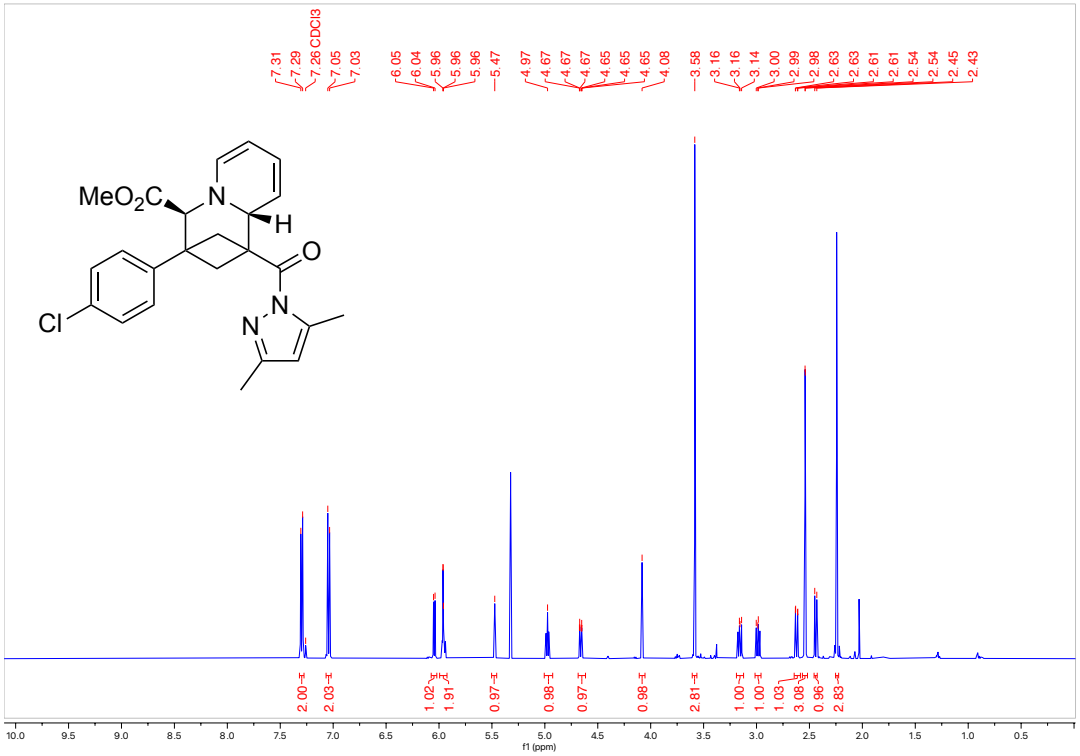

^{13}C NMR (126 MHz, $CDCl_3$, 292 K, ppm): δ 172.79, 172.01, 152.53, 144.09, 142.58, 135.67, 132.74, 128.50, 127.44, 127.42, 126.34, 111.27, 111.13, 98.31, 70.73, 59.28, 51.69, 49.61, 42.46, 40.28, 37.34, 14.40, 14.04.

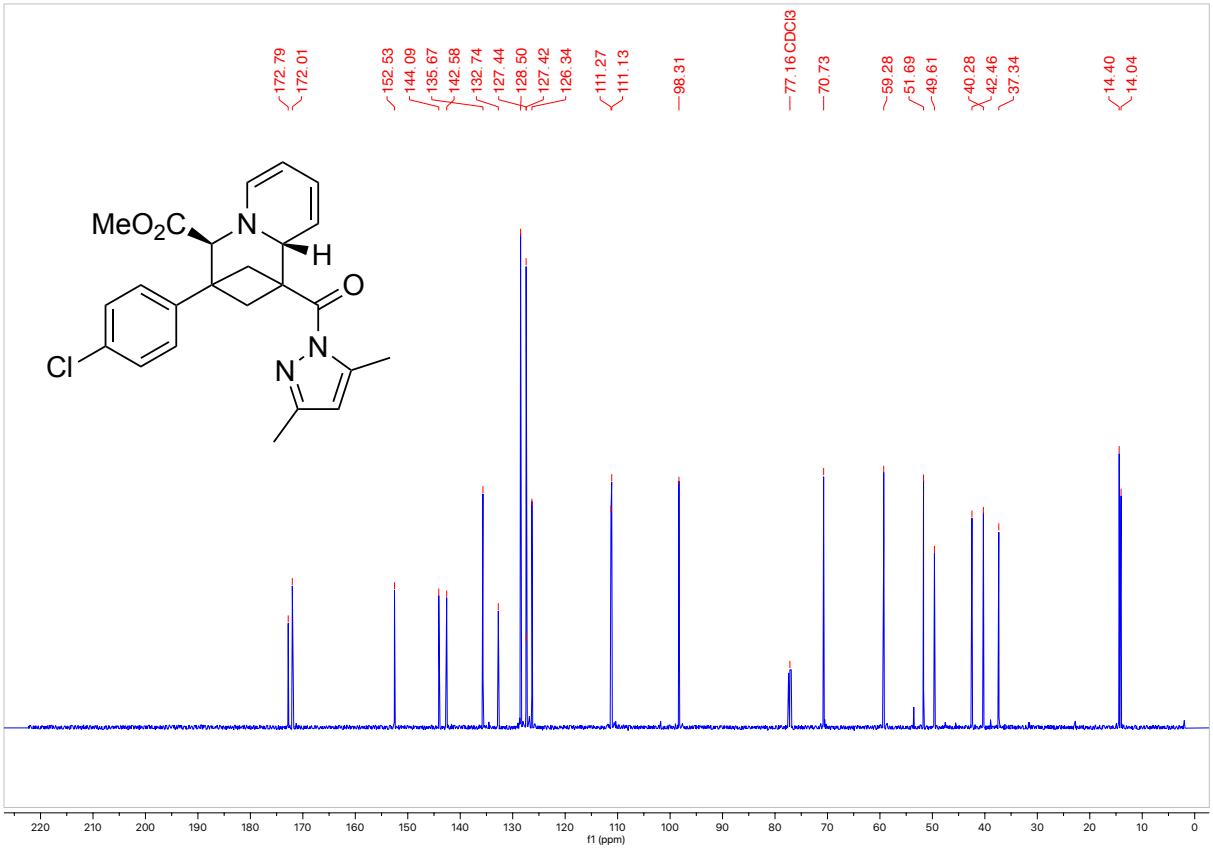

Methyl (3,5-dimethyl-1H-pyrazole-1-carbonyl)-3-(4-fluorophenyl)-1,3,4,9a-tetrahydro-2H-1,3-methanoquinolizine-4-carboxylate (3c)

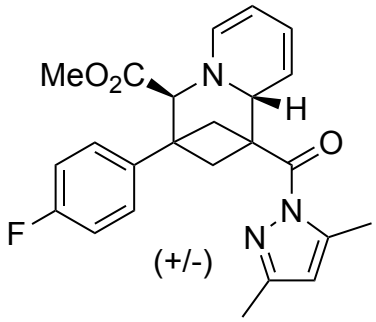

Product was synthesized following general procedure A on a 0.30 mmol scale. Reagent amounts used: bicyclobutane **1c** (81.1 mg, 0.30 mmol), pyridinium **2a** (1.25 equiv, 87.0 mg, 0.38 mmol), and K_3PO_4 (2.5 equiv, 159.2 mg, 0.75 mmol) in 1.2 mL acetonitrile (0.25 M). Isolated 89.0 mg of an orange solid (57% yield). Single crystals for X-ray diffraction were grown from a supersaturated solution of 3c in dichloromethane at −20 °C.

HRMS(ESI): calc'd for $[C_{24}H_{24}FN_3O_3 + H^+]$, 422.18745; found: 422.18770.

^{1}H NMR (500 MHz, $CDCl_3$, 292 K, ppm): δ 7.07 – 6.93 (m, 4H), 6.01 (d, J = 7.1 Hz, 1H), 5.92 (m, 2H), 5.46 – 5.40 (m, 1H), 4.94 (ddd, J = 6.9, 5.4, 1.3 Hz, 1H), 4.67 – 4.59 (m, 1H), 4.05 (s, 1H), 3.54 (s, 3H), 3.14 (dd, J = 10.2, 7.4 Hz, 1H), 2.94 (dd, J = 9.7, 7.4 Hz, 1H), 2.59 (d, J = 10.2, 1H), 2.50 (d, J = 1.0 Hz, 3H), 2.41 (d, J = 9.7 Hz, 1H), 2.21 (s, 3H).

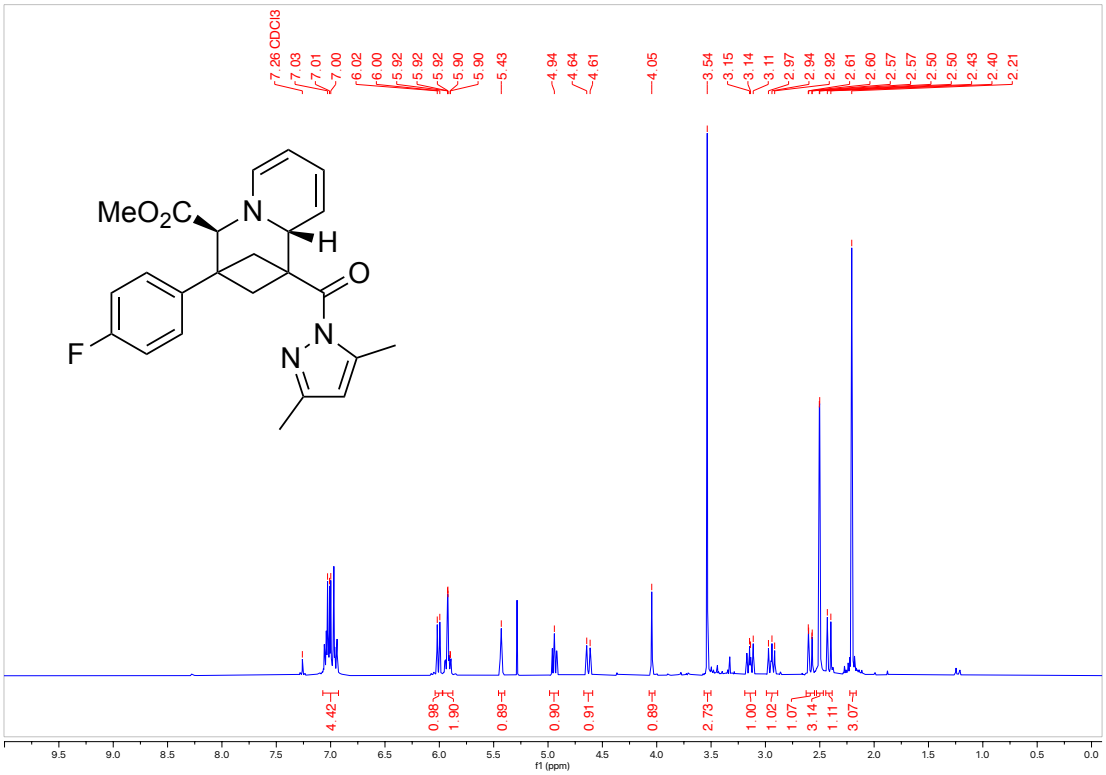

^{19}F NMR (500 MHz, $CDCl_3$, 292 K, ppm): δ 115.69.

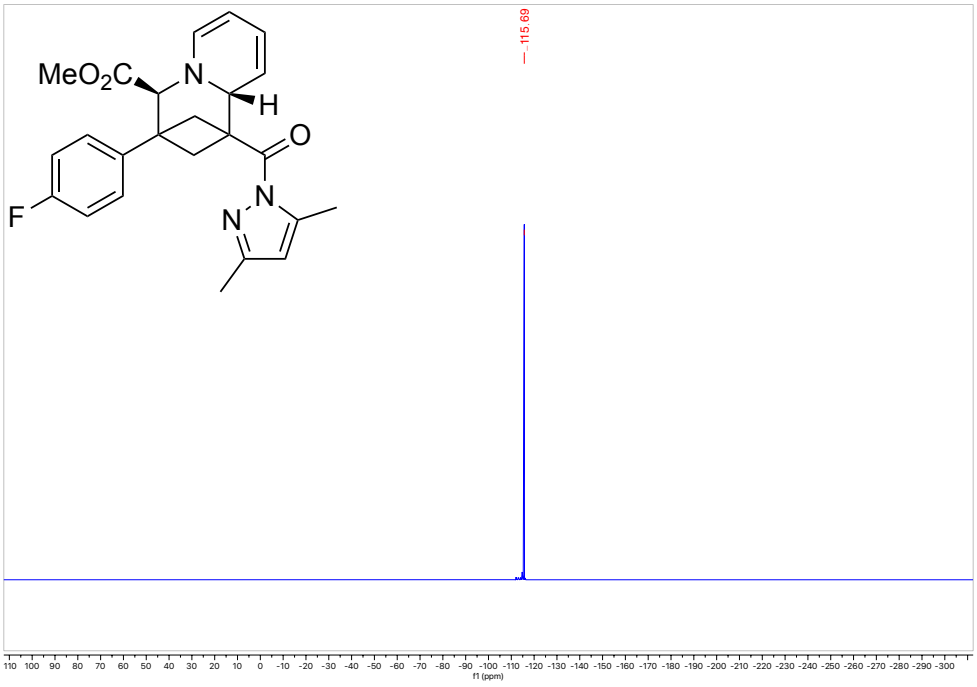

^{13}C NMR (126 MHz, $CDCl_3$, 292 K, ppm): δ 172.87, 172.11, 162.72, 160.77, 152.50, 144.09, 139.86, 139.83, 135.67, 127.63, 127.57, 126.34, 115.28, 115.11, 111.23, 111.11, 98.37, 70.93, 59.26, 51.64, 49.55, 42.36, 40.30, 37.42, 14.39, 14.03.

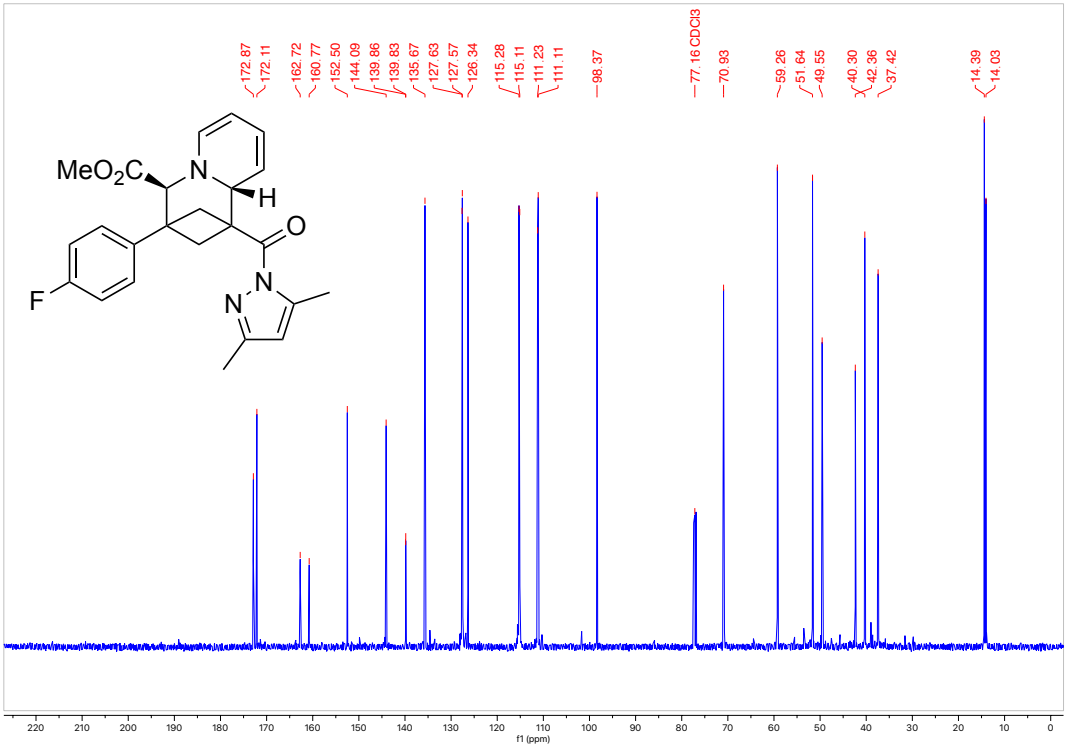

Methyl 1-(3,5-dimethyl-1H-pyrazole-1-carbonyl)-3-(3-methoxyphenyl)-1,3,4,9a-tetrahydro-2H-1,3-methanoquinolizine-4-carboxylate (3d)

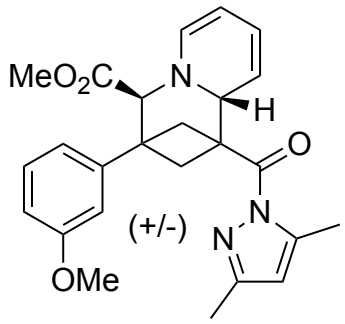

Product was synthesized following general procedure on a 0.30 mmol scale. Reagent amounts used: bicyclobutane **1d** (81.1 mg, 0.30 mmol), pyridinium **2a** (1.25 equiv, 86.7 mg, 0.38 mmol), and K_3PO_4 (2.5 equiv, 159.2 mg, 0.75 mmol) in 1.2 mL acetonitrile (0.25 M). Isolated 51.9 mg of an orange solid (32% yield).

HRMS(ESI): calc'd for [$C_{25}H_{27}N_3O_4$ + H^+], 434.20744; found: 434.20746.

^{1}H NMR (500 MHz, $CDCl_3$, 292 K, ppm): δ 7.20 (t, J = 7.9 Hz, 1H), 6.76 (dd, J = 8.1, 2.4 Hz, 1H), 6.66 (d, J = 7.7 Hz, 1H), 6.61 (m, 1H), 6.02 (d, J = 7.1 Hz, 1H), 5.96 – 5.90 (m, 2H), 5.44 (s, 1H), 4.94 (ddd, J = 6.9, 5.4, 1.3 Hz, 1H), 4.65 – 4.60 (m, 1H), 4.08 (s, 1H), 3.77 (s, 3H), 3.54 (s, 3H), 3.16 (dd, J = 10.2, 7.4 Hz, 1H), 2.94 (dd, J = 9.7, 7.4 Hz, 1H), 2.60 (d, J = 10.2 Hz, 1H), 2.51 (d, J = 1.1 Hz, 3H), 2.45 (d, J = 9.7 Hz, 1H), 2.22 (s, 3H).

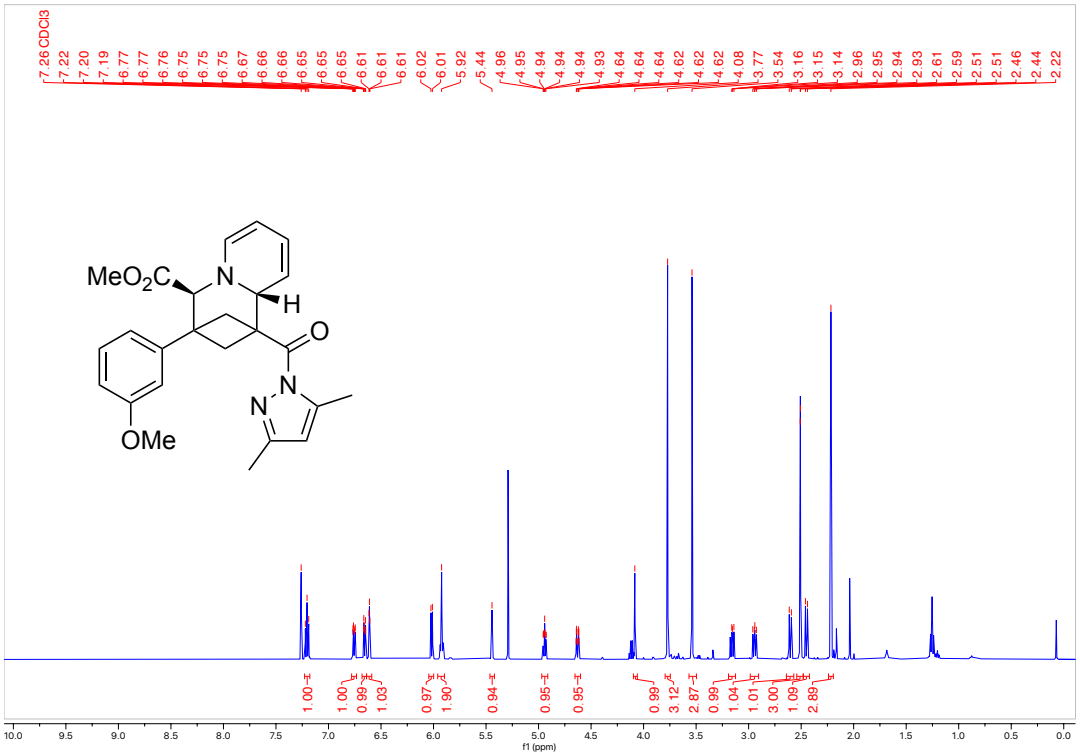

^{13}C NMR (126 MHz, $CDCl_3$, 292 K, ppm): δ 173.01, 172.25, 159.65, 152.47, 145.65, 144.09, 135.75, 129.36, 126.33, 118.34, 112.29, 111.76, 111.26, 111.08, 98.26, 70.88, 59.30, 55.30, 51.63, 49.57, 42.94, 40.27, 37.40, 14.42, 14.07.

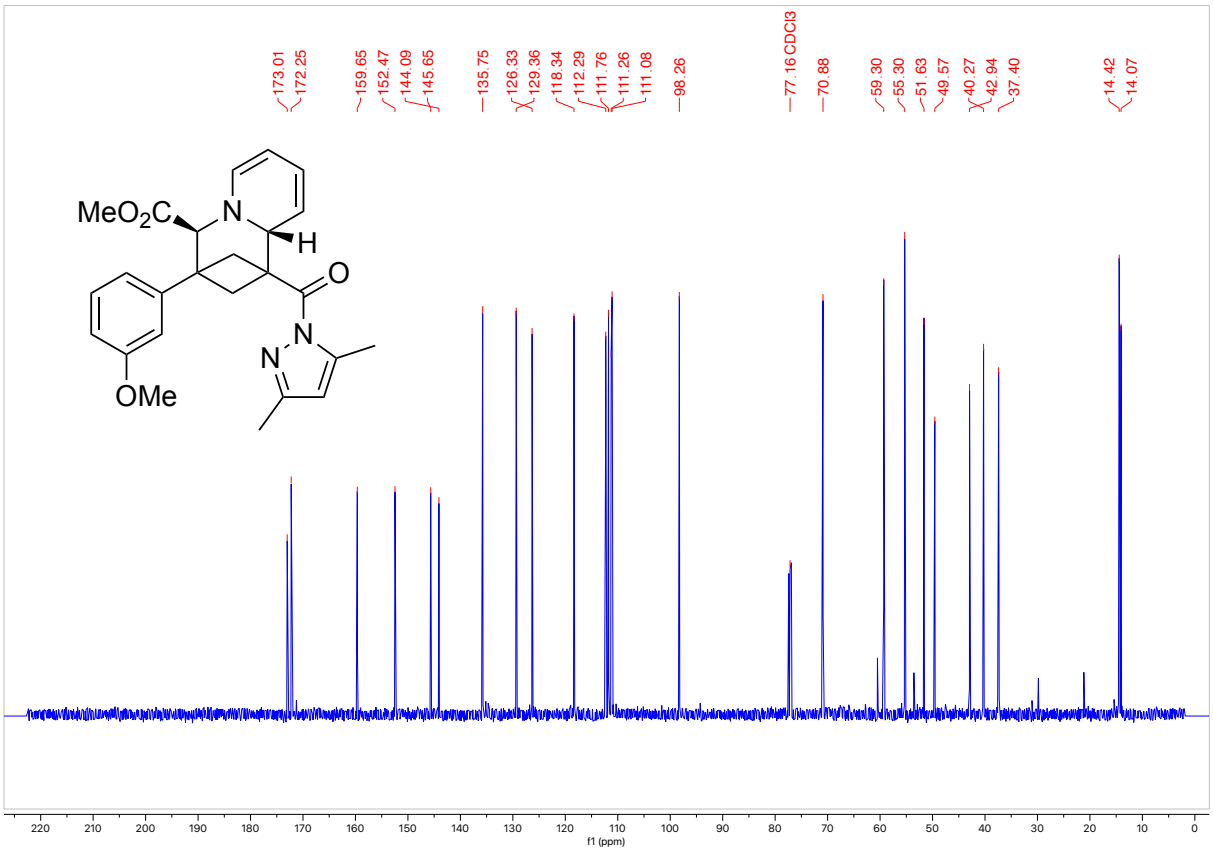

Methyl 1-(3,5-dimethyl-1H-pyrazole-1-carbonyl)-1,3,4,9a-tetrahydro-2H-1,3-methanoquinolizine-4-carboxylate (3e)

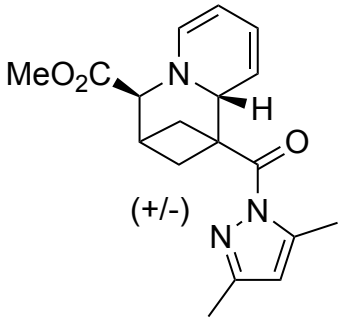

Product was synthesized following general procedure A on a 0.30 mmol scale. Reagent amounts used: bicyclobutane **1e** (52.9 mg, 0.30 mmol), pyridinium **2a** (1.25 equiv, 87.0 mg, 0.38 mmol), and K_3PO_4 (2.5 equiv, 159.2 mg, 0.75 mmol) in 1.20 mL acetonitrile (0.25 M). Isolated 43.0 mg of an orange oil (35% yield)

HRMS(ESI): calc'd for $[C_{18}H_{21}N_3O_3 + H^+]$, 328.16557; found: 328.16540.

^{1}H NMR (500 MHz, $CDCl_3$, 292 K, ppm): δ 6.08 – 6.03 (m, 1H), 5.93 – 5.84 (m, 2H), 5.31 (t, J = 2.1 Hz, 1H), 4.90 (ddd, J = 6.9, 5.4, 1.3 Hz, 1H), 4.53 (dddd, J = 9.4, 2.2, 1.3, 0.8 Hz, 1H), 4.07 (d, J = 4.1 Hz, 1H), 3.78 (s, 3H), 2.64 – 2.56 (m, 1H), 2.50 (d, J = 1.1 Hz, 3H), 2.48 – 2.33 (m, 3H), 2.24 – 2.17 (m, 1H), 2.15 (s, 3H).

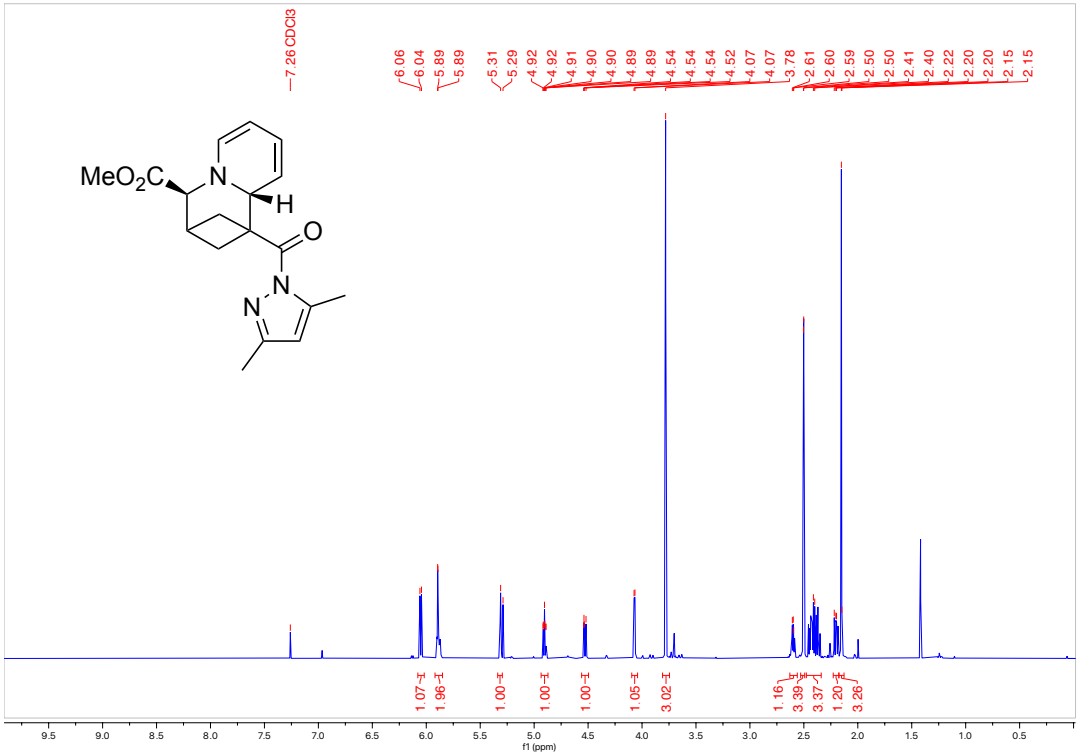

^{13}C NMR (126 MHz, $CDCl_3$, 292 K, ppm): δ 173.48, 173.11, 152.31, 143.98, 136.71, 126.39, 111.01, 110.96, 97.53, 64.96, 59.75, 52.34, 52.24, 37.93, 30.68, 30.16, 14.43, 14.43, 14.00.

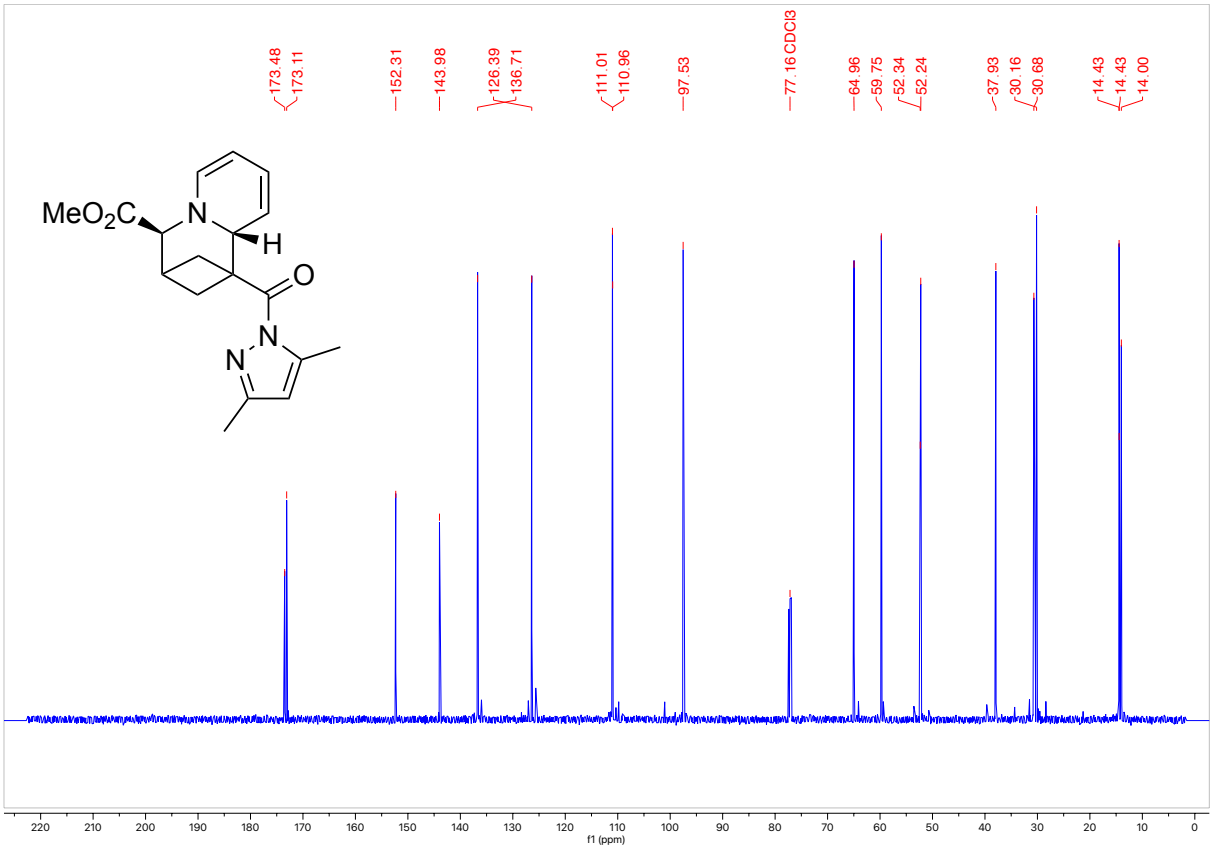

(4-benzoyl-3,4-dihydro-2H-1,3-methanoquinolizin-1(9aH)-yl)(3,5-dimethyl-1H-pyrazol-1-yl)methanone (3f)

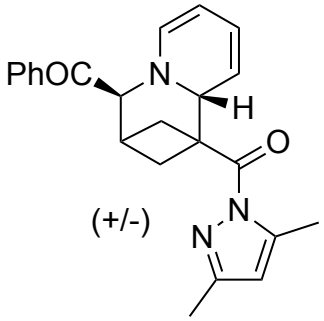

Product was synthesized following general procedure B on a 0.30 mmol scale. Reagent amounts used: bicyclobutane **1e** (52.9 mg, 0.30 mmol), pyridinium **2f** (1.25 equiv, 103.9 mg, 0.38 mmol), $NaPF_6$ (1.3 equiv, 65.5 mg), and K_3PO_4 (2.5 equiv, 159.2 mg, 0.75 mmol) in 1.2 mL acetonitrile (0.25 M). Isolated 27.8 mg of an orange solid as a mixture of diastereomers (25% yield, 6:1 d.r.).

HRMS(ESI): calc'd for $[C_{23}H_{23}N_3O_2 + H^+]$, 374.18631; found: 374.18672.

^{1}H NMR (500 MHz, $CDCl_3$, 292 K, ppm): δ 7.96 – 7.92 (m, 2H), 7.61 – 7.56 (m, 1H), 7.50 – 7.46 (m, 2H), 6.01 (d, J = 7.0 Hz, 1H), 5.95 (dddd, J = 9.3, 5.4, 2.2, 0.8 Hz, 1H), 5.90 (d, J = 1.2 Hz, 1H), 5.35 (t, J = 2.4 Hz, 1H), 5.09 (d, J = 3.6 Hz, 1H), 5.00 (ddd, J = 6.9, 5.4, 1.4 Hz, 1H), 4.63 – 4.58 (m, 1H), 2.67 – 2.62 (m, 1H), 2.58 – 2.44 (m, 5H), 2.33 – 2.24 (m, 2H), 2.18 (s, 3H).

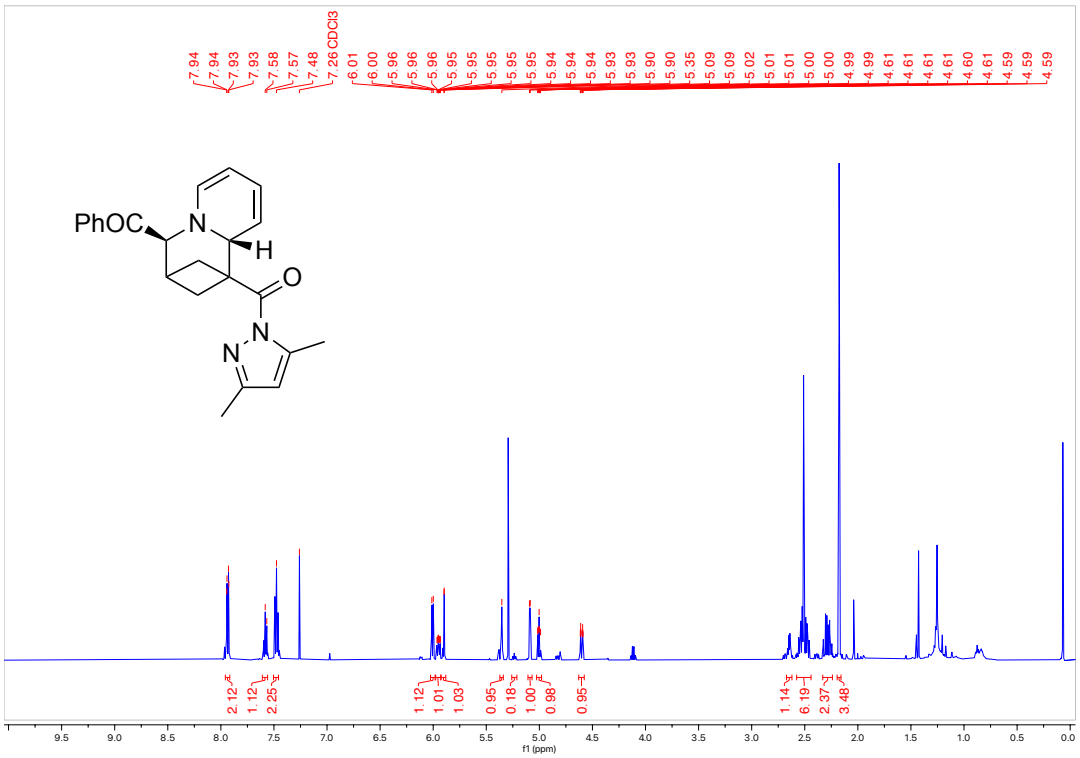

^{13}C NMR (126 MHz, $CDCl_3$, 292 K, ppm): δ 199.20, 173.60, 152.39, 143.98, 136.93, 135.64, 133.53, 133.51, 128.99, 128.96, 128.35, 128.34, 128.30, 126.68, 111.09, 110.39, 98.46, 67.76, 59.93, 52.02, 36.35, 31.51, 30.59, 29.84, 14.47, 14.05.

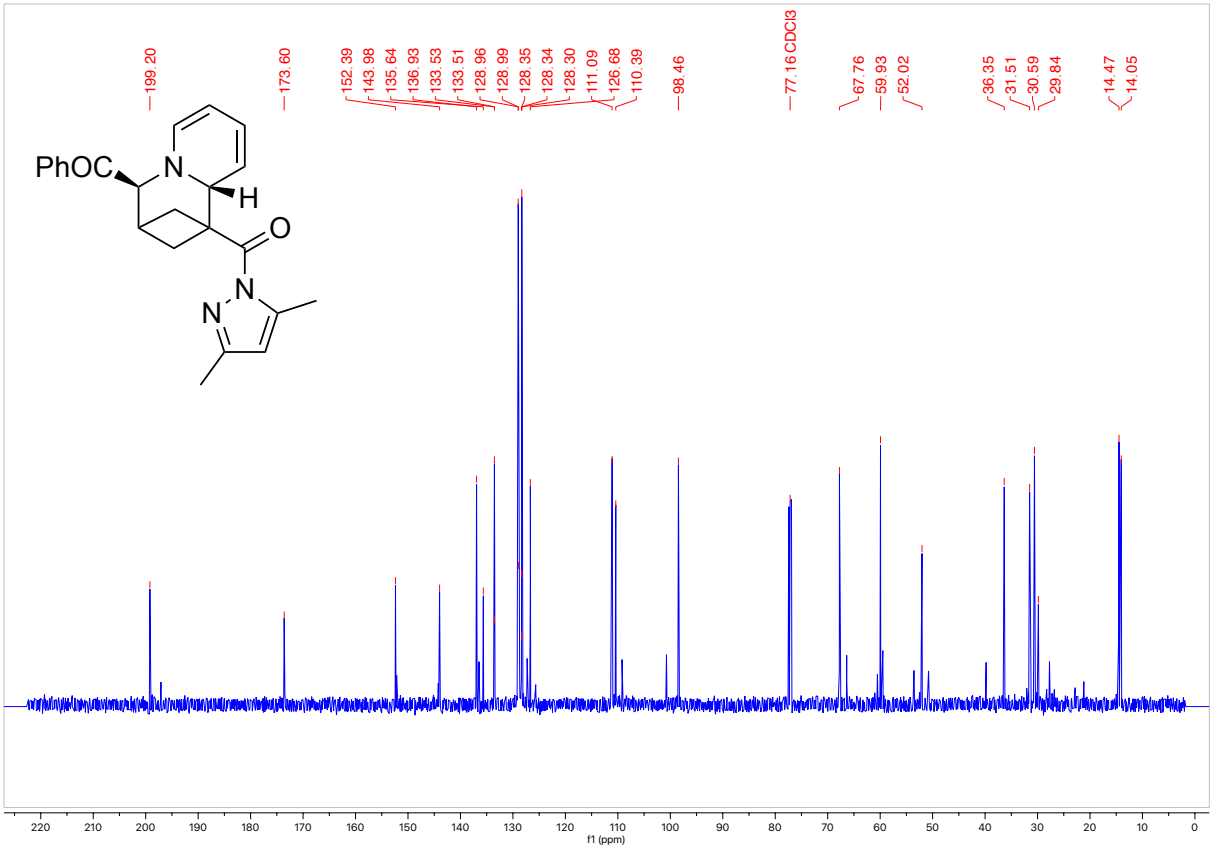

Methyl 1-(4-fluorobenzoyl)-1,3,4,9a-tetrahydro-2H-1,3-methanoquinolizine-4-carboxylate (3g)

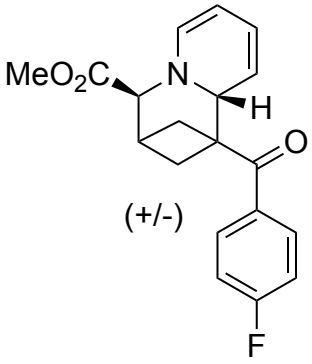

Product was synthesized following general procedure A on a 0.05 mmol scale. Reagent amounts used: bicyclobutane **1g** (8.8 mg, 0.05 mmol), pyridinium **2a** (1.25 equiv, 14.5 mg, 0.06 mmol), and K_3PO_4 (2.5 equiv, 26.5 mg, 0.13 mmol) in 0.2 mL d-MeCN (0.25 M). Solution yield determined by NMR spectroscopy using 1,3,5-trimethoxybenzene internal standard (72% solution yield, 5:1 d.r.).

HRMS(ESI): calc'd for $[C_{19}H_{18}FNO_3 + H^+]$, 328.13435; found: 328.13393.

^{1}H NMR (500 MHz, $CDCl_3$, 292 K, ppm): Product peak at 5.84 ppm.

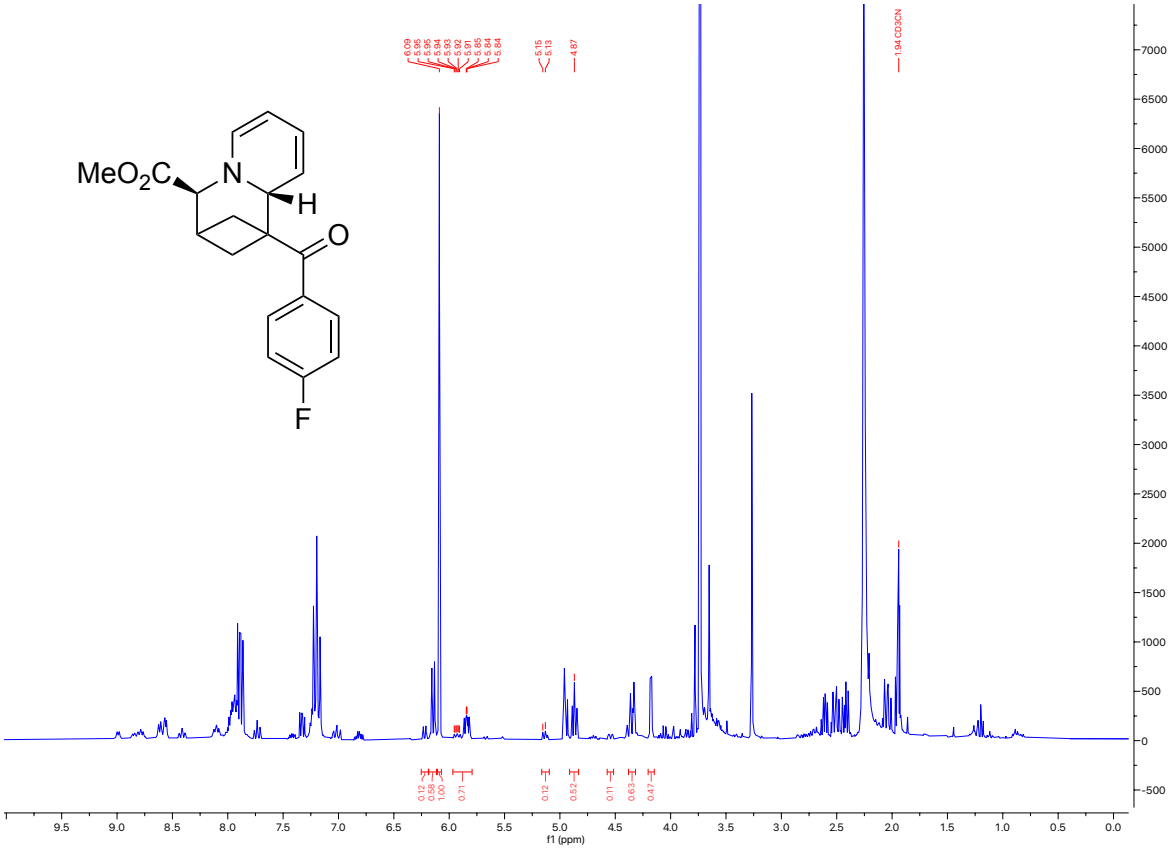

^{19}F NMR (300 MHz, $CDCl_3$, 292 K, ppm): 106.94, 106.97.

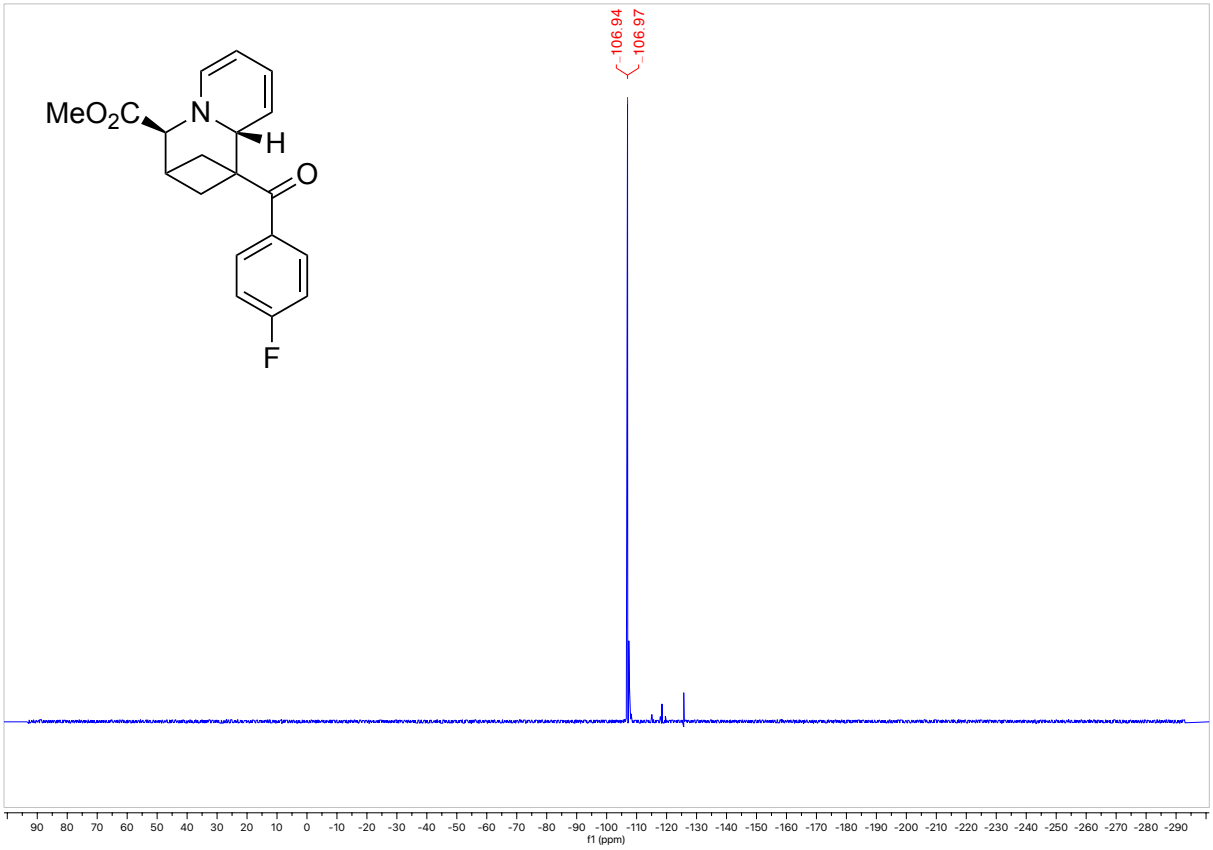

Methyl 3-phenyl-1-(4-(trifluoromethyl)benzoyl)-1,3,4,9a-tetrahydro-2H-1,3-methanoquinolizine-4-carboxylate (3h)

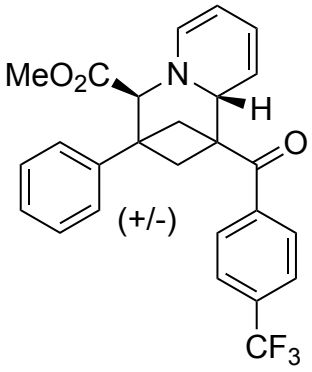

Product was synthesized following general procedure A on a 0.30 mmol scale. Reagent amounts used: bicyclobutane **1h** (90.7 mg, 0.30 mmol), pyridinium **2a** (1.25 equiv, 86.7 mg, 0.38 mmol), and K_3PO_4 (2.5 equiv, 159.2 mg, 0.75 mmol) in 1.8 mL acetonitrile (0.17 M). Isolated 32.1 mg of an orange oil (24% yield).

HRMS(ESI): calc'd for $[C_{26}H_{22}FNO_3 + H^+]$, 454.16246; found: 454.16208.

^{1}H NMR (500 MHz, $CDCl_3$, 292 K, ppm): δ 7.98 (d, J = 8.2 Hz, 1H), 7.71 (d, J = 8.2 Hz, 2H), 7.35 – 7.28 (m, 2H), 7.25 – 7.21 (m, 1H), 7.12 – 7.06 (m, 2H), 6.10 (dt, J = 7.0, 0.8 Hz, 1H), 6.03 (ddd, J = 9.0, 5.2, 2.2 Hz, 1H), 5.24 (ddd, J = 6.8, 5.3, 1.3 Hz, 1H), 4.79 (ddd, J = 8.9, 2.5, 1.2 Hz, 1H), 4.56 (t, J = 2.5 Hz, 1H), 4.43 (s, 1H), 3.32 (m, 4H), 2.79 – 2.69 (m, 2H), 2.55 (d, J = 10.0 Hz, 1H).

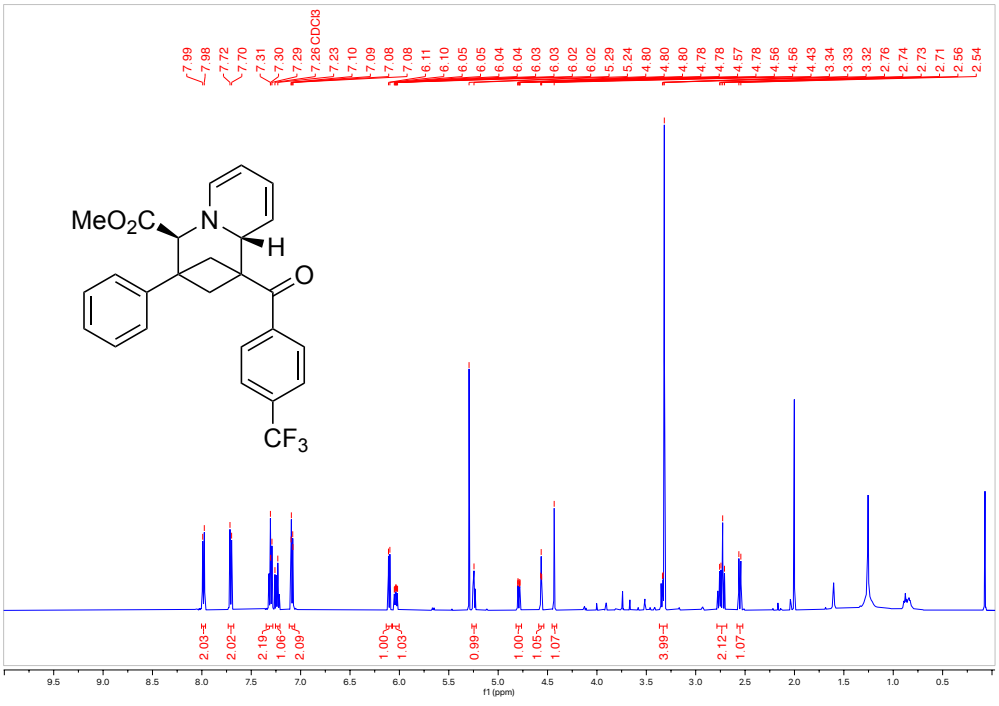

^{19}F NMR (300 MHz, $CDCl_3$, 292 K, ppm): δ 63.23

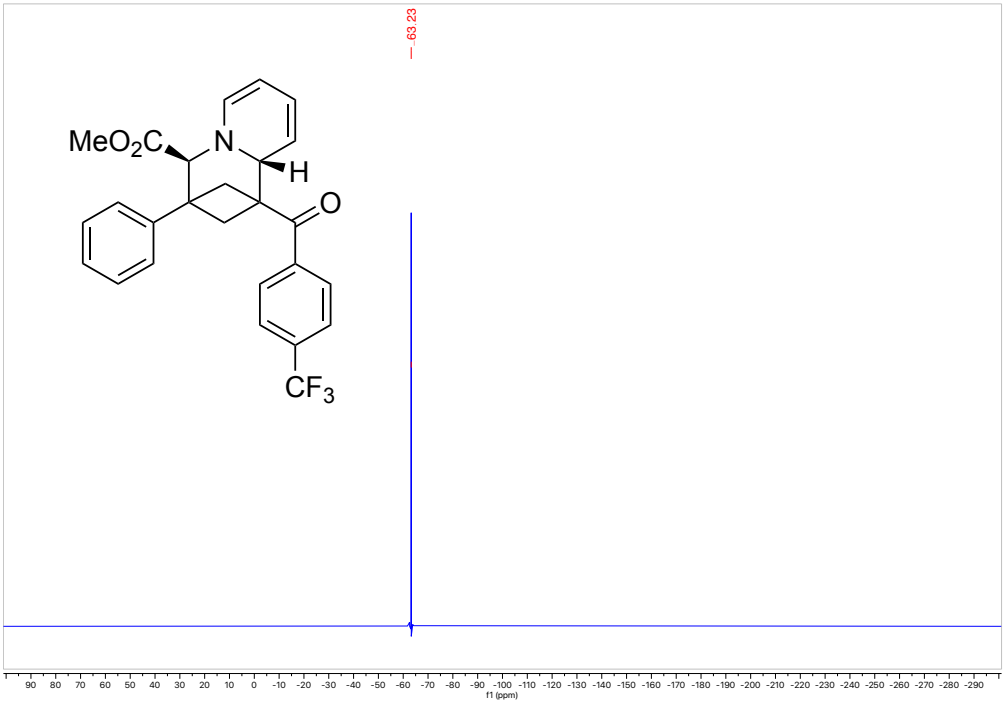

^{13}C NMR (126 MHz, $CDCl_3$, 292 K, ppm): δ 200.30, 171.21, 142.56, 138.60, 134.44, 129.17, 128.54, 127.51, 127.36, 125.88, 125.85, 125.82, 125.80, 109.79, 102.46, 70.81, 60.16, 51.73, 50.29, 45.07, 43.50, 31.45, 29.84.

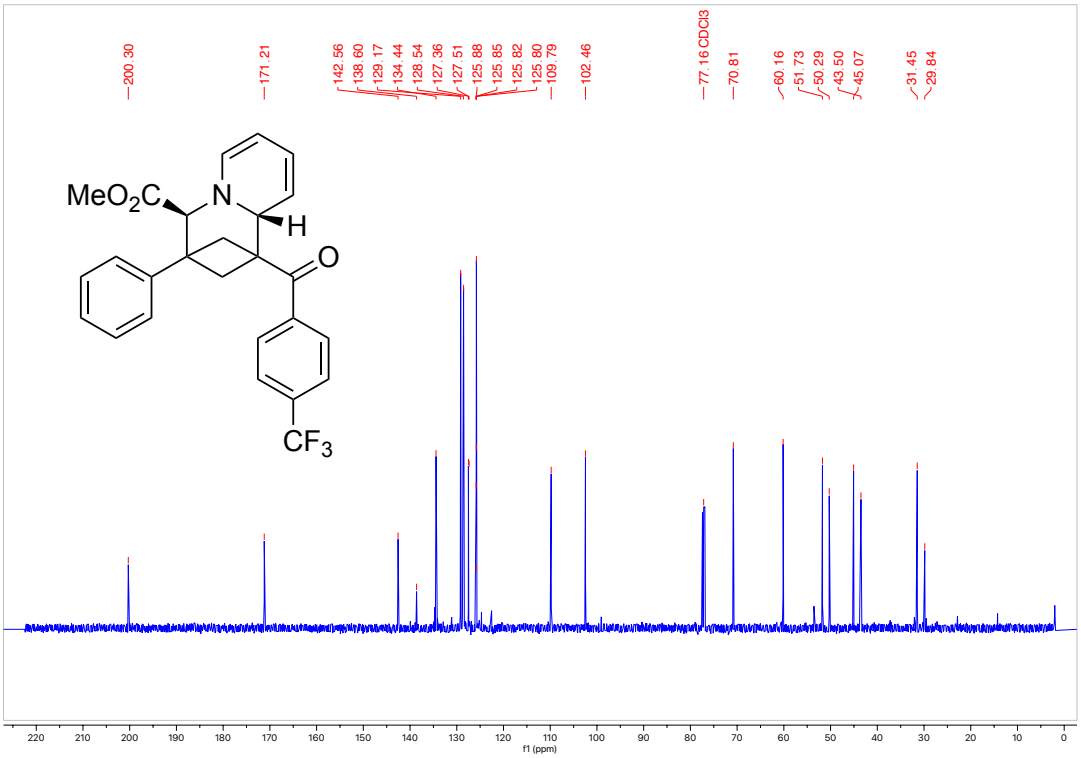

Methyl 1-(4-methoxybenzoyl)-3-phenyl-1,3,4,9a-tetrahydro-2H-1,3-methano-quinolizine-4-carboxylate (3i)

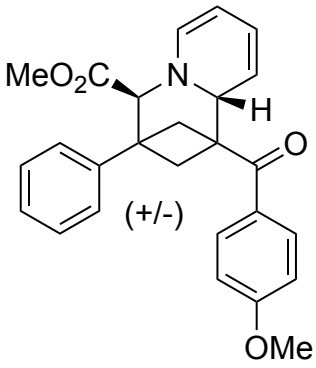

Product was synthesized following general procedure A on a 0.025 mmol scale. Reagent amounts used: bicyclobutane **1a** (6.6 mg, 0.025 mmol), pyridinium **2a** (1.25 equiv, 7.3 mg, 0.031 mmol), and K_3PO_4 (2.5 equiv, 13.3 mg, 0.063 mmol) in 0.1 mL acetonitrile (0.25 M). Solution yield determined by NMR spectroscopy using 1,3,5-trimethoxybenzene internal standard (65% solution yield).

HRMS(ESI): calc'd for $[C_{26}H_{25}NO_4 + H^+]$, 416.18564; found: 416.18549.

^{1}H NMR (500 MHz, $CDCl_3$, 292 K, ppm): Product peak at 6.11 ppm.

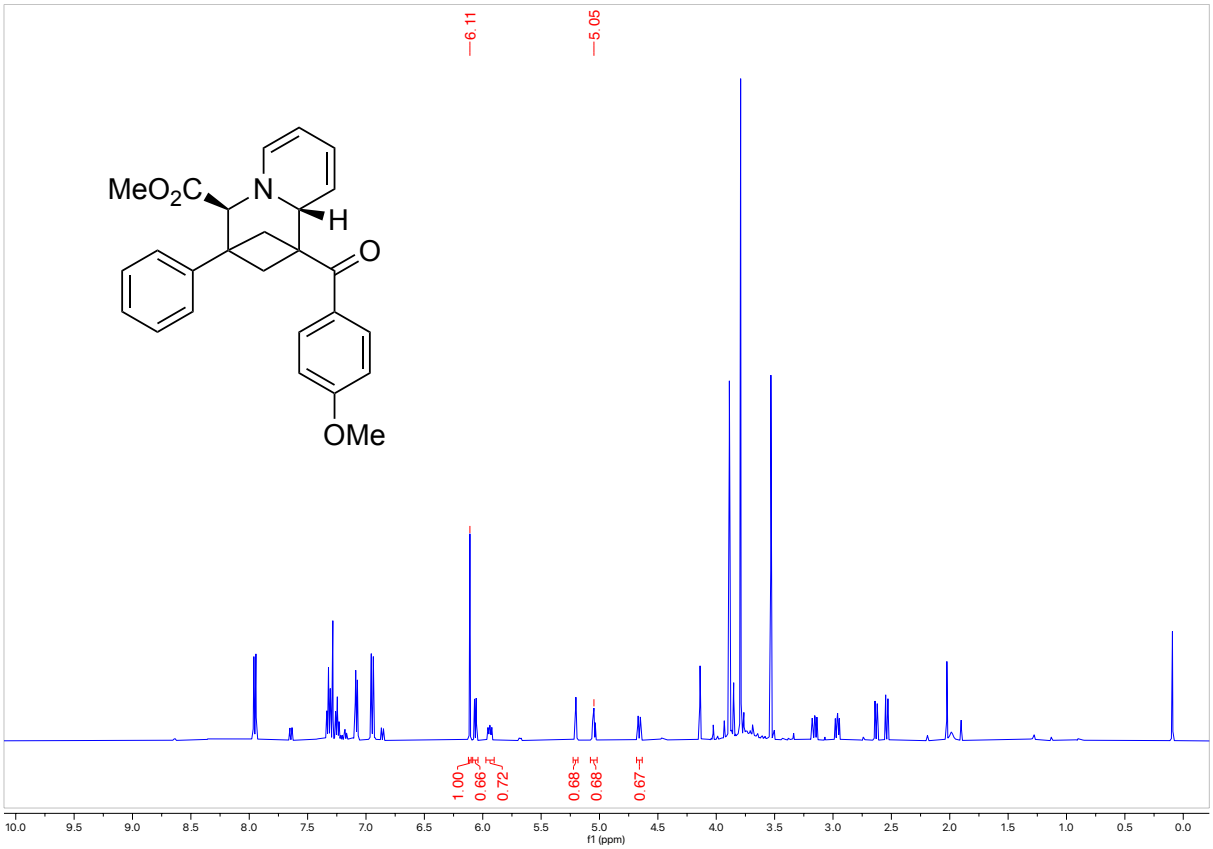

4-Benzoyl-3-phenyl-3,4-dihydro-2H-1,3-methanoquinolizin-1(9aH)-yl)(3,5-dimethyl-1H-pyrazol-1-yl)methanone (3m)

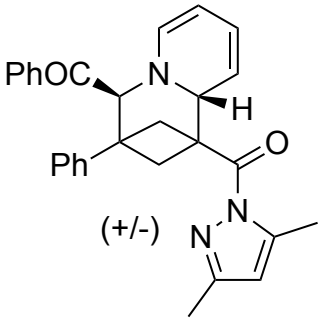

Product was synthesized following general procedure B on a 1.0 mmol scale. Reagent amounts used: bicyclobutane **1a** (252.3 mg, 1.0 mmol), pyridinium **2f** (1.25 equiv, 318.7 mg, 1.15 mmol), $NaPF_6$ (1.3 equiv, 218.3 mg, 1.30 mmol) and K_3PO_4 (2.5 equiv, 530.7 mg, 2.5 mmol) in 4.0 mL acetonitrile (0.25 M). Isolated 338.7 mg of an orange solid (75% yield).

HRMS(ESI): calc'd for $[C_{29}H_{27}N_3O_2 + H^+]$, 450.21761; found: 450.21745.

^{1}H NMR (500 MHz, $CDCl_3$, 292 K, ppm): δ 7.35 (m, 2H), 7.29 (m, 1H), 7.11 – 7.06 (m, 2H), 7.03 – 6.94 (m, 3H), 6.92 – 6.88 (m, 2H), 5.98 – 5.88 (m, 3H), 5.60 (t, J = 2.3 Hz, 1H), 5.15 (s, 1H), 4.95 (ddd, J = 6.9, 5.4, 1.4 Hz, 1H), 4.67 (ddt, J = 9.3, 2.2, 1.1 Hz, 1H), 3.32 (dd, J = 10.1, 7.4 Hz, 1H), 3.15 (dd, J = 9.5, 7.4 Hz, 1H), 2.55 – 2.48 (m, 5H).

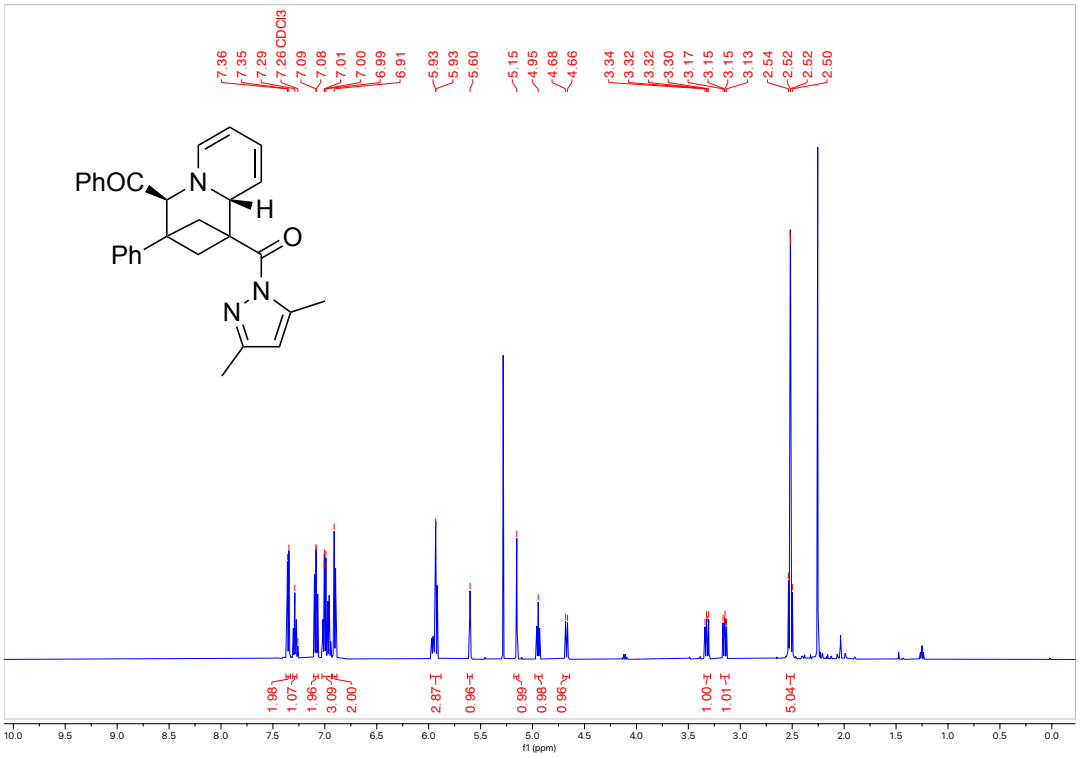

^{13}C NMR (126 MHz, $CDCl_3$, 292 K, ppm): δ 201.87, 173.19, 152.44, 144.00, 143.74, 137.86, 136.26, 132.66, 128.18, 128.04, 127.92, 126.74, 126.43, 126.26, 111.08, 110.76, 98.53, 70.76, 59.85, 49.51, 43.72, 39.33, 37.98, 14.42, 14.08.

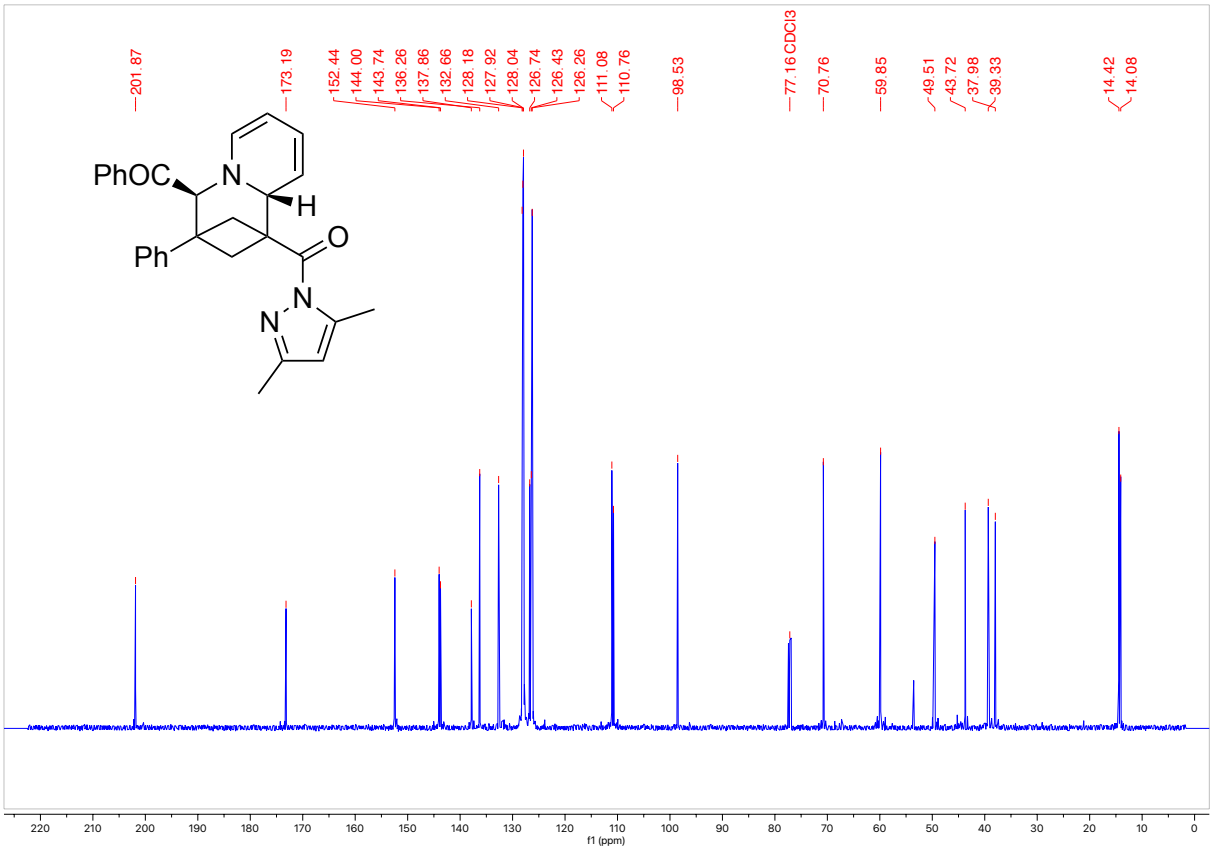

1-(3,5-Dimethyl-1H-pyrazole-1-carbonyl)-*N,N*-dimethyl-3-phenyl-1,3,4,9a-tetrahydro-2H-1,3-methanoquinolizine-4-carboxamide (3n)

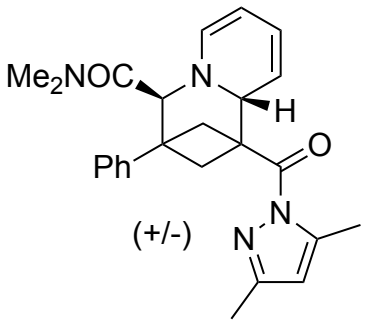

Product was synthesized following general procedure A on a 0.30 mmol scale. The reaction was conducted for 24 hours before a second charge of pyridinium and base was added, and stirred for another 24 hours. Reagent amounts used: bicyclobutane **1a** (75.7 mg, 0.30 mmol), pyridinium **2n** (2.5 equiv, 183.1 mg, 0.75 mmol, two portions), and K_3PO_4 (4 equiv, 254.7 mg, 1.20 mmol, two portions) in 1.2 mL acetonitrile (0.25 M). Product was purified by two successive elutions through a basic alumina plug. Isolated 42.3 mg of an orange oil (34% yield)

HRMS(ESI): calc'd for $[C_{25}H_{28}N_4O_2 + H^+]$, 417.22851; found: 417.22821.

^{1}H NMR (500 MHz, $CDCl_3$, 292 K, ppm): δ 7.31 – 7.24 (m, 2H), 7.24 – 7.16 (m, 1H), 7.14 – 7.05 (m, 2H), 5.96 – 5.86 (m, 3H), 5.50 (t, J = 2.5 Hz, 1H), 4.97 (ddd, J = 6.8, 5.3, 1.3 Hz, 1H), 4.68 – 4.59 (m, 1H), 4.43 (s, 1H), 3.72 (dd, J = 9.9, 7.4 Hz, 1H), 2.99 (dd, J = 9.5, 7.4 Hz, 1H), 2.78 (s, 3H), 2.53 (d, J = 9.5 Hz, 1H), 2.50 (d, J = 1.1 Hz, 3H), 2.40 (d, J = 9.9 Hz, 1H), 2.21 (s, 3H).

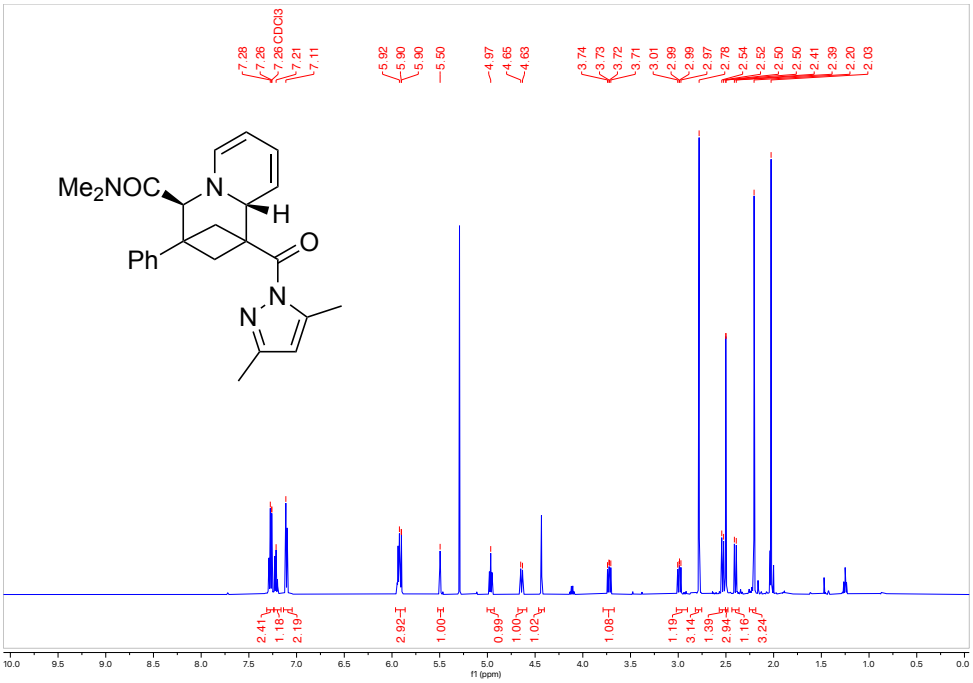

^{13}C NMR (126 MHz, $CDCl_3$, 292 K, ppm): δ 173.49, 171.52, 152.40, 144.27, 143.95, 135.62, 128.44, 127.08, 126.42, 126.27, 126.25, 111.08, 110.67, 98.82, 65.32, 59.41, 53.56, 49.44, 43.54, 39.82, 37.41, 36.58, 35.88, 14.46, 14.06.

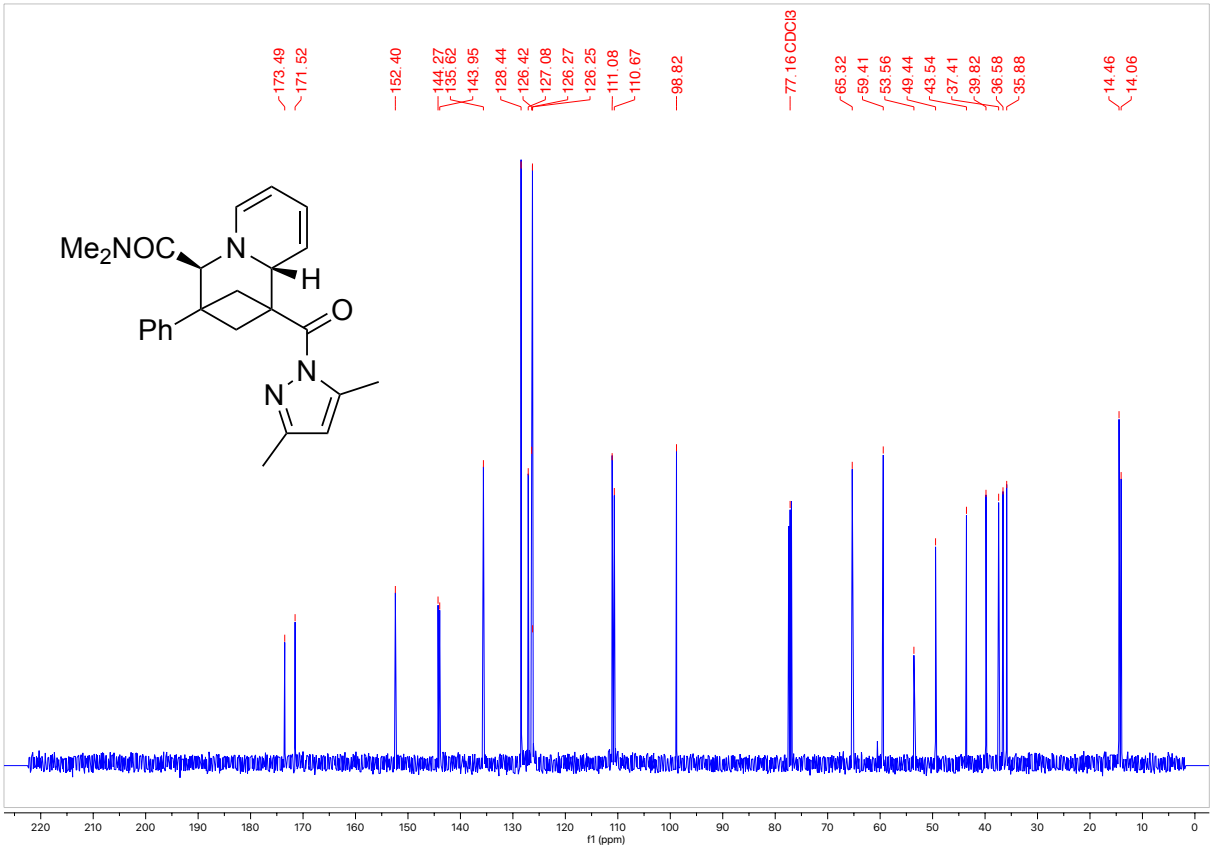

1-(3,5-dimethyl-1H-pyrazole-1-carbonyl)-3-phenyl-1,3,4,9a-tetrahydro-2H-1,3-methanoquinolizine-4-carbonitrile (3o)

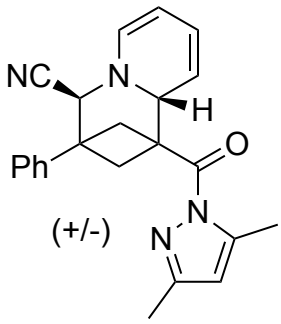

Product was synthesized following general procedure B on a 0.30 mmol scale with a 72 h reaction time. Reagent amounts used: bicyclobutane **1a** (75.7 mg, 0.30 mmol), pyridinium **2o** (1.25 equiv, 74.3 mg, 0.38 mmol), $NaPF_6$ (1.3 equiv, 65.5 mg, 0.39 mmol) and K_3PO_4 (2.5 equiv, 159.2 mg, 0.75 mmol) in 1.2 mL acetonitrile (0.25 M). Isolated 78.3 mg of a pale yellow oil (46% yield, additional 25% unreacted 1a).

HRMS(ESI): calc'd for [$C_{31}H_{31}N_3O_4$ + H^+], 371.18664; found: 371.18638.

^{1}H NMR (500 MHz, $CDCl_3$, 292 K, ppm): δ 7.38 – 7.27 (m, 5H), 6.18 (dd, J = 7.2, 1.0 Hz, 1H), 5.97 – 5.90 (m, 2H), 5.84 (d, J = 1.3 Hz, 1H), 5.36 (t, J = 2.3 Hz, 1H), 5.04 (ddd, J = 6.9, 5.4, 1.3 Hz, 1H), 4.73 (ddt, J = 9.5, 2.2, 1.1 Hz, 1H), 4.21 (s, 1H), 3.05 (dd, J = 10.6, 7.5 Hz, 1H), 2.95 (dd, J = 9.9, 7.5 Hz, 1H), 2.79 (dd, J = 10.6, 1.3 Hz, 1H), 2.52 (d, J = 1.1 Hz, 3H), 2.49 (d, J = 10.0 Hz, 1H), 2.24 (s, 3H).

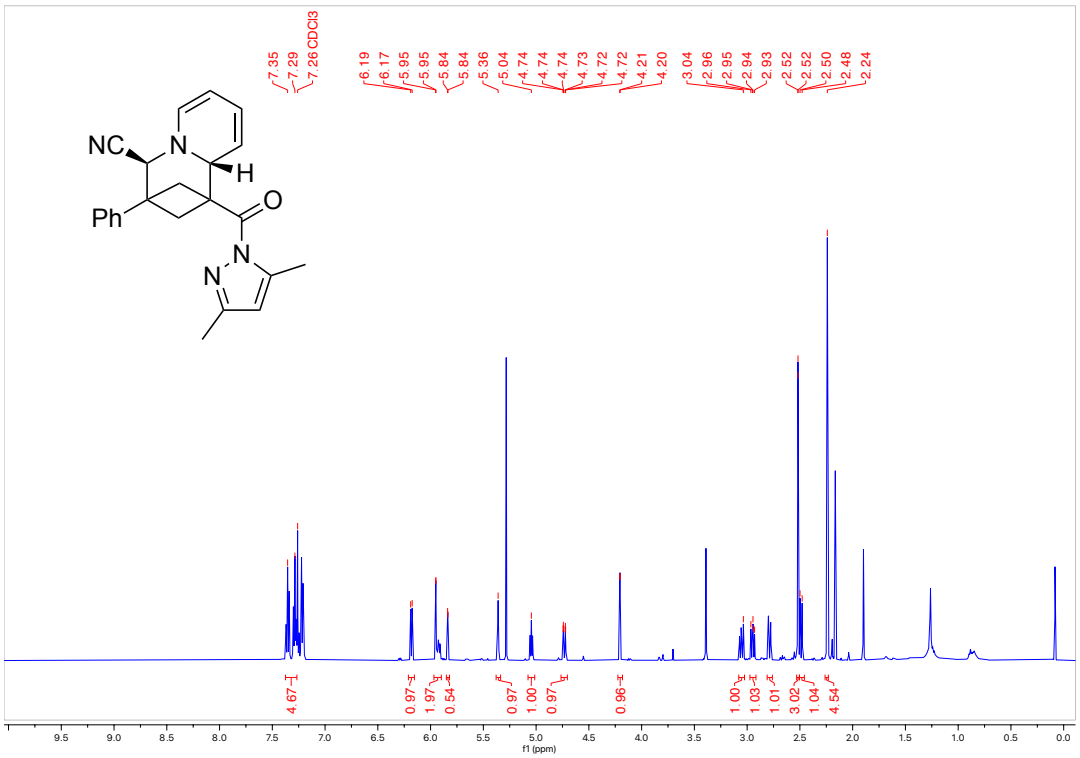

^{13}C NMR (126 MHz, $CDCl_3$, 292 K, ppm): δ 172.22, 152.92, 144.10, 141.76, 134.27, 128.85, 128.46, 127.80, 127.26, 126.39, 126.21, 126.06, 117.60, 113.07, 111.31, 110.08, 100.22, 61.69, 59.07, 49.45, 43.07, 42.79, 38.87, 34.13, 14.33, 14.03, 13.92, 13.88.

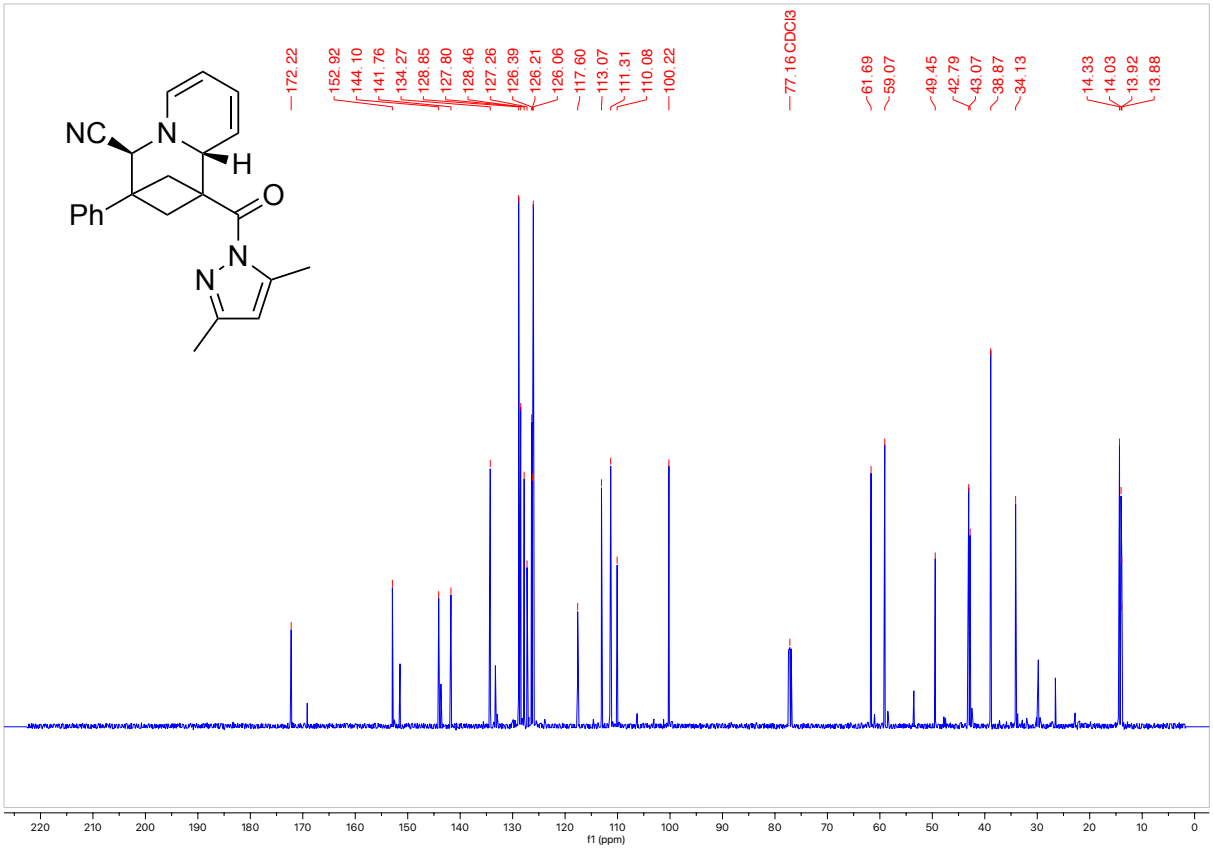

1'-(3,5-dimethyl-1H-pyrazole-1-carbonyl)-3'-phenyl-1',2',3',4,5,9a'-hexahydro-2H-spiro[furan-3,4'-[1,3]methanoquinolizin]-2-one (3p)

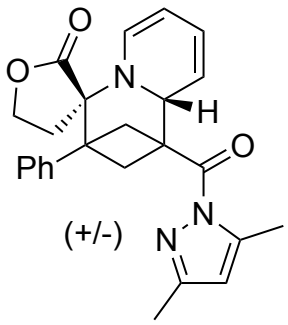

Product was synthesized following general procedure A on a 0.30 mmol scale with a reaction time of 72 h. Reagent amounts used: bicyclobutane **1a** (75.7 mg, 0.30 mmol), pyridinium **2p** (1.25 equiv, 91.5 mg, 0.38 mmol), and K_3PO_4 (2.5 equiv, 159.2 mg, 0.75 mmol) in 1.2 mL acetonitrile (0.25 M). Isolated 87.9 mg of an orange solid as a mixture of diastereomers (59% yield, 1.5:1 dr, additional 13% unreacted 1a).

HRMS(ESI): calc'd for [$C_{25}H_{25}N_3O_3$ + H^+], 416.19687; found: 416.19723.

^{1}H NMR (500 MHz, $CDCl_3$, 292 K, ppm): δ 7.32 (dd, J = 8.4, 7.6 Hz, 3H), 7.27 – 7.21 (m, 2H), 6.14 (d, J = 7.0 Hz, 0.6H), 6.04 (ddd, J = 9.0, 5.1, 2.2 Hz, 0.4H), 5.94 (m, 1H), 5.42 (ddd, J = 6.7, 5.1, 1.3 Hz, 0.6H), 5.31 – 5.27 (m, 0.4H), 5.01 (m, 1H), 4.95 (dddd, J = 8.9, 2.9, 1.3, 0.7 Hz, 0.6H), 4.88 – 4.81 (m, 0.4H), 3.98 – 3.88 (m, 1H), 3.74 (dd, J = 10.4, 7.2 Hz, 0.6H), 3.62 (dd, J = 10.2, 7.2 Hz, 0.4H), 3.00 (dd, J = 10.4, 7.2 Hz, 0.4H), 2.87 (dd, J = 10.1, 7.2 Hz, 0.6H), 2.81 (d, J = 10.3 Hz, 0.4H), 2.74 (ddd, J = 13.7, 7.7, 2.0 Hz, 0.4H), 2.65 (d, J = 10.1 Hz, 1H), 2.59 – 2.54 (m, 0.6H), 2.53 (dd, J = 2.4, 1.0 Hz, 3H), 2.50 (d, J = 10.4 Hz, 0.6H), 2.48 – 2.32 (m, 2H), 2.24 (d, J = 3.0 Hz, 3H).

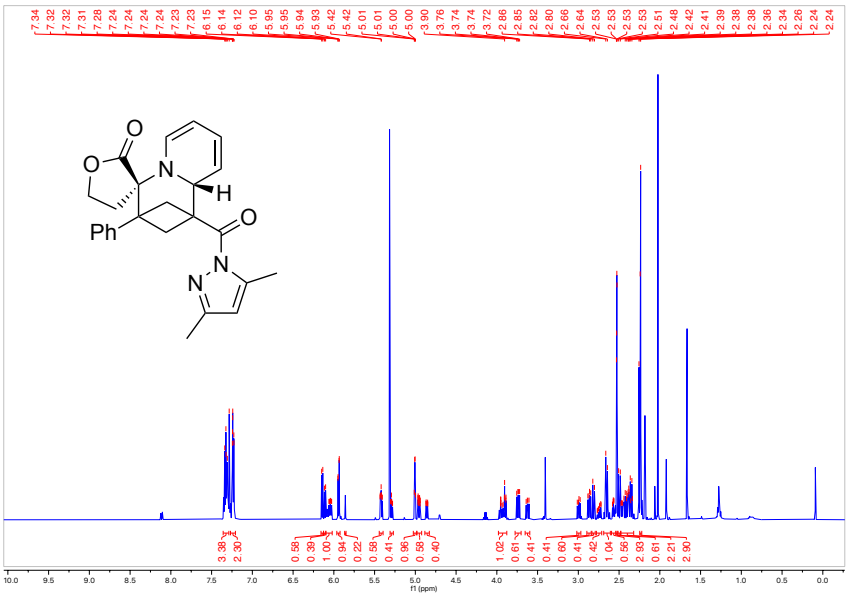

^{13}C NMR (126 MHz, $CDCl_3$, 292 K, ppm): δ 177.46, 175.91, 173.12, 172.68, 152.65, 152.33, 144.36, 144.09, 141.77, 141.52, 133.09, 131.52, 128.75, 128.50, 127.78, 127.75, 127.30, 127.04, 126.86, 126.81, 126.42, 111.82, 111.28, 111.09, 110.37, 110.12, 105.07, 102.75, 71.92, 70.63, 64.31, 64.10, 59.22, 59.18, 47.78, 47.63, 46.29, 45.74, 42.47, 40.74, 38.94, 38.91, 35.55, 33.71, 32.35, 30.82, 14.48, 14.46, 14.07, 13.91.

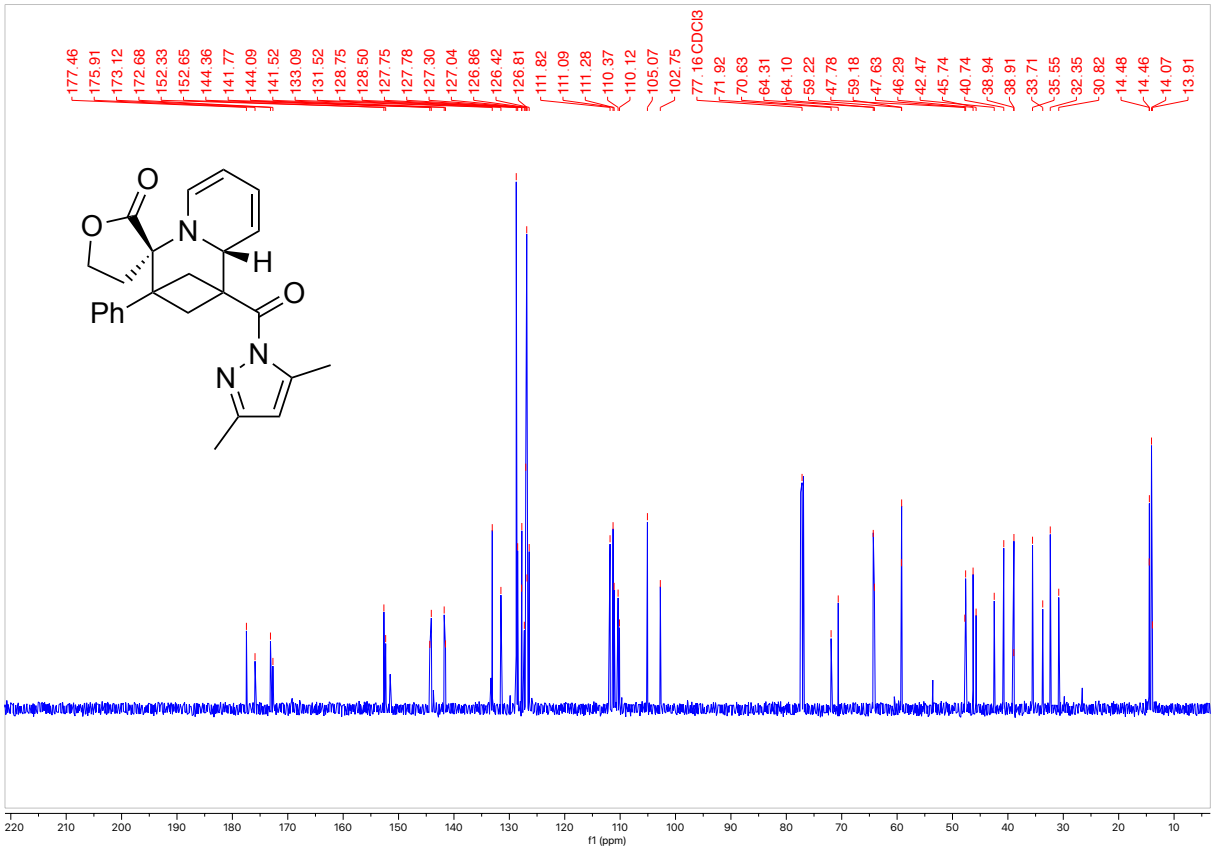

2-(Trimethylsilyl)ethyl 1-(3,5-dimethyl-1H-pyrazole-1-carbonyl)-3-phenyl-1,3,4,-9a-tetrahydro-2H-1,3-methanoquinolizine-4-carboxylate (3q)

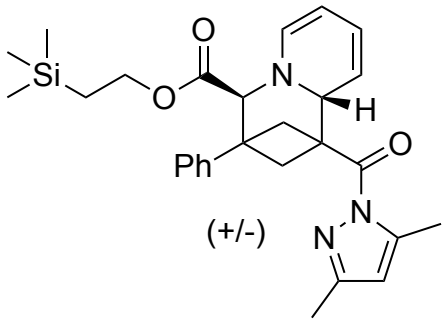

Product was synthesized following general procedure A on a 0.30 mmol scale. Reagent amounts used: bicyclobutane **1a** (75.7 mg, 0.30 mmol), pyridinium **2q** (1.25 equiv, 119.4 mg, 0.38 mmol), and K_3PO_4 (2.5 equiv, 159.2 mg, 0.75 mmol) in 1.2 mL acetonitrile (0.25 M). Isolated 124.0 mg of an orange oil (75% yield, additional 9% unreacted 1a).

HRMS(ESI): calc'd for $[C_{28}H_{35}N_3O_3Si + H^+]$, 490.25205; found: 490.25209.

^{1}H NMR (500 MHz, $CDCl_3$, 292 K, ppm): δ 7.32 – 7.26 (m, 2H), 7.25 – 7.17 (m, 1H), 7.11 – 7.06 (m, 2H), 6.03 (dt, J = 7.0, 0.9 Hz, 1H), 5.98 – 5.90 (m, 2H), 5.44 (d, J = 2.3 Hz, 1H), 4.95 (ddd, J = 6.9, 5.4, 1.3 Hz, 1H), 4.63 (dddd, J = 9.4, 2.3, 1.3, 0.9 Hz, 1H), 4.17 – 4.07 (m, 1H), 4.06 (d, J = 1.4 Hz, 1H), 3.93 (td, J = 10.9, 6.5 Hz, 1H), 3.21 (dd, J = 10.2, 7.4 Hz, 1H), 2.96 (dd, J = 9.7, 7.4 Hz, 1H), 2.65 – 2.59 (m, 1H), 2.51 (d, J = 1.1 Hz, 3H), 2.44 (d, J = 9.7 Hz, 1H), 2.21 (s, 3H), 0.78 – 0.66 (m, 2H), -0.04 (s, 9H).

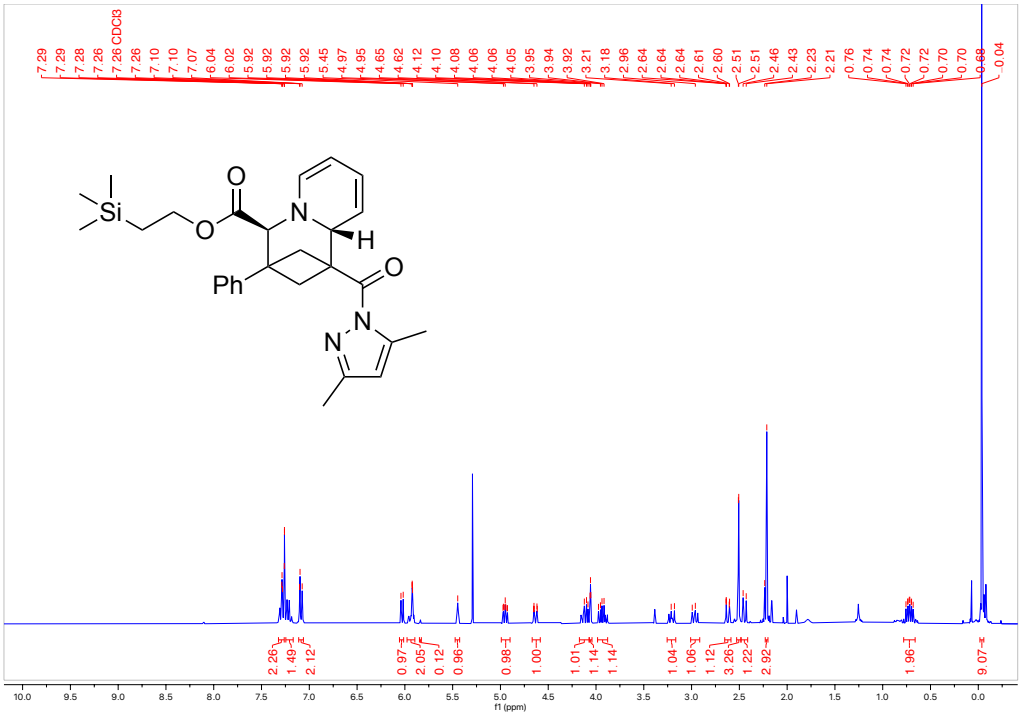

^{13}C NMR (126 MHz, $CDCl_3$, 292 K, ppm): δ 173.09, 171.93, 152.36, 144.06, 135.85, 128.48, 128.27, 126.82, 126.41, 126.35, 126.10, 111.10, 111.03, 98.20, 71.01, 63.02, 59.29, 49.62, 42.94, 40.08, 38.89, 37.55, 17.36, 14.41, 14.04.

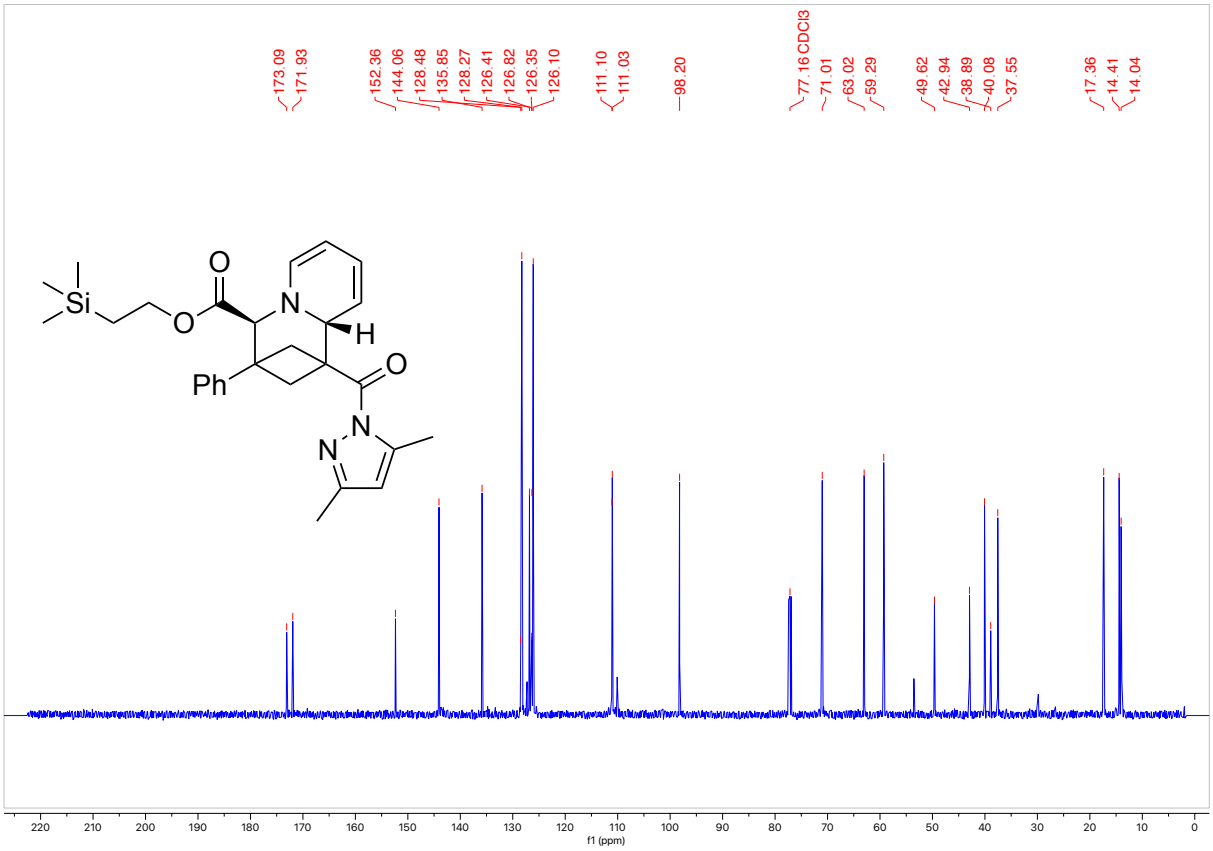

***Tert*-butyl 1-(3,5-dimethyl-1H-pyrazole-1-carbonyl)-3-phenyl-1,3,4,9a-tetrahydro-2H-1,3-methanoquinolizine-4-carboxylate (3r)**

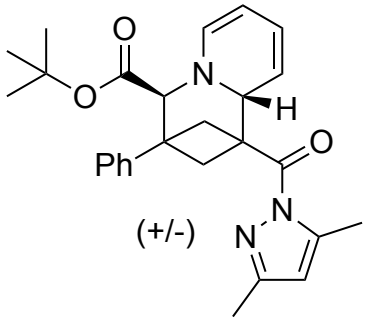

Product was synthesized following general procedure A on a 0.30 mmol scale. Reagent amounts used: bicyclobutane **1a** (81.1 mg, 0.30 mmol), pyridinium **2r** (1.25 equiv, 102.4 mg, 0.38 mmol), and K_3PO_4 (2.5 equiv, 159.2 mg, 0.75 mmol) in 1.2 mL acetonitrile (0.25 M). Isolated 101.7 mg of an orange oil (61% yield).

HRMS(ESI): calc'd for $[C_{27}H_{31}N_3O_3 + H^+]$, 446.24382; found: 446.24392.

^{1}H NMR (500 MHz, $CDCl_3$, 292 K, ppm): δ 7.31 – 7.27 (m, 2H), 7.24 – 7.18 (m, 1H), 7.14 – 7.07 (m, 2H), 6.04 (dd, J = 7.1, 0.9 Hz, 1H), 5.96 – 5.88 (m, 2H), 5.43 (t, J = 2.4 Hz, 1H), 4.95 (ddt, J = 6.7, 5.4, 1.2 Hz, 1H), 4.62 (ddt, J = 9.4, 2.3, 1.1 Hz, 1H), 4.02 (s, 1H), 3.17 (ddd, J = 10.2, 7.5, 2.9 Hz, 1H), 2.96 (dd, J = 9.6, 7.4 Hz, 1H), 2.66 (dd, J = 10.1, 1.2 Hz, 1H), 2.51 (d, J = 1.0 Hz, 3H), 2.40 (d, J = 9.6 Hz, 1H), 2.21 (s, 3H), 1.28 (s, 9H).

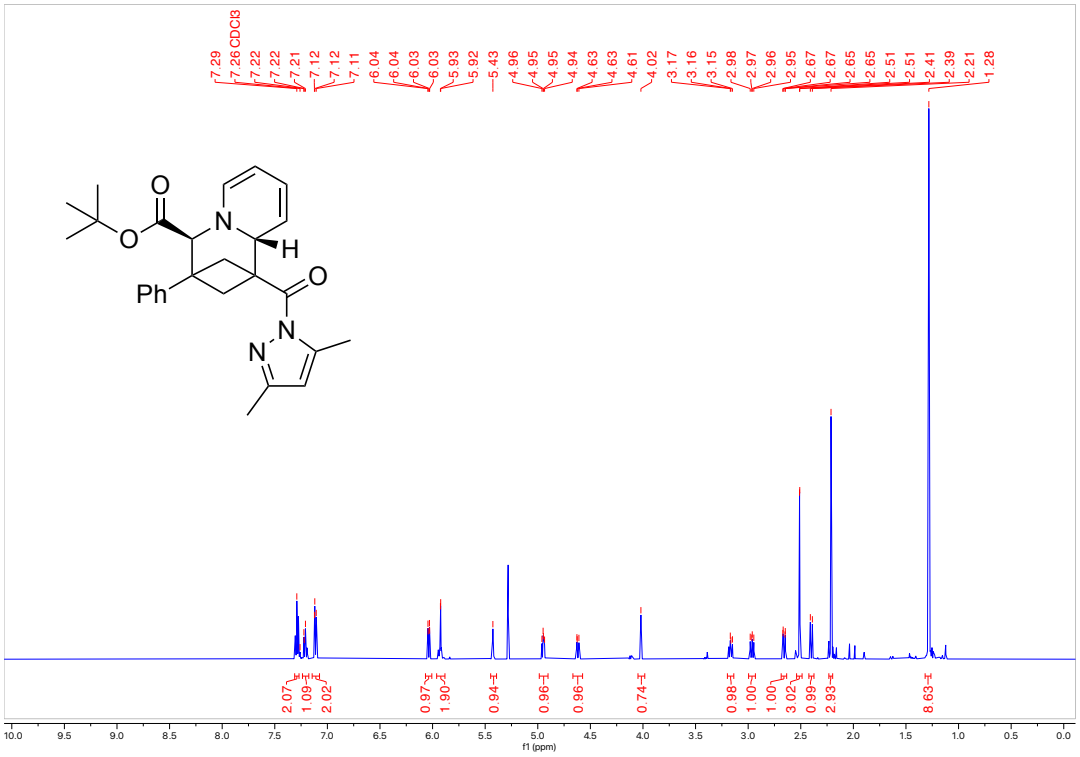

^{13}C NMR (126 MHz, $CDCl_3$, 292 K, ppm): δ 173.15, 170.71, 152.29, 144.02, 136.00, 135.96, 128.18, 128.17, 126.71, 126.36, 126.26, 110.97, 98.00, 97.98, 81.55, 71.32, 59.13, 59.11, 49.49, 42.80, 39.67, 39.64, 37.88, 37.85, 27.96, 14.39, 14.02.

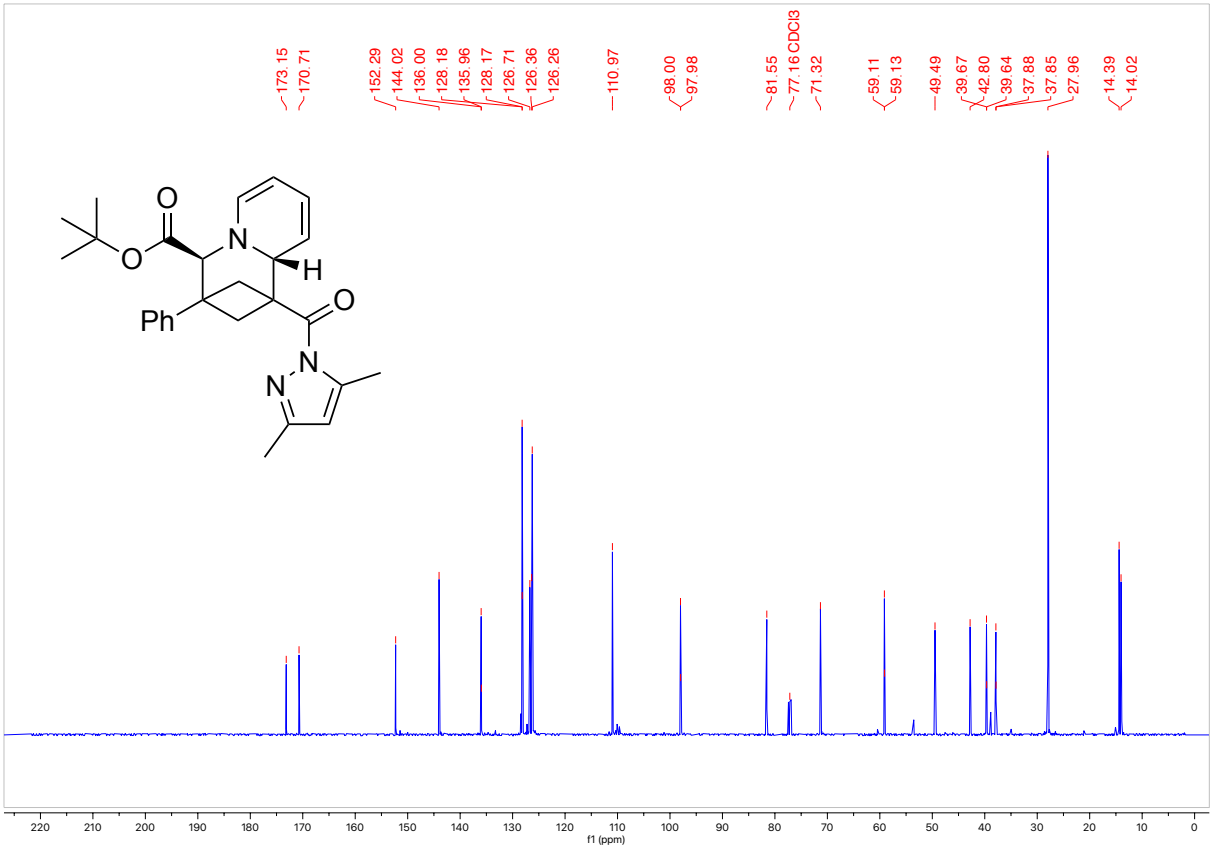

4-Methoxybenzyl 1-(3,5-dimethyl-1H-pyrazole-1-carbonyl)-3-phenyl-1,3,4,9a-tetrahydro-2H-1,3-methanoquinolizine-4-carboxylate (3s)

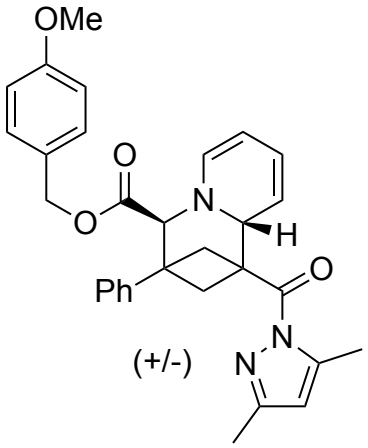

Product was synthesized following general procedure A on a 0.30 mmol scale. Reagent amounts used: bicyclobutane **1a** (81.1 mg, 0.30 mmol), pyridinium **2s** (1.25 equiv, 126.4 mg, 0.38 mmol), and K_3PO_4 (2.5 equiv, 159.2 mg, 0.75 mmol) in 1.2 mL acetonitrile (0.25 M). Isolated 136.2 mg of an orange oil (71% yield).

HRMS(ESI): calc'd for [$C_{31}H_{31}N_3O_4$ + H^+], 510.23874; found: 510.24009.

^{1}H NMR (500 MHz, $CDCl_3$, 292 K, ppm): δ 7.30 – 7.21 (m, 3H), 7.07 – 7.00 (m, 4H), 6.84 – 6.80 (m, 2H), 6.04 (d, J = 7.0,1H), 5.99 – 5.92 (m, 2H), 5.52 – 5.47 (m, 1H), 5.03 (d, J = 12.0 Hz, 1H), 4.97 (ddd, J = 6.9, 5.4, 1.3 Hz, 1H), 4.86 (d, J = 12.0 Hz, 1H), 4.67 (ddt, J = 9.4, 2.2, 1.1 Hz, 1H), 4.16 (s, 1H), 3.81 (s, 3H), 3.20 (dd, J = 10.2, 7.4 Hz, 1H), 2.99 (dd, J = 9.7, 7.4 Hz, 1H), 2.63 (d, J = 10.3, 1H), 2.54 (d, J = 1.1 Hz, 3H), 2.46 (d, J = 9.7 Hz, 1H), 2.24 (s, 3H).

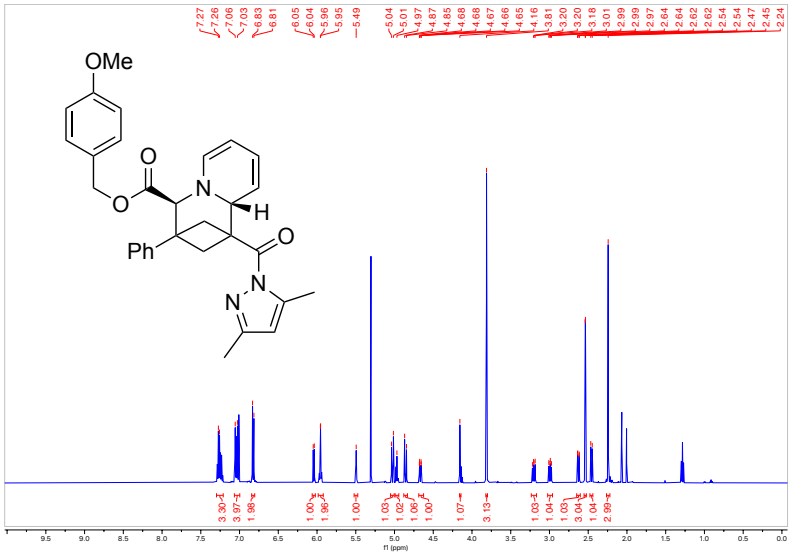

^{13}C NMR (126 MHz, $CDCl_3$, 292 K, ppm): δ 172.97, 171.72, 159.62, 152.34, 144.01, 143.83, 135.75, 130.13, 128.32, 127.49, 126.74, 126.31, 126.01, 113.78, 111.12, 111.00, 98.23, 70.87, 66.35, 59.23, 55.30, 49.55, 42.86, 39.98, 37.54, 14.36, 13.99.

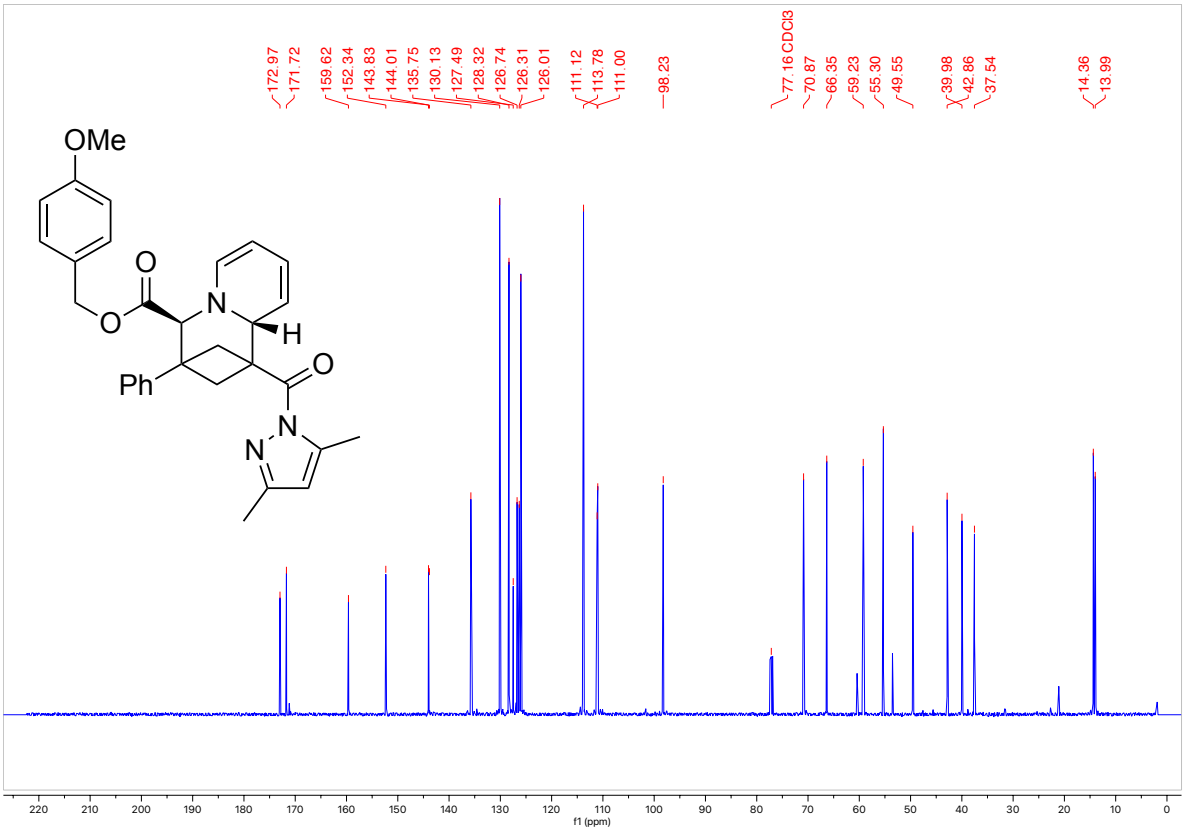

(*R*)-1-Phenylethyl 1-(3,5-dimethyl-1H-pyrazole-1-carbonyl)-3-phenyl-1,3,4,9a-tetrahydro-2H-1,3-methanoquinolizine-4-carboxylate (3t)

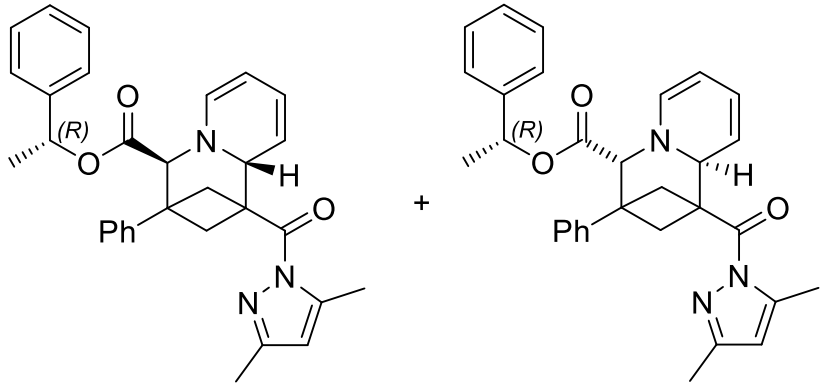

Product was synthesized following general procedure A on a 0.30 mmol scale. Reagent amounts used: bicyclobutane **1a** (81.1 mg, 0.30 mmol), pyridinium **2t** (1.25 equiv, 120.4 mg, 0.38 mmol), and K_3PO_4 (2.5 equiv, 159.2 mg, 0.75 mmol) in 1.2 mL acetonitrile (0.25 M). Isolated 120.2 mg of an orange oil (65% yield, 1:1.4 d.r.).

HRMS(ESI): calc'd for $[C_{31}H_{31}N_3O_3 + H^+]$, 494.24382; found: 494.24426.

^{1}H NMR (500 MHz, $CDCl_3$, 292 K, ppm): δ 7.37 – 7.25 (m, 5H), 7.23 – 7.03 (m, 5H), 6.05 (d, J = 7.0 Hz, 0.4H), 6.00 – 5.93 (m, 2.6H), 5.89 (q, J = 6.5 Hz, 0.4H), 5.77 (q, J = 6.6 Hz, 0.6H), 5.56 (s, 0.4H), 5.49 (s, 0.6H), 4.96 (dtd, J = 6.9, 5.3, 1.3 Hz, 1H), 4.67 (ddq, J = 9.1, 2.3, 1.3 Hz, 1H), 4.18 (d, J = 6.2 Hz, 1H), 3.25 (dd, J = 10.2, 7.5 Hz, 0.4H), 3.18 (dd, J = 10.2, 7.4 Hz, 0.6H), 3.02 (dt, J = 9.7, 7.7 Hz, 1H), 2.67 (td, J = 10.3, 1.1 Hz, 1H), 2.54 (d, J = 1.1 Hz, 3H), 2.45 (t, J = 10.1 Hz, 1H), 2.24 (s, 3H), 1.56 (d, J = 6.6 Hz, 1H), 1.25 (dd, J = 6.6, 2H).

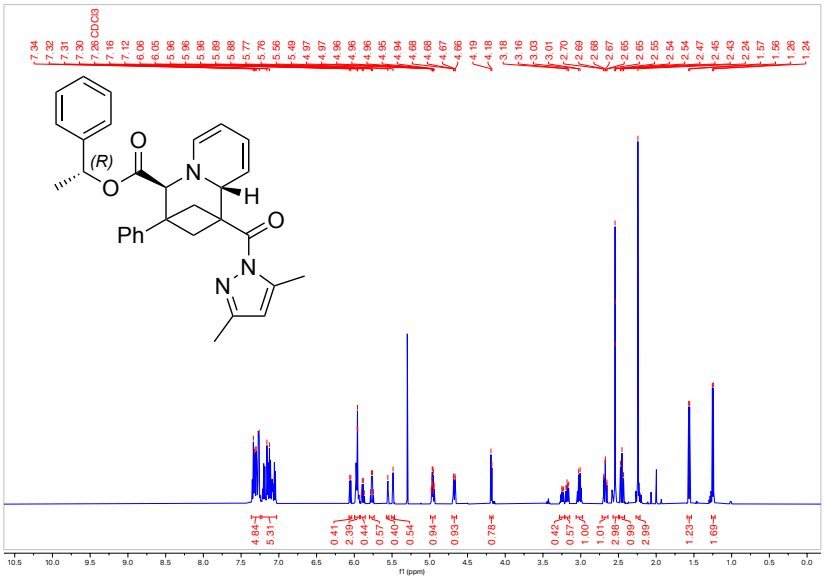

^{13}C NMR (126 MHz, $CDCl_3$, 292 K, ppm): δ 173.02, 173.00, 171.03, 170.97, 152.36, 152.31, 144.03, 143.87, 143.56, 141.36, 140.90, 135.85, 135.82, 128.50, 128.40, 128.38, 128.33, 127.98, 127.73, 126.82, 126.75, 126.35, 126.33, 126.22, 126.14, 126.10, 125.98, 111.24, 111.09, 111.02, 110.97, 98.32, 97.94, 73.34, 73.32, 73.12, 70.98, 70.88, 59.22, 59.19, 49.69, 49.46, 42.85, 42.82, 40.06, 39.78, 37.74, 37.71, 22.61, 22.25, 14.39, 14.37, 14.02.

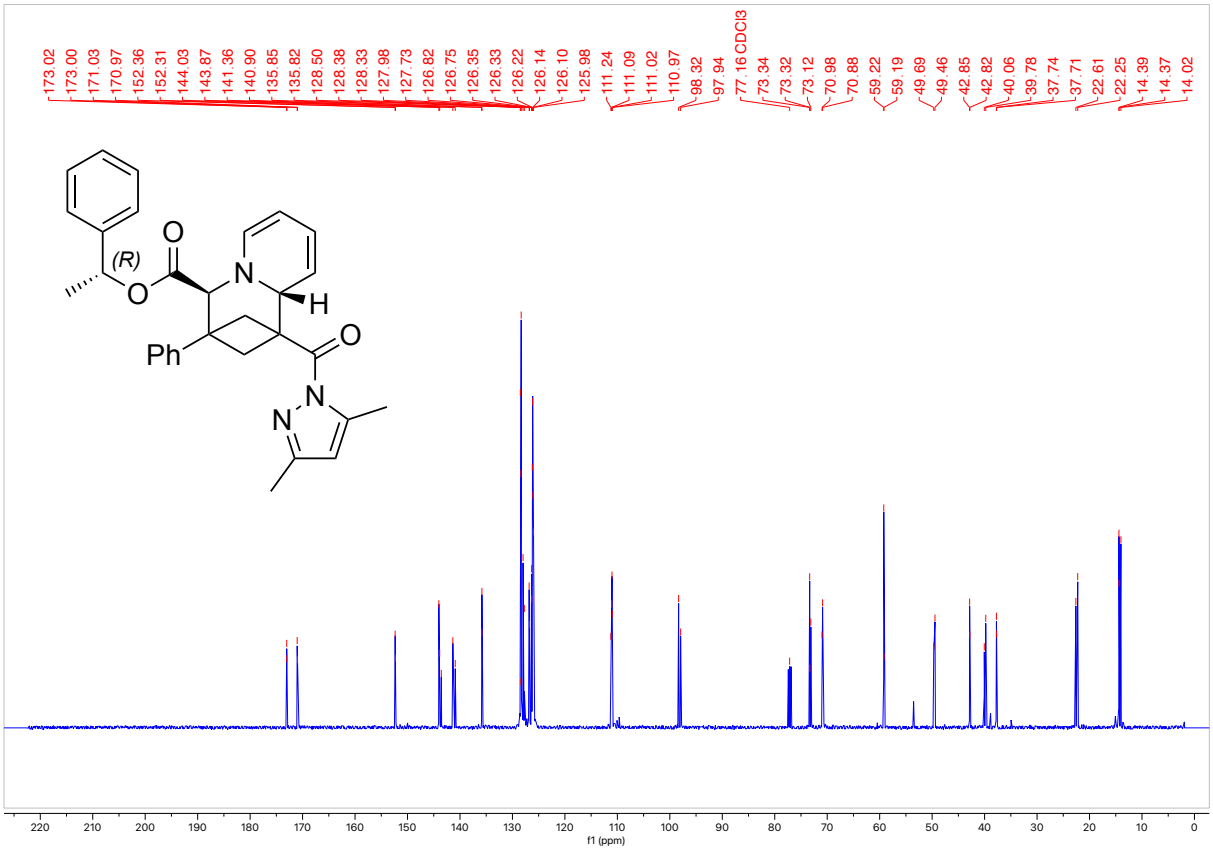

(*R*)-Tetrahydrofuran-3-yl 1-(3,5-dimethyl-1H-pyrazole-1-carbonyl)-3-phenyl-1,3, 4,9a-tetrahydro-2H-1,3-methanoquinolizine-4-carboxylate (3v)

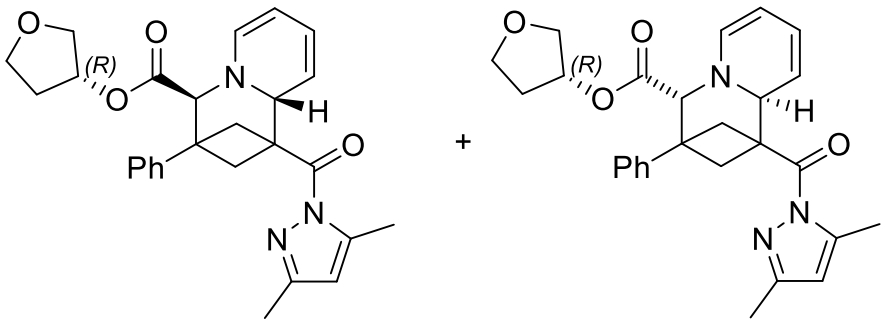

Product was synthesized following general procedure A on a 0.30 mmol scale. Reagent amounts used: bicyclobutane **1a** (75.7 mg, 0.30 mmol), pyridinium **2v** (1.25 equiv, 108.1 mg, 0.38 mmol), and K_3PO_4 (2.5 equiv, 159.2 mg, 0.75 mmol) in 1.2 mL acetonitrile (0.25 M). Isolated 67.2 mg of an orange oil as a mixture of diastereomers (70% yield, 1.2:1 d.r.).

HRMS(ESI): calc'd for [$C_{27}H_{29}N_3O_4$ + H^+], 460.22309; found: 460.22293.

^{1}H NMR (500 MHz, $CDCl_3$, 292 K, ppm): δ 7.29 (m, 2H), 7.22 (m, 1H), 7.13 – 7.06 (m, 2H), 6.00 (dd, J = 7.1, 2.6 Hz, 1H), 5.93 (s, 2H), 5.43 (d, J = 7.3 Hz, 1H), 5.17 (d, J = 17.0 Hz, 1H), 4.96 (q, J = 6.2 Hz, 1H), 4.65 (d, J = 9.6 Hz, 1H), 4.11 (s, 1H), 3.86 (dd, J = 10.6, 4.6 Hz, 0.5H), 3.79 – 3.67 (m, 2H), 3.62 (td, J = 8.7, 6.5 Hz, 0.5H), 3.54 (td, J = 8.7, 6.5 Hz, 0.5H), 3.33 – 3.26 (m, 0.5H), 3.14 (ddd, J = 29.3, 10.2, 7.4 Hz, 1H), 2.97 (ddd, J = 9.7, 7.4, 5.4 Hz, 1H), 2.66 (dd, J = 10.2, 2.7 Hz, 1H), 2.51 (s, 3H), 2.43 (dd, J = 9.7, 1.7 Hz, 1H), 2.22 (d, J = 1.5 Hz, 3H), 2.06 (dd, J = 14.1, 7.9 Hz, 0.5H), 1.96 – 1.79 (m, 1H), 1.48 (d, J = 13.4 Hz, 0.5H).

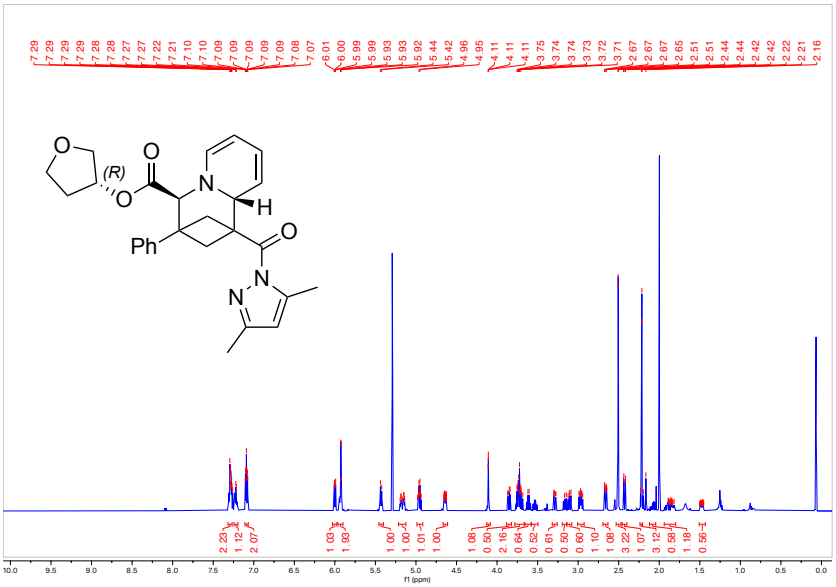

^{13}C NMR (126 MHz, $CDCl_3$, 292 K, ppm): δ 171.84, 171.83, 170.52, 170.47, 151.34, 142.98, 142.58, 142.55, 134.56, 134.43, 127.26, 125.85, 125.23, 125.21, 124.97, 124.93, 124.89, 110.24, 110.18, 109.95, 97.48, 97.29, 76.27, 76.02, 75.76, 74.28, 74.17, 72.10, 71.63, 69.66, 69.64, 65.82, 65.77, 58.14, 58.07, 52.41, 48.45, 48.37, 41.82, 41.80, 38.78, 38.65, 36.59, 36.53, 31.97, 31.33, 13.28, 12.92, 12.90.

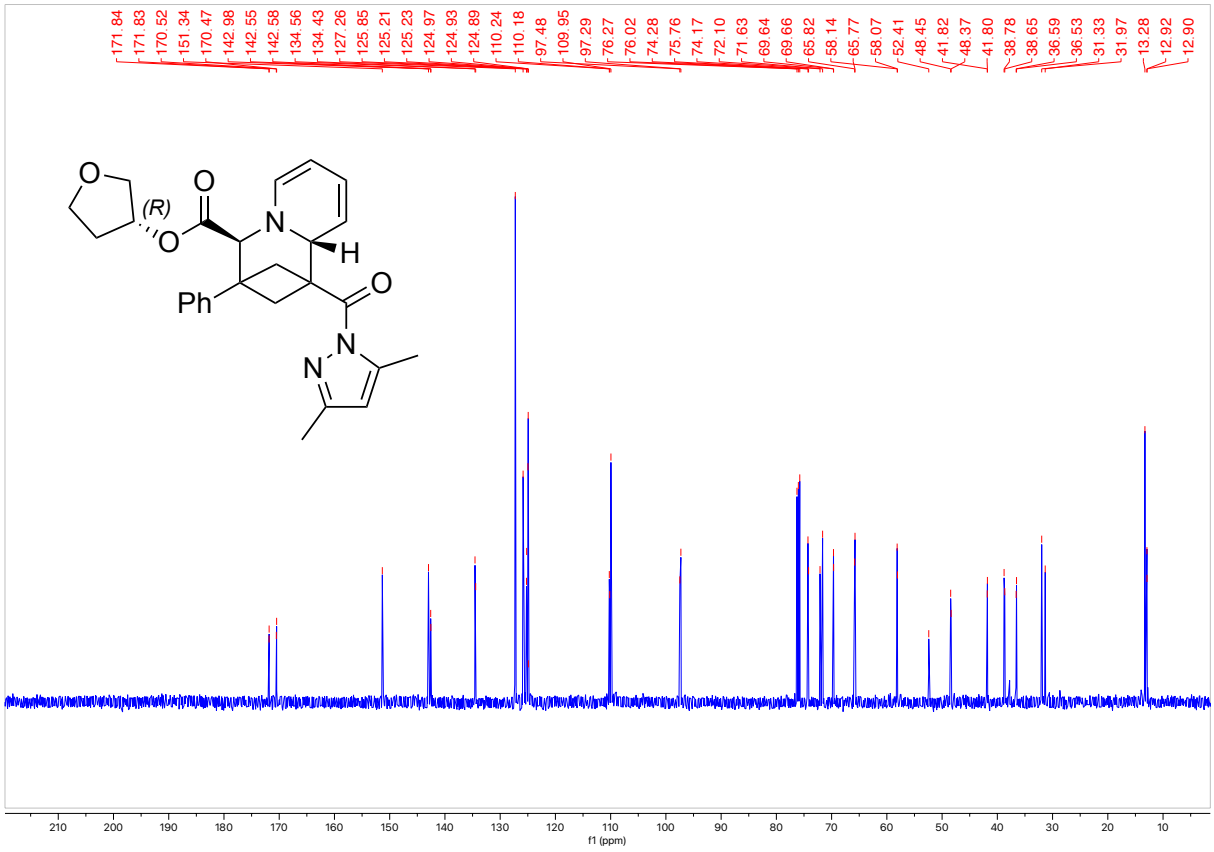

(3,5-Dimethyl-1H-pyrazol-1-yl)(3-phenyl-4-(thiophene-2-carbonyl)-3,4-dihydro-2H-1,3-methanoquinolizin-1(9aH)-yl)methanone (3w)

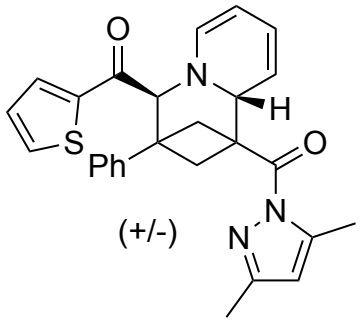

Product was synthesized following general procedure B on a 0.30 mmol scale. Reagent amounts used: bicyclobutane **1a** (75.7 mg, 0.30 mmol), pyridinium **2w** (1.25 equiv, 106.6 mg, 0.38 mmol), $NaPF_6$ (1.3 equiv, 65.5 mg), and K_3PO_4 (2.5 equiv, 159.2 mg, 0.75 mmol) in 1.2 mL acetonitrile (0.25 M). Isolated 21.7 mg of an orange solid (16% yield).

HRMS(ESI): calc'd for $[C_{31}H_{31}N_3O_4 + H^+]$, 456.17403; found: 456.17402.

^{1}H NMR (500 MHz, $CDCl_3$, 292 K, ppm): δ 7.44 (dd, J = 4.9, 1.1 Hz, 1H), 7.12 – 7.07 (m, 2H), 7.06 – 7.01 (m, 1H), 7.00 – 6.97 (m, 2H), 6.86 (dd, J = 3.9, 1.1 Hz, 1H), 6.72 (dd, J = 4.9, 3.9 Hz, 1H), 5.99 – 5.91 (m, 3H), 5.57 (s, 1H), 4.97 (ddd, J = 7.0, 5.5, 1.4 Hz, 1H), 4.85 (s, 1H), 4.69 (ddt, J = 9.5, 2.2, 1.1 Hz, 1H), 3.41 (dd, J = 10.3, 7.4 Hz, 1H), 3.11 (dd, J = 9.6, 7.4 Hz, 1H), 2.59 – 2.53 (m, 2H), 2.52 (s, 3H), 2.24 (s, 3H), 1.26 (s, 3H).

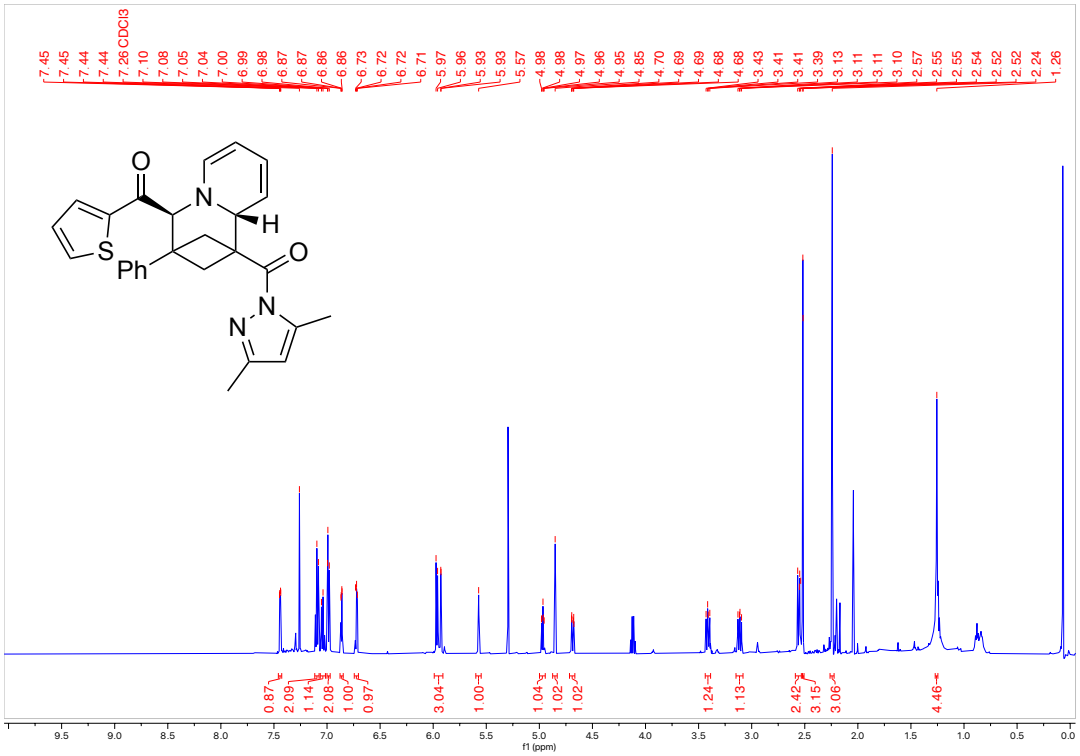

^{13}C NMR (126 MHz, $CDCl_3$, 292 K, ppm): δ 193.97, 173.22, 152.50, 144.62, 144.08, 144.06, 136.09, 134.31, 132.61, 128.30, 128.26, 128.01, 126.91, 126.45, 126.27, 126.23, 111.12, 111.04, 98.95, 72.74, 59.86, 49.53, 43.95, 39.46, 37.88, 29.85, 14.46, 14.11.

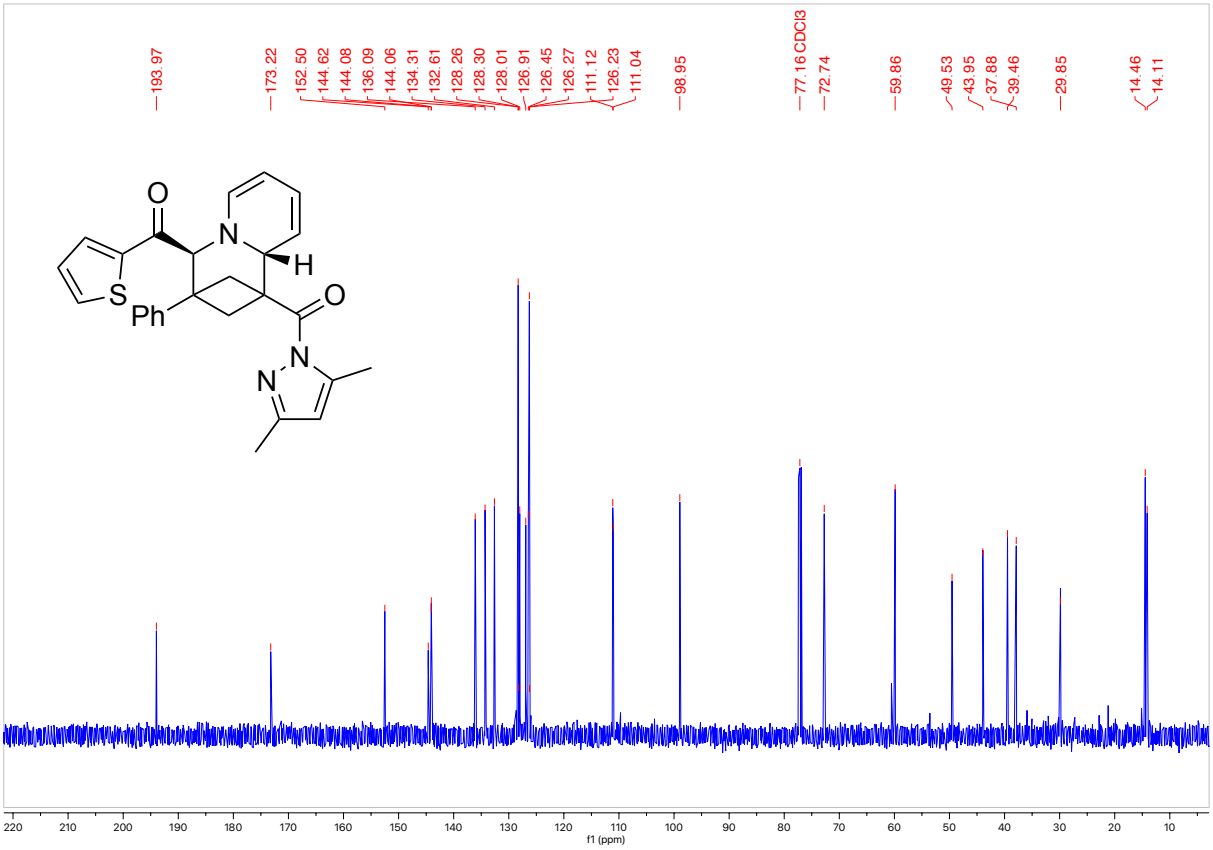

(3,5-Dimethyl-1H-pyrazol-1-yl)(-4-(4-methylbenzoyl)-3-phenyl-3,4-dihydro-2H-1,3-methanoquinolizin-1(9aH)-yl)methanone (3x)

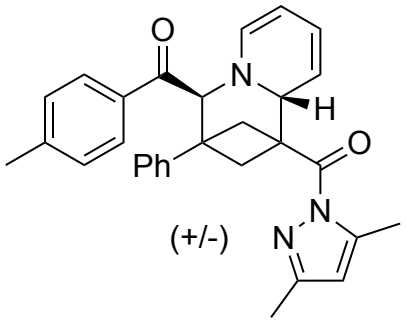

Product was synthesized following general procedure B on a 0.30 mmol scale. Reagent amounts used: bicyclobutane **1a** (75.7 mg, 0.30 mmol), pyridinium **2x** (1.25 equiv, 109.2 mg, 0.38 mmol), $NaPF_6$ (1.3 equiv, 65.5 mg, 0.39 mmol) and K_3PO_4 (2.5 equiv, 159.2 mg, 0.75 mmol) in 1.2 mL acetonitrile (0.25 M). Isolated 109.1 mg of an orange solid (78% yield).

HRMS(ESI): calc'd for $[C_{30}H_{29}N_3O_2 + H^+]$, 464.23326; found: 464.23339.

^{1}H NMR (500 MHz, $CDCl_3$, 292 K, ppm): δ 7.27 – 7.24 (m, 2H), 7.05 – 6.98 (m, 3H), 6.94 – 6.87 (m, 4H), 5.97 – 5.92 (m, 2H), 5.91 (d, J = 7.0 Hz, 1H), 5.59 (t, J = 2.4 Hz, 1H), 5.11 (s, 1H), 4.93 (ddd, J = 6.9, 5.4, 1.3 Hz, 1H), 4.66 (ddt, J = 9.2, 2.2, 1.0 Hz, 1H), 3.37 (dd, J = 10.1, 7.4 Hz, 1H), 3.14 (dd, J = 9.5, 7.4 Hz, 1H), 2.55 – 2.47 (m, 5H), 2.26 (s, 3H), 2.25 (s, 3H).

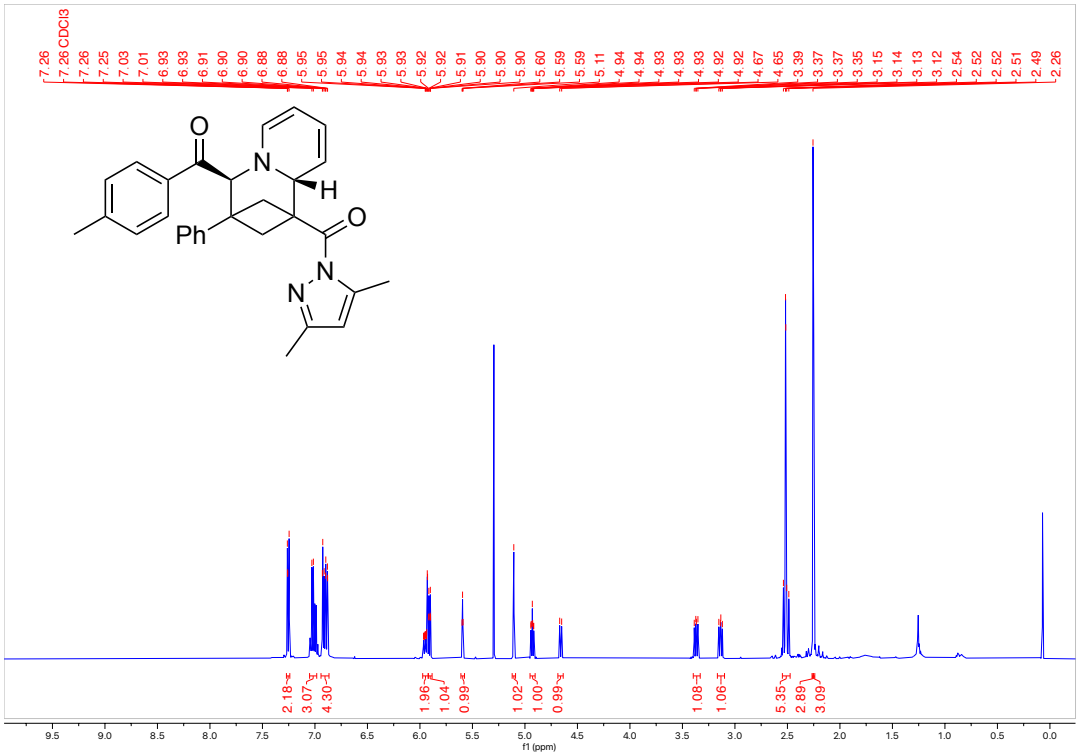

^{13}C NMR (126 MHz, $CDCl_3$, 292 K, ppm): δ 201.44, 173.33, 152.48, 144.06, 143.99, 143.59, 136.34, 135.44, 128.80, 128.77, 128.24, 128.16, 126.71, 126.46, 126.35, 111.11, 110.77, 98.47, 70.52, 59.91, 49.61, 43.83, 39.46, 38.04, 21.65, 14.48, 14.14.

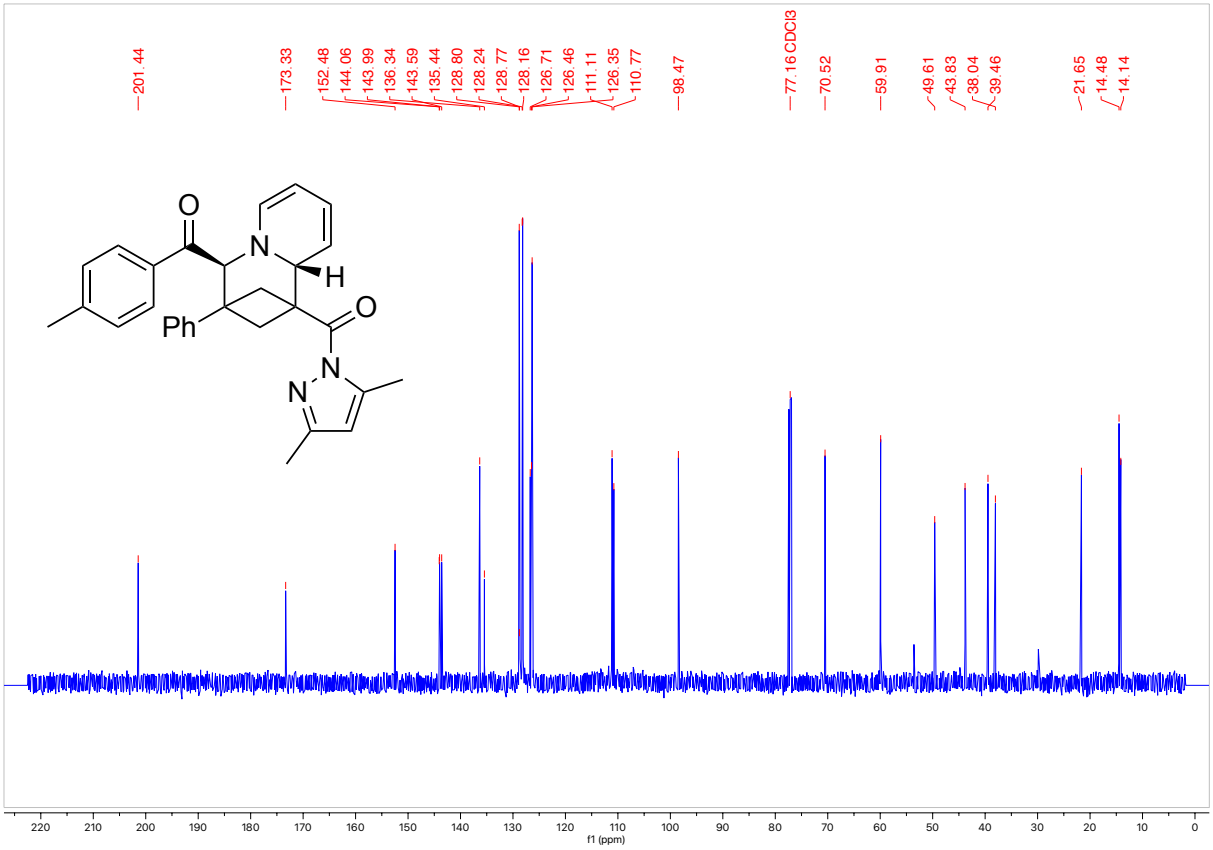

(4-(4-Chlorobenzoyl)-3-phenyl-3,4-dihydro-2H-1,3-methanoquinolizin-1(9aH)-yl)(3,5-dimethyl-1H-pyrazol-1-yl)methanone (3y)

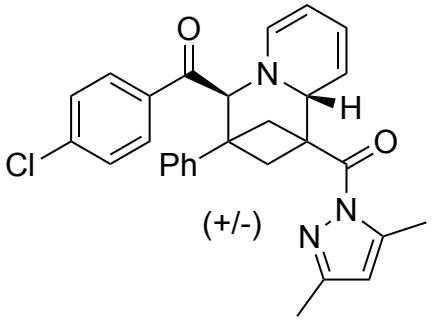

Product was synthesized following general procedure B on a 0.30 mmol scale. Reagent amounts used: bicyclobutane **1a** (75.7 mg, 0.30 mmol), pyridinium **2y** (1.25 equiv, 116.8 mg, 0.38 mmol), $NaPF_6$ (1.3 equiv, 65.5 mg, 0.39 mmol) and K_3PO_4 (2.5 equiv, 159.2 mg, 0.75 mmol) in 1.2 mL acetonitrile (0.25 M). Isolated 122.5 mg of an orange solid (84% yield).

HRMS(ESI): calc'd for $[C_{29}H_{26}ClN_3O_2 + H^+]$, 484.17863; found: 484.17963.

^{1}H NMR (500 MHz, $CDCl_3$, 292 K, ppm): δ 7.29 (dd, J = 8.7, 2.0 Hz, 2H), 7.10 – 7.04 (m, 5H), 6.95 – 6.90 (m, 2H), 6.00 – 5.94 (m, 2H), 5.91 (d, J = 7.0 Hz, 1H), 5.60 (s, 1H), 5.10 (s, 1H), 4.98 (ddd, J = 6.9, 5.4, 1.4 Hz, 1H), 4.70 (ddd, J = 9.4, 2.3, 1.1 Hz, 1H), 3.29 (dd, J = 10.2, 7.4 Hz, 1H), 3.16 (dd, J = 9.5, 7.4 Hz, 1H), 2.58 – 2.51 (m, 5H), 2.28 (s, 3H).

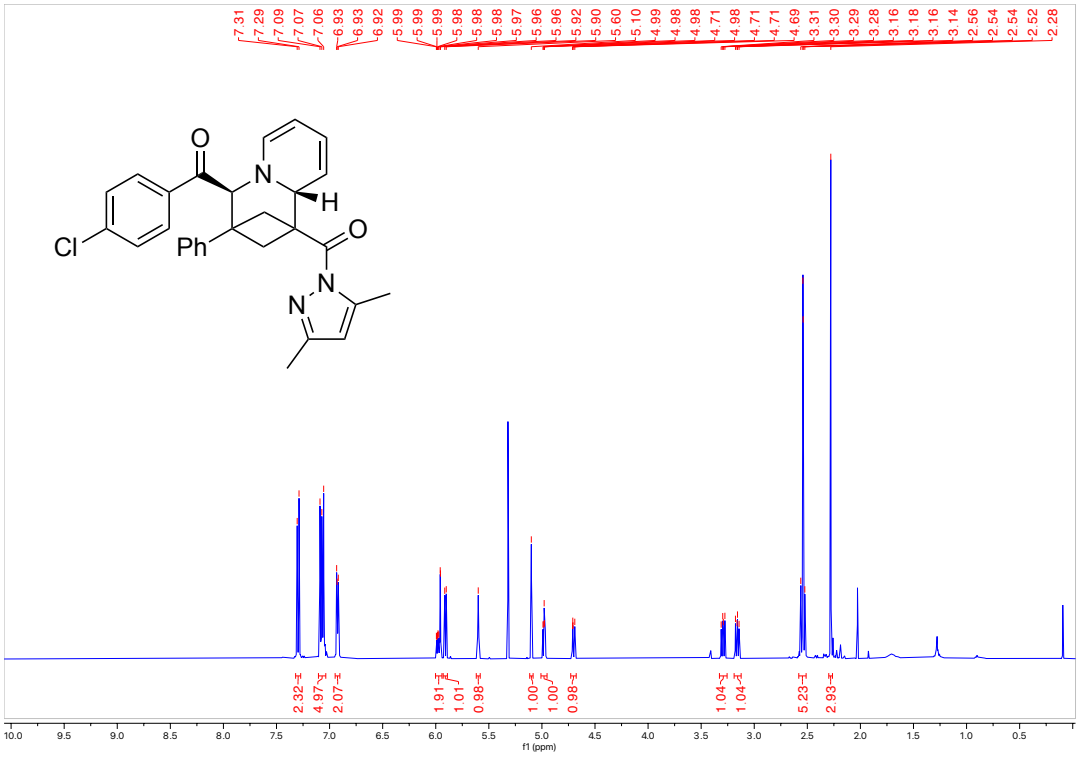

^{13}C NMR (126 MHz, $CDCl_3$, 292 K, ppm): δ 200.83, 173.15, 152.54, 144.10, 143.71, 139.24, 136.15, 136.11, 129.35, 128.43, 128.40, 128.39, 128.35, 127.00, 126.46, 126.30, 111.16, 111.03, 98.84, 71.05, 59.89, 49.51, 43.80, 43.80, 39.34, 37.97, 14.47, 14.14, 14.13.

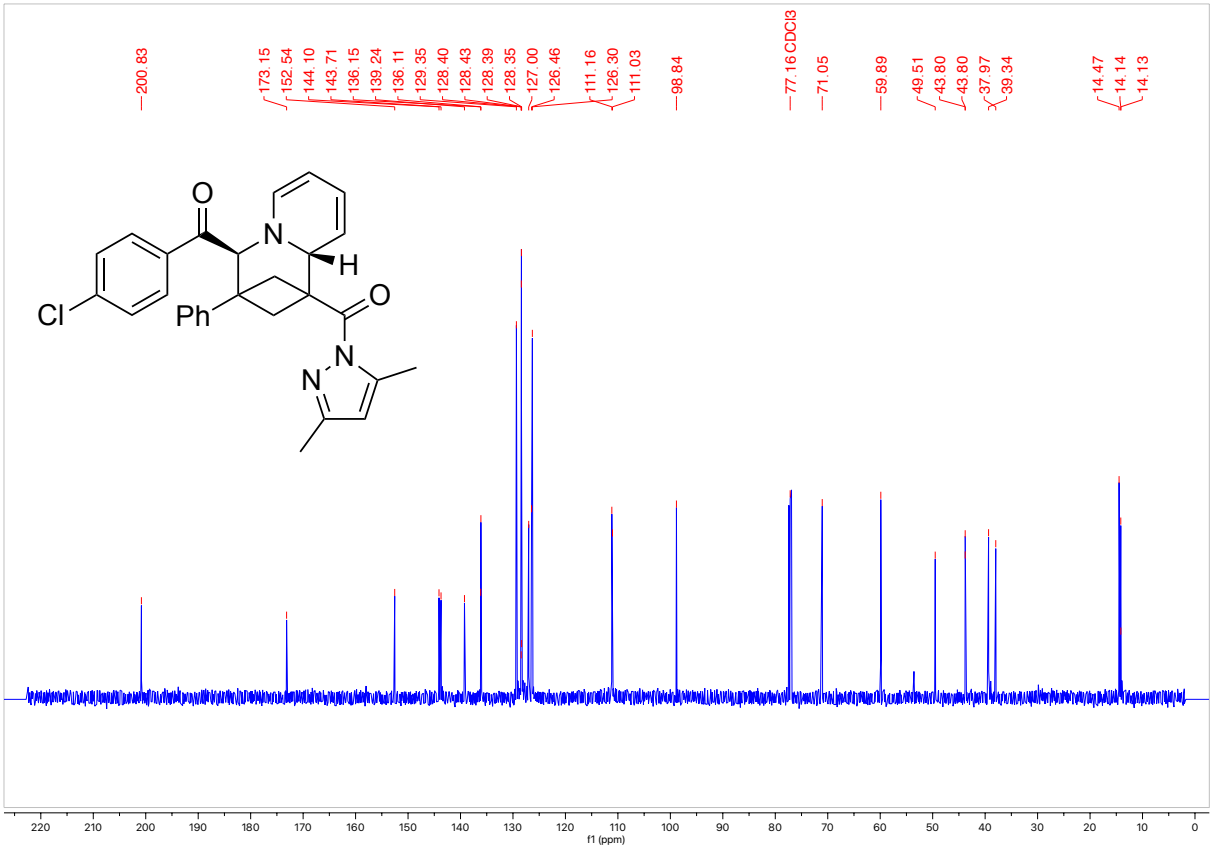

(3,5-Dimethyl-1H-pyrazol-1-yl)(4-(4-fluorobenzoyl)-3-phenyl-3,4-dihydro-2H-1,3-methanoquinolizin-1(9aH)-yl)methanone (3z)

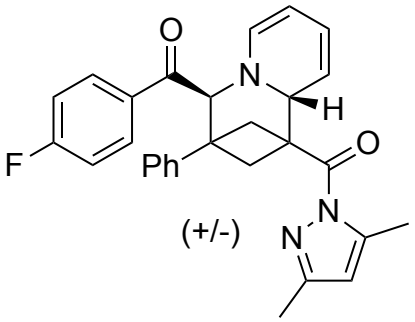

Product was synthesized following general procedure B on a 0.30 mmol scale. Reagent amounts used: bicyclobutane **1a** (75.7 mg, 0.30 mmol), pyridinium **2z** (1.25 equiv, 111.1 mg, 0.38 mmol), $NaPF_6$ (1.3 equiv, 65.5 mg), and K_3PO_4 (2.5 equiv, 159.2 mg, 0.75 mmol) in 1.2 mL acetonitrile (0.25 M). Isolated 101.7 mg of an orange oil (61% yield).

HRMS(ESI): calc'd for $[C_{31}H_{31}N_3O_4 + H^+]$, 468.20819; found: 468.20805.

^{1}H NMR (500 MHz, $CDCl_3$, 292 K, ppm): δ 7.20 – 7.11 (m, 2H), 6.75 (m, 3H), 6.67 (m, 2H), 6.58 – 6.48 (m, 2H), 5.77 (s, 1H), 5.73 – 5.62 (m, 2H), 5.26 (s, 1H), 4.97 (s, 1H), 4.61 (ddt, J = 7.7, 5.4, 1.1 Hz, 1H), 4.30 (dddd, J = 9.4, 2.3, 1.4, 0.8 Hz, 1H), 2.89 – 2.79 (m, 2H), 2.24 (m, 4H), 2.19 – 2.13 (m, 1H), 1.99 (d, J = 0.9 Hz, 3H).

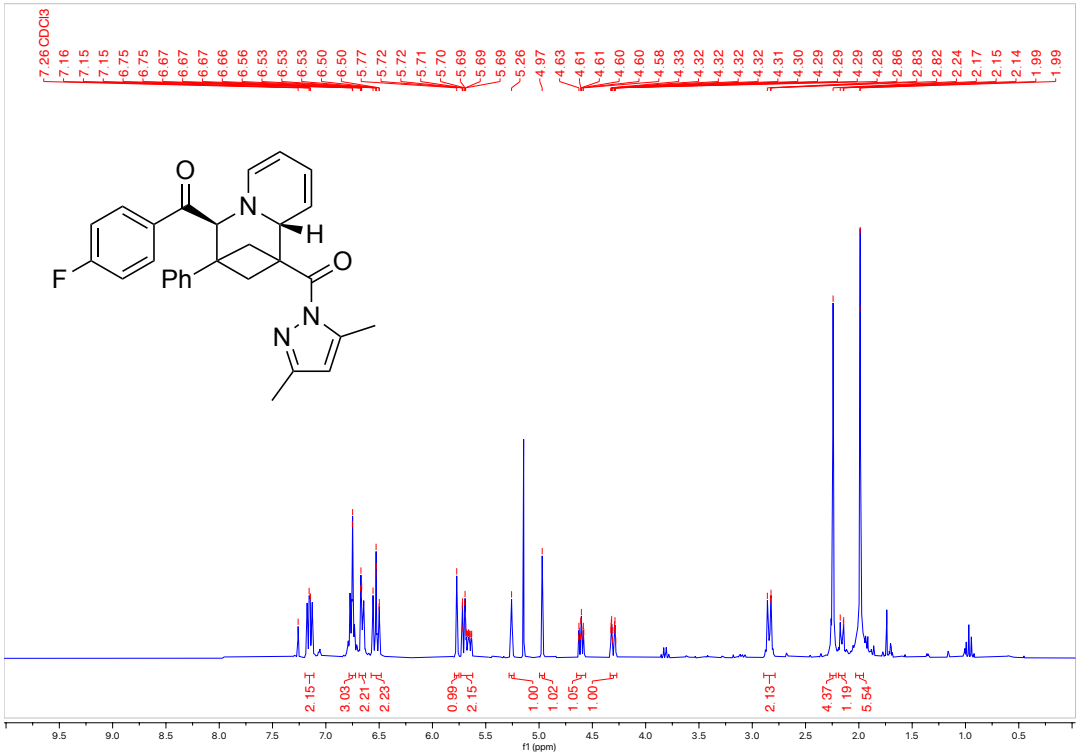

^{19}F NMR (300 MHz, $CDCl_3$, 292 K, ppm): δ 106.86.

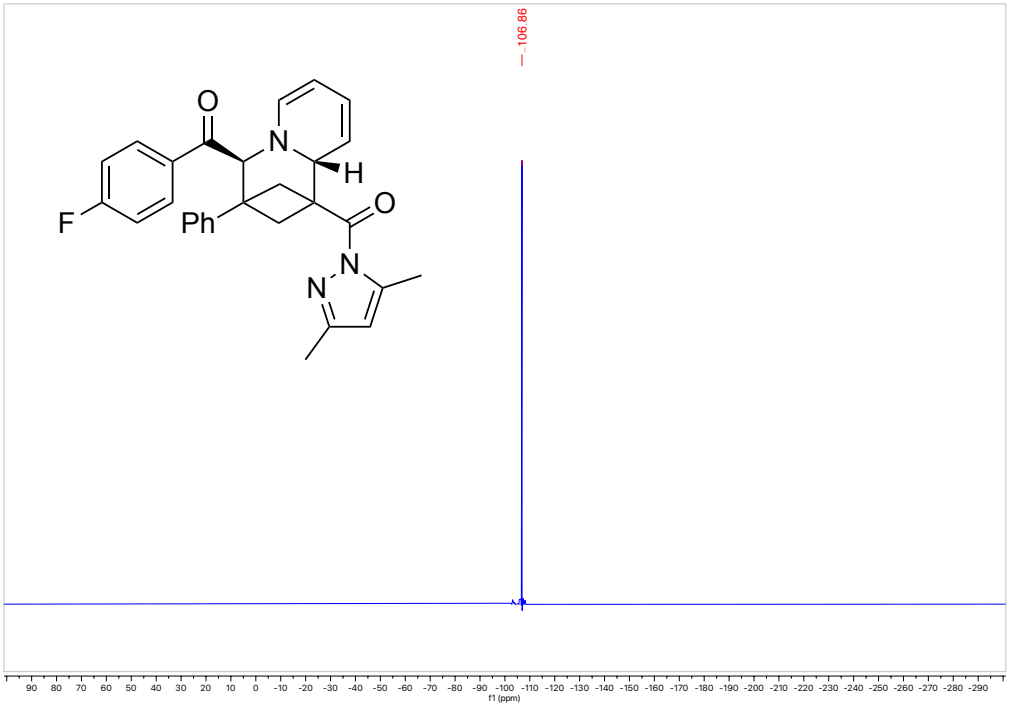

^{13}C NMR (126 MHz, $CDCl_3$, 292 K, ppm): δ 199.58, 172.01, 166.03, 162.68, 151.59, 143.35, 142.94, 136.02, 133.68, 133.65, 130.02, 129.90, 127.34, 125.89, 125.79, 125.55, 116.34, 114.28, 113.99, 110.23, 109.40, 96.63, 69.93, 59.17, 48.85, 42.70, 38.35, 37.12, 13.18, 12.78.

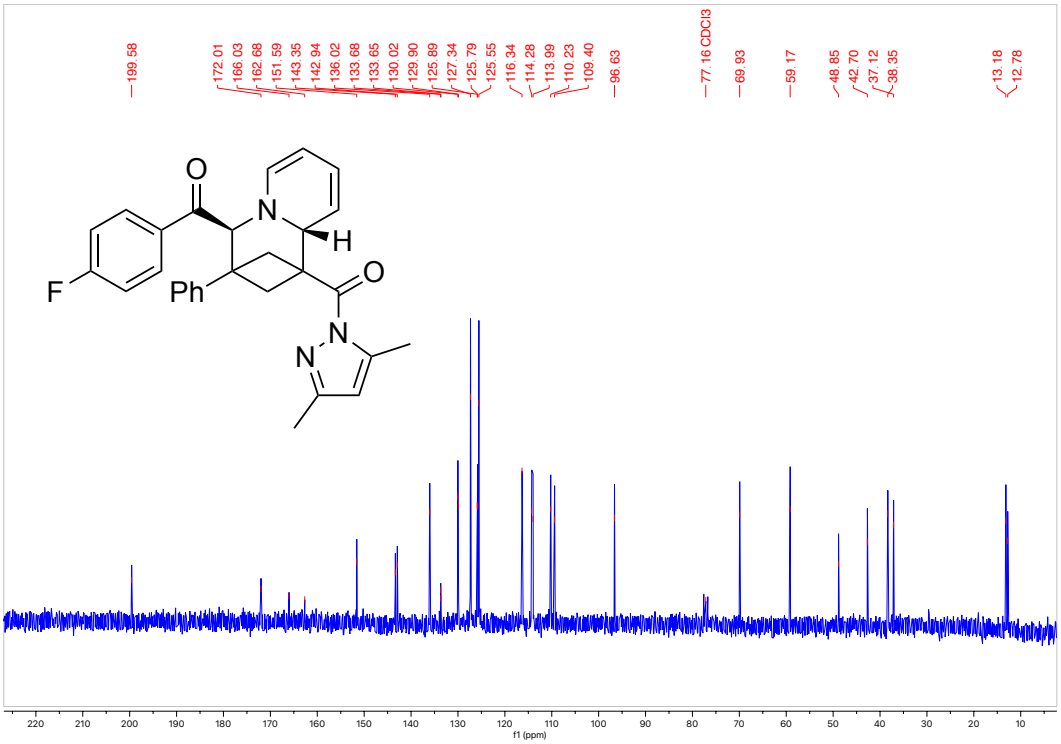

4-(Cyclopropanecarbonyl)-3-phenyl-3,4-dihydro-2H-1,3-methanoquinolizin-1-(9aH)-yl)(3,5-dimethyl-1H-pyrazol-1-yl)methanone (3aa)

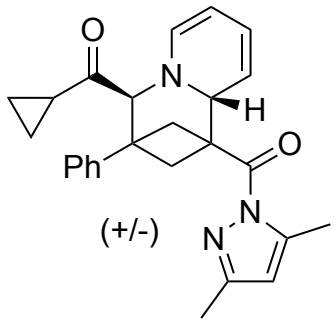

Product was synthesized following general procedure B on a 0.30 mmol scale. Reagent amounts used: bicyclobutane **1a** (75.7 mg, 0.30 mmol), pyridinium **2aa** (1.25 equiv, 90.8 mg, 0.38 mmol), $NaPF_6$ (1.3 equiv, 65.5 mg), and K_3PO_4 (2.5 equiv, 159.2 mg, 0.75 mmol) in 1.2 mL acetonitrile (0.25 M). Isolated 92.8 mg of an orange solid (75% yield).

HRMS(ESI): calc'd for $[C_{31}H_{31}N_3O_4 + H^+]$, 414.21761; found: 414.21722.

^{1}H NMR (500 MHz, $CDCl_3$, 292 K, ppm): δ 7.34 – 7.29 (m, 2H), 7.25 – 7.18 (m, 3H), 6.05 (d, J = 1.2 Hz, 1H), 5.97 (d, J = 7.0, 1H), 5.89 (dddd, J = 9.4, 5.5, 2.2, 0.9 Hz, 1H), 5.36 (t, J = 2.3 Hz, 1H), 4.83 (ddd, J = 6.9, 5.4, 1.3 Hz, 1H), 4.53 – 4.46 (m, 2H), 2.97 (dd, J = 9.5, 7.3 Hz, 1H), 2.78 (dd, J = 10.1, 7.3 Hz, 1H), 2.64 (dd, J = 10.1, 0.9 Hz, 1H), 2.47 (d, J = 1.1 Hz, 3H), 2.30 (d, J = 9.5 Hz, 1H), 2.18 (s, 3H), 1.23 – 1.16 (m, 1H), 0.85 – 0.80 (m, 2H), 0.81 – 0.74 (m, 1H), 0.50 – 0.41 (m, 1H).

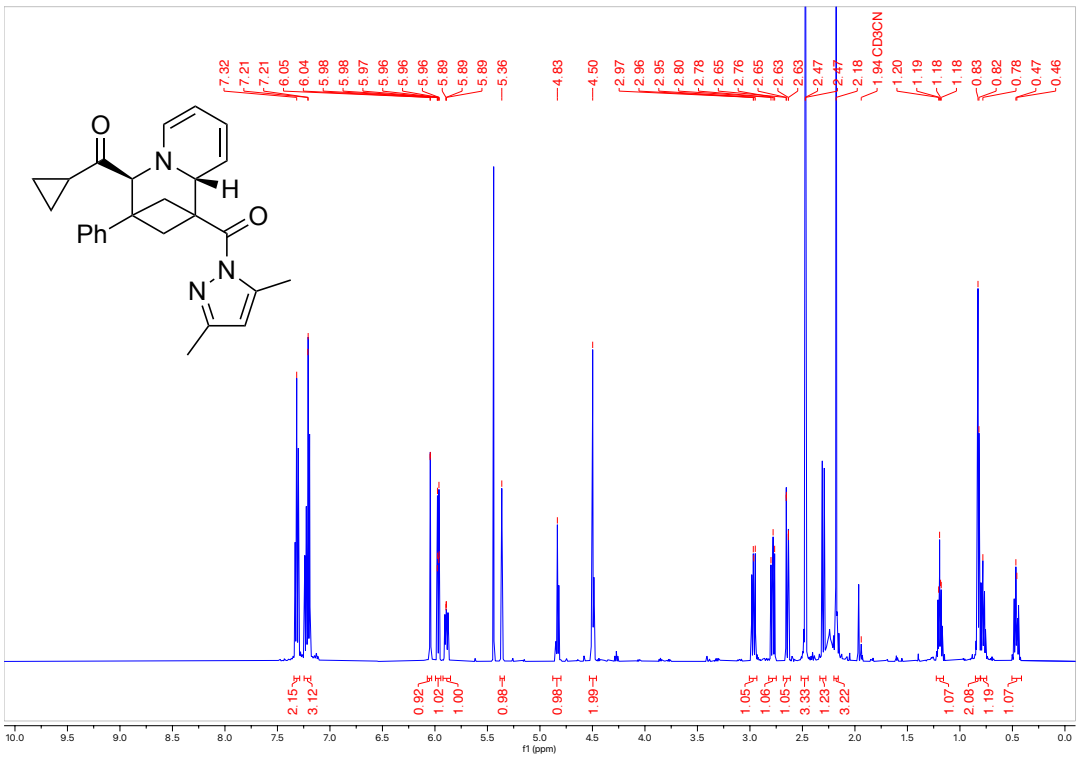

^{13}C NMR (126 MHz, $CDCl_3$, 292 K, ppm): δ 211.70, 173.55, 153.31, 145.25, 145.18, 137.89, 129.16, 127.71, 127.60, 127.31, 127.28, 118.27, 111.74, 110.62, 97.64, 78.03, 60.79, 50.51, 43.50, 43.49, 40.13, 39.09, 21.57, 14.48, 13.98, 13.14, 12.44.

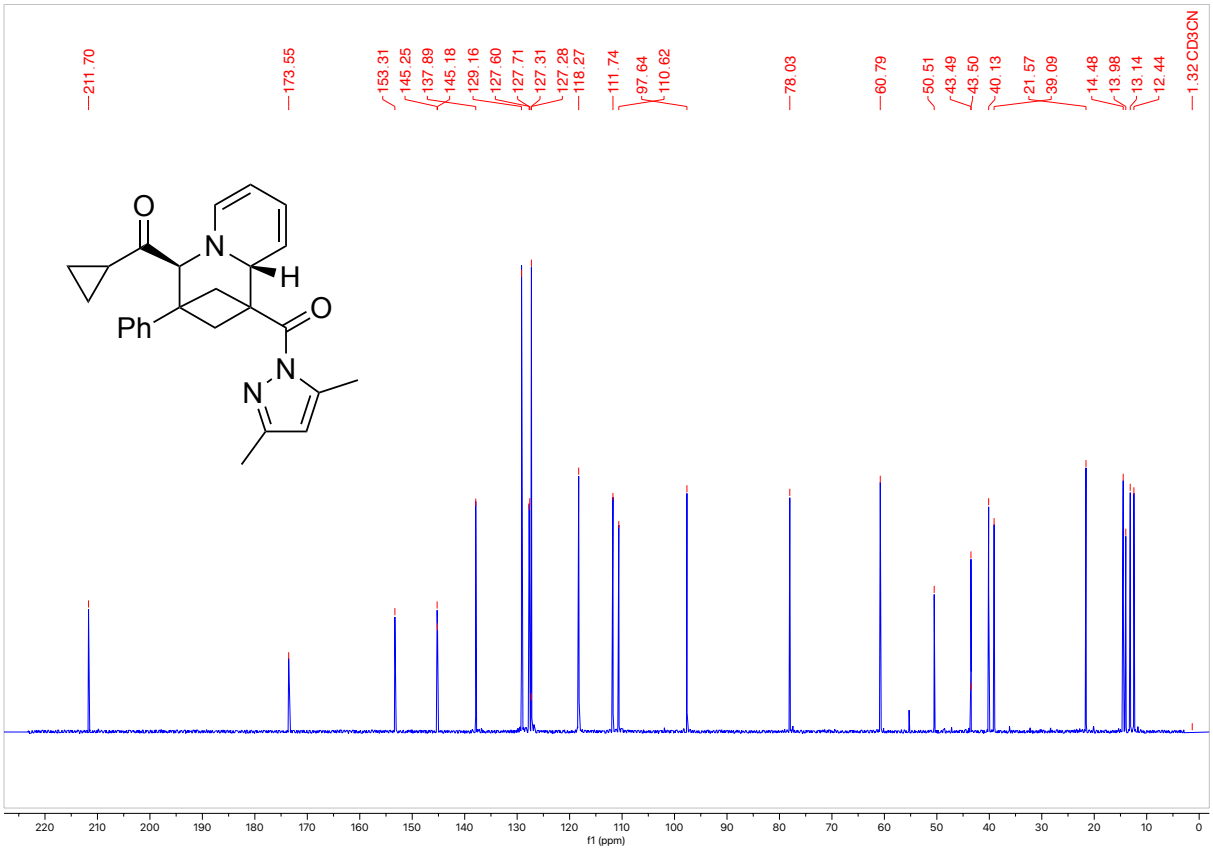

1-(1-(3,5-Dimethyl-1H-pyrazole-1-carbonyl)-3-phenyl-1,3,4,9a-tetrahydro-2H-1,3-methanoquinolizin-4-yl)-2,2-dimethylpropan-1-one (3ab)

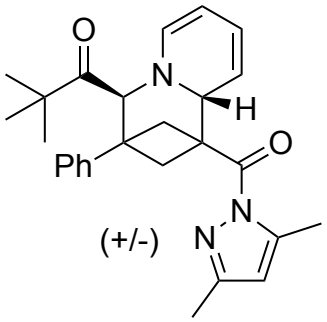

Product was synthesized following general procedure B on a 0.05 mmol scale. Reagent amounts used: bicyclobutane **1a** (12.6 mg, 0.05 mmol), pyridinium **2ab** (1.25 equiv, 16.1 mg, 0.06 mmol), $NaPF_6$ (1.3 equiv, 10.9 mg, 0.06 mmol) and K_3PO_4 (2.5 equiv, 26.4 mg, 0.13 mmol) in 0.2 mL acetonitrile (0.25 M). Solution yield determined by NMR spectroscopy using 1,3,5-trimethoxybenzene internal standard (48% solution yield, 5:1 d.r.).

HRMS(ESI): calc'd for $[C_{27}H_{31}N_3O_2 + H^+]$, 430.24891; found: 430.24905.

^{1}H NMR (500 MHz, $CDCl_3$, 292 K, ppm): Major diastereomer product peak at 5.6 ppm and minor at 5.2 ppm.

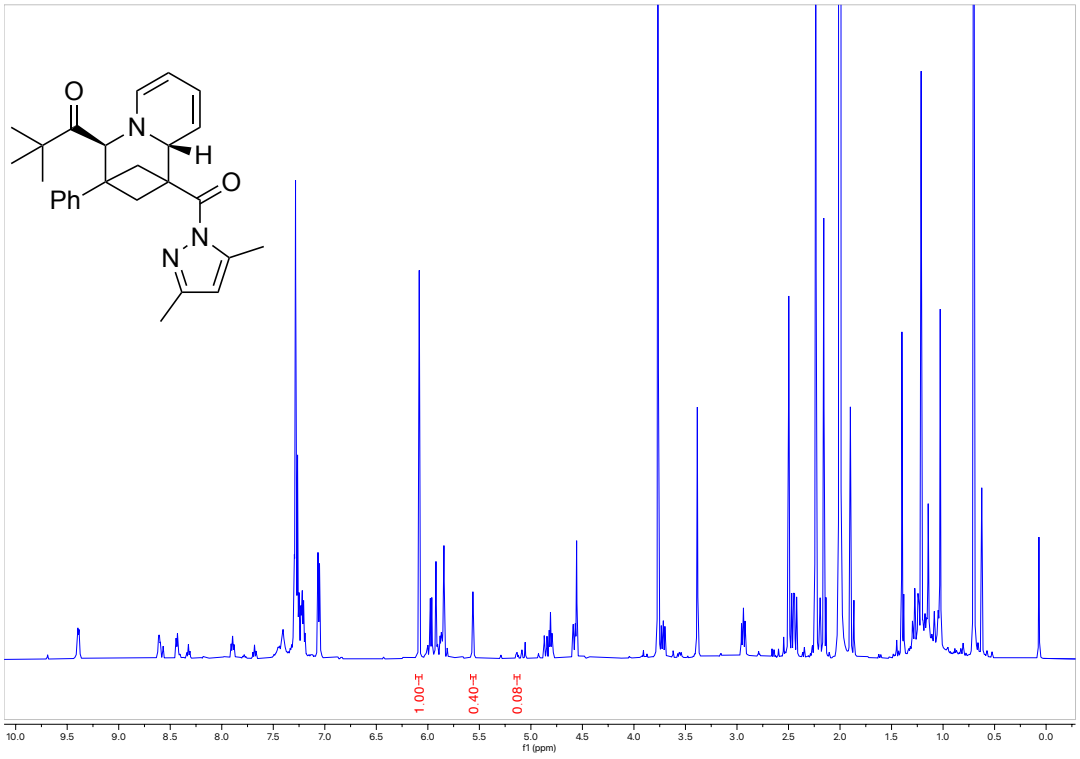

C.7 Larger Scale Synthesis

Methyl 1-(3,5-dimethyl-1H-pyrazole-1-carbonyl)-3-phenyl-1,3,4,9a-tetrahydro-2H-1,3-methanoquinolizine-4-carboxylate (3a)

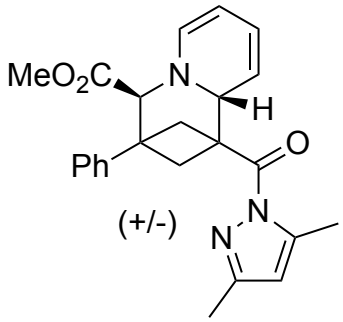

Product was synthesized following general procedure A on a 2.0 mmol scale. Reagent amounts used: bicyclobutane **1a** (504.6 mg, 2.0 mmol), pyridinium **2a** (1.25 equiv, 580.2 mg, 2.5 mmol), and K_3PO_4 (2.5 equiv, 1.0614 g, 5.0 mmol) in 8.0 mL acetonitrile (0.25 M). Isolated 655.0 mg of an orange solid (65% yield).

^{1}H NMR (500 MHz, $CDCl_3$, 292 K, ppm):

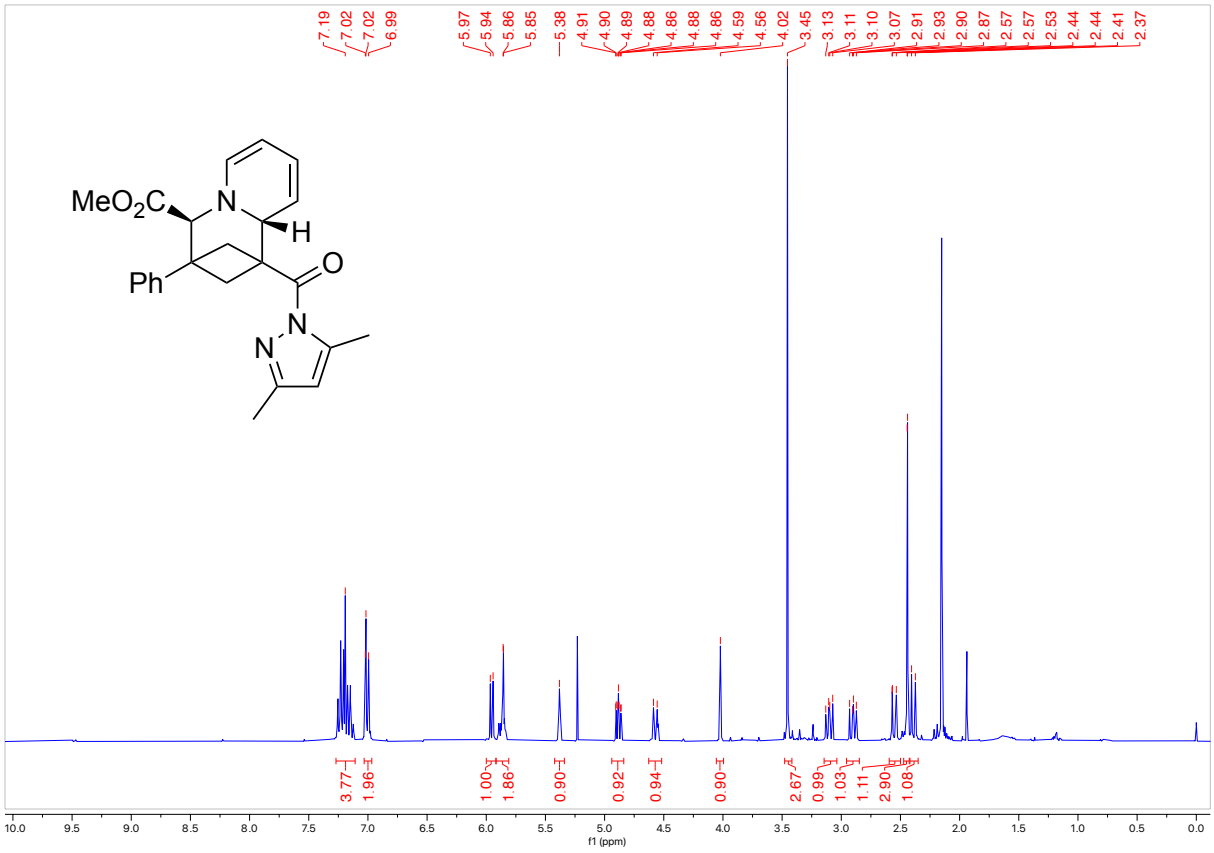

C.8 Diversification Reactions

Methyl 1-(4-methoxybenzoyl)-3-phenyl-1,3,4,6,7,9a-hexahydro-2H-1,3-methanoquinolizine-4-carboxylate (4i)

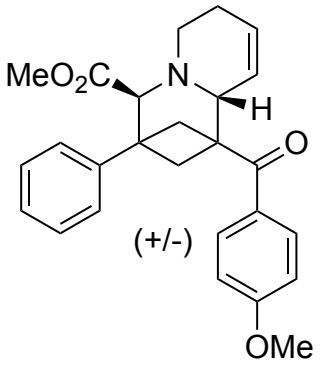

To a 4 mL vial was added the pyridinium salt **2i** (1.25 equiv, 46.2 mg, 0.20 mmol), K_3PO_4, (2.5 equiv, 84.9 mg, 0.40 mmol), bicyclobutane **1i** (1 equiv, 42.3 mg, 0.16 mmol) and a stir bar. Acetonitrile was added to the vial (0.64 mL, 0.25 M) and the reaction mixture was stirred for 24 hours at room temperature. The solvent was then evaporated, the residue redissolved in methanol and cooled down to 0 °C Then $NaBH_3CN$ (25.1 mg, 2.5 equiv, 0.40 mmol) and acetic acid (9.2 μL, 1 equiv, 0.16 mmol) was added to the cooled solution and it was allowed to warm to room temperature and left to stir overnight. The reaction mixture was quenched with $NaHCO_3$ (5 mL) and then extracted DCM (3 x 5 mL). The organic layers were combined then dried with Mg_2SO_4. The solution was filtered and the solvent was evaporated to give the crude product. The product was purified further by column chromatography (Biotage® Sfär 5g Column, 0-100% EtOAc/hexanes, eluted at 35% EtOAc) to obtain a white solid (16.5 mg, 25% Yield).

HRMS(ESI): calc'd for [$C_{26}H_{27}NO_4$ + H^+], 418.20129; found: 418.20115.

^{1}H NMR (500 MHz, $CDCl_3$, 292 K, ppm): δ 8.01 (d, J = 8.9 Hz, 2H), 7.26 (d, J = 15.0 Hz, 2H), 7.20 – 7.15 (m, 1H), 7.09 – 7.05 (m, 2H), 6.94 (d, J = 8.9 Hz, 2H), 5.97 (ddd, J = 7.1, 4.8, 2.8 Hz, 1H), 5.46 (ddt, J = 10.4, 2.9, 1.4 Hz, 1H), 4.56 (s, 1H), 3.88 (s, 3H), 3.83 (s, 1H), 3.64 – 3.59 (m, 1H), 3.30 (s, 3H), 3.14 (ddd, J = 14.0, 11.9, 4.1 Hz, 1H), 2.85 (dd, J = 14.1, 5.2 Hz, 1H), 2.45 – 2.34 (m, 3H), 2.26 (dd, J = 9.7, 7.4 Hz, 1H), 1.84 – 1.74 (m, 1H).

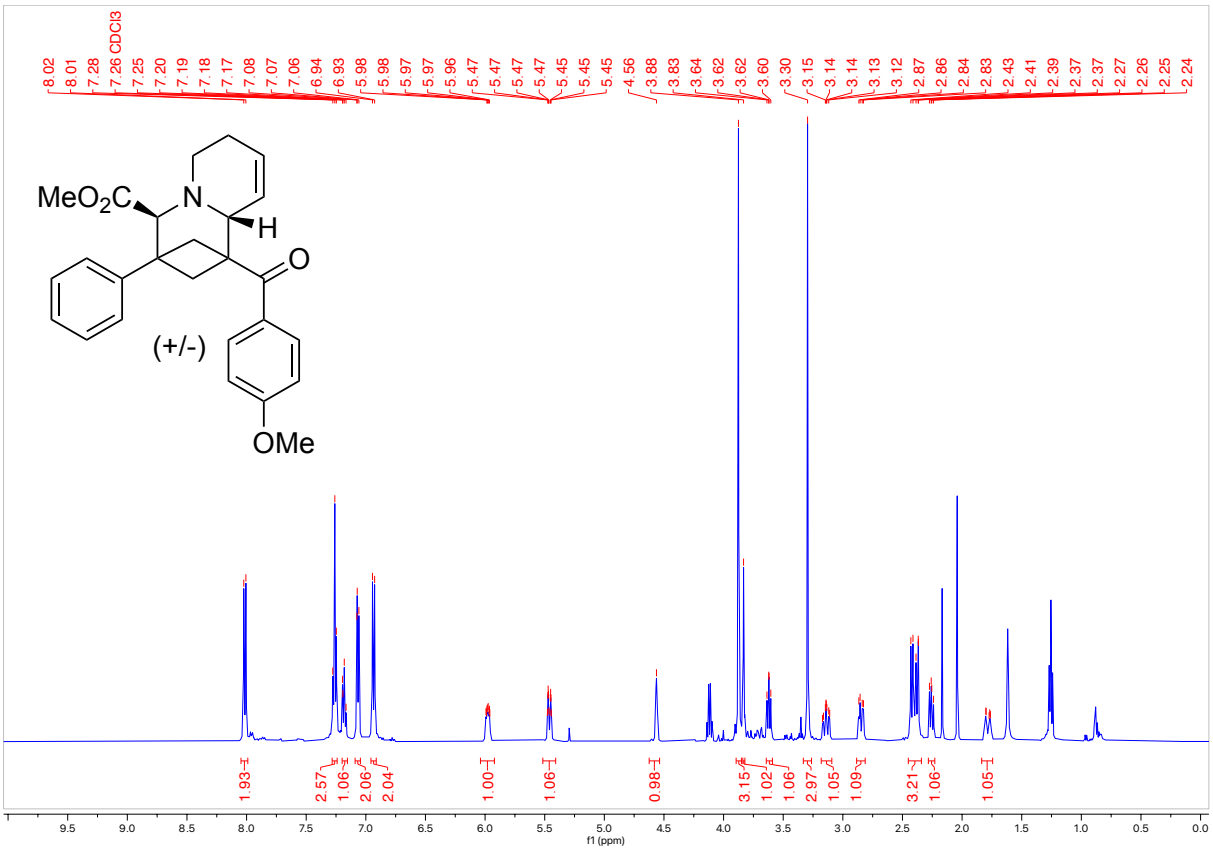

^{13}C NMR (126 MHz, $CDCl_3$, 292 K, ppm): δ 199.91, 173.29, 163.63, 143.88, 131.78, 128.21, 128.07, 127.93, 127.66, 126.83, 125.90, 113.89, 69.63, 58.51, 55.65, 51.53, 51.31, 46.08, 44.07, 38.71, 37.31, 19.42.

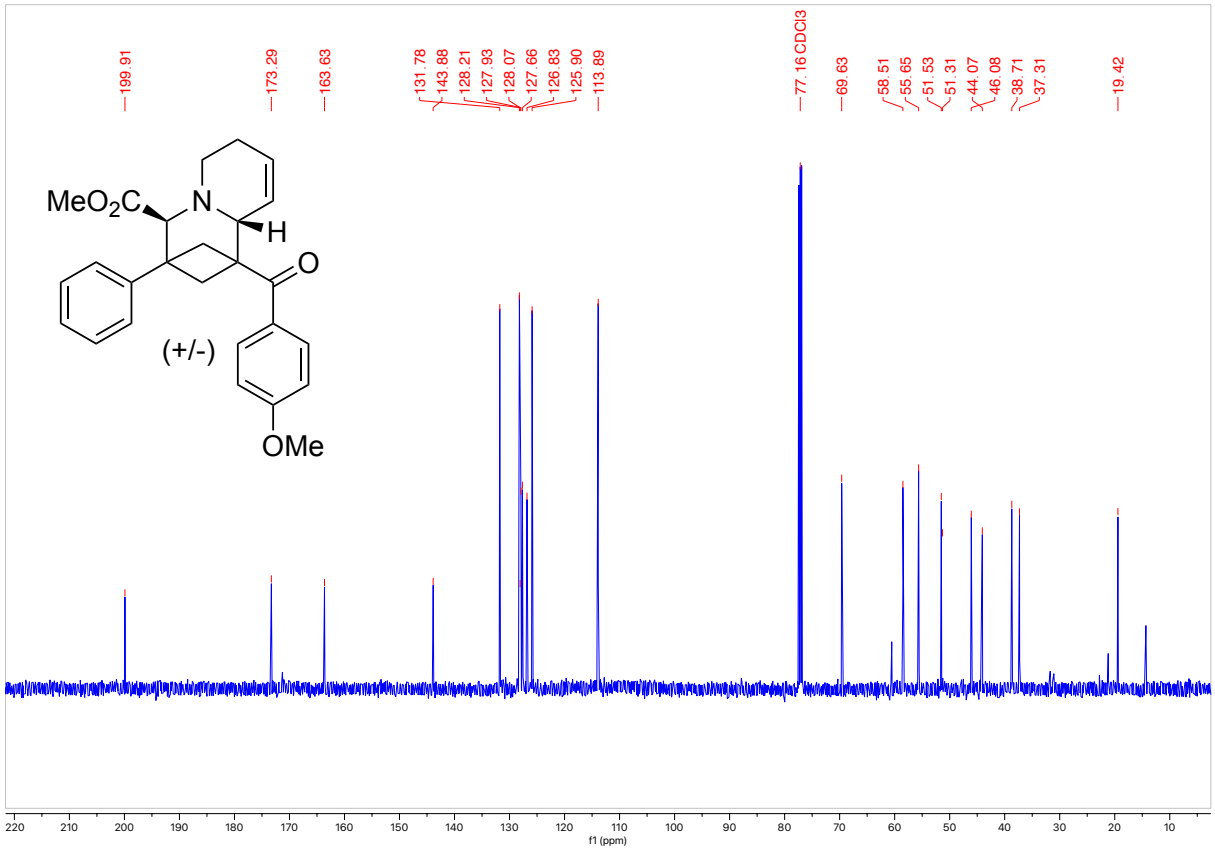

1-Methyl 4-(2-(trimethylsilyl)ethyl) 3-phenyl-3,4,7,9a-tetrahydro-2H-1,3-methano- quinolizine-1,4(6H)-dicarboxylate (4q)

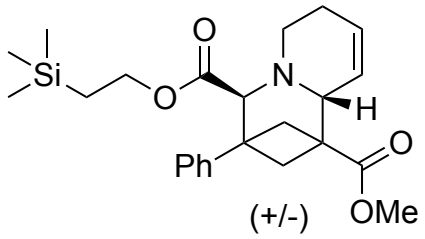

To a 4 mL vial was added the pyridinium salt **2q** (1.25 equiv, 119.4 mg, 0.38 mmol), K_3PO_4, (2.5 equiv, 159.2 mg, 0.75 mmol) and a stir bar. Acetonitrile (0.6 mL) was added, and the mixture stirred for 5 minutes at room temperature. Then, bicyclobutane **1a** (1 equiv, 75.7 g, 0.30 mmol) was weighed into a 1 mL vial. Using acetonitrile (0.6 mL), **1a** was quantitatively transferred to the reaction vial. The mixture was stirred for 24 hours at room temperature. Then, an equal volume of methanol (1.2 mL) and additional K_3PO_4 (1.0 equiv, 63.7 mg, 0.30 mmol) were added to the reaction mixture, which was stirred at rt for 24 hours. Then, the solvent was evaporated in vacuo and the residue was redissolved in methanol (3 mL), filtered quantitatively though a 0.45 μm syringe filter and the solution was cooled down to 0 °C. Then $NaBH_3CN$ (47.1 mg, 2.5 equiv, 0.75 mmol) and acetic acid (17.2 μL, 1 equiv, 0.30 mmol) was added to the reaction vial and it was allowed to warm to room temperature and left to stir overnight. The reaction mixture was quenched with $NaHCO_3$ (5 mL) and then extracted DCM (3 x 5 mL). The organic layers were combined then dried with Mg_2SO_4. The solution was filtered, and the solvent was evaporated to give the crude product. The product was purified further by column chromatography (Biotage® Sfär 5g Column, 0-100% EtOAc/hexanes, eluted at 25% EtOAc) to obtain a white solid (14.0 mg, 11% Yield over three steps).

HRMS(ESI): calc'd for [$C_{24}H_{33}NO_4Si + H^+$], 428.22517; found: 428.22500.

^{1}H NMR (500 MHz, $CDCl_3$, 292 K, ppm): δ 7.36 – 7.32 (m, 2H), 7.31 – 7.23 (m, 1H), 7.16 – 7.09 (m, 2H), 6.14 – 6.07 (m, 1H), 5.70 (ddt, J = 10.3, 2.8, 1.4 Hz, 1H), 4.53 – 4.44 (m, 1H), 3.90 (ddd, J = 11.8, 10.8, 5.7 Hz, 1H), 3.80 (s, 1H), 3.77 (s, 3H), 3.66 (ddd, J = 12.0, 10.8, 5.3 Hz, 1H), 3.30 – 3.17 (m, 2H), 2.89 (ddt, J = 14.1, 5.4, 1.2 Hz, 1H), 2.52 – 2.41 (m, 2H), 2.39 (d, J = 8.8 Hz, 1H), 2.15 (dd, J = 9.4, 7.5 Hz, 1H), 1.87 (ddt, J = 17.3, 4.2, 1.3 Hz, 1H), 0.62 (ddd, J = 13.7, 12.0, 5.7 Hz, 1H), 0.49 (ddd, J = 13.7, 11.8, 5.3 Hz, 1H), 0.00 (s, 9H).

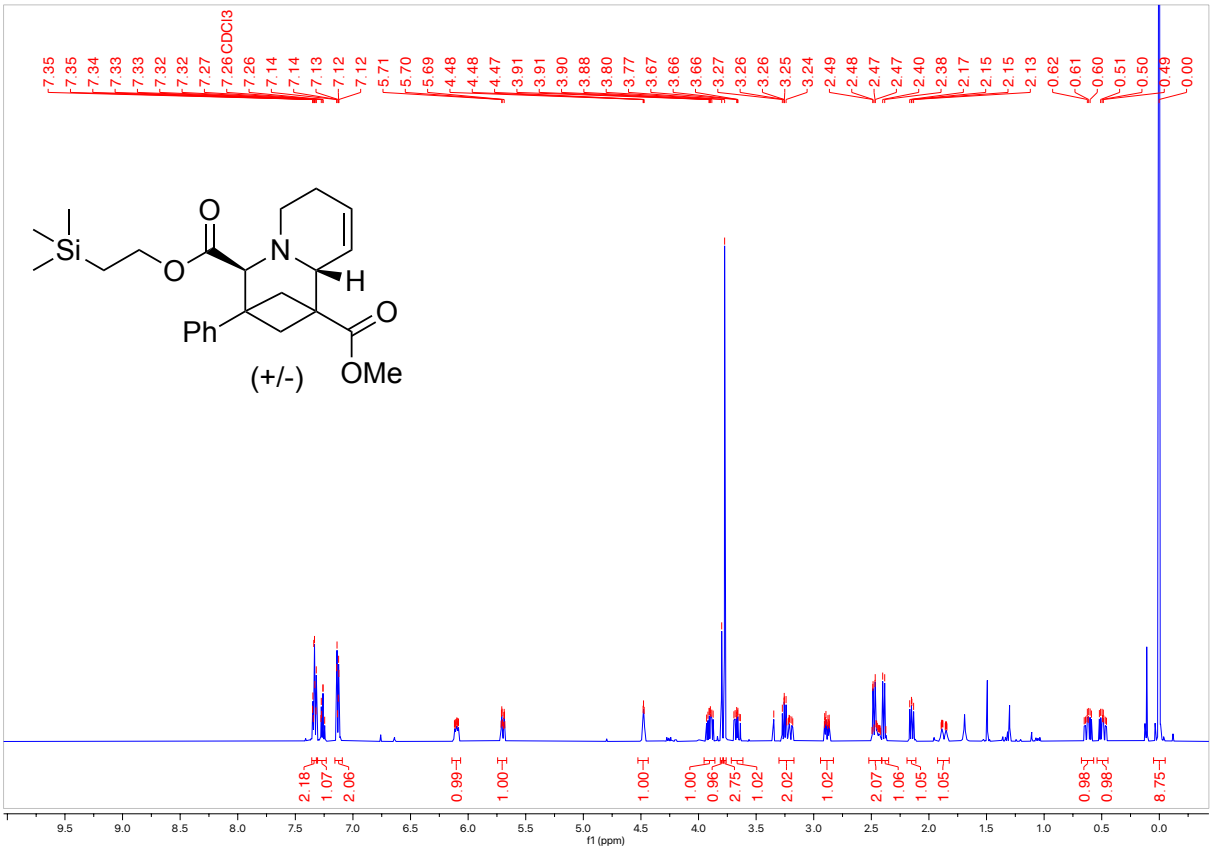

^{13}C NMR (126 MHz, $CDCl_3$, 292 K, ppm): δ 173.56, 172.89, 144.03, 128.82, 128.16, 128.14, 126.74, 126.07, 126.05, 69.23, 62.63, 57.20, 52.09, 45.89, 45.16, 44.71, 38.24, 35.76, 19.52, 17.02.

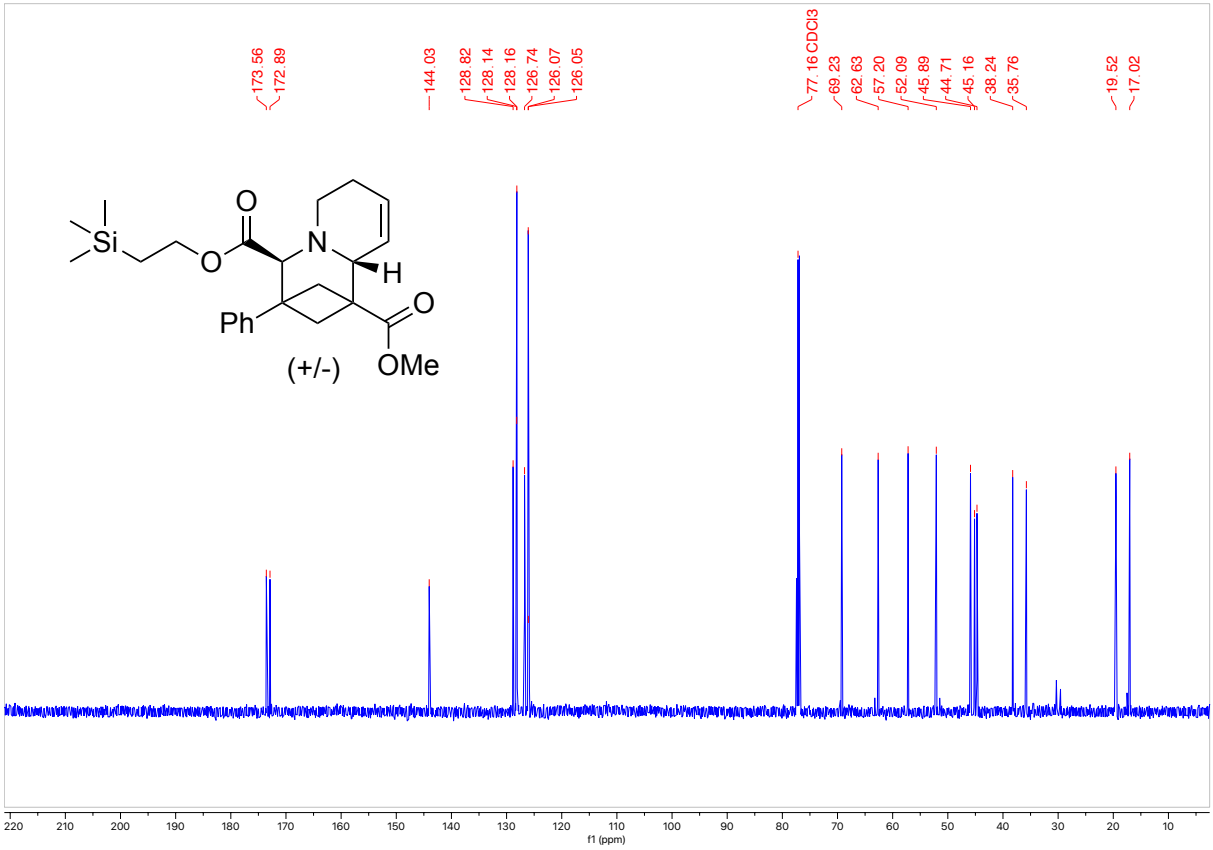

Methyl 3-phenyl-4-pivaloyl-3,4,7,9a-tetrahydro-2H-1,3-methanoquinolizine-1(6H)-carboxylate (4ab)

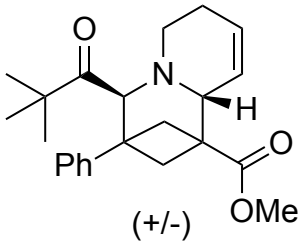

To a 4 mL vial was added the pyridinium salt **2ab** (1.25 equiv, 96.8 mg, 0.38 mmol), $NaPF_6$ (1.3 equiv, 65.5 mg, 0.39 mmol), and a stir bar. Acetonitrile (0.6 mL) was added, and the solution was stirred for 2 hours at room temperature. K_3PO_4, (2.5 equiv, 159.2 mg, 0.75 mmol) was added to the vial and the mixture stirred for 5 minutes at room temperature. Then, bicyclobutane **1a** (1 equiv, 75.7 g, 0.30 mmol) was weighed into a 1 mL vial. Using acetonitrile (0.6 mL), **1a** was quantitatively transferred to the reaction vial. The mixture was stirred for 24 hours at room temperature. Then, an equal volume of methanol (1.2 mL) and additional K_3PO_4 (1.0 equiv, 63.7 mg, 0.30 mmol) were added to the reaction mixture, which was stirred at rt for 24 hours. Then, the solvent was evaporated in vacuo and the residue was redissolved in methanol (3 mL), filtered quantitatively though a 0.45 μm syringe filter and the solution was cooled down to 0 °C. Then $NaBH_3CN$ (47.1 mg, 2.5 equiv, 0.75 mmol) and acetic acid (17.2 μL, 1 equiv, 0.30 mmol) was added to the reaction vial and it was allowed to warm to room temperature and left to stir overnight. The reaction mixture was quenched with $NaHCO_3$ (5 mL) and then extracted DCM (3 x 5 mL). The organic layers were combined then dried with Mg_2SO_4. The solution was filtered, and the solvent was evaporated to give the crude product. The product was purified further by column chromatography (Biotage® Sfär 5g Column, 0-100% EtOAc/hexanes, eluted at 25% EtOAc) to obtain a white solid (25.0 mg, 23% Yield (20% of the major diastereomer and 3% of the minor diastereomer isolated separately) over three steps).

HRMS(ESI): calc'd for [$C_{23}H_{29}NO_3$ + H^+], 368.22202; found: 368.22250.

^{1}H NMR (500 MHz, $CDCl_3$, 292 K, ppm): δ 7.29 – 7.22 (m, 2H), 7.22 – 7.12 (m, 1H), 7.05 – 6.95 (m, 2H), 6.08 – 5.96 (m, 1H), 5.61 (ddt, J = 10.4, 2.9, 1.4 Hz, 1H), 4.39 (m, 2H), 3.68 (s, 3H), 3.44 – 3.36 (m, 1H), 3.07 (ddd, J = 13.9, 11.9, 4.0 Hz, 1H), 2.78 – 2.68 (m, 1H), 2.46 – 2.32 (m, 2H), 2.23 – 2.12 (m, 2H), 1.89 – 1.77 (m, 1H), 0.63 (s, 9H).

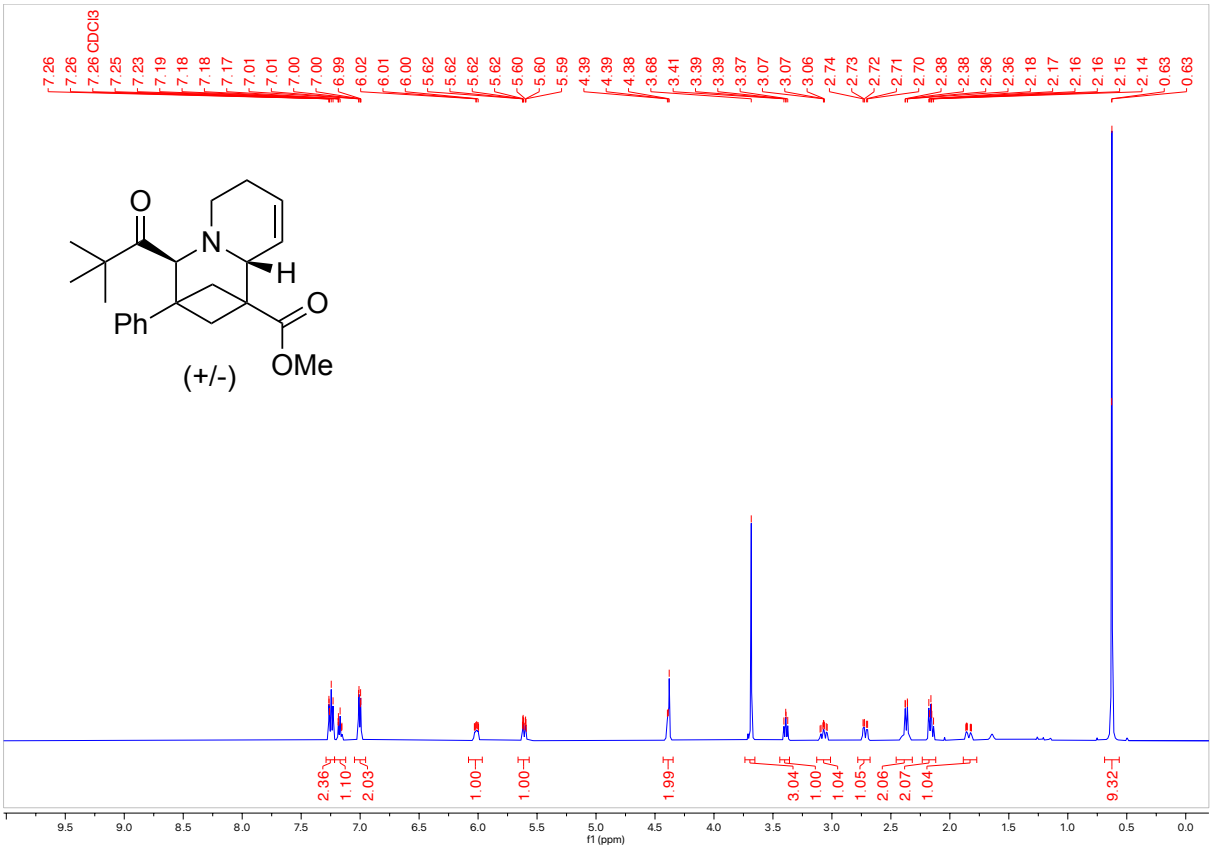

^{13}C NMR (126 MHz, $CDCl_3$, 292 K, ppm): δ 219.31, 173.62, 144.81, 129.15, 128.34, 127.77, 127.46, 126.91, 65.74, 57.74, 52.02, 46.25, 45.59, 45.18, 44.45, 38.34, 36.81, 26.96, 20.62.

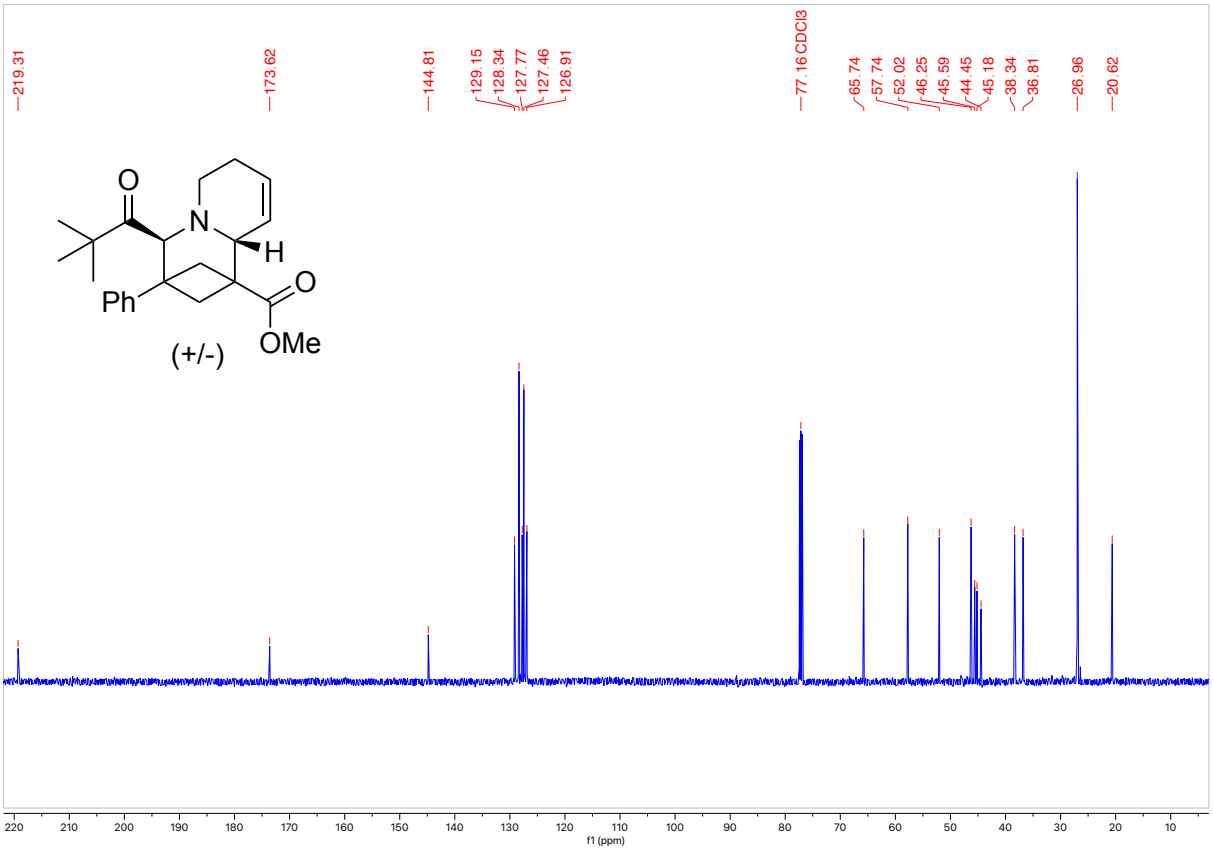

Methyl 3-phenyl-3,4-dihydro-2H-1,3-methanoquinolizine-1(9aH)-carboxylate (4o)

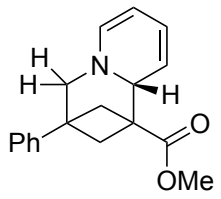

To a 4 mL vial was added the pyridinium salt **2o** (1.25 equiv, 74.3 mg, 0.38 mmol), K_3PO_4, (2.5 equiv, 159.2 mg, 0.75 mmol) and a stir bar. Acetonitrile (0.6 mL) was added, and the mixture stirred for 5 minutes at room temperature. Then, bicyclobutane **1a** (1 equiv, 75.7 g, 0.30 mmol) was weighed into a 1 mL vial. Using acetonitrile (0.6 mL), **1a** was quantitatively transferred to the reaction vial. The mixture was stirred for 24 hours at room temperature. Then, an equal volume of methanol (1.2 mL) and additional K_3PO_4 (1.0 equiv, 63.7 mg, 0.30 mmol) were added to the reaction mixture, which was stirred at rt for 24 hours. Then, the solvent was evaporated in vacuo and the residue was redissolved in methanol (3 mL), filtered quantitatively though a 0.45 μm syringe filter and the solution was cooled down to 0 °C. Then $NaBH_3CN$ (47.1 mg, 2.5 equiv, 0.75 mmol) and acetic acid (17.2 μL, 1 equiv, 0.30 mmol) was added to the reaction vial and it was allowed to warm to room temperature and left to stir overnight. The reaction mixture was quenched with $NaHCO_3$ (5 mL) and then extracted DCM (3 x 5 mL). The organic layers were combined then dried with Mg_2SO_4. The solution was filtered, and the solvent was evaporated to give the crude product. The product was purified further by column chromatography (Biotage® Sfär 5g Column, 0-100% EtOAc/hexanes, eluted at 35% EtOAc) to obtain a white solid (3.9 mg, 5% Yield over three steps).

HRMS(ESI): calc'd for [$C_{18}H_{21}NO_2$ + H^+], 284.16451; found: 284.16491.

^{1}H NMR (500 MHz, $CDCl_3$, 292 K, ppm): δ 7.34 – 7.29 (m, 2H), 7.25 – 7.16 (m, 1H), 7.17 – 7.11 (m, 2H), 6.03 – 5.95 (m, 1H), 5.66 – 5.57 (m, 1H), 4.13 (s, 1H), 3.70 (s, 3H), 3.11 (ddd, J = 13.7, 11.6, 4.2 Hz, 1H), 3.03 – 2.92 (m, 3H), 2.79 (t, J = 8.0 Hz, 1H), 2.44 – 2.31 (m, 2H), 2.26 (d, J = 8.3 Hz, 1H), 1.97 (dd, J = 9.0, 7.6 Hz, 1H), 1.83 – 1.71 (m, 1H).

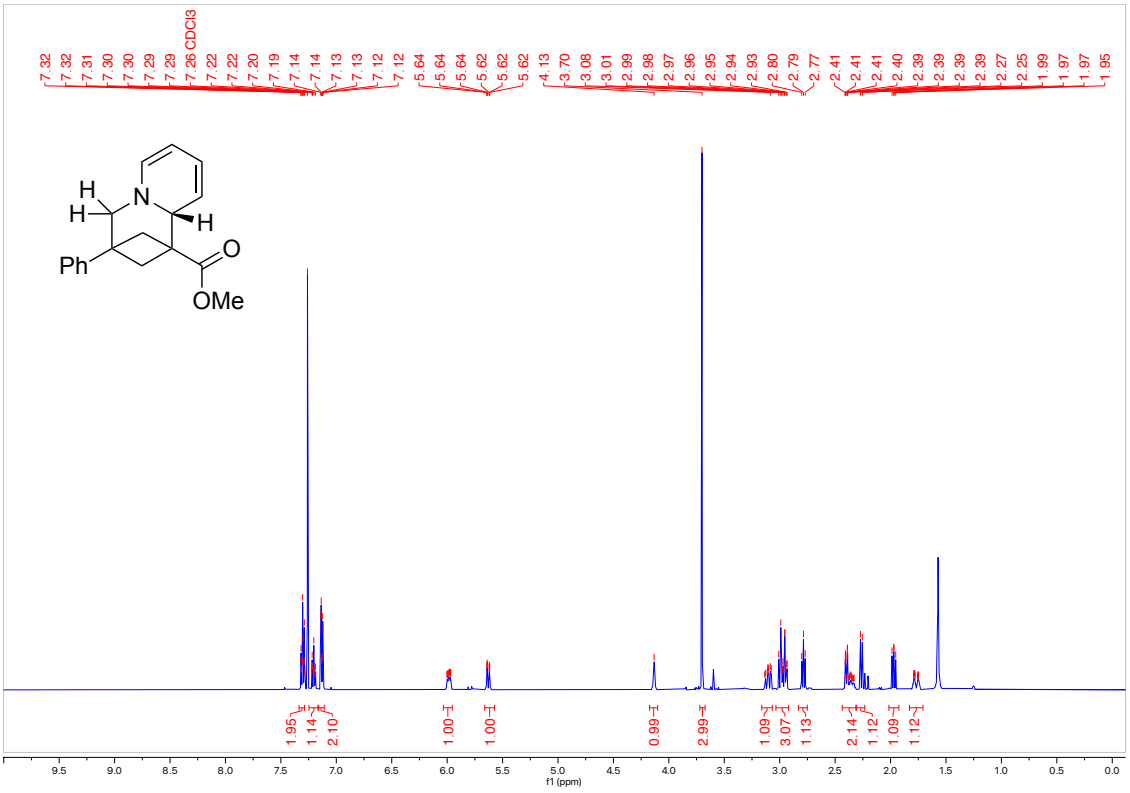

^{13}C NMR (126 MHz, $CDCl_3$, 292 K, ppm): δ 174.19, 146.57, 128.64, 128.43, 128.41, 127.91, 126.39, 125.31, 125.29, 59.00, 57.41, 52.02, 52.01, 46.94, 45.35, 42.19, 38.60, 37.09, 19.58.

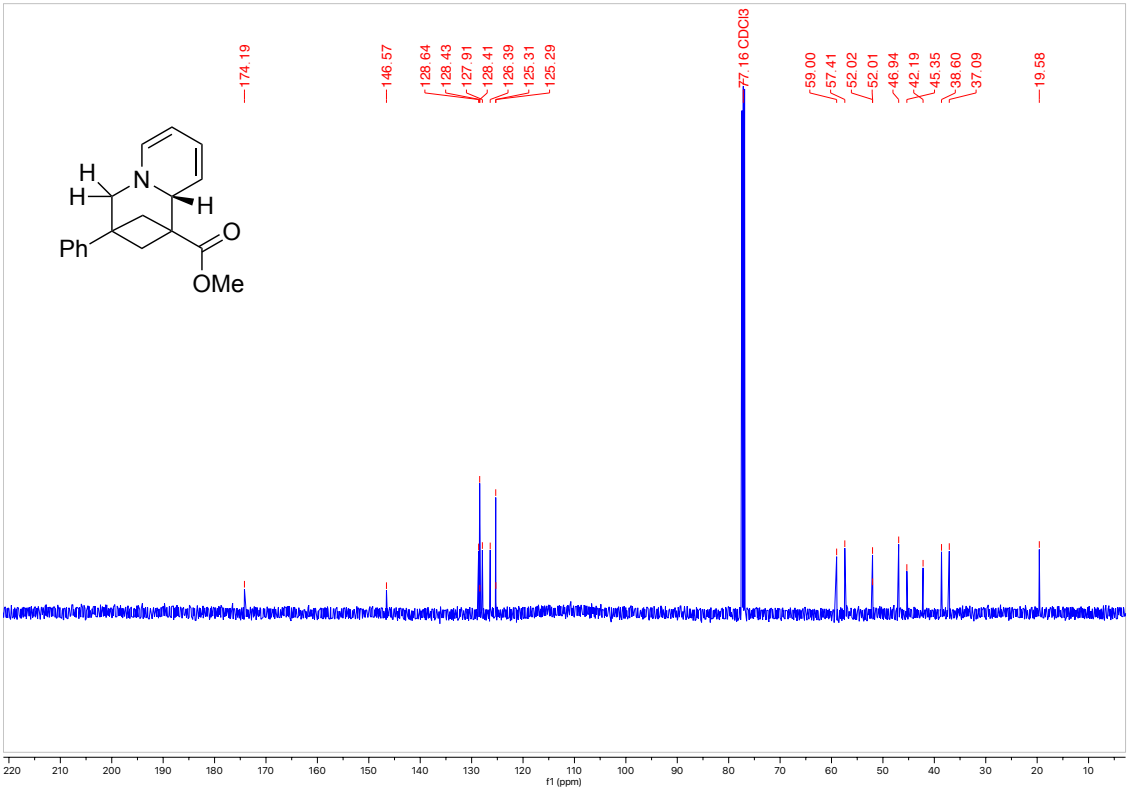

^{1}H-^{1}H COSY (4o):

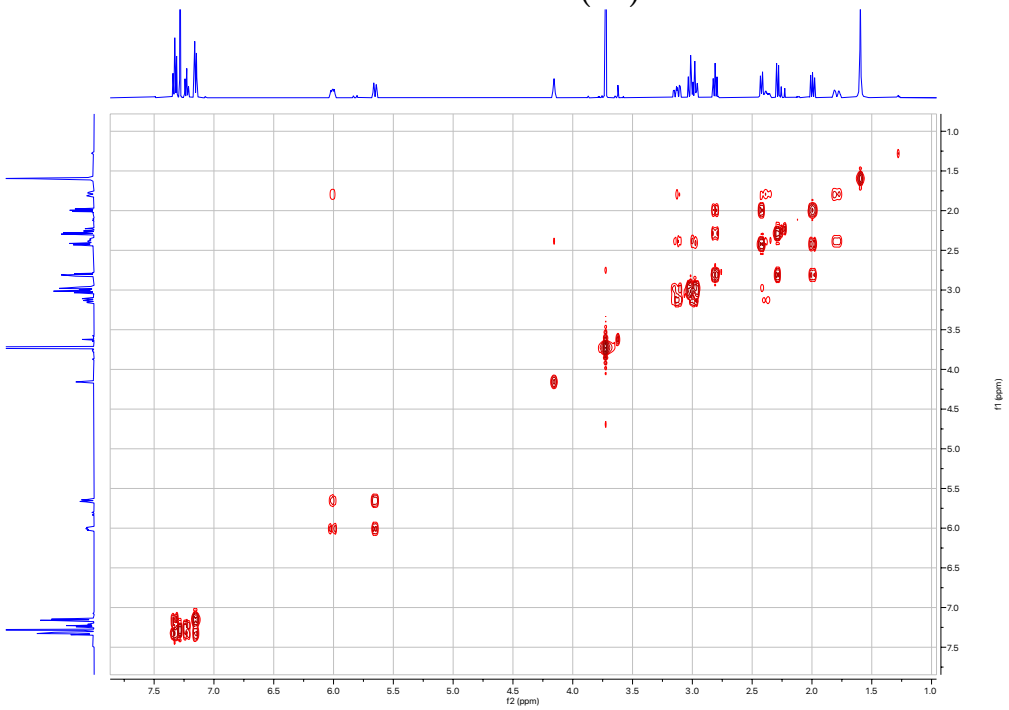

^{1}H-^{13}C HSQC (4o):

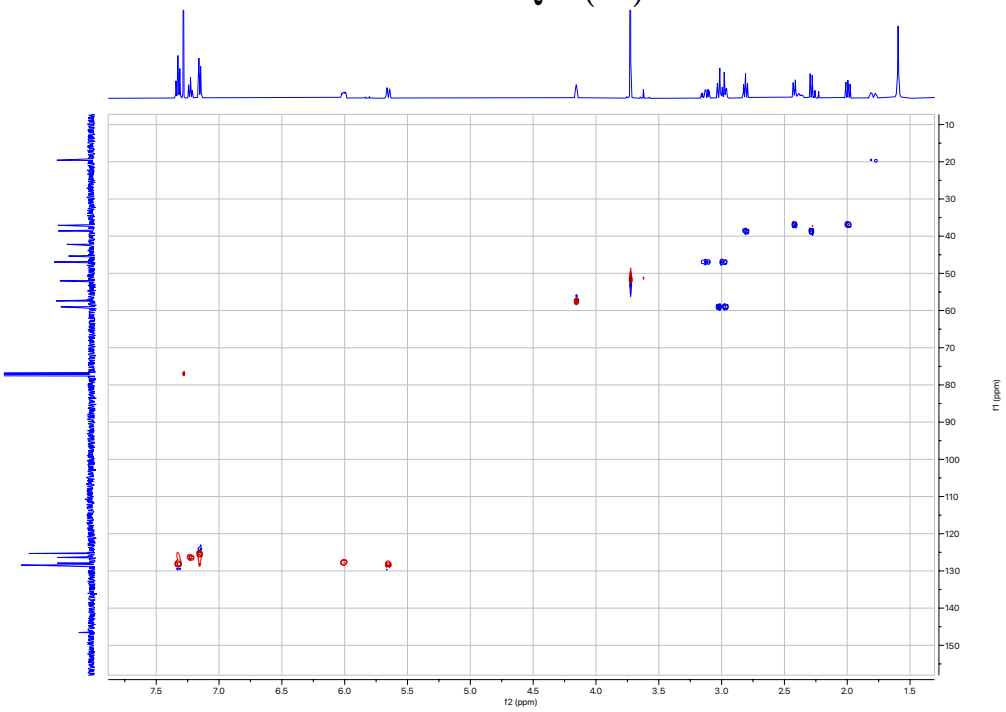

^{1}H-^{13}C HMBC (4o):

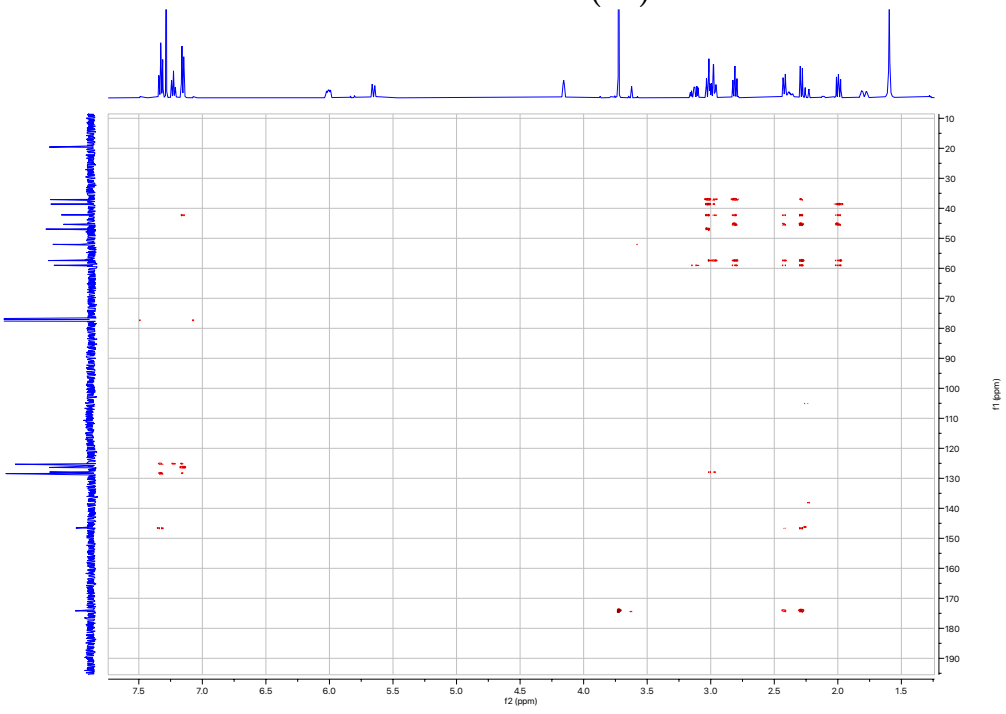

C.9 Tests for Other Ylide Additions to Bicyclobutane

C.9.1 Azomethine Ylides

General Procedure for Table 4.5:

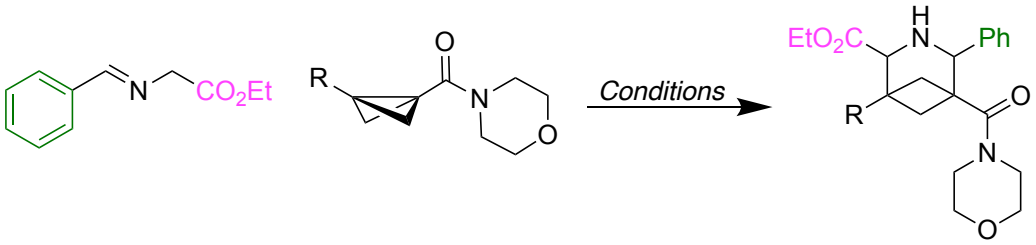

The imine (9.6 mg, 0.05 mmol, 1 equiv), Base, and catalyst/additive was added to a 1-dram vial and dissolved in solvent (0.50 mL, 0.10 M). The bicyclobutane (8.4 mg for mono-substituted or 12.2 mg for disubstituted, 0.05 mmol, 1 equiv) was then added to the reaction mixture and it was left to stir at the assigned temperature for 24 hours. The solvent was then evaporated and a ^{1}H NMR spectrum was taken in $CDCl_3$. No product observed.

^{1}H NMR 300 MHz in $CDCl_3$ for Table 4.5, Entry 1:

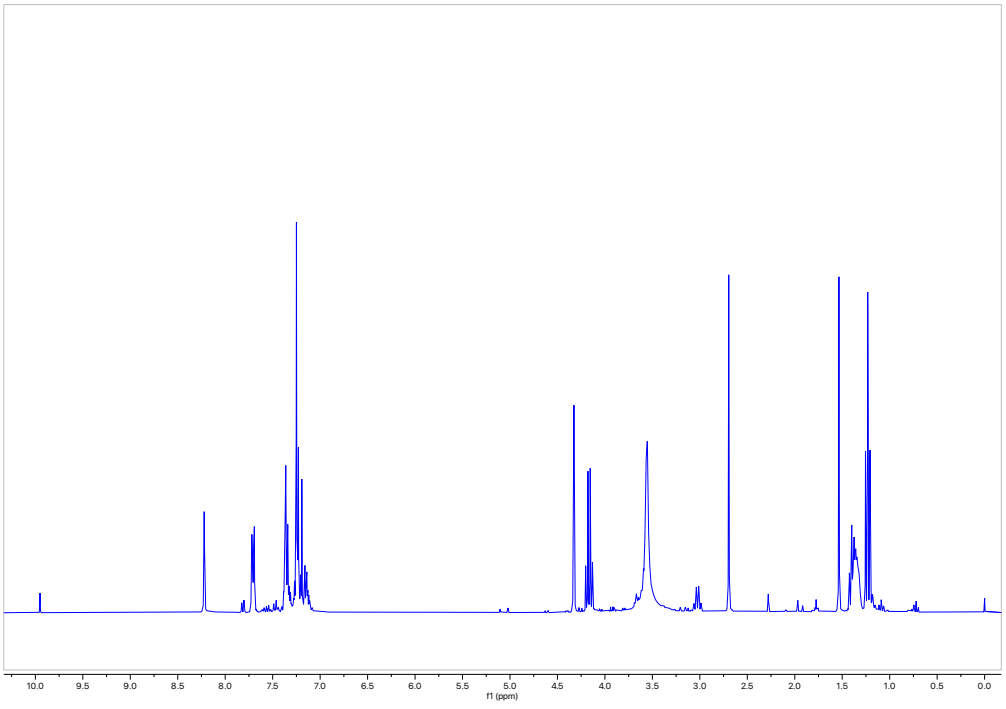

^{1}H NMR 300 MHz in $CDCl_3$ for Table 4.5, Entry 2:

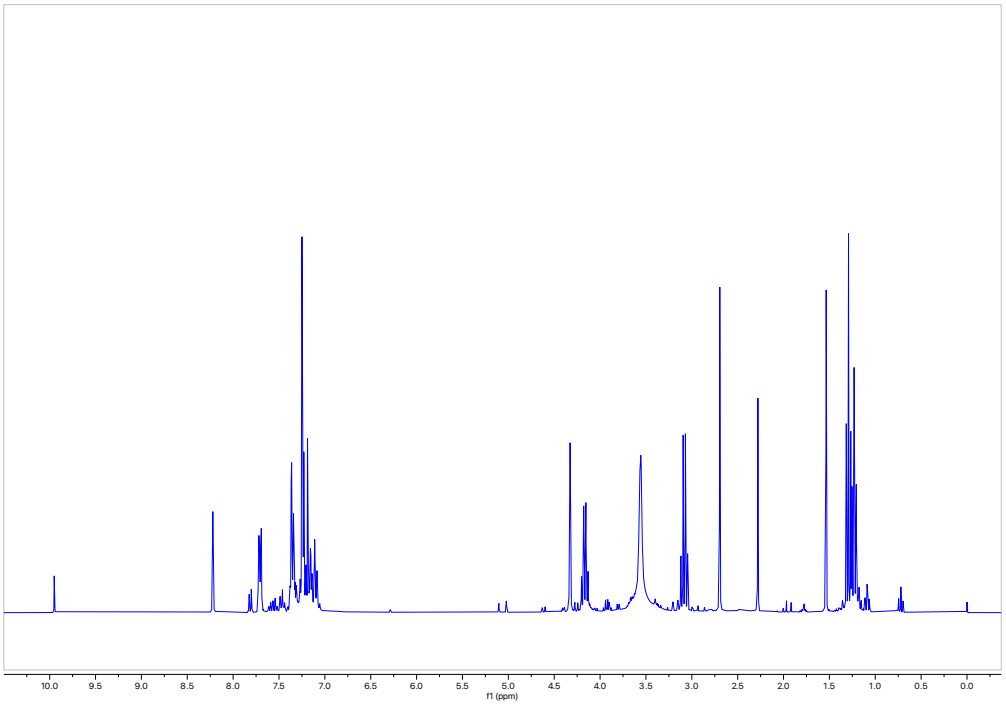

^{1}H NMR 300 MHz in $CDCl_3$ for Table 4.5, Entry 3:

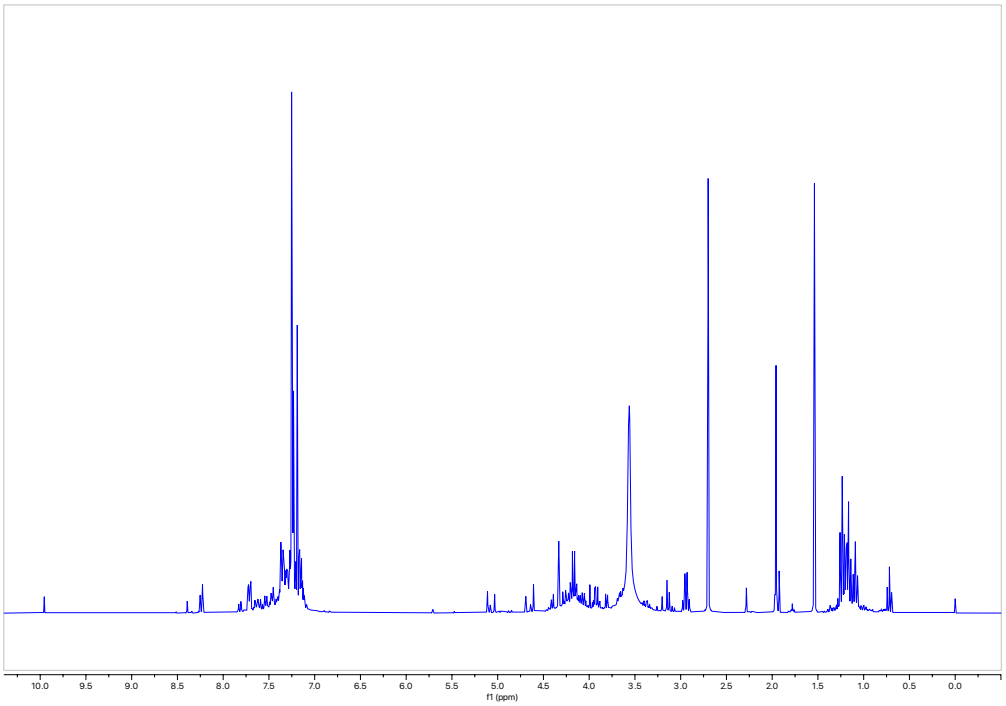

^{1}H NMR 300 MHz in $CDCl_3$ for Table 4.5, Entry 4:

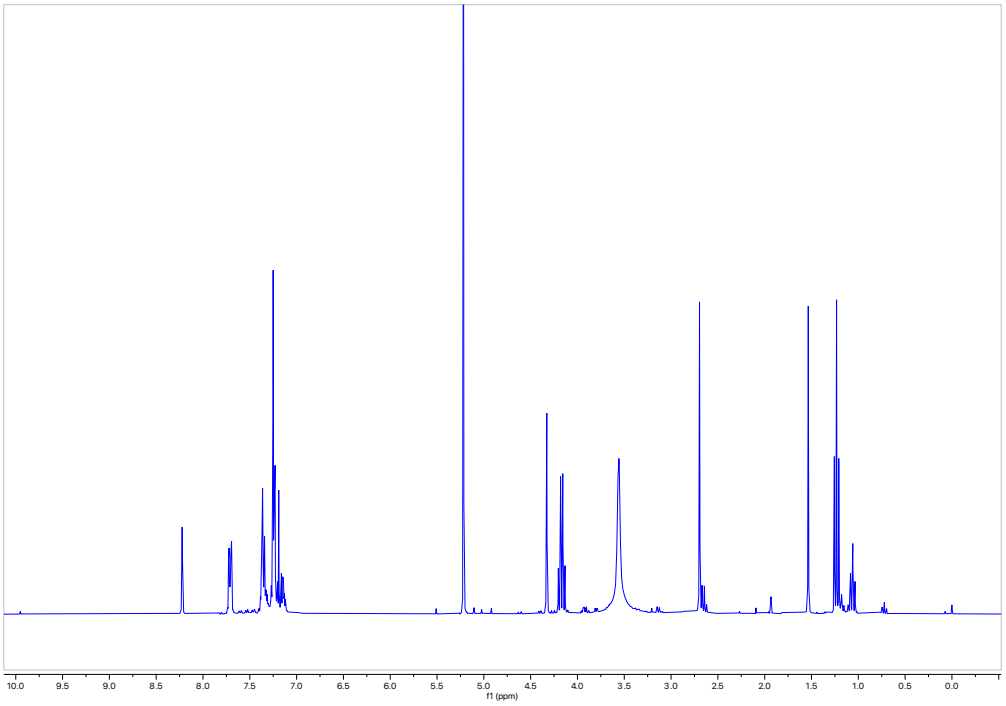

^{1}H NMR 300 MHz in $CDCl_3$ for Table 4.5, Entry 5:

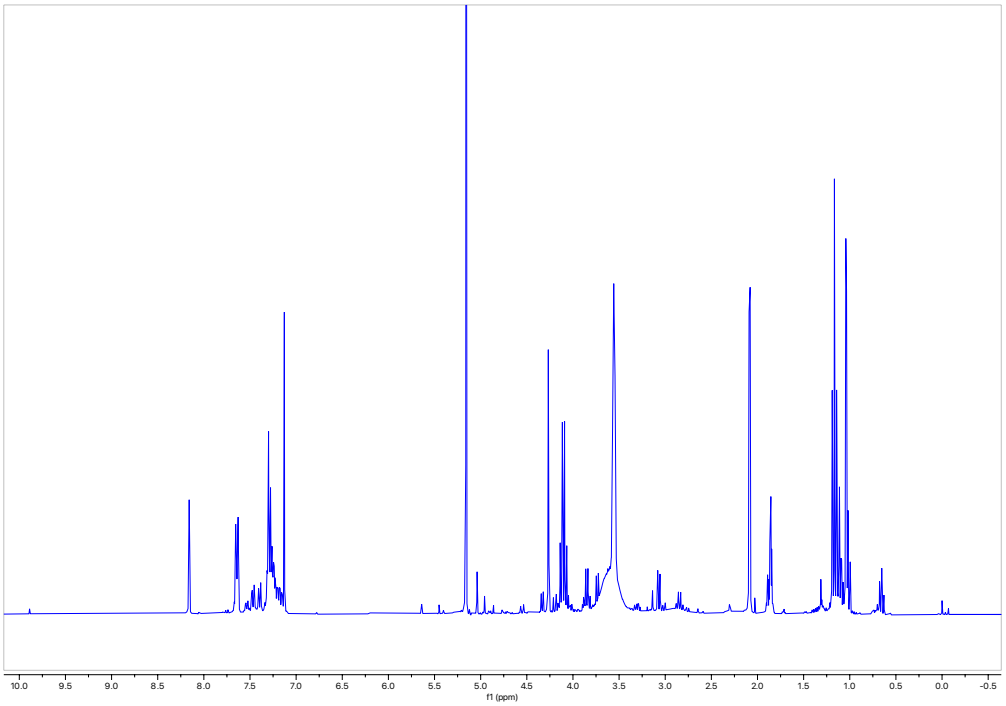

^{1}H NMR 300 MHz in $CDCl_3$ for Table 4.5, Entry 6:

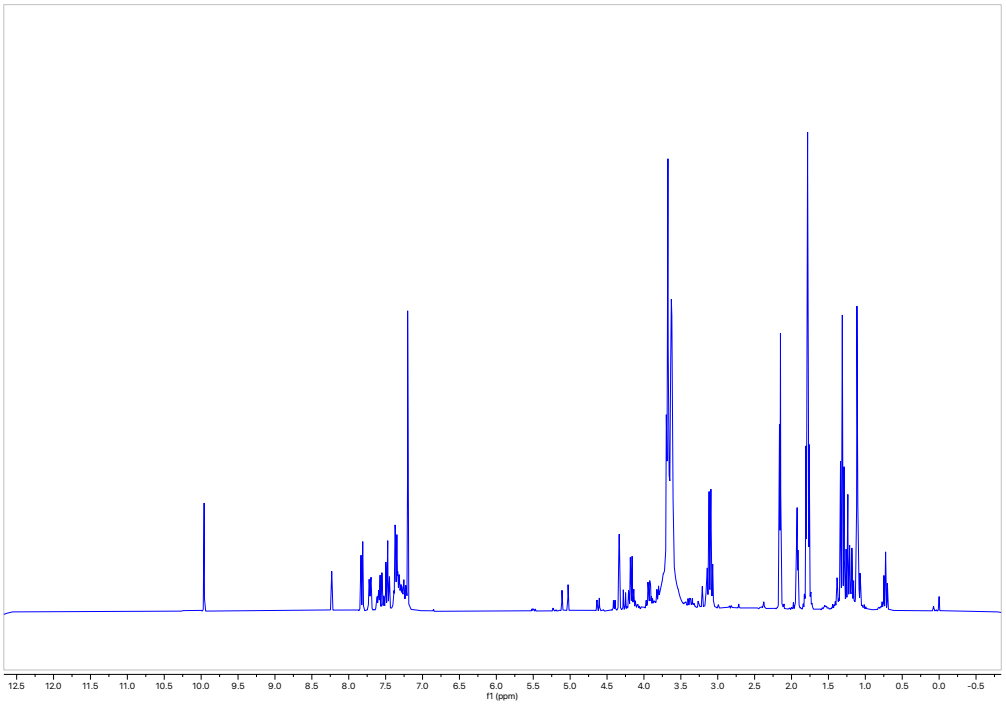

^{1}H NMR 300 MHz in $CDCl_3$ for Table 4.5, Entry 7:

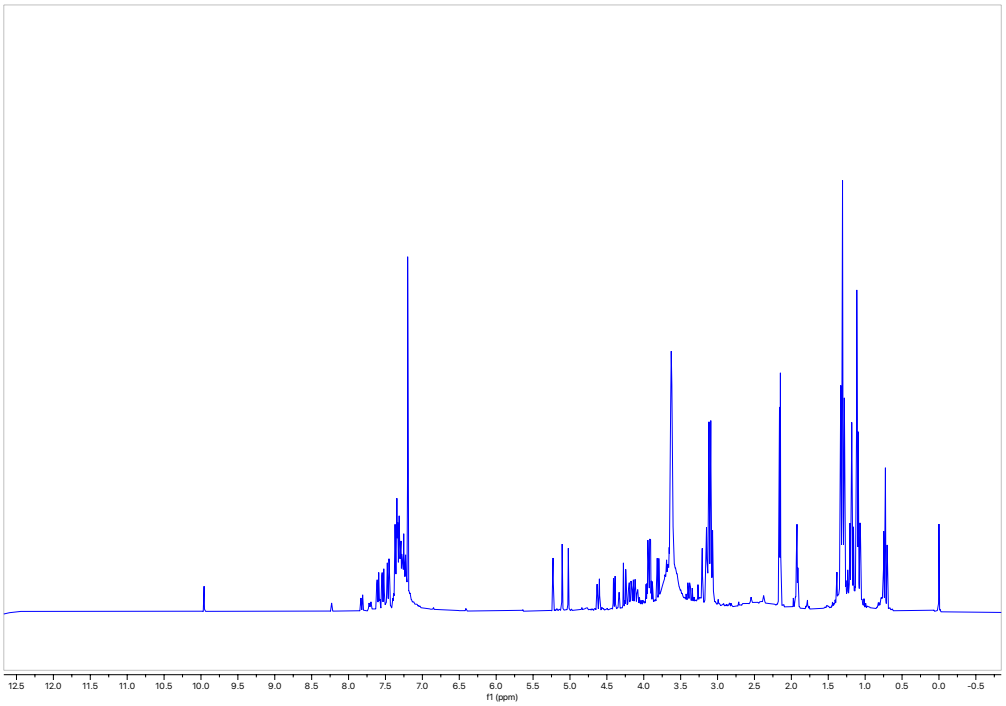

Appendix D

Supporting Information for Chapter 5

Contributions: The following data reported has been completed **independently** with supporting work from supervised undergraduate students.

D.1 General

Materials. All solvents and common organic reagents were purchased from commercial suppliers and used without further purification. Organic building blocks and starting materials were purchased from Oakwood Chemicals, Sigma Aldrich, or AmBeed and used as received. All Lewis acids were purchased from Strem Chemicals and used as received. All non-commerical compounds were prepared using literature procedures, or syntheses as described.

Analysis and Spectroscopy. All NMR spectra were acquired on either a Bruker AVANCE 300 MHz spectrometer or a Bruker AVANCE Neo 500 MHz spectrometer. All ^{1}H and ^{13}C NMR spectra chemical shifts are calibrated to residual protio-solvents, and ^{19}F NMR spectra chemical shifts are calibrated to an external standard.

D.2 Substrate Synthesis

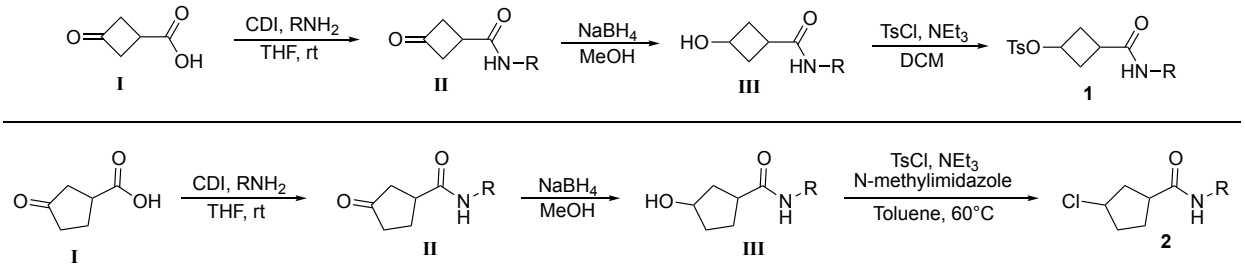

General Procedure 1: (Amidation) 3-Oxocyclobutane-1-carboxylic acid or 3-Oxocyclopentane-1-carboxylic acid **I** (1 equiv) was dissolved in THF (0.55 M) in a round bottom flask and the solution was cooled down to 0 °C. Carbonyl diimidazole (1.05 equiv) was added to the flask. The solution was warmed to room temperature and left to stir for 1 hour before the solution was cooled back down to 0 °C and the amine (1.05 equiv) was added dropwise. The solution was then warmed to room temperature and left to stir overnight. The reaction was then quenched with NH_4Cl and then extracted with ethyl acetate 3 times. The combined organic layers were dried with Mg_2SO_4, filtered and the solvent was evaporated. The compound **II** was purified by column chromatography in most cases.

General procedure 2 (Reduction)[212] The cyclobutanone or cyclopentanone amide **II** (1 equiv) was dissolved in methanol and cooled down to 0 °C. Sodium borohydride (0.5 equiv) was added portion-wise to the reaction mixture. The solution was allowed to warm to room temperature and left to stir for 2-3 hours at room temperature. The solution was quenched with NH_4Cl and extracted with ethyl acetate 3 times. The organic layer was dried with Mg_2SO_4, filtered and the solvent was evaporated to give the product **III** which was used without further purification.

General procedure 3 (Tosylation of cyclobutanols)[212] The cyclobutane or cyclopentane alcohol **III** (1 equiv) was dissolved in DCM and cooled down and 4-toluenesulfonyl chloride (1.2 equiv) was added to the reaction mixture followed by triethylamine (1.3 equiv). The solution was then heated to 40 °C for 24 hours. The reaction was quenched with NH_4Cl and then extracted with DCM 3 times. The organic solvent was dried with Mg_2SO_4, filtered and the solvent was evaporated to give the crude product **IV** . The compound was purified by column chromatography.

General procedure 3 (Tosylation of cyclopentanols)[212] The cyclopentane alcohol **III** was dissolved in toluene (0.53 M) followed by the addition of *N*-methylimidazole (1.0 equiv). 4-Toluenesulfonyl chloride (1.5 equiv) was then added, followed by triethylamine (1.5 equiv), and the mixture was stirred at 60 °C overnight. The reaction was quenched with saturated ammonium chloride and then extracted with toluene 3 times. The organic layers were combined, dried with Mg_2SO_4, filtered and then the solvent was evaporated to give the crude product **IV**. The compound was purified by column chromatography.

***N*-benzyl-3-oxocyclobutane-1-carboxamide**

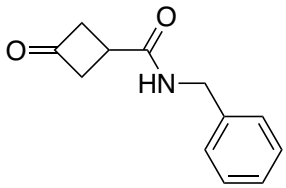

This product was prepared using **General Procedure 1** on a 44.8 mmol scale and 9.45 g of a beige solid was obtained (92% Yield). This product was carried forward without further purification.

^{1}H NMR (300 MHz, $CDCl_3$, 292 K, ppm): δ 7.50 – 7.13 (m, 5H), 5.93 (s, 1H), 4.49 (d, J = 5.7 Hz, 2H), 3.61 – 3.45 (m, 2H), 3.32 – 3.10 (m, 2H), 3.11 – 2.88 (m, 1H).

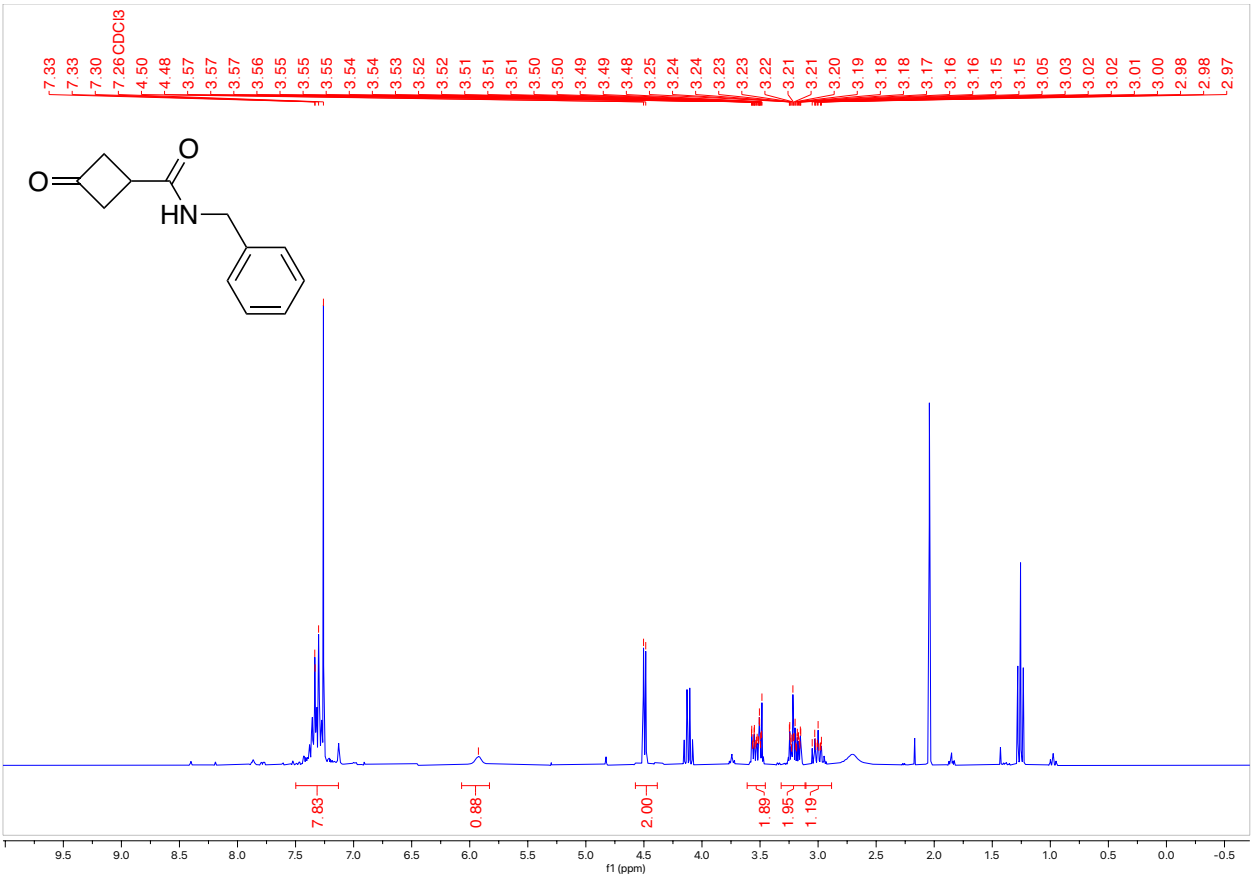

***N*-(4-methoxybenzyl)-3-oxocyclobutane-1-carboxamide**

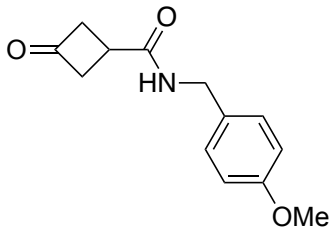

This product was prepared using **General Procedure 1** on a 4.4 mmol scale. The product was purified by column chromatography (Biotage® Sfär 10g Column, 0-100% EtOAc/ hexanes, eluted at 80% EtOAc) and 277.7 mg of a white solid was obtained (27% Yield).

^{1}H NMR (300 MHz, $CDCl_3$, 292 K, ppm): δ 7.24 – 7.17 (m, 2H), 6.88 (d, J = 8.8 Hz, 2H), 4.43 (d, J = 5.6 Hz, 2H), 3.81 (s, 3H), 3.60 – 3.43 (m, 2H), 3.27 – 3.11 (m, 2H), 3.03 – 2.89 (m, 1H).

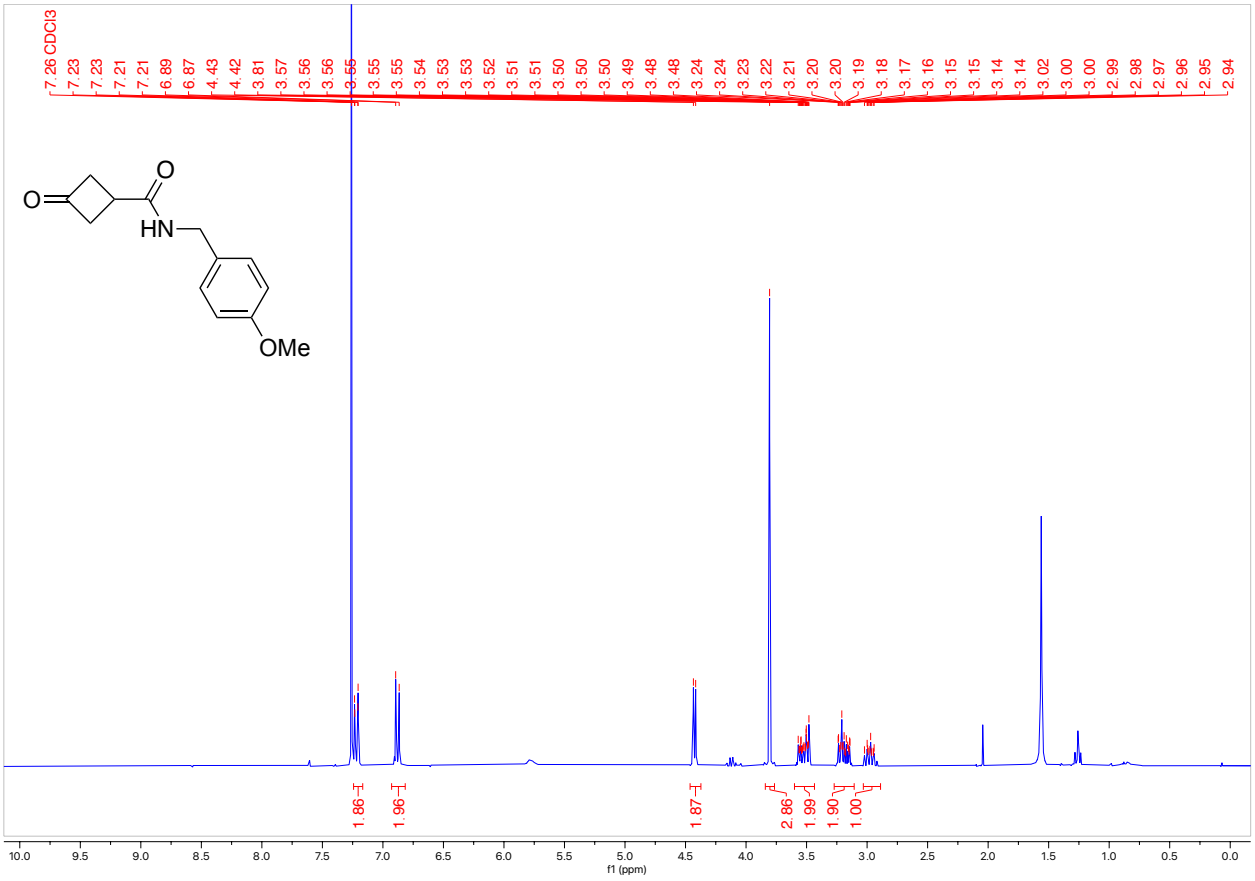

***N*-(4-fluorobenzyl)-3-oxocyclobutane-1-carboxamide**

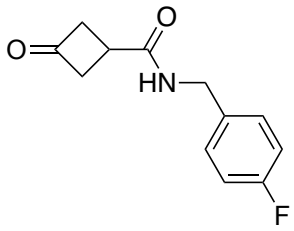

This product was prepared using **General Procedure 1** on a 4.4 mmol scale. The product was purified by column chromatography (Biotage® Sfär 10g Column, 0-100% EtOAc/ hexanes, eluted at 61% EtOAc) and 360.2 mg of a white solid was obtained (37% Yield).

^{1}H NMR (300 MHz, $CDCl_3$, 292 K, ppm): δ 7.24 – 7.17 (m, 2H), 6.88 (d, J = 8.8 Hz, 2H), 4.43 (d, J = 5.6 Hz, 2H), 3.81 (s, 3H), 3.60 – 3.43 (m, 2H), 3.27 – 3.11 (m, 2H), 3.03 – 2.89 (m, 1H).

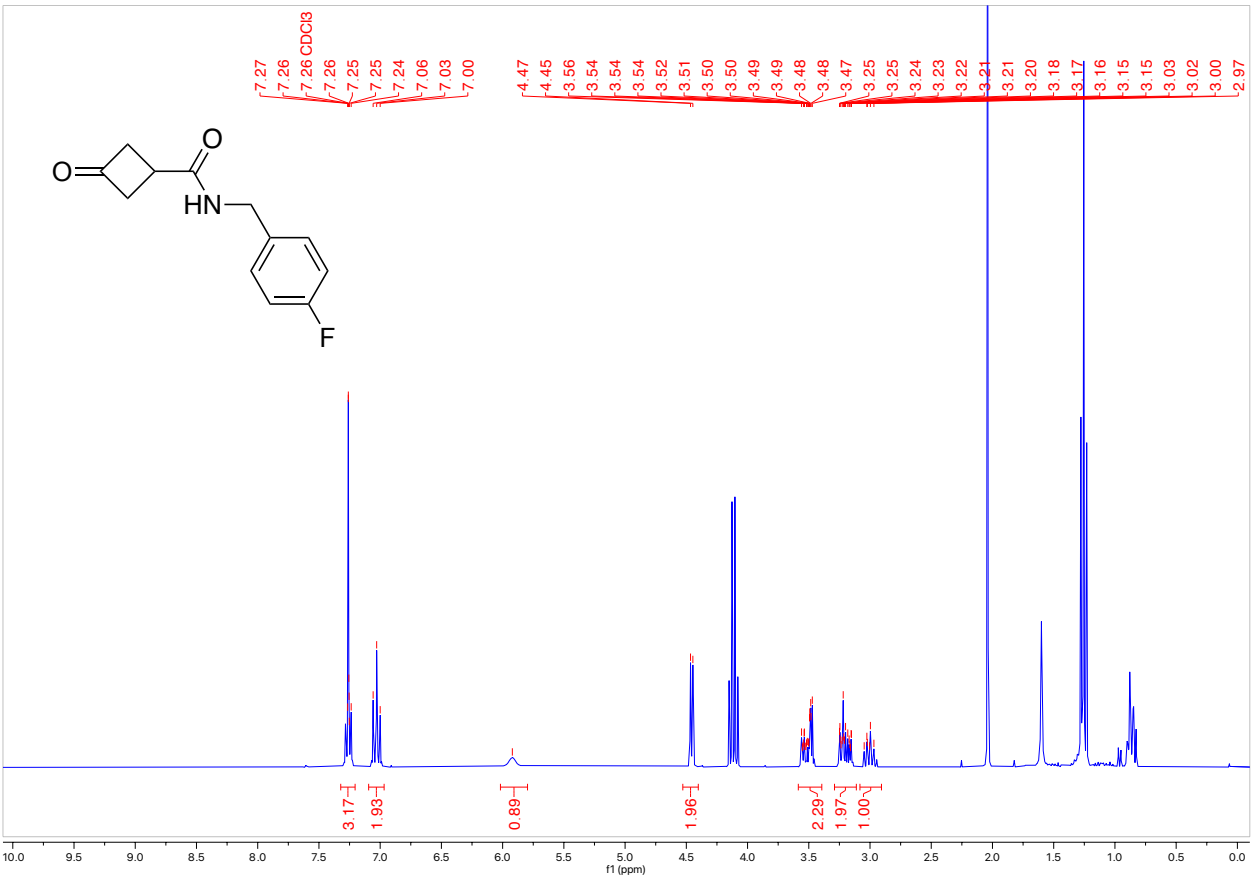

^{19}F NMR (300 MHz, $CDCl_3$, 292 K, ppm): δ 114.12.

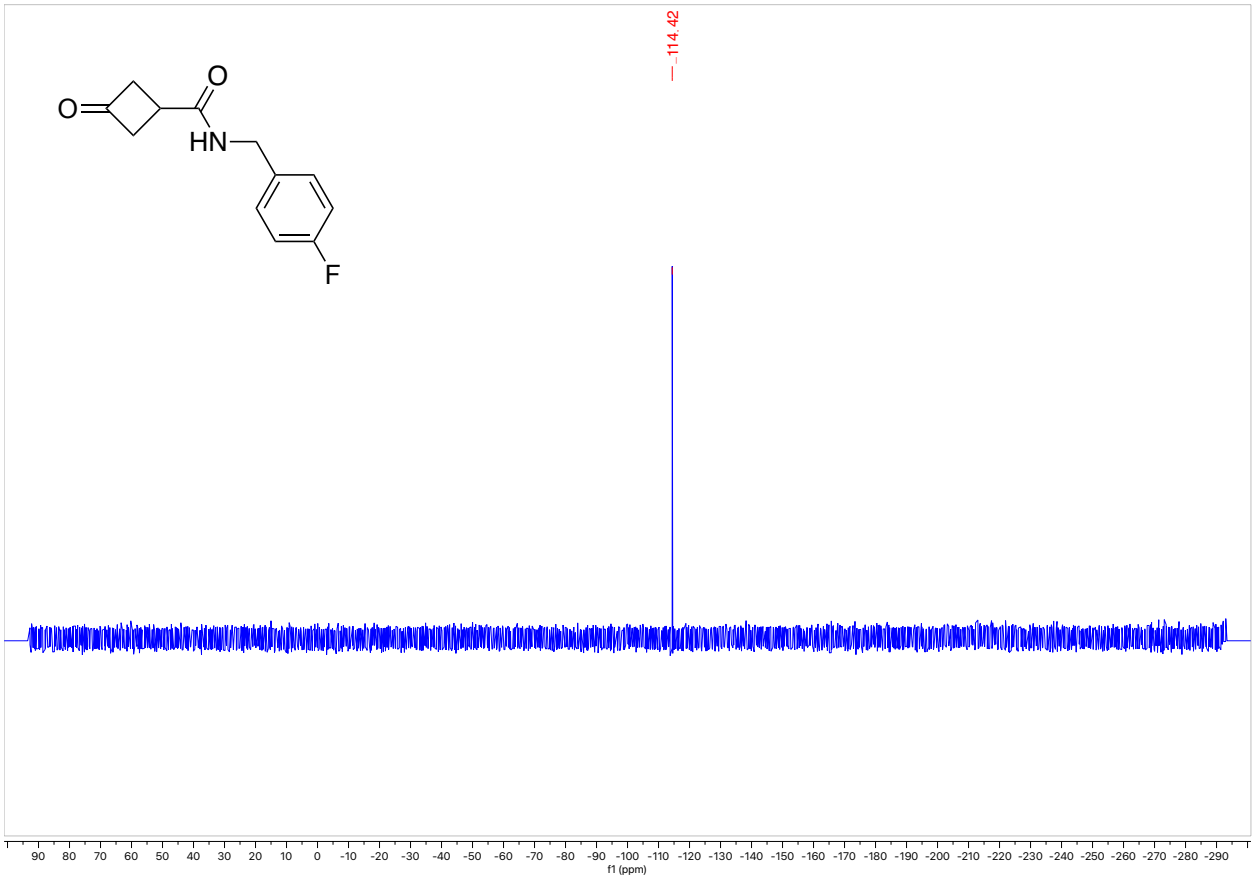

***N*-allyl-3-oxocyclobutane-1-carboxamide**

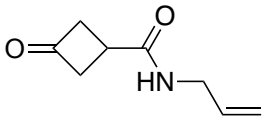

This product was prepared using **General Procedure 1** on a 4.4 mmol scale. The product was purified by column chromatography (Biotage® Sfär 10g Column, 0-100% EtOAc/ hexanes, eluted at 85% EtOAc) and 131.4 mg of a white solid was obtained (20% Yield).

^{1}H NMR (300 MHz, $CDCl_3$, 292 K, ppm): δ 5.86 (ddt, J = 17.1, 10.2, 5.8 Hz, 1H), 5.64 (s, 1H), 5.28 – 5.12 (m, 2H), 3.95 (tt, J = 5.8, 1.5 Hz, 2H), 3.61 – 3.42 (m, 2H), 3.30 – 3.12 (m, 2H), 3.08 – 2.91 (m, 1H).

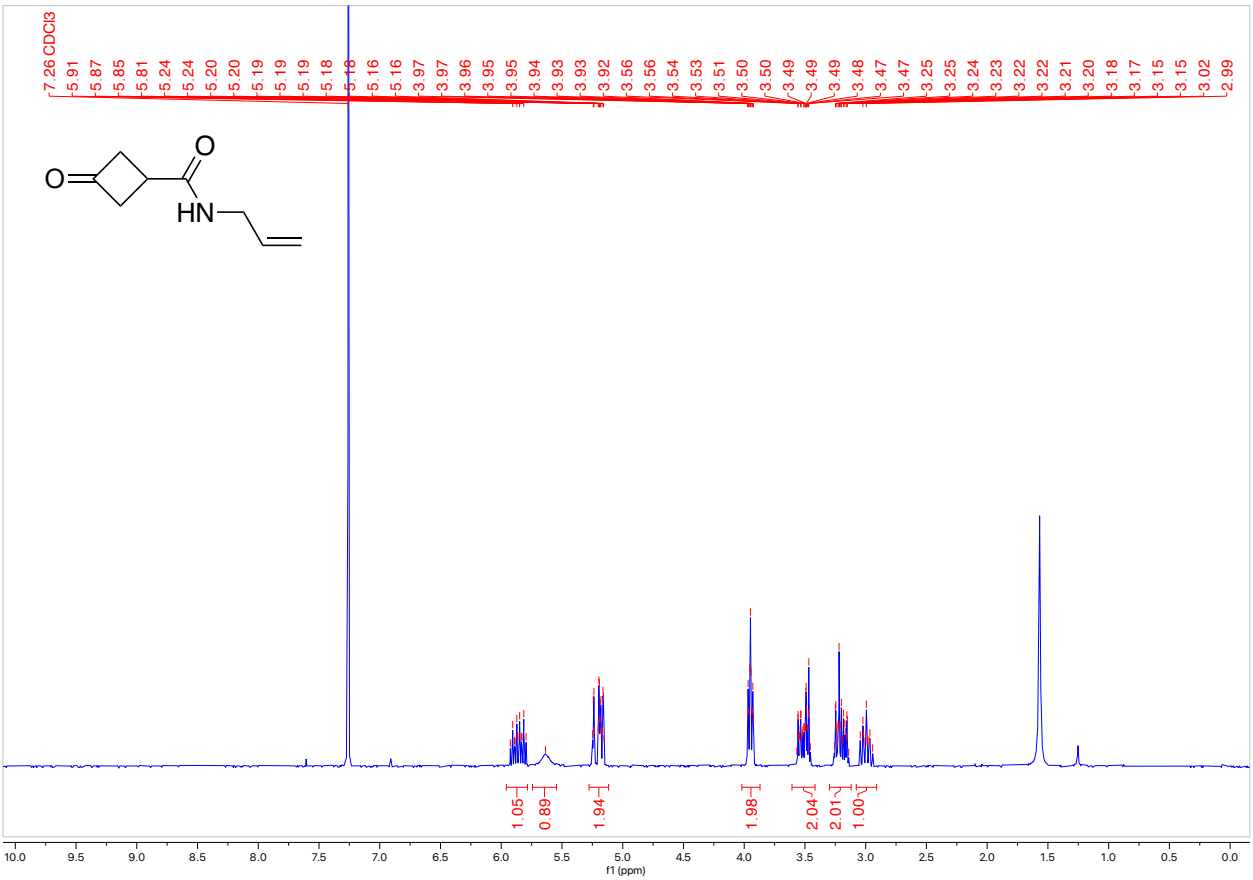

***N*-(*tert*-butyl)-3-oxocyclobutane-1-carboxamide**

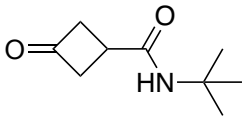

This product was prepared using **General Procedure 1** on a 4.4 mmol scale. The product was purified by column chromatography (Biotage® Sfär 10g Column, 0-100% EtOAc/ hexanes, eluted at 75% EtOAc) and 141.6 mg of a white solid was obtained (19% Yield).

^{1}H NMR (300 MHz, $CDCl_3$, 292 K, ppm): δ 3.54 – 3.34 (m, 2H), 3.24 – 3.03 (m, 2H), 2.99 – 2.78 (m, 1H), 1.38 (s, 9H).

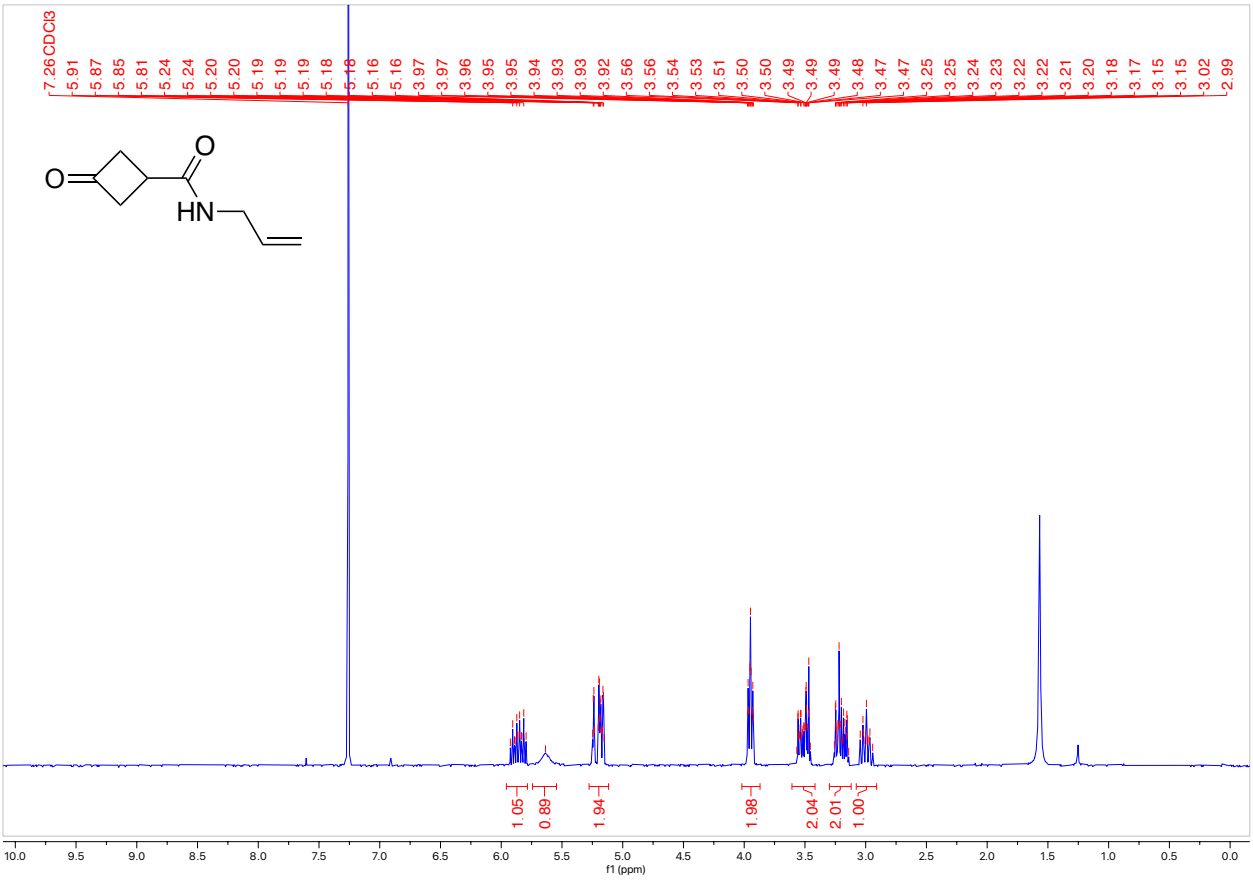

3-oxo-*N*-(2,2,2-trifluoroethyl)cyclobutane-1-carboxamide

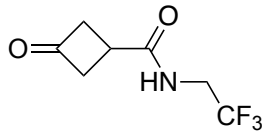

This product was prepared using **General Procedure 1** on a 1.75 mmol scale. The product was purified by column chromatography (Biotage® Sfär 10g Column, 0-100% EtOAc/ hexanes, eluted at 75% EtOAc) and 178.7 mg of a white solid was obtained (52% Yield).

^{1}H NMR (300 MHz, $CDCl_3$, 292 K, ppm): δ 5.86 (s, 1H), 3.99 (qd, J = 9.0, 6.5 Hz, 2H), 3.61 – 3.39 (m, 2H), 3.38 – 3.17 (m, 2H), 3.18 – 2.92 (m, 1H).

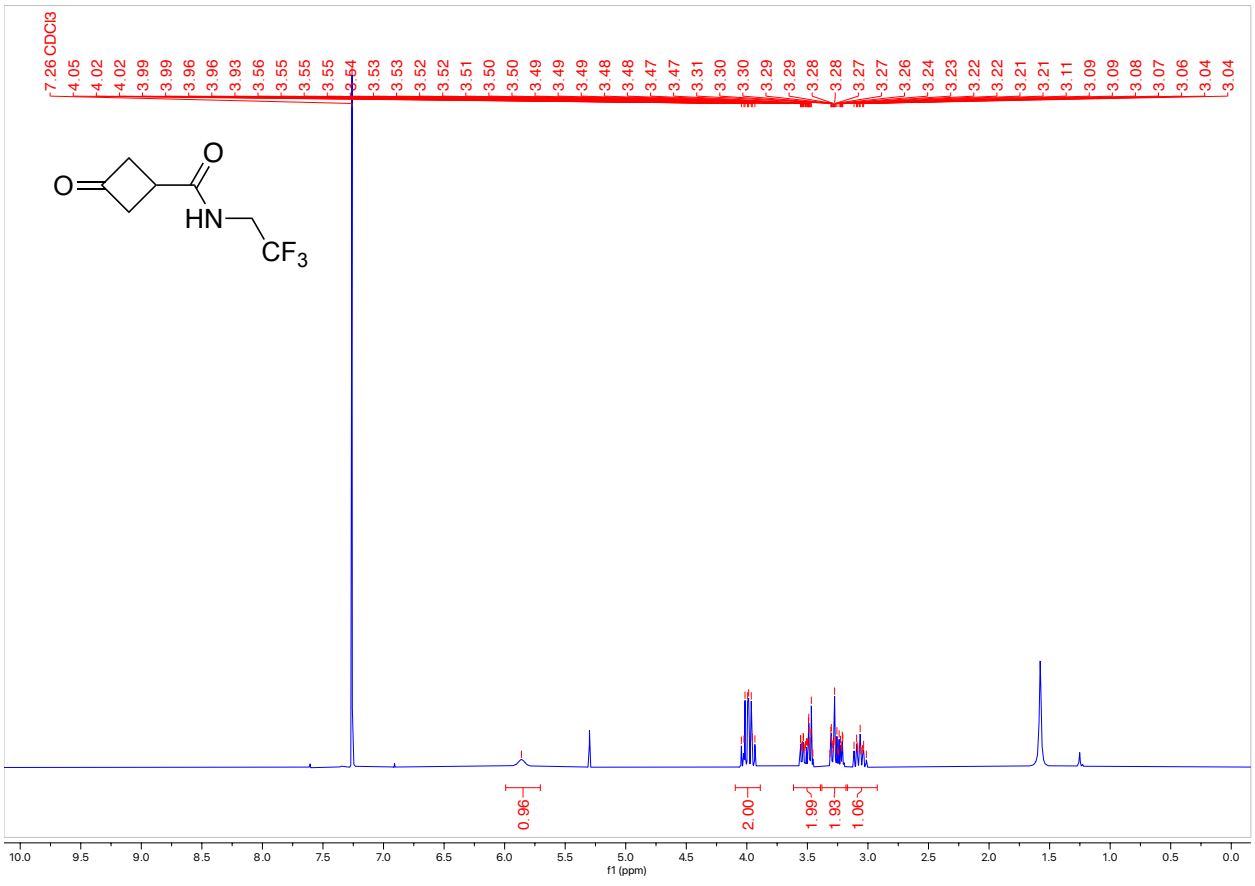

***N*-benzyl-3-oxocyclopentane-1-carboxamide**

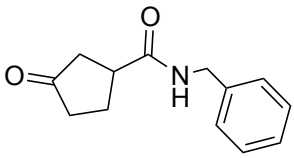

This product was prepared using **General Procedure 1** on a 3.4 mmol scale. The product was purified by column chromatography (Biotage® Sfär 10g Column, 0-100% EtOAc/ hexanes, eluted at 75% EtOAc) and 252.4 mg of a white solid was obtained (34% Yield).

^{1}H NMR (300 MHz, $CDCl_3$, 292 K, ppm): δ 7.38 – 7.17 (m, 6H), 7.06 (s, 1H), 4.42 – 4.29 (m, 2H), 3.02 – 2.90 (m, 1H), 2.48 (ddd, J = 18.3, 8.5, 1.5 Hz, 1H), 2.40 – 2.25 (m, 2H), 2.24 – 2.16 (m, 1H), 2.16 – 2.04 (m, 2H).

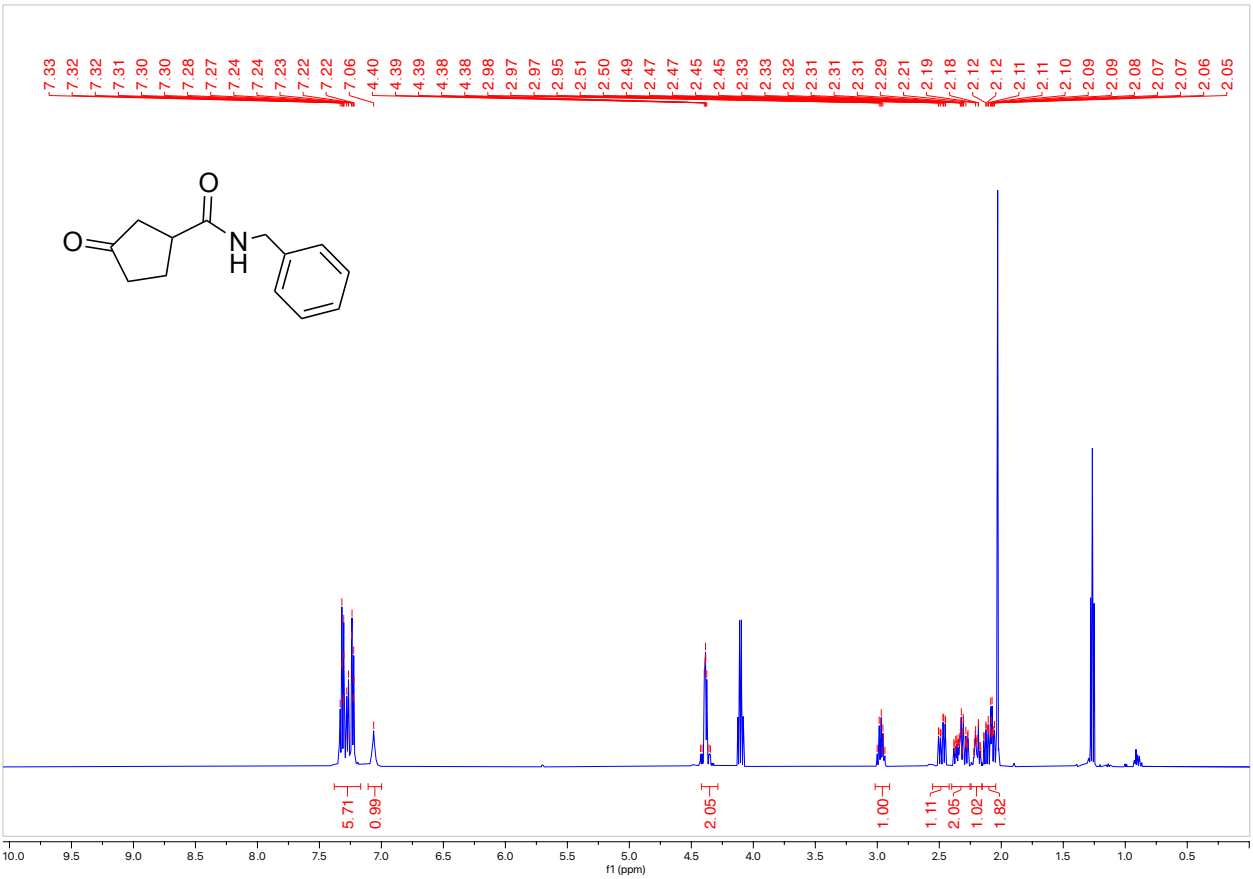

3-Oxo-*N*-phenylcyclopentane-1-carboxamide

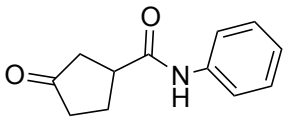

This product was prepared using **General Procedure 1** on a 3.9 mmol scale. The product was purified by column chromatography (Biotage® Sfär 10g Column, 0-100% EtOAc/ hexanes, eluted at 59% EtOAc) and 582.0 mg of a white solid was obtained (69% Yield).

^{1}H NMR (300 MHz, $CDCl_3$, 292 K, ppm): δ 7.56 – 7.48 (m, 2H), 7.34 (dd, J = 8.5, 7.4 Hz, 2H), 7.23 (s, 1H), 7.14 (t, J = 7.3 Hz, 1H), 3.04 (p, J = 8.0 Hz, 1H), 2.75 – 2.61 (m, 1H), 2.57 – 2.37 (m, 2H), 2.37 – 2.30 (m, 1H), 2.30 – 2.22 (m, 2H).

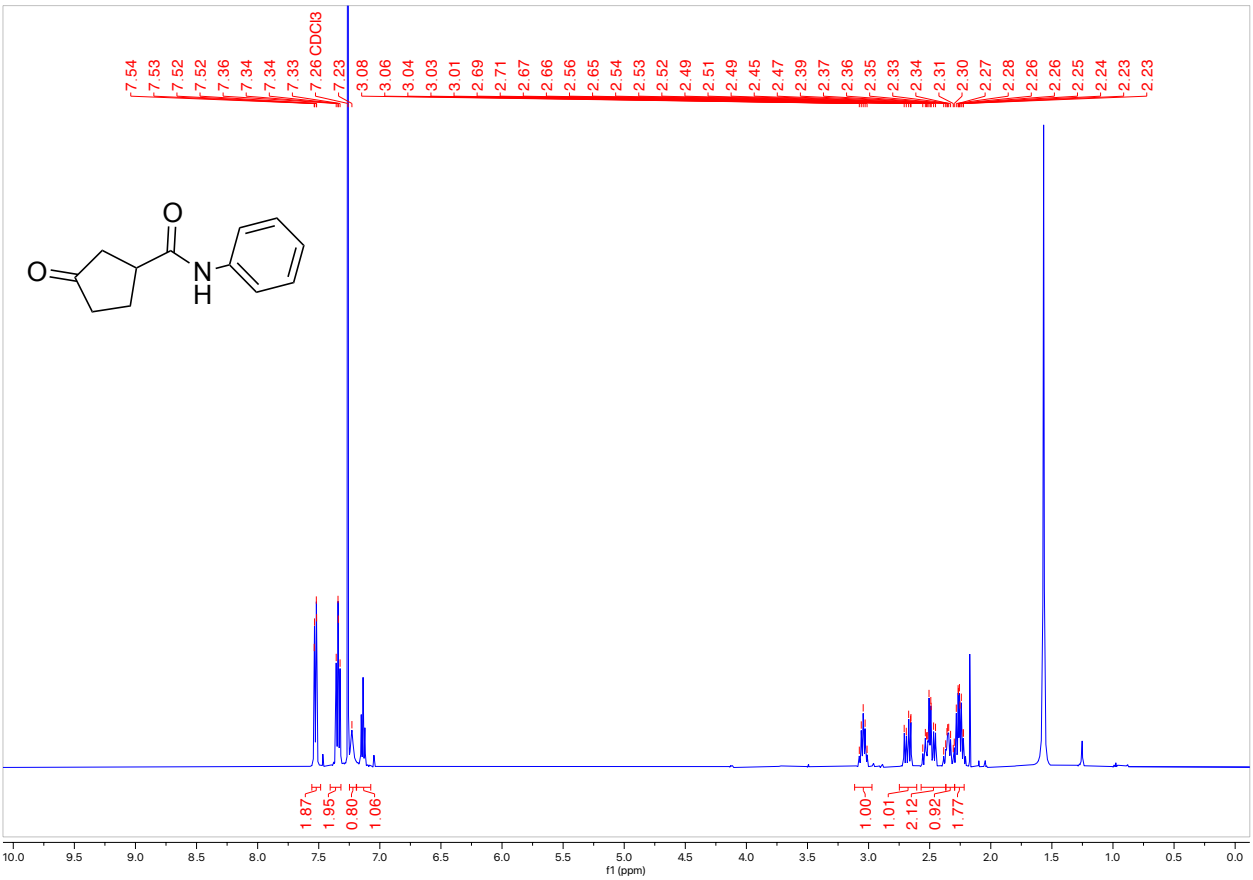

***N*-allyl-3-oxocyclopentane-1-carboxamide**

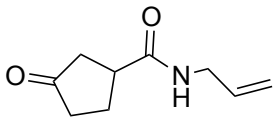

This product was prepared using **General Procedure 1** on a 3.9 mmol scale. The product was purified by column chromatography (Biotage® Sfär 10g Column, 0-100% EtOAc/ hexanes, eluted at 76% EtOAc) and 286.0 mg of a white solid was obtained (48% Yield).

^{1}H NMR (300 MHz, $CDCl_3$, 292 K, ppm): δ 5.85 (ddt, J = 17.1, 10.2, 5.7 Hz, 1H), 5.58 (s, 1H), 5.25 – 5.11 (m, 2H), 3.92 (ddt, J = 5.8, 4.2, 1.5 Hz, 2H), 2.94 – 2.81 (m, 1H), 2.58 (ddd, J = 18.4, 8.9, 1.5 Hz, 1H), 2.49 – 2.34 (m, 2H), 2.28 – 2.03 (m, 3H).

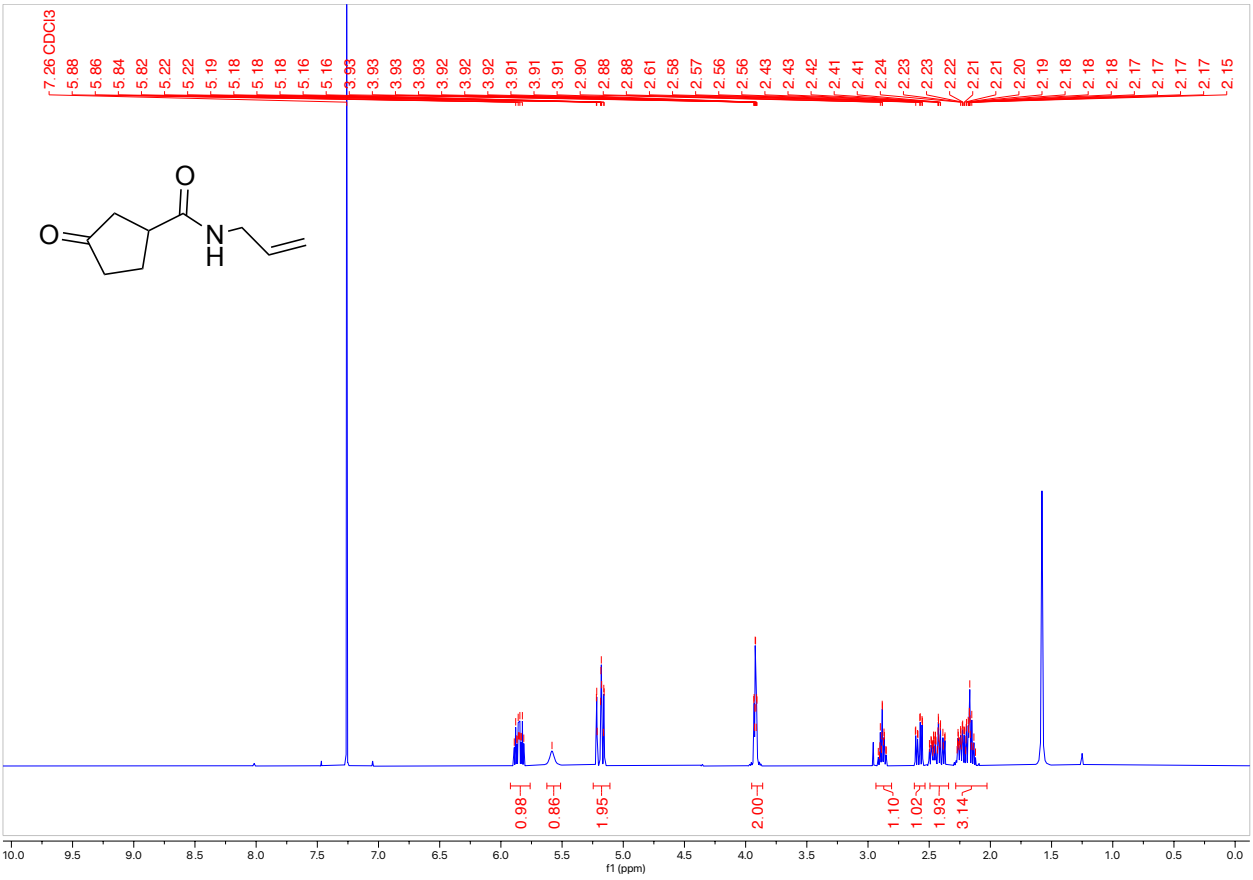

Methyl (3-oxocyclopentane-1-carbonyl)glycinate

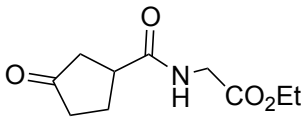

This product was prepared using **General Procedure 1** on a 3.9 mmol scale. The product was purified by column chromatography (Biotage® Sfär 10g Column, 0-100% EtOAc/ hexanes, eluted at 70% EtOAc) and 345.0 mg of a white solid was obtained (41% Yield).

^{1}H NMR (300 MHz, $CDCl_3$, 292 K, ppm): δ 6.07 (s, 1H), 4.24 (q, J = 7.2 Hz, 2H), 4.13 – 3.99 (m, 2H), 3.03 – 2.91 (m, 1H), 2.58 (ddd, J = 18.4, 8.7, 1.5 Hz, 1H), 2.50 – 2.36 (m, 2H), 2.31 – 2.09 (m, 3H), 1.30 (t, J = 7.1 Hz, 3H).

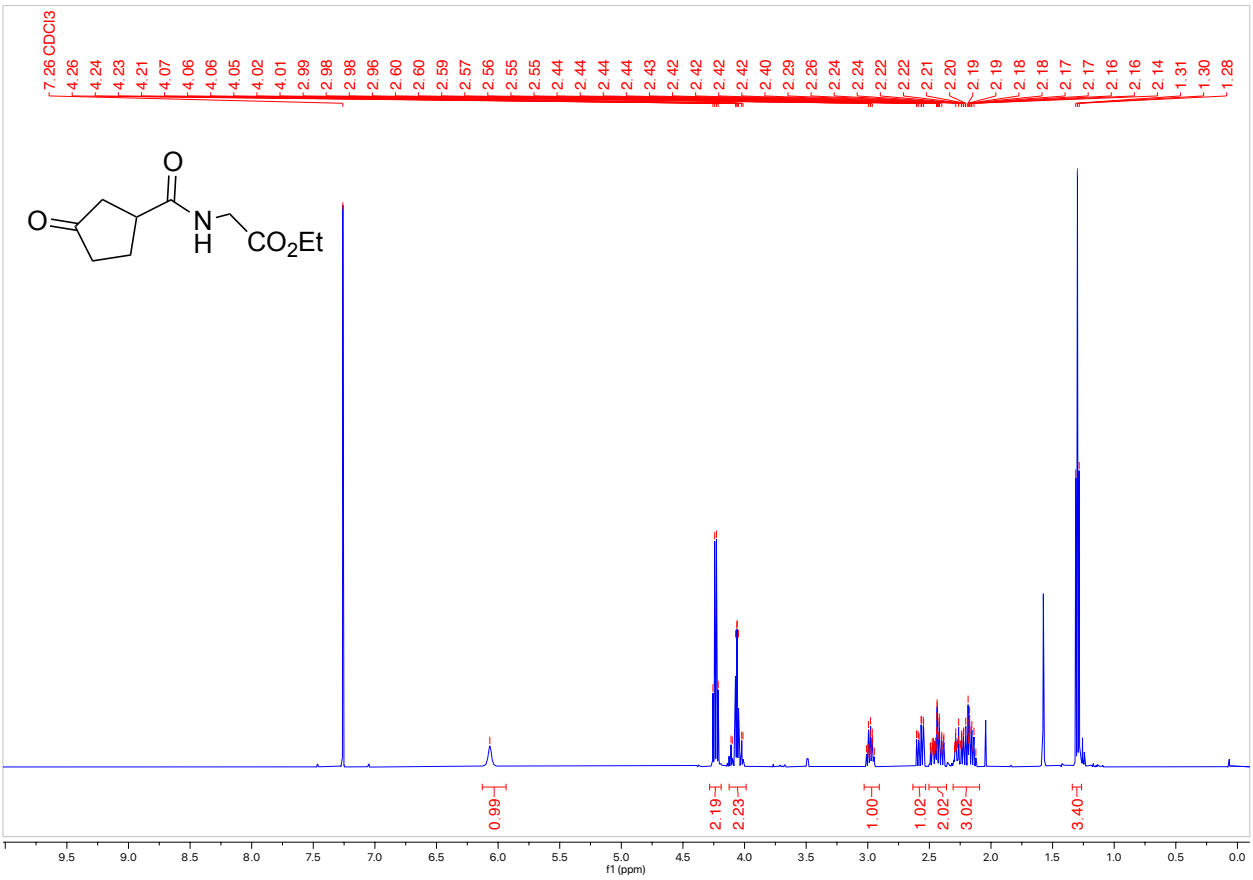

***N*-(*tert*-butyl)-3-oxocyclopentane-1-carboxamide**

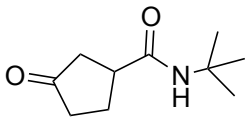

This product was prepared using **General Procedure 1** on a 3.9 mmol scale. The product was purified by column chromatography (Biotage® Sfär 10g Column, 0-100% EtOAc/ hexanes, eluted at 20% EtOAc) and 320.0 mg of a white solid was obtained (45% Yield). Note that some free imidazole is remaining after the column.

^{1}H NMR (300 MHz, $CDCl_3$, 292 K, ppm): δ 5.35 (s, 1H), 2.84 – 2.69 (m, 1H), 2.57 – 2.26 (m, 3H), 2.24 – 2.19 (m, 1H), 2.16 – 2.00 (m, 2H), 1.36 (s, 9H).

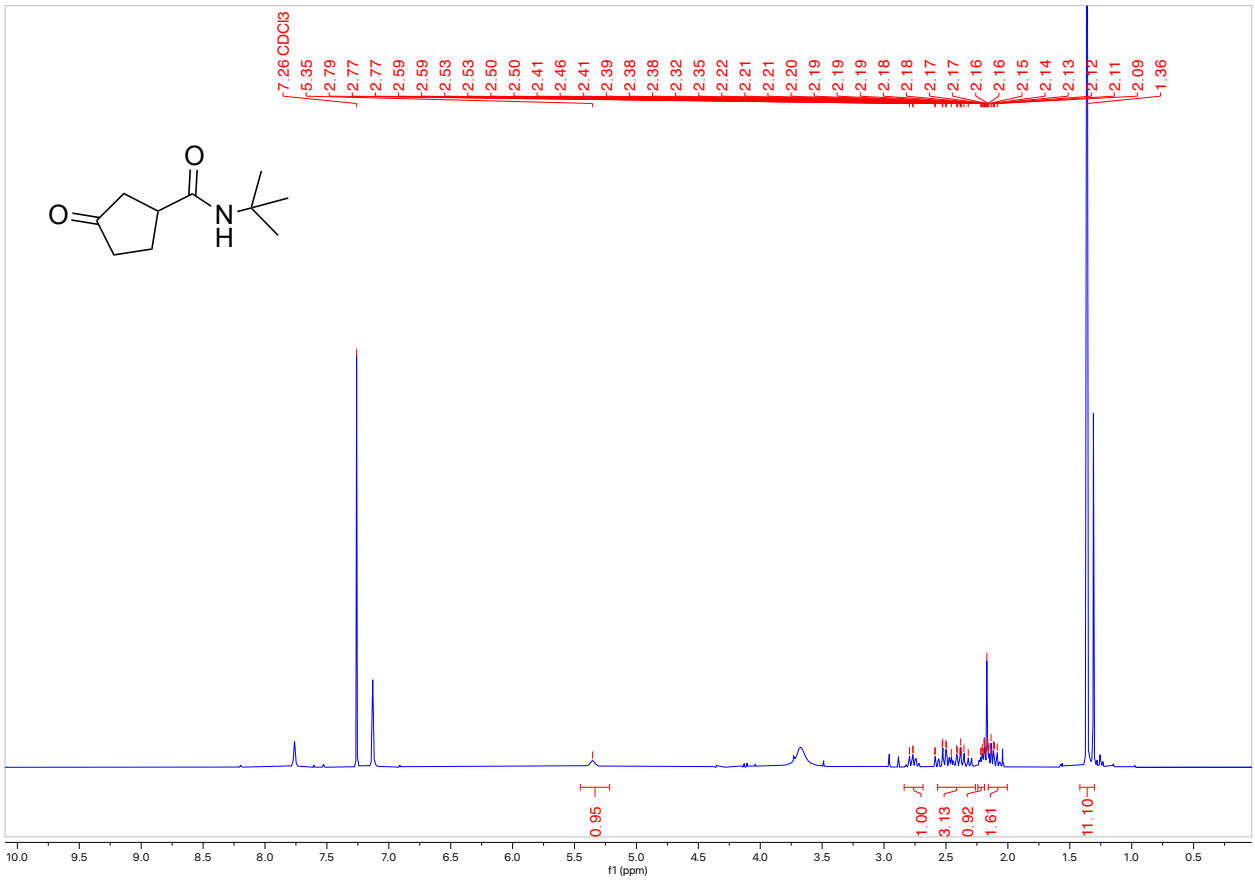

_N_-benzyl-3-hydroxycyclobutane-1-carboxamide

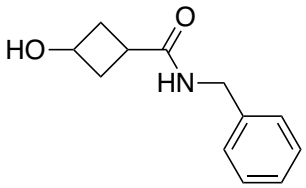

This product was prepared using **General Procedure 2** on a 50.3 mmol scale and 9.23 g of a white solid was obtained (89% Yield).

^{1}H NMR (300 MHz, $CDCl_3$, 292 K, ppm): δ 7.40 – 7.18 (m, 5H), 6.55 (s, 1H), 4.40 (d, J = 5.8 Hz, 2H), 4.10 (q, J = 7.1 Hz, 1H), 2.59 – 2.42 (m, 3H), 2.24 – 2.15 (m, 2H).

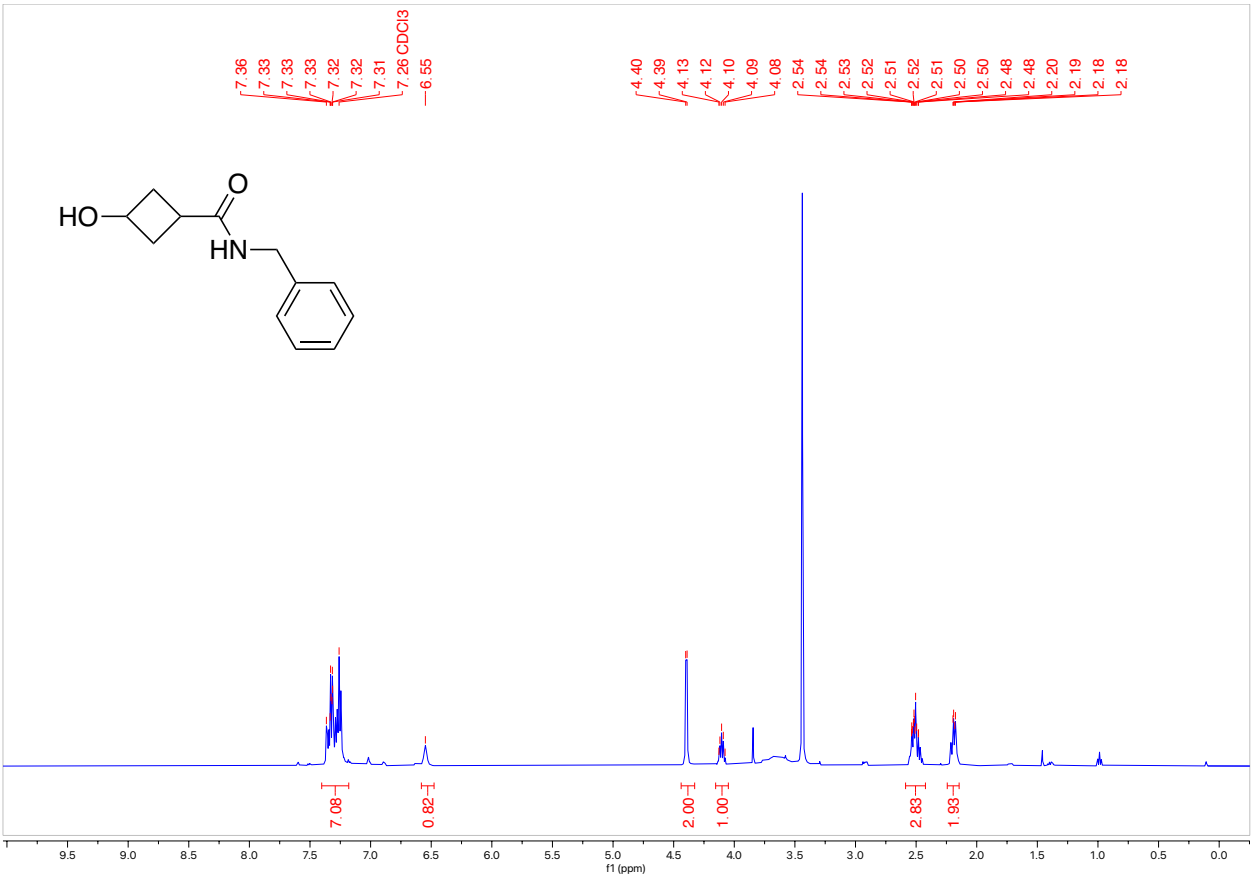

3-Hydroxy-*N*-(4-methoxybenzyl)cyclobutane-1-carboxamide

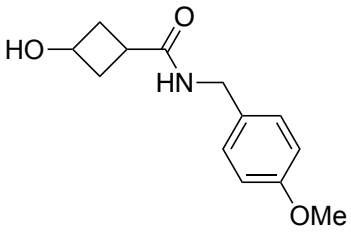

This product was prepared using **General Procedure 2** on a 1.2 mmol scale and 202.8 mg of a white solid was obtained (72% Yield).

^{1}H NMR (300 MHz, $CDCl_3$, 292 K, ppm): δ 7.24 – 7.13 (m, 2H), 6.87 (d, J = 8.7 Hz, 2H), 5.65 (s, 1H), 4.38 (d, J = 5.6 Hz, 2H), 4.25 – 4.11 (m, 1H), 3.80 (s, 3H), 2.68 – 2.42 (m, 3H), 2.26 – 2.08 (m, 2H).

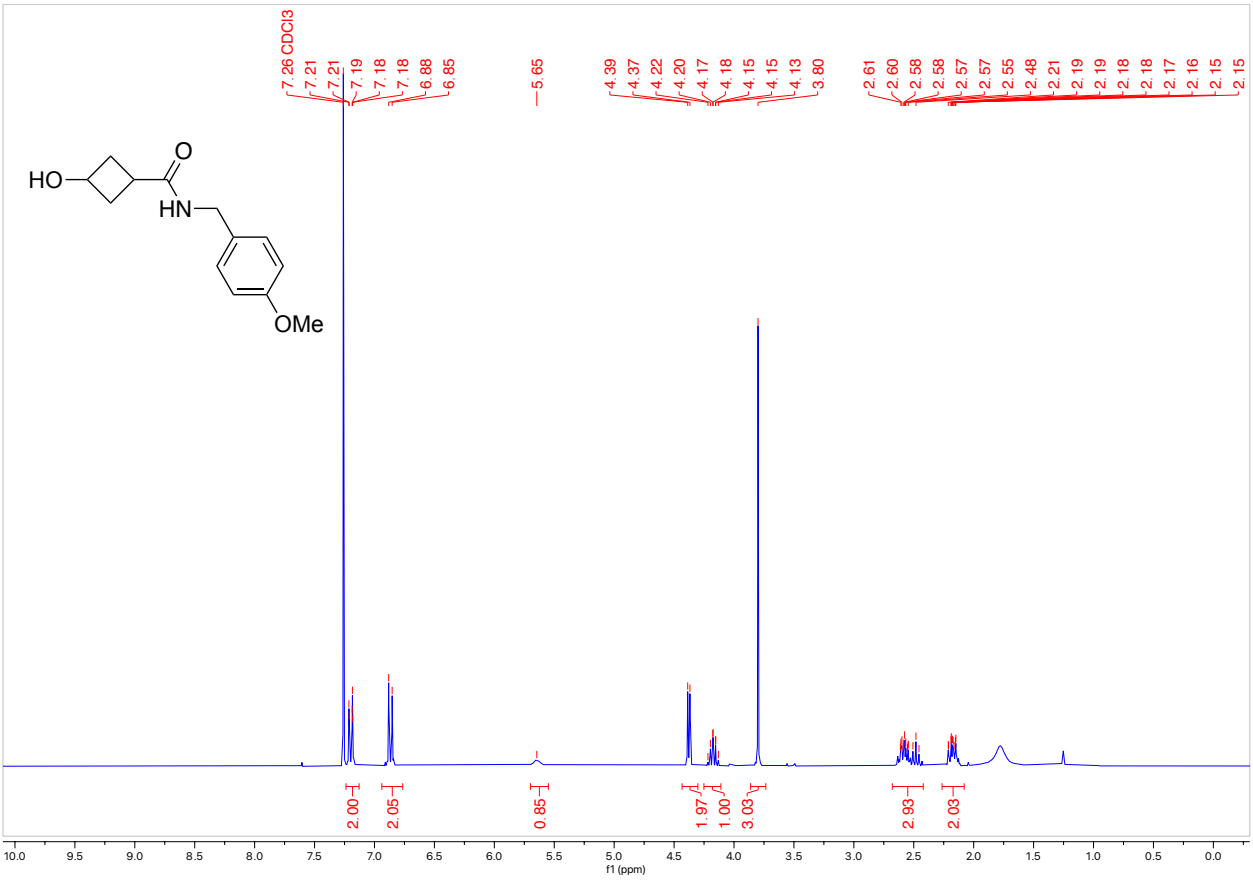

***N*-(4-fluorobenzyl)-3-hydroxycyclobutane-1-carboxamide**

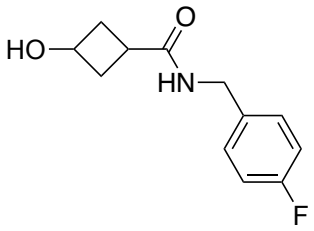

This product was prepared using **General Procedure 2** on a 1.6 mmol scale and 183.5 mg of a white solid was obtained (50% Yield).

^{1}H NMR (300 MHz, $CDCl_3$, 292 K, ppm): δ 7.22 (s, 2H), 7.02 (t, J = 8.7 Hz, 2H), 5.70 (s, 1H), 4.42 (d, J = 5.8 Hz, 2H), 4.26 – 4.13 (m, 1H), 2.69 – 2.43 (m, 3H), 2.23 – 2.07 (m, 2H).

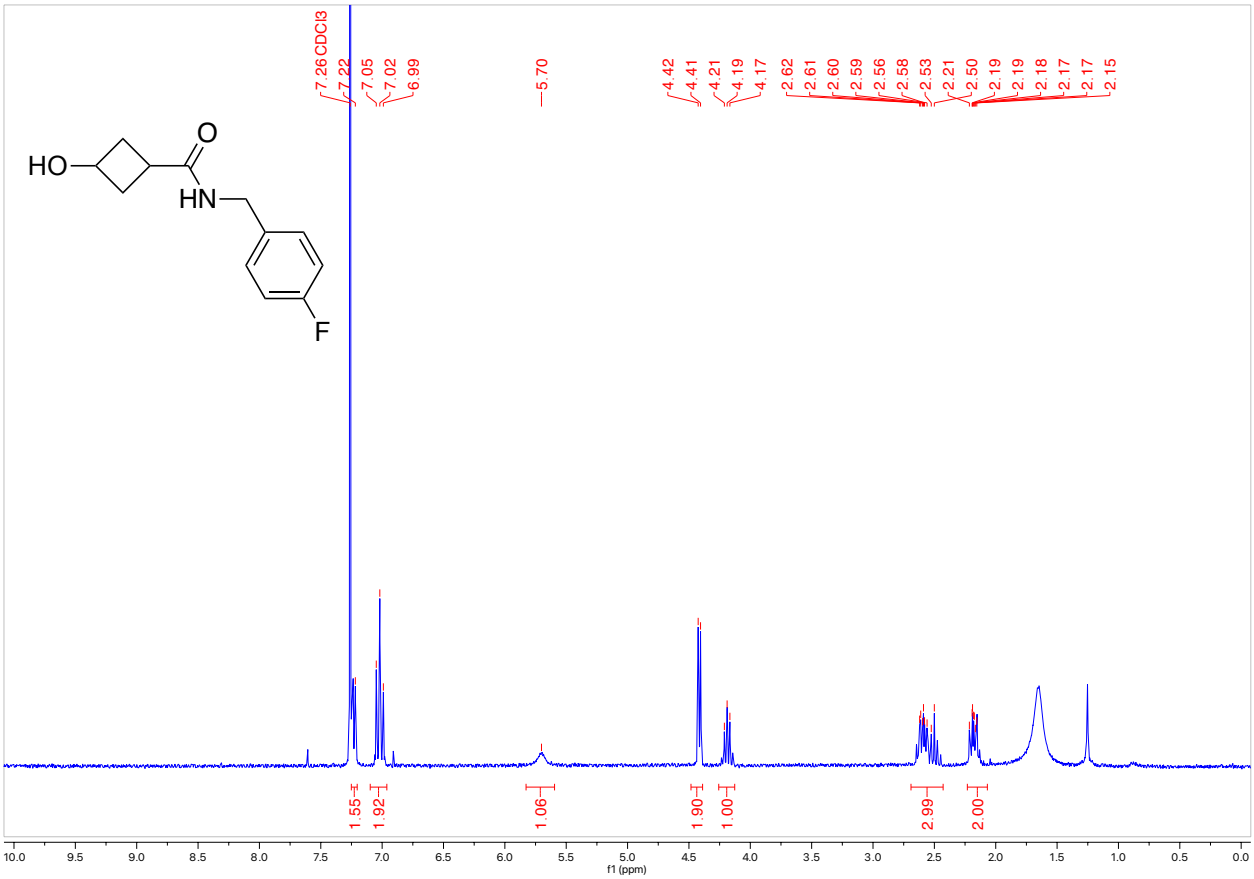

^{19}F NMR (300 MHz, $CDCl_3$, 292 K, ppm): δ 114.78.

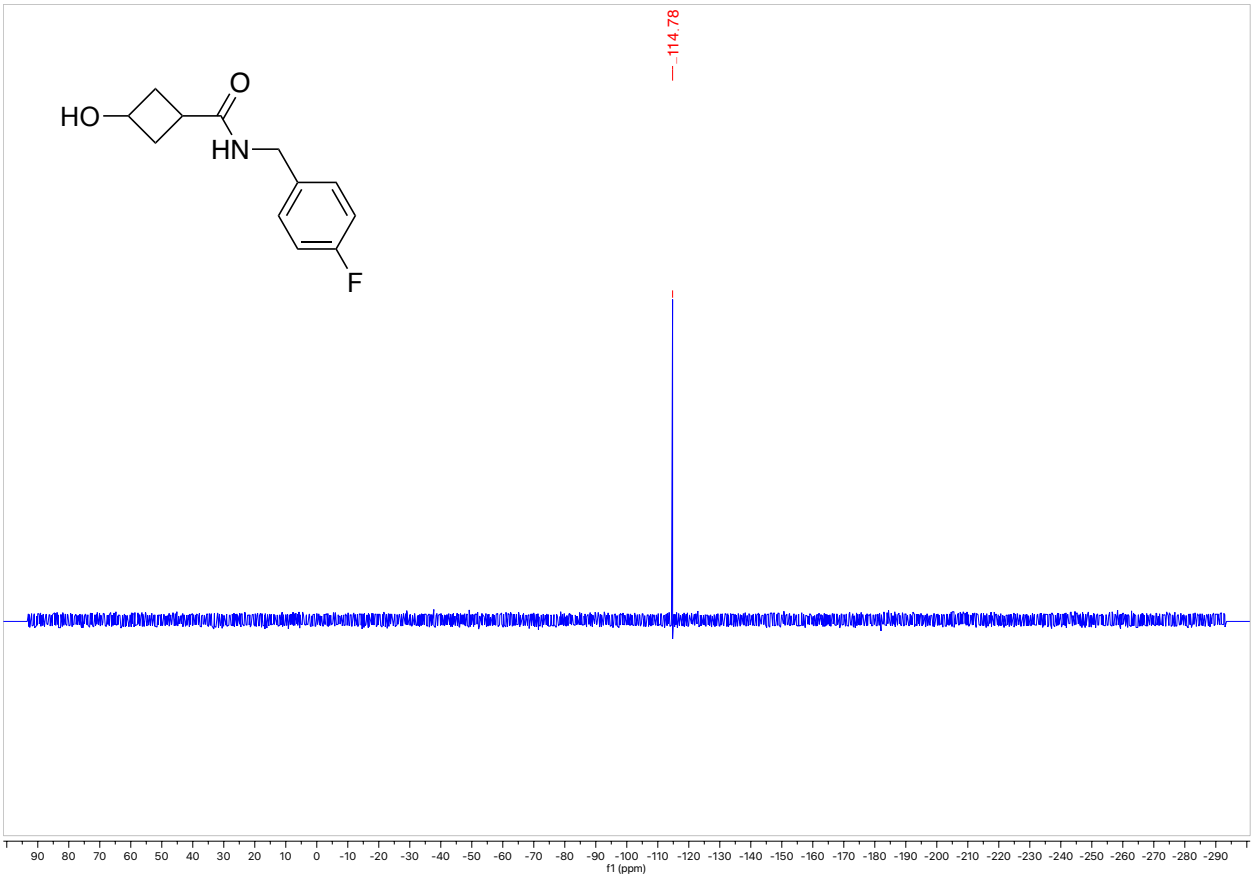

_N_-allyl-3-hydroxycyclobutane-1-carboxamide

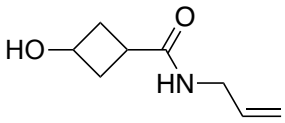

This product was prepared using **General Procedure 2** on a 0.86 mmol scale and 76.4 mg of a white solid was obtained (57% Yield).

^{1}H NMR (300 MHz, $CDCl_3$, 292 K, ppm): δ 5.96 – 5.72 (m, 1H), 5.49 (s, 1H), 5.28 – 5.04 (m, 2H), 4.18 (p, J = 6.5 Hz, 1H), 3.90 (tt, J = 5.8, 1.5 Hz, 2H), 2.70 – 2.40 (m, 3H), 2.24 – 2.08 (m, 2H).

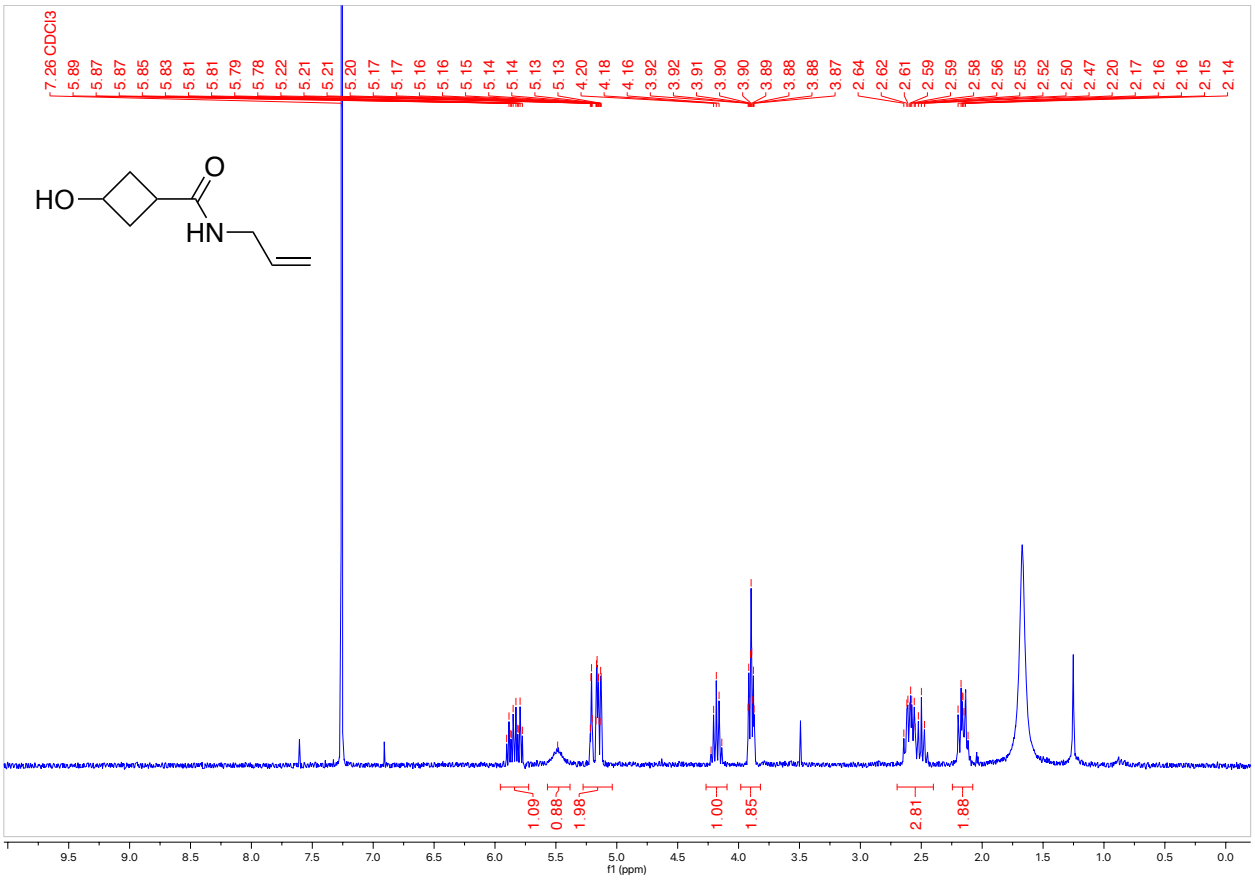

***N*-(*tert*-butyl)-3-hydroxycyclobutane-1-carboxamide**

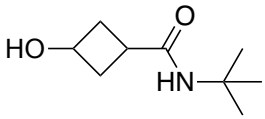

This product was prepared using **General Procedure 2** on a 0.84 mmol scale and 143.3 mg of a white solid was obtained (100% Yield).

^{1}H NMR (300 MHz, $CDCl_3$, 292 K, ppm): δ 5.25 (s, 1H), 4.14 (p, J = 6.6 Hz, 1H), 2.63 – 2.49 (m, 2H), 2.39 (t, J = 7.7 Hz, 1H), 2.20 – 2.02 (m, 2H), 1.35 (s, 9H).

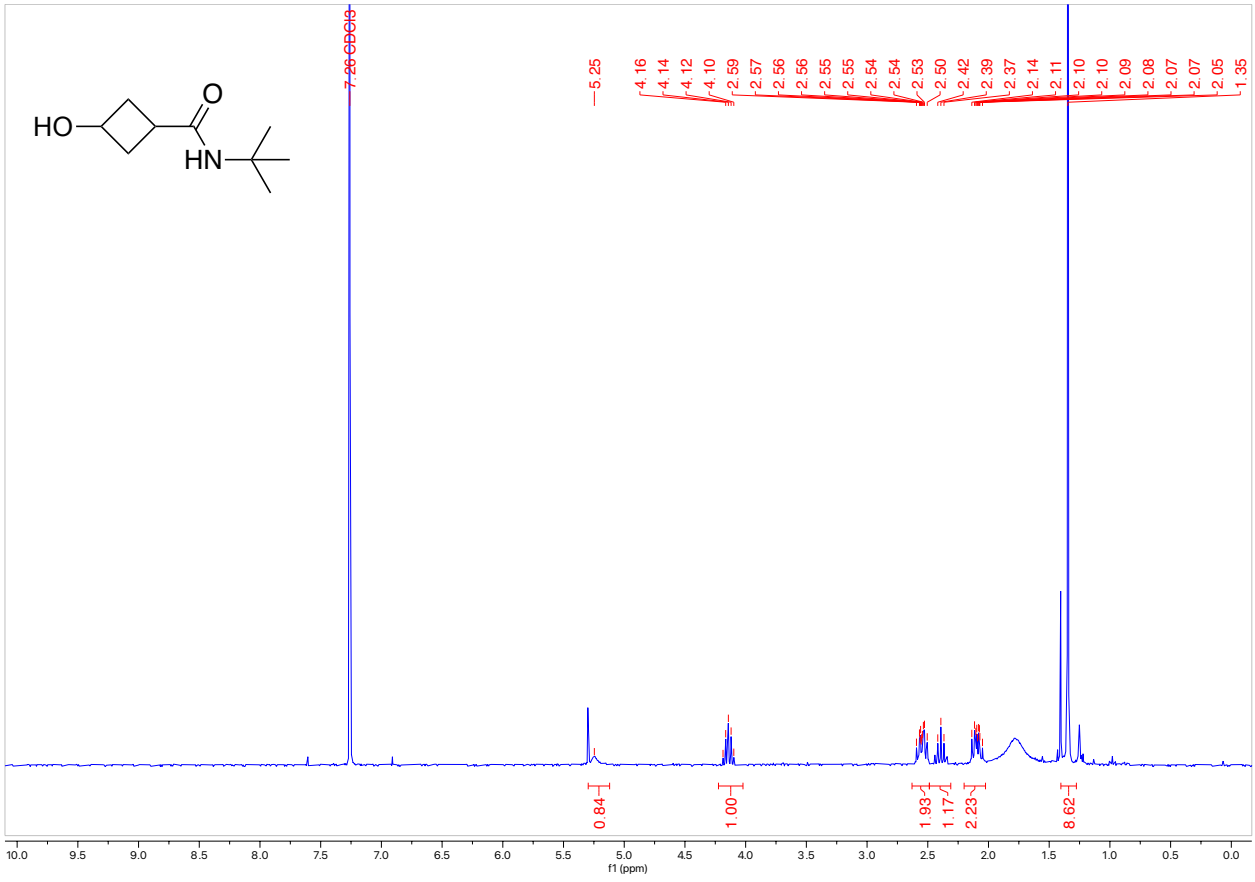

3-Hydroxy-*N*-(2,2,2-trifluoroethyl)cyclobutane-1-carboxamide

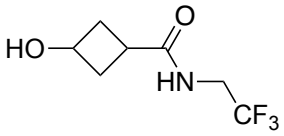

This product was prepared using **General Procedure 2** on a 0.92 mmol scale and 141.9 mg of a white solid was obtained (79% Yield).

^{1}H NMR (300 MHz, $CDCl_3$, 292 K, ppm): δ 5.71 (s, 1H), 4.20 (q, J = 6.9 Hz, 1H), 3.93 (qd, J = 9.1, 6.4 Hz, 2H), 2.69 – 2.44 (m, 3H), 2.28 – 2.03 (m, 2H).

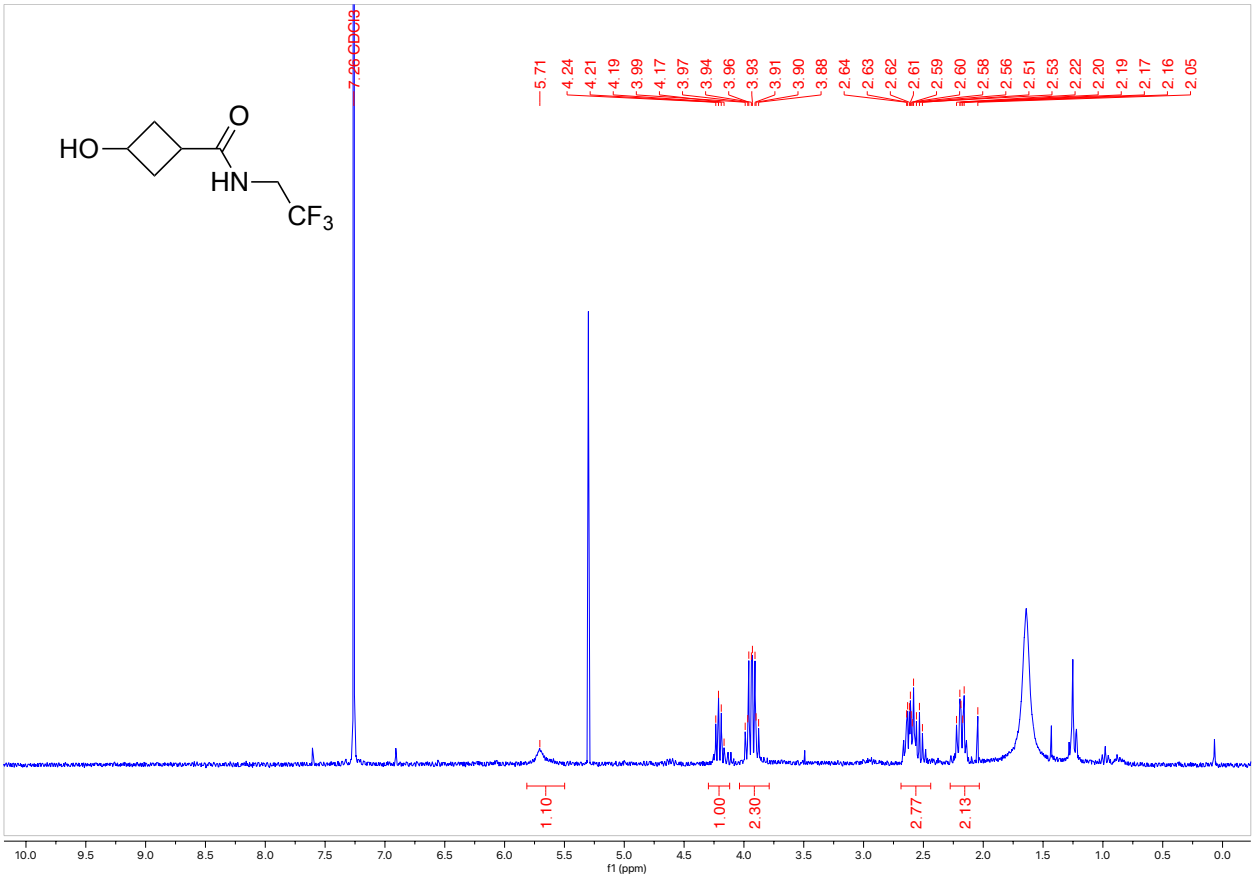

^{19}F NMR (300 MHz, $CDCl_3$, 292 K, ppm): δ 72.60, 72.71.

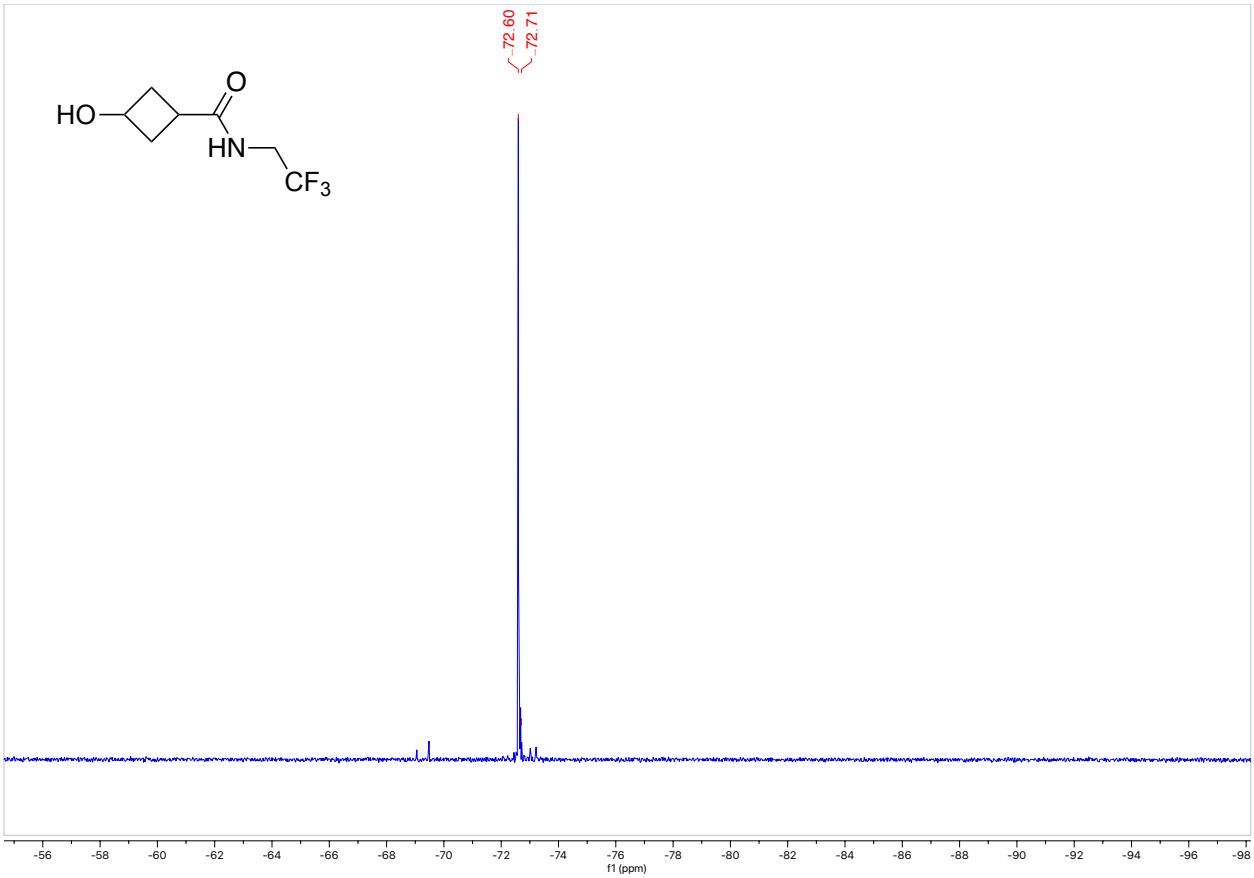

***N*-benzyl-3-hydroxycyclopentane-1-carboxamide**

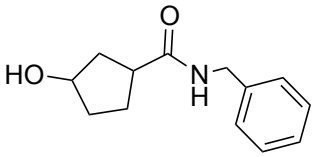

This product was prepared using **General Procedure 2** on a 0.82 mmol scale and 144.6 mg of a white solid was obtained (81% Yield).

^{1}H NMR (300 MHz, $CDCl_3$, 292 K, ppm): δ 7.40 – 7.25 (m, 5H), 6.16 (s, 1H), 4.44 (d, J = 5.8 Hz, 2H), 4.32 (ddd, J = 5.8, 4.3, 1.6 Hz, 1H), 2.83 – 2.63 (m, 1H), 2.03 – 1.86 (m, 6H).

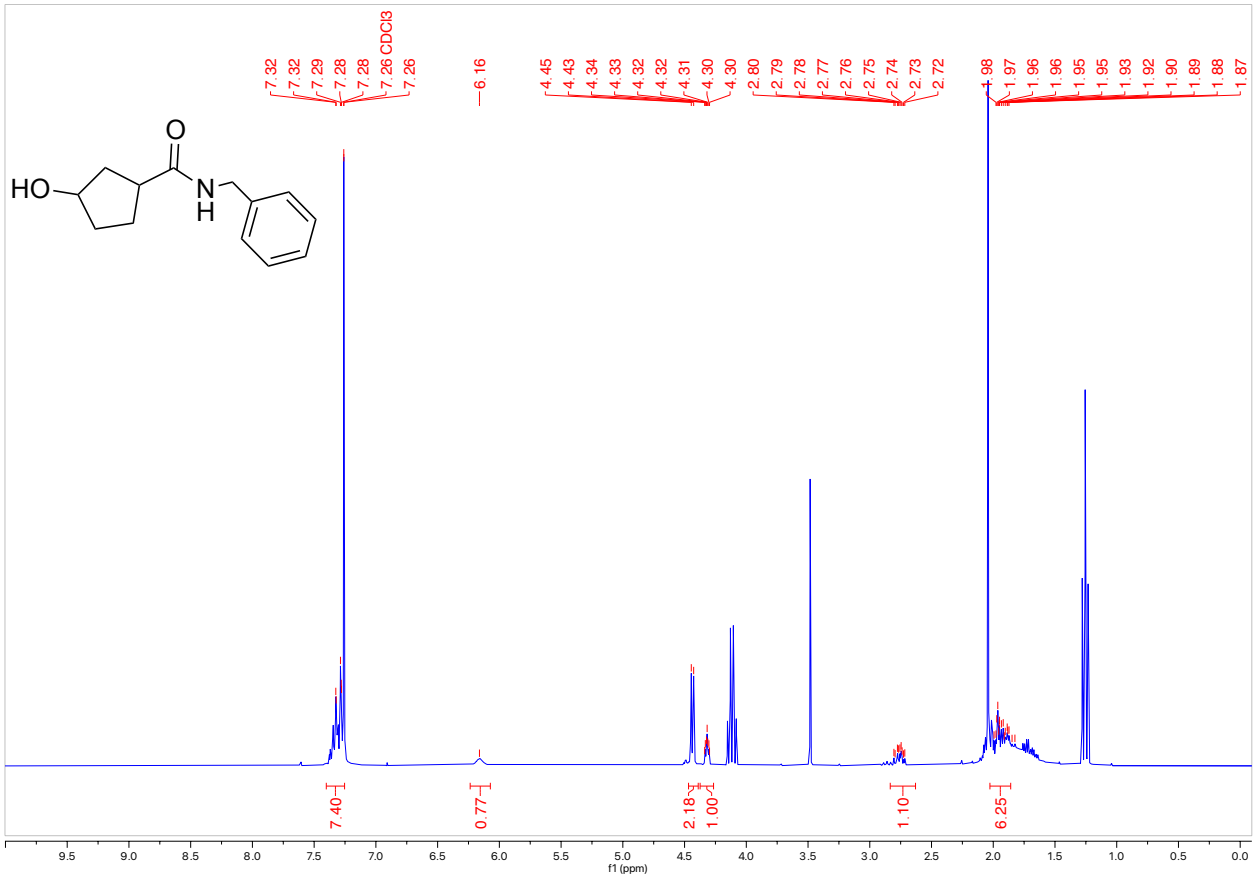

3-Hydroxy-*N*-phenylcyclopentane-1-carboxamide

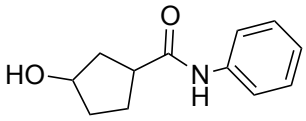

This product was prepared using **General Procedure 2** on a 2.86 mmol scale and 541.6 mg of a white solid was obtained (92% Yield).

^{1}H NMR (300 MHz, $CDCl_3$, 292 K, ppm): δ 7.57 – 7.47 (m, 2H), 7.37 – 7.31 (m, 2H), 7.15 – 7.07 (m, 1H), 4.42 (s, 1H), 2.93 (tdd, J = 9.2, 6.2, 2.6 Hz, 1H), 2.21 – 2.04 (m, 4H), 2.02 – 1.84 (m, 2H), 1.79 – 1.69 (m, 1H).

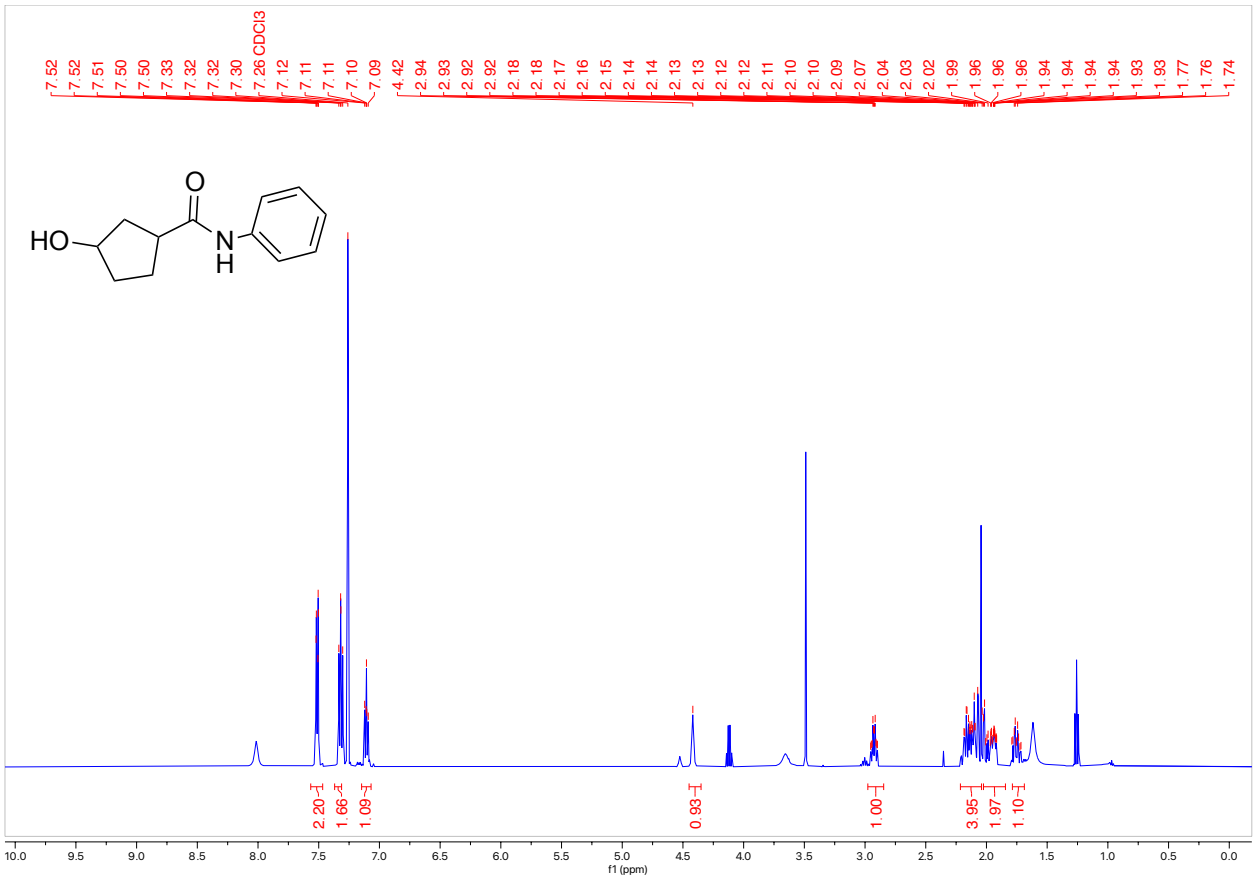

_N_-allyl-3-hydroxycyclopentane-1-carboxamide

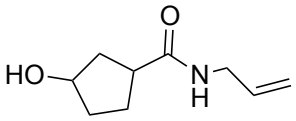

This product was prepared using **General Procedure 2** on a 1.71 mmol scale and 157.2 mg of a white solid was obtained (54% Yield).

^{1}H NMR (300 MHz, $CDCl_3$, 292 K, ppm): δ 7.57 – 7.47 (m, 2H), 7.37 – 7.31 (m, 2H), 7.15 – 7.07 (m, 1H), 4.42 (s, 1H), 2.93 (tdd, J = 9.2, 6.2, 2.6 Hz, 1H), 2.21 – 2.04 (m, 4H), 2.02 – 1.84 (m, 2H), 1.79 – 1.69 (m, 1H).

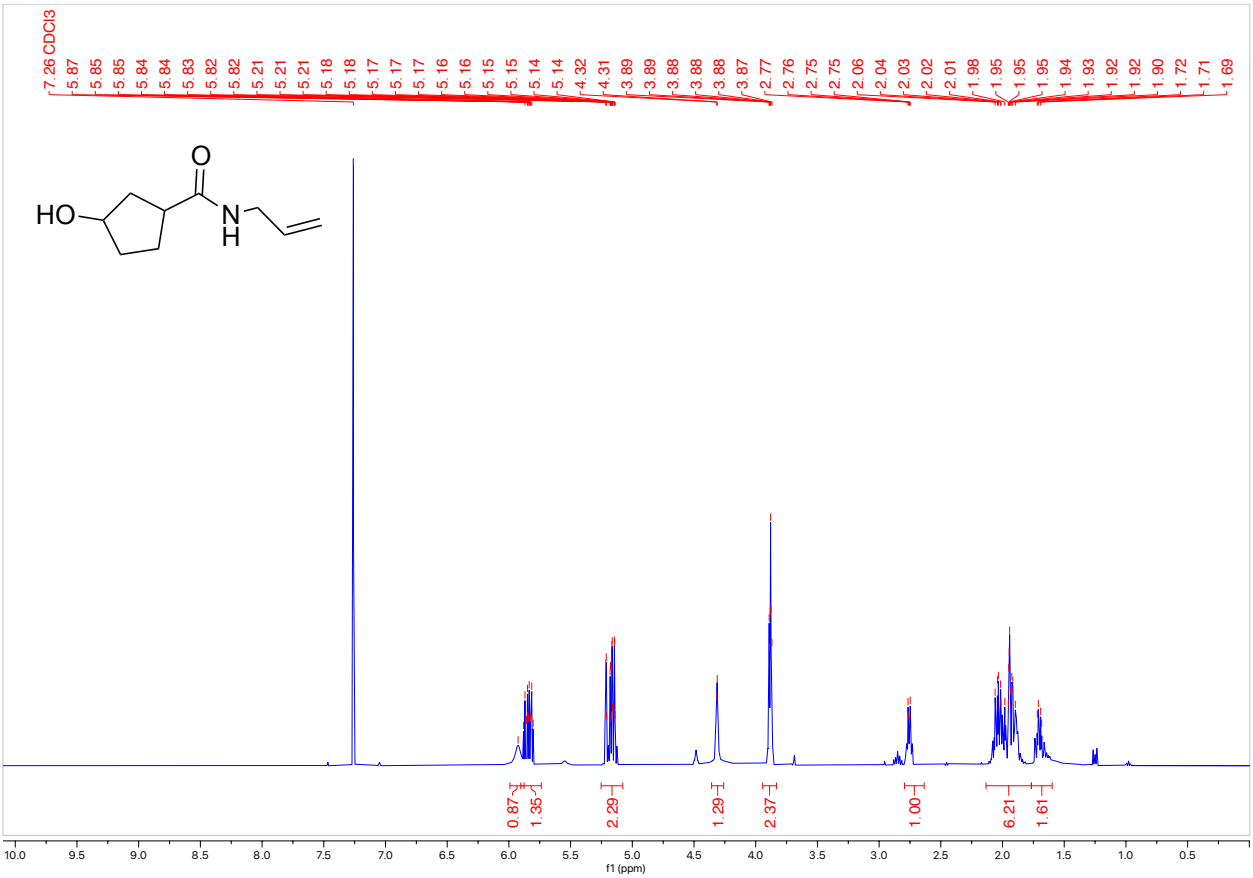

Methyl (3-hydroxycyclopentane-1-carbonyl)glycinate

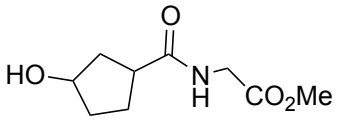

This product was prepared using **General Procedure 2** on a 1.62 mmol scale and 128.6 mg of a white solid was obtained. Transesterification of the ethyl ester occured to give the methyl ester product instead. (40% Yield).

^{1}H NMR (300 MHz, $CDCl_3$, 292 K, ppm): δ 6.43 (s, 1H), 4.36 (dt, J = 4.4, 2.4 Hz, 1H), 4.07 (dd, J = 5.2, 3.2 Hz, 2H), 3.80 (s, 3H), 2.91 – 2.80 (m, 1H), 2.06 (s, 3H), 2.01 – 1.96 (m, 2H), 1.96 – 1.88 (m, 1H), 1.80 – 1.70 (m, 1H).

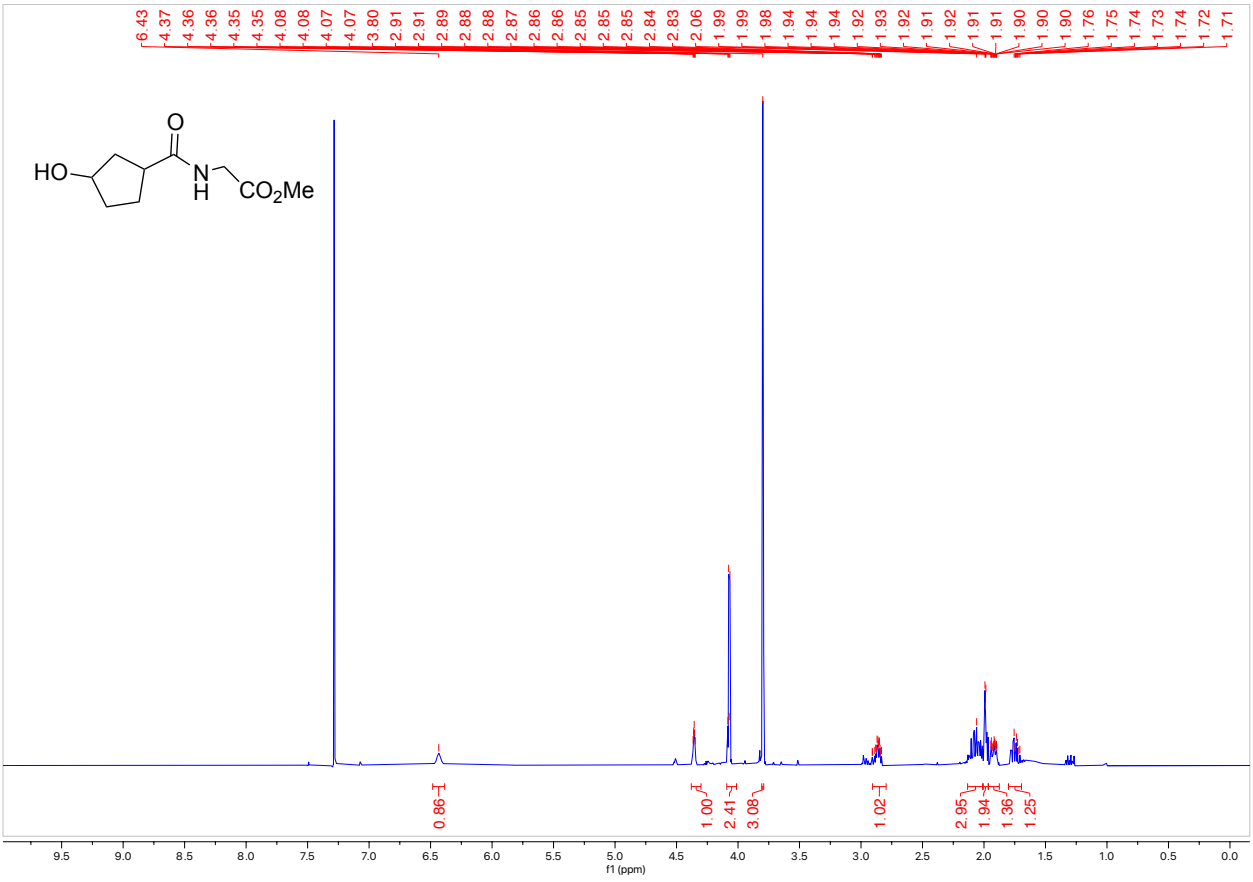

***N*-(*tert*-butyl)-3-hydroxycyclopentane-1-carboxamide**

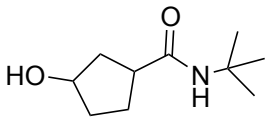

This product was prepared using **General Procedure 2** on a 1.75 mmol scale and 216.0 mg of a white solid was obtained. Transesterification of the ethyl ester occured to give the methyl ester product instead. (67% Yield).

^{1}H NMR (300 MHz, $CDCl_3$, 292 K, ppm): δ 5.58 (s, 1H), 4.27 (tt, J = 4.6, 1.3 Hz, 1H), 2.62 (tdd, J = 9.4, 5.3, 2.1 Hz, 1H), 2.05 – 1.73 (m, 5H), 1.73 – 1.52 (m, 1H), 1.35 (s, 9H).

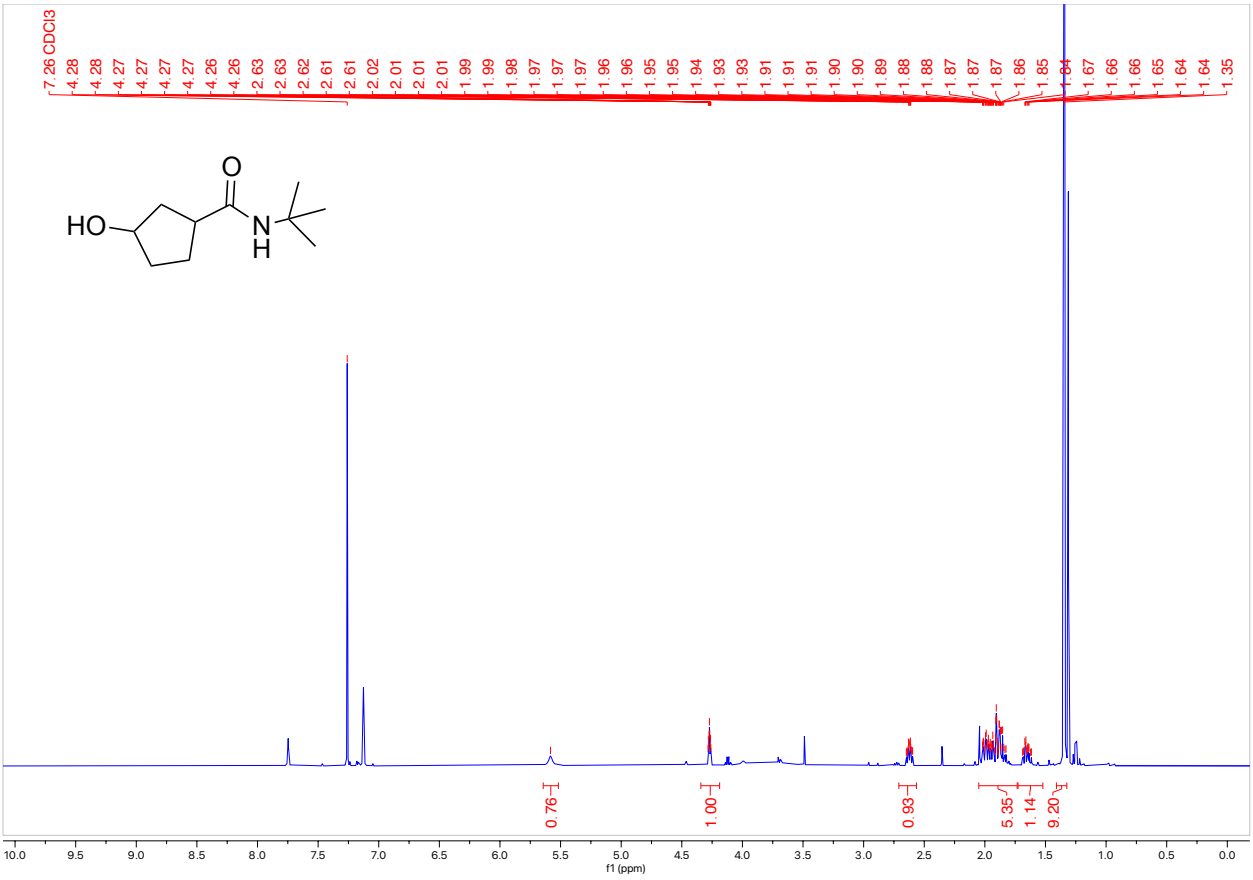

3-(Benzylcarbamoyl)cyclobutyl 4-methylbenzenesulfonate (1a)

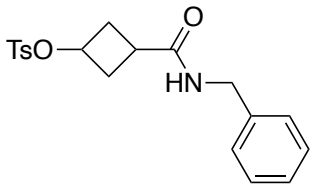

This product was prepared using **General Procedure 3** on a 4.9 mmol scale. The product was purified by column chromatography (Biotage® Sfär 25g Column, 0-100% EtOAc/ hexanes, eluted at 68% EtOAc) and 549.4 mg of a white solid was obtained (31% Yield).

^{1}H NMR (300 MHz, $CDCl_3$, 292 K, ppm): δ 7.78 (d, J = 8.3 Hz, 2H), 7.39 – 7.13 (m, 7H), 5.60 (s, 1H), 4.85 – 4.66 (m, 1H), 4.40 (d, J = 5.6 Hz, 2H), 2.56 – 2.35 (m, 8H).

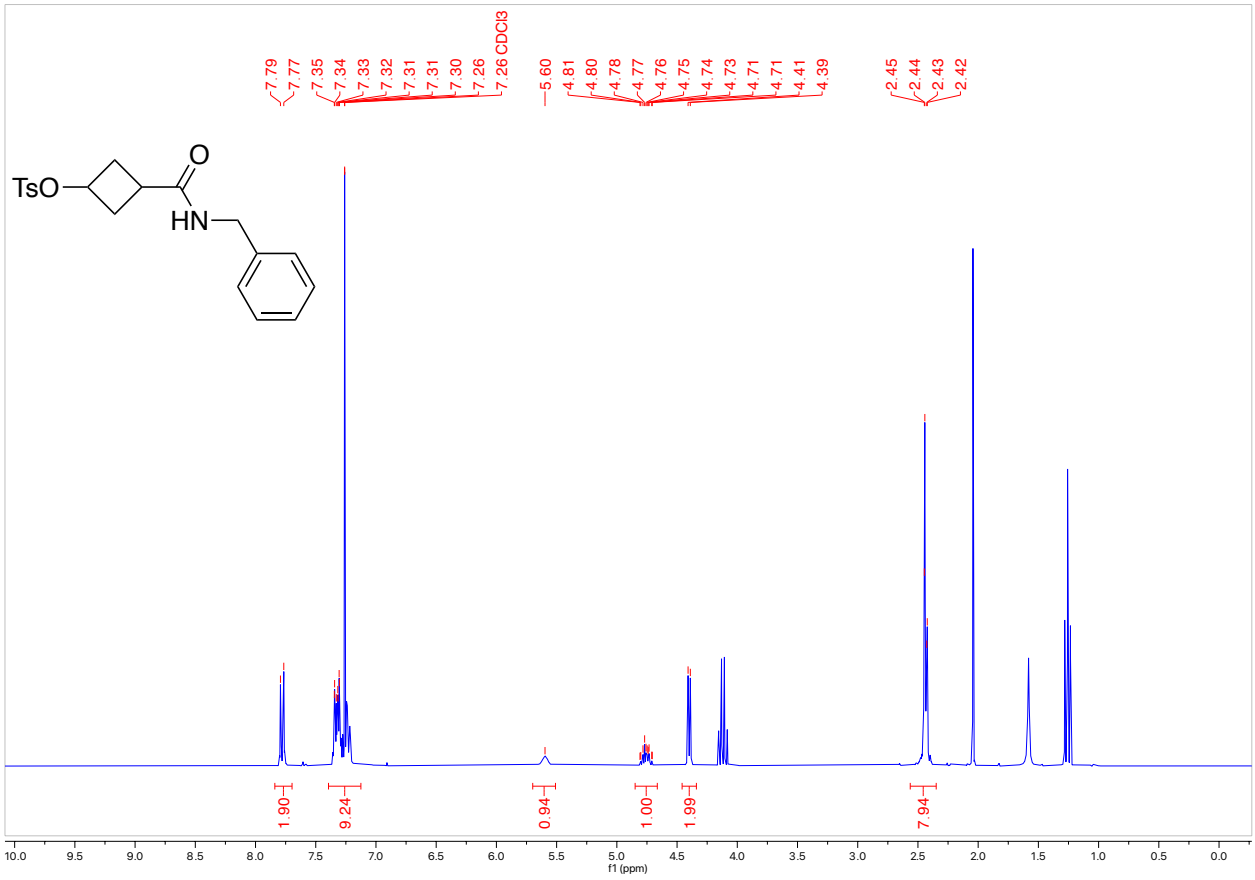

3-((4-Methoxybenzyl)carbamoyl)cyclobutyl 4-methylbenzenesulfonate (1b)

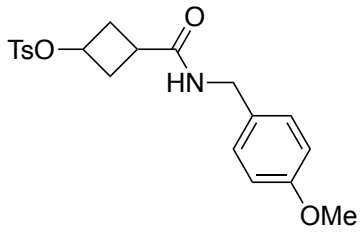

This product was prepared using **General Procedure 3** on a 0.86 mmol scale. The product was purified by column chromatography (Biotage® Sfär 10g Column, 0-100% EtOAc/ hexanes, eluted at 71% EtOAc) and 121.0 mg of a white solid was obtained (36% Yield).

^{1}H NMR (300 MHz, $CDCl_3$, 292 K, ppm): δ 7.78 (d, J = 8.3 Hz, 2H), 7.39 – 7.13 (m, 7H), 5.60 (s, 1H), 4.85 – 4.66 (m, 1H), 4.40 (d, J = 5.6 Hz, 2H), 2.56 – 2.35 (m, 8H).

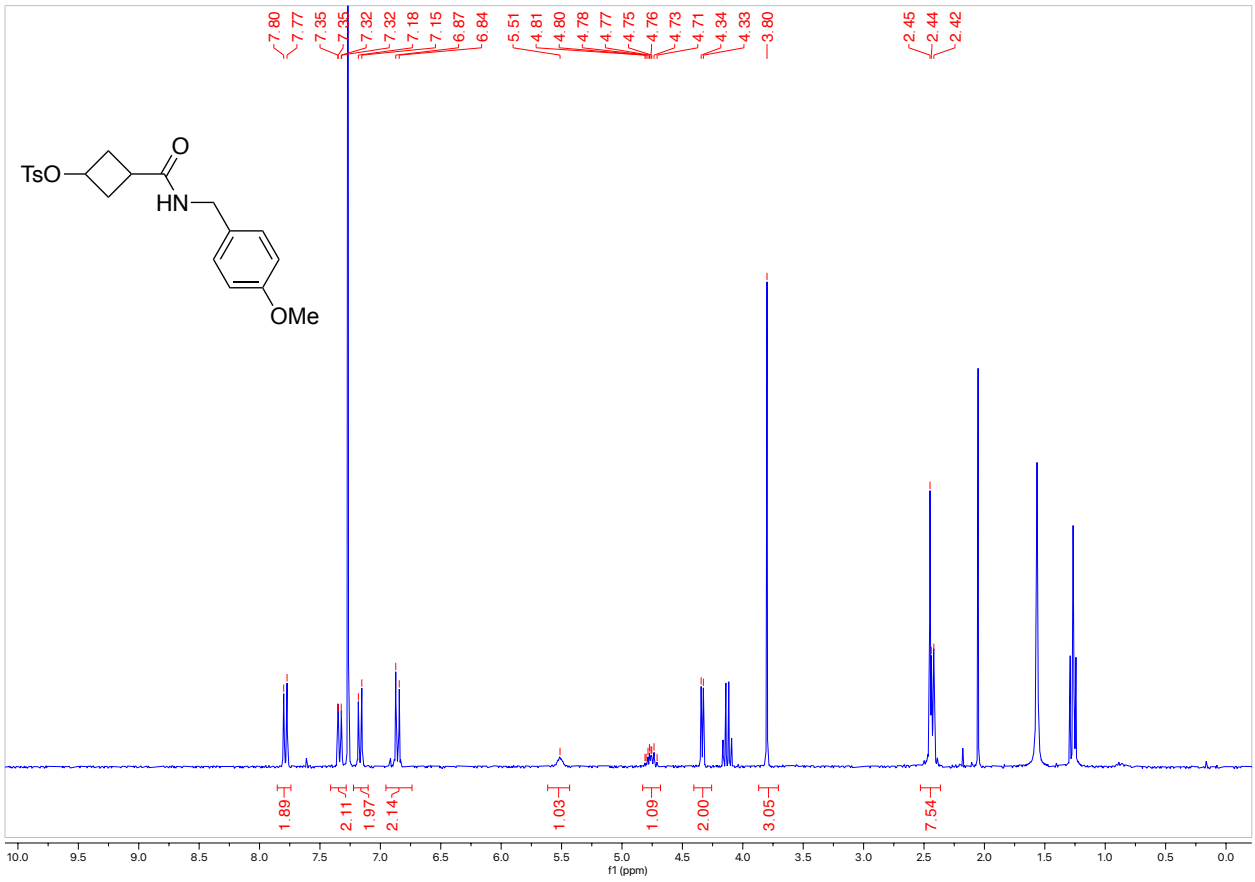

3-((4-Fluorobenzyl)carbamoyl)cyclobutyl 4-methylbenzenesulfonate (1c)

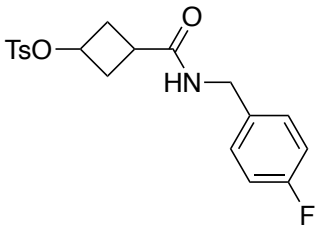

This product was prepared using **General Procedure 3** on a 0.82 mmol scale. The product was purified by column chromatography (Biotage® Sfär 10g Column, 0-100% EtOAc/ hexanes, eluted at 71% EtOAc) and 212.4 mg of a white solid was obtained (66% Yield).

^{1}H NMR (300 MHz, $CDCl_3$, 292 K, ppm): δ 7.78 (d, J = 8.3 Hz, 2H), 7.38 – 7.28 (m, 2H), 7.20 (dd, J = 8.5, 5.4 Hz, 2H), 7.00 (t, J = 8.7 Hz, 2H), 5.58 (s, 1H), 4.83 – 4.69 (m, 1H), 4.37 (d, J = 5.8 Hz, 2H), 2.51 – 2.37 (m, 7H).

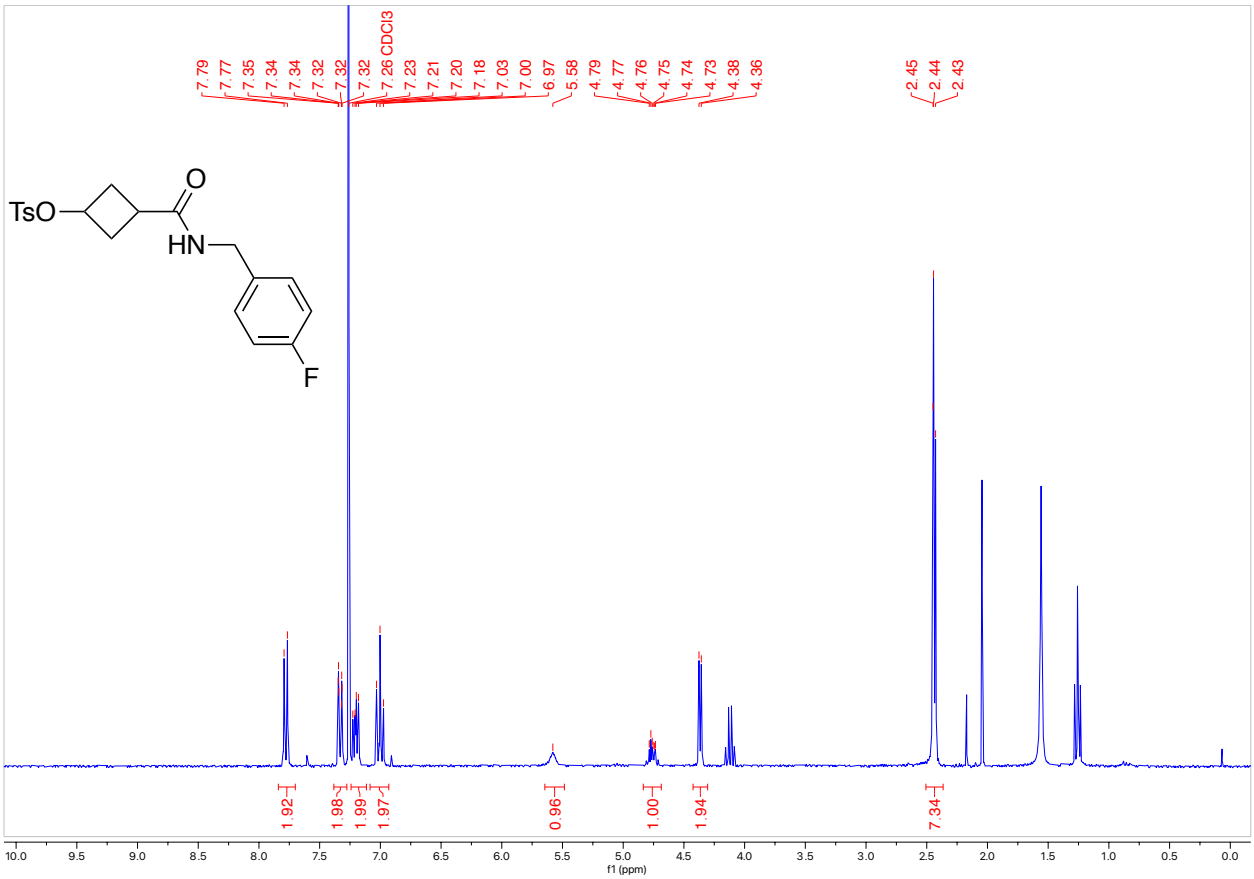

^{19}F NMR (300 MHz, $CDCl_3$, 292 K, ppm): δ 114.61.

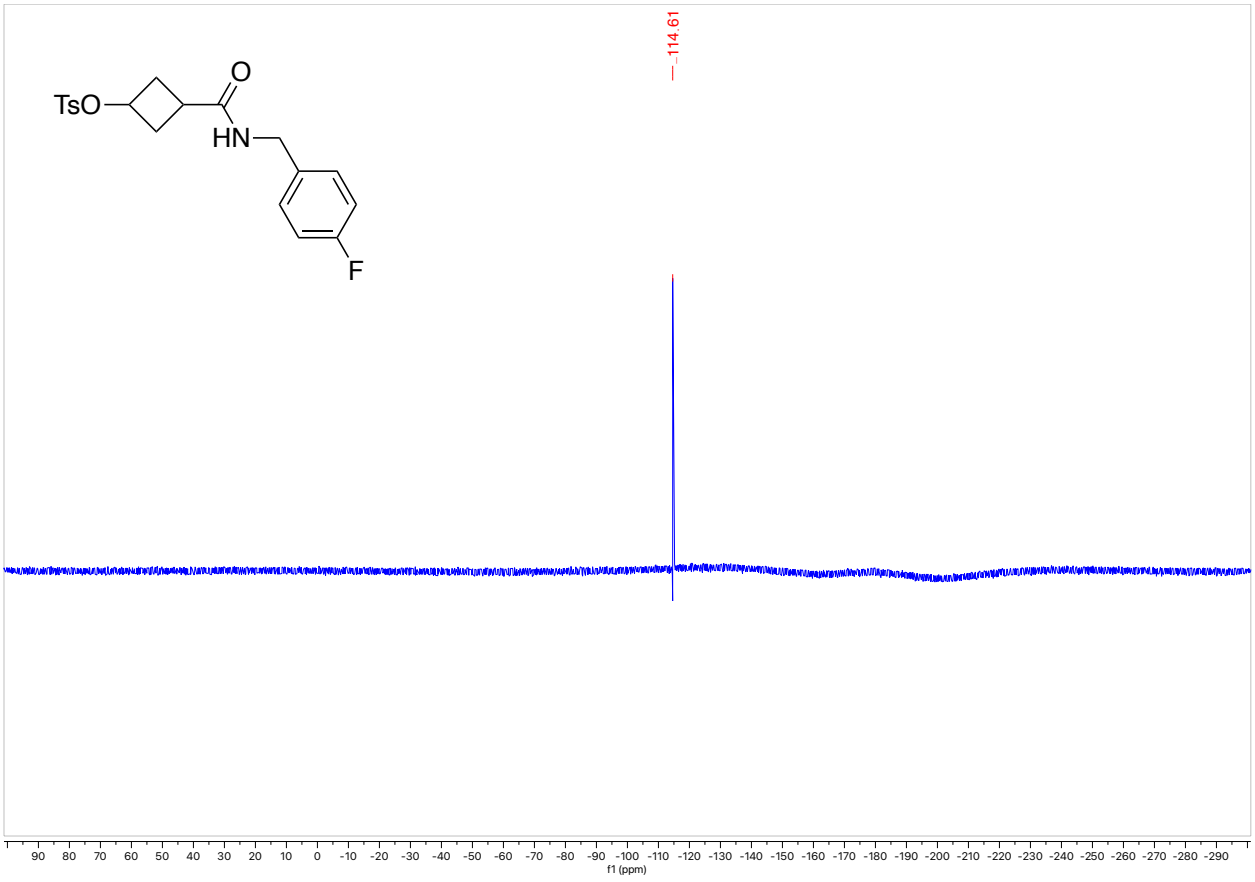

3-(Allylcarbamoyl)cyclobutyl 4-methylbenzenesulfonate (1d)

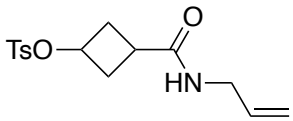

This product was prepared using **General Procedure 3** on a 0.49 mmol scale. The product was purified by column chromatography (Biotage® Sfär 10g Column, 0-100% EtOAc/ hexanes, eluted at 100% EtOAc) and 44.3 mg of a white solid was obtained (29% Yield).

^{1}H NMR (300 MHz, $CDCl_3$, 292 K, ppm): δ 7.78 (d, J = 8.3 Hz, 2H), 7.39 – 7.30 (m, 2H), 5.92 – 5.69 (m, 1H), 5.35 (s, 1H), 5.22 – 5.08 (m, 2H), 4.84 – 4.67 (m, 1H), 3.85 (tt, J = 5.8, 1.5 Hz, 2H), 2.50 – 2.34 (m, 7H).

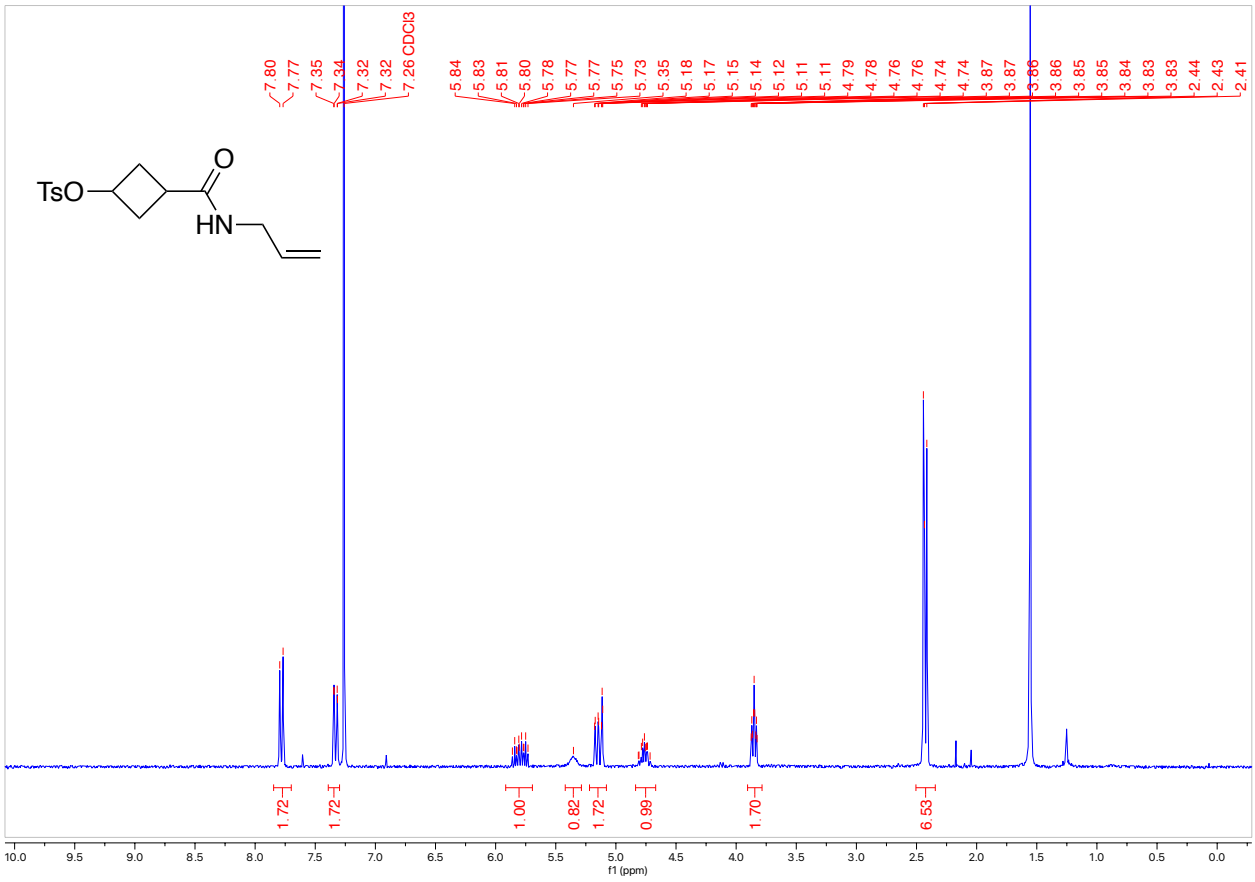

3-(*Tert*-butylcarbamoyl)cyclobutyl 4-methylbenzenesulfonate (1e)

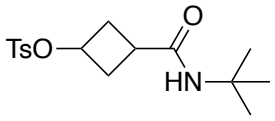

This product was prepared using **General Procedure 3** on a 1.2 mmol scale. The product was purified by column chromatography (Biotage® Sfär 10g Column, 0-100% EtOAc/ hexanes, eluted at 5% EtOAc) and 115.1 mg of a white solid was obtained (30% Yield).

^{1}H NMR (300 MHz, $CDCl_3$, 292 K, ppm): δ 7.78 (d, J = 8.3 Hz, 2H), 7.37 – 7.30 (m, 2H), 5.10 (s, 1H), 4.74 (p, J = 7.5 Hz, 1H), 2.44 (s, 3H), 2.41 – 2.25 (m, 5H), 1.31 (s, 9H).

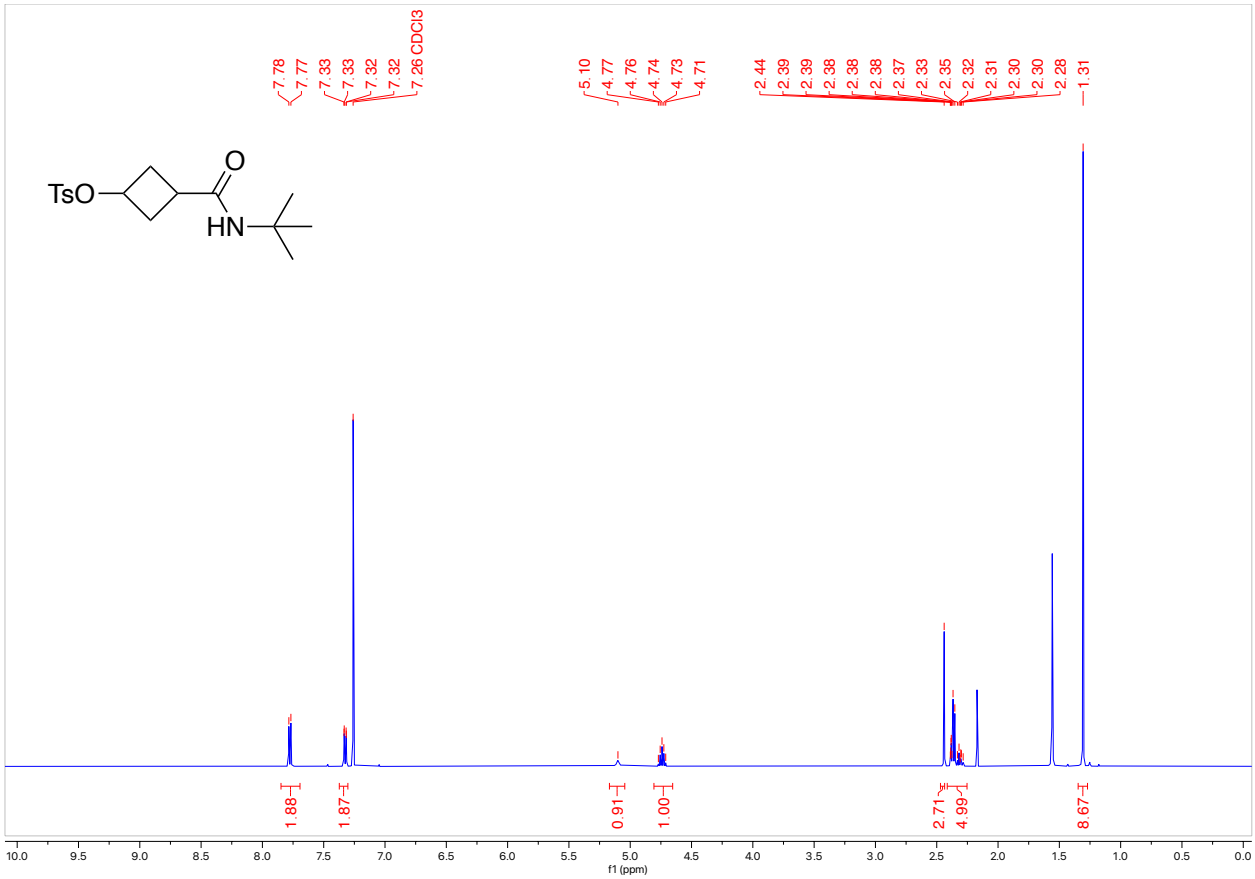

3-((2,2,2-Trifluoroethyl)carbamoyl)cyclobutyl 4-methylbenzenesulfonate (1f)

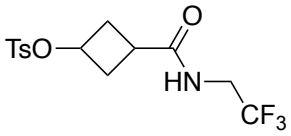

This product was prepared using **General Procedure 3** on a 0.72 mmol scale. The product was purified by column chromatography (Biotage® Sfär 10g Column, 0-100% EtOAc/ hexanes, eluted at 19% EtOAc) and 66.2 mg of a white solid was obtained (26% Yield).

^{1}H NMR (300 MHz, $CDCl_3$, 292 K, ppm): δ 7.78 (d, J = 8.3 Hz, 2H), 7.34 (dd, J = 8.7, 0.7 Hz, 2H), 5.57 (s, 1H), 4.83 – 4.71 (m, 1H), 3.89 (qd, J = 9.0, 6.4 Hz, 2H), 2.46 (d, J = 10.2 Hz, 8H).

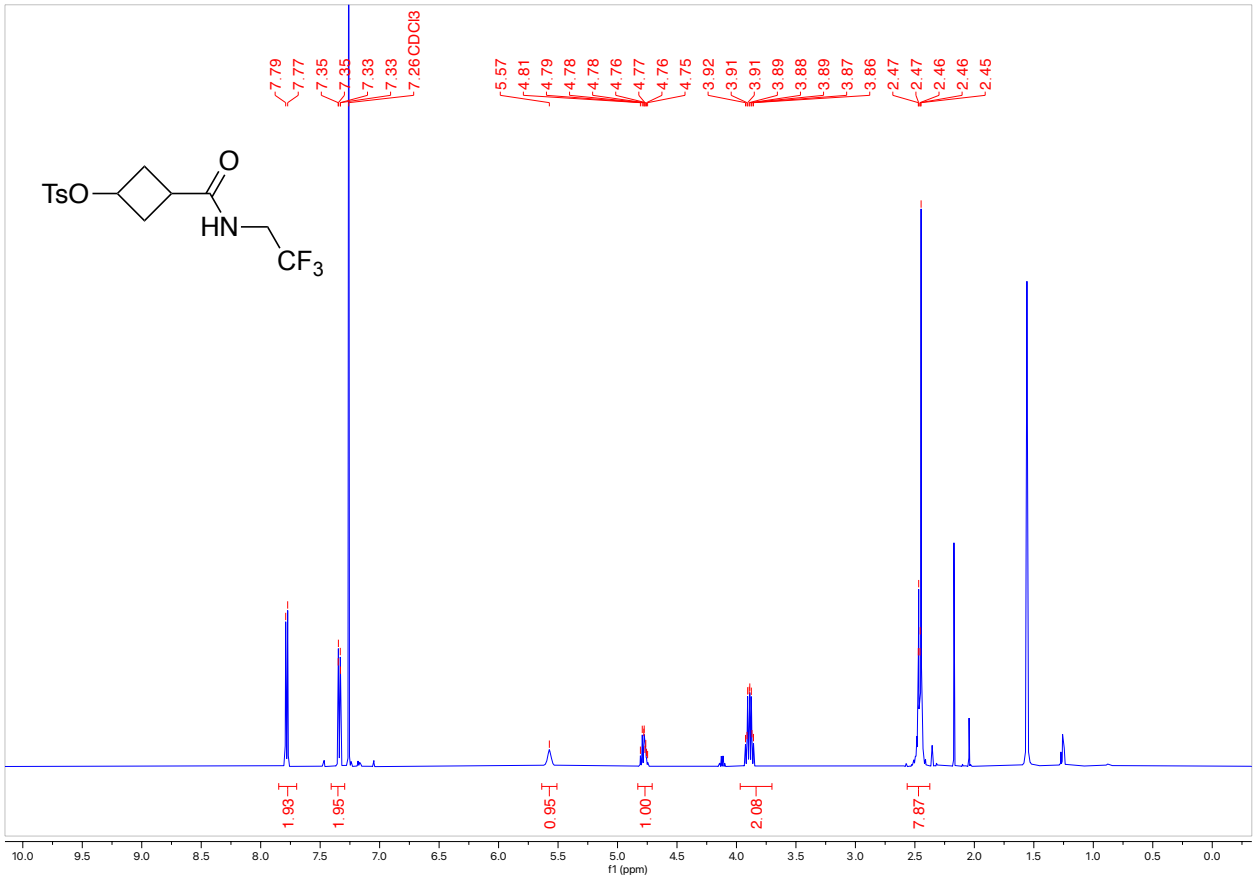

N-benzyl-3-chlorocyclopentane-1-carboxamide (4a)

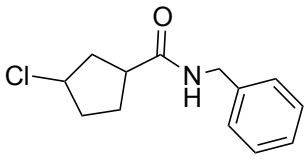

This product was prepared using **General Procedure 4** on a 6.41 mmol scale. The product was purified by column chromatography (Biotage® Sfär 25g Column, 0-100% EtOAc/ hexanes, eluted at 29% EtOAc) and 588.5 mg of a white solid was obtained (39% Yield).

^{1}H NMR (300 MHz, $CDCl_3$, 292 K, ppm): δ 7.40 – 7.26 (m, 5H), 5.75 (s, 1H), 4.57 (dq, J = 5.3, 2.6 Hz, 1H), 4.45 (d, J = 5.7 Hz, 2H), 2.96 (dt, J = 16.2, 8.3 Hz, 1H), 2.49 – 2.32 (m, 1H), 2.32 – 2.15 (m, 3H), 2.15 – 1.89 (m, 2H).

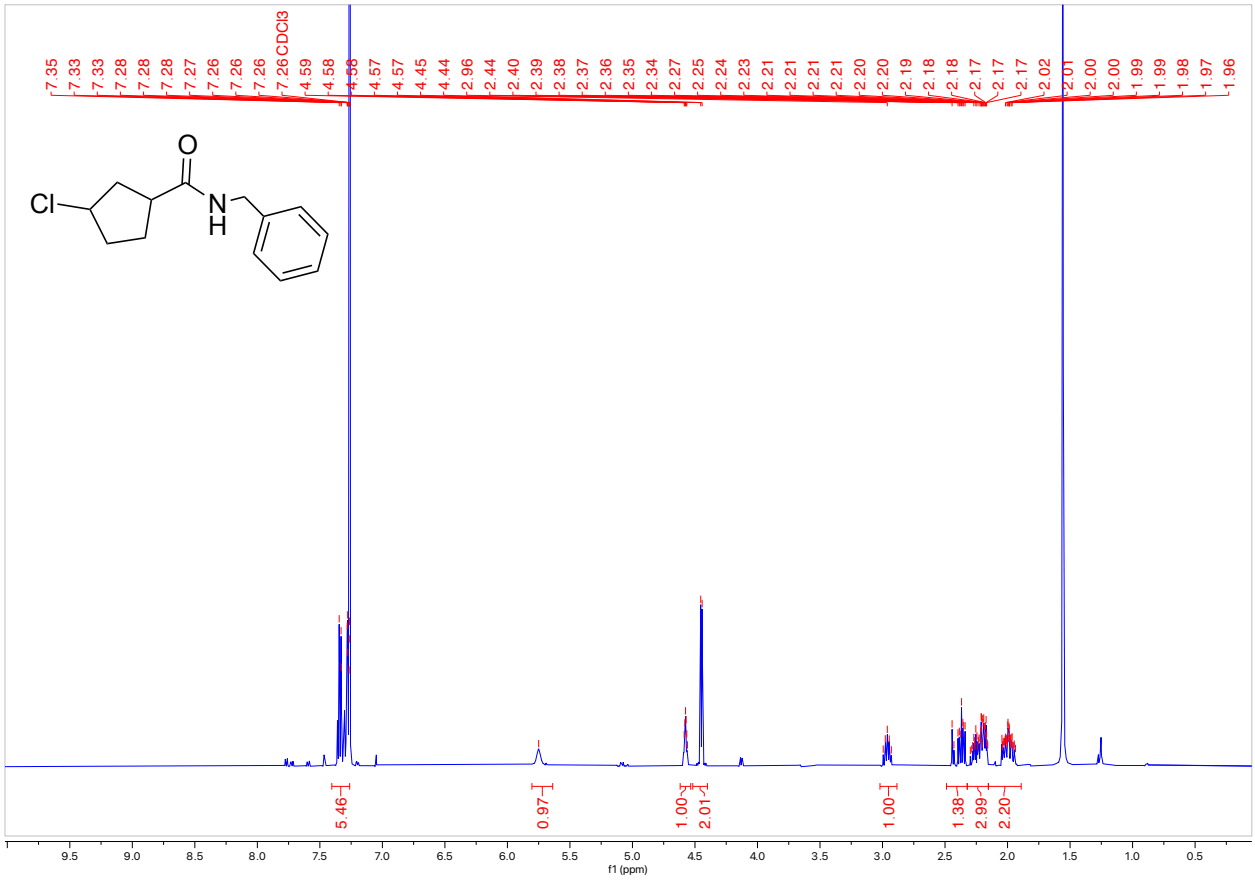

3-Chloro-*N*-phenylcyclopentane-1-carboxamide (4b)

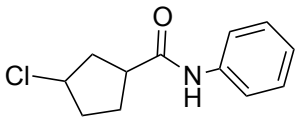

This product was prepared using **General Procedure 4** on a 2.64 mmol scale. The product was purified by column chromatography (Biotage® Sfär 25g Column, 0-100% EtOAc/ hexanes, eluted at 24% EtOAc) and 235.4 mg of a white solid was obtained (40% Yield).

^{1}H NMR (300 MHz, $CDCl_3$, 292 K, ppm): δ 7.57 – 7.48 (m, 2H), 7.33 (dd, J = 8.6, 7.3 Hz, 2H), 7.19 (s, 1H), 7.11 (s, 1H), 4.61 (q, J = 3.4 Hz, 1H), 3.11 (dd, J = 8.8, 5.7 Hz, 1H), 2.50 – 2.37 (m, 1H), 2.34 – 2.19 (m, 3H), 2.12 – 1.99 (m, 2H).

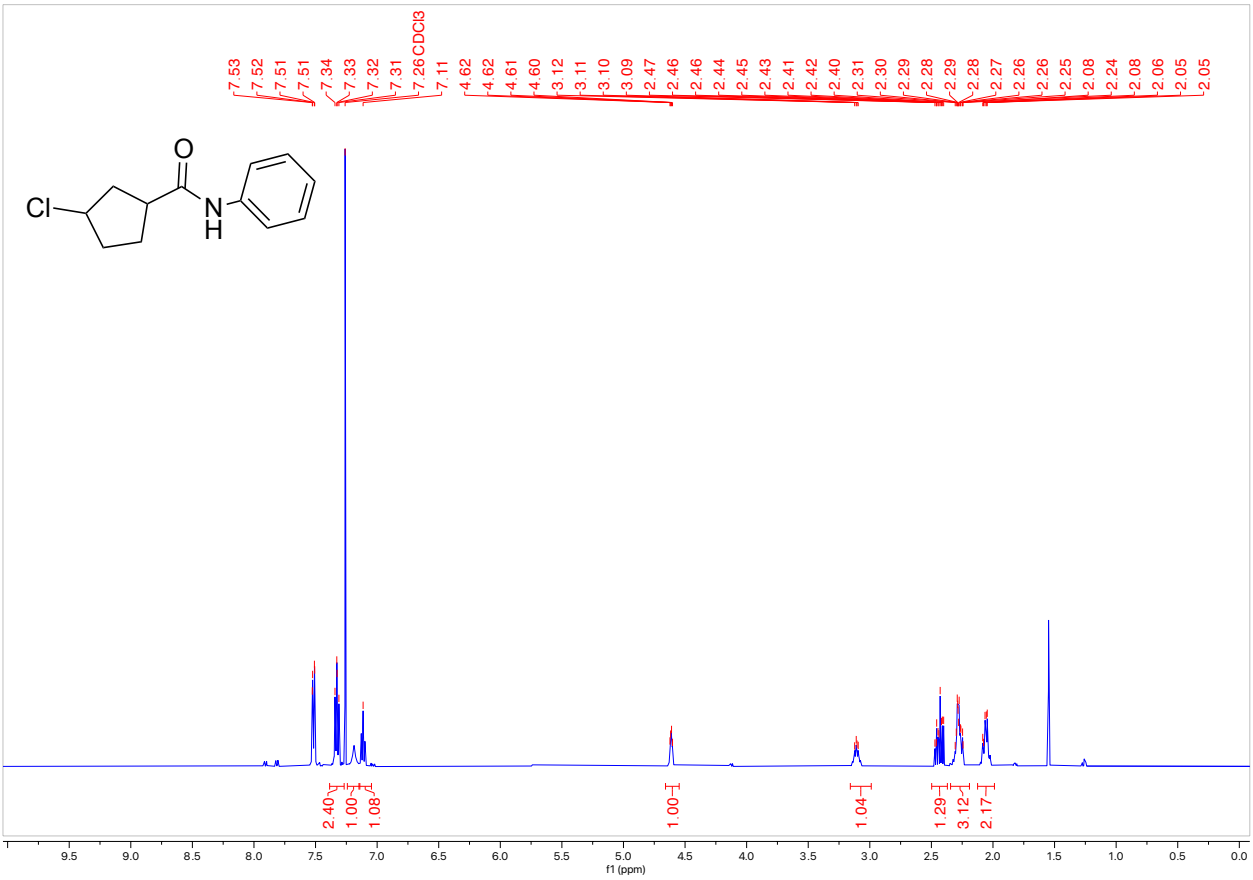

N-allyl-3-chlorocyclopentane-1-carboxamide (4c)

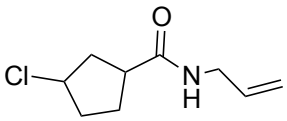

This product was prepared using **General Procedure 4** on a 0.93 mmol scale. The product was purified by column chromatography (Biotage® Sfär 25g Column, 0-100% EtOAc/ hexanes, eluted at 32% EtOAc) and 100.1 mg of a white solid was obtained (57% Yield).

^{1}H NMR (300 MHz, $CDCl_3$, 292 K, ppm): δ 5.84 (ddt, J = 17.2, 10.2, 5.7 Hz, 1H), 5.55 (s, 1H), 5.24 – 5.10 (m, 2H), 4.57 (tt, J = 5.1, 2.4 Hz, 1H), 3.89 (tt, J = 5.8, 1.6 Hz, 2H), 2.95 (tdd, J = 9.0, 7.4, 6.2 Hz, 1H), 2.34 (ddd, J = 14.2, 9.0, 5.4 Hz, 1H), 2.29 – 2.09 (m, 3H), 2.08 – 1.84 (m, 2H).

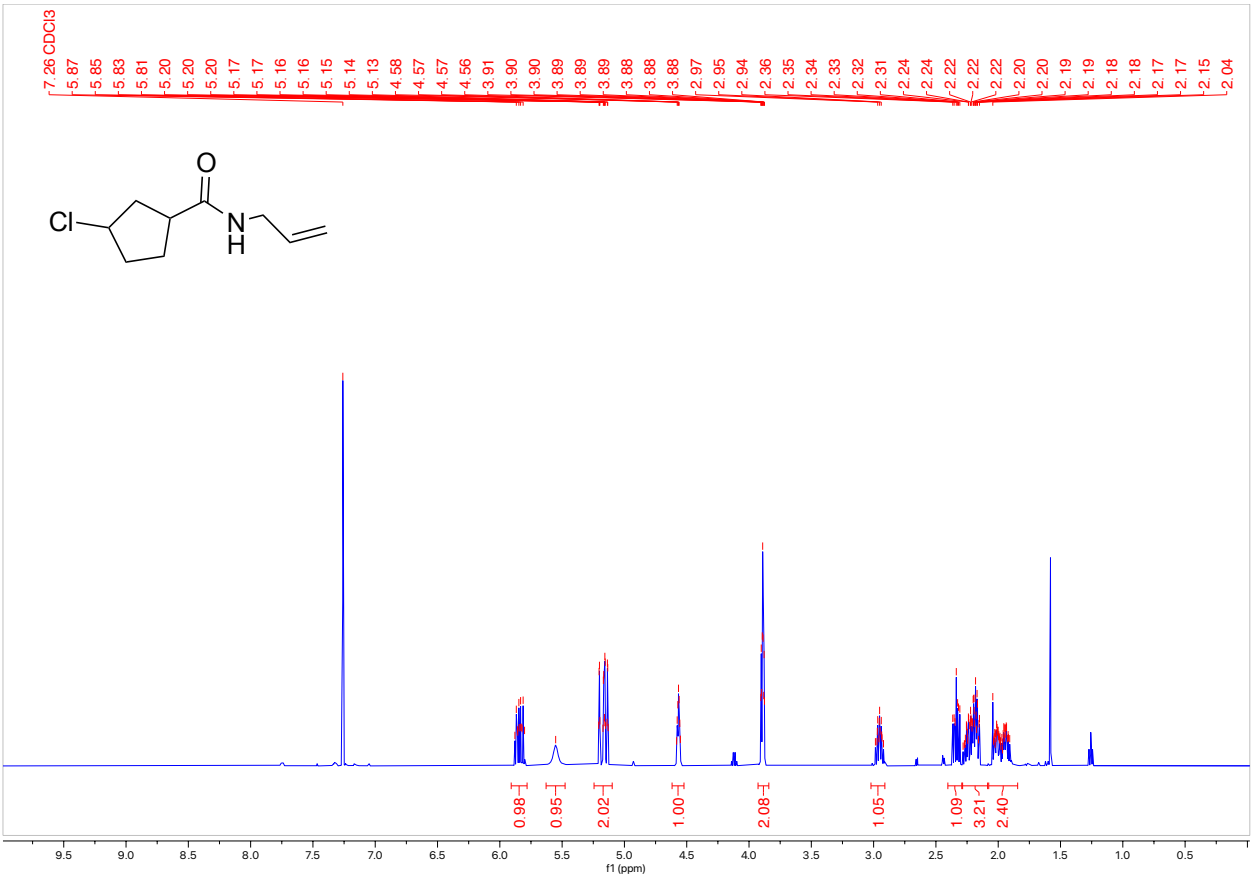

Methyl (3-chlorocyclopentane-1-carbonyl)glycinate (4d)

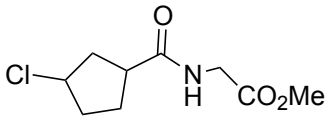

This product was prepared using **General Procedure 4** on a 0.60 mmol scale. The product was purified by column chromatography (Biotage® Sfär 25g Column, 0-100% EtOAc/ hexanes, eluted at 65% EtOAc) and 40.8 mg of a white solid was obtained (29% Yield).

^{1}H NMR (300 MHz, $CDCl_3$, 292 K, ppm): δ 6.07 (s, 1H), 4.55 (tt, J = 5.2, 2.3 Hz, 1H), 4.04 (dd, J = 5.2, 1.2 Hz, 2H), 3.76 (s, 3H), 3.09 – 2.97 (m, 1H), 2.32 (ddd, J = 14.1, 8.9, 5.4 Hz, 1H), 2.27 – 2.15 (m, 3H), 2.03 – 1.90 (m, 2H).

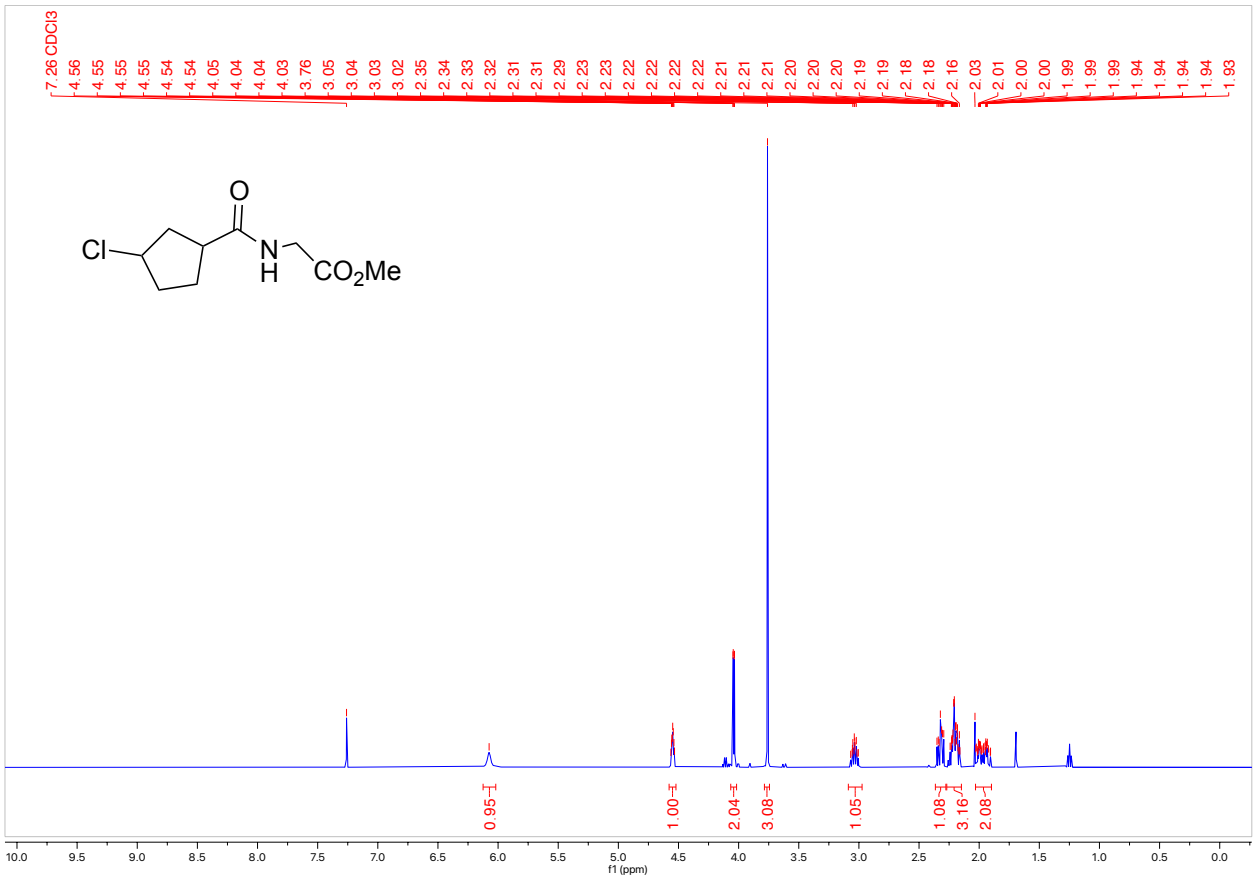

N-(*tert*-butyl)-3-chlorocyclopentane-1-carboxamide (4e)

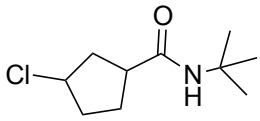

This product was prepared using **General Procedure 4** on a 1.17 mmol scale. The product was purified by column chromatography (Biotage® Sfär 25g Column, 0-100% EtOAc/ hexanes, eluted at 77% EtOAc) and 210.5 mg of a white solid was obtained (89% Yield).

^{1}H NMR (300 MHz, $CDCl_3$, 292 K, ppm): δ 5.29 (s, 1H), 4.55 (tt, J = 5.1, 2.4 Hz, 1H), 2.88 – 2.78 (m, 1H), 2.29 (ddd, J = 14.1, 8.9, 5.4 Hz, 1H), 2.25 – 2.17 (m, 1H), 2.17 – 2.09 (m, 2H), 2.02 – 1.95 (m, 1H), 1.93 – 1.85 (m, 1H), 1.34 (s, 9H).

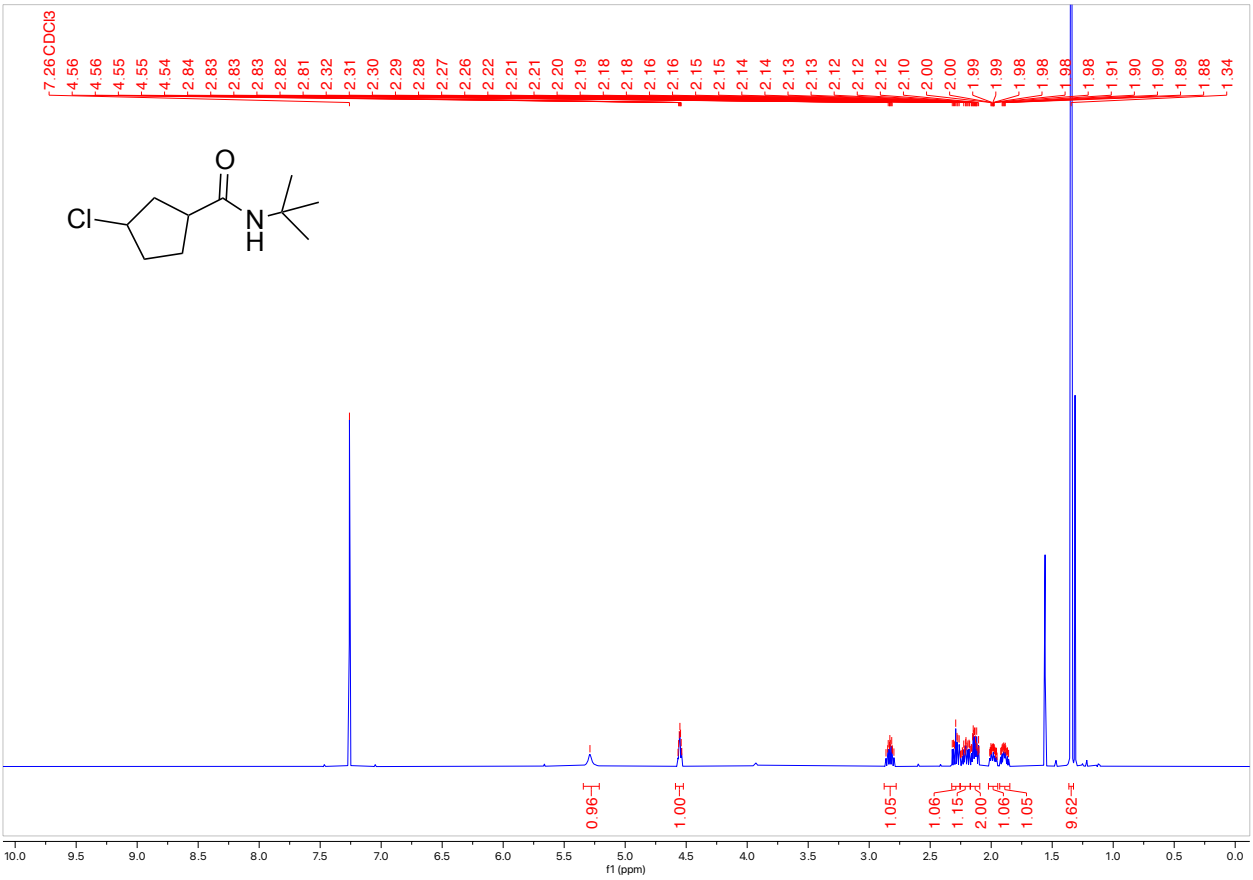

D.3 Optimization

Table 5.1 reaction conditions:

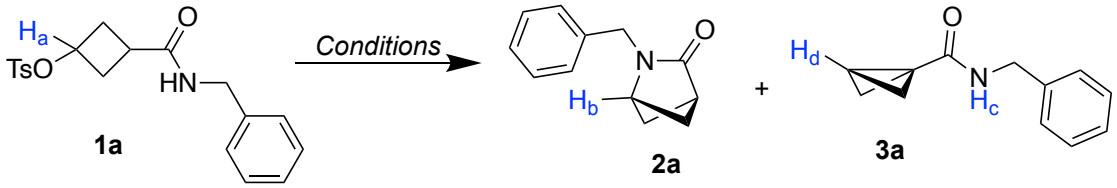

Table 5.1, Entry 1:

In a 1-dram vial, **1a** (18.0 mg, 0.05 mmol, 1 equiv) and 1,3,5-trimethyoxybenzene (2.8 mg, 0.33 equiv) was added and dissolved in THF (0.2 mL, 0.25 M). To the vial was added KOtBu (11.2 mg, 0.10 mmol, 2.0 equiv) and then the reaction was stirred at 40 °C for 24 hours. The reaction was quenched with 1 mL NH_4Cl and extracted twice with 1 mL of ethyl acetate. The organic layers were combined and dried with Mg_2SO_4, filtered and the solvent was evaported. The amounts of product and starting materials were determined by ^{1}H NMR spectroscopy relative to the internal standard (1,3,5-trimethoxybenzene). 0% **1a** (no peak at 4.68 ppm, H_a), 5% **2a** (3.38 ppm peak, H_b), and 20% **3a** (5.89 ppm peak, H_c).

^{1}H NMR (300 MHz, $CDCl_3$, 292 K):

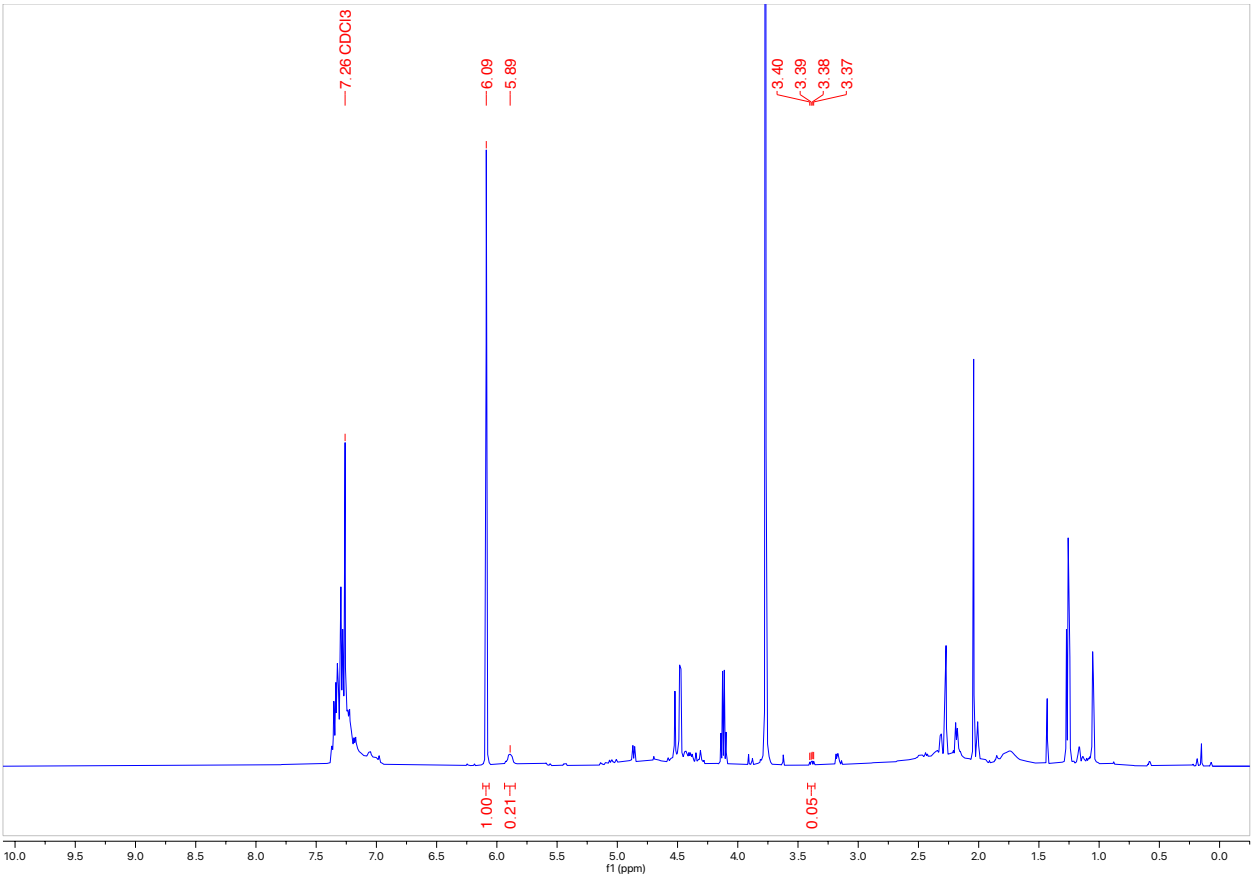

Table 5.1, Entry 2:

In a 1-dram vial, **1a** (18.0 mg, 0.05 mmol, 1 equiv) and 1,3,5-trimethyoxybenzene (2.8 mg, 0.33 equiv) was added and dissolved in THF (0.2 mL, 0.25 M). To the vial was added NaOtBu (5.3 mg, 0.055 mmol, 1.1 equiv) and then the reaction was stirred at 60 °C for 24 hours. The reaction was quenched with 1 mL NH_4Cl and extracted twice with 1 mL of ethyl acetate. The organic layers were combined and dried with Mg_2SO_4, filtered and the solvent was evaported. The amounts of product and starting materials were determined by ^{1}H NMR spectroscopy relative to the internal standard (1,3,5-trimethoxybenzene). 0% **1a** (no peak at 4.68 ppm, H_a), 0% **2a** (no peak at 3.38 ppm, H_b), and 59% **3a** (2.01 ppm peak, H_d).

^{1}H NMR (300 MHz, $CDCl_3$, 292 K):

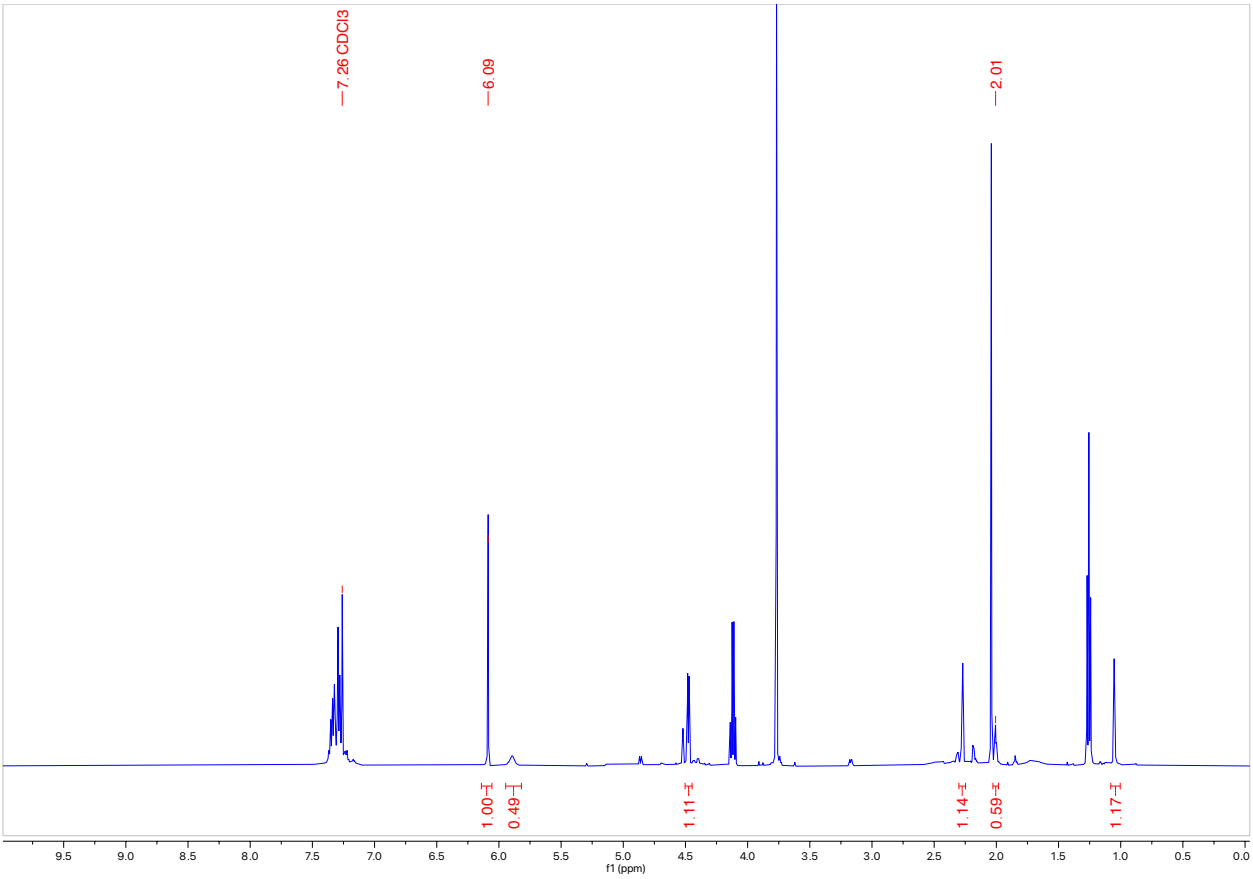

Table 5.1, Entry 3:

In a 1-dram vial, **1a** (18.0 mg, 0.05 mmol, 1 equiv) and 1,3,5-trimethyoxybenzene (2.8 mg, 0.33 equiv) was added and dissolved in THF (0.2 mL, 0.25 M). To the vial was added Cs_2CO_3 (17.9 mg, 0.055 mmol, 1.1 equiv) and then the reaction was stirred at 60 °C for 24 hours. The reaction was quenched with 1 mL NH_4Cl and extracted twice with 1 mL of ethyl acetate. The organic layers were combined and dried with Mg_2SO_4, filtered and the solvent was evaported. The amounts of product and starting materials were determined by ^{1}H NMR spectroscopy relative to the internal standard (1,3,5-trimethoxybenzene). 100% **1a** (4.68 ppm peak, H_a), 0% **2a** (no peak at 3.38 ppm, H_b), and 0% **3a** (no peak at 2.01 ppm, H_d).

^{1}H NMR (300 MHz, $CDCl_3$, 292 K):

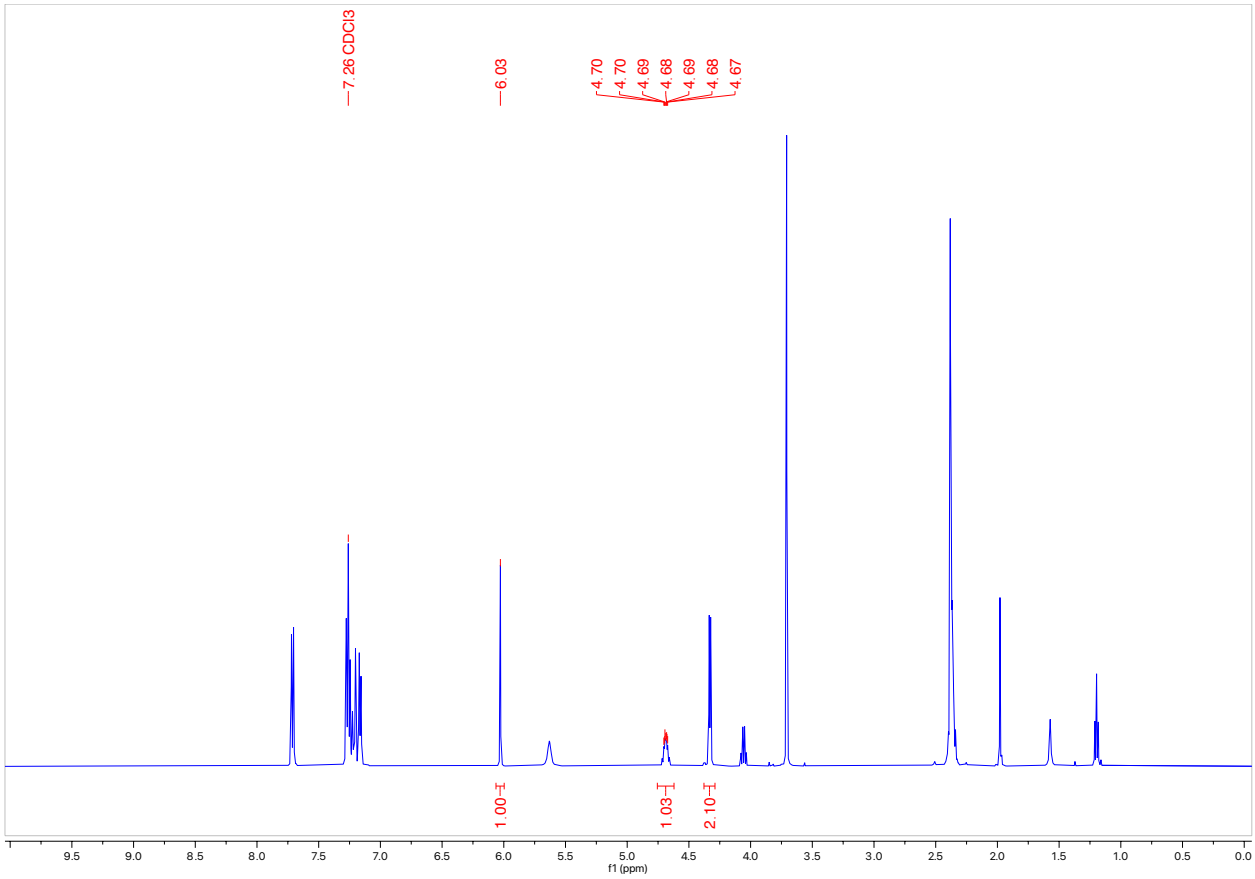

Table 5.1, Entry 4:

In a 1-dram vial, **1a** (18.0 mg, 0.05 mmol, 1 equiv) and 1,3,5-trimethyoxybenzene (2.8 mg, 0.33 equiv) was added and dissolved in THF (0.1 mL, 0.25 M). To another 1-dram vial was added n-BuLi in 2.5 M hexanes (40 μL, 0.10 mmol, 2.0 equiv) and THF (0.1 mL, 0.25 M) which was cooled down in the freezer. Then diisopropylamine (12.4 μL, 0.10 mmol, 2.0 equiv) was added to the base and it was stirred for 2 minutes before adding it to the vial contaning **1a**. The reaction was stirred at 60 °C for 24 hours. The reaction was quenched with 1 mL NH_4Cl and extracted twice with 1 mL of ethyl acetate. The organic layers were combined and dried with Mg_2SO_4, filtered and the solvent was evaported. The amounts of product and starting materials were determined by ^{1}H NMR spectroscopy relative to the internal standard (1,3,5-trimethoxybenzene). 0% **1a** (no peak at 4.68 ppm, H_a), 12% **2a** (3.13 ppm peak, H_b), and 0% **3a** (no peak at 2.01 ppm, H_d).

^{1}H NMR (300 MHz, $CDCl_3$, 292 K):

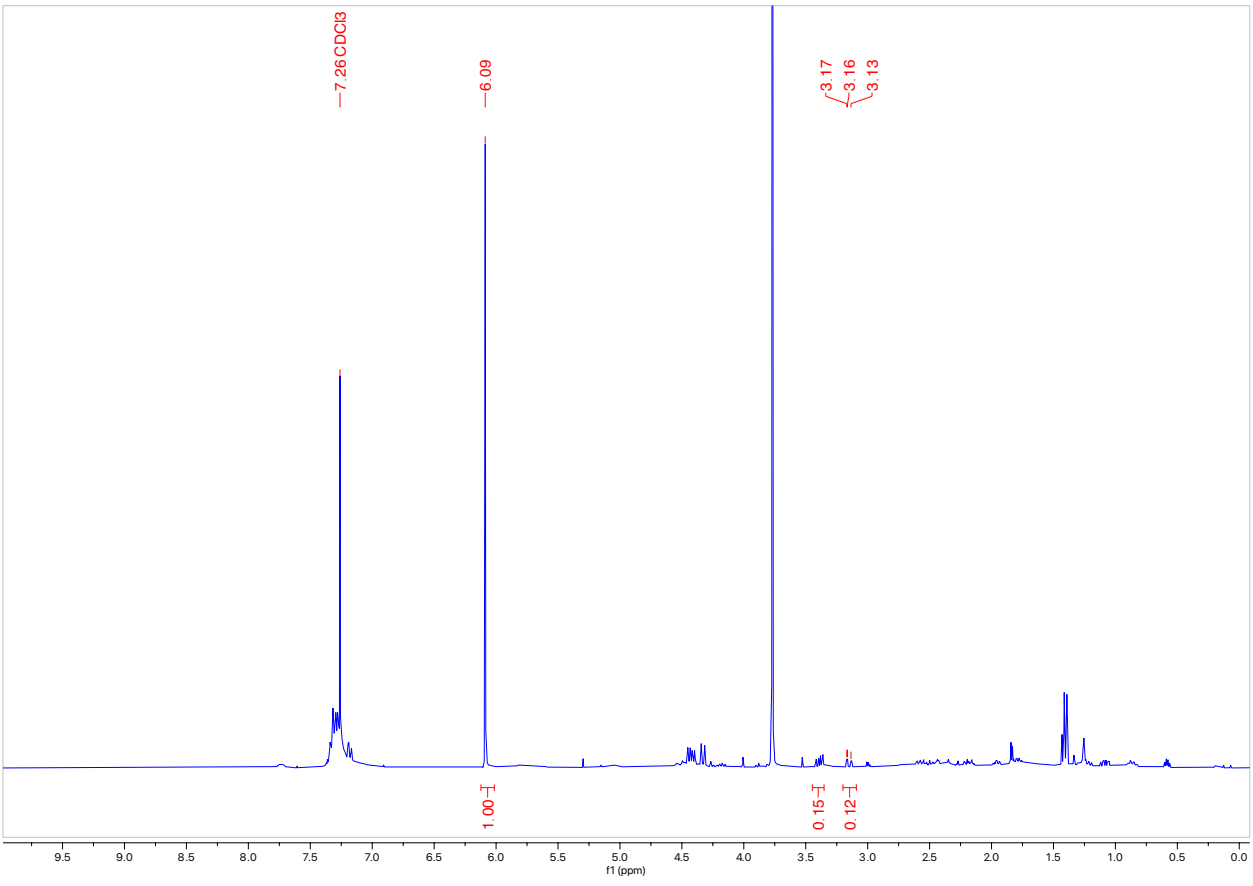

Table 5.1, Entry 5:

In a 1-dram vial, **1a** (18.0 mg, 0.05 mmol, 1 equiv) and 1,3,5-trimethyoxybenzene (2.8 mg, 0.33 equiv) was added and dissolved in THF (0.2 mL, 0.25 M). To the vial was added NaH (60% in mineral oil) (2.2 mg, 0.10 mmol, 2.0 equiv) and then the reaction was stirred at 60 °C for 24 hours. The reaction was quenched with 1 mL NH_4Cl and extracted twice with 1 mL of ethyl acetate. The organic layers were combined and dried with Mg_2SO_4, filtered and the solvent was evaported. The amounts of product and starting materials were determined by ^{1}H NMR spectroscopy relative to the internal standard (1,3,5-trimethoxybenzene). 84% **1a** (4.74 ppm peak, H_a), 0% **2a** (no peak at 3.38 ppm, H_b), and 0% **3a** (no peak at 2.01 ppm, H_d).

^{1}H NMR (300 MHz, $CDCl_3$, 292 K):

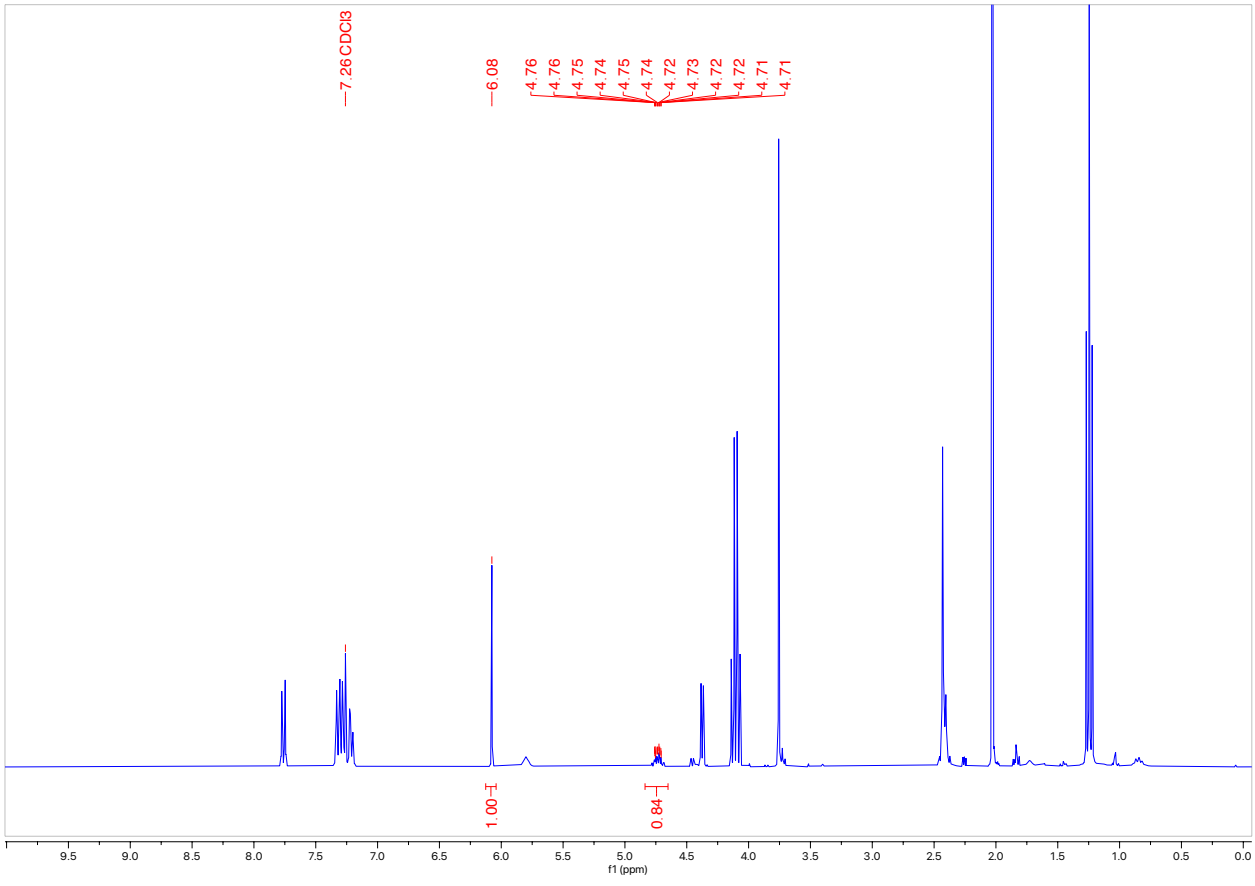

Table 5.1, Entry 6:

In a 1-dram vial, **1a** (18.0 mg, 0.05 mmol, 1 equiv) and 1,3,5-trimethyoxybenzene (2.8 mg, 0.33 equiv) was added and dissolved in THF (0.2 mL, 0.25 M). To the vial was added 1.0 M LiHMDS in THF (0.10 mL, 0.10 mmol, 2.0 equiv) and then the reaction was stirred at 60 °C for 24 hours. The reaction was quenched with 1 mL NH_4Cl and extracted twice with 1 mL of ethyl acetate. The organic layers were combined and dried with Mg_2SO_4, filtered and the solvent was evaported. The amounts of product and starting materials were determined by ^{1}H NMR spectroscopy relative to the internal standard (1,3,5-trimethoxybenzene). 0% **1a** (no peak at 4.68 ppm, H_a), 26% **2a** (3.13 ppm peak, H_b), and 0% **3a** (no peak at 2.01 ppm, H_d).

^{1}H NMR (300 MHz, $CDCl_3$, 292 K):

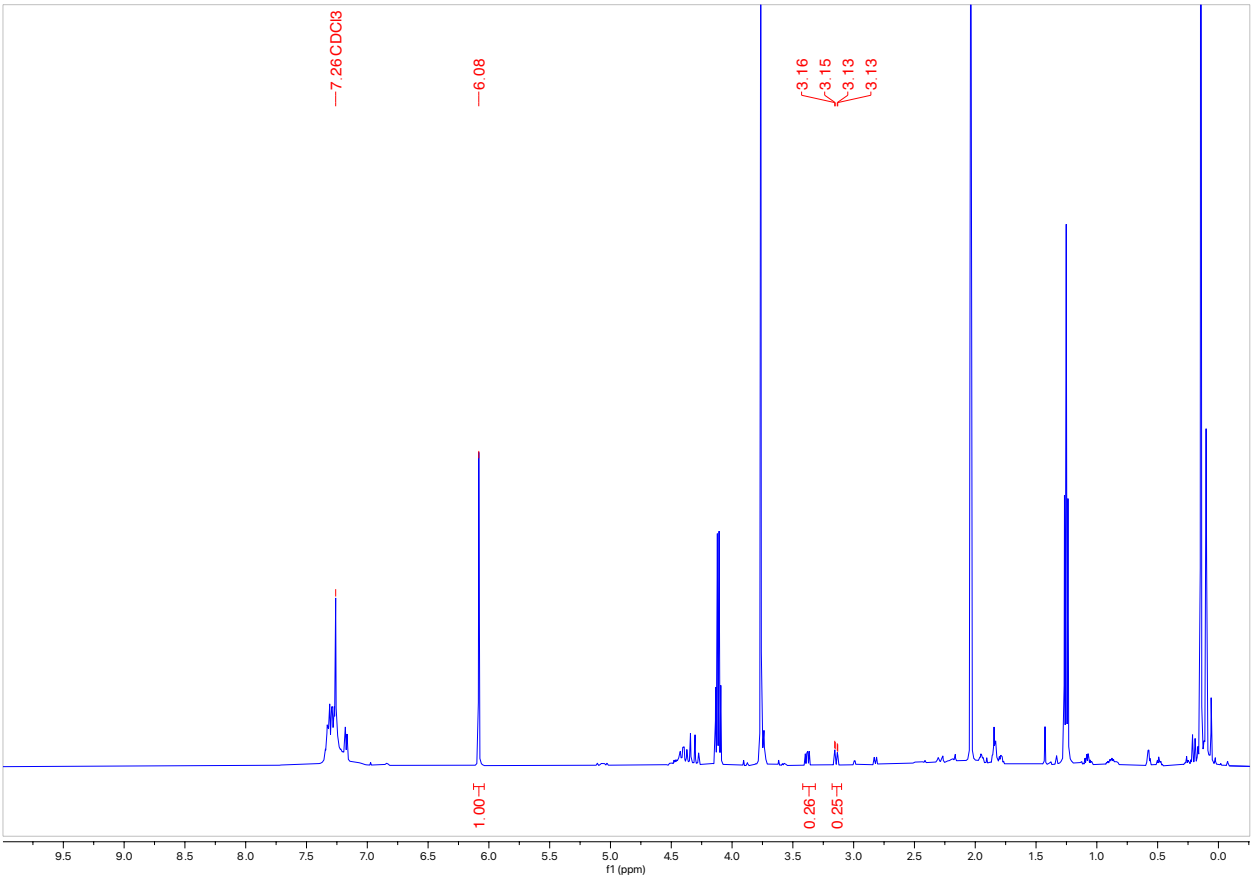

Table 5.1, Entry 7:

In a 1-dram vial, **1a** (18.0 mg, 0.05 mmol, 1 equiv) and 1,3,5-trimethyoxybenzene (2.8 mg, 0.33 equiv) was added and dissolved in THF (0.2 mL, 0.25 M). To the vial was added 1.0 M LiHMDS in THF (0.10 mL, 0.10 mmol, 2.0 equiv) and then the reaction was stirred at rt for 24 hours. The reaction was quenched with 1 mL NH_4Cl and extracted twice with 1 mL of ethyl acetate. The organic layers were combined and dried with Mg_2SO_4, filtered and the solvent was evaported. The amounts of product and starting materials were determined by ^{1}H NMR spectroscopy relative to the internal standard (1,3,5-trimethoxybenzene).67% **1a** (4.74 ppm peak, H_a), 6% **2a** (3.13 ppm peak, H_b), and 6% **3a** (2.12 ppm peak, H_d).

^{1}H NMR (300 MHz, $CDCl_3$, 292 K):

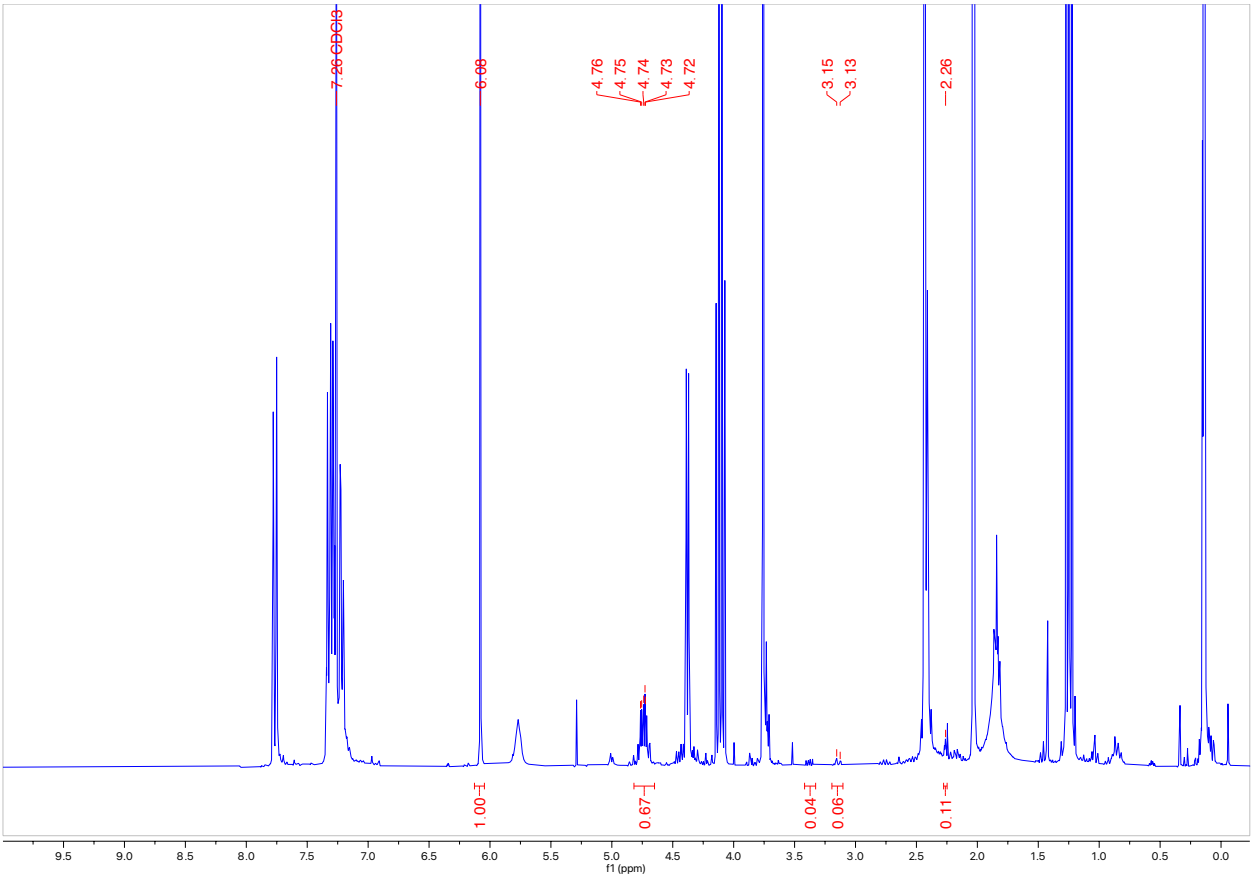

Table 5.1, Entry 8:

In a 1-dram vial, **1a** (18.0 mg, 0.05 mmol, 1 equiv) and 1,3,5-trimethyoxybenzene (2.8 mg, 0.33 equiv) was added and dissolved in THF (0.2 mL, 0.25 M). To the vial was added 1.0 M LiHMDS in THF (0.10 mL, 0.10 mmol, 2.0 equiv) and then the reaction was stirred at 40 °C for 24 hours. The reaction was quenched with 1 mL NH_4Cl and extracted twice with 1 mL of ethyl acetate. The organic layers were combined and dried with Mg_2SO_4, filtered and the solvent was evaported. The amounts of product and starting materials were determined by ^{1}H NMR spectroscopy relative to the internal standard (1,3,5-trimethoxybenzene). 24% **1a** (4.74 ppm peak, H_a), 19% **2a** (3.13 ppm peak, H_b), and 0% **3a** (no peak at 2.01 ppm, H_d).

^{1}H NMR (300 MHz, $CDCl_3$, 292 K):

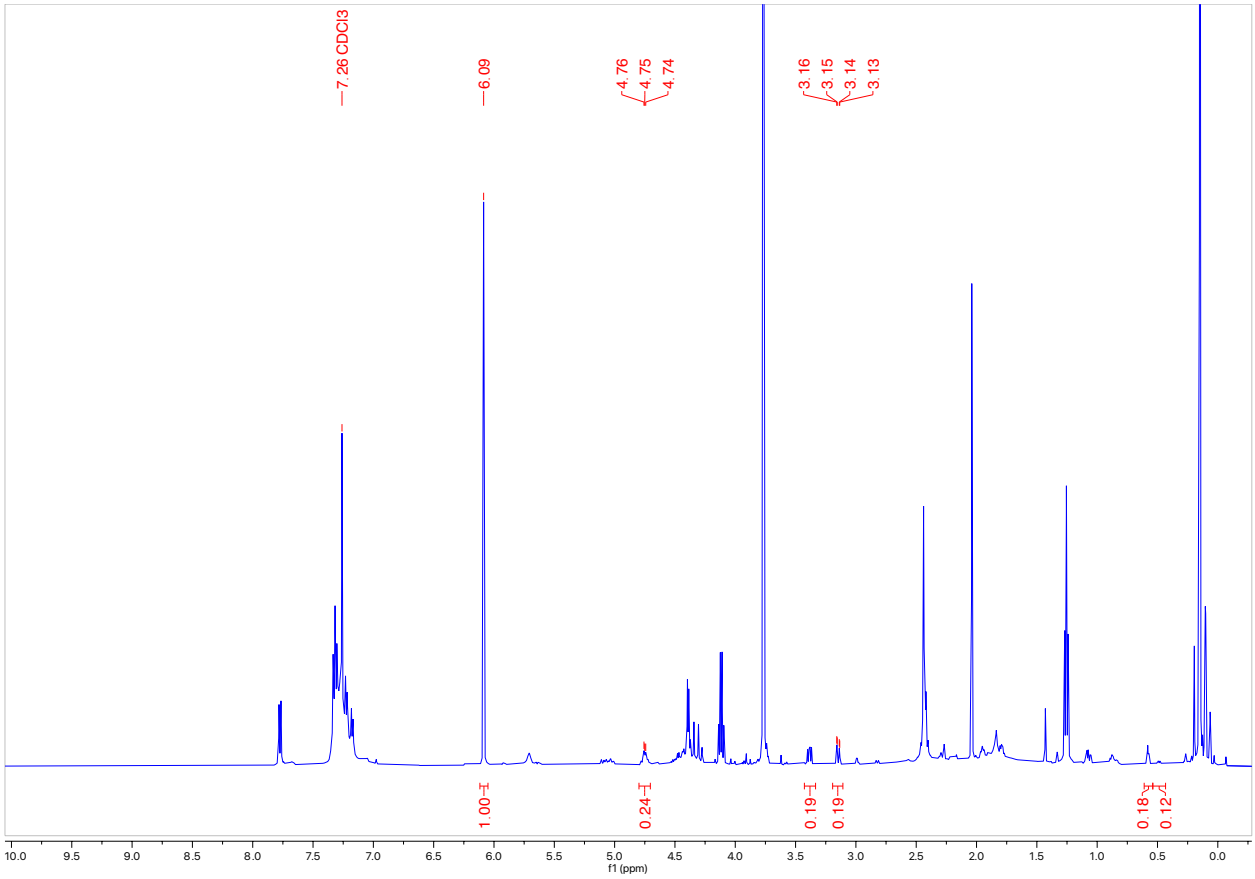

Table 5.1, Entry 9:

In a 1-dram vial, **1a** (18.0 mg, 0.05 mmol, 1 equiv) and 1,3,5-trimethyoxybenzene (2.8 mg, 0.33 equiv) was added and dissolved in THF (1.0 mL, 0.05 M). To the vial was added 1.0 M LiHMDS in THF (0.10 mL, 0.10 mmol, 2.0 equiv) and then the reaction was stirred at 60 °C for 24 hours. The reaction was quenched with 1 mL NH_4Cl and extracted twice with 1 mL of ethyl acetate. The organic layers were combined and dried with Mg_2SO_4, filtered and the solvent was evaported. The amounts of product and starting materials were determined by ^{1}H NMR spectroscopy relative to the internal standard (1,3,5-trimethoxybenzene). 0% **1a** (no peak at 4.68 ppm, H_a), 23% **2a** (3.13 ppm peak, H_b), and 0% **3a** (no peak at 2.01 ppm, H_d).

^{1}H NMR (300 MHz, $CDCl_3$, 292 K):

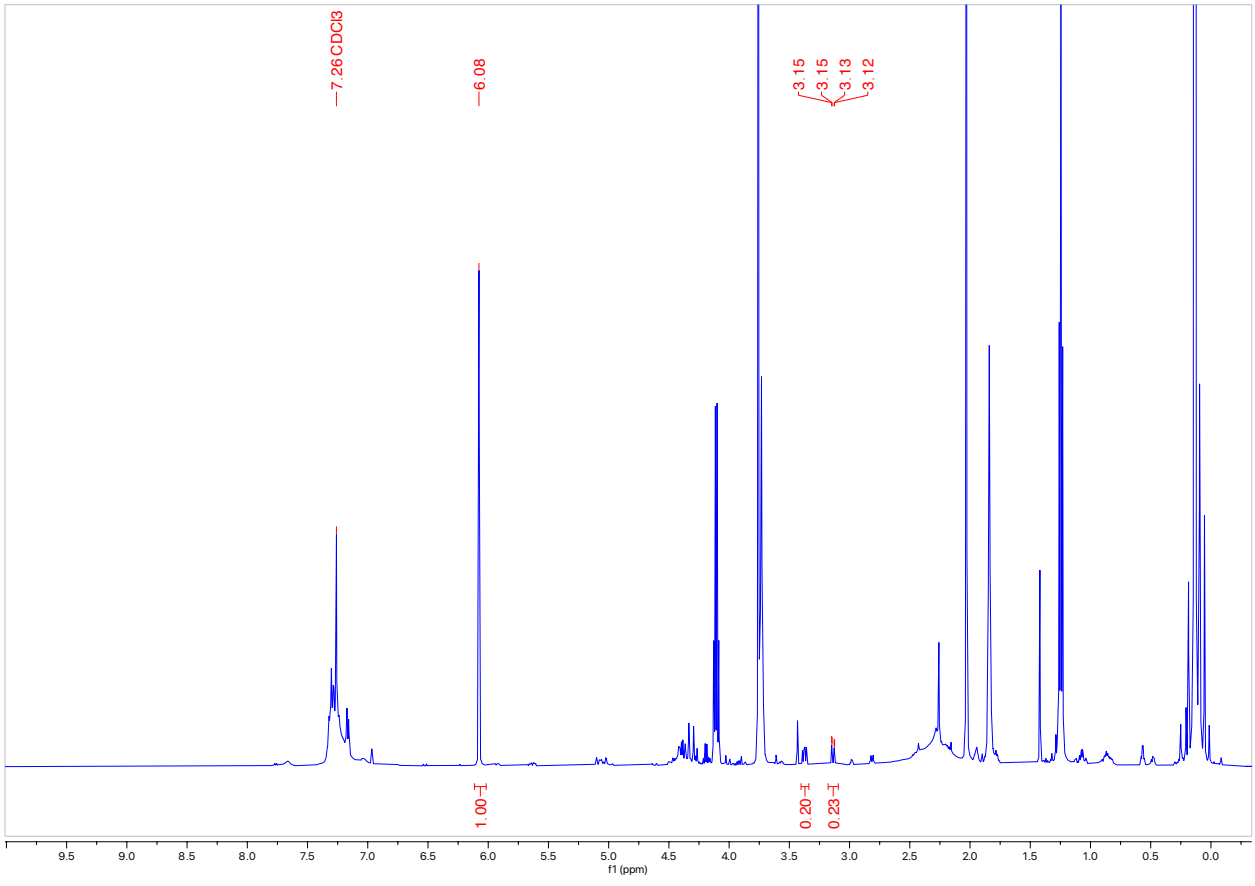

Table 5.1, Entry 10:

In a 1-dram vial, **1a** (18.0 mg, 0.05 mmol, 1 equiv) and 1,3,5-trimethyoxybenzene (2.8 mg, 0.33 equiv) was added and then 1.0 M LiHMDS in THF (0.10 mL, 2.0 equiv) was added. The reaction was stirred at 60 °C for 24 hours. The reaction was quenched with 1 mL NH_4Cl and extracted twice with 1 mL of ethyl acetate. The organic layers were combined and dried with Mg_2SO_4, filtered and the solvent was evaported. The amounts of product and starting materials were determined by ^{1}H NMR spectroscopy relative to the internal standard (1,3,5-trimethoxybenzene). 0% **1a** (no peak at 4.68 ppm, H_a), 21% **2a** (3.15 ppm peak, H_b), and 0% **3a** (no peak at 2.01 ppm, H_d).

^{1}H NMR (300 MHz, $CDCl_3$, 292 K):

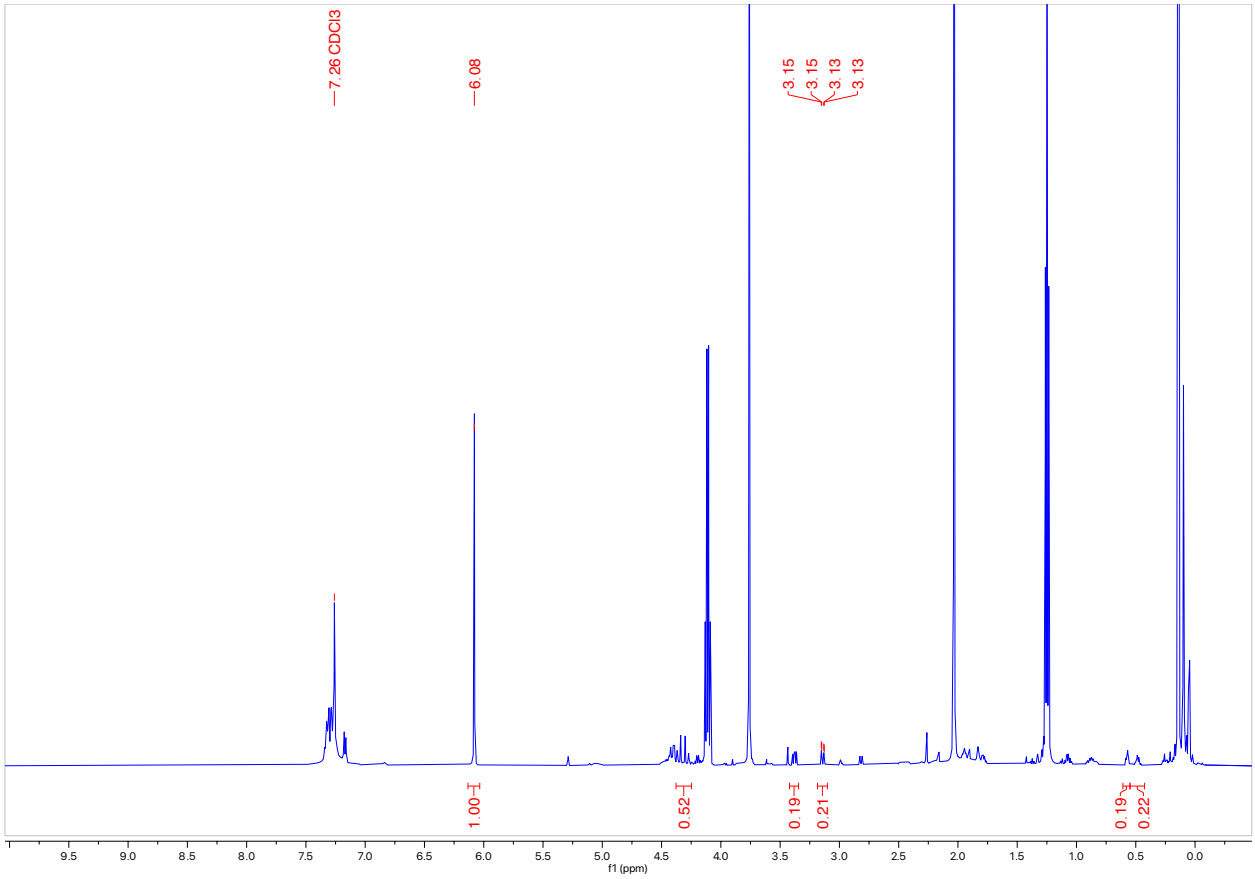

Table 5.1, Entry 11:

In a 1-dram vial, **1a** (18.0 mg, 0.05 mmol, 1 equiv) and 1,3,5-trimethyoxybenzene (2.8 mg, 0.33 equiv) was added and then trimethylsilyl trifluoromethanesulfonate (12.2 mg, 1.1 equiv) and DIPEA (9.6 μ, 1.1 equiv) was added. The reaction was stirred at 60 °C for 24 hours. The reaction was quenched with 1 mL NH_4Cl and extracted twice with 1 mL of ethyl acetate. The organic layers were combined and dried with Mg_2SO_4, filtered and the solvent was evaported. The amounts of product and starting materials were determined by ^{1}H NMR spectroscopy relative to the internal standard (1,3,5-trimethoxybenzene). 64% **1a** (4.70 ppm peak, H_a), 0% **2a** (no peak at 3.38 ppm, H_b) and 0% **3a** (no peak at 2.01 ppm, H_d).

^{1}H NMR (300 MHz, $CDCl_3$, 292 K):

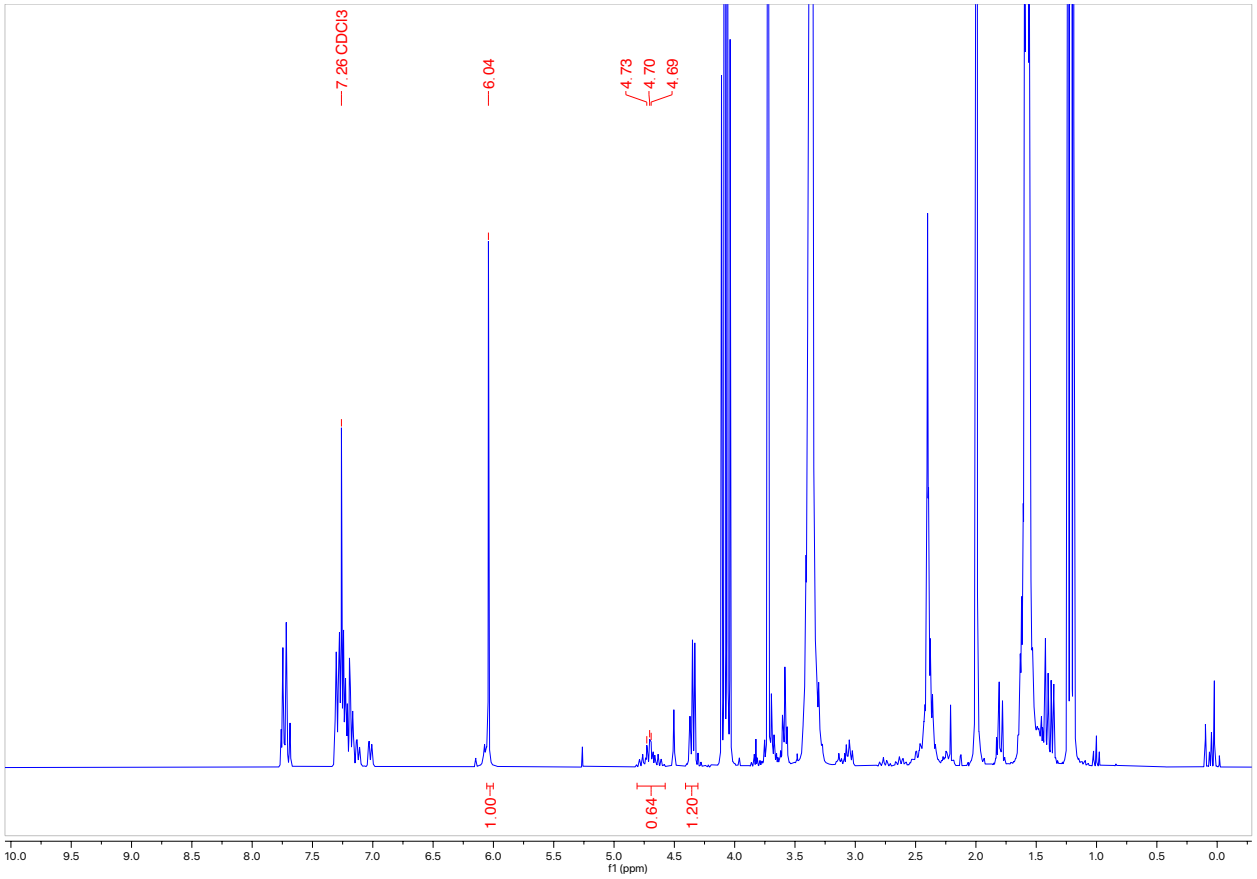

Synthesis of 2-benzyl-2-azabicyclo[2.2.1]heptan-3-one (5a)

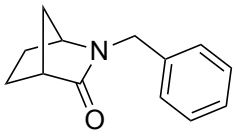

In a 2-dram vial, **4a** (111.9 mg, 0.50 mmol, 1 equiv) was added and dissolved in THF (2.0 mL, 0.25 M). To the vial was added 1.0 M LiHMDS in THF (1.0 mL, 1.0 mmol, 2.0 equiv) and then the reaction was stirred at 60 °C for 24 hours. The reaction was quenched with 3 mL NH_4Cl and extracted twice with 3 mL of ethyl acetate. The organic layers were combined and dried with Mg_2SO_4, filtered and the solvent was evaported. The product was purified by column chromatography (Biotage® Sfär 10g Column, 0-100% EtOAc/ hexanes, eluted at 29% EtOAc) and 38.5 mg of a white solid was obtained (41% Yield).

^{1}H NMR (300 MHz, $CDCl_3$, 292 K, ppm): δ 7.50 (dd, J = 8.8, 1.1 Hz, 2H), 7.34 (dd, J = 8.6, 7.5 Hz, 2H), 7.14 – 7.05 (m, 1H), 4.45 (s, 1H), 3.00 – 2.92 (m, 1H), 2.10 – 1.89 (m, 4H), 1.77 (d, J = 2.6 Hz, 1H), 1.53 (d, J = 9.5 Hz, 1H).

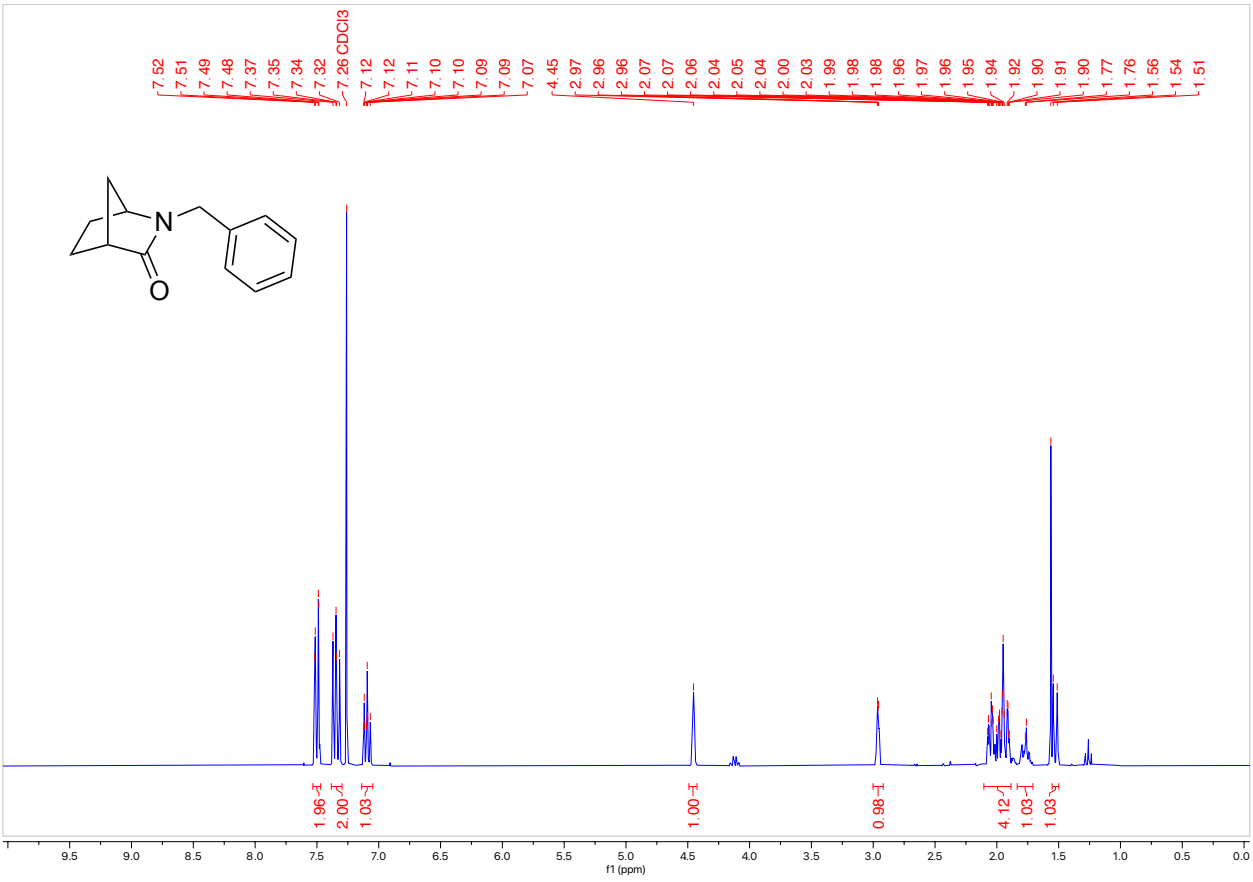

Test for synthesis of bicyclo[2.1.0]pentane 6a with conditions from Table 5.1, Entry 2:

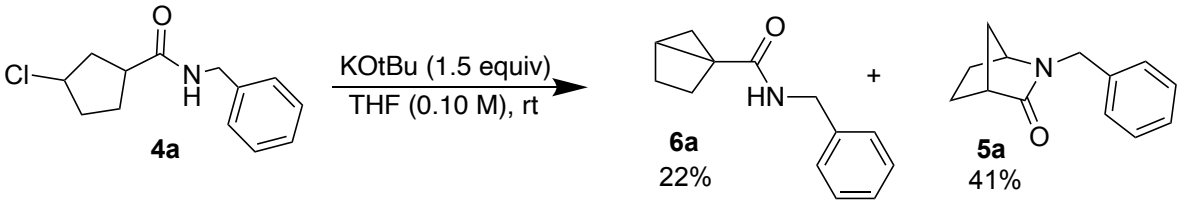

In a 1-dram vial, **4a** (12.1 mg, 0.05 mmol, 1 equiv) and 1,3,5-trimethyoxybenzene (2.8 mg, 0.33 equiv) was added and dissolved in THF (0.2 mL, 0.25 M). To the vial was added KOtBu (8.6 mg, 0.076 mmol, 1.5 equiv) and then the reaction was stirred at rt for 24 hours. The reaction was quenched with 1 mL NH_4Cl and extracted twice with 1 mL of ethyl acetate. The organic layers were combined and dried with Mg_2SO_4, filtered and the solvent was evaported. The amounts of product and starting materials were determined by ^{1}H NMR spectroscopy relative to the internal standard (1,3,5-trimethoxybenzene). 22% **6a** (4.52 ppm peak), and 41% **5a** (3.69 ppm peak).

^{1}H NMR (300 MHz, $CDCl_3$, 292 K, ppm):

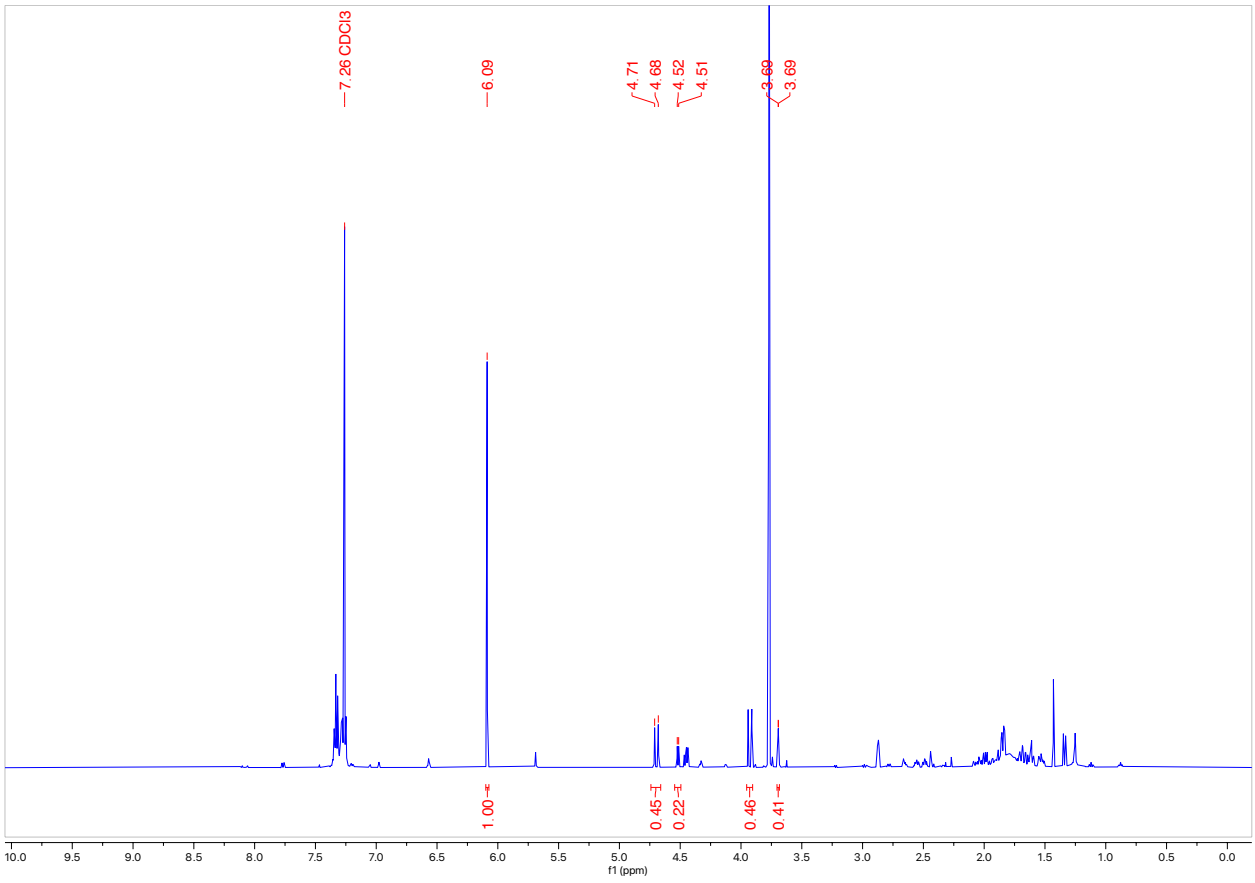

D.4 Reaction Scope

Substitution General Procedure In a 1-dram vial, **1** or **4** (0.05 mmol) and 1,3,5-trimethyoxybenzene (2.8 mg, 0.33 equiv, 0.017 mmol) was added and dissolved in THF (0.2 mL, 0.25 M). To the vial was added 1.0 M LiHMDS in THF (0.10 mL, 0.10 mmol, 2.0 equiv) and then the reaction was stirred at 60 °C for 24 hours. The reaction was quenched with 1 mL NH_4Cl and extracted twice with 1 mL of ethyl acetate. The organic layers were combined and dried with Mg_2SO_4, filtered and the solvent was evaported and then the sample was dissolved in $CDCl_3$. The % Yield was determined by ^{1}H NMR spectroscopy relative to the internal standard (1,3,5-trimethoxybenzene).

2-(4-Methoxybenzyl)-2-azabicyclo[2.1.1]hexan-3-one (2b)

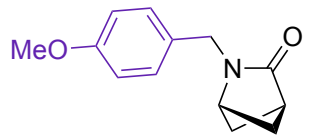

This product was prepared using the **Substitution General Procedure** and an 18% solution yield was obtained (3.36 ppm peak).

^{1}H NMR (300 MHz, $CDCl_3$, 292 K, ppm):

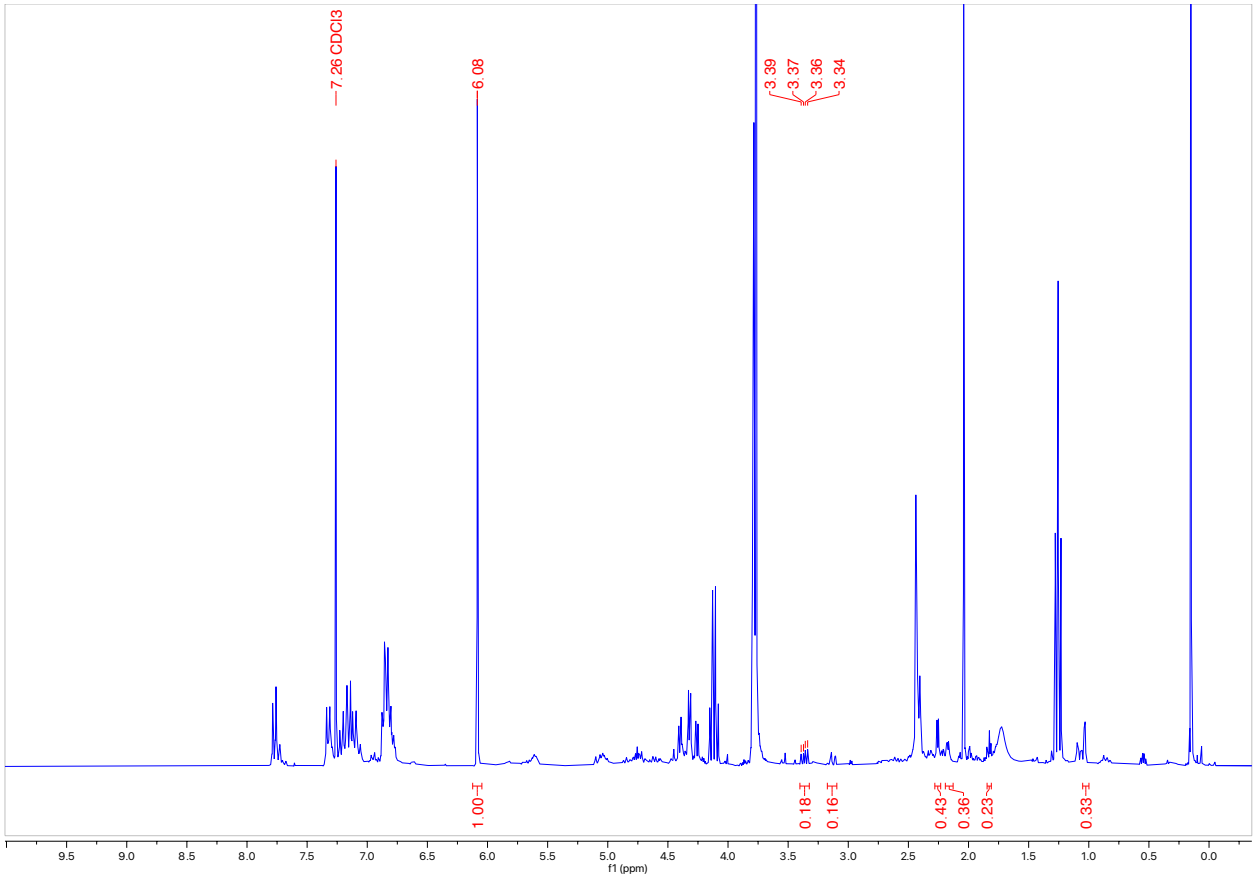

2-(4-Fluorobenzyl)-2-azabicyclo[2.1.1]hexan-3-one (2c)

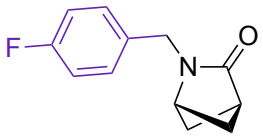

This product was prepared using the **Substitution General Procedure** and an 14% solution yield was obtained (3.37 ppm peak).

^{1}H NMR (300 MHz, $CDCl_3$, 292 K, ppm):

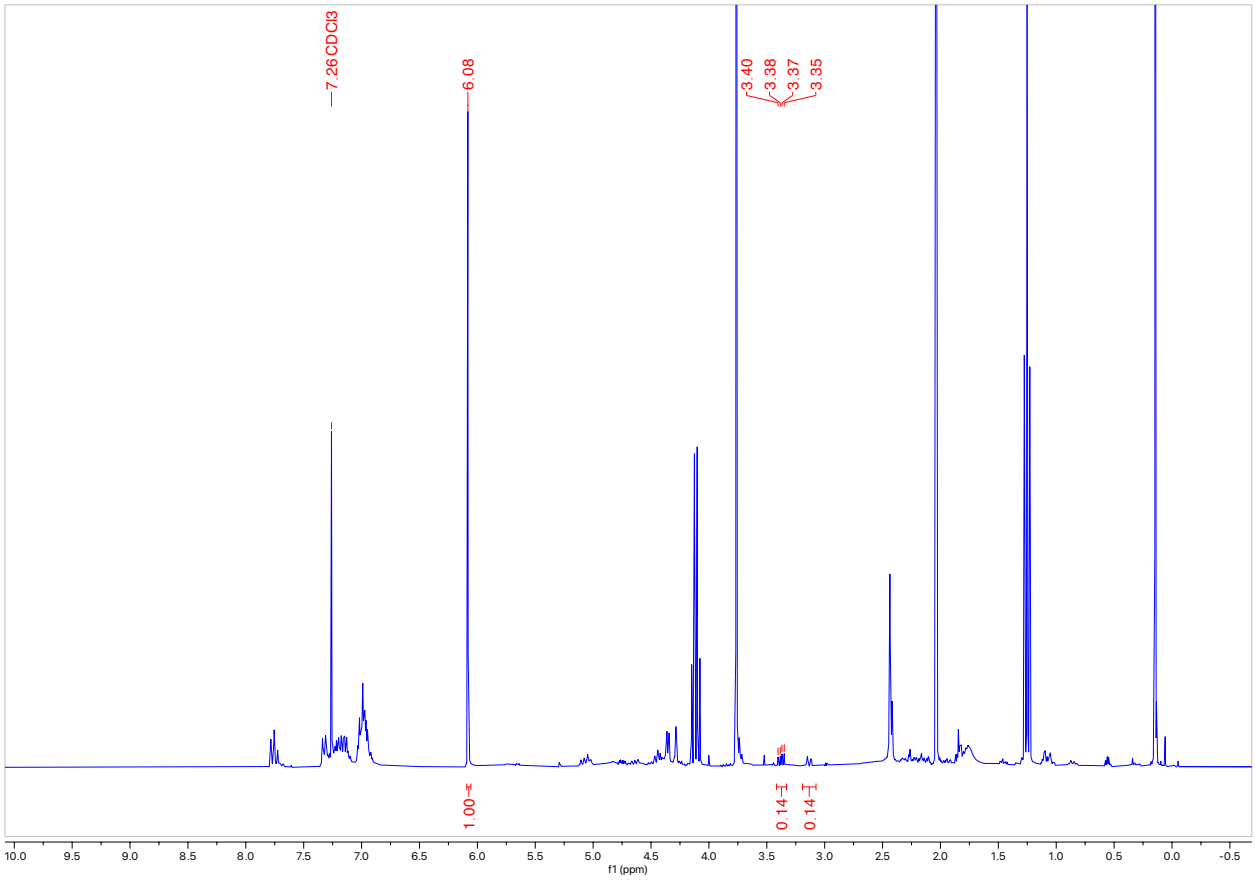

2-Allyl-2-azabicyclo[2.1.1]hexan-3-one (2d)

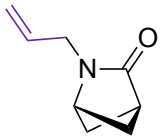

This product was prepared using the **Substitution General Procedure** and an 8% solution yield was obtained (3.46 ppm peak).

^{1}H NMR (300 MHz, $CDCl_3$, 292 K, ppm):

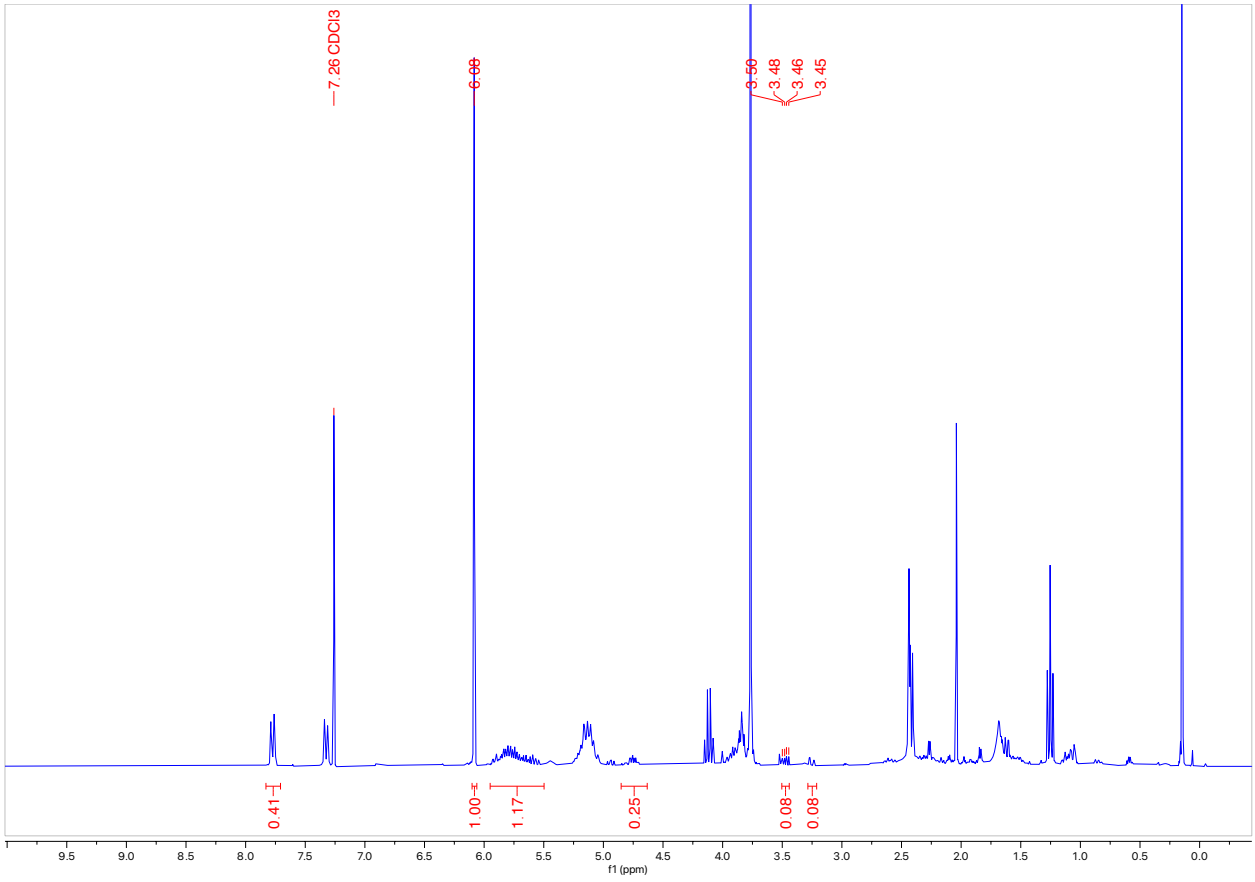

2-(*Tert*-butyl)-2-azabicyclo[2.1.1]hexan-3-one (2e)

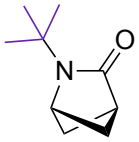

This product was prepared using the **Substitution General Procedure** and an 8% solution yield was obtained (3.39 ppm peak).

^{1}H NMR (300 MHz, $CDCl_3$, 292 K, ppm):

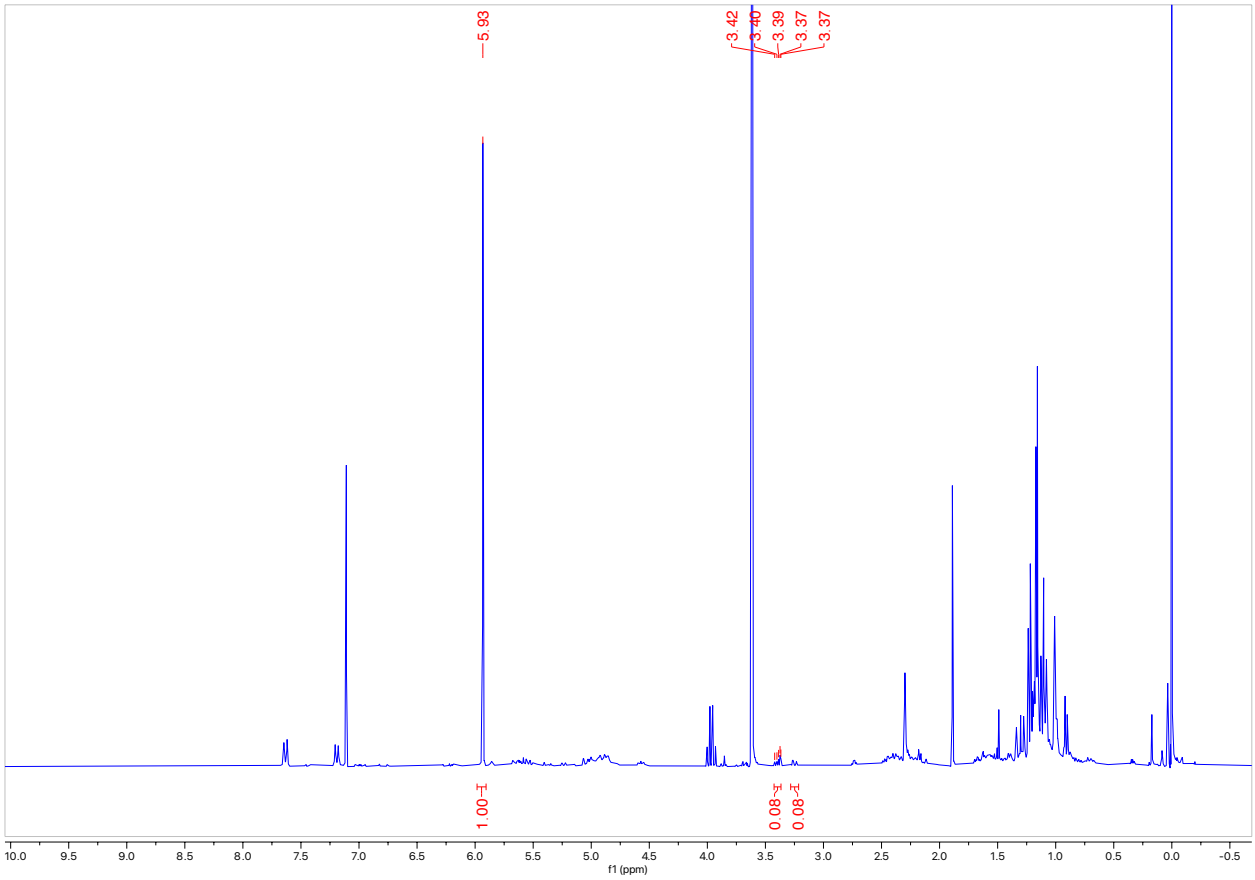

2-(2,2,2-Trifluoroethyl)-2-azabicyclo[2.1.1]hexan-3-one (2f)

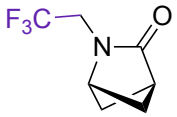

This product was prepared using the **Substitution General Procedure** and an 11% solution yield was obtained (3.00 ppm peak).

^{1}H NMR (300 MHz, $CDCl_3$, 292 K, ppm):

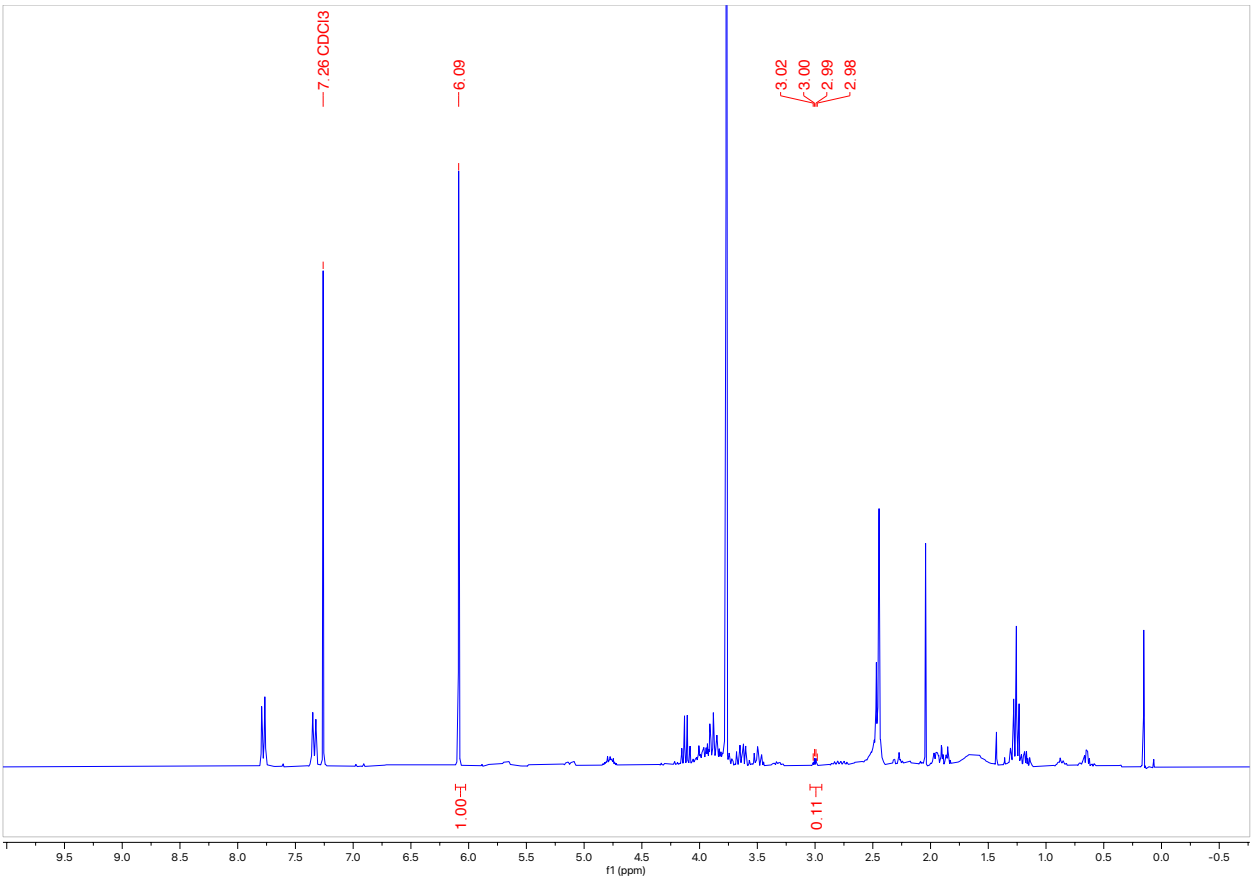

2-Phenyl-2-azabicyclo[2.2.1]heptan-3-one (5b)

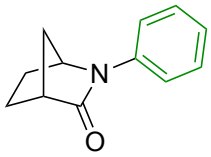

This product was prepared using the **Substitution General Procedure** and an 70% solution yield was obtained (2.96 ppm peak).

^{1}H NMR (300 MHz, $CDCl_3$, 292 K, ppm):

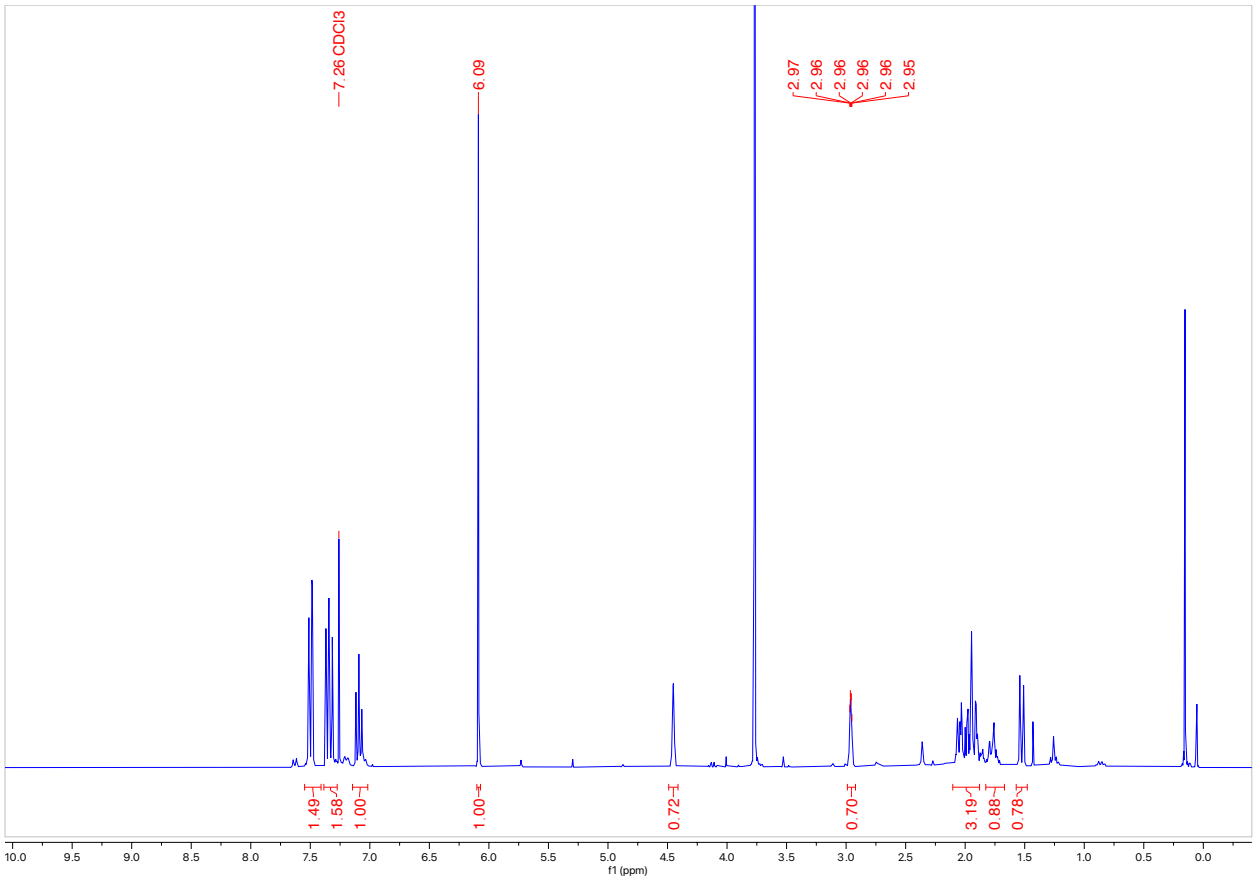

2-Allyl-2-azabicyclo[2.2.1]heptan-3-one (5c)

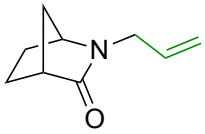

This product was prepared using the **Substitution General Procedure** and an 58% solution yield was obtained (2.83 ppm peak).

^{1}H NMR (300 MHz, $CDCl_3$, 292 K, ppm):

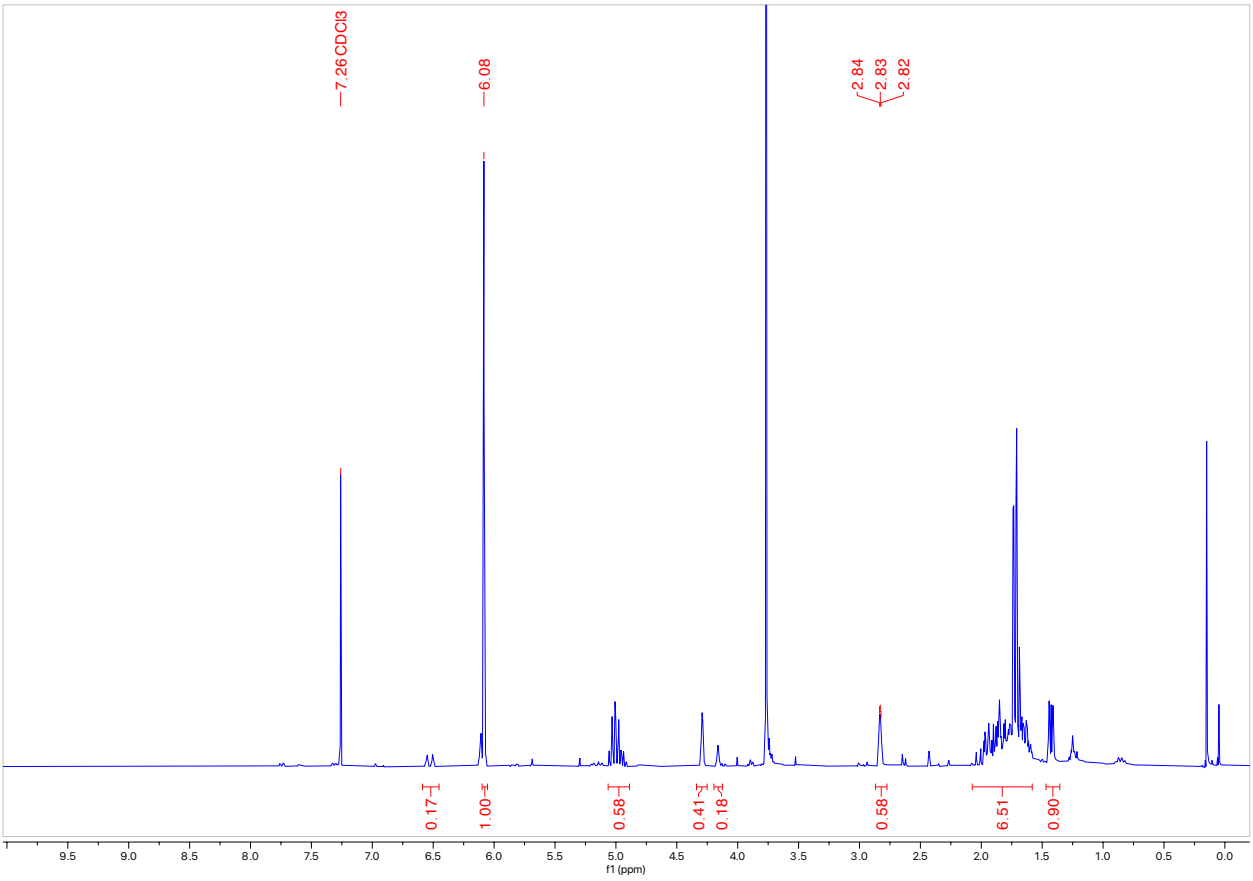

Methyl 2-(3-oxo-2-azabicyclo[2.2.1]heptan-2-yl)acetate (5d)

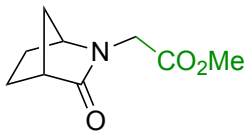

This product was prepared using the **Substitution General Procedure** and an 9% solution yield was obtained (2.80 ppm peak).

^{1}H NMR (300 MHz, $CDCl_3$, 292 K, ppm):

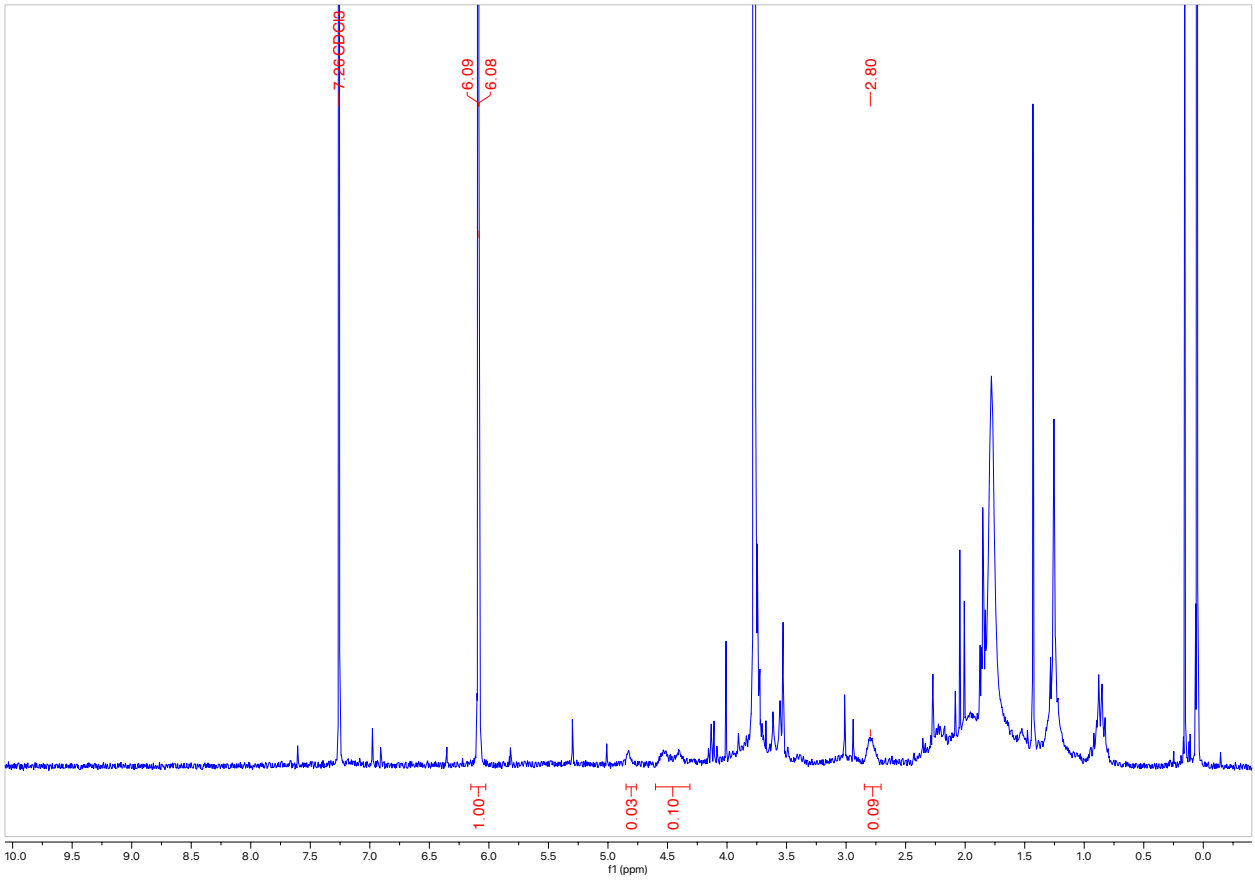

2-(*Tert*-butyl)-2-azabicyclo[2.2.1]heptan-3-one (5e)

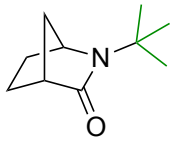

This product was prepared using the **Substitution General Procedure** and an 51% solution yield was obtained (2.69 ppm peak).

^{1}H NMR (300 MHz, $CDCl_3$, 292 K, ppm):

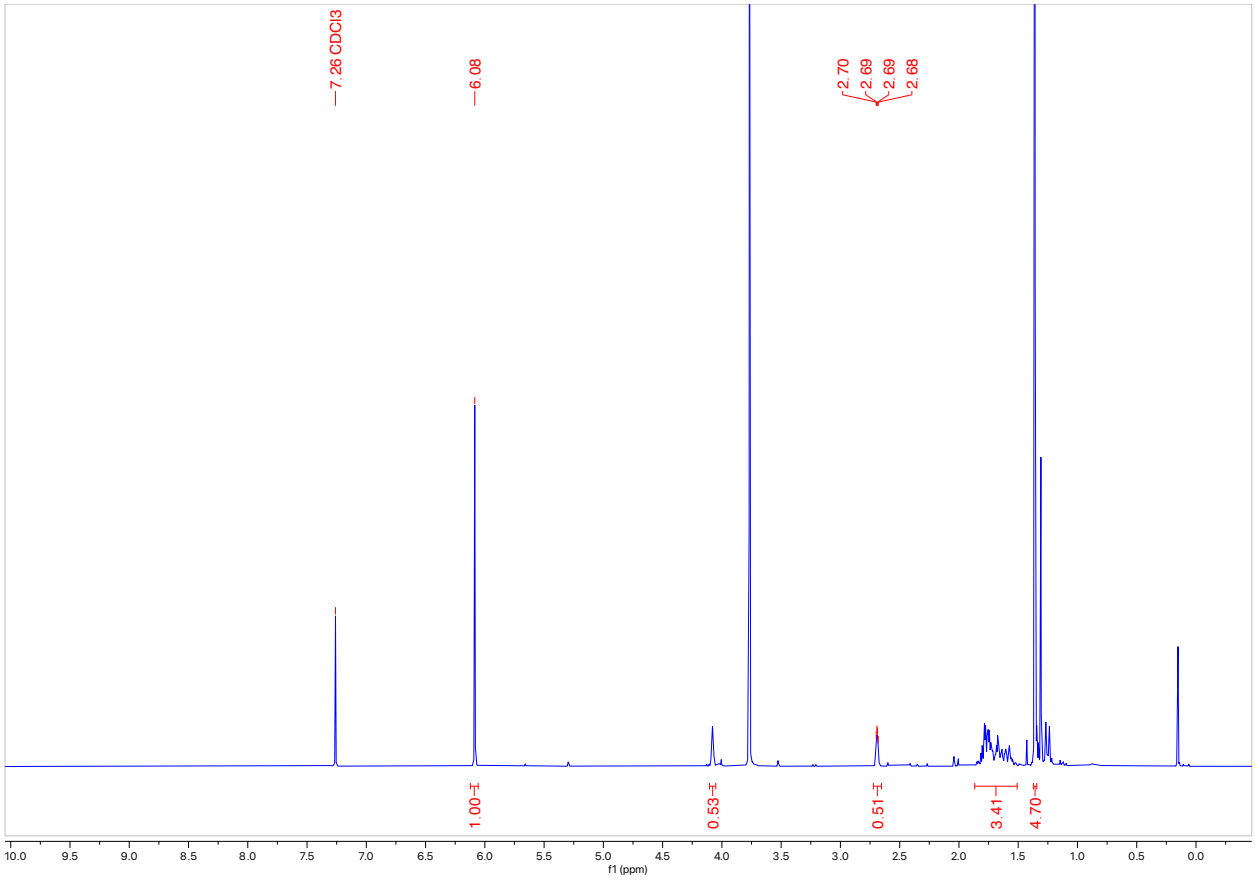

D.5 Additional Studies

Stereochemistry of *N*-benzyl-3-hydroxycyclobutane-1-carboxamide

^{1}H NMR (300 MHz, $CDCl_3$, 292 K, ppm):

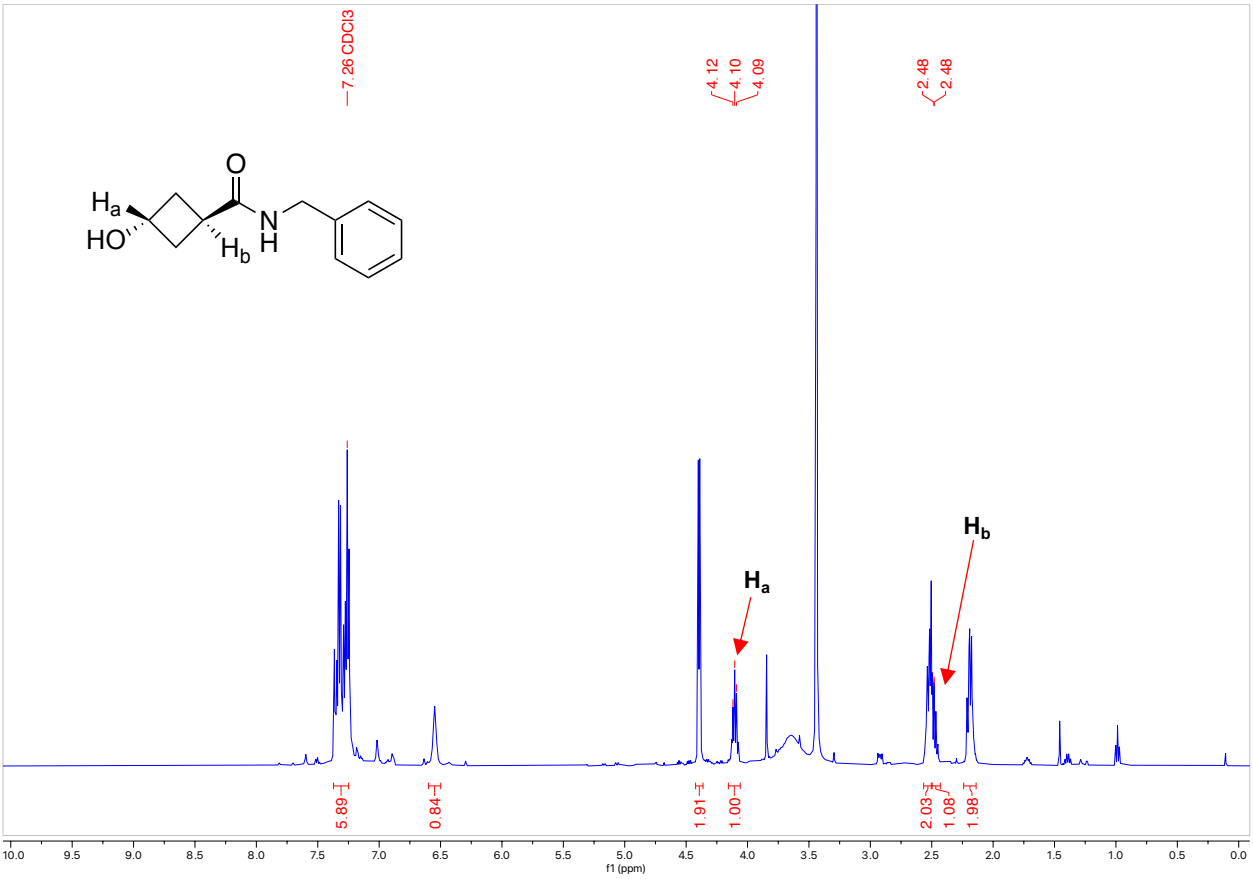

^{1}H-^{1}H NOESY: No correlation observed between H_a and H_b (4.1 and 2.5 ppm)

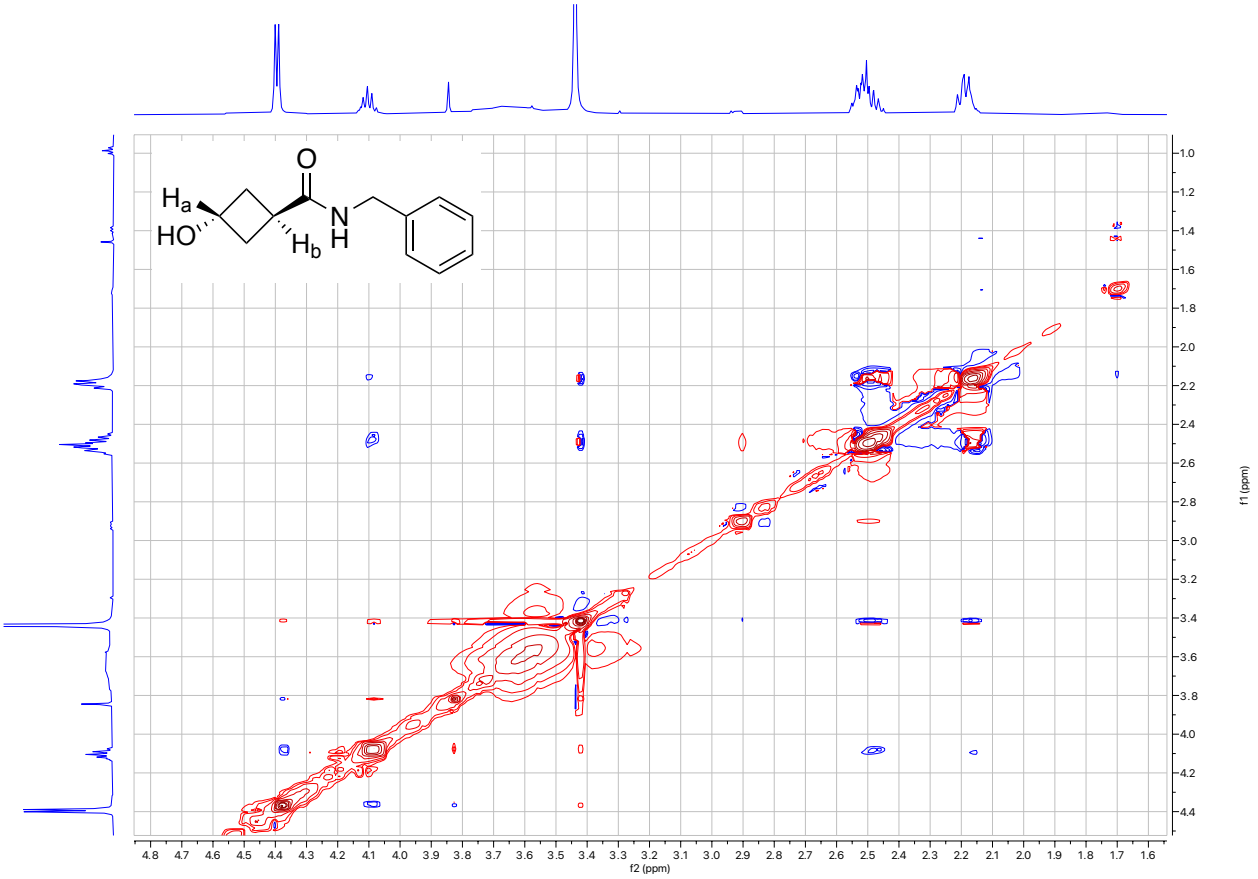

Bromination of *N*-benzyl-3-hydroxycyclobutane-1-carboxamide to *N*-benzyl-3-bromocyclobutane-1-carboxamide

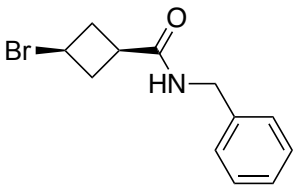

In a 4-dram vial, *N*-benzyl-3-hydroxycyclobutane-1-carboxamide (0.50 g, 2.44 mmol, 1 equiv) was added and dissolved in DCM (4.0 mL, 0.61 M). The vial was cooled down to 0 °C and then PBr_3 (76.3 μL, 0.33 equiv, 0.80 mmol) was added drop wise with stirring to the vial. The vial was warmed to room temperature and stirred overnight. The reaction was then quenched with $NaHCO_3$ and then extracted with DCM 3 times. The combined organic layers were dried with Mg_2SO_4, filtered and the solvent was evaporated. The product was purified by column chromatography Biotage® Sfär 10g Column, 0-100% EtOAc/ hexanes, eluted at 37% EtOAc) and 147.4 mg of a white solid was obtained (23% Yield).

^{1}H NMR (300 MHz, $CDCl_3$, 292 K, ppm):

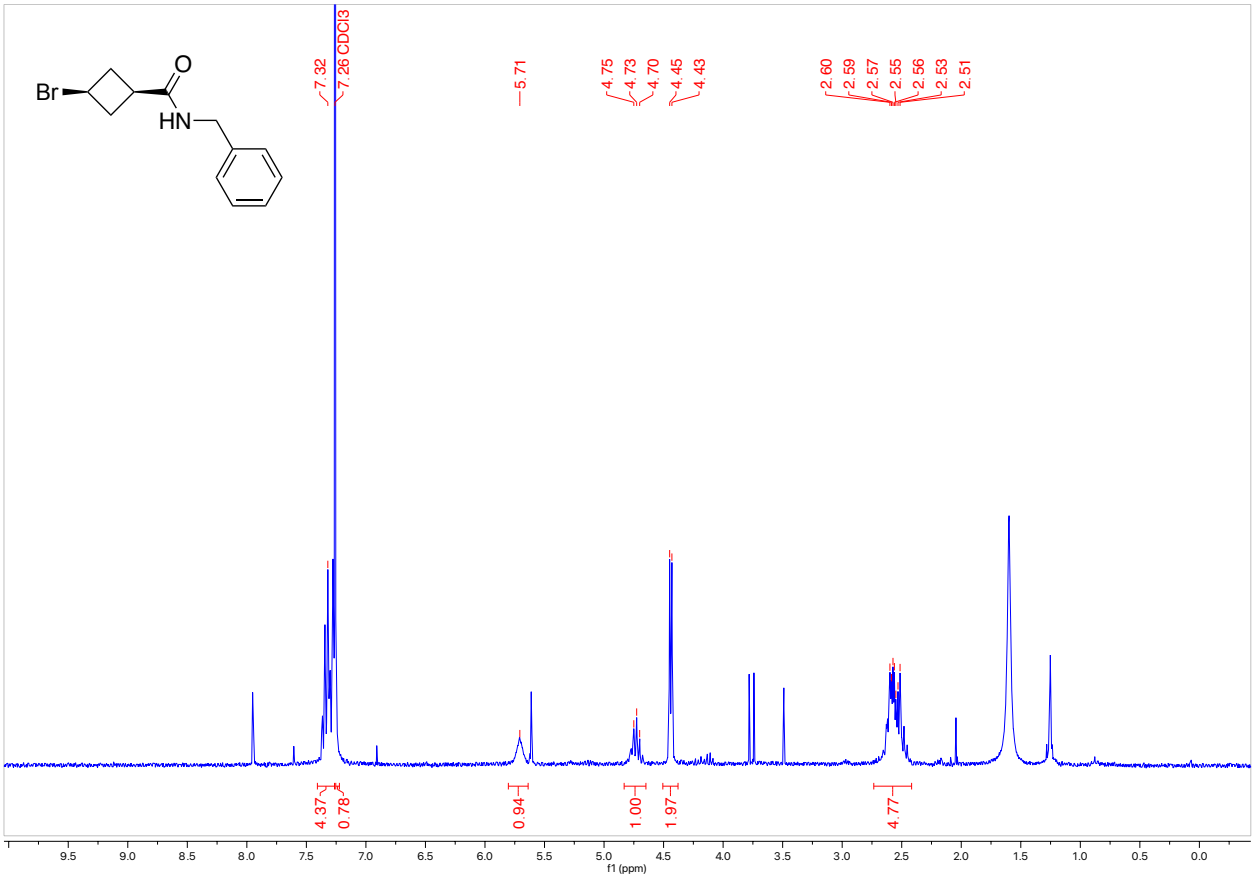

This product was subjected to the **Substitution General Procedure** and no azabicyclohexane product was observed.